

CONF - 780819
Volume 1
UC-70

PROCEEDINGS of the
15th DOE NUCLEAR AIR CLEANING CONFERENCE
held in Boston, Massachusetts
7 - 10 August 1978

Sponsors: U. S. Department of Energy
The Harvard Air Cleaning Laboratory

Editor
Melvin W. First

Published
February 1979

15th DOE NUCLEAR AIR CLEANING CONFERENCE

PROGRAM COMMITTEE:

W. L. ANDERSON

C. A. BURCHSTED

H. L. ETTINGER

D. W. MOELLER

R. R. BELLAMY

J. T. COLLINS

H. GILBERT

D. PENCE

R. BROWN

J. C. DEMPSEY

J. L. KOVACH

R. D. RIVERS

CONFERENCE CHAIRMAN:

MELVIN W. FIRST

HARVARD AIR CLEANING LABORATORY

15th DOE NUCLEAR AIR CLEANING CONFERENCE

TABLE OF CONTENTS

VOLUME I

Session I

INTRODUCTION TO THE NUCLEAR AIR CLEANING CONFERENCE: OBJECTIVES, NUCLEAR WASTE MANAGEMENT, RISK ASSESSMENT, AIR CLEANING FAILURES, AND STANDARDS FOR AIR AND GAS CLEANING INSTALLATIONS

Monday, August 7, 1978

CHAIRMAN: M. W. First

Harvard Air Cleaning Laboratory

WELCOME by M. W. First, Harvard Air Cleaning Laboratory..... 2

KEYNOTE ADDRESSES:

NUCLEAR WASTE MANAGEMENT AT DOE by A. Perge, Department of Energy..... 4

DISCUSSION..... 7

RISK-ASSESSMENT TECHNIQUES AND THE REACTOR LICENSING PROCESS by S. Levine,
U. S. Nuclear Regulatory Commission..... 8

DISCUSSION.....31

REVIEW OF FAILURES IN NUCLEAR AIR CLEANING SYSTEMS by D. W. Moeller, Harvard
Air Cleaning Laboratory.....32

DISCUSSION.....50

PROGRESS IN STANDARDS FOR NUCLEAR AIR AND GAS TREATMENT by C. A. Burchsted,
Oak Ridge National Laboratory.....51

REPORT ON ANSI/ASME NUCLEAR AIR AND GAS TREATMENT STANDARDS FOR NUCLEAR POWER
PLANTS by J. F. Fish, American Air Filter.....61

Session II

WASTE TREATMENT: VOLUME REDUCTION AND PREPARATION FOR STORAGE

Monday, August 7, 1978

CHAIRMAN: J. C. Dempsey

Department of Energy

OPENING REMARKS OF SESSION CHAIRMAN.....68

OPERATION OF LOW-LEVEL RADIOACTIVE WASTE INCINERATOR by E. C. Choi, T. S. Drolet,
W. B. Stewart, A. V. Campbell, Ontario Hydro.....70

DISCUSSION.....81

FLUIDIZED-BED CALCINATION OF LWR FUEL-REPROCESSING HLLW: REQUIREMENTS AND
POTENTIAL FOR OFF-GAS CLEANUP by R. E. Schindler, Allied Chemical Corp.....82

15th DOE NUCLEAR AIR CLEANING CONFERENCE

VOLATILIZATION FROM BOROSILICATE GLASS MELTS OF SIMULATED SAVANNAH RIVER PLANT WASTE by G. W. Wilds, Savannah River Laboratory.....	95
DISCUSSION.....	109
DISPOSAL OF HEPA FILTERS BY FLUIDIZED BED INCINERATION by D. L. Ziegler, A. J. Johnson, Rockwell International, Atomics International Division.....	111
DISCUSSION.....	115
VOLUME REDUCTION OF LOW-LEVEL COMBUSTIBLE TRANSURANIC WASTE AT MOUND FACILITY by W. H. Bond, J. W. Doty, J. W. Koenst, Jr., D. F. Luthy, Mound Facility.....	117
DISCUSSION.....	129
CLOSING REMARKS OF SESSION CHAIRMAN.....	130

Session III
TRITIUM, ¹⁴CARBON, OZONE
Tuesday, August 8, 1978
CHAIRMAN: D. Pence
Science Applications, Inc.

TRITIUM EFFLUENT REMOVAL SYSTEM by P. H. Lamberger, G. E. Gibbs, Mound Facility.....	133
DISCUSSION	140
MODIFICATION AND TESTING OF THE SANDIA LABORATORIES, LIVERMORE TRITIUM DECON- TAMINATION SYSTEMS by P. D. Gildea, H. G. Birnbaum, W. R. Wall, Sandia Laboratories.....	142
DISCUSSION.....	166
TRITIUM REMOVAL USING VANADIUM HYDRIDE by F. B. Hill, Y. W. Wong, Y. N. Chan, Brookhaven National Laboratory.....	167
DISCUSSION.....	194
STUDY ON THE TRITIUM REMOVAL FROM THE SODIUM IN LMFBR by K. Hata, Y. Nishizawa, Y. Osawa, Misubishi Atomic Power Industries, Inc.....	195
MONITORING AND REMOVAL OF GASEOUS CARBON-14 SPECIES by M. J. Kabat, Ontario Hydro.....	208
DISCUSSION.....	230
ON THE CATALYTIC REMOVAL OF OZONE PRODUCED IN RADIOACTIVE MEDIA by R.-D. Penzhorn, K. Günther, P. Schuster, Kernforschungszentrum Karlsruhe.....	231
DISCUSSION.....	243

15th DOE NUCLEAR AIR CLEANING CONFERENCE

Session IV
CONTAINMENT OF ACCIDENTAL RELEASES
Tuesday, August 8, 1978
CHAIRMAN: J. T. Collins
U. S. Nuclear Regulatory Commission

DEMONSTRATION OF AN EMERGENCY CONTAINMENT SYSTEM by T. M. Flanagan, M. L. Rogers, W. R. Wilkes, Mound Facility.....	245
STUDY OF THE CONTAINMENT SYSTEM OF THE PLANNED SNR-2 FAST BREEDER REACTOR by H. Bunz, Kernforschungszentrum Karlsruhe, and U. Scholle, INTERATOM.....	257
FISSION 2120: A PROGRAM FOR ASSESSING THE NEED FOR ENGINEERED SAFETY FEATURE GRADE AIR CLEANING SYSTEMS IN POST-ACCIDENT ENVIRONMENTS by G. Martin, Jr., D. Michlewicz, J. Thomas, Ebasco Services, Inc.....	266
DISCUSSION.....	278
IMPACT OF SOPHISTICATED FOG SPRAY MODELS ON ACCIDENT ANALYSES by S. P. Roblyer, United Nuclear Industries, Inc., and P. C. Owzarski, Sigma Research, Inc....	279
DISCUSSION.....	297

Session V
ADSORBENTS AND ABSORBENTS
Tuesday, August 8, 1978
CHAIRMEN: R. D. Rivers
American Air Filter
C. A. Burchsted
Oak Ridge National Laboratory

CONFIRMATORY RESEARCH PROGRAM--EFFECTS OF ATMOSPHERIC CONTAMINANTS ON COMMERCIAL CHARCOALS by R. R. Bellamy, U. S. Nuclear Regulatory Commission, and V. R. Deitz, Naval Research Laboratory.....	299
DISCUSSION.....	312
A NON-RADIOACTIVE DETERMINATION OF THE PENETRATION OF METHYL IODIDE THROUGH IMPREGNATED CHARCOALS by J. B. Romans, V. R. Deitz, Naval Research Laboratory.....	313
DISCUSSION.....	333
EFFECT OF PORE STRUCTURE ON THE ACTIVATED CARBON'S CAPABILITY TO SORB AIRBORNE METHYLRADIOIODIDE by A. J. Juhola, J. V. Friel, MSA Research Corporation...	335
METHYL IODIDE RETENTION ON CHARCOAL SORBENTS AT PARTS-PER-MILLION CONCENTRATIONS by G. O. Wood, C. A. Kasunic, Los Alamos Scientific Laboratory.....	352
DISCUSSION.....	367
EVALUATION AND CONTROL OF POISONING OF IMPREGNATED CARBONS USED FOR ORGANIC IODIDE REMOVAL by J. L. Kovach, L. Rankovic, Nuclear Consulting Services...	368

15th DOE NUCLEAR AIR CLEANING CONFERENCE

DISCUSSION.....	378
A DETERMINATION OF THE ATTRITION RESISTANCE OF GRANULAR CHARCOALS by V. R. Deitz, Naval Research Laboratory.....	379
DISCUSSION.....	392
THE DEVELOPMENT OF Ag ⁰ Z FOR BULK ¹²⁰ I REMOVAL FROM NUCLEAR FUEL REPROCESSING PLANTS AND PbX FOR ¹²⁰ I STORAGE by T. R. Thomas, B. A. Staples, L. P. Murphy, Allied Chemical Corporation.....	394
DISCUSSION.....	414
RADIATION-INDUCED IODINE MIGRATION IN SILVER ZEOLITE BEDS by A. G. Evans, Savannah River Laboratory.....	416
DISCUSSION.....	427
OPERATIONAL MAINTENANCE PROBLEMS WITH IODINE ADSORBERS IN NUCLEAR POWER PLANT SERVICE by C. E. Graves, J. R. Hunt, J. W. Jacox, J. L. Kovach, Nuclear Consulting Services, Inc.....	428
AECL IODINE SCRUBBING PROJECT by D. F. Torgerson, I. M. Smith, Atomic Energy of Canada, Ltd.....	437
DISCUSSION.....	445
DETERMINATION OF THE PHYSICO-CHEMICAL ¹³¹ I SPECIES IN THE EXHAUSTS AND STACK EFFLUENT OF A PWR POWER PLANT by H. Deuber, J. G. Wilhelm, Kernforschungs- zentrum Karlsruhe.....	446
DISCUSSION.....	475
CHAIRMAN BURCHSTED'S SUMMARY.....	475

Session VI
OFF-GAS TREATMENT
Tuesday, August 8, 1978
CHAIRMEN: R. R. Bellamy
U. S. Nuclear Regulatory Commission
R. Brown
Allied Chemical Company

OPENING REMARKS OF SESSION CHAIRMAN (R. R. Bellamy).....	476
BURNER AND DISSOLVER OFF-GAS TREATMENT IN HTR FUEL REPROCESSING by H. Barnert- Wiemer, M. Heidendael, H. Kirchner, E. Merz, G. Schröder, H. Vygen, Kerforschungsanlage Jülich.....	477
AEROSOL AND IODINE REMOVAL SYSTEM FOR THE DISSOLVER OFF-GAS IN A LARGE FUEL REPROCESSING PLANT by J. Furrer, J. G. Wilhelm, K. Jannakos, Kernforschungs- zentrum Karlsruhe.....	494

15th DOE NUCLEAR AIR CLEANING CONFERENCE

DISCUSSION.....	510
NOBLE GAS SEPARATION WITH THE USE OF INORGANIC ADSORBENTS by D. T. Pence, C. C. Chou, J. D. Christian, W. J. Paplawsky, Science Applications, Inc.....	512
DISCUSSION.....	519
NITROGEN OXIDE ABSORPTION INTO WATER AND DILUTE NITRIC ACID IN AN ENGINEERING-SCALE SIEVE-PLATE COLUMN WITH PLATES DESIGNED FOR HIGH GAS-LIQUID INTER-FACIAL AREA by R. M. Counce, W. S. Groenier, J. A. Klein, J. J. Perona, Oak Ridge National Laboratory.....	523
REMOVAL OF ^{14}C -CONTAMINATED CO_2 FROM SIMULATED LWR FUEL REPROCESSING OFF-GAS BY UTILIZING THE REACTION BETWEEN CO_2 AND ALKALINE HYDROXIDES IN EITHER SLURRY OR SOLID FORM by D. W. Holladay, G. L. Haag, Oak Ridge National Laboratory	547
DISCUSSION.....	568
MEASUREMENT OF RADIOACTIVE GASEOUS EFFLUENTS FROM VOLOXIDATION AND DISSOLUTION OF SPENT NUCLEAR FUEL by J. A. Stone, D. R. Johnson, Savannah River Laboratory.....	570
DISCUSSION.....	583
INVESTIGATION OF AIR CLEANING PROCESSES FOR REMOVING TRIBUTYL PHOSPHATE VAPORS FROM FUEL REPROCESSING OFF-GAS STREAMS by G. B. Parker, L. C. Schwendiman, Pacific Northwest Laboratory.....	584
DISCUSSION.....	598
A REVIEW OF SOME U.K.A.E.A. WORK ON GAS CLEANING IN FUEL REPROCESSING PLANTS by M. N. Elliott, U.K.A.E.A., Harwell, and E. Lilleyman, U.K.A.E.A., Dounreay..	600
DISCUSSION.....	613
ELIMINATION OF NO_x BY SELECTIVE REDUCTION WITH NH_3 by A. Bruggeman, L. Meyndonckx, W. R. A. Goossens, S.C.K./C.E.N., Mol, Belgium.....	614

VOLUME II

Session VII

NOBLE GAS SEPARATION

Tuesday, August 8, 1978

CHAIRMAN: D. Underhill

Harvard Air Cleaning Laboratory

OPENING REMARKS OF SESSION CHAIRMAN.....	626
DYNAMIC ADSORPTION OF RADON ON ACTIVATED CARBON by K. P. Strong, D. M. Levins, Australian Atomic Energy Commission.....	627
DISCUSSION.....	639
DEVELOPMENT OF A CRYOGENIC KRYPTON-SEPARATION SYSTEM FOR THE OFFGAS IF REPROCESSING PLANTS by R. v. Ammon, H. G. Burkardt, E. Hutter, G. Neffe, Kernforschungs-zentrum Karlsruhe.....	640

15th DOE NUCLEAR AIR CLEANING CONFERENCE

Session VIII
DAMAGE CONTROL
Tuesday, August 8, 1978
CHAIRMAN: W. L. Anderson
Naval Surface Weapons Laboratory

OPENING REMARKS OF SESSION CHAIRMAN.....	652
IN-DUCT COUNTERMEASURES FOR REDUCING FIRE-GENERATED-SMOKE-AEROSOL EXPOSURE TO HEPA FILTERS by N. J. Alvares, D. G. Beason, H. W. Ford, Lawrence Liver- more Laboratory.....	653
DISCUSSION.....	665
AIR CLEANING SYSTEM ISOLATION DURING TORNADO CONDITIONS by W. A. Pysh, T. A. Clements, Techno Corporation.....	666
DISCUSSION.....	686
EVALUATING NUCLEAR POWER PLANT VENTILATION SYSTEM ADEQUACY IN REDUCING AIRBORNE RADIOACTIVITY EXPOSURE by W. E. Jouris, King Faisal Specialist Hospital and Research Centre.....	688
AIR CLEANING SYSTEMS ANALYSIS AND HEPA FILTER RESPONSE TO SIMULATED TORNADO LOADINGS by W. S. Gregory, R. W. Andrae, K. H. Duerre, H. L. Horak, Los Alamos Scientific Laboratory, and P. R. Smith, C. I. Ricketts, W. Gill, New Mexico State University.....	694
DISCUSSION.....	705
CLOSING REMARKS OF SESSION CHAIRMAN.....	706

Session IX
AEROSOLS
Tuesday, August 8, 1978
CHAIRMAN: M. Tillery
Los Alamos Scientific Laboratory

CHARACTERIZATION OF AIRBORNE PLUTONIUM-BEARING PARTICLES FROM A NUCLEAR RE- PROCESSING PLANT by S. M. Sanders, Savannah River Laboratory.....	708
AGGLOMERATION CHARACTERISTICS OF FAST REACTOR HCDA AEROSOLS by G. W. Parker, G. E. Creek, A. L. Sutton, Jr., Oak Ridge National Laboratory.....	737
DISCUSSION.....	762
SODIUM OXIDE/HYDROXIDE AEROSOL PROPERTIES AND BEHAVIOR IN A LARGE VESSEL by R. K. Hilliard, J. D. McCormack, J. A. Hassberger, A. K. Potsma, Hanford Engineering Development Laboratory.....	764
DISCUSSION.....	791

15th DOE NUCLEAR AIR CLEANING CONFERENCE

ATTENUATION OF PARTICLES THROUGH LEAK PATHS by C. T. Nelson, R. P. Johnson, Atomics International.....	792
DISCUSSION.....	804

Session X
TEST METHODS
Wednesday, August 9, 1978
CHAIRMEN: J. L. Kovach, J. W. Jacox
Nuclear Consulting Services

THE NEW WASTE CALCINATING FACILITY PROCESS OFF-GAS FILTRATION SYSTEM AND REMOTE IN-PLACE DOP TEST by H. H. Loo, R. R. Smith, G. E. Bingham, Allied Chemical Corporation, and T. T. Allan, D. E. Wilcox, Flanders Filters, Inc.....	806
DISCUSSION.....	823
EVALUATION OF THE HEPA FILTER IN-PLACE TEST METHOD IN A CORROSIVE OFF-GAS ENVIRON- MENT by L. P. Murphy, M. A. Wong, R. C. Girton, Allied Chemical Corp.....	825
DISCUSSION.....	835
IN SITU TESTING OF TANDEM HEPA FILTER INSTALLATIONS WITH A LASER SINGLE PARTICLE SPECTROMETER SYSTEM by B. G. Schuster, D. J. Osetek, Los Alamos Scientific Laboratory.....	838
DISCUSSION.....	845
MEASUREMENTS WITH SELF-IDENTIFYING AEROSOLS by T. Kyle, B. G. Schuster, Los Alamos Scientific Laboratory.....	848
DISCUSSION.....	855
A METHOD FOR COMPARING AIR VELOCITIES BETWEEN BULK CARBON AND ASSOCIATED TEST CANISTERS by H. C. Parish, CVI Corporation.....	857
DISCUSSION.....	869
PERFORMANCE EVALUATION OF AN 18,000 CFM FILL-IN-PLACE ADSORBER UNIT by R. D. Porco, Mine Safety Appliances Co.....	871
DISCUSSION.....	891
EXPERIMENTAL DETERMINATION OF FISSION GAS ADSORPTION COEFFICIENTS by R. Lovell, D. Underhill, Harvard Air Cleaning Laboratory.....	893
DISCUSSION.....	899
A RADIOIODINE DETECTOR BASED ON LASER INDUCED FLUORESCENCE by A. P. Baronavski, J. R. McDonald, Naval Research Laboratory.....	901
DISCUSSION.....	914

15th DOE NUCLEAR AIR CLEANING CONFERENCE

AN INORGANIC RADIOIODINE ADSORBER WITH LOW NOBLE GAS RETENTION by C. Distenfeld, J. Klemish, Brookhaven National Laboratory.....	916
DISCUSSION.....	932
CLOSING REMARKS OF SESSION CHAIRMAN (J. L. Kovach).....	934

Session XI
LUNCHEON MEETING
Wednesday, August 9, 1978
CHAIRMAN: D. W. Moeller
Harvard Air Cleaning Laboratory

OPENING REMARKS OF SESSION CHAIRMAN.....	935
SOME PERSPECTIVES ON RADIATION PROTECTION by Dr. Warren K. Sinclair, National Council on Radiation Protection and Measurements.....	936

Session XII
NEW AIR CLEANING TECHNOLOGY FROM EUROPE
Wednesday, August 9, 1978
CHAIRMAN: D. W. Moeller
Harvard Air Cleaning Laboratory

OPENING REMARKS OF SESSION CHAIRMAN.....	946
NEW AIR CLEANING TECHNOLOGY IN THE UNITED KINGDOM by R. G. Dorman, Chemical Defense Establishment, United Kingdom.....	947
DISCUSSION.....	948
SOME DEVELOPMENTS IN NUCLEAR AIR CLEANING IN FRANCE by P. Sigli, Commissariat à l'Energie Atomique, France.....	950
DISCUSSION.....	955
GAS CLEANING RESEARCH AND ENGINEERING IN BELGIUM by W. R. A. Goossens, L. H. Baetslé, A. Bruggeman, G. Collard, S.C.K./C.E.N., Mol, Belgium.....	956
DISCUSSION.....	961
DEVELOPMENTS IN NUCLEAR AIR CLEANING IN GERMANY by J. G. Wilhelm, Kernforschungs- zentrum Karlsruhe.....	963
DISCUSSION.....	968
IAEA/NEA ACTIVITIES IN THE FIELD OF GASEOUS WASTES by J. Dubé, Organisation for Economic Co-Operation and Development, and Y. Zabaluev, International Atomic Energy Agency.....	971
CLOSING REMARKS OF SESSION CHAIRMAN.....	981

15th DOE NUCLEAR AIR CLEANING CONFERENCE

Session XIII
OPEN-END
Wednesday, August 9, 1978
CHAIRMAN: M. W. First
Harvard Air Cleaning Laboratory

OPENING REMARKS OF SESSION CHAIRMAN.....	982
USE OF INSTALLED TEST CANNISTERS FOR REPRESENTATIVE SAMPLING OF VENTILATION SYSTEMS CHARCOAL ADSORBERS by C. A. Moore, Florida Light and Power Co.....	984
DISCUSSION.....	986
A REMOTE SAMPLING SYSTEM FOR HEPA (1500 CFM) IN-PLACE FILTERS WITH A FLUORIDE (CHANNEL) SEAL SYSTEM by L. G. Musen, Idaho National Engineering Laboratory	987
DISCUSSION.....	997
RADIOACTIVE WASTE MANAGEMENT: THE NEED FOR MULTIPLE BARRIERS by J. Sokol, M. Cooper, Westinghouse Advanced Power Systems Divisions.....	998
DISCUSSION.....	1003
CSL ENGINEERING DESIGNER HANDBOOK by A. Shacter, Chemical Systems Laboratory, Aberdeen Proving Ground.....	1005
DISCUSSION.....	1014
CPP EXPERIMENTAL HEPA FILTER MEDIA by W. D. Hanson, Allied Chemical Corp.....	1015
DISCUSSION.....	1016

Session XIV
FILTRATION
Thursday, August 10, 1978
CHAIRMEN: R. Dorman
Chemical Defense Establishment, U.K.
H. Gilbert
Consultant

LOADING CAPACITY OF VARIOUS FILTERS FOR SODIUM OXIDE/HYDROXIDE AEROSOLS by J. D. McCormack, R. K. Hilliard, J. R. Barreca, Westinghouse Hanford Company.....	1018
DISCUSSION.....	1043
PERFORMANCE OF A WET CELL WASHER FOR SODIUM FIRE AEROSOLS by W. C. Hinds, J.M. Price, M. W. First, Harvard Air Cleaning Laboratory.....	1044
DISCUSSION.....	1056

15th DOE NUCLEAR AIR CLEANING CONFERENCE

ENHANCED FILTRATION PROGRAM AT LLL--A PROGRESS REPORT by W. Bergman, R. D. Taylor, H. H. Miller, A. H. Biermann, H. D. Hebard, R. A. daRoza, B. Y. Lum, Lawrence Livermore Laboratory.....	1058
DISCUSSION.....	1098
STUDIES ON PROLONGING HEPA FILTER SERVICE IN CHEMICAL APPLICATIONS by R. W. Woodard, K. Terada, O. I. Buttedahl, Rockwell International, Energy Systems Group.....	1100
DISCUSSION.....	1121
REPORT OF MINUTES OF GOVERNMENT-INDUSTRY MEETING ON FILTERS, MEDIA, AND MEDIA TESTING by W. L. Anderson, Naval Surface Weapons Center.....	1122
Appendix A A STUDY OF DIOCTYL PHTHALATE PARTICLES (DOP) GENERATED IN PENETROMETERS AND THE DEVICES USED CURRENTLY TO MEASURE THEIR SIZE by C. D. Skaats, Rockwell International, Atomics International Division.....	1127
Appendix B SIZE DISTRIBUTION OF "HOT DOP" AEROSOL PRODUCED BY ATI Q-127 AEROSOL GENERATOR by W. Hinds, M. First, D. Gibson, D. Leith, Harvard Air Cleaning Laboratory.....	1130
Appendix C FIBER DIAMETER DETERMAINTION OF FIBER GLASS SAMPLES by S. Gross, C. Cain, Johns-Manville.....	1145
EVALUATION OF DATA FROM HEPA FILTER QUALITY ASSURANCE TESTING STATIONS by J. T. Collins, R. R. Bellamy, J. R. Allen, U. S. Nuclear Regulatory Commission.....	1159
DISCUSSION.....	1173
PERFORMANCE AND ENVIRONMENTAL CHARACTERISTICS OF A COMPACT, HIGH-CAPACITY HEPA FILTER DESIGN by C. E. Rose, R. D. Rivers, American Air Filter.....	1176
DISCUSSION.....	1184
PERFORMANCE OF 1,000 AND 1800 CFM HEPA FILTERS ON LONG EXPOSURE TO LOW ATMOSPHERIC DUST LOADINGS by M. W. First, D. Leith, Harvard Air Cleaning Laboratory.....	1185
DECONTAMINATION OF HEPA FILTERS by J. W. Koenst, Jr., E. L. Lewis, D. F. Luthy, Mound Facility.....	1191
DISCUSSION.....	1225
INDEX OF AUTHORS AND SPEAKERS.....	1227
LIST OF ATTENDEES.....	1232

15th DOE NUCLEAR AIR CLEANING CONFERENCE

SESSION I

INTRODUCTION TO THE NUCLEAR AIR CLEANING CONFERENCE:
OBJECTIVES, NUCLEAR WASTE MANAGEMENT, RISK ASSESSMENT,
AIR CLEANING FAILURES, AND STANDARDS
FOR AIR AND GAS CLEANING INSTALLATIONS

Monday, August 7, 1978
CHAIRMAN: M. W. First

WELCOME M. W. First

KEYNOTE ADDRESSES:

NUCLEAR WASTE MANAGEMENT AT DOE A. Perge

RISK-ASSESSMENT TECHNIQUES AND THE REACTOR LICENSING PROCESS
S. Levine

REVIEW OF FAILURES IN NUCLEAR AIR CLEANING SYSTEMS
D. W. Moeller

PROGRESS IN STANDARDS FOR NUCLEAR AIR AND GAS TREATMENT
C. A. Burchsted

REPORT ON ANSI/ASME NUCLEAR AIR AND GAS TREATMENT STANDARDS FOR NUCLEAR POWER
PLANTS J. F. Fish

15th DOE NUCLEAR AIR CLEANING CONFERENCE

WELCOME

Melvin W. First
Harvard Air Cleaning Laboratory
Harvard School of Public Health
Boston, Massachusetts

My first pleasant duty is to welcome you on behalf of the U.S. Department of Energy and the Harvard Air Cleaning Laboratory, co-sponsors of this 15th Nuclear Air Cleaning Conference, and to express the wish that you will enjoy your stay in Boston. This conference started as the United States Energy and Development Administration Air Cleaning Conference and followed federal departmental reorganization by first becoming the 15th DOE Air Cleaning Conference and then the 15th DOE Nuclear Air Cleaning Conference when, much to our astonishment, we began to receive offers of papers on the subject of pulverized coal fly ash.

I hardly need tell you that a conference of this magnitude does not occur without the continuing efforts of many people. I know that I express your thanks as well as my own to the several members of the program committee of this conference who worked hard and well to put together the excellent groups of papers that we will listen to over the next several days and whose duties will not be completed until they have finished chairing the many technical sessions. The committee members are: W.L. Anderson, Clifford A. Burchsted, Harry L. Ettinger, Dade W. Moeller, Ronald R. Bellamy, John T. Collins, Humphrey Gilbert, Dallas Pence, Russ Brown, Jack C. Dempsey, Louis L. Kovach, and Richard D. Rivers.

Although this conference has always had a strong U.S. flavor because of the official sponsorship, we are delighted once again to greet and give a special welcome to those who join us from other countries. We have people here from Britain, from France, from West Germany, from Belgium, from Spain, from Sweden, from Saudi Arabia, from Australia, from Japan, and, although I have a hard time thinking of these people as from a foreign country, we have a fine delegation of our friends from Canada.

When I opened the Conference two years ago I expressed special concern that the opponents of nuclear energy were out-talking us by a considerable margin and reaching the small club groups as well as the national media very effectively with their strong "anti" messages. I am pleased to say I think we have done much better during the past two years to bring a positive message to the world about the benefits of nuclear energy as well as its safety and freedom from detrimental environmental impact. This is not to say we could not do much better, and I certainly hope we all will make a special effort to do so. Therefore, our current concerns have shifted to the topics we will discuss at this session. These are research and development in reactor safety, regulation to avoid accidents, and perhaps the most widely discussed topic of today, the matter of waste disposal. We are especially fortunate to have two keynote speakers of great stature to review the subject of nuclear research for us. The first speaker is from the Department of Energy, the second speaker from the Nuclear Regulatory Commission.

Our speaker from the Department of Energy is Mr. Alex Perge who received a chemical engineering degree from Case Institute of Technology in 1944 and then worked at K-25, the original Oak Ridge gaseous diffusion plant. He participated in A-bomb tests Able and Baker at Bikini and worked for General Electric at the Knowles Atomic Power Laboratory in fuel development and sodium purification systems

15th DOE NUCLEAR AIR CLEANING CONFERENCE

for what eventually became the SIR and the Seawolfe submarine reactors. At Knowles Atomic Power Laboratory he was involved in the development of the spent fuel processing system that was used in the Savannah River plant and he worked for the Atomic Energy Commission in the design, construction, and start-up of the Savannah River reprocessing plants. In addition, he worked in Washington for the Atomic Energy Commission where he was with the Production Division's development programs. He also worked for the Operational Safety Division and was concerned with the safety of all of the AEC's materials processing operations. In 1971, he organized the Atomic Energy Commission's division of waste management and transportation and has followed along with that program through all of the organizational changes from AEC to ERDA to DOE. As of May 1 of this year, Mr. Perge became the Manager of the Special Staff for the Director of the Office of Nuclear Waste Management.

Our second keynote speaker is Mr. Saul Levine. He is a graduate of the U.S. Naval Academy and in addition has degrees from MIT in electronics and nuclear engineering. He spent his early career in the submarine service. He was project officer for the USS Enterprise under Admiral Rickover so we know he had a very rigorous instruction period. He was responsible for directing all technical, financial, production, and administrative aspects of the reactor plant prototypes and the production plants for the first nuclear powered aircraft carrier, the Enterprise. From 1958 to 1962 he was with the Polaris missile system under Admiral Rayborne where he managed design integration, installation testing, and performance evaluation of the Polaris navigation system. Next, he was Assistant Director for Reactor Technology in the Division of Reactor Licensing, United States Atomic Energy Commission, where he was responsible for directing the development of nuclear safety review techniques for nuclear reactors, requirements for safety research and development, and technical safety reviews for reactors of all types. From 1970 to 1972 he was Assistant Director, Division of Environmental Affairs of the Atomic Energy Commission where he managed programs related to environmental impact associated with AEC's programs and assisted in the establishment of requirements for the implementation of NEPA in the AEC. From 1972 to 1975, Mr. Levine was Project Staff Director of the Reactor Safety Study of the United States Atomic Energy Commission. With Professor Rasmussen of MIT he provided the principal technical and management direction of the study entitled, An Assessment of Accident Risks in U.S. Commercial Nuclear Reactor Plants, a study with which I know all of you here are well familiar. From 1973 to 1975 he was Special Assistant to the Director of the Division of Reactor Safety Research. Most recently he has been Deputy Director, and is presently Director of research of the United States Nuclear Regulatory Commission. In this assignment, he manages a research program to confirm assessments used by the Commission in regulating the commercial uses of nuclear energy, in particular, the areas of nuclear safeguards and environmental aspects.

15th DOE NUCLEAR AIR CLEANING CONFERENCE

NUCLEAR WASTE MANAGEMENT AT DOE

Alex F. Perge
Office of Nuclear Waste Management
Department of Energy

The Department of Energy (DOE) is an organization that came into existence 10 months ago in October 1977. Most of the people came from two agencies, the Energy Research and Development Administration and the Federal Energy Agency. However, functions and a smaller number of people came from several other agencies. The agency operates with several functional components that are headed by Assistant Secretaries. I'll list the ones that are involved in efforts such as yours.

The Director of Energy Research is responsible for all basic research and also has primary responsibility in the Department for waste management policy. The Director is responsible for four national laboratories; they are, Brookhaven National Laboratory, Argonne National Laboratory, Lawrence Berkeley Laboratory, and the Ames Laboratory.

The Assistant Secretary for Energy Technology is responsible for the programs concerned with development of energy technology. That is, the transition from basic research to useable technology. This Assistant Secretary is responsible for the development programs for: Fossil Fuels, Geothermal Energy, Solar Energy, Fusion Energy, Nuclear Energy, and the Nuclear Waste Management Program. This Assistant Secretary is also responsible for five laboratories; i.e., Pacific-Northwest Laboratory, Oak Ridge National Laboratory, Savannah River Laboratory, Idaho National Engineering Laboratory, and the Hanford Engineering Development Laboratory.

The Assistant Secretary for Resource Applications is responsible for the commercialization of energy technology after the technology has been demonstrated. Additionally, this Assistant Secretary is responsible for a number of major operations; e.g., the uranium enrichment program.

The Assistant Secretary for Defense Programs is responsible for the operations and development programs concerned with the national defense effort. This Assistant Secretary is responsible for three national laboratories; i.e., Los Alamos Scientific Laboratory, Lawrence Livermore Laboratory, and Sandia Laboratory.

The Assistant Secretary for Environment is responsible for programs concerned with health, safety, and environmental aspects of all of the DOE programs.

The Office of Nuclear Waste Management was separated from the Nuclear Technology Program on May 1, 1978, and made a separate entity reporting directly to the Assistant Secretary for Energy Technology. This Office is responsible for most of the Agency's programs of concern to this conference.

The present DOE programs for airborne wastes are supporting the development of technologies for both defense and commercial needs. Technologies are being developed for the concentration, recovery, immobilization, storage, and monitoring of airborne wastes from the defense programs fuel cycle or the nuclear power fuel cycle. Nuclear reactors, irradiated fuel storage, fuel reprocessing, and weapons-related activities all produce airborne radioactive wastes.

15th DOE NUCLEAR AIR CLEANING CONFERENCE

The DOE operations are varied by type and scale. There are production operations and laboratory operations. There are reactors, chemical plants, metallurgical operations and mechanical operations. These extend in scale from very small to extremely large. The nature of the gaseous and airborne waste streams from these operations vary. There are large volumes of dry, moist, and wet gases which vary in nature from inert to very reactive. The temperatures and pressures vary from very low to very high resulting from either normal conditions or accident conditions; and, of course, there is a variation from radioactive gases to radioactive particulates.

DOE is responsible for interim storage for some of these wastes and for the disposal for most of them. Of the wastes that have to be managed, a significant part are a result of treatment systems and devices for cleaning gases. The best treatment devices do not always yield the best waste forms for either storage or disposal.

The long term waste management objectives place minimal reliance on surveillance and maintenance. Thus, the concerns about the chemical, thermal and radiolytic degradation of wastes require technology for converting the wastes to forms acceptable for long term isolation.

The strategy of the DOE airborne radioactive waste management program is to increase the service life and reliability of filters; to reduce filter wastes; and in anticipation of regulatory actions that would require further reductions in airborne radioactive releases from defense program facilities, to develop improved technology for additional collection, fixation, and long-term management of gaseous wastes.

Available technology and practices are adequate to meet current health and safety standards. The program is aimed primarily at cost effective improvements, quality assurance, and the addition of new capability in areas where more restrictive standards seem likely to apply in the future.

The current activities and objectives are as follows:

1) Filter Service Life Extension:

- o To reduce costs and waste, iodine absorbents are being developed that have substantially longer service life and can be regenerated.
- o More durable filters are being developed for service in off-gas streams from radioactive processes that emit acid vapors or high temperature gases.
- o Several prefilter concepts are being developed for capturing radioactive particulates near their source. These concepts will extend the service life of HEPA filters and thus reduce the costs for their replacement and their disposal. Costs of concern are not just monetary but also radiation exposure.

2) Gas Monitoring:

- o Improved monitoring systems are being demonstrated for specific long lived airborne radioactive constituents in the off-gas of waste treatment processes, particularly iodine-129, carbon-14 and tritium.
- o Improved particle measurement technology is being developed for high temperature applications.

15th DOE NUCLEAR AIR CLEANING CONFERENCE

3) Gaseous Waste Treatment:

- o Technology is being developed to remove tritium from air and water, to immobilize it and to store it safely.
- o The state-of-the-art for limiting emissions of iodine-129, krypton-85, and carbon-14 is being assessed. Studies are being made on the adaptation of advanced technology for use at DOE sites.

4) Filter Quality Assurance:

- o The operation of three filter test stations for testing HEPA filters prior to use in DOE facility filtration systems is continuing. The Hanford Station is being upgraded.
- o Improved filter test methods are being developed for the DOE radioactive iodine and particle removal filtration systems. This work also supports the development of filtration standards, regulations, and test procedures.

Effective use of the manpower and resources allocated to airborne waste management is our objective. We need:

- o Matching of program tasks to both specific and general waste management needs; i.e., why is the technology required?
- o Early review of technical, legal, and economic feasibility of proposed and existing programs--in the context of process, environmental, regulatory, and storage/disposal constraints.
- o Establishment of a relationship to other development activities; i.e., other Federal, private, and international activities.
- o Application of common criteria for decisionmaking at both the development and application stages of airborne waste management.

To aid in this, we are setting up a lead organization at the Idaho Operations Office to integrate the airborne radioactive waste management program. This office will review the program elements, analyze their technologies and objectives for technical merit, range of applicability, and for consistency with DOE program goals.

Before closing I would like to mention two more points that may be of interest to you.

At the direction of the President, an Interagency Review Group, commonly called the IRG, was formed to review all aspects of radioactive waste management. Every Government agency that has any tie, in any way, to any part of waste management, is involved. The IRG is charged with reporting back to the President by October 1, 1978, with a comprehensive evaluation of nuclear waste management. The IRG will recommend to the President what has to be done, when it should be done, and who has to do what to get it done.

Even though we feel that we have been working closely with the Environmental Protection Agency and the Nuclear Regulatory Commission in the past, the IRG review has caused the three agencies to work closer together. This should be of help to the nuclear air cleaning program.

15th DOE NUCLEAR AIR CLEANING CONFERENCE

There is a significant involvement in both the program and the attendance at this meeting from the international scene; that is, non-U.S. We recognize that airborne waste management is of international concern. Though there are problems of various types in international activities, we, as the U.S., and the DOE as one of the concerned U.S. agencies, have been working toward international cooperation. The pace is slow but I believe there is progress.

I'd like to leave with a repetition of an earlier comment. Air cleaning systems produce wastes. The costs of those wastes--for treatment (if required) and disposal--will be increasing very significantly.

DISCUSSION

FIRST: When are we going to get that stuff buried?

PERGE: For most of it, not very soon. However, the IRG program will be presenting the President with a broadly based and detailed evaluation of the present programs, plans, and alternatives. This will allow the administration to give Congress a program for resolving the waste management problem. Congress has indicated a desire to do its part in resolving this matter and the administration's recommendations, including a waste plan, have been promised to Congress by the end of the year. I can only hope that this process turns out to be the start of finally resolving the waste management problem.

I might add that the IRG program includes involvement to some extent of just about every identifiable special interest group, both technical and nontechnical, government (federal & state) and industrial, etc.

15th DOE NUCLEAR AIR CLEANING CONFERENCE

RISK-ASSESSMENT TECHNIQUES AND THE REACTOR LICENSING PROCESS

Saul Levine
Director, Office of Nuclear Regulatory Research
U.S. Nuclear Regulatory Commission

The principal subject of my talk is one that is of great interest to the nuclear community: the NRC's efforts to stabilize the reactor licensing process. I will start with a brief description of the Reactor Safety Study (WASH-1400), concentrating on the engineering aspects of the contribution to reactor accident risks. I will then go on to describe how we have applied the insights and techniques developed in this study to prepare a program, requested by Congress, to improve the safety of nuclear power plants. Finally, I will describe some new work we are just beginning on the application of risk-assessment techniques to stabilize the reactor licensing process.

An overview of the Reactor Safety Study is shown in Figure 1, and I am going to concentrate on step 3: fission-product source released from the containment. To define accidents in reactors, it is necessary to define the ways in which they can happen (i.e., accident sequences) and to assign probability values to those accidents. A set of processes is occurring within the reactor, and one must determine from those processes what fission products would be released from the containment. If we stop at this point, we can concentrate on the engineering insights that are applicable to reactor safety.

Figure 2 shows a typical simplified scheme that we use to define accident sequences. It starts with an initiating event, such as a pipe break or a transient, with which is associated a probability. What are the things that can work or fail that affect the course of events, given that initial failure? Of course, in the design-basis accident that is normally analyzed in the regulatory process one starts with the initial event, and all the engineered safety features that are provided are assumed to work. The result is a very small release of radioactivity with a probability that is the same as that of the pipe break. It is, of course, possible for any or all of these engineered safety features to fail. In fact, if the electrical power fails, none of the other systems can work. Therefore, the product $P_1 \times P_2$ gives a very large release of radioactivity: if there is a pipe break, no emergency core-cooling system, no fission-product removal, and no containment, a large amount of radioactivity will clearly be released. For instance, even if electrical power is available, the system can fail. There are then two alternatives: if the fission-product removal system works, there is one kind of release and probability, and if it does not work, there is a different kind of release and probability. These probabilities can be multiplied together if the conditional probabilities between the two events are taken into account.

BASIC SEVEN TASKS IN REACTOR SAFETY STUDY

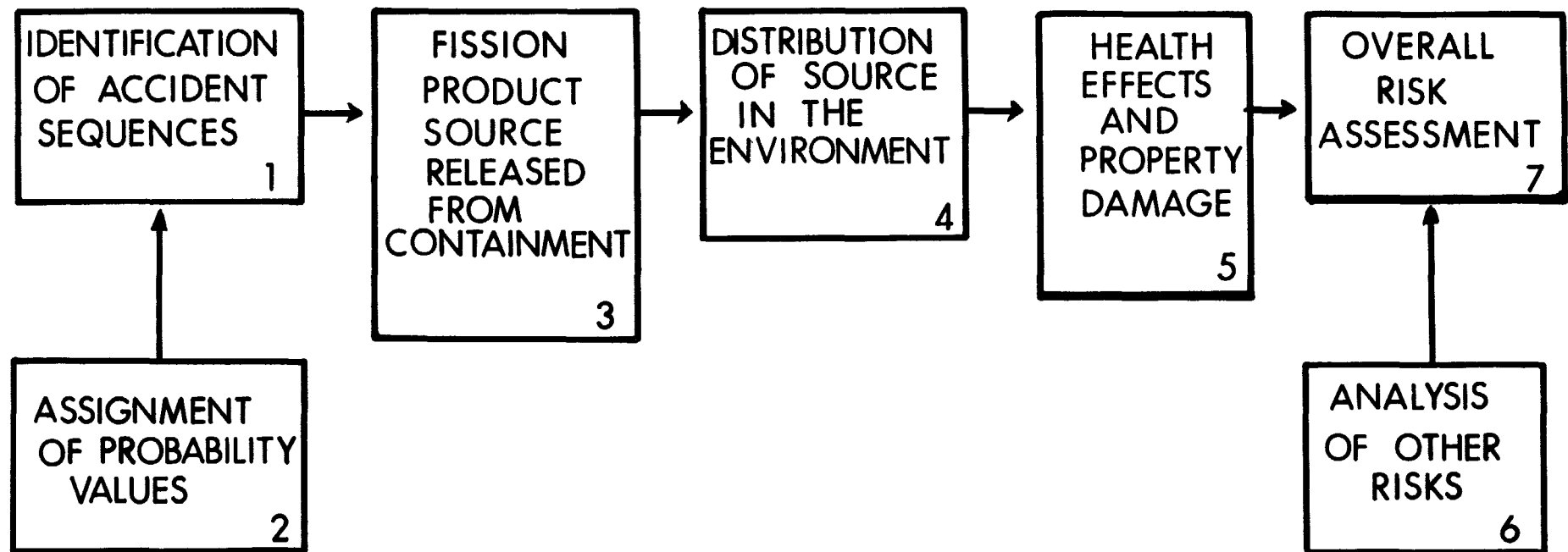


FIGURE 1

SIMPLIFIED EVENT TREE FOR A LOCA IN A TYPICAL NUCLEAR POWER PLANT

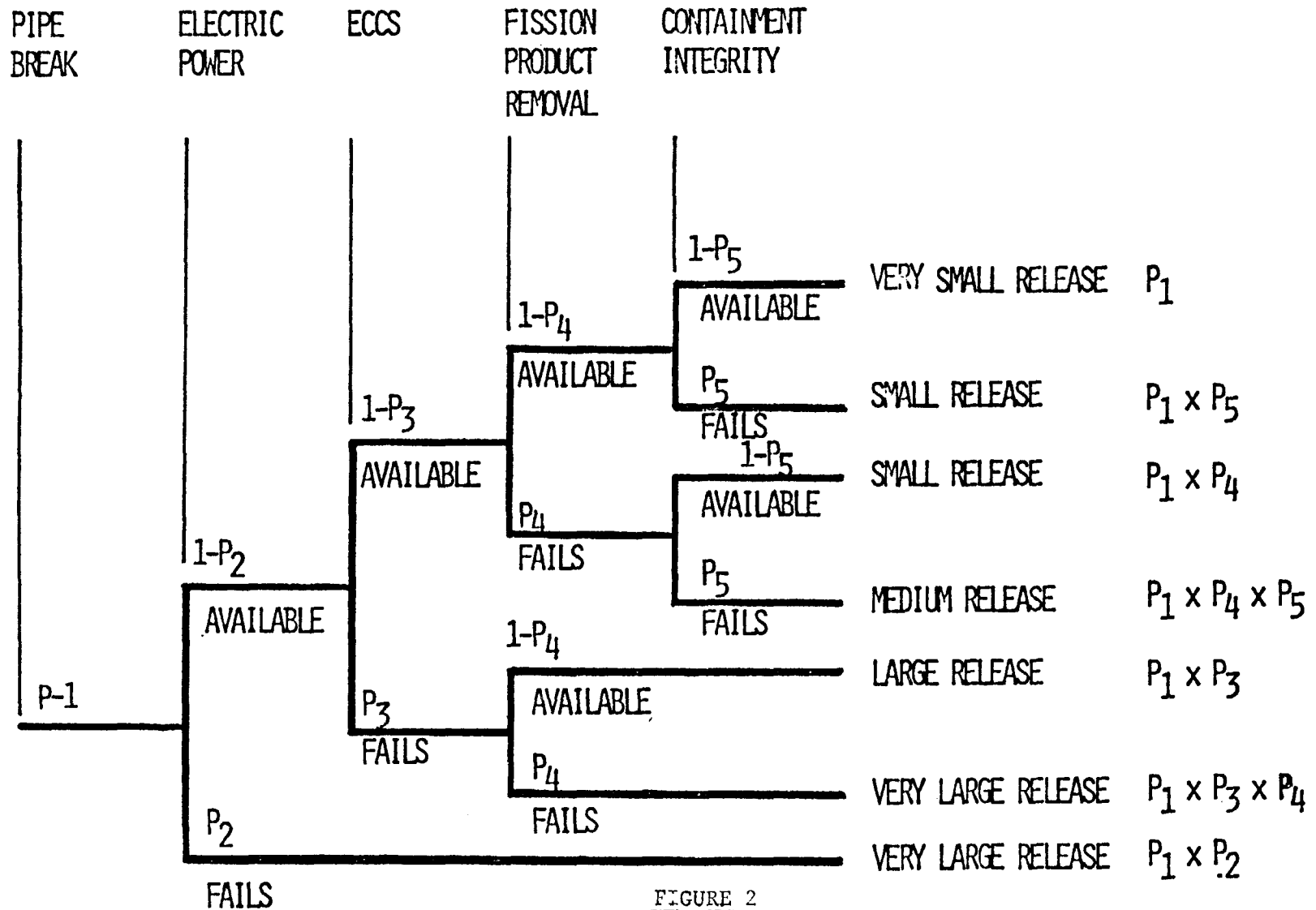


FIGURE 2

15th DOE NUCLEAR AIR CLEANING CONFERENCE

Figure 3 shows how the accident consequences can be categorized by size of release and then added within each category to get a histogram of consequences versus probability. This type of histogram was used to report the results of the Reactor Safety Study.

In making a risk assessment it is necessary to determine where to start. The most important factor is to prevent melting of the fuel because most of the radioactivity resides within the fuel. There are, however, only two ways to melt the fuel: there are loss-of-coolant events in which there is a loss of coolant that is not restored, and there are transient events in which the fuel is overpowered or the coolant flow is reduced to the point where the fuel melts.

The potential accidents analyzed in the Reactor Safety Study can be summarized as follows:

- A. Potential accidents that could involve the reactor:
 - 1. Event trees for events involving many systems
 - a. Large loss-of-coolant accident (LOCA): breaks >6 inches in equivalent diameter
 - b. Small LOCA 1: breaks 2 to 6 inches in equivalent diameter
 - c. Small LOCA 2: breaks 0.5 to 2 inches in equivalent diameter
 - d. Reactor-vessel rupture
 - e. Transient events
 - 2. External forces--earthquakes, tornadoes, floods, aircraft impacts, turbine missiles, tidal waves.
 - 3. Sabotage.
- B. Noncore accidents--spent-fuel storage pool and shipping casks, waste storage tanks, refueling operations.

We can see from the above that event trees are drawn for three different kinds of LOCA (large, small 1, and small 2) because they all have different combinations of systems to operate in case of need. In our study we considered all of these as carefully as we could except for sabotage because we did not know how to estimate the probability of successful sabotage.

Figure 4 shows the fundamental structure of a pressurized water reactor (PWR), and Figure 5 shows a reactor--a pressurized water reactor or a boiling water reactor--in which the main coolant pipes are broken. It is undergoing a LOCA. This simplified drawing shows the heart of the analysis. The emergency core-cooling water is starting to be pumped into the core to prevent core melting. What melts the core in the absence of water is the decay heat in the core.

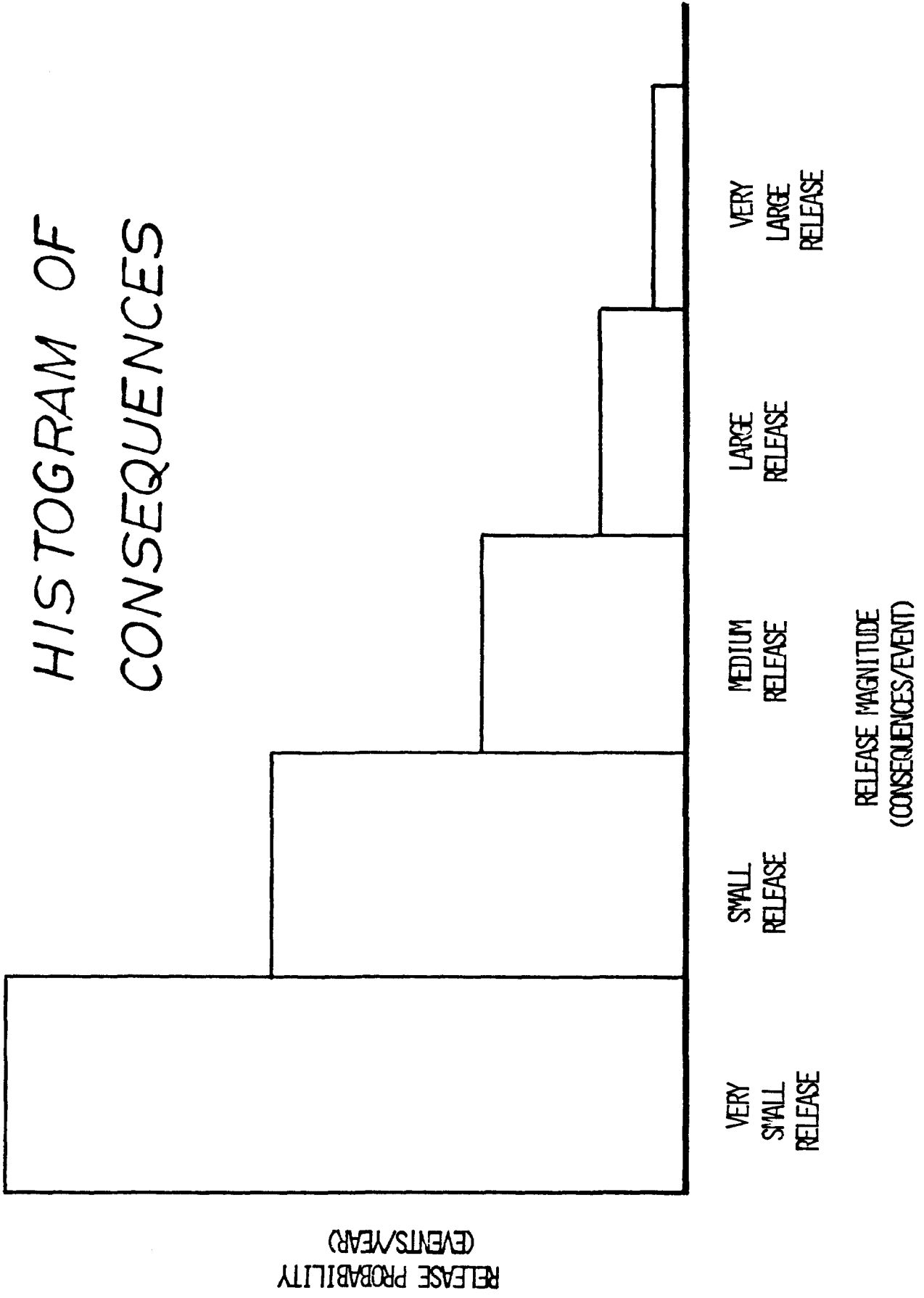


FIGURE 3

TYPICAL PRESSURIZED WATER REACTOR

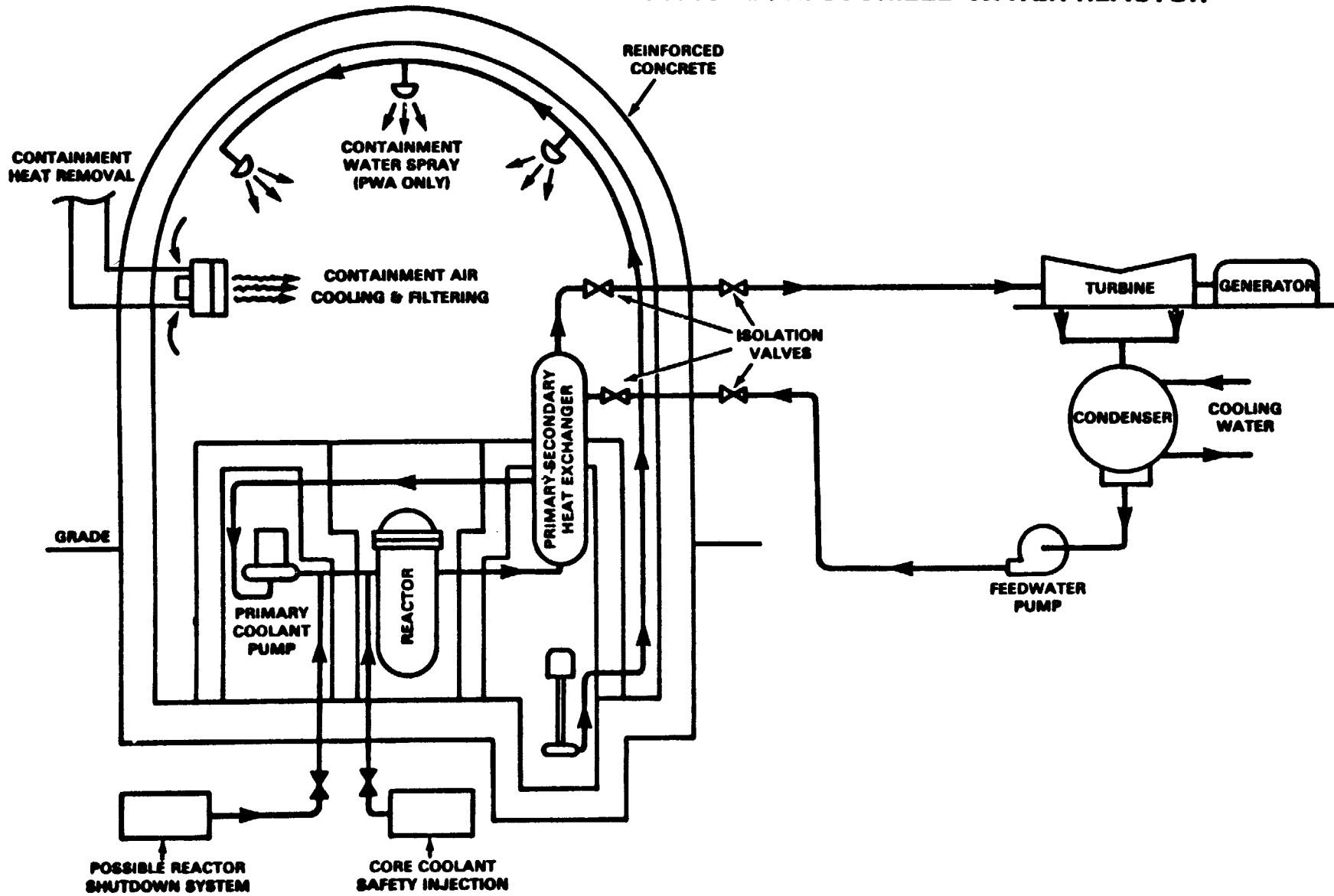
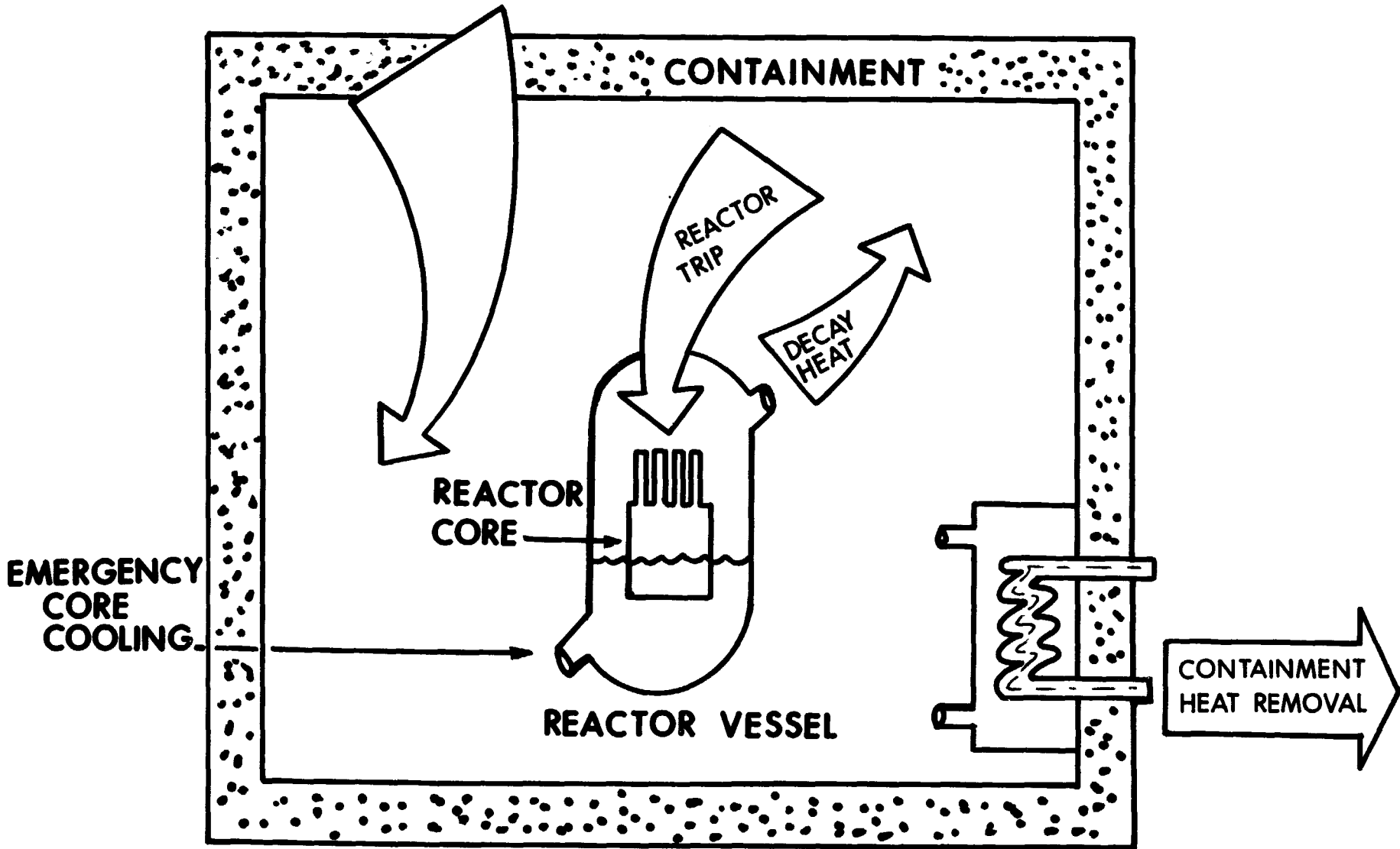


FIGURE 4

RADIOACTIVITY REMOVAL



14

15th DOE NUCLEAR AIR CLEANING CONFERENCE

FUNCTIONS OF ENGINEERED SAFETY FEATURES

FIGURE 5

15th DOE NUCLEAR AIR CLEANING CONFERENCE

The emergency core-cooling water is removing the decay heat and transferring it into the containment. The containment is sized to withstand the pressure and temperature associated with the blowdown of the stored energy in the primary coolant water. Constantly pumping decay heat into the containment will overpressure the containment or overheat it until it ruptures. A heat-removal system is therefore necessary to remove the decay heat from the containment. It is not enough to have the emergency core-cooling system work; heat must be removed from the containment because the containment is essentially an insulated box of steel and concrete. Obviously, if the heat is not removed from the containment, the containment will rupture, at about 120 psi, or twice its design pressure. The temperature will be in the neighborhood of 400°F and the emergency core-cooling system will then fail because it will be in the recirculation mode, where it is sucking water from the containment sump; this will in fact occur at 120 psi and 400°F, and when the pressure is relieved, the water will boil, the pump will cavitate and burn out, and the core will melt. It is possible to have an accident, therefore, in which first the containment ruptures and then the core melts--which is a rather bad accident. Reactor trip is also necessary to shut down thereafter in most accidents because when the core is reflooded, it will go critical again and generate power, which will defeat our purpose. And, of course, there are the radioactivity-removal system sprays and/or filters and the containment itself. These are not systems--these are simply functions to be performed.

Figure 6 is an event tree that is perfectly general, that shows all the functions with all possible combinations of success or failure. After going through some functional logic we can arrive at Figure 7, which shows not a symmetrical tree but a highly skewed tree that takes into account the dependencies and functional failures; hence the size of the tree has been reduced enormously, which is very important. We now have a tree that defines the functions and relationships among them. To quantify this tree we put systems along the top line and then construct fault trees for the systems to define the probability of failure. Figure 8 shows that for the functions along the top of the tree there are sets of systems that must perform those functions and that there are logical interrelationships among those systems, among the functions in fact, that must be taken into account. Taking into account the logic of the functional tree and the logical interrelationships with the systems, it is possible to draw another tree (Figure 9) that has the systems along the top and a correct representation of their interrelationships. It is important to know that, if one had not performed this removal of interrelationships in the correct way, the tree in Figure 9 would have contained 30,000 accident sequences. The fact that it has been reduced to 38 sequences means that there are "what if" questions about common-mode failures between systems that do not need answers.

Figure 9 has one of two outcomes. Either the core does not melt, such as in the design-basis accident, or enough things fail and the core does melt. It is necessary to define the relationship between the molten core and the containment-failure modes because the containment failure mode determines the release to the environment.

ILLUSTRATIVE EVENT TREE FOR LOCA FUNCTIONS

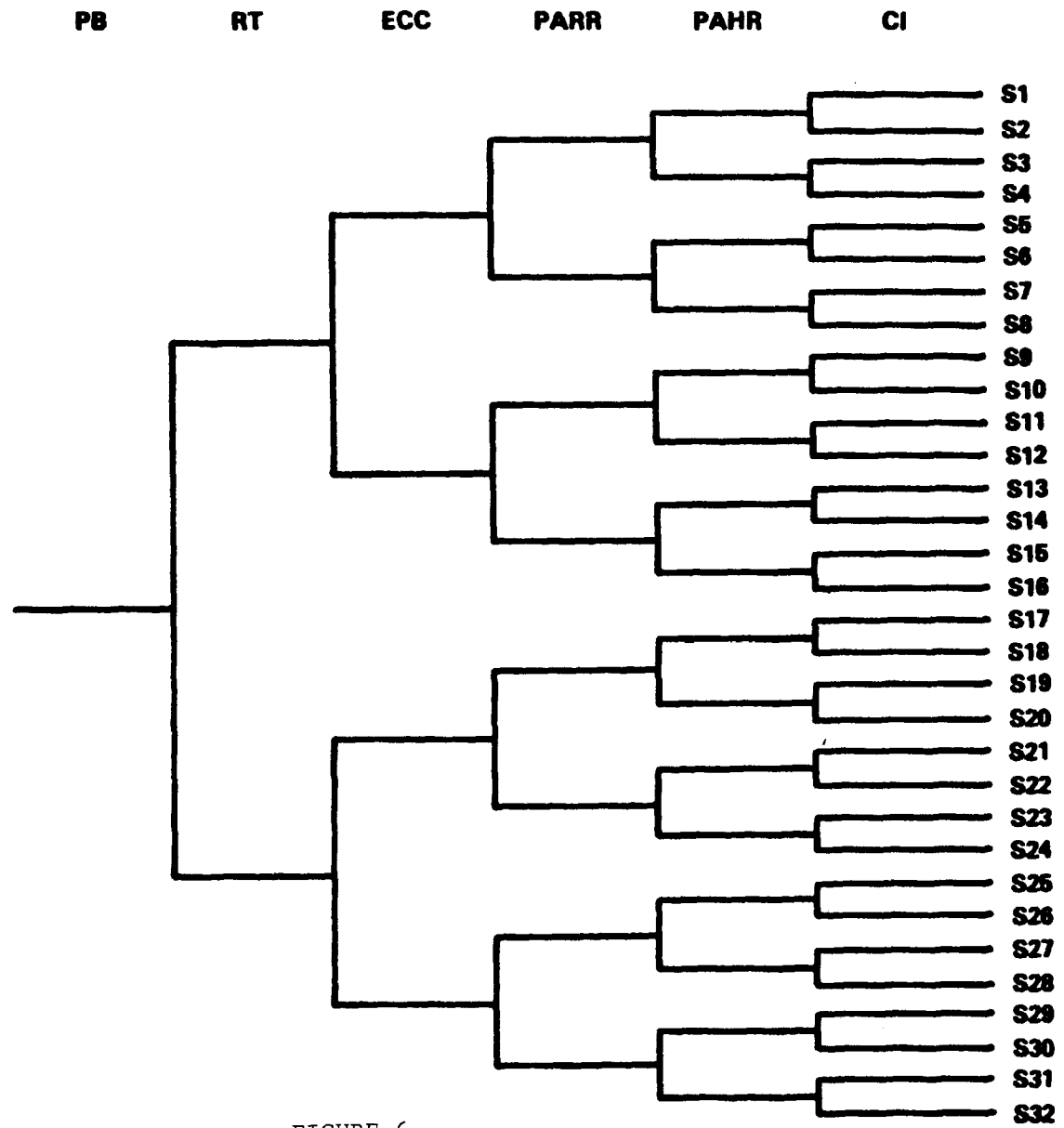
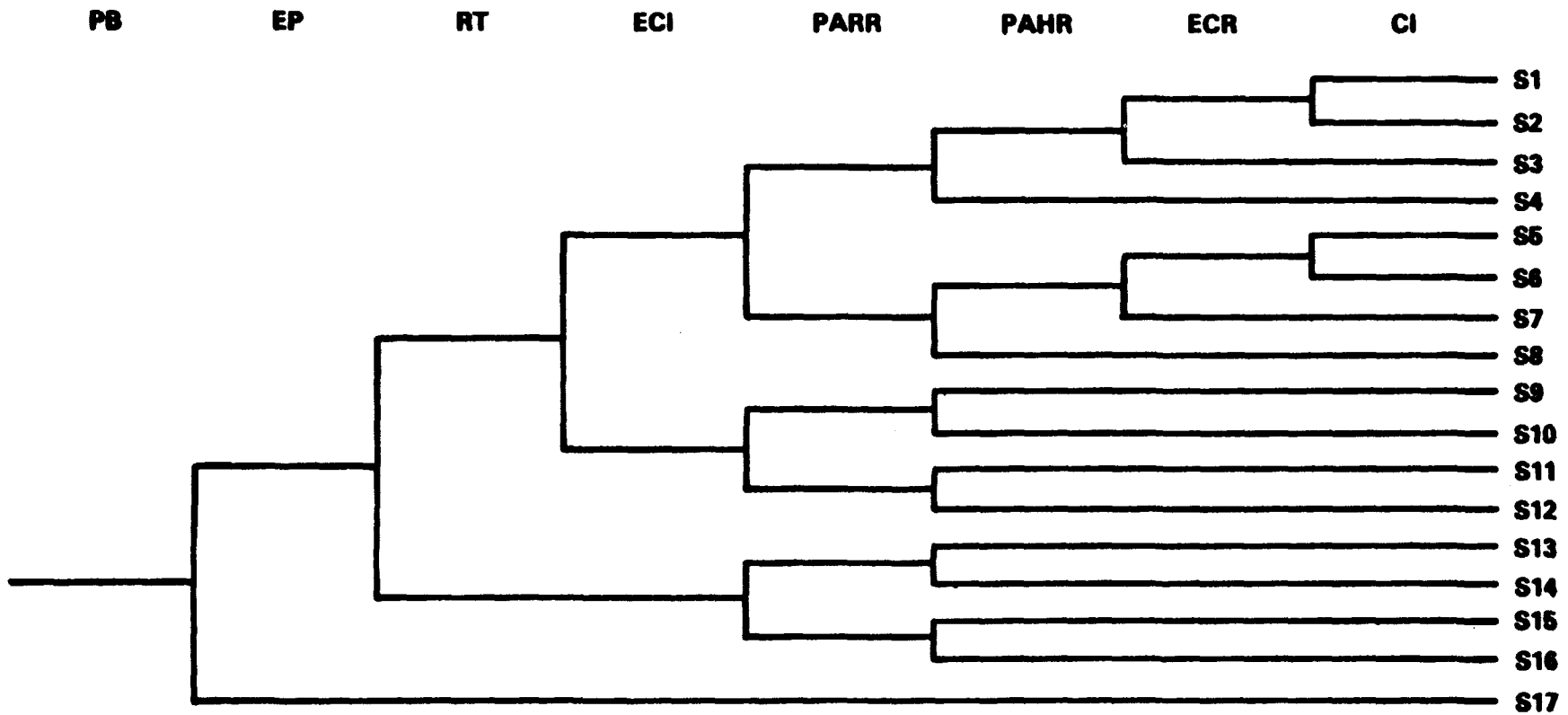


FIGURE 6

**FUNCTIONAL LOCAL EVENT TREE
SHOWING INTERRELATIONSHIPS WITH RT**



17

FIGURE 7

ESF FUNCTIONS TO ESF SYSTEM INTERRELATIONSHIPS

	RT	ECI	PARR	PAHR	ECR	
PWR LARGE LOCA >6" DIAM.		ACC AND LPIS	CSIS OR CSRS + SHA	CSRS AND CHRS	LPRS	}

PWR SMALL LOCA 2"-6" DIAM. BREAK	RPS	ACC AND HPIS	SAME	SAME	LPRS AND HPRS	}

PWR SMALL LOCA ½"-2" DIAM. BREAK	SAME	HPIS AND AFW	SAME	CSRS AND CHRS	SAME	}

FIGURE 8

PWR LARGE LOCA EVENT TREE

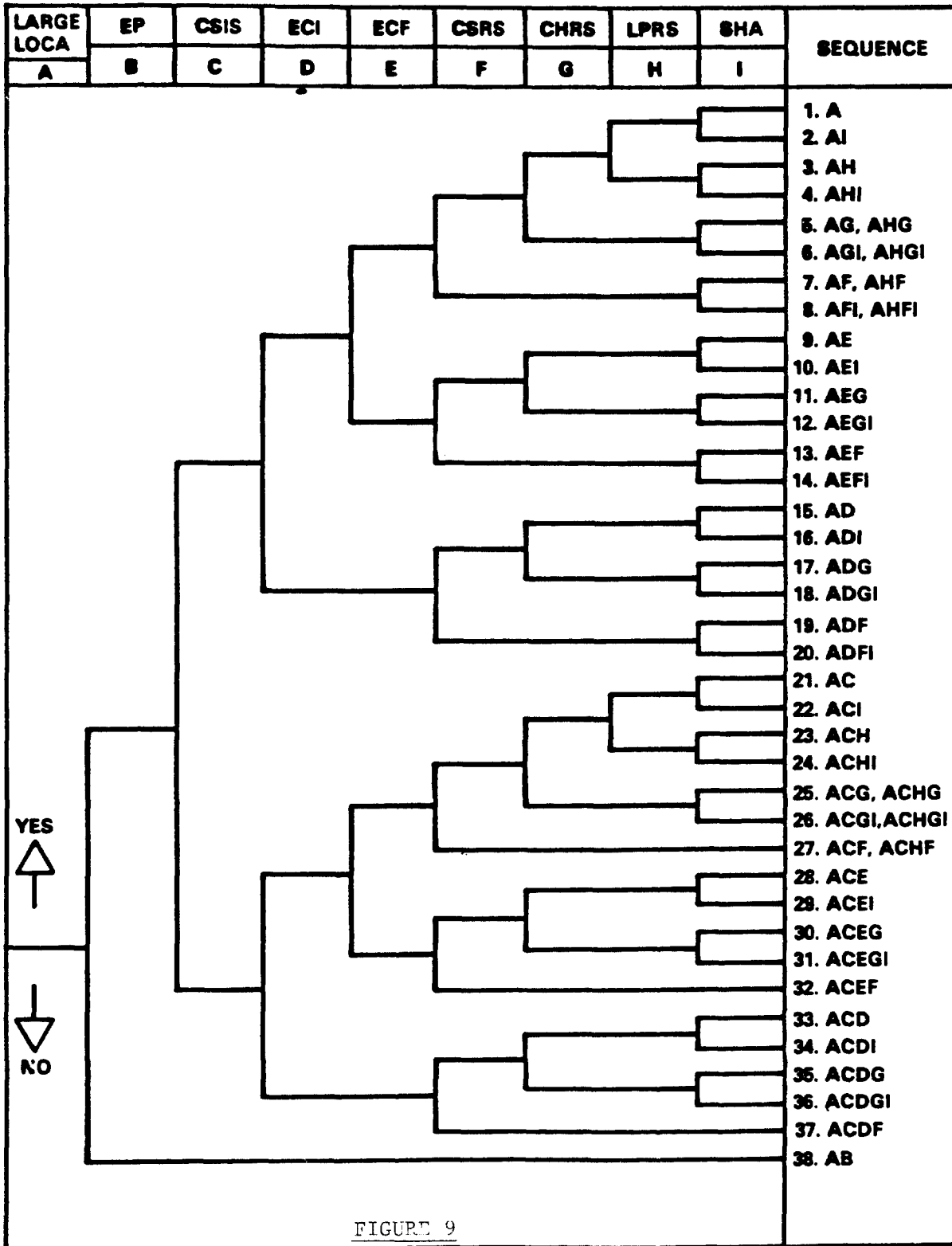


FIGURE 9

15th DOE NUCLEAR AIR CLEANING CONFERENCE

Figure 10 shows a containment event tree for which the inputs are the accident sequences from the last tree that resulted in containment rupture or in core melt. The various modes in which the containment can fail are examined. The containment can rupture because of a steam explosion in the reactor vessel. This would have to be a very large explosion, large enough to rip the head off the reactor vessel and blow it out through the top of the containment. That is a low-probability event, obviously. Containment failure can also result from failure to isolate it, in which case there would have to be a large enough hole so that the containment cannot be overpressurized. Another cause of containment failure is combustion and explosion of hydrogen generated by the reaction between stainless steel and water. If none of these things happen, the containment can rupture simply through failure of the heat-removal system. And, of course, there is one more mode of containment failure: the core will melt through the bottom of the reactor vessel, through the containment, and into the ground. These are the ways in which the containment can fail; each has a different probability and vastly different consequences.

Figure 11 indicates that we have to couple together the LOCA tree, or the transient tree, with the containment event tree to get the complete set of accident sequences. The form of the containment event tree changes depending on the a priori conditions of the LOCA tree.

From the large LOCA tree in the PWR combined with the containment event tree, there are 150 accident sequences possible (Figure 12). These are broken down in two ways: (1) by the size of the radioactivity release (1, 2, 3, 4, etc.) and (2) by probability. Probabilities are assigned to these sequences to determine the probability of each of the releases. Clearly, only a few sequences, anywhere from one to four or five, determine the probability of occurrence of any release. The probabilities of the other sequences are so much smaller than these few that they do not contribute. Thus a general case of 30,000 accident sequences in the large LOCA tree has reduced to 20. The same exercise can be done for each event tree that was considered in the study: the small LOCA tree and the transient tree. Figure 13 shows the top of the large LOCA tree, the two small LOCA trees, the reactor-vessel-rupture tree, and the transient tree. There are 80 sequences out of a possible total of 130,000. In fact, only two or three sequences dominate the risk.

Figure 14 shows the generalized form of the accident sequences. Each sequence has the probability of some initiating event x , the probability of some engineered safety system failing. In most cases this is a single system, but in a few cases it is more than one. Examples are the probability of a given containment-failure mode, the probability of a particular weather condition, and the probability of a particular population distribution being exposed. For a typical sequence the probability of a pipe break is 10^{-3} , the probability of a system failure is 10^{-2} , and the probability of a containment-failure mode is 10^{-1} . From the viewpoint of seeking to improve safety, it is obvious that the largest consequences come from the containment-failure mode in which the containment ruptures above the

LINKING OF ACCIDENT AND CONTAINMENT EVENT TREES

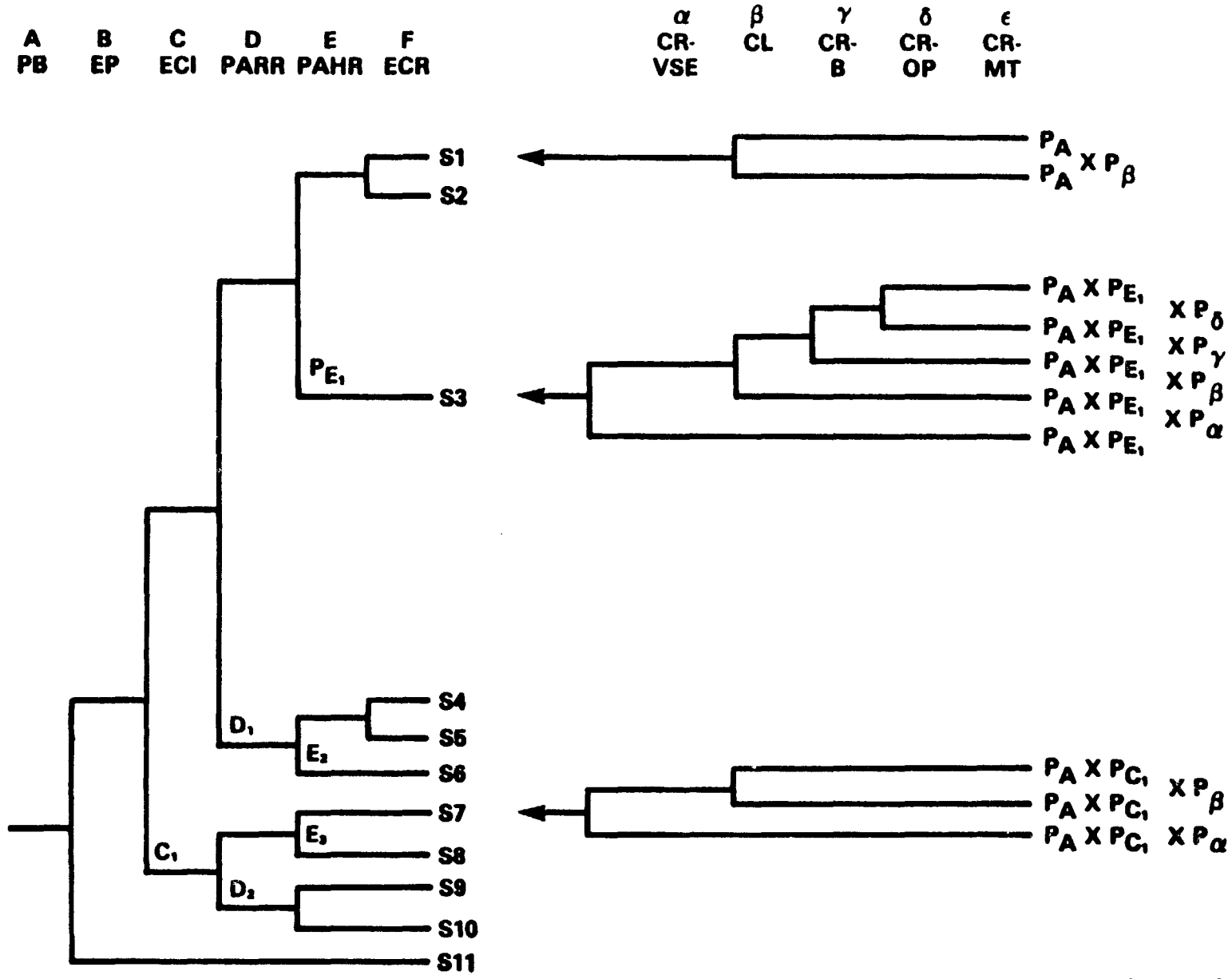


FIGURE 11

PWR LARGE LOCA ACCIDENT SEQUENCES VS. RELEASE CATEGORIES

Core Melt							No Core Melt	
CONSEQUENCE CATEGORIES								
1	2	3	4	5	6	7	8	9
DOMINANT LARGE LOCA ACCIDENT SEQUENCES WITH POINT ESTIMATES								
AB- α 1×10^{-11}	AB- γ 1×10^{-10}	AD- α 2×10^{-8}	ACD- β 3×10^{-11}	AD- β 9×10^{-9}	ACHF- ϵ 1×10^{-7}	AD- ϵ 2×10^{-6}	A- β 5×10^{-7}	A 1×10^{-4}
AF- α 1×10^{-10}	AHF- δ 2×10^{-10}	All- α 1.3×10^{-8}		AH- β 6×10^{-9}		AH- ϵ 1×10^{-6}		
ACD- α 5×10^{-11}		AF- δ 1×10^{-8}						
AG- α 9×10^{-11}		AG- δ 9×10^{-9}						
OTHER LARGE LOCA ACCIDENT SEQUENCES								
ACDGI- α AHFI- α ACHF- α ACDI- α ACDG- α AGI- α AFI- α ACG- α ACGI- α ACF- α ACDF- α ACEI- α ACEG- α ACEGI- α ACEF- α ACE- α AHF- α	ADF- β AHFI- δ ACHF- δ ACHF- γ ACDF- γ ACEF- γ AHFI- β ADFI- β ACHF- β ACDF- β AHI- γ AHFI- γ AB- δ AEF- β AEFI- β ACEF- β AEF- δ AEFI- δ ACEF- δ AB- β AHF- β	AHG- α AHGI- α ADF- α ADFI- α ACH- α ACHI- α ACHG- α ACHGI- α ACI- δ AFI- δ ACG- δ ACGI- δ ACF- δ AHI- α ADGI- α ADI- α ADG- α AE- α AEI- α AEF- α AEFI- α AEC- α AEGI- α	ACDGI- β ADG- β ACDI- β ACDG- β ADGI- β ACE- β ACEI- β ACEG- β ACEGI- β AEG- β AEGI- β	AHI- β AHG- β AHGI- β ADI- β ACH- β ACHI- β ACHG- β AE- β AEI- β	ADF- ϵ ACHGI- ϵ AHFI- ϵ ADFI- ϵ ACDF- ϵ ACDGI- ϵ AEF- ϵ AEFI- ϵ ACEF- ϵ ACEGI- ϵ AB- ϵ AHF- ϵ	ANG- δ AHGI- δ AHCI- ϵ ACH- ϵ ACHI- ϵ ACHG- δ ACHG- ϵ ACHGI- ϵ ACDI- ϵ ACDG- δ ACDG- ϵ ADG- δ ADGI- δ AHG- ϵ ADI- ϵ ADG- ϵ ACD- ϵ ADGI- ϵ AHI- ϵ AE- ϵ AEI- ϵ ACE- ϵ ACEI- ϵ ACEG- ϵ ACEG- δ ACEGI- δ ACHGI- δ AEG- δ AEGI- δ AEG- ϵ AEGI- ϵ	AI- β AC- β ACI- β	AI AC ACI

FIGURE 12

PWR DOMINANT ACCIDENT SEQUENCES VS. RELEASE CATEGORIES

	RELEASE CATEGORIES								
	Core Melt						No Core Melt		
	1	2	3	4	5	6	7	8	9
LARGE LOCA A	AB-a 1x10 ⁻¹¹ AF-a 1x10 ⁻¹⁰ ACD-a 5x10 ⁻¹¹ AC-a 9x10 ⁻¹¹	AB-γ 1x10 ⁻¹⁰ AMF-δ 2x10 ⁻¹⁰	AD-a 2x10 ⁻⁸ AM-a 1.3x10 ⁻⁸ AF-δ 1x10 ⁻⁸ AC-δ 9x10 ⁻⁸	ACD-δ 3x10 ⁻¹¹	AD-δ 9x10 ⁻⁸ AM-δ 6x10 ⁻⁸	ACMF-a 1x10 ⁻⁷	AD-γ 2x10 ⁻⁸ AM-γ 1x10 ⁻⁸	A-δ 5x10 ⁻⁷	A 1x10 ⁻⁴
A Probabilities	2x10 ⁻⁸	1x10 ⁻⁸	1x10 ⁻⁷	1x10 ⁻⁸	2x10 ⁻⁸	7x10 ⁻⁷	9x10 ⁻⁸	1x10 ⁻⁸	1x10 ⁻⁴
SMALL LOCA S₁	S ₁ B-a 3x10 ⁻¹¹ S ₁ CD-a 7x10 ⁻¹¹ S ₁ F-a 3x10 ⁻¹⁰ S ₁ G-a 2x10 ⁻¹⁰	S ₁ B-γ 2x10 ⁻¹⁰ S ₁ MF-δ 6x10 ⁻¹⁰ S ₁ B-δ 5x10 ⁻¹¹	S ₁ D-a 2x10 ⁻⁸ S ₁ H-a 4x10 ⁻⁸ S ₁ F-δ 3x10 ⁻⁸ S ₁ G-δ 2x10 ⁻⁸	S ₁ CD-δ 1x10 ⁻¹⁰	S ₁ H-δ 2x10 ⁻⁸ S ₁ D-δ 3x10 ⁻⁸	S ₁ DF-a 2x10 ⁻⁷	S ₁ D-γ 6x10 ⁻⁸ S ₁ H-γ 3x10 ⁻⁸	S ₁ γ 2x10 ⁻⁸	S ₁ 3x10 ⁻⁴
S₁ Probabilities	3x10 ⁻⁸	2x10 ⁻⁸	2x10 ⁻⁷	3x10 ⁻⁸	9x10 ⁻⁸	6x10 ⁻⁷	9x10 ⁻⁸	2x10 ⁻⁸	3x10 ⁻⁴
SMALL LOCA S₂	S ₂ B-a 1x10 ⁻¹⁰ S ₂ F-a 1x10 ⁻⁹ S ₂ CD-a 1x10 ⁻¹⁰ S ₂ G-a 9x10 ⁻¹⁰	S ₂ B-γ 1x10 ⁻⁹ S ₂ MF-δ 2x10 ⁻⁹	S ₂ D-a 1x10 ⁻⁷ S ₂ H-a 1x10 ⁻⁷ S ₂ F-δ 1x10 ⁻⁷ S ₂ C-δ 2x10 ⁻⁸ S ₂ G-δ 9x10 ⁻⁸	S ₂ DG-δ 1x10 ⁻¹¹	S ₂ D-δ 9x10 ⁻⁸ S ₂ H-δ 6x10 ⁻⁸	S ₂ B-γ 1x10 ⁻⁸ S ₂ CD-γ 2x10 ⁻⁸ S ₂ MF-γ 2x10 ⁻⁸	S ₂ D-γ 8x10 ⁻⁸ S ₂ H-γ 6x10 ⁻⁸		
S₂ Probabilities	7x10 ⁻⁸	4x10 ⁻⁷	3x10 ⁻⁸	4x10 ⁻⁷	2x10 ⁻⁷	2x10 ⁻⁸	2x10 ⁻⁸		
REACTOR VESSEL RUPTURE - R	RC-a 2x10 ⁻¹²	RC-γ 2x10 ⁻¹¹ RF-δ 1x10 ⁻¹¹ RC-δ 1x10 ⁻¹¹	R-a 1x10 ⁻⁸				R-a 1x10 ⁻⁷		
R Probabilities	2x10 ⁻¹¹	1x10 ⁻¹⁰	1x10 ⁻⁸	2x10 ⁻¹⁰	1x10 ⁻⁸	9x10 ⁻⁸	1x10 ⁻⁷		
INTERFACING SYSTEMS LOCA (CHECK VALVE) - V		V 4x10 ⁻⁸							
V Probabilities	4x10 ⁻⁷	4x10 ⁻⁸	4x10 ⁻⁷						
TRANSIENT EVENT - T	TMLB-a 3x10 ⁻⁸	TMLB-γ 4x10 ⁻⁷ TMLB-δ 1x10 ⁻⁷	TML-a 3x10 ⁻⁸ TKO-a 3x10 ⁻⁸ TKMO-a 1x10 ⁻⁸		TML-δ 6x10 ⁻¹⁰ TKO-δ 5x10 ⁻¹⁰	TLMB-a 2x10 ⁻⁸	TML-γ 3x10 ⁻⁸ TKO-γ 2x10 ⁻⁸ TKMO-γ 9x10 ⁻⁷		
T Probabilities	9x10 ⁻⁸	5x10 ⁻⁷	2x10 ⁻⁷	6x10 ⁻⁸	4x10 ⁻⁷	4x10 ⁻⁸	8x10 ⁻⁸		
(Σ) SUMMATION OF ALL ACCIDENT SEQUENCES PER RELEASE CATEGORY									
MEDIAN (50% VALUE)	7x10 ⁻⁷	5x10 ⁻⁸	5x10 ⁻⁸	5x10 ⁻⁷	1x10 ⁻⁸	1x10 ⁻⁸	6x10 ⁻⁸	4x10 ⁻⁸	4x10 ⁻⁴

FIGURE 13

SUMMARY OF ACCIDENTS INVOLVING CORE

RELEASE CATEGORY	PROBABILITY (Yr ⁻¹)	TIME OF RELEASE (Hr)	DURATION OF RELEASE (Hr)	WARNING TIME FOR EVACUATION (Hr)	ELEVATION OF RELEASE (Meters)	FRACTION OF CORE INVENTORY RELEASED							
						Xe-Kr	Org-1	I-Br	Cs-Rb	Te	Ba-Sr	Ru	La
PWR 1	7x10 ⁻⁷	1.5	0.5	1.5	25	0.8	6x10 ⁻³	0.6	0.4	0.4	0.05	0.4	3x10 ⁻³
PWR 2	6x10 ⁻⁶	2.5	0.5	1.5	0	0.8	7x10 ⁻³	0.7	0.5	0.3	0.06	0.02	4x10 ⁻³
PWR 3	6x10 ⁻⁶	2.0	1.0	1.5	0	0.8	6x10 ⁻³	0.2	0.2	0.3	0.02	0.02	3x10 ⁻³
PWR 4	6x10 ⁻⁷	2.5	3.0	1.5	0	0.5	2x10 ⁻³	0.09	0.04	0.03	6x10 ⁻³	3x10 ⁻³	4x10 ⁻⁴
PWR 5	1x10 ⁻⁶	2.5	4.0	1.5	0	0.2	2x10 ⁻³	0.03	9x10 ⁻³	6x10 ⁻³	1x10 ⁻³	6x10 ⁻⁴	7x10 ⁻⁵
PWR 6	1x10 ⁻⁵	12.0	10.0	1.5	0	0.2	2x10 ⁻³	8x10 ⁻⁴	7x10 ⁻⁴	1x10 ⁻³	9x10 ⁻⁵	7x10 ⁻⁵	1x10 ⁻⁵
PWR 7	6x10 ⁻⁵	10.0	10.0	1.5	0	5x10 ⁻³	2x10 ⁻⁵	2x10 ⁻⁵	1x10 ⁻⁵	2x10 ⁻⁵	1x10 ⁻⁶	1x10 ⁻⁶	2x10 ⁻⁷
PWR 8	4x10 ⁻⁵	0.5	0.5	N/A	0	2x10 ⁻³	6x10 ⁻⁶	1x10 ⁻⁴	6x10 ⁻⁴	1x10 ⁻⁶	1x10 ⁻⁸	0	0
PWR 9	4x10 ⁻⁴	0.5	0.5	N/A	0	3x10 ⁻⁶	7x10 ⁻⁹	1x10 ⁻⁷	6x10 ⁻⁷	1x10 ⁻⁹	1x10 ⁻¹¹	0	0

FIGURE 14

15th DOE NUCLEAR AIR CLEANING CONFERENCE

ground and releases a large cloud of airborne radioactivity. Let us see now whether or not the probability can be reduced significantly, say by an order of magnitude.

The three highest release categories, which in fact are the categories that determine the total risk, are 1, 2, and 3. The other categories are so small that there are extremely small consequences from them. The accident sequences that determine the probability of all three of these release categories--and whose probability determines the total probability of reactor accident risks in the PWR--are TMLB γ , TLMB δ , and S₂C δ (see Figure 13). The Greek letters denote the probability of failure of the containment from overpressure by failure of the containment heat-removal system and the probability of containment failure from hydrogen burning.

This suggests that if in fact those probabilities can be reduced, say by venting the containment through a filter so that it does not fail with that probability, the probabilities of these three categories and the overall risk can be reduced.

Figure 14 demonstrates this point in terms of radioactivity releases. The fraction of core inventory released is shown by fission-product release groups for the three highest categories: PWR 1, 2, and 3. One can see how large these three groups are in comparison with all the others. Nothing can be done to reduce the release fractions, but efforts can certainly be made to reduce the probabilities, which would then reduce the risks.

I am now going to talk about the second subject: improved safety research. In the Fiscal Year 1978 NRC Authorization Act, Congress asked the NRC to produce a plan for research to improve the safety of reactors. A wide range of sources were consulted for suggestions for improved safety, and a research review group was formed consisting of about 40 consultants, including antinuclear people. The most prolific source of suggestions was the Advisory Committee on Reactor Safeguards, although the NRC staff also made numerous suggestions. A report issued by the American Physical Society's (APS) Study Group on Reactor Safety contained a number of suggestions, as did a study sponsored by the Ford Foundation. Other suggestions were contained in the U.S. Atomic Energy Commission's ECCS Acceptance Criteria, written at the end of the 2-year ECCS hearing, and in a fairly comprehensive report by Environmental Quality Laboratories. In all there were over 200 suggestions, which were grouped into 16 research topics. To decide which of these 16 research topics are the most important, a set of criteria was set up, including the following: the breadth of support from this group, the risk-reduction potential (from the viewpoint of the Reactor Safety Study), applicability to existing and future reactors, applicability to BWRs and PWRs, and implementation cost. For lack of time the value-impact analysis was qualitative only.

The results are summarized in Figure 15, which shows the four evaluation criteria and the five topics that were selected. Vented containment, for instance, had high support, high risk-reduction potential, high applicability, and medium cost. (Medium cost was

	BREATH OF SUPPORT	RISK REDUCTION	APPLICABILITY	COST
VENTED CONTAINMENT	M	M	M	M
DECAY HEAT REMOVAL	M	M	M-H	M
ECCS SYSTEMS	M	M	M	L-M
ACCIDENT RESPONSE	M	M-M	M	L
SEISMIC DECOUPLING	M	M-M	L-M	M-H

FIGURE 15

15th DOE NUCLEAR AIR CLEANING CONFERENCE

defined as between \$10 to \$15 million per plant.) Decay-heat removal had high support, high risk-reduction potential, less clear applicability, and lower cost. One of the recommendations that was featured prominently in the APS report and the ECCS Acceptance Criteria was research on emergency core-cooling systems. It is well known how much effort has been and is still going into emergency core-cooling systems. Interestingly enough, though there is high support, there is only a moderate risk-reduction potential, moderate applicability, and large to medium costs. The risk-reduction potential is only moderate because it was established in the Reactor Safety Study that LOCA sequences are not among the three principal contributors to risk. Another topic selected for research is improved accident response within the plant, i.e., principally by the operators and by providing them with more analytical information than they now have. It turns out that the operators and maintenance personnel contribute significantly to accident risks. This topic had high support, high to medium risk-reduction potential, high applicability, and very low cost. There were a number of suggestions for decoupling seismic forces from the reactor plant, such as floating it in a pond or putting it in a muddy environment. This topic had moderate support, high to medium cost, and low general applicability (it would be applicable only to future plants and probably only in selected sites). The highest-priority topic and the one that seems to have the largest potential for risk reduction is the vented containment: if the core is melting, the containment is opened to the atmosphere through filters to prevent the large uncontrolled release of gaseous activity that occurs when the containment ruptures by itself. It is proposed to define a conceptual system configuration to determine feasibility, sizing, and cost and to perform a quantitative value-impact analysis. Concepts such as a separate building where the containment is vented through a pool of water, sand and gravel filters, or charcoal filters, will be explored. There is much information about the various concepts, and it is not sure that any physical research will be required. If it is, then the NRC will do it. Also studied will be some of the other containment improvements that can be made.

We have given a specific example of the application of risk-assessment techniques to improve the safety of nuclear power plants. There are many other examples of applications that have been made in solving specific licensing problems. The principal problem is associated with stabilizing the licensing process; that is, finding stopping places in the NRC review process.

Many believe that a major advance in licensing stability would be achieved if criteria for acceptable levels of risk were established. Presumably they feel that such criteria could provide a more rational basis for decisionmaking, both within the regulatory process and on a more broadly applicable societal basis. There are very real questions about the utility of such criteria in societal applications. Quantitative levels of acceptable risk have not been established in the United States regarding any human endeavor. There are some examples in other countries, but that does not change the problem of implementing such procedures in the United States. Furthermore, there is a body of opinion among social scientists, with some supporting evidence, that participation by divergent elements in an open

15th DOE NUCLEAR AIR CLEANING CONFERENCE

and local, and I emphasize local, decisionmaking process is the only way of determining societally acceptable risk levels. This viewpoint will not sit well with those of us in the physical sciences who have the traditional belief that somewhere there are some decisionmakers who will respond well to a fairly rational determination of acceptable levels of risk. It is likely that neither of these viewpoints is entirely correct.

If there is one place where criteria for acceptable risk levels would, on the surface, appear to be useful it is in the reactor licensing process. There are many examples of the difficulty involved in deciding how far to follow the path of a particular accident sequence in the review process. Clearly, there is some point at which the combined probability of the events postulated is so low as to make the consideration of additional events unnecessary. However, even there, if such criteria were available, one would have to face the problem of allocating portions of the allowable risks to the various safety features of the plant in order for the criteria to be usable. This is risk allocation, which is a whole separate and complicated subject of its own. The establishment of such risk allocations would be a formidable task, and even if feasible, would represent an additional limitation on freedom in design. Furthermore, it is not clear that such allocations would be more useful than other approaches. For instance, present NRC licensing activity already uses what is essentially a qualitative level of acceptable risk. The plants that are licensed have to meet NRC regulations and guidance embodied in standard review plans and regulatory guides. Moreover, the risk assessment in the Reactor Safety Study has in effect measured the accident risks in plants that the staff has found acceptable. Using this as a point of departure, in many cases a simple straightforward analysis can demonstrate that a particular accident sequence would or would not contribute to the overall accident risk defined in the Reactor Safety Study. The stopping places in licensing analysis can be found by this approach. The NRC's probabilistic analysis staff has demonstrated that in many cases matters that have been of concern to the regulatory staff and to the Advisory Committee on Reactor Safeguards have not in fact been significant contributors to the overall accident risk and could be ignored.

It is therefore clear that the quantitative risk-assessment techniques can be used to great advantage in stabilizing the licensing process without defining quantitative criteria for acceptable levels of risk. We are now just beginning to apply risk-assessment techniques to a whole variety of problems, and this should help significantly in stabilizing the licensing process. This is being done in close coordination between the Office of Nuclear Regulatory Research and the Office of Nuclear Reactor Regulation. I will just list five topics that we are looking at now. There are outstanding generic issues on reactor safety, 133 of them. We have reviewed these already, and it seems that perhaps 10 to 20 may significantly affect risk whereas the others do not matter very much. This has yet to be finished, promulgated, published, and accepted, but that is where we are today. We are beginning to look at the standard review plan, which guides individual reviewers and their review of reactors from a

15th DOE NUCLEAR AIR CLEANING CONFERENCE

risk-assessment viewpoint to determine which items considered may not be significant to risk. We are going to review those to find which are important to safety and which are not. We will look at technical specifications to find out which items are not significant to risk. There is also the systematic evaluation plan for evaluating the eleven oldest reactors in the country to find out what to do with them. And we are going to review them from a risk-assessment viewpoint to find out which items must be looked at and which items need not be looked at. I am very excited about this new work that we are just starting. It shows that the techniques of the Reactor Safety Study have come of age and have achieved broad acceptance both in the scientific community and in the NRC, and I hope we can do important things with it.

DISCUSSION

WILHELM: Could you give us some of the random conditions for a filter system of a vented containment with respect to temperature, pressure difference, dose, and relative humidity?

LEVINE: I am not able to define these conditions at this time since the study I mentioned has not yet been done. Obviously, a spectrum of conditions (i.e., flow rates, pressures, etc.) will have to be examined to optimize the system design.

WILHELM: You may be interested to learn that we calculated the conditions for such a vented containment filter system and the figures are rather shocking. The flow, calculated for a German 1300 megawatt electric pressurized water reactor, is 10,000 cubic feet/minute through the filter system. This is a problem when considering the use of sand bed filters. The temperature rises to 300° in the filter system and the amount of hydrogen in the containment amounts of some 10,000 cubic meters of hydrogen. With hydrogen present, you can't use silver zeolites for the adsorption of iodine because the iodine would react to form hydrogen iodide and desorb. Doses may rise to 10¹¹ rad on the adsorbent and the filter material, depending, of course, on the size of the filter system. I wish to mention these figures only to show the audience what kind of challenge it is to build such a system.

LEVINE: I can't quarrel with your numbers although I suspect your flow rate may be rather high. It turns out that to prevent a typical U.S. PWR containment from rupturing due to overpressure, requires a four or five inch hole. Now, you can't get adequate flowrates through a four inch hole to accommodate your flow rate, so I suspect there is some difference in the assumptions on which you made your calculations. You're certainly right about the challenge that would occur to a filter system, but there are filter systems in the United States that can handle very large flowrates and do so effectively. They're classified, unfortunately, so I can't talk much about them. It's a challenge, but I think it can be done.

KOVACH: I disagree with Mr. Wilhelm's analysis of the vented containment. If the venting is started early enough after a LOCA, a smaller than 10,000 CFM filter is required. We have presented such an analysis at the 14th Air Cleaning Conference. The quantities that were shown were a few thousand CFM, one to three, to prevent an overpressurization of the reactor. At that point, you have no hydrogen.

LEVINE: I agree with you.

FIRST: In view of the fact that Saul Levine has given us such an excellent review of how accident trees were used for making the assessments that he's covered so well, I've taken the privilege of slightly altering our program by asking Dade Moeller to give his talk next instead of waiting for the paper that was to go in between. The reason I've asked him to do this is that Saul Levine identified accidents sequences and talked about engineering safety system failure. Dr. Moeller's paper, entitled Review of Failures in Nuclear Air Cleaning Systems, fits very neatly with the papers we've just heard in terms of the practical applications. Dr. Moeller has spoken on this topic at previous meetings and the information he has brought to us has been not only excellent but quite startling, and I'm sure you will find what he has to say today equally interesting and important.

15th DOE NUCLEAR AIR CLEANING CONFERENCE

REVIEW OF FAILURES IN NUCLEAR AIR CLEANING SYSTEMS (1975 - 1978)*

Dade W. Moeller, Chairman
Department of Environmental Health Sciences
Harvard School of Public Health
Boston, Massachusetts

Abstract

During the period from January 1, 1975, through June 30, 1978, over 9,000 Licensee Event Reports (LERs) pertaining to the operation of commercial light water nuclear power plants in the U. S. were reported to the Nuclear Regulatory Commission. Of these reports, over 1,200 (approximately 13%) pertained to failures in air monitoring, ventilating and cleaning systems. For BWR installations, over half of the reported events related to failures in equipment for monitoring the performance of air cleaning systems as contrasted to failures in the systems themselves. In PWR installations, failures in monitoring equipment amounted to about 32% of the total. Reported problem areas in BWR installations included the primary containment and standby gas treatment and off-gas systems, as well as the High Pressure Coolant Injection and Reactor Core Isolation Systems. For PWR installations, reported problem areas included primary containment and associated spray systems and waste processing equipment. Although data on reported failures in power reactor installations can be interpreted in a variety of ways, one message is clear. There is a need for research on the development of more reliable equipment for sampling and monitoring air systems. Equipment that provides inaccurate data on the performance of such systems can lead to as many problems as inadequacies in the systems themselves.

I. Introduction

At the 13th Air Cleaning Conference in 1974, this author presented a paper⁽¹⁾ in which an analysis was performed of 55 failures that had been reported in nuclear air cleaning systems during the time period from 1966 through 1974. Of these failures, 28 had occurred in commercial nuclear power plants. Since that time, there has been a large increase in the number of commercial nuclear power plants in operation. In fact, during the period from January 1, 1975, through approximately June 30, 1978 (the time period covered by this study), over 9,000 additional Licensee Event Reports were submitted,⁽²⁾⁽³⁾⁽⁴⁾⁽⁵⁾⁽⁶⁾ of which over 1,200 pertain to failures in nuclear air systems. This paper presents a summary of observations made on the basis of an indepth review of these newer items. In evaluating this report, it should be noted that it differs in two basic ways from the earlier paper. First, this analysis was confined to events occurring within commercial nuclear power plants; second, it was broadened to include reports on air monitoring and ventilating, as well as air cleaning systems.

*This work was supported in part by the U.S. Department of Energy under contract EY 76 S 02-3049

15th DOE NUCLEAR AIR CLEANING CONFERENCE

Table I. Overall tabulation of licensee event reports

Year	Power Reactors		All Events		Air Cleaning Events*	
	Reactor Type	Number Operating**	Total Number	Number per Reactor	Total Number	Number per Reactor
1975	BWR	20	1169	58	121	6.0
	PWR	27	1097	41	141	5.2
1976	BWR	23	1253	54	227	9.9
	PWR	30	1264	42	131	4.4
1977	BWR	24	1190	50	152	6.3
	PWR	36	1678	47	210	5.8
1978	BWR	24	637***	53****	125***	10.4****
	PWR	41	1076***	52****	120***	5.9****

* Includes events pertaining to air monitoring, ventilating, and cleaning

** As of July 1 of the given year

*** Through approximately June 30, 1978

****Projected through December 31, 1978

15th DOE NUCLEAR AIR CLEANING CONFERENCE

As may be noted in Table I, there was a yearly average of 50 to 58 LERs per operating commercial Boiling Water Reactor (BWR) and 41 to 52 LERs per operating commercial Pressurized Water Reactor (PWR) during the three and one-half year period covered by this study. It should be observed, however, that these averages were calculated using a simplistic approach. That is, they were computed by dividing the total number of LERs for each year by the number of reactors operating as of July 1, of the same year. For BWR plants, approximately 10% to 20% of the reported events pertain to failures in air systems; for PWR plants, the range is from 10% to 13%. The higher average number of events pertaining to air systems in BWRs is to be expected since there are more opportunities for radioactive airborne releases from such facilities and the number of associated air monitoring, ventilating and cleaning systems is greater.

II. Review of Specific Failures

Details of LERs pertaining to air monitoring, ventilating and cleaning units within specific reactor systems for BWRs and PWRs are summarized in Tables II and III, respectively.

Problems in BWRs

As may be noted, the reported events for BWRs relate to the commonly expected areas such as primary and secondary containment, and standby gas treatment and off-gas systems, as well as to the less expected areas such as the High Pressure Coolant Injection (HPCI) and Reactor Core Isolation Cooling (RCIC) systems. Of particular note is the large number of reported events associated with the equipment designed to sample and monitor the performance of ventilating and air cleaning systems. In fact, an analysis of the data shows that 51% of all reported failures were in the equipment installed to monitor the performance of the air cleaning and ventilating systems. Further analyses show that, of the failures in air sampling and monitoring equipment in primary containment, 41% occurred as a result of deficiencies in the air sampling portion of the system, as contrasted to failures in the detector or analysis unit itself. Of the failures within the detectors and analyzers, 31% were with hydrogen and/or oxygen analyzers, 35% were with pressure sensors, 26% were with radiation monitors (gaseous and particulate), and about 9% were with temperature monitors. The relatively high frequency of failures in hydrogen and oxygen analyzers is of special significance in view of the importance of such monitors to warn of explosive mixtures within various BWR systems.

With respect to specific failures in air monitoring, ventilating and cleaning systems in BWRs, the following appear worthy of note.

Violation of Single Failure Criterion

During operation of one plant in 1975, it was discovered that an auto initiation signal for one standby gas treatment unit automatically closed the inlet valve to the second unit. As a result, if the inlet valve for the initiating unit failed, no inlet valve for either unit would be open. This proved to be a violation of the single failure criterion and the logic system was modified to remove this deficiency. This same problem was discovered at a second operating BWR in 1976 and again reported as an LER.

15th DOE NUCLEAR AIR CLEANING CONFERENCE

Table II. Summary of licensee event reports
Air Monitoring, Ventilating and Cleaning Systems
(Boiling Water Reactors, 1975 - 1978)

<u>System</u>	<u>Component</u>	<u>Nature of Problem</u>	<u>Number of Events</u>			
			<u>1975</u>	<u>1976</u>	<u>1977</u>	<u>1978*</u>
Primary contain- ment	Atmospheric sampling and moni- toring	Failure in sampling system	7	36	14	26
		Failure of detector or analysis unit	17	46	24	33
	Diluting, inerting, or venti- lating system	Deficien- cies in nitrogen purge or ventilating system	19	31	11	10
		Deficien- cies in filter system	0	0	0	2
Torus		Failure of vacuum breakers	10	10	9	3
		Improper water level or indicator malfunction	9	19	0	3
Contain- ment spray system		Deficiencies in operation of valves	2	8	0	0
		Failure of supporting equipment	2	4	1	1

*Through approximately June 30, 1978

15th DOE NUCLEAR AIR CLEANING CONFERENCE

System	Component	Nature of Problem	Number of Events			
			1975	1976	1977	1978*
Reactor cooling system	Coolant purification system	Excessive airborne release	0	2	2	0
		Hydrogen explosion	1	0	0	0
	Leak detection system	Failure of particulate sampler	0	0	1	0
	Injection and isolation system	Isolation of high pressure coolant injection system	1	6	13	0
		Isolation of reactor core isolation cooling system	1	3	1	0
Secondary containment (Reactor building)	Atmospheric sampling and monitoring system	Failure in sampling system	0	3	1	1
		Failure of radioactive gas monitor	6	5	7	8
	Diluting and ventilating system	Failure of blowers, isolation valves, or dampers, or cooling water flow	7	4	5	0

*Through approximately June 30, 1978

15th DOE NUCLEAR AIR CLEANING CONFERENCE

System	Component	Nature of Problem	Number of Events			
			1975	1976	1977	1978*
Standby gas treatment system	Air flow system	Failure of blowers, low flow, train overheated, excessive moisture	14	8	8	10
	Filter system	Adsorbers depleted or absent, filters plugged	2	2	2	2
	Fire protection system	Flooding of charcoal filters	0	1	0	3
Off-gas system	Sampling and monitoring system	Failure in sampling system	5	5	5	3
		Failure of detector or analysis unit	2	4	11	3
	Air flow system	Failure of drain line, leaks in line	2	4	8	2
	Filter system	Excessive pressure drop (plugged filter)	0	0	1	0
		Fires or explosions	2	5	2	1
	Combustible gas control	Excessive hydrogen concentration	1	2	2	1

* Through approximately June 30, 1978

15th DOE NUCLEAR AIR CLEANING CONFERENCE

<u>System</u>	<u>Component</u>	<u>Nature of Problem</u>	<u>Number of Events</u>			
			<u>1975</u>	<u>1976</u>	<u>1977</u>	<u>1978*</u>
Control room or building	Sampling and monitoring system	Failure in sampling system	0	1	0	0
		Failure of detector or analysis unit	1	4	1	0
	Ventilating system	Failure in emergency ventilating system	2	1	2	5
Turbine room	Atmospheric monitoring system	Failure of radiation monitor	0	0	1	0
	Airborne radioactive release control	Excessive airborne release	0	4	0	0
	Ventilating system	Lack of interlocks on supply and exhaust fans	1	0	0	0
Main stack discharge system	Sampling and monitoring system	Failure in sampling system	4	7	7	2
		Failure of detector or analysis unit	3	2	12	4
	Air flow system	Inadequate flow	0	0	1	2
TOTALS			121	227	152	125

* Through approximately June 30, 1978

15th DOE NUCLEAR AIR CLEANING CONFERENCE

Isolation of HPCI and RCIC Systems

An interesting set of failures has been the isolation of the High Pressure Coolant Injection (HPCI) and Reactor Core Isolation Cooling (RCIC) systems that has occurred as a result of inadequacies in the ventilating systems within several BWRs. One such event occurred in 1975, nine in 1976, and eleven in 1977. The basis of the problem is that the areas through which the piping from the HPCI and RCIC systems passes are equipped with temperature sensors which are designed to isolate these systems in case there is a steam leak in the lines. If, however, there is a malfunction in the ventilating systems for these areas, or a sudden change in the outdoor temperature which leads to the sensor indicating a steam leak, the two systems are automatically isolated. Correction of the problem appears to be to increase the capacity of the air ventilation systems for the affected areas.

Deficiencies in Control Room Ventilating System

In 1977, a worker was distracted while filling the caustic and acid tanks in the makeup demineralizer water room. The tanks overflowed and the acid and caustic interacted with each other and the concrete floor producing fumes. Since the exhaust fan in the room was inoperable, the fumes seeped into the Control Room ventilation system. Since the Control Room ventilation system was limited to a maximum of 10% outside (makeup) air, the operators shut off the ventilation system and transferred to the portable supplied air packs. Without the ventilation system on, the Control Room heated up and possible instrument failures were feared. As a result, the plant was put on Emergency Alert until the situation could be rectified.

Fires and Explosions in Off-Gas Systems

Fires and explosions continue to be a problem in BWR off-gas systems. There were two such events in 1975, five in 1976, two in 1977 and one has occurred in 1978. In 1975, a closed isolation valve in the off-gas system at one BWR forced off-gas from the steam jet air ejector through a loop-seal drainline from the holdup line to a sump and back to the dilution fans prior to being discharged through the elevated release point. The sump became pressurized and an explosion occurred when a health physicist removed a manhole cover to the sump and turned on a sampler to check for air contamination. Two people were injured as a result of this event. Later inspection showed that the control room valve position indicating lights and control switch showed the closed valve to be open. Errors in the electrical wiring to the valve were corrected.

In another event in 1975, catalyst pellets from the recombiners were somehow dislodged and transported, perhaps by system flushing, into the preheaters, a pressure valve, and two low point drains in an off-gas system. Later the pellets ignited and caused an explosion.

15th DOE NUCLEAR AIR CLEANING CONFERENCE

In 1976, a buildup of ice in the upper portion of the exhaust stack at a BWR resulted in backpressure and the accumulation of hydrogen in the off-gas building. Later, an explosion completely demolished the building. Corrective action included heat tracing and insulation of the upper portion of the elevated discharge pipe. In another case during the same year, an explosion occurred in the stack filter house at a BWR. This resulted from the improper positioning of a demister that permitted moisture to collect and freeze on a HEPA filter, causing a decrease in the flow rate. Pressure buildup resulted in the unseating of a number of off-gas loop seals, which permitted both airborne radioactive materials and hydrogen gas to enter the stack filter house. Corrective actions included proper positioning of the demister and other measures.

In another sequence of events in 1977, a welder's torch set off a hydrogen explosion in an off-gas delay line. Although the line was designed to withstand an explosion, the pressure wave caused water to be removed from the loop seals provided to draw condensation from the gaseous mixture in the off-gas pipe. Since the seals were not refilled, hydrogen built up in two unventilated rooms at the base of the plant stack. Later when a sump pump in the base of the stack was activated, the explosive mixture in the two rooms was ignited.

In early 1978, temperature transients were noted in six charcoal beds in an off-gas system. Because a drainline in the off-gas preheater was plugged, dilution steam condensed on the recombiner catalyst, preventing the recombination of the hydrogen and oxygen passing through the system. Ignition of the mix downstream of the recombiner apparently ignited the charcoal. Nitrogen purge was used to cool the charcoal and extinguish the fire. The drain line was unplugged and the beds returned to service.

Hydrogen Explosion in Acid Day Tank

In 1975, a hydrogen explosion occurred in the condensate demineralizer regeneration system acid day tank at a BWR power plant. The hydrogen was formed when moisture from the atmosphere interacted with concentrated sulfuric acid in the tank due to depletion of the dessicant in a vent line. The explosion, believed to have been ignited by a spark from a nearby welding operation, blew the top off the tank and broke the vent and fill piping. As a result of this event, acid was deposited on nearby equipment, cable trays and the floor.

Failures in Recombiners

The importance of recombiners in preventing the accumulation of explosive mixtures in off-gas and SGBT systems is well known. Proper operation of such units, however, is important from other aspects. For example, while attempting to return a recombiner system mechanical compressor to service after maintenance at one BWR in 1978, the operator left open the inlet-sump drain valve. This allowed radioactive gas to escape from the system to a ventilated sump and then through the vent stack. The resulting release of radioactive material was 4.7 times the Technical Specification limit for a short period of time.

15th DOE NUCLEAR AIR CLEANING CONFERENCE

Browns Ferry Fire

As is well known, the use of a candle for testing for penetration leakage in the wall between the cable spreading room and the reactor building in Browns Ferry, Unit 1, in March, 1975, led to a fire in the cable spreading room. As a result of this experience, many improvements and changes in fire protection procedures at nuclear power plants are now in effect. In addition to terminating the use of open flame for testing air leaks, recommendations resulting from this event include the requirement that (a) control and power cables for a ventilation system that is important in fire control should not be routed through areas the system must ventilate in case of fire; (b) ventilation designs should be provided with the capability of isolating fires by use of cutout valves and dampers; (c) capability for the control of ventilation systems to deal with fire and smoke should be provided, but such provisions should be compatible with requirements for the containment of radioactive materials.

Fire Protection Systems

Because of the long recognized possibility of fires in standby gas treatment systems, equipment has been installed to deluge the charcoal with water in case of a fire. In one instance in 1976 and three in 1978, shorts in the electrical wiring have caused this equipment to actuate unnecessarily and flood the charcoal, thereby requiring complete replacement of the adsorbent. This is particularly noteworthy inasmuch as equipment designed to prevent or correct problems has actually been a source of failure itself. Similar problems have occurred in diesel generator rooms where defective smoke detectors have led to the discharge of CO₂ fire protection systems.

Problems in PWRs

The reported events for PWRs relate to the commonly expected problems associated with primary containment and its associated spray system, as well as to the perhaps less expected problems associated with waste processing systems. Again, there is a large number of events related to equipment designed to sample and monitor the performance of ventilating and air cleaning systems. In this case, however, the percentage of such failures in terms of all reported failures was only 32%, as contrasted to 51% for BWRs. The percentage of air sampling and monitoring failures within the primary containment due to the sampling portion of the system was about 42%, essentially the same as the value (41%) for BWRs. Of the failures within the detectors and analyzers themselves, the data show that 61% were with gaseous and particulate radiation monitors, 30% were with pressure sensors, and 9% were with hydrogen and oxygen analyzers. There were no reported failures of temperature monitors.

With respect to specific failures in air monitoring, ventilating and cleaning systems in PWRs, the following appear to be worthy of note.

15th DOE NUCLEAR AIR CLEANING CONFERENCE

Table III. Summary of licensee event reports
 Air Monitoring, Ventilating and Cleaning Systems
 (Pressurized Water Reactors, 1975 - 1978)

<u>System</u>	<u>Component</u>	<u>Nature of Problem</u>	<u>Number of Events</u>			
			<u>1975</u>	<u>1976</u>	<u>1977</u>	<u>1978*</u>
Primary contain-ment	Atmospheric sampling and monitoring	Failure of sampling system	8	18	27	17
		Failure of detector or analysis unit	17	21	29	29
	Diluting or ventila-ting system	Deficien-cies in purge (ventila-tion) system	23	26	35	11
		Deficien-cies in filter system	4	1	7	6
		Deficien-cies in air cooling system	28	17	28	15
		Emergency combustible gas control	0	1	0	1
	Containment spray system	Spray system not available	11	5	13	8
		Performance degraded	6	7	12	6
	Containment isolation system	Vacuum breaker inoperable	2	2	3	0

*Through approximately June 30, 1978

15th DOE NUCLEAR AIR CLEANING CONFERENCE

<u>System</u>	<u>Component</u>	<u>Nature of Problem</u>	<u>Number of Events</u>			
			<u>1975</u>	<u>1976</u>	<u>1977</u>	<u>1978*</u>
Reactor cooling system (primary)	Pumps, valves, pressurizer, sensing lines, etc.	Excessive airborne release	10	7	12	5
Control room	Normal ventilating system	Failure of dampers or fans, or design error	0	2	7	4
		Failure of heaters, coolers, or compressors	0	2	1	2
	Emergency ventilating system	Failure of dampers or fans, or design error	1	0	3	1
		Leak in header	0	0	0	1
		Emergency sampling and monitoring system	Failure of chlorine or radiation detector	0	1	2
Enclosure building	Ventilating system	Water in off-gas pipe	1	0	0	0
Fuel storage building	Ventilating system	Degraded charcoal filter	0	0	0	1
Auxiliary building	Sampling and monitoring system	Failure of radiation monitor	0	0	0	3
		Failure of dampers, or fans, or loss of power	3	0	4	1
		Filter plugging or heater failure	0	1	1	0

*Through approximately June 30, 1978

15th DOE NUCLEAR AIR CLEANING CONFERENCE

<u>System</u>	<u>Component</u>	<u>Nature of Problem</u>	<u>Number of Events</u>			
			<u>1975</u>	<u>1976</u>	<u>1977</u>	<u>1978*</u>
Diesel generator room	Ventilating system	Failure of dampers or fans, or design error	3	2	2	0
		Failure of air cooler	0	1	0	0
Turbine building	Atmospheric sampling and monitoring	Failure of radiation monitor	0	0	1	0
Switch gear room	Ventilating system	Failure of air cooler	0	1	0	0
Waste processing system	Waste gas decay tank	Excessive airborne release	12	8	5	0
		Excessive airborne release	3	1	1	0
	Waste gas surge tank	Excessive airborne release	3	1	5	3
		Failure of radiation monitor on loop seal	0	0	2	0
	Liquid waste system	Excessive airborne release	3	1	1	0
Main stack discharge system	Sampling and monitoring system	Failure of sampling system	0	2	2	1
		Failure of radiation monitor	3	2	6	2
	Air flow system	Failure of exhaust fan	0	1	1	0
TOTALS			141	131	210	120

*Through approximately June 30, 1978

15th DOE NUCLEAR AIR CLEANING CONFERENCE

Excessive Airborne Releases

Normal procedures call for the venting of the mixed-bed demineralizer, using primary makeup water that contains no radioactive gases. Because of personnel error, venting at one PWR in 1975 was done with the demineralizer connected to the reactor coolant system. This resulted in the release of radioactive gases from the cooling system to the auxiliary building through a loose manhole cover on the equipment drain tank. As a result of this mishap, in which an estimated 63 curies of radioactive gases were released, the operating procedures have been upgraded and the manhole cover has been tightened. (3)

Ice Condenser Pressure Suppression System

Effective operation of the ice condenser system requires that an adequate amount of ice be maintained in the containment at all times. To accomplish this task, the ice bays are separated from the rest of containment by a panorama of doors which are designed to easily open to permit any steam released within containment to enter the ice chambers and be condensed. Initial operation of these systems has revealed some problems with ice forming on the doors and hinge mechanisms, through condensation on the outside and bottom of the door frame. Since lake water is used to cool the containment atmosphere in the specific plant in which this problem occurred, it is postulated that the higher ambient temperature during summer months led to the condensation of vapor from the atmosphere on the cold door frames. From there, the water seeped into the insulation where it subsequently froze. To alleviate the problem, the floor cooling system controls have been adjusted to increase the floor temperature, the soaked insulation has been replaced and periodic inspections of the doors have been instituted. (3)

Failures in Containment Spray Systems

One of the engineered safety features for dealing with a postulated loss of coolant accident in a PWR is the containment spray system. Initially, such a system will take water from the Raw Water Storage Tank (RWST) and pump it through the containment sprays. After being sprayed, the water collects in sumps at the bottom of containment. When the supply in the RWST has been exhausted, the spray system continues by recirculating the water from the sumps. As the spray cools the containment, however, the containment pressure decreases. Calculations performed in 1977 showed that this pressure decrease could lead to a reduction in the Net Positive Suction Head (NPSH) and result in cavitation in the recirculating pumps. Since proper performance of the pumps is essential to long term cooling of containment and the pumps could be damaged if operated for a period of time without water, this situation called for a thorough analysis of the implications of the NPSH problem to the overall performance of containment spray systems. The problem was solved by showing that NPSH would not be reduced to the point that the pumps would be damaged.

15th DOE NUCLEAR AIR CLEANING CONFERENCE

Because of pumps being locked out of service, valves misaligned, or loss of power, there were 37 events reported over the three and one half year period of this study in which the containment spray system was unavailable. Of these, over 90% were due to human error. In addition, there were 31 events in which the performance of this system was degraded. In the Reactor Safety Study⁽⁷⁾, it was estimated that there were about three chances in one thousand that both of the duplicate spray systems would be unavailable because the valves were not properly realigned after testing or the sensors that activate the systems were not properly calibrated. During the period covered by this study, there were approximately 113 reactor-years of operations. Assuming the containment spray systems in each PWR nuclear power plant were tested monthly, this means a total of about 1350 tests were conducted. Using these data, one can calculate that the 37 reports of unavailability over this period represent a probability of about 28 per thousand that one of the two containment spray systems would be unavailable. The probability that both systems would be unavailable would be about one in one thousand, which is substantially in agreement with the estimate given in the Reactor Safety Study.

Containment Purging Reduced to Alleviate Airborne Releases

Excessive airborne releases at one plant in 1977 led to a decision to reduce the frequency of containment purging. A factor entering into this decision was that the plant had 36 inch diameter purge lines and the NRC prefers not to permit continuous purging unless smaller 8 inch lines have been installed. As a result of the reduction in the frequency of purging, the plant's airborne releases were reduced. At the same time, however, this led to a reduction in the frequency with which containment could be entered for visual inspections of safety related equipment, such as piping, snubbers, etc. This is a good example of the interactions of various systems within nuclear power reactors and highlights the importance of good air cleaning equipment for the safe operation of such facilities.

Auxiliary Building Exhaust Fan Causes Reactor Trip

Another example of systems interactions was the instance in which an operator, in anticipation of taking an air flow reading, started the second auxiliary building ventilation fan. Because the discharge damper on the fan was leaking, back pressure from the operating fan caused the second idle fan to be rotating backwards. When it was switched on, a large starting current was demanded. This led, for unknown reasons, to tripping of the MCC-6 supply breaker, instead of the fan breaker, and caused a reactor trip and safety injection. The discharge damper was adjusted and the breakers examined.

Impact of Faulty Sensors

A review of the reported events revealed a number of instances in which failure of a sensor led to difficulties. For example, because of the failure of a temperature sensor in the air intake tunnel, the deluge fire protection system at one PWR plant activated. This led, in turn, to the loss of the building ventilation system for a period of two and one-half hours. In another situation, the

15th DOE NUCLEAR AIR CLEANING CONFERENCE

annulus emergency ventilation system was found to be inoperable. The problem was traced to an incorrect reading from a pressure sensor. The atmospheric pressure tap had been taped over during painting of the auxiliary building outside walls and had not been removed. In a related incident at another PWR power plant, the performance of the containment spray system was degraded because tape was left on the spray nozzles following painting of containment.

During the performance of preventive maintenance to verify operation of the deluge system on a shield building ventilation system, a heat gun was used to elevate the temperature of a heat detector. Activation of the detector, however, locked out train A of the shield building exhaust and recirculation fans, disabling that train. Since train B had not been tested, this violated the Technical Specifications. The procedure was inadequate in that it did not include evaluation of the consequences of activating the heat sensor.

In another occurrence at the same plant, a diesel generator was taken out of service concurrently with the outage of safeguards train A special zone ventilation fan. Subsequently, the special ventilation fan in safeguards train B was tested, with the operating personnel failing to recognize that a safeguards train A component was out of service prior to placing the safeguards train B emergency power out of service.

Violation of Single Failure Criterion

During a review of the electrical circuitry associated with the containment ventilation isolation valves, it was found that the single failure criterion could not be satisfied for a postulated short circuit or foreign voltage imposition in the control circuitry for these valves. All four valves were controlled from the same electrical circuit. The same condition existed for the three containment pressure relief valves. Modifications were made to provide independent circuitry to one supply and one exhaust valve and both pressure relief valves outside containment.

Failure of Hydrogen Recombiners

Although not frequent, there were several reports of failures of emergency recombiners during the period of this study. For example, during the semiannual operational check at one plant in 1976, it was found that a hydrogen recombiner could be loaded only to 43KW. The resulting heater temperature was 170°F below the Technical Specification limit. Preliminary inspection indicated that one phase of the heater was grounded. A similar failure was reported in 1978.

Ventilation and Instrument Performance

The importance of ventilation as a cooling source was well illustrated by an event in a PWR power plant in 1975 wherein a critical instrumentation bus grid was lost due to high ambient temperature. The cause was determined to be excessive ambient temperature during a high load on the inverter. The system was

15th DOE NUCLEAR AIR CLEANING CONFERENCE

redesigned to improve local ventilation. In another plant in 1977, the air ejector radiation monitor blower tripped off. The cause was an overheated condition in the monitor cabinet due to poor ventilation.

During a refueling outage at another plant, condensation built up and moisture shorted out the detector tube for the component cooling heat exchanger radiation monitor. The source was condensation buildup on the service water piping in the auxiliary building. Although the detector tube was replaced and the piping in the area of the monitor was subsequently insulated, the new detector tube failed, apparently because moisture had entered the detector tube chamber prior to installation of the insulation.

Ventilation Systems and Containment Pressure

In 1977, a shift in the wind over a lake led to an alteration in the water flow and a sudden change in the temperature of the cooling water flow to the circulating and service water pumps in a PWR plant. This resulted in an increase in the temperature and pressure within containment and caused two of the four containment high pressure signals to alarm, even though the actual pressure increase was only about 1 psi. To correct the situation, the containment was vented. In a contrasting event, a decrease in the outside ambient temperature and a concurrent decrease in the component cooling water temperature serving the containment recirculation fans at another PWR plant caused the containment temperature to drop below 100°F, which was in violation of the Technical Specifications. The fans were secured and service water to the component heat exchangers was throttled back to raise the component cooling water temperature.

Problems with Waste Gas Processing Systems

Although the number is decreasing, the frequency of excessive airborne releases from waste gas decay tanks in PWRs appears to be high. Twelve gases were reported in 1975, eight in 1976 and five in 1977. In addition, there were 22 reports of excessive airborne releases from other components within plant waste processing systems. When one considers that a typical PWR pressurized waste gas decay tank may contain a considerable radionuclide inventory (upwards of one third that in the charcoal beds of a BWR off-gas system), it may be that more attention to developing procedures for avoiding these releases is warranted.

III. Commentary

Although there is a variety of ways in which the data from this study can be interpreted, one message is clear. There is a need for research on the development of more reliable equipment for sampling and monitoring air systems. Equipment that provides inaccurate data on the performance of such systems can lead to as many problems as inadequacies in the systems themselves.

These analyses have also shown that LER data can be used to gain a better understanding of the various inputs required for studies of the risks associated with the operation of nuclear power

15th DOE NUCLEAR AIR CLEANING CONFERENCE

plants. One example was the observed frequency for the unavailability of containment spray systems within PWRs. The data from this study support the estimates used in the Reactor Safety Study. There are undoubtedly other instances in which LER data can be used to confirm or improve failure rate probability estimates for other safety systems.

As this author has pointed out in a previous report, (1) a review and analysis of LERs pertaining to air monitoring, ventilating and cleaning systems is a difficult task. One of the major reasons for this is that LERs pertaining to this subject area are not easy to extract from the totality of reported events. In addition, there are many variations in the way in which individual nuclear plant operators report LERs, as well as in the key words selected for recording them in the data bank. Events are classified under a variety of titles and frequently the titles are misleading from the standpoint of the air cleaning implications of the event. Many licensees, for example, appear to use the words, "reactor building," "shield building," and "containment" interchangeably. Others appear to take a similar approach to the use of the terms, "air cooling," "ventilation," and "purging," while others do not distinguish between systems for normal operation versus those for emergency situations.

Further compounding the problem is the fact that the indexes are not designed to be of maximum help to air cleaning specialists. For example, the index to the 1976 list of LERs for PWRs⁽⁵⁾ contains only one item under the subject of "air cleaning"; the corresponding list for BWRs⁽⁴⁾ contains only two items under this category. The reports for 1975 contain no items within this category.⁽²⁾⁽³⁾ Since the use and analyses of these data can yield a multitude of benefits in terms of improved nuclear air monitoring, ventilating and cleaning systems, it would appear that the Nuclear Regulatory Commission should be encouraged to conduct a study to determine and implement approaches to improve the methods by which LERs pertaining to this subject area are logged into the system.

IV. References

1. Moeller, D.W., "Performance of air cleaning systems in nuclear facilities," Proceedings of the 13th AEC Air Cleaning Conference, U.S. Atomic Energy Commission, Report CONF-740807, 1:10-28 (1975).
2. Scott, R.L. and Gallaher, R.B., "Annotated bibliography of safety-related occurrences in boiling-water nuclear power plants as reported in 1975," Report ORNL/NUREG/NSIC-126, Nuclear Safety Information Center, Oak Ridge National Laboratory, Oak Ridge, TN (1976).

15th DOE NUCLEAR AIR CLEANING CONFERENCE

3. Scott, R.L. and Gallaher, R.B., "Annotated bibliography of safety-related occurrences in pressurized-water nuclear power plants as reported in 1975," Report ORNL/NUREG/NSIC-127, Nuclear Safety Information Center, Oak Ridge National Laboratory, Oak Ridge, TN (1976).
4. Scott, R.L. and Gallaher, R.B., "Annotated bibliography of safety-related occurrences in boiling-water nuclear power plants as reported in 1976," Report ORNL/NUREG/NSCI-137, Nuclear Safety Information Center, Oak Ridge National Laboratory, Oak Ridge, TN (1977).
5. Scott, R.L. and Gallaher, R.B., "Annotated bibliography of safety-related occurrences in pressurized-water nuclear power plants as reported in 1976," Report ORNL/NUREG/NSIC-138, Nuclear Safety Information Center, Oak Ridge National Laboratory, Oak Ridge, TN (1977).
6. Private communication, Nuclear Safety Information Center, Oak Ridge National Laboratory, Oak Ridge, TN (1978).
7. Nuclear Regulatory Commission, "Reactor safety study: an assessment of accident risks in U.S. commercial nuclear power plants," Report WASH-1400 (NUREG-75-014), National Technical Information Service, Springfield, Virginia (1975).

DISCUSSION

GIBSON: What is being done about improving the reliability of air monitoring and sampling systems?

MOELLER: One step that has recently been taken is a reaffirmation of the American National Standards Institute Guide to "Sampling Airborne Radioactive Materials in Nuclear Facilities" (BSR N13.1-1969). On the basis of the data reported here today, however, I believe much more needs to be done. In particular, DOE and/or NRC need to sponsor a research program specifically directed to the types of failures in such systems as recorded in the LERs.

FIRST: In addition to engineering and careful design, we badly need standards which will point the way and avoid the kinds of accidents we have been hearing about. The next two speakers will describe the very active program of nuclear standards development which had been supported by the Atomic Energy Commission and ERDA and is now supported by the Department of Energy. Its importance is well recognized.

15th DOE NUCLEAR AIR CLEANING CONFERENCE

PROGRESS IN STANDARDS FOR NUCLEAR AIR AND GAS TREATMENT*

C. A. Burchsted
Nuclear Standards Office
Oak Ridge National Laboratory
Oak Ridge, Tennessee

Abstract

Standardization in nuclear air and gas treatment spans a period of more than 25 years, starting with military specifications for HEPA filters and filter media, and now progressing to the development of a formal code analogous to the ASME Boiler and Pressure Vessel Code. Whereas the current standard for components and installation of nuclear air cleaning systems is limited to safety related facilities for nuclear power plants, the proposed code will cover all types of critical ventilation and air and gas treatment installations for all types of nuclear facilities.

Introduction

Standards for ventilation and offgas-treatment in nuclear facilities span a period of at least 25 years, progressing from a standard specification for the basic high efficiency particulate air (HEPA) filter and filter medium to the present effort to develop a formal Code for the technology. The next paper of this conference will review the present status of the Code program. The purpose of this paper is to review the background that has led up to that Code.

Early Standards

The earliest standards in this field were military specifications MIL-F-51068 and MIL-F-51079 which covered requirements for HEPA filters and HEPA filter medium, respectively. To avoid the trap of distinguishing between a standard and a specification, these documents can be categorized as "standard specifications" -- that is, documented minimum requirements for performance, construction, and testing of the basic component that is at the heart of nearly every nuclear exhaust and process-offgas treatment system. Although these standards were developed by the Army's chemical warfare service to describe what was in the early 1950's a primarily military component, they have undergone considerable modification over the years to meet the needs of the nuclear industry. We are now at the point of issuing the fifth revision of MIL-F-51068 and the third revision of MIL-F-51079. MIL-STD-282, which provided the standard test for establishing the primary performance characteristic of the HEPA filter (the monodisperse dioctyl phthalate [DOP] particle-removal-efficiency test) was published concurrently with these standards. A new edition of that standard will be issued in the near future to reflect modifications of the test introduced by the nuclear industry.

About the time that the military standards were being issued, Underwriters Laboratories (UL), at the urging of Humphrey Gilbert of the U. S. Atomic Energy

*Research sponsored by the Division of Nuclear Power Development, U. S. Department of Energy under contract W-7405-eng-26 with the Union Carbide Corporation.

15th DOE NUCLEAR AIR CLEANING CONFERENCE

Commission (AEC), undertook the development of a series of tests to define and measure the minimum fire and hot air resistance of HEPA filters. This culminated in UL-586, Safety Standard for HEPA Filters, which has since been adopted as an American National Standard (ANSI/UL 586). With publication of UL-586 and a series of follow-on meetings at UL headquarters in Chicago aimed at unifying critical requirements of HEPA filters, a core of individuals concerned with standardization in the nuclear air cleaning field began to take form. This small group, which has been in large measure shepherded by Mr. Gilbert, has been largely responsible for the development standards for the nuclear air cleaning industry and remains central to its standards to this day. Gilbert seldom served directly on standards-writing work groups, but was often the prime mover in getting the standards started and in goading the work groups on to completion. This group included representatives of several AEC [now Department of Energy (DOE)] contractors, the Naval Research Laboratory, all of the HEPA filter manufacturers, and later the major manufacturers of nuclear grade activated carbon. It was, and still is, well balanced between producers and users in the industry.

During the 1960's the core group was called upon to work with the American Association for Contamination Control (AACC, since merged with the Institute of Environmental Sciences, or IES) to develop standards relating to clean rooms and clean air devices. Although this may appear anomalous, the AEC, as the nation's single largest user and operator of clean rooms at that time, had an important stake in the development of effective standards for critical aspects of those facilities. The AACC effort crystallized the core group of nuclear standards personnel, and it was to this group that the Nuclear Technical Advisory Board (NTAB, now the Nuclear Standards Management Board, or NSMB of the American National Standards Institute) turned to provide the expertise for the development of standards for the air cleaning facilities of commercial nuclear power plants. The closest thing to a system standard at that time was an AEC report, ORNL-NSIC-65,⁽¹⁾ and its emphasis was on the needs of AEC research reactors and laboratory facilities. The original charter of the committee initiated by NTAB, Nuclear Standards Committee N45-8, was to prepare a standard for boiling water reactor standby gas treatment systems. From the first meeting in the summer of 1971 it was obvious that this scope was much too narrow. The committee quickly broadened the scope to include all engineered safety feature (ESF) air cleaning systems for all nuclear power plants, this with the approval of NTAB. It was decided that the most effective approach to this project was to develop minimum specifications for each of the critical components of an ESF air cleaning system -- filters, adsorbers, demisters, housings, fans, ducts, dampers, etc. -- and procedures for the tests needed to evaluate the acceptability and performance of those components after they were installed. These became, in a sense, the basic building blocks of the standards. From this effort came the two standards which are basic to the nuclear air cleaning industry today, ANSI N509, *Standard for Nuclear Power Plant Air Cleaning Units and Components*, and ANSI N510, *Standard for Testing of Nuclear Air Cleaning Systems* (published 1976 and 1975, respectively).

Current Standards Activities

The earliest standards efforts stemmed from the need of users to define their requirements for critical components to industry, and the need of industry to have those requirements defined clearly, uniformly, and without equivocation so that competition among manufacturers could be on an equal footing. As the nuclear industry developed, other participants came into the picture -- architect-engineers (A-E's), utilities, nongovernment laboratories, consultants, and now, increasingly, the general public. There arose the need for more than simply specifying components

15th DOE NUCLEAR AIR CLEANING CONFERENCE

and equipment items. There arose the need for defining minimum requirements for and performance of integrated systems made up of these basic building blocks for specific applications in the interest of public safety. This took place, and is taking place, not only in air cleaning, but throughout the nuclear industry. It may be noted, however, that this branch of the nuclear industry appears to have anticipated the trend, being among the earliest in the nuclear standards "game".

The first response to the expanded interest in nuclear standards was seen in the AEC Safety Guides, now the Regulatory Guides (RG) of the Nuclear Regulatory Commission (NRC). The guide of major interest to us has been RG 1.52, *Design, Testing, and Maintenance Criteria for Atmosphere Cleanup System Air Filtration and Adsorption System Units of Light-Water-Cooled Nuclear Power Plants* (initial issue June 1973). This guide has undergone one revision and a second is in progress. Other guides dealing with non-ESF air cleaning systems are also coming. The Regulatory Guides, strictly speaking, are not standards but only recommendations of the NRC as to what they consider minimum requirements. Insofar as possible, NRC desires that the Regulatory Guides be little more than documents that invoke national standards developed under the voluntary consensus system. The guides were developed to fill the vacuum that existed because no suitable consensus standards were available; the guides may be phased out as suitable standards are developed.

Expansion of interest in nuclear standards has also led to the present effort under the American Nuclear Society (ANS) to develop a family of system standards covering requirements specific to certain types of air cleaning systems for each major category of reactor, for specific types of fuel manufacturing and processing facilities, hot cells, and so on. These will not duplicate the requirements for basic building blocks of such systems, and specified in ANSI N509 and N510, but will provide the framework for invoking the appropriate portions of those standards for specific applications. Although none of the ANS standards have been published to date, most are in one phase or another of the consensus process that leads to publication (see Appendix).

The most important current effort in the nuclear air cleaning standards arena is the development of a formal Nuclear Air and Gas Treatment (NA>) Code. Development of this Code, which has been assigned to the American Society of Mechanical Engineers (ASME), is an outgrowth of the NTAB-NSMB N45-8 activity. In the fall of 1976, N45-8 was transferred to sponsorship of ASME and became the ASME Committee on Nuclear Air and Gas Treatment (CONAGT). Although the committee's first efforts have been aimed at updating and correcting certain deficiencies of the current ANSI N509 and N510, its charter was the development of a code analogous to the ASME Boiler and Pressure Vessel Code which will eventually replace those standards. Whereas N509 was limited, by scope, to ESF systems of nuclear power generation plants, the proposed Code will cover all essential ventilation, air cleaning, and process-offgas treatment equipment for all types of nuclear facilities. The writing of the Code will not be an easy job and will involve inputs from a great number of technical and professional societies, trade associations, and governmental organizations. Mr. J. F. Fish, Chairman of CONAGT, will review the present status of the Code effort in the next paper.

As did ANSI N509, the NA> Code will draw upon existing technology. Wherever possible, requirements of the Code will be defined by reference to documents of other organizations. There will be no restating or inventing of requirements that have been previously, and perhaps better stated in existing standards. It will be recognized that components, procedures, and certain functional guides are basic building blocks of the industry, and that their requirements have been

15th DOE NUCLEAR AIR CLEANING CONFERENCE

adequately defined by various professional or technical societies (e.g., ASME, IEEE, ASTM) or trade associations (e.g., SMACNA, AMCA, ARI). The function of the Code will be to tie these together into a comprehensive whole, to eliminate (by exception) portions of the reference documents that are irrelevant or inadequate, and to supplement them as necessary to alleviate any shortcomings. Once invoked, together with any exceptions and/or supplementary requirements, these documents will assume the mandatory and legal status of the Code when applied within the framework of the Code. On the other hand, they will not have Code status when applied outside of the context of the Code, and therefore their usefulness and applicability in other industrial contexts will not be diminished. A list of organizations and relevant documents that could be considered for Code investment is given in the Appendix.

Codes vs Standards

Much fruitless effort has been expended in technical committees over the years in trying to make a distinction between what is a code and what is a standard. The following definitions from Webster may serve to avoid this trap in the furtherance of the current Code effort:⁽²⁾

- Standard - something that is established by authority or general consent as a model or example to be followed;
- Code - a set of rules of procedure and standards...designed to secure uniformity and protect the public interest. A set of rules for, or standards of professional practice set up by an organized group and...commonly having the force of law in a particular jurisdiction.

That is, a code is of itself a standard. But it is more. Whereas a standard is a model to be followed and implies some choice in its following, a code is mandatory and carries the force of law when invoked in the statutes of a political jurisdiction. Furthermore, it contains rules for professional practice and has the express purpose of protecting the public interest.

The stake of the public in nuclear air and gas treatment is substantially greater than in industrial ventilation and air pollution control. Much of the concern expressed by members of the public who fear nuclear energy can be reduced to a fear of the gaseous release of radioactivity. The gaseous release is the most probable mechanism by which the public would be exposed to radioactivity, both from the "expectable" malfunction that may occur in the normal operation of a nuclear plant and in the event of a "maximum credible accident". The equipment and systems covered by the proposed NA> Code constitute the single most important mechanism for countering any gaseous release. The importance of the program, therefore, is clear.

On the other hand, there has been a certain suspicion of standards in general, and codes in particular, on the part of industry over the years. Some manufacturers of equipment that has proven highly competent and reliable in the climate of industry have tended toward a *laissez faire* attitude in adapting those items to the requirements of the nuclear industry -- the products have withstood the test of time, why change now? Some feared that the restrictive requirements of the nuclear submarine program might be imposed on them, and openly resisted standardization efforts. These attitudes have been largely dispelled in this day, but there still remains a belief on the part of some scientists, engineers, and managers that the imposition of mandatory standards, in a free society,

15th DOE NUCLEAR AIR CLEANING CONFERENCE

may be stifling and perhaps would inhibit or prevent the exercise of proper technical judgment in particular situations calling for such judgment. There is also the feeling that standardization necessitates compromise and reduces technical judgment to the lowest common denominator of the standardizers; since, in our society and system of voluntary standards, anyone has the right to be heard in matters of standardization, this is considered to mean reduction to the lowest common denominator of the general public. But this is not true.

The consensus process by which codes and standards are reviewed, and eventually reach the stage of approval and publication, not only enables every voice to be heard, it also provides the means for resolving disputes and rejecting the unsound or irrational viewpoint or objection. Consensus does not mean unanimity. It is unanimity that reduces technology to a lowest common denominator, not consensus. Consensus does require compromise, but it is informed compromise. The typical standard first goes through a series of prescribed reviews and evaluations by the writing group and by whatever subcommittees and committees the sponsoring organization deems necessary to achieve the required level of competence and exposition. At that stage it can be adopted and published as an authorized standard of the sponsoring organization. To become an American National (ANSI) Standard, it must go through an additional, and broader series of reviews, including review by the general public under the auspices of ANSI, to ensure that all interested parties have had the opportunity to assess its implications or to appeal from its proposed requirements. This, briefly, is the consensus process. It provides for competent peer review, for all points of view to be exercised and ensures that elements that may have been overlooked by the experts are given due consideration.

Every supplier to the nuclear air and gas treatment industry has its own standards for controlling the work that he does. The mechanism of consensus and ANSI standards reduces the possibility that those supplier standards will bend to market-place pressures or the expediency of an immediate situation. There is concern in the private sector, however, that such national standards can become regulatory and cannot be changed when technical judgment indicates that change is needed. The public sector, on the other hand, is sometimes suspicious of the motives behind the technical judgments of industry and needs some way to have confidence that such judgments are based on the public interest. Standards, as noted earlier, even national standards, have an aura of choice; they imply an ability to deviate from agreed upon guidelines. Codes, on the other hand, are more rigid; when invoked they have the force of law. Although developed by the same competent people who develop standards, they necessarily are subject to the additional public review of an ANSI standard. Finally, they are developed and maintained in the traditional voluntary manner, not by lawmakers or regulatory agencies. The force of law comes only after the code has been developed to the satisfaction of all participant parties and has been invoked in the status of a political or regulatory jurisdiction.

The proposed NA> Code is a logical and evolutionary development of the previous standards efforts and of the concerns of both industry and the public. It provides a fundamental and necessary framework which, if properly understood and applied, should allay the fears of both the public and private sectors. There may still be the feeling on the part of individual engineers and scientists that, although the objectives of the Code are sound, he is somehow the victim of a system that will inevitably stifle his individuality. To that engineer or scientist, let it be said that no amount of standardization can hope to provide for all contingencies that will be met in its application. The Code can ensure that competent design and day-to-day processes and functions of the system are carried out

15th DOE NUCLEAR AIR CLEANING CONFERENCE

in the best possible manner, but beyond that lies an illimitable area for individual judgment and action. The requirements for original and creative thought and the exercise of technical judgment and responsibility remain undiminished. The writing and review of this Code will involve the donation of a great deal of time and effort over the next few years by a large number of people -- it is hoped that the members of this audience will respond appropriately when called upon.

References

1. C. A. Burchsted and A. B. Fuller, *Design, Construction and Testing of High-Efficiency Air Filtration Systems for Nuclear Application*, USAEC Report ORNL-NSIC-65, Oak Ridge National Laboratory, Jan. 1970.
2. *Webster's Third New International Dictionary*, G. and C. Meriam Co., Springfield, MA, 1959.

15th DOE NUCLEAR AIR CLEANING CONFERENCE

APPENDIX

STANDARDS ORGANIZATIONS AND DOCUMENTS RELEVANT TO THE PROPOSED ASME NUCLEAR AIR AND GAS TREATMENT CODE

American National Standards Institute (ANSI)

American Society of Mechanical Engineers (ASME)

ANSI N509	Nuclear Power Plant Air Cleaning Units and Components	(P)
ANSI N510	Testing of Nuclear Air Cleaning Systems	(P)
ANSI N45.2	Quality Assurance Programs for Nuclear Power Plants	(P)
ANSI N45.2.1	Cleaning of Fluid Systems and Associated Components for Nuclear Power Plants	(R)
ANSI N45.2.2	Packaging, Shipping, Receiving, Storage, and Handling of Items for Nuclear Power Plants	(P)
ANSI N45.2.6	Qualifications of Inspection, Examination, and Testing Personnel for Nuclear Facilities	(R)
ASME III	Boiler and Pressure Vessel Code, Nuclear Power Plant Components	(P)
III-ND	Class 3 Components	(P)
V	Nondestructive Examination	(P)
IX	Welding and Brazing Qualifications	(P)

American Nuclear Society (ANS)

ANSI N101.6	Concrete Radiation Shields	(P)
ANSI N101.2	Protective Coatings (Paints) for Light-Water Nuclear Reactor Containment Facilities	(P)
ANSI N101.4	Quality Assurance for Protective Coatings Applied to Nuclear Facilities	(P)
ANSI N512	Protective Coatings (Paints) for the Nuclear Industry	(P)
ANSI N202	Radioactive Gas Waste System for the Stationary Gas- Cooled Reactor Plant	(D)
ANSI N657	Gas-Cooled Reactor Plant Containment Atmospheric Clean-up System	(D)
ANSI N720	Gaseous Radioactive Waste Processing Systems for Light- Water Reactor Plants	(R)
ANSI N275	Containment Hydrogen Control	(D)
ANSI N276	Boiling Water Reactor Containment Ventilation Systems	(R)
ANSI N277	Pressurized Water Reactor Containment Ventilation Systems	(R)
ANSI N189	Safety-Related Ventilation Systems	(D)
ANSI N290	Design, Construction, and Operation of Ventilation Systems for Mixed Oxide (UO ₂ -PuO ₂) Fuel Fabrication Plants	(R)
ANSI N303	Guide for Control of Gasborne Radioactive Materials at Nuclear Fuel Reprocessing Facilities	(R)

Institute of Electrical and Electronic Engineers (IEEE)

ANSI C50.20	Test Code for Polyphase Induction Motors and Generators	(P)
ANSI N41.7	Guide for Seismic Qualification of Class 1 Electrical Equipment for Nuclear Power Generating Stations	(P)

(P) = Published, current edition; (D) = Under development; (R) = Under review.

15th DOE NUCLEAR AIR CLEANING CONFERENCE

ANSI C2	National Electrical Safety Code	(P)
IEEE 279	Criteria for Protection Systems for Nuclear Power Generating Stations	(P)
IEEE 323	Qualifying Class IE Equipment for Nuclear Power Generating Stations	(P)
IEEE 334	Type Tests of Continuous Duty Class IE Motors for Nuclear Power Generating Stations	(P)
IEEE 336	Installation, Inspection, and Testing Requirements for Instrumentation and Electric Equipment During the Construction of Nuclear Power Generating Stations	(P)
IEEE 338	Periodic Testing of Nuclear Power Generating Station Safety Systems	(P)
IEEE 344	Siesmic Qualification of Class I Electric Equipment for Nuclear Power Generating Station	(P)
IEEE 383	Type Test of Class IE Electric Cables, Field Splices, and Connections for Nuclear Power Generating Stations	(P)
IEEE 384	Criteria for Separation of Class IE Equipment and Circuits	(P)
IEEE 415	Planning of Pre-operational Testing Programs for Class IE Power Systems for Nuclear Power Generating Stations	(P)
IEEE 420	Guide for Class IE Control Switchboards for Nuclear Power Generating Stations	(P)

Institute of Environmental Sciences (IES)

IES/AACC CS 1	HEPA Filters	(P)
IES/AACC CS 8	High-Efficiency Gas-Phase Adsorber Cells	(P)

American Society of Heating, Refrigeration, and Air Conditioning Engineers (ASHRAE)

ASHRAE 52	Method of Testing Air Cleaning Devices Used in General Ventilation for Removing Particulate Matter	(P)
ASHRAE 37	Methods of Testing and Rating Unitary Air Conditioning and Heat Pump Equipment	(P)
ASHRAE 68P	Method of Testing Sound Power Radiated Into Ducts from Air Moving Devices	(P)
ASHRAE 62	Natural and Mechanical Ventilation	(P)

Underwriters Laboratories (UL)

UL 586	Safety Standard for High Efficiency Particulate Air Filters	(P)
UL 900	Safety Standard for Air Filter Units	(P)

Air Moving and Conditioning Association (AMCA)

AMCA 99	Standards Handbook	(P)
AMCA 201	Fan Application Manual - Fans and Systems	(P)
AMCA 202	Fan Application Manual - Troubleshooting	(P)
AMCA 203	Fan Application Manual - Field Performance Measurements	(P)
AMCA 210	Test Code for Air Moving Devices	(P)
AMCA 300	Test Code for Sound Rating	(P)
AMCA 500	Test Methods for Louvers, Dampers, and Shutters	(P)

American Welding Society (AWS)

AWS D 1.1	Structural Welding Code	(P)
-----------	-------------------------	-----

15th DOE NUCLEAR AIR CLEANING CONFERENCE

National Fire Protection Association (NFPA)

NFPA 90A	Installation of Air Conditioning and Ventilating Systems	(P)
NFPA 90B	Installation of Warm Air Heating and Air Conditioning Systems	(P)
NFPA 91	Installation of Blower and Exhaust Systems	(P)

Air Conditioning and Refrigerating Institute (ARI)

ARI 410	Standard for Forced Circulation Air Cooling and Air Heating Coils	(P)
ARI 680	Standard for Air Filter Equipment	(P)

National Electrical Manufacturers Association (NEMA)

IS 1.1	Enclosures for Industrial Controls and Systems	(P)
IS 2.2	Specification Guide for Industrial Motor Drive Systems	(P)
MG 1	Motors and Generators	(P)
MG 2	Safety Standard for Construction and Guide for Selection, Installation, and Use of Motors and Generators	(P)

American Society for Testing and Materials (ASTM)

ASTM A36	Specification for Structural Steel	(P)
ASTM A123	Specification for Zinc Hot-Galvanized Coatings on Products Fabricated from Rolled, Pressed, and Forged Steel Shapes, Plates, Bar, and Strip	(P)
ASTM A164	Specification for Electrodeposited Coating of Zinc on Steel	(P)
ASTM A167	Specification for Stainless and Heat-Resisting Chromium-Nickel Steel Plate, Sheet, and Strip	(P)
ASTM A283	Low and Intermediate Tensile Strength Carbon Steel Plates of Structural Quality	(P)
ASTM A525	Specification for Steel Sheet, Zinc-Coated (Galvanized) by the Hot-Dip Process, General Requirements	(P)
ASTM A526	Specification for Steel Sheet, Zinc-Coated (Galvanized) by the Hot-Dip Process, Commercial Quality	(P)
ASTM A527	Specification for Steel Sheet, Zinc-Coated (Galvanized) by the Hot-Dip Process, Lock Forming Quality	(P)
ASTM A570	Hot-Rolled Carbon Steel Sheet and Strip, Structural Quality	(P)
ASTM A606	Specification for Steel Sheet and Strip, Hot-Rolled and Cold-Rolled, High-Strength, Low-Alloy with Improved Corrosion Resistance	(P)
ASTM A607	Specification for Steel Sheet and Strip, Hot-Rolled and Cold-Rolled, High-Strength, Low-Alloy Columbium and/or Vanadium	(P)
ASTM A666	Specification for Austenitic Stainless Steel, Sheet, Strip, Plate and Flat Bar for Structural Applications	(P)
ASTM D2854	Specification for Test for Apparent Density of Activated Carbon	(P)
ASTM D2862	Specification for Test for Particle Size Distribution of Granulated Activated Carbon	(P)
ASTM E11	Specification for Wire Cloth Sieves for Testing Purposes	(P)
ASTM D2866	Test for Total Ash Content of Activated Carbon	(P)
ASTM D2867	Test for Moisture in Activated Carbon	(P)

15th DOE NUCLEAR AIR CLEANING CONFERENCE

ASTM Dxxxx	Test for Radioiodine Testing of Nuclear Grade Gas-Phase Adsorbents	(R)
ASTM Dxxxx	Test for pH of Activated Carbon	(R)
ASTM Dxxxx	Test for Ball Pan Hardness of Activated Carbon	(R)
ASTM Dxxxx	Analysis for Potassium and Iodine Impregnants in Activated Carbon	(R)
ASTM Dxxxx	Analysis for Tiethylenediamine (TEDA) Impregnant in Activated Carbon	(R)
ASTM A245	Specification for Flat-Rolled Carbon Steel Sheets	(P)
ASTM A479	Specification of Stainless and Heat-Resisting Steel Bars and Shapes	(P)
ASTM A499	Specification for Hot-Rolled Carbon Steel Bars and Shapes	(P)
ASTM A500	Specification for Cold-Formed Welded and Seamless Carbon Steel Structural Tubing in Rounds and Shapes	(P)
ASTM D1056	Specification for Sponge and Expanded Cellular Rubber Products	(P)
ASTM D3467	Method of Test for Carbon Tetrachloride Activity of Activated Carbon	(P)
ASTM D3466	Method of Test for Ignition Temperature of Activated Carbon	(P)

Sheet Metal and Air Conditioning Contractors National Association (SMACNA)

SMACNA	Round Industrial Duct Construction Standards	(P)
SMACNA	Rectangular Industrial Duct Construction Standards	(D)
SMACNA	High Velocity Duct Construction Standards	(P)
SMACNA	Manual for the Adjustment and Balancing of Air Distribution Systems	(P)

American Conference of Governmental Industrial Hygienists (ACGIH)

ACGIH	Industrial Ventilation	(P)
-------	------------------------	-----

Industrial Perforators Association (IPA)

IPA	Perforating Industry Standards and Practices Manual	(P)
-----	---	-----

U. S. Department of Defense (DOD)

MIL-F-51068	Filter, Particulate, High Efficiency, Fire-Resistant	(P)
MIL-F-51079	Filter Medium, Fire Resistant, High Efficiency	(P)
MIL-STD-282	Filter Units, Protective Clothing Gas Mask Components, and Related Products, Performance Test Methods	(P)

15th DOE NUCLEAR AIR CLEANING CONFERENCE

REPORT ON ANSI/ASME NUCLEAR AIR AND GAS TREATMENT STANDARDS FOR NUCLEAR POWER PLANTS

James F. Fish
Nuclear Environmental Systems
American Air Filter Co., Inc.
Louisville, Ky.

Abstract

Original "N" Committee, N45-8, has completed and published through the approved American National Standards Institute process two Standards, N-509 and N-510. This committee has been dissolved and replaced by ASME Committee on Nuclear Air and Gas Treatment with expanded scope to cover not only air cleaning, but thermal treatment equipment. Current efforts are directed to produce "Code" documents rather than "Standards" type publications. This report summarizes changed scope, current organization and sub-committee coverage areas.

I. Introduction

Proceedings of the Twelfth AEC Air Cleaning Conference at Oak Ridge, Tennessee August 28-31, 1972 contain an initial report by Leckie and Thompson on ANSI N45-8 Nuclear Gas Systems Treatment Standards.

Over the intervening six years, much has been accomplished. The organizational format has been changed and the scope and direction of the committee's activity has been greatly expanded.

II. Voluntary Standards Procedures in U.S., particularly for Nuclear Equipment.

Under the procedure controlling voluntary standards in the U.S., the American National Standards Institute recognizes three methods leading to a National Standard:

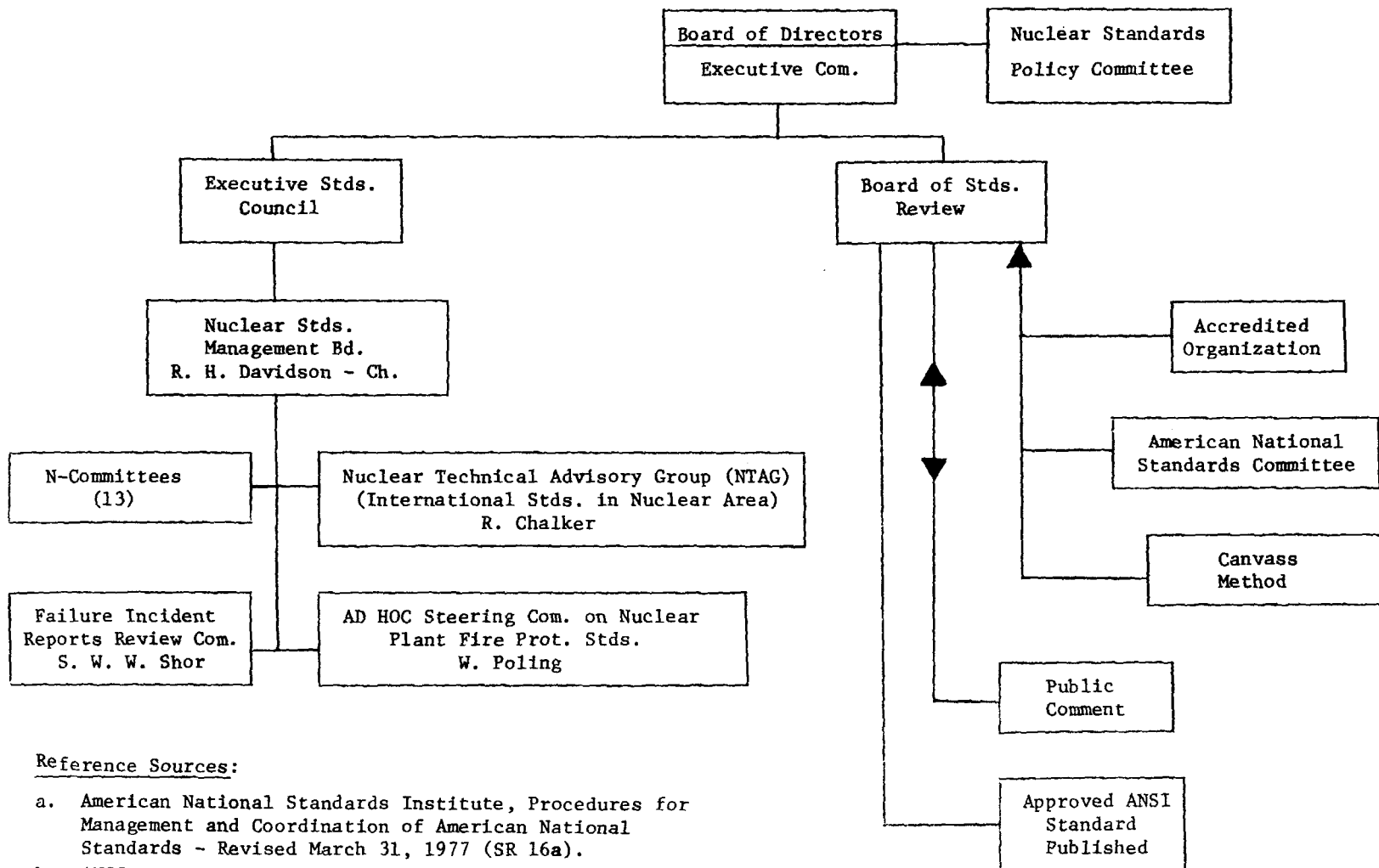
- 1) The ANSI Committee method; in the nuclear area, the N Committee.
- 2) The accredited organization method.
- 3) The canvass method.

The ANSI organizational structure applicable to Nuclear activity is shown in Table 1.

In 1971, this activity was organized under the "N" Committee method and assigned to American Society of Mechanical Engineers as the secretariat organization. Other "N" Committees covering other areas are assigned to other secretariates for standards action. Overall responsibility for such assignments was and is under American National Standards Institute.

AMERICAN NATIONAL STANDARDS INSTITUTE

NUCLEAR STANDARDS ACTIVITY ONLY



Ways to ANSI Standard

15th DOE NUCLEAR AIR CLEANING CONFERENCE

Reference Sources:

- a. American National Standards Institute, Procedures for Management and Coordination of American National Standards - Revised March 31, 1977 (SR 16a).
- b. ANSI Progress Report 1977 (PR25)
- c. Personal Communications

TABLE 1

JUNE 1978

15th DOE NUCLEAR AIR CLEANING CONFERENCE

For some time, national voluntary standards activity has been receiving a considerable amount of political attention. The basic question is "Should the Federal Government take over such activity?" under the banner of all concerned? ANSI activity has been carefully controlled and is documented to insure that all interested parties have full input access opportunity to any standard before any document is issued. To this end, the approved ANSI procedures are available in printed form with each required step documented in great detail.

When a secretariat professional organization has demonstrated structure in full accordance with these procedures, it becomes an "accredited organization". This means that the organization's procedures are also documented in detail, committees are balanced representing all interests, and ballot procedures are established to insure that all interests have full right of input, question and objection to any proposed document. When any draft standard is forwarded to ANSI's Board of Standards Review, it is also held open for comment by the general public for a rather extended period. All comments received require detailed consideration by the originating Committee and written response back to the originator of the comment or question.

III. Nuclear Air Cleaning Standards Activity to Present

N45-8

In June 1973, AEC first published Regulatory Guide 1.52 covering requirements for Engineered Safety Feature Air Cleaning Systems. ANSI Standards were not recognized as they did not, at that time, exist outside of Committee.

In 1975, the N45-8 Committee document ANSI N510 covering "Testing of Nuclear Air Cleaning Systems" was published following in 1976 by ANSI N509, "Nuclear Power Plant Air Cleaning Units and Components."

Therefore, in July 1976 and March 1978 when Revisions 1 and 2 to 1.52 were issued, N509 and N510 were extensively referenced, a practice continued with Regulatory Guide 1.140 for normal ventilation system filters first issued in March 1978. When satisfactory standards are available, it is the practice of NRC to reference them to the extent practicable.

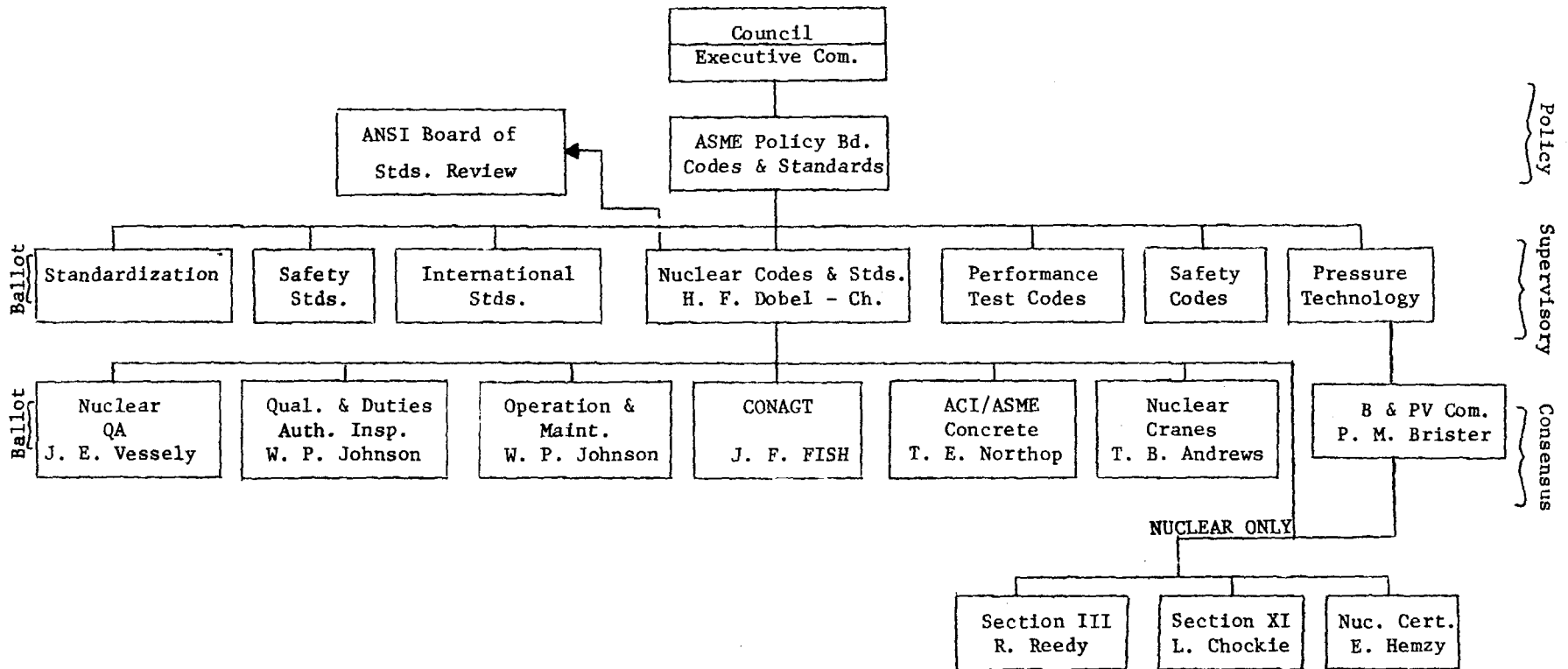
Meanwhile, the American Society of Mechanical Engineers, Nuclear Codes and Standards Supervisory Committee had achieved ANSI "accredited organization" status. The N45-8 organization was changed from "N" Committee status to "Accredited Organization" Status under this Committee after accreditation was achieved, see Table 2. The N45-8 Committee was then dissolved.

CONAGT

The new name is Committee on Nuclear Air and Gas Treatment, CONAGT, with approved scope as follows:

- "1. To Develop, review, maintain, and coordinate Codes and Standards for design, fabrication, installation, testing, and inspection of equipment for gas treatment for Nuclear Power Plants. As used herein "gas treatment" includes both HVAC and gas processing.

AMERICAN SOCIETY OF MECHANICAL ENGINEERS
 NUCLEAR CODES AND STANDARDS ACCREDITED ORGANIZATION



64

15th DOE NUCLEAR AIR CLEANING CONFERENCE

TABLE 2

JUNE 1978

15th DOE NUCLEAR AIR CLEANING CONFERENCE

- (a) HVAC - the moving and conditioning of air which is supplied exhausted, or recirculated into and from an enclosed space to maintain prescribe ambient conditions. These conditions include pressure, temperature, humidity, and contaminants.
 - (b) Gas Processing - the transportation of gas and the separation, isolation, and disposal of its constituents by physical, mechanical, chemical, delay, electrical and thermodynamic means.
2. Codes and Standards developed by this Committee will be supervised by the ASME Nuclear Codes and Standards Committee.
 3. This Committee will establish recommendations for ASME representation on Committees of organizations other than ASME developing interfacing Codes or Standards.
 4. This Committee will develop recommendations for ASME positions on interfacing or referenced Standards.
 5. This Committee will develop Codes and Standards in accordance with the Committee Procedures for Nuclear Projects approved by the American National Standards Institute under the Accredited Organization Method."

The original scope, limited to air cleaning, has now been greatly expanded.

Codes vs. Standards

At approximately the time this was taking place, pressure was being exerted to change over to a Code format rather than a Standard format. The Code concept goes back basically to the ASME Boiler and Pressure Vessel activity, firmly established by many years of operating experience. The reason for this change is that Codes are legally enforceable documents which can be adopted by political governing bodies to have the force of law. They specify minimum enforceable requirements. Standards on the other hand tend to be somewhat looser and do not lend themselves, in most cases, to legal status.

Organization

With the Committee scope broadened, it became obvious that a more complex organization, including additional breadth of knowledge, was required. Table 3 shows how the CONAGT Committee is currently organized within the ASME structure.

The Executive Committee under Dr. Wittke brings policy and or other considerations to the attention of the main committee for appropriate consideration. Because this CONAGT activity interfaces with the work of so many other Committees and organizations, the Coordinating Committee under Dr. Burchsted has its hands full attempting to stay abreast of developments and arranging CONAGT comment and input pertinent to other documents.

The breakdown of the Equipment Subcommittee under Mr. Miller is particularly interesting as it indicates the diversity of equipment now included under the Committee's surveillance. Subgroups cover: Fans, Dampers and Valves, Air Cleaning Equipment, Structures, Refrigeration Equipment, Conditioning Equipment and Gas Processing Equipment. The application of such items to nuclear plants involves many considerations not encountered in conventional industrial installations.

AMERICAN SOCIETY OF MECHANICAL ENGINEERS
 NUCLEAR CODES AND STANDARDS ACCREDITED ORGANIZATION
 COMMITTEE ON NUCLEAR AIR AND GAS TREATMENT

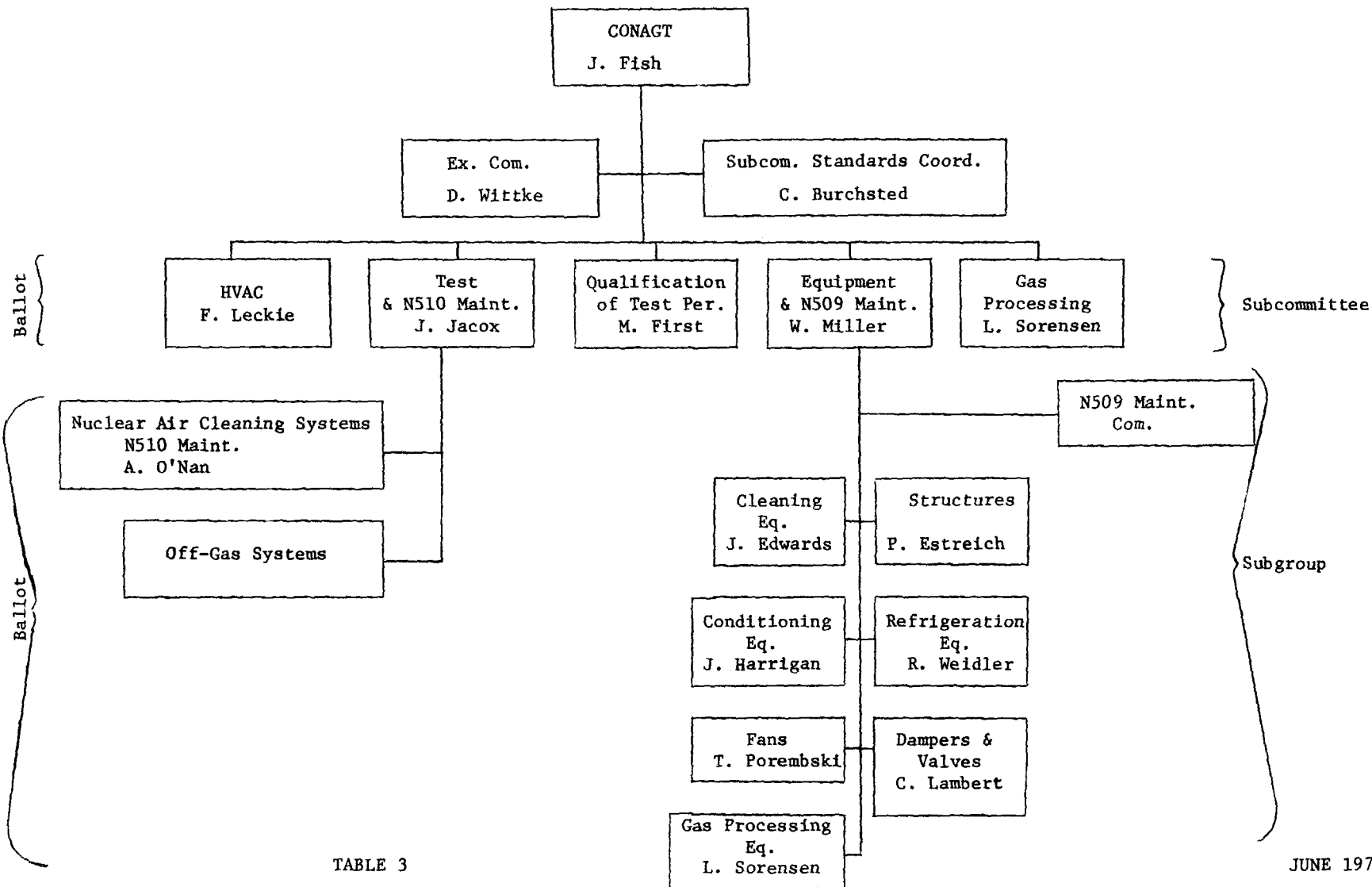


TABLE 3

JUNE 1978

15th DOE NUCLEAR AIR CLEANING CONFERENCE

The Testing Subcommittee's responsibilities under Mr. Jacox are currently directed towards air cleaning systems as initially covered in N510, but they are in the process of expanding their work to include off-gas system tests and will extend coverage to critical areas of other equipment as required.

The Qualification of Test Personnel Subcommittee under Dr. First is a most critical area and will eventually set forth requirements for both Lab and Field Test Personnel. Such tests are most important to protection of our overall environment. Therefore, it is considered prudent to carefully delineate the minimum required ability of persons engaged in such test activity.

Revisions to N509 and N510

As few words of man are so perfectly set forth as to require no revision, experience with both N509 and N510 has indicated that some changes are desirable. The problem, however, was that the N45-8 committee that produced these standards was no longer functioning. Also, of course, both documents will eventually be incorporated into Code documents with updating and inquiry procedures (code cases) being formalized. This will take some extended period of time.

Consequently, the Chairman of the Subcommittee on Equipment formed an ad hoc committee of his Sub Group Chairman to revise N509. The Chairman of the Subcommittee on Testing likewise formed an N510 ad hoc maintenance committee. These Committees will handle revisions to existing Standards pending issuance of Codes.

Both of these groups are in the process of completing their final drafts of Revision 1 to be balloted this year and if approved will go to Nuclear Codes and Standards and thence to ANSI Board of Standards Review, with formal issue estimated in early 1979.

Overall efforts are first directed at critical Engineering Safety Feature equipment and then to other non-ESF but critical items of hardware falling under the CONAGT scope.

When adequate standards exist or when other organizations are producing specific item requirements, we are very happy to reference them and not attempt to reinvent the wheel!! ASTM, for example, particularly the D28 Committee under Dr. Burchsted and specifically the D28.04 group under Mr. Rivers, have developed key input reference documents.

Summary

Codes and Standards are sometimes viewed as a painful reality. On the other hand, technical personnel use such references every day of their lives. Try to think for a moment what life would be like if there were not standards for all sorts of things we live with every day.

Now, almost eight years since the first get together at Engineering Society Headquarters in New York City, it requires effort to think of Nuclear Air Cleaning Equipment before Standards were drawn up, documented and enforced. Where would we be without codes and standards? With that thought, I leave you all to consider alternatives!!

15th DOE NUCLEAR AIR CLEANING CONFERENCE

SESSION II

WASTE TREATMENT : VOLUME REDUCTION AND PREPARATION FOR STORAGE

Monday, August 7, 1978
CHAIRMAN: J. C. Dempsey

OPERATION OF LOW-LEVEL RADIOACTIVE WASTE INCINERATOR

E. C. Choi, T. S. Drolet, W. B. Stewart,
A. V. Campbell

FLUIDIZED-BED CALCINATION OF LWR FUEL-REPROCESSING HLLW: REQUIREMENTS AND POTENTIAL FOR OFF-GAS CLEANUP

R. E. Schindler

VOLATILIZATION FROM BOROSILICATE GLASS MELTS OF SIMULATED SAVANNAH RIVER PLANT WASTE

G. W. Wilds

DISPOSAL OF HEPA FILTERS BY FLUIDIZED BED INCINERATION

D. L. Ziegler, A. J. Johnson

VOLUME REDUCTION OF LOW-LEVEL COMBUSTIBLE TRANSURANIC WASTE AT MOUND FACILITY

W. H. Bond, J. W. Doty, J. W. Koenst, Jr.,
D. F. Luthy

OPENING REMARKS OF SESSION CHAIRMAN:

The session we're starting is Waste Treatment: Volume Reduction and Preparation for Storage. By way of perspective, I've been a member of the Interagency Review Groups that have been mentioned in the previous session. The whole purpose is to come up with a work plan and to take care of the nation's wastes in a long-range way. High level waste, low level waste, transuranic waste, and all the rest. Whether processing liquids or solids, offgases are one of the technically vulnerable points in every case, from a technical as well as a control point of view. In that sense, we're working against a moving, or unknown, target because the regulations are being ratcheted in different ways. For example, EPA and NRC are meeting to prepare guides and regulations regarding what emissions will be permitted from DOE facilities. It is expected that this work will be completed about this time next year. So, all of the technology we will be talking about today should be considered in this context. We will be discussing incineration of low level transuranic waste, as well as calcination and vitrification of high level waste. There's no doubt about its being a national requirement. We have waste in-place and we must do something about it. The President has asked us to have a plan ready by October 1 in which all the aspects are outlined and what each agency has agreed upon as goals and timing. Of course, one of the major questions is, "When are you going to get it in the ground?" and that's one of the things we're concerned with. There is, as you know, a timetable that identifies calendar year 1985 as the starting date for a facility to accept DOE transuranic waste. And, to get there from here, the decision that must be made is whether to process all that waste by incineration. Therefore, 1985 looms very near when you consider that all this technology must be in-place and functioning by that time. I mention this to suggest that we have a new note of urgency about the technology that we will be talking about this afternoon.

15th DOE NUCLEAR AIR CLEANING CONFERENCE

The first paper is going to be by one of our colleagues from Canada. We're most interested to hear about their program, which apparently is very parallel to ours. The second paper is from the Allied Chemical Corporation in Idaho. It relates to the offgas treatment of high-level wastes. For several years Idaho has taken the lead in treating liquid wastes and is now moving to a still more elaborate treatment system. The third paper is also on the solidification of high-level waste; this time on vitrification, by Savannah River Laboratory. I'd just give you a bit of perspective here: I think it's public information that this program is also on the critical path of taking care of our nation's wastes. Solidifying these wastes is a major concern. Work has been going on for some time but now that the reports are coming in, we're sizing up the real magnitude of the problem. A plant to do this is now estimated well over 2 billion dollars and it will also be of concern in the Presidential report that is in preparation. All of us here have a vested interest in what Dr. Wilds has to say and it will perhaps impact on our children, as well. I think you'll agree that our final paper represents a fascinating and ingenious solution to a waste problem.

15th DOE NUCLEAR AIR CLEANING CONFERENCE

OPERATION OF LOW-LEVEL RADIOACTIVE WASTE INCINERATOR

E.C. Choi, T.S. Drolet, W.B. Stewart,
A.V. Campbell

Ontario Hydro

Toronto, Ontario, Canada

ABSTRACT

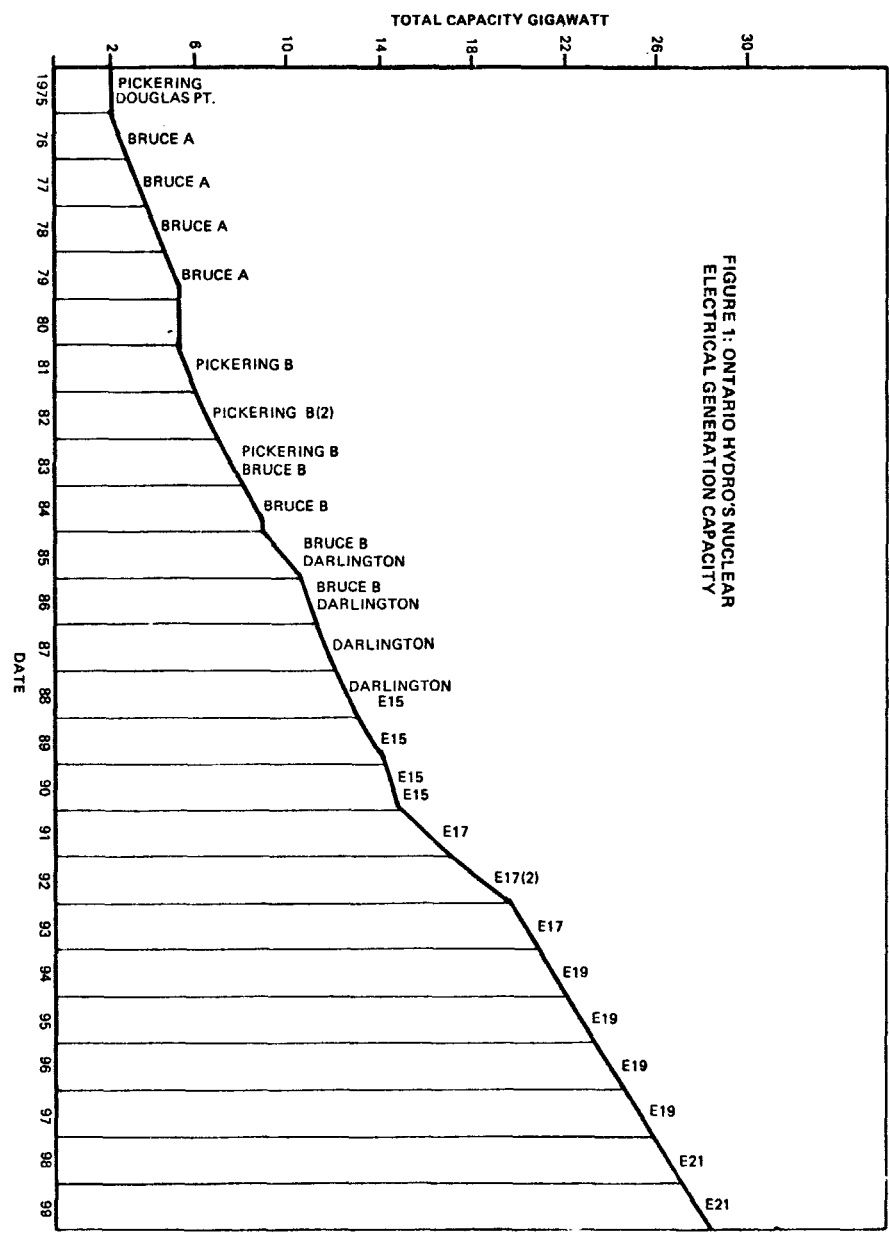
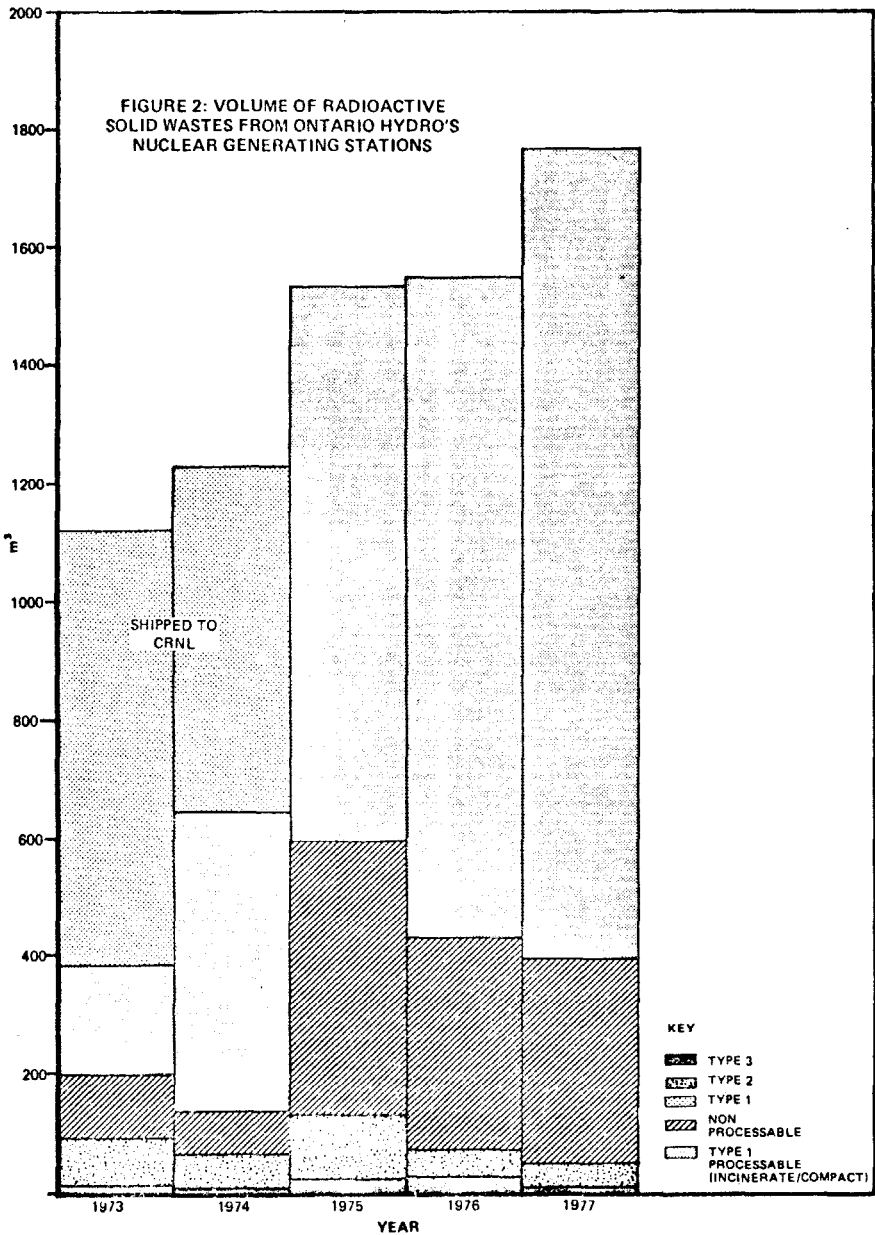
Ontario Hydro's radioactive waste incinerator designed to reduce the volume of low-level combustible wastes from nuclear generating station's was declared in-service in September 1977. Hitherto about 1500 m³ of combustible waste have been processed in over 90 separate batches. The process has resulted in 40:1 reduction in the volume and 12.5:1 reduction in the weight of the Type 1 wastes. The ultimate volume reduction factor after storage is 23:1. Airborne emissions has been maintained at the order of 10⁻³ to 10⁻⁵ percent of the Derived Emission Limits. Incineration of radioactive combustible wastes has been proven feasible, and will remain as one of the most important processes in Ontario Hydro's Radioactive Waste Management Program.

I. INTRODUCTION

Ontario Hydro is currently operating over 4000 MW(e) capacity of CANDU (Canadian Deuterium Uranium) generating stations. Another 15,000 MW(e) capacity will also be available by 1990 (Figure 1).

The radioactive solid wastes from the generating stations are processed and stored at the Radioactive Waste Storage Sites of the Bruce Nuclear Power Development Services (BNPDS) Department. Generally over 80% of the Type 1 wastes from the generating stations are classified as processable (Figure 2). The present storage cost of Type 1 solid wastes in fully engineered trenches is \$1060/m³ (~\$30/ft³). Due to this high cost, there is considerable economic incentive to reduce the volume of the radioactive wastes prior to storage.

The volume reduction processes selected are incineration for combustible wastes having less than 5 mR/h on contact, and compaction for wastes unsuitable for incineration. The low-level radioactive waste incinerator is located in the Waste Volume Reduction Facility (WVRF) of the BNPDS Department. The incinerator was commissioned in May 1977 and declared in-service in September of the same year.



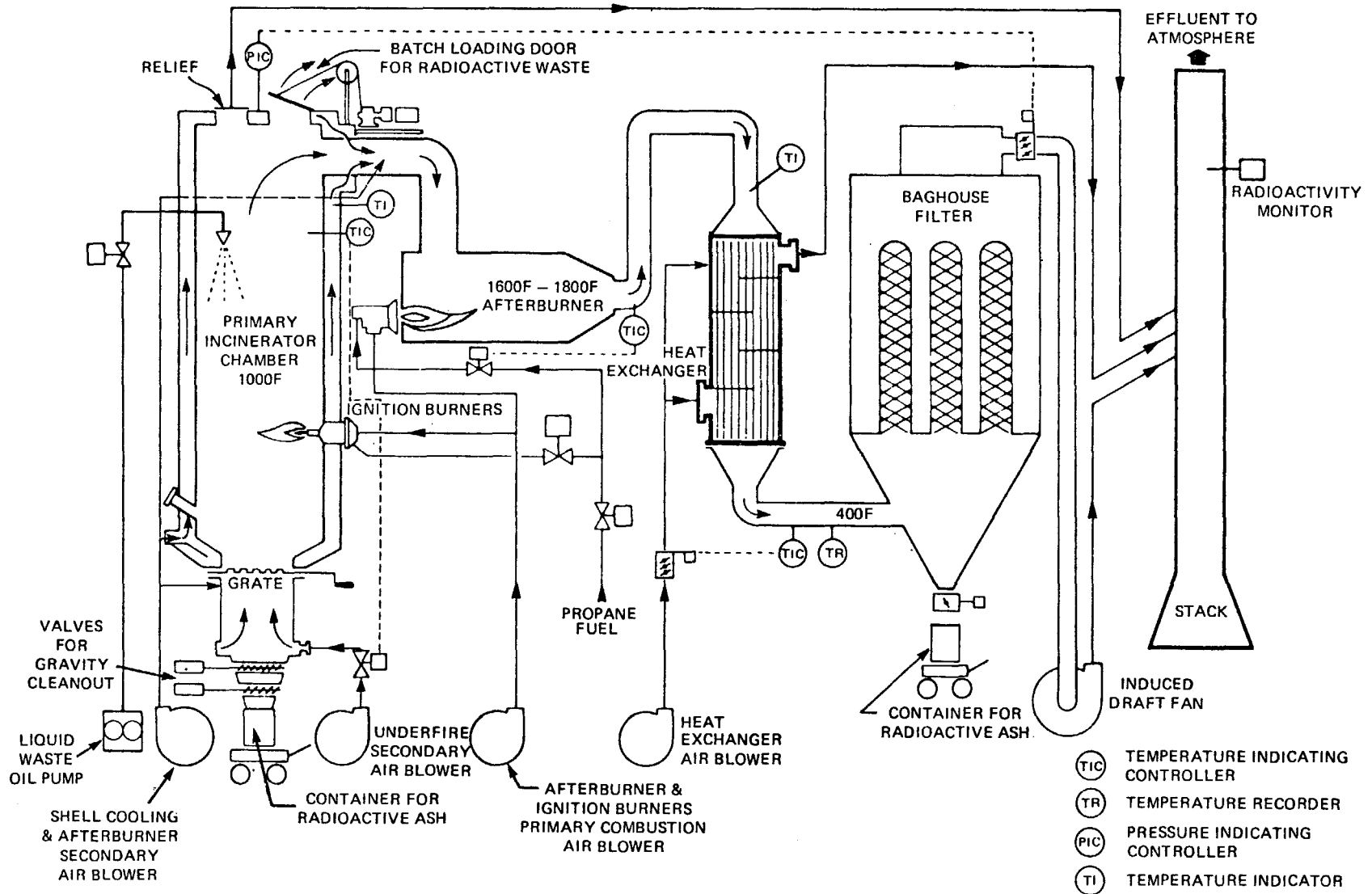


FIGURE 3 INCINERATOR SCHEMATIC

03460-0016

15th DOE NUCLEAR AIR CLEANING CONFERENCE

The wastes processed in this system may contain disposable cotton and plastic coveralls, gloves, cardboard, paper, wood pieces, oil absorbers, and mop heads, etc. Specific activity of the wastes is on the order of 10^{-4} Ci/m³. The wastes are generally packed in clear polyethylene bags with an average weight of about 5 kg/bag.

2.0 RADIOACTIVE WASTE INCINERATOR SYSTEM DESCRIPTION

Controlled air incineration is used to minimize radioactive particulate emissions (Figure 3). The incinerator's design capacity is 17 m³/burn (600 ft³/burn). About 2200 kg of wastes can be processed in each burn cycle.

The primary chamber of the incinerator is loaded in batch prior to ignition. Temperature in the primary chamber during the burn is maintained at 538°C (1000°F) by adjustment of the underfire air. The pyrolyzed gases generated in the primary chamber are further oxidized in the after-burner at 871°C to 982°C (1600°F to 1800°F) with the aid of a propane burner. The high-temperature flue gas from the after-burner is then cooled to 204°C (400°F), the limiting temperature of the baghouse. Despite the system's characteristically low particulate loading, a shaker type baghouse with Nomex bags is provided for further filtration prior to release. The incinerator is maintained at slightly negative pressure (-0.05 kPa(g) or -0.2 psig) by an induced draft fan.

Detailed design of the incinerator was discussed in a previous publication(1).

3.0 OPERATING EXPERIENCE

3.1 General

About 1500 m³ of Type 1 combustible wastes have been processed in more than 90 burns since the middle of 1977. The majority of the wastes processed had a contact field of less than 2 mR/h. Until the end of 1977 50 hours were required to completely process a batch of waste. This included:

- 2 hours for loading the primary chamber with wastes;
- 2 hours for warming-up the after-burner;
- 24 hours for burning (from primary chamber ignition to after-burner shut-down);
- 20 hours for cooling (from after-burner shut-down to ash unloading);
- 2 hours for ash unloading into 200 L drums.

The process time has since been reduced to about 36 hours eliminating the cooling period. Hot ash is now unloaded directly into 2.5 m³ rectangular carbon steel containers as soon as the burning cycle is completed.

The larger, rectangular container also have the advantage of holding several burns of ash, thus reducing the handling time, and providing maximum use of storage space.

TABLE 1

Radioactive Compositions of Incinerator Ash

SAMPLES OF ASH FROM EACH BURN	SPECIFIC ACTIVITY OF THE SAMPLE (mCi/m ³)	RADIOACTIVE COMPOSITIONS IN %							
		Ce-144	Cr-51	Cs-137	Zn-65	Co-60	Zr/Nb-95	Ru-106	Others
1	14.15	8.9	14.1	27.2	9.6	26.1	6.5	-	7.6
2	30.67	8.7	54	5.0	1.8	1.9	6.9		4.6
3	39.06	5.6	6.2	5.9	14.1	30.7	27.0		10.5
4	67.89	7.2	5.5	4.4	7.9	66.7	4.1		4.2
5	19.17	11	27	7	11	26	7		11
6	16	18	2.3	22.7	2.6	18.2	3.5		32.7
7	8	17	3	14	3	36	19		8
8	6	14	2	26	6	37	8		7

15th DOE NUCLEAR AIR CLEANING CONFERENCE

An average batch-load of waste ($\sim 16.4 \text{ m}^3$) produces about 0.4 m^3 of ash, giving an average volume reduction factor of 40 to 1. The average weight reduction factor is about 12.5 to 1. The ultimate volume reduction factor is 23:1 after storage of the 2.5 m^3 containers in engineered concrete trenches. One container occupies about 3.5 m^3 of trench space.

3.2 Characteristic of the Incinerator Ash And Heat Exchanger Deposit

Specific activity of the ash collected ranges from 5 to 100 mCi/m^3 depending on the type of wastes processed. Contact fields on most of the container surface is between 10 and 20 mR/h .

Analysis of the ash collected suggests that Co-60 is the predominant radionuclide. Other major radionuclides found are Ru-106, Cs-137 and Ce-144 (Table 1). This finding is consistent with the radionuclides found in other types of radioactive solid waste. It can be seen that these radionuclides are the activation and fission products generally found in the reactor systems. Since most of the solid wastes processed by the incinerator are generated during reactor maintenance, it is not surprising that they are contaminated with the above mentioned radionuclides.

Particle distribution analysis of a sample of ash collected in the baghouse suggests that 10% of the ash particles are under $10 \mu\text{m}$ and 50% under $30 \mu\text{m}$. The largest particle found is about $2000 \mu\text{m}$. The latter may be attributed to particle aggregation in the baghouse.

Samples of slag from the primary chamber, and deposits in the inside of the heat exchanger were analyzed for weight loss upon ignition at 1000°C , and the chemical composition. The results are summarized in Table 2.

Among the gamma-emitting radionuclides identified with the heat exchanger slag deposit, Cs-137, Zn-65, Cs-134 had notably higher concentrations than others such as Ru-106, Co-60.

3.3 Radioactive Airborne Emissions

The stacks of both the radioactive waste incinerator and the incinerator building ventilation system are equipped with radioactivity monitors. Tritium, iodine and particulates emissions are continuously monitored for operational control. The building ventilation also includes exhaust air from the compactor when it is in operation. Since the incinerator is maintained at negative pressure, its contribution to radioactivity emission via the building ventilation exhaust is not significant during the burn cycle. Some low-level, localized contamination of the room air may occur during the incinerator loading and ash unloading periods.

TABLE 2

Analyses of Incinerator Slag and Ash

SAMPLES	% Weight Loss Upon Ignition at 1000°C After 100 Minutes	Chemical Elements Identified			Compounds Identified In Crystalline Phase
		Major	Minor	Trace	
Heat Exchanger Tube Deposit	10-11	Fe,Zn,S,Cl	Cu,Ni,K,Ca,Cr Ma,As	Si,Ti	ZnS,CuO
Primary Chamber Slag Deposit	1	Fe,Cu,Ca	Al,Si,S,Cl,K Ti,V	Ni,Zn	CuO
Heat Exchanger Ash Deposit	1	Fe,Zn,S	Cu,Ni,K,Ca Ti,V,Ma,As	Si	Fe ₃ O ₄ ,ZnS,CuO

15th DOE NUCLEAR AIR CLEANING CONFERENCE

Emissions of radioactivity are usually expressed in percent of the Derived Emission Limits (DEL). The DEL of each radionuclide expressed in Ci/week is estimated from the maximum continuous release rate (Q) of that particular radionuclide. Q is in turn expressed as:

$$Q \text{ (Ci/sec)} = \text{MPCa/Ka} \quad (1)$$

where MPCa = the Maximum Permissible Concentration of the radionuclide in air (Ci/m³)
Ka = long term mean dilution factor (sec/m³) as a function of the effective stack height, the distance from the source and the weather.

The MPCa, Ka and DEL of the major radionuclides emitted from the incinerator and its building based on various pathways are given in Table 3.

Using the lowest limits given in Table 3, the DEL's for the radioactive incinerator and its building are:

I-131	0.72 Ci/wk
H-3	1.4 x 10 ⁵ Ci/wk
Particulates	1.8 Ci/wk

Airborne emissions from the incinerator and its building in 1977 and early 1978 have consistently been below 0.1% for particulates, 0.01% for I-131, 1% for H-3 (Figure 4). Airborne emissions in each burn via the incinerator stack are given in Figure 5. The variation from burn to burn is attributed to the origin and the type of wastes processed.

Tritium emissions have been consistently higher than other radionuclides mainly because of the higher tritium content in the wastes, and the volatile nature of tritium as tritium oxide upon incineration. Tritium concentrations in the reactor systems are increasing as a result of neutron activation of heavy water. The average tritium concentration at Pickering 'A' Generating Station's Moderator System was about 16 Ci/kg of heavy water at the end of 1977, compared to 11 Ci/kg at the end of 1975. Airborne emissions of tritium from Pickering 'A' were about 10 times higher than those from the Waste Volume Reduction Facility in 1977.

Emissions of I-131 and particulates have consistently been below 10⁻⁴ Ci for most of the burns. Analyses by the stack monitors suggest that Cs-137, Cs-134 and Zn-65 are the major radionuclides and constitute about 70% of the gross $\beta\gamma$ emission. It can be seen from Figure 5 that aside from tritium, emissions of radioactivity from the incinerator are sufficiently low that extensive flue gas treatment is not necessary with the type of wastes presently processed.

15th DOE NUCLEAR AIR CLEANING CONFERENCE

TABLE 3
Parameters Used for Airborne Emission Control

Radionuclides	Indirect Intake Via Food Chain		Direct Intake Via Inhalation or External Irradiation	
	($K_a = 5 \times 10^{-7} \text{ sec/m}^3$)		($K_a = 1.3 \times 10^{-6} \text{ sec/m}^3$ @ 1 km from source)	
	MPCa (Ci/m^3)	DEL (Ci/wk)	MPCa (Ci/m^3)	DEL (Ci/wk)
<u>I-131</u>	6×10^{-13}	0.72	3×10^{-11}	14
<u>H-3</u>	-	-	3×10^{-7}	1.4×10^5
<u>Particulates</u>				
Cs-137	5×10^{-11}	6.1	1.5×10^{-9}	700
Cs-134	1.5×10^{-11}	1.8	1×10^{-9}	470
Sr-90	1.5×10^{-12}	1.8	4×10^{-11}	19
Sr-89	1.5×10^{-11}	1.8	2×10^{-10}	93
Co-60	-	-	9×10^{-11}	42
Ru-106	-	-	4×10^{-11}	19
Unidentified Particulates	1.5×10^{-12}	1.8	4×10^{-11}	19

TABLE 4
Economic Analysis of the Radioactive Waste Incinerator

Annual Cost Without Incineration

Waste Processable/y	2000 m ³
Storage Cost ($\$1060/\text{m}^3$)	\$2,120,000

Annual Cost With Incineration

Ash Volume/y (Volume Reduction factor = 23:1)	87 m ³
Storage Cost ($\$1060/\text{m}^3$)	\$ 92,000

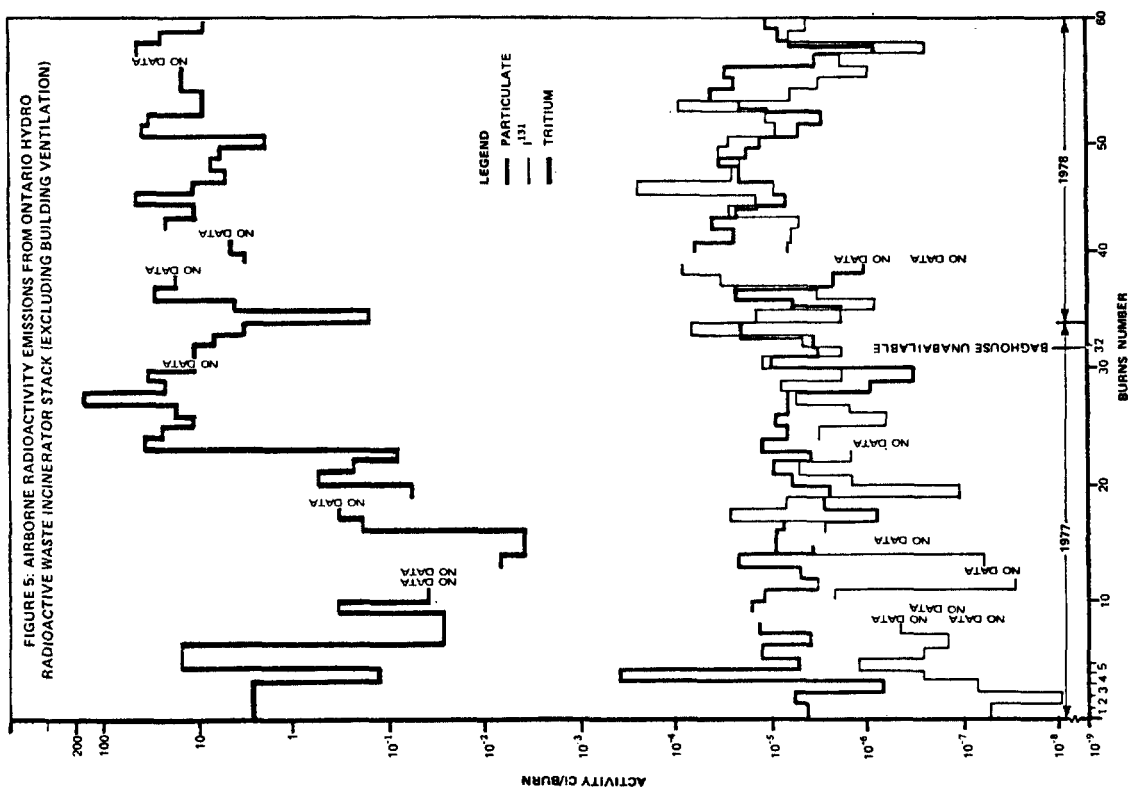
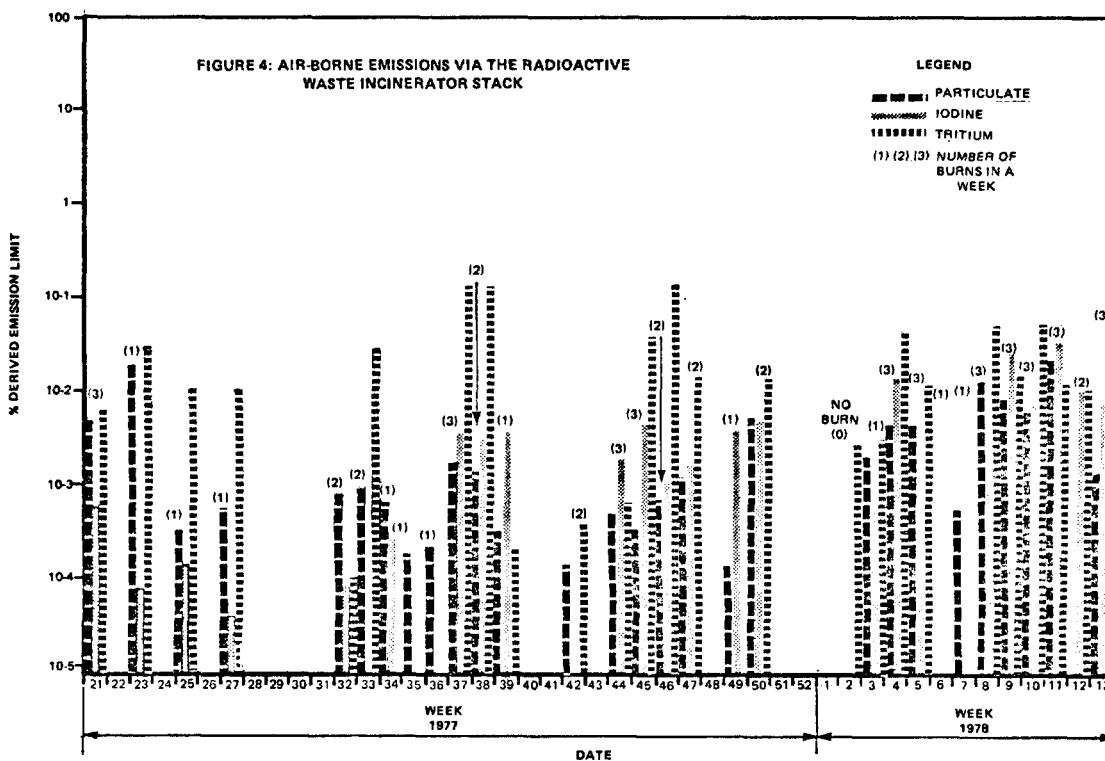
Annual Fixed Cost of the Incinerator (Total Capital Cost = \$3.7M, Capital Recovery Factor = 0.24 depreciated in 6 y, 11% interest rate)	\$ 875,000
---	------------

Annual Operating and Maintenance Cost Under Normal Conditions (Estimated)	\$ 600,000
---	------------

Total Annual Cost With Incineration	\$1,567,000
-------------------------------------	-------------

Annual Savings from Incineration	\$ 553,000
----------------------------------	------------

15th DOE NUCLEAR AIR CLEANING CONFERENCE



15th DOE NUCLEAR AIR CLEANING CONFERENCE

3.4 Other Airborne Emissions

The Environmental Protection Act of Canada⁽²⁾ limits the emissions of HCl (most restrictive among other contaminants such as Cl₂, SO₂) by requiring that its half-hour average ground level concentration at the site boundary (first point of impingement) be no more than 100 $\mu\text{g}/\text{m}^3$. This is equivalent to a maximum emission rate of 10 g/s under Type D Atmospheric Stability.

The Ontario Ministry of Health further requires that the air quality in the working environment be lower than the Threshold Limit Value of 7000 μg of HCl/ m^3 for an 8 hour working day, and 5 day working week. Time averaging is not allowed in this case. Under the hypothetical situation that the wind blows in the same direction as the line between the radioactive waste incinerator stack and the building ventilation intake, this is equivalent to a maximum emission rate of 2.6 g/sec. Emission rate of HCl has been kept below this level by restrictive burning of PVC wastes.

4.0 ECONOMIC ANALYSIS

With the impressive average volume reduction factor of 23:1 after final storage of the ash in engineered trenches, there can be significant savings in the storage cost of Type 1 combustible solid wastes. Detail estimates are given in Table 4. The annual saving can be even higher if longer useful life of the incinerator is applied in the depreciation estimate, and if higher capacity factor is achieved.

5.0 CONCLUSION

Ontario Hydro's radioactive waste incinerator has been in operation since mid-1977. Operating experience has proven that incineration is a viable process to reduce the volume of the wastes stored, and thus the storage cost.

Due to the low activity levels of the wastes processed, airborne emissions of radioactivity have been well below 1% of the Derived Emission Limits. More extensive off-gas treatment system may be required if wastes with higher levels of radioactivity and PVC are processed; but airborne emissions are expected to remain controllable if tritium levels in the wastes are not excessive. Incineration of highly tritiated wastes is not recommendable due to the volatility of tritium upon incineration.

15th DOE NUCLEAR AIR CLEANING CONFERENCE

REFERENCE

1. Drolet, T.S., J.A. Sovka, "An Incinerator For Power-Reactor Low-Level Radioactive Waste", presented at the 14th ERDA Air Cleaning Conference, Sun Valley, Idaho, August 2-4, 1976.
2. The Environmental Protection Act of Canada, 1971, Regulation 15.

DISCUSSION

HILLIARD: Would you care to comment on the experience you've had with the bag filter portion of your treatment?

CHOI: The airborne particulate emissions are very low (about 0.02 mCi/burn or 0.1 mCi/week) because of the controlled-air incineration process. At such low emission levels, the requirement for a baghouse is only marginal, and coating the filter bags for higher efficiency is not necessary. On the whole, the baghouse performance has been satisfactory.

15th DOE NUCLEAR AIR CLEANING CONFERENCE

FLUIDIZED-BED CALCINATION OF LWR FUEL-REPROCESSING HLLW: REQUIREMENTS AND POTENTIAL FOR OFF-GAS CLEANUP

R. E. Schindler
Allied Chemical Corporation, Idaho Chemical Programs
Idaho Falls, Idaho

Abstract

Fluidized-bed solidification (calcination) was developed on a pilot scale for a variety of simulated LWR high-level liquid-waste (HLLW) and blended high-level and intermediate-level liquid-waste (ILLW) compositions. It has also been demonstrated with ICPP fuel-reprocessing wastes since 1963 in the Waste Calcining Facility (WCF) at gross feed rates of 5 to 12 m³/day.

A fluidized-bed calciner produces a relatively large volume of off-gas. A calciner solidifying 6 m³/day of liquid waste would generate about 13 standard m³/min of off-gas containing 10 to 20 g of entrained solids per standard m³ of off-gas. Use of an off-gas system similar to that of the WCF could provide an overall process decontamination factor for particulates of about 2×10^{10} .

A potential advantage of fluidized-bed calcination over other solidification methods is the ability to control ruthenium volatilization from the calciner at less than 0.01% by calcining at 500°C or above. Use of an off-gas system similar to that of the WCF would provide an overall process decontamination factor for volatile ruthenium of greater than 1.6×10^7 .

I. Fluidized-Bed Calcination

Fluidized-bed calcination is one of the processes developed for calcination of liquid wastes from reprocessing of expended reactor fuels. A fluidized-bed calciner solidifies liquid wastes in a fluidized bed of hot, granular solids. The bed of granular solids is fluidized by forcing air upward through a distributor plate and through the bed of solids at a rate that suspends and causes a rapid mixing of the solids-- i.e., makes them behave like a fluid. The bed density is decreased by roughly 20% upon fluidization. The rapid mixing that accompanies fluidization results in uniform compositions and uniform temperatures throughout the bed. The liquid being calcined is sprayed into the calciner in the form of droplets, which calcine very rapidly upon impact on the surface of the hot bed granules. The solids are converted mostly to oxides; the water, nitrates, and other volatiles are evaporated and/or decomposed. The calcined solids generated in a fluidized-bed calciner consist of both granular bed particles with diameters of 0.2 to 1.0 mm and fines with particle diameters that are submicron to about 0.2 mm.

15th DOE NUCLEAR AIR CLEANING CONFERENCE

The process heat needed to evaporate and/or decompose the volatiles can be supplied by either in-bed combustion or indirect heating. With in-bed combustion (IBC), fuel and oxygen are introduced directly into the bed; combustion takes place in the fluidized bed. In-bed combustion functions efficiently at temperatures of 500°C and above and calcining wastes containing nitrates (which aid combustion). Advantages of in-bed combustion are: (1) a relatively simple installation, (2) suitability for high-temperature operation, and (3) efficient heat transfer. With indirect heating, the process heat is supplied by a heat-exchanger placed in the fluidized bed. With small calciners, heat can also be supplied through the calciner wall (the small calciners have a higher wall surface to bed volume ratio). Advantages of indirect heating are: (1) its suitability for low-temperature operation, and (2) a lower volume of calciner effluent (no combustion gases).

The Waste Calcining Facility (WCF) has demonstrated solidification of radioactive zirconium-fluoride and aluminum-nitrate wastes in a fluidized bed with a cross-section of about one m². Gross feed rates have ranged from 5 to 12 m³/day. Since 1963, the WCF has solidified approximately 13,000 m³ of radioactive liquid waste forming 1600 m³ of calcined solids.^{1,2,3,4,5} Process heat was supplied first by indirect heating with an in-bed heat exchanger^{1,2,3} and later by in-bed combustion.^{4,5}

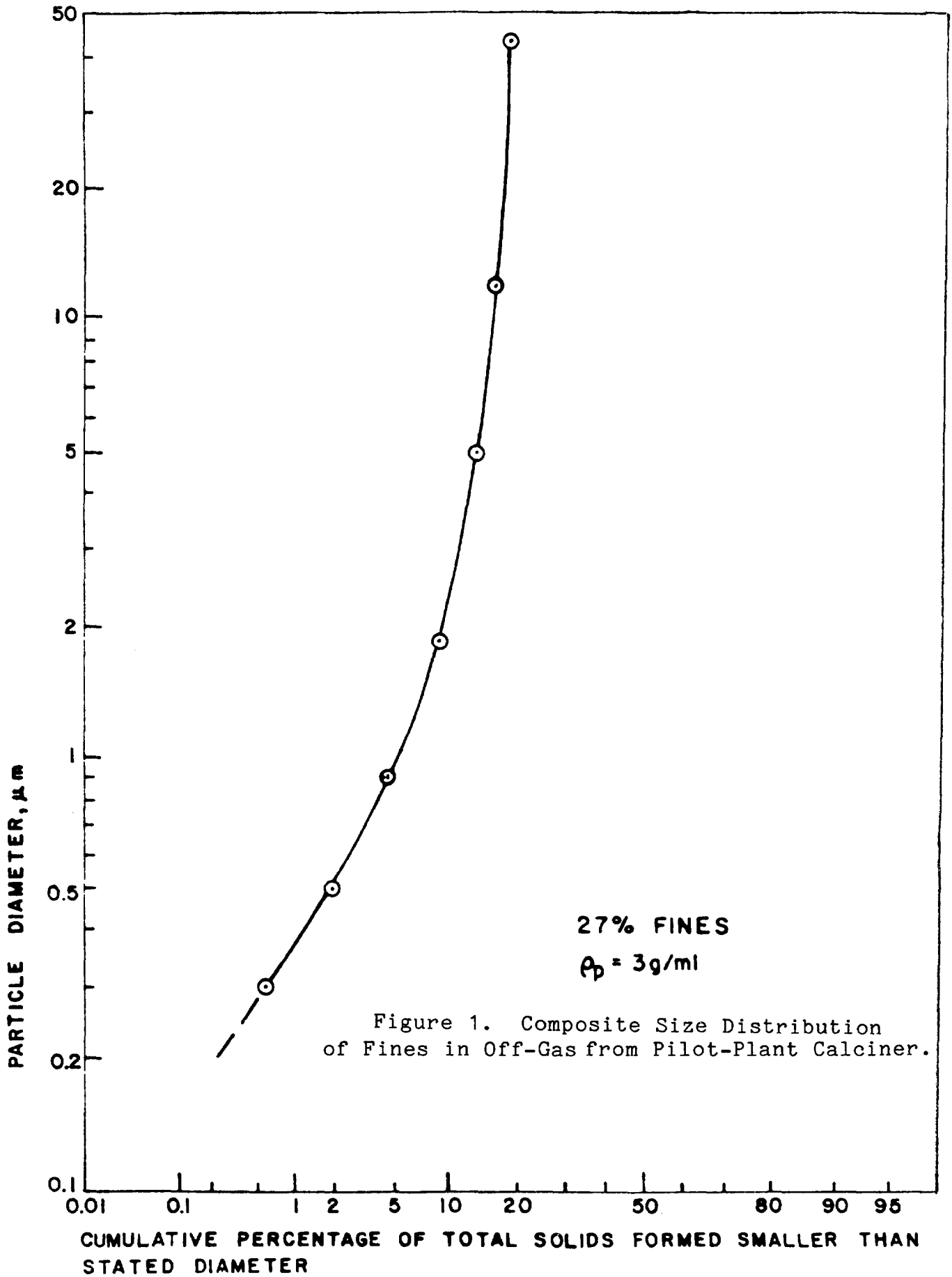
Flowsheets for calcination of radioactive liquid wastes from the reprocessing of commercial LWR fuels were developed on a pilot scale (10-cm and 30-cm-diameter calciners). Non-radioactive solutions simulating a variety of HLLW and HLLW-ILLW compositions were solidified.⁶ Most of the tests were made with solutions simulating the gadolinium-poisoned HLWW-ILLW once anticipated from the Barnwell Nuclear Fuel Plant (BNFP).

The potential advantages of fluidized-bed calcination are: (1) the demonstrated large calcining capacity, and (2) the demonstrated ability to control the formation of volatile ruthenium species.^{6,7} Disadvantages are: (1) the need to select and prepare the feed carefully--e.g., the sodium concentration must be kept below 1 M to prevent agglomeration of the bed caused by the formation of molten sodium compounds--and (2) the relatively large volume of off-gas requiring cleanup.

II. Characterization of Off-Gas

A. Physical Characteristics

The design requirements for a calciner off-gas system depend largely on the characteristics of the off-gas being



15th DOE NUCLEAR AIR CLEANING CONFERENCE

cleaned. The off-gas described in Table I is postulated for a relatively large fluidized-bed calciner designed to provide 50% excess or catch-up capacity for a 5 MTU/day fuel-reprocessing plant using a gadolinium-poisoned flowsheet. It would solidify 6 m³/day of waste to about 1100 kg/day of calcined solids. Heat would be supplied by in-bed combustion at 500°C.

Table I

Calciner Off-Gas Characteristics

Flow, standard condition, m ³ /min	13
Flow at 500°C, m ³ /min	38
Composition	
Air, %	50
Combustion gases (CO ₂ , CO, H ₂ ,) %	8
Water vapor, %	42
NO _x , ppm	14,000
Solids, g/std m ³	10-20

The off-gas composition of Table I is a flowsheet composition based on operating conditions in the WCF and in the pilot plant calciners. Most of the air is fluidizing air. The NO_x concentration is a value measured in a pilot plant test⁶ calcining simulated LWR HLLW-ILLW; it is about half the stoichiometric concentration of NO_x based on the nitrate input in the feed.

The solids concentration is based on pilot plant measurements of solids carryover from the calciner. Solids carryover from a plant calciner will depend on the calciner design: disengaging height, baffles, and calciner diameter. Figure 1 shows a size distribution of the fines in the off-gas of a pilot plant calciner. The size analysis is a composite of: (1) a cascade-impactor analysis of the fines penetrating the cyclone, (2) a screen analysis of the fines collected by the cyclone, and (3) a cascade-impactor analysis of the smaller-than-325-mesh fraction of the collected fines after redispersal with a sonic ejector. At the point they were sampled, the fines were probably agglomerating rapidly; the estimated particle concentration is in the 10¹² to 10¹³ particles/m³ range. Agglomeration during transport of the off-gas through a length of pipe into another cell and through a cyclone and a quench vessel would shift the tail of the curve upward--i.e., to larger particle sizes.

B. Volatile Components

Ruthenium volatility during solidification is a major concern. A potential advantage of fluidized-bed calcination over other solidification methods is that ruthenium volatilization from the calciner can be controlled by calcining at 500°C or above.^{6,7,8}

Figure 2 shows the measured^{6,7,8} percent of ruthenium in the feed that is volatilized with heating by in-bed combustion at 500°C or above, plotted as a function of (dual abscissa) acidity and nitrate concentration. At nitrate concentrations below 6.5 M and acidity below 4 N, the ruthenium volatility is mostly below 0.01%--0.001 to 0.01%. High nitric acid concentrations result in increased ruthenium volatility. No definite effect of other parameters--e.g., temperature and composition variations--could be observed. However, limits in the sensitivity of the analytical methods used would not permit the detection of volatiles below 0.001%.

The volatility of ruthenium when calcining low-acid feeds (0 to 3N) with indirect heating was investigated over the temperature range from 300°C to 570°C with short-term calcining tests. The test results are plotted in Figure 3. The ruthenium volatility decreased rapidly with increasing temperature between 300°C and 500°C dropping from 76-78% at 300°C to less than 0.01% at temperatures of 500°C and above. The ruthenium volatility appeared to level out at temperatures above 500°C; however, this may be an artifact resulting from vapor concentrations below the analytical detection limits. The cause of the factor-of-a hundred data spread at 390°C and 400°C is not known.

Feed denitration with formic acid was evaluated as a potential means of reducing ruthenium volatility when calcining at lower temperatures with indirect heating. As shown in Figure 3, feed denitration reduced ruthenium volatility by a factor of about 10^4 in short-term tests. However, long-term calcining tests with the denitrated feed (HLLW-ILLW) were unsuccessful because of bed agglomeration. The main problem with denitration was that it also deacidified the feed. The basic, sodium-bearing, HLLW-ILLW then agglomerated⁶ when calcined.

When calcining fluoride wastes with in-bed combustion, ruthenium appears to behave as a semi-volatile species. The volatile ruthenium forms a particulate when cooled in a spray quench tower. The net result is that the fraction of the ruthenium from the feed that is in the fine particles carried in the off-gas is 10- to 40-times higher than that of the particulate fission products--e.g., strontium and cerium. This behavior was not observed in pilot plant tests with simulated LWR

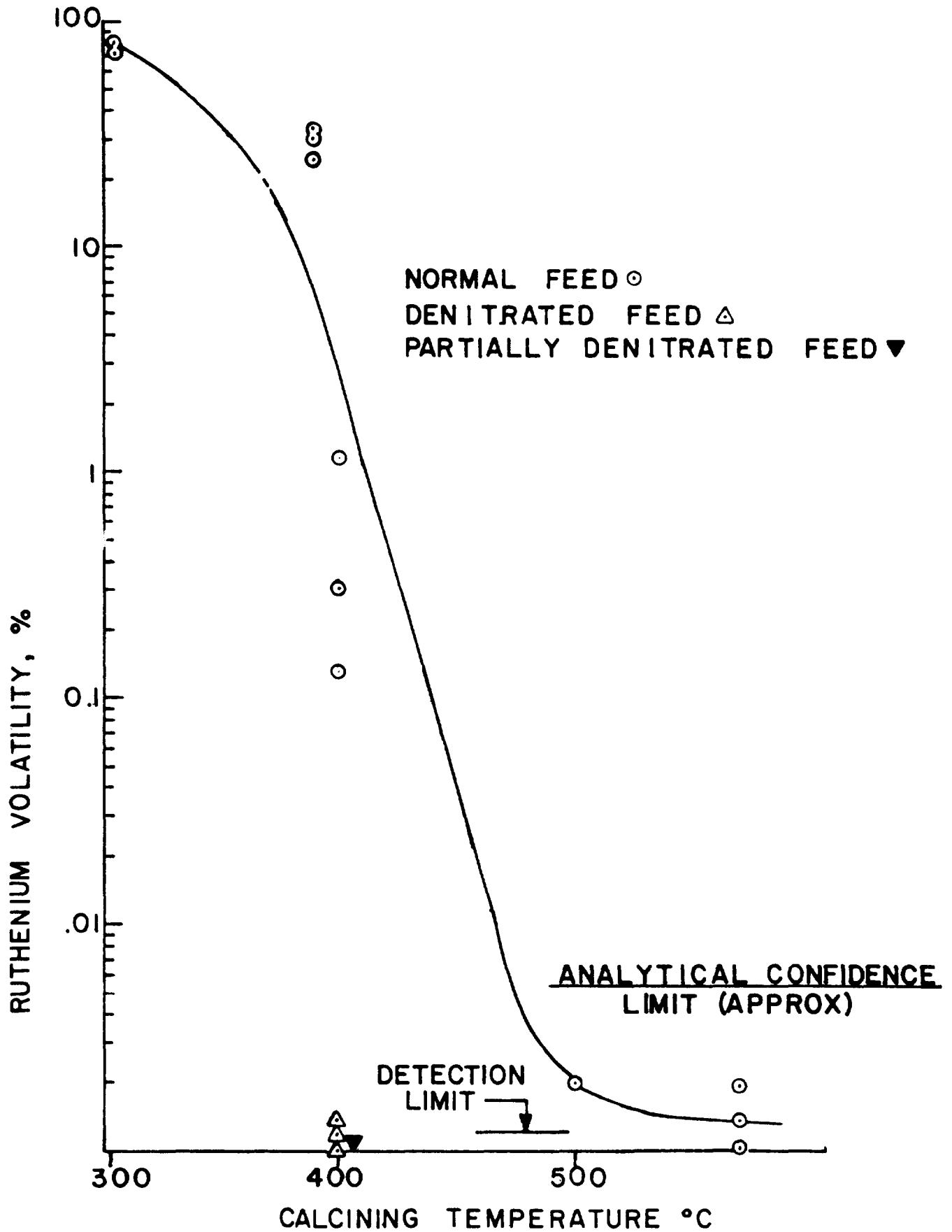


Figure 3. Ruthenium Volatility When Calcining Low-Acid, HLLW-ILLW with Indirect Heating.

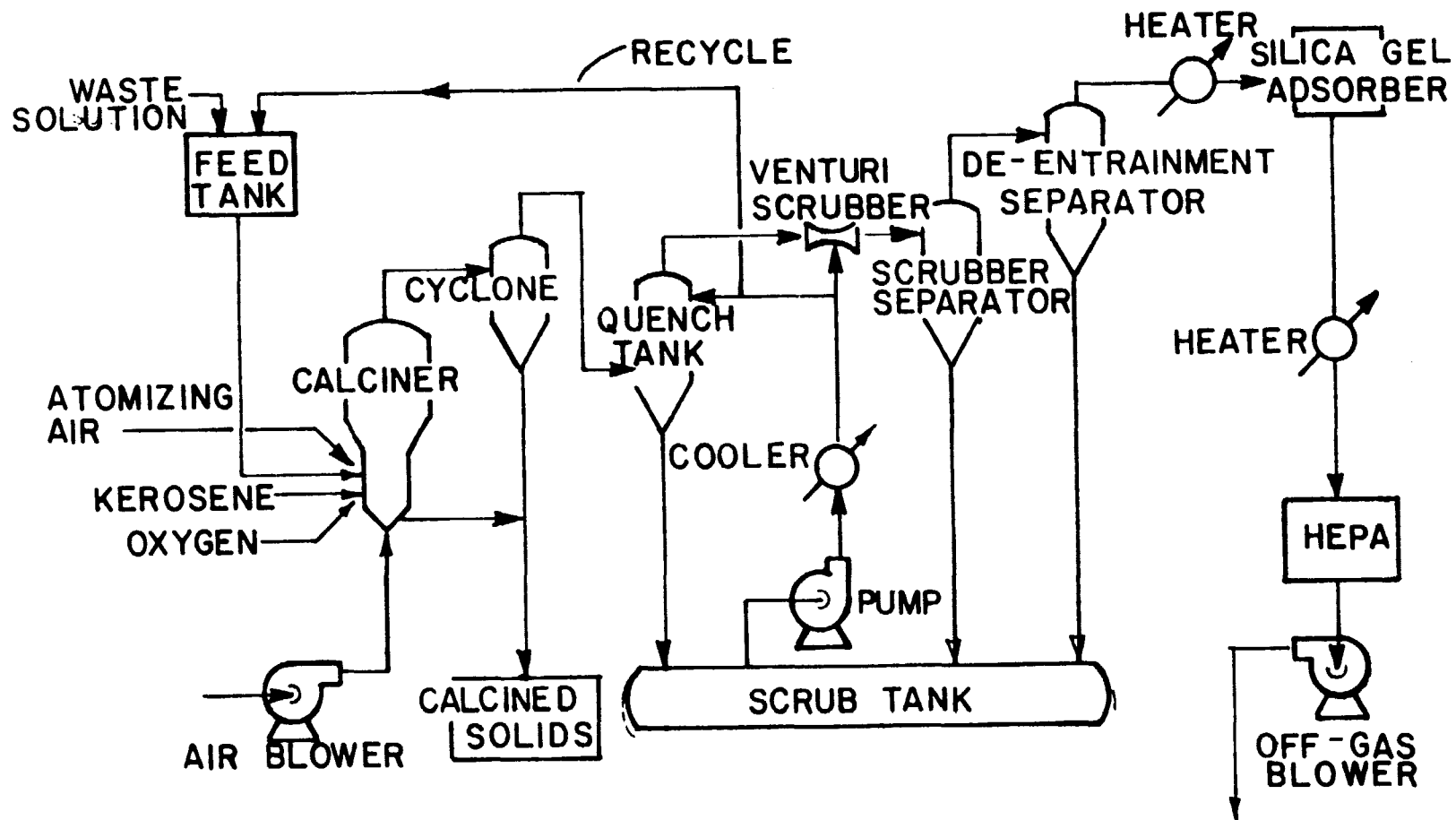


Figure 4. Schematic Flowsheet of a Commercial Calcining Facility.

15th DOE NUCLEAR AIR CLEANING CONFERENCE

HLLW-ILLW; however, it was not thoroughly checked. Christian⁸ argues that this should not be expected with non-fluoride wastes.

There are also some indications of semi-volatile behavior of cesium during the WCF campaigns with in-bed combustion at 500°C. The fraction of cesium released from the calciner and penetrating through the off-gas system was a factor of about six higher than that of the particulate radionuclides. Cesium behavior was not evaluated in the pilot plant tests. The possibility of partial volatility of cesium should be considered in the design of an off-gas system for a fluidized-bed calciner operating at 500°C or above.

III. Off-Gas Systems

The WCF off-gas system⁹ is of potential application to a calciner for LWR HLLW-ILLW. A schematic diagram is shown in Figure 4. Principal components are a cyclone, a venturi scrubber, a silica-gel ruthenium adsorber, and HEPA filters.

Figure 5 shows the predicted flow of solids through the off-gas system and the estimated airborne solids concentrations. The most sensitive components of the off-gas system are the HEPA filters which can deteriorate in service due to age and to contact with moisture. If filter performance is monitored, and deteriorating filters are replaced when necessary, a set of filters in series can probably provide essentially any required collection efficiency. The basis for the assumed filter-system DF of 10^6 is: (1) the filter system contains a pair of HEPA filters in series followed by a backup filter system containing another HEPA filter, and (2) two of the 3 HEPA filters are in good condition providing a DF of 10^3 each. The DF values for the other off-gas components are based on WCF^{1,2,3,4,8,9} and/or pilot plant⁶ data. The overall DF for particulates is 2×10^{10} . The DF's for any particulate fission product would be the same as shown in Figure 5. For example, the calciner feed would contain about 560,000 Ci/day of strontium of which about 30×10^{-6} Ci/day would be released with the off-gas.

The predicted flow of volatile ruthenium vapors (with 1-yr-cooled waste) through the off-gas system is shown in Figure 6. The component DF's are conservative values as might be used in a safety analysis:

- (1) The calciner DF of 10^4 is based on ruthenium volatility of 0.01%, which is roughly an upper limit value for the data in Figure 2. The actual volatility may be lower; however, refined experimental methods will be required to demonstrate a lower volatility value

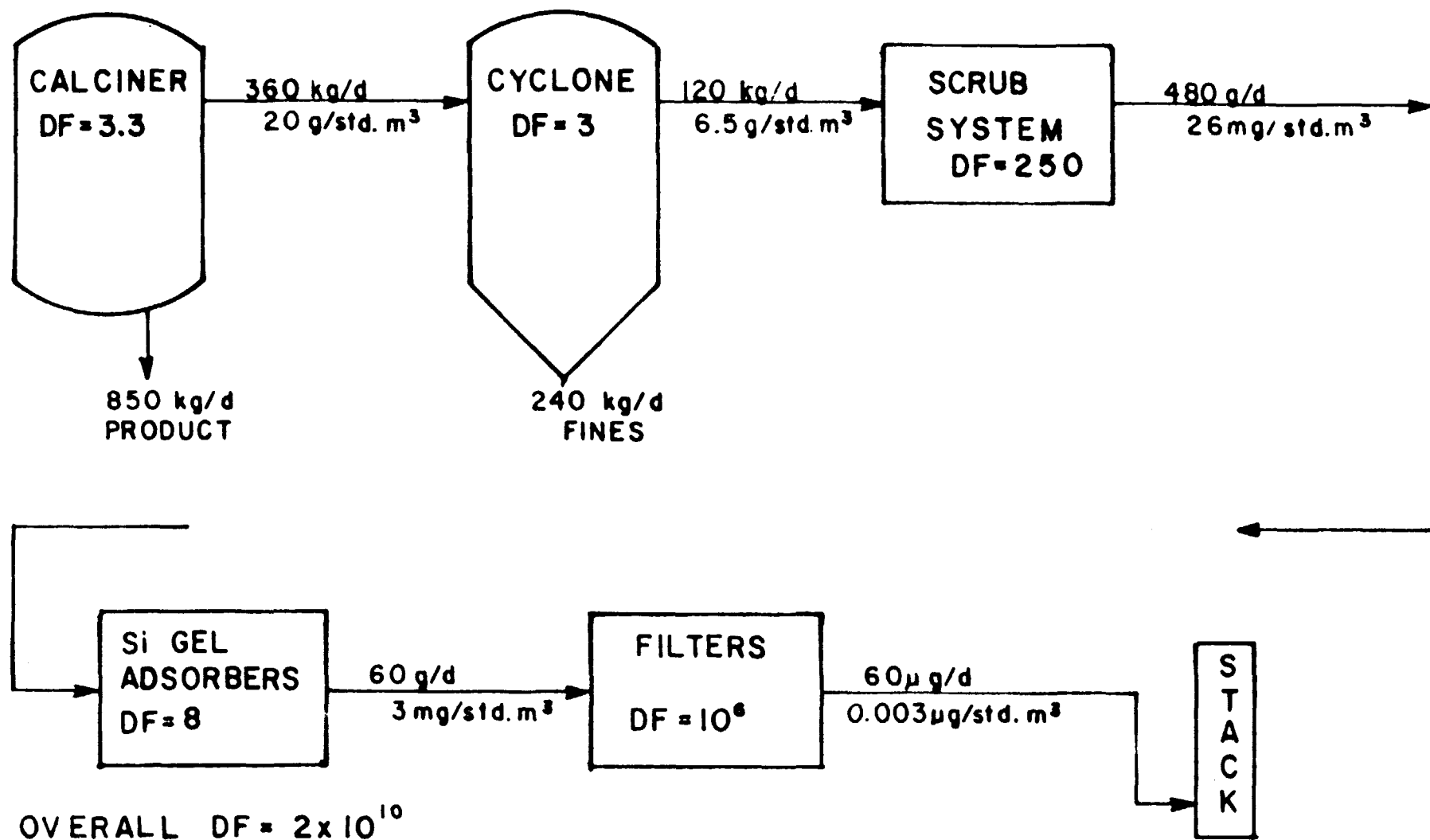
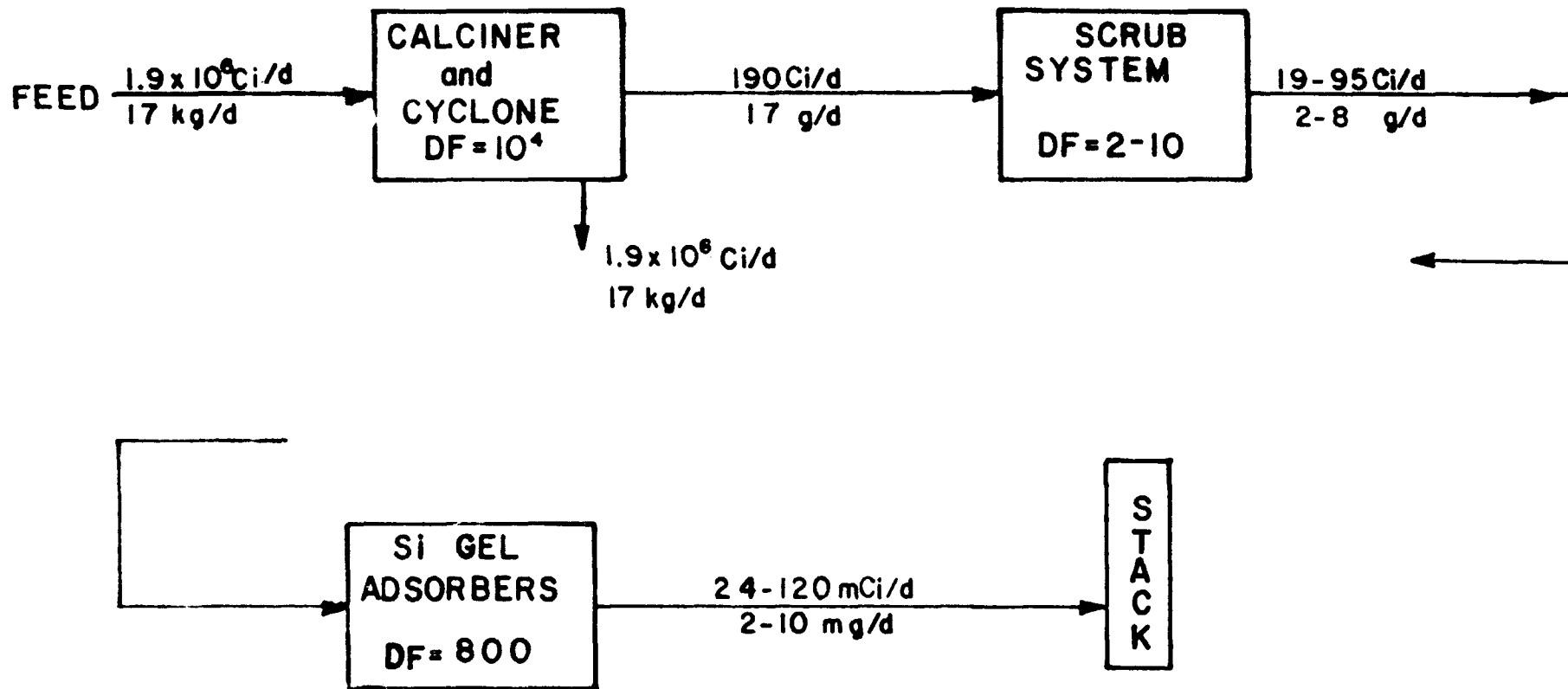


Figure 5. Flow of Solids through Candidate Off-gas Cleanup System.



OVERALL DF = $1.6-8 \times 10^7$
 1-YR.-COOLED WASTE
 7.5 MTU/DAY

Figure 6. Flow of Volatile Ruthenium through Candidate Off-Gas System.

15th DOE NUCLEAR AIR CLEANING CONFERENCE

- (2) The scrubbing system DF of 2 was measured⁶ in a pilot plant scrubbing system which uses a venturi scrubber without a quench tower. Christian and Rhodes⁸ estimate a DF of 10 for a scrubbing system with a quench tower and scrubber.
- (3) The adsorber DF of 800 is based on observed^{1,2,3,8} performance of the WCF adsorber during operation with indirect heating

The overall DF for volatile ruthenium is 1.6×10^7 to 8×10^7 . The release of volatile ruthenium would be 120 mCi/day or less (with 1-yr-cooled waste). A second stage of ruthenium adsorbers would provide additional ruthenium adsorption if required.

In conclusion, an off-gas system similar to the one used in the WCF would probably be satisfactory for a large fluidized-bed calciner for LWR HLLW-ILLW. Alternative designs may offer improvements.

References

1. R. E. Commander et al., Operation of the Waste Calcining Facility with Highly Radioactive Aqueous Waste, IDO-;4662 (June 1968).
2. G. E. Lohse and M. P. Hales, Second Processing Campaign in the Waste Calcining Facility, IN-1344 (March 1970).
3. C. L. Bendixsen et al., The Third Processing Campaign in the Waste Calcining Facility, IN-1474 (May 1971).
4. J. A. Wielang et al., The Fourth Processing Campaign in the Waste Calcining Facility, FY-1972, ICP-1004 (March 1972).
5. J. A. Wielang and W. A. Freeby, The Fifth Processing Campaign in the Waste Calcining Facility, FY-1972, ICP-1021 (June 1973).
6. R. E. Schindler et al., Development of a Fluidized-Bed Calciner and Post-Treatment Processes for Solidification of Commercial Fuel Reprocessing Liquid Wastes, ICP-1136, (1977).
7. J. D. Christian, Process Behavior and Control of Ruthenium and Cerium, ANS-AIChE Conference on "Controlling Air-Borne Effluents from Fuel Cycle Plants", (August 1976).

15th DOE NUCLEAR AIR CLEANING CONFERENCE

8. J. D. Christian and D. W. Rhodes, Ruthenium Containment During Fluid-Bed Calcination of High-Level Waste from Commercial Nuclear Fuel Reprocessing Plants, ICP-1091, (1977).
9. R. E. Schindler, Removal of Particulate Solids from the Off-Gas of the WCF and NWCF, ICP-1157, 1978.

15th DOE NUCLEAR AIR CLEANING CONFERENCE

VOLATILIZATION FROM BOROSILICATE GLASS MELTS OF SIMULATED SAVANNAH RIVER PLANT WASTE*

G. W. Wilds
Savannah River Laboratory
E. I. du Pont de Nemours & Co.
Aiken, South Carolina 29801

Abstract

Laboratory scale studies determined the rates at which the semivolatile components sodium, boron, lithium, cesium, and ruthenium volatilized from borosilicate glass melts that contained simulated Savannah River Plant waste sludge. Sodium and boric oxides volatilize as the thermally stable compound sodium metaborate, and accounted for ~90% of the semivolatiles that evolved. The amounts of semivolatiles that evolved increased linearly with the logarithm of the sodium content of the glass-forming mixture. Cesium volatility was slightly suppressed when titanium dioxide was added to the melt, but was unaffected when cesium was added to the melt as a cesium-loaded zeolite rather than as a cesium carbonate solution. Volatility of ruthenium was not suppressed when the glass melt was blanketed with a nonoxidizing atmosphere.

Trace quantities of mercury were removed from vapor streams by adsorption onto a silver-exchanged zeolite. A bed containing silver in the ionic state removed more than 99.9% of the mercury and had a high chemisorption capacity. Beds of lead-, copper-, and copper sulfide-exchanged zeolite-X and also an unexchanged zeolite-X were tested. None of these latter beds had high removal efficiency and high chemisorption capacity.

I. Introduction

One process being studied for long term management of Savannah River Plant (SRP) high-level waste sludge is incorporation into a borosilicate glass matrix by spray calcination and electric melting. Several components of the melt will volatilize during the high temperature vitrification process. Savannah River Laboratory (SRL) has therefore initiated studies to determine the types and quantities of species that vaporize during fixation of SRP waste into glass. These studies provide basic data that are required to design an off-gas clean-up system for a vitrification process. This paper discusses laboratory-scale studies of the vaporization of sodium, lithium, boron, cesium, and ruthenium from glass melts. The chemical form in which these semivolatiles vaporize, the rates of vaporization, and some of the factors that influence volatility are discussed. All results were obtained with glasses that contained simulated non-radioactive sludges.

15th DOE NUCLEAR AIR CLEANING CONFERENCE

Based on previous studies at SRL, all of the mercury in SRP waste is expected to volatilize during vitrification. A process was developed to remove trace quantities of mercury from gaseous streams by adsorption onto a bed of silver-exchanged zeolite. This process is discussed in the second part of this paper.

II. Experimental Procedure

Sodium, Lithium, Boron, and Cesium Compounds

The apparatus used to measure the volatility of Na, Li, B, and Cs is shown schematically in Figure 1. The crucible, collection tube, lid assembly, and hypodermic tubing were all fabricated from platinum. The transfer line from the collection tube to the scrubber was made of stainless steel, and the scrubber was made of glass. Volatility was determined by mixing the required proportions of glass frit/simulated sludge in the platinum crucible, which was then placed in the furnace. Normal melting conditions consisted of holding a 2-g sample at 1150°C for three hours. Nitrogen gas (750 mL/min) was introduced through the hypodermic tubing and across the melt. A vacuum was applied to the scrubber to insure that all volatilized species were removed from the crucible.

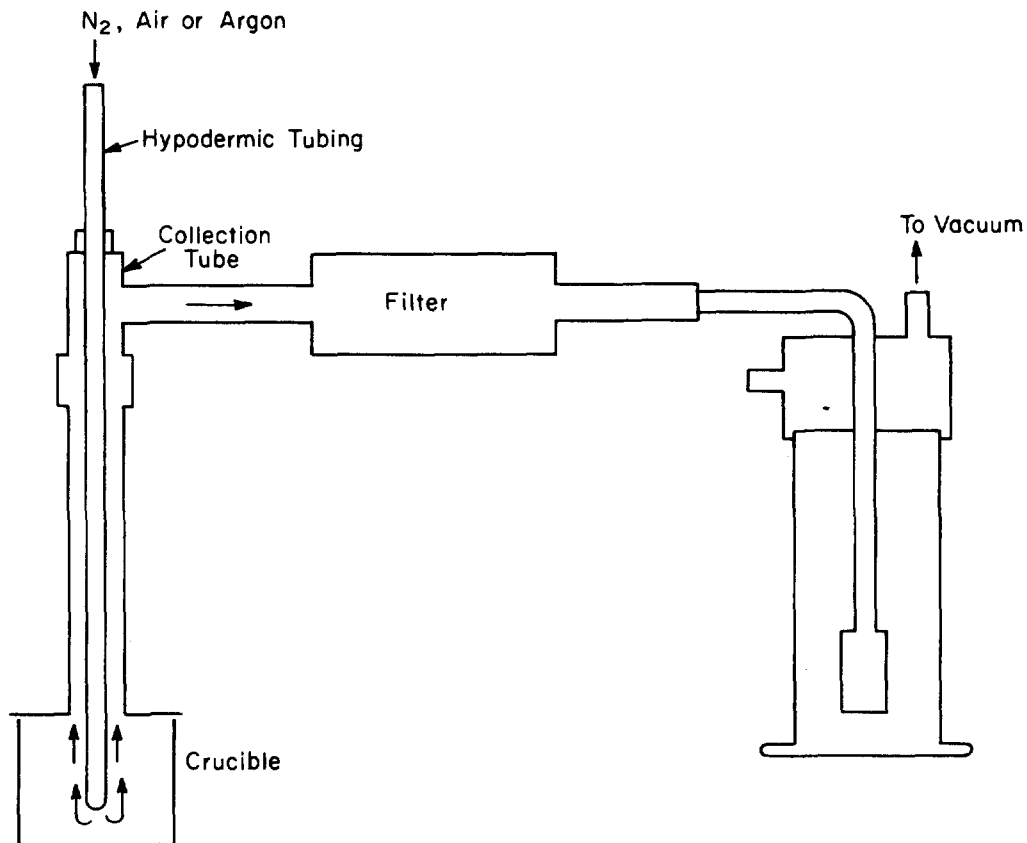


FIGURE 1
VOLATILITY APPARATUS

15th DOE NUCLEAR AIR CLEANING CONFERENCE

Compounds of Li, B, Na, and Cs condensed at the top of the collection tube, on the hypodermic tubing, in the transfer lines, and on the surface of the filter. Less than 1% of the semivolatiles penetrated through the filter; these were collected in the scrubber. The condensed gases were washed from the various parts of the apparatus and analyzed for Li, B, Na, and Cs by atomic absorption spectrophotometry (AA). A solution of 0.1M HNO₃ was used both for washing out the apparatus and as a scrubber solution.

Ruthenium Compounds

The apparatus and procedure described above were used to measure ruthenium volatility, except that a 6-g sample size was used and the in-line filter was removed. To minimize plating-out of ruthenium on the walls of the platinum collection tube, the inside of the tube was polished just prior to running each sample. This procedure prevented buildup of ruthenium in the transfer line. The collection tube was washed out after each sample was run, and residual ruthenium was removed from the walls. The washings containing the residual ruthenium were combined with the scrubber solution prior to analysis. This technique did not distinguish between particulate and volatile ruthenium, nor did it measure the extent to which ruthenium plates out.

The ruthenium was analyzed by a modification of the spectrophotometric technique developed by Woodhead.⁽¹⁾ This technique measures the absorbance at the isosbestic point (415 nm) of a RuO₄²⁻/RuO₄⁻ mixture. Ruthenium was converted to the mixture by the action of K₂S₂O₈ in the presence of boiling KOH. The method detected ruthenium concentrations as low as 0.3 ppm in 100 mL of solution, which covered the range of ruthenium concentrations in the scrubber solutions.

III. Glass Compositions

Table I lists the two borosilicate glass-forming frits used in these studies. The high Fe, high Al, and average simulated calcined

Table I. Frit compositions.

<u>Component</u>	<u>Concentration, wt %</u>	
	<u>Frit 21</u>	<u>Frit 18</u>
SiO ₂	52.5	52.5
Na ₂ O	18.5	22.2
B ₂ O ₃	10.0	10.0
TiO ₂	10.0	10.0
CaO	5.0	5.0
Li ₂ O	4.0	—

15th DOE NUCLEAR AIR CLEANING CONFERENCE

sludges were prepared by mixing quantities of the dried metal oxides in the proportions required to give the compositions shown in Table II. The compositions are based on actual analyses of SRP waste sludge^(2,3) and represent sludges from waste tanks with typically high Fe concentrations, Al concentrations, and an overall average for all tanks sampled.

Table II. Composition of simulated calcined sludges.

Metal Oxide	Metal Oxide in Sludge, wt %		
	High Fe	High Al	Average
Fe ₂ O ₃	61.4	6.0	43.5
Al ₂ O ₃	5.6	86.3	25.8
MnO ₂	4.1	4.9	11.7
U ₃ O ₈	14.2	1.5	11.0
CaO	4.2	0.4	3.0
NiO	10.5	0.9	5.0

The cesium content of SRP waste glass was calculated to be 0.06 wt % (as Cs₂O). Because this small amount of material could not be added in solid form to the 2-g samples, cesium was added by either adsorption of the cesium onto zeolite or by adding aliquots of a cesium carbonate solution to the glass-forming mixture. In cases where cesium was added from solution, the sample was dried to remove excess water before placing the loaded crucible into the furnace. Pre-drying prevented entrainment of particulates in the steam that would result from placing the wet mixture in the furnace heated to 1150°C.

Ruthenium was incorporated into the glass-forming mixture by adding the volume of a 3 g/L solution of Ru(NO)(NO₃)₃ required to give 0.05 or 0.15 wt % Ru in the final glass. The Ru(NO)(NO₃)₃ solution was prepared by dissolving Ru(NO)(OH)₃ in 4M HNO₃. After addition of the Ru(NO)(NO₃)₃ solution, the glass-forming mixture was dried at 115°C to drive off excess water to prevent entrainment of ruthenium.

IV. Specific Element Volatility

Sodium, Boron, and Lithium Volatilities

Volatilities of Na, Li, and B are discussed together because these species vaporized from the melt as alkali borates. The thermally stable compound sodium metaborate (Na₂O·B₂O₃) accounted for ~90% of the semivolatiles that vaporized. Trace quantities of LiBO₂, LiNaBO₂, Na₂BO₂, and B₂O₃ were also detected in the vapor above the melt by Knudsen cell - mass spectrometer measurements. In the condensed phase, the species that volatilized were determined from the molar ratios of Na/B and (Li + Na)/B in the condensate. A ratio of one would indicate the metaborate, a ratio of two would indicate the

15th DOE NUCLEAR AIR CLEANING CONFERENCE

diborate, and a mixture of the two compounds would be indicated by a ratio between one and two. The ratio of Na/B should be less than one when the melt contains lithium, because only part of the boron is associated with sodium; the remaining boron forms a lithium borate. The ratio of (Li + Na)/B would equal one, however, if $\text{Li}_2\text{O}\cdot\text{B}_2\text{O}_3$ and $\text{Na}_2\text{O}\cdot\text{B}_2\text{O}_3$ are the compounds that volatilize. A melt that contains sodium (but no lithium) should give a Na/B ratio of 1 if $\text{Na}_2\text{O}\cdot\text{B}_2\text{O}_3$ is the vaporizing species. When Frit 21, which contained both sodium and lithium, was used to prepare glasses (Table III), the molar ratio of Na/B was 0.89, and that of (Na + Li)/B was 1.02. Off-gasses from glasses prepared from Frit 18, a frit that contains no lithium, gave a Na/B ratio of 1.05 (Table IV). These three ratios are

Table III. Volatility of Na, Li and B from Frit 21 glass melts.

Code	Na ₂ O in Glass, mole %	Volatility, mg/cm ²			Molar Ratios	
		Na ₂ O	Li ₂ O	B ₂ O ₃	Na ₂ O/B ₂ O ₃	(Na ₂ O + Li ₂ O)/B ₂ O ₃
21-Avg-25		0.4	0.04	0.4	1	1.0
-35		0.4	0.05	0.5	1	1.1
-45	13.6	0.9	0.14	1.2	0.84	0.97
21-Fe-25	17.1	1.4	0.20	1.5	0.99	1.1
-35	15.7	1.4	0.20	2.0	0.82	0.93
-45	14.2	0.7	0.13	1.0	0.83	0.98
21-A1-25	16.1	1.3	0.16	2.0	0.74	0.84
-35	14.5	0.7	0.13	1.0	0.84	1.0
-45	12.6	0.5	0.08	0.5	1	1.2
				Avg	0.89	1.02

Table IV. Volatility of Na and B from Frit 18 glass melts.

Code	Na ₂ O in glass, mole %	Volatility, mg/cm ²		Molar Ratio, Na ₂ O/B ₂ O ₃
		Na ₂ O	B ₂ O ₃	
18-Avg-25	21.2	2.6	3.0	0.97
-35	19.4	1.9	1.9	1.1
-45	17.1	1.5	1.6	1.1
18-Fe-25	21.6	1.8	1.9	1.1
-35	19.9	2.2	2.3	1.1
-45	17.7	1.0	1.4	0.86
18-A1-25	20.4	0.7	0.7	1.1
-35	18.2	1.5	1.9	0.93
-45	15.8	1.2	1.2	1.2
			Avg	1.05
Frit 18	22.7	4.0	4.5	
Frit 21	17.8	1.7		

consistent with a mechanism of alkali and boron volatilization as the compounds $\text{Na}_2\text{O}\cdot\text{B}_2\text{O}_3$ and $\text{Li}_2\text{O}\cdot\text{B}_2\text{O}_3$. Solomin⁽⁴⁾ and Walmsley,⁽⁵⁾ in their work on borosilicate glass volatility, also concluded that alkalis volatilize from borosilicate melts as thermally stable alkali borates.

The quantity of $\text{Na}_2\text{O}\cdot\text{B}_2\text{O}_3$ evolved increased exponentially when the mole % of sodium in the glass melt was increased (Figure 2). Measurements were made over a range of 12 to 23 mole % Na_2O in the glass. Volatility varied from 1.5 mg/cm^2 (at 12 mole % Na_2O) to 8.5 mg/cm^2 (at 23 mole % Na_2O). The linear relationship between the logarithm of weight loss and Na_2O content of the melt is similar to that obtained by Kolykov⁽⁶⁾ when he studied the system $\text{Na}_2\text{O}-\text{B}_2\text{O}_3-\text{SiO}_2$. Barlow⁽⁷⁾ also concluded that sodium volatilizes from a borosilicate glass melt as either sodium metaborate or sodium diborate, and that volatility increases as the logarithm of sodium concentration.

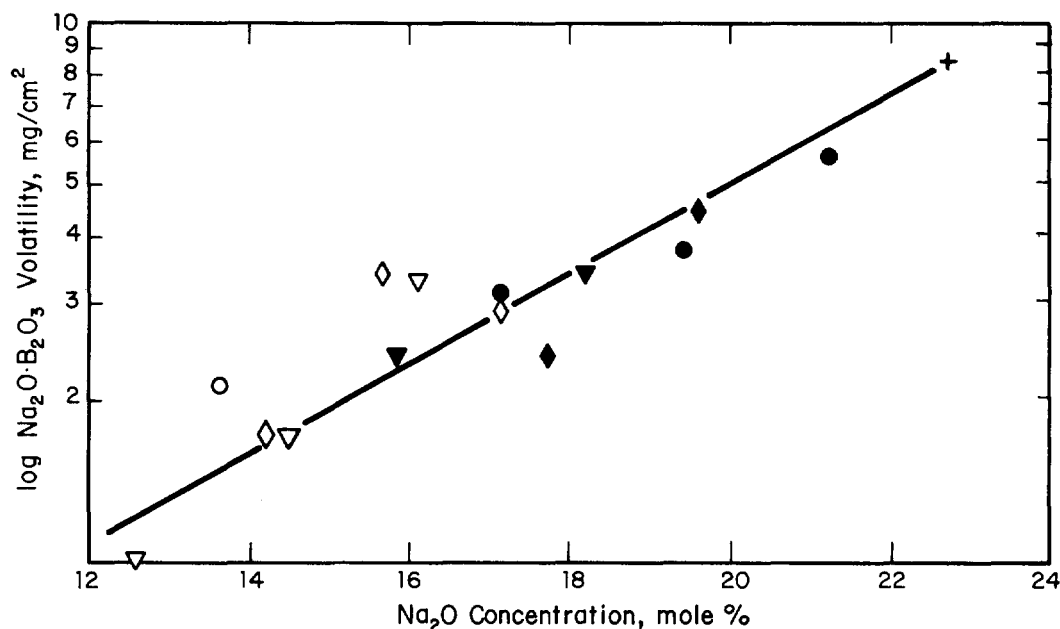


FIGURE 2
EFFECT OF Na_2O CONCENTRATION ON $\text{Na}_2\text{O}\cdot\text{B}_2\text{O}_3$ VOLATILITY

Lithium metaborate volatility was about 1/10 that of sodium borate. Changes in melt composition or in melting conditions had no appreciable effect on lithium volatility.

The type sludge, the type frit, and the concentration of other glass components affected volatility only to the extent that changes in these variables affected changes in the mole % of Na_2O in the glass melt.

Cesium

Cesium, which volatilized from the melt as either elemental cesium or as some oxide of cesium, is the most volatile of the three alkali metals studied. An average of 0.11 mg/cm^2 of cesium (as Cs_2O) volatilized from samples that contained a range of 0.03 to 0.09 wt %

15th DOE NUCLEAR AIR CLEANING CONFERENCE

cesium. Because previous workers⁽⁸⁾ have reported that addition of TiO_2 , B_2O_3 , or MoO_3 to glass melts reduces cesium volatility, one part of the current work compared cesium volatilization from glass melts prepared from frits that contained 0, 5, and 10 wt % of TiO_2 . Also, a comparison between cesium volatility from melts which contained cesium as a cesium-loaded zeolite and as a cesium carbonate solution was made.

Tables IV through VII summarize the effect on cesium volatility of the wt % TiO_2 added, the form of cesium addition, and the concentration of cesium in the melt. The high volatilities in these tests reflect the high surface-area-to-weight ratios for the small samples used and should not be interpreted as a direct measure of the amount of cesium expected to volatilize from a full-scale melter. If these levels of volatility are scaled up to a 2.2 ton/day melter, they

Table V. Effect of addition of TiO_2 on cesium volatility.

<u>Cesium Added as</u>	<u>Cs₂O in Glass, wt %</u>	<u>TiO₂ in Frit, wt %</u>	<u>Volatility, mg/cm²</u>
Zeolite	0.03	0	0.08
Zeolite	0.03	10	0.06
Carbonate	0.03	0	0.08
Carbonate	0.03	10	0.06

Table VI. Effect of form of addition on cesium volatility.

<u>Cesium Added as</u>	<u>Cs₂O in Glass, wt %</u>	<u>TiO₂ in Frit, wt %</u>	<u>Volatility, mg/cm²</u>
Zeolite	0.03	0	0.08
Carbonate	0.03	0	0.08
Zeolite	0.03	10	0.06
Carbonate	0.03	10	0.06
Zeolite	0.09	10	0.10
Carbonate	0.09	10	0.15

Table VII. Effect of Cs₂O concentration on cesium volatility.

<u>Cs₂O in Glass, wt %</u>	<u>TiO₂ in Frit, wt %</u>	<u>Volatility, mg/cm²</u>
0.03	0	0.08
0.03	10	0.06
0.06	5	0.11
0.06	5	0.13
0.09	0	0.21
0.09	10	0.15

15th DOE NUCLEAR AIR CLEANING CONFERENCE

represent volatilization of 0.05% of the cesium in the melter charge. Battelle Northwest Laboratories (BNWL), by comparison, measured ~0.3% volatility when they vitrified simulated light-water-reactor (LWR) waste that contained 0.2 wt % of Cs_2O .⁽⁹⁾ A melting temperature of 1050°C for 6 hours was used in the BNWL study.

The slight suppression of cesium volatility by titanium dioxide can be seen by comparing samples in Table V. The volatility is decreased so slightly that it would not significantly reduce problems of cesium vaporization during glass melting. The failure of titanium dioxide to significantly reduce cesium volatilization can be explained by the work of Rastogi, et al.,^(10,11) who found that reductions in cesium volatility were obtained only at temperatures below 1000°C and for vitrification times ≤ 1 hour. They found, for example, that the compound $\text{Cs}_2\text{O}\cdot 4\text{TiO}_2$ does not volatilize at 400°C, but that 31% of this compound volatilizes at 1200°C. Other work by Rudolph, et al.⁽⁸⁾ and by Kupfer and Schulz⁽¹²⁾ report that titanium dioxide effectively suppresses cesium volatilization, but in the 1000 to 1050°C temperature range. Another probable cause of the failure of titanium dioxide to suppress cesium volatility significantly is the large amounts of boric oxide present in the melt compositions used for SRP glasses. Rudolph, et al.⁽⁸⁾ found that boric oxide, though not as effective as titanium dioxide, does reduce the volatility of cesium. The effect of titanium dioxide, then, is probably reduced when the melt contains boric oxide as a constituent.

Incorporation of cesium into the glass as cesium-loaded zeolite (0.02 g Cs/g zeolite), rather than as a cesium carbonate solution, did not increase cesium volatility from the glass melt. The insensitivity of cesium volatility to the form of cesium addition is shown in Table VI. Kelley, in his work on radionuclide vaporization from SRP waste,⁽¹³⁾ also found that volatility of cesium was unchanged when cesium-loaded zeolite was substituted for direct addition of cesium carbonate.

Total cesium volatility increased when the total amount of cesium in the melt was increased (Table VII). The increase in volatility was proportional to the increased cesium concentration, suggesting that cesium vaporizes by diffusion from the melt surface.

The Knudsen cell studies conducted as a part of the experiments in this report did detect elemental cesium above the melt at a temperature of 1200°C. No cesium borates were detected.

Ruthenium

The high alumina, high iron, and composite sludges (Table II) along with Frit 21 were used to study ruthenium volatility. The two gases used to blanket the melt, air and argon, showed the effect of the oxygen on ruthenium volatilization. Each sludge-atmosphere combination was run in duplicate, and the result was interpreted by the analysis of variance method. For these experiments, nitrate-free simulated sludge was used. Neither the composition of the sludge nor the atmosphere over the melt affected the volatilization of ruthenium. Table VIII shows the per cent of ruthenium volatilized for the various combinations of sludges and atmospheres above the melt. The failure

15th DOE NUCLEAR AIR CLEANING CONFERENCE

Table VIII. Effect of sludge type and atmosphere over melt on ruthenium volatility.

<u>Sludge Type</u>	<u>Cover Gas</u>	<u>Ru Volatilized, %</u>
High Al	Argon	5.5
	Air	6.3
High Fe	Argon	2.8
	Air	7.4
Composite	Argon	7.5
	Air	5.3

of oxygen to increase ruthenium volatility, indicates that volatilization of ruthenium depends on the bulk rather than surface conditions of the melt. This result also indicates that atmospheric oxygen is not the only oxidant for ruthenium. This is consistent with previous work⁽¹³⁾ that identified manganese dioxide as one component of SRP sludges that oxidizes ruthenium. All three sludges contained an excess of manganese dioxide relative to the ruthenium content.

The effect of nitrate concentration on ruthenium volatility depended on the level of ruthenium in the melt. Figure 3 summarizes

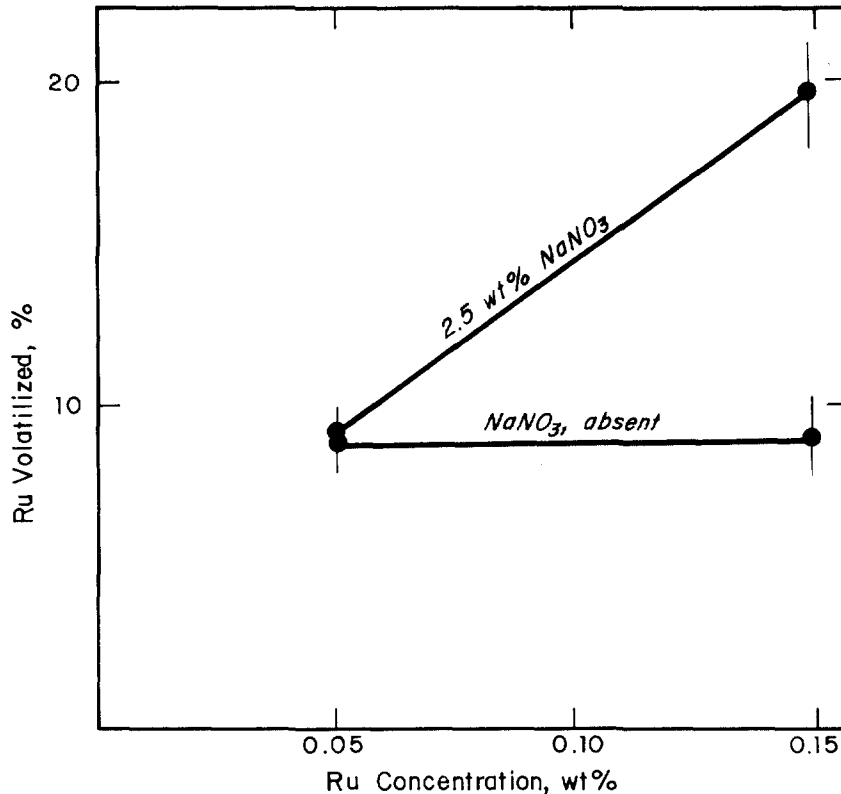


FIGURE 3
EFFECT OF SODIUM NITRATE CONCENTRATION ON RUTHENIUM

15th DOE NUCLEAR AIR CLEANING CONFERENCE

the volatility dependence on the level of ruthenium and the concentration of nitrate in the waste. Neither increasing the nitrate concentration at a low ruthenium concentration nor increasing the ruthenium concentration in nitrate-free melts caused increased ruthenium volatilization. However, a sharp increase in volatility was obtained when both the nitrate and ruthenium contents were increased. The nature of the nitrate/ruthenium concentration interaction has not been defined. These results do show, however, that acceptable nitrate levels for SRP waste sludges may depend on the amount of ruthenium present in composite (blended) SRP sludge.

V. Solid Sorbents for Mercury Vapor

It is estimated that 2.3 lbs/hr of mercury will be vaporized from the calciner/melter during vitrification of SRP waste. The calciner/melter off-gas system will include a quench column and a condenser that is cooled to 5°C to reduce the mercury vapor concentration to $\sim 3 \times 10^{-9}$ g/cm³. Laboratory data show that the final traces of mercury can be removed by adsorption onto silver-exchanged zeolite. A bed of Ag⁺ exchanged zeolite irreversibly chemisorbed 0.190 g Hg/g of bed at an adsorption efficiency of >99.9%.* Over the temperature range of 20 to 400°C, the efficiency of the silver zeolite bed remained >99.9%; at 500°C, efficiency dropped to 92%.

Preparation of Zeolite and Analytical Method

The Na, Ag⁺, Ag⁰, Pb²⁺ and the CuS forms of zeolite were available from previous studies.⁽¹⁴⁾ The Cu²⁺ zeolite was prepared by exchanging Cu²⁺ from a saturated cupric acetate solution with *Linde Type 13X*[®] molecular sieve for 10 days at 80°C. After exchange, the Cu²⁺ zeolite was thoroughly washed to remove any residual cupric acetate solution and then dried.

Mercury vapor concentrations were measured with a mercury analyzer previously used in a study of the dispersion of buried elemental mercury.⁽¹⁵⁾ The analyzer is shown schematically in Fig. 4 and is more fully described in Reference 15. In these experiments, the accessory mercury vapor source is replaced by the adsorption bed being tested. A septum, through which known amounts of air saturated with mercury vapor can be injected, is placed just upstream from the bed.

Capacities of adsorption beds were measured by passing mercury vapor through the bed at a face velocity of ~ 3 m/min and measuring the weight of the bed until no further weight gain was recorded. After constant weight was attained, argon was passed through the bed and the weight loss recorded. The weight lost to the argon stream was assumed to be physically adsorbed mercury, while the remaining weight gain by the bed was assumed to be chemisorbed mercury. During desorption of physisorbed mercury, the bed was placed in line with the specific mercury analyzer, and the evolution of mercury was measured.

* Efficiency is defined as the % of mercury in the vapor stream that is trapped by the adsorbent bed.

15th DOE NUCLEAR AIR CLEANING CONFERENCE

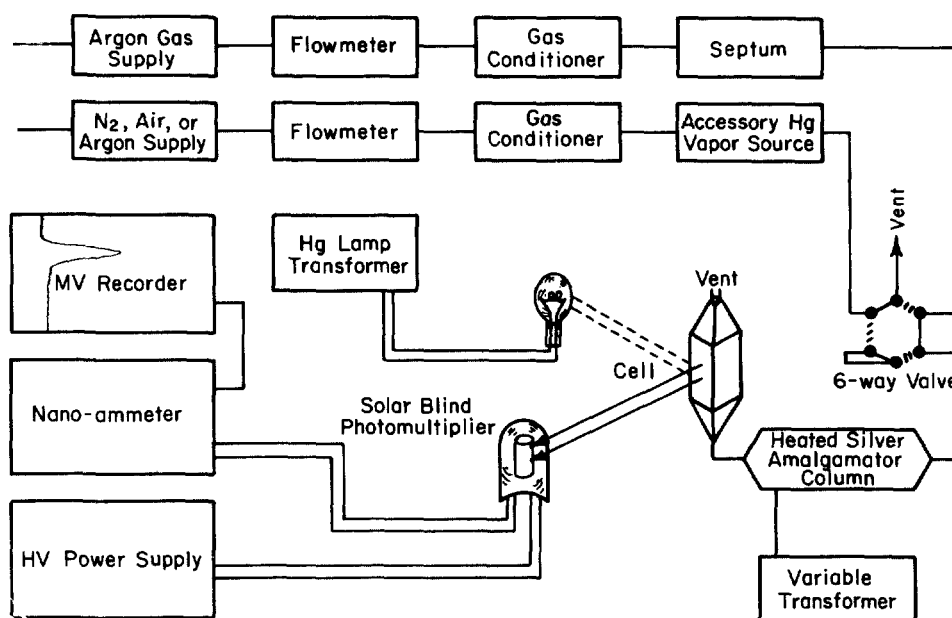


FIGURE 4
SCHEMATIC DIAGRAM OF MERCURY ANALYZER

Screening Tests

The adsorption efficiency of the beds was first measured at room temperature ($\sim 20^{\circ}\text{C}$). The results in Table IX show that only Ag^+ , Ag^0 , and CuS exchanged beds have a high adsorption efficiency for mercury. Table IX also shows that apparent residence times* influence mercury adsorption efficiency. The importance of residence time is shown by comparing the efficiencies of the Ag^+ exchanged bed at various residence times. The efficiency of $>99.9\%$ at 0.04 seconds apparent residence time decreased to 80% at 0.0006 sec. In these experiments, the lower detection limit for mercury was 0.1%, so that an efficiency of at least 99.9% may be assigned for the cases where no mercury was detected in the vapor. This assumption gives a lower limit of $\sim 10^3$ for the mercury decontamination factor for cases in which no detectable mercury vapor was found exiting the adsorption bed.

Effect of Temperature on Efficiency

The effect of bed temperature on adsorption efficiency for Ag^+ , Ag^0 , and CuS exchanged zeolite beds was measured over a temperature range of 20 to 500°C (Table X). Beds were first heated to the desired temperature, and then the mercury vapor was passed through the adsorbent. Of the three beds, the Ag^+ form was least affected by temperature, showing an adsorption efficiency of $>99.9\%$ up to 400°C . The Ag^0 bed had $>99.9\%$ efficiency up to 200°C , while the CuS bed had this level of efficiency only up to 50°C . These results are consistent with work reported by Barrer and Whiteman,⁽¹⁶⁾ who found that sorption of mercury onto metal-exchanged zeolites was inversely proportional to temperature.

* Apparent residence time is defined as the bed volume divided by the volume flow rate of the vapor stream.

15th DOE NUCLEAR AIR CLEANING CONFERENCE

TABLE IX. Efficiency of mercury adsorption beds.

<u>Sorbent^a</u>	<u>Apparent Residence Time, sec</u>	<u>Hg Vapor Adsorbed, %</u>
None	0.04	0
Shredded Rubber	0.04	0
Na-X	0.04	0
Pb-X	0.04	15
Cu-X	0.04	0
CuS-X	0.04	>99.9 ^b
Ag ⁰ -X	0.04	>99.9 ^b
Ag ⁺ -X	0.04	>99.9 ^b
Ag ⁺ -X	0.0002	98
Ag ⁺ -X	0.001	95
Ag ⁺ -X	0.0006	80

a. X = A near-faujasite type of zeolite.

b. No mercury was detected in the gas exiting the bed; percent adsorption taken by using minimum detection level of 0.1%.

Table X. Effect of temperature on efficiency of mercury adsorption beds.

<u>Bed Temperature, °C</u>	<u>Adsorption Efficiency, % Hg Adsorbed</u>		
	<u>CuS-X</u>	<u>Ag⁺-X</u>	<u>Ag⁰-X</u>
20 to 25	>99.9	>99.9	>99.9
50	>99.9	>99.9	>99.9
100	97	>99.9	>99.9
200	79	>99.9	>99.9
300	59	>99.9	92
400	39	>99.9	88
500	-	92	-

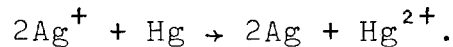
Adsorption Capacity

The capacity of a zeolite adsorption bed depends on the bed depth, the face velocity of the gas stream entering the bed, and the nature of the sorbent. The capacities of Ag⁺, Ag⁰ and CuS beds were measured for a bed depth of 1.5 cm and a superficial face velocity of ~3m/min.

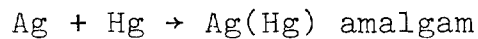
The only bed with an appreciable adsorption capacity was the Ag⁺ exchanged zeolite which chemisorbed 0.190 g of Hg/g of bed and physisorbed another 0.0264 g Hg/g of bed before a constant weight was

15th DOE NUCLEAR AIR CLEANING CONFERENCE

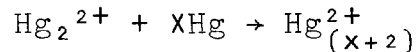
achieved. The irreversible chemisorption of mercury is attributed to the reaction,



Barrer and Whiteman⁽¹⁶⁾ studied adsorption of mercury onto several zeolites. At low mercury concentrations, the exchange between silver and mercury reached 63% of the value calculated for complete exchange. At mercury concentrations higher than those expected to be encountered in the calciner/melter off-gas system adsorption beds, the reactions,



and



can also occur.

The adsorption capacities of Ag^0 and CuS exchanged zeolite beds are quite low under the conditions of these experiments (Table XI). No detectable weight gain was recorded for either bed. Therefore, the smallest measurable weight gain (0.1 mg) was used to calculate the upper limits on capacities shown in Table XI. Even though the capacities are very low, Ag^0 and CuS exchanged zeolite beds efficiently removed mercury vapor at low concentrations. However, Ag^+ zeolite beds are recommended for plant processing because less frequent replacement is required.

Table XI. Capacities of mercury adsorbent beds.

Sorbent	Bed Length, cm	Bed Weight, g	Mercury Adsorbed, g Hg/g Bed	
			Total	Chemisorbed
Ag^+-X	1.5	0.1525	0.2164	0.190
$\text{CuS}-\text{X}$	1.5	0.1495	$<7 \times 10^{-4}$	-
Ag^0-X	1.5	0.1505	$<7 \times 10^{-4}$	-

VI. Acknowledgement

The information contained in this article was developed during the course of work under contract No. AT(07-2)-1 with the U.S. Department of Energy.

15th DOE NUCLEAR AIR CLEANING CONFERENCE

VII. References

1. J. L. Woodhead, A Spectrophotometric Method for the Determination of Ruthenium as Ruthenate-Perruthenate Mixtures, AERE-R 3279 (May 1960).
2. J. A. Stone, J. A. Kelley, and T. S. McMillan, Sampling and Analyses of SRP High-Level Waste Sludges, USERDA Report DP-1399 (August, 1976).
3. J. A. Stone, Separation of SRP Waste Sludge and Supernate, USERDA Report DP-1441 (November, 1976).
4. N. V. Solomin, "Chemical compounds in borate glasses;" Structure of Glass Symposium I, Leningrad, November 23-27, 1953.
5. D. Walmsley, B. A. Sammons, and J. R. Grover, Volatility Studies of Glasses for the Fingal Process, AERE-R5777 (July, 1969).
6. G. A. Kolykov, "Selective volatilization of components of the System $\text{Na}_2\text{O}-\text{B}_2\text{O}_3-\text{SiO}_2$ as a method for studying the glassy state;" Structure of Glass Symposium I, Leningrad, November 23-27, 1953.
7. D. F. Barlow, "Volatilization of fluorides, borates and arsenic from glass;" VIIIth International Congress on Glass, Brussels, June 28-July 2, 1965.
8. G. Rudolph, et al., "Lab scale R&D work on fission product solidification by vitrification and thermite processes;" Symposium on the Management of Radioactive Wastes from Fuel Reprocessing, KFK-1743, OECD-NEA and IAEA, Paris, November 27 - December 1, 1972.
9. J. E. Mandel, et al., Annual Report on the Characteristics of High Level Waste Glasses, USERDA Report BNWL-2252 (June 1977).
10. R. C. Rastogi, J. D. Schgal, and K. T. Thomas, Investigation of Materials and Methods for Fixation of Low and Medium Level Radioactive Waste in Stable Solid Media, BARC-304 (1967).
11. R. C. Rastogi, J. D. Schgal, and K. T. Thomas, Investigation of Materials for Fixation of Low and Medium Level Radioactive Waste in Stable Media, AEET-250 (1966).
12. M. J. Kupfer and W. W. Schulz, The Endothermic Process-Application to Immobilization of Hanford in-Tank Solidified Waste, ARH-2800 (July, 1973).
13. J. A. Kelley, Evaluation of Glass as a Matrix for Solidification of Savannah River Plant Waste: Nonradioactive and Tracer Studies, USERDA Report DP-1382 (May, 1975).
14. G. H. Thompson and J. A. Kelley, Evaluation of Methods for Retention of Radioiodine During Processing of Irradiated ^{237}Np , USERDA Report DP-1373 (June, 1975).

15th DOE NUCLEAR AIR CLEANING CONFERENCE

15. E. G. Orebaugh and W. H. Hale, Jr., Dispersion Study of Buried Elemental Mercury, USERDA Report DP-1401 (July, 1976).
16. R. M. Barrer and J. L. Whiteman, "Mercury uptake in various cationic forms of several zeolites;" Chem Soc., 19, (1967).

DISCUSSION

DEMPSEY: How does your program relate to the similar work underway at Pacific Northwest Laboratory? Do you see any insurmountable obstacles in control of off-gases from the vitrification process?

WILDS: First, the two programs have several common areas. For example, PNL is currently conducting large scale tests with simulated SRP waste. We expect to obtain data on sodium borate volatility and particle sizes of volatile species from that work.

Second, the answer is no. I believe that with our current research and development programs, we are well on our way to defining an adequate off-gas clean-up system.

GIRTON: What are your Hg concentrations in the off-gas?

WILDS: The concentration of mercury will depend on the particular waste being processed since, as I previously mentioned, the composition of SRP waste is quite variable. However, the initial concentration of mercury from an average waste composition is expected to be $\sim 4 \times 10^{-4}$ g/l. This concentration will be reduced to 3×10^{-6} g/l prior to entering the mercury adsorber bed. The temperatures of the off-gas stream are 300°C initially and $\sim 20^\circ\text{C}$ entering the adsorber.

McFEE: Have you speculated as to the mechanism of sodium metaborate volatility? Is it simply vaporization of sodium metaborate, or is there another mechanism going on?

WILDS: We haven't done a lot of work trying to determine the exact mechanism, but I believe it is sodium metaborate that vaporizes. We're using a premelted frit so we're not simply putting the material in as sodium carbonate and boric acid. The frit we put into our glasses has already been melted so, presumably, we have sodium and boron already in a network and I think it's simply volatilizing as a compound.

McFEE: Have you tried to check the vapor pressure of sodium metaborate against your results?

WILDS: We have done a little of this in our Newton cell measurements. It's in a very early stage of development.

McFEE: I'm aware that the orthoboric acid is nonvolatile but in the presence of water vapor becomes volatile. Are you seeing the same effect?

15th DOE NUCLEAR AIR CLEANING CONFERENCE

WILDS: I really don't know. The only indication we've had is when we had a melt with boric acid present, or some sodium tetraborate present, we would get volatilization as boric acid and not as the sodium metaborate. We have tested that. I think I should be very careful in stating that when we get sodium metaborate, we get it from the premelted fret. When we use batch chemicals, we do not get sodium metaborate. We do get crystals of boric acid and, presumably, some boric oxide coming off as well. We have made limited measurements of sodium metaborate vapor pressures. These studies indicate that the mechanism of sodium borate volatility is simple vaporization. References 4, 6, and 7 of this paper confirm that sodium metaborate vaporizes without decomposition up to temperatures of 1400°C.

15th DOE NUCLEAR AIR CLEANING CONFERENCE

DISPOSAL OF HEPA FILTERS BY FLUIDIZED BED INCINERATION

Donald L. Ziegler and Andrew J. Johnson
Rockwell International
Atomics International Division
Rocky Flats Plant
Golden, Colorado

Introduction

High efficiency particulate air filters (HEPA) are used in virtually all nuclear facilities, the majority in main production building exhaust plenums and others on smaller unit operations. These filters must be periodically changed, due to radioactive contamination or flow restriction by trapped particulates. Used, and/or radioactively contaminated HEPA filters constitute a high volume, low density waste stream that must be disposed of by a safe and efficient method. Presented in Table I, are approximations of the HEPA filter usage in some of the nuclear facilities which gives some idea of the magnitude of this waste stream.

Table I. HEPA Filter Use At DOE Facilities
Calendar Year 1977 Partial Listing

<u>Facility</u>	<u>Filter Size</u>	
	<u>Plenums</u> <u>2 ft x 2 ft x 1 ft</u>	<u>Unit Operation</u> <u>Other Smaller Size</u>
Hanford	500	-
Livermore	200	-
Lovelace	250	-
LASL	500	1500
Mound	100	350
Oak Ridge	150	525
Sandia	85	15
Savannah River	-	325
Rocky Flats	2600	1300
Total	4385	4015

One factor that must be considered in the development of a method for HEPA filter disposal is the waste acceptance criteria now being established for the waste isolation repository. It is highly unlikely that unit HEPA filters will be acceptable under proposed criteria on flammability, gas generation, and leachability.

Discussion

The HEPA filter, packaged as a unprocessed unit, occupies a comparative large volume, estimated at about 85% empty volume. The general composition of a HEPA filter, given in Table II, illustrates this point.

15th DOE NUCLEAR AIR CLEANING CONFERENCE

Table II. HEPA Filter Composition
Size: 2 ft x 2 ft x 1 ft

<u>Component</u>	<u>Weight (lbs.)</u>	<u>Volume (ft³)</u>	<u>Density (lbs./ft³)</u>
Frame	25.1	0.5	50.1
Media	<u>16.1</u>	<u>3.5</u>	<u>4.6</u>
Unit Filter	41.2	4.0	10.3

Frame: 3/4 inches plywood or particle board - phenolic resin bonded.
Media: Fiberglass and fibrous asbestos with corrugated asbestos paper separators.

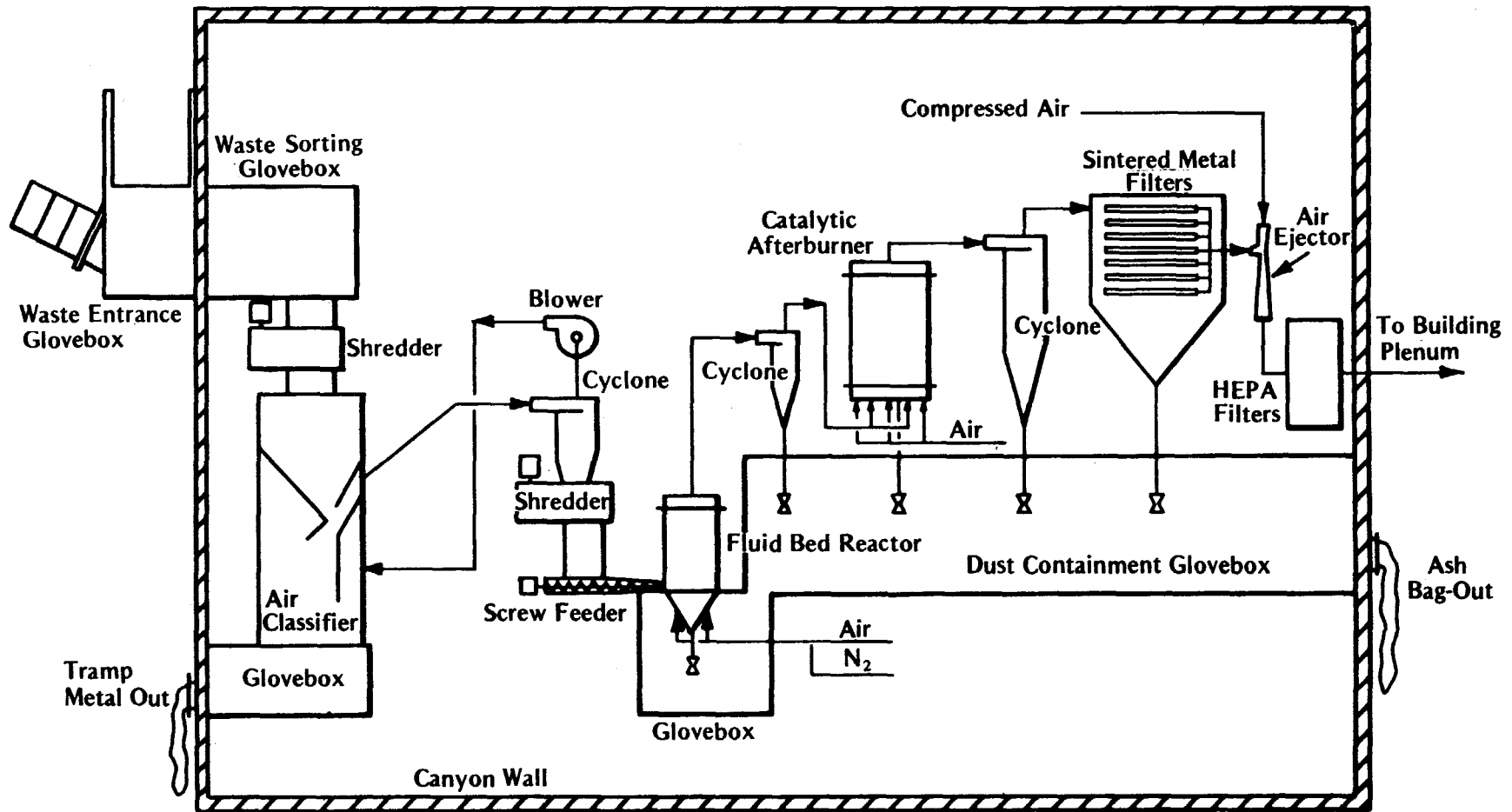
Present methods of HEPA filter disposal vary according to the level of contained radioactivity. The large 24 inch by 24 inch by 12 inch filters from building exhaust plenums usually fall into the low level TRU Waste category. A simple arbor press is used to break the filter into an elongated diamond configuration, the pressed filter is wrapped with a wire tie, and plastic bagged before packing in a crate for shipment. The compression allows only a few more filters to be packed per crate. Filters containing significant levels of radionuclides are generally the smaller size used on unit operations and gloveboxes. The present disposal method used at Rocky Flats is to cut the media out of the frame with a reciprocating saw, send the media to reprocessing, and incinerate the frame. A method being developed is to punch the media from the frame with a hydraulically operated ram and an extruding die. This process will provide a separation of the frame from the media and result in a significant volume reduction of the media.

The applicability of these disposal methods for future use must be assessed in light of the proposed criteria for the permanent waste storage repository. A study on the content of filters that had been in use for direct filtration of unit operations indicated the presence of absorbed H₂O, HF, and HNO₃.⁽¹⁾ These components could also react with particulate matter trapped in the media. It is evident that outgassing, or gas generation from HEPA filters is a distinct possibility. Another matter of concern is leachability. The same study also included the measurement of weight loss due to water leaching. In addition to the constituents leached, the leach solution was found to be acidic. This could cause problems when contacting other stored materials.

Incineration Process

The incineration of the entire filter would offer advantages over other present methods of disposal. It would be a one step operation, material trapped in the media would be destroyed, and the residue would be in an ideal form for further reprocessing. The fluidized bed incinerator used for test burns of HEPA filters is shown in Figure 1. The small nails used in the filter frame cause no problem either to the shredder or the screw, which feeds into the incinerator. Shredding of used filters does generate some dusting, but the low speed cutters hold this to a minimum. As the dust is about 95% non-combustible asbestos and glass fibers, no dust explosive hazard is presented.

As mentioned earlier, only the wooden frame comprising about 61% of the filter weight is combustible. This results in a large amount of residue, or ash, from the incineration. Reduction, by incineration, was approximately 4.4 to 1 in volume and 2 to 1 by weight. The residue, collected from the cyclone separators



FLUIDIZED BED INCINERATION PILOT UNIT
FIGURE 1

15th DOE NUCLEAR AIR CLEANING CONFERENCE

and sintered metal filters, is a fine powdery material. Without further treatment this material may be unacceptable for storage in the waste repository. Proposed criteria does not allow material present as respirable fines.

Immobilization of HEPA Filter Ash

Various methods of waste immobilization have been tested at the Rocky Flats Plant over the past few years. For our use, and because it appears to best meet repository acceptance criteria, vitrification was selected as the most promising immobilization method. The composition of HEPA filter media, shown in Table III, appears to be an ideal feed for a vitrification process. Two vitrification alternatives were tested, 1) punching out the media, feeding it into the vitrification process, and incinerating the frame, and 2) incinerating the entire filter and vitrifying the incinerator residue.

Table III. Composition of
HEPA Filter Media

Component	Weight Percent		
	Fiber Glass Filler	Crocidolite Filler	Crysolite Separators
SiO ₂	60	51.1	46.7
MgO	13	2.3	50.7
Al ₂ O ₃	21	-	0.2
CaO	6	-	-
FeO	-	35.8	0.8
Na ₂ O	-	6.9	-
H ₂ O	-	3.9	-
Fe ₂ O ₃	-	-	1.6
Weight Represented	23.5	1.5	75

The first alternative was tried in a series of crucible tests. Heating HEPA filter media at 1100°C, with no fluxing aids added, did not produce a glass. By the addition of 20% boric oxide and 10% sodium oxide, a glass with a workable viscosity range could be obtained only after holding the melt at 1150°C for one hour. In all the tests, the media was first pulverized using a laboratory ball mill; unground media was impossible to vitrify under any of the test conditions. The necessity of the ball milling step, and the 1150°C operating temperature, diminished the desirability of reacting HEPA filter media separately.

Incineration of HEPA filters can be handled by "campaigning" the filters or by incinerating them with a mix of general solid waste. The first batch of filters incinerated were "campaigned", producing a residue from filters alone. This ash was used for another series of crucible vitrification tests. The present Rocky Flats bench scale vitrification system uses an Inconel 690 reactor vessel, and it is desirable to hold the process temperature around the 1050°C operating level. For this reason, these crucible tests were limited to a 1050°C maximum temperature.

The initial test was made with 20% boric oxide and 10% sodium oxide added to the filter residue as fluxing aids. This mixture, at 1050°C, would not produce a pourable melt. However, mixtures of 50% HEPA filter ash with 50% general solid waste ash was found to produce a good viscosity range glass at 1050°C when 20% boric oxide and 10% sodium oxide was added. The incineration of mixtures of HEPA

15th DOE NUCLEAR AIR CLEANING CONFERENCE

filters and general waste appears to offer a residue amenable to vitrification in the Rocky Flats Plant vitrification process.

A major advantage of vitrification is the volume reduction obtained by immobilizing waste in a glass matrix. The residue from incineration of solid waste has about the same density as HEPA filter residue, roughly 0.5 on the average. By the addition of 20% boric oxide and 10% sodium oxide, glass with a density of 2.5 can be produced. The volume of additives will be about 30% of this, leaving a volume reduction factor of 3.75 for going from ash into a glass waste form.

Conclusions

1. Present methods of handling HEPA filters produces a waste probably unacceptable at a permanent repository.
2. HEPA filters can be successfully incinerated using a fluidized bed incinerator.
3. Separation of the frame from the media and incinerating only the frame is an unnecessary operation.
4. The residue from incineration of HEPA filters can be processed into a glass acceptable under proposed repository criteria.

Reference

1. R. W. Woodard, K. J. Grossaint, and T. L. McFeeters, "Exhaust Filtration on Gloveboxes Used for Aqueous Processing of Plutonium", Proceedings of the Fourteenth ERDA Air Cleaning Conference, Sun Valley, Idaho, 1976, USERDA Report CONF-760822 (1977). (Reviewed as RFP-2495)

DISCUSSION

MURROW: Most of the nuclear power plant regulatory guides require a metal frame. Can you separate the frames from the media and do something with the two components separately?

JOHNSON: At our plant, we have worked on a combination punch and compressor to merely punch the medium out of the frame. So, if you have to use a metal frame, you could go that route. Then you'd have the metal left over as contaminated material that you might be able to decontaminate by electropolishing or other methods. In our plant we use all wooden frames.

CHOI: Do you see any advantage in using fluidized bed incinerators for the HEPA filter?

JOHNSON: For HEPA filters alone, maybe not. But since we have one operating and we use it for all types of waste, we generally just combine the filter waste with the rest of the waste.

15th DOE NUCLEAR AIR CLEANING CONFERENCE

CHOI: So there's no real advantage or disadvantage in using other types of incinerators for the HEPA filter.

JOHNSON: Probably not. Although, our residue comes out as extremely fine particles that are ideal for mixing with the flux to make a glass.

CHOI: The point that you made at the end of the session was that industry really needs a type of HEPA filter that can be processed and, indeed, we find that this is the best solution for Ontario Hydro. We have to change over 1,000 HEPA filters a year at just two stations and we will have more stations in the future. At \$30 per cubic foot, that's a lot of money. That's why Ontario Hydro is seeking types of filters that are processable. In other words, we will try to avoid metal parts as much as possible in the HEPA filter.

BURCHSTED: That was one of the points I was also going to make. People here are probably using metal frame filters instead of wood and that presents a different situation when considering incineration. The other point is that most of the people here are using either aluminum separators or a separatorless construction so this magnesium oxide you talked about probably would not be a problem for most other organizations. I think you're the biggest user of asbestos separators today.

JOHNSON: Yes, we are by far. We used over half of those I mentioned.

BURCHSTED: Yes, the absence of asbestos separators does simplify the problem for other people considerably.

JOHNSON: Yes, it does. Thin aluminum would give us no problem in our shredding operations or in vitrification.

DEMPSEY: Does the small size of the particles inherent in the glass making process pose any special problems?

JOHNSON: Right now we are working on our vitrification unit. We are using a modified moving bed filter. Yes, it is a problem. The effluent from glass making pots does produce offgases that are very difficult to handle. And we do get vaporized sodium chloride as one of our main compounds. Off-gas filtration has been a problem in all vitrification processes.

15th DOE NUCLEAR AIR CLEANING CONFERENCE

VOLUME REDUCTION OF LOW-LEVEL, COMBUSTIBLE, TRANSURANIC WASTE AT MOUND FACILITY

W. H. Bond, J. W. Doty, J. W. Koenst, Jr. and D. F. Luthy
Mound Facility*
Miamisburg, Ohio 45342

Abstract

Low-level combustible waste (<100 nCi per g of waste) generated during plutonium-238 processing is collected and stored in 55-gallon (200-liter) drums. The composition of this waste is approximately 32 wt % paper, 46% plastic, 16% rubber and cloth, and 6% metal. Treatment of this waste is initiated by burning in the Mound Cyclone Incinerator, which consists of a burning chamber, deluge tank, venturi scrubber and blower.

During the two years of operating the Cyclone Incinerator, experiments have been performed on particle distribution throughout the system using various mixtures of feed material. Measurements were taken at the incinerator outlet, after the spray tank, and after the venturi scrubber. An average emission of 0.23 g of particles per kg of feed at the venturi outlet was determined.

The distribution of chlorine from the combustion of polyvinyl chloride was studied. Analyses of the off-gas and scrubber solution show that approximately 87 wt % of the chlorine was captured by the scrubber solution and approximately 0.6 wt % remained in the off gas after the venturi scrubber. Measurements of the amount of NO_x present in the off-gas were also made during the chloride studies. An average of approximately 200 ppm NO_x was produced during each incineration run.

Immobilization of the incinerator ash is being studied with regard to long-term behavior of the product. The immobilization matrix which looks most promising is ash mixed with Portland 1A cement in a 65/35 wt % ash-to-cement ratio. This matrix exhibits good mechanical properties while maintaining a maximum volume reduction.

Cyclone Incineration

The Mound Cyclone Incinerator project, funded by the Division of Waste Management of the U. S. Department of Energy, has as its goal the development of processes that will reduce combustible, low-level radioactively contaminated waste to a compact, inert material suitable for long-term storage or burial. At present, combustible waste, contaminated to <100 nCi of plutonium-238 per gram of waste,

*Mound Facility is operated by Monsanto Research Corporation for the U. S. Department of Energy under Contract No. EY-76-C-04-0053.

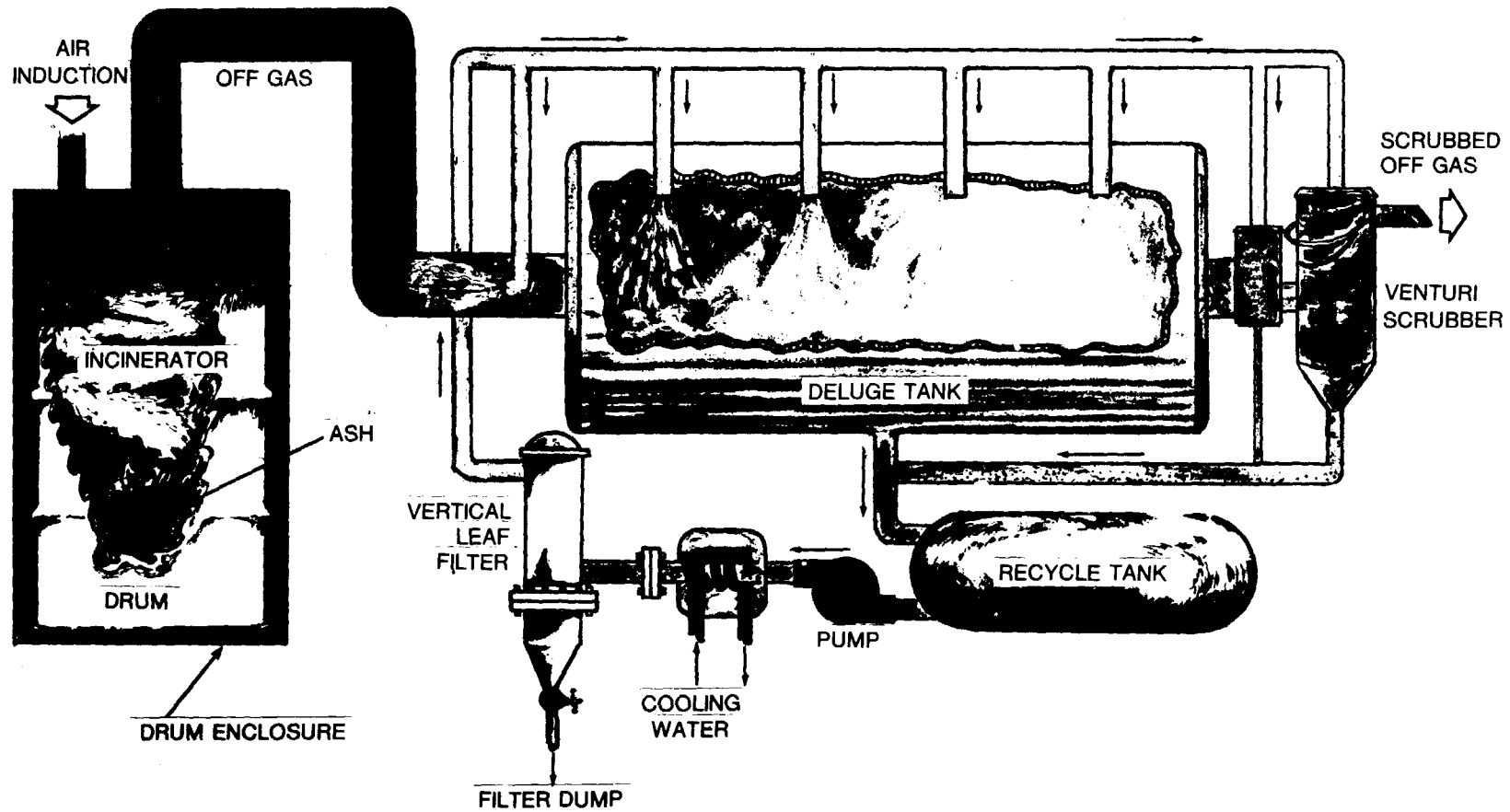


Figure 1—Mound Cyclone Incinerator

15th DOE NUCLEAR AIR CLEANING CONFERENCE

is being incinerated on a routine basis. To date, a quantity of contaminated waste in excess of 5,000 kg has been incinerated. This waste was generated in the course of plutonium processing at Mound. The ash resulting from incineration receives further treatment to achieve immobilization during long-term storage.

Details of the Cyclone Incinerator are shown in Figure 1. The Cyclone Incinerator normally uses a 55-gallon (200-liter) drum as the burning chamber. The advantages of using the drum in which the waste has been shipped or stored are that 1) radioactive waste handling is reduced to removing the lid from the drum; and that 2) the drum, which is subjected to destructive thermal shock during combustion, is expendable, providing an inexpensive, easily replaceable burning chamber.

Previously, combustion air was introduced to the primary burning chamber through a single adjustable inlet (see Figure 2). Vertical movement of the inlet was provided to follow the burning interface as it progressed down the drum. Movement about the vertical axis was made possible to experimentally determine the optimum angle of air introduction. This angle is vital to the creation of the cyclone effect -- the heart of the cyclone incinerator. The cyclone effect produces a spiraling airflow down the inside burning chamber surface which cools the metal while preheating the air. When the airstream reaches the fuel surface, it not only supplies oxygen for combustion, but also agitates the top layers of fuel, resulting in a thorough mixing of oxygen and fuel in the combustion zone. The air sweeps across the fuel surface to the center of the chamber and rises to exit through the centrally located exhaust at the top of the chamber. The products of initial combustion, which include particles of unburned fuel and combustible gases (see Tables I and II), are retained in a high-temperature environment by the cyclone effect in the primary burning chamber. Combustion is continued in a secondary burning chamber which incorporates a baffle to prolong particle retention time in the hot zone.

Table I Characteristics of the off-gas stream.

	<u>mg/m³</u>
Combustion Chamber Outlet	504.9
Deluge Tank Outlet	236.6
Venturi Scrubber Outlet	18.4
Primary HEPA Filter Outlet	Nil
	<u>°C</u>
Temperature, Average at Outlet	1090
Temperature, Maximum at Outlet	1320

More recently, an experimental lid assembly has replaced the upper burn chamber. The air inlets are placed 90° apart around the cylinder to provide a smoother air flow and are directed toward the side of the cylinder both to cool the metal and to initiate the swirling action that was previously found to be so important to burning in a drum.

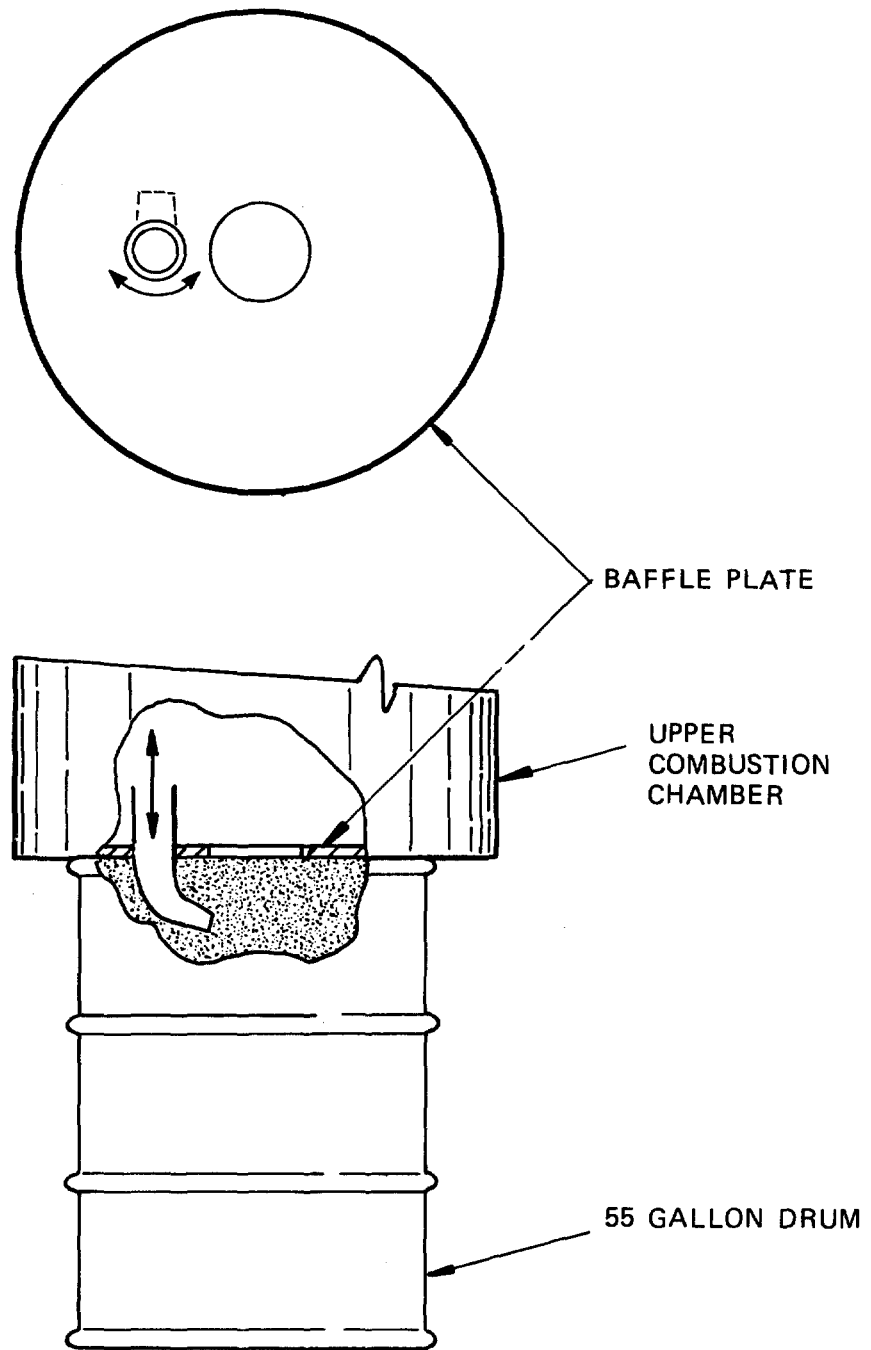


Figure 2 - Adjustable air inlet.

15th DOE NUCLEAR AIR CLEANING CONFERENCE

Table II Analysis of cyclone incinerator off-gas.

<u>Component</u>	<u>Treated Off-Gas</u>
Carbon Dioxide	9.0 wt %
Oxides of Nitrogen	10-600 ppm
Oxygen	13.5 wt %
Sulfur Dioxide	Not Detectable

The lid was installed to improve combustion characteristics such as burning rate, amount of combustible material in the ash, and particle carry-over to the off-gas system. Experiments conducted with the new lid assembly show improvements in the burning rate and in the amount of combustible material in the ash. Particle carry-over measurements are inconclusive so far.

Treatment of the incinerator off-gas begins with a deluge tank which cools the off-gas, neutralizes the acid agases, and removes a high percentage of the particles entrained in the off-gas. Further particle removal is accomplished by a high-energy venturi scrubber. The liquid used in the deluge tank and venturi scrubber is a sodium carbonate or sodium hydroxide solution which is recirculated through a heat exchanger for cooling and a vertical leaf filter for suspended solids removal.

The exhaust gas, cooled to about 65°C, passes through a HEPA filter before being discharged by a blower to the building exhaust. The blowers provide the airflow for the combined incinerator/off-gas system and maintain the system at a negative pressure relative to the room, thus simplifying contamination control and operational safety.

Volume and Weight Reduction

One of the ultimate goals of waste reduction is to achieve a maximum volume reduction, although the performance of waste reduction processes cannot be accurately measured by using volume reduction alone. Waste densities vary considerably and directly affect reduction measurements. Not only does tightly packed waste contain less volume than the same amount of loosely packed waste, it also requires longer combustion times. Therefore, both weight and volume reduction measurements are necessary to fully evaluate the performance of a waste reduction system. To determine the volume/weight reduction of the Cyclone Incinerator a series of 45 drums of waste was incinerated. The results are summarized in Table III.

The "incinerator ash" includes the remains in the combustion chamber but excludes metals present in the feed material. The "solids in the scrubber solution" consist of fly ash and precipitated salts formed during neutralization; they are collected in the vertical leaf filter. The sodium carbonate scrubber solution is controlled to a pH of approximately 9 by the addition of fresh carbonate solution. When the dissolved solids (NaCl, Na₂SO₄, and NaHCO₃) reach a maximum of 210 g per liter (solubility limitation), the scrubber solution is replenished. The "solid from waste treatment" is sludge generated during the chemical treatment that removes radionuclides from the spent scrubber solution. This treated scrubber solution is combined with other waste streams, and discharged to the environment.

15th DOE NUCLEAR AIR CLEANING CONFERENCE

Table III Volume/weight reduction for the cyclone incinerator.

Input		Material	Output	
Wt(kg)	Vol(m ³)		Wt(kg)	Vol(m ³)
1574	9.172	Incinerator Ash	86.9	0.153
		Solids in Scrubber Solution	76.6	0.086
		Solid from Waste Treatment	<u>3.3</u>	<u>0.004</u>
		Total	166.8	0.243
		% Reduction	89.4	97.4

Using feed material containing approximately 18 wt % chloride and 2 wt % sulfur, the spent scrubber solution has been found to contain 14.9 wt % NaCl, 4.3 wt % Na₂SO₄ and 1.4 wt % NaHCO₃. Considering these primary and secondary waste streams, a total of 1574 kg of waste was reduced to 166.8 kg, giving a reduction factor of 9.4 to 1. The volume reduction accomplished was 97.5% (volume reduction factor of 37.8 to 1).

Mode of Operation

The cyclone system can be operated in a batch or continuous mode using solid or liquid feed. The batch method is ideally suited for wastes from storage or those requiring transportation, because it allows in-situ burning in the original drums. This is the normal mode of operation for waste currently being processed at Mound.

Continuous feeding is preferred when sufficient amounts of waste are generated in one place and packaging in drums would be a needless operation. Advantages of continuous feeding are that 1) total pollutants per quantity of feed burned are fewer, because most pollutants come from the cyclone incinerator during startup and shutdown and that 2) the metals in the incinerator will last longer because of fewer thermal cycles. The disadvantage of continuous feeding is increased capital and operating costs for an additional step, since the feed must be sorted and shredded in order to be fed to the incinerator.

The first attempt at continuously feeding the Cyclone Incinerator was made by dropping shredded feed into an air inlet line with a rotary valve fed from a bin. Jamming of the rotary valve was the major fault of the system. The second attempt will be with a screw feeder and a revised bin. Feed rates up to 50 kg/hr were achieved with the rotary valve system.

Experiments have shown that the cyclone system can also reduce volumes of combustible liquids. For example kerosene, kerosene/tributyl phosphate and vacuum pump oils have been burned.

15th DOE NUCLEAR AIR CLEANING CONFERENCE

For burning combustible liquids, a commercial oil burner, designed to burn all types of fuel oils, was chosen as the primary combustion unit. The steel drum combustion chamber was modified somewhat with the addition of a castable refractory liner and the installation of the oil burner at the base of the drum. Interchanging the burn chambers is a practical way of providing multiple fuel burning capabilities with minimum effort. The induced air current is as useful as in the solid-batch incineration; it prolongs retention time in the high-temperature zone so that all necessary secondary combustion can be completed. No changes were considered to be necessary in the off-gas handling system.

Several safety devices have been installed to protect against a possible local concentration of flammable vapors. A propane pilot flame with automatic ignition was installed to initiate liquid burning. In the event that an oil flame would extinguish through blow-out, feed cut off, etc., an ultraviolet sensor automatically re-ignites this pilot flame.

Tests using liquid feed have shown that mixtures of tributyl phosphate (TBP) and kerosene burn readily, at least in the percentages used. It was found that igniting kerosene alone, prior to feeding the mixture, resulted in a superior initial burning of the mixture. The feed rate, after ignition, was 15 liters per hour. At this feed rate, the scrubber cooling system approached capacity. Increased cooling capacity would, therefore, be necessary for a higher feed rate. The primary conclusion of this experiment was that the incinerator system can handle the mixture of 30% TBP-70% kerosene common to the nuclear industry.

Off-Gas Composition

We have extensively monitored the exhaust from the Cyclone Incinerator to determine the effectiveness of the scrubbers in removing acid gases generated in the combustion of materials commonly used in nuclear operations. The data in Table IV were collected during the incineration of waste containing 18 wt % chloride and 2 wt % sulfur. Because no externally fueled burner is utilized for solid waste combustion in the Cyclone Incinerator, the composition of the waste determines the peak temperatures of combustion which range from 1100 to 1300°C.

Table IV Typical off-gas analysis for cyclone incinerator.

<u>Component</u>	<u>Treated Off-Gas</u>
Carbon Dioxide	9.0 wt %
Oxides of Nitrogen	10-600 ppm
Nitrogen	66.2 wt %
Hydrogen Chloride	1-13 ppm
Oxygen	13.5 wt %
Sulfur Dioxide	Not detectable
Water	11.0 wt %

15th DOE NUCLEAR AIR CLEANING CONFERENCE

A series of chloride mass balance runs was made to define more clearly the disposition of chlorides generated during the combustion of polyvinyl chloride (PVC) in the cyclone incinerator. Known amounts of PVC were burned. Before the first run and after each succeeding run, the scrubber solution was sampled for chloride. A collection train monitored the off-gas prior to the HEPA filter. Chemical analysis indicated that 87 wt % of the chlorides in the PVC went into the scrubber solution and a statistical average of 0.6 wt % showed up in the off-gas. The remaining 12 wt % is unaccounted for, but most likely some remained with the ash and some was attached to solids removed from the scrubber solution by the liquid filter.

We have also monitored the off-gas during liquid incineration. A solution of potassium hydroxide was cycled through the deluge tank and venturi scrubber to remove phosphates from the flue gas stream. The scrubber system effectively removed phosphates from the off-gas. Measurement of phosphates in the flue gas indicated a range of from 0.3 to 2.1 ppm at an average phosphate concentration of 1.3 ppm.

Extensive particle monitoring was performed at appropriate points in the incineration system during combustion of simulated wastes to assess the effect of adjustments to the system, to determine the effectiveness of the off-gas system components and to estimate the HEPA filter life expectancy. The HEPA filter, unlike the off-gas system components, is not self-cleaning and must be replaced when loaded. A low loading rate is desirable from operating cost and volume reduction aspects.

Radioactive contamination of actual waste has made particle sampling more difficult, but at points where comparisons have been made, the size and distribution of particles are nearly identical for all types of feed.

Immobilization

Controlled experiments were conducted on the selected pressed-pellet matrix chosen for the immobilization process of incinerator ash residue. The experiments were designed to provide data for evaluation and selection of the best pellet matrix for incinerator ash and Portland Type 1A cement.

Certain process parameters previously determined and evaluated during screening studies with the pressed ash-cement matrix were fixed throughout the entire experimental sequence. The parameters in the process which were held constant are:

1. Pressing pressure of 25,000 psi for 1-min duration.
2. Three-gram matrix weight.
3. One-half inch pressing die, which, with a 3-g charge, produces a relatively standard 1/2-in. diameter by 1/2-in. high pellet (L/D ratio approximately 1).
4. Dry Cure Cycle - two days (48 hr) in open atmosphere.
5. Wet Cure Cycle - four-day (96 hr) cure in distilled water followed by a two-day cure in open atmosphere.

15th DOE NUCLEAR AIR CLEANING CONFERENCE

Five groups of waste matrices samples were evaluated during the controlled experiments. Pellets were pressed with 60%, 65%, 70%, 80% and 0% ash residue (100% Portland 1A cement). The pure cement pellets were pressed for control comparison conditions. The water-to-cement ratio was varied in each sample group to determine the water-to-cement ratio which would produce acceptable pressed pellets. Normally, six water-to-cement ratios were evaluated ranging from a too dry condition (fracturing pellet matrix after pressing) to a wet condition (excess water ejected from die during pressing operation).

The control condition matrix (100% Portland 1A cement) containing 0% incinerator ash at acceptable water-to-cement ratios produced nearly identical pressed pellets. The dry-cure method produced pressed pellets of uniform compressive strength, density, and final weight. Based on the final weight of the pellets, the calculated percentage of water remaining in the matrix is approximately 2% for the dry-cure method. Similarly the wet-cure method produced pressed pellets also of uniform but higher compressive strength, density, and final pellet weight. However, the wet-cure method retained approximately 10% water in the matrix form.

The data shown in Table V for the 60%, 65%, 70% and 80% ash-cement pressed matrices are given only for the two best water-to-cement ratios even though four acceptable and tested water-to-cement ratios were attained. The data clearly indicate that the wet-cure method produces ash-cement matrix having higher compressive strength than pellets which were dry cured. In general, the compressive strength increased as the percent of ash in the matrix decreased. This result was expected since the cement (binder) contributes significantly to the pellet compressive strength.

As the percent of incinerator ash was increased, the water-to-cement ratio also increased. This was also expected as observed in past screening studies conducted on the ash-cement pressed matrices. Although a small portion of water must be required for cement interaction and blending, the ash requires significant amounts of water to wet the ash because of its hydrophilic characteristic. Although this condition exists, the final pellet weights after curing are close in final weight value as the 0% ash matrix final weight. The 60/40 ash-cement matrix after wet-cure processing, however, gained weight; the reason for this is presently being investigated.

The density of the various ash-cement pressed pellets increased as the percent of ash decreased. The density ranged from 83-88% of the 0% ash-cement pressed matrix; however, the density values calculated for the ash-cement various matrices were taken, and the radiographs clearly show that no void, crack, or fissure exists in any of the ash-cement pressed pellet matrices.

Mechanical strength and corresponding percent weight loss of the various pressed pellets were also determined. The pressed pellets were placed in stainless steel containers which were clamped into a Model BT Wrist Action Shaker. The shaker was set at the maximum 10° shake angle to vibrate the samples in a circular motion inside the fixed container. The shaking action was continued for 50 hr, and the weight loss was determined. The resulting weight losses are also shown in Table V. All the samples experienced a slight rounding of

the edge that contacted the stainless steel container; one slight abrasion occurred on the walls of the samples. Figures 3 and 4 are photographs of the 100% cement pressed pellet before and after the shake test. Radiographs of the pellets taken before and after the shake test showed that the pellets were still homogeneous and contained no voids, cracks, or fissures. Although the percent weight loss is higher for the 60%, 70% and 80% ash-cement pressed matrices as compared to the 100% cement pressed matrices, this result would be expected based on the lower compressive strength values.

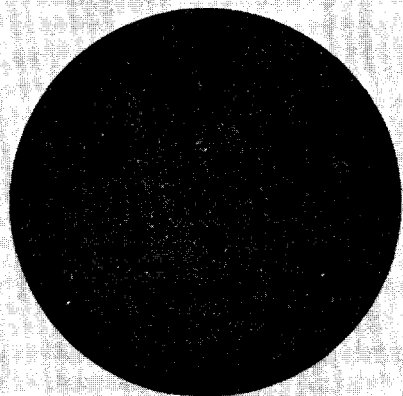


Figure 3 Pellet before shake test.

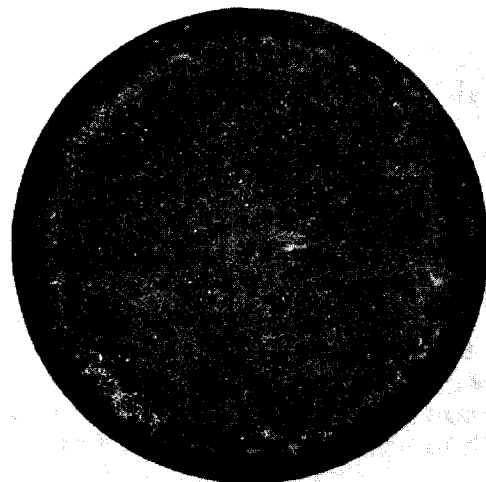


Figure 4 Pellet after shake test.

Volume Reduction Efficiency

Prior to the initiation of the controlled experimentation on the ash-cement matrix process, a new batch of incinerator ash was prepared with the cyclone incinerator. The composition of the incinerator feed was Type I, which consisted of 32 wt % paper, 9 wt % PVC, 29 wt % polyethylene, 8 wt % polypropylene, 13 wt % rubber, 3 wt % cloth, and 6 wt % metal. A total of 11.2 kg (24.6 lb) of the uncompacted combustible composition (2.2 ft³) was burned in a 55-gal drum. The resulting ash, containing approximately 20% carbon, was then sintered for 1 hr at 800°C to reduce the carbon content to approximately 0.04% carbon. After grinding and sizing, the sintered ash weighed 340 g and contained a volume of 570 cm³.

Based on the pelletization process for a pressed ash-cement matrix ratio of 70/30, approximately 162 pressed pellets could be produced. These pellets would weigh approximately 494 g if dry cured and approximately 534 g if wet cured. The resulting volume of the immobilized matrix would be approximately 252 cm³ for the dry-cure product and approximately 256 cm³ for the wet-cure method. This analysis is based on the preliminary data obtained during the experimentation controlled processes (Table V).

15th DOE NUCLEAR AIR CLEANING CONFERENCE

Table V Pressed Ash-Cement Pellet Matrix
Controlled Experimental Process

Ash Type	Percent Ash	Percent Cement	Water/ Cement	Cure		Average Loss During Cure (wt %)	Density (gm/cm ³)	Compressive Strength (psi)	Shaking Loss (wt %)
				Dry	Wet				
	0	100	0.10	x		5.9	2.29	3635	
	0	100	0.125	x		6.1	2.30	3661	
	0	100	0.15	x		6.5	2.32	3668	0.50
	0	100	0.175	x		6.7	2.33	3670	
	0	100	0.10		x	2.1	2.43	4580	
	0	100	0.125		x	2.0	2.45	4330	
	0	100	0.15		x	1.5	2.47	4192	0.84
	0	100	0.175		x	1.2	2.49	4293	
I	60	40	0.45	x		6.2	2.00	3470	4.45
I	60	40	0.45		x	(4.1)	2.30	3600	3.21
I	60	40	0.50	x		8.9	2.00	3470	0.62
I	60	40	0.50		x	(3.5)	2.29	3620	4.33
II	65	35	0.60	x		11.8	1.90	3484	
I	65	35	0.60		x	5.5	2.21	3583	
II	65	35	0.60	x		7.9	2.51	3605	
II	65	35	0.60		x	5.2	2.56	3911	
III	65	35	0.25	x		2.7	2.47	3618	
S-UK*	65	35	0.60	x		7.4	2.08	3619	
S-UK*	65	35	0.60		x	3.3	2.18	3733	
I	70	30	0.70	x		11.0	1.96	2480	1.78
I	70	30	0.70		x	4.9	2.01	3640	3.70
I	70	30	0.75	x		11.1	1.96	3470	2.27
I	70	30	0.75		x	3.2	2.11	3625	3.63
I	80	20	1.10	x		7.1	1.92	2480	3.72
I	80	20	1.10		x	3.3	2.08	3600	3.84
I	80	20	1.15	x		7.9	1.92	2480	1.85
I	80	20	1.15		x	2.9	2.08	3570	4.45
I	80	20	0.70	x		9.0	2.03	~2507	
I	80	20	0.70		x	2.7	2.15	~3640	
I	80	20	0.85	x		9.0	2.04	~2500	
I	80	20	0.85		x	5.6	2.10	~3670	

*S-UK denotes pellets containing 3 wt % Na₂SiO₃ that were made with "unknown type" ash

15th DOE NUCLEAR AIR CLEANING CONFERENCE

The data indicate the overall process efficiency starting with uncompacted combustible Type I composition through incineration and immobilization is approximately 95% in weight reduction and approximately 99% in volume reduction.

The selected fixation process, which is a cement/ash pressed pellet matrix, was chosen on the basis of the waste matrix meeting known WIPP acceptance criteria and, also, with respect to simplicity of the process in terms of processing, process equipment, and operating costs. Figure 5 shows a flowsheet for the pelletization process of incinerator ash residue.

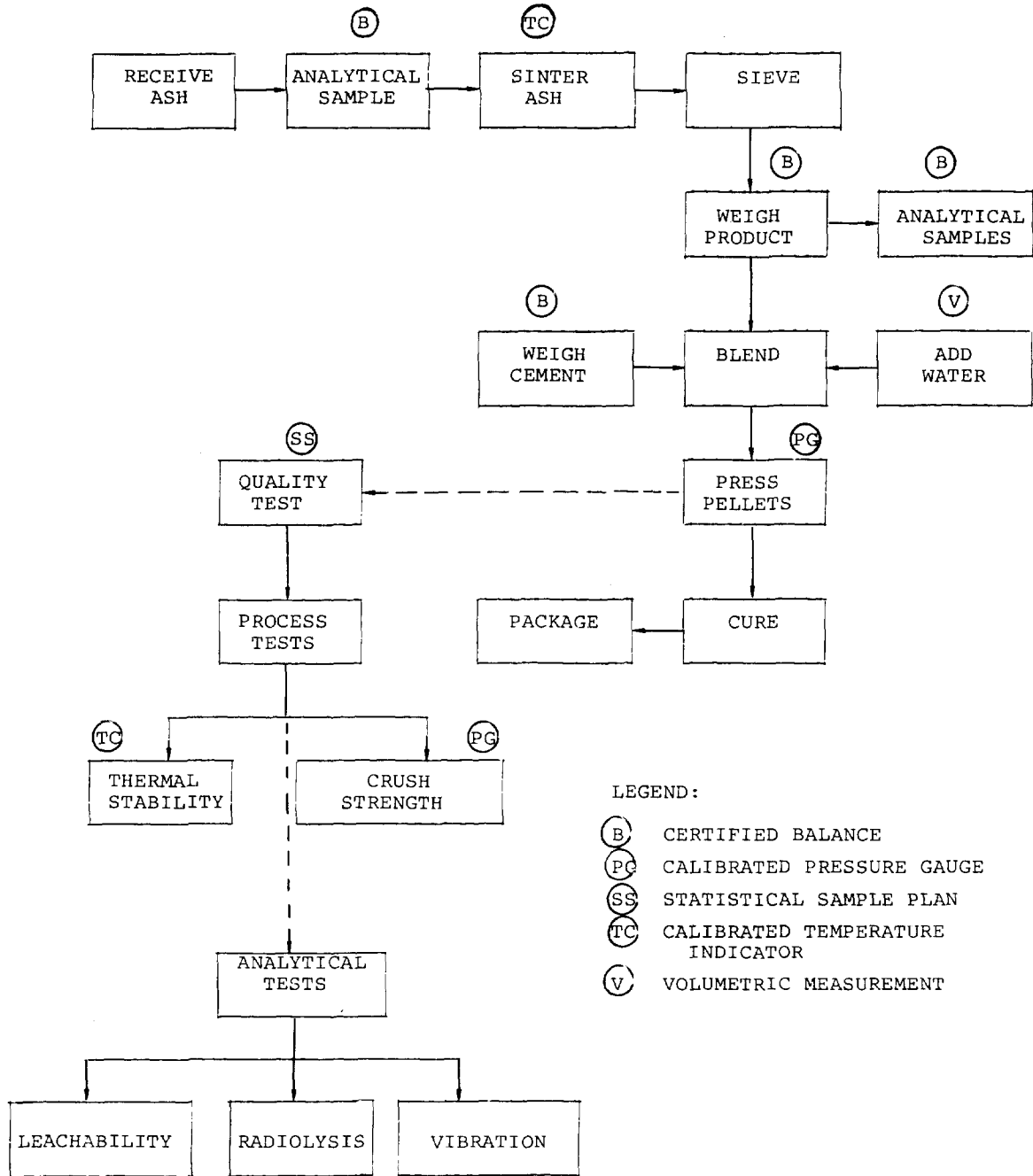


Figure 5 - Proposed Pelletization Flow Sheet.

15th DOE NUCLEAR AIR CLEANING CONFERENCE

DISCUSSION

BURCHSTED: I'd like to make an observation and ask two questions. First, I assume that the Venturi effluent efficiency of 95% for submicron particles is based on mass, and that the number efficiency would be closer to 5 or 10%.

BOND: That is correct. We have not measured numbers of particles in the submicron range.

BURCHSTED: Now, as to the HEPA filter, what was the air temperature?

BOND: That was the same as the scrubber outlet which was about 60°C.

BURCHSTED: Have you tried incineration of HEPA filters?

BOND: We have tried it. We, also, have only wooden frames that burn beautifully, but the asbestos, naturally, does not. It does, however, disintegrate. The reduction ratio is not as good as with more combustible waste. The filter must be broken up to fit inside a 55 gallon drum.

BURCHSTED: The comments I made before about aluminum separators would apply here, too?

BOND: Yes.

MURROW: The 60°C offgas, after going through the scrubber, would be pretty well saturated with water. Do you have any trouble with water condensation in the HEPA filter?

BOND: Yes, at one time we had a small amount of trouble. Subsequently, we added a heating element in the offgas line between the Venturi scrubber and HEPA filter which heats the offgas sufficiently to keep the water vaporized. The temperatures quoted in the talk were taken prior to the addition of the heater.

MURROW: Is your temperature high enough to avoid carbonaceous effluent from the materials you're burning, such as oils or plastics or rubber?

BOND: We have not detected any material of this sort coming from the combustion chamber. The design of the combustion chamber provides a cyclone action to both the incoming and exiting air which allows sufficient time for complete combustion of carbonaceous material.

MURTHY: Could you tell us what you do with the scrubber liquor that you get from both scrubbers?

BOND: Yes, at Mound facility the scrub liquor from the deluge tank and Venturi scrubber is combined in the recycle tank. The spent solution, at Mound, is processed in the plant waste disposal system. After processing, it is clean enough to be dumped into the river. We are working on a treatment method that will, when developed, provide an accessory to the cyclone system for use in applications where waste disposal facilities are not available, but we have not tested it yet. In fact, we haven't bought it yet.

ALVARES: What is used to measure aerosol at various incinerator stages? What reservations do you have about your efficiency results?

15th DOE NUCLEAR AIR CLEANING CONFERENCE

BOND: Leeds & Northrup Cascade impactors are used. We have no reservations. These data were taken over many incinerator runs with a wide variety of feeds. The results are consistently within a narrow range.

DEMPSEY: What are the binders in the pressed pellets that you spoke about? Do you press them without any binder at all? What binder do you use in the ideal pellets that you spoke about? What is the difference between "concrete pellets" and "pressed pellets"--if the latter also have concrete in them?

BOND: We use a small amount of water as a binder which is taken up by the cement and forms almost a concrete type of pellet. The second pellets were cast concrete. We mixed ash and cement with sufficient water to form concrete and these were then cast in molds. The others have just enough water to act as a binder and they are pressed in a die so that the water content is quite a bit lower.

DEMPSEY: Does the cement actually hydrate in the second case? Is it just a stoichiometric amount of water but not enough to be free water?

BOND: I'm not sure, but I believe that is the case.

COLLINS: Have you tried this on typical wastes from light water reactors; sludges and slurries? What about waste contaminated with iodine?

BOND: There were three types of waste that we have done experiments with, primarily paper, wood, leather, and rubber. We have tried a small amount of sludge mixed with the regular feed. The results were good, i.e., satisfactory burning. We hope to look into this problem more deeply in the future. Iodine contaminants are a recognized problem. One current project of ours is directed toward iodine removal, but we have not yet reached the experimentation stage. The liquids we have burned have been tributyl phosphate and kerosene mixtures primarily. Also vacuum pump oils.

CHOI: We have drums of oil, as in your case. How would it be burned in situ in the drums? For example if the drum is filled with oil?

BOND: The liquid can be pumped from any tank or drum and fed through our liquid burner. We have successfully burned mixtures of tributyl phosphate and kerosene, kerosene and vacuum pump oils. We expect to try liquids such as Hyprez and others commonly found in the nuclear industry.

CHOI: So, it would be different from what you have shown on the slides.

BOND: Yes, it's a different set-up completely.

CLOSING REMARKS OF SESSION CHAIRMAN:

We are done with the day, and I have no words of wisdom. Some of you who are not involved with this technology may wonder why we keep hearing of all these different types of incinerators. Why doesn't everyone use or purchase one particular unit and get on with it? The DOE is now supporting development of five. There were seven different types before. The intention is to keep narrowing the number down and we have narrowed it down a little. Now, we're coming to the end of Phase 2; namely, the pilot process where we have conducted tracer tests. Now, the narrowing down process really becomes in earnest as we prepare to process massive amounts of waste. Two years from now, I think there will be still another story with regard to this technology. However, each of the units you've heard about is finding its own

15th DOE NUCLEAR AIR CLEANING CONFERENCE

little niche in small-scale, on-site-type applications even though they may not be suitable for a very large incineration center requirement.

15th DOE NUCLEAR AIR CLEANING CONFERENCE

SESSION III

TRITIUM, ¹⁴CARBON, OZONE

Tuesday, August 8, 1978

CHAIRMAN: D. Pence

- | | |
|--|---|
| TRITIUM EFFLUENT REMOVAL SYSTEM | P. H. Lamberger, G. E. Gibbs |
| MODIFICATION AND TESTING OF THE SANDIA LABORATORIES, LIVERMORE TRITIUM DECONTAMINATION SYSTEMS | P. D. Gildea, H. G. Birnbaum, W.R. Wall |
| TRITIUM REMOVAL USING VANADIUM HYDRIDE | F. B. Hill, Y. W. Wong, Y. N. Chan |
| STUDY ON THE TRITIUM REMOVAL FROM THE SODIUM IN LMFBR | K. Hata, Y. Nishizawa, Y. Osawa |
| MONITORING AND REMOVAL OF GASEOUS CARBON-14 SPECIES | M. J. Kabat |
| ON THE CATALYTIC REMOVAL OF OZONE PRODUCED IN RADIOACTIVE MEDIA | R.-D. Penzhorn, K. Günther, P. Schuster |

15th DOE NUCLEAR AIR CLEANING CONFERENCE

TRITIUM EFFLUENT REMOVAL SYSTEM

P. H. Lamberger and G. E. Gibbs
Monsanto Research Corporation
Mound Facility*
Miamisburg, Ohio 45342

Abstract

An air detritiation system has been developed and is in routine use for removing tritium and tritiated compounds from glovebox effluent streams before they are released to the atmosphere. The system is also used, in combination with temporary enclosures, to contain and decontaminate airborne releases resulting from the opening of tritium containment systems during maintenance and repair operations. This detritiation system, which services all the tritium handling areas at Mound Facility, has played an important role in reducing effluents and maintaining them at 2% of the level of 8 yr ago.

The system has a capacity of $1.7 \text{ m}^3/\text{min}$ (60 cfm) and has operated around the clock for several years. A refrigerated in-line filtration system removes water, mercury, or pump oil and other organics from gaseous waste streams. The filtered waste stream is then heated and passed through two different types of oxidizing beds; the resulting tritiated water is collected on molecular sieve dryer beds. Liquids obtained from regenerating the dryers and from the refrigerated filtration system are collected and transferred to a waste solidification and packaging station. Component redundancy and by-pass capabilities ensure uninterrupted system operation during maintenance. When processing capacity is exceeded, an evacuated storage tank of 45 m^3 (1600 ft^3) is automatically opened to the inlet side of the system.

The gaseous effluent from the system is monitored for tritium content and recycled or released directly to the stack. The average release is $<1 \text{ Ci/day}$. The tritium effluent can be reduced by isotopically swamping the tritium; this is accomplished by adding hydrogen prior to the oxidizer beds, or by adding water to the stream between the two final dryer beds.

Introduction

One of the principal goals of Mound Facility is to keep tritium discharges as low as practicable. To achieve this goal, concentrated gaseous effluents from any application or process involving tritium must be discharged to a tritium removal system. Mound conducts a variety of operations involving tritium, including the recovery of tritium from many kinds of wastes generated by U. S. Department of Energy contractors. This recovered tritium is put into gaseous form and separated from other hydrogen isotopes in thermal diffusion columns. Tritium effluents from Mound to the atmosphere have been reduced to about 2% of the level of 8 yr ago.

*Mound Facility is operated by Monsanto Research Corporation for the U.S. Department of Energy under Contract No. EY-76-C-04-0053.

15th DOE NUCLEAR AIR CLEANING CONFERENCE

The major operating system in use at Mound for tritium removal from concentrated gaseous effluents is the Effluent Removal System (ERS). The ERS has a 1.7 m³/min processing capability for tritium removal from gaseous effluents prior to their release to the atmosphere. This tritium removal is accomplished by the oxidation of tritium and tritium-containing compounds to water, followed by the collection of the water on drying beds. Effluents contaminated with tritium come to the ERS from such sources as flushing of passboxes, purges of glovebox atmospheres, regeneration of glovebox inert atmosphere purification systems, vacuum pump exhausts, relief of glovebox overpressures, solvent vapors from boxline decontamination operations, purges of space between double layer drybox gloves, discharges of unrecoverable tritium in contaminated waste gases, and a variety of maintenance operations.

The wide spectrum of gases processed by the ERS includes argon, nitrogen, air, helium, hydrogen, water vapor, and various organic compounds such as several types of solvent and vacuum pump oil vapors. The introduction of halogen-containing compounds is forbidden because of the corrosion that would result from the formation of various corrosive agents within the system.

Use in Maintenance Operations

The capability of the ERS to move substantial amounts of gas is used at Mound to greatly reduce or eliminate tritium releases to the atmosphere. Various maintenance operations require the opening of tritium-contaminated lines or equipment and exposing the interior to the laboratory air. During these operations, the release of tritium to the atmosphere is inevitable without some type of containment and decontamination of effluents. At Mound, the item to be opened is enclosed in flexible plastic sheet supported on a metal frame. The enclosure is exhausted to the ERS through plastic tubing connected to one of the ERS inlet lines. Sufficient air flow is maintained through the enclosure to prevent tritium migration to the room air. All the tools and equipment needed to perform the operation are placed inside the enclosure prior to the start of the maintenance work.

There are two types of temporary enclosures used at Mound. In situations where high concentrations of tritium could be present, an enclosure with built-in gloves is erected. The repair work is performed through these gloves by the operating and maintenance personnel. For low tritium levels where the volume to be contained is large an enclosure large enough to allow operating and maintenance personnel to work inside is used. While inside the enclosure, a worker wears a plastic bubblesuit with supplied breathing air so that all physical contact with tritium is avoided.

Several methods are used to decontaminate or reduce the quantities of tritium in lines and equipment if they must be opened for maintenance. If liquid could be present, the item is fitted with a specially designed piercing valve. This valve makes a small hole and the liquid drains into a container without any release of tritium. If welding is involved in the maintenance operation, external heat is applied to the area while a small flow (0.05 m³/min) of air is flushed through the line. This vaporizes moisture and liberates sorbed tritium in the vicinity of the repair and carries it to the ERS. For general decontamination of lines, equipment or enclosures, moist air is more effective than dry gases.

15th DOE NUCLEAR AIR CLEANING CONFERENCE

During the maintenance operation, air flow from the enclosure to the ERS is limited to only that necessary for tritium containment. At times, this type of operation requires the maximum capacity (1.7 m³/min) of the ERS for several hours. Not only is the enclosure ventilated, but, whenever possible, open contaminated lines are directly purged to the ERS. The intent is to move air from the room, through the enclosure, into the open equipment and process lines, and then into the ERS.

These simple but very effective methods have helped considerably in reducing tritium releases to the atmosphere and have contributed to reducing personnel exposures to tritium by a factor of 16 over the past several years.

System Description

The tritium handling operations are connected to the ERS through an inlet collection system consisting of 2, 3 and 4-inch copper trunklines (see Figure 1). This inlet system is maintained at a pressure of 600 torr. In the event that the capacity of the compressors is temporarily exceeded causing trunkline pressure to exceed 700 torr, the system influent is automatically diverted to a 45 m³ evacuated storage tank. The tank inlet valve, which is controlled by a pressure switch, opens and closes when necessary to maintain the trunkline pressure. This pressure control is very important as a pressure above atmospheric could seriously harm certain operations and equipment serviced by the ERS, resulting in a possible release of tritium to the atmosphere.

A pressure of 100 torr is automatically maintained inside the storage tank by a vacuum pump. If influent flow continues at a high rate for an extended period and fills the tank, it is isolated from the ERS trunkline when the pressure reaches 720 torr. Any additional flow to the ERS in excess of its processing capacity is then released directly to the stack. This has occurred only once in the past 6 yr.

Each branch of the inlet collection system is equipped with a gas flowmeter whose output is displayed and recorded on a strip chart. Each branch is periodically sampled for tritium concentration which is also recorded. This branch monitoring permits administrative control by operating personnel in case of system overloads and also provides an historical record.

Downstream of the point where the various branch trunklines merge into a single process line, a series of two filters (30 μ m and 10 μ m) remove particulate material and liquid droplets from the incoming gases. The purpose of this filtration is to protect the Teflon piston rings of the compressors against abrasive materials. The collected liquid and solids from the filters are held in storage tanks while awaiting disposal (1).

The next processing step is the cooling of the incoming gas by refrigerated heat exchangers. Here the contaminated gas is dried to a dew point of -50°C. Two shell and tube heat exchangers are used alternately, one cooling the gas while the other is being heated to defrost the collected condensate which is then stored in a stainless steel tank and later packaged for burial(1). The heat transfer fluid

EFFLUENT REMOVAL SYSTEM

LEGEND

-  FLOW CONTROL VALVE
-  AIR OPERATED BALL VALVE
-  SOLENOID VALVE
-  COMBUSTION GAS MIXTURE DETECTOR
-  FINNED COOLING SECTIONS

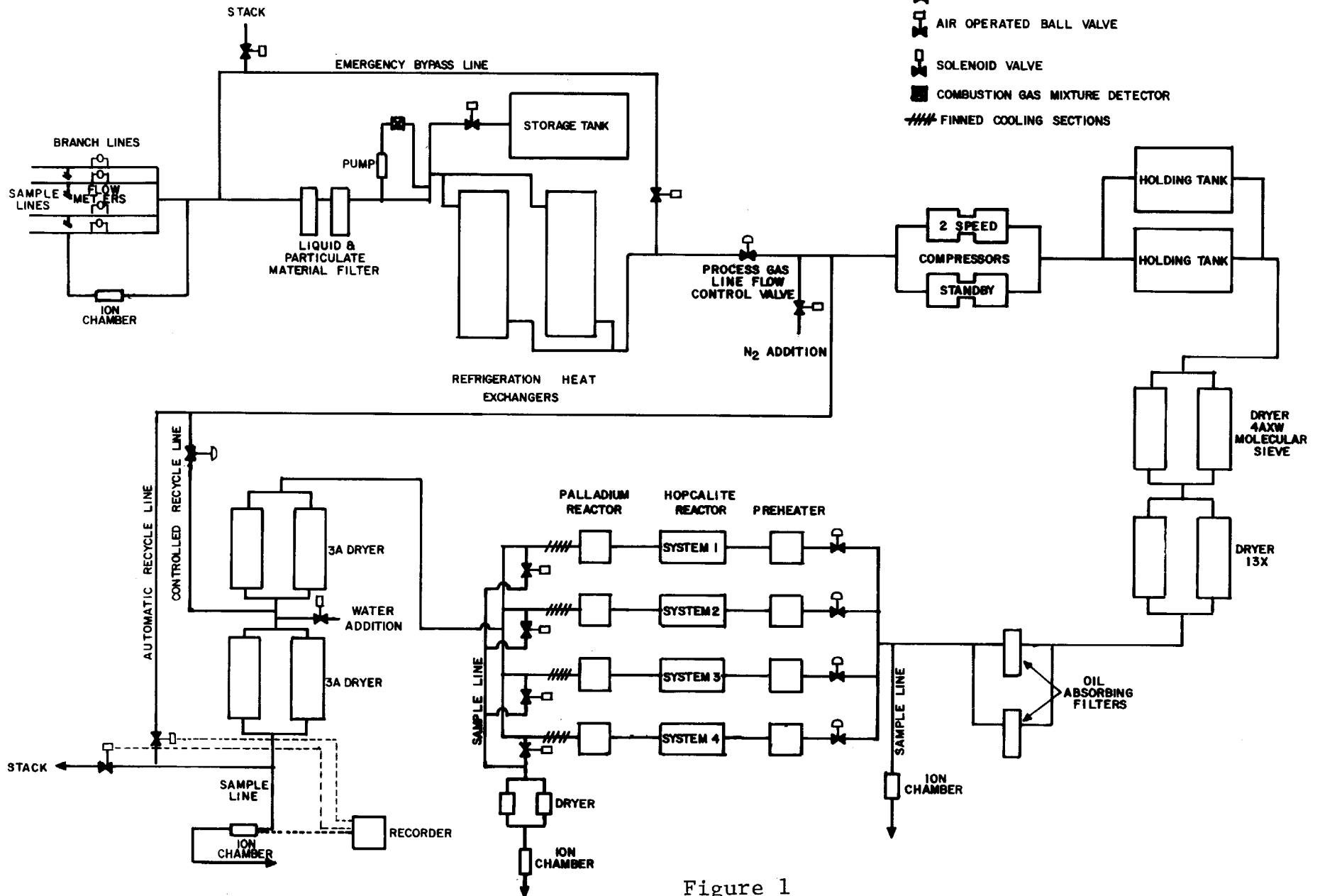


Figure 1

15th DOE NUCLEAR AIR CLEANING CONFERENCE

is cooled to -55°C by a cascade refrigeration compressor system. Steam is used to supply heat for the defrost cycle.

The flow of contaminated gas and heat transfer fluid through the heat exchangers is automatically governed by a programmable step selector. A cycle timer with adjustable settings is used to advance the selector. This allows for variation in time intervals between the defrost and gas cooling cycles.

Prior to the heat exchanger switching from the defrost cycle to the gas cooling cycle, a three-step time interval is devoted to pre-cooling the hot heat exchanger. This provides for constant cooling of the gas during the switching process. The system has built-in failsafe features to ensure uninterrupted operation. In the event of a valve failure, gas will automatically bypass the refrigeration system.

A combustible gas detector is installed on the gas line; its purpose is to warn of the presence of a combustible mixture of hydrogen and oxygen. The detector will alarm when the mixture of hydrogen and oxygen reaches 25% of the lower explosive limit. When the mixture reaches the 75% level, nitrogen gas is added automatically for dilution purposes.

An automatic flow control valve is located in the process line for the purpose of regulating gas flow to maintain the gas inlet header at a pressure of 600 torr. The pressure downstream of the control valve normally is maintained at 510 torr by the addition of recycled gas from within the system. A pressure controller is used to operate this recycle flow control valve which is similar to the process line control valve. The purpose of this controlled recycle gas is to provide the positive displacement compressors with sufficient gas to maintain the inlet pressure at 510 torr. The compressors have the capability of reducing the inlet pressure to 310 torr which could cause damage to the diaphragms in the compressor inlet valves.

Gas is moved through the ERS by either of two oil-less-head compressors connected in parallel. This type of compressor was chosen because the introduction of oil into the system would require additional filtration to protect the Hopcalite oxidizing reactors. Oil vapor has a tendency to coat the Hopcalite and seriously reduce its effectiveness. One compressor of $0.85\text{ m}^3/\text{min}$ capacity is maintained in standby condition. Should the normally operating compressor become inoperative the standby unit is automatically activated. The active compressor has a capacity of either 0.85 or $1.7\text{ m}^3/\text{min}$ and is equipped with a two-speed motor, which changes to high speed automatically when the gas flow rate exceeds the low speed capacity or the gas line pressure increases to 670 torr.

The gas discharged by the compressor is fed to two 4.25 m^3 holding tanks which are normally held at 2000-2300 torr. This pressure provides the driving force for gas flow through the remainder of the system. Following the holding tanks are two dual-tower, automatic, self-regenerating dryers using molecular sieve as the desiccant. The first dryer is filled with 4AXW molecular sieve to remove trace amounts of water vapor. The second dryer is filled with type 13X molecular sieve for hydrocarbon removal. It is important that halogenated hydrocarbons be removed from the gas stream prior to its entry into the hot oxidizing

15th DOE NUCLEAR AIR CLEANING CONFERENCE

reactors since decomposition of the halogen compounds leads to the formation of corrosive agents.

After the gas exits the 13X dryer, it is passed through an oil absorbing filter. The gas is now considered completely free of any vapor which will harm the oxidizing reactors or produce corrosive agents at the high temperatures of the reactors. At this point, a 28 liter/min sample is fed through an ion chamber which measures the tritium concentration of the gas prior to entering the reactor system.

The ERS is equipped with four identical parallel reactor systems, which have the function of oxidizing hydrogen isotopes and compounds into water. Each reactor system consists of a preheater, a Hopcalite reactor and a palladium reactor. An automatic ball-valve switching mechanism is used to select any two reactor systems for processing gas contaminated with tritium. The other two reactors are held in a hot standby condition. A gas flow control valve is located on each reactor system and the gas flow can be regulated from 0.17 to 0.43 m³/min as desired. A pressure switch, located on the holding tanks, will automatically introduce gas to the two standby reactors when the tank pressure reaches 2400 torr. This switch will also return the two reactors to standby status upon the reduction in tank pressure to 1950 torr.

An electric preheater raises the temperature of the incoming gas to 400°C prior to entering the Hopcalite (15% CuO and 85% MnO₂) reactors. Here the hydrogen is oxidized by the CuO, and the MnO₂ acts as a catalyst for the reaction. The CuO provides an oxygen supply if the incoming gas stream does not contain any air. There is normally sufficient oxygen in the gas to maintain the copper in the oxidized state; but as a precaution, air is routinely introduced into the system to avoid oxygen depletion. A second reactor downstream of each Hopcalite reactor contains a palladium catalyst held at 600°C. The purpose of this palladium reactor is for oxidizing tritiated organic compounds, such as radiolytically generated methane, for which the Hopcalite is ineffective.

The efficiency of each reactor can be determined by automatically sampling the gas leaving each reactor, drying the gas and measuring the tritium content with an ionization chamber.

The gas is passed through air-cooled, finned, copper heat exchangers before entering another pair of dual-tower dryers. These two dryers use type 3A molecular sieve. The water collected in these dryers was produced in the oxidation process of the reactors. Upon regeneration of the dryers, the accumulated water is collected and packaged for burial.

Additional removal of tritiated water from the gas is achieved by the use of isotopic swamping. This is accomplished by periodically loading the final dryer with several kilograms of natural water. Since there is rapid exchange between water in the adsorbed and vapor phases, the HTO is adsorbed and H₂O is released resulting in the virtual elimination of HTO from the discharge of the second dryer. Periodically, the dryer is regenerated and, after cooling, is again loaded with clean water.

15th DOE NUCLEAR AIR CLEANING CONFERENCE

A hydrometer is used to measure the trace amounts of water vapor in the gas entering and leaving the third dryer, and leaving the final dryer. This information is useful for troubleshooting during brief and rare periods of system inefficiency. By combining the information from the tritium concentration monitors, the explosive mixture monitor, and the hydrometer, the cause of most problems can be determined and corrective action taken.

As the decontaminated gas exits the final dryer, the tritium concentration is measured with an ion chamber whose output is fed to a recorder equipped with an alarm set point. If the tritium concentration reaches the set point, a series of valves will automatically divert the contaminated gas back into the compressor inlet line for recycle. This recycling continues until the tritium concentration is less than the set point. When this point is reached, the valves automatically reverse to the normal position and the gas is discharged to the atmosphere.

Detritiation factors of 10^5 can be attained by use of the ERS. In tests with tritium concentrations of 10 ppm (25 Ci/m^3) in the influent, tritium concentrations in the output or discharge were less than $250 \text{ } \mu\text{Ci/m}^3$.

Engineering Data

The system is relatively large and complex because of its capacity, redundancy of critical components and safety features. Current replacement cost is \$1.5 million. The ERS was designed for, and is operating on, a continuous 24-hr/day basis with almost no downtime. Normal maintenance of the system can be performed without seriously reducing its capacity or efficiency.

Containment of tritium, operating life and ease of maintenance are the main design criteria when selecting materials and equipment for the ERS. The lines not subjected to elevated temperatures are copper tubing joined with silver solder. The lines exposed to high temperatures are 316 stainless steel, and the reactors and preheaters are constructed from 304H rerolled stainless steel. Heliarc welding in an argon atmosphere is used for fixed stainless steel joints. Flexible bellows connections, which allow for thermal expansion, are used between the Hopcalite reactors and the preheaters. The stainless steel bellows are welded to stainless steel flanges and when assembled are in a state of stress. Upon thermal expansion of the reactors during operation, the stress in the bellows is relieved. A special gold-plated, K-shaped gasket is used between these flanges. Flanges were selected for use in these locations to allow the reactor or preheater to be removed easily.

The finned cooling sections are fabricated from oxygen-free copper (OFC) tubing to resist corrosion. Viton, which has high resistance to tritium, is used as gasket material for flanges where temperatures are not greater than 100°C .

Many different thermal insulating materials are used in the ERS. In the refrigeration system, the holding tank containing the heat-transfer fluid is insulated with foam glass. The refrigerant transfer lines are insulated with foam rubber and fiberglass. The Hopcalite reactors

15th DOE NUCLEAR AIR CLEANING CONFERENCE

and preheaters are enclosed with rigid, 23-cm thick, pressed fiber insulation. The palladium reactors are insulated with high-temperature, evacuated glass beads contained within a stainless steel enclosure.

Several of the significant improvements of the present system, built in 1972, compared to the original system, are the following: The capacity has been increased by a factor of 10. The addition of the refrigerated heat exchangers has provided for an essentially dry system resulting in more reliable operation and less hazard to maintenance personnel from tritiated condensates. The absence of tritiated liquids requires less preparation before maintenance work can start, resulting in decreased system downtime. The use of effective filters and condensers and proper control of the cooling water has extended the operating time of the compressors between overhauls from ~600 hr to ~15,000 hr. Improved tritiated liquid handling equipment has reduced losses to the atmosphere. The addition of the palladium reactors has given the system the capability to oxidize tritiated organic compounds which otherwise would be released to the environment; this has resulted in reduced effluents and in increased flexibility in choosing decontaminating solvents. Improved pressure, temperature, and gas flow instrumentation has improved the control and efficiency of the system.

Conclusion

There are two methods of disposing of tritiated effluents -- releasing them to the environment or exhausting them to an effluent decontamination system. Mound has shown, through use of the ERS, that most effluents need not be discharged to the environment and that an effluent goal of "as low as practicable" can truly be achieved.

Acknowledgement

The authors thank T. B. Rhinehammer for many helpful discussions and comments.

Reference

1. E. A. Mershad, W. W. Thomasson, and J. J. Dauby, "Packaging of Tritium Contaminated Liquid Waste," Nuc. Tech., 32:1, 53-59 (1977).

DISCUSSION

O'BRIEN: First, is the output of the ERS linearly related to the input or is the output concentration the same no matter what the input concentration? Second, what becomes of the water absorbed on the drying beds?

LAMBERGER: The output is constant over a wide range of inputs but does increase when the input concentration reaches very high levels. The answer to your second question is that the dryers are regenerated and the water moved to storage tanks. Ultimately, the water is solidified, using Portland cement, and packaged in a series of three drums with a very low release rate.

PARISH: Why are you using a Hopcalite catalyst in series with a precious metal?

15th DOE NUCLEAR AIR CLEANING CONFERENCE

LAMBERGER: The oxygen in CuO is available to oxidize hydrogen in case insufficient oxygen is present in the incoming gas stream.

CARTER: In what form is the tritium released from the stack? Is the input to the cleanup system all tritium gas rather than tritiated water vapor? Finally, what is the effective decontamination factor for plastic suits?

LAMBERGER: Tritium is released from the stack both as elemental hydrogen and as the oxide. The input to the cleanup system contains tritium gas and oxide in varying amounts. I don't know what decontamination factor applies to plastic suits. We have a publication on the subject that contains the data you are seeking.

15th DOE NUCLEAR AIR CLEANING CONFERENCE

MODIFICATION AND TESTING OF THE SANDIA LABORATORIES LIVERMORE TRITIUM DECONTAMINATION SYSTEMS*

P. D. Gildea, H. G. Birnbaum and W. R. Wall
Sandia Laboratories
Livermore, California 94550

Abstract

Sandia Laboratories, Livermore, has put into operation a new facility, the Tritium Research Laboratory. The laboratory incorporates containment and cleanup facilities such that any tritium accidentally released is captured rather than vented to the atmosphere. This containment is achieved with hermetically sealed glove boxes that are connected on demand by manifolds to two central decontamination systems called the Gas Purification System (GPS) and the Vacuum Effluent Recovery System (VERS). The primary function of the GPS is to remove tritium and tritiated water vapor from the glove box atmosphere. The primary function of the VERS is to decontaminate the gas exhausted from the glove box pressure control systems and vacuum pumps in the building before venting the gas to the stack. Both of these systems are designed to remove tritium to the few parts per billion range.

Acceptance tests at the manufacturer's plant and preoperational testing at Livermore demonstrated that the systems met their design specifications. After preoperational testing the Gas Purification System was modified to enhance the safety of maintenance operations. Both the Gas Purification System and the Vacuum Effluent Recovery System were performance tested with tritium. Results show that concentration reduction factors (ratio of inlet to exhaust concentrations) much in excess of 1000 per pass have been achieved for both systems at inlet concentrations of 1 ppm or less.

Introduction

Sandia Laboratories, Livermore, has put into operation a new facility, the Tritium Research Laboratory (TRL). The laboratory (Figure 1), designed for a wide range of experiments using multi-gram amounts of tritium, entered its start-up phase on October 1, 1977. In addition to the usual pressure-gradient-controlled once-through ventilation system, the Tritium Research Laboratory provides for both personnel safety and environmental protection by employing a glove box secondary containment system connected to the two central decontamination systems, the Gas Purification System (GPS) and the Vacuum Effluent Recovery System (VERS).

This paper describes the glove boxes and operating principles of the GPS and VERS. It gives their performance specifications, and details Sandia's modifications to the manufacturer's design to enhance the safety of maintenance operations. Performance tests, preoperational and with tritium, are also discussed.

*Work supported by the Department of Energy under Contract AT(29-1)-789.

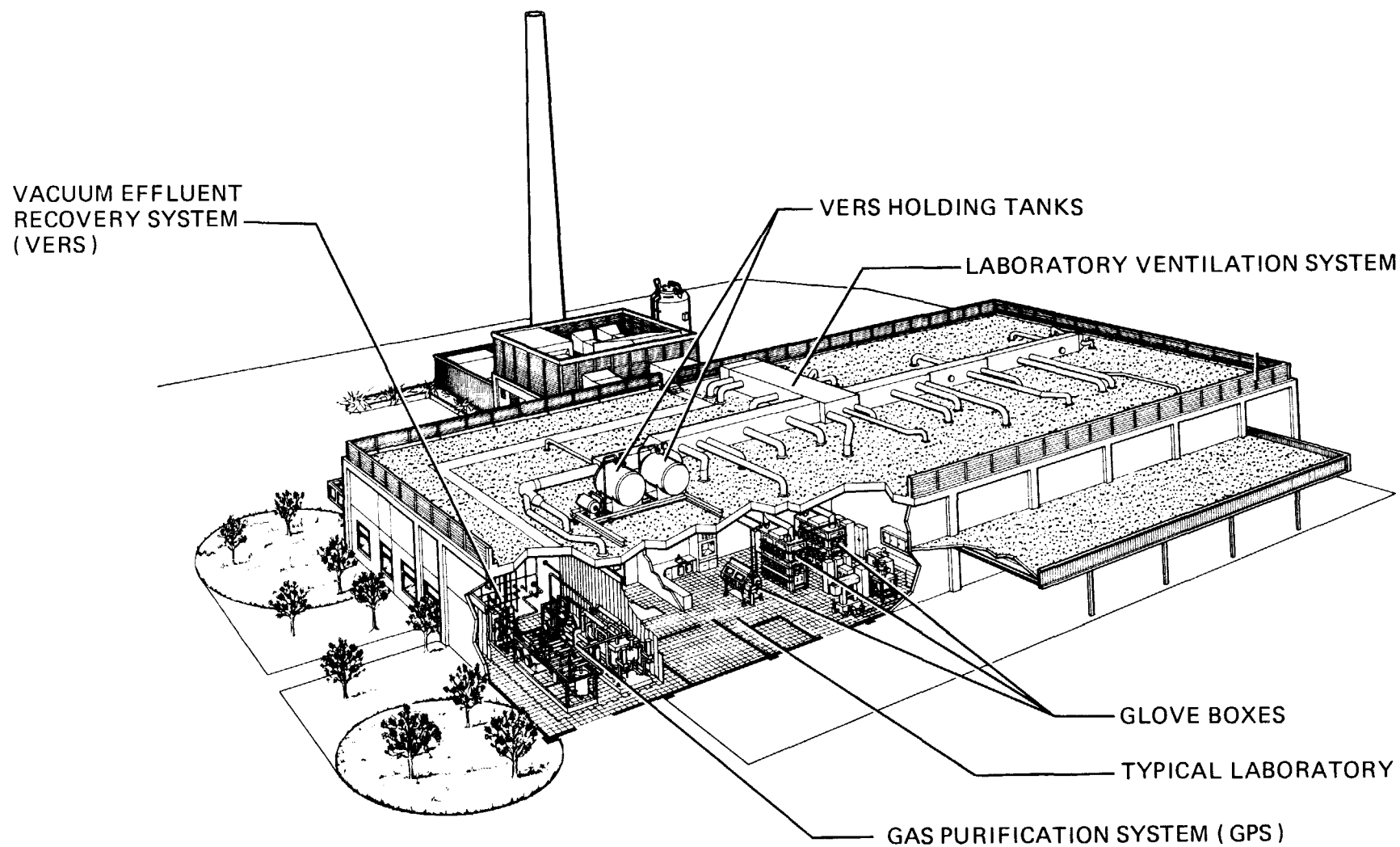


Figure 1 The TRL building at Livermore, showing the arrangement of some of the major systems and a typical experiment station.

Containment

All experiments are secondarily contained in sealed stainless steel glove boxes of welded construction (Figure 2). Each box is equipped with glove ports, viewing windows, and an air lock pass-through; and on each end there are removable panels for the installation of large items. Both regular utility and emergency electrical power are provided to the box. Also, there are feed-through provisions for instrumentation and inert gas pressure connections, and a cooling system to remove the heat generated by experiments. Both tritium concentration and humidity control are maintained by processing the glove box atmosphere through the GPS. Normally, the glove boxes are operated with dry nitrogen maintained by the box pressure control system at a pressure of -0.25 to -1.0 kPa with respect to the room. However, the box can be operated with an argon or air atmosphere if desired.

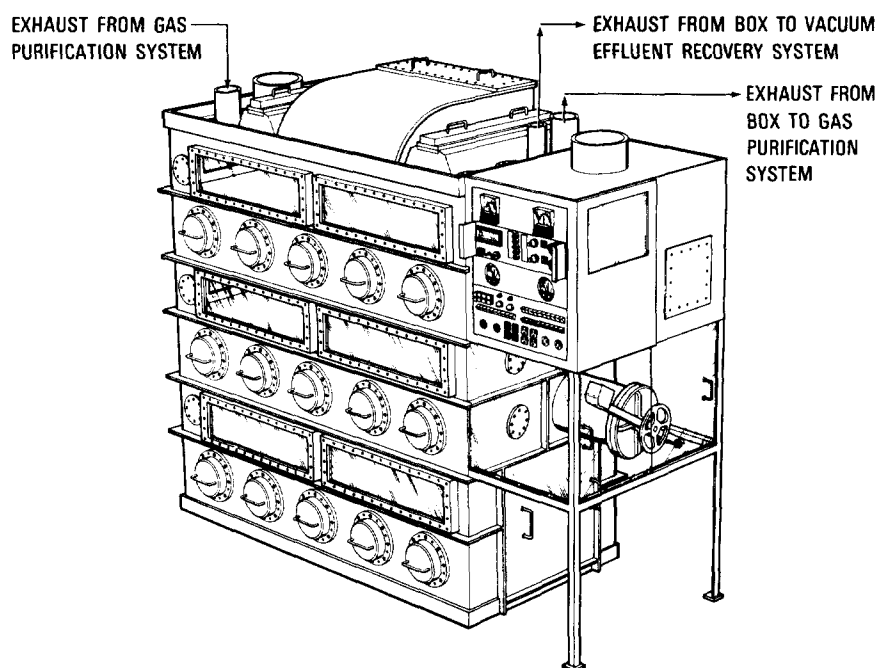


Figure 2 Sealed glove box.

Decontamination

Decontamination is accomplished by two centralized systems. (1) The first of these, the Gas Purification System (GPS), removes tritium and tritiated water vapor from the glove box atmospheres. The second, the Vacuum Effluent Recovery System (VERS), removes tritium, tritiated water vapor, and tritiated hydrocarbons from gases exhausted from the glove box pressure control systems and laboratory vacuum systems before the decontaminated residue gases are vented to the stack. The original systems were manufactured to a Sandia performance specification by Engelhard Industries Systems Department, Union, New Jersey. Both systems were designed to reduce tritium concentrations to a few parts per billion. The tritium removed by the decontamination systems is contained, either for recovery or for disposal, as solid waste on Type 4A molecular sieves.

Gas Purification SystemDesign and Operation

The Gas Purification System (GPS), conceptually illustrated in Figure 3, removes tritium from the glove box atmosphere in the event of either an accidental release or a slow buildup of background concentration.

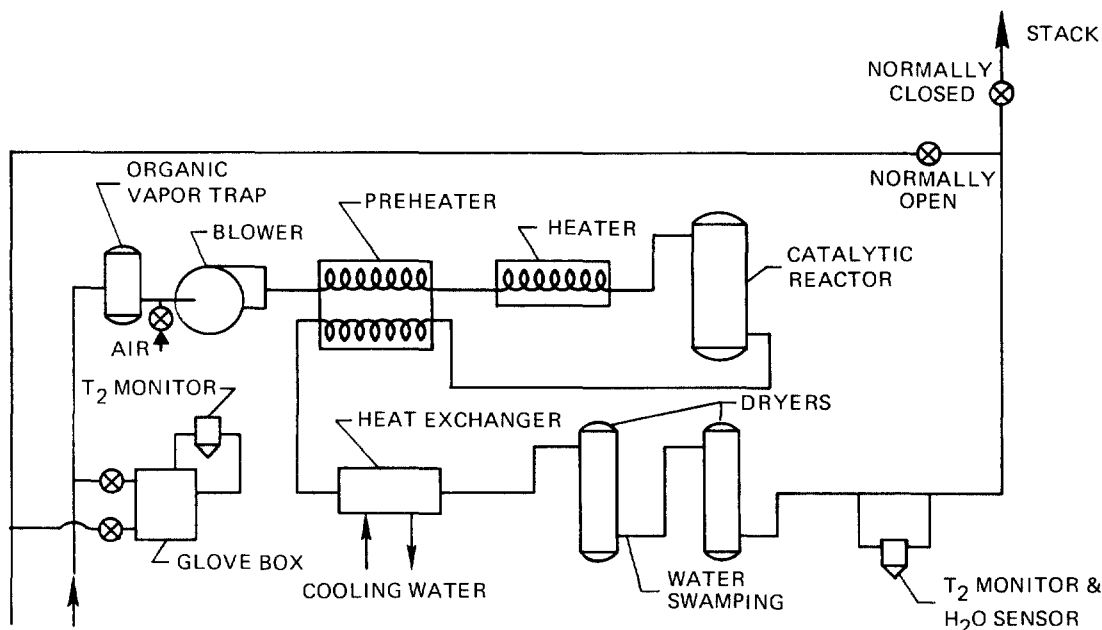


Figure 3 Gas purification system schematic.

The GPS consists of a central manifold connected to each of the laboratory glove boxes, a catalytic reactor to oxidize the tritium, two molecular sieve dryers in series to collect the tritiated water, a blower to circulate the glove box atmosphere through the system, and a control and diagnostics system to provide both automatic and manual control and to assess operational status. Redundant prime function components, i. e., blowers, heaters, and catalyst and dryer beds are provided for reliability. A dryer regeneration system provides for removal of water from a loaded dryer while the GPS is operating with the use of the other two dryers. Entry and exit nozzles allow safe removal and replacement of both catalyst and sieve material while the system remains operational by the use of a redundant flow path. Major system performance criteria are summarized in Table I.

The GPS can be operated either in a recirculation mode or in a stacking mode. In the recirculation mode, the normal method of operation, the glove box gases are pumped from the box, through the GPS, and back to the box until tritium contamination is reduced to an acceptable level. The stacking mode is similar to the recirculation mode with the exception that the glove box atmosphere is not recirculated but stacked after passing through the GPS. This is accomplished by drawing clean box atmosphere gas into the manifold ahead of the glove box and venting the GPS effluent to the ventilation exhaust. This mode of operation may

15th DOE NUCLEAR AIR CLEANING CONFERENCE

Table I GPS performance criteria.

Processing Capacity	340 m ³ hr ⁻¹
Catalytic Reactor	
Operating Temperature	783 K
Standby Temperature	783 K
Catalyst	Engelhard Minerals and Chemicals No. A-16648
Tritium Concentration Reduction Factor*	1000 per pass for concentrations from 20,000 ppm to 1 ppm.
Molecular Sieve Dryer	
Capacity	37 moles of water while maintaining less than 1 ppm water at exit
Regeneration Time	6 hours
Regeneration Temperature	589 K
Molecular Sieve	Type 4A
Startup Operating Time	30 s
Glove Box Pressure Control	-0.25 to -1.0 kPa relative to the laboratory
System Leak Rate	1 x 10 ⁻¹⁰ m ³ (STP)s ⁻¹ maximum helium at 98 kPa differential

*Ratio of inlet to outlet tritium concentrations.

be used to backfill the glove box with dry nitrogen or argon when an inert atmosphere is required. It can also be used to drive the glove box concentration to low levels when it is necessary to clean up a box for reentry.

GPS Modifications

The GPS as originally received from the manufacturer is shown in Figures 4 and 5.

As a result of experience gained during preoperational testing of the GPS in the TRL, it became apparent that system changes were required primarily to increase the safety of maintenance operations. Modifications were necessary to reduce to a minimum the volume of the GPS opened up to the room during such operations as valve seat, heater, catalyst, and sieve removal and replacement. The diagnostics and control systems were also modified at this time. To achieve

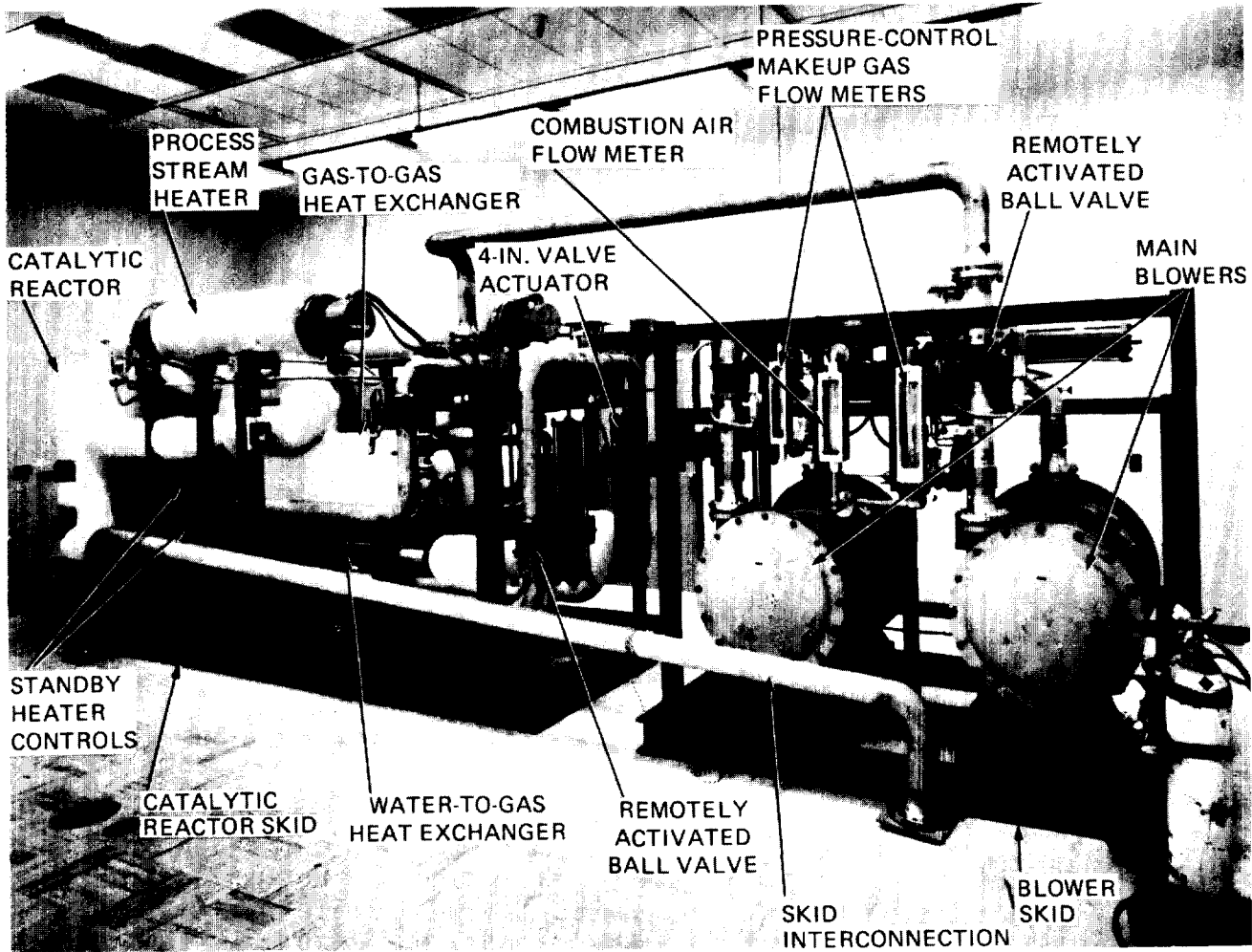


Figure 4 GPS blower and catalytic reactor skids, as received from manufacturer.

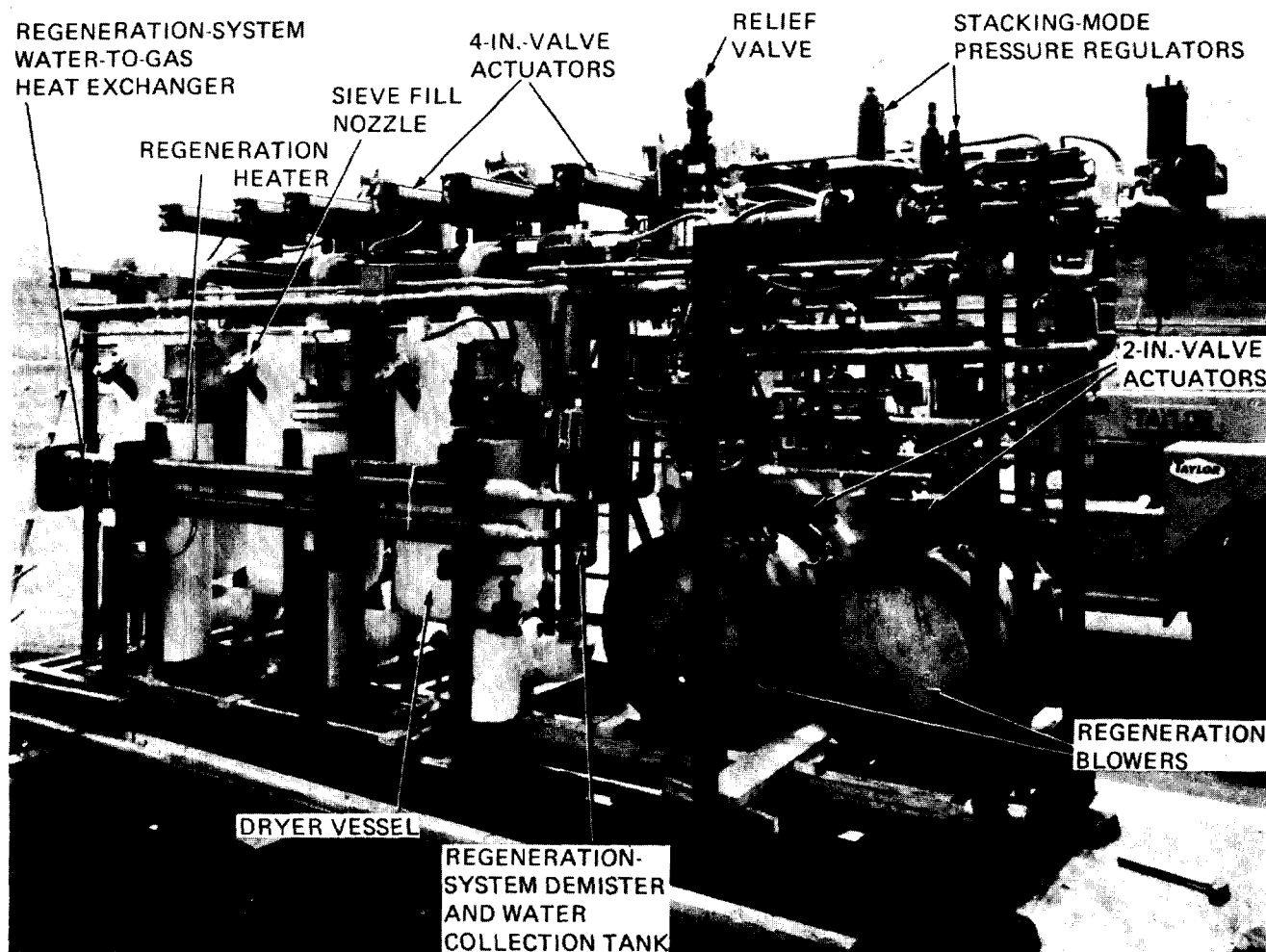


Figure 5 GPS dryer skid as received from manufacturer.

this end the GPS was removed from the laboratory and modified after completion of preoperational testing but prior to tritium testing. The major modification problem encountered was finding a suitable arrangement of the dryer skid that would allow space for placement of isolation valves on both sides of the eleven 4-in. and thirteen 2-in. remotely actuated ball valves on the skid.

Mechanical Modifications. The three skids were disassembled and modified as follows:

1. Isolation valves and purge ports were added on either side of all remotely actuated valves and on the catalyst and sieve vessel entry and exit nozzles.
2. A sealing surface was added to the main heater vessel to allow for installation of a glove box for heater removal.
3. Raceways were installed on the outside of the main heater and catalyst vessels for ease of replacement of standby heating elements.

15th DOE NUCLEAR AIR CLEANING CONFERENCE

4. The catalytic reactor skid was split into two separable independent skids to allow replacement of one complete flow path without major interruption of system operation.
5. A bypass was added to the catalytic reactor skid to allow system operation without flow through the catalyst and to allow isolation of the catalyst when the system is not operating.

Figures 6, 7, and 8 show the three skids after completion of the mechanical modifications. The purge port arrangement used on the dryer vessel sieve fill nozzle is shown in Figure 9.

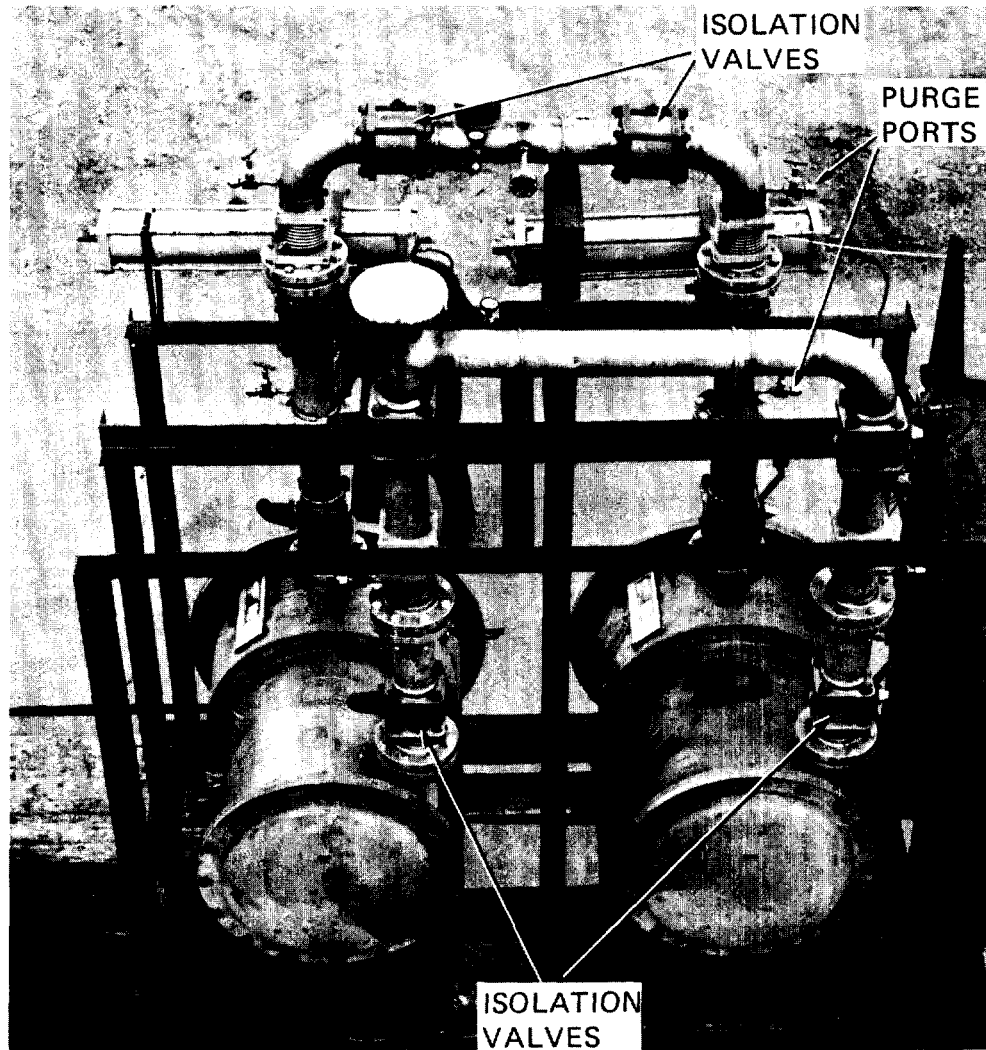


Figure 6 Modified GPS blower skid.

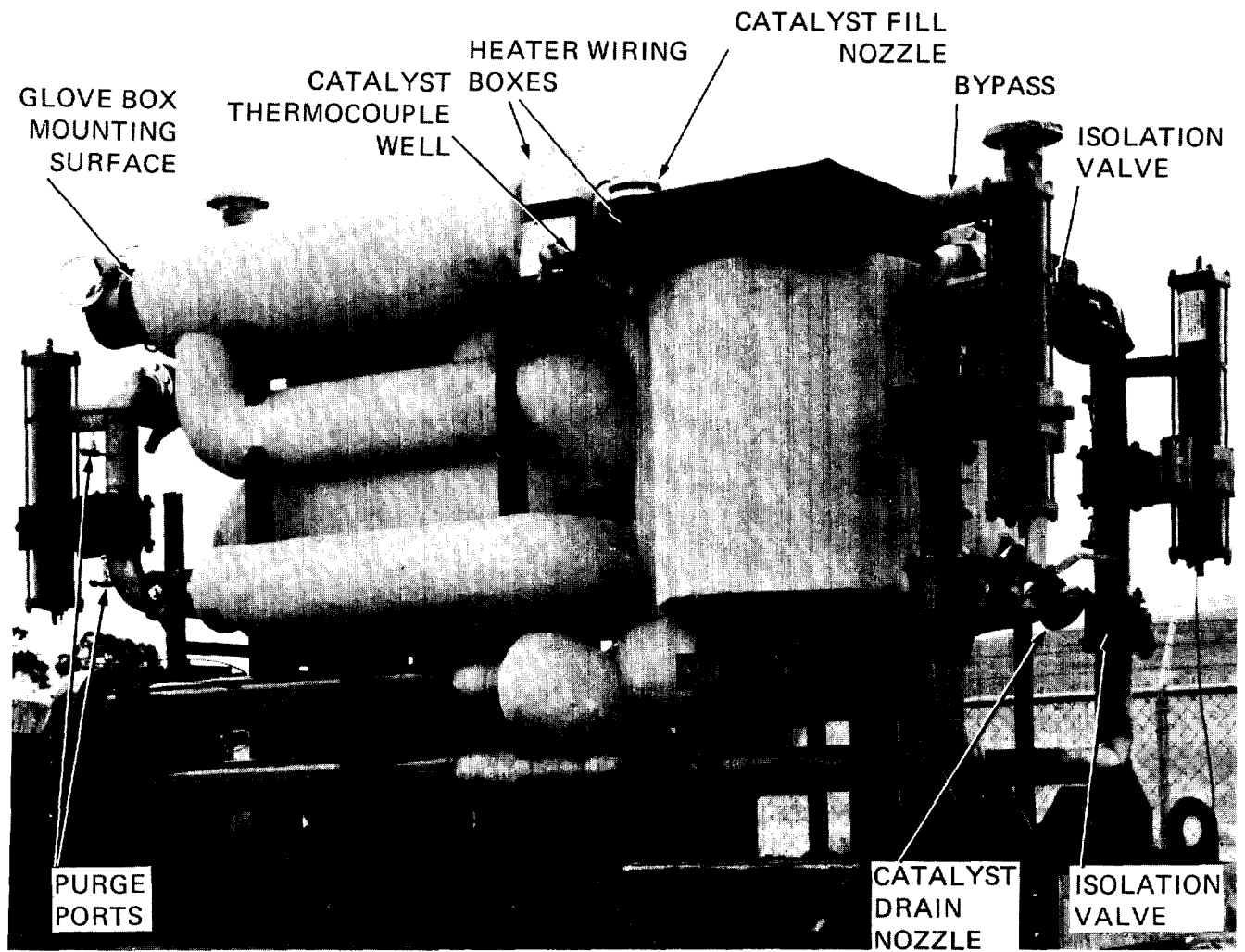


Figure 7 Modified GPS catalytic reactor skid.

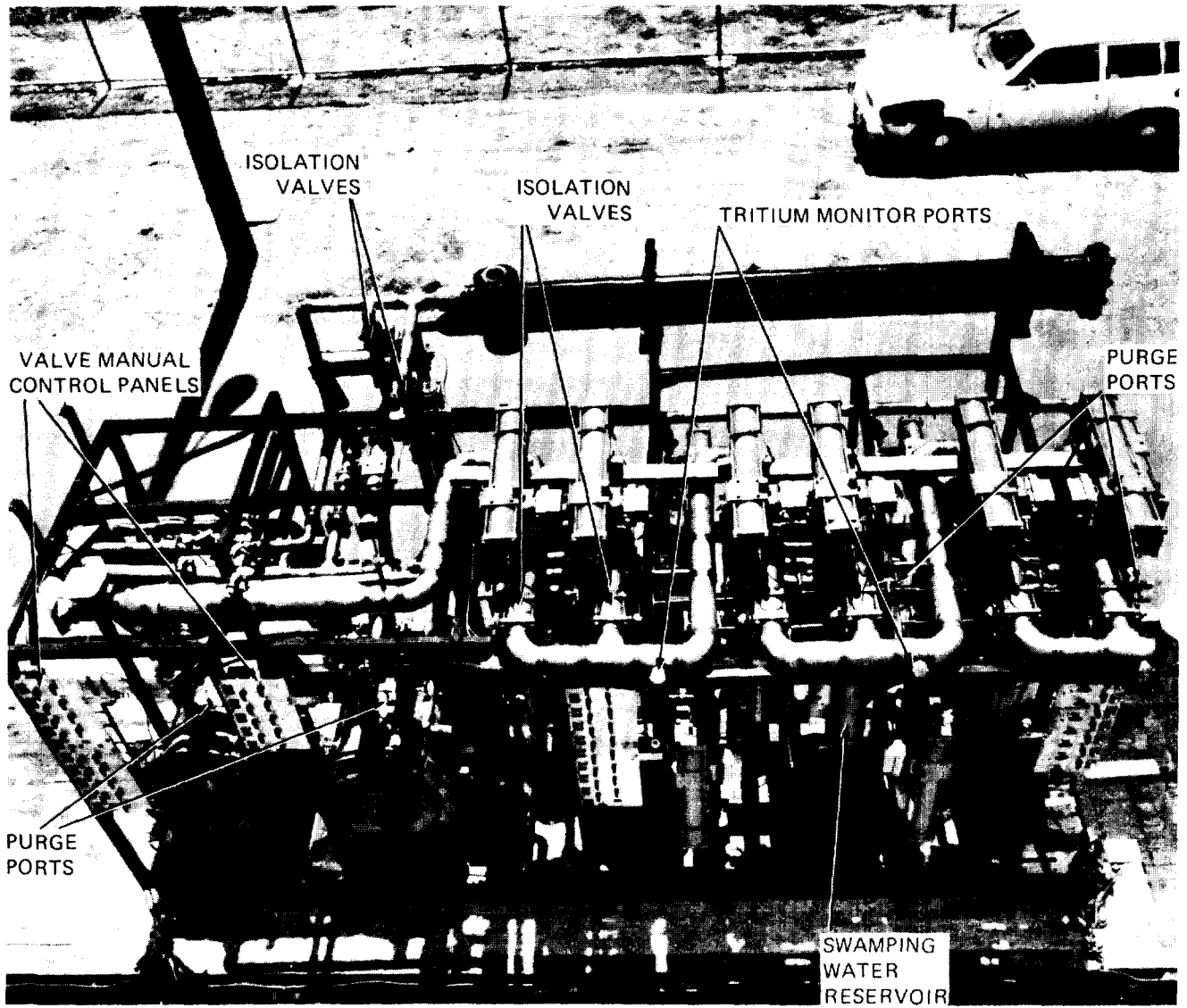


Figure 8 Modified GPS dryer skid.

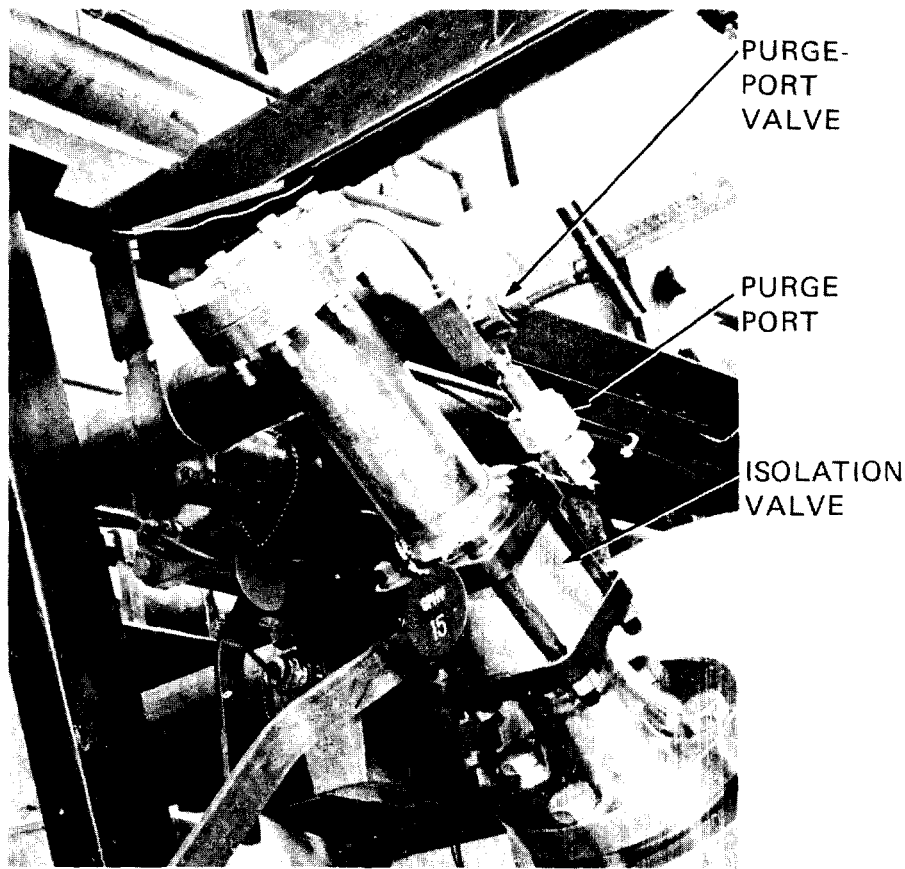


Figure 9 Dryer fill nozzle purge port configuration.

Instrument and Control System Modifications. To enhance both reliability and ease of maintenance, the diagnostics and control systems were changed as follows:

1. The mechanical relay control system was replaced by a microprocessor controlled solid state system to provide increased flexibility and reliability.
2. All heater, motor, and valve control elements except disconnects were removed from the skids and placed outside the hood surrounding the GPS to allow ease of maintenance.
3. The Variac standby heater controls were replaced with silicone controlled rectifier units to achieve better temperature control.
4. Thermocouples were placed in the catalyst bed to provide more accurate temperature control and allow assessment of catalyst performance. Thermocouples were also added at the dryer inlet to provide more accurate determination of regeneration completion.

The GPS control panel in the TRL control room is shown in Figure 10; the wall mounted GPS combustion air and makeup gas flow instrumentation and control valves are shown in Figure 11. The catalytic reactor standby heater and thermocouple mounting arrangements are presented in Figure 12.

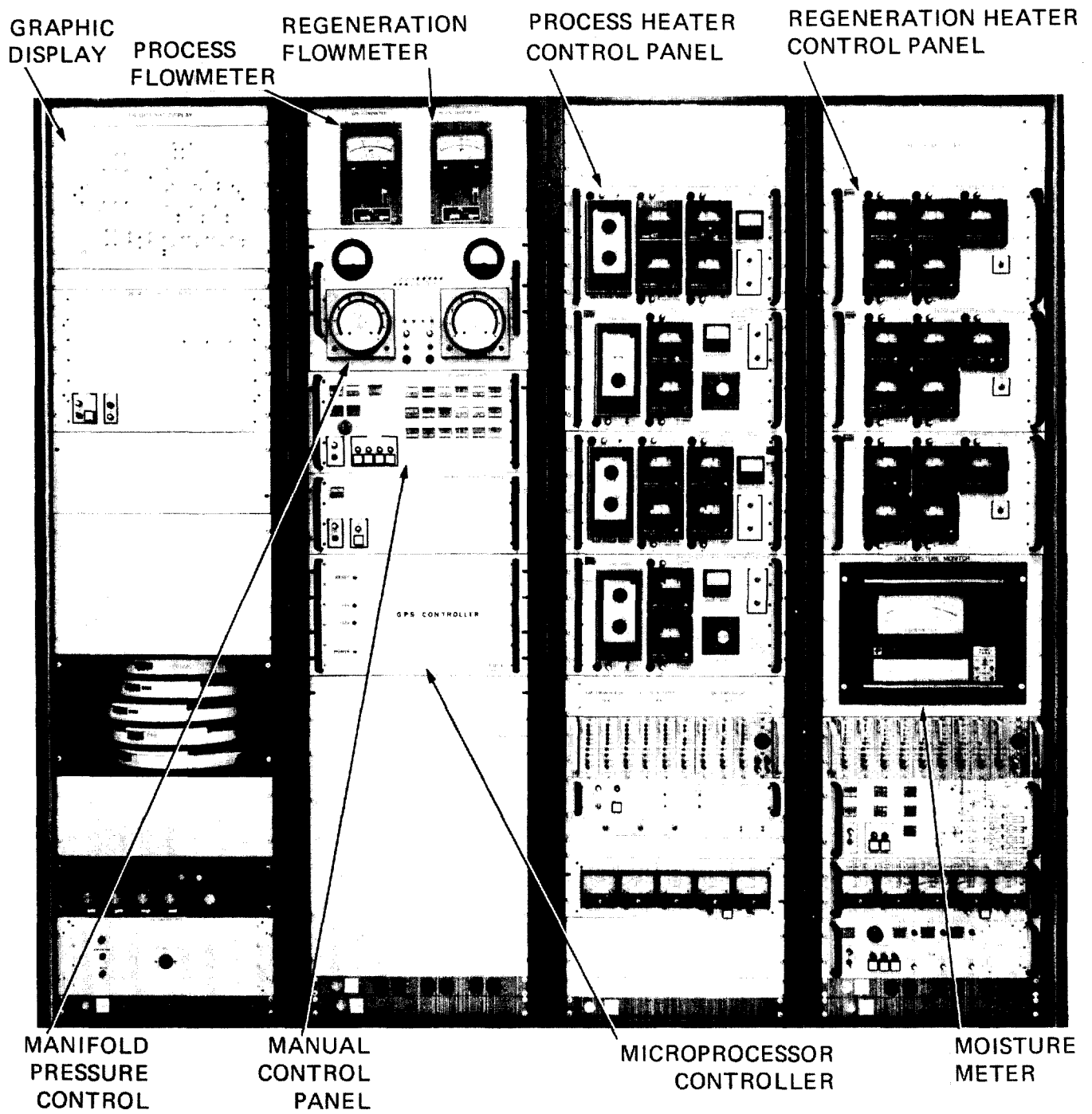


Figure 10 GPS control panel.

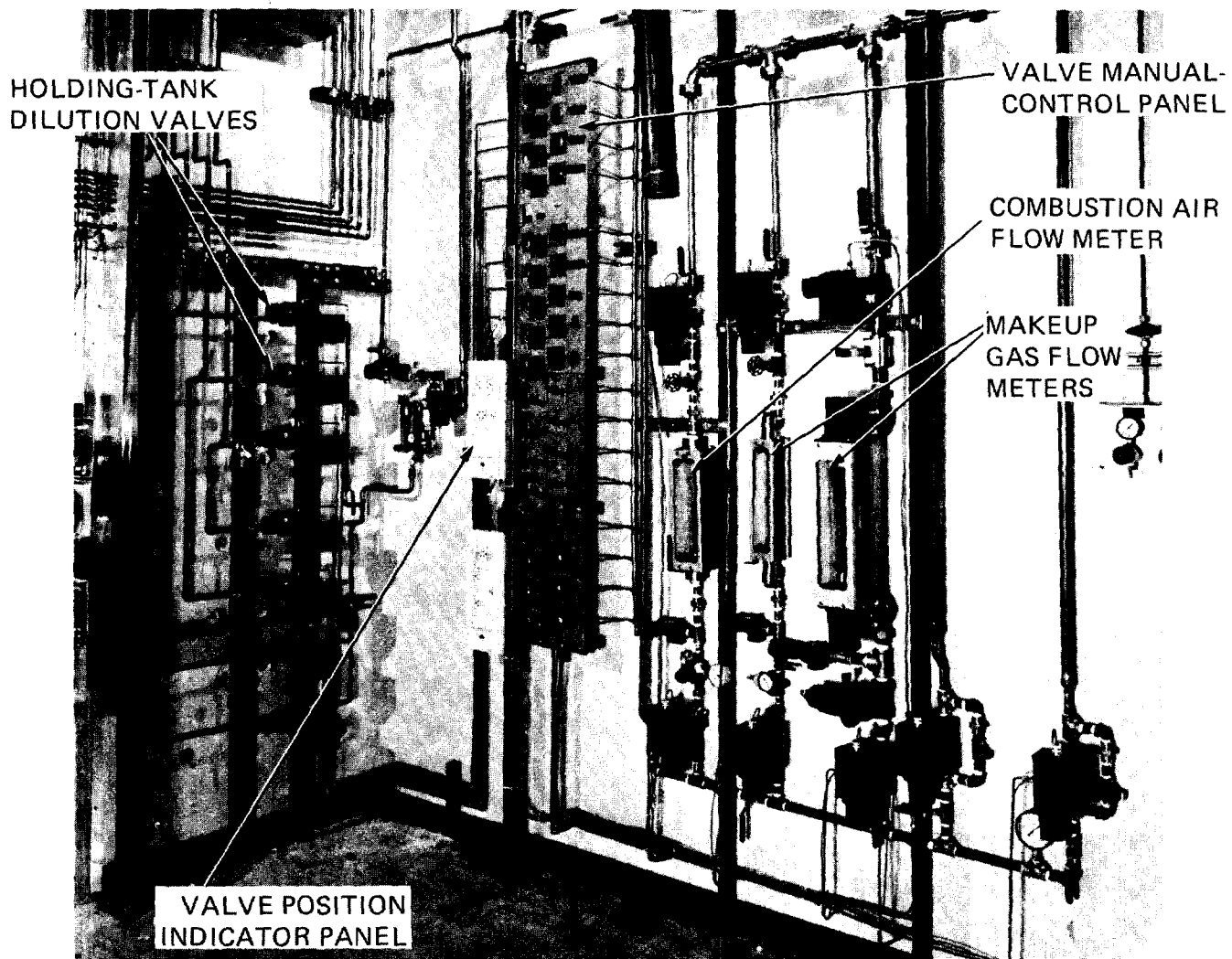


Figure 11 GPS gas flow instrumentation and control valves.

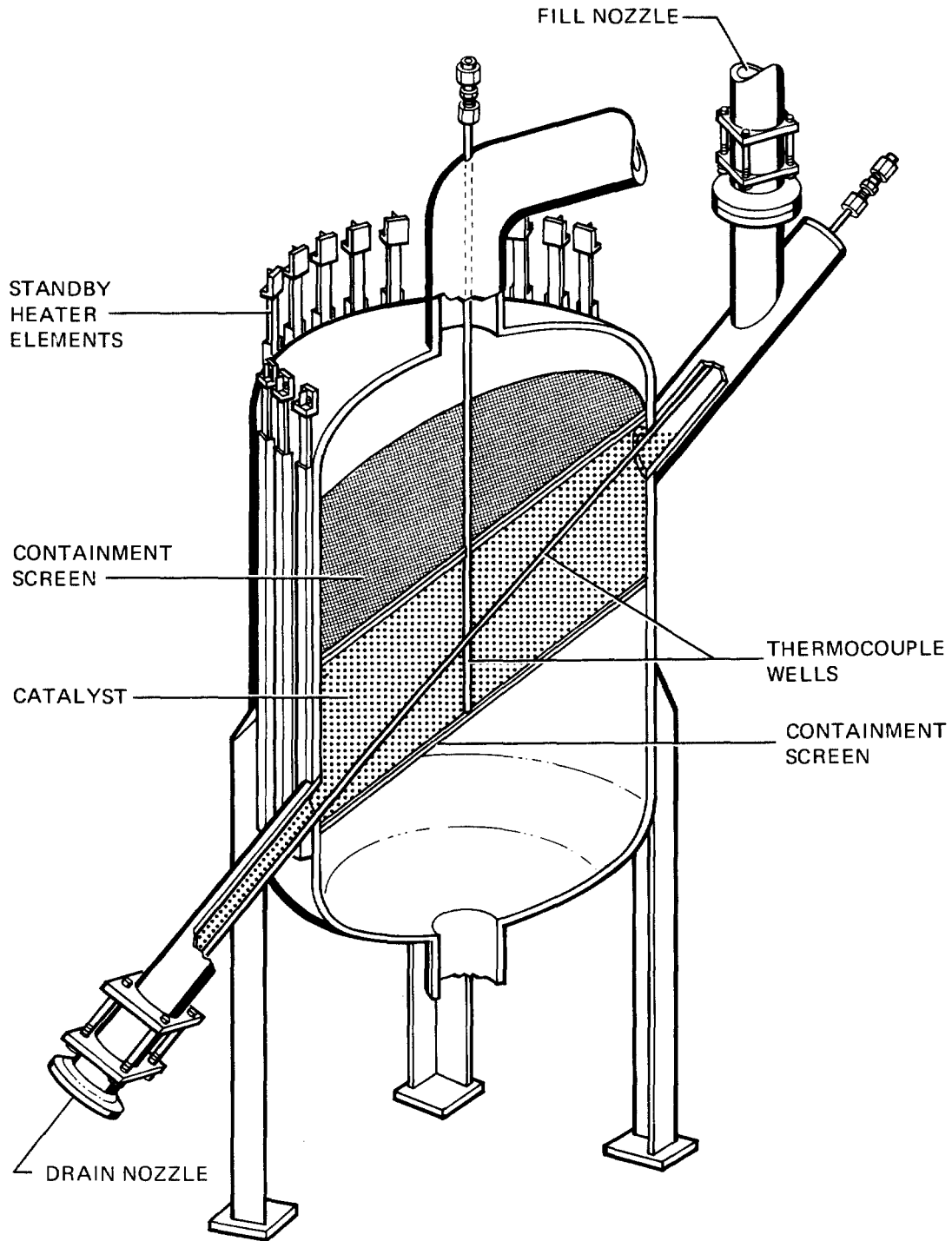


Figure 12 GPS catalytic reactor.

Vacuum Effluent Recovery SystemDesign and Operation

The VERS, conceptually shown in Figure 13, is used to remove tritium from the exhaust gases of the laboratory vacuum systems before venting to the stack. The VERS removes tritium in the same manner as the GPS and uses the same precious metal catalyst. The system consists primarily of a laboratory vacuum manifold and two holding tanks to collect the contaminated waste gases, a catalytic reactor to oxidize the tritium, two molecular sieve dryers connected in series to collect the tritiated water, the necessary pumps to evacuate the laboratory manifold and transfer the waste gas through the system, and a control and diagnostics section to provide both automatic and manual operation and to assess operational status. That portion of the VERS containing the heater, catalytic reactor, heat exchanger, dryers, and transfer pump is referred to as the "decontamination section."

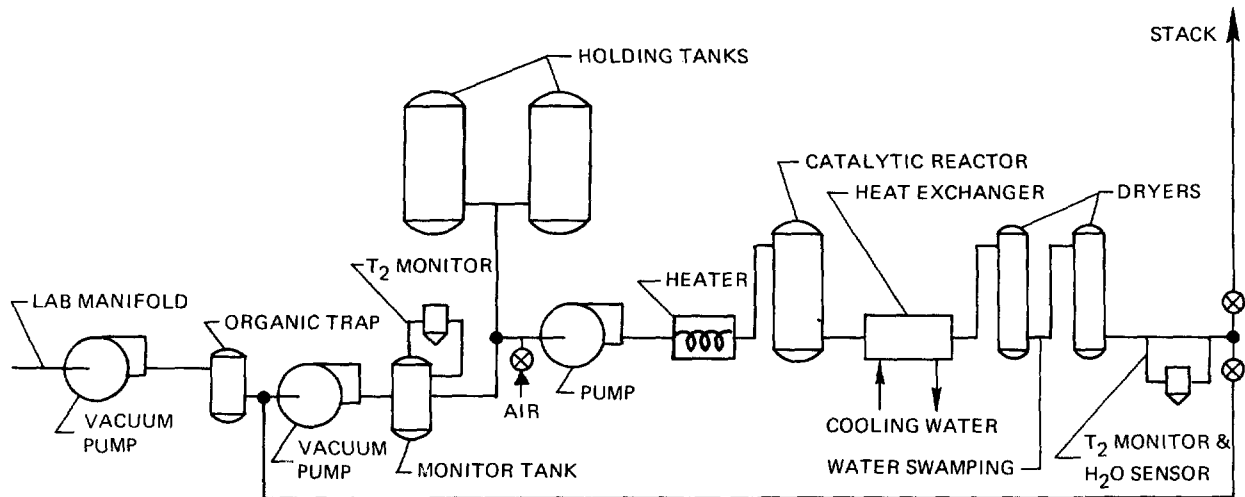


Figure 13 Vacuum effluent recovery system schematic.

The VERS catalytic reactor like that of the GPS is maintained at an elevated temperature (783 K) in standby condition to ensure combustion of tritiated hydrocarbons and readiness to begin processing upon receipt of a start signal. Because holding tank capacity provides adequate time for most maintenance operations, redundant components are limited to the vacuum and gas transfer pumps. Major system performance criteria are summarized in Table II.

The VERS is normally operated in a batch processing mode. The laboratory vacuum manifold is maintained at an average pressure of approximately 3.3 kPa. The effluent exhausted to the manifold is pumped into a 0.3 m³ tank, where its contamination level is monitored. To minimize VERS operating time, the effluent of the 0.3 m³ tank is divided into two levels of tritium concentration which are collected in separate 5.7 m³ holding tanks. The lower concentration is selected such that effluent can be vented directly to the stack while the effluent with the higher tritium concentration is decontaminated before stacking.

Effluent is collected until the holding tank pressure reaches 86 kPa. The decision to stack the holding tank contents is made by control room personnel and

15th DOE NUCLEAR AIR CLEANING CONFERENCE

Table II VERS performance criteria.

Processing Capacity	18 m ³ hr ⁻¹
Holding Capacity	9.5 m ³ at 86 kPa
Catalytic Reactor	
Operating Temperature	783 K
Standby Temperature	783 K
Catalyst	Engelhard Minerals and Chemicals No. A-16648
Tritium Concentration Reduction Factor*	1000 per pass for concentration from 20,000 ppm to 1 ppm
Molecular Sieve Dryer	Will use GPS dryers
Molecular Sieve	Type 4A
System Operating Pressure	13 to 86 kPa
System Leak Rate	1 x 10 ⁻¹⁰ m ³ (STP)s ⁻¹ maximum helium at 98 kPa differential

*Ratio of inlet to outlet tritium concentrations.

must be initiated manually. The decision to process the holding tank contents through the decontamination section is automatically made by the VERS control system. The tritium monitor at the exit of the decontamination section generates a signal, depending upon the tritium concentration, either to recirculate the effluent through the VERS or to direct it to the stack.

When a holding tank is to be processed through the decontamination section, the VERS control system alerts the control room by means of an alarm light and begins circulation of the holding tank contents through the decontamination section. When the holding tank pressure is reduced below 13 kPa, the system shuts down. The VERS has the capability for being operated in a continuous stacking and processing mode. However, the decision to use this mode will depend upon operational experience still to be gained.

VERS Modifications

The decontamination section of the VERS is shown in Figure 14 as originally received from the manufacturer.

With the exception of the decontamination section, the VERS was designed and fabricated by Sandia. A major task was to integrate the decontamination section into the rest of the system. Because of space limitations, the manufacturer's skid was disassembled and the major components, with the exception of the catalytic reactor, were mounted on the Sandia skid. A new catalytic reactor was built to provide a larger flow capacity and catalyst entry, and exit nozzles

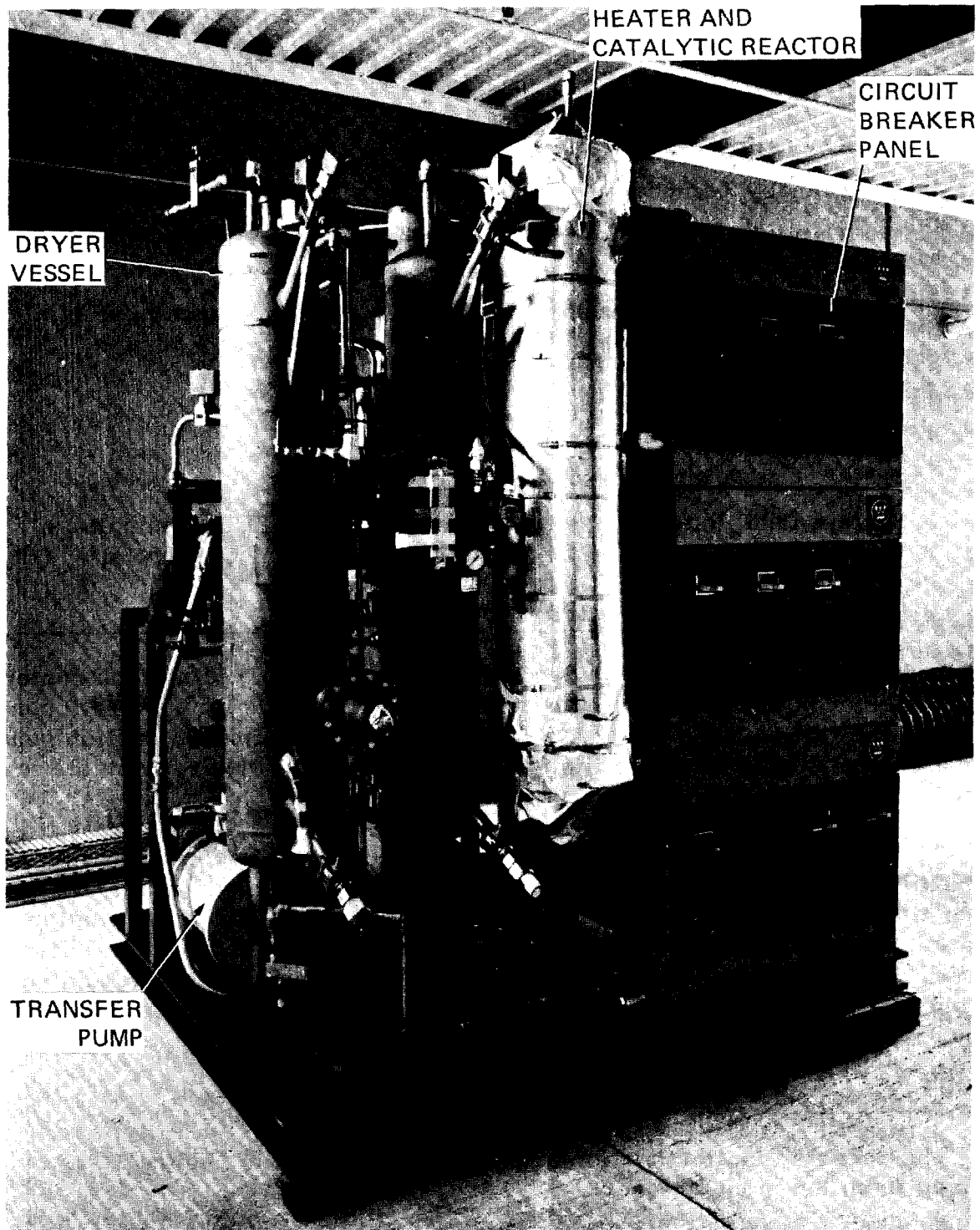


Figure 14 VERS decontamination section as received from manufacturer.

15th DOE NUCLEAR AIR CLEANING CONFERENCE

were relocated to facilitate catalyst addition and removal. The VERS exhaust was interconnected to the GPS so that GPS dryers could be used for water collection.

Where possible the control system elements used for acceptance testing of the skid were integrated with the microprocessor controlled solid state system designed by Sandia. As with the GPS, all of the control elements except disconnects were removed from the skid and mounted outside the air hood. The heater control was changed to a silicone controlled rectifier unit, and thermocouples were placed in the catalytic reactor to allow for more accurate temperature control and to provide a means for monitoring catalyst performance. The final VERS skid configuration is shown in Figure 15, and the control panel located in the TRL control room is shown in Figure 16.

Test Program

The GPS and VERS were subjected to acceptance tests at the manufacturer's plant, and preoperational and tritium tests in the TRL. Acceptance testing at the manufacturer's plant verified the ability of the two systems to meet the performance criteria required by the specification (Tables I and II), with the exception of the concentration reduction factors, which required tritium testing for verification. Hydrogen was combusted as part of the acceptance testing to demonstrate that the catalyst was operating and to provide a source of moisture for loading the first dryer. The swamping system was used to load the second and third dryers.

Preoperational testing of the systems in the TRL included essentially a repeat of the manufacturer's acceptance tests. These tests demonstrated that the systems installed in the TRL met the processing capacity, pressure control, and startup operating time, etc., specifications in the actual laboratory operating configuration. The preoperational testing also included a series of catalyst performance tests with hydrogen and methane.⁽²⁾ These tests were run to provide confidence that the catalytic reactors in both systems were operating properly before tritium was introduced and also to determine the appropriate catalyst operating temperature.

The final series of tests was made with tritium and tritiated methane⁽²⁾ to determine that the systems were capable of achieving the design requirement of a single-pass concentration reduction factor (ratio of inlet to exhaust concentration) of 1000 per pass for inlet concentrations of 1 part per million. Sensitivity limitations of gas chromatography required that this confirmation be made with tritium as the test gas. Tests were run with methane and tritiated methane because tritiated hydrocarbons are expected to be present in both systems,⁽³⁾ particularly in the VERS.

GPS and VERS Hydrogen and Methane Tests

The GPS tests were performed first. Approximately ten runs were made to assess the system operation before the parameters were selected for tests measuring temperature effects upon catalyst performance. The VERS test parameters were selected as a result of this experience. The test parameters used are

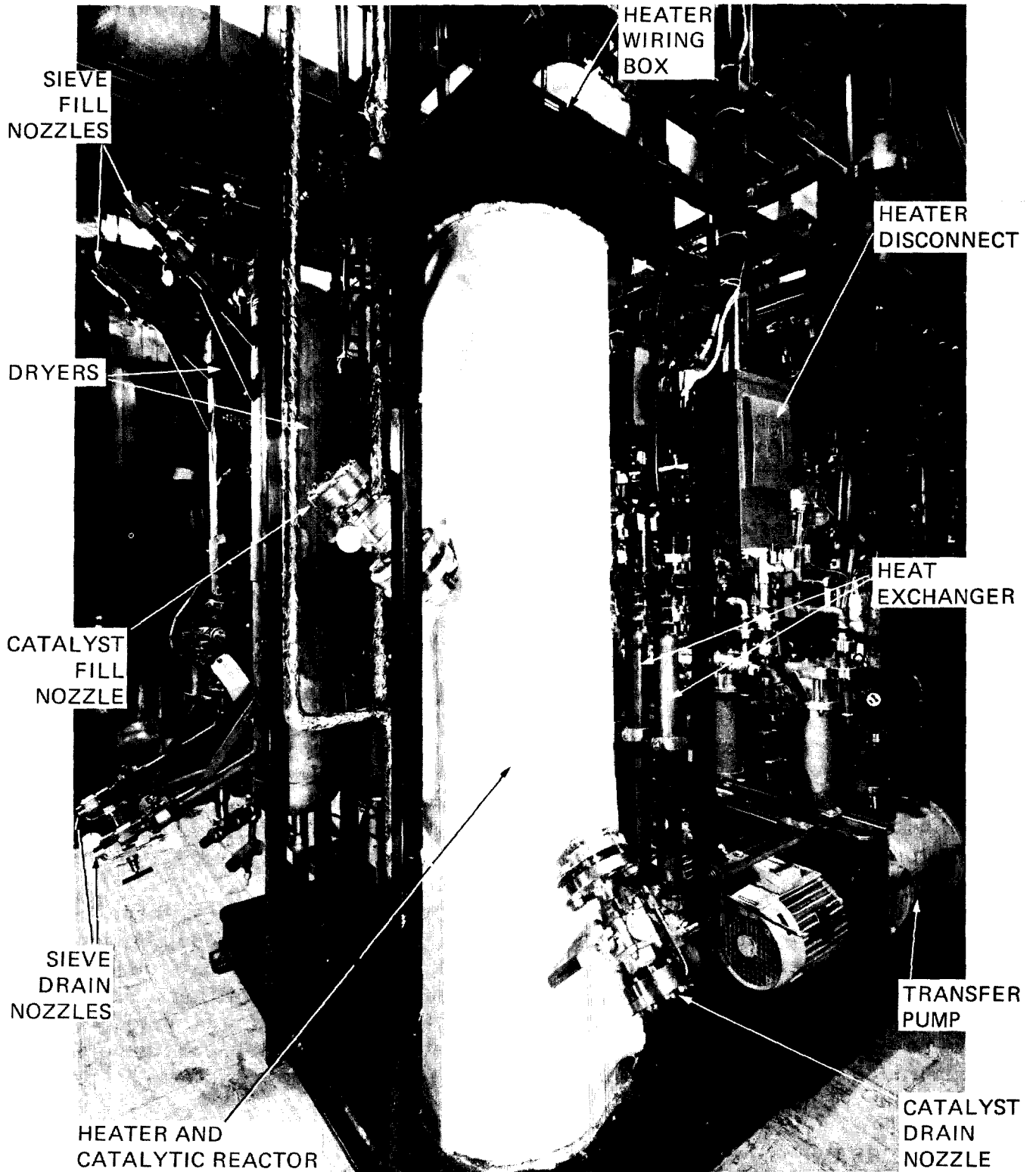


Figure 15 VERS skid final configuration.

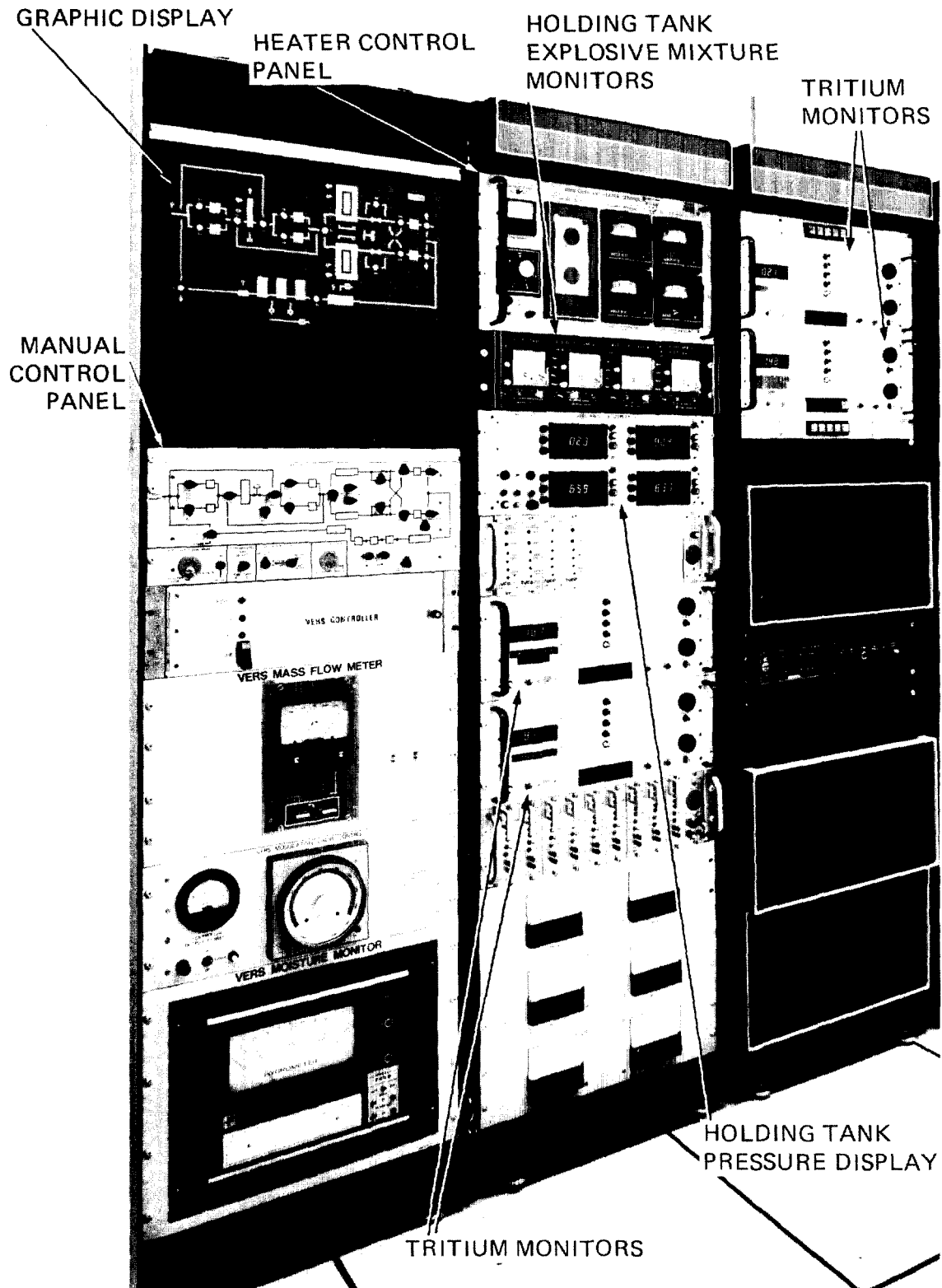


Figure 16 VERS control panel.

15th DOE NUCLEAR AIR CLEANING CONFERENCE

summarized in Table III. Inlet concentrations were chosen to provide a reasonable range of detection for the gas chromatograph.

Table III Hydrogen and methane test parameters.

System	Test Gas	Flow Rate (std m ³ hr ⁻¹)	Inlet Concentration (ppm)	Catalyst Temperature (°K)
GPS	Hydrogen	340	120	316-743
GPS	Methane	261	700	316-810
VERS	Hydrogen	16.4	100	302
VERS	Methane	13.3	2000	302-810

The test gases along with nitrogen and combustion air were injected upstream of the catalytic reactor, and inlet and exhaust concentrations were measured with a gas chromatograph upstream and downstream of the catalytic reactor, respectively. Combustion air was injected in excess of stoichiometric requirements. The results of the GPS catalyst temperature tests are displayed in Figure 17 for both hydrogen and methane. Temperatures below 316 K were not achievable because of the heat of compression generated by the circulation blowers.

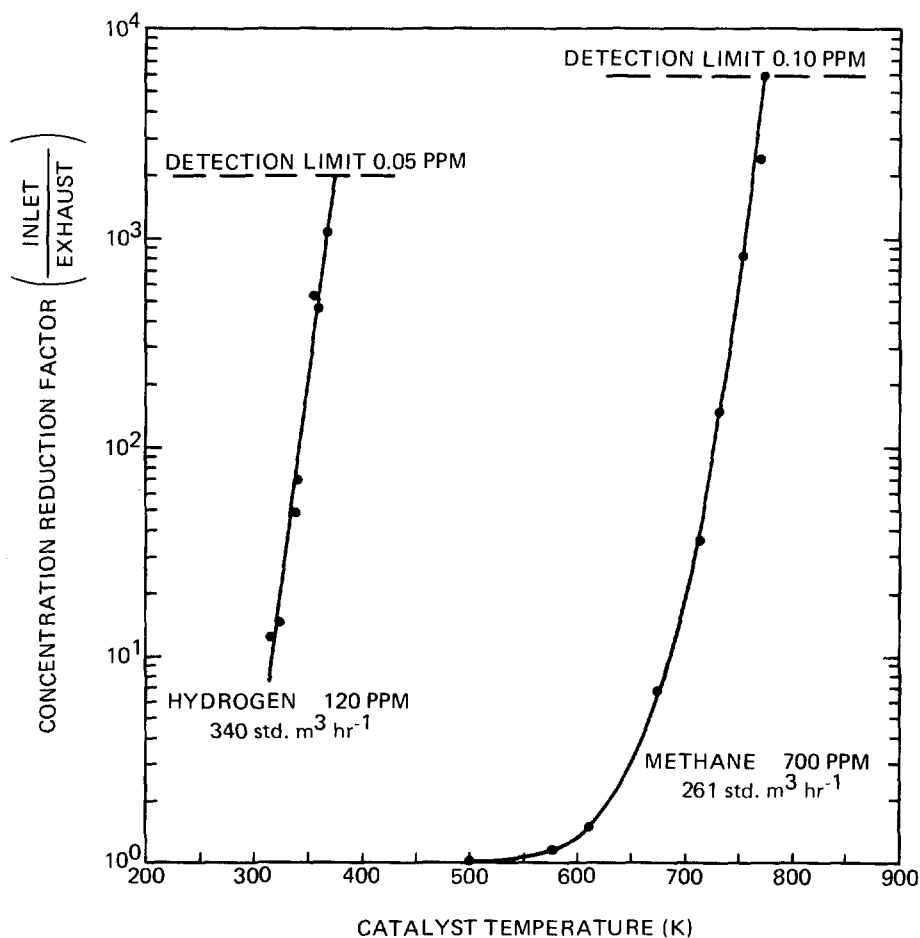


Figure 17 Effect of GPS catalyst temperature on concentration reduction factor.

15th DOE NUCLEAR AIR CLEANING CONFERENCE

A glove box cleanup test was also run with methane to determine the rate at which a contaminant could be removed from the glove box atmosphere. Methane was injected into a nitrogen filled glove box until an initial concentration of 500 ppm was achieved. The box atmosphere was then processed by the GPS. The results are presented in Figure 18.

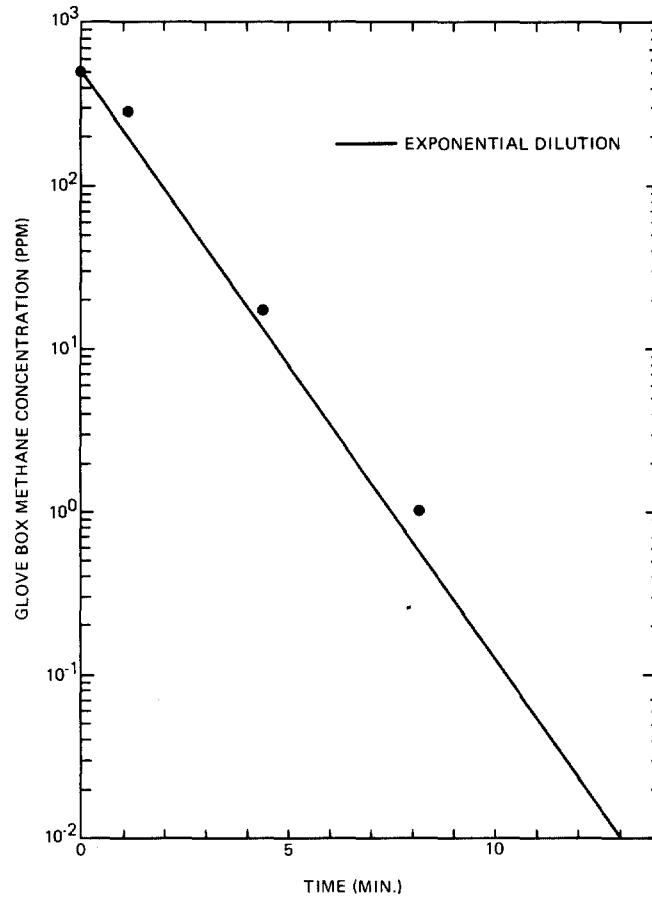


Figure 18 Glove box cleanup test results.

The VERS test results, though similar, cannot be directly compared to those for the GPS since the catalyst residence time for the VERS is approximately 2.5 times that for the GPS. At 320 K, the lowest temperature achievable, the VERS exhaust hydrogen concentration was below the detection limit of the chromatograph, 0.1 ppm. The results of the methane test were essentially the same as for the GPS (Figure 16) and show that to achieve concentration reduction factors greater than 1000, the catalyst must be operated at temperatures in excess of 750 K for methane.

GPS and VERS Tritium Tests

After the preoperational tests and GPS system modifications had been completed, both systems were tested with tritium to verify their ability to achieve concentration reduction factors of 1000 per pass at inlet concentrations of 1 ppm.

15th DOE NUCLEAR AIR CLEANING CONFERENCE

Four tritium tests were run on the GPS at a catalyst temperature of 783 K and a flow rate of 340 std m³ hr⁻¹. Seven tests, four with tritium and three with tritiated methane, were run on the VERS at a catalyst temperature of 783 K and a flow rate of 17.0 std m³ hr⁻¹. Hydrogen was added to some test runs to simulate tritium processing at higher concentrations. All of the tests were run without water added ahead of the second dryer. The GPS test gases were injected into a sealed glove box while the VERS test gases were injected into one of the 5.7 m³ holding tanks and then processed through the system. The test results are summarized in Tables IV and V for the GPS and VERS, respectively. Concentration reduction factors were calculated by dividing the maximum inlet tritium concentration by the maximum exhaust tritium concentration.

Table IV GPS tritium test summary.

Test Designation	Sample Composition	Inlet Tritium Concentration Ci m ⁻³	Exhaust Tritium Concentration μCi m ⁻³	Concentration Reduction Factor
GPS T-1	T ₂ in Nitrogen	0.14	2.0	7.0 x 10 ⁴
GPS T-2	T ₂ in Nitrogen	1.3	15.0	8.7 x 10 ⁴
GPS T-3	T ₂ & 2.0% H ₂ in Nitrogen	9.4	1020.0	9.2 x 10 ³
GPS T-4	T ₂ in Nitrogen	115.0	250.0	4.6 x 10 ⁵

Table V VERS tritium test summary.

Test Designation	Sample Composition	Inlet Tritium Concentration Ci m ⁻³	Exhaust Tritium Concentration* μCi m ⁻³	Concentration Reduction Factor
VERS T-1	T ₂ in Nitrogen	0.18	≤ 1.0	≥ 1.8 x 10 ⁵
VERS T-2	T ₂ in Nitrogen	0.18	≤ 1.0	≥ 1.8 x 10 ⁵
VERS CH ₃ T-1	CH ₃ T in Nitrogen	0.18	≤ 1.0	≥ 1.8 x 10 ⁵
VERS CH ₃ T-2	CH ₃ T in Nitrogen	1.8	≤ 1.0	≥ 1.8 x 10 ⁶
VERS CH ₃ T-4	CH ₃ T & 0.5% H ₂ in Nitrogen	7.4	≤ 1.0	≥ 7.0 x 10 ⁶
VERS T-5	T ₂ & 0.5% H ₂ in Nitrogen	13.2	≤ 1.0	≥ 1.3 x 10 ⁷
VERS T-6	T ₂ & 2.0% H ₂ in Nitrogen	132.0	≤ 1.0	≥ 1.3 x 10 ⁸

*1.0 μCi m⁻³ is the least count of the tritium monitor.

15th DOE NUCLEAR AIR CLEANING CONFERENCE

An uncertainty of approximately 30 percent should be applied to the GPS concentration reduction factors because of inaccuracies both with tritium measurements and data acquisition methods.

An uncertainty of approximately 50 percent should be applied to the VERS concentration reduction factors because of inaccuracies with tritium measurements at the $1 \mu\text{Ci m}^{-3}$ level of concentration.

Summary

The concept of providing both personnel safety and environmental protection from tritium on a laboratory-wide basis by employing a secondary containment system of sealed glove boxes connected to two central decontamination systems has been implemented by Sandia Laboratories Livermore. Acceptance tests at the manufacturer's plant and preoperational tests in the Tritium Research Laboratory have demonstrated that the systems meet their design specifications and that glove box cleanup rates approaching exponential dilution can be achieved.

The tritium test program to date has demonstrated that both the Gas Purification System and Vacuum Effluent Recovery System perform 10-1000 times better than required by the design specifications, and that tritium removal systems can be designed to achieve concentration reduction factors much in excess of 1000 per pass at inlet concentrations of 1 part per million or less for tritium and for tritiated methane.

References

1. P. D. Gildea et al., "A Tritium Systems Test Facility Volume II: Appendixes," Sandia Laboratories, Livermore, SAND76-8053, October 1976, pp. 57-59.
2. P. D. Gildea, W. R. Wall, and V. P. Gede, "Results of Tritium Tests Performed on Sandia Laboratories Decontamination System," Sandia Laboratories, Livermore, SAND77-8766, May 1978.
3. J. C. Bixel and C. J. Kershner, "A Study of Catalytic Oxidation and Oxide Adsorption for the Removal of Tritium From Air," in Proceedings of the Second AEC Environmental Protection Conference, WASH-1332(74), April 16-19, 1974.

15th DOE NUCLEAR AIR CLEANING CONFERENCE

DISCUSSION

KAPASI: How was the tritiated moisture removed from the dryer beds, as liquid or solid?

GILDEA: Water is removed from the dryers in the liquid form by a regeneration system. The liquid water is collected in a room temperature separator and then drained into a mole sieve trap for disposal.

KAPASI: Was swamping used in achieving the decontamination factor you cited?

GILDEA: The equipment provides the capability for water swamping ahead of the second dryer. However, swamping was not used on the tests reported in this paper.

FREEMAN: Are your systems located in an open room with only arrangements for a glove box for removal of the heater?

GILDEA: That is essentially correct. The equipment is located in the equivalent of a walk-in hood. However, this hood does not provide for personal protection during maintenance operations. A glove box mounting arrangement is provided for heater removal/replacement since it requires opening a very large volume of the system to the room.

FREEMAN: Do you anticipate problems with contamination when performing other maintenance procedures?

GILDEA: The isolation valve-purge port arrangement is expected to minimize contamination problems for most maintenance operations.

ANON.: Will the N_2 used to regenerate the molecular sieves be reused since there will be some tritium oxide left in the gas stream even after moisture removal by condensation?

GILDEA: Yes, the nitrogen in the regeneration system is just left there until the next regeneration cycle is required. However, the majority of the moisture picked up by the nitrogen is put back on the sieve bed during the cooldown part of the cycle.

BRUGGEMAN: Please comment on the time scheme you use for the regeneration of your GPS dryers.

GILDEA: The regeneration process takes from 6-8 hours. Hot nitrogen is circulated through the sieve beds until the bed reaches 600°F, at which time the cool down cycle starts.

BRUGGEMAN: Do you have to add oxygen anywhere in your systems?

GILDEA: We add air ahead of the system blowers in order to provide oxygen for combustion of the tritium.

15th DOE NUCLEAR AIR CLEANING CONFERENCE

TRITIUM REMOVAL USING VANADIUM HYDRIDE*

F. B. Hill, Y. W. Wong, and Y. N. Chan
Department of Energy and Environment
Brookhaven National Laboratory
Upton, NY 11973

Abstract

The results of an initial examination of the feasibility of separation of tritium from gaseous protium-tritium mixtures using vanadium hydride in cyclic processes are reported. Interest was drawn to the vanadium-hydrogen system because of the so-called inverse isotope effect exhibited by this system. Thus the tritide is more stable than the protide, a fact which makes the system attractive for removal of tritium from a mixture in which the light isotope predominates. The initial results of three phases of the research program are reported, dealing with studies of the equilibrium and kinetics properties of isotope exchange, development of an equilibrium theory of isotope separation via heatless adsorption, and experiments on the performance of a single heatless adsorption stage.

In the equilibrium and kinetics studies, measurements were made of pressure-composition isotherms, the HT-H₂ separation factor and rates of HT-H₂ exchange. This information was used to evaluate constants in the theory and to understand the performance of the heatless adsorption experiments.

A recently developed equilibrium theory of heatless adsorption⁽¹⁷⁾ was applied to the HT-H₂ separation using vanadium hydride. Using the theory it was predicted that no separation would occur by pressure cycling wholly within the β phase but that separation would occur by cycling between the β and γ phases and using high purge-to-feed ratios.

Heatless adsorption experiments conducted within the β phase led to inverse separations rather than no separation. A kinetic isotope effect may be responsible. Cycling between the β and γ phases led to separation but not to the predicted complete removal of HT from the product stream, possibly because of finite rates of exchange.

Further experimental and theoretical work is suggested which should ultimately make possible assessment of the feasibility and practicability of hydrogen isotope separation by this approach.

I. Introduction

Isotope effects are commonly observed in metal hydrides. The usual finding is that stability increases in the order tritide, deuteride, protide. The vanadium-hydrogen system is one of the few exceptions in that stability increases in the reverse order. An inverse isotope effect may be of value in separating mixtures of

* This work was supported by the Division of Chemical Sciences, U.S. Department of Energy, Washington, D.C., under Contract No. EY-76-C-02-0016.

15th DOE NUCLEAR AIR CLEANING CONFERENCE

hydrogen isotopes consisting mainly of protium with a trace of a heavier isotope, deuterium or tritium.

With this viewpoint in mind, an investigation of the feasibility of removal of tritium from a gaseous protium-tritium mixture using vanadium hydride has been undertaken. The investigation was formulated and is being carried out with the idea in mind of using cyclic processes such as heatless adsorption (cycling pressure) or cycling zone adsorption (cycling temperature) to carry out the separation. Heatless adsorption has been the process studied to date. Three topics have been examined and are discussed in the present paper: equilibrium and kinetics properties of isotope exchange in the vanadium-hydrogen system, the theory of isotope exchange via heatless adsorption, and the performance of a single heatless adsorption stage.

II. Equilibrium and Kinetics Studies

Experimental information needed for development of a theory of isotope separation via heatless adsorption using vanadium hydride and in general needed for the design and analysis of isotope separation processes using this system includes pressure-composition isotherms for H₂, the HT-H₂ separation factor, and information on rates of attainment of equilibrium in isotope exchange. Experimental studies to obtain this information are described briefly in this section. Details are available elsewhere.⁽¹⁾

Materials

Hydrogen was obtained from the Matheson Gas Co., Rutherford, N.J., with a purity of 99.999%. Gaseous tritium was obtained from the New England Nuclear Corp., Boston, Mass., in the form of a one-curie ampoule, carrier free. A master batch of tritiated hydrogen (approximately 4×10^{-9} mole fraction HT in H₂) was prepared by diluting the tritium with $\sim 3 \text{ m}^3$ of the Matheson hydrogen. Ingots of vanadium were obtained from the Gallard-Schlesinger Chemical Manufacturing Corp., Carle Place, N.Y. The vanadium purity was 99.5% V minimum with major impurities in percent, 0.15 Si, 0.05 Fe, 0.04 N, 0.02 O, 0.03 C, 0.01 all other metals. Upon receipt the ingots were partially hydrided to facilitate crushing and sizing with standard sieves.

Pressure-Composition Isotherms

These measurements were made using the techniques and apparatus of Reilly and Wiswall.⁽²⁾ Measurements were made in the VH_{0.6} - VH_{1.8} region at temperatures from 0° to 250°C, and pressures from approximately atmospheric to 7000 kPa (1000 psi). The results are shown in Figure 1. The plateau pressures, corresponding to dihydride dissociation, were approximately twice those reported by Reilly and Wiswall⁽³⁾ for hydride made from zone-refined V, thus reflecting the strong influence of impurities. Hydrogen content of hydrides made from commercial grade V was lower than that for hydrides from zone refined V. Impurities were found to exert no significant influence on the temperature dependence of the plateau pressures, confirming the earlier findings of Reilly and Wiswall.⁽⁴⁾

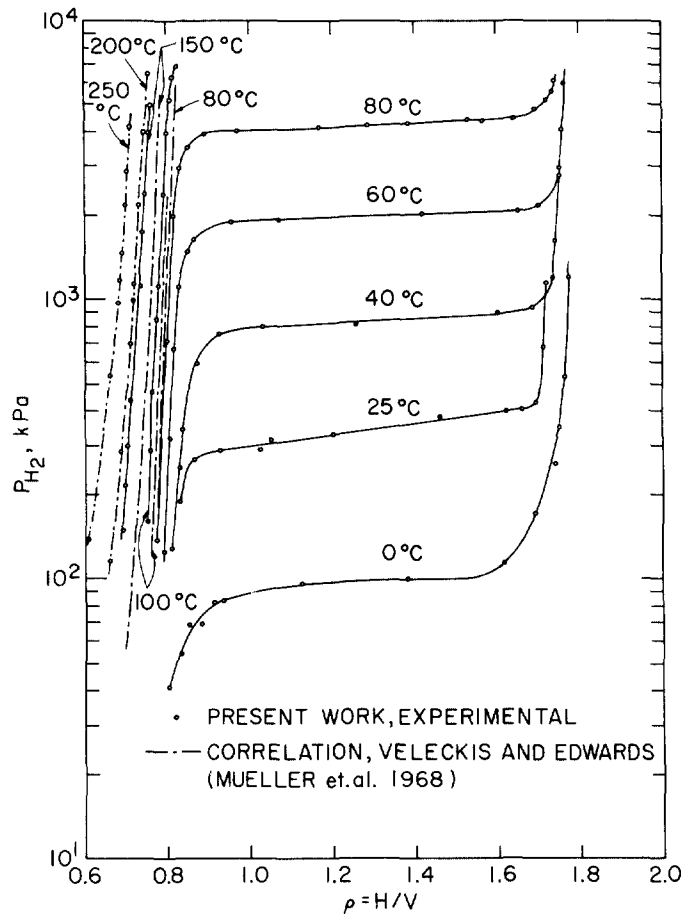


Figure 1. Pressure-composition isotherm data for the vanadium (commercial grade)-hydrogen system.

Also shown in Figure 1 is a comparison of the present data with the predictions of a semi-empirical formula due to Veleckis and Edwards: (5)

$$\ln p_{\text{mm}}^{\frac{1}{2}} = 10.283 + 1.0598 \ln \frac{\rho}{0.89 - \rho} + \frac{1}{T}(-3489.2 - 3269.0\rho + 2563.0\rho^2 - 732.39\rho^3 + 4818.3\rho^4) \cdot \quad (1)$$

Agreement with this relation is good at high temperature and at pressures below the dihydride dissociation pressure. Equation (1) was developed by fitting pressure-composition data for the α phase to a model based on simple interstitial solution of hydrogen atoms in a perfect crystalline lattice. Thus this model appears to apply also to the β phase at higher temperatures.

The distribution coefficient for H_2 , $K_{H_2} = C_H/C_{H_2}$, was calculated from the isotherm data as follows. From the perfect gas law,

15th DOE NUCLEAR AIR CLEANING CONFERENCE

$$C_{H_2} = \frac{P}{RT} \quad (2)$$

The equilibrium concentration of hydrogen atoms in the solid phase is given by

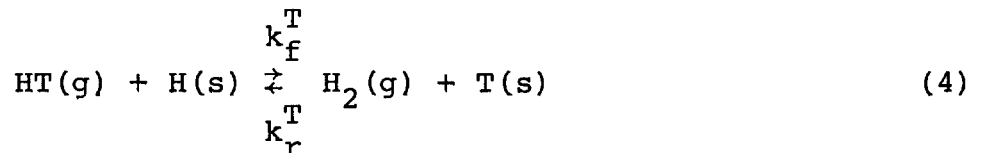
$$C_H = \rho / \left[\frac{50.95 + 1.008\rho}{\rho_s} \right] \quad (3)$$

where ρ is the hydrogen-to-vanadium ratio corresponding to the pressure P on the isotherm, 50.95 and 1.008 are the atomic weights of V and H and ρ_s is the density of vanadium hydride in g/cm^3 . As indicated above, the distribution coefficient is the quotient, C_H/C_{H_2} .

Chromatography Experiments

Separation factors and rate information were obtained from chromatography experiments in which pulses of tritiated hydrogen were eluted from a column packed with vanadium hydride particles. The eluted pulses were detected by means of an internal proportional counter. First and second moments of these pulses were determined in an extensive series of experiments in which particle size, temperature, pressure and hydrogen flow rate were variables.

The first and second moment data were interpreted in terms of a theoretical model of mass transfer and exchange reaction. In this model the exchange reaction occurring at the gas-solid interface is



The overall exchange process is postulated to occur in the following steps in series: diffusion of HT through a gas film surrounding a hydride particle, exchange at the gas-solid interface via reaction (4), and diffusion of T atoms into the interior of the particle. Also dispersion of HT in the gas phase occurs in the axial direction.

For this model it can be shown that the first absolute moment (elution time) and second central moment (variance) are related to equilibrium and rate constants of the constituent processes of the model by the following relations:

$$\mu_1'(h) = \left(1 + \frac{1-\epsilon}{\epsilon} \frac{\alpha}{2} K_{H_2} \right) \frac{h}{u} + \frac{t_0}{2} \quad (5)$$

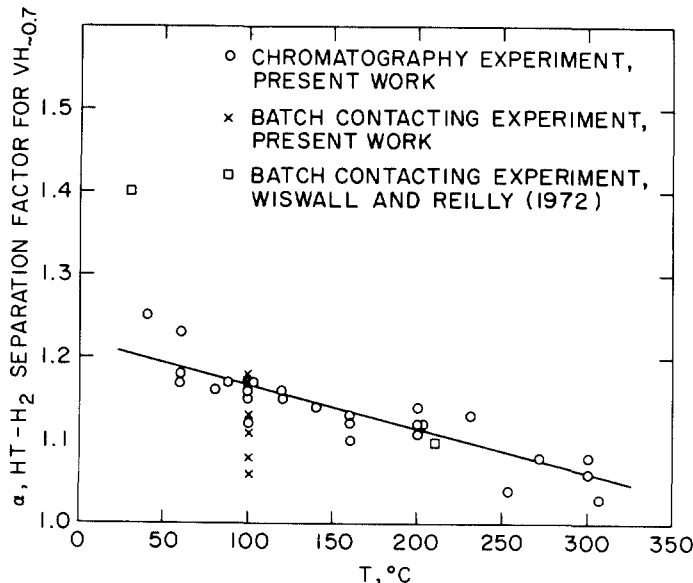
$$\begin{aligned} \mu_2(h) = & \left\{ \frac{1-\epsilon}{\epsilon} \frac{\alpha}{2} K_{H_2} \left[\left(\frac{\alpha}{2} K_{H_2} \right) \frac{1}{3D_{HT-H_2}} + \frac{1}{15D_s} \right] r_p^2 \right. \\ & \left. + \frac{\alpha}{2} \frac{K_{H_2}}{k_f^T C_H^*} \right\} + E_z \left(1 + \frac{1-\epsilon}{\epsilon} \frac{\alpha}{2} K_{H_2} \right)^2 \frac{1}{u^2} \left\{ \frac{2h}{u} + \frac{t_0^2}{12} \right\} \quad (6) \end{aligned}$$

15th DOE NUCLEAR AIR CLEANING CONFERENCE

An assumption implicit in Equation (6) is that the flow in the column is laminar.

By inspection of Equation (5) it is apparent that by using values of $\mu_1^*(h)$, K_{H_2} , h , u , and t_0 in this equation one can evaluate α , the HT-H₂ separation factor. The distribution coefficient, K_{H_2} , is obtained for this purpose from the pressure-composition isotherms as indicated in the previous section. Similarly, Equation (6) can be used to evaluate rate information. The details of this evaluation are given by Wong and Hill.⁽¹⁾

The chromatography experiments were conducted over the temperature range 40° to 307°C and over the pressure range 210 to 1030 kPa (30 to 150 psi). Hydrogen flow rates were varied from 80 to 400 standard cm³/min. Four particle sizes were used: 40/45 mesh (380 μ m geometric average diameter), 30/40 (500), 20/25 (770), and 16/20 (1000). Values of the separation factor, α , determined from first moment data are plotted versus temperature in Figure 2. It may be



9-228-78

Figure 2. HT-H₂ separation factors for β vanadium hydride.

shown that α is not a function of pressure.⁽¹⁾ This behavior is expected since α is held to be related to the Einstein vibration frequencies of the isotopes in the metal lattice⁽⁶⁾ and hence should be a function of lattice structure and temperature only. It is generally true that isotope effects disappear, i.e., $\alpha \rightarrow 1$, at high temperature.⁽⁷⁾ As a result, the magnitude of the measured α was expected to decrease with temperature. This was found to be so experimentally. It is interesting that there is no discontinuity in the variation of α with temperature in the range 160° to 180°C where a transition from the β to the α phase occurs.⁽⁸⁾ Also shown in Figure 2 are separation factors obtained by Wiswall and Reilly⁽⁹⁾ and in this work using the batch contacting technique of Tanaka, Wiswall and Reilly.⁽¹⁰⁾ Good agreement exists between the data for

15th DOE NUCLEAR AIR CLEANING CONFERENCE

the two types of experiments, thus demonstrating as did Schneider and Smith(11) that values of equilibrium properties can be accurately determined from kinetic measurements. Also agreement is good between data for hydrides derived from pure and commercial grade V (Wiswall and Reilly's data are for zone refined V). The presence or absence of impurities seemed to have no influence on separation factor.

By suitable representation of second moment data it was possible to show that the term in square brackets in Equation (6) did not vary with particle size and thus that this term was essentially equal to $\frac{\alpha}{2} K_{H_2} / (k_F^T C_H^*)$. This term represents the resistance due to the exchange reaction. The terms multiplied by r_p^2 represent the resistances due to external diffusion and solid phase diffusion. The implication is that the exchange reaction is controlling.

With knowledge that the first term in square brackets in Equation (6) is small compared with the second, this equation was used in combination with values of ϵ , α , and K_{H_2} to determine values of $k_F^T C_H^*$ for each set of temperature and pressure conditions. For purposes which will become apparent below each value of $k_F^T C_H^*$ was then multiplied by $C_{H_2}^* = P/RT$, where the values of P and T were those corresponding to the experiments from which the value of $k_F^T C_H^*$ was derived. Values of $k_F^T C_H^* C_{H_2}^*$ so determined are shown in Figure 3. The

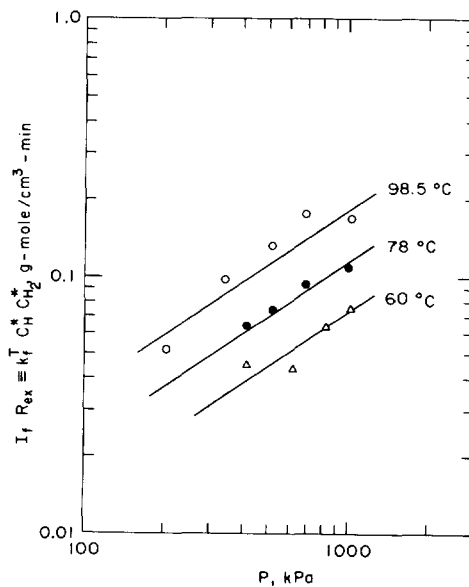


Figure 3. Pressure and temperature dependence of the exchange reaction rate.

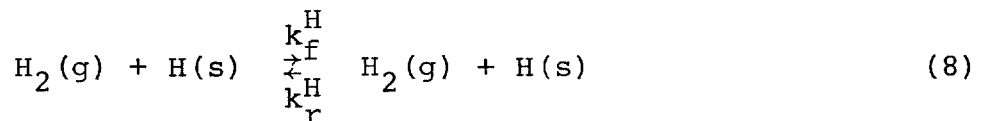
15th DOE NUCLEAR AIR CLEANING CONFERENCE

temperature and pressure dependence of $k_f^T C_H^* C_{H_2}^*$ was found to be given by

$$k_f^T C_H^* C_{H_2}^* = 4.06 P^{0.7} \exp\left(-\frac{24600}{RT}\right) \text{ gm mole/cm}^3\text{-min}, \quad (7)$$

where P is in kPa and the activation energy is in joule/gm-mole.

For the purpose of examining the significance of the temperature and pressure dependence of the exchange reaction rate it is convenient to proceed as follows. The rate of disappearance of HT is given by $k_f^T C_H^* C_{HT}^*$. This rate may be expressed in terms of the rate of the hydrogen exchange reaction



as follows:

$$\begin{aligned} k_f^T C_H^* C_{HT}^* &= \frac{k_f^T}{k_f^H} k_f^H C_H^* C_{H_2}^* \frac{C_{HT}^*}{C_{H_2}^*} \\ &= I_f R_{ex} \frac{C_{HT}^*}{C_{H_2}^*} \end{aligned} \quad (9)$$

As one can see, the product of the hydrogen exchange rate, R_{ex} , and the forward isotope effect, I_f , is identically the left hand side of Equation (7). The forward isotope effect is independent of pressure and is a slowly varying function of temperature.⁽⁷⁾ Hence all of the pressure dependence and substantially all of the temperature dependence of Equation (7) may be ascribed to the hydrogen exchange rate R_{ex} . The pressure dependence of the hydrogen exchange reaction rate may range from P^0 to P^1 according to the detailed nature of the mechanism of chemisorption and reaction of H_2 . Three such mechanisms together with their pressure dependencies are those of Bonhoeffer and Farkas (P^0), Rideal-Eley, two site ($P^{0.5}$), and Rideal-Eley, single site (P^1). A pressure dependence given by $P^{0.7}$ can be ascribed to a mixture of contributions from all three mechanisms. Alternately, the explanation of Scholten and Konvalinka⁽¹²⁾ may be valid. They found a pressure dependence of $P^{0.64}$ for the rate of hydrogen exchange on β palladium hydride. This pressure dependence closely approximated the variation with $P^{2/3}$ found for a mechanism based on a surface composition of Pd_3H_2 (approximately the composition of $PdH_{0.68}$ used experimentally) and the assumption that the rate of reaction was proportional to the number of H_2 collisions with the surface and the chance of encounter with a free Pd atom. The same argument would apply to the β vanadium hydride system with its approximate composition V_3H_2 .

15th DOE NUCLEAR AIR CLEANING CONFERENCE

The temperature dependence of the hydrogen exchange rate is in the range expected for activated chemisorption. (13)

Also obtainable from second moment data are values of the axial dispersion coefficient, E_z . These were found to be just slightly greater than expectations based on molecular diffusion only. Thus some additional mechanism of axial mixing appeared to have been present.

III. Theory

In this section an equilibrium theory of hydrogen isotope separation via heatless adsorption using vanadium hydride is presented. First a brief description of the heatless adsorption process is given.

Heatless adsorption is a cyclic separation process involving two adsorption beds. Each cycle consists of four steps (Figure 4). In

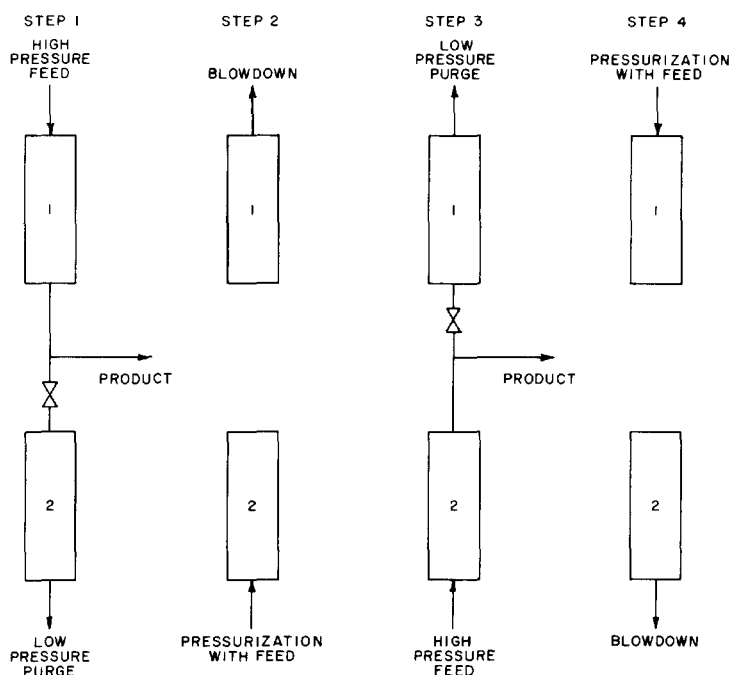


Figure 4. Steps in a cycle of heatless adsorption.

the first step, a high pressure feed mixture is continuously supplied to Bed 1, and during this step sorbable components are taken up. A portion of the purified Bed 1 effluent is taken off as product and the remainder is throttled down to a lower pressure and is supplied to Bed 2 and serves to purge previously sorbed species. In the second step Bed 2 is pressurized with the feed and Bed 1 undergoes depressurization or blowdown to the purge pressure. The third and fourth steps are the same as the first two except that the points of feed introduction and purge and blowdown removal are reversed with respect to Beds 1 and 2. Heatless adsorption has the unusual characteristic that if a sufficiently high fraction of the feed is used as purge and if the cycle time is sufficiently long then at steady state the product stream will be completely free of adsorbable or preferentially adsorbable components.

15th DOE NUCLEAR AIR CLEANING CONFERENCE

Shendalman and Mitchell⁽¹⁴⁾ have presented an equilibrium theory of heatless adsorption. Their theory was based on the following assumptions.

1. The feed consists of a nonadsorbing carrier gas containing a trace amount of an adsorbing component.
2. The adsorbing component obeys a linear distribution law.
3. Equilibrium is instantaneously established between phases.
4. The system is isothermal.
5. Dispersion axially is negligible.
6. Flow and composition are uniform radially.
7. The frictional pressure drop across a bed due to flow is negligible.
8. The ideal gas law is valid.

Development of the theory proceeded along the lines of the theory of parametric pumping.⁽¹⁵⁾ The penetration distance concept⁽¹⁶⁾ was employed. The novel feature in heatless adsorption which it was necessary to treat was the presence of pressurization and blowdown steps.

The theory presented by Shendalman and Mitchell is conceptually valid in its prediction of the rate of movement of concentration characteristics during the feed and purge step, concentration changes occurring within the column as the result of pressure changes, and the critical purge-to-feed ratio (the minimum value required for complete column cleanup). However an error was made in the calculation of sorbing component uptake during pressurization, which can lead to significant overestimation of that quantity and consequently to incorrect values of the average blowdown and purge concentrations.

The calculation of sorbing component uptake during pressurization was recently correctly described by Chan, et al.⁽¹⁷⁾ and the complete corrected theory was presented. Also the theory was extended to the case in which the carrier is also adsorbed.

In this section of the paper the theory of Chan, et al.⁽¹⁷⁾ is applied to the removal of a trace level of HT from a stream of H₂ using vanadium hydride. The principal modification of the original theory required is the introduction of the proper isotherm. For the sake of brevity, the theory will be presented in outline form for a separation conducted wholly within the β phase.

In the β phase, ($V_{H_2 0.6} - V_{H_2 0.8}$) a pressure-composition isotherm for H₂ (see Figure 1) may be represented by

$$\ln P = a C_H + b \quad (10)$$

where a and b are functions of temperature.

15th DOE NUCLEAR AIR CLEANING CONFERENCE

We define the HT-H₂ separation factor as follows:

$$\alpha = \left(\frac{C_T}{C_H} \right) / \left(\frac{C_{HT}}{2C_{H_2}} \right) \quad (11)$$

where α is a function of temperature.

A balance for H₂ over a differential length of a column is

$$\epsilon \left[\frac{\partial C_{H_2}}{\partial t} + \frac{\partial (u C_{H_2})}{\partial z} \right] + (1-\epsilon) \frac{1}{2} \frac{\partial C_H}{\partial t} = 0 \quad (12)$$

A similar balance for T atoms is

$$\epsilon \left[\frac{\partial C_{HT}}{\partial t} + \frac{\partial (u C_{HT})}{\partial z} \right] + (1-\epsilon) \frac{\partial C_T}{\partial t} = 0 \quad (13)$$

With the use of Equations (10) and (11) and the perfect gas law, expressions for $\frac{\partial C_H}{\partial t}$ and $\frac{\partial C_T}{\partial t}$ may be derived. By using these expressions, the perfect gas law, and assumption 7 in Equations (12) and (13) the following equations may be obtained:

$$\left[\frac{\epsilon}{RT} + \frac{(1-\epsilon)}{2aP} \right] \frac{\partial P}{\partial t} + \frac{\epsilon P}{RT} \frac{\partial u}{\partial z} = 0 \quad (14)$$

$$\left[\frac{\epsilon P}{RT} + (1-\epsilon) \frac{\alpha}{2} C_H \right] \frac{\partial y}{\partial t} + \frac{\epsilon u P}{RT} \frac{\partial y}{\partial z} - (1-\epsilon) \frac{1-\alpha}{2} \frac{y}{aP} \frac{\partial P}{\partial t} = 0 \quad (15)$$

The method of characteristics is applied to these equations (Shendalman and Mitchell,⁽¹⁴⁾ Chan, et al.⁽¹⁷⁾) with the following results. During process steps occurring at constant pressure (feed and purge steps) the movement of characteristics is described by

$$\frac{dz}{dt} = \frac{\frac{\epsilon P}{RT}}{\frac{\epsilon P}{RT} + (1-\epsilon) \frac{\alpha}{2} C_H} u \quad (16)$$

Let

$$B = \frac{\frac{\epsilon P}{RT}}{\frac{\epsilon P}{RT} + (1-\epsilon) \frac{\alpha}{2} C_H} \quad (17)$$

Then the penetration distances for high and low pressure concentration fronts are

$$L_H = B_H u_H \Delta t \quad (18)$$

$$L_L = B_L u_L \Delta t \quad (19)$$

15th DOE NUCLEAR AIR CLEANING CONFERENCE

During pressure changes the movement of characteristics and changes in concentration are given by

$$\ln \frac{z_2}{z_1} = - \int_{P_1}^{P_2} \frac{\frac{\epsilon}{RT} + \frac{(1-\epsilon)}{2aP}}{\frac{\epsilon P}{RT} + (1-\epsilon) \frac{\alpha}{2a} (\ln p - b)} dP \quad (20)$$

$$\ln \frac{Y_2}{Y_1} = \int_{P_1}^{P_2} \frac{(1-\epsilon) \frac{1-\alpha}{2aP}}{\frac{\epsilon P}{RT} + (1-\epsilon) \frac{\alpha}{2a} (\ln p - b)} dP \quad (21)$$

or, defining $E(P_2, P_1)$ and $F(P_2, P_1)$ as the exponentials of the right hand sides of Equations (20) and (21),

$$z_H = E(P_H, P_L) z_L \quad (22)$$

$$Y_H = F(P_H, P_L) Y_L \quad (23)$$

The net displacement of a concentration front during a complete cycle of operation can be shown to be

$$\Delta L = L_L - E(P_L, P_H) L_H \quad (24)$$

For $\Delta L = 0$,

$$\frac{L_L}{L_H} = E(P_H, P_L) \quad (25)$$

The fraction of the feed which is rejected as purge when $\Delta L = 0$ may be calculated from this equation by multiplying by the ratio, P_L/P_H . This fraction is called the critical purge-to-feed ratio:

$$G_{crit} = E(P_H, P_L) \frac{P_L}{P_H} \quad (26)$$

When $L_L/L_H \geq G_{crit}$ and $L_H \leq h$, it may be shown that

$$\lim_{n \rightarrow \infty} y_n^{Pr} = 0 \quad (27)$$

or that the product stream will be completely free of preferentially sorbable component at steady state.

During the pressurization step the HT contained within the column at the outset of the pressure change will move as dictated by Equation (20) and will experience concentration changes in accordance with Equation (21). In particular, HT at $z = h$ when $t = t_1$ (see Figure 5) will move to $z = A$ by the time $t = t_2$. Therefore at the end of the pressurization step the section of the column defined by

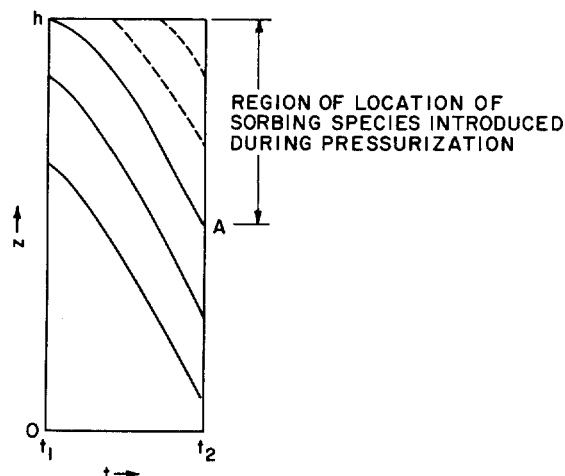


Figure 5. The pressurization step in heatless adsorption.

$A < z \leq h$ will be occupied by all of the HT which entered the column during the pressurization step. Shendalman and Mitchell assumed the gas phase mole fraction within this section would be uniformly equal to the feed mole fraction, y_F . That this cannot be so may be shown simply as follows. During pressurization as one moves from left to right along $z = h$ in Figure 5, the pressure is increasing continuously. Therefore gas introduced into the column at different times will "see" different initial pressures with the result that the lower limit on the integrals in Equations (20) and (21) changes along $z = h$. The mole fraction of HT at $t = t_2$ then varies within the section of the column of interest from a value at A resulting from a low pressure limit of P_L in Equation (21) to the value y_F at $z = h$ corresponding to $P_1 = P_H$.

In the case of a linear isotherm⁽¹⁷⁾ an analytical relation defining the mole fraction distribution within $A \leq z \leq h$ can be obtained. In the present case Equations (20) and (21) are integrated numerically with $z_1 = h$ and $y_1 = y_F$ for values of P_1 between P_L and P_H . Pairs of values $\{y_i, z_i\}$ along $t = t_2$ are thereby obtained which can be fitted satisfactorily by a regression procedure. This method does lead to a good mass balance between HT introduced to the column during pressurization and the HT contained in $A \leq z \leq h$ after pressurization.

Using the relations obtained thus far a difference equation may be derived relating the purge mole fraction after n cycles of operation to the feed mole fraction, to y_{av} , the average mole fraction introduced during pressurization, and to product mole fractions of earlier cycles. The difference equation is obtained by tracing the movement of concentration fronts through the column:

$$y_n^{Pg} = \frac{\left[h - (h-L_H) \frac{1}{E(P_H, P_L)} \right] \frac{1}{F(P_H, P_L)} y_F}{L_L} + \frac{h}{L_L} \left[\frac{1}{E(P_H, P_L)} - 1 \right] y_{av} + q \frac{\Delta L_L}{L_L} y_{n-r-1}^{Pr} + (1-q) \frac{\Delta L_L}{L_L} y_{n-r}^{Pr} \quad (28)$$

Enrichment ratios can now be found. For the blowdown, for instance, the total amount of protium and the total amount of tritium in the column before and after blowdown are calculated. From this information the average mole fraction of HT in the blowdown may be calculated. The same procedure is followed for the purge. Enrichment ratios are then the ratio of the average mole fraction of HT in the blowdown or purge to the feed mole fraction. Thus the blowdown enrichment is

$$E_b = \frac{\left\{ \left[\frac{\epsilon P_H}{RT} + (1-\epsilon) \frac{\alpha C_H^H}{2} \right] \frac{L_H}{h} - \left[\frac{\epsilon P_L}{RT} + (1-\epsilon) \frac{\alpha C_H^L}{2} \right] \right\} \left[h - (h-L_H) / E(P_H, P_L) \right] \frac{1}{h} \cdot \frac{1}{F(P_H, P_L)}}{\frac{\epsilon}{RT} (P_H - P_L) + (1-\epsilon) \frac{1}{2} (C_H^H - C_H^L)} \quad (29)$$

The purge enrichment is by definition

$$E_{Pg} = \frac{y_n^{Pg}}{y_F} \quad (30)$$

For purposes of comparison with experiments to be described in the next section, calculations were made of the performance of the heatless adsorption process using equations from the above development. All of the calculations were made for apparatus having the shortest possible columns necessary for complete removal of HT from the product stream. This condition is realized when the column height is set equal to the low pressure penetration distance,

$$h = L_L \quad (31)$$

and when at the same time the column height is equal to the pressurization displacement ($h-A$ in Figure 5) plus the high pressure penetration distance:

$$h = h-A + L_H$$

or

$$A = L_H \quad (32)$$

Enrichment in such a column is the maximum obtainable. Enrichment in longer columns will be the same or smaller.

Calculations were made for conditions approximating or bracketing those used in experiments to be described in the next section. For all calculations $h = 45.7$ cm, $S = 0.472$ cm², and $\epsilon = 0.5$.

15th DOE NUCLEAR AIR CLEANING CONFERENCE

Single Phase Operating Mode

Separation experiments may be conducted wholly within the β phase by cycling the pressure at constant temperature between limits such that operation occurs along a vertical segment of a pressure-composition isotherm for which the hydride composition is in the range $VH_{\sim 0.6}$ to $VH_{\sim 0.8}$ (see Figure 1). This means, for instance, if pressures are restricted to the range, say, 100 to 1000 kPa (~ 15 to ~ 150 psi) that experiments may be conducted at temperatures of 60°C or higher.

Table I. Calculated performance of heatless adsorption operating in single phase mode.

<u>T, °C</u>	<u>α</u>	<u>G_{crit}</u>	<u>E_{ov}</u>
100	1.17	0.9985	1.0072
118	1.16	1.001	1.0044
150	1.14	0.9977	1.0076
200	1.12	0.9974	1.0074
250	1.09	0.9966	1.0078

Table I presents the results of calculations of performance in the single phase region. There it is seen that for temperatures ranging from 100°C to 250°C the critical purge-to-feed ratios are so high that they are tantamount to total reflux. In a corresponding way the overall enrichments (average value in the combined purge and blowdown) are extremely small. Thus essentially no separation is predicted for this mode of operation. For all intents and purposes this is because the equilibrium hydrogen content of the solid in the β region varies very little with pressure and the HT-H₂ separation factor does not change at all with pressure. For example, with respect to hydrogen content, as indicated in Figure 1 for the 100°C isotherm, the hydrogen-to-vanadium ratio, ρ , increases only by 7 percent between 100 and 1000 kPa.

Two Phase Operating Mode

Significant changes in hydrogen content and separation factor are possible at lower temperatures where operation over the same pressure range involves cycling between the β and γ phases. Thus, as an example, at 40°C ρ would vary from about 0.8 at 100 kPa to approximately 1.7 at 1000 kPa, more than a factor of 2. From Wiswall and Reilly⁽⁹⁾ the HT-H₂ separation factor in the γ phase is about 1.7 at 40°C. From Figure 2, it is 1.20 in the β phase at this temperature.

Calculations of process performance when cycling between the β and γ phases were carried out for three different temperatures: 16, 25 and 40°C. The isotherms were represented by a number of straight lines. The details of this representation were dependent on the particular low and high pressures chosen for the calculation. The lines chosen for the 40°C isotherm for instance are shown in

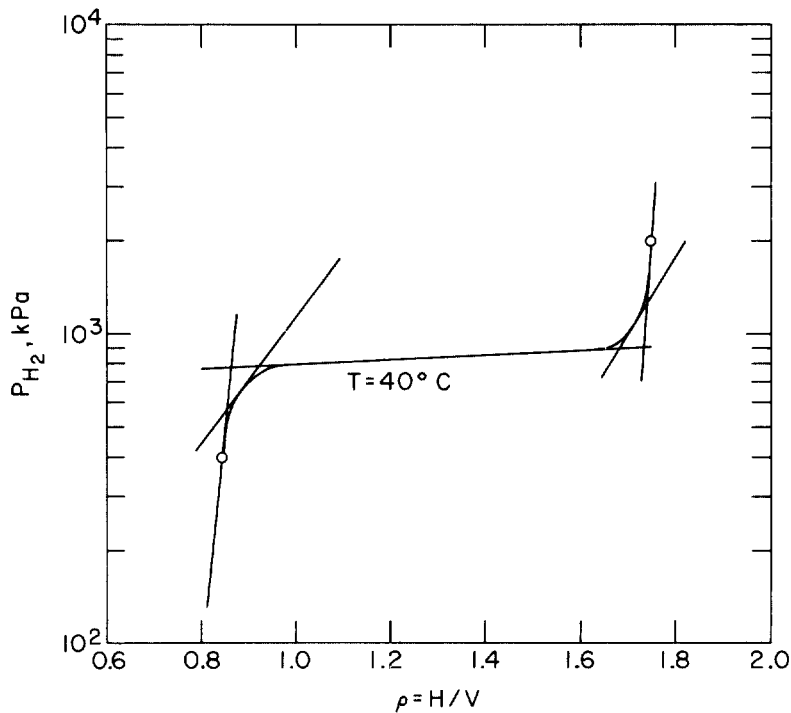


Figure 6. Representation of pressure-composition isotherms for operation in the two phase region.

Figure 6. In making the calculation it was assumed that the separation factor varied continuously in the two phase region from its value in the β phase to that in the γ phase according to the lever rule. All of the equations for process performance were modified to accommodate the two phase isotherm and the accompanying separation factor variation.

Table II. Calculated performance of heatless adsorption operating in two phase mode.

Feed flow rate = 250 sccm
Cycle time = 40 min

$T, ^\circ\text{C}$	P_L, kPa	$\alpha, \beta\text{-phase}$	P_H, kPa	$\alpha, \gamma\text{-phase}$	G_{crit}	$\frac{E}{\text{ov}}$
0	40	1.22	200	1.89	0.766	2.06
25	200	1.21	1000	1.75	0.819	1.41
40	400	1.20	2000	1.66	0.840	1.35

The results of the calculation are given in Table II. There it may be seen that the critical purge-to-feed ratio ranges from 0.77 to 0.84 as the temperature increases from 0° to 40°C. HT is thus completely removed from the product stream which ranges in total amount from 23 to 16 percent of the feed introduced during the high pressure continuous flow step. Overall enrichment decreases with temperature from 2.06 to 1.35.

IV. Performance of a Single Heatless Adsorption Stage

In this section experiments are described on a single heatless adsorption stage and the results are discussed in the light of predictions of the equilibrium theory and of the findings of the chromatography experiments.

Apparatus

A schematic diagram of the apparatus is shown in Figure 7. Each column was made of stainless steel, had an inside diameter of 0.775 cm, and contained 59.4 grams of vanadium hydride particles. The packed bed had a void fraction of 0.5 and a length of 45.7 cm. The bed was supported at the bottom by a stainless steel filter. Stainless steel wool was used to fill the space above the bed. The temperature of the column was maintained constant by means of a jacket and constant temperature circulating bath. Resistance heating wires wrapped around the outside of the jacket were used to raise the column temperature to levels as high as 450°C for the purpose of activating the vanadium particles. Hydrogen gas at high pressure was directed into one column and purge gas at low pressure was introduced into the other. This was achieved by a so-called feed and purge flow

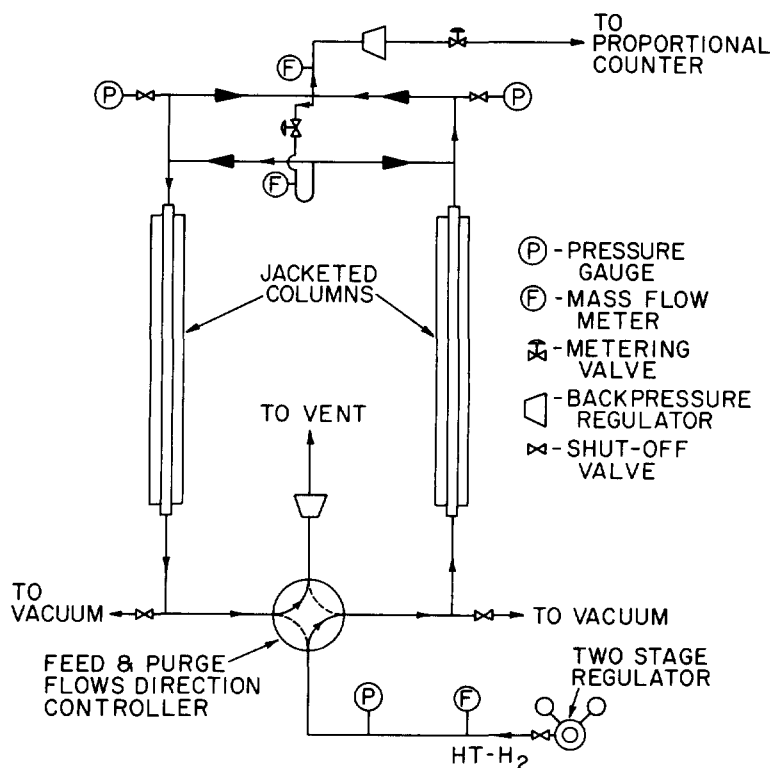


Figure 7. Schematic diagram of heatless adsorption apparatus.

15th DOE NUCLEAR AIR CLEANING CONFERENCE

direction controller on the feed side and check valves on the product side. The flow direction controller consisted of an arrangement of four air-operated valves actuated by solid state timers. The valves were operated in such a way that one column was fed while the other was purged and vice versa.

The purge was derived from the high pressure product stream. Thus part of the stream emerging from the high pressure column was withdrawn as product and the rest was let down to a lower pressure and introduced into the low pressure column as purge. The lowering of the pressure was a direct result of the pressure drop across a fine metering valve. The high pressure stream was prevented from entering the low pressure column by a check valve. The pressure levels at the two columns were maintained by the feed gas regulator and the respective back pressure regulators. The column pressures and the pressure drops across the columns were measured by three high precision pressure gauges. The flow rates of the feed, the product and the purge were monitored by mass flow meters. All the valves used, except the fine metering valve, were bellows-sealed valves. A flow-through proportional counter of the kind described by Bernstein & Ballantine⁽¹⁸⁾ was used to monitor the tritium level in either the product or the purge streams. The gas flowing through the counter was a mixture of the product gas and P-10 counting gas. They were combined and mixed in a gas proportioner.

Materials

The materials used were the same as those used in the equilibrium and kinetic studies described earlier, with one addition. The mixture used as feed in the present experiments was obtained by diluting 0.07 m³ of the master batch of tritiated hydrogen with about 3 m³ of pure hydrogen.

Procedure

The bed was activated in the following way. After charging the vanadium particles to the column, the bed was outgassed at 450°C until a vacuum better than 7×10^{-4} Pa was attained. The bed was then cooled to room temperature and pressurized with hydrogen to 1030 kPa. Hydrogen adsorption was very rapid and was accompanied by rapid heat release. A bed temperature rise of 100°C was not unusual. After carrying out this procedure twice, the bed was considered to be fully activated. Prior to each pressure cycling run, column 1 was saturated with feed gas at high pressure P_H and column 2 was saturated with the same gas at low pressure P_L . This was achieved by feeding tritiated hydrogen gas at P_H to column 1 at a rate of 200 sccm and allowing the emerging stream to bleed down to low pressure P_L and flow through column 2. The effluent of column 2 was monitored by the internal proportional counter until a steady state count rate was reached. The feed, product and purge flow rates were then adjusted to the conditions desired for the experimental run. The run was started by activating the solid state timers which controlled the switching of the air-operated valves. At half cycle intervals, this valve switching alternately directed feed into one column while allowing purge to escape from the other. The concentration of tritium in the product stream was monitored continuously during the whole run. The heatless adsorption runs were conducted over two distinct regions of the

pressure-composition diagram of the vanadium-hydrogen system, namely, the single phase β region and the two phase β - γ region. In the monohydride (β) region, the structure of the hydride phase remained the same at the two extreme pressure conditions. Also, the change in hydrogen content of the hydride was small. In the two phase region the hydride changed from a body-centered tetragonal lattice structure at low pressure to a face-centered cubic one at high pressure. The change in hydrogen content was appreciable in this case. The pressure cycling runs were carried out to study the isotope separation as a function of pressure ratio $\frac{P_H}{P_L}$, feed to purge ratio, temperature, and cycle time.

Results and Discussion

Single Phase Operating Mode. The results of the pressure cycling runs in the β phase were completely unexpected. Whereas according to equilibrium theory concepts slight depletion of tritium in the product stream would be expected to occur at small G , in fact appreciable enrichment was found. This enrichment was commonly of the order of 40 percent at steady state and reached a maximum value of 54 percent in one run. Concentration transients for runs conducted in the β phase are shown in Figures 8 to 10. The ordinate in these figures is the mole fraction in the product stream divided by the mole fraction in the feed. The abscissa is the number of cycles of operation. In all runs a steady state was reached after an initial transient period of operation. The transients remained cyclic in nature for those runs with the smaller purge-to-feed ratios, longer cycle times, and higher feed flow rates. Purge-to-feed ratio (Figure 8) is seen to have no well defined effect on enrichment. Thus the enrichment with no purge ($G = 0$) is little different from that with substantial purge ($G = 0.85$). This is advantageous, for the fraction of the feed which is enriched is greater with $G = 0$. At $G = 0$ the depleted stream consists only of the blowdown. The

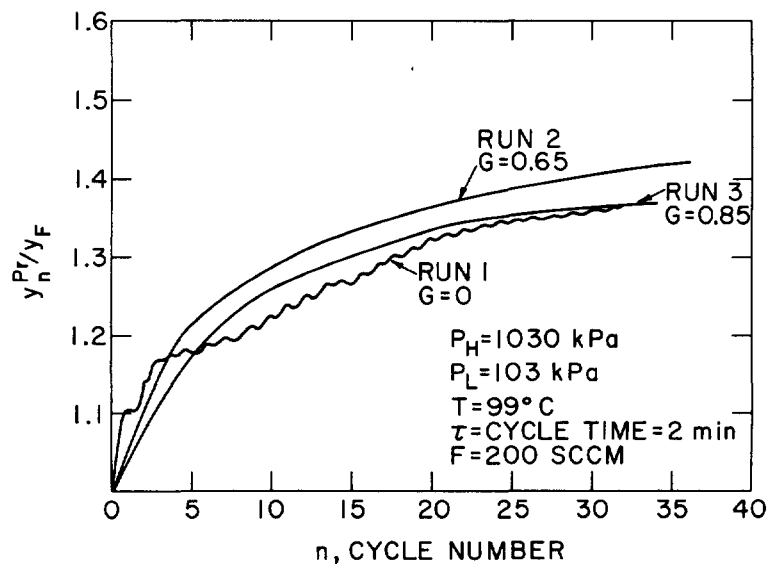


Figure 8. Transients in product concentration for heatless adsorption experiments conducted in the β phase: effect of purge-to-feed ratio.

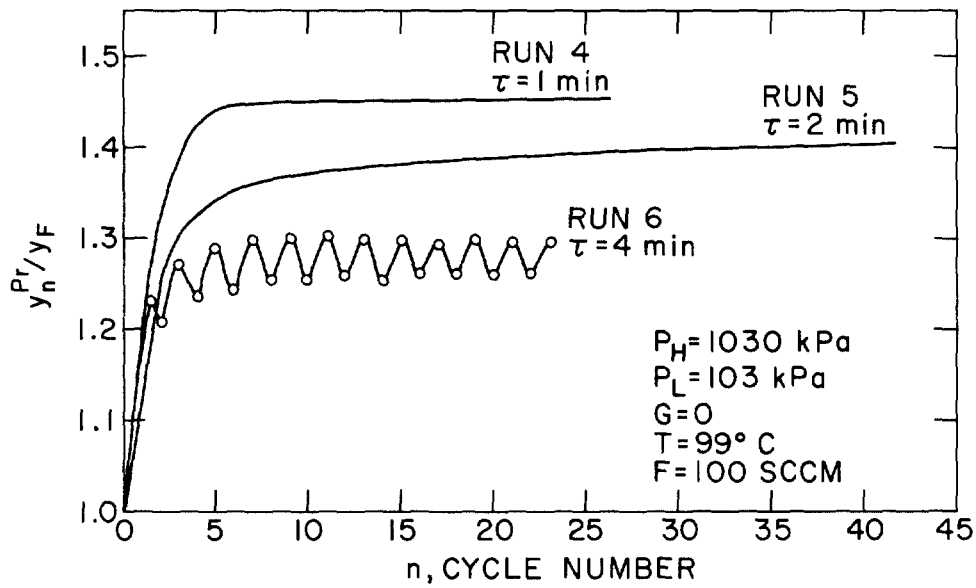
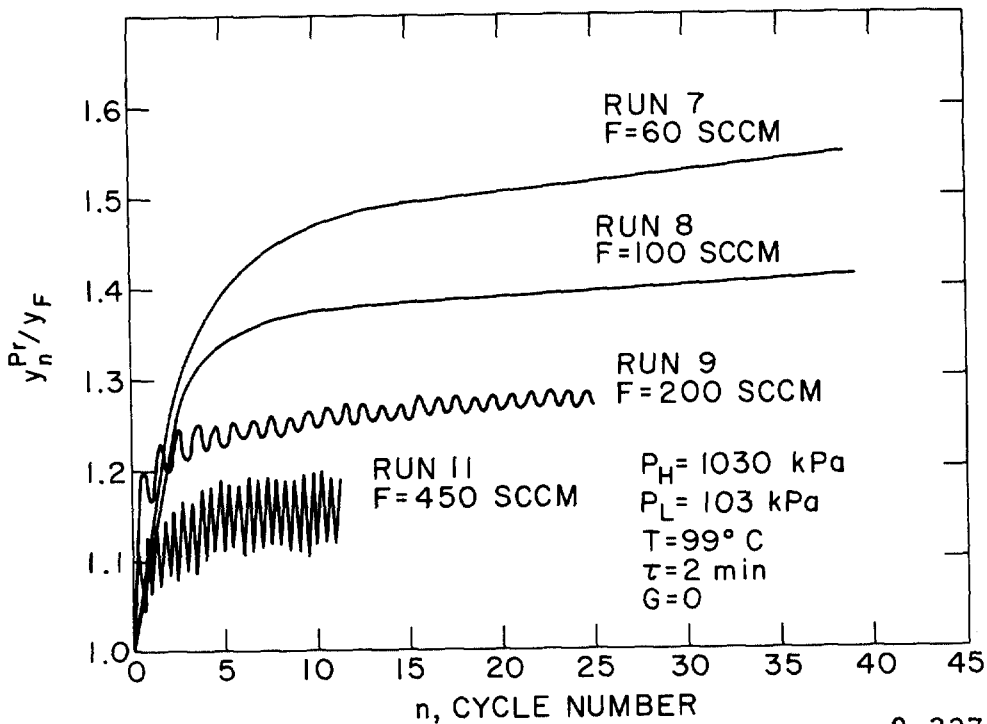


Figure 9. Transients in product concentration for heatless adsorption experiments conducted in the β phase: effect of cycle time.



9-227-78

Figure 10. Transients in product concentration for heatless adsorption experiments conducted in the β phase: effect of feed flow rate.

15th DOE NUCLEAR AIR CLEANING CONFERENCE

blowdown in turn consists of the same volume of H₂ per cycle regardless of the value of G. Because of this fact the remaining experiments described for the β phase were all conducted with no purge.

Product enrichment increases as the cycle time decreases (Figure 9) and as the feed flow rate decreases (Figure 10). Data (not shown) for runs exploring the influence of variation of the high pressure and the temperature show that product enrichment increases with both variables but appears to approach a limit (~45 percent) as the high pressure approaches 1400 kPa (~200 psi).

The depletion in the blowdown was not measured because of experimental difficulty but the amount of the blowdown per cycle was measured. For Run 8, for instance, P_H = 1030 kPa, P_L = 103 kPa and T = 100°C, the blowdown amounted to 0.02 moles H₂, in good agreement with the value calculated from the pressure-composition isotherm. Using this value and the measured steady state enrichment in the product (1.41), we calculate the depletion of HT in the blowdown for a feed flow rate of 100 sccm to be 9 percent. The total quantity of product amounts to about 18 percent of the feed. Hydrogen and tritium balances for this run are shown in Table III. From this table it is apparent that recycle may be beneficial in increasing the amount of product enriched and in increasing the depletion in the blowdown. This possibility is being investigated.

Table III. Hydrogen and tritium balances in single phase operating mode (Run 8).

<u>Stream</u>	<u>Moles H₂</u>	<u>Percent of feed</u>	<u>y/y_F</u>
Product	$\frac{100 \text{ sccm} \times 1 \text{ min}}{22400} = 0.0045$	0.18	1.41
Purge	0.0	0.00	----
Blowdown	0.02	0.82	0.91
Total feed	0.0245	1.00	1.00

It should be noted that Runs 1 (Figure 8) and 9 (Figure 10) were conducted under nominally identical conditions and yet the ultimate enrichments obtained were noticeably different. The difference between them was that Run 1 was conducted with freshly activated beds whereas Run 9 was in fact conducted long after activation. This difference points up the fact that the beds deteriorate with use, probably as the result of introduction of impurities such as water vapor or oxygen which cause inactivation. Activation after every few runs was required to obtain good reproducibility.

Additional experiments are required to determine the origin of the inverse separation. A possible cause may be a kinetic isotope effect. Enrichment of the product stream may result if H₂ is more rapidly absorbed than HT. The inverse separation may well not be associated with the feed and purge steps in the process. This is because the time scales of the exchange reaction estimated from the chromatographic data discussed earlier are somewhat smaller than the

15th DOE NUCLEAR AIR CLEANING CONFERENCE

half-cycle times. Thus $\frac{\alpha}{2} K_{H_2} / (k_F^T C_H^*)$, the chemical reaction time in Equation (6), at 1030 kPa and 100°C is 17 s. From this result one would expect that exchange taking place during a half cycle of duration, say, 30 s or more, would be likely to take place under conditions near equilibrium. The inverse separation may therefore arise in the pressurization and blowdown steps. Those steps are known to occur very rapidly, perhaps in less than 1 s. A quantitative investigation of the rates of H₂ and HT absorption and desorption in these steps may disclose whether a kinetic isotope effect may give rise to the inverse separation. Tritium may be more slowly absorbed and desorbed than protium.

Two Phase Operating Mode. Experiments were conducted in this mode by using temperatures of 16° to 50°C and pressures in the range 100 to 1600 kPa (15 to 240 psi). Rates of absorption, desorption and exchange were known to be small in the γ phase and therefore cycle times of the order of 30 min to 1 hr were used.

This mode of operation did lead to depletion of tritium in the product stream as expected for the process and as predicted by equilibrium theory. The maximum depletion found in any run at steady state was 65 percent.

Transients in HT concentration in the product stream for runs conducted at 25°C are shown in Figures 11 and 12. The ordinate is the mole fraction ratio as before but the abscissa is the time of

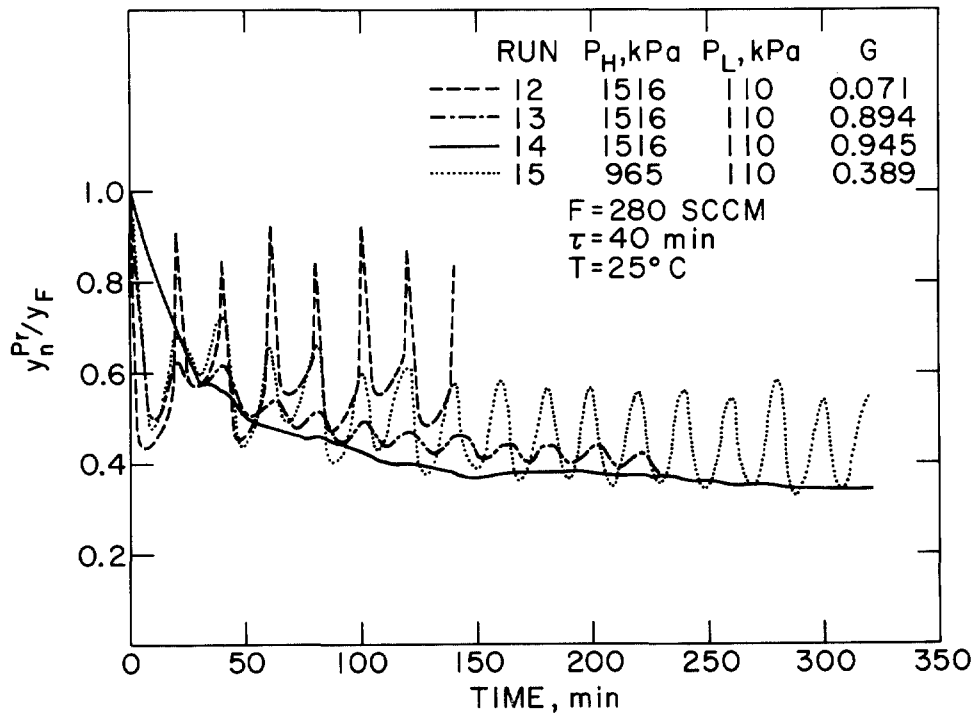


Figure 11. Transients in product concentration for heatless adsorption experiments conducted in the β and γ phases: effect of purge-to-feed ratio.

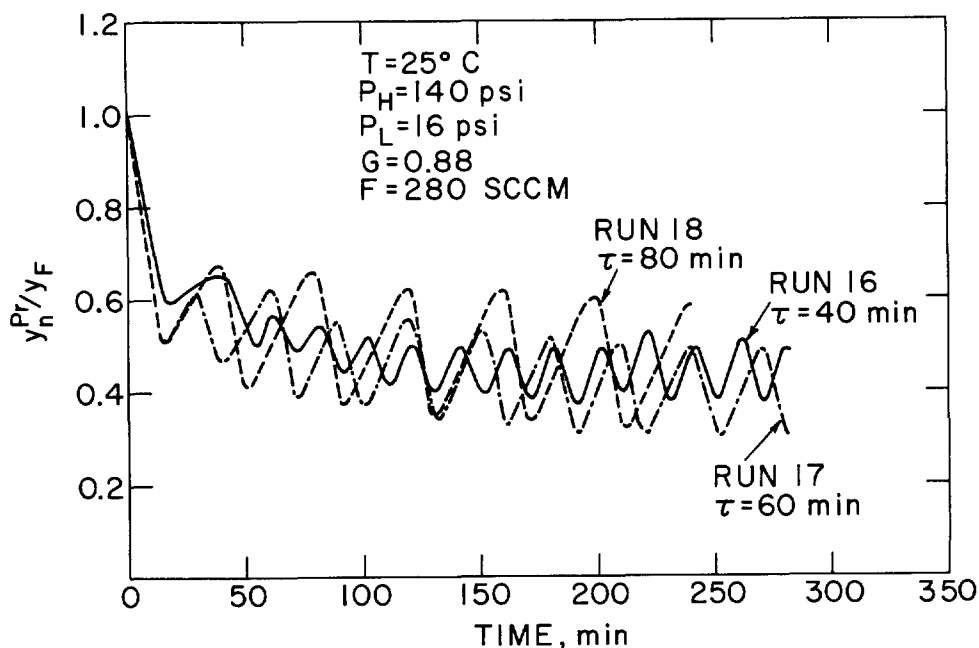


Figure 12. Transients in product concentration for heatless adsorption experiments conducted in the β and γ phases: effect of cycle time.

operation. In all cases a steady state is approached after an initial transient. In all runs but one (Figure 11, Run 14) a cyclic variation persists throughout the run. The effect of purge-to-feed ratio is shown in Figure 11. For $G = 0.071$ (Run 12) the sharp high peaks are regarded as indicative of incipient feed breakthrough into the product stream. Depletion in the product stream generally increases with increasing G . As indicated in the Theory section for $P_H = 1000$ kPa, $P_L = 200$ kPa, at 25°C , $G_{\text{crit}} = 0.82$. Therefore only for Runs 13 and 14 where $G > 0.82$ might complete removal of HT from the product stream have been expected. Even for these runs steady state non-zero concentrations were found. Concentration front spreading resulting from finite rates of exchange and from axial dispersion may have contributed to the failure to achieve complete HT removal.

The transients shown in Figure 12 indicate no dependence of depletion on cycle time for cycle times in the range 40 to 80 min.

Additional runs (data not shown) were made to examine the influence of temperature and high and low pressures. Little change in depletion was brought about by changes in these variables. The principal factors in these runs then were (a) cycling across the dissociation plateau and (b) purge-to-feed ratio. As long as the temperature and high and low pressures were such as to require cycling between the β and γ phases and as long as G was relatively high, significant depletion was found in the product stream.

15th DOE NUCLEAR AIR CLEANING CONFERENCE

While it was found possible to obtain depletions of HT in the product stream of up to 65 percent, at the same time the product stream represented a small fraction of the feed. Most of the feed was rejected as slightly enriched purge and blowdown gas. This circumstance may dictate as with single phase operation the use of recycle of most of the combined purge and blowdown streams, with the recycle stream being recompressed to the feed pressure. This concept is currently being explored.

As an example of the relative amounts of purified product and enriched purge and blowdown, consider Run 14, Figure 11. The amount of the blowdown gas per column per cycle calculated from the pressure-composition isotherm for the temperature and pressure conditions used and for the vanadium charge in a column is 0.536 moles H₂. A like amount of feed must be supplied during repressurization. During continuous supply of feed at high pressure the amount of feed introduced per column per cycle is 280 sccm x 20 min = 5600 scc or 0.25 mole H₂. With G = 0.945 the number of moles of H₂ in the purge and product streams may be calculated. Hydrogen and tritium balances for the process are given in Table IV. The need for substantial recycle is apparent. Less recycle would be needed at smaller purge-to-feed ratios without great change in depletion.

Table IV. Hydrogen and tritium balances in two phase operating mode (Run 14).

Stream		Moles H ₂	Percent of feed	Y/Y _F
Product	0.055 x 0.25 =	0.014	2	0.35
Purge	0.945 x 0.25 =	0.236	30	} 1.01
Blowdown		0.536	68	
Total feed		0.786	100	1.00

In addition to recycle another factor to be considered in the further development of a process based on the two phase operating mode is particle attrition. The large change in hydrogen content of the particles resulting from cycling between the β and γ phases can bring about substantial attrition after many cycles of operation. Indeed such attrition was found in the columns used in the present work. Attrition is commonly found in the cyclic operations employed in the use of metal hydrides in hydrogen storage. Much effort is currently being expended to overcome this problem.⁽¹⁹⁾ Continued attrition in cyclic processes can lead to excessive pressure drop and to deformation of confining vessels if vessel design and operation do not properly allow for this phenomenon.

V. Summary and Concluding Remarks

1. An experimental study of the equilibrium and kinetics properties of hydrogen isotope exchange on vanadium hydride has been conducted. For hydrides made from commercial grade V, pressure-composition isotherms for the β and γ phases, HT-H₂ separation factors for the β phase, rates of HT-H₂ exchange for the β phase, and

15th DOE NUCLEAR AIR CLEANING CONFERENCE

axial dispersion coefficients have been determined.

2. An equilibrium theory of hydrogen isotope separation via heatless adsorption using vanadium hydride has been developed. Constants in the derived theoretical expressions were evaluated using the pressure-composition and separation factor data obtained as indicated above. The theory was then used to calculate process performance for HT-H₂ separation in two operating modes. In the single (β) phase mode, it was predicted that over a wide temperature range (100° to 250°C) essentially no separation would be obtained. For the two (β - γ) phase mode, complete removal of HT from the product stream was predicted for purge-to-feed ratios ranging from 0.77 to 0.84 as the temperature increased from 0° to 40°C. Overall enrichment in the combined purge and blowdown decreased from 2.06 to 1.34 for the same temperature range.

3. Experiments were conducted on the performance of heatless adsorption apparatus in separating HT-H₂ mixtures using vanadium hydride. In the single phase mode, enrichment in the product (up to 54 percent) was found whereas no change was expected. A kinetic isotope effect may be responsible for the inverse separation. Depletion in the product (up to 65 percent) was found as expected when operating in the two phase mode. For both modes of operation, performance may be enhanced by recycle of the combined purge and blowdown.

4. Future experimental work will involve study of rates of HT and H₂ absorption and desorption during blowdown and repressurization, investigation of the use of recycle, and examination of the efficacy of temperature cycling. Theoretical effort will be concentrated on the performance of temperature cycling processes and on the effect of finite rates of exchange. Completion of this work will make possible a conclusive assessment of the usefulness of hydrogen isotope separation via cyclic processes based on the use of vanadium hydride.

Notation

a	=	empirical constant in Equation (10)
A	=	z-coordinate of maximum penetration of fresh feed during pressurization
b	=	empirical constant in Equation (10)
B	=	fraction of tritium in gas phase
C _i	=	concentration of species i
C _H ^H , C _H ^L	=	concentration of hydrogen atoms in hydride particles at high and low pressures, respectively
D _{HT-H₂}	=	diffusion coefficient of HT in H ₂
D _p	=	particle diameter
D _s	=	diffusion coefficient of tritium atoms in hydride particles

15th DOE NUCLEAR AIR CLEANING CONFERENCE

E_i	= enrichment in stream i
$E(P_2, P_1)$	= exponential of right hand side of Equation (20)
E_z	= axial dispersion coefficient
F	= feed flow rates
$F(P_2, P_1)$	= exponential of right hand side of Equation (21)
G	= fraction of feed introduced during high pressure flow step which is rejected as purge
h	= packed height of column
I_f	= forward kinetic isotope effect
k_f^H, k_r^H	= forward and reverse rate constants for reaction (8)
k_f^T, k_r^T	= forward and reverse reaction rate constants for reaction (4)
k_g	= gas phase mass transfer coefficient
K_{H_2}	= hydrogen distribution coefficient
L	= penetration distance of HT concentration front
n	= number of cycles of heatless adsorption process
r	= the minimum non-negative number such that $(1+r)L_L - rE(P_H, P_L)L_H \geq h$
P_{mm}	= hydrogen pressure, mm Hg
P	= hydrogen pressure
q	= a number such that $(r+q)[L_L - E(P_H, P_L)L_H] = h - E(P_H, P_L)L_H$
r_p	= particle radius
R	= gas constant
R_{ex}	= rate of reaction (8)
S	= column cross sectional area
t	= time
t_0	= pulse duration
T	= temperature
Δt	= half cycle duration
u	= superficial gas velocity

15th DOE NUCLEAR AIR CLEANING CONFERENCE

y = mole fraction of HT in H_2
 z = axial distance coordinate

Greek Letters

α = HT- H_2 separation factor
 ϵ = bed void fraction
 θ = h/u , bed residence time
 μ_1 = first absolute moment (mean)
 μ_2 = second central moment (variance)
 ρ = hydrogen-to-vanadium atom ratio
 ρ_s = density of vanadium hydride
 τ = cycle time

Superscripts

* = pertains to surface
Pr = product
Pg = purge

Subscripts

b = blowdown
crit = critical
F = feed
H = high
L = low
n = pertains to n-th cycle
ov = overall
Pg = purge

15th DOE NUCLEAR AIR CLEANING CONFERENCE

References

1. Wong, Y. W. and F. B. Hill, "Equilibrium and kinetics studies of hydrogen isotope exchange on vanadium hydride," submitted to A.I.Ch.E. Journal.
2. Reilly, J. J. and R. H. Wiswall, Jr., "The reaction of hydrogen with alloys of magnesium and copper," Inorg. Chem. 6, 2220 (1967).
3. Reilly, J. J. and R. H. Wiswall, Jr., "The higher hydrides of vanadium and niobium," Inorg. Chem. 9, 1678 (1970).
4. Reilly, J. J. and R. H. Wiswall, Jr., "The effect of minor constituents on the properties of vanadium and niobium hydrides," Brookhaven National Laboratory Report BNL 16546 (1972).
5. Mueller, W. M., J. P. Blackledge, and G. G. Libowitz, "Metal hydrides," Academic Press, New York, p. 601 (1968).
6. Ebisuzaki, Y. and M. O'Keefe, "The solubility of hydrogen in transition metals and alloys," Prog. Solid State Chem. 4, 187 (1967).
7. Melander, L., "Isotope effects on reaction rates," The Ronald Press Company, New York (1960).
8. Schober, T. and H. Wenzl, "Structures, phase diagrams, phase morphologies and preparation methods of V-, Nb-, and Ta-hydrogen systems," in Alefeld, G., ed., "Hydrogen in metals," to be published by Springer-Verlag, Berlin.
9. Wiswall, Jr., R. H. and J. J. Reilly, "Inverse hydrogen isotope effects in some metal hydride systems," Inorg. Chem. 11, 1691 (1972).
10. Tanaka, J., R. H. Wiswall, and J. J. Reilly, "Hydrogen isotope effects in titanium alloy hydrides," Inorg. Chem. 17, 498 (1978).
11. Schneider, P. and J. M. Smith, "Adsorption rate constants from chromatography," A.I.Ch.E. Journal 14, 762 (1968).
12. Scholten, J. J. F. and J. A. Konvalinka, "Hydrogen-deuterium equilibrium and parahydrogen and orthodeuterium conversion over palladium: kinetics and mechanism," J. Catalysis 5, 1 (1966).
13. Flanagan, T. B., "Kinetics of hydrogen absorption and desorption," presented at the International Symposium on Hydrides for Energy Storage, Norway (1977).
14. Shendalman, L. H. and J. E. Mitchell, "A study of heatless adsorption in the model system CO₂ in He, I," Chem. Eng. Sci. 27, 1449 (1972).
15. Pigford, R. L., B. Baker, III, and D. E. Blum, "An equilibrium theory of the parametric pump," Ind. Eng. Chem. Fundamentals 8, 144 (1969).

15th DOE NUCLEAR AIR CLEANING CONFERENCE

16. Chen, H. T. and F. B. Hill, "Characteristics of batch, semi-continuous and continuous parametric pumps," Separation Sci. 6, 411 (1971).
17. Chan, Y. N. I., F. B. Hill, and Y. W. P. Wong, "Equilibrium theory of heatless adsorption," in preparation.
18. Bernstein, W. and R. Ballantine, "Gas phase counting of low energy betz-emitters," Rev. Sci. Instr. 21, 158 (1950).
19. Strickland, G., T. Milau, and Wen-Shi Yu, "The behavior of iron titanium hydride: long term effects, heat transfer and modeling," Brookhaven National Laboratory Report BNL 20876.

DISCUSSION

CHOI: This process can be best used in detritiating reactor water which usually has tritium oxide in parts per million range; is there any variation in the separation (decontamination) factor with the inlet concentration in that range?

WONG: The concentration level of tritium used in our elution chromatography experiment was $\sim 10^{-6}$ Ci/cm³. The separation factors obtained agreed quite well with those obtained in a batch reactor in which the tritium level was about one order of magnitude higher. However, it is a good idea to investigate further the concentration effect on the separation factor.

KNECHT: What do you see as a commercial application of this method? An estimate of the scale required for a D₂O reactor or reprocessing plant water clean-up system would be useful.

WONG: This process has the potential to recover deuterium or tritium from a hydrogen stream with the protium being used in an ammonia synthesis process to make the economics of one process more attractive. This process is useful in decontaminating tritiated water from nuclear reactors. First, the water has to be split into hydrogen and oxygen by an electrolytic process. The hydrogen then can be separated by this process. Finally, the concentrated tritium can be stored as stable tritides for safe disposal. We are now working on a single stage process. Multiple-stage processes will be investigated in the future. At that time, scale of operation and economic feasibility will be looked at.

15th DOE NUCLEAR AIR CLEANING CONFERENCE

STUDY ON THE TRITIUM REMOVAL FROM THE SODIUM IN LMFBR

K. Hata, Y. Nishizawa, Y. Osawa
Mitsubishi Atomic Power Industries, Inc.
Omiya, Japan

Abstract

Removal of tritium in the sodium coolant of LMFBR, is important for achieving the release of radioactivities as low as reasonably achievable. It is well known that cold trap should be an effective method for controlling tritium in sodium. To develop an effective tritium trapping system with "reactive getter (chemical trap)", in-sodium hydrogen absorption behavior has been studied.

The absorption experiment was conducted by dipping some test materials into sodium on which cover gas was composed of an Ar-H₂ mixture. Hydrogen analysis and metallographic examination for the test materials were made after the experiment.

From these experiments, it was concluded that Yttrium canned with Nickel or Niobium was the most suitable as "reactive getter". Further investigation to develop the "chemical trap" made from these materials for practical application has been in progress.

I. Introduction

Tritium is produced in LMFBR core by three primary mechanisms; (1) ternary fission of the fuel, (2) activation of boron in the B₄C control rods, and (3) activation of boron and lithium impurities presented in the fuel and sodium. Most of the tritium generated in the reactor core, is expected to be released into the coolant sodium. For achieving the release of radioactivities to the environment as low as reasonably achievable, tritium is one of the most difficult radioactive isotopes to control in LMFBR. Because, as an isotope of hydrogen, it diffuses easily through the structural materials at the LMFBR temperatures.

Cold trap is well known to be an effective method in containing tritium and preventing its release. Although this method is employed efficiently, however, it is estimated that a considerable amount of tritium would be released¹.

For the purpose of developing a tritium trapping method with "reactive getter", which should be more effective than the usual cold trap method, the screening test of the materials which might be suitable as the getter, has been performed.

This paper describes the results of the test for some materials, with respect to their in-sodium hydrogen absorption behavior and their feasibility as the getter.

15th DOE NUCLEAR AIR CLEANING CONFERENCE

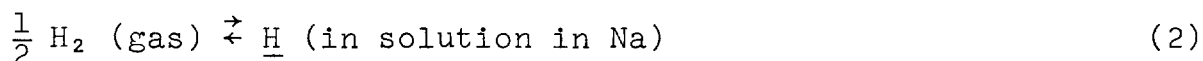
II. Principle of Chemical-Trapping Method

In the sodium-hydrogen system, the solubility of hydrogen in sodium has been recently reported by D. R. Vissers et al.², as follows.

$$S = 1.0 \times 10^{-3} \exp \left(- \frac{6550}{T} + 61.52 \right) \quad \{ \text{atoms-H/g-Na} \} \quad (1)$$

Substitution of a cold trap temperatures ($^{\circ}\text{K}$) for T in equation (1) gives the minimum hydrogen concentrations in sodium that can be attained by the cold trap method. For example, it is shown in FIG.2 that they come to $\sim 1 \times 10^{17}$ (atoms-H/g-Na) when cold trap is controlled at 150°C .

In the unsaturated solution ranges of the Na-H system, equilibrium would be established between hydrogen in gas phase and hydrogen in solution;



The equilibrium can be expressed by the following equation;

$$C = K \cdot P^{\frac{1}{2}} \quad (3)$$

where C: concentration of hydrogen in the solution
 K: Sievert's constant
 P: hydrogen pressure

Equation (3) is known as Sievert's law which states that the solubility of hydrogen in sodium is proportional to the square root of the hydrogen pressure. The Sievert's constant for the sodium-hydrogen system was reported as follows, and to be insensitive to small variation in temperature³.

$$K = 8.3 \times 10^{19} \quad \left\{ \frac{\text{atoms-H/g-Na}}{(\text{atm})^{\frac{1}{2}}} \right\} \text{ at } 450^{\circ}\text{C} \quad (4)$$

In a metal-hydrogen system, if the system forms hydride phase, pressure-composition isotherms such as those shown in FIG. 1 are generally obtained.

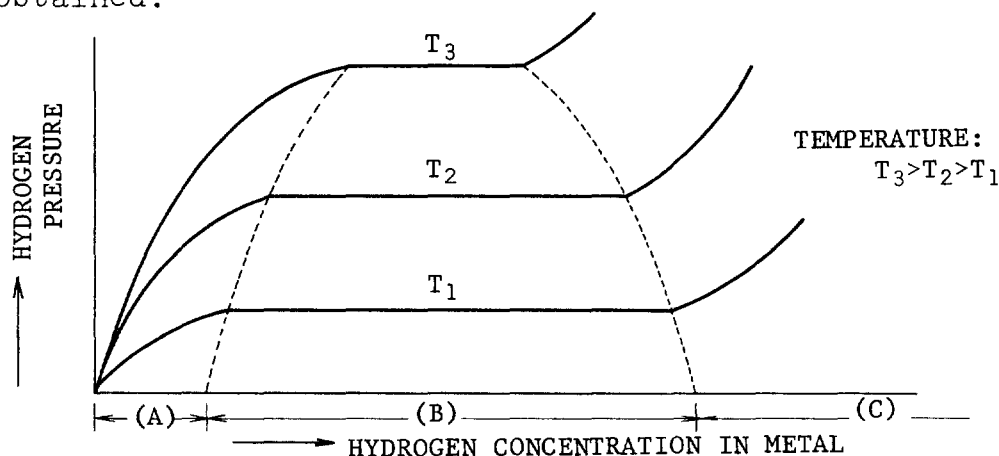


FIGURE 1 GENERAL PRESSURE - COMPOSITION ISOTHERMS FOR AN M-H SYSTEM

15th DOE NUCLEAR AIR CLEANING CONFERENCE

In FIG. 1 the region (A) shows solid solution of hydrogen in a metal, and the region (B) shows 2-phase coexistence of saturated solid solution and a hydride. In the plateau-pressure region (B), $\log P$ vs. $1/T$ can be expressed in the following equation which is sometimes called Van't Hoff isochore.

$$\log P = -\frac{A}{T} + B \tag{5}$$

where P: hydrogen dissociation pressure

T: temperature ($^{\circ}K$)

A, B: constants

A and B in equation (5) have been reported in many metal-hydrogen system⁴.

If a metal, which has a strong tendency to combine with hydrogen and accordingly exhibits a low hydrogen plateau-pressure, were sufficiently added to the sodium-hydrogen system at temperature T_1 , some hydrogen in solution in sodium would be removed into the metal to form the hydride. Finally, equilibrated hydrogen concentration in the sodium can be calculated from equation (3), (4), (5), as follows.

$$C_1 = K \cdot 10^{\frac{1}{2}(-\frac{A}{T_1} + B)} \tag{6}$$

This is the principle which chemical trap method is based on. The graphs, $\log C$ vs. $1/T$ for some metals, which form stable hydrides, are shown in FIG. 2 together with the hydrogen solubility curve of equation (1).

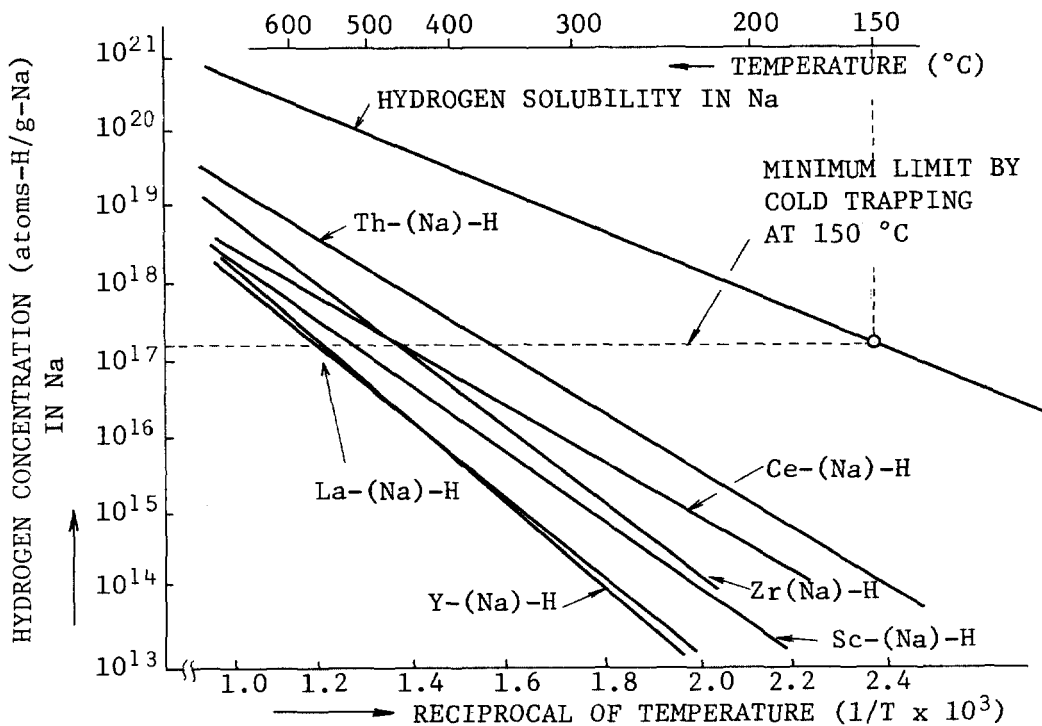


FIGURE 2
CALCULATED HYDROGEN CONCENTRATION vs. RECIPROCAL OF TEMPERATURE
FOR SOME HYPOTHETICAL M-Na-H EQUILIBRIUM SYSTEM

III. Experimental

Apparatus

The apparatus for the in-sodium hydrogen absorption experiment is shown in FIG. 3. The main constituents were a charge tank (160 dia. x 230 height), a test tank (160 dia. x 230 height) and piping/valves (21.7 dia.). The electric heating system and the cover-gas supply/evacuate system were also attached. The apparatus was composed entirely of 304 stainless steel except for zirconium-foil arranged in the charge tank.

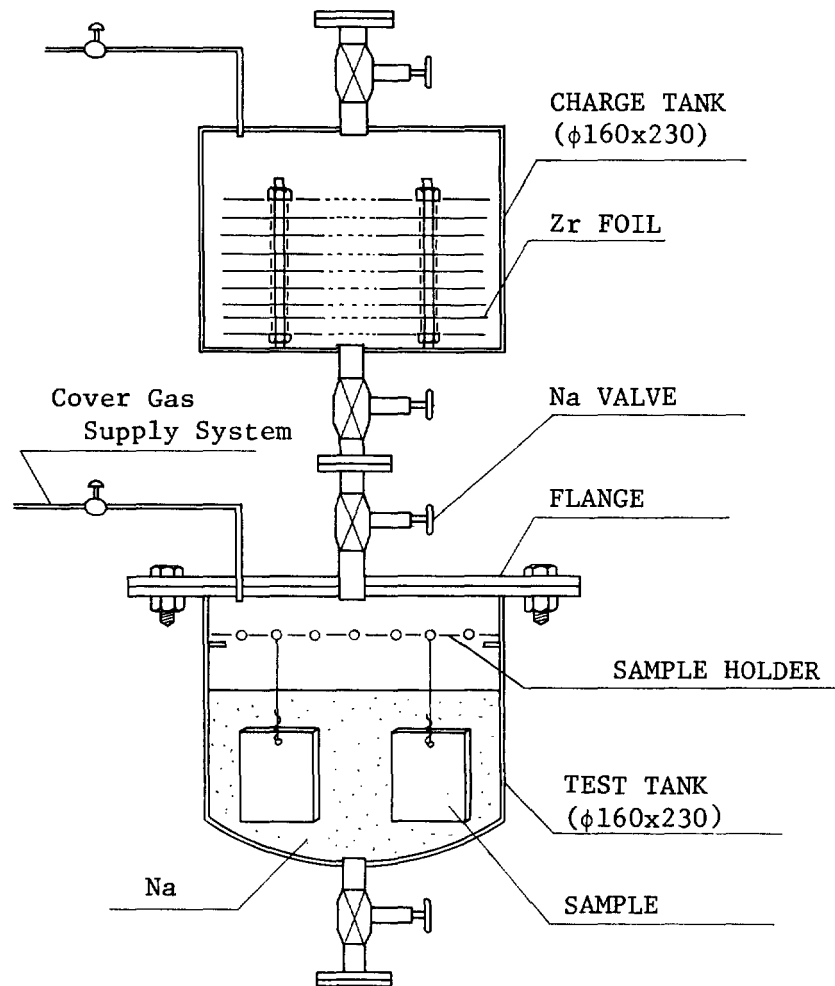


FIGURE 3
EXPERIMENTAL APPARATUS

Sample Preparation

Test materials for the experiment were selected in consideration of their hydrogen affinity, their compatibility with hot sodium, and their availability.

15th DOE NUCLEAR AIR CLEANING CONFERENCE

Titanium (Ti) exhibits a wide solid solution region (~ 10 at %H, at $300 \sim 600$ °C), and is often used as good hydrogen absorbent. Zirconium (Zr) is a stable hydride former. (See FIG. 2) Ti and Zr are commonly available and compatible with hot sodium. Ti and Zr have a tendency to be oxidized in sodium which contains some oxygen. Generally surface oxide film is known to sometimes interfere, and/or reduce the permeation of hydrogen. Therefore, to examine an effect of surface oxide film on hydrogen absorption, we prepared, as test samples, Ti/Zr with and without surface oxide film, respectively.

Yttrium (Y) and cerium (Ce) as well as other rare earth metals, although they have attractive property of forming very stable hydrides (see FIG. 2), are hardly compatible with hot sodium. By this reason, they can't be used in direct contact with hot sodium. Modifying this poor compatibility by the methods of alloying or canning, we prepared the test samples of Ti-5 % Ce alloy and of Y canned with Ni. Ni is compatible with hot sodium and through Ni, hydrogen can easily permeate at high temperature. The test samples prepared for the experiment are summarized as follows and are also shown in FIG. 4.

(Test Samples)

- (1) Ti
- (2) Ti with oxide film (0.3μ thickness)
- (3) Zr
- (4) Zr with oxide film (0.2μ thickness)
- (5) Ti-5 % Ce alloy
- (6) Y canned with Ni

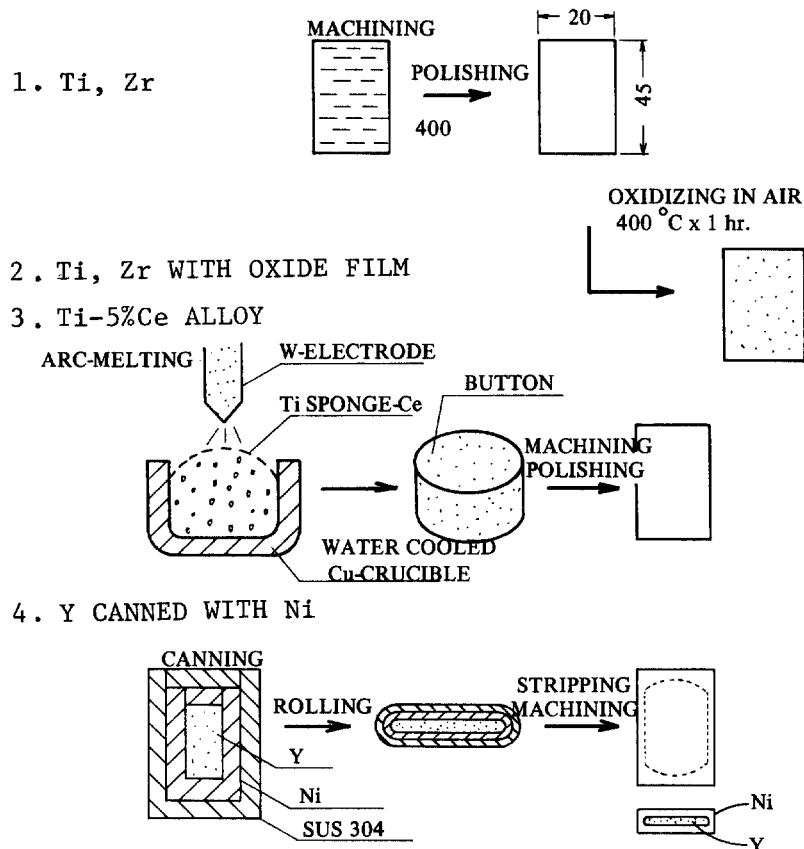


FIGURE 4
TEST SAMPLES PREPARATION

15th DOE NUCLEAR AIR CLEANING CONFERENCE

From the results of those experiments, Y canned with Ni was expected to be very attractive as getter materials. To accumulate more data on the hydrogen absorption behavior of these canning materials, additional in-sodium hydrogen absorption experiments of which test samples were composed of Ce or Y for meat and Ni or Nb for cladding has been performed. Test sample for the additional experiments is shown in FIG. 5.

i.	Y Canned with Ni
ii.	Ce " Ni
iii.	Y " Nb

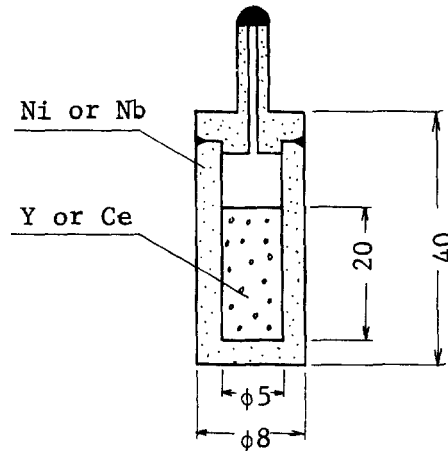


FIGURE 5
TEST SAMPLE FOR ADDITIONAL EXPERIMENTS

In-sodium Hydrogen Absorption

Test samples were hanged with small wire (SUS 304) from the holder in the test tank. (see FIG. 3) Sodium was poured from the charge tank into the test tank. Then cover-gas was replaced from a pure Ar to an Ar-H₂ mixture gas. Then, in-sodium hydrogen absorption experiments were conducted at constant temperature.

The experimental parameters were summarized in Table I.

Table I Experimental parameters

Dipping Time (Hr.) Dipping Temperature (°C)	100	200	400
350	*	*	*
450	*	*	*
550	*	-	-

*: conducted
-: not conducted

(Additional experiments)

° Dipping Temperature (°C): 500

° Dipping Time (hr): 74, 170, 510, 820

15th DOE NUCLEAR AIR CLEANING CONFERENCE

Sodium. Prior to the in-sodium hydrogen absorption experiment, the sodium was purified at 600 °C for 100 hr in the charge tank, where zirconium-foil was arranged as getter. The sodium inventory was 2.5 Kg and the surface area of the foil was $7 \times 10^3 \text{ cm}^2$. By this purification treatment, most impurities contained in the sodium (such as O, N, C, H) have been removed.

Cover-gas. Ar-H₂ mixture gas was used for the in-sodium experiment, so as to keep the hydrogen concentrations in sodium at constant values. The compositions of the Ar-H₂ mixture gas were shown in Table II. The pressure of cover gas was kept at 0.1 (Kg/cm². gauge) throughout the experimental periods. Therefore, hydrogen concentrations in the sodium were supposed to be as follows for all the experimental periods.

$$C = K \cdot P^2 \approx 4 \times 10^{17} \quad \{\text{atom-H/g-Na}\}$$

Table II Ar-H₂ mixture gas composition

Argon	99.9 % up
Hydrogen	23.9 ^{±1} p.p.m. (for additional experiments) 19.3 ^{±1} p.p.m.
Oxygen	<1 p.p.m.
Moisture	<1 p.p.m.

Examination

After the experiments, sodium in the test tank was drained off and the samples were drawn up from the tank. They were completely washed by ethylalcohol and demineralized water to remove the stuck sodium. Then, the samples were examined as follows.

- (1) surface observation and weight change measurement
- (2) metallographic examination
- (3) hydrogen analysis

IV. Results

Surface observation

Throughout the experiments, the samples of Ti, Zr, and Ti-Ce Alloy considerably reduced their initial metallic luster, respectively. The samples of Ti/Zr with oxide film also reduced their luster of light-brownish color. Ni had essentially no changes in its aspect. By additional experiments, Nb turned its surface color from metallic gray to blackish gray, perhaps by oxidation.

The weight changes of test samples were plotted as the function of dipping time and temperature, shown in FIG. 6, 7, 8. From these figures and surface observation mentioned above, it was concluded that the compatibility of all tested materials with hot sodium

15th DOE NUCLEAR AIR CLEANING CONFERENCE

(350 ~ 550 °C) seemed to be good. Nb exhibited a relatively high weight gains, perhaps through its oxidation, but as the oxide film formation rate was about $10\mu/200$ hr. for initial period and seemed to obey in parabolic law (see FIG. 8), therefore Nb might be also feasible in hot sodium (500 °C) for this application.

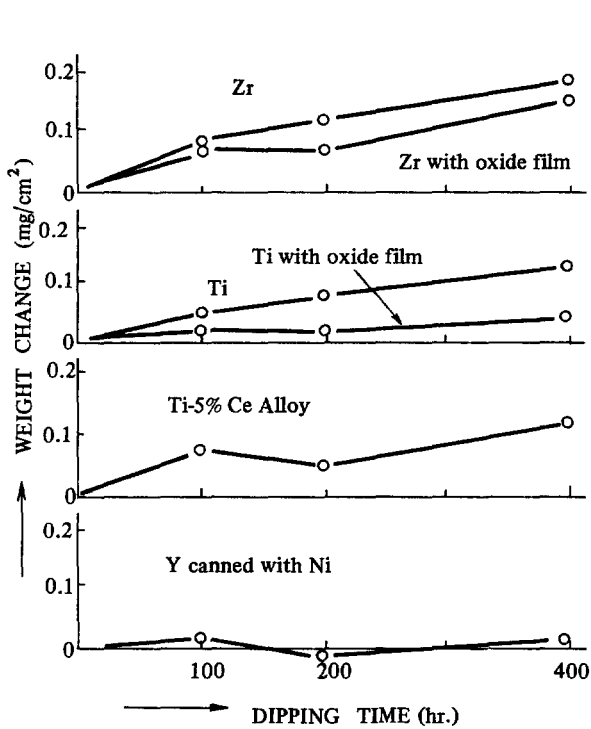


FIGURE 6
WEIGHT CHANGE
(Sodium Temp. = 450 °C)

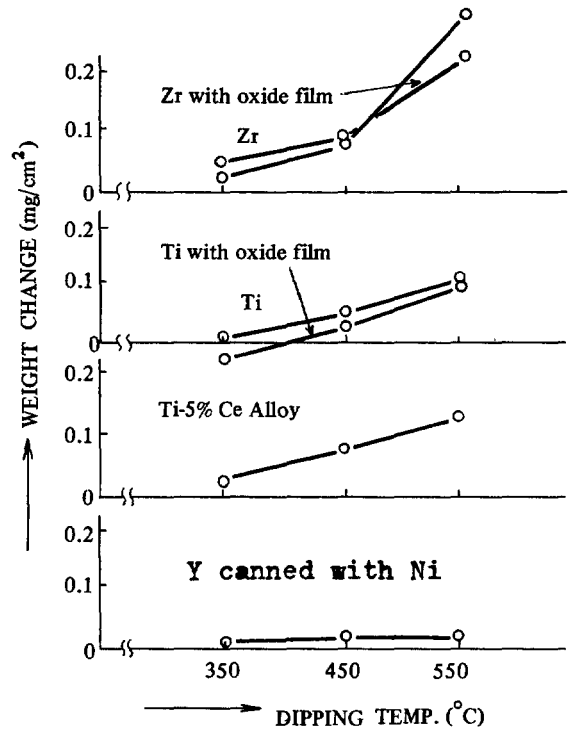


FIGURE 7
WEIGHT CHANGE
(Dipping Time = 100 hr.)

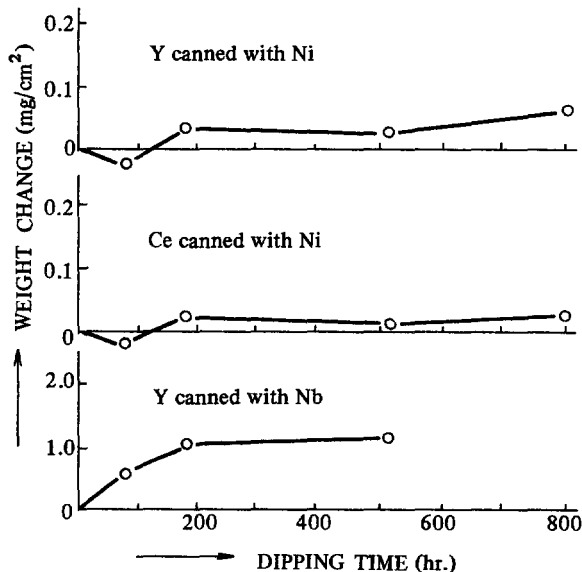


FIGURE 8
WEIGHT CHANGE
(Sodium Temp. = 500 °C)

Metallography

For those samples of Ti, Zr with/without an oxide film on the surface, and of Ti-Ce Alloy, there were little changes in their microstructures throughout the in-sodium hydrogen absorption experiments. As for Ni, there were no changes in its microstructure.

In additional experiment, at the outer surface of the samples (Na-Ni or Na-Nb interfaces), there were no changes in their microstructures. On the other hand, at the inner surface of the samples composed of Y (Y-Ni or Y-Nb interfaces), there were little changes in their microstructures of Ni and Nb, but at the inner surface of the samples of Ni-Ce couple there exhibited a considerable interaction between Ce and Ni. This is shown in PHOTO.1. It can be seen that Ce was aggressive upon Ni at tested temperature (500 °C), causing a matrix attack and an intergranular attack.

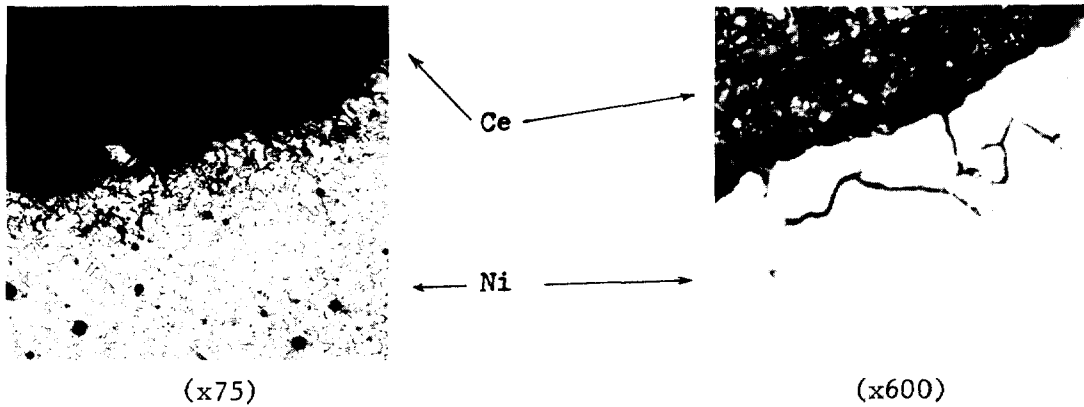


PHOTO. 1
MICROSTRUCTURE OF Ni CONTACTED WITH Ce

This result is also supported by the phase diagram of Ni-Ce, in FIG. 9 which shows that Ni-Ce system forms an eutectic compound with low melting points (455 °C). The same behavior would be also shown between Ni and the other lanthanide elements which form the stable hydrides.

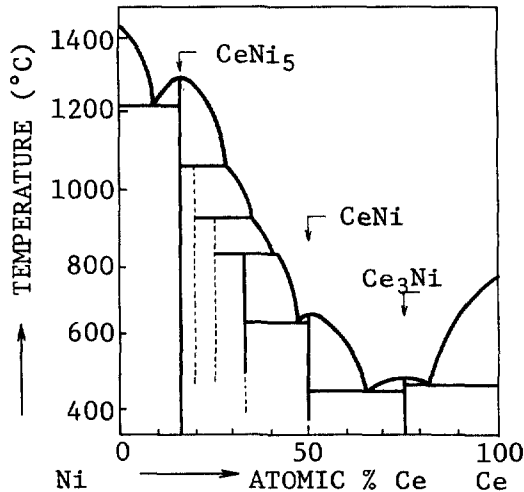


FIGURE 9
Phase Diagram for Ni-Ce

15th DOE NUCLEAR AIR CLEANING CONFERENCE

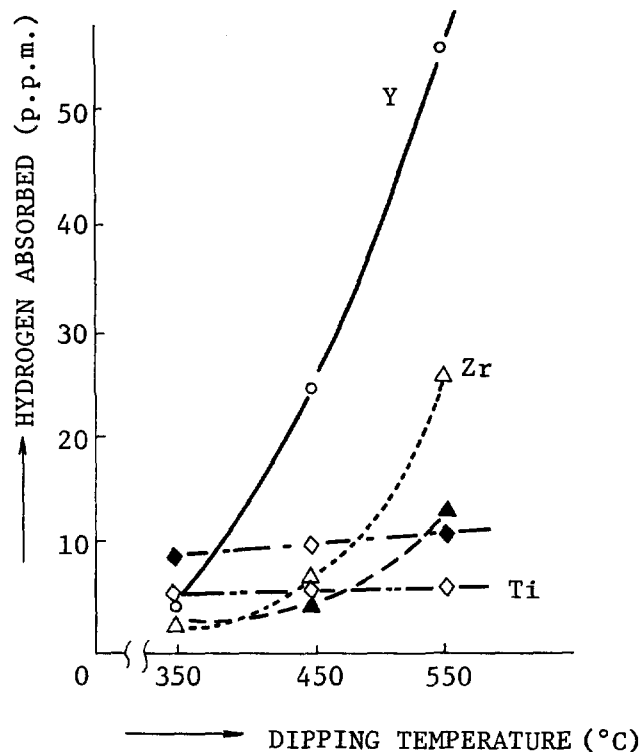
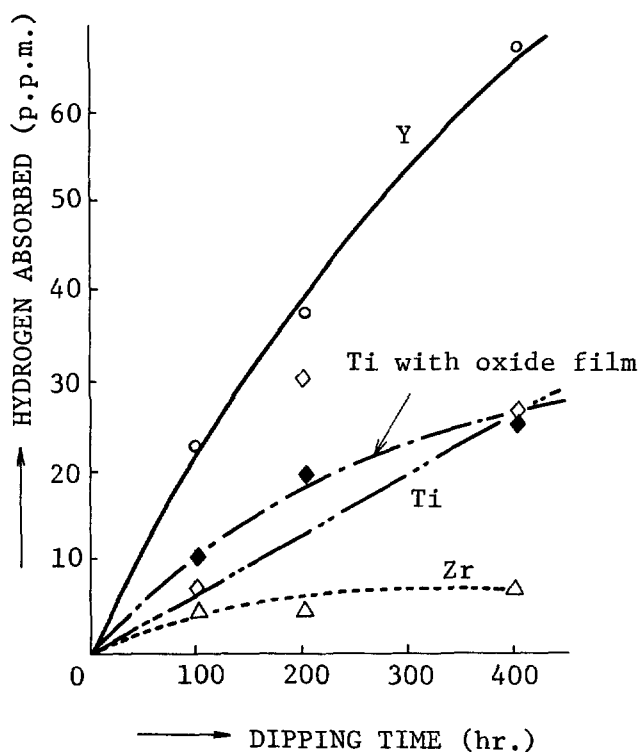
Through the experiments, Y and Ce had a tendency to be pulverized, perhaps forming a hydride phase.

From these results of metallographic examination together with those results of weight change measurements, it was concluded that Ti, Zr, Ti-Ce Alloy and canning materials which were composed of Y or Ce (also other lanthanide elements) for meat and Ni or Nb for cladding were all excellent in the view point of compatibilities, except for Ni-Lanthanide couples.

Hydrogen Analysis

Hydrogen analyses were conducted on the samples of pre-, and post-, in-sodium hydrogen absorption experiments by using the vacuum-outgassing technique.

Those results were plotted versus dipping time and dipping temperature, shown in FIG. 10, 11. The results of Ti-Ce Alloy sample were not included there, because they were so scattered perhaps due to its high initially absorbed gas contents.



LEGEND {

- Y canned with Ni
- △ Zr
- ▲ Zr with oxide film
- ◇ Ti
- ◆ Ti with oxide film

FIGURE 10
HYDROGEN ABSORPTION BEHAVIOR
(Dipping Temp. = 450 °C)

FIGURE 11
HYDROGEN ABSORPTION BEHAVIOR
(Dipping Time = 100 hr.)

As can be seen from FIG. 10, 11, Y canned with Ni is expected to be very attractive as "hydrogen getter". Although Zr absorbed a considerable amount of hydrogen at 550 °C, but as shown in FIG. 2, minimum attainable hydrogen concentration in sodium is nearly equal both in case of using the Zr getter (550 °C) and the cold trap (150 °C). Accordingly Zr seemed to be not so attractive as "hydrogen getter".

Hydrogen contents were also analyzed of the additional experiments which have been conducted on the materials of Y-Ni, Y-Nb, and Ce-Ni couples at temperature 500 °C. The results are shown in FIG. 12.

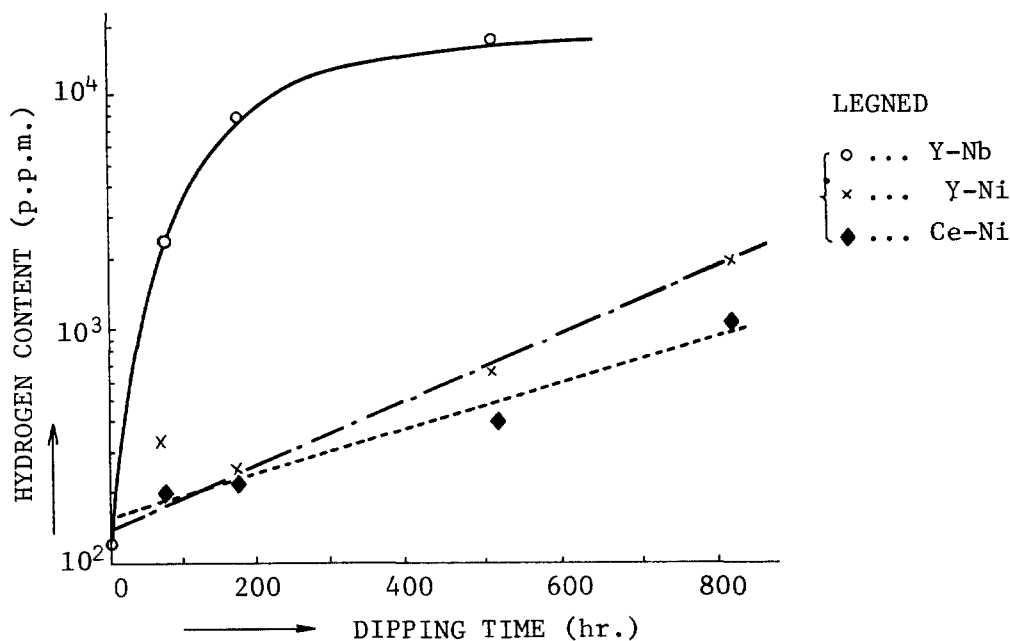


FIGURE 12
HYDROGEN ABSORPTION BEHAVIOR
(Sodium Temp. = 500 °C)

From FIG. 12, it can be seen that: Hydrogen absorption rates of Y and Ce are not decreased with increases of hydrogen contents by absorption. Y canned with Nb is shown to be saturated at the value of 2×10^4 p.p.m. hydrogen. This is nearly coincident with $YH_{1.9}$, which is yttrium dihydride exhibited by Y-H phase diagram, shown in FIG. 13.

The difference of hydrogen absorption rate between Y-Nb and Y-Ni would be due to the hydrogen permeation rates though Nb and Ni. i.e., through Nb, it is much higher than through Ni by 1 ~ 2 order of magnitude at those temperatures.

From these experiments, it was concluded that Y canned with Ni or Nb would be the most suitable as "hydrogen (tritium) getter" in sodium.

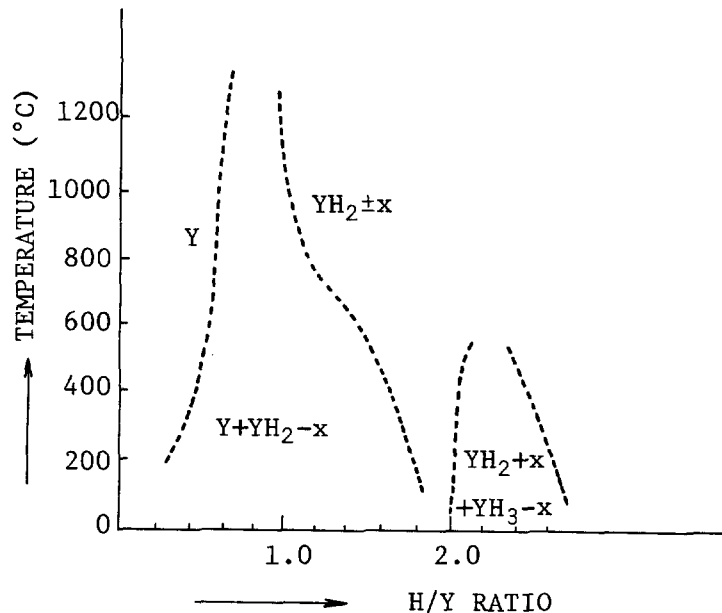


FIGURE 13
PHASE DIAGRAM FOR Y-H

V. Conclusion

(1) Chemical trap with reactive getter was found to be a promising method for the tritium removal in sodium coolant of LMFBR.

(2) Chemical trap with Y is expected to reduce the tritium concentration in sodium to more than one order of magnitude lower, as compared with cold trap. This means that tritium releases from the primary sodium coolant would be also lowered by more than one order of magnitude. Y getter has a so much capacity as absorbing hydrogen to about 2 wt. % of the Y. Further it would be more safe and easy to manage the "spent chemical trap", compared with that of cold trap.

(3) Chemical trap is also applicable for hydrogen removal in sodium of secondary coolant of LMFBR and for tritium removal in lithium coolant of CTR.

(4) For Nb, as canning material, indeed it is superior in hydrogen permeation, but it is necessary to be more investigated in compatibility study because it has a tendency to be oxidized in sodium solving some oxygen.

Developing the chemical trap for practical application, more quantitative informations are necessary. Further developments are in progress to accumulate the more quantitative data and informations on practical application of the tritium trapping system.

15th DOE NUCLEAR AIR CLEANING CONFERENCE

Acknowledgment

This work was performed under contract with Power Reactor and Nuclear Fuel Development Corp. (PNC).

The authors wish to express their appreciations to Dr. K. Mochizuki, senior engineer, FBR Development Project (PNC), and Mr. K. Akagane, assistant senior engineer, FBR Development Project (PNC), for their valuable suggestions. Technical contributions from K. Kasahara, T. Kamei, H. Taki are gratefully acknowledged.

References

1. Erdman C.A., "Radionuclide production, transport, and release from normal operation of LMFBRs" EPA-520/3-75-019, November 1975
2. D. R. Vissers, J. T. Holmes, L. G. Bartholme and P. N. Nelson, J. Nuclear Technology Vol. 21, March 1974
3. R. Kumar, "Tritium transport in an LMFBR" ANL-8089, August 1974
4. W. H. Meuller, J. P. Blackledge, G. G. Libowitz, "Metal Hydrides" 1968

15th DOE NUCLEAR AIR CLEANING CONFERENCE

MONITORING AND REMOVAL OF GASEOUS CARBON-14 SPECIES

M.J. Kabat
Ontario Hydro
Health Physics Department
Toronto, Ontario

Abstract

A simple and efficient method was developed for the monitoring of low level carbon-14 in nuclear power station areas and gaseous effluent. Gaseous carbon compounds (hydrocarbons and CO) are catalytically oxidized to CO₂, which is then absorbed on solid Ca(OH)₂ at elevated temperatures. The ¹⁴C collected is quantitatively liberated by thermal decomposition of CaCO₃ as CO₂, which is either measured directly by flow-through detectors or absorbed in alkali hydroxide followed by liquid scintillation counting.

The method can also be used for the removal of gaseous ¹⁴C. The Ca¹⁴CO₃ can be immobilized in concrete for long term disposal. Ca(OH)₂ is an inexpensive absorber. It is selective for CO₂ and has high capacity and efficiency for its absorption and retention.

A theoretical evaluation of the optimum conditions for CO₂ absorption and liberation is discussed and experimental investigations are described. There is good agreement between theoretical predictions and experimental findings.

I. Introduction

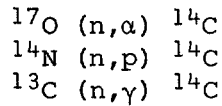
With the growth of the nuclear industry throughout the world, there is increasing concern with the global and regional impact associated with the discharge of long-lived radionuclides. Carbon-14 is one of the most significant radionuclides in this group. Considerable efforts have been made in industrial countries in the last decade to determine its global impact, emission standards, monitoring and control techniques and adequate long term disposal. In CANDU, power stations nitrogen gas has been removed from the annulus between pressure and calandria tubes in all recently built reactors, but a significant amount of ¹⁴C is still produced in moderator systems. Therefore, a project is currently in progress in the Ontario Hydro Health Physics Department to develop adequate techniques for monitoring and control of ¹⁴C in power station systems, areas and effluents with the prospect of its safe long term disposal.

II. Carbon-14 Production and Releases from Nuclear Facilities

Production Rates

Carbon-14 is produced in nuclear reactors by neutron activation of N, O and C in the coolant and moderator and impurities in reactor systems and components. The basic reactions are:

15th DOE NUCLEAR AIR CLEANING CONFERENCE



The yield of ${}^{14}\text{C}$ from other reactions is negligible.

Major sources of ${}^{14}\text{C}$ in CANDU reactors are the moderator system (large quantity of D_2O) and the nitrogen filled annulus gas systems. Carbon-14 production rates calculated for two operating CANDU power reactors, 540 MWe units at the Pickering NGS and 750 MWe units at the Bruce NGS are listed in Table I with data on ${}^{14}\text{C}$ production in other reactors derived by W. Davis Jr. in publication (1). The CANDU production rates were calculated from core-averaged Westcott fluxes and 200 m/s cross-sections of 0.235 b, 1.81 b, and 0.9 mb respectively for the above reactions.

Table I
Estimated Production Rates of ${}^{14}\text{C}$ in Various Reactor Types

Reactor	Carbon-14 Production Rates - Ci/GWe-yr			
	Coolant	Other Systems - Ci/GWe-yr	Fuel (Average Values)	
CANDU - 540 MWe	9	Moderator D_2O	440	15
		N_2 Annulus System	430	
750 MWe	10	Moderator D_2O	547	20
		CO_2 Annulus System	0.02	
BWR	4.7	Cladding & Struct. Mater.	43.3-60.4	17.6
PWR	5.0	Cladding & Struct. Mater.	30.5-41.6	18.8
LMFBR	nil	Cladding & Struct. Mater.	12.8	6.3
HTGR	nil	Cladding & Struct. Mater.	< 190	12

Chemical Forms

Reactor Systems. Carbon-14 was identified in reactor systems as a mixture of CO_2 , CO and hydrocarbons. Their ratio depends on the chemistry of the respective reactor system. C.O. Kunz et. al. reported in publication (2) that a major portion of ${}^{14}\text{C}$ measured in PWR systems was present as hydrocarbons and only small amounts as carbon oxides because D_2 is maintained in the primary coolant as a cover gas. The above authors also reported in publication (3) that in BWR

15th DOE NUCLEAR AIR CLEANING CONFERENCE

station more than 90% of ^{14}C was present as CO_2 . It was also suggested that the predominant mechanism appears to be oxidation of carbon to CO_2 and CO by oxygen radicals formed from radiolytic decomposition of the coolant water.

An annulus gas sample (N_2) from a CANDU reactor was analyzed in the NY State Department of Health Laboratory. In this sample > 75% of ^{14}C was present as hydrocarbons, as expected, because of the presence of D_2 in the annulus gas (from the coolant). Samples of primary coolant off-gas (D_2) and moderator cover gas (He) have not yet been analyzed but from chemical conditions it can be assumed that hydrocarbons are the major ^{14}C compounds in the primary coolant and significant portions of ^{14}C in the moderator system are in oxide forms.

Fuel. It was suggested in publication (1) that ^{14}C produced in UO_2 fuel might become bound to uranium as carbide, remain as impurity atoms, or be converted to carbon monoxide or dioxide. It was also assumed that major portion of ^{14}C in the fuel will be converted to CO_2 in dissolving operations at the fuel reprocessing plant.

Carbon-14 Releases

It was reported in publication (2) that combined gaseous ^{14}C effluent from a 1000 MWe PWR would be approximately 6 Ci/year. The BWR release rate of approximately 8 Ci/GWe-year was estimated from measurements, described in publication (3). No other experimental data on ^{14}C effluents is available at present. The magnitude of ^{14}C releases through all potential pathways from PWR and BWR stations was estimated in publication (9) and ^{14}C release from the HTGR reprocessing facility evaluated in publication (10). Measurements of ^{14}C release from CANDU reactors are in progress and will be reported in the near future.

Carbon-14 production can be greatly reduced by avoiding the presence of nitrogen in high neutron flux systems and areas. Releases of ^{14}C can be further reduced by removing it from power station and fuel reprocessing plant systems and effluents, transferring it to a solid form, chemically stable, and for permanent disposal.

III. Present Status in Monitoring and Control of Gaseous Carbon-14 Releases

Monitoring and Control Requirements

No regulatory requirements have yet been issued on monitoring and control of ^{14}C effluents. However, from the carbon-14 environmental impact analysis performed by the Commission of the European Communities (4), US-EPA (5), and several authors (6,7,8) it is evident that the requirements on the control and monitoring of ^{14}C release will be formulated in the near future. Also in Ontario Hydro, work is in progress on deriving ^{14}C release limits.

Carbon-14 Monitoring Methods

Several methods were developed for "carbon dating" which are not directly applicable for ^{14}C monitoring in nuclear facilities. However, the practice of CO_2 purification with heated CaO , applied in some ^{14}C dating procedures, was further developed for direct collection of gaseous ^{14}C in nuclear facilities as described later in this paper. The well known method of CO_2 collection in alkaline solutions was used on several occasions for $^{14}\text{CO}_2$ sampling. However, this method is not selective for CO_2 since other carbon compounds can be partially

15th DOE NUCLEAR AIR CLEANING CONFERENCE

absorbed and other radionuclides can interfere with ^{14}C measurement. A heated catalyst must be added when "total ^{14}C " is to be collected and evaporation or spills of alkaline solution can introduce significant experimental errors.

A sophisticated laboratory method was developed in the NY State Department of Health Laboratory (11) for ^{14}C analysis. Carbon-14 gaseous compounds are separated with a gas chromatograph and radiometrically evaluated. This method was successfully applied in PWR and BWR effluents and also a CANDU sample evaluation. Unfortunately, it is too complex for routine monitoring of ^{14}C in nuclear facilities operational field.

Carbon-14 Removal Methods

All proposed methods for ^{14}C removal are based on converting it to CO_2 and solidification as CaCO_3 for disposal. In publication (12) a detailed evaluation was made on $^{14}\text{CO}_2$ fixation methods and available options for CaCO_3 disposal. The dry CO_2 - CaO process for CO_2 fixation was rejected and the following aqueous processes were considered.

1. The direct reaction of CO_2 with a slaked lime slurry.
2. A double alkali process where CO_2 is absorbed in NaOH solution and then transferred to CaCO_3 by reaction of Na_2CO_3 with slaked lime slurry.

The simpler direct CO_2 fixation process was recommended. It was suggested that ^{85}Kr was the controlling radiation hazard in the ^{14}C fixation and disposal processes. It was also concluded that shallow land burial of CaCO_3 appears to be the optimal disposal method available.

In publication (9) all available techniques with the potential for ^{14}C removal were reviewed. A system for ^{14}C removal from LWR effluents was proposed and the cost of fixation and disposal processes evaluated. The assumption was also made in this report that direct reaction of CO_2 with solid CaO is not practical for this purpose.

It was recognized from operational experience with similar systems in the chemical industry that a number of technical difficulties must also be expected in operating the systems for absorption of CO_2 in alkaline liquids, i.e. complexity and size of the equipment, possibility of contamination from leaking liquids, foaming of liquids, plugging the column with CaCO_3 , presence of gamma emitting radionuclides causing building of radiation fields on $\text{Ca}^{14}\text{CO}_3$ containers, etc.

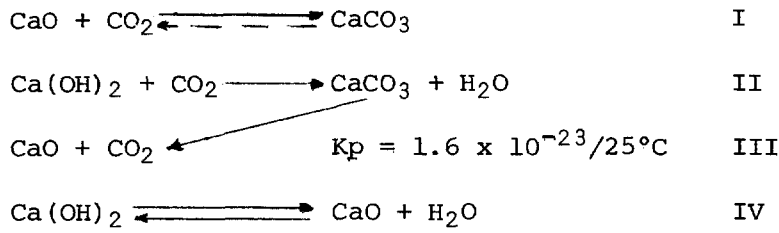
Chemistry of $\text{CaO}/\text{Ca}(\text{OH})_2$ Reactions with CO_2

The methods referred to in Carbon-14 Removal Methods are based on reactions of disassociated forms of $\text{Ca}(\text{OH})_2$ or NaOH with CO_2 in aqueous solutions. The direct reaction of solid CaO with CO_2 , which is much slower under normal temperature and pressure conditions, was not considered for CO_2 fixation on an industrial scale.

From some "carbon dating" procedures and data from chemical publications and physico-chemical considerations it is evident that the rate of the direct reaction of gaseous CO_2 with solid CaO and $\text{Ca}(\text{OH})_2$ significantly increases with temperature. Therefore, in publication (13), a proposal was made to fix $^{14}\text{CO}_2$ on solid CaO at a higher temperature.

15th DOE NUCLEAR AIR CLEANING CONFERENCE

The following reactions are involved in the process of CO₂ fixation on solid CaO and Ca(OH)₂:



Reactions I and II are practically irreversible at temperature up to 300°C because in reaction III the thermal dissociation of CaCO₃ can be neglected at this temperature. Reaction III was discussed in detail in several publications while very little data on the kinetics of reactions I and II have been found in chemical literature. In publication (14) the equilibrium constant of reaction III ($K_p = 1.6 \times 10^{-23}$) was given and it was suggested that "metal oxide (solid) carbon dioxide (gas) reactions, which might in theory yield the carbonate, are often too slow in practice, possibly because of inactivity of the oxide surface."

J. Johnson in publication (15) derived an equation for CO₂ pressure above CaCO₃ which was well in agreement with experimental findings:

$$\log p = -9340 T^{-1} + 1.1 \log T + 0.0012 T + 8.882$$

The temperature dependence of both CO₂ pressure above CaCO₃, calculated from the above equation, and water vapour pressure above Ca(OH)₂ from data in publication (16) are illustrated in Figure 1.

Rapid absorption of CO₂ with moist Ca(OH)₂ and no CO₂ absorption with dry CaO at normal temperature when moisture was excluded, was reported in publication (17). According to several authors, referred to in this publication, "dry calcium oxide absorbs no CO₂ in the cold, but a reaction occurs when the temperature is raised to 420°C". Also that "crystalline CaO combines with CO₂ very slowly while the porous variety combines rapidly with the same gas." Also, "no absorption of nitric oxide on CaO" is reported in publication (19).

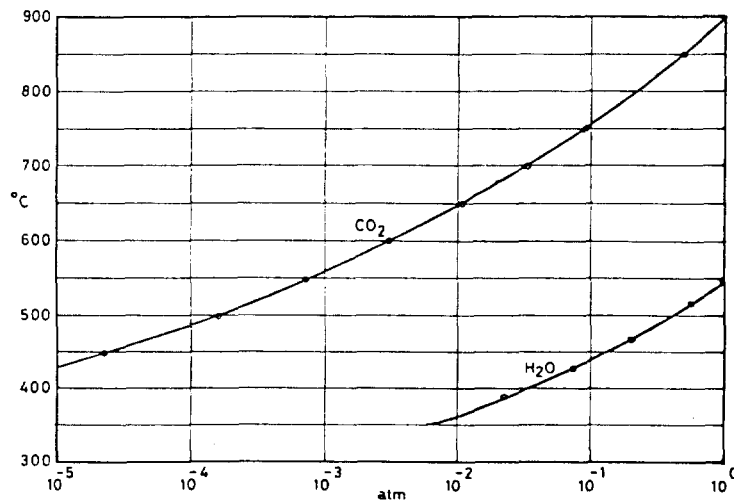


Figure 1

15th DOE NUCLEAR AIR CLEANING CONFERENCE

It was deduced from the above information that the direct reaction of solid $\text{Ca}(\text{OH})_2$ (rather than CaO) with gaseous CO_2 could be sufficiently fast at increased temperatures for efficient absorption of CO_2 for both ^{14}C monitoring and removal at nuclear facilities.

V. Proposal for CO_2 Absorbent

Performance Requirements

Sampling of $^{14}\text{CO}_2$:

- Collection efficiency for CO_2 of $\geq 99\%$ at reasonably low residence time, $< 500^\circ\text{C}$ temperature and CO_2 concentration range of 0.1 - 1000 ppm.
- Sufficient capacity for sampling air, with 350 ppm CO_2 , for a one week period.
- Simple equipment and procedure involving minimal sampling error in the field.
- High collection selectivity for CO_2 , minimum retention of noble gas radionuclides.
- Quantitative desorption of ^{14}C in a form suitable for its radio-metric evaluation.
- Minimum release of other radionuclides in the process of ^{14}C desorption.

Removal of $^{14}\text{CO}_2$:

- Collection efficiency for CO_2 of $> 90\%$ at temperatures $< 500^\circ\text{C}$, and CO_2 concentrations of 0.1 - 1000 ppm.
- Large volume reduction factors for CO_2 .
- Operationally simple collection process.
- Minimal possibility of radioactive contamination arising from processing the used absorbent for disposal.
- Minimal radiation field at the disposal containers surface.
- Negligible release of radionuclides from the containers during long term storage.

Proposal for CO_2 Collection Method

From the above requirements, the absorption of gaseous CO_2 on solid $\text{Ca}(\text{OH})_2$ was the logical choice for both ^{14}C sampling and removal.

The proposal for the CO_2 collector was based on the following considerations:

1. In order to obtain both adequate absorption velocity and maximum capacity:
 - The operating temperature was to be $> 300^\circ\text{C}$ but should not exceed approximately 500°C when significant decomposition of $\text{Ca}(\text{OH})_2$ occurs.

15th DOE NUCLEAR AIR CLEANING CONFERENCE

- The $\text{Ca}(\text{OH})_2$ absorbent must have a large absorption surface.
 - Reasonable residence time (0.1 - 1 s) should be allowed for the chemical reaction to be efficient.
2. The selectivity of CO_2 adsorption results from the specific affinity of $\text{Ca}(\text{OH})_2$ for CO_2 . No noble gas retention can occur at increased temperature. Tritiated water vapour present in the gas sample could be partially absorbed in $\text{Ca}(\text{OH})_2$ through isotopic exchange process. However, tritium can be separated later by fractional desorption; it desorbs from the absorbent at $< 600^\circ\text{C}$ temperature, at which no significant CaCO_3 decomposition occurs.
 3. Carbon-14 can be selectively desorbed as CO_2 at approximately 900°C . A low purge of inert gas accelerates the process of CaCO_3 decomposition by continuously removing the gaseous reaction product (CO_2). Coincidentally, the purge provides a gas carrier for transferring $^{14}\text{CO}_2$ for radiometric evaluation.
 4. The spent absorbent, a solid mixture of $\text{CaCO}_3 + \text{Ca}(\text{OH})_2$ can be easily sealed without any handling of loose contaminated material. Negligible amounts of other radionuclides would be present with ^{14}C in the disposal containers and negligible leaching of ^{14}C from containers would occur during their long term storage.

To evaluate the above concept, a laboratory system was built and the absorption of CO_2 tested, with both CaO and $\text{Ca}(\text{OH})_2$ as described in the next section.

VI. Experimental Studies on Carbon-14 Monitoring

Process Description

In most field applications, gaseous organic compounds and CO are first oxydized to CO_2 by catalytic combustion. Carbon dioxide absorption on CaO and $\text{Ca}(\text{OH})_2$ was evaluated by injecting $^{14}\text{CO}_2$ into an air stream containing approximately 330 ppm of nonradioactive CO_2 and passing the air through test columns containing the absorbents. From the measured $^{14}\text{CO}_2$ concentration upstream and downstream of the column the efficiency and capacity of both CaO and $\text{Ca}(\text{OH})_2$ for CO_2 absorption was evaluated within a wide range of experimental conditions. The temperature and gas purging effects on Ca-CO_3 dissociation were then evaluated by continuous measurement of $^{14}\text{CO}_2$ concentrations in the purge gas downstream of the column and also by collecting CO_2 in NaOH solution followed by liquid scintillation counting of ^{14}C .

Equipment Description

The experimental system is shown in Figures 2 and 3. It contains the following components.

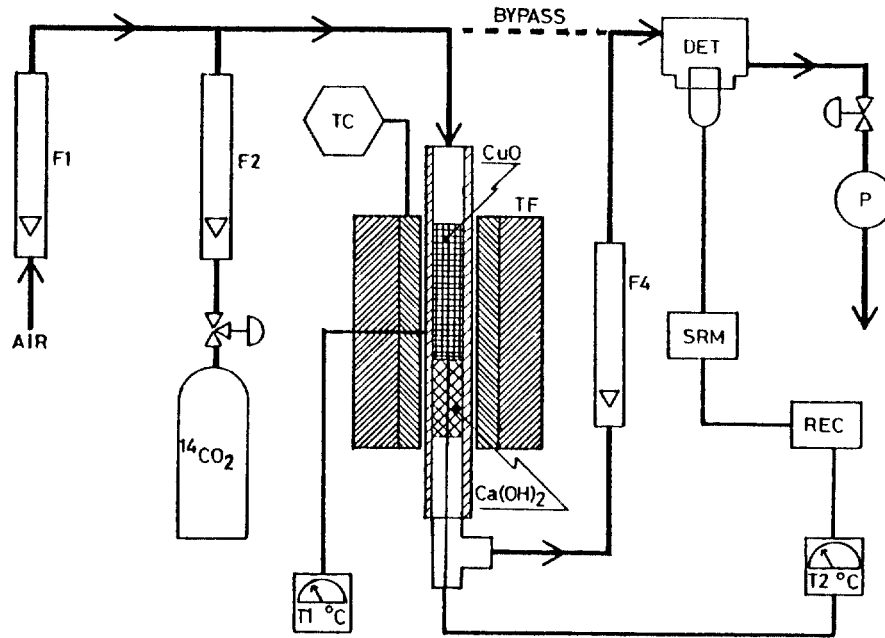


Figure 2

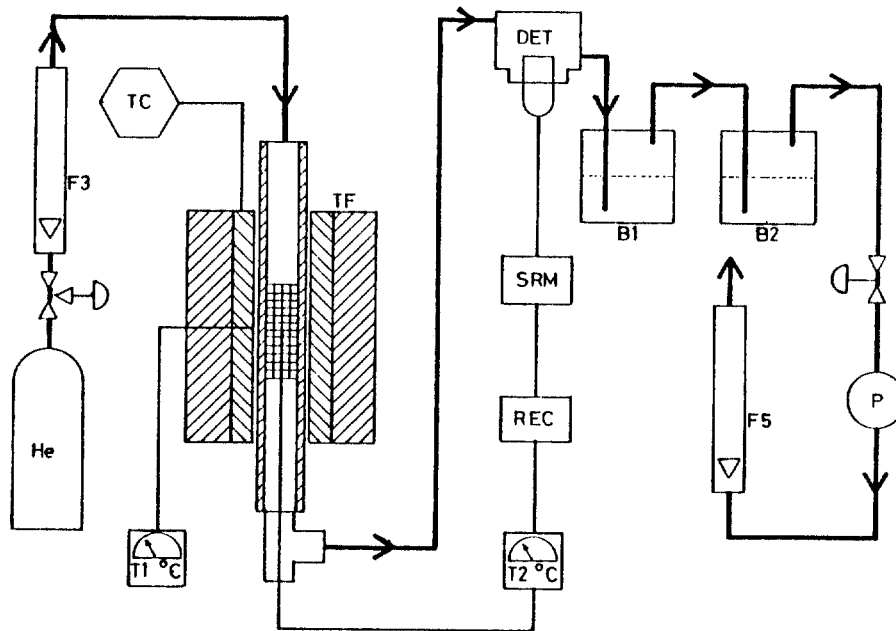


Figure 3

- Carbon-14 and purge gas supply.
- Systems for measurement and control of operational parameters (flow, temperature).

15th DOE NUCLEAR AIR CLEANING CONFERENCE

- Catalyst for combustion of ^{14}C species and CO_2 absorber.
- ^{14}C monitors (upstream and downstream of the CO_2 absorber).

Carbon-14 and Purging Gas. The carbon dioxide ($^{14}\text{CO}_2$) used for CaO testing was generated from the Pickering NGS annulus gas as follows:

A stream of N_2 from the annulus gas system containing ^{14}C (mostly as CH_4) was passed through CuO at approximately 400°C and the resulting $^{14}\text{CO}_2$ was then absorbed on $\text{Ca}(\text{OH})_2$ at the same temperature. When approximately 20 mCi of ^{14}C was accumulated as $\text{Ca}^{14}\text{CO}_3$, the temperature of the column was increased to 900°C and the $^{14}\text{CO}_2$ produced from CaCO_3 thermal dissociation was transferred into an evacuated stainless steel bomb which was then filled with N_2 to approximately 7 MPa (1000psi) pressure.

Nitrogen from the bomb, containing 10 - 100 μCi of $^{14}\text{CO}_2/\text{L}$ was then injected into air or other gas stream and carried into the tested column.

Helium, nitrogen or air were used for purging desorbed CO_2 from the absorber column in testing the process of CaCO_3 thermal decomposition.

Measurement and Control of Operational Parameters. In most experiments, laboratory air containing 330 ± 15 ppm of CO_2 was drawn through the tested column with the pump P at the flow rate of 5 Lpm. Carbon-14 ($^{14}\text{CO}_2$ in nitrogen) was injected into the air stream from the pressurized stainless steel bomb at the rate of 10 - 30 mL/m.

The gas flows and the column temperatures were continuously measured and controlled for both the CO_2 absorption and the CaCO_3 dissociation.

Calibrated flow meters F_1 , F_2 and F_3 measured gas flow rates at the inlet and F_4 , F_5 installed downstream of the columns, was used to monitor system leaks.

Thermocouple T_1 detected the temperature of the tubular furnace TF equipped with the temperature controller TC.

The temperature inside the absorbent was detected with the thermocouple T_2 installed axially of the absorption column and recorded.

The Catalyst and Absorbent Columns. Cupric oxide, prepared in our laboratory, was used in our experiments. In the experimental setup, both the catalyst column (CuO) and the absorbent column [CaO or $\text{Ca}(\text{OH})_2$] were contained in a quartz tube, 25 mm diameter and separated with a stainless steel screen. The column length was: 50-100 mm of CuO and 30-50 mm of CaO . The grain size of CuO was 10-40, while two size ranges of CaO and $\text{Ca}(\text{OH})_2$, 10-20 and 20-40, were tested separately.

Carbon-14 Monitors. Continuous on line measurement of ^{14}C concentration was performed with a thin wall ($< 2 \text{ mg/cm}^2$) GM detector D installed in through-flow chambers (50 and 1000 mL volume) installed upstream and downstream of the absorber column. Both the count rate and accumulated counts were measured with an NE-SR5 scaler/rate meter (SRM) and the ^{14}C count rate was recorded. In desorption experiments, $^{14}\text{CO}_2$ was also absorbed in NaOH solution and measured with a liquid scintillation counter.

15th DOE NUCLEAR AIR CLEANING CONFERENCE

Materials. Most of the system was assembled of quartz and glass tubing. Plastic tygon tubing was only used for connecting system components. Thermo-couple sheath and the screens separating the catalyst and the absorbent columns were made of stainless steel. A polyethylene flow chamber was used for monitoring low concentrations of ^{14}C in the collection process and a glass chamber for counting high concentrations of ^{14}C in the desorption process.

Catalytic Oxidation of ^{14}C Species

Catalyst Performance Requirements. The basic requirements on the catalysts performance for hydrocarbons and CO oxidation are as follows:

1. For ^{14}C sampling:
 - a) Combustion efficiency of $> 97\%$ for hydrocarbons at 0.1 - 1000 ppm concentrations and temperature range 350-450°C.
 - b) No significant retention of any chemical form of carbon.
 - c) At least one week lifetime for hydrocarbons oxidation from air under typical sampling conditions.
 - d) At least 24 hours capacity for hydrocarbons oxidation from gas containing no oxygen (which requires CuO type catalyst).
2. For ^{14}C removal:
 - a) Combustion efficiency $> 90\%$ in oxygen free gas within 350-450°C and CH_4 concentration 0.1-500 ppm.
 - b) Capacity for $>$ one week of continuous oxidation of methane at an average concentration of 10 ppm, from gas containing no oxygen.
 - c) Regeneration capability (when applied for ^{14}C removal from gas containing no oxygen).

Testing of Catalysts. The GM-AC converter catalyst type number 78925 and two Hopcalite samples (from MSA and Safety Supply), which were tested in our laboratory with a gas chromatograph did not comply with the requirements 1b, 1d, 2a, 2b, and 2c. Also, CuO from Fisher Scientific, prepared by the oxidation of Cu wire, was not adequately efficient.

Development of the catalyst was not originally intended in this project. However, when no commercially available catalyst was found to perform as needed for the quantitative sampling of ^{14}C , cupric oxide was prepared in our laboratory by precipitation from hot CuSO_4 solution, ground and tested with a gas chromatograph under the assumed sampling conditions. This material satisfied all the above requirements for ^{14}C sampling and removal, except its regeneration capability.

The measured performance of this catalyst for methane combustion was as follows:

1. The minimum temperature for efficient combustion of methane in air is 270°C at the residence time of 3 seconds. A slightly higher temperature - approximately 300°C - is needed for complete CH_4 combustion from oxygen free gas.
2. The measured efficiency values for combusting CH_4 (1000 ppm) over a one week period in air at 310°C were:

15th DOE NUCLEAR AIR CLEANING CONFERENCE

- > 99.5% at > 3 second residence time
- > 99% at > 2 second residence time
- > 97% at > 1 second residence time

The total volume of air, with 1000 ppm of CH₄ was > 10⁵ volumes of the catalyst. It is expected that the catalyst lifetime is significantly longer than one week under the above conditions.

3. For combustion of methane in nitrogen, the available oxygen from one volume of CuO oxidized 5000 volumes of 0.1% CH₄ in N₂. The efficiency was > 97% at the residence time of approximately six seconds and temperature of 320°C.
4. At low methane concentrations (< 1 ppm), its combustion was still improved and also the catalyst's lifetime proportionally increased.
5. The catalyst, in agreement with experimental data in publication (18), was more efficient for CO than for CH₄ combustion at the same temperature and residence time.
6. The combustion efficiency increases with the catalyst temperature (measured up to 600°C) but temperature cycling has a detrimental effect on the catalyst.
7. Carbon-14 retention of < 0.1% was measured on the precipitated CuO catalyst after passing large volumes of gas containing a mixture of ¹⁴CO₂, ¹⁴CO and ¹⁴C hydrocarbons.
8. Once the catalyst was exhausted it cannot be reoxidized to regain its original efficiency for methane combustion, probably because of its restructured surface.

Testing Of ¹⁴CO₂ Absorption on CaO and Ca(OH)₂

Materials Tested. Three grades of commercially available CaO were tested in the original CaO form and also as Ca(OH)₂ prepared in our laboratory.

The technical quality and purified CaO lumps from Fisher Scientific were ground and two grain sizes, 10-20 and 20-40 mesh, selected for our measurements.

The analytical grade CaO was not tested in its original powdered form.

Further, both the purified and analytical CaO were converted to solid, granulated Ca(OH)₂ by slaking CaO with distilled water, drying the sludge, grinding and selecting 10-20 and 20-40 mesh sizes. In this process, BaO, SrO and solid impurities were further removed from the "purified" CaO. From the measured weight loss of the "reprocessed CaO" after heating to 600°C, it was evident that the original CaO was quantitatively converted to Ca(OH)₂ through the above process. Also, the specific weight of this material was reduced. The average specific weight values of the tested absorbents are listed in Table II.

15th DOE NUCLEAR AIR CLEANING CONFERENCE

Table II

<u>Absorbent Type</u>	<u>Mesh Size</u>	<u>Specific Weight g/cm³</u>
CaO - technical	20-40	0.87
CaO - purified	20-40	0.85
CaO - purified	10-20	0.8
Ca(OH) ₂ - from both purified and analytical CaO	20-40	0.4
Ca(OH) ₂ - from both purified and analytical CaO	10-20	0.35

Testing Conditions. Experimental conditions applied in the evaluation of CaO and Ca(OH)₂ absorbents were as follows:

The efficiency and capacity for CO₂ absorption was tested within the temperature range of 20°C to 550°C.

Laboratory air (approximately 50% RH) containing 330 ± 15 ppm of CO₂, with the addition of approximately 0.1 ppm of ¹⁴CO₂ was applied in most measurements. At a flow rate of 5 Lpm and absorbent volume of 30-50 cm³ the "residence time" was 0.36 - 0.6 seconds. To confirm references to the slow reaction of dry CaO with CO₂, the efficiency of both Ca(OH)₂ and dry CaO for absorption of CO₂ from dry nitrogen was evaluated.

The collection capacity was calculated from the total amount of air passed through the absorber until its efficiency for CO₂ removal was reduced to approximately 95%. From air volume, CO₂ concentration and absorbent weight, the portion of CaO or Ca(OH)₂ converted to CaCO₃ was calculated.

The penetration of 5% ¹⁴CO₂ was radiometrically monitored with better than ± 10% accuracy at the 95% confidence level.

Absorption of CO₂. Results of absorbers' efficiency and capacity testing with air containing 330 ± 15 ppm of CO₂ are summarized in Table III.

Results of Ca(OH)₂ and dry CaO efficiency testing with CO₂ in dry nitrogen are given in Table IV.

The time dependence of CO₂ penetration through absorber containing 30 mL (approximately 11 g) Ca(OH)₂ is illustrated in Figure 4.

The efficiency of powdered, analytical grade CaO could not be evaluated because under typical experimental conditions its flow resistance was too high and it developed channelling of the sample which caused erroneous results.

Table III

<u>Absorbent</u>	<u>Mesh Size</u>	<u>Temp. (°C)</u>	<u>Residence Time (Sec.)</u>	<u>Total Air Volume at 5% Penetr. (m³)</u>	<u>Collect Capacity (%* at 98% eff.)</u>	<u>Average Collect Capacity (%* at 95% eff.)</u>
1. CaO - technical	10-20	400	0.6	0.23		0.5
2. CaO - purified	10-20	20-200	2.0	0.14		0.3
3. CaO - purified	10-20	400	0.6	0.9		2.0
4. CaO - purified	20-40	400	0.6	2.2		4.8
5. Ca(OH) ₂ from purified CaO	10-20	300	0.6	0.7	5.5	7.0
6. Ca(OH) ₂ from purified CaO dried out 700°C	10-20	300	0.6	0.35	3.0	3.5
7. Ca(OH) ₂ from purified CaO	10-20	400	0.6	4.2	42	43
8. Ca(OH) ₂ repeated use (after CaCO ₃) thermal dissociation.	10-20	400	0.6	1.2	10	12
9. Ca(OH) ₂ from purified CaO	20-40	400	0.6	4.4	44	45
10. Ca(OH) ₂ from analytical CaO	20-40	400	0.6	4.4	44	45
11. Ca(OH) ₂ from purified CaO	10-20	20-250	0.36	0.4	3.0	4.0
12. Ca(OH) ₂ from purified CaO	10-20	350	0.36	2.6	25	27
13. Ca(OH) ₂ from purified CaO	10-20	400	0.36	3.7	37	38
14. Ca(OH) ₂ from purified CaO	10-20	450	0.36	5.9	58	60
15. Ca(OH) ₂ from purified CaO dried out 650°C	10-20	450	0.36	1.1	10	11

* Percent of the theoretical capacity calculated from stoichiometric ratio.

15th DOE NUCLEAR AIR CLEANING CONFERENCE

Table IV

Absorbent	Size	Concentration of CO ₂ in N ₂ (ppm)	Residence Time (Sec.)	Temperature (°C)	CO ₂ Absorption Efficiency (%)
Ca(OH) ₂ from purified CaO	10-20	1	0.6	360 - 380	≥ 99.7
				400	99.5
				450	99
				550	< 90
CaO from Ca(OH) ₂ dried at 700°C	10-20	330	0.6	400	nil
				500	nil
				600	nil

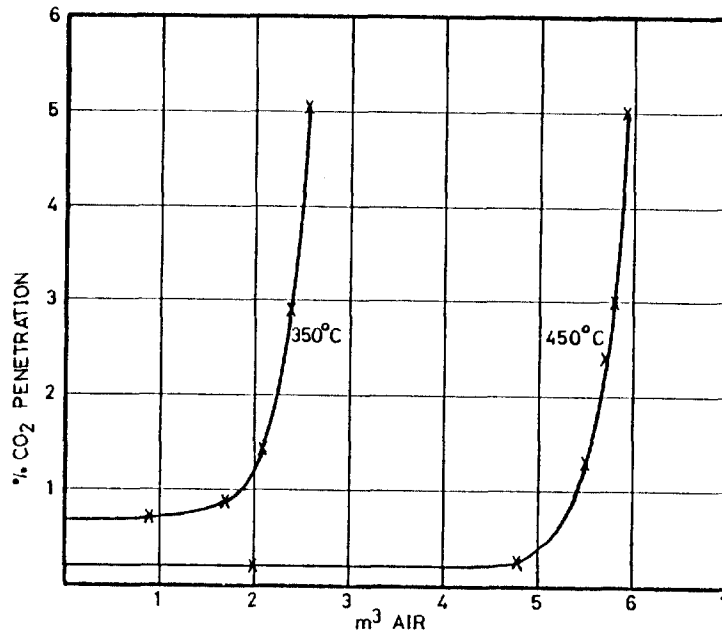


Figure 4

Thermal Dissociation of CaCO₃

The graph on Figure 1 shows that the equilibrium CO₂ pressure above CaCO₃ reaches 1 atm at a temperature of approximately 900°C. Therefore, the rate of Ca¹⁴CO₃ dissociation was experimentally evaluated within 700-950°C.

After CO₂ penetration exceeded 5% in the absorption period, ¹⁴CO₂ flow was terminated, a low purge flow (50-100 mL/m) of inert gas was maintained and the column temperature continuously increased. In the temperature range 500-650°C water was released from the column due to decomposition of remaining Ca(OH)₂. With further column temperature increase noticeable decomposition of CaCO₃ started at ≥ 700°C and rapid and complete decomposition of CaCO₃ occurred at 900°C.

15th DOE NUCLEAR AIR CLEANING CONFERENCE

No significant effect of the purge gas quality was found in our experiments. Helium was used in most experiments, but using N₂, dry or humidified air did not cause any significant difference in the CO₂ desorption from the column.

CO₂ Absorption on System Components

It was found from the experiments that ¹⁴CO₂ reacts with plastic materials and metals used in the experimental setup. It can be assumed that physical absorption, chemisorption and isotopic exchange are involved.

Any ¹⁴C hold-up on the system components is undesirable in the sampling process. Therefore, ¹⁴CO₂ sorption on stainless steel was investigated. Slugs of stainless steel wire were exposed to ¹⁴CO₂/N₂ at a residence time of approximately 0.5 minutes, for 30 minutes at temperatures of 20°C and 400°C. The system was then purged with pure He and the temperature increased to 900°C. The amount of ¹⁴C, desorbed from the stainless steel wire, was then measured. Results are summarized in Table V.

It was also determined that ¹⁴CO₂ from the gaseous sample was partially sorbed on the mylar foil covering the GM detector and subsequently desorbed using a pure gas purge, with a half-life of approximately 15 minutes.

Significant sorption of both ¹⁴CO₂ and ¹⁴CH₄ on PVC tygon tubing was also observed.

As expected, no measureable ¹⁴C sorption occurred on quartz, Vycor glass and pyrex glass components.

Radiometric Determination of ¹⁴C Gaseous Species

Both direct and indirect counting methods were applied in our laboratory for ¹⁴C measurement.

Table V

<u>Absorption Temperature (°C)</u>	<u>¹⁴CO₂ Through The S.S. Slug (μCi)</u>	<u>Desorption Temperature (°C)</u>	<u>¹⁴C Desorbed (% of CO₂ Passed)</u>	<u>Total ¹⁴CO₂ Desorbed (%)</u>
20	67.6	20 - 400	3.7	
		400 - 950	2.6	6.65
		1000	0.35	
400	338	400	0.76	
		400 - 950	1.2	2.25
		1000	0.29	

Plastic scintillation cell NE802 with a photomultiplier or a thin wall (< 2 mg/cm²) GM detector installed in flow-through chambers, 50 mL and 1 L volume were applied for direct counting of gaseous forms of ¹⁴C.

When a low activity of ¹⁴C in a small volume of gaseous sample was to be measured, the sample was transferred into the cell and the detector counts were integrated with a scaler for the time period required for adequately low

15th DOE NUCLEAR AIR CLEANING CONFERENCE

statistical error.

The GM chambers were applied in most "continuous flow" measurements, particularly in CO₂ absorption/desorption experiments. Specific activity of ¹⁴C was evaluated from the detector count rate and the "total ¹⁴C" from integration of detector counts.

Tritium or other radionuclides did not interfere with ¹⁴C measurements.

A liquid scintillation counting method was used in cases when very low activity of ¹⁴C was to be measured, the water condensate from Ca(OH)₂ decomposition was to be included in the ¹⁴C evaluation or when tritium was present in the sample. Carbon dioxide and water desorbed from Ca(OH)₂ was absorbed in 0.5 N NaOH solution which was then mixed with Aquasol 2 scintillator and measured with a three-channel liquid scintillation counter.

Detection efficiencies of our counting cells for ¹⁴C are listed in Table VI.

Table VI

<u>Detector</u>	<u>Cell Volume</u> <u>cm³</u>	<u>Net cpm From</u> <u>1 μCi ¹⁴C/L</u> <u>cpm</u>	<u>Detection Efficiency</u> <u>For ¹⁴C</u> <u>%</u>
GM Detector	50	3670	3.3
GM Detector	1000	5560	0.25
NE802	11	4320	17.8
Liquid Scintillation Counter	5 mL NaOH Solution + 15 mL Aquasol 2	--	85

VII. Discussion of Results

Oxidation of ¹⁴C Compounds

The results of our experiments show that the efficiency of precipitated CuO for oxidation of carbon monoxide and hydrocarbons is sufficient for both ¹⁴C sampling and its removal. It also has an adequate lifetime for combustion of hydrocarbons and CO from gas containing oxygen. The capacity for combusting hydrocarbons from oxygen free gas is at least 20 Ci of pure ¹⁴CH₄/kg of CuO or a proportional quantity of high hydrocarbons. No significant retention of ¹⁴C on the CuO was measured under typical sampling conditions.

This catalyst is particularly suitable for ¹⁴C sampling. It can be also used in ¹⁴C removal from gas containing at least an equivalent concentration of oxygen.

Use of another catalyst, with a regeneration capability, would be more economical in industrial application where hydrocarbons are to be combusted from oxygen free gas and carbon retention does not cause any difficulties.

15th DOE NUCLEAR AIR CLEANING CONFERENCE

Absorption of CO₂

From the results of CaO and Ca(OH)₂ testing, the following conclusions have been drawn:

1. Only Ca(OH)₂ has a high efficiency and capacity for absorption of gaseous CO₂ within the temperature range 350-450°C. Practically no CO₂ can be absorbed from a dry carrier gas on dry CaO within the above temperature range and residence time of ≤ 1 second.
2. There is no difference in the efficiency and capacity between Ca(OH)₂ made of purified or analytical grade CaO.
3. Calcium hydroxide, 10-20 mesh, is more suitable for field application than the 20-40 mesh which has much higher flow resistance and is only slightly more efficient for CO₂ absorption.
4. The optimum temperature range for CO₂ collection is 350-450°C. Lower temperatures (360-400°C) are more suitable for CO₂ at < 1 ppm concentration. The absorbent lifetime increases almost proportionally to reduced CO₂ concentration. A temperature of 450°C is more practical when the CO₂ concentration exceeds 100 ppm.
5. At 550°C, a significant portion of Ca(OH)₂ is dehydrated to an inactive CaO. At this temperature, the efficiency of the absorbent is less than 90% at the beginning of the collection period.
6. It is evident from Table III and Figure 4 that within the recommended temperature range, Ca(OH)₂ maintains its high collection efficiency until a rapid CO₂ breakthrough occurs.

Decomposition of CaCO₃

In our experiments, the course of CaCO₃ thermal decomposition was well in agreement with that theoretically predicted.

The optimum parameters for desorption of CO₂ are 900-950°C column temperature and 50-100 mL/m gas purge (N₂ or He). Under these conditions, the process of CaCO₃ decomposition can be completed in less than 15 minutes.

If tritium was absorbed (through an isotopic exchange with OH¹) on Ca(OH)₂ in the sampling process, it can be selectively desorbed by increasing the absorbent temperature to 600°C for approximately 15 minutes and purged off with N₂ or He. No loss of CO₂ occurs at this temperature. Then CO₂ is desorbed from the absorbent with the second increase of column temperature to $> 900^\circ\text{C}$.

For radiometric evaluation of ¹⁴C the previously described direct counting method with a GM detector in continuous flow regime is suitable for measurement of medium activity ¹⁴C.

A plastic scintillator and GM low volume cells in the scaler counting mode are more convenient for measurement of medium to low activity of ¹⁴C in small volumes.

Absorption of ¹⁴CO₂ in NaOH solution and liquid scintillation counting gives the best results for measuring large volume samples with a wide range of ¹⁴C

15th DOE NUCLEAR AIR CLEANING CONFERENCE

concentrations and $^{14}\text{CO}_2$ samples containing a water condensate.

VIII. Field Applications

Theoretical considerations and the experimental work on this project were oriented toward demonstration of the potential of this method for both sampling and removal of ^{14}C in nuclear field operations.

From the results discussed above, the following proposals were made:

Carbon-14 Sampler

1. The proposed field sampler for "total ^{14}C " is illustrated in Figure 5.

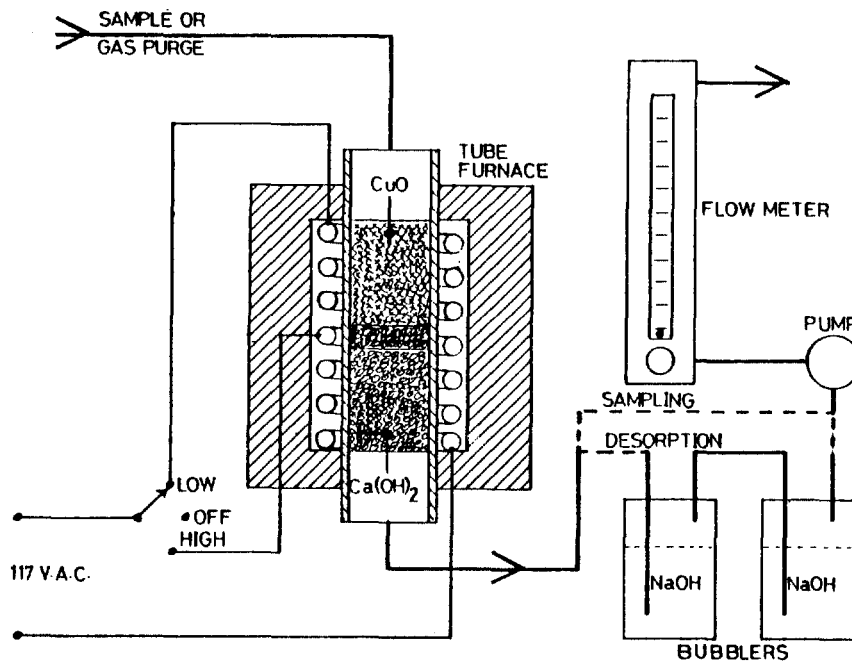


Figure 5

Both the catalyst (CuO) and the absorbent [$\text{Ca}(\text{OH})_2$] are loaded in the quartz or Vycor tube QT, separated with quartz fibre or stainless steel screen and surrounded with the heating element H. The element is assembled of two parts, heating the CuO and $\text{Ca}(\text{OH})_2$ columns separately. The resistance of the heaters is selected in such a way that in the sampling process they are in series (the switch S is in the position a) and both columns are heated to 400°C .

For CO_2 desorption, the switch is in position b, and full power is applied to heat only the absorbent column to 950°C .

In the collection period, the sampling pump P is connected to the outlet of the $\text{Ca}(\text{OH})_2$ and the sample flow is measured with the flowmeter F. For CO_2 desorption, the first bubbler inlet I is connected downstream of the absorbent and the pump inlet to the outlet O of the second bubbler.

15th DOE NUCLEAR AIR CLEANING CONFERENCE

An identical assembly, but without the catalyst (CuO) can be used for selective sampling of $^{14}\text{CO}_2$ from other gaseous ^{14}C compounds.

Several different alternatives of this sampler can be built for specific needs, containing separate catalyst and absorbent columns, automatic control and readout of column temperature, constant flow controller, particulate filter at the sampler inlet, direct $^{14}\text{CO}_2$ detection in the desorption process, etc. For best performance, the size of the sampler should be optimized for both the sampling flow and period required. The optimum sampling parameters and column loads are recommended in Table VII.

Procedure for ^{14}C Sampling and $^{14}\text{CO}_2$ Desorption

After filling columns with appropriate amounts of catalyst and absorbent, a flow meter is connected to the CuO column inlet and a pump to the outlet of the absorber. Heaters on both columns are switched on and the system left for an adequate time period (depending on type of heaters and size of the column) to equilibrate the catalyst and absorbent temperature. Then sample flow is initiated and maintained for the selected time period.

When ^{14}C sampling is completed, two bubblers filled with 100 mL of 0.5 N NaOH each, are connected in series between the absorbent column and sampling pump. A purge gas flow of 100 mL/m is established and temperature of the absorber increased to 950°C. This temperature is then maintained for 15-20 minutes while continuing to purge at 100 mL/m. When CO_2 desorption is completed, the ^{14}C in the solutions is evaluated by liquid scintillation counting.

Carbon-14 Removal System

The removal system principle is identical to that of the above sampler. The material choice is not critical in this application. The whole system can be made of carbon steel because its operational temperature does not exceed 450°C and retention of ^{14}C on system components does not have any negative effect.

The catalyst choice depends on the character of both the carrier gas and ^{14}C compounds to be removed. Commercially available catalyst which can be re-generated is preferable for systems removing ^{14}C components from oxygen free gas.

Only a heated cartridge with an adequate quantity of $\text{Ca}(\text{OH})_2$ is required when $^{14}\text{CO}_2$ is to be removed from systems or gaseous effluents at a nuclear facility. The recommended loads and temperatures of the absorbent are given in Table VIII.

The recommended purification flow limit is 10 L/s (~ 20 cfm) per kilogram of $\text{Ca}(\text{OH})_2$. This value is independent of CO_2 concentration and gives $\geq 99\%$ efficiency for CO_2 removal throughout the operational period as calculated from Table VIII.

The principle of the removal process is very simple. The process does not form by-products or involve handling loose contamination. Carbon dioxide can be removed from high pressure gaseous systems, its adsorption is very selective, therefore the used absorbent cartridges will cause negligible gamma fields. No handling of loose $\text{Ca}^{14}\text{CO}_3$ is necessary, the absorber cartridges can be disposed directly or fixed in concrete for disposal. The high capacity of $\text{Ca}(\text{OH})_2$ for CO_2 results in low volume waste to be disposed. The remaining $\text{Ca}(\text{OH})_2$ in the disposed cartridge will absorb CO_2 eventually penetrating into the container and

15th DOE NUCLEAR AIR CLEANING CONFERENCE

reduce the possibility of ^{14}C leak.

Table VII

Sample	Carbon Compounds		Flow (Lpm)	Total Sample Volume (m ³)	Recommended Loads*		Column Temp. (°C)
	CO ₂ (ppm)	Hydrocarb. + CO (ppm)			CuO (g)	Ca(OH) ₂ (g)	
Air (or gas containing O ₂)	330	300 - 1000	1	≤ 1.5	50	15	450
			5	≤ 1.5	150	15	450
Air (or gas containing O ₂)	330	0 - 300	1	≤ 3.0	50	15	450
			5	≤ 3.0	150	15	450
Air (or gas containing O ₂)	330	0 - 300	1	< 0.5	50	5	450
			5	< 0.5	150	10	450
Oxygen free gas	50-500	50 - 500	1	≤ 1.5	100	15	450
			5	≤ 1.5	300	15	450
Oxygen free gas	1-50	1 - 50	1	≤ 5.0	70	10	400
			5	≤ 5.0	300	10	400
Oxygen free gas	< 1	< 1	1	≤ 5.0	70	5	380
			5	≤ 5.0	300	7	380
Oxygen free gas	0-500	0 - 500	1	< 0.5	100	5	400
			5	< 0.5	300	5	400

* A smaller load than recommended can cause inadequate sampling efficiency and capacity.

A significantly larger load of the absorbent column can slow down the process of desorption.

Table VIII

CO ₂ Concentration (ppm)	Absorbent Temperature (°C)	Absorbent Load [kg Ca(OH) ₂ Per kg CO ₂ Removed]
> 100	450	3.5
1 - 100	400	4.5
< 1	370	5.0

15th DOE NUCLEAR AIR CLEANING CONFERENCE

IX. Conclusions

The method described for CO₂ collection on solid Ca(OH)₂ is applicable in two ways:

1. For ¹⁴C monitoring purposes for selective ¹⁴CO₂ or "total ¹⁴C" sampling in nuclear facilities and their environment. At present, systematic investigations of ¹⁴C levels in CANDU station systems, areas and effluents are in progress, applying the above described techniques. The sampling equipment will be further simplified as operating experience is obtained.
2. This method has good potential for ¹⁴C removal. Large amounts of ¹⁴C can be solidified directly during collection. The highly concentrated ¹⁴C as CaCO₃ can be hermetically sealed and easily disposed of. A purification loop prototype will be tested in the field and possibly used in the future for ¹⁴C control in CANDU reactor moderator systems.

Acknowledgments

The author wishes to acknowledge the assistance of co-workers J.L. Hartwell on carrying the absorbents testing and B.C. Neil and G. McCann on catalysts testing.

15th DOE NUCLEAR AIR CLEANING CONFERENCE

References

1. W. Davis Jr.
"Carbon-14 Production in Nuclear Reactors"
ORNL/NUREG/TM-12, February 1977
2. C. Kunz, W.E. Mahoney, T.W. Miller
"C-14 Gaseous Effluents from Pressurized Water Reactors"
Health Physics Society, Symposium on Population Exposures,
Knoxville, October 1974
3. C. Kunz, W.E. Mahoney, T.W. Miller
"¹⁴C Gaseous Effluents from Boiling Water Reactors"
Annual Meeting of the American Nuclear Society, New Orleans,
June 1975
4. G.N. Kelly, J.A. Jones, Pamela M. Bryant and F. Morley
"The Predicted Radiation Exposure of the Population of the European
Community Resulting from Discharges of Krypton-85, Tritium, Carbon-14
and Iodine-129 from the Nuclear Power Industry to the Year 2000"
V/2676/75 Commission of the European Communities, Luxemburg,
September 1975
5. T.W. Fowler, R.L. Clark, J.M. Gruhlke, J.L. Russell
"Public Health Considerations of Carbon-14 Discharges from the Light
Water-Cooled Nuclear Power Reactor Industry"
ORP/Tad-76-3, U.S. Environmental Protection Agency, July 1976
6. R.O. Pohl
"Nuclear Energy: Health Impact of Carbon-14"
Rad. and Environmental Biophys. 13, 315-237 (1976)
7. H. Bonka, K. Brusserman, G. Schwartz, V. Willrodt
"Production and Emission of Carbon-14 from Nuclear Power Stations and
Reprocessing Plants and its Radiological Significance"
Paper No. 281, The Fourth International Congress of the IRPA, Paris, April 1977
8. P.J. Magno, C.B. Nelson, W.H. Ellett
"A Consideration of the Significance of Carbon-14 Discharges from the
Nuclear Power Industry"
13th AEC Air Cleaning Conference, San Francisco, August 1974
9. G.R. Bray, Ch. L. Miller, T.D. Nguyen, J.W. Rieke
"Assessment of Carbon-14 Control Technology and Cost for the LWR Fuel
Cycle"
Rep. EPA 520/4-77-013, September 1977
10. J.W. Snider, S.V. Kaye
"Process Behaviour and Environmental Assessments of ¹⁴C Releases from an
HTGR Fuel Reprocessing Facility"
Controlling Airborne Effluents from Fuel Cycle Plants,
ANS-AlChE Meeting, Sun Valley, August 1976
11. C. Kunz, N.Y. State Department of Health Laboratory,
Private Communication

15th DOE NUCLEAR AIR CLEANING CONFERENCE

12. A.G. Croft
"An Evaluation of Options Relative to the Fixation and Disposal of ^{14}C --Contaminated CO_2 as CaCO_3 "
ORNL/TM-5171, UC-77, April 1976
13. M.J. Kabat
Consideration on Control of Tritium and Carbon-14 in Nuclear Power Stations
Rep. Air Cont. 3.1/75, October 1975
14. Comprehensive Inorganic Chemistry
Vol. 1, pg. 1235, Pergamon Press
15. J. Johnston
"The Thermal Dissociation of Calcium Carbonate"
Journ. Amer. Chem. Soc., 32, 938-946, 1910
16. J. Johnston
"The Free Energy Changes Attending the Formation of Certain Carbonates and Hydroxides"
Journ. Amer. Chem. Soc., 30, 1357-1365, 1908
17. Mellor
A Comprehensive Treatise on Inorganic and Theoretical Chemistry
Vol. 3, pg. 664

DISCUSSION

COLLINS: Do you intend to install this in all effluent release points in your CANDU reactors?

KABAT: Carbon-14 purification is being considered for reactor systems in which a major quantity of ^{14}C is generated, i.e. moderator cover gas and some annulus gas systems in CANDU reactors.

COLLINS: Is AECL doing anything about establishing limits for ^{14}C in reactor effluent?

KABAT: The work on establishing ^{14}C release limits is in progress in the Health Physics and the Radiation Monitoring and Environmental Protection Departments of Ontario Hydro.

HAAG: My question is directed toward the role of relative humidity with respect to CO_2 fixation and the effect of pressure drop problems when scaling up.

KABAT: A detailed explanation has been given in this paper of the negligible humidity effect on CO_2 fixation by $\text{Ca}(\text{OH})_2$ at temperatures up to 450°C . Moderately large mesh absorbent can be used in scaling up the absorbent bed to reduce pressure drop. It can be assumed from the results of comparing 20-40 mesh with 10-20 mesh that no significant loss in efficiency will result from increasing the absorbent particle size.

15th DOE NUCLEAR AIR CLEANING CONFERENCE

ON THE CATALYTIC REMOVAL OF OZONE PRODUCED IN RADIOACTIVE MEDIA

R.-D. Penzhorn, K. Günther and P. Schuster

Kernforschungszentrum Karlsruhe, Institut für Radiochemie,
7500 Karlsruhe, Postfach 3640, Federal Republic of Germany

Abstract

Eighteen materials and catalysts were tested for their catalytic efficiency in decomposing ozone. The best results at 80°C and linear flow velocities of O₂/O₃ mixtures between 0 and 0.9 (m/s) were obtained with catalysts containing silver or palladium. Catalysts containing platinum proved to be particularly inactive. A Ag on Al₂O₃ catalyst removed ozone with 100 % efficiency from a 700 l/h gas stream carrying approx. 35 g O₃/l even at temperatures as low as -80°C. For several catalysts a further decrease in temperature, i.e.: below -60°C, was accompanied by an increase in the rate of ozone removal. The highest efficiency at cryogenic temperatures was obtained with a silver catalyst.

From a systematic investigation of the inhibiting effect of nitrogen oxides on the catalytic ozone destruction, it was concluded that catalysts containing palladium are most resistant to N_xO_y poisoning.

Ozone and oxygen can be eliminated simultaneously, down to the ppm range, from a process gas with a previously reduced copper catalyst. For this purpose Al₂O₃ is a better metal carrier than SiO₂, the specific area providing a good criterion for catalyst selection. N_xO_y poisoning of Cu catalysts is reversible and comparatively insignificant.

I Introduction

Beams of fast electrons as well as powerfull γ -sources in air are known to generate ozone and nitrogen oxides in quantities that may represent health hazards 1/. Explosions have often resulted from experiments that involve the irradiation of liquid air or liquid nitrogen containing oxygen as an impurity. The usual cause of an explosion in a closed system is the evaporation of nitrogen which permits the accumulation of ozone, oxygen and oxides of nitrogen due to differences in their boiling points. In open systems oxygen accumulates in liquid nitrogen due to lique-

15th DOE NUCLEAR AIR CLEANING CONFERENCE

faction of oxygen from the air 2,3/. Very high concentrations of ozone were also reported during cryogenic recovery and purification of fission noble gases 4/.

The G values for ozone formation from oxygen have been widely investigated. They varie from 2-5 at 4 K in the solid phase 5/, 6-12 at 77 K in the liquid phase 5-8/ and 7-17 at room temperature in the gas phase 6,8,9/, depending mainly upon the total dose and dose rate 9/. To account for the dependancy on the dose rate, a detailed mechanism has been proposed that is based on reactions of ionic and neutral oxygen species 6/. The ozone yields in mixtures of oxygen with N₂ or noble gases, in which most of the energy is absorbed by the diluents, are considerably higher than those expected from a mechanism involving only oxygen species. This observation is particularly true at high oxygen dilutions. Obviously, radiation induced excited and ionic species of the diluents are formed which in turn are capable of generating, via energy transfer reactions, ozon precursors such as O₂⁺ and O.

From spark initiated measurments of explosion limits it has been found that, at room temperature and pressure, concentrations below 9-12 mol % O₃ in O₂ are not explosive 10-14/. These values increase to 14.3 and 35 mol % ozone at 200 and 100 K respectively and decrease to 8.8 mol % O₃ when argon is used instead of O₂ 14,15/. Out of safety considerations the ozone concentration should however be kept well below these limits, because of the unknown effects of chemical explosion inciting agents like for instance N₂O₅, Cl₂, H₂O₂, unsaturated hydrocarbons, etc. 16,17/. It is in this context that we examined the catalytic decomposition of ozone over a variety of catalysts and experimental parameters.

II Catalytic ozone decomposition at or above room temperature

After preliminary tests on the ozone destruction efficiency with a variety of catalysts, a selection of the more promising was investigated in greater detail. These catalysts, whose characteristics have been summarized in Table 1, were either directly purchased from the manufactors or kindly made on request by the indicated firms.

Several conventional stainless steel gas flow apparatuses were build to carry out the experiments. Depending upon the desired concentration, the ozon was generated, either with a Fischer Model 504 (max. 1 m³/h and 35 g O₃/h) or a Model 501 (max. 0.1 m³/h and 3 g O₃/h) silent discharge ozon generator. Ozon analysis was carried out directly in the gas flow - before and after the catalyst bed - either by UV absorpction with a Cary 15 spectrophotometer or with a home made chemiluminiscence

Tab. 1: Characteristics of investigated catalysts.

Identification code	Origin	Support material	Active metal	Surface area (m^2/g)		Pellet dimension \emptyset x length (mm)
				new	after treatment with O_3	
AG-RKO-1	Merck	none	Ag	---	---	0.06 wire
AG-MKO-12	Heraeus	Al_2O_3	Ag	99.8	98.3	3.2 x 3.4
PD-MKO-4	Fluka	Asbest	Pd	10.2	n.d.	fibers
PD-MKO-9	Degussa	Al_2O_3	Pd	263	268.9	3.7 - 2.8*
PD-RKO-11	Fluka	none	Pd	---	---	sponge
MO-MKO-7	Degussa	none	Metalloxides	114.9	n.d.	3.8 x ~ 4.3
PT-MKO-8	Heraeus	Al_2O_3	Pt	114	112	3.2 x 3.4
CU-MKO-3	Merck	none	Cu	---	---	wire
BTS	Fluka	Al_2O_3	Cu	202	113	4.3 x 1.0
R-3-11	BASF	Al_2O_3	Cu	181.6	108.2	4.8 x 2.8
Actimet-13	Doduco	Al_2O_3	Cu	56.0	65.3	5.0 x 5.1
Cu MKO-30	Degussa	SiO_2	Cu	258.1	n.d.	irregular \approx 4

* spheres

n.d. = not determined

15th DOE NUCLEAR AIR CLEANING CONFERENCE

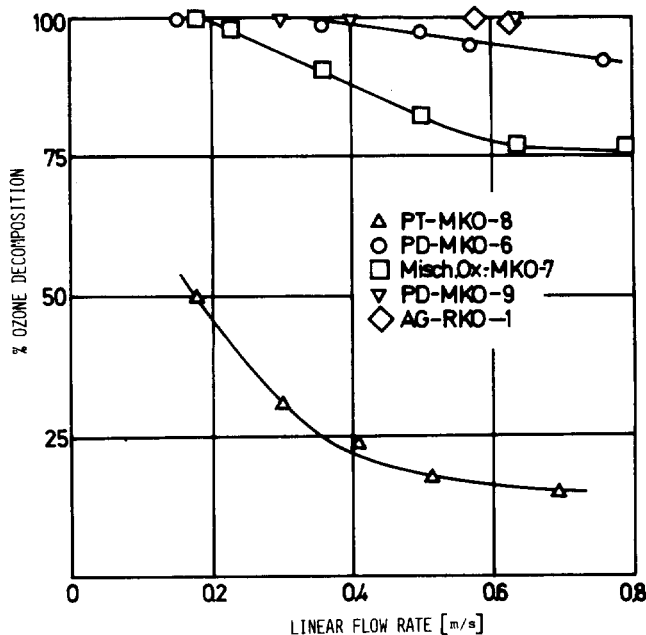
detector coupled via a 4-way valve and a sample loop to the gas stream. The determination of oxygen was accomplished with a Magnos 2T as well as with a D5/2000 Simec oxygen analyser. By using reactors of several dimensions - all provided with numerous thermocouples, a cooling mantle and T01 mini heating lines - it was possible to vary the flow dynamics within a wide range.

The efficiency of ozone removal with 2 g of various catalysts at 80°C as a function of the linear flow velocity (0-0.9 (m/s)) of a oxygen gas stream containing 22.3 g O₃/l is shown in Fig. 1.

It is seen that catalysts having Ag or Pd as the active metal are much more efficient than those having Pt.

Silver can be employed either as a film on a long glass spiral (silver mirror), as a wire (AG-MKO-1) or on a support material such as Al₂O₃ (AG-MKO-12). The first two are convenient when high stream velocities are required. The catalytic nature of the ozone destruction on silver is apparent from the fact that 1.15 mol ozone were decomposed on 9·10⁻² mol Ag at room temperature without significant loss in efficiency. Confirming the earlier observation of Schwab and Hartmann 18/ that the oxides of silver are at least as effective as the pure metal, we also observe that after an initial induction period a black oxide is formed (Ag₂O and or AgO) that in turn exhibits strong catalytic activity. From several runs at 25 and 80°C on 0.7-8.4 g AG-MKO-1 and linear flow velocities up to 0.9 (m/s) it could be shown that the min. weight m_{Ag} in (g) of catalyst that is necessary to destroy 100 % of the ozone can be estimated from the following relationship

$$f = \frac{k \cdot v}{m_{Ag}}$$



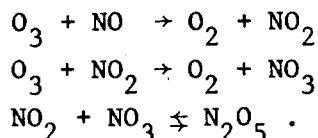
OZONE DECOMPOSITION AS A FUNCTION OF FLOW RATE.

Fig. 1

where v is the flow rate in (l/h) and k is a proportionality constant having values of 2.6 ± 0.9 and 1.4 ± 0.4 (g·h/l) at 25 and 80°C respectively.

III Catalyst poisoning by nitrogen oxides

Since nitrogen oxides are usually formed together with ozone during the radiolysis of N_2-O_2 mixtures, the inhibiting effect of N_xO_y on the catalytic ozone destruction was more closely examined. The N_xO_y partial pressure was determined by ozone titration. In excess ozone the following reactions can take place

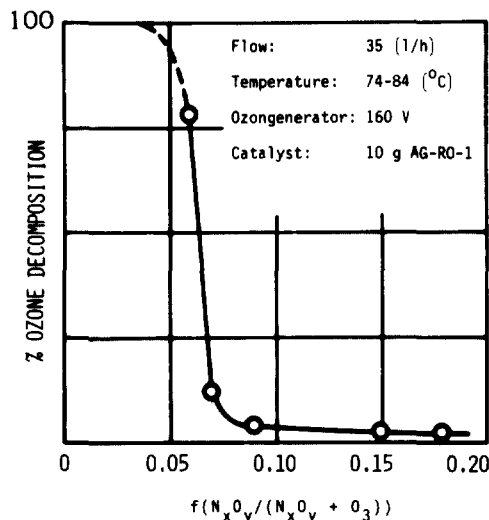


In view that neither NO nor NO_2 could be detected by Second Derivative UV-Spectroscopy in the gas stream we conclude that nitrogen pentoxide is the only nitrogen species present. The results of the effect of the fraction

$$f = \frac{N_2O_5}{N_2O_5 + O_3}$$

on the ozone breakdown efficiency of the AG-MKO-1 catalyst are shown in Fig. 2.

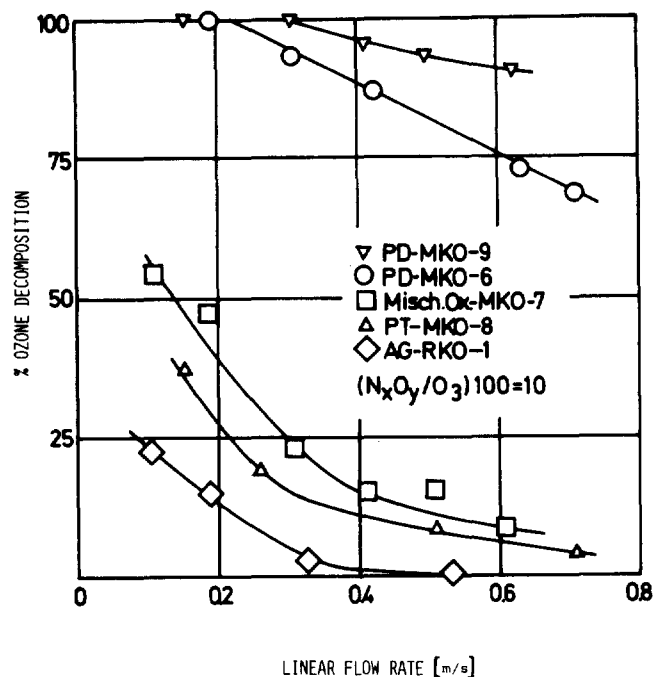
Relatively low partial pressures of N_xO_y ($f \cong 0.09$) are sufficient to stop the catalytic activity. It was observed however that whereas the AG-MKO-1 catalyst is irreversibly poisoned at 20°C, it completely recovers at 80°C. A systematic investigation on the influence of the linear flow velocity (0-0.7 m/s) on the heterogeneous O_3 decomposition efficiency at 80°C and $f = 0.05$ showed that all the tested catalysts are sensitive to the presence of N_xO_y , the least affected being those



CATALYST POISONING BY N_xO_y .

Fig. 2

containing Pd (see Fig. 3).



OZONE DECOMPOSITION AS A FUNCTION OF FLOW RATE AND N_xO_y

Fig. 3

IV Activation energies

The temperature dependency of the percent ozone decomposition on several catalysts in the temperature range from -70 up to 80°C is shown in Fig. 4. In this temperature range the thermal contribution to the ozone decomposition rate is negligible. As expected, most catalyst show a low temperature activity limit, the limit (as opposed to the activation energy) being strongly dependent upon the structure of the catalyst. Only the PD-MKO-9 catalyst seemed to reach a plateau value of 10 % at $T < -50^\circ\text{C}$.

Since the rate of ozone decomposition over the catalysts AG-MKO-1, AG-MKO-12, BTS, PT-MKO-8 and PD-MKO-9 was found to be, at several temperatures, directly proportional to the ozone partial pressure in the gas stream it is concluded that the overall kinetics is first order, i.e.:

$$-\frac{d O_3}{dt} = k \cdot O_3 \quad (I)$$

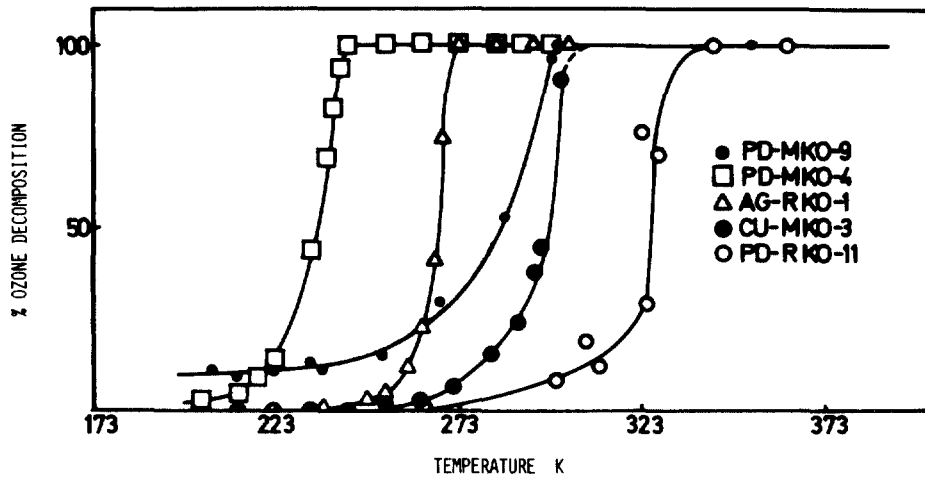
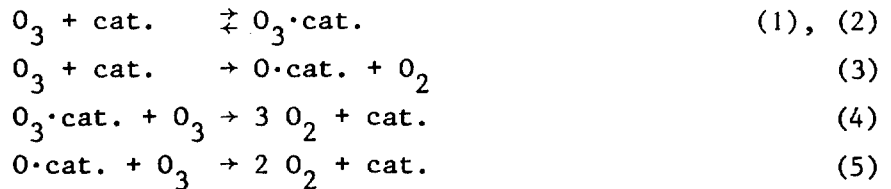


Fig. 4 OZONE DECOMPOSITION ON VARIOUS CATALYSTS AS A FUNCTION OF TEMPERATURE

Fig. 4

The following reaction mechanism adequately describes the catalytic ozone removal



From steady state considerations the rate equation

$$- \frac{d \text{O}_3}{dt} = 2 k_1 \cdot \text{O}_3 \left(1 - \frac{k_2}{k_2 + k_3 + k_4 \cdot \text{O}_3} \right) \quad (II)$$

can be derived. At low ozone partial pressures $k_2 + k_3 \gg k_4 \cdot \text{O}_3$ and equation (II) reduces to

$$- \frac{d \text{O}_3}{dt} \approx 2 k_2 \left(1 - \frac{k_2}{k_2 + k_3} \right) \cdot \text{O}_3 \quad (III)$$

in accordance with the experimentally observed reaction order. Arrhenius plots for the AG-MKO-1, AG-MKO-12, PD-MKO-9 catalysts in the temperature range 280-370 K yielded good straight lines. The estimated overall activation energies have been compiled in Tab. 2 together with some values found in the literature.

15th DOE NUCLEAR AIR CLEANING CONFERENCE

Tab. 2: Activation energies

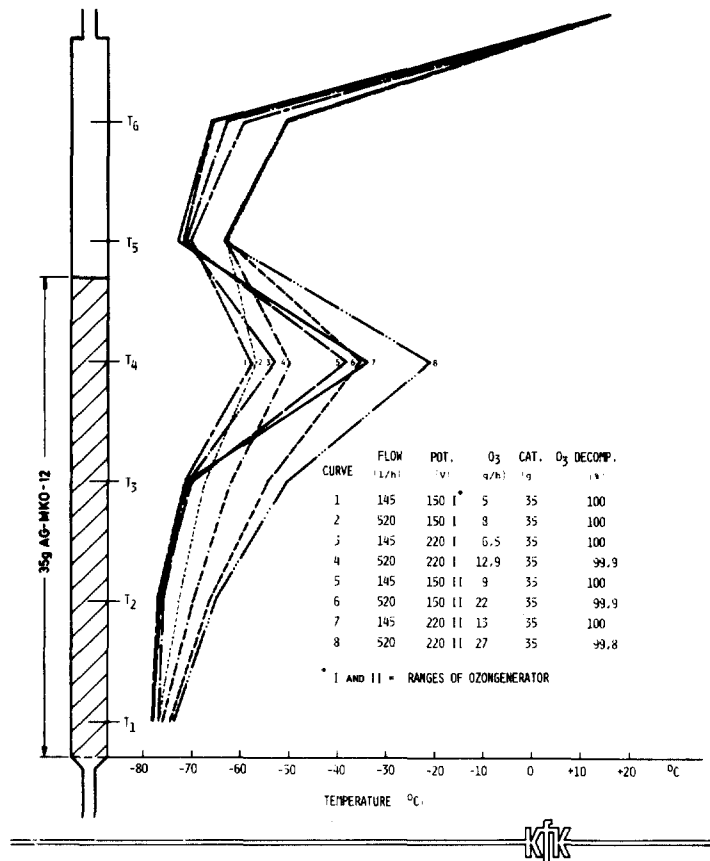
Catalyst	Temp. range (K)	Apparent ΔE (kcal/mol)	Reference
Pt black	77.4 - 90	0.5	20
	77.4 - 90	1.0	19
	310 - 380	3.8	18
PT-MKO-8	280 - 370	4.4 ⁺	this work
	210 - 260	0	this work
Pd black	77.4 - 90	active, n.d.	20
PD-MKO-9	280 - 330	4.7	this work
	225 - 250	0	this work
Ag black	77.4 - 90	active, n.d.	20
AG-MKO-1	280 - 370	1.1	this work
AG-MKO-12	280 - 370	1.6	this work
Ag O	290 - 360	2.2	18
Cu ₂ O	>353	active	
Cu, CuO	77.4 - 90	inactive	20
CuO	290 - 370	2.2	18
BTS	280 - 330	3.8	this work
	210 - 250	0	this work

V Ozone decomposition at cryogenic temperatures

In view that frequently high level irradiation experiments are carried out at cryogenic temperatures and that there the explosion danger is greatest, it seemed of interest to examine the catalytic ozone decomposition at low temperature. To avoid the danger of ozone accumulation, temperatures below -135°C were avoided in these experiments⁺. Several catalysts, i.e.: PD-MKO-9, AG-MKO-12 and PT-MKO-8 efficiently decomposed ozone at these temperatures. Fig. 5 shows the temperature profil, due to the exothermicity of the O₃ decomposition, within a AG-MKO-12 catalyst bed when up

⁺ The O₃/O₂ phase diagram at 1 atm. indicates that a gaseous mixture containing 3 mol % will coexist at -145°C with a 98 % ozone liquid phase 21,22/.

to 27 g O₃/h at a flow rate of up to 0.5 m³/h are passed over 35 g of pellets at -80°C. The effluent gas contains no ozone and reaches a temperature that is lower than that of the feed gas. The other catalysts showed similar profiles, also when cooling to much lower temperatures i.e.: -135°C. Surprisingly, with the exception of the AG-MKO-12 catalyst (not jet measured), the reaction rate increases at temperatures below -60°C with decreasing temperature. Apparently, whereas at cryogenic temperatures van der Waals adsorption requiring practically no activation energy predominates, at the higher temperatures chemisorption involving a definite activation energy is primarily responsible for the catalytic activity. In accordance with this assumption the k-T data could be fitted with an equation of the form



CATALYTIC DECOMPOSITION OF OZONE AT LOW TEMPERATURES.

Fig. 5

with this assumption the k-T data could be fitted with an equation of the form

$$k = \frac{A}{T} e^{-\Delta E' / RT} \tag{1V}$$

where ΔE' equals ΔE and 0 (kcal/mol) (see Tab. II) at temperatures above and below ~ -60°C respectively.

VI Oxygen and Ozone removal

In some applications it is of interest to remove simultaneously ozone and oxygen. An area of concern is for instance the enhancement of alkali metal corrosion by O₃/O₂ during long term storage of Kr-85.

From the literature it is well known that reduced copper catalysts remove O₂ from a process gas down to the ppm range. The oxygen absorption capacity M_{O₂} in STP l/kg varies linearly with the residence time s according to

15th DOE NUCLEAR AIR CLEANING CONFERENCE

$$M_{O_2} = A + B \cdot s \quad (5)$$

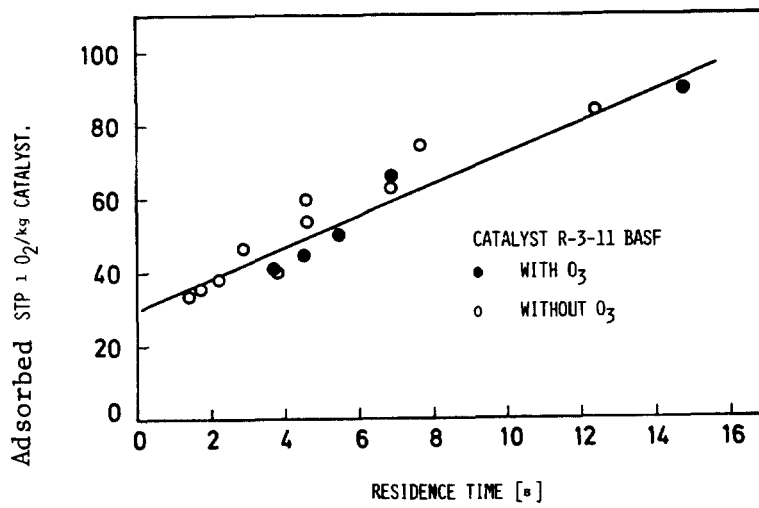
where A and B are catalyst specific constants having units of (1/kg·sec) and (1/kg) respectively (Fig. 6 shows data obtained with 50-150 g catalyst).

The results shown in Table 3, were obtained at 250°C, using input flow rates between 0.08 and 0.5 m³/h, a 26.3 % O₂ in He feed gas and 0.05-0.15 kg of catalyst. The various investigated Cu catalysts were in their reduced form, obtained by passing CO over the catalyst bed at 150°C until the gas chromatographically measured CO₂/CO peak ratio in the effluent gas dropped to zero. From Table 3 it is apparent that Al₂O₃ is a better catalyst carrier than SiO₂ and that the specific surface area (see also Tab. 1) is directly proportional to A_{S→O}. Thus, for a particular catalyst carrier the specific area provides a good criterion for catalyst selection.

Tab. 3: Comparison of the O₂ absorption capacity of various catalysts

Catalyst	B (1/kg sec)	A (1/kg)
Actimet 13	2.7	10
Degussa	2.6	15
R-3-11	5.9	27
BTS	4.8	33

When the feed gas contained up to 0.4 % O₃ only a slight temperature increase in the catalyst bed was noticed and the same total amount of O₂ was adsorbed (see Fig. 6). No O₃ could be detected by UV absorption in the effluent gas. The presence of up to 5 % NO in the previously described feed gas reduced the amount of adsorbed O₂ by only a few percent. Since furthermore this poisoning is reversible, it is of little concern.



REMOVAL OF O₂ AND O₃.

Fig. 6

15th DOE NUCLEAR AIR CLEANING CONFERENCE

- 1/ M.T. Dmitriev, O.P. Yurasova
Gigiena i Sanitariya 32, 112, (1967)
- 2/ P.T. Perdue
Health Physics 21, 116, (1972)
- 3/ J.D. Gault, K.W. Logan, H.R. Danner
Nuclear Safety, 14, 446, (1973)
- 4/ C.L. Bendixsen, F.O. German, R.R. Hammer
ICP-1023, (1973)
- 5/ D.B. Brown, L.A. Wall
J. Phys. Chem. 65, 915, (1961)
- 6/ C. Willis, A.W. Boyd, M.J. Young, D.A. Armstrong
Can. J. Chem. 48, 1505, (1970)
- 7/ J.F. Riley
ORNL 3488, 42, (1963)
- 8/ M.T. Dimitriev
Zhurnal Prikladnoi Khimii 41, 39, (1968)
- 9/ J.F. Kircher, J.S. McNulty, J.L. McFarling, A. Levy
Rad. Research, 13, 452, (1960)
- 10/ E.H. Riesenfeld
Z. Elektrochemie 29, 119, (1923)
- 11/ H.T. Schumacher
An. Asoc. Quim. Arg. 41, 230, (1953)
- 12/ G.A. Cook, E. Spadinger, A.D. Kiffer, C.V. Klumpp
Ind. Eng. Chem. 48, 736, (1956)
- 13/ G.M. Platz, C.K. Hersh
Ind. Eng. Chem. 48, 742, (1956)
- 14/ V.V. Yastrebov, N.I. Kobozev
Russian J. Phys. Chem. 33, 118, (1959)
- 15/ R.O. Miller
J. Phys. Chem. 63, 1054, (1959)
- 16/ S.W. Benson, A.E. Axworthy
J. Chem. Phys. 26, 1718, (1956)
- 17/ J.E. Douglas, L.C. Bratt, E.M. Kinderman
J. Chem. Phys. 31, 1416, (1959)
- 18/ G.M. Schwab, G. Hartmann
Z. Phys. Chem. (Neue Folge) 6, 72, (1956)
- 19/ G.J. Emel'yanova, V.P. Lebedev, N.I. Kobozev
Kataliticheskie reakcii v zhidkoi faze Trudy Vsesoyvznoi konferentsii, Alma-Ata
(1962)

15th DOE NUCLEAR AIR CLEANING CONFERENCE

20/ G.J. Emel'yanova, V.P. Lebedev, N.I. Kobozev
Vestnik Moskovskogo Universiteta, ser II, khimiya 4, 31, (1961)

21/ A.C. Jenkins, F.S. DiPaolo, C.M. Birdsall
J. Chem. Phys. 23, 2049, (1955)

22/ C. Brown, A.W. Berger, C.K. Hersh
J. Chem. Phys. 23, 1340, (1955)

DISCUSSION

CHENG: It has been known for quite some time that commercially available synthetic zeolites, such as molecular sieve 10X, can serve effectively as a catalyst for ozone destruction. Do you have any comment on that?

PENZHORN: Although I am aware that zeolites have been reported to be good catalysts, we have not investigated them so far. Our present work has been limited to metal-based catalysts.

VON AMMON: Catalysts which are active for the decomposition of ozone at the low temperatures you mentioned have a tremendous potential for application in a cryogenic krypton separation system for the offgases from reprocessing plants. It is not possible to imagine such a system without ozone formation because O₂ will always be present, even in case of O₂ separation prior to the cryogenic part. Traces of O₂ in the ppm-range will always pass the reduction catalyst during normal operation (not to speak of malfunctions). The question, whether or not such a step is necessary, cannot be answered conclusively at the moment. I wonder if some of the catalysts are active enough to be used in the liquid phase of a Kr-Xe mixture (at 180-200 K, or so) in a cryogenic column? In this case, evaporation of the gas mixture for the ozone decomposition could be avoided.

PENZHORN: Our results indicate that ozone can be destroyed efficiently even at temperatures as low as 130 K. In our experiments we have observed that at this temperature the gas flow suddenly becomes highly unsteady. From the ozone-oxygen phase diagram, we know that at temperatures in the region of 130 K a liquid, whose composition is almost 100% ozone, will condense. Since in these experiments no ozone could be detected in the effluent gas--a sign of 100% ozone decomposition--I believe that there are good chances for the catalytic removal of ozone from Kr/Xe/O₂/O₃ liquid mixtures at the temperatures you mention.

BRUGGEMAN: Considering an integrated dissolver offgas purification system, would it be necessary to remove nitrogen oxides and oxygen before the cryogenic separation of the noble gases, or would it be sufficient to remove only the nitrogen oxides in combination with catalytic ozone removal anywhere in the cryogenic installation?

PENZHORN: This question goes somewhat beyond the scope of my talk and would perhaps be better asked again this afternoon during the presentation of Dr. v. Ammon. However, it certainly is the aim of our work to develop a process whereby ozone can be continuously eliminated from cryogenic liquids. If this can be demonstrated successfully, your alternative process becomes more feasible.

15th DOE NUCLEAR AIR CLEANING CONFERENCE

SESSION IV

CONTAINMENT OF ACCIDENTAL RELEASES

Tuesday, August 8, 1978
CHAIRMAN: J. T. Collins

DEMONSTRATION OF AN EMERGENCY CONTAINMENT SYSTEM

T. M. Flanagan, M. L. Rogers,
W. R. Wilkes

STUDY OF THE CONTAINMENT SYSTEM OF THE PLANNED SNR-2 FAST BREEDER REACTOR

H. Bunz, U. Scholle

FISSION 2120: A PROGRAM FOR ASSESSING THE NEED FOR ENGINEERED SAFETY FEATURE GRADE
AIR CLEANING SYSTEMS IN POST-ACCIDENT ENVIRONMENTS

G. Martin, Jr., D. Michlewicz,
J. Thomas

IMPACT OF SOPHISTICATED FOG SPRAY MODELS ON ACCIDENT ANALYSES

S. P. Roblyer, P. C. Owzarski

15th DOE NUCLEAR AIR CLEANING CONFERENCE

DEMONSTRATION OF AN EMERGENCY CONTAINMENT SYSTEM

T. M. Flanagan, M. L. Rogers and W. R. Wilkes

Monsanto Research Corporation
Mound Facility*
Miamisburg, Ohio

Abstract

A system called an Emergency Containment System (ECS) to be used for tertiary containment of tritium was reported at the 13th Air Cleaning Conference. This system was part of the Tritium Effluent Control Laboratory then under construction at Mound Facility. A series of experiments has recently been conducted to evaluate the performance of an ECS in capturing tritium accidentally released into an operating laboratory.

The ECS is an automatically actuated laboratory air detritiation system utilizing a catalytic oxidation reactor and presaturated oxide adsorption/exchange columns. In the event of an accidental release of tritium into the laboratory, the ECS is automatically activated, and quick-acting pneumatic dampers divert the laboratory air supply and exhaust through the ECS until room concentrations are returned to safe operating levels.

The experiments involved the release of elemental tritium into a 560 m³ laboratory. Concentrations, which initially were in excess of 5000 $\mu\text{Ci}/\text{m}^3$, were reduced to less than 5 $\mu\text{Ci}/\text{m}^3$ in about two hours. During the experiments, data were obtained on the buildup of tritium oxide in the laboratory air, and swipes were taken on several surfaces to determine tritium deposition.

The results of the experiments have shown that a tertiary containment of tritium is feasible. In the event of a catastrophic accident, the ECS is capable of preventing the release of a large quantity of tritium to the environment.

Introduction

Mound Facility began a Tritium Effluent Control Technology Project in January 1972. A goal of this project was to develop and demonstrate technology and equipment to maintain tritium emissions to the atmosphere below 10% of the Radiation Concentration Guide (RCG) levels. Kershner et al. (1) described the "Tritium Effluent Control Laboratory" at the 13th AEC Air Cleaning Conference. A major part of this program was to develop and demonstrate a tritium containment system capable of preventing tritium from reaching the biosphere in the event tritium is released into a typical laboratory.

*Mound Facility is operated by Monsanto Research Corporation for the U. S. Department of Energy under Contract No. EY-76-C-04-0053.

15th DOE NUCLEAR AIR CLEANING CONFERENCE

Since 1973 accidents at major nuclear installations in the United States have resulted in excess of one-half (2-4) million curies of tritium reaching the environment. In each case it was determined that the impact on the general public and the environment did not exceed appropriate guidelines (2-4). But the increased emphasis on radioactive emissions and the tightening of regulations indicate that similar incidents in the future may be both politically and legally unacceptable.

An indication of the extent to which standards can be raised is evident in the U. S. EPA Interim Primary Drinking Water Regulations (5). The EPA reduced the acceptable level in drinking water from 3 $\mu\text{Ci/liter}$ to 0.02 $\mu\text{Ci/liter}$ or a reduction of 150 times.

The EPA has also established total quantity limits on specific radionuclides associated with the uranium fuel cycle (6). In the Final Environmental Statement for 40 CFR 190, the EPA states "Similarly, as knowledge becomes available concerning the capability of technology to limit environmental releases of tritium and carbon-14, the appropriate levels of these radionuclides will be carefully considered by the Agency."

The national effort to develop fusion as an alternative energy supply will result in megacurie quantities of tritium being handled. The Tritium Systems Test Assembly at Los Alamos Scientific Laboratory and the Tokamak Fusion Test Reactor at Princeton (7-8) have incorporated large-scale tritium containment systems. Mound Facility has completed conceptual design of a similar emergency containment system, as described in this paper, for its major tritium facility.

System Design

The Emergency Containment System (ECS) is an automatically actuated, room air detritiation system utilizing a catalytic oxidation reactor and presaturated oxide adsorption/exchange columns. In the event of an accidental release of tritium to the laboratory, the ECS is automatically activated and the quick-acting pneumatic dampers divert the room air supply and exhaust through the ECS until the tritium concentration in the room air is returned to a safe operating level. The air stream is heated to a temperature of 175°C before it enters the catalyst to meet the design goal of 99.9% oxidation of tritium in air at inlet concentrations of 0.5 ppm. The air is cooled to near 20°C before entering the adsorption columns. The oxidized tritium is captured and contained on the adsorption columns in the oxide form. The ECS is designed to provide the oxidation and adsorption capacities for a single pass decontamination factor of 1000:1 in a 0.66 m^3/s air flow containing as high as 1 Ci/m^3 tritium and 0.5 ppm natural hydrogen background. The adsorber section of the ECS consists of two stainless steel vessels containing 1730 kg of Alcoa alumina H151 adsorbent, saturated at 100% relative humidity. These vessels were sized to provide 10 hr of operation with an inlet activity of 1 Ci/m^3 before a defined breakthrough of 100 $\mu\text{Ci}/\text{m}^3$ occurs. A Spencer turbine controls gas flow for the ECS.

15th DOE NUCLEAR AIR CLEANING CONFERENCE

Experiment Design

The efficiency of the ECS to capture tritium released into an operating area was evaluated by releasing three elemental tritium samples into the laboratory. The automatic start-up of the ECS was controlled by a 20-liter ionization chamber monitoring the laboratory. The exhaust from the area was also monitored by a 20-liter ionization chamber. Bubbler-type tritium monitors containing ethylene glycol (9) sampled the laboratory exhaust, the area adjacent to the exterior doors, and the supply to the room coming from the ECS adsorber beds. These monitors provided data on the quantity of tritium oxide at the various sampling locations. Fifteen 100-cm² areas at various locations throughout the laboratory were marked off to determine tritium deposition on laboratory surfaces. Tritium deposition was determined after the tritium release by wiping the areas with dry Metrical filter paper. The wipes were counted by liquid scintillation counting.

After each experiment the adsorber bed used was regenerated by purging it with an air stream heated to 100°C. An ethylene glycol bubbler monitor sampled the effluent air stream to determine the quantity of tritium captured on the bed.

First Experiment

In the first experiment 0.87 Ci of elemental tritium was released with 20 cm³ of hydrogen. The container was flushed with a nitrogen purge to ensure that all the tritium and hydrogen were released. The 20 cm³ of hydrogen increased the hydrogen concentration to approximately 0.03 ppm above the natural abundance of 0.5 ppm. The hydrogen release simulated an accident where the average room concentration would be 0.1 Ci/m³ or 10% of the design criteria of 1 Ci/m³.

Figure 1 is a plot of the tritium concentration in the laboratory resulting from the first experiment. It required 70 min for the laboratory tritium concentration to return to less than 5 μCi/m³. The ECS was automatically activated approximately 10 sec after the sample was released. The air stream was at the design temperature of 175°C after 10 min. Figure 2 shows the effluent levels during the experiment. During the first 2 min of the experiment 0.08 Ci was released to the environment. This release is attributed to tritium that escaped before the dampers closed. The 2 min required for the monitoring system to respond to the tritium release in the first 10 s is attributed to the travel time from the dampers to the monitoring probe which sampled the room exhaust. A large filter-bank between the dampers and the probe is effectively a holding tank which increases the time of travel.

In addition to the 0.08 Ci which escaped before the dampers closed, 0.28 Ci was released which is attributed to leakage through the dampers. The dampers used are fast-acting, conventional ventilation dampers with an estimated leakage rate of 10% per hour. The total quantity lost to the exhaust system was 0.36 Ci or 41% of the quantity released. These data show the importance of fast-acting low-leakage dampers located far enough downstream to accommodate the time required to activate the system.

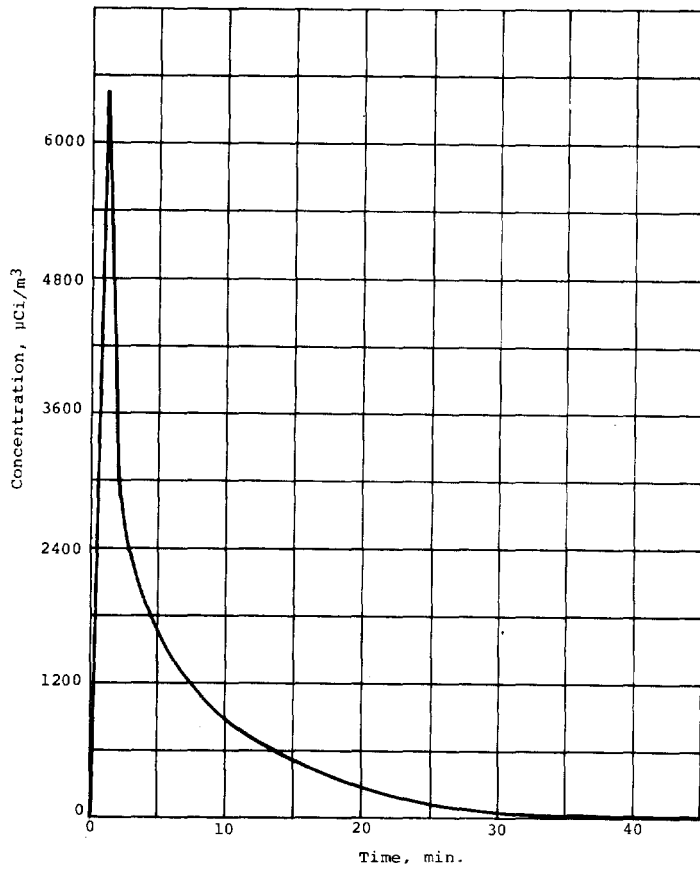
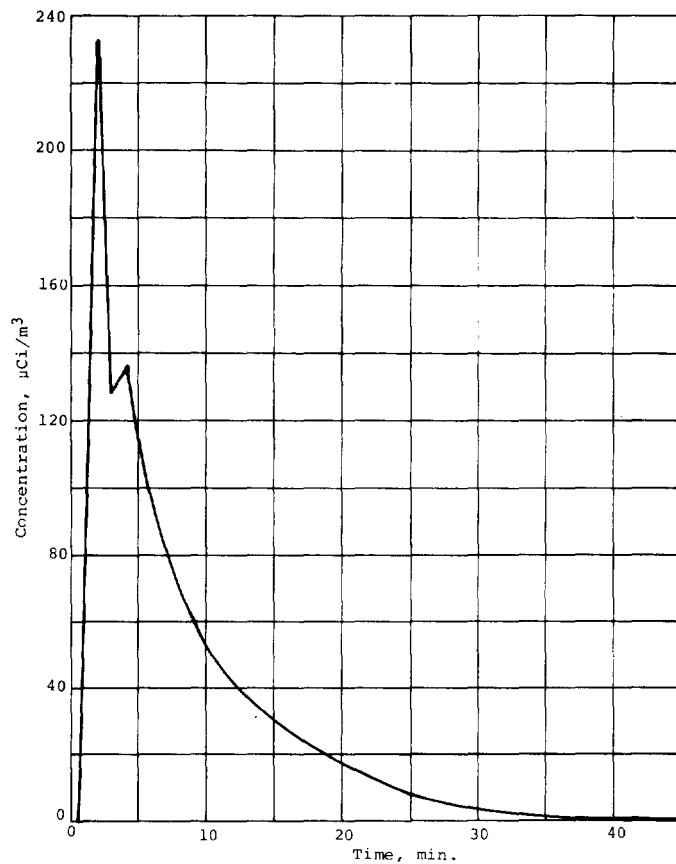


FIGURE 1

ECS EXPERIMENT 1; LABORATORY
CONCENTRATION AS A FUNCTION
OF TIME

FIGURE 2

ECS EXPERIMENT 1; EXHAUST
SYSTEM CONCENTRATION AS A
FUNCTION OF TIME



15th DOE NUCLEAR AIR CLEANING CONFERENCE

The tritium oxide concentration in the laboratory increased during the experiment to $2.9 \mu\text{Ci}/\text{m}^3$ or 60% of the Radiation Concentration Guide. The tritium oxide concentration measured just outside the laboratory doorways was less than $7 \times 10^{-3} \mu\text{Ci}/\text{m}^3$. This indicates that the doors, which have refrigeration gasketing and metal door sweeps, were effective in preventing tritium leakage. Sampling the exhaust leaving the adsorber bed indicated that 0.006 Ci of tritium oxide was returned to the laboratory by the ECS.

Examination of individual samples taken from the adsorber bed exhaust showed the data did not follow the pattern predicted by a breakthrough phenomenon, i.e., concentration increase as a function of time. Instead, the data showed that the outlet concentration was dependent on the inlet concentration, indicating that the tritium oxide recycled into the laboratory was not the result of breakthrough but channeling through the bed. After the experiment, the bed was regenerated by first flowing 100°C dry air through the bed to remove the tritium oxide and then passing saturated air at 20°C through the bed. At this temperature, approximately 95% of the tritium should be removed by the drying step. Sampling of the bed exhaust during regeneration indicated that 0.37 Ci or 42% of the quantity released had been captured on the bed. For this experiment 88% of the original 0.87 Ci release could be accounted for. Tritium deposition on laboratory surfaces is shown in Table 1.

Table 1. Tritium deposition on Laboratory surfaces (Experiment 1).

<u>Surface</u>	<u>Tritium Deposited (dis/min/100 cm²)</u>
Iron	Nondetectable
Sheet Metal	Nondetectable
Plexiglas	Nondetectable
Glass	Nondetectable
Bench Top	Nondetectable
Glass	Nondetectable
Desk	9
Bench Top	Nondetectable
Sheet Metal	Nondetectable
Glass	5
Wood	Nondetectable
Tile	2
Tile	Nondetectable
Desk Top	Nondetectable
Tile	Nondetectable

Second Experiment

In the second experiment 0.86 Ci of elemental tritium was released followed by five liters of hydrogen (diluted with nitrogen to maintain a hydrogen concentration below 50% of the lower explosive limit). The five liters of hydrogen released into the 560 m³ room raised the hydrogen concentration to approximately 10 ppm, equivalent to a tritium concentration of ~30 Ci/m³ or 30 times design criteria. To determine the impact of not heating the air stream to 175°C the preheater was shut off. The only heat supplied to the system was the heat of compression of the turbine blower. The air stream reached a temperature of 80°C from the heat of compression. Figures 3 and 4 show the laboratory concentration and the effluent concentration during Experiment 2. The ECS was automatically activated approximately 20 s after the release.

During the first 3 min 0.15 Ci was released. An additional 0.39 Ci was released during the remaining time. The total tritium lost to the exhaust system was 0.54 Ci or 61% of the quantity released. Tritium oxide concentration in the laboratory averaged 3.5 μCi/m³. The total tritium oxide recycled into the laboratory was 0.007 Ci. The concentration data again appeared to be a function of inlet concentration and not that associated with breakthrough. The total quantity of tritium oxide released through the exhaust system was 0.024 Ci or approximately three times that observed being recycled. This experiment required 120 min to reduce the tritium concentration to less than 5 μCi/m³ as compared with the 60-70 min required for the previous experiment.

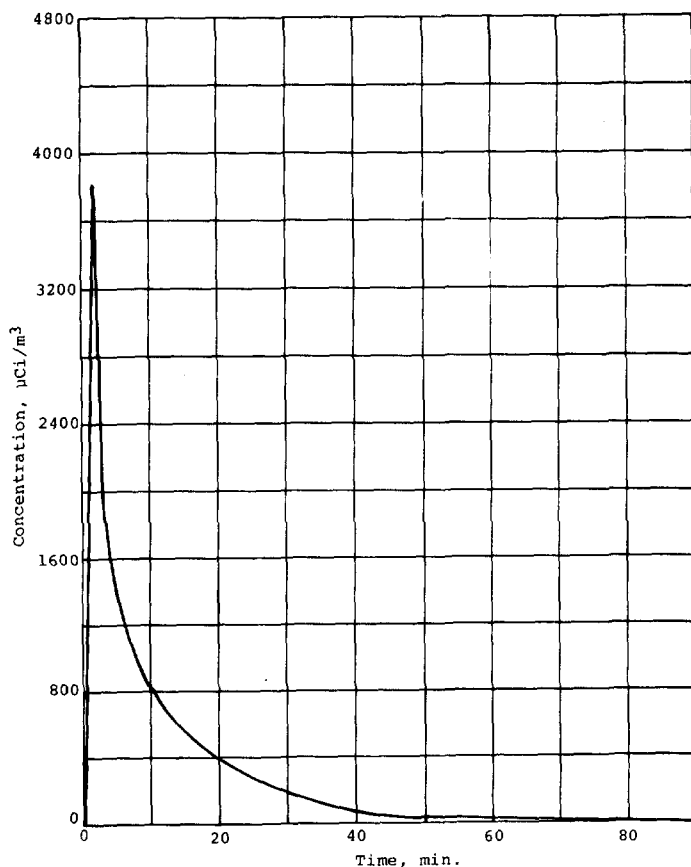


FIGURE 3

ECS EXPERIMENT 2; LABORATORY CONCENTRATION AS A FUNCTION OF TIME.

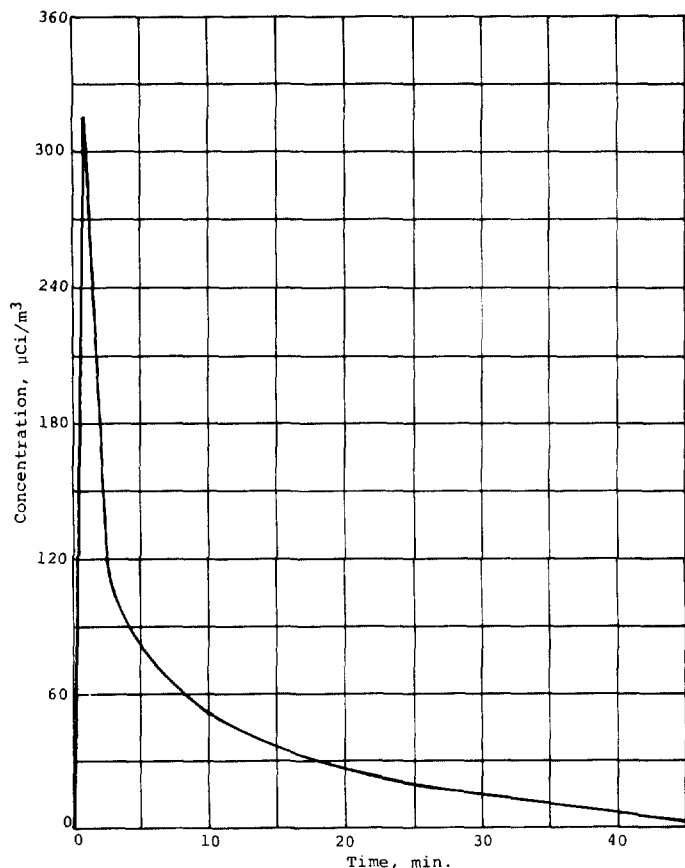


FIGURE 4

ECS EXPERIMENT 2; EXHAUST SYSTEM CONCENTRATION AS A FUNCTION OF TIME.

Table 2 shows the tritium deposition on laboratory surfaces for the second experiment. The deposition on the liquid nitrogen dewar during the second experiment indicates a significant increase in surface contamination on wet or cold surfaces. This is consistent with earlier predictions by Maroni (10). The higher surface contamination after this experiment can be explained by the fact that high airborne concentrations persisted for longer times than in the earlier experiment. Regeneration of the adsorber bed removed 0.61 Ci or 69% of the release. The bed used for this experiment had been contaminated as a result of prior work including Experiment 1. The apparent inventory greater than the release is attributed to this prior work.

Third Experiment

A third experiment was performed to simulate a system in which low leakage dampers would be located at a sufficient distance downstream to prevent any tritium from passing the dampers before they closed. In this experiment 0.88 Ci of elemental tritium was released with no additional hydrogen. Prior to the release, the laboratory supply and exhaust were shut down and weather balloons were inflated inside the exhaust and supply ducts to provide a tight seal. The ECS was manually activated before releasing the tritium to prevent any tritium loss during the time required for the monitoring systems to activate the ECS.

15th DOE NUCLEAR AIR CLEANING CONFERENCE

Table 2. Tritium deposition on laboratory surfaces (Experiment 2).

<u>Surface</u>	<u>Tritium Deposited (dis/min/100 cm²)</u>
Iron	48
Sheet Metal	26
Plexiglas	55
Glass	35
Bench Top	33
Glass	19
Desk	21
Bench Top	84
Sheet Metal	21
Glass	31
Wood	36
Tile	22
Tile	36
Desk Top	21
Tile	
Liquid Nitrogen Dewar	3388
Ice on Liquid Nitrogen Dewar	26704

Figure 5 shows the laboratory concentration of tritium during the third experiment. The tritium concentration was reduced to less than 5 $\mu\text{Ci}/\text{m}^3$ in 120 min. The exhaust monitoring system level increased to 2 $\mu\text{Ci}/\text{m}^3$ after 10 min and returned to background in another 10 min. There was no measurable air flow at the sampling location and, therefore, the total quantity released was insignificant. The average tritium oxide concentration in the laboratory was 0.52 $\mu\text{Ci}/\text{m}^3$ during the experiment. Sampling of the exterior areas showed no detectable concentrations of tritium. The bubbler system monitoring the adsorber bed indicated that a total of 0.005 Ci was recirculated into the laboratory. Table 3 shows the surface contamination levels for the 15 wipe areas. Regeneration of the adsorber bed accounted for 0.59 Ci or 66% of the quantity released.

Data Analysis

The concentration data obtained during the three ECS experiments were used to determine the efficiency and decontamination factor for the ECS. If a well-mixed atmosphere is assumed, the fraction of tritium remaining in the room can be expressed by Equation 1 and the fraction released to the environment can be expressed by Equation 2.

$$T = e^{-(\gamma_L + \epsilon\gamma_R)t} \quad (1)$$

15th DOE NUCLEAR AIR CLEANING CONFERENCE

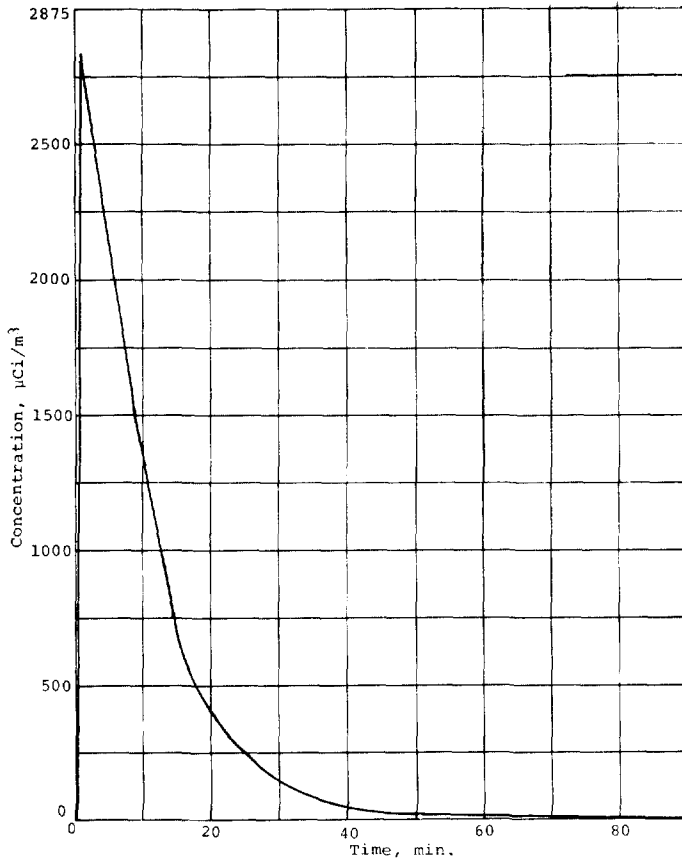


FIGURE 5

ECS EXPERIMENT 3; LABORATORY CONCENTRATION AS A FUNCTION OF TIME.

Table 3. Tritium deposition on laboratory surfaces (Experiment 3).

<u>Surface</u>	<u>Tritium Deposited (dis/min/100 cm²)</u>
Iron	72
Sheet Metal	104
Plexiglas	95
Glass	111
Bench Top	85
Glass	137
Desk	91
Bench Top	97
Sheet Metal	96
Glass	81
Wood	79
Tile	137
Tile	96
Desk Top	103
Tile	105

15th DOE NUCLEAR AIR CLEANING CONFERENCE

$$T' = \frac{\gamma_L}{\gamma_R \epsilon \gamma_L} [1 - e^{-(\gamma_R \epsilon + \gamma_L)t}] \quad (2)$$

where T = the fraction of the tritium initially present that remains in the room after time t.

T' = the fraction of the tritium initially present that is leaked to the environment in time t.

t = time, hr.

γ_R = removal time constant, $\text{hr}^{-1} = 4.2$.

γ_L = leak time constant, hr^{-1} . This is not known directly, but may be determined from the values of T and T'.

ϵ = system tritium removal efficiency. This too must be calculated from T and T'.

The decontamination factor (DF) is defined as the reciprocal of the fraction of tritium initially present which remains uncontained after time t.

$$DF = \frac{1}{T + T'} \quad (3)$$

After 25 min during Experiment 1, the entire area serviced by the ECS was at a uniform concentration of $110 \mu\text{Ci}/\text{m}^3$ as determined by the fact that two air monitors at different parts of the laboratory showed the same concentration. The total quantity of tritium in the 560-m^3 area at that time was 0.06 Ci. The concentration then decreased to 0.009 of the original or $1 \mu\text{Ci}/\text{m}^3$ in 0.75 hr. The quantity released to the effluent during this time period was 0.01 Ci or 0.17% of the initial quantity of tritium in the area.

Substituting these values into Equations (1) and (2), one finds that the calculated efficiency of the ECS is 1.4. An efficiency greater than one is presumably the result of incomplete mixing, i.e., the tritium concentration in the laboratory was not uniform.

The decontamination factor for Experiment 1 was calculated to be 6.

A uniform concentration of $38 \mu\text{Ci}/\text{m}^3$ was assumed after 60 min during Experiment 2. It required 1 hr more to decrease the concentration to $1 \mu\text{Ci}/\text{m}^3$. During this period 0.003 Ci of the 0.021 Ci in the room at the beginning of the period was released to the ventilation system. The calculated efficiency of the ECS system was 0.7. The calculated efficiency of the catalysts at 80°C is 0.9 (11). The decontamination factor during Experiment 2 was determined to be 6.

The equilibrium concentration during the third ECS experiment occurred in 25 min and was $266 \mu\text{Ci}/\text{m}^3$. After 1.6 hr the concentration was $1 \mu\text{Ci}/\text{m}^3$ or 0.003 of the original concentration. No measurable quantity of tritium was released to the ventilation system. The efficiency of the system was determined to be 0.9. The decontamination factor during the 1.6 hr was 333. The decontamination factor for

15th DOE NUCLEAR AIR CLEANING CONFERENCE

the entire 2-hr experiment was 1800. The predicted decontamination factor using the model was 1900. Note here that the decontamination factor increases with time. In Experiments 1 and 2, because of leakage, the decontamination factor approaches a limiting value after long clean-up times.

The third ECS experiment has shown that the ECS will function as designed if low leakage dampers are installed.

Summary

These experiments have shown that the ECS is capable of capturing tritium released into a laboratory before it reaches the biosphere. The ECS is capable of removing tritium at levels that approach natural abundance hydrogen concentration. The importance of low-leakage dampers and their locations were also demonstrated. Experiment 2 showed the ECS will function with only the heat of compression from the blower but with a longer cleanup time. Excessive surface contamination was not observed except on a low-temperature surface. The mathematical model developed for design criteria was shown to be capable of predicting experimental results.

References

1. C. J. Kershner and J. C. Bixel, "Tritium Effluent Control Laboratory," presented at the 13th USAEC Air Cleaning Conference, CONF-740807, San Francisco, California, August 1974.
2. Environmental Monitoring at Major U. S. Energy Research and Development Agency Contractor Sites, ERDA 77-104/2, 1976.
3. Environmental Monitoring at Major U. S. Energy Research and Development Agency Contractor Sites, ERDA-76-74, 1975.
4. Environmental Monitoring at Major U. S. Energy Research and Development Agency Contractor Sites, ERDA-54, 1974.
5. "Interim Primary Drinking Water Regulations," U. S. Environmental Protection Agency, 40 CFR Part 141, 1976.
6. Environmental Radiation Protection Requirements for Normal Operations of Activities in the Uranium Fuel Cycle, Final Environmental Statement, U. S. Environmental Protection Agency, EPA 520/4-76-016, 1976.
7. K. E. Lind et al., "Tritium Handling Systems for TFTR and PITR," Third Topical Meeting on The Technology of Controlled Nuclear Fusion, Santa Fe, New Mexico (May 1978).
8. M. E. Muller, "Conceptual Design of an Emergency Tritium Clean-Up System," Third Topical Meeting on the Technology of Controlled Nuclear Fusion, Santa Fe, New Mexico (May 1978).

15th DOE NUCLEAR AIR CLEANING CONFERENCE

9. W. E. Sheehan, M. L. Curtis and D. C. Carter, "Development of a Low-Cost Versatile Method for Measurement of HTO and HT in Air," presented at the 20th Annual Conference on Bioassay, Environmental and Analytical Chemistry, Cincinnati, OH, September 24-25, 1974, MLM-2205 (Feb. 1975).
10. V. A. Maroni, Private Communication; R. G. Clemmer, et al., "Simulation of Large Scale Air Detritiation Operations by Computer Modeling and Bench-Scale Experimentation," Seventh IEEE Symposium on Engineering Problems of Fusion Research, Knoxville, Tennessee (October 1977).
11. J. C. Bixel and C. J. Kershner, "A Study of Catalytic Oxidation and Oxide Adsorption for the Removal of Tritium from Air," in Proceedings of the Second AEC Environmental Protection Conference, April 16-19, 1974, WASH-1332 (74), Sandia Laboratories, Albuquerque, NM, pp. 261-284, MLM-2140(OP).

15th DOE NUCLEAR AIR CLEANING CONFERENCE

STUDY OF THE CONTAINMENT SYSTEM OF THE PLANNED SNR-2 FAST BREEDER REACTOR

Helmut Bunz

Kernforschungszentrum Karlsruhe GmbH
Laboratory for Aerosol Physics and Filter Technology

Ulrich Scholle
INTERATOM, Bensberg

Abstract

Research is presented concerning the behaviour of four possible containment concepts for the planned Fast Breeder Reactor SNR-2 under the conditions of a HCDA. Detailed descriptions and calculations are given dealing with the acceptable leakages and the filter loads reached. The transport of the aerosol-type as well as the gaseous activity through the different compartments into the environment is calculated and from this the resulting accident doses. To cover the uncertainties of the accident course a wide range of accident parameters is examined.

1. Introduction

Research was carried out to find a containment concept for the planned 1300 MW Fast Breeder Reactor SNR-2. As part of a preliminary study four possible concepts for a more detailed quantitative examination were selected. This paper describes part of the research dealing with the demands made on the containment system after a HCDA (Bethe-Tait-accident). As this accident very probably has the greatest hazard potential, it was considered to be of prime importance in designing the containment system. The primary enclosure will be designed in such a way that a disruption is impossible. Criteria are the requirements concerning the acceptable leakage of the containment enclosures, the ventilation and filter system, accessibility to containment areas after an accident, and radiological effects on the environment. It is impossible to consider these items independent from each other because the necessity to respect the radiological limits in the surrounding environment, for example, has a direct effect upon the required ability of the containment to restrain the activity. In order to do this, first the release factor of each radionuclide was estimated conservatively and then the transfer of the gaseous and the aerosol-type activity through the different compartments was calculated, and by use of these results the effect on the environment.

The calculations concerning the behaviour of the aerosols were made by the code Pardiseko IIIb, whose predecessor was reported about in [1, 2, 3].

2. Containment concepts

The difference between the four containment concepts (fig. 1) lie only in the

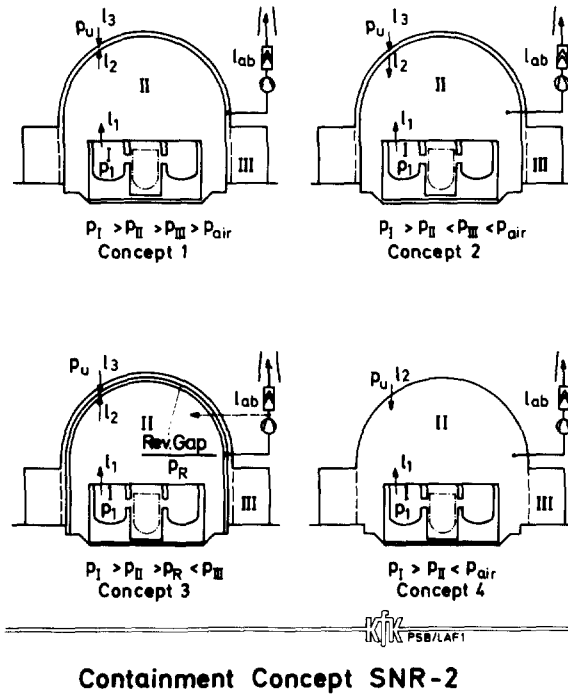
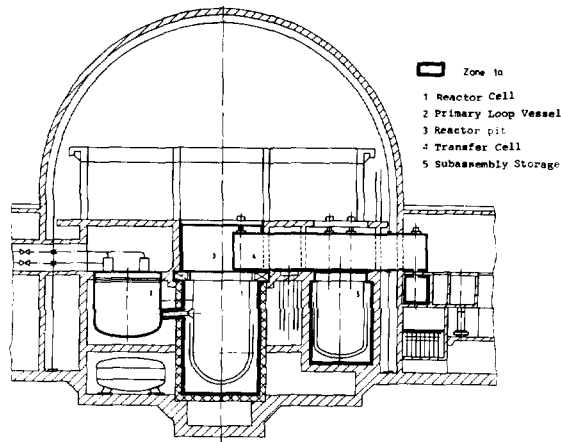


Fig. 1



LAF 1
 Reactor Building SNR-2

Fig. 2

15th DOE NUCLEAR AIR CLEANING CONFERENCE

outer containments. The concepts 1 and 2 are in principle developed from those of the KWU-LWRs and the KNK-II Fast Breeder Reactor which have already stood the test. The outer containment consists of a double containment. This has an outer enclosure consisting of reinforced concrete protecting against external impacts (e.g. airplane crash, sabotage etc.) and an inner enclosure made of steel which is relatively leakproof and is intended to hold the activity back during an accident. In the case of concept 1 the underpressure is kept in the ring gap (space III) and in the case of concept 2 in the outer containment (space II) which determines the path of the activity. From there the gas is discharged through filters into the environment. Concept 3 basically represents the concept of the SNR-300 which had to be examined again for purposes of comparison since its realization was proved to be possible during the licencing procedure for the SNR-300. The underpressure is kept in the ring gap by repumping the gas in the outer containment by a special blower (reventing system). After a period of several days the maximum pressure of the outer containment is reached caused by the several thermodynamic effects and the gas leakage from the environment into the gap. Then the gas has to be discharged from the outer containment through filters into the environment (exventing). Therefore there is a time with zero release after the accident [5].

In the case of concept 4 the underpressure (always compared with the inner containment and the surrounding space) is kept in the outer containment where the gas is directly pumped through filters into the environment. The enclosure is made of reinforced concrete, so a relatively high leakage from the exterior has to be taken into account. The research of this concept allows a comparison of a single outer containment with the double outer containment concepts.

In all containment concepts the inner containment (space I) (Fig. 2) is the boundary of the inertized area and the inner barrier for the activity. It surrounds all areas which contain the primary sodium circuit like the reactor itself, the four primary circuits, the sodium-filled storage for irradiated elements, cleaning systems etc. It consists of the reactor enclosure and the four primary circuit containers and is made of steel. The environment of the containers is filled with air and is not leakproof. For a more detailed description see [4].

3. The accident taken as a basis for the study

The design basic accident for the SNR-2 is not yet established, but in this containment study it was assumed that the design parameters of the containment system were derived from the effects of a Bethe-Tait-excursion accident (HCDA). The reactor tank and the primary enclosure remain intact following the mechanical loading produced by the excursion energy. Decay heat from the damaged core is dissipated by means of the emergency cooling system and the primary heat removal chain.

The reaction zone contains liquid, solid and gaseous fuel, liquid and gaseous sodium as well as fission products. In this accident it was assumed that only at the beginning active nuclides and gaseous sodium are released to the inner containment following the pressure decrease. Then the released activity is transported by leakages (l_1) into the outer containment. To be conservative the release fractions of fuel and fission products were estimated to be high and those of sodium to be low. Being low in the case of sodium is therefore conservative as a high aerosol concentration causes a faster decay of the aerosol-type activity. Table 1 shows the estimated release fractions used as basic values for the calculations. They lead to an initial aerosol mass concentration in the inner containment of 132,4 g/m³.

15th DOE NUCLEAR AIR CLEANING CONFERENCE

	Release Fraction [%]	Released Activity [Ci]
Noble gases (Xe, Kr)	100	$1.8 \cdot 10^8$
Halogens (J)	50	$3.9 \cdot 10^8$
Volatile fission products (Cs, Te)	50	$7.1 \cdot 10^7$
Solid fission products (Sr, Y, Zr, Ru, Ba, Ce)	5	$5.7 \cdot 10^7$
Fuel (U, Pu), Transuranic Elements	5	$4.8 \cdot 10^6$
Sodium	500 kg	$1.9 \cdot 10^4$

} 2500 kg



Table 1 Release from the reactor tank after HCDA

Criterion Cont. concept	Acceptable leakage* [Vol%/d]	Accessible cont. area	Filter load [g]
1	$l_2 \leq 4$ for $l_1 = 100$	—	≤ 200
2	$l_2 \leq 0.1$ for $l_1 = 100$	area 3	≤ 1000
3	$l_3 \leq 4$ for $0 < l_1 < 50$	area 3	$\ll 200$
4	$l_2 < 0.1$ for $l_1 = 100$	—	≤ 15000



Table 2 Pros and cons of the 4 containment systems

* Maximum external γ -dose: 5 rem

4. Transport of the activity and the aerosols through the containment

The aerosol mass concentrations in the different compartments were calculated by the code Paradiseko III b. This describes the same aerosol-physical effects as the program Paradiseko III /1/, /2/, /3/, this is the coagulation, sedimentation, diffusion and thermophoresis but it is different in their numerical treatment. Instead of a distribution function the particle size distribution is approximated by a number of monodisperse particle fractions. Thus it was possible to change the integro-differential equation system into a pure differential equation system. By these means the numerical problems of Paradiseko III could be removed and the running time could be reduced by a factor 10. The particle source for the inner containment is taken to be the instantaneous release of the fuel, the fission products and the primary sodium in the quantities given in chapter 3. The particles leaking from the inner containment are the source for the outer containment. To do this the leak rates for each particle class and at each time step are stored on a magnetic tape and read again for the calculation of the second compartment. It should be noted that it is not necessary to make restrictions regarding the particle size distribution for example the restriction on log-normal distributions. Fig. 3 shows the dependence of the mass concentration in the outer containment on that in the inner containment with given leakage parameters.

The leak rates were varied over a wide range of values according to the following list:

leak rate of the inner containment l_1 :	1	to	100	[vol %/d]
leak rate of the outer containment l_2				
	for concept 1 and 2 :	0.1	to	10 [vol %/d]
	for concept 3 :	0.1	to	1 [vol %/d]
	for concept 4 :	10	to	100 [vol %/d]

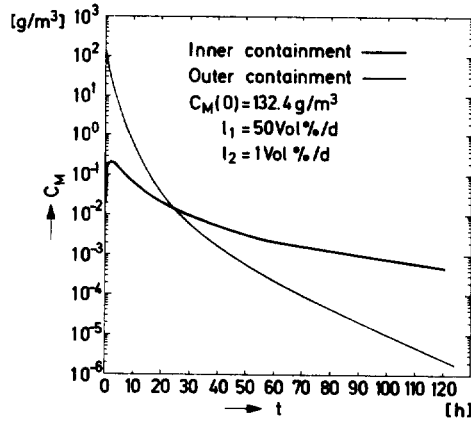
These average leak rates were estimated with thermodynamic considerations and the construction of the containment. In order to be conservative a filter factor was not taken into account during the passage of the aerosol through the leakages. To investigate the dependence of the mass released into the environment and the filter load on the initial concentration a second set of calculations was made using a value of 13.2 g/m^3 as initial mass concentration in the inner containment instead of the reference value of 132.4 g/m^3 . As it can be seen in fig. 4 the dependence on the initial release is relatively weak compared with the dependence on the leak rates. The values calculated in the study generally show that a decrease of the initial release affects the filter load only by a factor of 2 to 3 but the effect of an increase of the leak rates is directly proportional to them.

Therefore, it can be deduced that the exact determination of the release from the reactor tank is less important for the aerosol-type activity than the quality of the containment enclosures and of the filter equipment.

The release of the gaseous activity was calculated by means of the estimated pressure course and the leakage parameters.

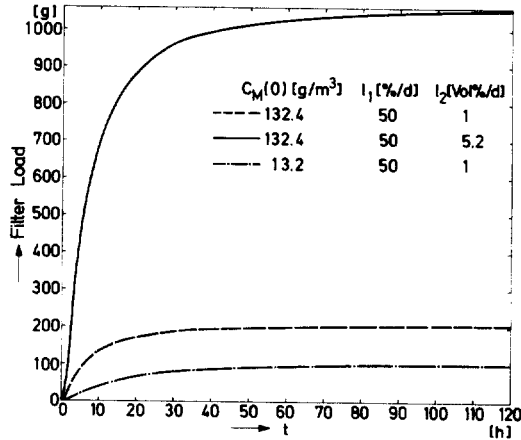
5. Radiological effects on the environment after the accident

The behaviour of the radioactive nuclides during their transport through the containment system can be described by a system of coupled first order differential



Aerosol mass concentration in the inner and the outer containment

Fig. 3



Aerosol Load of the Exhaust Air Filter Equipment

Fig. 4

15th DOE NUCLEAR AIR CLEANING CONFERENCE

equations. Its solution gives the time function of the activity load in the different compartments and the effluent of activity from the reactor equipment. For the aerosol-type activity the "plate-out" rates computed in the aerosol-physical calculations are used as input.

The dispersion parameters and the dose rates in the environment are calculated using the equations and statements in [6]. They refer to the points of maximum dose rate and the most unfavourable meteorological situation.

The results of the radiological analysis generally show that the dose for each organ integrated over the whole accident time is determined by the release of the gas type activity. The 2h-dose as well as the 24h-dose, however, are mainly influenced by the release of the aerosol-type activity (mainly Pu). The reason is that the aerosol physical decay processes cause an appreciable reduction of the dose made by the aerosol type activity. The filter efficiency for the aerosols is assumed as 99 % and for the noble gases as 0 %.

In nearly all parameter cases considered the external γ -submersion dose from the exhaust air cloud is the most critical dose.

The calculated accident doses have to be compared with the limit of 5 rem acceptable in view of the radiological protection regulation. Additionally the fact has to be taken into account that the calculated dose should be reasonably lower than the above mentioned limit. Therefore, it is possible to draw conclusions how leakproof the containment enclosures of the considered containment should be (see Fig. 5). The figure shows the 1-rem isodose line and the 5-rem isodose line depending on the leakage parameters of the inner (l_1) and the outer containment (l_2). It can be seen from the figure that containment concept 1 keeps the activity back best because of the two activity barriers. In the case of failure of the inner enclosure (l_1 large) the activity emission is much more limited by the outer enclosures in this concept than in the others. Fig. 6 shows a comparison of the accident dose as a function of the leakage of the inner containment for concept 1, 2 and 4. The concepts 2 and 4 react quite sensitively on an increase of the leakages of the inner containment. Therefore, concept 4 can only be realized if the leakage l_1 is less than some Vol. %/d. In this concept the relatively high inlet leakages badly influence the emission rate and therefore the period of time which the nuclides spend in area 2.

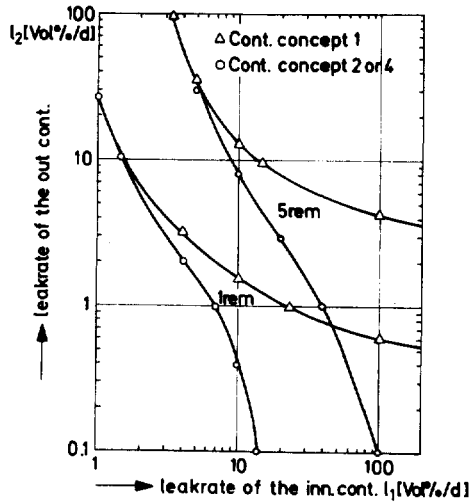
6. Assessment of the containment concepts

It should be emphasized that these assessments only relate to this study and that other problems (finances, engineering) are not considered.

A summarization of the pros and cons of the 4 containment concepts is shown in table 2.

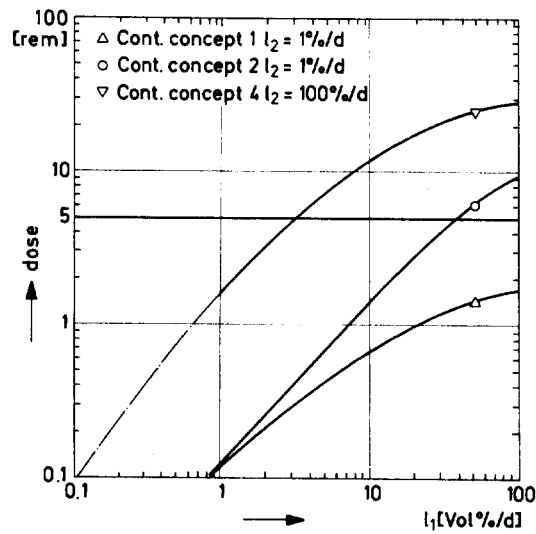
Concepts 1 and 3 have the greatest advantages to keep the activity back, but concept 3 has the disadvantage of doing it by active components (the reventing blowers). The differences of the concepts concerning this point are described in details in chapter 5.

The accessibility to the different containment areas strongly depends on the ventilation system, therefore it is bad for concepts 1 and 4. Since the construction of concepts 1 and 2 is quite similar, it is possible to combine the two concepts to select the ventilation depending on the accident occurring and so to



Maximum external γ -dose dependant on the leakage parameters

Fig. 5



Maximum external γ -dose dependant on the leakage of the inner containment

Fig. 6

15th DOE NUCLEAR AIR CLEANING CONFERENCE

avoid the disadvantage of inaccessible areas in many cases.

Regarding the filter loads the disadvantage of concept 4 is obvious because it has a filter load of 15000 g, whereas all other concepts have filter loads less than or equal to 1000 g. This point is strongly correlated to the point of release of aerosol-type activity to the environment. The high filter load in concept 4 is caused by the high inlet leakage of the simple outer containment enclosure.

7. Conclusion

The results of the study show that a combination of the concepts 1 and 2 could be the basic concept:

- an inner enclosure for the inertized area
- an outer steel enclosure relatively leakproof
- a reinforced concrete enclosure surrounding the steel enclosure to protect against external impacts
- a ventilation system allowing the air to be led alternatively according to concept 1 (underpressure in the ring gap) or concept 2 (underpressure in the outer containment).

This concept keeps the activity sufficiently back even if greater leakages of the inner containment exist, and the filter load produced thereby can be disposed of without too much effort.

References

- [1] W.O. Schikarski, "On the State of the Art in Aerosol Modelling for LMFBR Safety Analysis", Int. Meeting Fast Reactor Safety and Related Physics, Chicago (1976)
- [2] H. Jordan, W. Schikarski, H. Wild, "Nukleare Aerosole im geschlossenen System" KFK 1989 (1974)
- [3] H. Jordan, C. Sack, "Pardiseko III, A Computer Code for Determining the Behavior of Contained Nuclear Aerosols", KFK 2151 (1975)
- [4] H. Hillekum, "SNR-2 - Innere Sicherheitseinschlüsse", Reaktortagung Hannover (1978)
- [5] H. Oeynhausien, F. Morgenstern, U. Scholle, L. Lange, G. Waldhör, "Design Requirements for the SNR-300 Containment System", Int. Meeting Fast Reactor Safety and Related Physics, Chicago (1976)
- [6] "Allgemeine Berechnungsgrundlagen für die Bestimmung der Strahlenexposition durch Emission radioaktiver Stoffe mit der Abluft", Empfehlung der Strahlenschutzkommission - BMI (1977)

15th DOE NUCLEAR AIR CLEANING CONFERENCE

FISSION 2120: A PROGRAM FOR ASSESSING THE NEED FOR ENGINEERED SAFETY FEATURE GRADE AIR CLEANING SYSTEMS IN POST ACCIDENT ENVIRONMENTS

G. Martin, Jr., D. Michlewicz and J. Thomas
Ebasco Services Incorporated
New York, New York

Abstract

A computer program FISSION 2120, has been developed to evaluate the need for various Engineered Safety Feature grade air cleaning systems to mitigate radiation exposures resulting from accidental releases of radioactivity. Those systems which are generally investigated include containment sprays with chemical additives, containment fan coolers with charcoal filters, and negative pressure maintenance systems for double barrier containments with either one-pass filtration or recirculation with filtration. The program can also be used to calculate the radiation doses to control room personnel. This type of analysis is directed towards the various protection aspects of the emergency ventilation system and involves the modeling of the radiological source terms and the atmospheric transport of the radioactive releases. The modeling is enhanced by the inherent capability of the program to accommodate simultaneous release of activity from several sources and to perform a dose evaluation for a wide range of the design characteristics of control room emergency air filtration systems.

Use of the program has resulted in considerable savings in the time required to perform such analyses and in the selection of the most cost-effective Engineered Safety Features.

I. Introduction

The licensing of a nuclear power plant requires an evaluation of the radiological consequences of a spectrum of postulated accidents. The spectrum should include an accident whose consequences are not exceeded by any other accident which is considered credible. A major loss-of-coolant accident (LOCA) is the most limiting credible occurrence which is presently considered. The results of such an evaluation provide a significant contribution to the selection of the design specifications for components and systems from the viewpoint of protecting the public health and safety. As an aid in the performance of safety analyses, the FISSION 2120 computer program has been written to evaluate the radiological consequences of the various postulated accidents. Using this program, one can investigate the need for various Engineered Safety Features (ESF) by analytically evaluating the effects on the plant, its associated personnel, and the public of the simultaneous failure of various components of the facility and some of its redundant safety systems.

The adequacy of the ESFs is measured by their capability to limit the release of radioactive materials into the environment to the extent that the radiation exposures to an individual at the plant

15th DOE NUCLEAR AIR CLEANING CONFERENCE

exclusion area boundary (EAB) distance and low population zone (LPZ) will not exceed the guidelines of 10CFR Part 100 (1). In addition, the program is a useful tool in establishing the design requirements of the control room emergency air filtration system for conformance with the radiological exposure guidelines of General Design Criterion 19 of Appendix A to 10CFR Part 50 (2). The most economical design, with respect to cost and necessity for periodic testing, may be determined by calculating doses to control room operators following a hypothetical Design Basis Accident as a function of filter efficiency, air handling capacity and other parameters.

II. The FISSION 2120 Radioactivity Releases and Dose Calculation Computer Program

FISSION 2120 was developed to model the release of airborne radionuclides from the containment and to calculate resulting doses to individuals at chosen locations. It was recognized that the program possessed the potential of being used as a design tool, particularly in establishing the specifications of dose mitigating ESFs relative to the atmospheric characteristics of a specific site. As a result, the capability to parametrically vary the ESF design variables was incorporated into the program enabling one to study the dose mitigating effects of various combinations of ESFs.

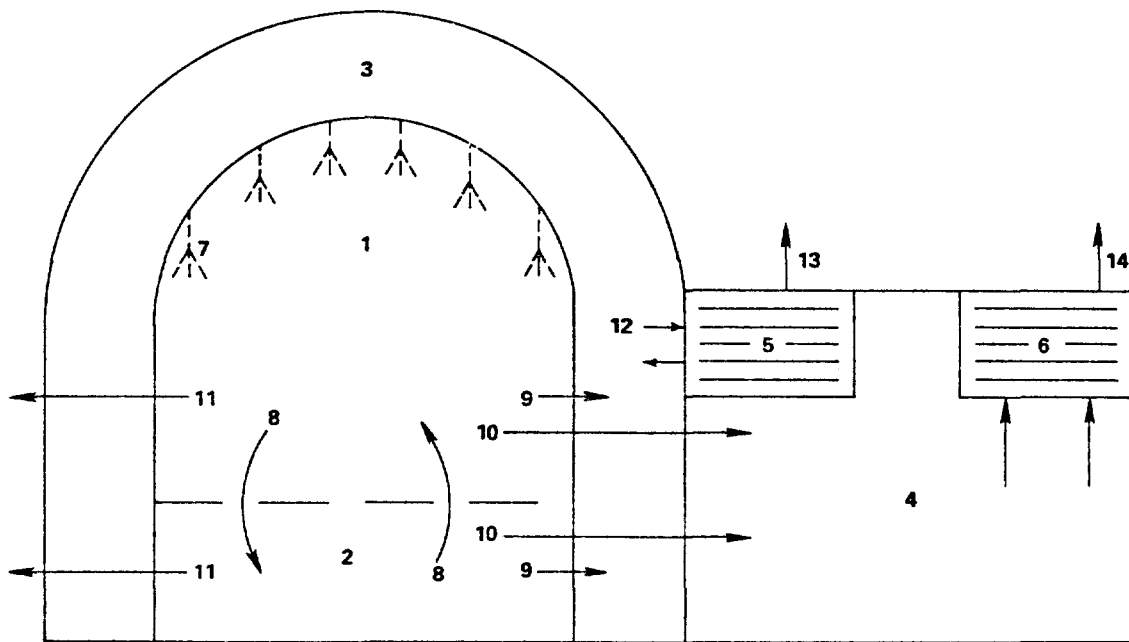
The parametric aspect is characteristic throughout the program and is especially useful in the following two areas:

1. containment design characteristics, ESF requirements and site suitability studies;
2. control room emergency air filtration system design and operating modes.

Figure 1 is a diagram of the FISSION 2120 containment leakage model indicating the transport pathways of airborne radionuclides from one compartment to another and to the environment. Also presented in this figure are examples of the ESFs whose design variables can be parametrically studied using the program.

The model shown in Figure 1 is a dual-compartment containment leakage model. This model takes into account the partial coverage of the containment volume by the containment sprays and the mixing that takes place between the sprayed and unsprayed regions. One would normally use this model when taking credit for the iodine scrubbing action of certain chemicals added to the spray solution. In the case of pressurized water reactors, the volume of the containment below the operating deck contains compartments which are essentially excluded from the direct action of the sprays. Consequently, iodine scrubbing either does not take place or occurs at a much reduced rate in those situations where an air exchange exists between the sprayed and the obstructed lower zone.

**FIGURE 1
CONTAINMENT LEAKAGE MODEL**



- | | |
|---|---|
| 1. CONTAINMENT SPRAYED VOLUME | 8. AIR EXCHANGE BETWEEN REGIONS 1 AND 2 |
| 2. CONTAINMENT UNSPRAYED VOLUME | 9. LEAKAGE INTO THE SHIELD BUILDING ANNULUS |
| 3. SHIELD BUILDING ANNULUS | 10. LEAKAGE INTO THE NEGATIVE PRESSURE AREA OF THE REACTOR AUXILIARY BUILDING |
| 4. NEGATIVE PRESSURE AREA OF THE REACTOR AUXILIARY BUILDING | 11. BYPASS LEAKAGE |
| 5. SHIELD BUILDING VENTILATION SYSTEM | 12. SHIELD BUILDING VENTILATION SYSTEM RECIRCULATION |
| 6. CONTROLLED VENTILATION AREA SYSTEM | 13. SHIELD BUILDING VENTILATION SYSTEM RELEASE |
| 7. CONTAINMENT SPRAYS | 14. CONTROLLED VENTILATION AREA SYSTEM RELEASE |

Activity Transport and Dose Calculation Equations

The transport of activity from the containment to the environment and the control room is represented by a set of equations which describe the conservation of activity within the various compartments.

The change in activity with respect to time in the sprayed and unsprayed regions of the containment, respectively, is given by:

$$\frac{dA}{dt}_s = - (\lambda + R_s + L_1 + \frac{E}{V}_s) A_s + \frac{E}{V}_u A_u \quad (1)$$

$$\frac{dA}{dt}_u = - (\lambda + R_u + L_1 + \frac{E}{V}_u) A_u + \frac{E}{V}_s A_s \quad (2)$$

where:

A_s = activity in sprayed region of containment (Ci)

A_u = activity in unsprayed region of containment (Ci)

15th DOE NUCLEAR AIR CLEANING CONFERENCE

t = time (sec)

λ = radioactive decay constant (sec^{-1})

R_s, R_u = first order removal coefficient of the ESFs inside the sprayed and unsprayed regions of the containment (sec^{-1})

L_1 = primary containment leak rate coefficient (sec^{-1})

E = air exchange rate between sprayed and unsprayed region (m^3/sec)

V_s, V_u = volumes of sprayed and unsprayed regions (m^3).

For a secondary enclosure (e.g. the shield building annulus), the time rate of change of activity is expressed as:

$$\frac{dA}{dt} = L_1(A_s + A_u) - (\lambda + L_2 + R_2)A_2 \quad (3)$$

where:

A_2 = activity in secondary containment (Ci)

R_2 = first order removal coefficient of the shield building annulus recirculation system (sec^{-1})

L_2 = secondary containment vent rate coefficient (sec^{-1}).

The activity, Q_2 (Ci), which is released from the secondary enclosure to the environs is given by:

$$Q_2(t) = L_2 \int_0^t A_2(t') dt' \quad (4)$$

The calculation of this quantity permits the calculation of the offsite integrated concentration, or exposure, given by:

$$\psi_2 = Q_2 \left(\frac{X}{Q} \right)_2 \quad (5)$$

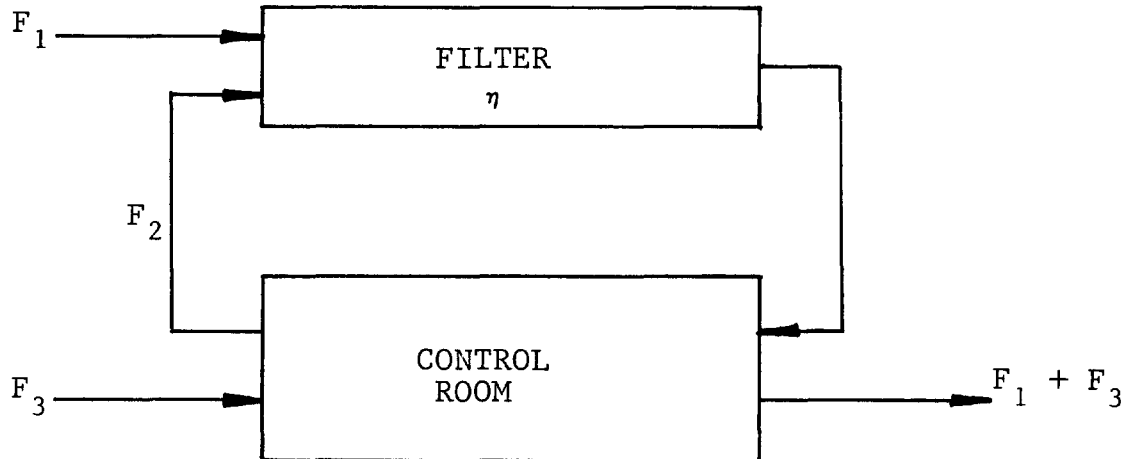
where:

ψ_2 = offsite exposure ($\text{Ci}\cdot\text{sec}/\text{m}^3$)

$\left(\frac{X}{Q} \right)_2$ = offsite atmospheric dispersion factor (sec/m^3).

Figure 2 shows the model which is used in the dose analysis of a control room emergency air filtration system ⁽³⁾. The model is general in nature and can represent a control room in either the pressurized or totally isolated mode.

FIGURE 2
CONTROL ROOM EMERGENCY FILTRATION SYSTEM



F_1 = rate of filtered outside air intake

F_2 = rate of filtered air recirculation

F_3 = rate of unfiltered outside air infiltration

η = filter efficiency

The activity in the control room is a function of the activity released from the containment, the atmospheric dispersion that takes place between the source and the point of intake, the intake rate of air into the control room, and the degree of air filtration provided.

The change of activity in the control room is given by the following equation:

$$\frac{dA}{dt} = L_2 A_2 \left[\left(\frac{X}{Q} \right)_1 F_1 (1-\eta) + \left(\frac{X}{Q} \right)_3 F_3 \right] - \left[\lambda + \frac{F_1 + (1-\eta)F_2 + F_3}{V} \right] A_3 \quad (6)$$

where:

A_3 = activity in the control room emergency HVAC envelope (Ci)

$L_2 A_2$ = the rate of release of activity into the environment from the secondary containment (Ci/sec)

F_1 = rate of filtered outside air intake (m^3/sec)

F_2 = rate of filtered air recirculation (m^3/sec)

F_3 = rate of unfiltered outside air infiltration (m^3/sec)

15th DOE NUCLEAR AIR CLEANING CONFERENCE

V = volume of control room emergency HVAC envelope (m³)

λ = radioactive decay constant (sec⁻¹)

η = efficiency of the control room emergency filtration system charcoal adsorber

$\left(\frac{X}{Q}\right)_1, \left(\frac{X}{Q}\right)_3$ = atmospheric dispersion factors representative, respectively, of dilution between the activity release point and main control room air intake and point of unfiltered inleakage (sec/m³).

The integrated activity concentration in the control room atmosphere, ψ_3 (Ci-sec/m³), is given by:

$$\psi_3 = \frac{1}{V} \int_0^t A_3(t') dt' \quad (7)$$

The exposure is used to calculate the skin, thyroid and whole body doses, in rem, to offsite receptors and control room personnel according to the following equations:

$$\text{Skin Dose} = \text{SDCF} \cdot \psi \cdot K$$

$$\text{Thyroid Dose} = B \cdot \text{TDCF} \cdot \psi \cdot K \quad (8)$$

$$\text{Whole Body Dose} = \text{WDCF} \cdot \psi \cdot K$$

where:

SDCF = skin dose conversion factor (rem/sec/Ci/m³)

TDCF = thyroid dose conversion factor (rem/Ci-inhaled)

WDCF = whole body dose conversion factor (rem/sec/Ci/m³)

B = breathing rate (m³/sec)

K = a modifying factor which accounts for the effects of in-transit decay, depletion and effects of finite geometry, as applicable.

The analytical solutions to the above equations are incorporated into the FISSION 2120 program. Input of problem dependent parameters such as filter efficiency and X/Q permits the calculation of offsite doses for up to eight time intervals following the start of the accident.

The FISSION 2120 program is written in FORTRAN IV, requires 18 K words of core storage space and, depending on the extent of the problem, runs about 18 seconds on a Burroughs B7760 computer.

15th DOE NUCLEAR AIR CLEANING CONFERENCE

III. Containment Design Characteristics and Plant Requirements in Site Suitability Studies

Offsite doses resulting from a large LOCA are the major factors which are considered in any containment design. 10CFR Part 100 specifies the dose limits as 300 rem to the thyroid from iodine exposure and 25 rem immersion dose to the whole body. However, at the construction permit stage of licensing, the Nuclear Regulatory Commission (NRC) guideline values are 150 and 20 rem, respectively (4,5). These exposures are calculated for an individual located at any point on an exclusion area boundary (EAB) for two hours immediately following the onset of the postulated fission product release, and on the outer boundary of a low population zone (LPZ) during the entire period of the radioactive cloud passage.

In general, the thyroid dose received at the EAB in the first two-hour period following the accident has been observed to be the controlling factor when using the activity release fractions specified by the NRC (4,5). An examination of the containment leakage model and the dose calculation equations reveals that the thyroid dose is a function of several factors, which in turn are related to the containment, the type of ESFs and the site. These are:

1. containment design leak rate;
2. overall iodine decontamination factor (IDF);
3. atmospheric dispersion factor, X/Q.

In these calculations the offsite thyroid dose is directly proportional to the containment leak rate; with leak rates ranging from 0.1% to 0.5% of the containment volume per day currently being used.

The IDF as used here is defined as the ratio of the integrated releases of a plant without dose reduction features to those of the same plant including such features and, hence, is a function of the type, the size and the effectiveness of the ESFs provided for iodine removal. It is in the development of the IDFs that the FISSION 2120 program proves to be an effective practical design tool. The dose reduction features may consist of internal containment sprays with additives, filter removal systems, external filter system used in conjunction with a double barrier containment or, as is usually the case, a combination of these features. Table I lists the IDFs for various combinations of these ESFs. In the development of these values, the "base" case (with the IDF equal to 1) has been taken as a plant with a single barrier containment, with a design leak rate of 0.5% per day, and without any ESFs.

The atmospheric dispersion factor, X/Q, is a measure of the dilution of the released fission products at a distance from the point of emission. It is dependent on site meteorology and distance and, in general, its value decreases as the distance increases. The offsite doses are directly proportional to the X/Q value.

15th DOE NUCLEAR AIR CLEANING CONFERENCE

TABLE I

Iodine Removal Effectiveness
of
Various Engineered Safety Features

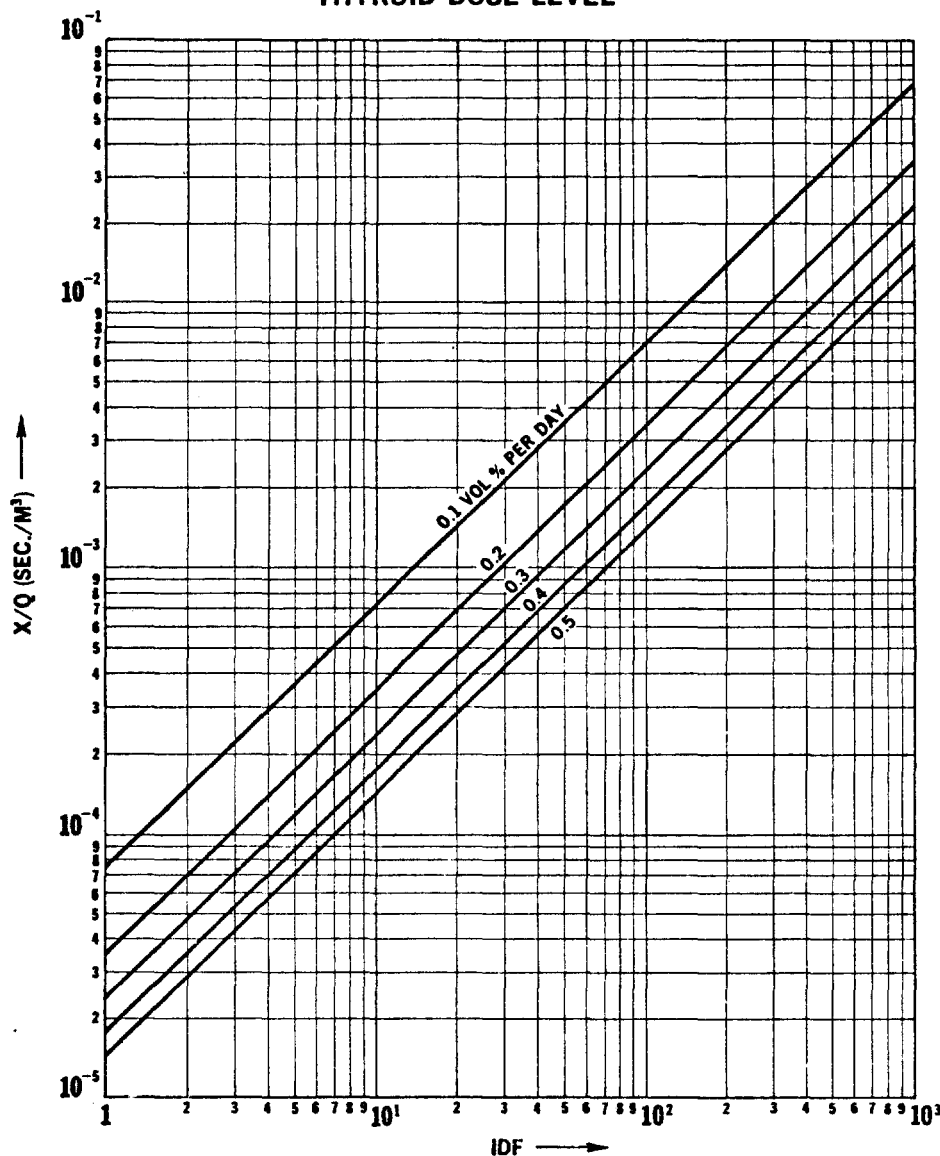
<u>Engineered Safety Features</u>	<u>Iodine Decontamination Factor</u>
1. Single barrier containment without iodine spray removal system.	1.0
2. Single barrier containment with iodine spray removal system.	7.0
3. Double barrier containment with external once-through filtration system with 95% efficiency charcoal adsorber.	21.0
4. Double barrier containment with external once-through filtration system with 99% efficiency charcoal adsorbers.	100.0
5. Double barrier containment with iodine spray removal system and external once-through filtration system with 95% efficiency charcoal adsorbers.	158.0
6. Double barrier containment with iodine spray removal system and external once-through filtration system with 99% efficiency charcoal adsorbers.	658.0

Figure 3 is a plot of the IDFs versus X/Q values for a family of 150 rem thyroid isodose curves evaluated for containment leak rates varied over the range of 0.1% to 0.5% per day. Ideally, the development of such a graph should be undertaken as soon as reliable onsite meteorological data are available and should precede, or, at least coincide with, the preliminary design phases of the nuclear plant. Knowledge of site meteorological characteristics could, through the use of a graph similar to Figure 3, help determine the distance to the EAB, the LPZ and the corresponding plant ESFs required to ensure that the LOCA doses will be below the limits established by the NRC. Using such an approach, economic studies can be performed whereby the cost of installing progressively more expensive ESFs would be measured against that of acquiring additional land.

15th DOE NUCLEAR AIR CLEANING CONFERENCE

The results presented in Figure 3 can also provide the basis for setting the technical specifications for the containment leak rate. Examination of Figure 3 will show that choosing a design basis containment leak rate of 0.1% per day will result in either the installation of a minimum number of ESFs and/or a shorter EAB. For example, the choice of the smallest leak rate of 0.1% per day at a site with an EAB X/Q equal to 5×10^{-4} sec/m³ would require a combination of Engineered Safety Features with an IDF of about 7. Table I indicates that this can be achieved by a single barrier containment with an iodine spray removal system. However, one should be aware that the choice of such a small leak rate may introduce problems in engineering, construction, plant operation and maintenance.

FIGURE 3
X/Q AS A FUNCTION OF IDF FOR A 150 REM
THYROID DOSE LEVEL



15th DOE NUCLEAR AIR CLEANING CONFERENCE

IV. Emergency Air Filtration Design Requirements For Control Room Habitability

The protection requirements of control room personnel against radiation exposure under accident conditions are specified in General Design Criterion 19 (GDC 19) of Appendix A to 10CFR 50 (2). As stated in GDC 19, "a control room shall be provided from which actions can be taken to operate the nuclear power unit safely under normal conditions and to maintain it in a safe condition under accident conditions, including loss-of-coolant accidents." Consequently, the evaluation of the performance requirements of a protection system for a control room is based on the same LOCA source term which is used in the assessment of compliance with 10CFR Part 100 dose criteria. Therefore, the control room activity and dose model is a natural extension of the containment leakage model. The evaluation of compliance with GDC 19 is generally directed toward the emergency ventilation system and involves modeling of the radiological source term, the atmospheric transport of the radionuclides released, along with the various protection aspects of the control room ventilation system.

The FISSION 2120 control room model is similar to that of Murphy and Campe (3) and Byoun and Conway (6). The major difference is that this model does not assume the existence of equilibrium conditions. The calculation of doses is based on the exact solutions of the mass balance equations. Consequently, the dose mitigating effect of slow build-up of activity in an isolated control room followed by a rapid purge, is automatically accounted for without having to resort to the calculation of a purge factor (3).

The control room part of the program is very versatile due to the fact that virtually all the necessary input data can be treated parametrically. For example, a control room may be designed to operate in either a pressurized or an isolated mode under accident conditions. However, in some cases, pressurized control rooms actually go into an isolated mode initially, followed by a time lag, which may be significant, before attaining proper pressurization. This case can be analyzed to provide information relative to the selection of a manual or automatic system and operational flexibility within the control room. An associated aspect is the control room emergency system filters. The filter efficiency can be treated parametrically and be turned "ON/OFF" over specified time intervals to account for time lags required to get the emergency system operational or to attain the specified pressurization. Similarly, the filtered air intake rate for the pressurized mode, the unfiltered inleakage and the emergency filtration system recirculation capacity can be treated as parametric variables.

The program can accommodate specific atmospheric dispersion factors (X/Q) for both the filtered air intake and unfiltered inleakage, as well as X/Qs for simultaneous multi-point releases. This is done by assigning a pair of X/Qs to each source of activity release; one for filtered air intake and one for unfiltered inleakage into the control room. Points of release which can be considered include filtered releases from the Standby Gas Treatment System, unfiltered

15th DOE NUCLEAR AIR CLEANING CONFERENCE

containment bypass leakage as well as releases from the Emergency Core Cooling System equipment rooms kept at negative pressure. The X/Qs may be evaluated according to the models of Murphy and Campe⁽³⁾. By considering various combinations of release to intake X/Qs one can optimize the location of control room emergency outside air intakes with respect to minimizing potential personnel doses.

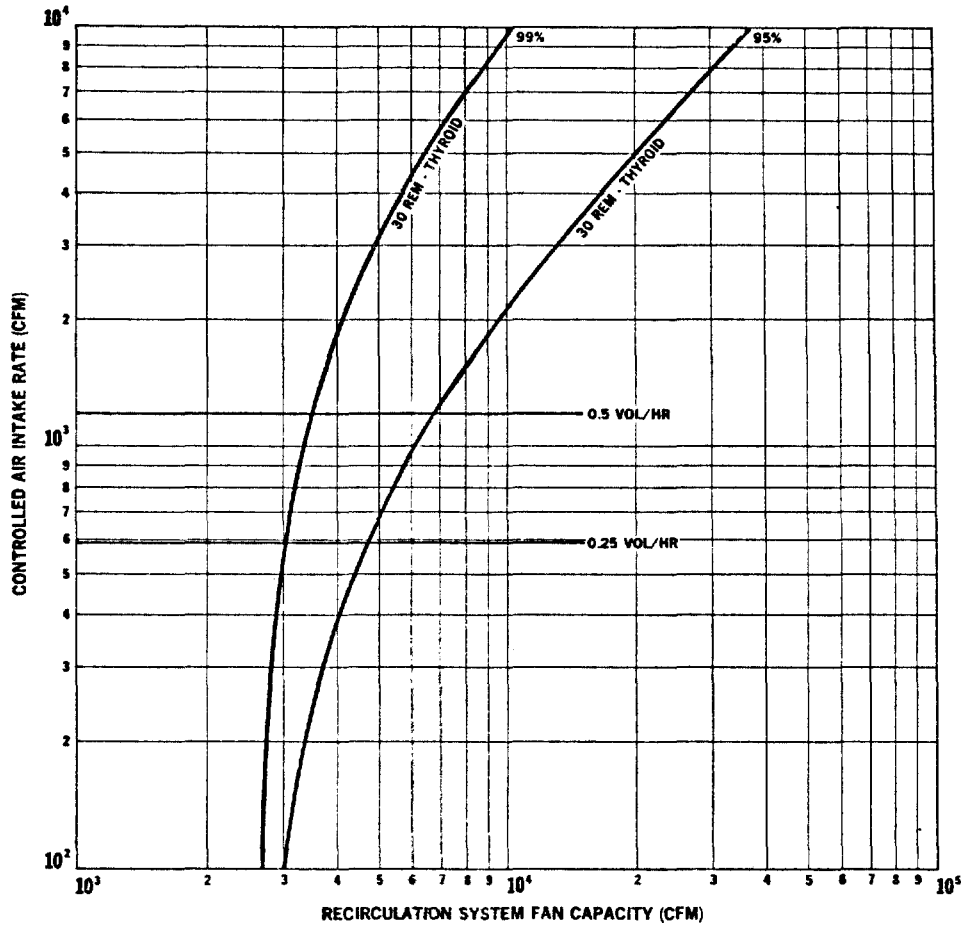
Another aspect of design which can be investigated by this program is the choice between automatic and manual isolation of a control room following a LOCA. This choice is particularly significant because the NRC is currently permitting large reduction in the dispersion factors for well separated dual air intakes, and manual or automatic isolation⁽⁷⁾. These reduction factors apply to the determination of the five percentile X/Q for dual inlets located on Seismic Category I structures, for which the current NRC practice is as follows:

1. For well separated dual fresh air intakes the X/Q is obtained from Eq. 6 in Ref. (3) for the intake closest to the point of release and then reduced by a factor of 2.
2. If active manual control over source of makeup air has been provided by installing radiation monitors at the inlets and by training control room operators to switch to the cleaner inlets, the X/Q is obtained from Eq. 6 in Ref. (3) for the farthest air inlet and then reduced by a factor of 4.
3. If active automatic control over source of makeup air has been provided by means of radiation monitors and control logic, the X/Q for the farthest air inlet is reduced by a factor of 10.

The reductions in the values of the X/Qs lead to corresponding reductions in calculated doses to control room operators.

The results of the control room dose evaluation, generally presented graphically, define the ventilation system requirements in the form of an "envelope". In this manner the designer can readily select system parameters with assurance that the resulting design would be acceptable from a radiological point of view and also be aware of the testing requirements being imposed. Figure 4 is a graphical representation of the curves that form the "envelopes" for acceptable combinations of the major design parameters, (filter efficiency, makeup air intake rate and filtered air recirculation rate) of a pressurized control room emergency air filtration system. Regions of Figure 4 lying to the right of and below the isodose curves indicate values of air makeup rate and recirculation system fan capacity at which the radiological protection criteria of GDC 19 would not be exceeded. The 0.5 volume/hour and 0.25 volume/hour horizontal lines indicate regions of different requirements for verifying control room leak tightness, as specified in Standard Review Plan 6.4,⁽⁸⁾ and provide an added constraint on the sizing of the emergency air filtration system.

FIGURE 4
30 DAY 30 REM THYROID ISODOSE CURVE



V. Conclusion

Use of the FISSION 2120 program has resulted in considerable savings in the time and cost required to perform accident analyses, and in the selection of the most cost effective Engineered Safety Features. This program has proven to be a useful tool for the radiological assessment engineer in advising the designer, the safety and licensing engineer and the environmental engineer through the various stages of the plant design.

References

1. Reactor Site Criteria, 10CFR Part 100.
2. Control Room, General Design Criterion 19, General Design Criteria For Nuclear Power Plants, Appendix A to 10CFR Part 50.

15th DOE NUCLEAR AIR CLEANING CONFERENCE

3. K.G. Murphy & K.M. Campe, Nuclear Power Plant Control Room Ventilation System Design For Meeting General Criterion 19, 13th AEC Air Cleaning Conference (1973).
4. Regulatory Guide 1.3; "Assumptions Used for Evaluating The Potential Radiological Consequences Of A Loss-Of-Coolant Accident For Boiling Water Reactors."
5. Regulatory Guide 1.4; "Assumptions Used For Evaluating The Potential Radiological Consequences Of A Loss-Of-Coolant Accident For Pressurized Water Reactors."
6. T.Y. Byoun & J.N. Conway, Evaluation of Control Room Exposure, 14th ERDA Air Cleaning Conference (1976).
7. Personal communications with K.G. Murphy and K.M. Campe, NRC, 1977-1978.

DISCUSSION

MOELLER: Does your program provide a quantitative estimate of the source term required to yield the 150 rem thyroid dose limit?

MICHLEWICZ: The program can be used to calculate the source term. However, the source term would depend on containment design and site conditions.

COLLINS: In considering cost did you factor in operating and maintenance cost or only capital cost?

MICHLEWICZ: We considered both costs. For example, in the design of a control room ventilation system, the costs of periodic testing of that system are considered in the selection of the system parameters.

15th DOE NUCLEAR AIR CLEANING CONFERENCE

IMPACT OF SOPHISTICATED FOG SPRAY

MODELS ON ACCIDENT ANALYSES

by

S. P. Roblyer, United Nuclear Industries, Inc.
Richland, Washington

P. C. Owzarski, Sigma Research, Inc.
Richland, Washington

Abstract

In the analysis of postulated accidents involving a primary coolant pipe break and subsequent release of fission products, the detailed mechanisms of plateout, washout by fog sprays and filtering are evaluated as a means of removing fission products from the atmosphere inside the reactor building. The N Reactor confinement system release dose to the public in a postulated accident is reduced by washing the confinement atmosphere with fog sprays. This allows a low pressure release of confinement atmosphere containing fission products through filters and out an elevated stack.

The current accident analysis required revision of the CORRAL code and other codes such as CONTEMPT to properly model the N Reactor confinement into a system of multiple fog-sprayed compartments. In revising these codes, more sophisticated models for the fog sprays and iodine plateout were incorporated to remove some of the conservatism of steam condensing rate, fission product washout and iodine plateout than used in previous studies.

The CORRAL code, which was used to describe the transport and deposition of airborne fission products in LWR containment systems for the Rasmussen Study, was revised to describe fog spray removal of molecular iodine (I_2) and particulates in multiple compartments for sprays having individual characteristics of on-off times, flow rates, fall heights, and drop sizes in changing containment atmospheres. During postulated accidents, the code determined the fission product removal rates internally rather than from input decontamination factors. A discussion is given below of how the calculated plateout and washout rates vary with time throughout the analysis. The results of the accident analyses indicated that more credit could be given to fission product washout and plateout. An important finding was that the release of fission products to the atmosphere and adsorption of fission products on the filters was significantly lower than previous studies had indicated.

15th DOE NUCLEAR AIR CLEANING CONFERENCE

I. Introduction/Summary

The CORRAL code was chosen to be used in the accident analyses for N Reactor. This decision was made because the capabilities of the code were suitable for modeling the complex confinement system of N Reactor. The N Reactor confinement system has a low pressure design which will relieve pressure from major pipe accidents during the initial pressure transient.

The confinement building is categorized as four compartment volumes which are interconnected by ventilation flow paths. Each compartment of the confinement building has its unique volume, wall and floor area and temperatures, vapor pressures and pressure transients during the course of the accident. In three of the compartments, 11 unique fog sprays are described. Intercompartmental flow rates and flow rates through a filtered release and building leakage are specified as a function of time. It was therefore clear in considering the complexity of the N Reactor confinement system during postulated accidents that a sophisticated model of the confinement system was needed to properly analyze the postulated accidents.

CORRAL is a complex computer model (developed for the Rasmussen Reactor Safety Study (WASH-1400)) of light water reactor containment space that describes the transport, deposition and leakage of airborne fission products during postulated accidents. CORRAL handles the airborne fission products in four basic models based on their physical and chemical properties. These groups are particulates, elemental iodine, methyl iodine and noble gases. Natural deposition of particulates and I_2 as well as spray washout are modeled to apply to each individual (of N total) compartments' unique features and existing thermodynamic states. The compartments are tied together via cross flows. In the compartments the code is used to account for the mass balance of each fission product group. The resulting 3N time dependent differential mass balances are solved exactly over a specified time interval. Complete inventories of these fission products are computed for each compartment and reprinted as fractions: remaining airborne, deposited and/or washed out, present on filters and lost to the environment by ground or stack level leaks.

The CORRAL code was successfully applied to the fuel ejection accident described in this paper, and other accidents considered in the N Reactor safety analysis report. The code accounted for the distribution, depletion and release to the environs of the above four fission product groups as a function of time. The release fractions of these fission product groups were used as the basis to calculate the release of fission products and the accident doses.

II. Airborne Fission Product Depletion Mechanisms and Their Models in a LWR Containment System

The rates of processes controlling the depletion of airborne fission products depends on the physical and chemical properties of the individual species. These properties allow grouping all important products into four major categories:

15th DOE NUCLEAR AIR CLEANING CONFERENCE

- elemental iodine (as a vapor)
- methyl (organic) iodide
- noble gases
- aerosol particles

Detailed description of the models and mechanisms are described in Reference (1) of the Rasmussen Report. Summaries of the mechanisms and models follow.

II.1 Noble Gases

Although means for collecting noble gases have been proposed, none have yet been implemented in LWR containment systems, so no removal terms were added to the differential equations for the material balances of noble gases.

II.2 Methyl (organic) Iodide

The airborne alkyl halides that can form following a postulated accident are relatively unreactive. Special treated activated charcoal filters, thiosulphate sprays, and special reactive paints can remove these species at rates faster than the very slow water hydrolysis reaction. None of these were present in systems analyzed for N Reactor, so methyl iodide was treated as a noble gas in the present CORRAL calculations. CORRAL is easily amenable to organic halide depletion mechanisms if desired.

II.3 Elemental Iodine

Airborne elemental iodine (I_2) can exist in both vapor and particulate forms. The quantity in the vapor phase usually predominates and is discussed below. Particulate iodine becomes part of the composition of the solid aerosol particles and is treated as such.

Two mechanisms exist for the depletion of elemental iodine: one is referred to as natural deposition or "plateout" and the other is spray washout. Natural deposition can occur on nearly all exposed surfaces below a certain temperature (250°C). The rate of deposition is limited by diffusion through a gas boundary layer along the surface of the containment system. A preferred model for boundary layer resistance involves natural convection that is driven by the temperature difference between containment gas phase and walls. The natural deposition removal constant $\lambda(\text{hr}^{-1})$ for a given compartment is thus

$$\lambda_{\text{ND}} = \frac{k_g A}{V} = \frac{A D_g}{V L} a (\text{Gr Sc})^b \quad (1)$$

15th DOE NUCLEAR AIR CLEANING CONFERENCE

where k_g = gas phase mass transfer coefficient
 V, A = compartment volume and surface area
 D_g = iodine diffusivity in the gas phase
 L = vertical height along convective boundary
 Gr = Grashov number for heat transfer
 Sc = Schmidt number for mass transfer
 a, b = constants ($a = 0.13, b = 1/3$ for Laminar $Gr < 1.5 \times 10^8$ and $a = 0.59, b = 1/4$ for turbulent $Gr > 10^{10}$)

Spray removal of I_2 can be accomplished much faster than natural deposition. A conservative model for spray removal employs a stagnant gas film around the drop and a well mixed drop interior. The resulting spray lambda is

$$\lambda_s = \frac{FH}{V} \left\{ 1 - \exp \left[\frac{-6 k_g t_e}{d \left(H + \frac{k_g}{k_e} \right)} \right] \right\} \quad (2)$$

where F = spray flow rate
 H = equilibrium partition coefficient
 t_e = drop terminal falling velocity
 d = drop diameter
 k_g = gas phase mass transfer coefficient
 $= \frac{D_g}{d} \left(2 + 0.6 Re^{0.6} Sc^{0.33} \right)$
 Re = drop Reynolds number
 k_l = liquid phase mass transfer coefficient
 $= 2\pi^2 D_g/3d$

Limitations on this spray drop model are discussed by Postma and Pasedag (2). The equilibrium partition coefficient, H , has the following applicable values (2):

- for neutral to pH = 5 (Boric acid), $H = 200$
- for caustic, pH = 9, $H = 5000$
- for basic sodium thiosulphate, $H = 10^5$

15th DOE NUCLEAR AIR CLEANING CONFERENCE

Equation (2) holds until iodine concentrations are reduced to about 1% of the initial airborne amount. After this, the iodine removal rate is independent of the spray volume rate and a pseudo-equilibrium sets in where H becomes dependent on time and a positive dH/dt leads to a slower rate of scrubbing. Each spray solution has its own pseudo-equilibrium pattern. CORRAL is presently programmed for three of these: pH = 5-7, pH = 9, and no spray.

II.4 Particulates

Airborne particulates also have two removal mechanisms: natural settling on all up-facing horizontal surfaces and spray removal. Natural settling from a well mixed compartment has the removal coefficient

$$\lambda_p = U_t A_h / V \quad (3)$$

where U_t is the terminal particle velocity, A_h = horizontal area component of all up-facing surfaces in compartment of volume V. CORRAL is programmed to determine a U_t given an initial particle size at the moment the particulates are airborne; then CORRAL linearly interpolates between that particle size and another input size at some later time. Based on CSE data (1)* the usual inputs were: initial size = 15×10^{-6} meter, final size = 5×10^{-6} meter beginning four hours later.

Spray removal of particulates is modeled using non-interacting drops that sweep out particles in their falling paths with efficiency E. This model gives

$$\lambda_{sp} = \frac{3h F E}{2 dV} \quad (4)$$

where h = spray fall height. The efficiency E monotonically decreases with an increasing value in the integrated dimensionless spray volume Ft/V . The CSE experiments determined an initial $E = 0.06$ which became 0.0015 for $Ft/V > 0.02$. This spray aging is programmed into CORRAL for each possible spray group.

III. Quantitative Comparison of Mechanisms in a Single Compartment

To show the relative effects of the various depletion mechanisms using the models discussed above, a single compartment was chosen for this case study. This compartment has the following typical PWR parameters: 10^6 ft³ volume, 50 ft height, 2×10^4 effective floor area, 10^6 ft² total surface area. This compartment has one spray type: 0.1 cm diam drops or 0.0465 cm, 50 ft fall height, 8×10^5 ft³/hr liquid flow rate,

* CSE: Containment Systems Experiments - Several references to work done here are listed in Reference (1).

15th DOE NUCLEAR AIR CLEANING CONFERENCE

and spray liquid is water, pH = 5-7 (H= 200). The compartment conditions following the spike release of airborne fission products are: p = 1 atm absolute; T = 180°F initially changing to 75° after one hour; atmosphere saturated with steam at the compartment pressure and temperature.

III.1 Particulate Behavior

Figure 1 is a plot of \log_{10} of the fraction of the initial particulate aerosol cloud that remains airborne in the compartment versus time. No leaks or radioactive decay were assumed. Each of the six curves represents a different removal in the basic depletion equation

$$\frac{d \ln C/C_0}{dt} = -\lambda \quad (3)$$

where C/C_0 is the fraction of particulates remaining airborne.

Curve A represents C/C_0 for the single removal mechanism of natural settling. Here the particles were 15×10^{-6} meters initially changing with time to 5×10^{-6} meters after four hours. Here $\lambda \approx 1.5 \text{ hr}^{-1}$. The nonlinearity of $\log_{10} C/C_0$ reflects the influence of this changing particle size and changing compartment conditions on λ .

Curves B-D show how an internal compartment filter could compare to natural settling. These curves represent 100% efficient filtering of particles through filters at flow volumes of one, two and three compartment volumes per hour (or 17,000, 33,000 and 50,000 ACFM).

Curves E and F compare two drop sizes, 0.1 cm and 0.0465 cm (1/10 mass of 0.1 cm drop). Here the removal λ 's are about 40 and 70 hr^{-1} . The curves terminate at $C/C_0 = 0.01$ reflecting an observed zero washout rate at that point in the CSE experiments. Equation (4) shows the direct influence of drop size on λ and this is apparent on the observed λ 's. The nonlinearity of the curves (F does not show any due to only one computed C/C_0) is due to the decreasing scrubbing efficiency in Figure 4 as sprays continue as well as the changing compartment conditions. These conditions would primarily affect the terminal drop velocity through the gas viscosity changes with compartment temperature.

For combined mechanisms in the compartment, one needs to simply add the various λ 's. If these are constant over a time interval, t_1 to t_2 , the differential equation solution is

$$C_{t_2}/C_{t_1} = \exp (-\Sigma \lambda)(t_2 - t_1) \quad (5)$$

However, if one needs to consider multiple mechanisms that change with time, the use of CORRAL for even a single compartment becomes advantageous for the accuracy delivered.

15th DOE NUCLEAR AIR CLEANING CONFERENCE

Single Compartment Behavior of Particles Showing the Effects of Three Depletion Mechanisms - Natural Settling, Spray Washout and Internal Filtration

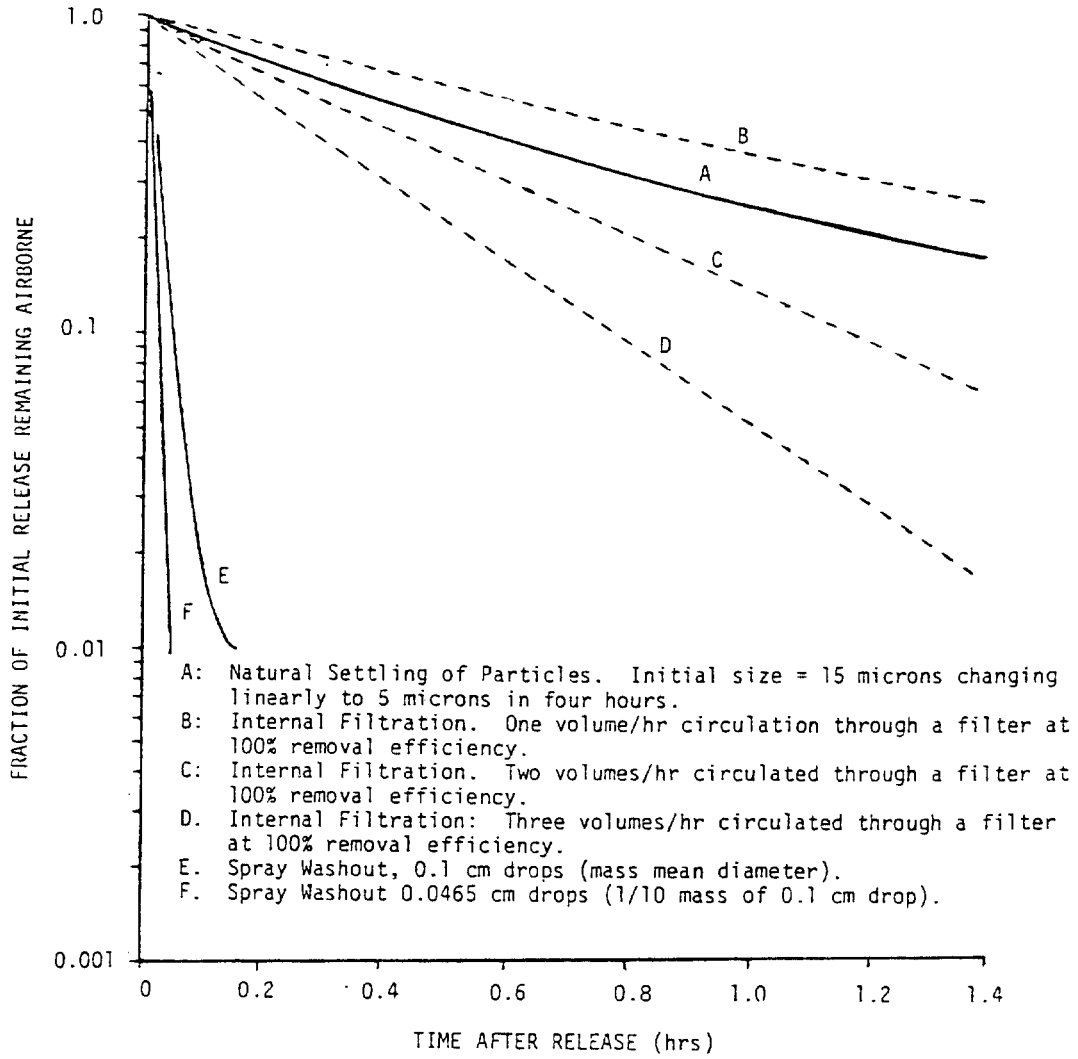


Figure 1

15th DOE NUCLEAR AIR CLEANING CONFERENCE

III.2 Elemental Iodine Behavior

Figure 2 is a plot similar to Figure 1 but for I_2 behavior in a single compartment. Curves A and B are $\log_{10}C/C_0$ versus time for natural deposition. The driving force for depletion is the bulk gas wall temperature difference and is modeled by equation (1). Here the typical initial temperature differences were 60°F and 30°F respectively. These differences changed linearly to 0.1°F at one hour and remained there. Since this λ is proportional to the temperature difference to the $1/3$ or $1/4$ power, the difference between curves A and B is small. The average λ was generally of the order of one hr^{-1} for the first hour and gradually became less after that. Curve C shows that internal filtration at 1.2 hr^{-1} can equal typical natural deposition processes.

Curves D and E compare the pH 5-7 ($H = 200$) spray removal mechanism using equation (2) for two drop sizes: 0.1 cm and $.0465 \text{ cm}$. Here the drop diameter affects the λ in the exponent (Equation (2)) and the λ 's are about 5 and 18 respectively over the first hour. For $C/C_0 > 0.01$ the nonlinearity in curves D and E is due solely to changing compartment conditions. For $C/C_0 < .01$, the pseudoequilibrium conditions hold and this removal mechanism in these cases resulted in a fairly smooth transition at the cutoff point ($C/C_0 = .01$)

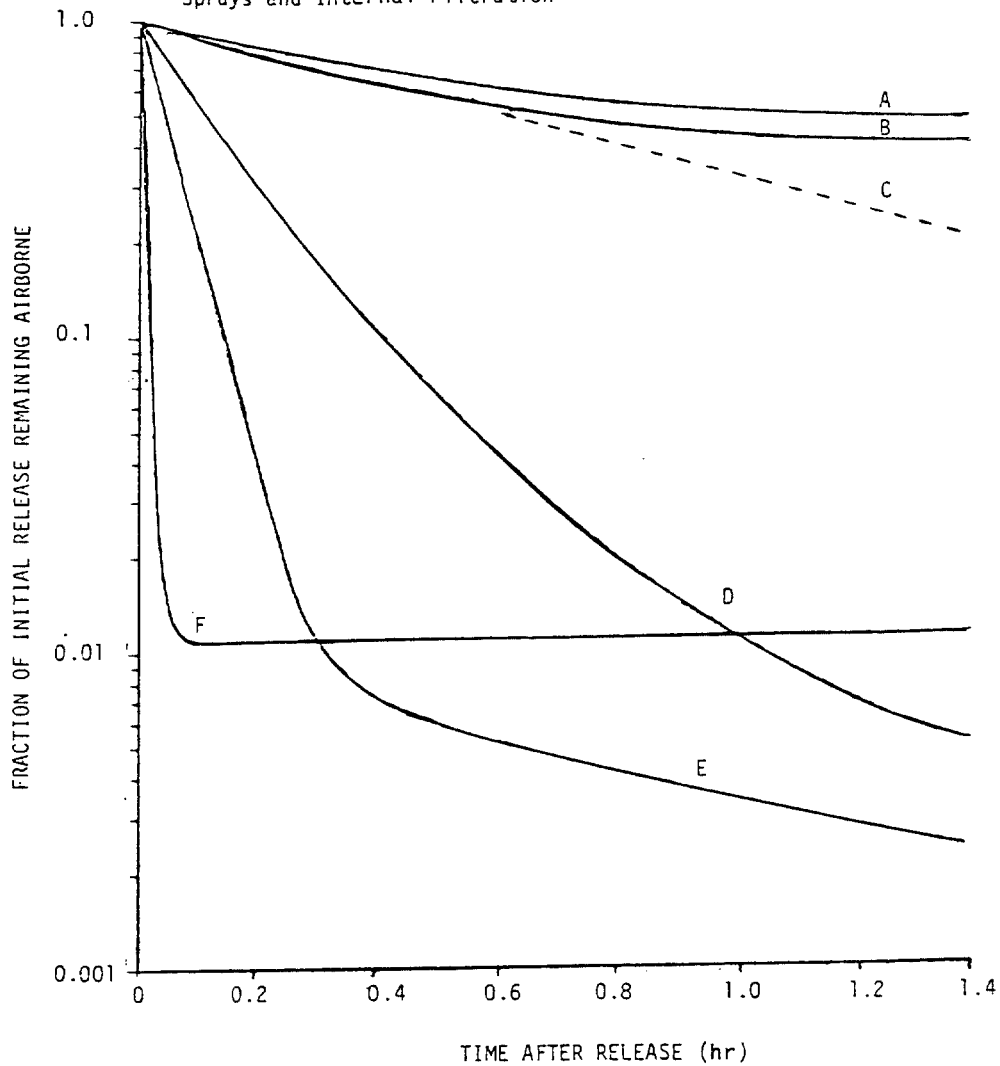
Curve F is like D except caustic (pH = 9) replaced the pH 5-7 spray. Here the resulting $\lambda = 125 \text{ hr}^{-1}$ until the cutoff $C/C_0 = .01$. At that point the removal halts for 100 minutes and then the pseudoequilibrium condition begins to remove I_2 slowly. The net effect is that the neutral and caustic sprays produce identical C/C_0 conditions at one hour via much different paths. This can greatly affect net fission product losses, depending on when the leakage occurs to the environment.

Again, as with sprayed particles, combined mechanisms can be handled by just adding component λ 's together. In the case of combined natural deposition and sprays, it can be argued that spraying negates the other. This would seem to be so if the sprays destroyed the temperature difference driving force as well as convective flow patterns. In the comparison here, any natural deposition can be neglected in terms of the overwhelming spray washout.

The use of CORRAL for I_2 washout can easily give more accurate answers than using average λ 's over large time periods. This is particularly important if the containment system is breached and the airborne contents (if under positive pressure) can directly puff to the environment. Average λ 's could give airborne concentrations that are more than 50% in error if the λ is averaged over one or more hours.

15th DOE NUCLEAR AIR CLEANING CONFERENCE

Single Compartment Behavior of Molecular Iodine (I_2) Showing Effects of Three Depletion Mechanisms - Natural Deposition, Spray Washout with Neutral or Boric Acid and with Caustic Sprays and Internal Filtration



Legend:

- A. Natural Deposition: Driving force temperature difference initially 30°F falling linearly to 0.1°F on one hour.
- B. Natural Deposition. Driving force initially 60°F falling linearly to 0.1°F in one hour.
- C. Internal Filtration. One volume/hour circulated through a filter at 100% removal efficiency.
- D. Spray Washout with neutral or boric acid sprays, 0.1 cm drops (mass mean diameter).
- E. Spray Washout with neutral or boric acid sprays, 0.0465 cm drops.
- F. Spray Washout with caustic pH = 0.5, 0.1 cm drops.

Figure 2

15th DOE NUCLEAR AIR CLEANING CONFERENCE

IV. Multicompartment Application in a Complex Postulated Accident

The CORRAL code was used as part of the accident analysis of N Reactor. One of the postulated accidents is a fuel ejection accident.

N Reactor differs significantly from commercial reactors in that it's core is composed of metallic fuel elements which lie in 1003 horizontal pressure tubes inside a graphite moderator which measures 39'-5" by 33'-0" by 33'-4 1/2". Water is circulated through the pressure tubes at high pressure which cools the fuel elements.

The N Reactor confinement Model used by the CORRAL code is shown in Figure 3 having the reactor core surrounded by the 105-N building front and rear compartments. An adjacent 109-N building pipe space and steam generator cells are connected to the 105-N building rear compartment by atmospheric flow paths. A flow path through filters and out an elevated stack is shown leading from the 105-N building front compartment.

The fuel ejection accident assumes the front nozzle of a single pressure tube fails and fuel is discharged from the pressure tube into 105-N building front by the primary coolant back pressure. A single fuel element is assumed to lodge in piping or structure where it is uncooled by fog sprays or contact with the floor.

The confinement building is pressurized as shown in Figure 4, to a peak pressure of 0.6 psig by steam flashing to hot water from the nozzle discharge. The sequence of events of the confinement are tabulated in Table 1. The rate of condensation by the fog sprays increase as steam is dispersed throughout the building until the pressure falls to 3 inches W.C. after 20 minutes and flow is established through filters and out a 230 ft. stack.

Building leakage also occurs during the pressurization and filter release stages of the accident. The leakage rate is assumed to be 200 cfm at a corresponding pressure of 0.1 inch W.C. The leakage rate was assumed to be proportional to the square root of the confinement atmospheric pressure and proportional to the volume of each compartment.

The total release during the filtered release stage is equal to the pool displacements from the fog sprays and nozzle spills. The building leakage rate is 5 percent of the total release rate and is also assumed proportional to the compartment volumes.

Fission products are released from the uncooled fuel element beginning 292 seconds after the accident and are completely released after 468 seconds.

CORRAL CONFINEMENT MODEL

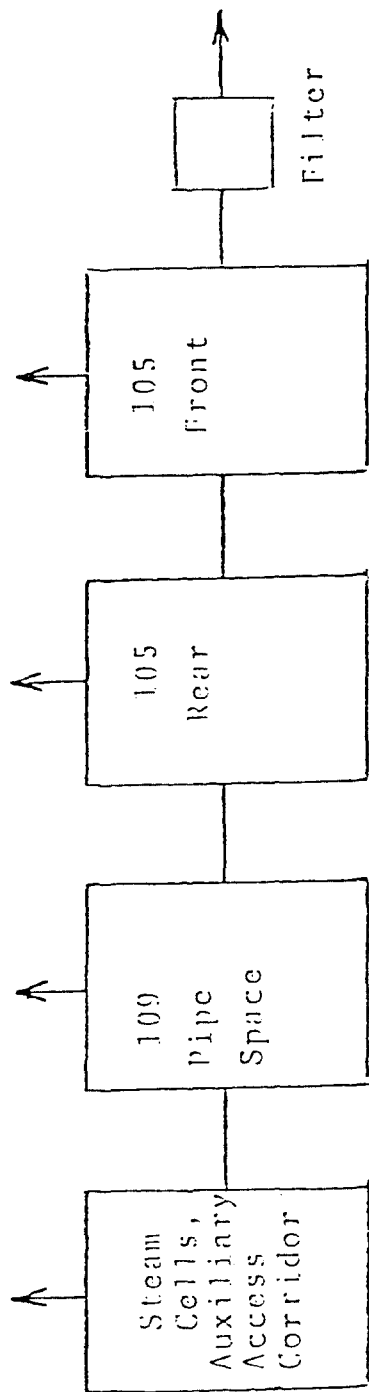


Figure 3

FUEL EJECTION ACCIDENT CONFINEMENT PRESSURE
VERSUS TIME

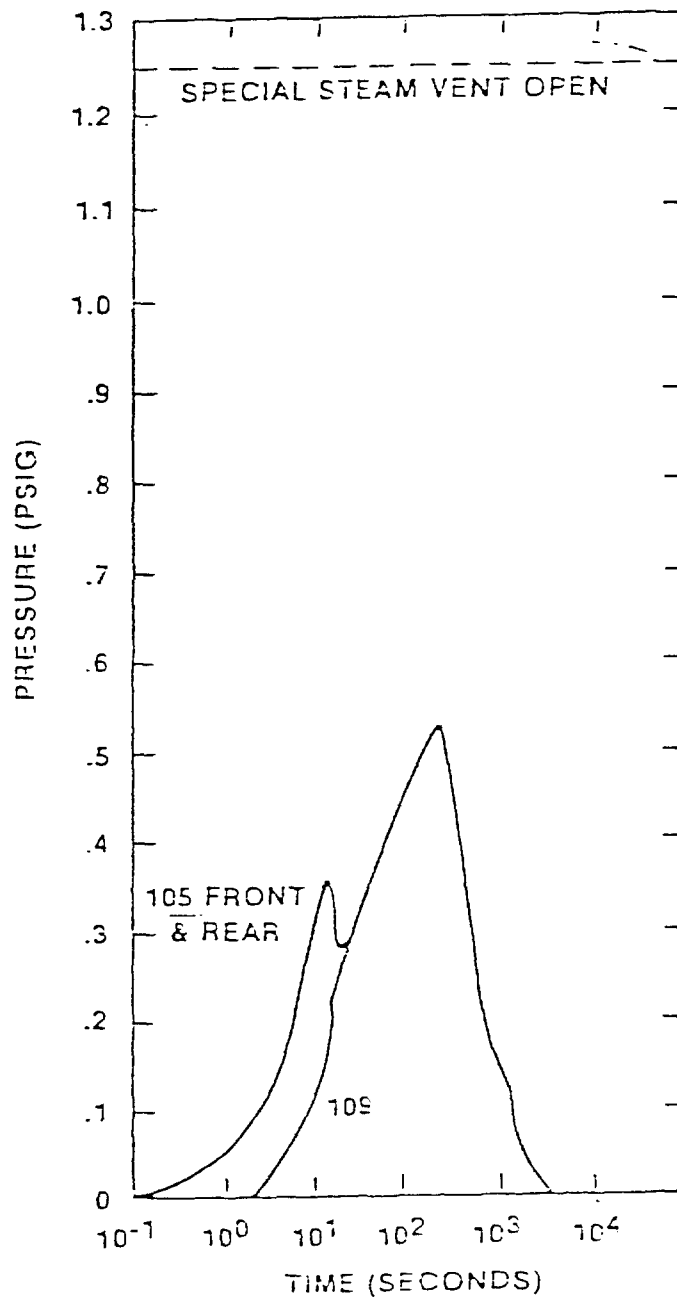


Figure 4

15th DOE NUCLEAR AIR CLEANING CONFERENCE

TABLE I
SEQUENCE OF EVENTS
FUEL EJECTION ACCIDENT

<u>Time (Sec)</u>	<u>Event</u>
0	Front nozzle fails and fuel is ejected.
0.5	Flow monitor actuates low flow trip.
0.7	Insertion of control rods begins.
2.2	Control rods 90 percent inserted.
2.5	105-N confinement trip at set pressure of 2 inches w.g.
3.5	105-N Zone I ventilation exhaust valves closes to 80 degrees
4.5	105-N Zone I ventilation supply valves closes to 80 degrees.
7.0	109-N confinement trip at set pressure of 2 inches w.g.
12.0	109-N ventilation exhaust and supply valves close.
15.0	Fog sprays in 105-N come on at 12 inches w.g.
56.7	Fog sprays in 109-N come on at 10 inches w.g.
280.0	Peak confinement pressure of 0.54 psig reached.
292.0	Ejected fuel begins to fail and release fission products to confiner atmosphere.
468.0	Fuel failure ends and no more fission products are released to confiner atmosphere.
1100.0	105-N Zone I exhaust valves open at 3 inches w.g. and filtered flow is established at 1740 cfm with a leak rate of 87 cfm.

15th DOE NUCLEAR AIR CLEANING CONFERENCE

The fog sprays consist of two nozzle types in the 105-N building and a third type in the 109-N building. Table 2 gives a breakdown of flows, fall heights and droplet sizes which represent the fog spray system for the accident analysis.

The compartment volumes, wall areas and floor areas are shown in Table 3. The compartment air temperatures are assumed to be ambient and the differential temperature between the compartment air and walls is 0.1°F for times greater than 2 hours after the accident.

The washout and plateout of elemental and particulate iodine is shown in Figure 5 as a function of time for unit amounts of elemental and particulate iodine released to the confinement atmosphere.

The fraction of noble gas and methyl iodine contained in the confinement atmosphere versus time is shown in Figure 6. Similarly, the fractions of elemental iodine and particulates are shown in Figures 7 and 8 respectively.

The removal of elemental iodine and particulate iodine by the filters is 95 percent and 99.95 percent respectively. No removal of noble gas or methyl iodine by the filter was assumed. The fraction of noble gas and methyl iodine, elemental iodine and particulate iodine, released to the atmosphere from filtered release are shown in Figures 9 through 11 respectively.

Similarly, the release by building leakage to the atmosphere is shown for noble gas and methyl iodine, elemental iodine and particulates in Figures 12 through 14 respectively.

It is evident in Figures 5 and 6 that the fog sprays and plateout of N Reactor are effective in removing iodine from the confinement atmosphere. The elemental iodine decreases to about 2 percent of the original value in about 1 hour. The removal of particulates is almost instantaneous. These removal mechanisms for iodine and particulates show a significant decrease in the building release fractions compared to the noble gas release. A similar comparison is seen for the filtered release where the filter removals are also factored into the results.

The results of the releases to the atmosphere versus time were used to calculate accident doses for individual isotope releases to the confinement atmosphere. Appropriate depletion by radioactive decay during holdup on the confinement building was taken into account to arrive at release rates of isotopes as a function of time which were used to calculate doses.

15th DOE NUCLEAR AIR CLEANING CONFERENCE

Table 2 Fog Spray Parameters for Fuel Ejection Accident

<u>Compartment</u>	<u>Spray Height (ft)</u>	<u>Drop Diam. (ft)</u>	<u>Spray Flow Rate (lb/sec)</u>
105-N front	74.5	0.043	42.24
105-N front	74.5	0.055	0.0
105-N front	18.0	0.043	309.76
105-N front	18.0	0.055	0.0
105-N rear	8.0	0.043	21.12
105-N rear	8.0	0.055	81.01
105-N rear	74.0	0.043	178.34
105-N rear	74.0	0.055	324.04
105-N rear	20.0	0.043	152.53
105-N rear	20.0	0.055	253.15
109-N pipe space	51.0	0.0665	152.73

Table 3 Compartment Volumes, Wall and Floor Areas of CORRAL Confinement Building Model

<u>Compartment</u>	<u>Volume (ft³)</u>	<u>Wall Area (ft²)</u>	<u>Floor Area (ft²)</u>
105-N front	3.58 x 10 ⁵	4.2 x 10 ⁴	8.5 x 10 ³
105-N rear	3.92 x 10 ⁵	4.7 x 10 ⁴	7.2 x 10 ³
109-N pipe space	7.22 x 10 ⁵	7.6 x 10 ⁴	1.39 x 10 ⁴
109-N steam gen. cells, aux. cell and access corridor	1.51 x 10 ⁶	1.39 x 10 ⁵	2.0 x 10 ⁴

15th DOE NUCLEAR AIR CLEANING CONFERENCE

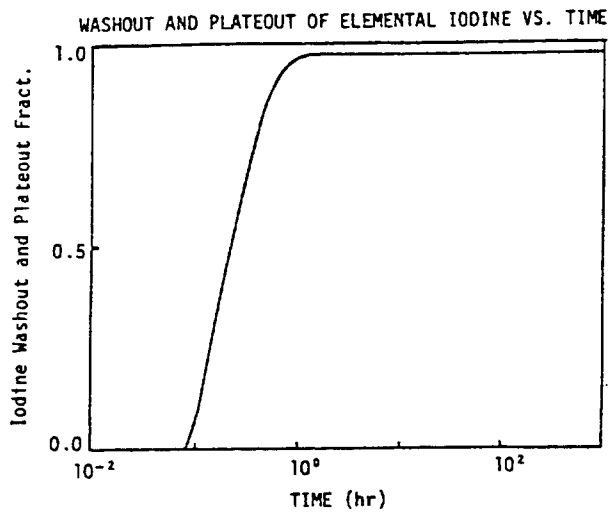


FIGURE 5

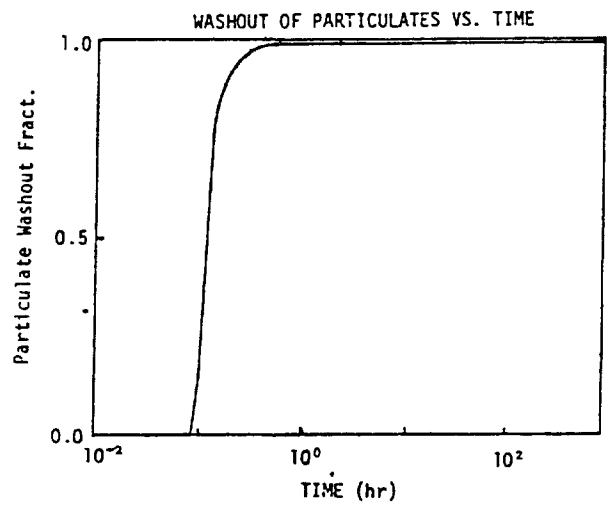


FIGURE 6

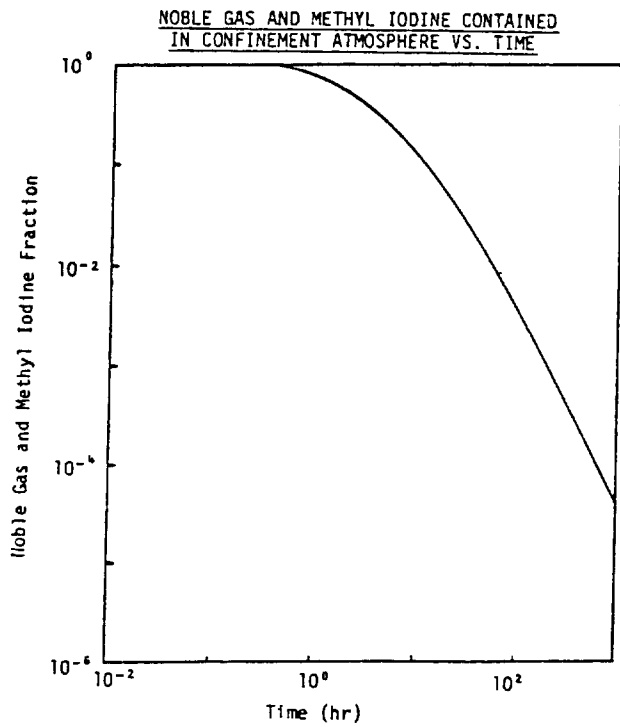


FIGURE 7

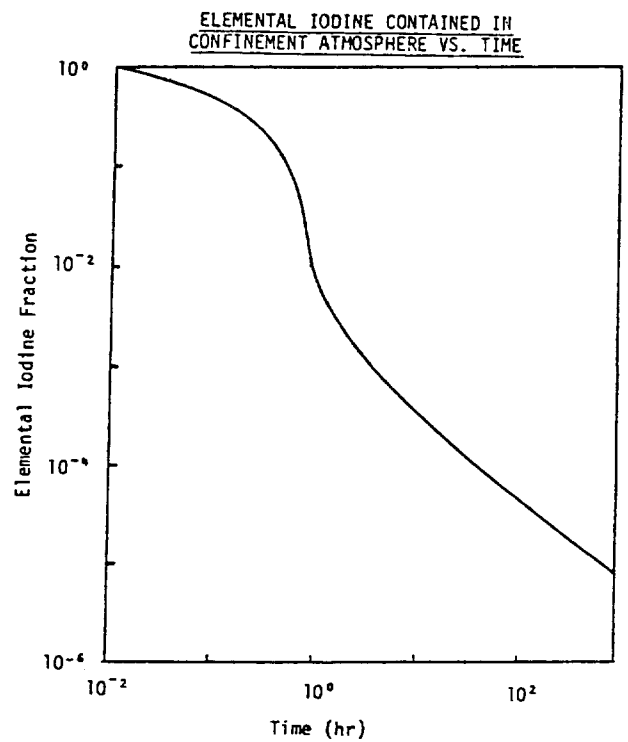


FIGURE 8

15th DOE NUCLEAR AIR CLEANING CONFERENCE

PARTICULATES CONTAINED IN CONFINEMENT
ATMOSPHERE VS. TIME

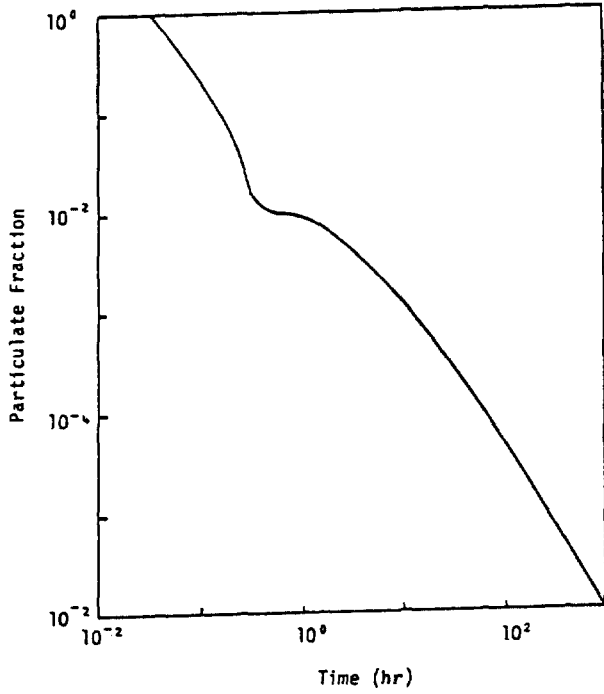


FIGURE 9

RELEASE OF NOBLE GAS AND METHYL IODINE
THROUGH FILTERS VS. TIME

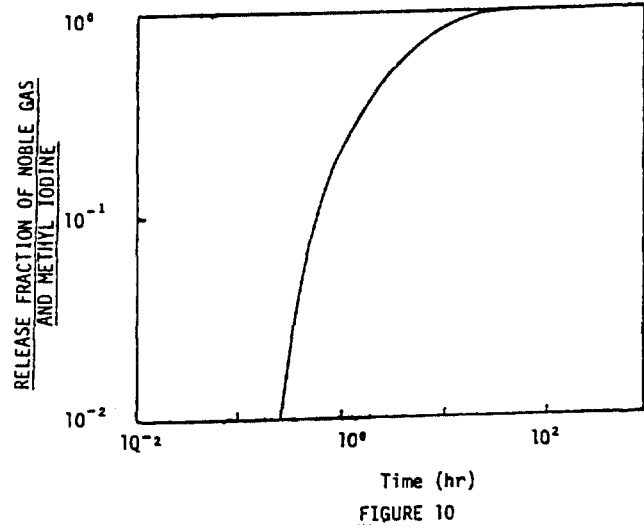


FIGURE 10

RELEASE OF ELEMENTAL IODINE THROUGH
FILTERS VS. TIME

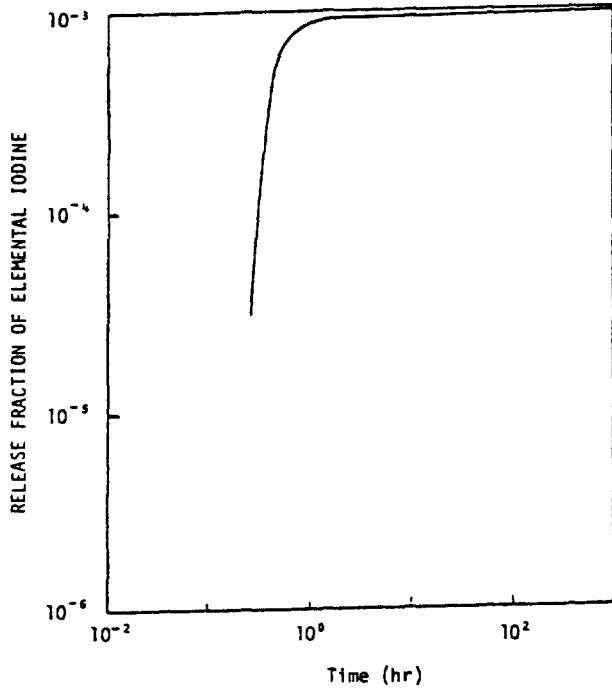


FIGURE 11

RELEASE OF PARTICULATES THROUGH
FILTERS VS. TIME

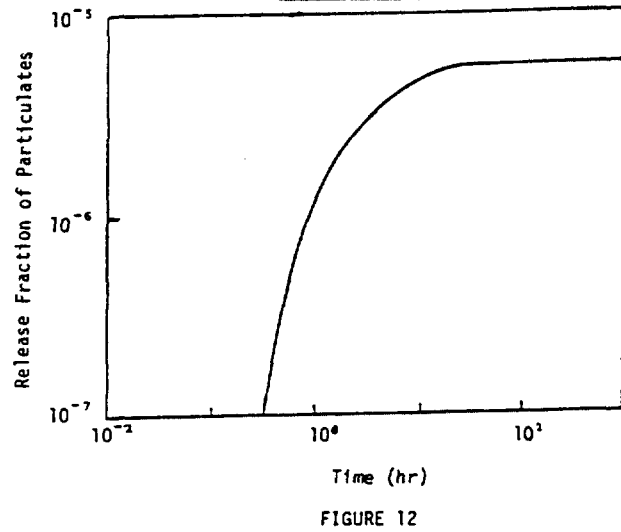


FIGURE 12

15th DOE NUCLEAR AIR CLEANING CONFERENCE

RELEASE OF NOBLE GAS AND METHYL IODINE THROUGH BUILDING LEAKAGE VS. TIME

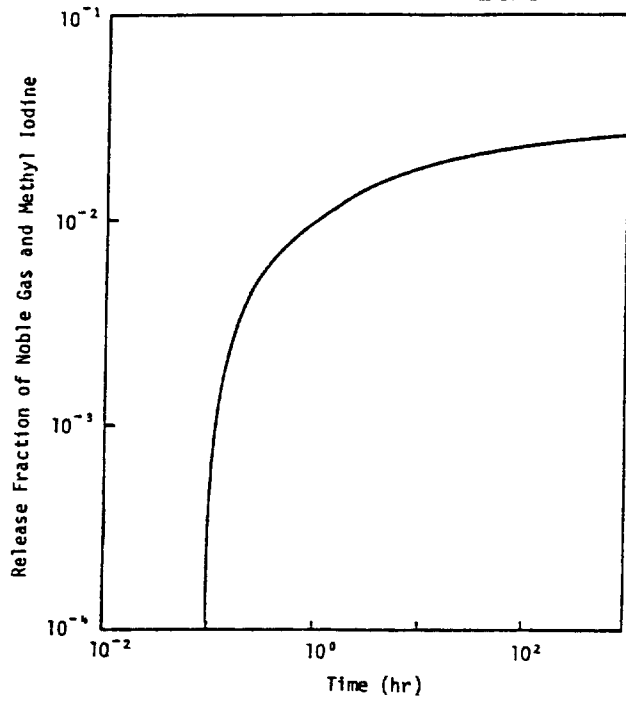


FIGURE 13

RELEASE OF ELEMENTAL IODINE THROUGH BUILDING LEAKAGE VS. TIME

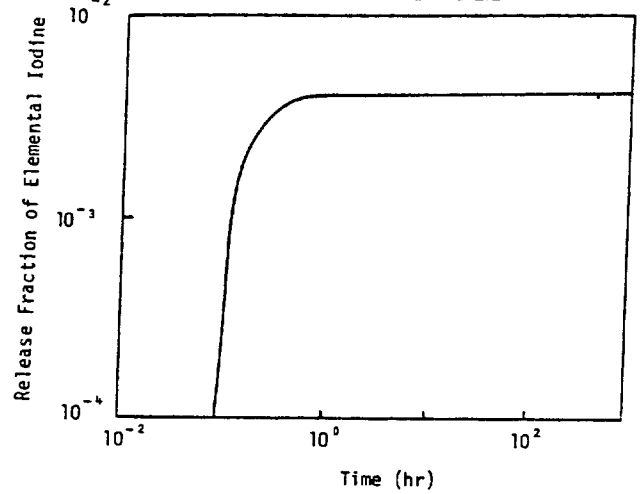


FIGURE 14

RELEASE OF PARTICULATES THROUGH BUILDING LEAKAGE VS. TIME

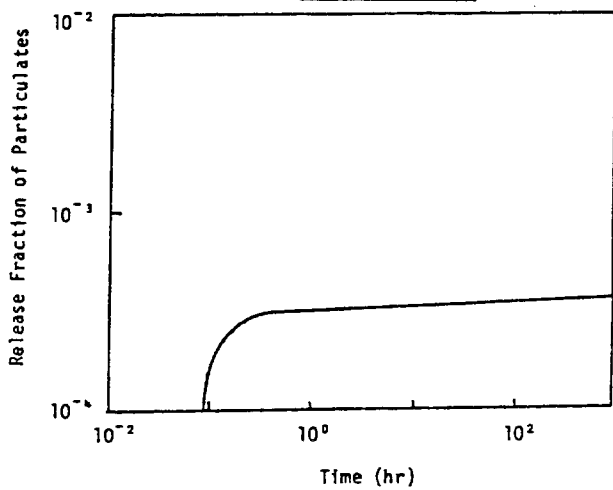


FIGURE 15

15th DOE NUCLEAR AIR CLEANING CONFERENCE

References

- (1) A.K. Postma, P.C. Owzarski, and D.L. Lessor, "Transport and Deposition of Airborne Fission Products in Containment Systems of Water Cooled Reactors Following Postulated Accidents," Appendix J of Appendix VII, WASH-1400 (Nureg 75/014), U.S. Nuclear Regulator Commission, October 1976.
- (2) A.K. Postma and W.F. Pasedag, "A Review of Mathematical Models for Predicting Spray Removal of Fission Products in Reactor Containment Vessels," BNWL-B-268, Battelle-Northwest, Richland, WA (1973).

DISCUSSION

ALVARES: Has there been any experimental verification of the model?

ROBLYER: Yes. The removal models in the CORRAL code are based on the work of A. K. Postma and W. F. Pasedag in WASH-1329 dated June, 1974. Their mathematical models were based on the Confinement Systems Experiment conducted on the Hanford Site.

SHAW: Would you explain the inverse relationship of particle radius for your spray efficiency and what is the average droplet size?

ROBLYER: The removal rate is proportional to the ratio of flow rate and drop diameter and is proportional to the droplet removal efficiency. The droplet diameters from the non-clogging nozzles at Hanford N Reactor range from 0.11 to 0.17 cm which is much larger than those of most commercial reactors.

SCHIKARSKI: The CORRAL code is a very nice tool to handle fission product transport problems. However, in its present state its treatment of the behavior of particulates is poor. It contains only the removal by wash-out and settling but neglects coagulation, diffusion, and thermophoresis. Therefore, it underestimates particulate removal by orders of magnitude. Are you going to improve the code in that respect?

ROBLYER: We have no plans to incorporate these models into the CORRAL code because the dose from particulates is relatively small for our problems. However, I am sure that Dr. Owzarski, who now works for Pacific Northwest Laboratories in Richland, Washington, could incorporate these models into the CORRAL code to suit your individual needs.

15th DOE NUCLEAR AIR CLEANING CONFERENCE

SESSION V

ADSORBENTS AND ABSORBENTS

Tuesday, August 8, 1978

CHAIRMEN: R. D. Rivers, C. A. Burchsted

- CONFIRMATORY RESEARCH PROGRAM--EFFECTS OF ATMOSPHERIC CONTAMINANTS ON COMMERCIAL CHARCOALS
R. R. Bellamy, V. R. Deitz
- A NON-RADIOACTIVE DETERMINATION OF THE PENETRATION OF METHYL IODIDE THROUGH IMPREGNATED CHARCOALS
J. B. Romans, V. R. Deitz
- EFFECT OF PORE STRUCTURE ON THE ACTIVATED CARBON'S CAPABILITY TO SORB AIRBORNE METHYL RADIODIODE
A. J. Juhola, J. V. Friel
- METHYL IODIDE RETENTION ON CHARCOAL SORBENTS AT PARTS-PER-MILLION CONCENTRATIONS
G. O. Wood, C. A. Kasunic
- EVALUATION AND CONTROL OF POISONING OF IMPREGNATED CARBONS USED FOR ORGANIC IODIDE REMOVAL
J. L. Kovach, L. Rankovic
- A DETERMINATION OF THE ATTRITION RESISTANCE OF GRANULAR CHARCOALS
V. R. Deitz
- THE DEVELOPMENT OF Ag^0Z FOR BULK ^{120}I REMOVAL FROM NUCLEAR FUEL REPROCESSING PLANTS AND PbX FOR ^{120}I STORAGE
T. R. Thomas, B. A. Staples,
L. P. Murphy
- RADIATION-INDUCED IODINE MIGRATION IN SILVER ZEOLITE BEDS
A. G. Evans
- OPERATIONAL MAINTENANCE PROBLEMS WITH IODINE ADSORBERS IN NUCLEAR POWER PLANT SERVICE
C. E. Graves, J. R. Hunt, J. W. Jacox,
J. L. Kovach
- AECL IODINE SCRUBBING PROJECT
D. F. Torgerson, I. M. Smith
- DETERMINATION OF THE PHYSICO-CHEMICAL ^{131}I SPECIES IN THE EXHAUSTS AND STACK EFFLUENT OF A PWR POWER PLANT
H. Deuber, J. G. Wilhelm

15th DOE NUCLEAR AIR CLEANING CONFERENCE

CONFIRMATORY RESEARCH PROGRAM - EFFECTS OF ATMOSPHERIC CONTAMINANTS ON COMMERCIAL CHARCOALS *

Ronald R. Bellamy
U.S. Nuclear Regulatory Commission
Washington, D.C. 20555

Victor R. Deitz
Naval Research Laboratory
Washington, D.C. 20315

ABSTRACT

The increased use of activated charcoals in engineered-safety-feature and normal ventilation systems of nuclear power stations to continually remove radioiodine from flowing air prior to release to the environment has added importance to the question of the effect of atmospheric contaminants on the useful life of the charcoal. In January of 1977 the Naval Research Laboratory (NRL) began an investigation** to determine the extent to which atmospheric contaminants in ambient concentrations degrade the efficiency of various commercially-available charcoals for removing methyl iodide. A report summarizing the FY77 effort has been published as NUREG/CR-0025, "Effects of Weathering on Impregnant Charcoal Performance."⁽¹⁾ This paper will briefly summarize that report and present the results available from the FY78 investigations.

The approach employed by NRL is two-fold. First, charcoal samples are exposed to unmodified outdoor air for periods of one to nine months, then examined for methyl iodide retention, increase in weight, and the pH of water extract. The atmospheric contaminants are identified by the NRL Air Quality Monitoring Station, and concentrations of the various contaminants (ozone, SO₂, NO₂, CO₂, methane and total hydrocarbons) are also available. Moisture content data is obtained from a neighboring station (Washington National Airport) of the U.S. Department of Commerce. Second, additional charcoal samples are exposed to the same pollutants under controlled laboratory conditions in various pollutant combinations.

Results from FY77 indicate that the water vapor-charcoal interaction is an important factor in the degradation of the commercial charcoals. Laboratory results indicate the pollutant sulfur dioxide plus water vapor can result in significant charcoal deterioration, as did ozone plus water vapor. Conversely, carbon monoxide did not appear to affect the charcoal. Also, differences were observed for various charcoals. The FY78 laboratory work will expand the pollutants to include a hydrocarbon mixture, use various concentrations of pollutants, verify differences in charcoals, and attempt to determine if the effects are because of the base charcoal, the impregnation, or both.

*Paper to be presented at the 15th DOE Air Cleaning Conference, Boston, Mass, August 7-10, 1978.

**Work performed under contract for the U.S. Nuclear Regulatory Commission under Interagency Agreement No. AT(49-24)-9006.

15th DOE NUCLEAR AIR CLEANING CONFERENCE

The outdoor exposures at NRL consider the integrated and accumulative effect of the pollutants. FY77 results indicate more degradation after three months than after one month exposure for the same charcoal; FY78 results will extend the exposure time to nine months for various charcoals. FY77 preliminary results indicate two different charcoals differ in their ability to survive the weathering process over time; FY78 results will include up to twelve different charcoals.

This paper will discuss the progressive effect of the pollutants through the charcoal bed. Both the laboratory and outdoor samples were layered to allow analysis of weight increase, methyl iodide removal, and pH of water extract as a function of bed depth. These results on exposed charcoals are compared to the known semi-logarithmic dependence of decrease in penetration with increased bed depth for unexposed charcoals.

This paper will also present the proposed scope of work for the remainder of FY78 and FY79, including a discussion of plans to examine the weathering effects exhibited by spent charcoals of known history from power reactors.

I. INTRODUCTION

The impregnated activated carbon installed in engineered-safety-feature and normal ventilation systems at nuclear power stations to remove radioiodine prior to release to the environment will not adsorb radioiodine indefinitely. The active sites on the carbon surface have a finite capacity for adsorption, and once that capacity is reached, the carbon is saturated and will no longer remove radioiodine from flowing air. The adsorption sites can be blocked by atmospheric contaminants, quickly destroying the adsorption capacity of the carbon. Commonly termed "weathering", there has not been (as of January 1977) an in-depth engineering analysis of the problem, to determine the extent to which atmospheric contaminants in ambient concentrations degrade the efficiency of various commercially - available charcoals for removing radioiodine. Recognizing this deficiency, the U.S. Nuclear Regulatory Commission contracted with the Naval Research Laboratory to perform such confirmatory research. Results on various carbons are not to be interpreted as a recommendation of any manufacturer's carbon, but are presented to illustrate the effect of the carbon base and impregnant. This paper will discuss the results obtained to date, the work in progress, and the experiments planned for the remainder of the fiscal year, 1978, and 1979.

A two-fold approach has been undertaken to obtain the necessary data. First, charcoal samples are exposed to unmodified outdoor air for various periods of time, and then examined for changes in methyl iodide retention capability, weight and pH of water extract. This approach allows no control over the concentration or type of atmospheric contaminant. Second, additional charcoal samples (of the same charcoal as used for the outdoor exposures) are exposed to the same pollutants under controlled laboratory conditions in various pollutant combinations. This approach allows pollutant types, concentrations, and combinations to be varied and controlled under the discretion of the investigator.

II. Accomplishment in Fiscal Year 1977

There are two elements of the procedure for analysis of weathered samples that can significantly affect the results and conclusions, yet are unrelated to the weathering phenomenon. The first is related to the preparation of weathered samples for subsequent laboratory analysis for methyl iodide retention, the second is related to the laboratory procedures employed for the methyl iodide retention analysis.

15th DOE NUCLEAR AIR CLEANING CONFERENCE

There are three methods available for preparation of weathered samples for laboratory methyl iodide analysis:

- A. The weathered samples are prepared in four separate layers, each 4 inches in diameter and 0.5 inches high. Each layer may be tested separately and independently by transferring each layer (with mixing) to a test canister 2 inches in diameter and 2 inches high.
- B. One-fourth of each layer of the weathered sample can be used to construct a test bed in which the same sequence of entrance to exit is preserved in the bed, again yielding a test canister 2 inches in diameter and 2 inches high.
- C. Examine the weathered sample without removal of the charcoal from the exposure configuration. This requires exposure canisters 2 inches in diameter and 2 inches high which are presently being fabricated.

The preferred procedure depends on the information that is desired. Procedure A yields information on the gradient within the bed brought about by weathering, while Procedures B and C yield information on the lifetime of the exposed carbon. Results to date have been determined using Procedure A, in order to elicit as much information as possible from one weathering exposure.

The second element that will effect the results but is not directly associated with the weathering phenomenon is the laboratory procedure employed for the methyl iodide retention analysis. Testing procedures are being established by the American Society for Testing and Materials⁽²⁾ (ASTM) for both new (unexposed) and weathered carbons. For laboratory determination of methyl iodide penetration for new carbons, the test temperatures, relative humidities and periods of equilibration (with water vapor), feed (with methyl iodide), and purge (with air) are well-defined. However, the proposed procedures for testing of weathered carbons are only preliminary, and are being tried in various laboratories today.

As Table 1 illustrates, for new carbons there is considerably less penetration without prehumidification (the charcoals performed better). This effect is reversed for exposed carbons, as the prehumidification period cleans and regenerates the carbon, leading to better performance with prehumidification. Accordingly, the proposed ASTM procedures recommend static temperature equilibrium with no flow. This results in temperature excursions of 20°C or more when the 95% RH air enters the charcoal bed, due to the heat of adsorption.⁽³⁾ To obtain consistent results, NRL weathered samples are today being prehumidified for 1 hour or until the temperature rise is less than 1°C.

An alternate procedure under investigation is to statically equilibrate the carbon in an oven containing a water source until the carbon has adsorbed sufficient moisture to eliminate any significant temperature excursion.

A. Exposures To Outdoor Air

In FY77 there were 8 different commercially-available charcoals weathered on the roof of the NRL Chemistry Building. Most of those were only exposed for one month, however, there were two carbons exposed for periods of one, two, and three months to examine accumulative effects. Samples of the same charcoal were exposed for various one-month periods to analyze monthly weathering variations, and different charcoals were exposed for the same one-month period to begin an analysis of the effect of the base material and impregnant complex. FY77 results will be briefly

15th DOE NUCLEAR AIR CLEANING CONFERENCE

TABLE 1

METHYL IODIDE PENETRATION FOR NEW COCONUT-BASE
COMMERCIAL CHARCOALS AT 21°C

	Nominal Size	Water Extract pH	Penetration, %	
			Prehumidification 16 Hours	None
BC 717	8 X 16	9.5	0.99	0.05
BC 727	8 X 16	9.5	4.8, 4.0	0.014
MSA 463563	8 X 16	8.5	2.5	0.13
NACAR G-615	8 X 16	9.8	0.27, 0.23	0.05
NACAR G-617	8 X 16	9.3	3.8	0.1
NACAR G-617-A	8 X 16	9.3	5.7	0.07

discussed to aid in the explanation of the work in progress and future plans.

The two charcoals for periods one, two and three months were Barnebey-Cheney BC-727 (cocoanut base with KI impregnant) and North American Carbon NACAR G-615 (cocoanut base with KI and TEDA impregnant).

The entrance layer showed the greatest degradation for all tests, both in a higher penetration of methyl iodide and a lower pH of the water extract.⁽⁴⁾ The charcoal in the three subsequent layers exhibited less penetration than the first layer, indicating the initial layer acting as a guard bed. However, there is no monotonic decrease in penetration with the bed depth, as experienced for unexposed charcoals. Of these two charcoals, NACAR G-615 performed better than BC-727 for the same exposure period (Table 2). Additional tests are required before the role of the impregnation complex can be identified with confidence. Also, an increase in exposure time resulted in greater penetration for the first bed layer, but not always in subsequent layers. In general the longer exposure time did weather the entire bed to a greater extent. These results are presented in Table 2.

Identical charcoals exposed different months showed that dryer months result in less weathering than wet months. It is not clear if this effect can be attributed to the total water vapor content during the month, or the water vapor content during the last 2-3 days prior to termination of weathering. It is planned to study this effect in the laboratory under controlled conditions.

15th DOE NUCLEAR AIR CLEANING CONFERENCE

TABLE 2

GRADIENTS IN THE PENETRATIONS (P) OF METHYL IODIDE AND THE pH OF WATER EXTRACTS AFTER 1, 2, AND 3 MONTHS EXPOSURE

Exposure	First Layer		Second Layer		Third Layer		Fourth Layer			
	pH	P	pH	P	pH	P	pH	P		
NACAR G-615										
5016	1	month	9.3	1.77	9.5	0.64	9.6	0.34	9.7	0.70
5031	2	"	8.2	3.42	9.8	1.32	10.0	0.86	10.0	1.02
5022	3	"	7.5	8.62	9.8	1.38	10.0	1.19	10.0	0.81
BC 727										
5014	1	month	8.8	2.67	9.3	1.20	9.3	0.68	9.3	1.31
5032	2	"	7.3	5.81	9.3	2.58	9.5	3.09	9.5	3.45
5020	3	"	7.0	21.6	9.4	5.4	9.5	5.0	9.5	5.7

Available data for pollutant concentrations at NRL were obtained from the NRL Air Quality Monitoring Station. The pollutants identified and the range of monthly average concentrations include ozone (0.007 to 0.04 volume parts per million), sulfur dioxide (0.020 to 0.052 ppm), nitrogen dioxide (0.018 to 0.12 ppm), total hydrocarbons (1.8 to 3.1 ppm), methane (1.5 to 2.5 ppm), and carbon monoxide (0.6 to 1.9 ppm). For one-month continuous exposures these concentrations yield integrated insults on the order of hundredths of grams (see Table 18 in Reference 1).

B. Laboratory Exposures

Concentrations of pollutants for laboratory exposures were chosen in an attempt to represent the magnitudes prevalent in the outdoor exposures. Water vapor was added since in magnitude the water vapor constituent is present in far greater amounts than any other pollutant (kilograms for 100-hour exposures compared to grams for one-month exposures). Of the many possible combinations of pollutants to study, FY77 work was limited to single component (water vapor) weathering or binary mixtures (water-vapor plus contaminant). In addition, only two charcoals (BC-727 and NACAR G-615) have been examined.

Testing with water vapor as the only pollutant was performed at 50, 70 and 90% RH. The carbons increased in weight by approximately 50% after 100 hours exposure. Significant penetrations of methyl iodide were observed, as high as 16% for the entrance layer of BC 727; pH of water extract values did not drop significantly. In the cases evaluated, the NACAR G-615 carbon performed better than the BC-727

15th DOE NUCLEAR AIR CLEANING CONFERENCE

carbon (Table 9a in Reference 1), but these are only two of the carbons to be tested, and no conclusion as to a more suitable carbon or impregnant can be made at this time.

A water vapor (70 and 90% RH) plus sulfur dioxide (0.5 ppm SO₂) combination was used to weather the two carbons for 100 hours. In all cases, no sulfur dioxide was evident in the exit gases from the test bed, and the penetrations of methyl iodide (as high as 66% for the first layer) and the pH of water extract values (as low as 2.7 for the first layer) indicate drastic deterioration of the carbon. Total SO₂ insult was determined to be approximately 0.75 gm, which is significantly higher (by approximately a factor of 10) than expected due to ambient concentrations. Future work will attempt to reach the expected ambient concentration in the insult mixture.

Similarly to sulfur dioxide, no ozone was detected in the exit gases when 1-3 ppm were combined with 70 and 90% RH air. High penetrations for methyl iodide were observed (as high as 21.5% for the fourth layer), but pH values were not significantly affected (Table 9b of Reference 1). Lower inlet concentrations will be achieved in future work.

Converse to sulfur dioxide and ozone, carbon monoxide (2.5 ppm in 90% RH air), passed through the charcoal unadsorbed. No change in carbon monoxide concentration from inlet to outlet of the test bed was observed.

In summary, the laboratory results obtained in FY77 show that the three pollutants water vapor, water vapor plus sulfur dioxide, and water vapor plus ozone degrade the two charcoals significantly in a short time, while carbon monoxide showed no degradation of the carbon.

III. Work in Progress and Results

Present efforts are directed towards weathering various carbons to outdoor exposures and to laboratory pollutant mixtures.

A. Exposures to Outdoor Air

Outdoor exposures are obtained by drawing air through the carbon samples as explained in Reference 1. The number of independent exposure positions has been increased to allow 12 samples to be weathered simultaneously.

Table 3 indicates the entire outdoor weathering program under evaluation. Entries in the table indicate the number of repetitive samples for the same charcoal that will be exposed for each time period listed, and entries in parentheses indicate that the exposures have not been completed.

Partial results are available for those samples that have completed their outdoor exposures in FY78. Values of the pH of water extract have been determined, but penetrations of methyl iodide are not yet available due to the procedural questions of equilibration for laboratory methyl iodide determinations as previously discussed in Section II of this paper. These results covering the NRL progress in FY78, will be published by December 1978.

Table 4 presents the results available on the two carbons BC 727 and NACAR G-615 that have been weathered for 6 months on the roof of the NRL Chemistry Building. The results for 1, 2, and 3 months from Table 2 are included for completeness. Using a lower pH value as indicating additional degradation, the monotonic decrease in expected carbon performance as exposure time increases is illustrated for the

15th DOE NUCLEAR AIR CLEANING CONFERENCE

TABLE 3

OUTDOOR WEATHERING PROGRAM

Exposure	EXPOSURE PERIOD, MONTHS				
	1	2	3	6	9
NACAR G-615	1	1	(4)	1	(1)
BC 727	(10)	2	1	1	(1)
SS 207	(5)	0	1	(1)	(1)
MSA 463563	2	0	1	1	(1)
2701	2	0	1	(1)	(1)
KITEG	1	0	1	(1)	(1)

Entries indicate the number of independent exposure periods.
 Parentheses indicate tests not completed.

first bed layer, but it appears that the pollutants are not reaching subsequent layers of the bed to any great extent (pH of water extract values for unweathered carbons are 9.8 for NACAR G-615 and 9.5 for BC 727). These conclusions should be substantiated when 9-month exposure data are available and when the penetrations of methyl iodide for the exposed carbons are available.

Table 4 also includes the available data for the carbon MSA 463563. The indicated degradations for 3 and 6 months are values obtained during FY78; 1 month values are included for completeness from Reference 1. The expected increase of degradation with increased weathering time is observed, and it also appears that the pollutants are reaching the second layer to a significant degree after 6 months exposure (initial pH of water extract for unexposed MSA 463563 is 8.5). Results for 9 month exposures and for all penetrations of methyl iodide will be published by December 1978.

Three month outdoor exposures have also been completed for Sutcliffe Speakman 207B plus 5% TEDA (coal based, with an initial pH of water extract of 8.8), and KITEG (initial pH of 8.2). These results are presented in Table 5, including the 3-month data for NACAR G-615 and BC 727, to illustrate the effect of the carbon base, the impregnant, and the effect of the type of exposure (winter versus summer, wet versus dry period).

The meteorological conditions and pollutants, and the additional penetration of methyl iodide data will be published when available. The results presented for carbons MSA 463563 and 2701 are for the same exposure period, and for carbons Sutcliffe Speakman and KITEG are for the same exposure period.

15th DOE NUCLEAR AIR CLEANING CONFERENCE

TABLE 4

GRADIENTS IN THE PENETRATIONS (P) OF METHYL IODIDE AND THE pH OF WATER EXTRACTS AFTER 1, 2, AND 3 MONTHS EXPOSURE

Exposure	First Layer		Second Layer		Third Layer		Fourth Layer			
	pH	P	pH	P	pH	P	pH	P		
NACAR G-615										
5016	1	month	9.3	1.77	9.5	0.64	9.6	0.34	9.7	0.70
5031	2	"	8.2	3.42	9.8	1.32	10.0	0.86	10.0	1.02
5022	3	"	7.5	8.62	9.8	1.38	10.0	1.19	10.0	0.81
5056	6	"	3.8		9.4		9.6		9.6	
BC 727										
5014	1	month	8.8	2.67	9.3	1.20	9.3	0.68	9.3	1.31
5032	2	"	7.3	5.81	9.3	2.58	9.5	3.09	9.5	3.45
5020	3	"	7.0	21.6	9.4	5.4	9.5	5.0	9.5	5.7
5056	6	"	3.1		8.9		9.1		9.0	
MSA 463563										
5015	1	month	7.45	4.0	7.65	1.9	7.65	3.6	7.8	2.1
5021	1	"	6.7	15.5	8.2	8.0	8.2	8.8	8.2	8.4
5060	3	"	3.4		7.5		7.7		7.8	
5059	6	"	2.5		6.9		7.8		8.0	

TABLE 5

GRADIENTS IN THE PENETRATION (P) OF METHYL IODIDE
AND THE pH OF WATER EXTRACTS AFTER 3 MONTHS EXPOSURE

Exposure	First Layer		Second Layer		Third Layer		Fourth Layer	
	pH	P	pH	P	pH	P	pH	P
5022 NACAR G 615	7.5	8.62	9.8	1.38	10.0	1.14	10.0	0.81
5020 BC 727	7.0	21.6	9.4	5.4	9.5	5.0	9.5	5.7
5060 MSA 463563	3.4		7.5		7.7		7.8	
5063 SS	4.5		8.7		8.9		8.9	
5061 2701	3.6		8.2		8.5		8.6	
5069 KITEG	2.8		7.2		7.3		7.4	

The final results available for FY78 are additional one-month and two-month exposures for BC 727. Table 6 presents the pH of water extract values, and comparative values for FY77 exposures are included. From the two-month exposures, it appears that two winter months degrade the carbon to a greater degree than two summer months. An identical type of profile for the two month (February - March 1978) period is observed as was reported in Reference 1. That is, the first layer appears to act as a guard bed to remove the bulk of the contaminants, then any migration of impregnant complex will lead to a decrease in penetration for the subsequent layer, except for the fourth layer for which the penetration could increase due to the net loss of impregnant in the expelled air.

B. Laboratory Exposures

There are now two independent installations available to conduct the laboratory weathering experiments, allowing a greater accumulation of data in less time. Laboratory exposures that have been completed in FY78 have used water vapor as the single pollutant, and all exposures have been for 100 hours. Charcoals MSA 463563, AAF 2701, KITEG, and Sutcliffe Speakman have been exposed to air with both 50% and 90% RH. Table 7 lists the results available for the 90% RH exposures, including BC 727 and NACAR G-615 results as published in Reference 1, and Table 8 lists identical information for the 50% RH exposures. The penetration of methyl iodide values listed for MSA 463563 and NACAR G-617 carbons were evaluated according to Method B as discussed in Section II of this paper, i.e., use of one-fourth of each layer of the weathered sample to construct a test bed preserving the same entrance-to-exit sequence, and performing one methyl iodide penetration test on the 2-inch deep bed. Future tests for penetrations of methyl iodide to complete Tables

15th DOE NUCLEAR AIR CLEANING CONFERENCE

TABLE 6

CHARCOAL BC 727 EXPOSURES

Exposures	First Layer		Second Layer		Third Layer		Fourth Layer	
	pH	P	pH	P	pH	P	pH	P
5014 June 77	8.8	2.67	9.3	1.20	9.3	0.68	9.3	1.31
5070 April 78	8.3		9.2		9.2		9.2	
5032 Aug-Sept 77	7.3	5.81	9.3	2.58	9.5	3.09	9.5	3.45
5065 Feb-Mar 78	7.3	13.4	9.3	5.4	9.2	5.1	9.4	6.0

TABLE 7

LABORATORY EXPOSURES AT 90% RH

Exposures	First Layer		Second Layer		Third Layer		Fourth Layer	
	pH	P(%)	pH	P(%)	pH	P(%)	pH	P(%)
5036 BC 727	8.2	12.7	9.1	5.1	9.1	7.3	9.2	3.4
5037 NACAR G-615	9.5	2.0	9.5		9.4		8.8	2.1
5072 SS	8.6		8.7		8.7		8.7	
5074 NACAR G-617 P*=9.2%	9.6		9.6		9.6		9.6	
5076 KITEG	7.8		7.7		7.7		7.7	
5086 MSA 463563	8.3		8.3		8.3		8.2	

*= Penetration for a two-inch bed.

15th DOE NUCLEAR AIR CLEANING CONFERENCE

TABLE 8

LABORATORY EXPOSURES AT 50% RH

Exposures	First Layer pH	Second Layer pH	Third Layer pH	Fourth Layer pH
5053 BC 727	9.5	9.5	9.5	9.6
5054 NACAR G-615	9.9	9.9	9.9	9.9
5071 2701	9.0	9.0	9.1	9.1
5073 MSA 463563 P* = 4.7%	8.2	8.3	8.3	8.3
5075 KITEG	8.4	8.4	8.4	8.4
5085 SS	8.4	8.4	8.4	8.4

*= Penetration for a two-inch bed.

7 and 8 will also be performed according to Method B. From the pH of water extract values listed there does not appear to be sufficient variation to draw any meaningful conclusions.

IV. FUTURE WORK

Plans for future experimentation include outdoor exposures at NRL, laboratory exposures, examination of spent charcoals of known weathering history, and outdoor exposures at locations other than NRL.

A. Exposures to Outdoor Air

Table 3 indicates the charcoal samples that will be weathered in outdoor air at NRL. At the end of the program, all charcoals listed will have been weathered for 1, 3, 6 and 9 month periods. A number of charcoals will have been weathered for the same time periods, and one carbon (BC 727) will be weathered for nine 1-month periods to observe any seasonal variations. Selected exposed samples will be tested for methyl iodide penetration according to Method A (test each layer after mixing to obtain the profile), but most samples will be tested for methyl iodide penetration according to Method B, (use one-fourth of each layer of the weathered sample to construct a test bed preserving the same entrance-to-exit sequence and determine only one methyl iodide penetration). Samples will also be tested for methyl iodide penetration according to Method C (test without disturbing the weathered sample), once fabrication of appropriate canisters is complete.

15th DOE NUCLEAR AIR CLEANING CONFERENCE

Two carbons (BC 727 and Sutcliffe Speakman) will also be evaluated to determine any influence of "resting" a sample. For these tests, samples will be exposed for one month, held dormant (no weathering-inactive) for one month, then exposing for one additional month, and then analyzed for pH of water extract and penetration of methyl iodide values.

The sequence expose-inactive-expose-inactive-expose-test (resulting in a total of three months weathering) will also be examined.

B. Laboratory Exposures

Laboratory exposures are to be completed using water vapor as the single pollutant for the carbons MSA 463563, Sutcliffe Speakman, 2701, KITEG and NACAR G-617 at 70% RH, for 2701 at 90% RH, and for NACAR G-617 at 50% RH. This will result in all the carbons under study being evaluated at 50, 70 and 90% RH for 100 hours exposures.

An atmospheric pollutant will be added to the water vapor plus air mixture. First, hexane (2.5 to 5 ppm) will be added to 50, 70 and 90% RH air and used as the insult gas for BC 727 and NACAR G-615 carbons. Hexane will also be added to 70% RH air and used as the insult gas for MSA 463563, Sutcliffe Speakman, 2701, KITEG and NACAR G-617 carbons. Hexane is chosen to represent the total hydrocarbon (including methane) pollutant in the environment. Second, methyl isobutyl ketone will be added to 70% RH air and used as the insult gas for BC 727 and NACAR G-615 carbons. Methyl isobutyl ketone is chosen to represent a paint solvent pollutant. Third, ozone levels of 0.1 ppm will be achieved and added to 90% RH air for use as the insult gas for BC 727 and NACAR G-615 carbon. All of the above exposures will be for 100 hours.

Laboratory work will include cycling water vapor levels. For BC 727 and NACAR G-615 carbons, 50% RH air will be used as the insult gas for 50 hours followed by 90% RH air for 50 hours, and then evaluated (after the total exposure of 100 hours). The reverse order of RH values will then be examined; i.e., 90% RH air for 50 hours followed by 50% RH air for 50 hours.

Finally, selected synergistic combinations of pollutants (water vapor plus sulfur dioxide plus hydrocarbon, water vapor plus ozone plus hydrocarbon) will be used as the insult gas.

For all the above analysis of laboratory-exposed carbons, selected samples will be evaluated for penetrations of methyl iodide according to Method A (evaluate each one-half inch layer independently), but the majority will be evaluated for penetration of methyl iodide using Method B (use one-fourth of each layer of the weathered sample to construct a test bed preserving the same entrance-to-exit sequence and performing one penetration test on the 2-inch deep bed). The pH of water extracts and weight gains will be evaluated for all carbons exposed as a function of bed layer.

C. Outdoor Exposures at Locations Other Than NRL

Due to variation of contaminants in the atmosphere in both time and location, it is desirable to expose the carbons to outdoor air at locations other than NRL. General weather considerations will aid in the selection of suitable sites (the dry southwest, the humid southeast, industrial versus non-industrial areas), and data on the contaminants must also be available. Sites in close proximity to nuclear

15th DOE NUCLEAR AIR CLEANING CONFERENCE

power stations will be chosen. The exposed charcoals will be changed periodically and returned to the laboratory for examination of penetrations of methyl iodide, PH of water extract and weight gains. It is also planned to attempt to regenerate the spent carbon to recover methyl iodide trapping efficiency, and to analyze the carbon for the pollutants that have accumulated on the carbon (analysis of volatiles on programmed heating), and to determine the ignition temperature.

D. Examination of Charcoals in Different Stages of Service

Charcoals that have been in service at nuclear installations will be procured and will be analyzed similiarly to those carbons exposed at outdoor locations other than NRL. This information, with an indication of what service the carbon has experienced, will aid in correlating laboratory versus outdoor exposure data in order to predict the useful life of carbons.

V. Conclusions

Recognizing the need to determine the effect of atmospheric contaminants on the useful life of activated charcoal, the U.S. Nuclear Regulatory Commission contracted with the Naval Research Laboratory (Surface Chemistry Branch) to determine the extent to which such contaminants degrade commercially - available charcoals. The work is in the second year; results for FY77 have been published in NUREG/CR-0025, "Effects of Weathering on Impregnated Charcoal Performance", March 1978. This paper has briefly summarized the FY77 results, and also highlighted two problems with the evaluation of exposed carbons; the configuration to be employed for the laboratory determinations of the penetration of methyl iodide, and the equilibrium procedure used for such laboratory analysis. The pollutants water vapor, ozone and sulfur dioxide have been seen to seriously degrade the carbons, whereas carbon monoxide did not. It has also been shown that the longer the exposure, the more the carbon degrades, but this effect has not proved to be monotonic with bed depth. The laboratory and outdoor exposure work in progress has been summarized, which extends the time of exposure and the number and type of carbons to be tested. Future work will include different combinations of three (and more) pollutants as the insult gas, outdoor exposures at various U.S. locations, and examination of spent charcoal from nuclear power installations.

REFERENCES

1. U.S. Nuclear Regulatory Commission NUREG/CR-0025, "Effects of Weathering on Impregnated Charcoal Performance," V. R. Deitz (Naval Research Laboratory), March 1978.
2. American Society for Testing and Materials, "Standard Method for Radioiodine Testing of Nuclear Grade Gas-Phase Adsorbents," Draft Version, October 14, 1977.
3. Letter to H. Brockelsby, Reactor and Technology Support Division, Oak Ridge Operations Office, DOE from V. R. Deitz and J. B. Romans, Naval Research Laboratory, "Activities for March 1978, Project KZ, 03 04 03," 6170-211, May 1, 1978.
4. A. G. Evans, "Effect of Service Aging on Iodine Retention of Activated Charcoals," Proceedings of the Fourteenth ERDA Air Cleaning Conference, Sun Valley, Idaho, 2-4 August, 1976, USDOE Report CONF-760822, pp. 251-263.

15th DOE NUCLEAR AIR CLEANING CONFERENCE

DISCUSSION

EVANS: Why does charcoal weather faster in the winter?

BELLAMY: Additional data will be gathered during future work, but it appears that the combination of low temperature and moisture weathers the carbon to a greater degree than high temperature and moisture.

DEMPSEY: It appears that an in situ radioiodine test might be carried out through the charcoal samples now that you have accurate proportional flow data, i.e., a sufficiently small amount of radioiodine might be used to permit licensing. Do you think this would be possible?

BELLAMY: The present state of mind of the public with regard to the release of radioactivity to the atmosphere is such that these tests are impractical unless there is a very strong overriding technical reason for using a radioactive in-place test in preference to the standard in-place leak test with Freon and the corresponding laboratory radiotest for the carbon.

15th DOE NUCLEAR AIR CLEANING CONFERENCE

A NON-RADIOACTIVE DETERMINATION OF THE PENETRATION OF METHYL IODIDE THROUGH IMPREGNATED CHARCOALS DURING DOSING AND PURGING

J. B. Romans and Victor R. Deitz
Naval Research Laboratory
Washington, D.C. 20375

Abstract

A laboratory procedure is described using methyl iodide-127 which had the same linear flow of air (12.2 m/min) and contact time (0.25 sec.) as the RDT M16 Test Procedure. Only one-fourth of the charcoal was used (in a bed 2.54 cm diameter and 5.08 cm high) and the required dose of methyl iodide-127 was reduced from 5.25 to 1.31 mg. The inlet concentrations were determined with a gas chromatograph and the effluent concentrations with a modified microcoulombmeter. Two calibration procedures were used: (1) known vapor pressure of iodine crystals, and (2) quantitative pyrolysis of the methyl iodide-127 delivered from certified permeation tubes. Five charcoals and three impregnations were used in this study. Typical behaviors are given in 90% RH air with the charcoals either prehumidified for 16 hours at 90% RH or without the prehumidification. The breakthrough curves, concentration versus time, rose very slowly for the first 120 minutes and then more rapidly for an additional time. It is possible to determine the accumulated breakthrough for 120 minutes; good agreement was then found with the penetration for the same impregnated charcoals evaluated by the RDT M16 procedure with methyl iodide-131. It is concluded that the use of methyl iodide-127 is a feasible procedure to evaluate penetration. The lack of a dependence on the magnitude of the dose is compatible with a catalytic trapping mechanism. In the case of KI_x impregnations, there was excess emission of iodine during purging over that introduced as methyl iodide-127 which must have originated in the reservoir of iodine contained in the impregnation.

15th DOE NUCLEAR AIR CLEANING CONFERENCE

I. Introduction

Plant-scale and laboratory processes for the removal of airborne iodine by charcoal are examples of kinetic systems in gas adsorption. The iodine breakthrough behavior over the complete range of penetration is very complex (1,2,3). However, it has been demonstrated (4) that for small penetration (less than 2%), where only the beginning of the general sigmoidal dependence (Figure 1) is pertinent, some simplification is possible. The RDT Standard M16-1T, 1977, Test Procedure (5) is based on the total radioactive count in the sample and back-up beds after both the introduction of the methyl iodide dose and the 2-hour elution or purge period. The fraction of the penetration that occurs in each of these periods is not known and one objective of this paper is to obtain the magnitude for each fraction using several impregnated charcoals. The purge behavior is a most important safety feature of the charcoal trapping process.

The ability to make penetration measurements with non-radioactive iodine has several advantages. The necessary health physics requirements for radioactive materials are eliminated, a continuous monitoring of the methyl iodide concentration is possible, the cost of the radioactive methyl iodide is avoided, and in-place testing to monitor plant-scale charcoals filters is without restrictions. The quantity of methyl iodide-127 in a challenge gas is very large relative to that of methyl iodide-131, being in many cases of the order of magnitude of 10^4 . Consequently, the detection of the non-radioactive species is favored and this helps to compensate for the higher sensitivity of radioactive counting.

The test procedure for the penetration of radioactive methyl iodide entails separate physical operations. First, the charcoal sample may be prehumidified for 16 hours before the introduction of methyl iodide or it may have been subjected to some systematic weathering program. Second, a specified dose of methyl iodide may have been introduced during a known period either continuously or intermittently. The third operation is an air purge of the charcoal for a specified time. At this point the efficiency of the trapping process is generally determined. These operations have a sequential dependence and, therefore, another objective of this paper is to observe the behavior after each operation. The experimental parameters are: the magnitude of the methyl iodide dose, the relative humidity of the air flow, the duration of the purge period, and variations in the impregnation formulation and the base charcoal. All of these variations are readily followed using the non-radioactive technique and the results will be compared where possible with the trapping determined with methyl iodide-131.

2. Experimental Procedure

2.1 Scaling Factors

A dynamic test procedure was developed to study the penetration of non-radioactive methyl iodide. The scaling factor retained the RDT-M16 specification for linear flow, namely 12.2 m/min. (40 feet/min.) and the residence time of 0.25 seconds. A comparison is given below:

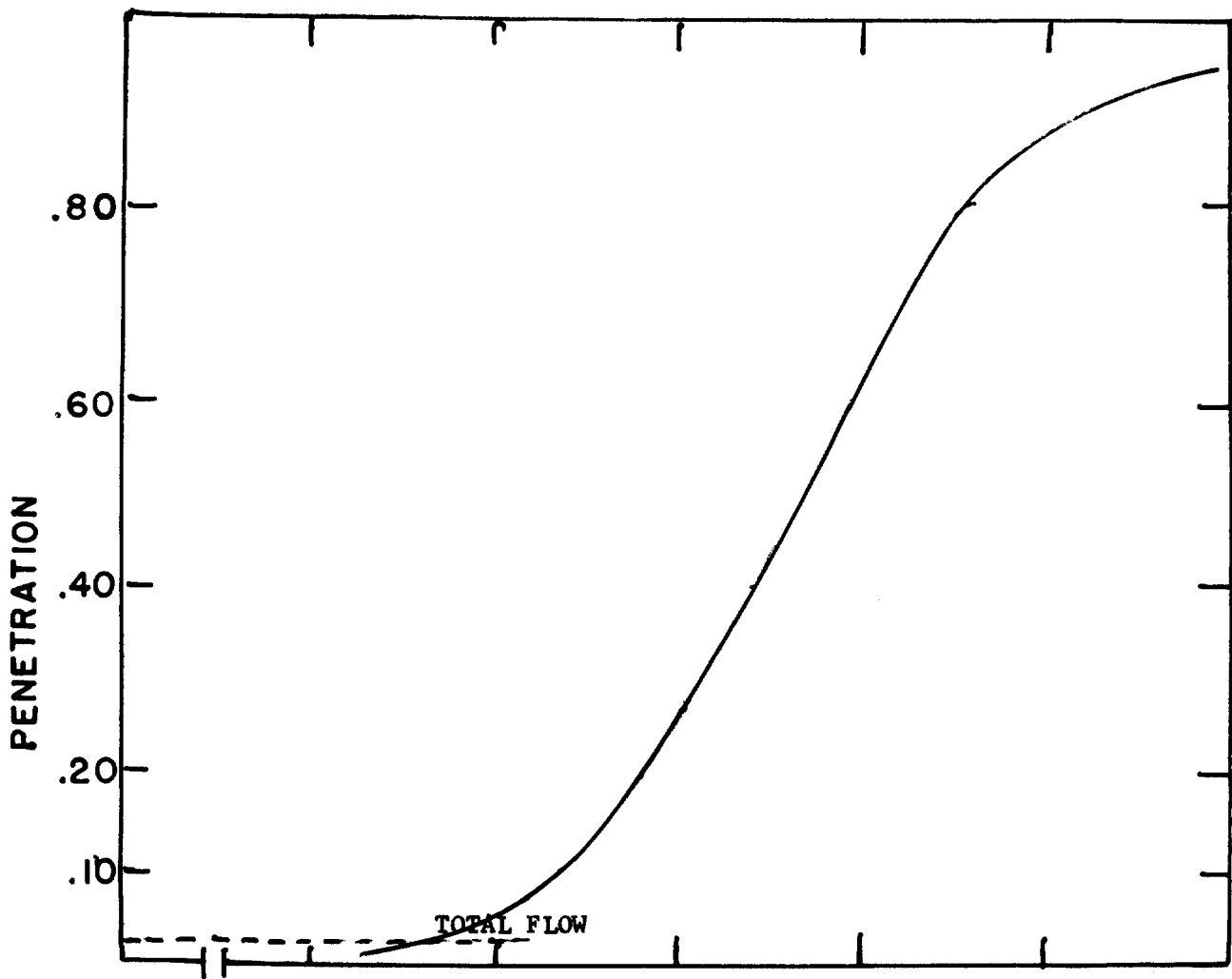


Figure 1: General dependence of fractional penetration over the complete range of breakthrough concentration (dotted line signifies a permissible upper level for satisfactory performance)

15th DOE NUCLEAR AIR CLEANING CONFERENCE

	RDT-M16	NRL Laboratory
bed diameter (cm)	5.08	2.54
bed height (cm)	5.08	5.08
linear air velocity (m/min)	12.2	12.2
residence time (sec)	0.25	0.25
volume flow (ℓ/min)	25	6.2
total methyl iodide (mg)	5.25	1.31
total methyl iodide (nm)	36900	9230
temperature °C	30	30

2.2 Schematic Flow Diagram

The air flow (6.2 ℓ/min) passed in sequence (Figure 2) through: (1) regulator and control valve(s), (2) dry test meter (American DTM 115), (3) particulate and charcoal filter, (4) humidifier, (5) electric hygrometer element, (6) mixing chamber, (7) gas sample opening to chromatograph, (8) thermostated container for the charcoal sample, (9) exit to detection elements, (10) exit to trap and vent. The cylindrical tube (8) was maintained at constant temperature by a surrounding split resistance heater with the controlling thermocouple located beneath the center of the bottom plate holding the charcoal. Additional thermocouples were located at the center of the bottom charcoal support and at the top center of the charcoal. The air flow could be sent either upward or downward through the charcoal; the present results were obtained with upward flow. Two side outlets (2 mm i.d. tubing) were available to sample the gases emerging from the mixing chamber (7) and at the outlet side of the charcoal (9). A mixture of methyl iodide and nitrogen was pressurized in a stainless steel bottle and metered as desired into the mixing chamber through a pressure regulator and a microneedle valve.

2.3 Detector and Calibration

A certified permeation tube containing liquid methyl iodide was used to calibrate a modified Hewlett-Packard gas chromatograph (5710 A series) equipped with a flame-ionization detector. The vapor permeates through the Teflon wall of the tube at a constant rate and the weight loss at constant temperature over a given time period served as the primary standard. The air flow across the tube (maintained at 30.0°C) was varied 100-fold and the corresponding chromatographic peak heights (h) were measured. Typical data and the calculated concentration, \underline{c} , at 25°C are given in Table 1. A least squares linear regression analysis gave the following relationship:

$$\underline{c} \text{ (ppm)} = 0.342 \underline{h} - 0.139 \dots (1)$$

In order to realize a dose of methyl iodide of 1.31 mg in two hours, an average concentration of 0.30 ppm (V/V) would have to be maintained. At unit attenuation this concentration corresponds to a peak height of 20.5 chart divisions.

The detector for iodine in the charcoal effluent stream was a modified microcoulombmeter (Mast Instrument Co. Model 724-2). Two independent calibrations were made. One was based on the known vapor pressure of iodine crystals and the second on the quantitative pyrolysis of the methyl iodide delivered from the certified permeation tube. Figure 3 is a schematic flow diagram of the calibration source of air + iodine vapor. Air was passed through charcoal and drierite and at position A entered the tube B containing Anhydrone (barium perchlorate). The dried air was then passed over iodine crystals in flask C

15th DOE NUCLEAR AIR CLEANING CONFERENCE

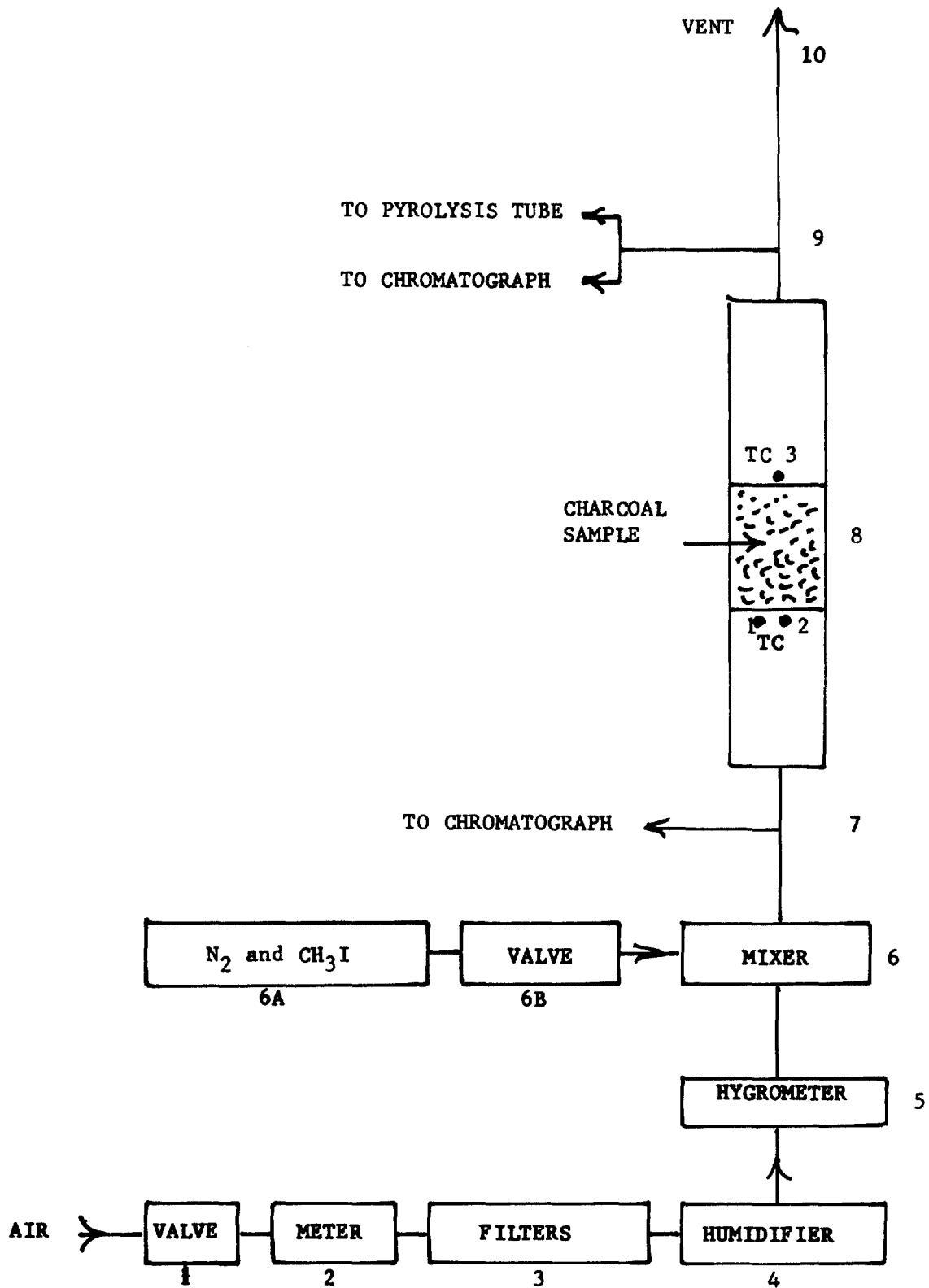


Figure 2: Flow Diagram for Methyl Iodide-127 Experimentation

15th DOE NUCLEAR AIR CLEANING CONFERENCE

Table 1: Calibration of gas chromatograph with a Certified Permeation Tube of methyl iodide held at 30.0°C.

Air Flow ml/min	Concn. ppm	Peak Height (attenuation 16) chart-divisions
199	0.23	0.4
203	0.23	0.3
56.7	0.82	1.9
20.9	2.23	6.5
9.80	4.75	14.1
7.01	6.63	19.8
3.64	12.8	36.8
31.7	1.45	5.6
12.3	3.74	13.9
12.7	3.63	13.7
5.2	8.85	28.4
13.4	3.44	10.1
2.6	17.4	51.6
3.6	12.8	34.6
58	0.79	1.4

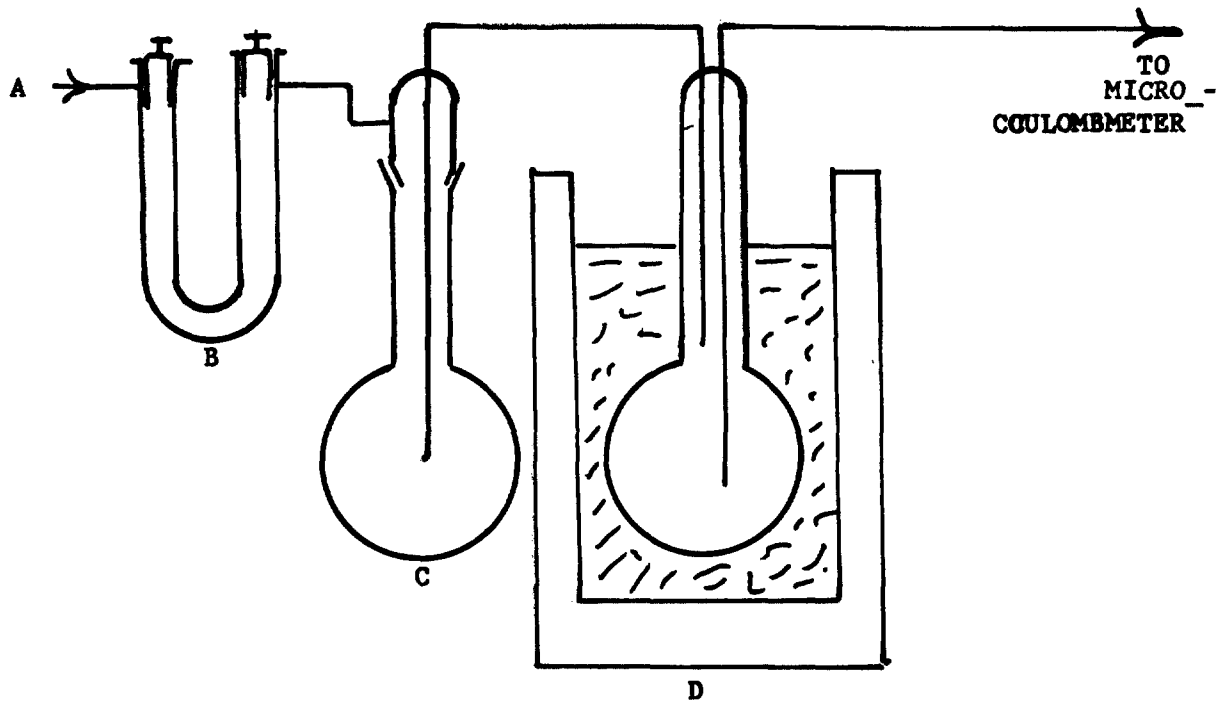


Figure 3: Calibration Source of Air and Iodine Vapor by Passage of Purified Air Over Iodine Crystals Held at Constant Temperature

Table 2: Pyrolysis of Methyl Iodide in Air Flows

Heating Current (amp.)	Temperature (center of tube)	Mast Coulombmeter mv	I ₂ (ppm)		% Conversion
			Mast	Permeation Tube (calc.)	
1.4	448	0.08	.0005	.072	0.7
1.6	527	3.69	.056	"	78.
1.8	612	4.24	.067	"	93.
2.0	686	3.99	.062	"	86.
2.2	745	3.58	.054	"	75.

15th DOE NUCLEAR AIR CLEANING CONFERENCE

at room temperature and then into a second flask, D, held under the liquid level of a cryostat maintained at the desired temperature. Thus, the approach to the equilibrium vapor pressure of iodine was from a higher vapor pressure, a procedure found necessary to attain steady states.

The published data for the vapor pressure of iodine crystals at and below room temperature were reviewed and a least square linear regression analysis gave equation (2):

$$\ln p_{I_2} \text{ (torr)} = - 8148.4/T^{\circ}K + 26.361 \dots (2)$$

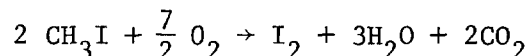
The output of the microcoulombmeter was shunted across a resistance of 5250 Ω and the voltage drop (mv) was record. A plot of $\ln \underline{mv}$ was made as a function of the reciprocal cryostat temperature ($^{\circ}K$) and a least square linear regression analysis gave equation (3):

$$\ln \underline{mv} = 6663/T + 31.736 \dots (3)$$

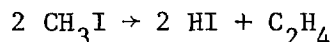
Combining equations (2) and (3) the following calibration formula was obtained

$$\ln p_{I_2} = 1.2229 \ln \underline{mv} - 12.449 \dots (4)$$

The second calibration was based on the formation of I_2 in the pyrolysis of methyl iodide. It was necessary to regulate the temperature of the quartz tube within a narrow range in order to obtain a quantitative decomposition. The desired mechanism is given by



When the temperature of pyrolysis is too high, a second mechanism of decomposition occurs, i.e.



The results for one series of pyrolysis experiments are given in Table 2. When the tube furnace around the quartz tube was held at $650 \pm 20^{\circ}C$ (inside temperature of the tube), the conversion was practically quantitative (Table 3). The plot of methyl iodide introduced (ppm) as a function of iodine produced (Figure 4) gave a slope of 2 in agreement with theory.

2.4 Impregnated Charcoals

The results given in this report are concerned with five charcoals and three kinds of impregnation, Table 4. Additional studies with other charcoals and impregnations are in progress.

3.0 Results

3.1 Penetration during Introduction of Methyl Iodide

The breakthrough data can be presented as a function of time in terms of concentration (nanomoles/unit flow) or as the accumulated methyl iodide up to a specified time, \underline{t} . The latter at $\underline{t} = 120$ minutes is required to make comparisons with the results obtained using radioactive methyl iodide-131. Typical behaviors are given (Figures 5, 6, 7) for charcoal BC 727 in air of 90% RH, either prehumidified for 16 hours at 90% RH or without prehumidification. The influence of prehumidification is to increase the penetration as previously

15th DOE NUCLEAR AIR CLEANING CONFERENCE

Table 3: Pyrolysis of Methyl Iodide-Air Mixtures at Optimum Temperature of 650°C

Mast Microcoulombmeter		Calcd. from Permeation Tube	% Conversion
(mv)	Iodine (I ₂) ppm		
3.14	.063	.073	87
3.82	.081	.087	93
4.74	.105	.106	99
4.91	.109	.114	96
4.89	.109	.115	95
4.86	.108	.116	93
9.05	.161	.162	99
9.20	.164	.162	100
9.37	.168	.162	100
9.0	.160	.162	99
9.0	.160	.161	99
3.54	.073	.075	99

Table 4: Summary of charcoals studied in this report

Notation	Base charcoal	Impregnation
BC 727	coconut	KI + xI ₂ = KI _x
NACAR 615	coconut	KI and TEDA
NRL 4314	coal, ACC	KIO ₃ + KI + K ₃ PO ₄ + HMTA
NRL 4315	coal, 207A	ditto
NRL 4316	coal, BPL	ditto
BC 727	8 x 16, Barnebey Cheney	
NACAR 615	8 x 16, North American Carbon Inc.	
ACC	6 x 14, Columbia Activated Carbon	
207A	8 x 16, Sutcliffe, Speakman Co. Ltd.	
BPL	8 x 20, Activated Carbon Division, Calgon Corp.	
TEDA	≡	triethylenediamine
HMTA	≡	hexamethylenetetramine

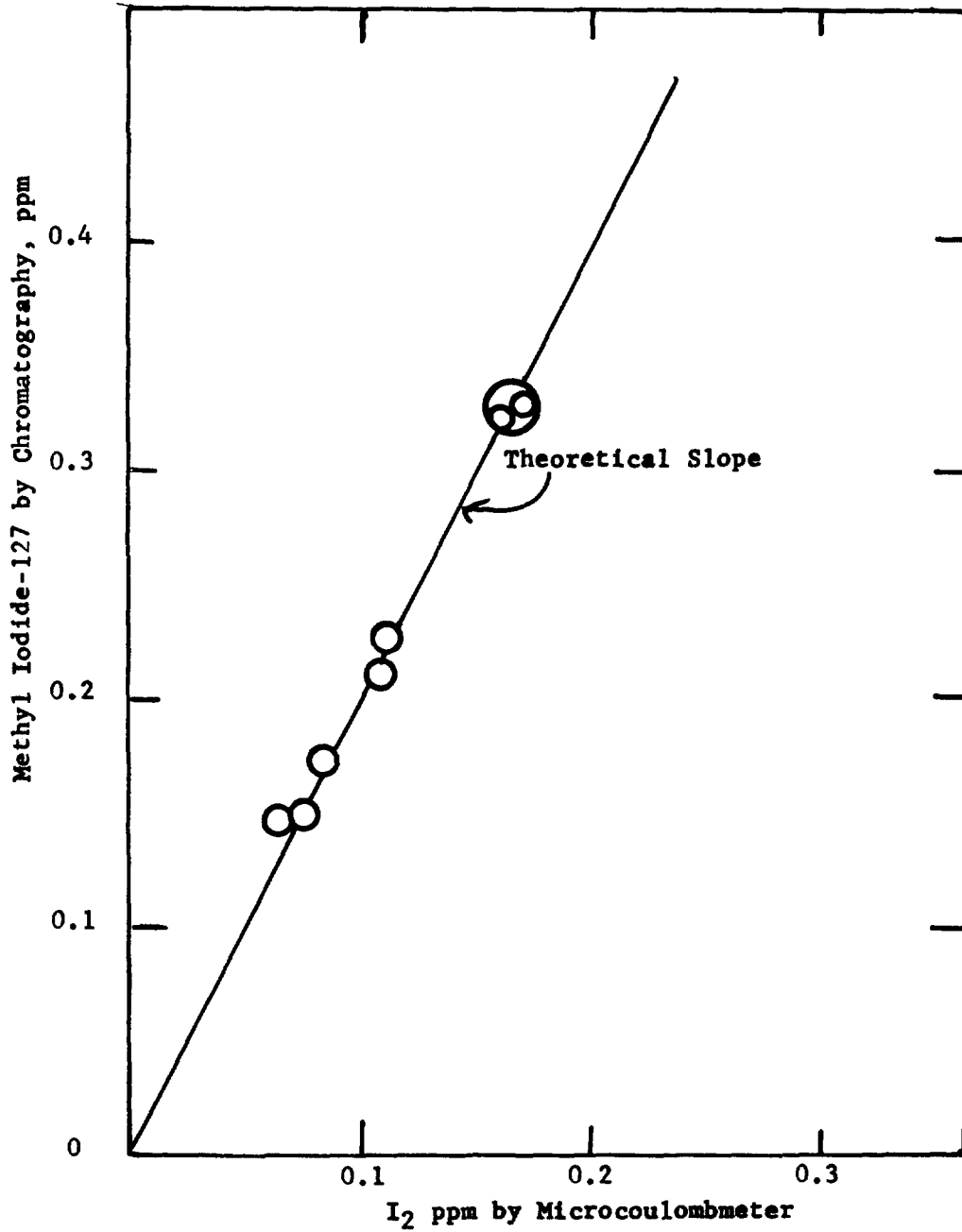


Figure 4: Correlation of CH₃I by Chromatography with I₂ by Microcoulombmeter

15th DOE NUCLEAR AIR CLEANING CONFERENCE

reported (6). The effluent concentrations at a specified time (Figure 5) were greater using prehumidification even though the average initial concentration of methyl iodide (21.8 nano m/liter) was less than for the experiment with prehumidification (33.2 nano m/liter). The measurements for the latter case, were also extended beyond 120 minutes.

The same experimental results are also presented in Figure 6 by the ratio of C_0/C as a function of time. The ratio is related to the decontamination factor K and is seen to decrease steadily with the magnitude of the incident dose.

The penetration of methyl iodide (Figure 7) was calculated as follows for a given time t :

$$\text{penetration (\%)} = 100 \frac{\text{Summation of effluent to time } t}{\text{Summation introduced to time } t}$$

When the charcoal sample was prehumidified, the penetration at $t = 120$ minutes was determined to be 2.1%. At this point the methyl iodide introduced was 16600 nanom. The point R on Figure 7 is the penetration (2.2%) observed with radioactive methyl iodide-131 for a sub-sample of the identical charcoal. This value was determined by the RDT test procedure in which 36,900 nm was introduced in 120 minutes. The corresponding points for the non-prehumidified sample given in Figure 7 are of the correct magnitude.

A comparison of the penetrations at 120 minutes is given for the five charcoals in Table 5. The agreement between the nonradioactive procedure and the RDT M-16 test is rather good. Although procedures use the same residence times and the same linear air velocity, the amount of methyl iodide required for the nonradioactive test is scaled to one fourth, i.e. 9230 nanomoles. It appears, therefore, from these results that the penetration for any given charcoal is independent of the methyl iodide concentration over approximately a 3-fold dose range.

3.2 Elution of Methyl Iodide during Purging

After the introduction of methyl iodide, the iodine in the effluent air stream was further monitored for the period required to reach the base line of the detector. With dry air as a carrier, there was not indication of a detectable penetration during the purge for any of the 5 charcoals. Also, with 90% RH air, there was no appreciable penetration with NACAR 615 charcoal. However, different behaviors were observed for the other charcoals; these are summarized in Table 6.

The effluent iodine from BC 727 (test 3287) continued to increase after the addition of methyl iodide was discontinued. The air flow was maintained at 6.2 L/min and the temperature at 30°C. As shown in Figure 8, it required about 20 hours for the total emission to level off. During the early stages the characteristic chromatographic peak of methyl iodide was observed. A summation of 28000 n moles of iodine were obtained from the time when the CH_3I was discontinued to the time when the detector base line was reached. This magnitude exceeded that introduced and can only have come from the reservoir of iodine in the charcoal impregnant (KI_x). The excess is approximately 1% of that in the charcoal sample.

The effluent iodine from charcoal 4316 (Figure 9) also continued to increase for about 2 hours after the methyl iodide was discontinued. During the early stages the characteristic chromatographic peaks of methyl iodide were observed.

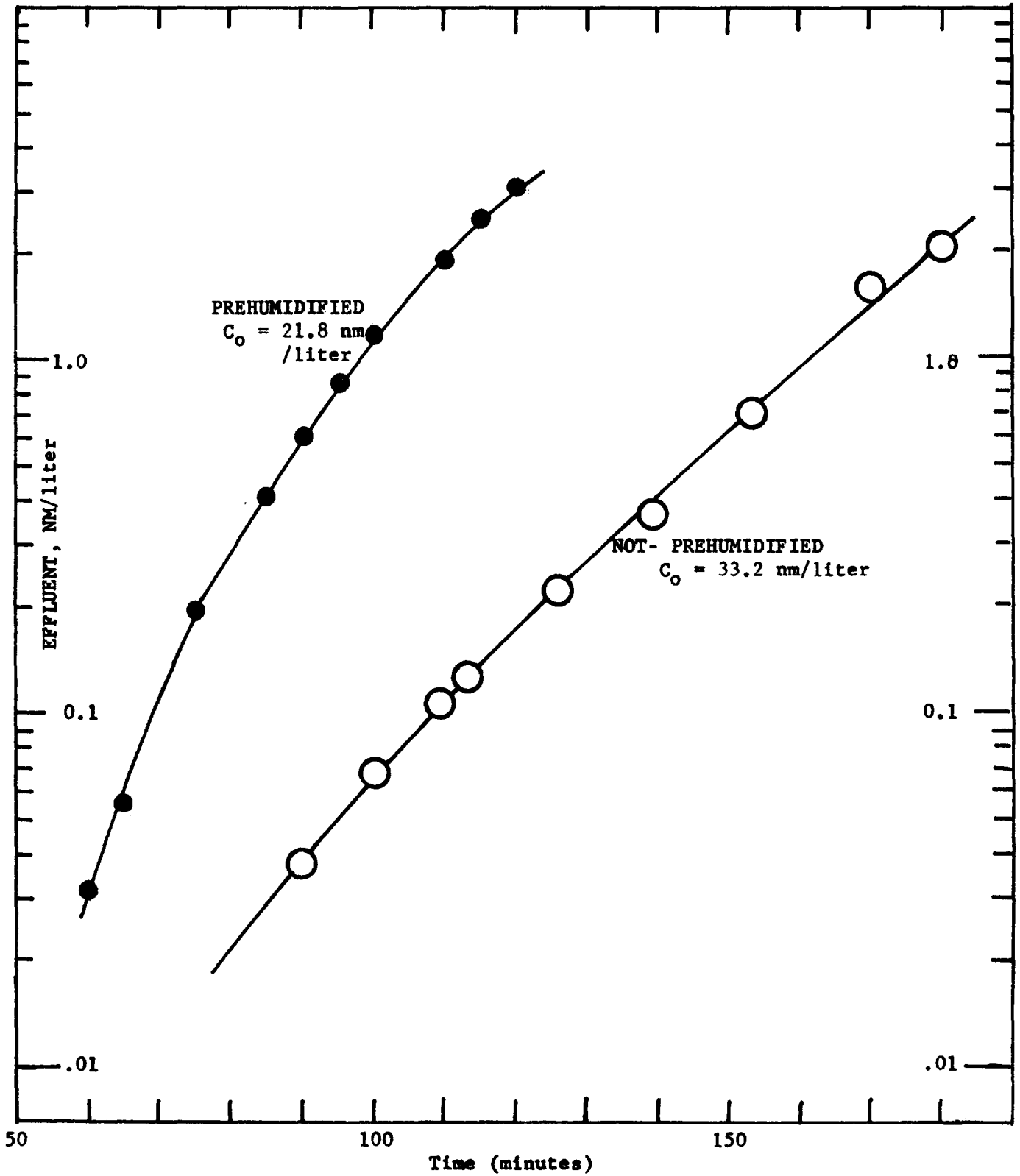


Figure 5: Effluent Concentration of Methyl Iodide-127 as a Function of Time During the Continuous Loading of BC 727 in 90% RH Air with (Test 3287) and without (Test 3283) Prehumidification

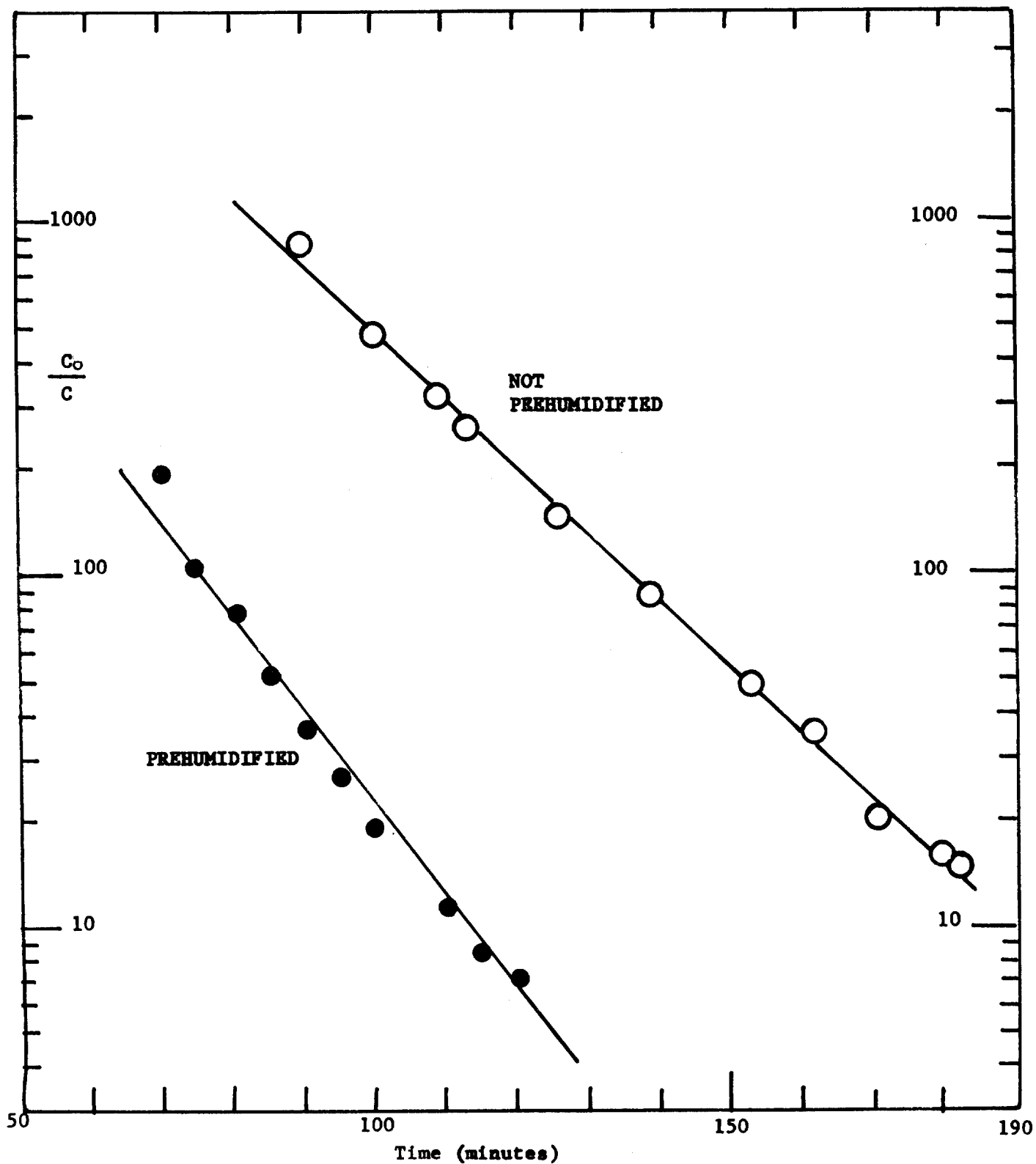


Figure 6: Dependence of C_0/C on Time when Charcoal BC 727 was Challenged Continuously with Methyl Iodide-127 in 90% RH Air with (Test 3287) and without (Test 3283) Prehumidification

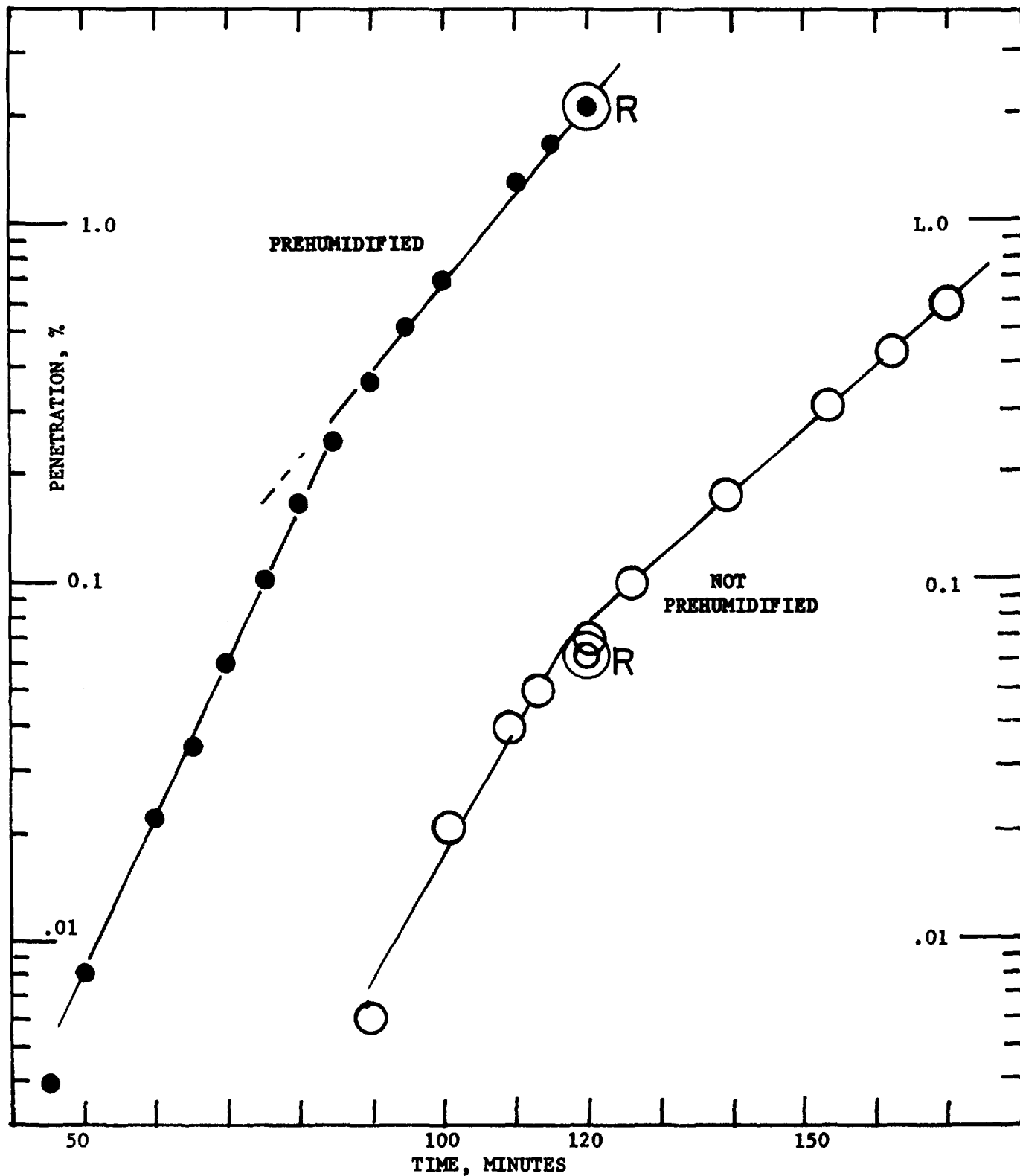


Figure 7: Penetration of Methyl Iodide-127 through BC 727 in 90% RH Air with (Test 3287) and without (Test 3283) Prehumidification. R denotes Independent Results with Methyl Iodide-131.

15th DOE NUCLEAR AIR CLEANING CONFERENCE

Table 5: Comparison of Penetrations at 120 minutes for five charcoals in 90% RH air

Charcoal	Procedures	Prehumidification	Test	Introduced n moles	Penetration %
727	CH ₃ I-131 (EET)	yes		36900	2.2
	non-radioactive	yes	3287	16600	2.1
	CH ₃ I-131 (EET)	no		110700	0.056
	non-radioactive	no	3283	26000	0.07
	non-radioactive	no	3276	19300	0.14
4314	CH ₃ I-131 (EET)	yes		36900	1.73
	CH ₃ I-131 (NRL)	yes		36900	1.54
	CH ₃ I-131 (NRL)	yes		36900	1.82
	CH ₃ I-131 (NRL)	no		36900	0.57
	non-radioactive	no	3269	31100	0.38
	CH ₃ I-131 (NRL)	no		36900	0.10
4315	CH ₃ I-131 (EET)	yes		36900	0.14
	CH ₃ I-131 (NES)	yes		36900	0.24
	CH ₃ I-131 (NES)	yes		36900	0.53
	CH ₃ I-131 (NRL)	yes		36900	0.26
	CH ₃ I-131 (NRL)	no		36900	< 0.01
	non-radioactive	no	3285	18400	.008
4316	CH ₃ I-131 (NRL)	yes		36900	0.90
	non-radioactive	no	3286	16600	0.10
	CH ₃ I-131 (NRL)	no		36900	0.051
NACAR	CH ₃ I-131 (NRL)	yes		36900	0.27
615	CH ₃ I-131 (NRL)	no		36900	0.05
	non-radioactive	no	3277	12900	0.00

EET Environmental Engineering & Testing

NES Nuclear Environmental Services

NRL Naval Research Laboratory

15th DOE NUCLEAR AIR CLEANING CONFERENCE

The total of 957 nanomoles realized in the purge corresponds in this case to only 4% of that introduced as methyl iodide to the charcoal.

The five charcoals (Table 6) show quite different behaviors which must be related to both the charcoals and the chemical properties of the impregnant. The moisture concentration in the carrier air is definitely a factor, and for a given charcoal and moisture content of the air, the amount of methyl iodide introduced influences the quantity purged.

The emission of iodine on a programmed heating of impregnated charcoals is another problem and the results of such measurements will be treated in a subsequent report.

4.0 Discussion

In so far as evaluation of the penetration of methyl iodide through impregnated charcoals is concerned, the use of non-radioactive methyl iodide appears to be feasible. The use of a detector of suitable sensitivity will eliminate the need for the preliminary pyrolysis of low-level methyl iodide that was used in the present work. Chromatographic systems using electron capture detectors have been demonstrated to be useful in atmospheric studies and preparations are in progress at NRL to use this system in future iodine penetration studies with impregnated charcoals.

The lack of a strong dependence of penetration on the magnitude of the methyl iodide dose is useful and points to a trapping mechanism which has catalytic attributes. Nevertheless, the adsorption of the reaction products and the unavoidable presence of atmospheric contaminants creates a situation where both adsorptive and catalytic properties are involved.

The excess emission of iodine over that introduced to charcoal as methyl iodide can be explained in part by the reactivity of catalytic surface complexes with the iodine contained in the impregnation formulation. A sequence of reactions results in the gasification of a fraction of the impregnated iodine and the reaction products can readily be detected using the non-radioactive technique. The gasification of impregnated iodine might have an important advantage in expediting an isotope exchange which, in view of the large excess of normal iodine-127 in the impregnation, would contribute significantly to the overall trapping of iodine-131.

Three series of measurements were made with methyl iodide-131 in which the back-up beds were replaced by new material periodically - after the introduction of the dose and after each hour of the purging period. Thus, the total penetrations could be divided into the fraction during the dosing and that during the purge periods. The results (Table 7, using BC-727 prehumidified, BC-727 not prehumidified, and NACAR 615 prehumidified) demonstrate that the major penetration takes place during the introductions of methyl iodide-131 and in relatively much smaller amounts during purging. The sample of BC-727 gave a small steady penetration during purging, much smaller, however, than that observed with CH_3I -127. The sample not prehumidified was challenged with three times the dose (15 mg CH_3I -131) and had considerably more activity (total count 800000 cps). Nevertheless, the purging behavior was almost identical for both prehumidified and not prehumidified samples.

15th DOE NUCLEAR AIR CLEANING CONFERENCE

Table 6: Comparison of the Quantities of Methyl Iodide Purged After the Dosing

	Test	Introduced		Purge		
		Total (nano m)	RH %	Time (min)	Total n moles	RH%
BC 727	3283	36900	90	2900	78,800	dry
	3287 (prehumidified)	16600	90	1210	28,000	90
	3276	29800	90	1125	23,090	90
4314	3268	101700	dry	---	< 1	dry
	3274	13260	dry	1022	< 1	dry
	3273	32960	53	184	945 (incompleted)	50
	3272	54560	90	990	7,840	90
4315	3285	26200	90	670	1,400	90
4316	3286	22480	90	1160	957	dry
NACAR 615	3277	19650	90	4020	< 1	90
	3284	24290	90	1120	< 1	90

Table 7: Penetration (%) of Methyl Iodide-131 During the Dosing and the Purging Periods

	Time (hrs)	BC 727 Prehumidified	BC 727 Not Prehumidified	NACAR 615 Prehumidified
Introduction	2	2.178	0.0557	0.382
1st Purge	1	.0333	.0272	.010
2nd Purge	1	.0063	.0086	.000
3rd Purge	1	.0054	.0053	.000
4th Purge	1	nd	.0067	.000
5th Purge	1	nd	.0080	nd

Acknowledgement is made to EET for these measurements; nd ≡ not determined

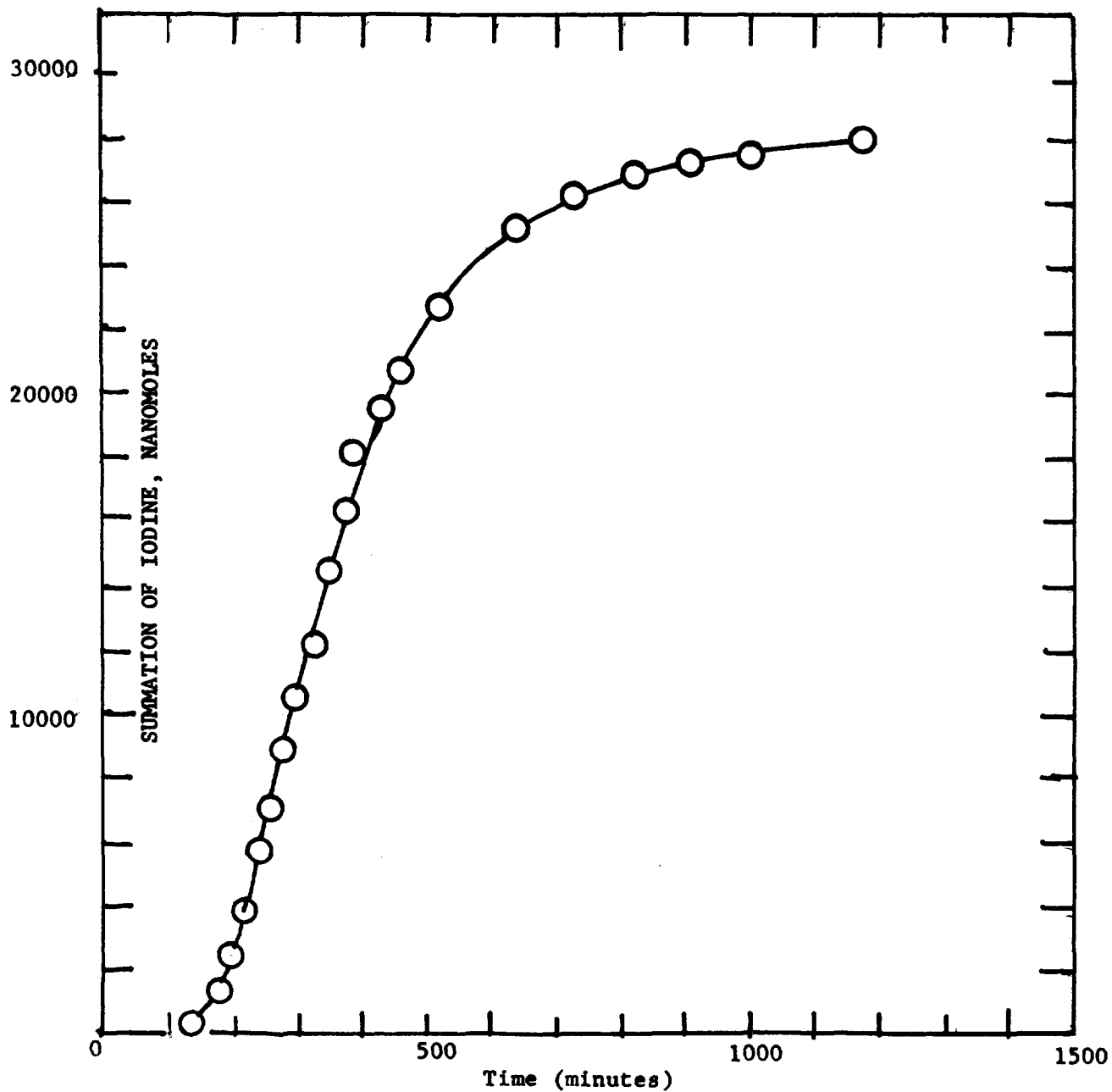


Figure 8: Purging of Charcoal BC 727 (Test 3287) after the Introduction of 16620 nanomoles of CH_3I in 120 minutes

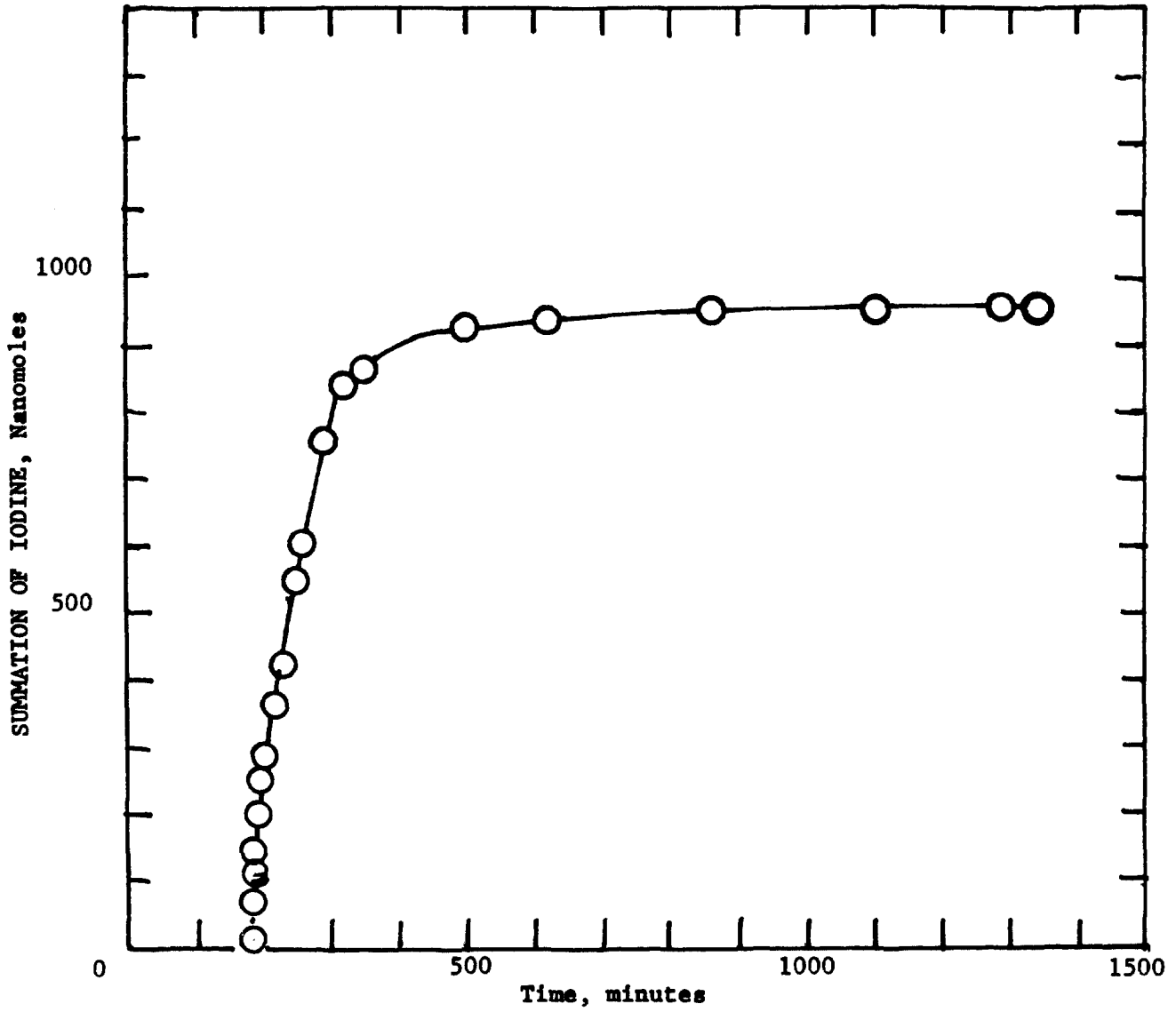
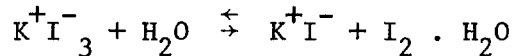


Figure 9: Purging of Charcoal 4316 (Test 3286) after the Introduction of 22480 nanomoles of CH_3I in 180 minutes

15th DOE NUCLEAR AIR CLEANING CONFERENCE

Impregnations on charcoals that contain KI_x as part of the formulation could have a special behavior due to the reactions



During the purge in the presence of water vapor the small fraction present as molecular iodine will have greater mobility and would in part become airborne. As previously mentioned, in the absence of water vapor there is no release of iodine. Hill and Marsh (7) have shown that the free iodine species and not the total iodine concentration controls the rate of adsorption processes in solutions, but in vapor phase adsorption additional processes may be involved. The iodide species, I^- , on the surface of a charcoal may be slowly oxidized to elementary iodine and the resulting iodine while mostly chemisorbed may also partly gasify. In the absence of water vapor the dominant species at the interface with charcoal is $K^+I_3^-$ and this prevents gasification of both impregnated and adsorbed iodine species. Gasification, of course, is a mechanism that can slowly exhaust the original level of iodine in the impregnation.

Very important questions remain as to the influence of contaminants on both the dosing and purging mechanisms. The kinetics of desorption does not follow a simple exponential decrease and further study is warranted on this important safety feature of the iodine trapping process.

5.0 Conclusions

The use of methyl iodide-127 is a feasible procedure to evaluate penetration. The same results are obtained as with CH_3I -131 which uses a counting technique. One may conclude that the charcoal efficiency in trapping methyl iodide is independent of the iodine isotope species; in fact, the major fraction of the iodine present in a dose of CH_3I -131 is of course CH_3I -127. Moreover, the surface reactions responsible for trapping are independent of the iodine specie. The particular choice of technique may rest on the available instrumentation, i.e. counting equipment or sensitive chromatographic detection. Nevertheless, the charcoal is a sink for all iodine specie and it is important to follow the changes in the major component, i.e. I-127.

The purging of a charcoal with air can be effectively followed using CH_3I -127. The moisture concentration in the carrier is definitely a factor and, for a given charcoal and moisture content of the air, the quantity purged depends on the magnitude of the methyl iodide introduced. The purging of a KI_x impregnated charcoal after dosing with CH_3I -131 (Table 7) shows qualitatively similar behavior to CH_3I -127. The count rate per hour did not appreciably change in the last four hours of purge which is compatible with the purge after the CH_3I -127 challenge. The attainment of an exchange equilibrium between CH_3I -127 and CH_3I -131 when in contact with charcoal is the main problem for the correctness of the results of this analysis.

Acknowledgement

The sponsorship of the Division of Nuclear Fuel Cycles and Production, D.O.E. and the complete cooperation of John C. Dempsey, Contract Manager, are gratefully acknowledged.

15th DOE NUCLEAR AIR CLEANING CONFERENCE

References

- (1) Klotz, I. M. Chem. Rev. 39, 244 (1946).
- (2) Wheeler, A. "Advances in Catalysis" Vol. III, 249-327 Reinhold Publishing Co., New York, N.Y. 1951.
- (3) Jonas, L. A. "Gas Adsorption Kinetics," 1970 Thesis to the Graduate Faculty of the University of Maryland in fulfillment for the degree of Doctor of Philosophy.
- (4) Deitz, V. R. and Jonas, L. A. Nuclear Technology 37, 59-64 (1978).
- (5) RDT Standard, M16-IT, 1977 DOE, Division Nuclear Power Development.
- (6) Deitz, V. R. and Blachly, C. H. Proc 14th ERDA AIR CLEANING Confr. 2, 836-843/1976).
- (7) Hill, A. and Marsh, H. CARBON 16, 31-39 (1968).

DISCUSSION

KOVACH: What is the difference or improvement in your work using the Mast instrument over the data reported in the 9th Air Cleaning Conference?

DEITZ: The improvements produced by the use of the Mast instrument over that used by Hoffman and Thompson were:

- (a) Repeated calibration using (1) the vapor pressure of iodine crystals and (2) the quantitative pyrolysis of methyl iodide from calibrated permeation tubes.
- (b) The solutions in the coulomb meter were changed to minimize and to stabilize the base line signal.
- (c) Adjusted resistance in the electronics to optimize the response of the recorder used.
- (d) Use of glass tubing only, with minimum Teflon tubing for connections.
- (e) The Mast instrument avoids exposure to too-high concentrations of iodine and never saturates the electrode.
- (f) A one-way clutch drive on the pump for mechanical convenience.

The detection limit of our modified instrument is estimated to be 0.01 mv and the precision about 0.05 mv.

KOVACH: How does your procedure show up $\text{CH}_3^{131}\text{I}$ removal by isotope exchange on KI_x -impregnated carbons?

DEITZ: The use of both $\text{CH}_3^{127}\text{I}$ and $\text{CH}_3^{131}\text{I}$ show the same qualitative behavior with a KI_x -impregnated charcoal. The effluent iodine in the purging periods continued at a constant concentration level. The purging with $\text{CH}_3^{127}\text{I}$ was followed for 20 hours (Figure 8) and that for $\text{CH}_3^{131}\text{I}$ on the same sample for 5 hours (Table 7). The surface reactions involve a heterogenous isotope-exchange

15th DOE NUCLEAR AIR CLEANING CONFERENCE

mechanism.

We have not located any published account of an iodine release during the purging of impregnated charcoals with air following a challenge of methyl iodide. It is important to understand that the iodine release occurs only after a challenge of methyl iodide. Before the challenge, no trace of released iodine was observed in the air flow. We postulate that the surface complex, formed in the trapping mechanism of methyl iodide, persists and there is sufficient surface mobility at high relative humidity to gasify the iodine of impregnation.

15th DOE NUCLEAR AIR CLEANING CONFERENCE

EFFECT OF PORE STRUCTURE ON THE ACTIVATED CARBON'S CAPABILITY TO SORB AIRBORNE METHYLRADIOIODINE

A. J. Juhola and J. V. Friel
MSA Research Corporation
Evans City, PA 16033

Abstract

A study was conducted to determine the effect pore structure of activated carbons has on their capability to sorb airborne methylradioiodine. Six de-ashed carbons of very diverse pore structure were selected for study. Batches of each were impregnated with (1) 4.3% I_2 , (2) 5.6% KI, (3) 2% KI, (4) 3% KI - 2% I_2 , (5) 2% I_2 , and (6) 3.4% KIO_3 . Some carbon was reserved for testing without impregnant. Standard procedures at ambient temperature and pressure were followed in the methyl iodide testing, with some changes only made to meet the requirements of the specialized study.

Since water is adsorbed by capillary condensation, the adsorbed water fills the pores to different levels depending on the relative humidity at which the carbon was equilibrated, thus leaving an open-pore volume available for the methyl iodide sorptive processes. The surface area of the open-pore volume, for KI impregnated carbons, determined the sorptive efficiency. This relationship is expressed by the equation

$$\ln p = \ln a - ks$$

where p is the fraction of methyl iodide penetrating the bed and s the surface area. The quantity (a) is associated with the macropore properties, and determines the capability of the carbon to sorb at very high humidities (>95% RH). Constant k is to a large degree dependent on the mean diameter of the micropores.

Elemental iodine impregnated carbons were considerably less effective than those impregnated with KI, and their sorption of methyl iodide did not follow the above equation. Their activity could be increased by a second impregnation with KOH. KI impregnated carbons lost their activity when treated with HCl on converting the KI to I_2 . The conversion of KI to I_2 by acid gases in nuclear power plants offers an explanation for the cause of carbon aging.

I. Introduction

It has been amply substantiated that in common usages of activated carbons, such as in solvent recovery, gas masks, sugar refining, waste water treatment, air purification, water purification, and air pollution control, the pore size distribution is the determining factor in the suitability of the carbon for the intended use. The manner in which the pore structure functions in this respect was discussed in a recent lecture by Juhola.⁽¹⁾ Except for the survey conducted by Dietz and Burchsted,⁽²⁾ no attempts appear to have been made to establish a relationship between pore structure and organic iodide sorption, although, on the basis of observations made in the above mentioned other applications, the pore structure should be a very important factor.

The results presented in this paper are preliminary observations on an in-depth study of the effect of the pore size distributions of several diverse types of activated carbons on their capability to sorb methyl iodide. The ultimate objective is that the results of the study will determine the optimum pore structure.

15th DOE NUCLEAR AIR CLEANING CONFERENCE

II. Experimental

Methyliodide Test

Standard procedures at ambient temperature and pressure were followed as far as possible, with some changes made only to meet the requirements of the specialized study. A one-inch test bed depth was used, rather than the standard two-inch, to get a larger count in the backup bed, and thereby, improve the accuracy of the test results. Methyliodide injection period was 90 min followed by 90 min pure air flow. Concentration was maintained at a level to deliver 2.0 μ l of methyliodide into the carbon beds in the 90 min. For each carbon, tests were conducted at different water contents, from almost dry to saturated state (\sim 99% RH). Sieve size of the carbons was 8 to 16 U.S. standard.

Activated Carbons

Six carbons of very diverse pore structure were selected for study. They were repeatedly leached with HCl, HF, and water to reduce the ash content to low levels to avoid contributions to methyliodide sorption other than that due to pore structure or added impregnants. Table I presents properties, other than pore structure, of the six carbons to indicate the low level of ash attained and diversity of the carbons in other respects.

Table I. Properties of the carbons

Carbon	Base material	Bulk density, g/cc	Ash, %	Total surface area, m ² /g		Pore vol, cc/g
				from pore dist.	from I ₂ No.	
1	Coal	0.55	0.4	820	730	0.42
2	Coconut	0.49	0.3	1160	1170	0.72
3	Coconut	0.40	0.2	1360	1380	1.10
4	Coal	0.51	0.8	1070	1070	0.69
5	Coal	0.29	0.1	1260	1330	1.60
6	Lignite	0.36	1.4	800	650	1.10

Carbons 2 and 3 are frequently used in nuclear power plants.

Total surface area measurements are included in the table since the area is one of the first properties that many investigators attempt to correlate with whatever sorptive property is being investigated. It is also one of the specifications given for carbons used in the nuclear power plants.

The surface areas from pore size distribution curves were calculated using the equation

$$\text{Surface area, m}^2 = \sum_{\substack{\bar{D} = 100,000 \\ \bar{D} = 10}} 40,000 \Delta V / \bar{D} \quad (1)$$

15th DOE NUCLEAR AIR CLEANING CONFERENCE

where ΔV in cc is a small increment of pore volume having an average diameter \bar{D} in Å.

The surface areas from I_2 No. were calculated using the equation⁽³⁾

$$\text{Surface area, m}^2/\text{g} = [I_2 \text{ No. (mg/g)} - 17] / 1.07 \quad (2)$$

The iodine number is determined by liquid phase adsorption from a solution of 0.1 N in I_2 and 0.116 N in KI. It is given in mg/g carbon when final solution concentration is 0.02 N.

The BET surface area was determined only for carbon No. 2 and was 1280 m²/g. BET surface areas for carbons are generally incorrect on the high side, and the error becomes larger as the area is larger. Areas have been reported of over 3,000 m²/g although the theoretical maximum is 2,630 m²/g. BET areas were not used in this study.

Impregnation

Various batches of carbons were impregnated with: (1) 3% KI, 2% I_2 , (2) 5.6% KI, (3) 2% KI, (4) 4.3% I_2 , (5) 2% I_2 , and (6) 4.3% KIO_3 . Tests were also made on carbons with no impregnant added. To determine the effect of acidity and basicity, some carbons impregnated with 4.3% I_2 were again impregnated with KOH, and some carbons impregnated with 5.6% KI were treated with HCl acid. Several runs were made on unleached carbon No. 3 impregnated with 3% I_2 to determine the effect of alkaline ash.

The elemental iodine was sublimed into the carbon by placing the weighed mixture into a sealed rotating jar, and rotating it for 3 hr.

The KI, KI- I_2 , KOH, KIO_3 were sprayed on from water solutions using the rotating jar to get uniform distribution of solution on the carbon. An attempt was made to use only enough solution to just wet the exterior surface of the granules when all the solution had been sprayed. The pore volumes given in Table I were used as guide in determining the amount of solution needed. However, it was found that the exterior of the granules started to get wet with less solution than that required to fill the pore space. The amount of solution required varied from carbon to carbon, but satisfactory results were obtained when solution volume was 80% of pore volume. The slightly surface-wet carbon was then dried until the granules were surface-dry by blowing an air stream into the rotating jar. Drying was completed in an air convection oven at 110°C.

Analyses were made on several of the carbons impregnated with the 3% KI - 2% I_2 mixture to determine whether any changes in chemical composition occur to the mixture because of contact with the carbon surface or interaction with the remaining ash. The dry, weighed carbon sample was first leached with hot water and then dried and weighed to get weight decrease. The sample was then leached with hot NaOH solution and hot pure water, and then dried and weighed to get second weight decrease. The rationale of the procedure is that pure water only removes KI and iodides formed by reaction of the elemental iodine with the remaining ash, and the NaOH solution removes the elemental iodine. The results of these measurements are given in Table II.

15th DOE NUCLEAR AIR CLEANING CONFERENCE

Table II. Measurements to determine chemical changes in 3% KI - 2% I₂ impregnated carbons

	% wt. decrease, based on final wt.				
	Carbon 1	2	3	4	6
Water soluble	2.3	2.5	3.3	2.5	2.3
NaOH sol'n soluble	<u>2.8</u>	<u>2.7</u>	<u>2.3</u>	<u>3.2</u>	<u>3.6</u>
Totals	5.1	5.2	5.6	5.7	5.9

On carbons 1, 2, 4, and 6 there appears to be a conversion of the iodide to the elemental form, while no change occurred in carbon 3. The final leach on de-ashing of carbons 1, 2, 4, and 6 was HF and water until neutral to litmus paper while the final leach on carbon 3 was NaOH and water until neutral. Apparently, enough acidity remained in carbons 1, 2, 4, and 6 to cause conversion of the iodide to iodine.

The weight decrease for each carbon is larger than the 5% impregnant initially added. This may in part be explained by further loss of ash and also by chemical reactions where there is a possible release of H₂O or O₂.

These determinations emphasize the fact that when impregnants are added to even relatively ash-free carbons, the impregnants can undergo chemical changes when subjected to moisture and elevated temperatures during drying. To recognize these possibilities is important to the interpretation of the methyl iodide sorption test results.

Pore Size Distribution Curves

Figures 1 and 2 present the pore size distribution curves of the six carbons studied. The pore size distributions were determined from water adsorption data according to the methods developed by Juhola and Wiig,^(4,5) with some recent modifications added to the procedures. These are (1) the diameter distribution of the pore cavities are now calculated from the adsorption branch of the water adsorption, and (2) a correction is made for helium adsorption in the helium displacement determinations.⁽⁶⁾ The broken line curves represent the distribution of cavity diameters, and the solid line curves the distribution of the constriction diameters. For future reference, micropore volume is defined as volume of pores of diameter less than 30Å on the constriction distribution curve, and of pores that are larger, as macropore volume. The point of division is marked by X on each distribution curve.

The water-adsorption method is effective from about 10Å, at P/P₀ = 0.3 on the adsorption isotherm, to about 2000Å, at P/P₀ = 0.995. In pores of less than 10Å, the restrictive size of the pores prevents normal hydrogen bonding between water molecules, hence the vapor pressure of adsorbed molecules in these pores is higher than normal. When the Kelvin equation is used to calculate pore size of carbons with molecular sieve size pores, the pore diameters derived are then erroneously large. However, commercial activated carbons are generally activated to the level where very small volumes of pores less than 10Å are present.

In pores larger than 2,000Å, the mode of water adsorption appears to change from capillary condensation to multilayer, hence, the exterior surface of the carbon granules become visibly wet before enough water has been adsorbed to fill the pore space. This is of academic interest in isotherm determinations, since meas-

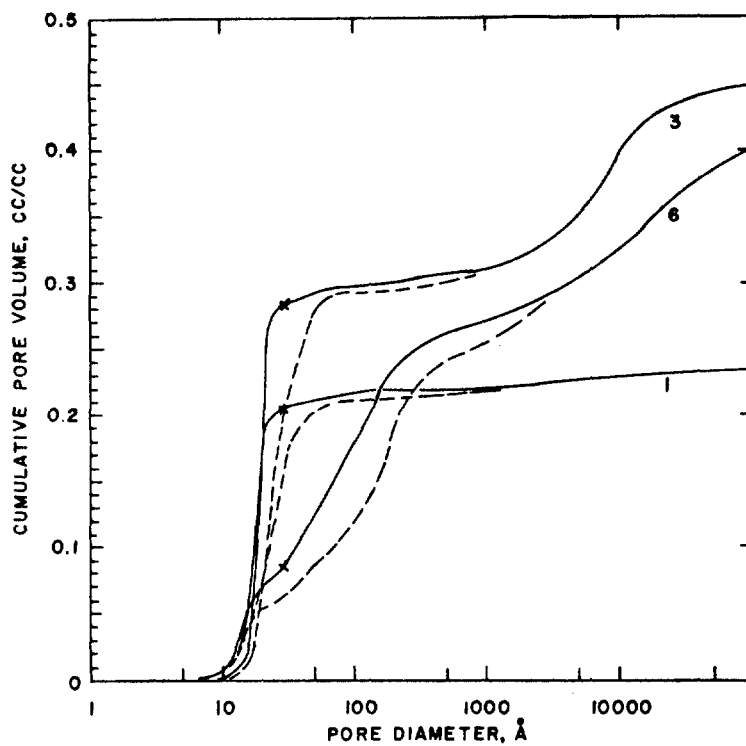


Figure 1 Pore size distribution of activated carbons.

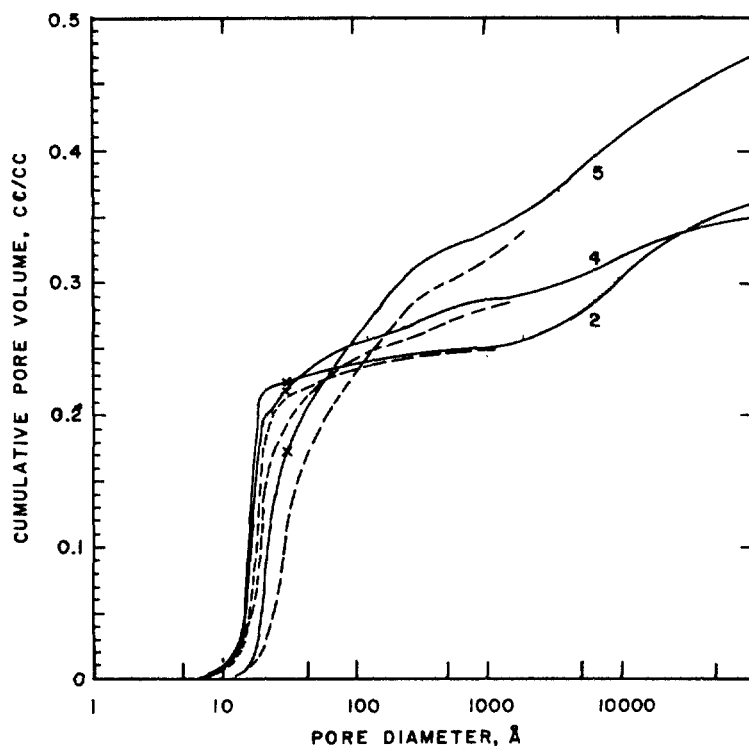


Figure 2 Pore size distribution of activated carbon.

15th DOE NUCLEAR AIR CLEANING CONFERENCE

measurements at P/P_0 over 0.995 are too difficult to attain any degree of accuracy. However, in nuclear power plant applications, humidities above 0.995 P/P_0 are attainable, and as will be shown later in this report, this has a large effect on methyl iodide sorption.

Available Pore Volume and Surface Area

Since water is adsorbed by capillary condensation, at any water content there is a measurable pore volume and an associated surface area that are available for interreaction with the methyl iodide molecules. Figure 3 shows the relationship between these two properties for each carbon. The point of division between micro- and macropores is again marked by X. Macropores are to the left of X on the pore volume scale and micropores to the right. The highest point on each curve represents the total surface area or pore volume of the dry carbon.

In calculating available pore volume, 0.90 g/cc was used for the density of adsorbed water to convert adsorbed weight of water to volume. This volume was then subtracted from total pore volume as determined by helium and mercury displacement measurements.⁽⁵⁾ Equation 1 was then used to calculate the surface area associated with the available pore volume.

As is apparent from the location of the X marks on the curves in Figure 3, only a small fraction of the total surface area is in macropores. Table III gives the numerical values of these pore volumes and surface areas.

Table III. Volume and surface area of micro- and macropores of each carbon bed, 5l cc bed volume.

<u>Carbon</u>	<u>Pore vol, cc/bed</u>			<u>Surface area, m²/bed</u>		
	<u>Micro</u>	<u>Macro</u>	<u>Total</u>	<u>Micro</u>	<u>Macro</u>	<u>Total</u>
1	10.7	1.1	11.8	22,830	170	23,000
2	11.7	6.3	18.0	28,300	700	29,000
3	14.4	8.2	22.6	27,430	720	28,150
4	11.4	6.7	18.1	26,900	1200	28,100
5	8.6	15.1	23.7	15,100	3800	18,900
6	5.0	15.2	20.2	11,700	3200	14,900

The micropores fill with water at 0.80 P/P_0 , hence, the micropore volume given in column 2 is also the volume of water in the carbon bed. The macropore volume is the available pore volume for methyl iodide sorption at high humidities, and, correspondingly, the macropore surface areas are available for methyl iodide sorption. Since acceptance tests are done at P/P_0 over 0.80 and the performance, at crucial times, is expected to occur at these high humidities, the macropore volume and area are important properties of the carbons. Carbon 1 has the smallest macropore area, carbons 2 and 3 (which at present are used in nuclear power plants) have intermediate areas, (carbon 4 is not too greatly different from 2 and 3 and may be a candidate for nuclear power plant usage), and carbons 5 and 6 have large macropore areas.

Location of Impregnant in the Pores

Iodine type impregnants are proven necessities for methyl iodide sorption,

15th DOE NUCLEAR AIR CLEANING CONFERENCE

hence, to be effective they must be located in the pores in such a manner that the methyl iodide can react with them, whether directly or in conjunction with the carbon surface.

Elemental iodine sublimed onto ash-free carbon adsorbs by pore filling, starting with the smallest pores, and as more is adsorbed, larger pores fill up.⁽⁷⁾ Iodine adsorbed from a KI-I₂ water solution adsorbs by surface coverage. The KI does not appear to be adsorbed but remains dissolved in the solution.⁽⁷⁾

What happens to adsorbed elemental iodine when water is adsorbed by the carbon is not definitely known, but it does not desorb when the carbon is leached with hot water. KI in carbons leaches out readily while elemental iodine adsorbed from aqueous phase does not. Although KI is very soluble in water, it must, at some point, start to crystallize out on the carbon surface when the water is desorbed. Whether it is actually adsorbed or just lays down, presumably in a very fine crystalline aggregate form, is not known.

Another factor that should be considered is the variable amount of impregnant on the different carbons because of difference in density. Table IV presents figures on the amount of impregnant on each carbon impregnated with 3% KI and 2% I₂. Also included are estimates of the fraction of pore volume filled and surface area covered, assuming surface adsorption occurs.

Table IV. Amount of impregnant added to carbon, fraction of pore volume filled and fraction of surface covered, for 3% KI, 2% I₂ impregnant.

<u>Carbon</u>	<u>Impregnant added, g</u>	<u>Fraction pores filled</u>	<u>Fraction surface covered</u>
1	1.40	0.033	0.041
2	1.25	0.019	0.029
3	1.02	0.013	0.024
4	1.30	0.020	0.031
5	0.74	0.009	0.026
6	0.92	0.013	0.041

Carbon 1 has the most impregnant, 5 and 6 the least, and 2, 3, and 4 are in the intermediate range. Approximately 1% to 3% of the pore space is filled with impregnant, or 2.5% to 4.0% of the surface is covered if surface adsorption occurs. There is a preponderance of impregnant; i.e., ~1.0 g impregnant to 0.0046 g methyl iodide sorbed, but the impregnant is either widely dispersed or concentrated in the smallest pores. It can easily be submerged under water unless soluble, and become available by migrating through the solution.

Since nothing definite could be determined regarding location of impregnant, attempts to correlate methyl iodide sorption with impregnant content by itself or in conjunction with pore structure were abandoned early in the study. Pore volume and surface area were then considered.

15th DOE NUCLEAR AIR CLEANING CONFERENCE

III. Experimental Results and Discussion

Correlation of Available Pore Volume with Methyl iodide Sorption

Figure 4 shows the relationship between available pore volume and methyl iodide penetration. It was apparent from the curves that other properties than pore volume control the methyl iodide sorption.

Correlation of Available Surface Area with Methyl iodide Sorption

Carbons Impregnated with 3% KI, 2% I₂. Figures 5 and 6 show the relationship between available surface area and methyl iodide penetration through the carbon bed. Within experimental error, the straight line correlation shows a close dependence of methyl iodide sorption on the available surface area. The relationship obeys the equation

$$\ln p = \ln a - ks \quad (3)$$

where p is the fraction penetrated, s is the available surface area, a and k are constants for each carbon. The correlation extends from s equal to virtually zero to the total surface area for carbons 1, 3, 5, and 6. For carbon 2, a change in slope occurs at 10,000 m², and for carbon 4 at 6,400 m². This break in slope occurs at a mean pore diameter of 20Å, indicating that pores of less than 20Å in diameter are less effective for methyl iodide sorption than the larger pores for these two carbons, but does not apply to other carbons. Carbons 1, 3, 5, and 6 have considerably less pore volume and/or surface area in pores less than 20Å in diameter, which explains the absence of slope change in their graphs.

The quantity (a) is the fraction of methyl iodide penetrating the carbon bed when s is zero. It was possible to check (a) on several runs at $P/P_0 = 0.99$, where s is virtually zero; but, when the exterior of the carbon granules became wet on other attempts, the fraction of penetration was much larger than (a). (a) is then the fraction of penetration when the pores are filled with water to the point where the available surface area is virtually zero, but the external surface of the granules is not wet. However, on those runs where high humidities were maintained without causing surface wetness, the amount of water in the carbon was not enough to fill the pore space. Even those carbons that were slightly wet still had available pore space.

Unimpregnated and Carbons Impregnated with KI or I₂. Figures 7, 8, and 9 show the relationship between s and p when the carbon is not impregnated or when impregnated with KI or I₂.

Carbons impregnated with KI give straight line plot close to those observed for carbons impregnated with 3% KI and 2% I₂, Figures 7, 8, and 9.

With no impregnant the plots have considerable curvature; the sorption does not follow equation 3. Methyl iodide is adsorbed by physical or van der Waal's forces where the preferred sorption occurs in the smallest pores. Since these pores fill with water first on humidification, the carbon loses much of its adsorptive capacity at low water contents.

The sorption pattern of elemental iodine impregnated carbons in some cases follows one that is between those of the unimpregnated and KI impregnated carbons and in other cases is similar to the unimpregnated. In every case observed, the elemental iodine impregnant is considerably less effective than the KI. Apparently, the small amount of iodine impregnant is adsorbed in the smallest pores, and when

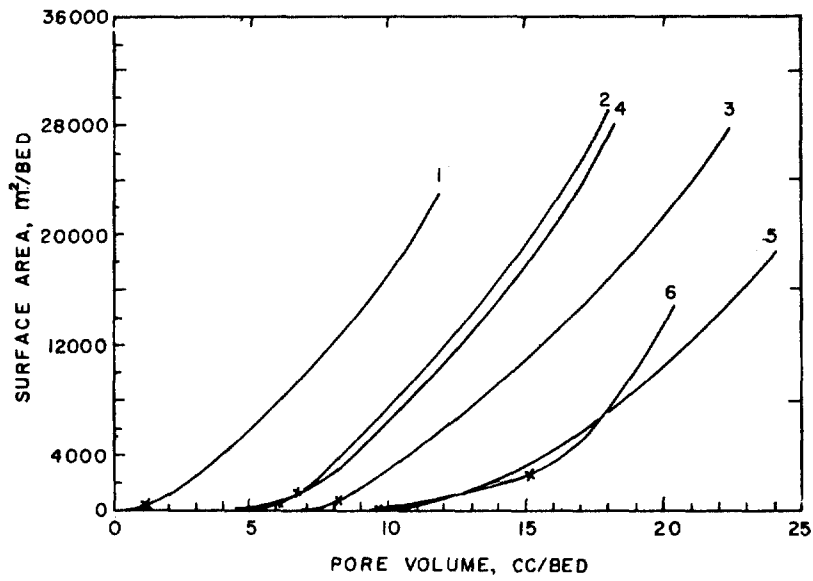


Figure 3 Available surface area as function of available pore volume in carbon bed.

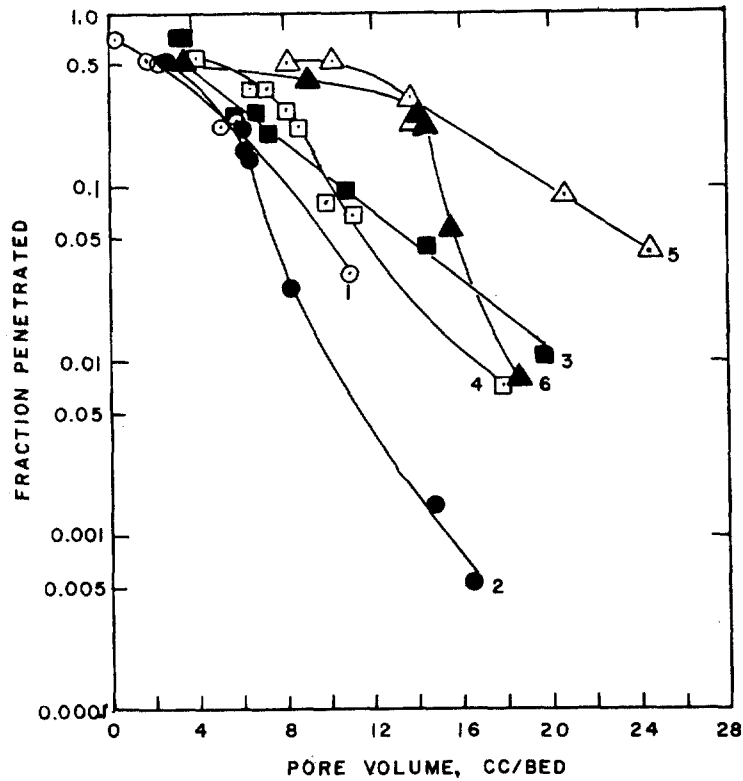


Figure 4 Methyl iodide penetration as function of available pore volume of carbons impregnated with 3% KI, 2% I₂

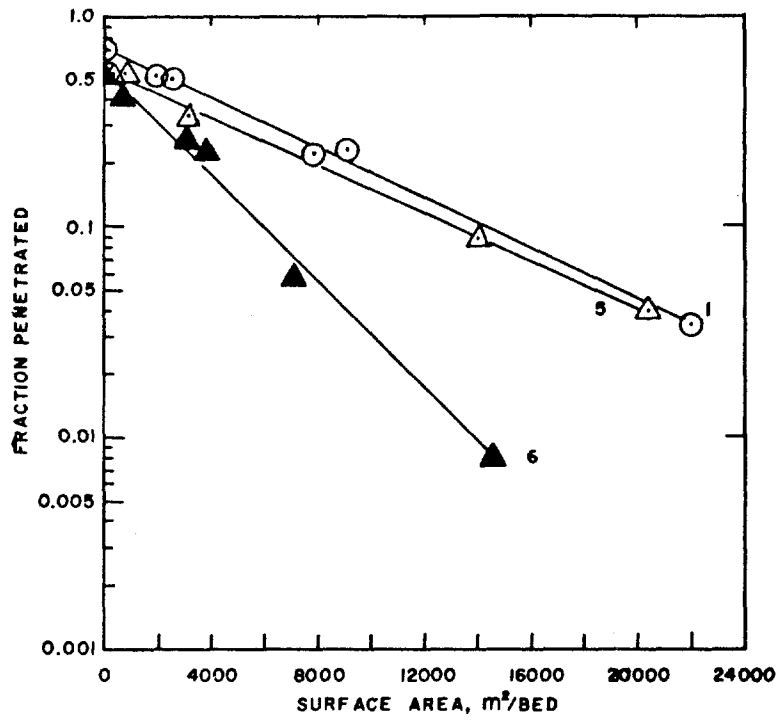


Figure 5 Methyl iodide penetration as function of available surface area of carbons impregnated with 3% KI, 2% I₂

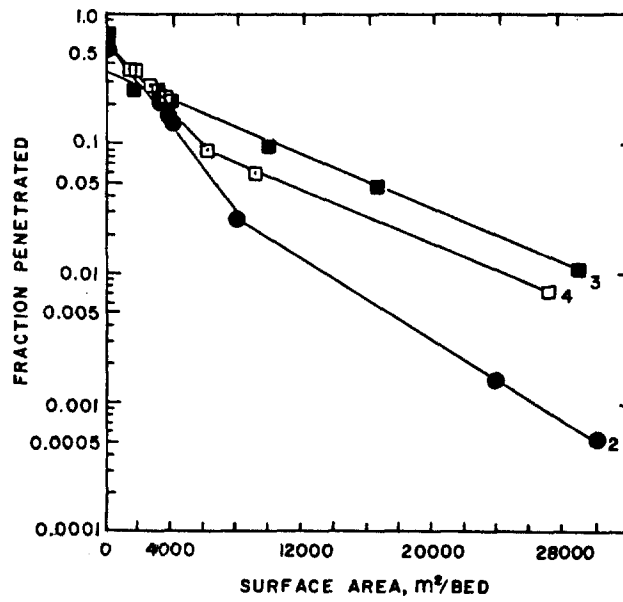


Figure 6 Methyl iodide penetration as function of available surface area of carbons impregnated with 3% KI, 2% I₂

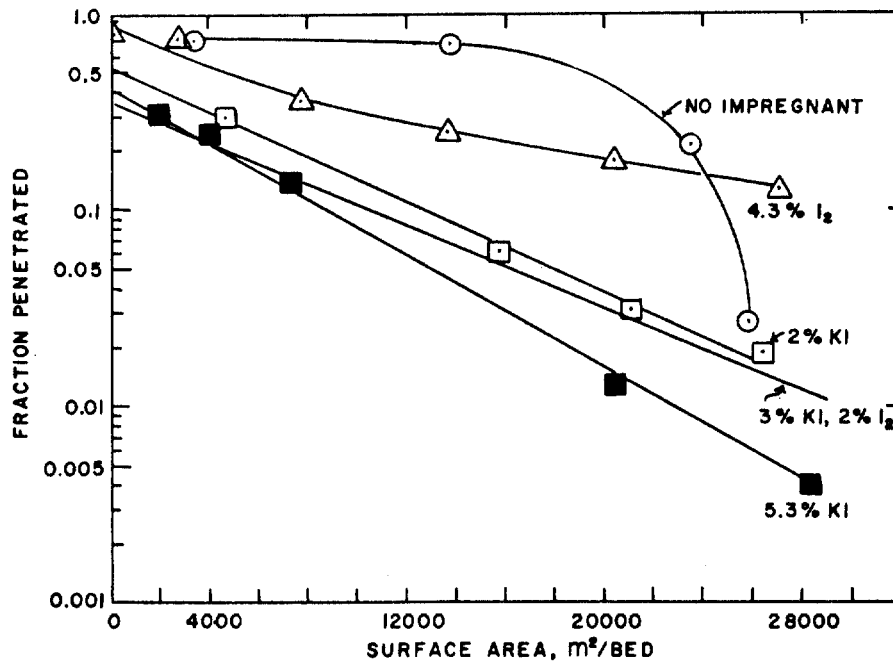


Figure 7 Methyl iodide penetration as function of available surface area of carbon No.3 with various impregnants.

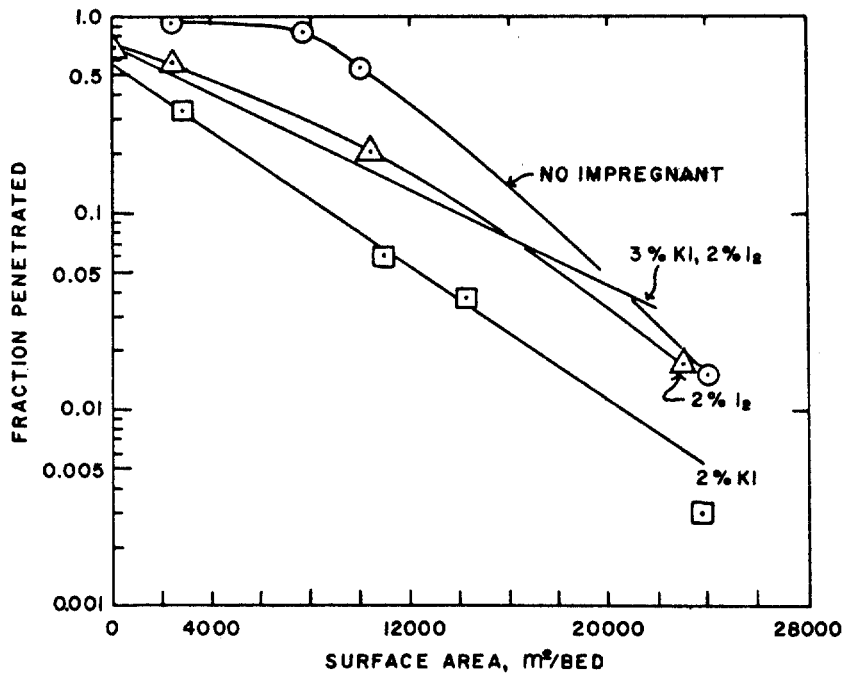


Figure 8 Methyl iodide penetration as function of available surface area of carbon No.1 with various impregnants.

15th DOE NUCLEAR AIR CLEANING CONFERENCE

water is adsorbed, the iodine is submerged or blocked off from external contact. This explanation accounts for the rapid loss of sorptive capacity of carbon 6, Figure 9. Carbons 1 and 3 show some activity.

Effect of Ash, HCl, and KOH

The effect of ash, HCl, and KOH were determined for KI and I₂ impregnated carbon No. 3. The results of these determinations are shown in Figure 10.

The effect of ash was determined by subliming 3% I₂ into the unleached carbon, which has 2.6% ash, mostly alkaline. The lowest curve in Figure 10 has two experimental points, one determined at about 80% RH, at the upper left end, and one at 13% RH, at the lower right end. To determine the lower point, the dry carbon, with the sublimed I₂, was first equilibrated to 90% RH and then dried with a dry air stream. The methyl iodide test was then run at 13% RH. When the dry carbon was tested directly, without the 90% pretreatment, the methyl iodide penetration was much greater as indicated by the higher experimental point. Moisture is needed to cause the iodine to react with the ash to form KI, NaI, KOI, NaOI and possibly some iodates. Without ash, the curve of the iodine treated carbon would have been near the 4.3% I₂ curve. When the carbon was humidified until the granules were surface-wet, the penetration was higher than would have been predicted by extension of the curve to zero surface area, as indicated by the point at 0.4 penetration.

When a sample of 5.6% KI impregnated carbon was treated with 1.2% HCl, the acid converted the iodide to elemental iodine causing methyl iodide penetration to increase from 0.24 to 0.74. This is considerably above the curve for the 4.3% I₂ impregnated carbon.

When a sample of 4.3% I₂ impregnated carbon was treated with 1.9% KOH, the elemental iodine was converted to a mixture of KI, KOI, and KIO₃, causing a decrease of methyl iodide penetration from 0.50 to 0.33.

Carbon impregnated with 3.4% KIO₃ gave a penetration of 0.39. The short line beneath the point is for 2% KI impregnated carbon. Although the KIO₃ has the same amount of iodine as 2% KI, the KIO₃ form does not appear to be as effective as KI. KIO₃ is considerably less soluble than KI, hence less mobile in the adsorbed water. This may in part account for its lower activity.

Two observations can be made on the basis of this phase of the study. The presence of acid vapors in the air stream can convert the active KI to inactive I₂, and the carbon bed loses its capacity to sorb methyl iodide. Ash can greatly alter the composition of impregnants added to the carbon, thus introducing an unknown variable. Any research program on the effects of impregnants should take into consideration the effect of the ash on the impregnant.

Effect of Impregnant on pH

Since ash, and addition of HCl or KOH affect the sorptive properties of the carbon by causing changes in impregnant composition, this phase of the overall program was investigated further in regard to pH. It has been observed that loss of sorptive capability is accompanied by decrease of pH of the carbon as measured on the water extract from the carbon.

Table V presents the results of the impregnant versus pH measurements. The tendency is for the pH to increase when the impregnant added to the carbon con-

15th DOE NUCLEAR AIR CLEANING CONFERENCE

tains KI. When only I₂ is added, the pH decreases. For initially neutral carbons, such as 3 and 4, the addition of KI produced essentially no change, while the addition of I₂ alone produced a very large decrease in pH.

These results raise an academic question. Is the decreased activity of carbons with low pH due to a high hydrogen ion concentration, or due to the conversion of KI to I₂?

Table V. Effect of impregnant on pH

<u>Carbon</u>	<u>Impregnant</u>	<u>pH</u>
1	none	3.9
1	3% KI, 2% I ₂	5.1
1	2% KI	6.2
1	2% I ₂	3.3
2	none	4.4
2	3% KI, 2% I ₂	6.8
2	2% KI	7.0
2	2% I ₂	3.3
3	none	6.9
3	3% KI, 2% I ₂	7.1
3	2% KI	6.8
3	5.6% KI	7.0
3	4.3% I ₂	3.0
4	none	7.1
4	3% KI, 2% I ₂	7.0
5	none	5.0
5	3% KI, 2% I ₂	5.7
6	none	2.5
6	2% KI	3.6
6	2% I ₂	2.4
6	none	5.0
6	3% KI, 2% I ₂	5.8

Constants a and k

The constants a and k of equation 3 were further investigated in their relationship to pore structure. From the study two equations were evolved.

$$a = f / (S_m \times \text{pH}^2) \quad (4)$$

$$k = f / \bar{D} \quad (5)$$

where S_m is the area of pores larger than 2000Å diameter and \bar{D} is the mean micropore diameter. Table VI presents the numerical values of (a), k, and \bar{D} for the KI and KI-I₂ impregnated carbons.

Figure 11 summarizes graphically the results which show the dependence of (a) on S_m and pH, equation 4. For carbon 3 which has the largest S_m, the effect of pH is very pronounced. At 6.8 pH (a) was 0.5, but at 9.4 pH (a) had decreased to 0.22, or 0.108 units decrease of (a) per unit of pH increase. For carbon 6, which has a

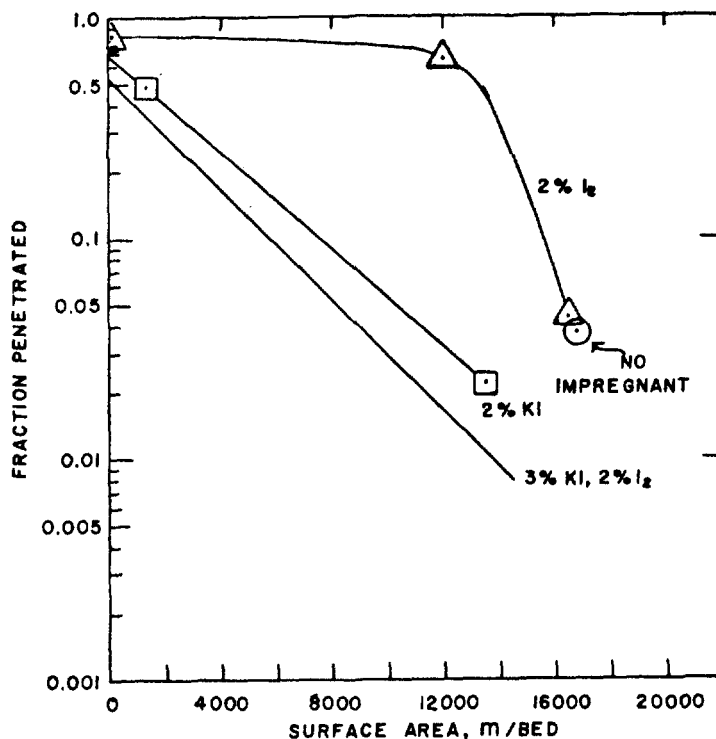


Figure 9 Methyl iodide penetration as function of available surface area of carbon No. 6 with various impregnants.

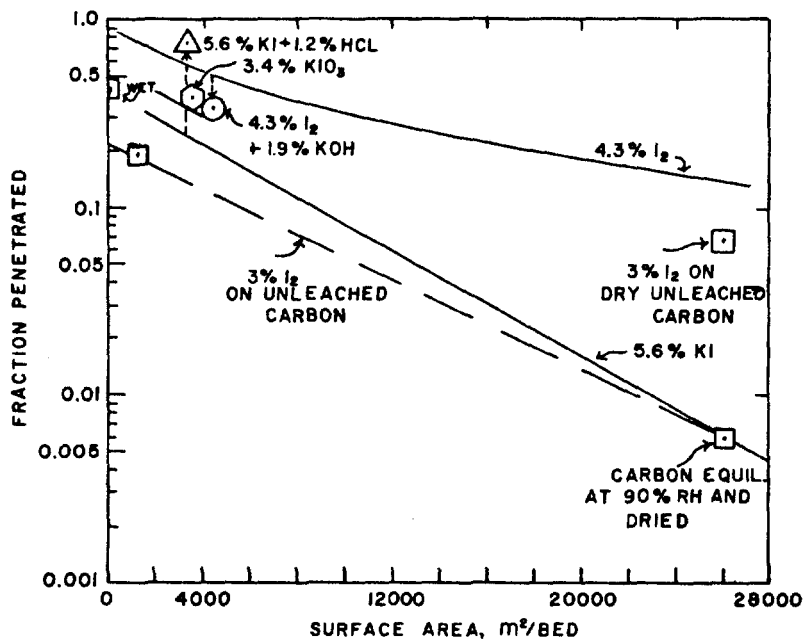


Figure 10 Effect of HCL, KOH, and ash on methyl iodide sorption, carbon No. 3.

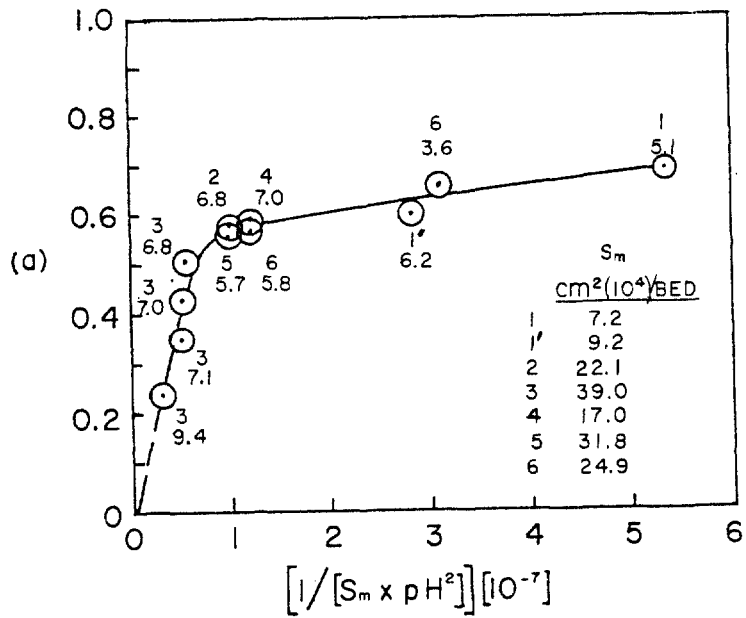


Figure 11 (a) as function of pH^2 and of surface area, S_m , of pores larger than 2000Å diameter

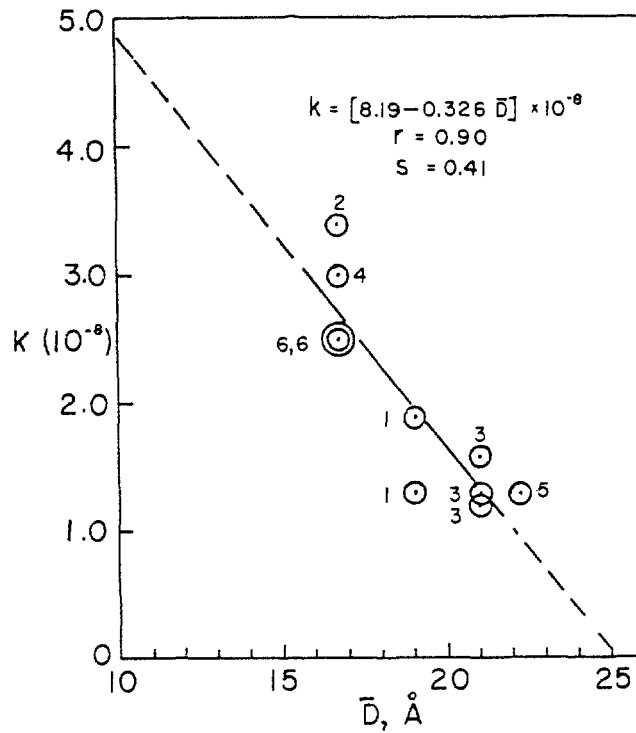


Figure 12 k as function of micropore mean diameter, \bar{D}

15th DOE NUCLEAR AIR CLEANING CONFERENCE

smaller S_m , the effect of pH is less pronounced. At 3.6 pH (a) was 0.66 and at 5.8 pH (a) decreased to 0.56, or 0.045 units decrease of (a) per unit pH increase. Carbon 1 appears to follow the same pattern. If more data were available for verification, it is probable the carbons of different S_m would have characteristic curves dependent on pH.

Table VI. Constants a and k of equation 3

<u>Carbon</u>	<u>Impregnant</u>	<u>a</u>	<u>$k(10^{-8})$</u>	<u>$\bar{D} \text{ \AA}$</u>
1	3% KI, 2% I ₂	0.69	1.3	19
2	" "	0.58	3.4	17
3	" "	0.35	1.2	21
4	" "	0.59	3.0	17
5	" "	0.56	1.3	22
6	" "	0.56	2.5	17
1	2% KI	0.55	1.9	19
6	"	0.66	2.5	17
3	"	0.54	1.6	21
3	5.6% KI	0.43	1.3	21

Figure 12 shows the dependence of k on \bar{D} , equation 5. The coefficient of correlation, r , is 0.90 and standard error of estimate, s is 0.41.

VII. Conclusions

Pore Structure Effects

The methyl iodide penetration, p , through a KI impregnated carbon bed is a function of the available carbon surface area, s , at various levels of moisture content as expressed by the equation

$$\ln p = \ln a - ks$$

(a) is the penetration at high humidities where s is very small. It is inversely proportional to the surface area of pores larger than 2000Å diameter. Constant k is inversely proportional to the mean micropore diameter.

An ideal carbon would have the micropore characteristics of carbon 2, to give a large k , and the macropore characteristics of carbon 3, to give a small (a). Such a carbon would be most effective at all levels of moisture content.

Impregnant Effects

The potential performance of a carbon with the favorable pore structure can be nullified or enhanced by the state of the impregnant and/or pH of the carbon. With decreasing pH, methyl iodide penetration increases. Whether this is a direct effect of the hydrogen ion concentration or due to the conversion of alkaline iodide to elemental iodine is not known. It may be due in part to both. By increasing the pH, as by adding caustic, methyl iodide penetration is decreased, but there are limits to the amount of caustic that can be added because of its effect on the ignition temperature. In nuclear power plants, acid vapors in the air stream drawn through the carbon bed can in time convert KI to I₂, or decrease pH, and cause in part, the observed loss of sorptive capability.

15th DOE NUCLEAR AIR CLEANING CONFERENCE

The amount of KI impregnant in the 2% to 5.6% range did not appear to have any effect on sorptive capability; the critical range must be considerably below 2%.

References

1. Juhola, A. J., "Manufacture, pore structure, and application of activated carbons," Kemia 4, No. 11, pp 543; No. 12, pp 653 (1977).
2. Dietz, V. R. and Burchsted, C. A., "Survey of domestic charcoals for iodine retention," NRL Memorandum Report 2960, Naval Research Laboratory, Washington, D.C. (Jan. 1975).
3. Grant, R. J., "Basic concept of adsorption on activated carbon," an internal report of Pittsburgh Activated Carbon Company (1951).
4. Juhola, A. J. and Wiig, E. O., "Determination of micropore size distribution," J. Am. Chem. Soc., 71, 2069 (1949).
5. Wiig, E. O. and Juhola, A. J., "Determination of macropore size distribution," J. Am. Chem. Soc., 71, 2078 (1949).
6. Juhola, A. J., "Organic vapor adsorption and micropore structure of activated carbons," MSAR Report 78-52 (1977).
7. Juhola, A. J., "Iodine adsorption and structure of activated carbons," Carbon, 13, pp 437 (1975).

15th DOE NUCLEAR AIR CLEANING CONFERENCE

METHYL IODIDE RETENTION ON CHARCOAL SORBENTS AT PARTS-PER-MILLION CONCENTRATIONS*

G. O. Wood, G. J. Vogt, and C. A. Kasunic
Los Alamos Scientific Laboratory
University of California
Los Alamos, New Mexico 87545

Abstract

Breakthrough curves for charcoal beds challenged by air containing parts-per-million methyl iodide (I-127) vapor concentrations were obtained and analyzed. A goal of this research is to determine if sorbent tests at relatively high vapor concentrations give data that can be extrapolated many orders of magnitude to the region of interest for radioiodine retention and removal. Another objective is to identify and characterize parameters that are critical to the performance of a charcoal bed in a respirator cartridge application. Towards these ends, a sorbent test system was built that allows experimental variations of the parameters of challenge vapor concentration, volumetric flow rate, bed depth, bed diameter, and relative humidity. Methyl iodide breakthrough was measured at a limit of 0.002 ppm using a gas chromatograph equipped with a linearized electron capture detector.

Several models that have been proposed to describe breakthrough curves were tested against experimental data. Only the equations of a Theory of Statistical Moments, including the first three moments, adequately described the breakthrough curves over the entire three orders of magnitude in breakthrough concentration. These moments, which are easily calculated by data fitting, have physical significance and can be related to measurable parameters. A variety of charcoals used or proposed for use in radioiodine air filtration systems have been tested against 25.7 ppm methyl iodide to obtain these parameters and protection (decontamination) factors.

Effects of challenge concentration, relative humidity, and bed diameter were also investigated. Significant challenge concentration dependence was measured (more efficiency at lower concentration) for two types of charcoals. Increased relative humidity greatly decreased breakthrough times for a given protection factor. Increased bed diameter greatly increased breakthrough times for a given protection factor. Implications of these effects for a test method are discussed.

*Work supported by the Nuclear Regulatory Commission and performed at the Los Alamos Scientific Laboratory operated under the auspices of the U. S. Department of Energy, Contract No. W7405 ENG-36.

15th DOE NUCLEAR AIR CLEANING CONFERENCE

I. Introduction

A question that is being raised more frequently is the adequacy of air-purifying respirators for personal protection against airborne radioiodine. The degree of protection that can be expected due to facial fit under a variety of work exercises is becoming better defined by research done at Los Alamos and other places. However, the efficiency of charcoal beds in the form of respirator cartridges remains much in doubt. Therefore, we have undertaken the responsibilities to (1) develop acceptance criteria for an air-purifying respirator to protect against forms of airborne radioiodine and (2) develop test methods for certifying respirator cartridges for such a use.

We have selected for initial investigation the approach of using nonradioactive (I-127) methyl iodide at parts-per-million concentrations for testing the performance of charcoal beds. The big question that appears is how does sorbent efficiency at ppm levels relate to efficiency at much lower ($\sim 10^{-7}$ ppm) levels of concern with radioiodine. In the first phase of our research we have attempted to define performance of sorbents at ppm concentrations of methyl iodide and identify the parameters critical to this performance. In the future we will investigate identical sorbent beds at lower challenge concentrations using radioiodine (I-131) species and counting measurement techniques. Then we should have an answer to the question of validity of extrapolation of charcoal bed efficiencies over orders-of-magnitude differences in challenge vapor concentrations.

Some differences must be recognized between the uses of charcoal beds for radioiodine removal. These mostly involve the ranges of parameters to be considered. For respirator cartridges bed size, weight, and pressure drop are more critical considerations. Also, airflows are cyclical and may range widely depending on the workload of the user. The complete range of relative humidities must be considered in both cases. However, only ambient temperatures must be considered for respirator cartridge beds, since radioiodine loadings must be kept low. Equilibration of a respirator cartridge to ambient humidity and airflows may vary from none to the lifetime of its use, depending on the regulations regarding its preparation, storage, use, and replacement.

The application of a sorbent bed in the form of a respirator cartridge is similar in many ways to the application of a much larger sorbent bed for high volume ambient air cleaning. In fact, the radioiodine air cleaning literature has been most valuable in beginning our investigations. Effects of parameters such as challenge vapor concentration, relative humidity, and airflow velocity on bed performance and testing procedures are similar. Therefore, we are presenting our experimental results and conclusions in this forum with the expectation that they will add to the understanding of charcoal bed performance in both applications.

II. Experimental

Figure 1 is a schematic of the apparatus that was used to measure the performance of charcoal beds for methyl iodide removal. Pressurized air was regulated, filtered, and humidified to obtain

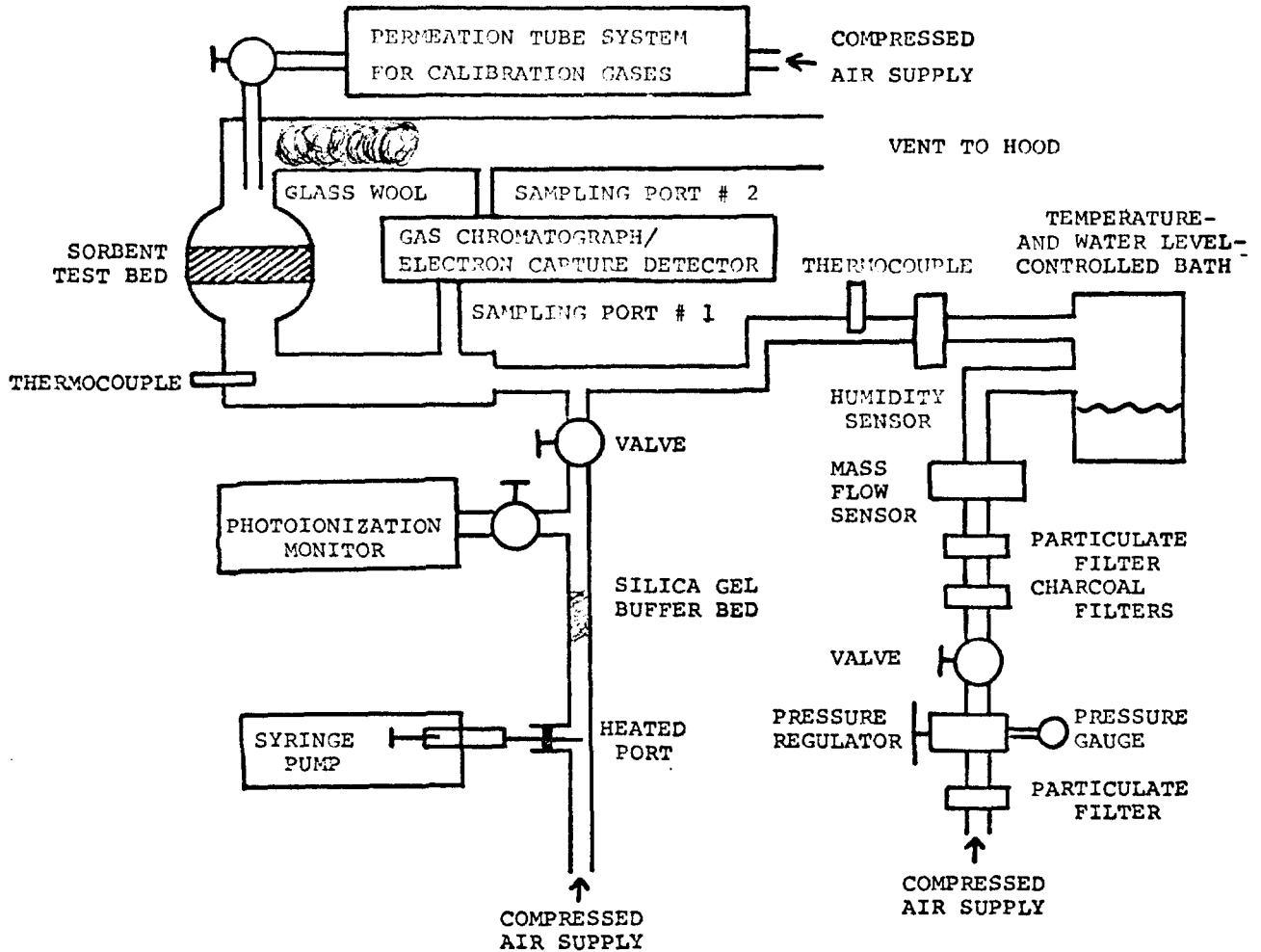


Figure 1 Schematic of the sorbent test flow system.

the conditions desired. A calibrated electronic flow meter and an electronic humidity meter were used to monitor, and in the case of the latter, to control these conditions. Liquid methyl iodide was metered at a calibrated rate by a syringe pump into a heated port where it vaporized and was swept into the main airstream by an auxiliary (0.2 L/min) airstream. From this point in the apparatus to the sorbent bed, all tubing was 2.5-cm glass. An air monitor with a photoionization detector was used to monitor the output of the syringe pump generation system. Air entering the charcoal bed and effluent air were alternately sampled by an automated gas sampling valve with Teflon loops. Such samples were introduced into a gas chromatograph, separated on a silicone OV-7 (15% on 100/120-mesh Chromosorb G) column (4-mm i.d. x 1.8-m long, 100°C, 20 cm³/min 19:1 Ar/CH₄) and measured for methyl iodide with a Ni-63 linearized electron capture detector. An electronic peak integrator was used to quantitate the methyl iodide peaks and to record elapsed times. Teflon and glass was used throughout the sampling and analysis system except for the sampling valve, which was Hastalloy C, and the detector, which was stainless steel (300°C).

15th DOE NUCLEAR AIR CLEANING CONFERENCE

The valve-gas chromatograph-electron capture measuring system was frequently calibrated using Teflon permeation tubes containing liquid methyl iodide. The outputs of these permeation tubes, maintained at constant ($\pm 0.3^\circ\text{C}$) temperatures, were quite constant over periods of many months, as determined by weekly weighings. These known methyl iodide outputs were mixed in known airflows to produce known methyl iodide concentrations (0.03-26 ppm). Calibration indicated that the detector response was indeed linear over at least 3 orders of magnitude and methyl iodide concentration was proportional to measured peak area. The response of the measurement system was affected slightly by relative humidity of the air. The limit of measurement was about 2 parts-per-billion methyl iodide in air.

The experimental procedure was as follows. The airflow (20-40 L/min) was stabilized at a selected relative humidity. The syringe pump was started and its output was diverted to the photoionization monitor. Meanwhile, the output of a calibrated permeation tube was introduced at 1 L/min into the main airstream. The detector system was recalibrated in this way. The flow from the permeation tube to the main airstream was stopped. A charcoal bed was prepared by weight in a cylindrical glass tube of selected diameter. This was placed in the flow system. After 5 min, the syringe pump output was diverted into the main airstream and the experiment was begun. After significant breakthrough (10-20%) of the test bed had occurred, the experiment was terminated.

III. Interpretation of Breakthrough Curves

The raw data obtained from the experiments described above were in the form of peak areas vs elapsed time (t_B). Syringe pump output and volumetric airflow rates were used to calculate challenge concentrations (C_O) in ppm. Detection system calibration factors obtained from permeation tube outputs were used to convert peak areas to breakthrough methyl iodide concentrations (C_B) in ppm. The data were then converted to fractional breakthrough (C_B/C_O) vs elapsed time (t_B) for further analysis.

Several models that have been proposed to describe breakthrough curves were tested against the experimental methyl iodide breakthrough data. The most common descriptions of breakthrough curves are based on the Mecklenburg equation, which has the basic form:

$$t_B = \frac{a_1}{C_O} (b_1 - h) \quad (1)$$

where h is the "dead layer" depth or the "critical" bed depth, i.e., that value below which breakthrough would be instantaneous. In this equation and those following a_i and b_i refer to combinations of parameters that are constant for a given breakthrough curve. The many variations of the Mecklenburg equation that have been proposed have differed primarily in the expression used to calculate h . For example, the Klotz, Sillen, Van Dongen, Wheeler, and Jonas equations have $h = -a_2 \ln (C_B/C_O)$. The Danby equation has $h = -a_3 \ln [C_B/(C_O - C_B)]$, which is equivalent in form to the others for $C_B/C_O < 0.1$. All these variations of the Mecklenburg equation predict that a plot of t_B vs $\ln (C_B/C_O)$ or vs $\log (C_B/C_O)$ would be linear. Figure 2 shows

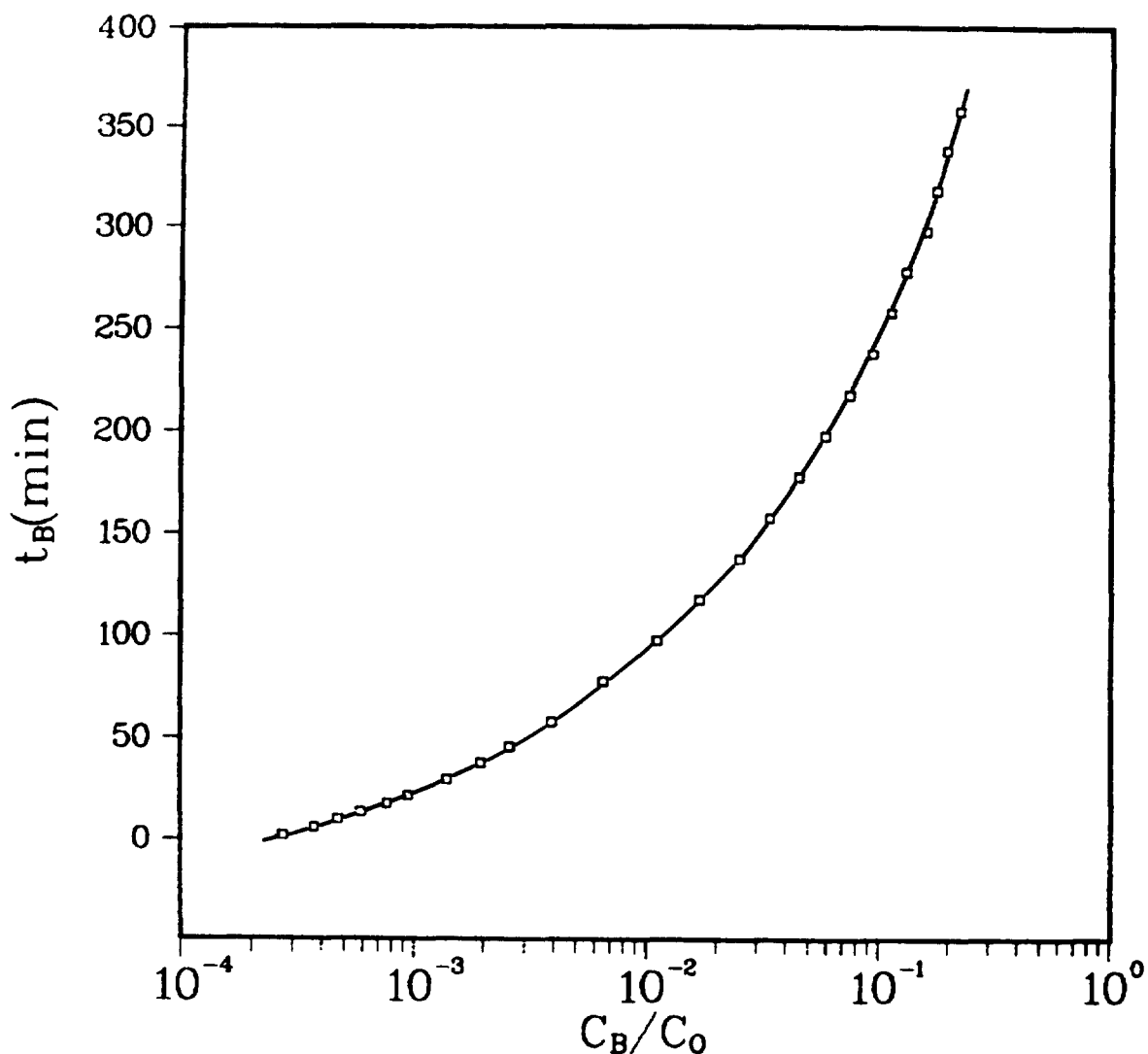


Figure 2 Semilog plot of the breakthrough curve data.

such a plot for data obtained in an experiment with a bed of Barnebey Cheney 487 charcoal (5% TEDA impregnated) at these conditions:

25.7 ppm methyl iodide challenge concentration
 20 L/min airflow rate at $21 \pm 1^\circ\text{C}$, 585 torr
 50 % relative humidity
 4.1-cm-diam x 2.5-cm-deep bed.

Every fifth data point of 90 obtained was plotted in this graph. This plot is clearly nonlinear over the entire range of data. Therefore, the variations of the Mecklenburg equation with $h = -a_2 \ln(C_B/C_0)$ do not adequately describe the breakthrough of methyl iodide in this experiment.

The second description attempted for methyl iodide breakthrough was an empirical relationship,

$$t_B = a_4 (C_B/C_0)^{b_4} \quad (2)$$

This implies that a plot of $\log t_B$ vs $\log (C_B/C_0)$ is linear. Such a plot (Fig. 3) for the same set of data was linear only in the range $C_B/C_0 = 0.005$ to 0.22 and, therefore Equation 2 is not adequate. Furthermore, the parameters from such a data fit have no known physical significance.

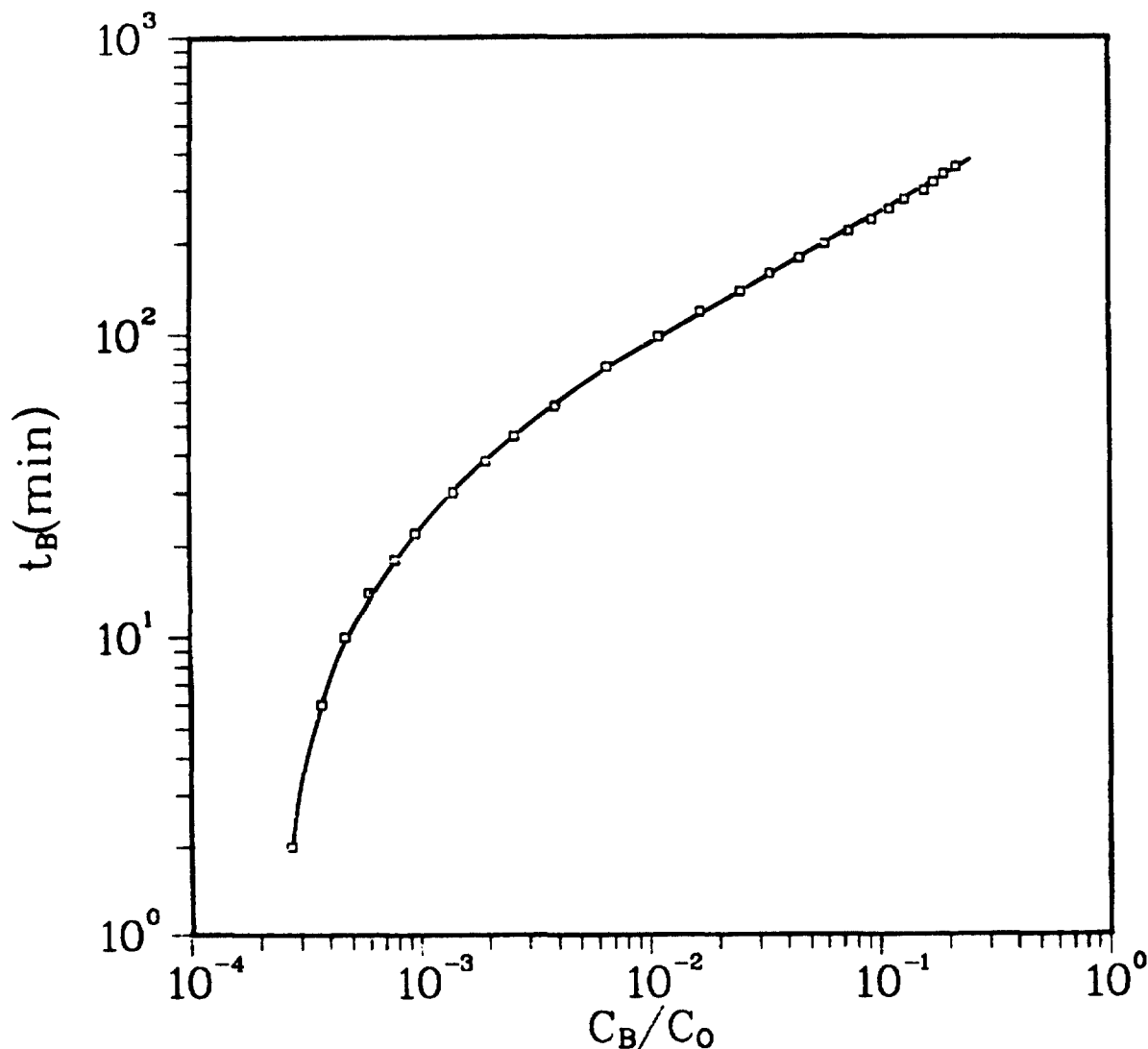


Figure 3 Log-log plot of the breakthrough curve data.

The most successful fit of this set of breakthrough data was obtained using the equations developed for a Theory of Statistical Moments by Otto Grubner and Dwight Underhill.⁽¹⁻²⁾ By this theory the breakthrough curve can be generated from its moments by a series such as the Gram-Charlier series. Simplifications of the adsorption mechanism are required to obtain analytically useful equations whose parameters are related to parameters of physical significance. The references cited provide further explanation. A basic equation obtained by retaining the first three statistical moments (m_1, m_2, m_3) is

$$t_B = m_1 + \sqrt{m_2} (X_B) + \frac{m_3}{6m_2} (X_B^2 - 1), \quad (3)$$

where

$$C_B/C_O = \frac{1}{\sqrt{2\pi}} \int_{-\infty}^{X_B} \exp \left[\frac{-x^2}{2} \right] dx. \quad (4)$$

Equation 4 is the normal probability integral whose values of X_B for C_B/C_O are readily available in tabulated form or may be calculated on a programmable calculator. Equation 3 predicts a parabolic relationship between t_B and X_B for 3 statistical moments and a linear relationship if 2 statistical moments are sufficient. Figure 4 shows a plot of t_B vs X_B for the same set of data considered previously. This plot is linear only for $-X_B < 1$ or $C_B/C_O > 0.16$. However, a parabolic fit of the data by least-squares regression to $t_B = a_0 + a_1 X_B + a_2 X_B^2$ produced a curve such as that drawn through the data points. Such a fit is excellent over the entire range of the data with $m_1 = 578 \text{ min}$, $\sqrt{m_2} = 274 \text{ min}$, and $m_3/6m_2 = 34.36 \text{ min}$.

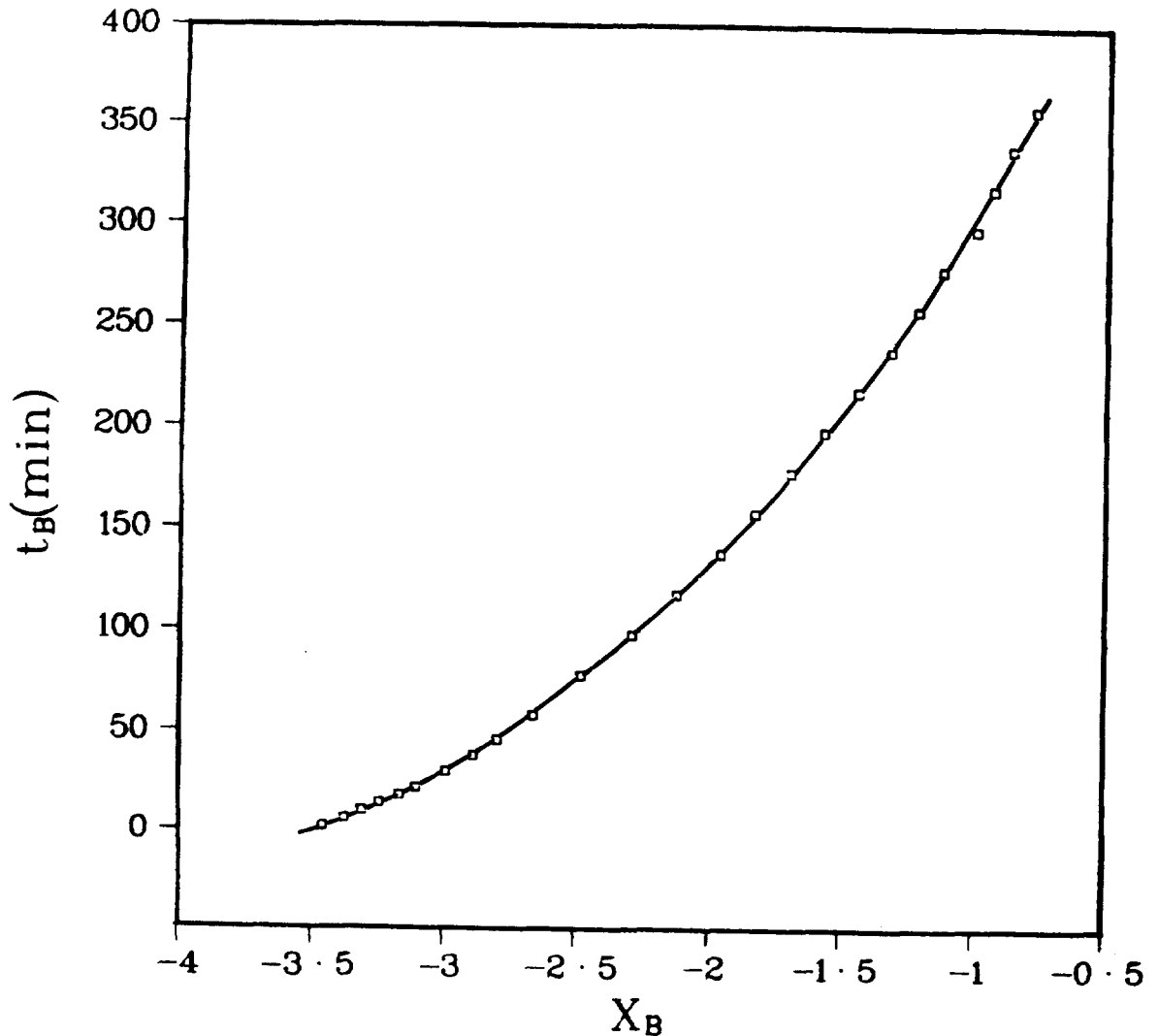


Figure 4 Probability plot of the breakthrough curve data.

15th DOE NUCLEAR AIR CLEANING CONFERENCE

Fits of the parabolic form of the Theory of Statistical Moments to breakthrough curves for two other charcoals are shown in Fig. 5. The triangles represent data for a bed of Union Carbide ACC nonimpregnated charcoal and the circles represent data for a bed of North American Carbon G615 KI/TEDA-impregnated charcoal. Experimental conditions were:

- 25.7 ppm challenge concentration
- 20 L/min airflow rate
- 33% relative humidity
- 6.9-cm-diam x 2.5-cm-deep bed.

The curves drawn through the experimental points are representative of those calculated from parameters m_1 , m_2 , m_3 obtained by least-squares fitting of the data. Again, the theory described the breakthrough curve very well for these different types of charcoals.

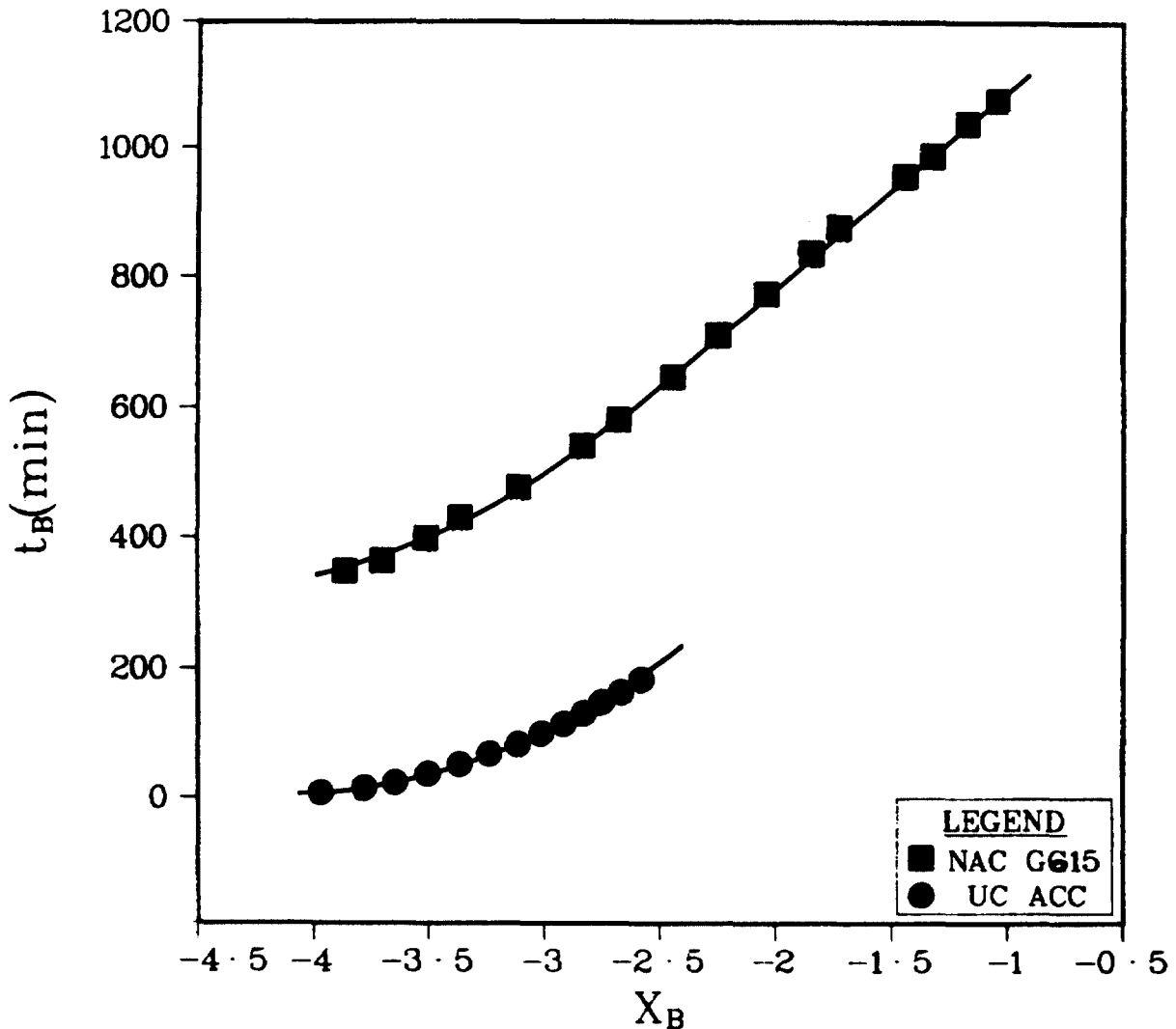


Figure 5 Probability plots of breakthrough curve data for a KI/TEDA-impregnated charcoal (NAC G615) and a non-impregnated charcoal (UC ACC).

15th DOE NUCLEAR AIR CLEANING CONFERENCE

One advantage of having such a good description of the breakthrough curve is that it allows interpolation and limited extrapolation of experimental data. Another advantage of the use of the Theory of Statistical Moments is that the parameters obtained in fitting data have physical significance. The first statistical moment, m_1 , corresponds approximately to the mean of the breakthrough curve, where $C_B/C_0 = 0.5$,

$$t_{0.5} = m_1 - \frac{m_3}{6m_2} \quad (5)$$

The second statistical moment, m_2 , equals the variance (σ^2) which describes the spread of the breakthrough curve. And the third statistical moment, m_3 , corresponds to the symmetry of the breakthrough curve. An effective adsorption bed capacity can be calculated as

$$F = 1 + \frac{\sqrt{m_2}}{m_1} (X_B) + \frac{m_3}{6m_1 m_2} (X_B^2 - 1) \quad (6)$$

A fractional bed capacity loss due to mass transfer is

$$M = -\frac{\sqrt{m_2}}{m_1} (X_B) - \frac{m_3}{6m_1 m_2} (X_B^2 - 1) \quad (7)$$

When appropriate assumptions are made, the parameters obtained by the Theory of Statistical Moments can be further related to measurable factors. For example, the assumption that mass transfer resistance is controlled by internal (pore) diffusion yields

$$\frac{\sqrt{m_2}}{m_1} = \left(\frac{2 R^2 u}{15 \epsilon D_i L} \right)^{1/2} \quad (8)$$

$$\frac{m_3}{6m_1 m_2} = \left(\frac{R^2 u}{21 \epsilon D_i L} \right) \quad (9)$$

where

- R = adsorbent particle radius
- u = carrier gas face velocity
- L = bed length
- D_i = effective pore diffusion coefficient
- ϵ = internal/total porosity ratio.

More details of such relationships are available. (1-2) However, this brief review suggests the possibilities of using this theory, which so well describes the experimental breakthrough curves. Among other things, it can permit the bed designer or tester to predict t_B , F, and M as functions of measurable factors such as those listed above.

15th DOE NUCLEAR AIR CLEANING CONFERENCE

IV. Experimental Results

Comparisons of Sorbents

Breakthrough curves were obtained for 6 activated charcoals and 4 impregnated charcoals of the type used in radioiodine air cleaning applications. The conditions were kept constant:

25.7 ppm methyl iodide challenge concentration
 20 L/min airflow rate
 33% relative humidity at $21 \pm 1^\circ\text{C}$
 6.9-cm-diam x 2.5-cm-deep bed

These sets of data were fit to the statistical moments equation (3) to give the parameters listed in Table I. Breakthrough times corresponding to protection factors (decontamination factors) of 10, 100, and 1000 are also listed in Table I.

Table I Parameters and protection factors.

Source	Sorbent		Calculated Parameters (min)			Breakthrough Times (min)		
	Designation	Impregnant	m_1	$\sqrt{m_2}$	$m_3/6m_2$	For Protection Factors		
Union Carbide	ACC	None	1005	417	43.6	10	100	1000
			1268	571	67.9	499	228	88
			1179	458	45.2	580	241	85
			1501	675	80.2	621	314	149
Westvaco	WV-H	None	1034	473	58.2	688	286	101
Witco	337	None	1017	416	43.7	466	192	70
Pittsburgh AC	BPL	None	1239	493	49.5	512	243	105
Narbada	NG	None	1619	727	88.1	640	312	139
Fisher	5-685-B	None	1374	585	65.4	744	318	125
North American Carbon	G-618	TEDA	3295	1240	123.4	667	304	126
	G-615	KI/TEDA	1533	429	32.7	1786	958	517
Barnebey Cheney	487	TEDA	2480	800	62.4	1005	682	488
Sutcliffe-Speakman	208C	TEDA	2923	983	94.2	1497	899	543
						1725	1055	691

Reproducibility of these early experiments is shown by the four replicate experiments with Union Carbide ACC charcoal. Within this reproducibility, the nonimpregnated adsorbents were similar in performance. The impregnated sorbents were much better for methyl iodide retention. The order of results shown in Table I was not surprising. However, this does demonstrate one use of breakthrough curve fitting by statistical moments.

Challenge Concentration Effects

Breakthrough curves were obtained for two charcoals to study the effects of challenge vapor concentrations on protection factors. The first series used Union Carbide ACC charcoal at the experimental conditions listed immediately above, but with challenge methyl iodide concentrations from 0.90 to 25.7 ppm. Results were plotted as $\log t_B$ vs $\log C_0$ for protection factors of 10, 100, and 1000 in Fig. 6.

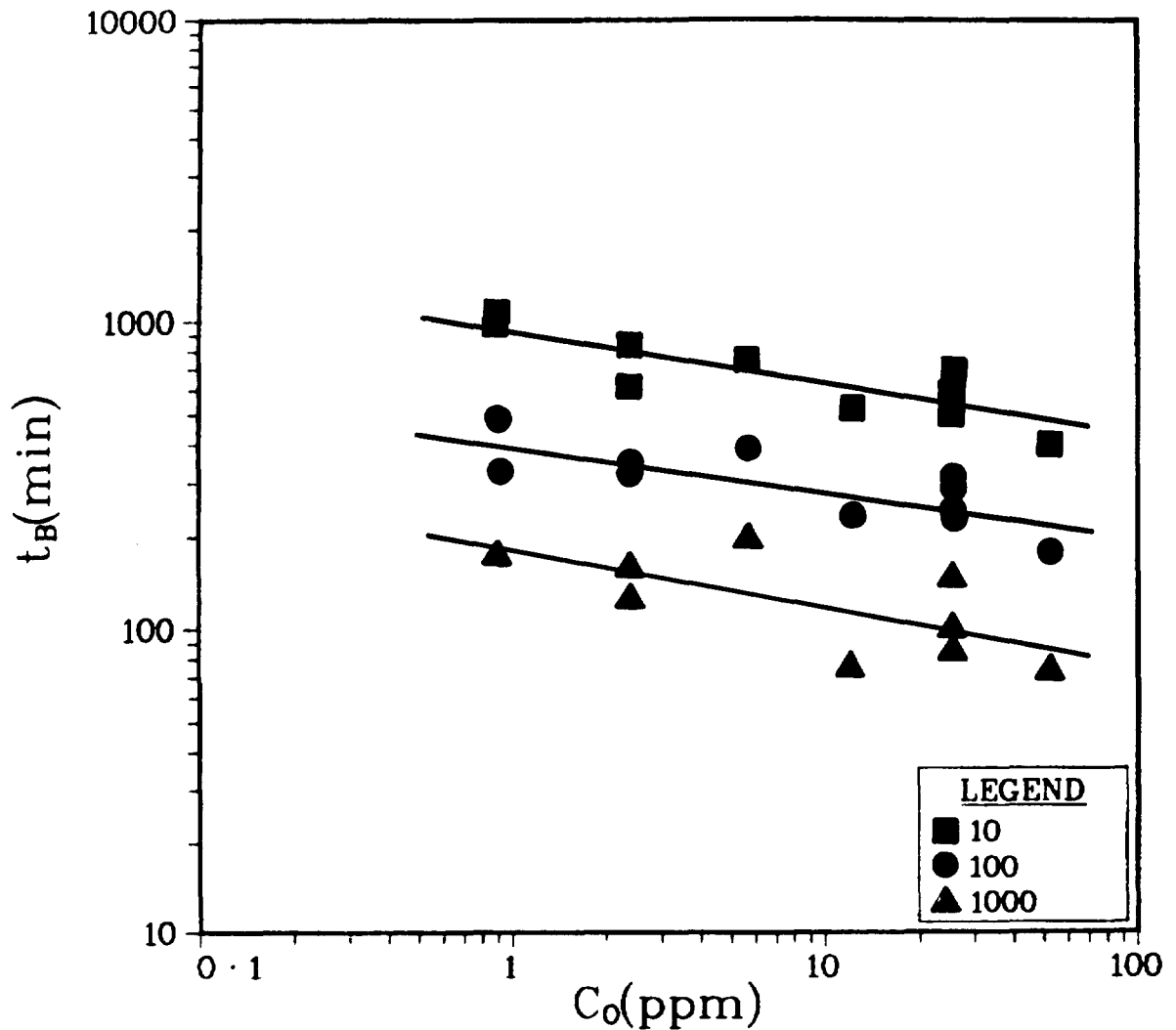


Figure 6 Challenge concentration dependence for protection factors from tests with Union Carbide ACC non-impregnated charcoal.

Since these plots were apparently linear, the following relationships were calculated by linear least-squares fitting:

$$PF = 10, \quad t_B = (940 \pm 81) C_0^{-0.17 \pm 0.09}$$

$$PF = 100, \quad t_B = (390 \pm 38) C_0^{-0.15 \pm 0.04}$$

$$PF = 1000, \quad t_B = (180 \pm 32) C_0^{-0.19 \pm 0.07}$$

The \pm values refer to standard deviations calculated for 11 experimental points. The relative values of the standard deviations confirm that the dependence of protection factors on challenge concentration is real.

A similar series of experiments was done with Barnebey Cheney 487 5% TEDA-impregnated charcoal at challenge methyl iodide concentrations from 0.87 to 29.0 ppm. Other conditions were:

15th DOE NUCLEAR AIR CLEANING CONFERENCE

40 L/min airflow rate
50% relative humidity
4.1-cm-diam x 2.5-cm-deep bed

Breakthrough times for protection factors of 10 and 100 were plotted in Fig. 7 as $\log t_B$ vs $\log C_0$. Reproducibility was much improved for these experiments as seen by the overlapping of duplicate points at 12.1, 20.6, and 29.0 ppm. Again, these plots were apparently linear with the results:

$$PF = 10, t_B = (2720 \pm 290) C_0^{-1.06 \pm 0.04}$$

$$PF = 100, t_B = (290 \pm 44) C_0^{-0.80 \pm 0.06}$$

and, again, a significant challenge concentration effect was observed.

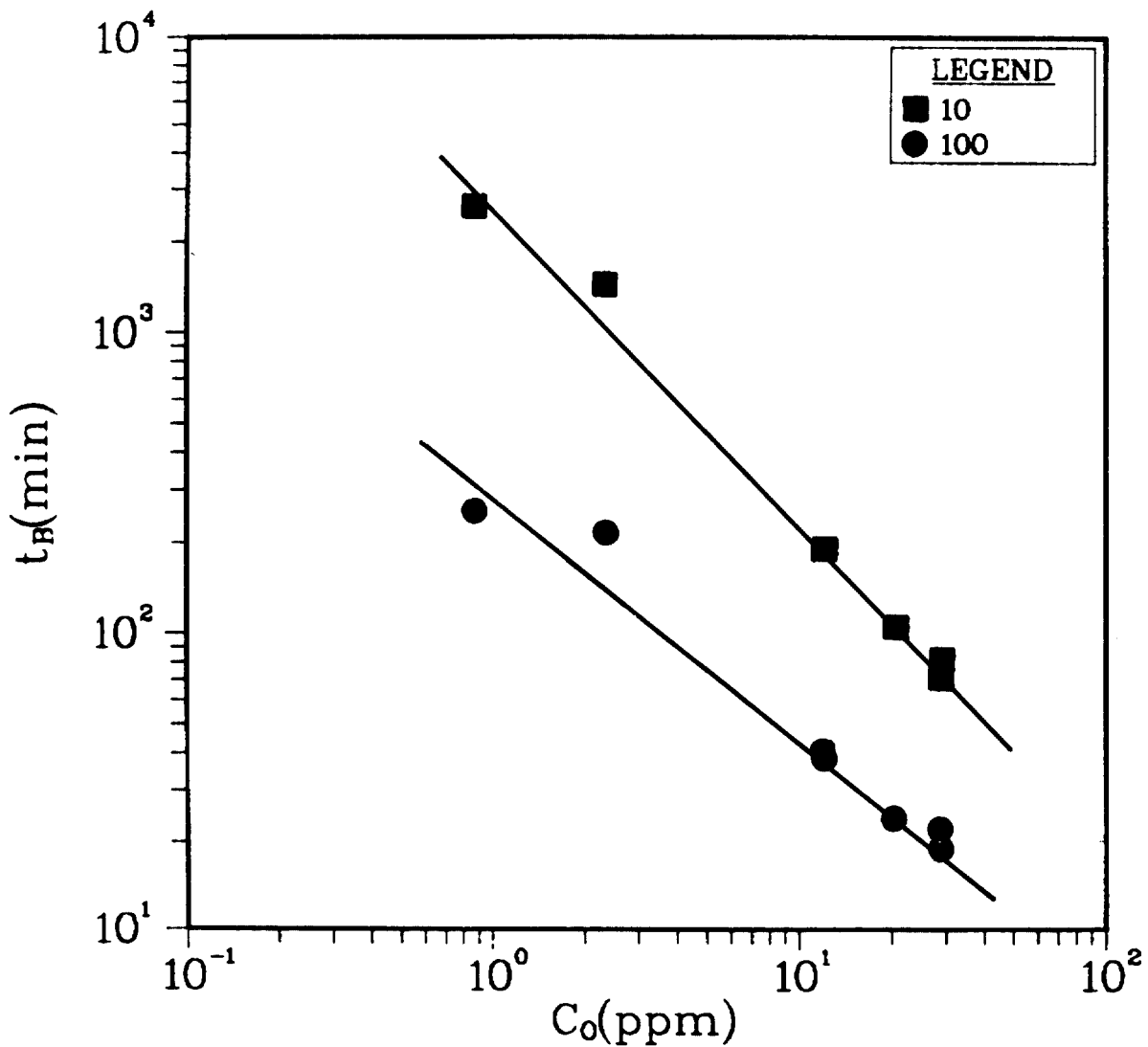


Figure 7 Challenge concentration dependence for protection factors from tests with BC 487 TEDA-impregnated charcoal.

Bed Diameter Effects

Bed diameters were varied for a fixed 2.5-cm depth of Barnebey Cheney 487 charcoal under these constant conditions:

- 25.7 ppm challenge concentration
- 20 L/min air flow rate
- 50 % relative humidity

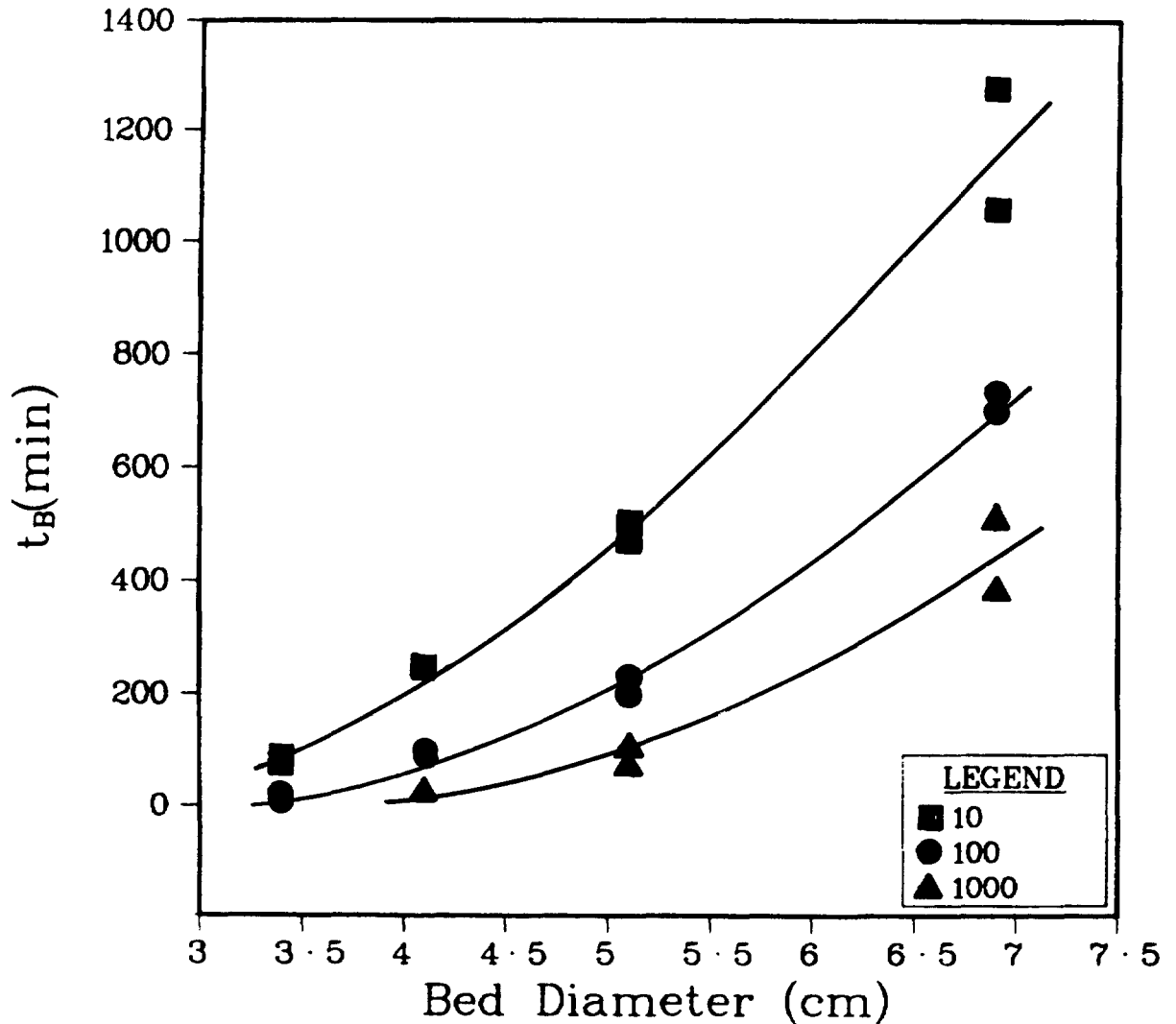


Figure 9 Protection factors as functions of bed diameter for a TEDA-impregnated charcoal (BC 487).

Plots of breakthrough times vs bed diameter for three protection factors are shown in Fig. 9. The effects of increased bed diameter in increasing breakthrough times are large. This is not surprising since increasing bed diameter for a fixed bed depth not only reduces linear flow velocity, but also increases the amount of sorbent in the bed. An interesting observation from Fig. 9 is the apparent convergence of all three protection factor curves to a bed diameter value of 3-3.5 as t_B approaches zero. This suggests that a "critical" bed diameter exists.

Relative Humidity Effects

Variations of protection factors with relative humidity were also investigated for the Barnebey Cheney 487 charcoal under these conditions:

- 25.7 ppm challenge concentration
- 20 L/min air flow rate
- 4.1-cm-diam x 2.5-cm-deep bed

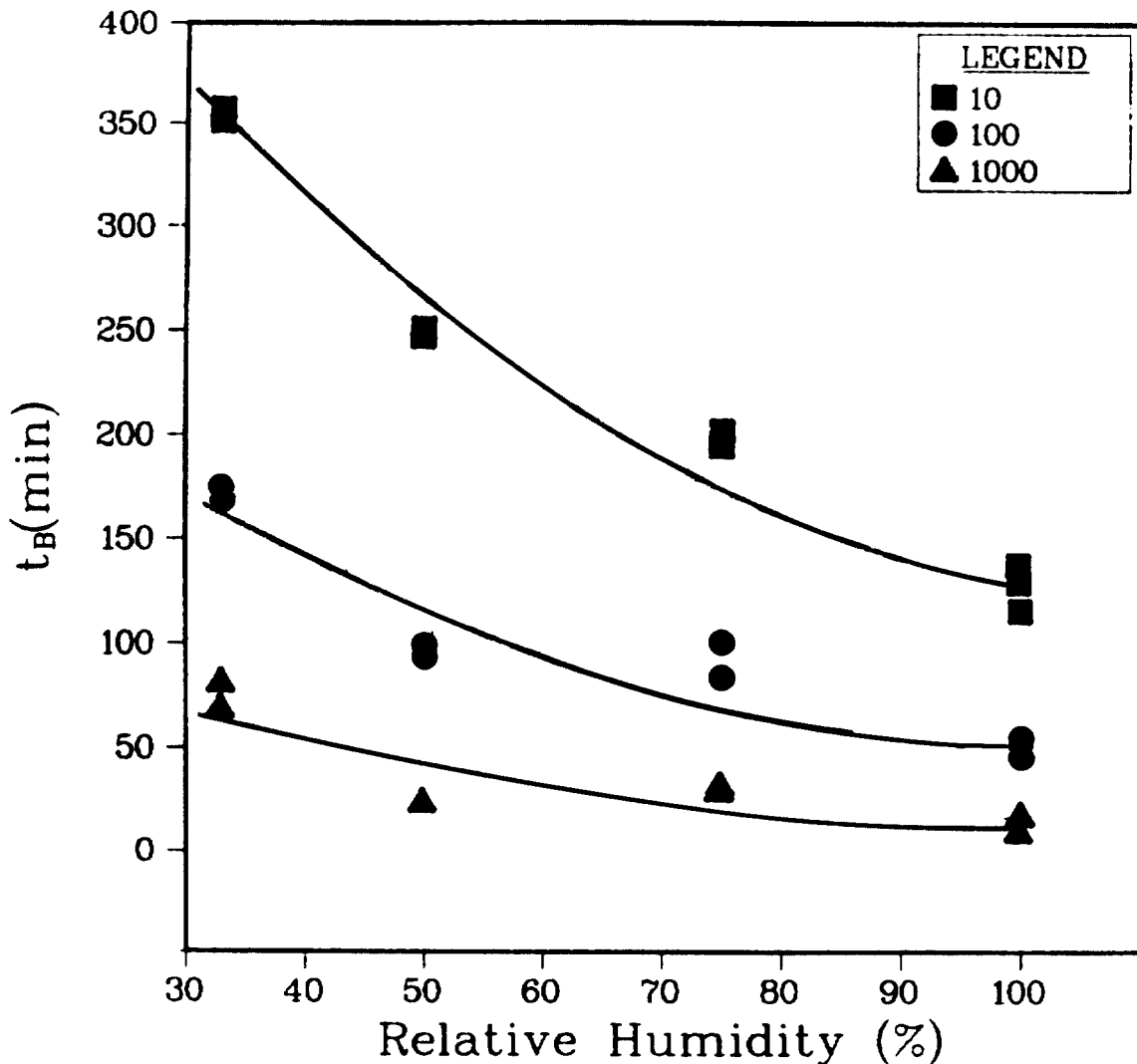


Figure 8 Protection factors as functions of relative humidity for a TEDA-impregnated charcoal (BC 487).

Figure 8 shows plots of breakthrough times vs relative humidities (21 ± 1 °C) for three protection factors. Increased relative humidity greatly decreased the breakthrough times for a given protection factor. Or, stated otherwise, increased relative humidity decreased the protection (or decontamination) afforded after a given time.

15th DOE NUCLEAR AIR CLEANING CONFERENCE

V. Conclusions

1. The Theory of Statistical Moments best described breakthrough curves for charcoal beds obtained at ppm methyl iodide challenge concentrations. Parameters obtained from data fitting with this theoretical model have useful, physical significance.
2. Breakthrough curves were useful for comparing the performances of sorbent beds using protection factors.
3. Significant increases in breakthrough times for decreasing challenge concentrations were measured for two charcoal sorbents. If further studies show that this concentration dependence continues to the levels of interest in radioiodine removal, bed testing at ppm methyl iodide concentrations would produce ultraconservative protection factors (bed efficiencies). A challenge concentration effect also has other implications for bed testing procedures. For example, the rate at which a given amount of methyl iodide is released into an air stream will determine its concentration and, thereby, the efficiency measured for a bed downstream.
4. Increased relative humidity resulted in decreased performance of a sorbent bed. This effect is also significant above 50 %. Therefore, a respirator cartridge or other sorbent bed should be tested at 100 % relative humidity or limited in use to the maximum humidity at which it was tested successfully.
5. The effect of increased sorbent bed performance with increased bed diameter was mainly due to decreased air flow velocity. Such a dependence is especially important for a respirator cartridge application, since the air flow in actual use can vary widely, depending on the workload of the user. Therefore, a respirator cartridge or other sorbent bed should be tested at the maximum expected flow velocity or should be limited in its use to certain flow velocities.

VI. References

- (1) O. Grubner. "Statistical moments theory of gas chromatography: diffusion controlled kinetics." Advances in Chromatography, Vol. 6. Marcel Dekker, Inc., New York, N.Y., 1968.
- (2) O. Grubner and D.W. Underhill. "Calculation of adsorption bed capacity by the theory of statistical moments." Separation Science, 5, pp. 555-582.

DISCUSSION

KOVACH: The velocity used in your experiments is above that used in reactor air cleaning applications. Whereas at gas mask velocities (above ~ 80 fpm) pore diffusion is the rate controlling step, below that velocity, bulk diffusion is the rate controlling step.

WOOD: The linear velocities we used are of the same order of magnitude as the 12 m/min in the RDT M-16 test procedures. The Equations (8) and (9) were cited only as examples of how statistical moments can be related to physical parameters. Actually, more recent data developed by varying face velocity, show that the velocity dependence of the statistical moment ratios is not that shown in these equations.

TADMOR: Since your paper was not distributed, I did not have the privilege of seeing all your equations. From the equations shown in the slides, I didn't see an explicit expression for the adsorption coefficient. Is it hidden within the effective diffusion coefficient, or is it explicitly expressed?

WOOD: The adsorption coefficient does not appear in Equations (8) and (9), which are for a given sorbent and sorbate. However, the adsorption coefficient and isotherm can be obtained from the breakthrough data using the Theory of Statistical Moments. I refer you to the paper of Grubner and Underhill that we cited.

15th DOE NUCLEAR AIR CLEANING CONFERENCE

EVALUATION AND CONTROL OF POISONING OF IMPREGNATED CARBONS USED FOR ORGANIC IODIDE REMOVAL

J. Louis Kovach and L. Rankovic
Nuclear Consulting Services, Inc.
Columbus Ohio

Abstract

By the evaluation of the chemical reactions which have taken place on impregnated activated carbon surfaces exposed to nuclear reactor atmospheric environments, the role of various impregnants has been studied. The evaluation shows several different paths for the aging and poisoning to take place. The four major causes were found to be:

- a) Organic solvent contamination.
- b) Inorganic acid gas contamination.
- c) Formation of organic acids on carbon surface.
- d) Formation of SO_2 from carbon sulfur content.

It was found that the prevention of poisoning by path a and b can be accomplished only by procedural changes within the facility. However poisoning paths b, c and d can be controlled to some extent by the selection of carbon pretreatment techniques and the type of impregnant used.

Results were generated by evaluating used carbons from 14 nuclear power plants and by artificial poisoning of laboratory impregnated carbons.

It was found that impregnants which have antioxidant properties, besides reaction with organic iodides, can increase the life of the impregnated activated carbons.

I. Introduction

The two major impregnants used to enhance the organic iodine removal efficiency of activated carbons are iodine and tertiary amine compounds. The initial use of these impregnants was somewhat accidental. The carbons impregnated with these compounds were not initially developed for organic radioiodine removal but for mercury vapor, SO_2 , and halide containing war gas removal. It is only recently that conscious effort was being made in the evaluation of existing impregnants or the development of new improved impregnants for organic iodine control. (1)(2)

While most commercial impregnated adsorbents perform well in fresh form, the efficiency of these adsorbents can be reduced in several different manners.

- a) Organic solvent contamination.
- b) Inorganic acid gas contamination.
- c) Formation of organic acids on carbon surface.
- d) Formation of SO_2 from carbon sulfur content.

15th DOE NUCLEAR AIR CLEANING CONFERENCE

In the following each of these effects are evaluated in relation to their practical occurrence and potential preventive methods.

II. Organic Solvent Contamination

Carbon disulfide extraction of impregnated carbons used in various areas of commercial power reactors indicated the presence of the following contaminants.

Paint Solvents: Toluene
Methyl Ethyl Ketone
Methyl Isobutyl Ketone
C₆-C₁₀ Straight Chain Hydrocarbons

Degreasing Solvents: Trichloroethylene
Perchloroethylene
Acetone

Welding Fume Decomposition Products:
C₈-C₁₅ Aliphatic and Aromatic Hydrocarbons

Organic Acids (probably generated on carbon surface)
Formic
Acetic
Butyric

Additionally, carbon samples from banks of laboratory exhaust hoods showed a very large number of unidentified organic components.

The adsorption of organic solvents on the adsorbent surface results in several paths of decreasing the organic iodide removal efficiency of impregnated carbons and in some cases can actually enhance the formation of organic iodides, while in rare cases the deposition of adsorbed organics can improve the efficiency of these carbons.

As an accelerated laboratory impregnant styrene-butadiene mixtures were tried as simulated poisons, because such mixtures result in plugging of the carbons pore structure. Such poisoning even at severe pore volume and surface area reductions resulted in good methyl iodide removal.

The control of these contaminants is twofold. First it is very important that the administrative control be improved from current practice to lessen exposure of stored or installed adsorbents to paint fumes, degreasing and cleaning solvents and welding fumes. However if exposure of the adsorbent bed to these compounds is unavoidable, such as the case of continuously operated systems, the use of guard beds is highly recommended. Guard beds are unimpregnated beds of carbon (or adsorbents impregnated to control non-radioactive impurities) installed in separate beds. While the use of guard beds will not prevent the transmission of all organic compounds it still gives a very good protection to the main adsorber beds with the exception of possible short durations. The reason for this is that the low molecular weight organics which easily penetrate the guard bed will pass through the main bed relatively fast also. While compounds which are strongly adsorbed and would constitute permanent poisons will be removed at a high efficiency by the guard beds.

15th DOE NUCLEAR AIR CLEANING CONFERENCE

III. Inorganic Acid Gas Contamination

The exposure of carbons to SO₂, NO and NO₂ depends primarily in the proximity of the facility to coal fired plants, paper mills, reprocessing facilities, etc. Again, the degree of exposure is more severe in cases of continuously operated systems.

The result of adsorption and/or reaction with acid gases of the impregnant and the carbon can lower organic iodide removal efficiency by several means. As the initial alkalinity of the impregnant (or the adsorbent in case of vegetable base carbons) decreases, iodide compounds are converted to free iodine forms, which are not as strongly retained on the adsorbent particularly at elevated temperatures.

NO_x compounds can react with triamines resulting in either carcinogenic and mutagenic nitrosamines (3), or in the formation of explosives. Such an example is the formation of hexogen or octagen from hexamethylene tetramine in NO₂.

While the NO_x compounds particularly attack the triamine type impregnant the SO₂ reacts with the iodide impregnants.

Additionally NO₂ can also attack the carbon surface itself and result in the oxidation of the carbon surface:



While not all of the CO would be released, the oxidation of the carbon surface would eventually also result in surface acidification as discussed later.

This type of contamination is very difficult to control by protective and nearly impossible by administrative measures. However impregnant composition can be varied to greatly lessen the effect of the poisons. Two different additive forms have been successfully evaluated by NUCON to decrease the poisoning effects. These are coimpregnating the carbon - in addition to CH₃ ¹³¹I control impregnants - with a buffer solution which can hold the carbon pH at 10 and the use of small quantities of urea which decomposes both NO and NO₂ to nitrogen, CO₂ and water.

The use of these coimpregnants have increased by more than 50% the life of impregnated carbons exposed to artificially generated NO_x and SO₂ levels under accelerated conditions. The addition of these impregnants have not resulted in the degradation of other properties of the carbon.

Because of the preferential reaction of NO_x with amids compared with amines the urea and other amid compounds results in the lowering of CH₃ ¹³¹I reactant impregnant loss also.

IV. Formation Of Organic Acids On The Carbon Surface

All commercial activated carbons contain carbon-oxygen complexes at the solid-gas interface. These are commonly called surface oxides. The type and quantity of surface oxides depends on the history of the carbon, particularly its exposure to oxygen at various temperatures.

15th DOE NUCLEAR AIR CLEANING CONFERENCE

Oxygen present in the form of surface oxides is not physically adsorbed oxygen but chemisorbed. Typical coconutshell carbons used as base for impregnation have approximately 1,000-1300 m²/g surface area. Chemisorbed oxygen forms can exist in up to 25% of the surface coverage, i.e., 200-300 m²/g carbon surface filled with various oxygen compounds.

While these surface oxides have very little or no influence on the adsorption of polar compounds they can exert either beneficial or undesirable action on the adsorption of polar compounds, surface acidity and water adsorption. (4) (5) (6) (7)

Formation and/or conversion of these surface oxides is one of the main causes of aging of impregnated carbons. That is, the loss in efficiency during storage of carbons.

As an example the water adsorption isotherm of new and two year aged coconutshell carbon is shown on Figure 1. The shift toward higher water adsorption capacity at all relative humidities is obvious. The effect of humidity on adsorption, isotope exchange and other chemical reactions of CH₃ ¹³¹I is a well known fact and not discussed here in detail.

The presence of the surface oxides does not affect the nitrogen surface area or carbontetrachloride adsorption of activated carbons, thus their presence or form is not directly established by the current test requirements of Regulatory Guide 1.52 or ANSI N509, other than possible different CH₃ ¹³¹I removal efficiency.

In relation to water adsorption at low relative humidities, water adsorption is due to the formation of hydrogen bonds between the water molecules and the most active surface locations. The thus adsorbed water represents secondary adsorption centers which can retain additional water molecules by hydrogen bonds. This leads to the formation of dimeric complexes on the surface. At increasing relative humidity the adsorption will increase based on the number of these secondary adsorption centers. The sharp rise in the water adsorption isotherm at mid range relative humidity is caused by the formation of dimeric groups of water molecules which fuses into the completion of the monomolecular layer. Further increase in RH results in multilayer adsorption thru capillary condensation in the filling of the micropores of the activated carbon.

Surface oxides can be both basic and acidic in character. While carbons exposed to oxygen above 700°C result in an initially basic surface oxide; exposure to oxygen at lower temperature and aging of basic surface oxides results in acidic groups on the surface. In the absence of sufficient alkalinity or buffering on the carbon surface all carbons will show a decreasing pH with aging. (8) (9) (10)

While from a CH₃ ¹³¹I removal standpoint the presence of surface oxides is detrimental, they do have desirable effects also. Similarly to oxide layers on some metal surfaces they do protect the carbon from further oxidation. The carbon is most vulnerable to fast oxidation and subsequent ignition when all surface oxides are removed and the carbon is exposed to oxygen again.

The formation and/or conversion to acidic surface oxides was postulated by several methods. (11) (12) The acidic group formation can proceed from the adsorption of molecular oxygen and its conversion to peroxide group which when hydrated becomes an acid group or through the formation of and oxidation of aldehyde groups on the surface.

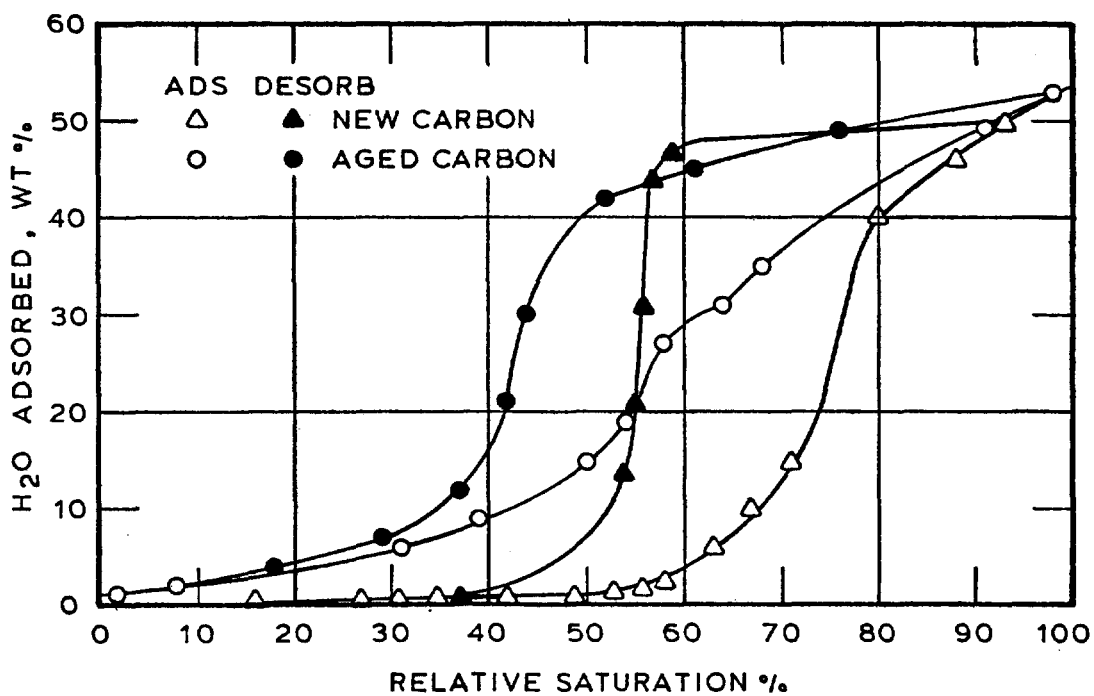


Figure 1 Water adsorption isotherm of new and two year aged unimpregnated coconutshell carbon, 8X16 mesh, $1050 \pm 50 \text{ m}^2/\text{g}$.

15th DOE NUCLEAR AIR CLEANING CONFERENCE

Although impregnated activated carbons can be stored by the manufacturer in oxygen free atmospheres, after they are filled into adsorbers or installed are impossible to protect from oxygen exposure.

However again impregnant selection or addition can decrease the formation of acidic surface by reaction with the surface aldehyde groups or by prevention or decomposition of the peroxide intermediate.

Urea, the impregnant successfully employed to counteract NO_x degradation, also reacts with surface aldehyde groups and can prevent their conversion to surface acid groups. Additional impregnants can also be used to prevent peroxide type oxidation. Some of those tried have detrimental effect on the adsorption or other means of removal of iodine compounds. These are: H_3PO_4 , phenol, several organic sulfur compounds. While others have neutral or positive effect in addition to their antioxidant properties. Compounds of the latter group which were evaluated and found acceptable are 4-tert-Butylcatechol, N,N-Diphenyl-p-phenylenediamine, p-Hydroxydiphenylamine, p-Methoxydiphenylamine, benzidine, diphenylamine, phenothiazine, alkylamidinoisurea. (11)

In general the antioxidant selection is based on the following criteria

- a) compatibility with other impregnants
- b) antioxidant effective
- c) neutral or positive effect on organic iodide removal
- d) lack of explosive or other adverse chemical formation

The formation of surface oxides does not stop with the generation of chains attached to the bulk carbon, but can result in the formation of detachable, identifiable organic compounds.

Compounds identified as probably originating due to surface oxide formation and decomposition in 0.0001-0.1 $\mu\text{g/g}$ concentrations:

- Benzene
- Toluene
- Furan
- Methyl alcohol
- Ethyl alcohol
- Actone
- Methyl isobutyl ketone
- Acetaldehyde
- Ethyl acetate
- 1 Butene
- C2 - C7 Organic acids
- CO_2
- i Propyl alcohol
- i Butyl alcohol

To avoid inclusion of incidental contamination results, the compounds shown are those which occurred in all carbon samples tested from various manufacturers' unimpregnated carbons. Compounds which were detected only on one or two carbons were not included in list.

15th DOE NUCLEAR AIR CLEANING CONFERENCE

V. Formation Of SO₂ From Carbon Sulfur Content

Numerous activated carbons are prepared from raw materials which contain sulfur (coal, petroleum, coke). It was found that such carbons can slowly release low concentration SO₂ for long times. The reason for the evaluation was the observation of faster aging of a petroleum base carbon identically impregnated to a coconut carbon. Evaluation of the base carbon has shown that the sulfur dioxide is continuously generated. The carbon was evacuated four times at 250°C in less than 10 um Hg vacuum. Even after the fourth evacuation SO₂ was detected in the outgas residue. The residual SO₂ was in the range of 1.0-1.5 µg/g carbon. Similar tests on coconut based carbon resulted only in the decomposed surface oxide residues, no sulfur was detected. Subsequently it was found that a NASA study has resulted in similar findings.(12) That same study identified close to 40 organic compounds in trace quantities removable from the surface of unused carbon. Most of these compounds can be identified as generated by the surface oxidation route and decomposition products surveying the activation process rather than being post production contaminants.

The generation, albeit in trace levels, of SO₂ by activated carbon containing carbon bound sulfur or inorganic sulfides requires the addition of extra alkali or the variation of the buffering composition to assure that the carbon will not reach an undesirably low pH level while in storage or in use. For some of the carbons this would require the addition of so large a quantity of alkali (2-4% by wt) that the ignition temperature of the carbon can not be maintained above the ANSI required level (350°C).

The application of non-vegetable based carbons as base materials for organic radioiodine removal impregnations is dependent on their non-sulfate sulfur content.

VI. Evaluation Of Used Carbons

Often test conditions used in the past have not resulted in pinpointing the degree of poisoning because test pre-equilibration resulted in partial or full regeneration of the carbon. However evaluation of condensate obtained during 130°C tests and CS₂ extraction of carbon samples results in the following observations.

- 1) The major cause of poisoning is organic solvent contamination, 85% of failed tests showed high organic content. In one case organics in excess of 5.0% by weight were present. Failure rate was approximately 15% of 74 samples tested at 130°C.
- 2) In 55% of used carbons tested, even though the carbon passed under old test conditions, the condensate collected contained organics corresponding to 14.0-260.0 mg/g carbon.
- 3) Inorganic acids HNO₃ and H₂SO₄ were identified in all samples from systems operating continuously when nuclear power station is located within approximately 10 miles of a coal fired station.
- 4) Organic acids were identified in all samples which were in place for longer than 1 year.

15th DOE NUCLEAR AIR CLEANING CONFERENCE

5) Carbons containing tertiary amines showed higher $\text{CH}_3 \text{}^{131}\text{I}$ residual efficiency than KI or KI_3 carbons at equal contaminant levels.

Figure 2 shows the aging and poisoning rate of in-place power plant carbons. Figure 3 shows artificial accelerated exposure response of several different impregnation carbons.

The results of in-place carbons can be evaluated only in a trend basis because of great divergence in housekeeping and care exercised for the filter-adsorption systems.

The simulated laboratory exposure consisted of air stream at 85-95% RH, 5-25 ppm organics and 1.0-1.5 ppm NO_x at 40 ± 2 fpm superficial face velocity on 8X16 mesh carbons.

The carbon types used were:

- 1) KIG (iodine impregnated coconut)
- 2) TEG (tertiary amine impregnated coconut)
- 3) KITEG (iodine and tertiary amine impregnated coconut with buffering)
- 4) KITEG(CO) (same as No. 3 but coal base)
- 5) KITEG II (iodine and tertiary amine impregnated with buffering and antioxidant)

VII. Summary And Conclusions

Four major poisoning paths of impregnated carbons used for organic radio-iodine control were evaluated. The most commonly occurring poisoning in continuously operated systems is due to organic solvent contamination which is the most difficult to control by technical means.

The effect of other poisoning paths can be greatly lessened by the selection of $\text{CH}_3 \text{}^{131}\text{I}$ reacting impregnants which act as antioxidants and/or by the addition of other impregnants for the control of inorganic acid, carbon surface oxide and sulfur decomposition. The data generated indicates that by selection of impregnants for the specific purpose rather than employing impregnated carbons developed for other application the carbon efficiency and life can be optimized.

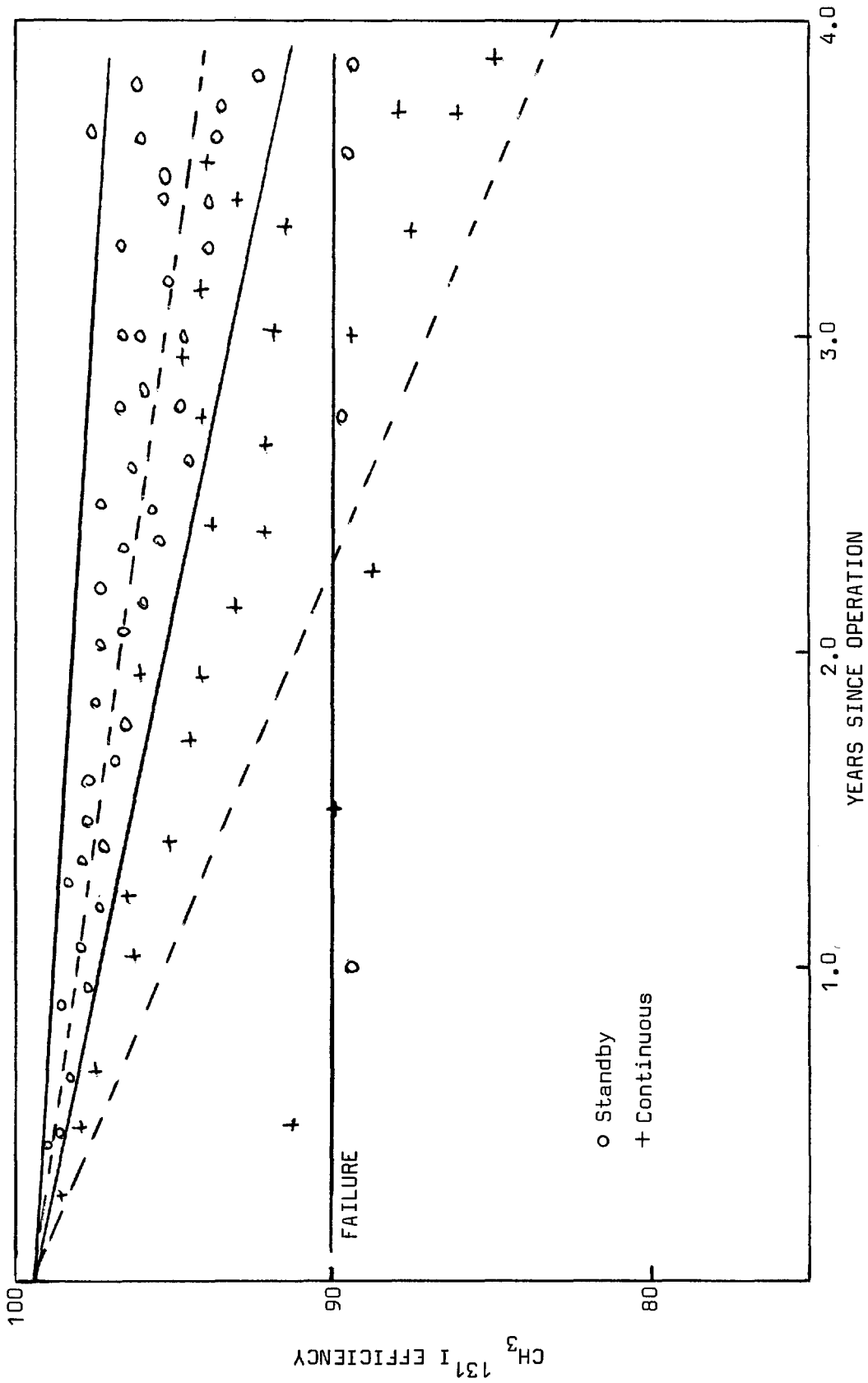


Figure 2 Poisoning rate of plant installed impregnated carbons.

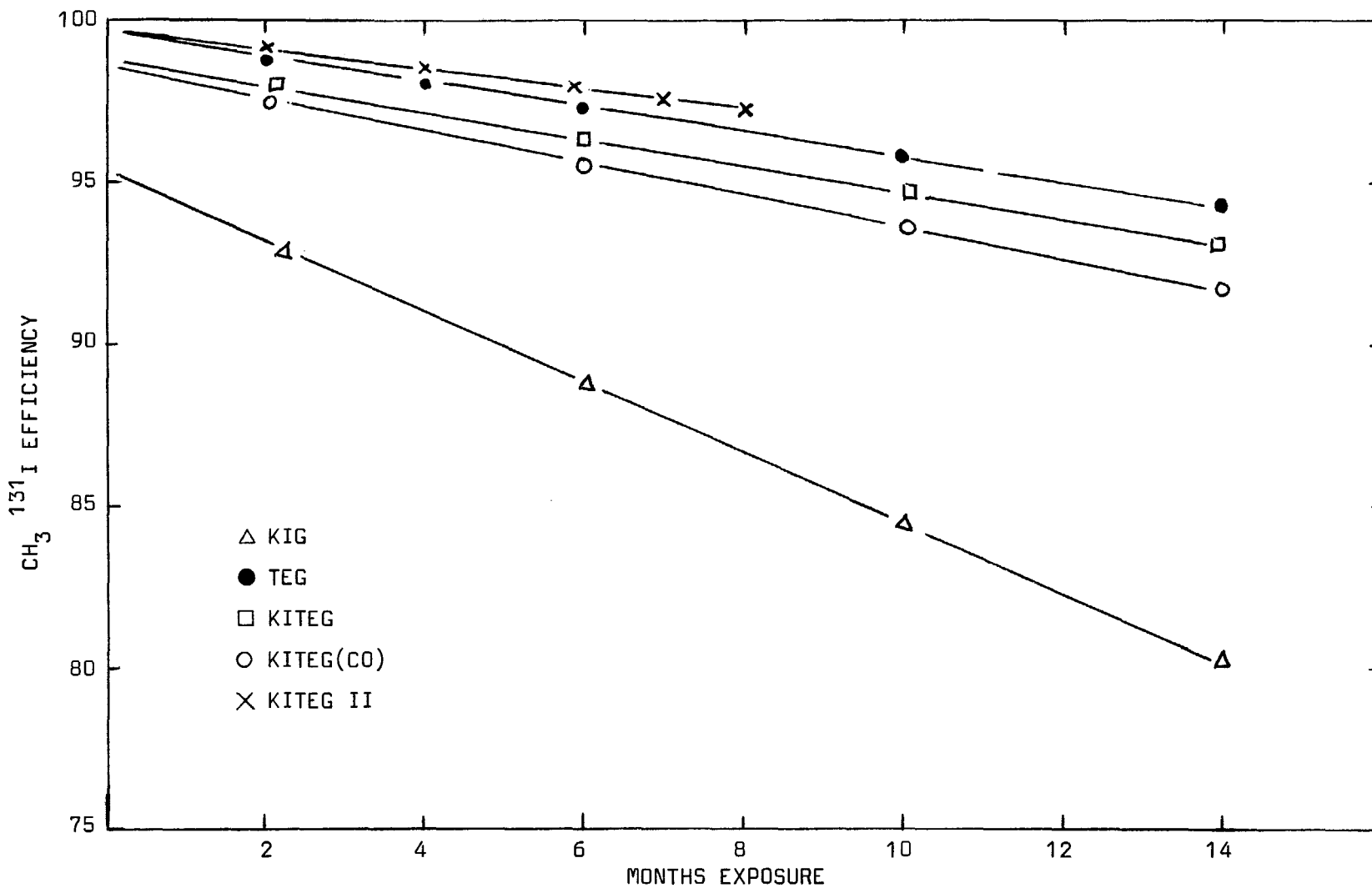


Figure 3 Methyl iodide removal efficiency vs exposure: 25°C, 95% RH, 2.0 inch bed, 40 FPM.

15th DOE NUCLEAR AIR CLEANING CONFERENCE

References

- 1) Deitz, V. R. and Blackley, C. H. ERDA Report CONF-760822 (1977)
- 2) Evans, A. G. ERDA Reports 1403, 1463 (1975 & 1976)
- 3) Magee, P. N. and Barnes, J. M. Advances of Cancer Research 10,163 (1967)
- 4) Sihvonon, V. Trans. Farad. Soc. 34, 1062, (1938)
- 5) Lendle, A. Zhur. Phys. Chem. A172, 77, (1935)
- 6) Garten, V. A. and Weiss, D. E. Austral, J. Chem. 8, 68 (1953)
- 7) Garten, V. A. and Weiss, D. E. Austral, J. Chem. 10, 295 (1957)
- 8) Puri, B. R. Chemistry & Physics of Carbon Vol 6, M. Dekker (1970)
- 9) Kruyt, H. R. and deKadt, G. S. Koll. Zblatt. 47, 44 (1929)
- 10) Strickland-Constable, R. F. Trans. Farad Soc. 34, 1075, (1938)
- 11) Patent applied for by Nuclear Consulting Services, Inc. (1978)
- 12) NASA Report CR-115202, Analytical Research Laboratories, Inc. (1971)

DISCUSSION

DEUBER: From the laboratory tests on the retention efficiency of aged carbons, one often gets biased results. With preconditioning, the pollutants are desorbed. Without preconditioning, exact conditions cannot be assured. The best results are to be expected with in-plant tests using radioiodine species samplers and the ^{131}I of the plant.

KOVACH: If the iodine species and concentrations existing in-plant are identical to those expected in accidental releases, then testing with those iodine species will result in a correct approximation of efficiency. However, even without preequilibration, if the test is run long enough to obtain steady state conditions, then laboratory testing is also valid.

PAULING: What, in your opinion, is the advantage and economic value of using a non-impregnated charcoal in a guard bed of a continuously operating system?

KOVACH: The use of a properly designed, testable deep bed system with guard beds has significant advantages. Generally, organic compounds which are only weakly adsorbed on the guard bed will not permanently poison the main bed either, whereas compounds which would permanently poison the main bed would be strongly adsorbed on the guard bed. The economics depend on the particular contamination level in the influent air stream. Adsorbents in unimpregnated form cost approximately 1/3 of the impregnated carbon.

15th DOE NUCLEAR AIR CLEANING CONFERENCE

A DETERMINATION OF THE ATTRITION RESISTANCE OF GRANULAR CHARCOALS

Victor R. Deitz
Naval Research Laboratory
Washington, D. C. 20375

Abstract

A laboratory procedure has been developed to evaluate the attrition of granular adsorbent charcoals on passing an air flow through the bed. Two factors observed in plant operations were selected as relevant: (1) the characteristic structural vibrations in plant scale equipment (motors, fans, etc.) that are transmitted to charcoal particles and cause the particles to move and rub each other, and (2) the rapid air flow that results in the movement of the attrited dust. In the test a container for charcoal [50 mm diameter and 50 mm high] was vibrated at a frequency of 60 Hz and at a constant energy input manually controlled using a vibration meter in the acceleration mode. Simultaneously, air was applied and exited through glass fiber filter paper. The quantity of dust trapped on the exit filter was then determined, either optically or gravimetrically. The dust formed per minute (attrition coefficient) was found to approach a constant value. The plateau-values from sequential determinations varied with the source of the charcoal; a 5-fold difference was found among a large variety of commercial products. The first testing of a sample released the excess dust accumulated in previous handling of the charcoal. The plateau values were then attained in the succeeding tests and these were characteristic of the material. The results were compared with those obtained for the same charcoals using older test methods such as the Ball and Pan Hardness Test described in RDTM16-1T (October 1973).

I. Introduction

The evaluation of the mechanical integrity of charcoal granules is admittedly a very difficult problem. Many studies^(1,2,3,4) have been based on measurements of particle breakdown and the simultaneous

15th DOE NUCLEAR AIR CLEANING CONFERENCE

formation of dust, which in many applications is undesirable. Dust, an imprecise term, refers to particulates capable of temporary suspension in the fluid (air); it may also refer to particles smaller than an arbitrarily selected particle size used for a specified application⁽⁵⁾. Charcoal granules can fragment into smaller pieces and the total material remain in a useful size range, however, some dust is always formed whenever a particle is broken. In addition, neighboring particles have been observed to rub each other more-or-less gently and in the friction process generate small amounts of dust. This paper is concerned with a procedure for quantifying the amount of dust that is formed by the latter process and some results are presented for a number of granular carbon adsorbents.

The published test procedures used to evaluate the attrition of granular charcoals are attempts to simulate the interparticle forces under service conditions. None of these procedures has proven to be generally satisfactory; this fact alone indicates the great complexity of the attrition process in actual applications. The ball and pan hardness test^(3,4), developed over 50 years ago, has a considerable backlog of experience which is of value for some producer-user specifications, but the action of steel balls in constant collision with the much smaller charcoal particles is not a good simulation of the mechanical forces at work in an overall adsorbent application.

The proposed procedure is directed to the formation of dust when typical air flows (12 m/min) are passed through beds of granular charcoals. In the selection of relevant factors for modeling, it was observed that plant operations are conducted under engineering conditions that do abrade individual charcoal particles. There are characteristic vibrations in plant scale equipment that are transmitted to the containers that house the charcoal; these vibrations originate in the operating machinery (conveyors, motors, fans, etc.). The charcoal granules subjected to these forces may oscillate and move within the bed as mentioned above. The rapid air flow can then carry the attrited particles from the bed. The present procedure

15th DOE NUCLEAR AIR CLEANING CONFERENCE

endeavors to simulate this behavior in a laboratory evaluation of the attrition of charcoals.

II. Experimental

The charcoal container was made of a 50 mm (i.d.) aluminum cylinder with 1/4 inch wall (Figure 1). The bottom was a stainless steel disc (5.6 mm thick) perforated by approximately 225 holes per square inch (0.8 mm diameter). The charcoal sample was placed on a fine mesh wire cloth securely fastened above the retaining disc. The openings of the wire cloth (between 0.17 and 0.21 mm) thus placed a limit on the largest size of particle that could leave the sample. For comparison, the openings of No. 70 and No. 80 U.S. Standard sieves are 0.21 and 0.18 mm, respectively.

The assembly is mounted on a vibration table (Buffalo Dental Mfg. Co., Inc., Brooklyn, New York) which is rated 40 watts at 115 volts, 60 Hz; the different sections were clamped together with 6 mm o.d. tie rods. The vibration table was monitored by controlling the current required to maintain a vibrational intensity at 5g acceleration, the latter being determined by an attached transducer such as the Endevco Accelerometer (Model 2251) with a Signal Conditioner (Model 4416).

The air stream was maintained in a steady downward flow (7ℓ/minute) and upon leaving the charcoal was passed through a Gelman glass fiber filter, Type A/E, 63.5 mm diameter. The filter completely trapped all charcoal dust particles (no darkening of the opposite side occurred) and a weighable deposit of dust was obtained. For smaller deposits of dust, the white filter paper was viewed with a Gardner Colorgrade Portable Reflectometer for measurement of diffuse reflectance (see ASTM Method E 97-55). The illumination was at 45° and viewing at 0° and the spectral response closely approximated the CIE luminosity function Y. The instrument was supplied with a sensor, digital panel meter, and power supply. A ceramic reflectance standard furnished with the instrument was used at frequent intervals to maintain the light intensity at a constant value.

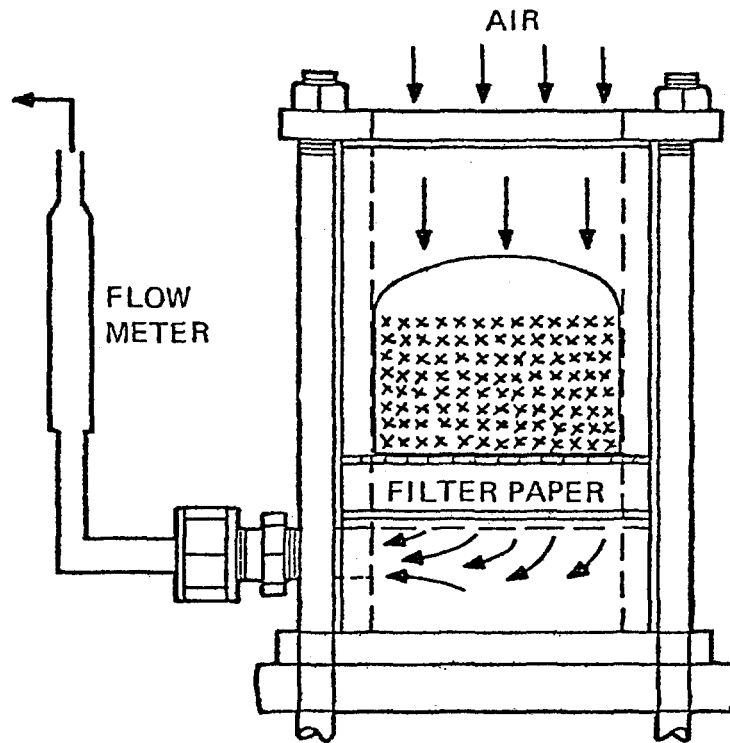


Figure 1: Sketch of a Unit for the Determination of the Attrition of Granular Charcoals

15th DOE NUCLEAR AIR CLEANING CONFERENCE

The experimental parameters that may be adjusted are the volume of charcoal, the energy input of the vibrator, the flow of air, the duration of dust collection, and the particle size range accepted as the definition of "dust". The lower limit on particle size is fixed by the Type A/E glass fiber filter rated at 99.9% efficiency (0.3 μm) by the dioctyl phthalate penetration (DOP) test. The upper limit is the opening of the wire cloth described above. A large number of measurements were made with a steady downward air flow of 7 ℓ/min . The vibrator current was maintained at 200 ma and, referring to the calibration curve (Figure 2), this current corresponded to an acceleration value of 5g for the vibrator at 60 Hz. This fixed the energy and the momentum transfer (and therefore the force) between the vibrator and the contacting charcoal particles.

III. Results

Six commercial charcoals were evaluated by the same procedure and the results in Table I align the samples in an increasing

Table I: Dust Formation for Five Granular Charcoals -
Repetitive Measurements with Same Sample
(Units Based on Relative Reflectance)

	G-210	GX 158	G104	Granular Darco	CAL
1	1.49**	<u>4.61**</u>	3.46**	<u>4.80**</u>	<u>4.78**</u>
2	<u>0.38*</u>	3.56	<u>2.87**</u>	4.48	3.26
3	1.06	3.64	1.69	3.77	3.82
4	1.17	3.73	1.40	4.16	3.38
5	1.07	3.34	1.61	3.98	3.50
6	0.84	3.61	1.57	4.21	3.50
7	0.87	3.17	1.58	4.36	3.25
8				3.80	
9				4.54	
Average	1.00	3.51	1.57	4.16	3.45

* No vibration, air pulse only; ** The first use of the sample releases excess dust accumulated in previous handling; these values were excluded from the average.

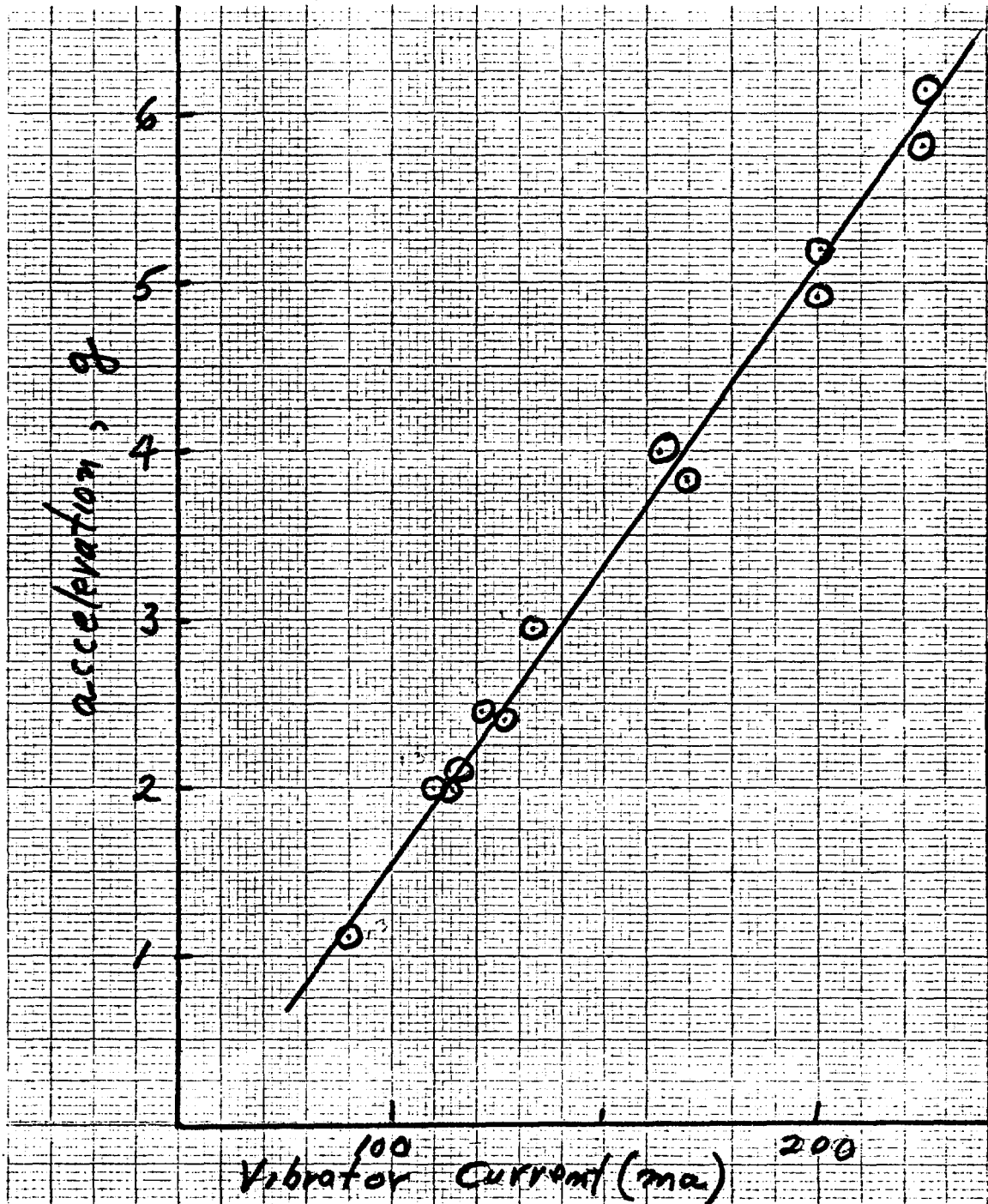


Figure 2: Calibration of the Vibrator Unit Using an Endevco Accelerometer

15th DOE NUCLEAR AIR CLEANING CONFERENCE

sequence of dust formation. In these measurements the values are based on the change in reflectance of the initial paper and the same paper plus the dust deposit. The alignment, seen in Figure 3, shows that a coconut shell charcoal, G 210, had the lowest attrition in these tests and one of the coal-base charcoals appears to have a four-fold greater value.

The above preliminary measurements may be considered in terms of known interactions among particles in a vibratory conveying system⁽⁶⁾. The frictional coefficient and the mass of the particles are controlling factors in the motion of particles at constant frequency. The particle translation increases with increase of the frictional coefficient. The observations with charcoal particles in a vibrating bed of constant volume may be summarized as follows:

(1) "Dust" fractions, fragments of the larger particles of charcoal, are generated at a constant rate when an air stream is passed through a vibrating bed.

(2) Very little dust is removed from the charcoal by the air flow when the vibrator is turned off.

(3) The observed dust formation can be used to align samples of different commercial sources in a several-fold variation.

The energy imbalance of the impact and frictional forces result in particle movements which can be viewed when the charcoal is placed in a transparent plastic container. The movement is more rapid with particles of equal size and in those positions in the bed removed from the nodes of the vibrations. When viewed stroboscopically, the frequencies of the particle oscillations cover a continuous range from 60 Hz to rest position.

Additional measurements were made on a number of gas adsorbent charcoals. Series I of Table II was studied with the sample (G 210) loosely packed in a cloth bag; Series II made use of the same sample in loose packing resting on a stretched layer of the same cloth. In the second configuration it is necessary to be alert to possible leakage past the peripheral edge. G-210, a coconut charcoal, has been vibrated about 50 times with little trend in the magnitude of the attrition coefficient. GX-158 is a coal-base charcoal, Granular

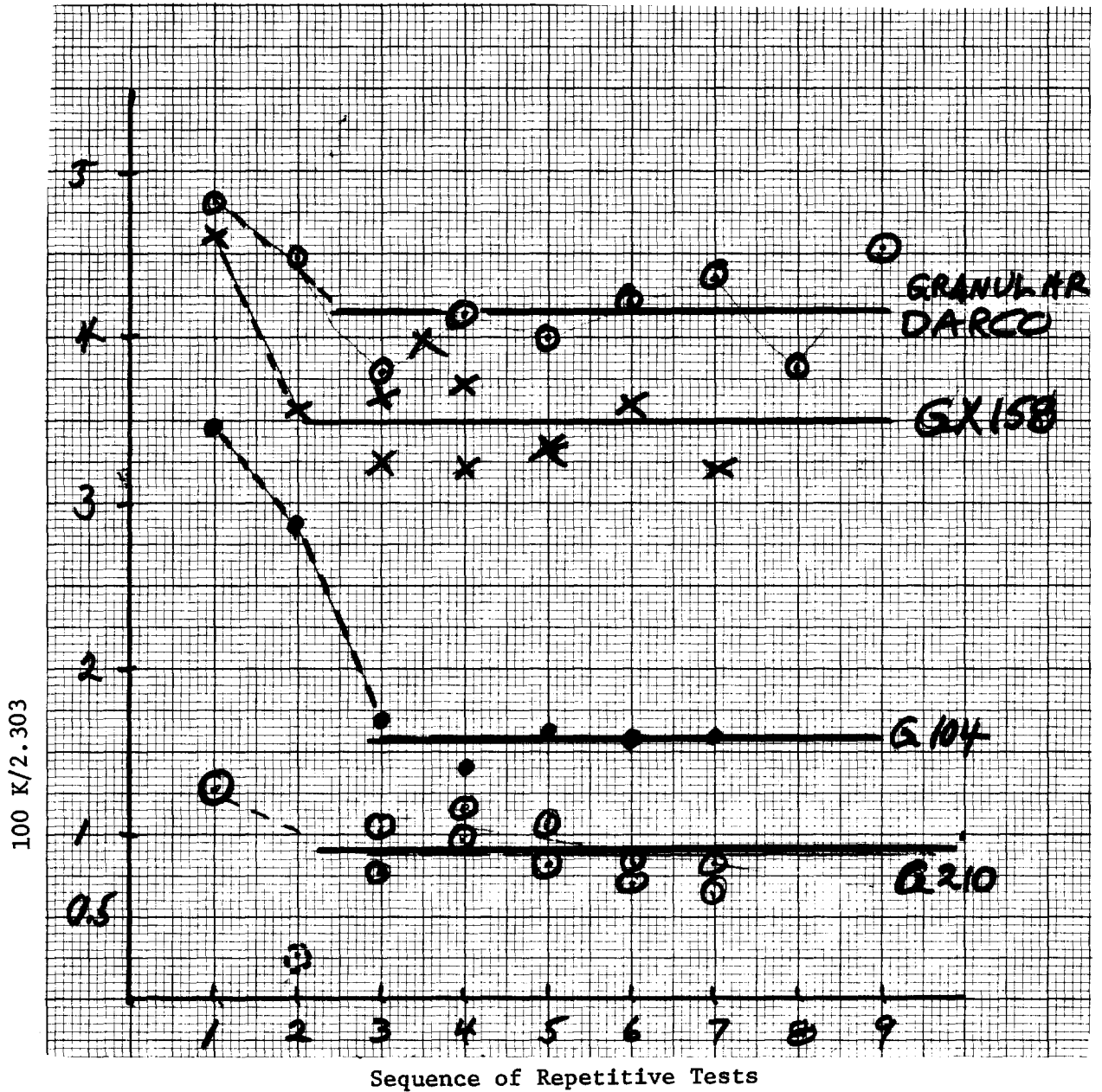


Figure 3: Alignment of Some Granular Charcoals in Formation of Dust

15th DOE NUCLEAR AIR CLEANING CONFERENCE

Darco is a lignite-base charcoal and G-104 is a wood-base charcoal. The results in Table II show approximately a 7-fold difference in attrition coefficients (mg/10 minutes).

Table II: Attrition Coefficients (mg per 10 minute vibration) of Some Gas Adsorbent Charcoals (loose packing)

G-210 Coconut Charcoals (25 g)		GX-158 Coal Base (10.0 g)	Granular Darco wt.	G-104 Wood-Base (15 g)
		4.83	10g	8.45
I	1.47	5.64	10	7.71
	1.18	3.78	15	8.91
	1.30	4.16	15	8.01
	1.11	3.16	20	9.27
	1.22	2.40	20	9.02
		<u>4.0 av.</u>		<u>1.10</u>
				<u>1.2 av.</u>
II	1.49		25	10.3
	1.58		25	9.4
				<u>8.9 av.</u>
	1.34			
	1.53			
	<u>1.33</u>			
	<u>1.35 av.</u>			

The dependence of the results on the total weight of the sample is not thoroughly understood. The results for a pelleted coal-base charcoal (G-352) are shown in Figure 4. Repetitive use of a 15 g sample lead to an attrition coefficient of about 4 mg/10 minutes. When additional sample, 10 g, was added, the same value was obtained. One explanation is based on the observation that some fraction of the charcoal particles is really at rest in the node positions of 3-dimensional vibrations. As a consequence, charcoal samples must be compared on a constant volume basis, of fixed dimensions.

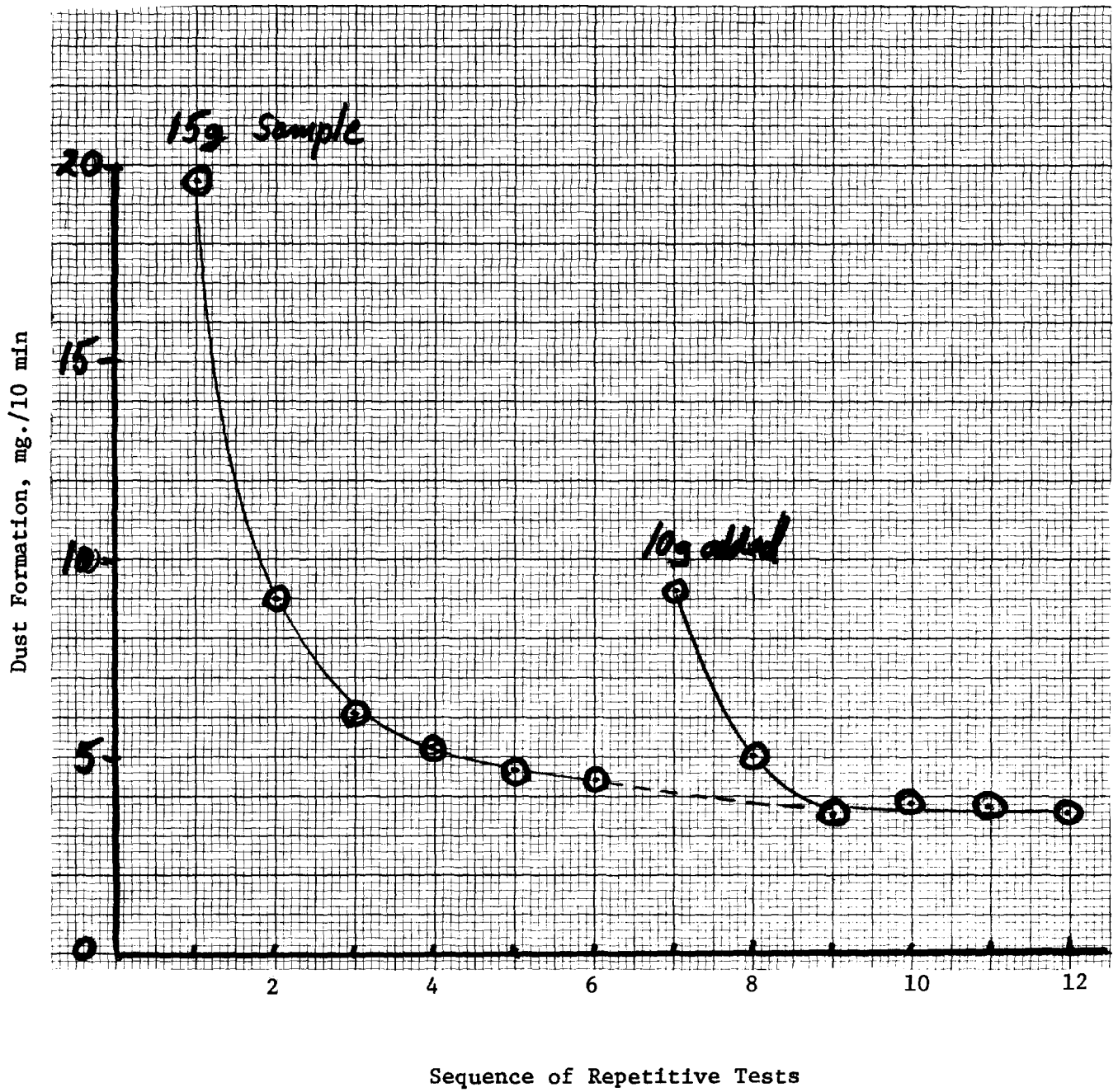


Figure 4: Attrition of a Pelleted Charcoal (G 352, 1/8" cylinders) in Sequential Testing

15th DOE NUCLEAR AIR CLEANING CONFERENCE

Some samples were contained in a cloth bag in which the sizes of the rectangular openings varied from 0.1 to 0.25 mm. It may be noted that the opening of a No. 100 U.S. Standard sieve is 0.149 mm and that of a No. 60 sieve is 0.25 mm; thus, no particles greater than that of a No. 60 sieve were counted in the formation of dust. Indeed, in most cases very few individual particles greater than a No. 100 sieve opening were collected on the filters. The same cloth was in other cases stretched across the top of the charcoal-support disc and wedged tightly around the circular edge of the support.

A most interesting behavior was found when a cloth bag containing a charcoal was tightly packed; this configuration markedly reduced the formation of dust. When the closure of the bag was relaxed, the charcoal particles assumed a loose packing and the dust formation then increased to a characteristic value. Typical results are given (Table III) for a Cane CAL sample kindly supplied by the California and Hawaiian Refinery. The marked difference between the tightly-packed and a loosely-packed sample is evident in Table III. The first use of a sample frequently released excess dust that had accumulated in the previous handling of the material in transportation, manufacture, or laboratory operations, but the plateau value formed upon repetitive measurements was characteristic of the charcoal.

Table III: Dusting Coefficient (mg/10 minutes) of Cane CAL:
Dependence on Packing during Vibration (Samples
Supplied by the C & H Refinery)

	New Cane CAL tightly packed	CAL loosely packed	Regenerated Cane CAL tightly packed	CAL loosely packed
	8.5*	12.8	2.3	10.1
	----- 3.7	6.1	1.5	9.3
	2.4	10.2	0.2	8.0
	<u>1.7</u>	<u>10.1</u>	<u>0.5</u>	<u>7.2</u>
Av.	2.5	9.5	1.1	8.6

*NOTE: The first use of a sample in the vibrator often releases excess dust accumulated in previous handling.

IV. Discussion

Charcoal particles fracture in a brittle manner, i.e. by a process with little or no plastic deformation. In this respect, the behavior is like most ceramics. Experimentally, the strength of porous ceramics decreases nearly exponentially with increase in the volume fraction of pores⁽⁷⁾. Hence, highly porous charcoal particles can be expected to show a correlation between the friction and attrition mechanism. The factors that increase the friction between charcoal particles should likewise increase the attrition, i.e. the dust formed.

A fundamental treatment of the fracture of charcoal particles is beyond the scope of the present paper. Instead, one application of the findings is to formulate a test procedure whereby different charcoals can be evaluated for use in some individual application. The requirements of a test procedure for technical control purposes are:

1. The experimental details should be relevant to the adsorption application.
2. The results must be adequately precise.
3. The test should be conducted with minimum technician time and maximum simplicity.
4. The maintenance should be practical in time and capital investment.

A test procedure is now being prepared for consideration by the ASTM Committee D-28. The procedure is based on the increase in weight of the glass fiber filter observed during specified parameters.

The present study has been directed to the attrition of charcoal and the generation of dust in adsorbent applications, but the procedure might also be used to estimate the dust already in a sample. The boundary of a charcoal granule is a very rough surface and there are many nooks and crannies to hold small dust particles. It is not known to what degree these are released in the vibrating sample and carried away by the flow of air. A plausible assumption

15th DOE NUCLEAR AIR CLEANING CONFERENCE

is that a steady state is soon attained. It is, of course, necessary to specify the time interval on the vibrating unit that is to be used in the estimate of initial dust in a sample.

There does not appear to be a significant correlation of the attrition coefficient with Ball & Pan Hardness. The latter is concerned with both particle breakdown and attrition and both processes form dust. The new procedure given in this report forms dust alone. There is need to obtain a correlation with some plant experience. Qualitatively, it is possible to align different charcoals by the visual appearance of the cloud of dust obtained by allowing a sample of charcoal to fall about 3 feet. The alignment is subjective, but appears to be in direct proportion to the attrition coefficient. It may be noted that a vibrated sample of charcoal is remarkably free of dust as judged by appearance in free fall.

There is no satisfactory correlation among samples from different sources with the bulk density or weight per particle. This is understandable since the source of the dust originates from the dynamic process of particles rubbing each other.

Further studies now in progress are concerned with many aspects of the above work: vibrations 20 to 120 Hz, closely sieved fractions of charcoals, methods to maintain tight packings, correlation with published test procedures, and theoretical models for vibrating beds of charcoals with kinetic equations of motion.

V. Acknowledgements

The sponsorship of the Division of Nuclear Fuel Cycle and Production, Department of Energy, and the cooperation of John C. Dempsey are gratefully acknowledged. Many profitable discussions with Frank R. Schwartz, Jr., North American Carbon, Inc. were very helpful.

VI. References

1. Black, R. F., "Hardness Determination by the Shaking Test", 11th Annual Meeting Sugar Industry Technicians, 1951.

15th DOE NUCLEAR AIR CLEANING CONFERENCE

2. Carpenter, F. G., "Development of a New Test for the Abrasion Hardness of Bone Char", 1957, Proc. Tech. Sess. Bone Char, 99-135.
3. Military Specification MIL-C-17605B (SHIPS), 21 March 1966, Charcoal, Activated, Technical, Unimpregnated.
4. RDT Standard, Dept. of Energy, Division of Nuclear Power Development RDT M-16-1T, December 1977. Appendix F: "Standard Method of Test for Determining Ball-Pan Hardness of Activated Carbon", 49-53.
5. ANSI/ASTM D2652-76, "Standard Definitions of Terms Relating to Activated Carbon".
6. Hayashi, H., Suzuki, A. and Tanaka, T., Powder Technology 6, 353-362 (1972).
7. Ryshkewitch, E., J. Am. Ceram. Soc. 36, 65-68 (1953).

DISCUSSION

MURROW: Could vibration possibly circulate the carbon from the lower layers toward the top, or inlet?

DEITZ: The vibrated charcoal particles in a 2-inch bed were observed to circulate from the bottom to the top and then follow another path to the bottom. As mentioned in the text, there were regions where the particles did not move and these were identified under stroboscopic illumination to be the nodes of 3-dimensional vibrations of the charcoal bed.

MURROW: Would you anticipate as much circulation in deep bed systems which have a "head" of carbon out of the air stream?

DEITZ: The "head" of carbon could be a factor if some close-packing arrangement of particles were attained. However, the applied forces on the charcoal in a commercial installation originate at the closest metal parts of the filter installation and these will vary with the vibrational modes and the geometry of the structure.

I would like to raise a question for the HEPA filter engineers, and ask how much charcoal dust has been observed to collect on the filtering surfaces when they follow a charcoal installation.

SCHURR: Have you done size and shape studies of attrited charcoal particles to determine if attrition rates are likely to remain constant over a long period?

DEITZ: The dust that was collected on several glass filter papers was observed with an optical microscope (100X) and found to have only normal features. Extruded charcoal gives some curved particles. Cylindrical and spherical particles generated least dust per unit time, as might be expected in a wear-friction process. As mentioned in the text, a particular coconut charcoal was vibrated in 50 separate experiments with only a slight trend towards smaller values of the attrition coef-

15th DOE NUCLEAR AIR CLEANING CONFERENCE

ficients. Determinations are planned using closely-sieved fractions from some charcoals. However, the friction of porous and rough charcoal particles rubbing each other in a vibrating bed could be expected to continue to abrade at the relatively small constant rate that is observed.

Our plans are to make ten vibrating devices similar to that described in the paper and these will be made available, at cost, to would-be investigators. Please write to the author at: Code 6170, Naval Research Laboratory, Washington, D.C. 20375, if your laboratory is interested.

15th DOE NUCLEAR AIR CLEANING CONFERENCE

THE DEVELOPMENT OF Ag^{OZ} FOR BULK ^{129}I REMOVAL FROM NUCLEAR FUEL REPROCESSING PLANTS AND PbX FOR ^{129}I STORAGE*

T. R. Thomas, B. A. Staples, and L. P. Murphy
Allied Chemical Corporation
Idaho Chemical Programs - Operations Office
Idaho National Engineering Laboratory
Idaho Falls, Idaho

ABSTRACT

Tests were conducted to develop silver-exchanged mordenite (AgZ) for removal of gaseous ^{129}I from nuclear fuel reprocessing plants. The effects of bed depth and hydrogen pretreatment on the elemental (I_2) iodine loading of AgZ were examined. The tests indicated that reduced AgZ (Ag^{OZ}) had about twice the capacity for iodine as AgZ , and at least 15-cm bed depths should be used for loading tests.

The effects of $\text{H}_2\text{O}(\text{g})$, NO , NO_2 , and bed temperature on the iodine loading of Ag^{OZ} were determined. The highest loadings were obtained with NO in the gas stream. Using simulated dissolver off-gas streams, loadings of about 170 mg I_2/g Ag^{OZ} and decontamination factors of 10^3 to 10^4 were obtained. This represents about 72% conversion of the silver to silver iodide. The data indicate that NO keeps the silver in the metallic state until silver iodide is formed. In the absence of NO , NO_2 may partially oxidize the silver to silver oxide and/or nitrate to cause lower iodine loadings. Water vapor and bed temperature appeared to have no effect on the iodine loadings.

Tests were conducted to develop a dry method for in situ regeneration of iodine-loaded Ag^{OZ} . A test bed of Ag^{OZ} was recycled 13 times by loading it with I_2 and stripping the I_2 (as HI) with H_2 . A 20% loss in iodine capacity was observed by the fourteenth loading. More tests are needed to determine if iodine loadings continue to decrease or become constant beyond the thirteenth cycle.

The iodine loadings of lead-exchanged zeolites, which were used to chemisorb HI during the recycle tests, were measured. Loadings up to 408 mg HI/g substrate were obtained. This represents about 90% use of the lead to form chemisorbed iodine. The iodine vapor pressures at 20°C over the substrates were predicted to be 10^{-6} , 10^{-8} , and less than 10^{-16} atm for lead-exchanged mordenite, lead-exchanged faujasite and reduced lead-exchanged faujasite, respectively.

A process-flow diagram was formulated for iodine recovery. Two parallel beds of Ag^{OZ} are used to permit continuous iodine recovery. While one is being regenerated the other recovers iodine. The iodine is chemisorbed as silver iodide, stripped as hydrogen iodide, and chemisorbed on the lead bed as a form of lead iodide. The silver beds were sized for a 30-day operation in a fuel reprocessing plant before regeneration. About 5 days would be needed for regeneration. About 2 m^3 of iodine-loaded lead-exchanged faujasite would be

*Work performed under USDOE Contract EY-76-C-07-1540.

15th DOE NUCLEAR AIR CLEANING CONFERENCE

generated each year. The lead bed would be contained in canisters to permit transfer in and out of the bed holder and storage in 0.2 m³ (55 gal) drums.

INTRODUCTION

The objectives of the ¹²⁹I Adsorbent and Storage Program conducted at the Idaho Chemical Processing Plant (ICPP) were to develop:

- (a) Silver-exchanged zeolites for bulk ¹²⁹I removal from the dissolver off-gas (DOG) of Light Water Reactor (LWR) fuel reprocessing plants.
- (b) A dry method for in situ regeneration of spent silver-exchanged zeolites.
- (c) Lead-exchanged zeolites for the collection of iodine during regeneration of the silver-exchanged zeolites and as a final storage medium for immobilization of ¹²⁹I.

In the previous Air Cleaning Conference,¹ we reported a dry method for in situ regeneration of spent silver-exchanged faujasite (AgX). The data indicated a 50% loss in iodine loading occurred after five regenerations. Later investigations with silver-exchanged mordenite (AgZ) indicated no loss in iodine loadings after five regenerations. The efforts of the program were shifted to developing AgZ for bulk ¹²⁹I recovery. The objectives were:

- (a) Determine the effect of hydrogen-pretreatment on the elemental-iodine (I₂) loading of AgZ.
- (b) Determine the effects of water vapor, NO, and NO₂ on the iodine loadings of hydrogen-pretreated silver-exchanged mordenite (Ag⁰Z).
- (c) Conduct recycle tests using a bed of Ag⁰Z in which the iodine was repeatedly loaded as I₂ and stripped as hydrogen iodide (HI).
- (d) Perform iodine-loading tests on lead-exchanged zeolites with HI.
- (e) Measure the iodine vapor pressures of chemisorbed iodine in lead-exchanged zeolites.

EXPERIMENTAL PROCEDURE

The lead-exchanged faujasite (PbX) was prepared by ion exchange with 1.6 mm spheres of Linde Molecular Sieve, Type 13X. The lead-exchanged and silver-exchanged mordenites (PbZ and AgZ) were prepared by ion-exchange with the sodium form of 10-20 mesh Norton Zeolon 900. A plug-flow procedure was developed for ion exchange. The method and apparatus are described elsewhere.² Fresh Ag⁰Z (i.e., not regenerated) and Pb⁰X were prepared by exposing 500 g batches of the AgZ or PbX to pure H₂ (5 L/min) at 500°C for 24 hours.

15th DOE NUCLEAR AIR CLEANING CONFERENCE

The test apparatus and general test procedure used for iodine-loading studies were described in the previous Air Cleaning Conference.¹ The apparatus used for regenerating the iodine-loaded Ag⁰Z (AgIZ) and transferring the iodine to PbX is described elsewhere.²

Recycle Tests on Ag⁰Z

Iodine-loading and stripping tests were run repeatedly on a test bed of Ag⁰Z. The Ag⁰Z was loaded with iodine in a simulated DOG stream, the bed dismantled, the iodine content determined, and the bed transferred to the regeneration-test apparatus. The recycle test conditions are given in Table I. Lead-exchanged zeolites were used downstream of the AgIZ during regeneration to recover desorbed iodine. The lead-exchanged zeolites tested were PbX, PbZ and PbX reduced to the metal (Pb⁰X). Experimental conditions for these adsorbents were the same as those indicated for iodine stripping of AgIZ except for a 150°C bed temperature and 8 m/min superficial face velocity.

TABLE I
CONDITIONS FOR RECYCLE TESTS ON Ag⁰Z

<u>Experimental Variable</u>	<u>Iodine Loading</u>	<u>Iodine Stripping</u>
Bed diameter (cm)	5	5
Bed depth (cm)	15	15
Particle size (mesh)	10-20	10-20
Superficial face velocity (m/min)	15	15
Bed temperature (°C)	150	500
Inlet pressure (mm Hg ⁰)	700	760
Carrier gas	air	hydrogen
Iodine conc. at 21°C and 1 atm (mg/m ³)	1500	7400
NO ₂ concentration (%)	2	0
NO concentration (%)	2	0
Dew point (°C)	35	nil
Iodine flux to and from bed (mg/min·cm ²)	1.5	4.5

Iodine Vapor Pressure over Zeolites

The method for measuring the HI vapor pressure over silver-exchanged zeolites was reported in the previous Air Cleaning Conference.¹ Tests were also conducted to determine the vapor pressure of iodine loaded on PbX, Pb⁰X, and PbZ (PbIX, Pb⁰IX and PbIZ, respectively). Samples were taken from beds of these materials used to

15th DOE NUCLEAR AIR CLEANING CONFERENCE

chemisorb HI during the regeneration of AgIZ. The sodium form of the substrate (NaX) was loaded with airborne-elemental iodine (NaIX) to serve as a reference case for the vapor pressure studies. The NaIX samples contained smaller amounts of iodine (4 wt%) than did Pb^oIX (38 wt%), PbIX (40 wt%), and PbIZ (38 wt%). Static-gas blankets of air, hydrogen and nitrogen were used in the iodine-vapor pressure studies. Adsorbent samples were placed in the heated cell, and the absorbance by I₂(g) in the cell was measured as a function of temperature. The experimental procedure and apparatus are described elsewhere.³

EXPERIMENTAL RESULTS

The Effect of H₂-Pretreatment on I₂ Loading

The effects of contact time and hydrogen pretreatment on the I₂ loading of AgZ were examined using an airstream face velocity of 15 m/min, a bed temperature of 100°C, and a dew point of 23°C. The test beds were pretest purged for 16 hr. The results along with the distribution of iodine from the top to the bottom of the bed are shown in Table II.

TABLE II
EFFECT OF CONTACT TIME AND H₂-PRETREATMENT ON THE
I₂ LOADING OF AgZ

Total Bed Depth(cm)	(mg I ₂ /g Ag in each 2.5 cm segment)						(mg I ₂ /g AgZ) ^b Average
	1	2	3	4	5	6	
5	57	10	-	-	-	-	33 ± 7
5 ^a	60	12	-	-	-	-	36 ± 7
15	71	70	68	67	47	9	56 ± 7
15 ^a	138	136	123	94	34	5	88 ± 7

a H₂-pretreated

b Duplicate tests were run in all cases; the 95% confidence interval is based on a pooled variance.

The data indicate that the mass transfer zone (MTZ) is 7.5 to 10-cm deep under these conditions. In the 15-cm-deep beds, an effect due to hydrogen pretreatment is observed. In the saturation zone (i.e., the top 5 to 7.5 cm of the bed) the iodine loading of the hydrogen pretreated AgZ (Ag^oZ) is about twice that of the untreated AgZ.

Iodine Loading on Ag^oZ

The effects of water vapor, NO, and NO₂ on the iodine loading of Ag^oZ were studied. All tests were run in airstreams using the following conditions: bed weight, 270 g; bed depth, 15 cm; bed diameter,

15th DOE NUCLEAR AIR CLEANING CONFERENCE

5 cm; superficial face velocity, 15 m/min; bed temperature, 150°C; airborne-elemental iodine concentration, about 1500 mg I₂/m³; and decontamination factor at breakthrough, 10³ to 10⁴.

The iodine loadings and distribution throughout the bed are given in Table III. The data indicate that the first 5 to 7.5 cm of the test bed attains a saturation loading; the distribution of iodine is about constant. The remaining 7.5 cm is in the mass-transfer zone. In Table IV the average iodine loadings, along with the saturation- and mass-transfer zone loadings are given.

An analysis of the saturation-zone data based on a three-level factorial design and the 95% confidence interval for an effect indicate:

- (a) NO effect = 40±12 mg I₂/g Ag⁰Z; adding NO to the gas stream enhances the iodine loading.
- (b) NO₂ effect = -12±12 mg I₂/g Ag⁰Z; within the confidence limits of an effect, the negative influence of NO₂ is not clearly established.
- (c) H₂O effect = -4±12 mg I₂/g Ag⁰Z; the presence or absence of water vapor has no significant effect on the iodine loadings.
- (d) NO x NO₂ interaction = 25±12 mg I₂/g Ag⁰Z; the interaction between NO and NO₂ is large; at low levels of NO the effect of increasing NO₂ is a reduction in loading. At higher NO levels, the NO₂ effect becomes small.
- (e) H₂O x NO₂ interaction = 11±12 mg I₂/g Ag⁰Z; the interaction between water and NO₂ is insignificant.
- (f) H₂O x NO = 7.5±12 mg I₂/g Ag⁰Z; the interaction between water and NO is insignificant.

A similar analysis of the data in the mass-transfer zone and the overall average loading both indicate a large positive effect due to NO. However, no other main effects or interactions were significant.

Recycle Tests on Ag⁰Z

The recycle of a bed of Ag⁰Z was stopped after 13 cycles. The experimental conditions used are given in Table I. Table V shows the results of the loading tests and the distribution of the iodine throughout the bed.

During the regeneration tests, the desorbed HI from the AgIZ bed was chemisorbed on lead-exchanged zeolites downstream. Table VI gives the results of the loading tests. The data indicate that the best loadings are obtained on PbX and about 90% of the lead is being used to chemisorb HI. The loading on Pb⁰X appears to be about half of that on PbX and PbZ under the same test conditions.

15th DOE NUCLEAR AIR CLEANING CONFERENCE

TABLE III
IODINE LOADING AND DISTRIBUTION vs. CONTAMINANT GASES

Test Conditions			mg I ₂ /g Ag ⁰ Z in each 2.5 cm Segment ^b						Avg. Loading (mg I ₂ /g Ag ⁰ Z)
Water Vapor (%) ^a	NO ₂ (%)	NO (%)	1	2	3	4	5	6	
0	0	0	174	160	141	121	69	15	113
6	0	0	155	136	123	89	35	3	91
0	2	0	97	100	91	73	39	9	67
6	2	0	125	127	119	121	81	17	98
0	0	2	163	171	170	134	93	22	129
6	0	2	169	167	143	123	74	10	115
0	2	2	187	181	185	169	103	21	141
6	2	2	181	172	163	129	65	9	120

^a Dew point = 35°C

^b The average value of duplicate or triplicate tests

TABLE IV
IODINE LOADINGS IN SATURATION AND MASS-TRANSFER
ZONES vs. CONTAMINANT GASES

Test Conditions			Loadings (mg I ₂ /g Ag ⁰ Z) ^a		
Water Vapor (%)	NO ₂ (%)	NO (%)	Saturation Zone ^b	Mass-Transfer Zone ^c	Overall Average
0	0	0	159 ± 17	69 ± 17	113 ± 12
6	0	0	138 ± 17	43 ± 17	91 ± 12
0	2	0	96 ± 17	41 ± 17	68 ± 12
6	2	0	124 ± 17	73 ± 17	98 ± 12
0	0	2	168 ± 14	90 ± 14	129 ± 10
6	0	2	159 ± 17	69 ± 17	115 ± 12
0	2	2	185 ± 14	98 ± 14	141 ± 10
6	2	2	171 ± 17	67 ± 17	119 ± 12

^a The error limits represent the 95% confidence interval for duplicate or triplicate tests based on a pooled variance.

^b The average loading on the first three segments in Table III.

^c The average loading on the last three segments in Table III.

15th DOE NUCLEAR AIR CLEANING CONFERENCE

TABLE V
IODINE LOADING ON Ag⁰Z vs. NUMBER OF RECYCLES

Cycle	mg I ₂ /g Ag ⁰ Z in each 2.5 cm Segment						Avg. Loading (mg I ₂ /g Ag ⁰ Z)
	1	2	3	4	5	6	
0	179	174	164	132	60	7	119
1	182	170	161	127	71	10	120
2	212	201	178	147	76	13	138
3	192	192	180	150	70	5	131
4	194	189	179	145	67	8	130
5	191	180	176	147	80	10	131
6	169	166	154	142	94	21	124
7	188	174	169	139	61	12	124
8	165	182	158	142	47	8	117
9	137	129	125	88	46	11	89
10	149	143	128	103	42	6	95
11	141	117	154	85	95	36	105
12	137	130	129	114	70	18	100
13	143	140	131	107	51	13	98

TABLE VI
HYDROGEN IODIDE LOADINGS ON LEAD-EXCHANGED
ZEOLITES IN DRY HYDROGEN AT 150°C

Zeolite	No. of Tests	Iodide Loadings (mg HI/g Zeolite)	
		Average	Range
PbX ^a	5	408 ± 22 ^d	378 - 436
Pb ⁰ X ^b	1	192	-
PbZ ^c	2	380	361 - 398

^a Lead-exchanged faujasite

^b PbX exposed to H₂ at 500°C for 24 hr

^c Lead-exchanged mordenite

^d The 95% confidence interval of the average

15th DOE NUCLEAR AIR CLEANING CONFERENCE

HI Vapor Pressure over AgIZ

Prior to the Ag⁰Z recycle tests, the vapor pressures of HI (P_{HI}) over AgIZ vs. bed temperature and superficial face velocity were measured. The P_{HI} ranged from 1x10⁻⁴ to 2x10⁻³ atm, and the stripping rates of HI were calculated by:

$$\frac{(P_{HI}) (\text{cm}^3 \text{ H}_2/\text{min}) (128 \text{ mg HI}/24.1 \text{ cm}^3)}{(\text{cross-sectional area of the test bed})} = \text{mg HI}/\text{min}\cdot\text{cm}^2$$

where the flow of H₂ and the P_{HI} were measured at one atm pressure and 21°C.

The response surface (see Figure 1) of the stripping rate vs. the two test variables was obtained by fitting the data to the second order model:

$$Y = 0.585 + 0.456 X_1 + 0.477 X_2 + 0.064 X_1^2 + 0.0045 X_2^2 + 0.352 X_1 X_2$$

where Y = mg HI/min·cm², X₁ = (temp-475)/75, and X₂ = (face velocity-369)/246.

The coordinates at which duplicate data points were obtained are shown by the symbol "o" in Figure 1. At the 95% confidence level, all observed stripping rates for AgIZ agree within ± 11% of the predicted rate by the above equation. Possible changes in the response surface due to recycling Ag⁰Z were not studied.

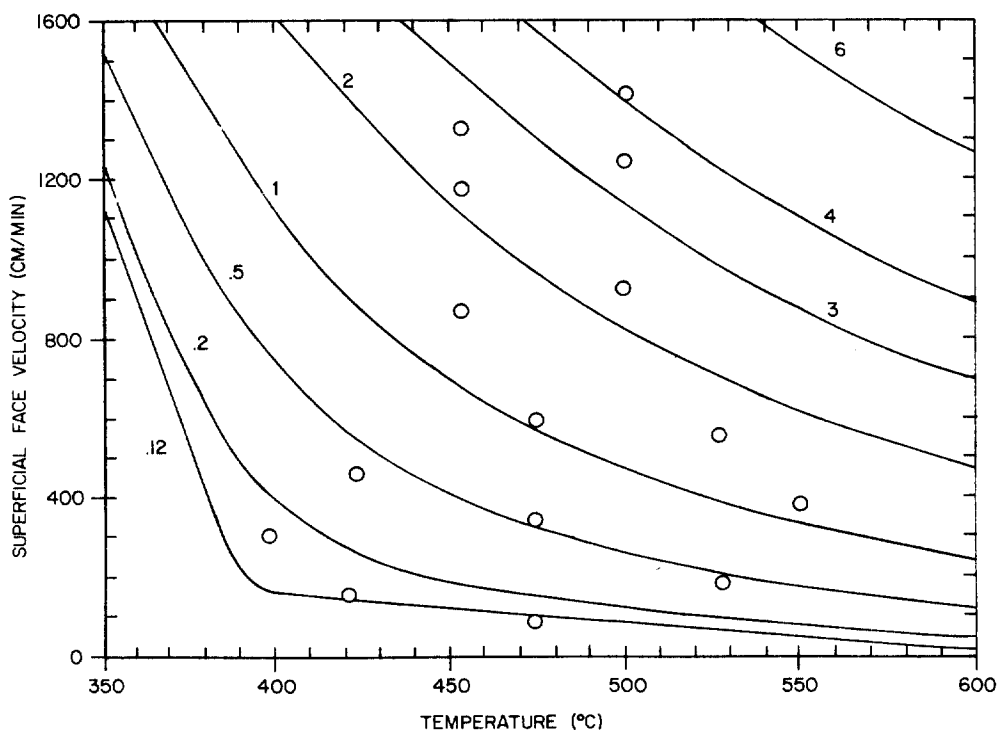


Figure 1. Stripping rate of HI from AgIZ
(mg HI/min·cm²)

15th DOE NUCLEAR AIR CLEANING CONFERENCE

I₂ Vapor Pressure over Lead-Exchanged Zeolites

Results of the iodine-vapor pressure studies were fitted by least squares to the equation:

$$\ln P_{I_2} = A - B/T$$

where P is the vapor pressure of elemental iodine in atmospheres and T is in K. The experimental data and curves are published elsewhere.³ The values of A and B are given in Table VII. The values for P_{I₂} at 20°C were estimated by extrapolation.

TABLE VII
IODINE VAPOR PRESSURE DATA FOR CHEMISORBED
IODINE ON LEAD-EXCHANGED ZEOLITES

<u>Substrate</u>	<u>Gas Blanket</u>	<u>A</u>	<u>B</u>	<u>P_{I₂} at 20°C (atm)</u>
PbIX	Air	15.3	9.47 x 10 ³	4.0 x 10 ⁻⁸
	Nitrogen	17.3	1.01 x 10 ⁴	3.4 x 10 ⁻⁸
Pb ⁰ IX	Air	44.5	2.65 x 10 ⁴	9.5 x 10 ⁻²¹
	Nitrogen	51.6	3.02 x 10 ⁴	2.3 x 10 ⁻¹⁶
PbIZ	Air	6.6	5.53 x 10 ³	4.4 x 10 ⁻⁶
	Nitrogen	8.0	6.20 x 10 ³	1.8 x 10 ⁻⁶

I₂ Solubility Studies

In the solubility studies, about 70% of the iodine on the NaIX beds was eluted by hexane, indicating physisorption of elemental iodine. No iodine could be found in the hexane effluent from columns of Pb⁰IX and PbIX. Previous tests have indicated that the water solubility of PbIX is less than that of PbI₂ (Ref. 1) which indicates that HI is not physisorbed. Thus, the results of the solubility studies suggest chemisorption of iodine by Pb⁰IX and PbIX as some form of lead iodide.

DISCUSSION OF RESULTS

The Effect of H₂-Pretreatment on AgZ

As the data in Table II indicate, the effect of H₂-pretreatment only shows up in the 15-cm-deep beds. In the 5-cm-deep beds, the shape of the MTZ is probably cancelling out the effect of the increased iodine-loading capacity of Ag⁰Z. As the reaction rate becomes slower, the MTZ increases and breakthrough occurs sooner, all other variables being equal. Consequently, tests should be conducted on deep beds to eliminate reaction rate as a variable.

15th DOE NUCLEAR AIR CLEANING CONFERENCE

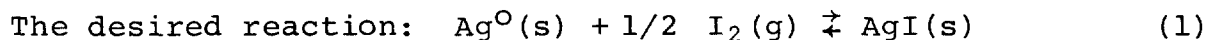
In the saturation zone of test beds, Ag^{OZ} has about twice the iodine-loading capacity as AgZ (TABLE II). To conserve charge balance, half the iodine in AgZ must be bonded to Ag and the other half to the framework oxygens. There are eight cation sites per unit cell in mordenite.⁴ Our substrate contains 20% silver by weight. Thus, if all the silver were converted to AgI and an equal amount were bonded to the framework, the mordenite could contain 448 mg I_2/g AgZ . A loading of 71 mg I_2/g AgZ represents about 16% of total capacity. This amounts to slightly more than one silver atom (12.5%) per unit cell forming AgI . Very little information is available on the location of the cation sites in mordenites. Four sodium sites have been located⁴ in the 8-membered rings which interconnect the main channels (12-membered rings). Only the main channels are considered accessible for most molecules. Thus, at least 50% of the silver is not accessible. Perhaps two or three of the remaining four sites are within the interconnecting framework which could also account for the apparent 16% use of exchanged silver in AgZ .

Considerable work has been done to determine the state of the metal⁵ when the metal-exchanged zeolite is exposed to hydrogen. Reduced metals become extremely mobile. The metals Cd, Hg, and Zn volatilize from the substrate. The metals Pt, Ni, and Ag migrate to the surface and form aggregates. In faujasites, reduction of the silver by H_2 at 250°C causes silver aggregates, which average 170 angstroms in diameter, to form.⁶ The fraction of silver which remains within the zeolite framework was not determined. As the results in Table II indicate, about 60% of the silver is used in Ag^{OZ} . Since the charge imbalance on the framework oxygens has already been satisfied by protonation, the iodine must be bonded only to the silver.

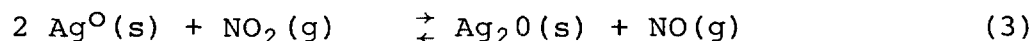
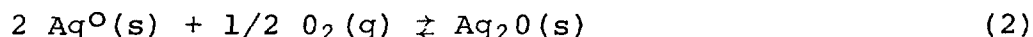
At least five of the eight silver atoms per site may become available by migration from restrictive framework cavities to the surface of the substrate. In our recycle tests on Ag^{OZ} (Table V) about seven out of eight silver atoms per site were used after the third exposure to hydrogen.

Iodine Loading on Ag^{OZ}

A graphical presentation (Figure 2) of the data in Table IV illustrates the positive influence of NO on the iodine loadings. In the absence of NO, NO_2 has a negative influence. However, the large NO x NO_2 interaction (i.e., 25±12 mg I_2/g Ag^{OZ}) identified in the effect tests prevents a clear statistical interpretation of the positive and negative effects of NO and NO_2 , respectively.



has a driving force of about -14.6 kcal/mol at 150°C. In the presence of O_2 and NO_x , there are three more reactions to consider.



15th DOE NUCLEAR AIR CLEANING CONFERENCE

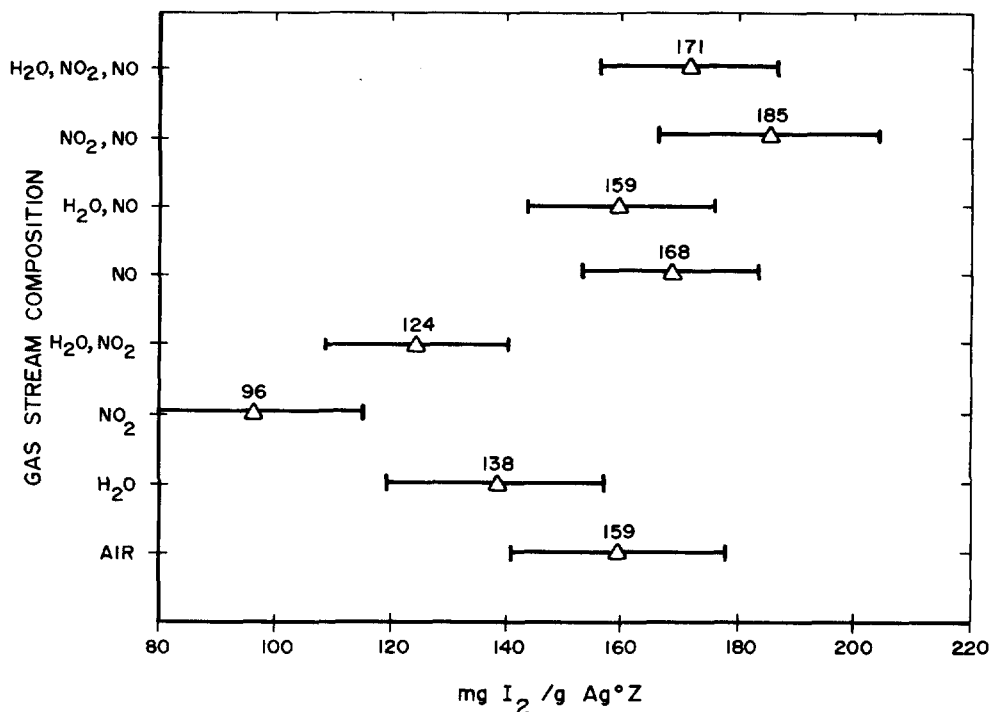


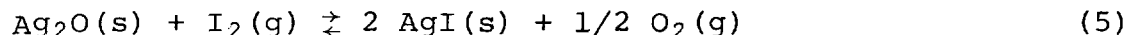
Figure 2. Iodine loadings in the saturation zone of Ag^oZ vs. gas stream composition at 150°C

The reaction free energies (ΔG) for reactions (2) through (4) are, respectively: -0.6, 5.6, and -12.3 kcal. Reaction (3) is probably the reason for the large NO x NO₂ interaction. As long as NO is present, any Ag₂O formed by reaction (2) should be reduced via reaction (3). The equilibrium pressure of NO(g) is given by:

$$\Delta G = -RT \ln P_{NO}/P_{NO_2}$$

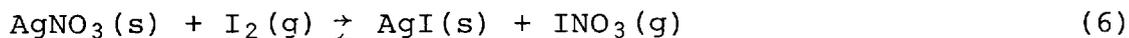
Substituting $\Delta G = 5.6$ kcal and $P_{NO_2} = 0.02$ atm, yields $P_{NO} = 3 \times 10^{-5}$ atm. For partial pressures of NO greater than 3×10^{-5} atm, Ag₂O should not form. In the absence of NO, the driving force to form AgNO₃ is about the same to form AgI from Ag^o(s).

Even though it is plausible that the oxide and nitrate may be involved, it is not clear why their formation would reduce the iodine loading in Ag^oZ. The reaction:



has about the same driving force per mole of AgI formed as reaction (1). Up to 95% of the silver in AgNO₃-impregnated amorphous silicic acid will react with I₂(g) in the saturation zone.⁷ Mechanistic studies indicate that iodine nitrate (INO₃) is formed via the reaction:⁸

15th DOE NUCLEAR AIR CLEANING CONFERENCE



The INO_3 then reacts with more AgNO_3 to form the iodate, or decomposes to NO_2 , O_2 , and I_2 . Also, mixtures of AgNO_3 , AgI , and AgIO_3 are known to form eutectic mixtures with melting points⁸ as low as 76°C . These facts present at least two possible explanations for the low iodine loading on Ag°Z when only NO_2 is present. The INO_3 may find insufficient AgNO_3 to complete the reaction to the iodate. A eutectic melt may replace the silver aggregates and cover some of the available silver.

The effect of NO_2 on Ag°Z will be a moot point for DOG applications. The primary NO_x species in the DOG of reprocessing plants will be NO . Consequently, the Ag°Z should remain in the reduced state and the maximum loadings in Figure 2 should be obtained. A loading of $171 \text{ mg I}_2/\text{g Ag}^\circ\text{Z}$ represents about 72% conversion of the Ag° to AgI .

As indicated by the data in Table IV, water vapor did not affect the iodine loadings of Ag°Z . There is no obvious reaction that should occur between Ag° and $\text{H}_2\text{O}(\text{g})$. Test results also indicate the absence of a temperature effect. The iodine loading of $132 \text{ mg I}_2/\text{g Ag}^\circ\text{Z}$ at 100°C and 3% H_2O (the upper 7.5 cm in Table II) is the same as $138 \pm 17 \text{ mg I}_2/\text{g Ag}^\circ\text{Z}$ at 150°C and 6% H_2O (in Figure 2). A comparative test was also made in dry airstreams containing 2% NO_2 . At 250°C the iodine loading was $88 \text{ mg I}_2/\text{g Ag}^\circ\text{Z}$ which is statistically the same as $96 \pm 17 \text{ mg I}_2/\text{g Ag}^\circ\text{Z}$ at 150°C in Figure 2.

Recycle Tests on Ag°Z

Figure 3 illustrates the iodine loadings in the saturation zones (the upper 7.5 cm loadings from Table V) vs. the number of recycles. The iodine loading on the thirteenth recycle is about 20% less than the initial loading. Linear extrapolation of the data indicates a 50% decrease in the initial loading would occur on the eighteenth recycle. However, further tests are needed to verify the extrapolation. The actual curve may be leveling out as indicated by the similar loadings obtained beyond Recycle 9. The increase in iodine loadings up to Recycle 2 is attributed to further reduction and/or migration of the silver to the surface of the substrate during regeneration. Beyond the second recycle, reduction in loading is attributed to pore collapse, which blocks access to Ag° remaining in the pores, and/or formation of multi-layered silver aggregates which block access to the lower layers. Both of these processes should reach a point of no further effect; the amount of surface silver available for reaction should reach a steady state. However, the lower limit has not been established.

Iodine loadings and Vapor Pressure on Secondary Adsorbents

The iodine vapor pressures over PbIZ , Pb°IX , and PbIX in H_2 increase rapidly with temperature. For example, the P_{I_2} over PbIX is 1×10^{-4} and 3×10^{-3} atm at 150 and 200°C , respectively² (i.e., a

15th DOE NUCLEAR AIR CLEANING CONFERENCE

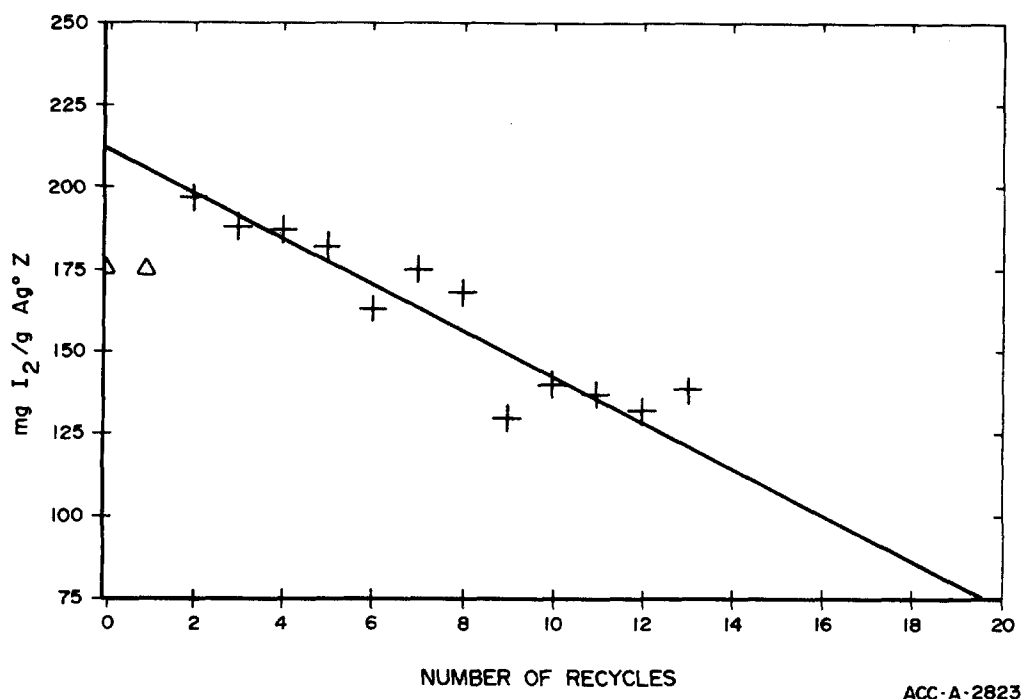


Figure 3. Iodine loadings of recycled Ag²OZ in the saturation zone

30-fold increase in P_{I_2}). While lower temperatures should result in higher decontamination factors, the bed temperature must be kept above 100°C to avoid condensation (in the PbX bed) of the water vapor desorbed from the AgIZ bed. The temperature effect on the HI loading of PbX was not studied. Our results indicate about 90% of the lead in PbX was used to chemisorbed HI at 150°C. Therefore, increasing the bed temperature could provide only a small increase (i.e., up to 10%) in the iodine loading. Since the low loading on Pb^{OX} is attributed to pore collapse, higher bed temperatures would probably have little effect on increasing the iodine loading. The iodine loadings on PbZ exceeded the stoichiometric ratio based on the lead content (i.e., a maximum of 247 mg HI/g PbZ for PbI₂ formation) which may be due to some physisorbed iodine or higher forms of lead iodide (i.e., H₂PbI₄). The best bed temperature for HI chemisorption on the lead-exchanged zeolites appears to lie somewhere between 100 and 150°C when both the instantaneous decontamination factor and the iodine loadings are considered. However, further testing is needed to confirm this, especially in the case of PbZ.

HI Vapor Pressure over AgIZ

The vapor pressure of HI over iodine-loaded AgX (AgIX) is close to that predicted for pure AgI.¹ The temperature-dependent vapor pressure curves for AgI and AgIZ are almost identical between 400 and 550°C. The data fitted to the equation $P_{HI} = e^A e^{-B/T}$, where $T = K$, is shown in Figure 4. We have found no basic difference between the

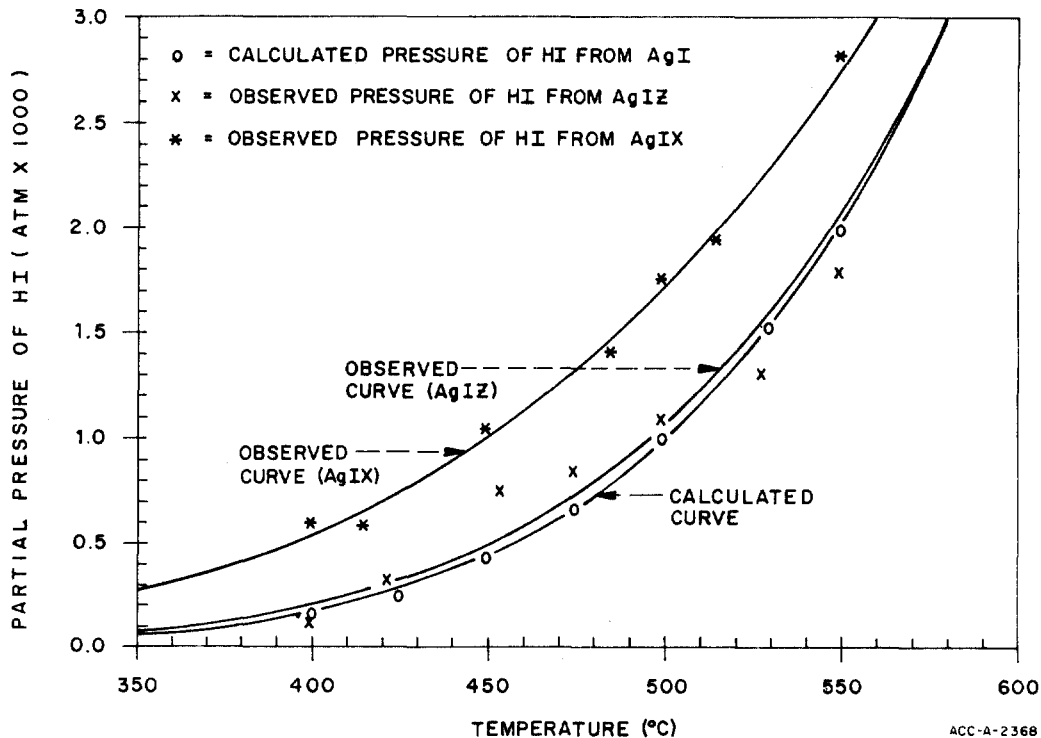
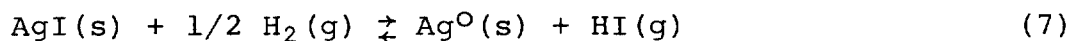


Figure 4. Vapor pressure of HI over AgI, AgIZ, and AgIX

HI vapor pressures over iodine loaded on AgX or Ag^OX and on AgZ or Ag^OZ. This observation seems inconsistent with the concept that half the iodine in AgZ or AgX is bonded to the framework oxygens. However, it is inconsequential how the iodine is bonded in AgX and AgZ. Upon exposure to H₂ at 500°C, most of the silver ions are rapidly converted to the metal. Then the equilibrium:

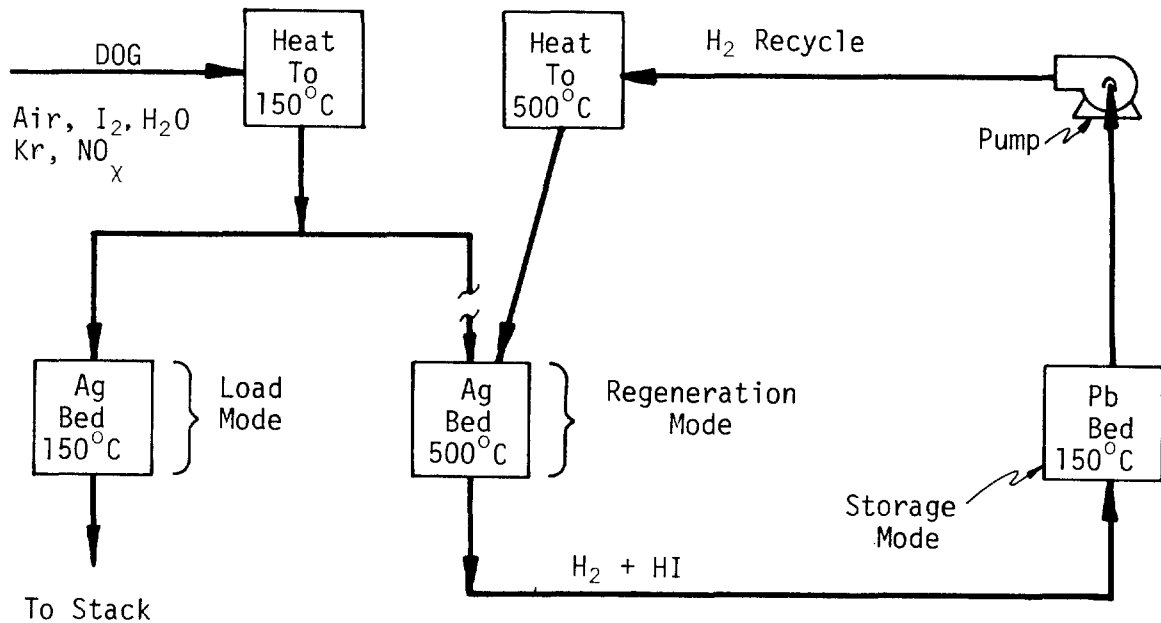


is established regardless of the source of HI(g). If HI could be easily formed from the iodine bonded to the framework oxygens, any amount in excess of the equilibrium pressure of HI(g) in equation (7) would be converted to AgI. Our data have indicated that this equilibrium is instantaneous because the partial pressure of HI is almost independent of the H₂ flow throughout the bed.

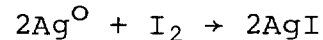
15th DOE NUCLEAR AIR CLEANING CONFERENCE

APPLICATION OF ADSORBENT TECHNOLOGY

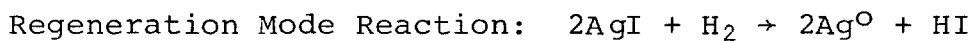
The application of adsorbent technology to include regeneration and recycle of Ag^{OZ} is illustrated by a block diagram in Figure 5 and a process-flow diagram in Figure 6. The assumed operational characteristics of a typical LWR fuel reprocessing plant are given in Table VIII. The fundamental data obtained from laboratory observations and used for calculations in the flow diagram are given in Table IX. The design criteria for the Ag^{OZ} and PbX beds are given in Table X.



Load Mode Reaction:



Regeneration Mode Reaction:



Storage Mode Reaction
Approximated by:

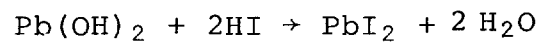
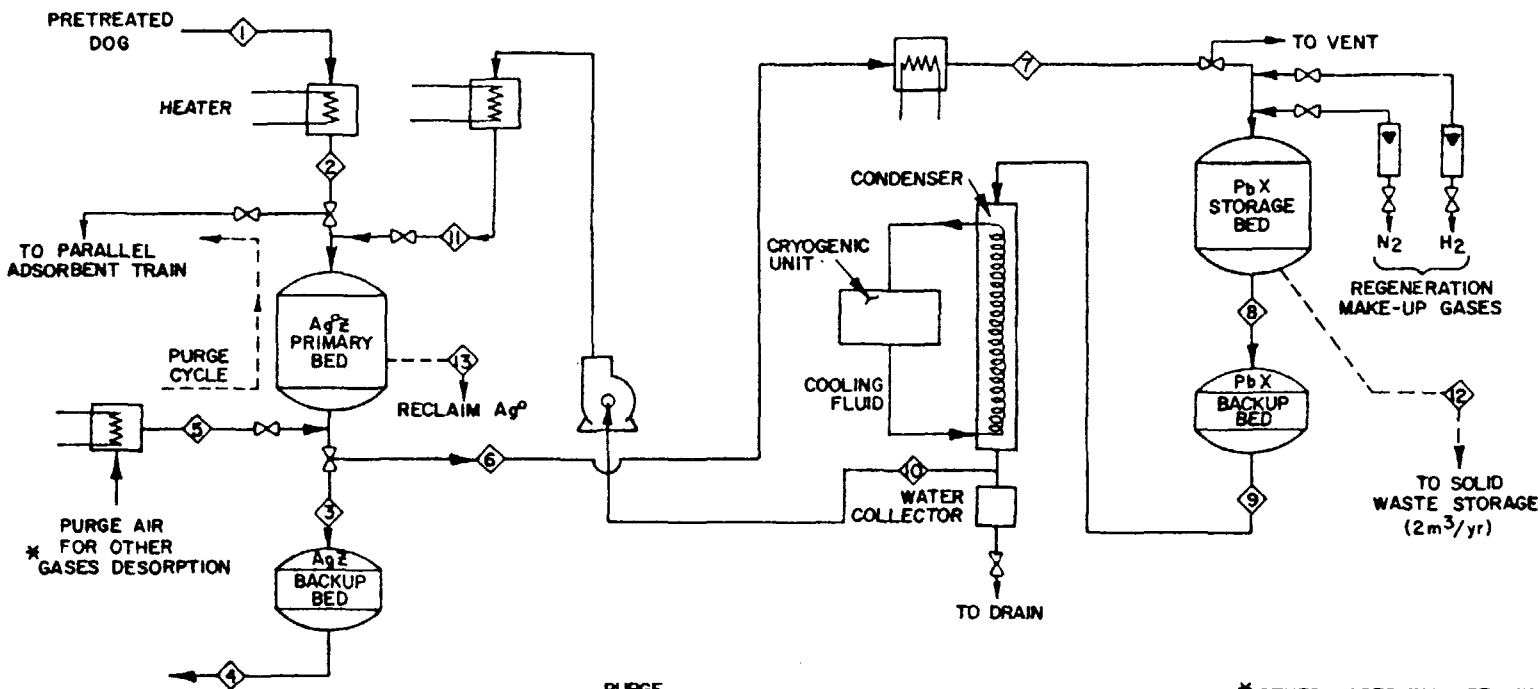


Figure 5. Block diagram of iodine recovery process



409

STREAM NO.	LOADING CYCLE = 30 DAYS				PURGE CYCLE 2 DAYS	REGENERATION CYCLE = 3 DAYS					
	1	2	3	4	5	6	7	8	9	10	11
PRESSURE (atm)	1.0	1.0	0.8	0.75	1.1	0.94	0.94	0.87	0.85	0.85	1.0
TEMPERATURE (°C)	45	150	150	150	300	500	150	150	150	0	500
FLOW (m ³ /h)	209	278	346	369	56	296	161	174	178	114	278
FLOW (kg/h)	233	233	233	233	38	9.6	9.6	9.6	9.6	9.6	9.6
NITROGEN	166	166	166	166	28	0	0	0	0	0	0
OXYGEN	51	51	51	51	9	0	0	0	0	0	0
OTHER GASES *	14.6	14.6	14.6	14.6	0.5	>0.6	>0.6	>0.6	>0.6	<0.6	<0.6
HYDROGEN	0	0	0	0	0	9	9	9	9	9	9
IODINE	7.1x10 ⁻²	7.1x10 ⁻²	7.1x10 ⁻⁴	7.1x10 ⁻⁶	0	0.26	0.26	2.6x10 ⁻³	2.6x10 ⁻⁶	2.6x10 ⁻⁶	2.6x10 ⁻⁶

* OTHER GASES INCLUDE: WATER VAPOR, NO_x, ARGON, AND KRYPTON AT 4.3, 7.4, 2.8 AND 0.09 kg/hr RESPECTIVELY.

** FLOWS FOR CLOSED LOOP. ABOUT 4 kg/yr H₂ NEEDED TO TRANSFER IODINE AS HI FROM Ag² TO PbX.

◊12 SPENT PbX TO WASTE STORAGE

◊13 LIFETIME OF Ag² UNKNOWN.

ACC-A-2622

Figure 6. Process flow diagram for iodine recovery from dissolver off-gas

15th DOE NUCLEAR AIR CLEANING CONFERENCE

TABLE VIII

ASSUMED OPERATIONAL CHARACTERISTICS OF AN
LWR FUEL REPROCESSING PLANT

1. Plant capacity	2000 tonne/yr
2. Fuel burnup	28,700 MWd/tonne
3. Cooling period	1.5 yr
4. Plant on-stream time	300 d/yr
5. Airflow through dissolver at 0°C and 1 atm press	2.83 m ³ /min
6. DOG pretreatment systems before iodine removal	H ₂ O/NO _x scrubber, deentrainer silica gel, and HEPA
7. NO _x conc. after pretreatment	≤ 2%
8. H ₂ O dew point after pretreatment	35°C
9. Volatility of I ₂ from dissolver	> 99%
10. Halide inventory from burnup:	
¹²⁹ I + ¹²⁷ I	470 kg/yr
⁸¹ Br	27 kg/yr
⁸¹ Br normalized to ¹²⁹ I	43 kg/yr
Total halides as ¹²⁹ I	513 kg/yr

TABLE IX

FUNDAMENTAL DATA FROM LABORATORY OBSERVATIONS

1. Iodine loading on Ag ⁰ Z	≥ 100 mg I ₂ /g Ag ⁰ Z
2. Iodine loading on PbX	≥ 300 mg I ₂ /g PbX
3. Dry density of Ag ⁰ Z	0.79 g/cm ³
4. Dry density of PbX	0.85 g/cm ³
5. Desorption rate of HI from Ag ⁰ Z at 500°C, 1 atm and 15 m/min face velocity	4.5 mg HI/min·cm ² in pure H ₂
6. Pressure drop across Ag ⁰ Z at 150°C and 15 m/min face velocity	0.097 atm/m in air
7. Pressure drop across Ag ⁰ Z at 500°C and 15 m/min face velocity	0.03 atm/m in hydrogen
8. Pressure drop across PbX at 150°C and 11 m/min face velocity	0.02 atm/m in hydrogen

15th DOE NUCLEAR AIR CLEANING CONFERENCE

TABLE X
DESIGN CRITERIA FOR Ag^OZ and PbX BEDS

	face velocity (m/min)	diam (m)	length (m)	volume (m ³)	weight (Mg)	iodine loading (kg)
1. Ag ^O Z primary	15	0.63	2.1	0.65	0.51	51
2. AgZ backup	19	0.63	0.5	0.15	0.12	12 ^b
3. PbX storage ^a	11	0.55	3.2	0.76	0.64	192
4. PbX backup	12	0.55	0.8	0.19	0.16	48 ^b

^a PbX storage bed consists of 4 self-contained cartridges designed to fit in 55 gal drums. Number of cartridges needed per/yr ~11.

^b During normal operation, the backup beds would not be loaded with iodine.

The Ag^OZ primary bed was sized for a 30-day loading operation. During the adsorption of iodine, the bed would attain some saturation loading of H₂O, NO_x, HNO₃, and ⁸⁵Kr. Based on the work done by Sundaresan and coworkers,⁹ we have assumed an upper limit of 51 kg of H₂O and 36 kg of NO₂ for 0.65 m³ of Ag^OZ. During the 48-hr purge cycle, an average of 1.8 kg/hr NO_x/H₂O would be added to the 11.7 kg/hr NO_x/H₂O already present in the DOG. The combined load would increase the NO_x/H₂O flow to the parallel Ag^OZ primary bed (not shown in flow diagram) by about 13% over normal operation. The two parallel Ag^OZ adsorbent trains permit continuous iodine recovery while one of the beds is being regenerated.

After the purge cycle, the Ag^OZ bed is isolated from the DOG and opened to streams 6-11. The air in the bed is purged off with nitrogen and vented just before the nitrogen inlet. Hydrogen is added to the nitrogen until the regeneration gas consists of 100% H₂. The Ag^OZ primary bed is brought up to temperature, and the iodine stripped as hydrogen iodide. Any chemisorbed bromine would also be removed as HBr, but at a rate 100 times faster than iodine. The desorbed iodine and bromine are chemisorbed as some form of lead halide on the PbX. Residual water on the AgZ and the PbX beds would be partially removed by the condenser. The regeneration process is a closed loop in which the H₂ is recirculated. Although 9 kg H₂/hr would be recycled, only 4 kg H₂/hr would be required to transport the halides as HI and HBr to the PbX.

The transfer of iodine to the PbX would be discontinued when iodine is detected in stream 8. The self-contained cartridges in the PbX storage bed would be removed and placed in 55-gal drums for

15th DOE NUCLEAR AIR CLEANING CONFERENCE

storage. The PbX backup-bed cartridge would be repositioned at the top of the PbX storage-bed holder and new cartridges placed below it and in the backup-bed holder. This would provide a fresh backup bed for every new set of cartridges placed in the PbX storage-bed holder.

After regeneration of the $\text{Ag}^{\text{O}}\text{X}$ bed, it would be placed on standby status to remove iodine from the DOG when the parallel $\text{Ag}^{\text{O}}\text{Z}$ bed is saturated with iodine. With this design, the two $\text{Ag}^{\text{O}}\text{Z}$ beds would be regenerated five times a year. The long-term life of the $\text{Ag}^{\text{O}}\text{Z}$ beds has not been determined.

CONCLUSIONS AND SUGGESTED FUTURE WORK

The conclusions based on the experimental results and interpretation of the data are as follows:

1. In simulated DOG streams, elemental iodine loadings of 171 ± 17 mg I_2/g $\text{Ag}^{\text{O}}\text{Z}$ can be obtained; about 72% of the Ag^{O} is converted to AgI .
2. NO has a positive effect on the iodine loading of $\text{Ag}^{\text{O}}\text{Z}$; conversion to the oxide or nitrate by NO_2 is blocked.
3. The iodine loading of AgZ (silver in the oxide form) is about half the iodine loading of $\text{Ag}^{\text{O}}\text{Z}$.
4. Water vapor up to a 35°C dew point and bed temperatures between 100 and 250°C have little or no effect on the iodine loading of $\text{Ag}^{\text{O}}\text{Z}$.
5. Regeneration and recycle of $\text{Ag}^{\text{O}}\text{Z}$ is a practical concept; the $\text{Ag}^{\text{O}}\text{Z}$ loses about 20% of its initial iodine-loading capacity after 13 recycles. Extrapolation of the data indicates no greater than 50% and no less than 20% loss in the loading capacity would occur after 18 recycles.
6. Storage of ^{129}I on PbX is a practical concept; iodine loadings of 408 mg I_2/g PbX with iodine vapor pressures less than 4×10^{-8} atm are obtainable.
7. $\text{Pb}^{\text{O}}\text{Z}$ may give the best combination of a high iodine loading and low iodine vapor pressure.

It is recommended that additional studies be done:

1. Measure the loading capacity of $\text{Ag}^{\text{O}}\text{Z}$ for airborne-organic iodides.
2. Conduct design verification studies on the regeneration and recycle of $\text{Ag}^{\text{O}}\text{Z}$ in pilot-plant studies.
3. Search for other silver-loaded substrates that might be more suitable for regeneration and recycle than $\text{Ag}^{\text{O}}\text{Z}$.

15th DOE NUCLEAR AIR CLEANING CONFERENCE

4. Complete the evaluation of the recycle life of Ag^{OZ} , i.e., measure the complete life of the adsorbent.
5. Determine the hydrogen iodide loading and iodine vapor pressure of Pb^{OZ} .

REFERENCES

1. B. A. Staples, L. P. Murphy, and T. R. Thomas, "Airborne elemental iodine loading capacities of metal zeolites and a dry method for recycling silver zeolite," Proceedings of the 14th ERDA Air Cleaning Conference, CONF-760822, p. 363 (August 1976).
2. T. R. Thomas, et al., "Airborne elemental iodine loading capacities of metal zeolites and a dry method for recycling silver zeolite," ICP-1119, Idaho National Engineering Laboratory, Idaho Falls, Idaho (July 1977).
3. L. P. Murphy, et al., "The development of Ag^{OZ} for bulk ^{129}I removal from nuclear fuel reprocessing plants and PbX for ^{129}I storage," ICP-1135, Idaho National Engineering Laboratory, Idaho Falls, Idaho (December 1977).
4. D. W. Breck, "Zeolite molecular sieves," John Wiley & Sons, New York, NY, pp.120-124 (1974).
5. Kh. M. Minachev and Ya. I. Isakov, "Catalytic properties of metal-containing zeolites," Zeolite Chemistry and Catalyst, ACS Monograph 171, J. A. Rabo, Ed., pp. 552-611 (1976).
6. D. J. C. Yates, "The stability of metallic cations in zeolites," J. Phys. Chem., Vol. 69, p. 1676 (1965).
7. J. G. Wilhelm and J. Furrer, "Head-end iodine removal from a reprocessing plant with a solid sorbent," Proceedings of the 14th ERDA Air Cleaning Conference, CONF-760822, p. 447 (August 1976).
8. K. C. Patil, et al., "The silver nitrate-iodine reaction: iodine nitrate as the reaction intermediate," J. Inorg. Nucl. Chem., Vol. 29, p. 407 (1967).
9. B. B. Sundaresan, et al., "Adsorption of nitrogen oxides from waste gas," Environ. Sci. and Tech., Vol. 1, p. 151 (February 1976).

15th DOE NUCLEAR AIR CLEANING CONFERENCE

SYMBOLS

AgX	Silver-exchanged faujasite
AgZ	Silver-exchanged mordenite
Ag ⁰ Z	Ag in AgZ reduced with H ₂
AgIX	AgX loaded with iodine
AgIZ	AgZ loaded with iodine
NaX	Sodium form of Type 13X faujasite
NaIX	NaX loaded with iodine
PbX	Lead-exchanged faujasite
PbZ	Lead-exchanged mordenite
PbIX	PbX loaded with iodine
PbIZ	PbZ loaded with iodine
Pb ⁰ X	Pb in PbX reduced with H ₂
Pb ⁰ IX	Pb ⁰ X loaded with iodine

DISCUSSION

MIDLIK: It is my understanding that there is a problem with in-place testing of silver zeolite filtration systems. Is there a test plan or test procedure that is satisfactory to NRC? Our problem is related to type of agent used for leak testing.

T. R. THOMAS: This question is not relevant to my paper.

PICOULT: Current leak testing on silver zeolite adsorbents is being accomplished through the use of Freon.

HALLIGAN: I would like to comment on in-place testing of silver zeolite (AgZ) adsorbents. We have had some experience in this area. Our efforts using Freons, R-11 and R-112, were unsuccessful due to rapid breakthrough. We did, however, resort to the use of CH₃¹²⁷I as the challenge agent and obtained performance test data with no difficulty.

VAN BRUNT: One might expect that unmixed beds might have a different and lower recycle efficiency than the mixed adsorbent beds used in your tests. Can you comment on this?

T. R. THOMAS: I anticipate that a bed regenerated and recycled in situ will perform better. In the lab tests, it was necessary to reassemble the bed repeatedly to load and strip the iodine. This caused attrition and dusting from bed handling that would otherwise not occur.

HAAG: Please comment on the operation of a silver zeolite regeneration step and the possible hazards involved with high hydrogen concentrations at high temperatures (500°C) in a reprocessing plant.

15th DOE NUCLEAR AIR CLEANING CONFERENCE

T. R. THOMAS: I think we have the capability to handle pure hydrogen safely. It is done in private industry to produce pure hydrogen in pressurized cylinders and in reactor technology to recombine radiolytic hydrogen. The safety requirements that might be imposed on the nuclear industry might make the recycle technology economically unattractive.

BROWN: How much hydrogen would be required to handle the annual recycle requirement in a 2000 MT/year fuel reprocessing plant?

T. R. THOMAS: About nine standard, size A, pressurized cylinders of H₂ would be required to transfer the iodine from the silver zeolite to a PbX bed. This is based on the stoichiometry of the stripping reaction.

FURRER: Have you made loading and recycling tests of your silver zeolite in real DOG? Maybe you have a loading of organics in your silver zeolite from the recycled acid?

T. R. THOMAS: No, we have not tested silver zeolite in actual DOG streams. Organics would interfere only if they condense and form a tar-like layer. If degradation products from tributylphosphate are found to be a problem, an additional adsorbent, specific for organic compounds, would be positioned upstream of the iodine adsorbent.

WILHELM: Did you measure the removal efficiency of the silver zeolite with metallic silver for organic iodides? Experiments in Karlsruhe showed that this material would not remove organic iodides.

T. R. THOMAS: No, we didn't make the measurements, but they are going to be made at another laboratory; and until they are, we won't know whether these materials will efficiently recover organic iodides.

15th DOE NUCLEAR AIR CLEANING CONFERENCE

RADIATION-INDUCED IODINE MIGRATION IN SILVER ZEOLITE BEDS*

A. G. Evans
Savannah River Laboratory
E. I. du Pont de Nemours & Co.
Aiken, SC 29801

Abstract

The radiation stability of iodine-loaded, silver-exchanged zeolite (AgX) was evaluated under dynamic flow conditions in the radiolysis facility at the Savannah River Laboratory. A series of three tests was conducted in which 1-in.-deep beds of 10×16 mesh AgX beads were loaded to approximately 6 mg ^{131}I -tagged elemental iodine per mg AgX over a 1-hr period. Test conditions included an intense radiation field (absorbed dose rate of $\sim 1.5 \times 10^7$ rads/hr), a steam-air mixture (80°C and 95% relative humidity) and a face velocity of 55 ft per minute. Iodine passing through the beds was collected on backup beds located outside the radiation field to determine the penetration occurring during the irradiation period. In the first test, radiation exposure was terminated at the end of the 1-hr loading period. In the second test, irradiation and gas flow continued for an additional 4 hr (total exposure of 5 hr). In the third test, the total exposure period was increased to 105 hr. At the end of each test the test bed was counted, then sectioned into $\sim 1/8$ -in.-deep segments and recounted to determine the spatial distribution of ^{131}I activity in the irradiated assembly. Two additional tests were conducted at I_2 loadings of ~ 0.6 mg/g and an exposure period of 5 hr. The test bed was loaded with AgX in one test and with GX-176 carbon in the other test to determine the spatial distribution of I_2 at a lighter loading.

The long-term test (105-hr exposure) showed that little iodine migration occurred after an accumulated exposure of $\sim 1.6 \times 10^9$ rads (the cumulative penetration of ^{131}I was 0.7% for the entire test). Analysis of the irradiated test bed showed that more than 30% of the iodine activity remaining on the bed was located in the downstream half of the bed. About 3.9% of the iodine migrated to the last $1/8$ -in. section of the bed. The other tests, using shorter irradiation periods and lighter loadings, showed that the gross migration of iodine into the downstream sections of the bed was the result of the high iodine concentration in the gas stream during the loading phase (~ 400 mg I_2/m^3 air during loading). Comparison of activity distributions after short-term and long-term irradiation indicates that up to 10% of the iodine was redistributed within the bed after prolonged exposure to intense radiation and flowing air. However, downstream migration from radiolytic decomposition of silver-iodine complexes is less important to the iodine distribution than is the rapid heavy loading.

Introduction

Silver-exchanged zeolite is currently used to adsorb airborne radioiodine in locations where hostile environments prevent the use of carbon-based adsorbents (for example, where oxidizing gases or elevated temperatures could cause ignition of carbon). Use of AgX has also been proposed in reactor applications where high-intensity radiation fields could be encountered should a major accident occur.

* The information contained in this article was developed during the course of work under Contract AT(07-2)-1 with the U. S. Department of Energy.

15th DOE NUCLEAR AIR CLEANING CONFERENCE

In view of the fact that silver halide compounds are used as photosensitive agents in photographic and x-ray film emulsions, some reservations have been expressed about the effectiveness of AgX in these latter applications. The principal concern was the possible chromatographic migration of iodine through the adsorber beds under dynamic flow conditions in the high-intensity radiation environment. The radiation stability tests of AgX were conducted in the SRL Radiolysis Facility^{1,2} at the request of the Department of Energy to determine whether such migration occurs.

Discussion

A single, long-term exposure test was initially planned and executed. In this test, elemental iodine was loaded onto commercial AgX* over a 1-hr period in a high-intensity radiation field. This was followed by an extended (104-hr) desorption period in the radiation field with continued air flow. Iodine desorbed from the irradiated test bed was collected on backup beds which were changed at regular intervals to evaluate time-dependent desorption rates during the irradiation. The iodine loading on the test bed was about 6 mg I/g AgX on the 1-in.-deep test bed. Air flow was maintained at 55 ft/min face velocity and the adsorbed dose rate in the test bed was $\sim 1.5 \times 10^7$ rads/hr. A steam-air mixture (80°C and $\sim 95\%$ RH) was employed during the loading phase and for the first 4-hr desorption period. Except for two 4-hr periods, the remainder of the test was run at 35°C and ambient humidity (ranging from 20% to 35% RH at 35°C). Air at 45°C and 75% RH was intentionally introduced for 4 hr after 45-hr and 69-hr exposure to evaluate the effects of increased humidity on the desorption rate.

The specific test bed loading was chosen to be within the dynamic loading range of 1 to 10 mg I/g AgX found in the literature.³⁻⁶ The 1-in. bed depth was dictated by the design of the radiolysis test facility, and the dose rate dictated by the specific activity of the ⁶⁰Co in the facility.

At the end of the radiation exposure period, the test bed was counted to determine the residual radioactive content, then carefully sectioned into $\sim 1/8$ -in.-thick layers. Each of the layers was weighed and counted to determine the iodine distribution within the test bed.

Results of the desorption phase of the test showed that little migration of iodine occurred as a result of prolonged radiation exposure. The total penetration measured during the 105-hr test period was 0.743%. Measured desorption rates during the test are shown in Figure 1. Examination of the data shows that the desorption rates decreased with increasing accumulated exposure except for periods when high-humidity air was intentionally introduced. The desorption rates during the last 25 to 30 hr of the test remained fairly constant at about 1% of the peak desorption rate observed during the initial loading phase.

Analysis of the distribution of activity in the test bed showed that about 37% of the iodine remained in the front 1/4 in. of the bed and that nearly 4% had migrated to the last 1/8-in. segment of the test bed. The shape of the activity distribution curve (Figure 2) strongly suggests a "normal distribution" similar to that seen in ion exchange columns when an ionic species is moving through the resin beds. Numerical data are presented in Table I.

* 10 x 20 mesh beads, >98% exchanged. Purchased from CTI Nuclear, Inc., Denver, Colorado.

15th DOE NUCLEAR AIR CLEANING CONFERENCE

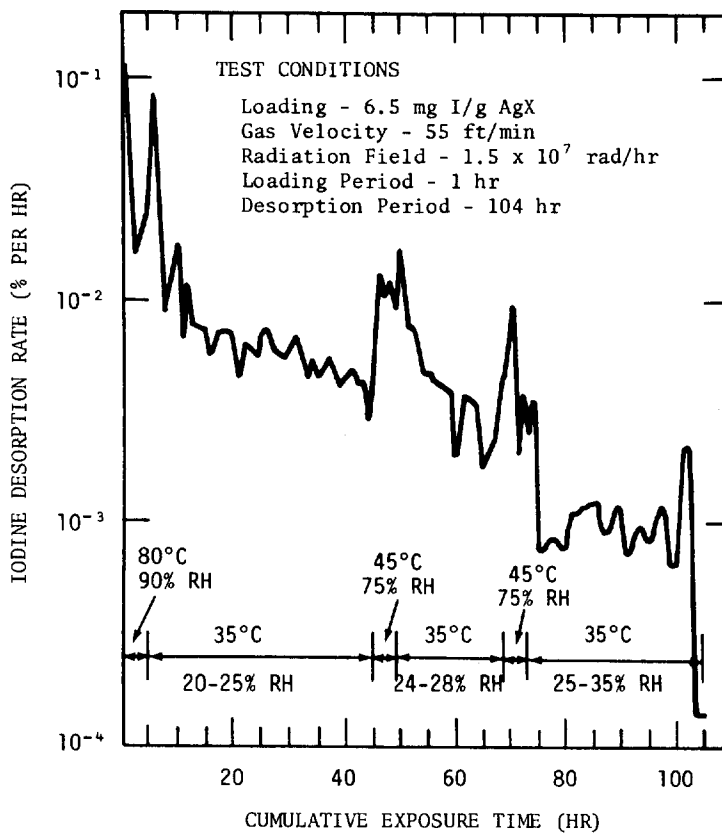


FIGURE 1
IODINE DESORPTION RATES FROM IRRADIATED AgX

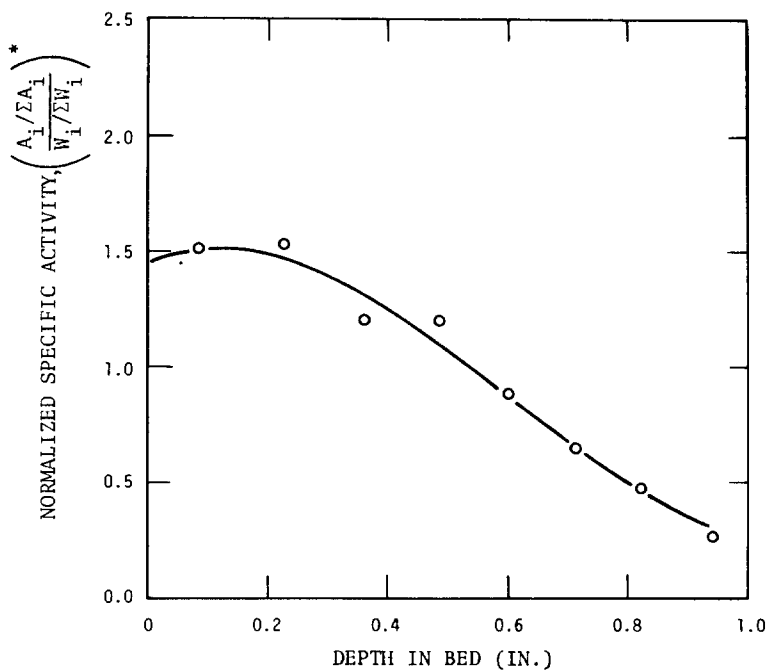


FIGURE 2
ACTIVITY DISTRIBUTION IN AgX BED AFTER 105-HR IRRADIATION

* see text

15th DOE NUCLEAR AIR CLEANING CONFERENCE

Table I. Radioactivity Distribution in AgX Bed After 105-hr Exposure.

Depth to Middle of Section, in.	Normalized ^a Specific Activity, (A _i /ΣA _i)/(W _i /ΣW _i)
0.083	1.504
0.227	1.520
0.351	1.203
0.486	1.192
0.602	0.881
0.716	0.647
0.827	0.482
0.944	0.262

a. Iodine loading - 6.5 mg I/g AgX, see text for discussion of normalization function.

This evidence of movement of activity in the test bed suggested additional tests in which shorter irradiation periods were employed to determine rate constants. A bed-sectioning experiment was also performed for GX-176* carbon for comparison (at a loading of 0.6 mg I/g C to stay within design loading limits).

The activity distributions in adsorber beds after 5-hr exposure (1-hr loading, 4-hr desorption) are shown in Table II and Figure 3 for GX-176 carbon (0.6 mg/g loading), AgX at 0.6 mg/g loading and AgX at ~6 mg/g loading. Since adsorber weights and activity levels were not constant, it was necessary to normalize the data to allow direct comparisons. The normalization was made using the function

$$\frac{A_i/\Sigma A_i}{W_i/\Sigma W_i}$$

where: A_i = activity in an individual segment, c/s

W_i = weight of adsorber in that segment, g

ΣA_i = total activity in the test bed, c/s

ΣW_i = total weight of adsorber in the test bed, g

The data in Figure 3 show that the activity level in carbon decreases exponentially with increasing bed depth at 0.6 mg/g loading. At 0.6 mg/g loading some penetration into the AgX bed is evident. These data suggest a somewhat slower reaction rate for airborne iodine removal in the AgX than is the case for carbon. At a loading of 6 mg/g, AgX exhibits considerable migration. This migration into AgX is consistent with recently published data which indicates a reaction zone of up to 5 cm depth when inlet concentrations of ~500 mg I/m³ air are encountered.⁷

Thus, at least a portion of the activity found in the deeper layers of adsorber in the 105-hr irradiation test can be attributed to the high inlet iodine concentration and heavy loading.

* North American Carbon Company, Columbus, Ohio.

15th DOE NUCLEAR AIR CLEANING CONFERENCE

Table II. Radioactivity Distribution in Test Beds After 5-hr Exposure.

GX-176 Carbon ^a (0.65 mg I/g C)		AgX ^b (0.68 mg I/g AgX)		AgX ^b (6.2 mg I/g AgX)	
Depth, in. ^c	Normalized Activity ^d	Depth, in. ^c	Normalized Activity ^d	Depth, in. ^c	Normalized Activity ^d
0.072	5.604	0.069	3.661	0.080	1.827
0.192	1.590	0.188	2.828	0.228	1.478
0.289	0.340	0.293	1.464	0.347	1.294
0.405	0.0571	0.422	0.314	0.457	1.076
0.543	0.0085	0.561	0.0364	0.589	0.711
0.671	0.0020	0.686	0.0044	0.719	0.573
0.778	0.0005	0.807	0.0007	0.826	0.467
0.914	0.0000	0.933	0.0002	0.938	0.257

- a. Product of North American Carbon Company, Columbus, Ohio.
- b. Type III, 10 × 20 mesh beads, >98% exchanged, Product of CTI Nuclear, Inc., Denver, Colorado.
- c. Depth to middle of bed section.
- d. $(A_i/\Sigma A_i)/(W_i/\Sigma W_i)$, see text for discussion.

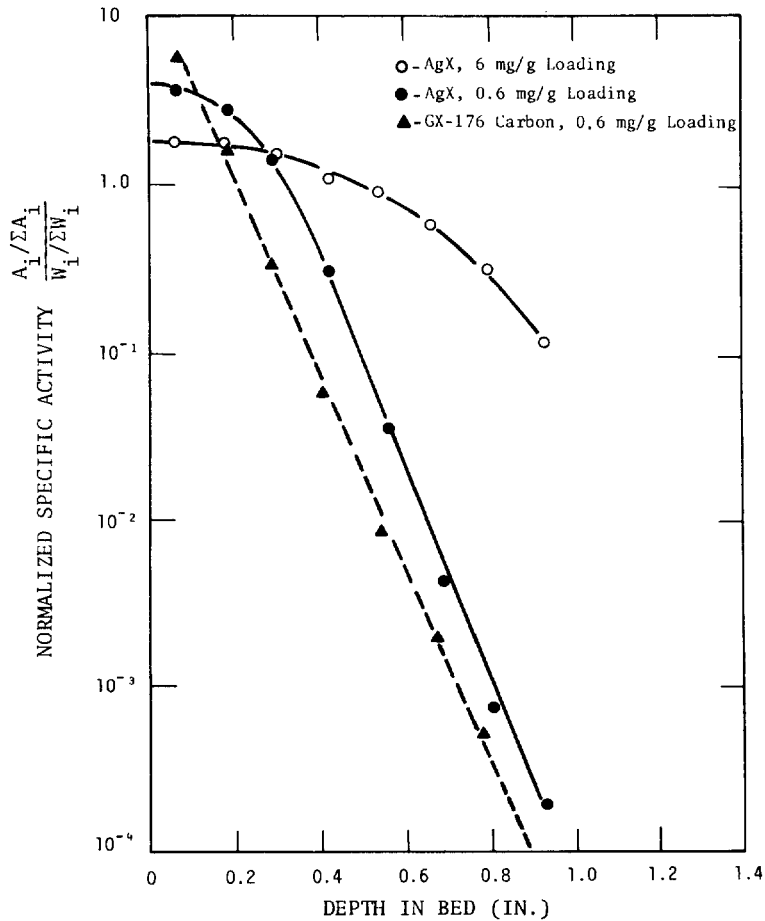


FIGURE 3
IODINE DISTRIBUTION IN TEST BEDS AFTER 5 HOURS EXPOSURE

15th DOE NUCLEAR AIR CLEANING CONFERENCE

To separate the heavy loading effects from the possible radiation effects, a third heavy loading experiment was performed in which the exposure time was reduced to 1 hr (the loading period only, with no subsequent desorption). Data for the three heavy loading (~ 6 mg/g) experiments are shown in Table III and Figure 4. The curves fitted to each set of data points were obtained by least squares methods assuming a normal distribution function (see Appendix).

Table III. Activity Distribution in Heavy Loaded AgX Beds After Irradiation.

1-hr Exposure (6.6 mg I/g AgX)		5-hr Exposure (6.2 mg I/g AgX)		105-hr Exposure (6.5 mg I/g AgX)	
Depth, in. ^a	Normalized Activity ^b	Depth, in. ^a	Normalized Activity ^b	Depth, in. ^a	Normalized Activity ^b
0.061	1.831	0.080	1.827	0.083	1.504
0.179	1.797	0.228	1.478	0.227	1.520
0.303	1.524	0.347	1.294	0.361	1.203
0.426	1.103	0.457	1.076	0.486	1.192
0.540	0.911	0.589	0.711	0.602	0.881
0.665	0.592	0.719	0.573	0.716	0.647
0.797	0.326	0.826	0.467	0.827	0.482
0.932	0.119	0.938	0.257	0.944	0.262

a. Depth to mid-section.

b. $(A_i/\Sigma A_i)/(W_i/\Sigma W_i)$, see text for discussion.

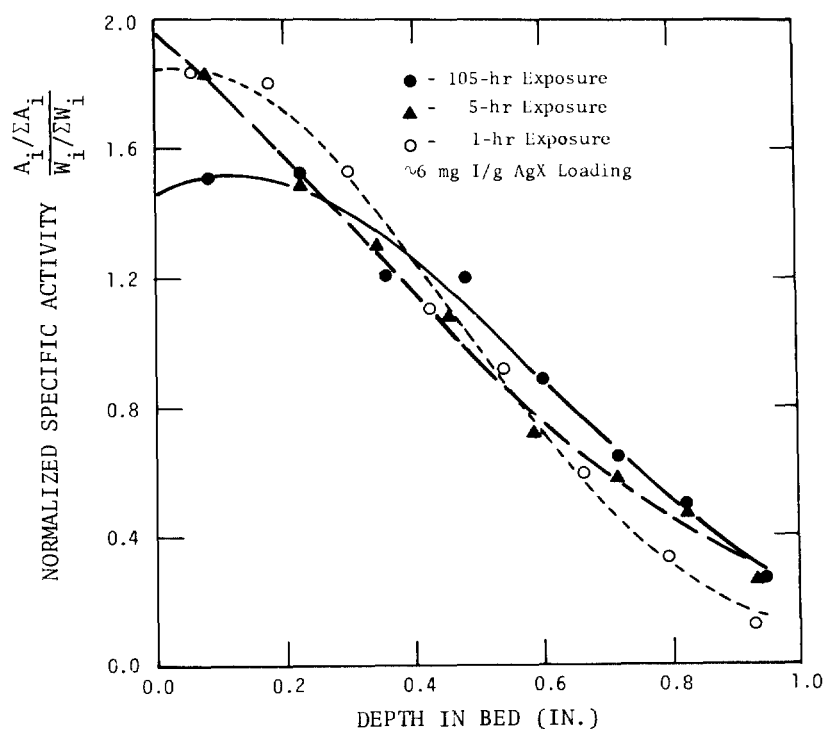


FIGURE 4
ACTIVITY DISTRIBUTION IN IRRADIATED AgX BEDS

15th DOE NUCLEAR AIR CLEANING CONFERENCE

Examination of the curves in Figure 4 shows that some discernible movement of activity from the front toward the rear of the test beds has occurred between each of the exposure periods. The magnitude of the movement cannot be obtained directly from the data as presented because of differences in segment depths, uncertainties in the effect of slightly different loadings and the magnitude of the experimental error, and because data cannot be expressed as specific activity of a bed segment.

Approximate numerical comparison of activity migrations can be made, however, if one assumes that the equations obtained in the curve fitting process (see Appendix) are reasonable approximations of the true iodine distributions. The equation for each curve can be integrated between the limits of $X = 0$ and $X = 1$ in. using the method shown in the Appendix. Corrections for activity desorbed from the the bed can now be made as shown below.

$$\frac{\int_0^1 f(x) dx}{1 - P} = T$$

where $\int_0^1 f(x) dx$ = total activity fraction on test bed
P = total activity fraction passing through test bed (penetration)
T = normalized total activity in test

Each equation can then be reintegrated between discrete limits and divided by T to obtain estimates of the normalized activity contained in equal depth segments of the bed. Calculated estimates of the activity contained in equal, 1/8-in.-deep segments (corrected for penetration) are given in Table IV.

Numerical estimates of the movements of iodine within the test bed can be made by determining the intersection points for each pair of curves (1-hr vs. 5-hr, 1-hr vs. 105-hr, and 5-hr vs. 105-hr exposures), then integrating the area under each curve from the bed front to the intersection point. The difference in integrated area plus the difference in desorbed iodine for each pair of curves is then the estimate of the total iodine migration between each exposure time. Calculated data are shown in Table V. The data indicate that between 1-hr and 105-hr exposures approximately 9.3% of iodine initially located in the first 0.41 in. of the bed moved to the rear of the bed. Another 0.6% of the iodine initially located in the rear of the bed moved out of the bed so that a total of about 9.9% of the total iodine migrated within or out of the 1-in.-deep bed as a result of radiation exposure. Similar comparisons in the time interval from 1-hr to 5-hr exposures indicate a migration of about 5.4% of the iodine, and that approximately 6.2% of the iodine was redistributed between 5-hr and 105-hr exposures.

In the proposed reactor applications, AgX adsorber beds of at least two inches depth would be used. Thus, an internal redistribution of ~10% of the iodine in the first inch of bed depth would not compromise the integrity of the adsorber system.

15th DOE NUCLEAR AIR CLEANING CONFERENCE

Table IV. Estimated Iodine Content of Equal Test Bed Segments.

Segment Depth, in.	Estimated Iodine Content of Each Segment, %		
	1-hr Exposure	5-hr Exposure	105-hr Exposure
0.000-0.125	22.97	22.87	18.44
0.125-0.250	21.70	19.89	18.46
0.250-0.375	18.57	16.61	17.13
0.375-0.500	14.40	13.32	14.76
0.500-0.625	10.12	10.25	11.81
0.625-0.750	6.45	7.58	8.76
0.750-0.875	3.73	5.38	6.04
0.875-1.000	1.95	3.66	3.86
Thru Bed	0.11	0.44	0.74

Table V. Estimated Iodine Migration in Irradiated AgX Test Beds^a

	Fraction of Total Iodine, %		
	Curve 1	Curve 2	C(1)-C(2)
<u>1-hr vs. 105-hr</u>			
Test Bed Iodine ^b	67.60	58.31	+9.29
Desorbed Iodine	0.11	0.74	-0.63
Total Migration	-	-	9.92
<u>5-hr vs. 105-hr</u>			
Test Bed Iodine ^c	45.39	39.51	+5.88
Desorbed Iodine	0.44	0.74	-0.30
Total Migration	-	-	6.18
<u>1-hr vs. 5-hr</u>			
Test Bed Iodine ^d	82.01	76.96	+5.05
Desorbed Iodine	0.11	0.44	-0.33
Total Migration	-	-	5.38

a. One-in.-deep beds loaded to ~6 mg I/g AgX, superficial face velocity of 55 ft/min and an absorbed dose rate of $\sim 1.5 \times 10^7$ rads/hr.

b. Fraction of iodine contained in the first 0.409 in. of the test bed.

c. Fraction of iodine contained in the first 0.268 in. of the test bed.

d. Fraction of iodine contained in the first 0.548 in. of the test bed.

15th DOE NUCLEAR AIR CLEANING CONFERENCE

References

1. A. G. Evans and L. R. Jones, *Confinement of Airborne Radioactivity - Progress Report: January 1971 - June 1971*. USAEC Report DP-1280, E. I. du Pont de Nemours and Co., Savannah River Laboratory, Aiken, SC (1971).
2. A. G. Evans and L. R. Jones, *Confinement of Airborne Radioactivity - Progress Report: July 1971 - December 1971*. USAEC Report DP-1298, E. I. du Pont de Nemours and Co., Savannah River Laboratory, Aiken, SC (1972).
3. D. T. Pence, F. A. Duce, and W. J. Maeck, "A Study of the Adsorption Properties of Metal Zeolites for Airborne Iodine Species," *Proceedings of the Eleventh AEC Air Cleaning Conference*, Richland, Washington, August 31-September 3, 1970, p 581, USAEC Report CONF 700816, NTIS, Springfield, VA (1970).
4. D. T. Pence, F. A. Duce, and W. J. Maeck, "Developments in the Removal of Airborne Iodine Species with Metal-Substituted Zeolites," *Proceedings of the Twelfth AEC Air Cleaning Conference*, Oak Ridge, Tennessee, August 28-31, 1972, p 417, USAEC Report CONF 720823, NTIS, Springfield, VA (1973).
5. J. G. Wilhelm and H. Schuttelkopf, "Inorganic Absorber Materials for Trapping of Fission Product Iodine," *Proceedings of the Eleventh AEC Air Cleaning Conference*, Richland, Washington, August 31-September 3, 1970, p 568, USAEC Report CONF 700816, NTIS, Springfield, VA (1970).
6. J. G. Wilhelm and H. Schuttelkopf, "An Inorganic Absorber Material for Off-Gas Cleaning in Fuel Reprocessing Plants," *Proceedings of the Twelfth AEC Air Cleaning Conference*, Oak Ridge, Tennessee, August 28-31, 1972, p 540, USAEC Report CONF 720823, NTIS, Springfield, VA (1973).
7. T. R. Thomas, B. A. Staples, L. P. Murphy, and J. T. Nichols, *Airborne Elemental Iodine Loading Capacities of Metal Zeolites and a Method for Recycling Silver Zeolite*. USERDA Report ICP-1119, Allied Chemical Corporation, Idaho Chemical Programs Operations Office, Idaho Falls, ID (July 1977).

Appendix

Curve Fitting Method

Depth distribution curves for the AgX test series were obtained by assuming that the general equations for the normal distribution curve best fit the experimental data

$$y = Ae^{-\frac{1}{2}\left(\frac{x-B}{C}\right)^2}$$

where: y = normalized specific activity functions

x = depth in test bed, in.

A = constant representing maximum value of y

B = constant related to depth displacement in bed

C = constant related to spread in data

15th DOE NUCLEAR AIR CLEANING CONFERENCE

A computer code was written in which the observed values of \bar{x} (XOBS) and \bar{y} (YOBS) were used for each test. In the program, a value for \bar{A} , \bar{B} , and \bar{C} was assumed and a new value for \bar{Y} (YCALC) was calculated for each XOBS value. The function

$$\Delta^2 = \sum_{i=1}^8 (\text{YCALC}_i - \text{YOBS}_i)^2$$

was then evaluated. New values for B and C were then assumed and new \bar{y} values calculated to obtain a new Δ^2 value. The process was repeated until the minimum value for Δ^2 was obtained for a constant value of A. The calculations were then repeated assuming a new value for A and an array of values for B and C. The equations obtained for each test represent the best fit found when values of A were incremented at intervals of 0.001 units and values of B and C were incremented at intervals of 0.0005 units. The "best-fit" constants found in this manner are given in Table AI.

Table AI. "Best-Fit" Constants for Depth Distribution Curves.

<u>Test Duration, hr</u>	<u>Best Value Found For Constant</u>		
	<u>A</u>	<u>B</u>	<u>C</u>
1	1.850	0.0520	0.3970
5	2.200	-0.3030	0.6185
105	1.510	0.1260	0.4560

Integration of Curves

To obtain the area under each curve, it is necessary to evaluate the integral

$$dy = A \int_0^1 e^{-\frac{1}{2} \left(\frac{x-B}{C} \right)^2} dx = \int_0^1 f(x) dx$$

$$\text{Let } a = \frac{1}{2C^2} \quad \text{and} \quad w = x - B$$

then $dw = dx$

$$\text{and } \int_0^1 f(x) dx = A \int_{-B}^{1-B} e^{-aw^2} dw$$

$$\text{but } \int_0^Z e^{-aw^2} dw = \frac{\sqrt{\pi}}{2\sqrt{a}} \left[\text{erf}(Z\sqrt{a}) \right]$$

where $\text{erf}(Z\sqrt{a})$ = the error function of a number whose value is $(Z\sqrt{a})$

15th DOE NUCLEAR AIR CLEANING CONFERENCE

$$\text{therefore: } A \int_{-B}^{1-B} e^{-aw^2} dw = \frac{A\sqrt{\pi}}{2\sqrt{a}} \left\{ \text{erf} \left[(1-B)\sqrt{a} \right] + \text{erf} \left[B\sqrt{a} \right] \right\}$$

$$\text{substituting: } \int_0^1 f(x) dx = \frac{A\sqrt{\pi}}{2\sqrt{2C^2}} \left\{ \text{erf} \left[(1-B)\sqrt{\frac{1}{2C^2}} \right] + \text{erf} \left[B\sqrt{\frac{1}{2C^2}} \right] \right\}$$

$$\int_0^1 f(x) dx = AC\sqrt{\frac{\pi}{2}} \left[\text{erf} \left(\frac{1-B}{C\sqrt{2}} \right) + \text{erf} \left(\frac{B}{C\sqrt{2}} \right) \right] \quad (1)$$

Equation 1 is the form used to integrate the curves for the 1-hr and 105-hr tests since both equations have positive values for B (the apex of the curve occurs within the limits of $x = 0$ to $x = 1$). For the 5-hr test, as well as evaluation of sections of test beds between the limits of x and $x + \Delta x$, the equation

$$\int_x^{x+\Delta x} f(x) = AC\sqrt{\frac{\pi}{2}} \left[\text{erf} \left(\frac{x + \Delta x - B}{C\sqrt{2}} \right) - \text{erf} \left(\frac{x-B}{C\sqrt{2}} \right) \right] \quad (2)$$

was used.

For the 5-hr test, $x = 0$ and $\Delta x = 1.0$.

For the bed sectioning data, $x =$ front boundary of section (0.250 in.) and $\Delta x =$ depth of section (0.125 in.).

The calculated fraction of iodine in any bed segment (corrected for penetration) can be determined from the equation

$$\frac{\int_x^{x+\Delta x} f(x) dx}{\int_0^1 f(x) dx / (1 - \text{Penetration})} \quad (3)$$

Thus, to find the fraction of iodine in the last 1/8-in.-deep segment of the test bed from the 1-hr test, from Equation 2 and Table A-I

$$\begin{aligned} \int_{0.875}^{1.000} f(x) dx &= (1.850) (0.3970)\sqrt{\frac{\pi}{2}} \left[\text{erf} \left(\frac{1-0.0520}{0.3970\sqrt{2}} \right) - \text{erf} \left(\frac{0.875-0.0520}{0.3970\sqrt{2}} \right) \right] \\ &= 0.9205 \left[\text{erf}(1.6885) - \text{erf}(1.4659) \right] \\ &= 0.01954 \end{aligned}$$

15th DOE NUCLEAR AIR CLEANING CONFERENCE

From Equation 1,

$$\begin{aligned}\int_0^1 f(x) dx &= (1.850)(0.3970) \sqrt{\frac{\pi}{2}} \left[\operatorname{erf}\left(\frac{1-0.0520}{0.3970\sqrt{2}}\right) + \operatorname{erf}\left(\frac{0.0520}{0.3970\sqrt{2}}\right) \right] \\ &= 0.9205 \left[\operatorname{erf}(1.6885) + \operatorname{erf}(0.0926) \right] \\ &= 1.0008\end{aligned}$$

1-hr penetration = 0.10631%

$$\text{or } \frac{(0.01954)(1-0.00106)}{(1.0008)} = 0.01950 = 1.95\%$$

The complete list of calculated distribution values for all three tests is shown in Table IV.

DISCUSSION

WILHELM: Do you think that the low desorption rate will be valid on doses 10 to 100 times higher than you reached in your experiments?

EVANS: I have no reason to believe there would be higher desorption rates at higher dose rates.

DEITZ: A few observations have been made on the thermal stability of a sample of silver zeolite after exposure to methyl iodide-127 in the RDT M-16 configuration at 30°C. The sample which had retained all of the methyl iodide was subjected to programmed heating (2.7°C/min.) with continuation of the air flow. Emission of iodine started suddenly at 130°C and became catastrophic at about 350°C. These observations indicate that the retention of iodine in the zeolite cage may not be as tight as some would wish.

15th DOE NUCLEAR AIR CLEANING CONFERENCE

OPERATIONAL MAINTENANCE PROBLEMS WITH IODINE ADSORBERS IN NUCLEAR POWER PLANT SERVICE

C. E. Graves, J. R. Hunt, J. W. Jacox and J. L. Kovach
Nuclear Consulting Services, Inc.
Columbus Ohio

Abstract

The start-up and inservice testing of adsorber systems and components and their maintenance show several problems which can be prevented by change in design, installation and operation procedures.

Major problems relate to:

- a) Testability of systems and components to existing standards.
- b) The accidental initiation of fire control water sprays and their consequences.
- c) Severe corrosion developing in systems subjected to wetting or high moisture condition resulting in total mechanical failure of components.
- d) Adsorbent settling and degradation occurring in storage and use of the components.

Each of the problems and their occurrence and partial or total prevention techniques are discussed.

I. Introduction

This paper is based on actual field maintenance and testing in addition to data and observations gathered during routine design, manufacture and servicing of iodine adsorber systems and components used in nuclear power plant applications.

Discussed are the most commonly encountered problems in start-up (acceptance) testing, inservice (surveillance) testing and maintenance of iodine adsorbers as well as a number of surprising yet predictable and avoidable difficulties.

It is hoped that this paper will aid the manufacturer, service and test personnel and, most importantly, the final user in avoiding pitfalls where possible and initiating the most effective corrective action when necessary.

II. Testability of Systems and Components to Existing Standards

In recent years manufacturers have become increasingly aware of the necessity of designing not only functionally acceptable adsorber systems but systems which can be safely and easily tested without requiring massive redesign and backfitting after field installation.

Hopefully the era of systems with adsorber trays welded to the mounting frame with safe access requiring complete system disassembly is only a dim memory of a maturing industry's infancy.

As systems are designed and built to current standards (ANSI N509-76) and, therefor, testable to current standards (ANSI N510-75) many problem areas will be eliminated. But what about yesterday's systems and components which are to a

15th DOE NUCLEAR AIR CLEANING CONFERENCE

large extent today's problems?

Consider the following descriptions of equipment recently encountered in the field. A number of the problems discussed apply to system components or sections other than specifically the adsorber section itself.

1. "It leaks --- It doesn't leak". A system blower was found literally hanging from the ceiling, suspended by steel cables. It was a small (approx. 1000 cfm) HEPA - Adsorber - HEPA design.

The first problem encountered was accurate measurement of flow. The problem was not lack of a straight duct run as is often the case, but rather a puzzling oscillation of flow. This oscillation, coupled with another problem to be discussed later, created an interesting morning of testing.

The flow oscillations were quickly traced to the flexible blower - plenum connection. Since the blower was freely suspended it was free to swing. The period of blower swing matched and caused the flow oscillation.

When the system was halide leak tested a significant "leakage" was detected. A retest (without system modification) showed insignificant (i.e., within specification limits) leakage. Detailed investigation of the system and its relationship to its environment determined that the system was "breathing". The area in which it was installed was randomly changing from a positive to negative pressure relative to the system due to the opening and closing of a personnel access door in a near-by room. At some point during the halide injection of the first test the system "exhaled" (became positive with respect to the surrounding area) and halide was expelled into the general system area to be picked up downstream of the adsorber through inleakage through the sheet metal and showed up as bypass leakage.

Often systems are tested prior to full flow balancing of the entire plant ventilation systems.

Even if an initial complete flow balance is performed to ensure a system operates within its design specifications, changes in other systems during plant operation may effect the subject system so design specifications cannot be met without a plant wide rebalance.

2. Deep Bed Adsorbers. The use of deep bed (gasketless) adsorbers is becoming more common. They offer many advantages such as:

- A) Higher fission product removal efficiencies, particularly for organic forms.
- B) Ease of maintenance with less frequent adsorbent changeout and absence of gaskets as potential leak paths.
- C) Use of guard beds to prevent (or minimize) poisoning of the expensive impregnated main bed adsorbent.
- D) On-site refilling.
- E) Longer effective adsorbent life.

With these benefits there are also potential problems. Manufacturers must exercise extreme care in shop testing of these systems. If a leak is detected after field installation it is virtually impossible to pinpoint and repair. This is because the inlet and outlet flow paths are usually only a few inches wide and may be many feet deep. Such flow paths cause turbulence that makes scanning for leaks practically impossible and repair of a leak deep in the slot actually

15th DOE NUCLEAR AIR CLEANING CONFERENCE

impossible (without major structural disassembly usually requiring cutting). Guard beds are usually separated from the main bed by a single sheet of perforated metal which limits the ability to test or repair them individually and causes abrasion problems to be discussed later in this paper.

One recently tested system was found to have the perforated stainless steel screen installed with the rough side facing the adsorbent. Another was supplied by the manufacturer with a grain thief only 24" long. This did not reach past the blanked off top section which provides a carbon "head" so the carbon sampled was not exposed to system flow.

Many deep bed systems with guard beds have only 2" guard beds. Experience in testing the adsorbents from these systems shows that this is often insufficient to protect the main bed. One guard bed had such a high solvent loading that it was caked almost solid. An interesting point to be pondered and investigated is whether the presence of a guard bed creates a false sense of security in the minds of some users. Guard beds are designed to protect the main bed but will not mitigate the effects of painting or other sources of gross contamination in the area ventilated.

3. Zeolites.

Occasionally manufacturers will utilize conventionally designed adsorber units for zeolites. If the unit is sufficiently over designed to handle the increased weight of the zeolite the result can be satisfactory. Often the heavier zeolite causes problems of distortion, cell-frame interfacing and handling. Further the poor retention of halides by zeolites makes field leak testing very difficult. Currently R-112 (or R-112A) is the halide of choice since, of the halides approved for leak testing, it is retained the longest by zeolites. Unfortunately unless the zeolite is very dry and the air stream is low RH the retention is so short that a fully valid test is marginal. Designers and users of zeolite systems are cautioned about this problem. Additional study is required to determine the specific parameters of dryness of zeolite and RH of the airstream vs R-112 delay (retention) time on zeolites and investigation of other possible challenge agents.

4. Halide Background Interference During Halide Leak Testing.

High halide background concentrations due to use of degreasers, dye penetrants, propellents, refrigerants, etc., are a constant source of concern during testing.

Occasionally one can literally be sitting on the problem. One system tested was plagued by uncommonly high halide interference. Inspection and testing of the area ventilated by the system did not reveal any substantial source of halide. The source of the problem in this case was an air conditioner unit located in the same room as the system - a common practice with control room emergency systems. This particular system had a make-up air grill in the same room as the air conditioner. The test team used its halide sensor to locate the compressor leak (which plant personnel had been unable to locate for several years) and then successfully tested the system.

III. Accidental Initiations Of Water Sprays And Their Consequences

Accidental initiation of water spray systems designed to mitigate the consequences of adsorbent fire may be caused by (but not limited to) the following:

- A) Routine testing of electrical systems.

15th DOE NUCLEAR AIR CLEANING CONFERENCE

B) Inadvertent application of a heat source to system heat sensors during maintenance, repair or inspection.

C) Improper setting of thermo switches.

D) Flow failure with humidity control heaters energized.

E) High light levels in a unique system with photosensors for flame detection.

All these sources of accidental water spray initiation can be eliminated by proper initial design, attention to control sequence and interlocks and operating (maintenance) procedures.

Given the nightmare of an accidentally flooded deep bed (or any adsorbent) system, additional study and attention should be paid to non-water spray approaches, such as simply sealing the adsorber section off from air flow to extinguish by O₂ depletion and CO₂ creation or use of commercial halogenated hydrocarbon fire suppression systems. Both have shown excellent results in various industrial applications and appear to have significantly fewer drawbacks compared to water sprays.

IV. Corrosion Due To Wetting Of Adsorbers

Since almost all current adsorbents used for I131 control are impregnated with iodine any wetting causes immediate and severe corrosion problems. Everyone is aware of chloride corrosion and considerable effort is made to eliminate chloride contamination. All too few recognize that iodide corrosion is chemically similar and almost as bad as chloride. (Figure 1) Of course if there is no water there is no problem. In addition to the water spray problems just discussed the following are observed mechanisms whereby the adsorbent can (and has) been wetted.

A) Hydro testing of the system with adsorbers (and HEPAs) installed.

B) Unprotected fresh air intakes.

C) Area flooding.

D) Uninsulated duct runs resulting in condensation.

E) Poorly drained (or blocked) moisture separators.

F) Water leaks in cooling coils.

G) Improper adsorber storage.

H) Condensation from high RH in conjunction with cycling systems during testing.

The consequences of wetting of the impregnated adsorbent by any of these, or other, mechanisms is costly. (Figure 2) Examples are:

A) Impregnant leachout and spread of radioisotopes.

B) Loss of efficiency to control organic forms of I131.

C) Formation and spread of contaminated corrosion products.

D) Mechanical failure from corrosion. (Figure 3)

Since the majority of accidental adsorber wettings occur in systems not contaminated with significant radioactivity they can be spared irreparable damage and component and system failure can be avoided.

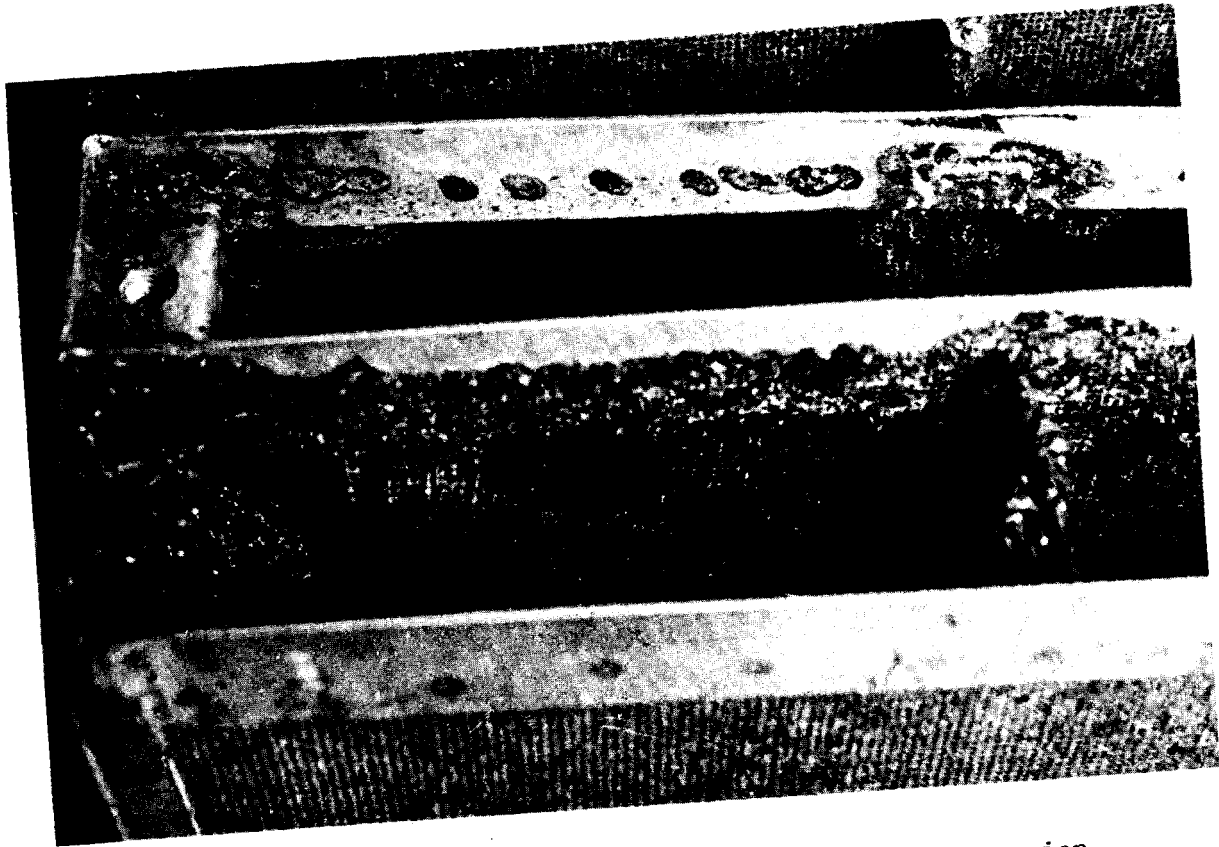


Figure 1 Tray type adsorber damaged by iodine corrosion.

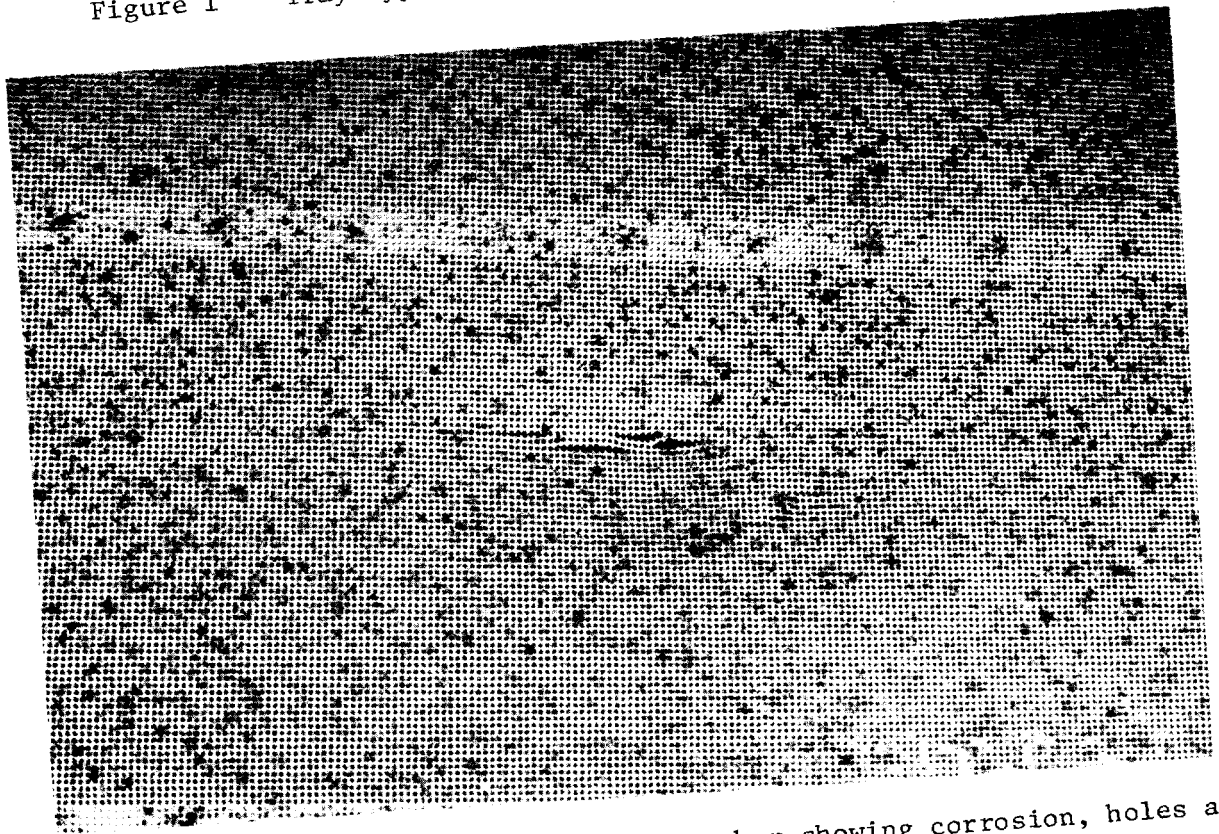


Figure 2 Perforated area of tray type adsorber showing corrosion, holes and a tear.

15th DOE NUCLEAR AIR CLEANING CONFERENCE

First the fact that the component or system has been wetted must be known. This requires a thorough understanding of each system in all modes. Detailed administrative procedures are required to ensure prompt reporting and action when wetting is suspected or confirmed.

The first step is of course to remove the wet cell or carbon. This removes the source of iodine from the system. The system must be carefully cleaned to remove any iodide contaminated material or water. This can be an extensive project in a deep bed or badly flooded tray type system. After gross clean-up of sludge and rinse with utility water, the wetted surfaces must be rinsed with deionized water treated with 0.1% sodium nitrite solution.

Badly corroded cells should be set aside for repair. Other cells should be rinsed in deionized water treated with sodium nitrite (0.1% solution). They should then be dried and passivated per ASTM A380 Table A2 Part II Code G. They may then be refilled for reuse.

V. Adsorbent Settling And Degradation

Experience has shown the principle causes of adsorbent settling and degradation to be:

- A) Improper filling (Figure 4 and Figure 5).
- B) Improper adsorber design.
- C) Improper adsorbent particle size.
- D) Improper pretreatment of air.
- E) Ventilation of poisoned atmosphere.

During on-site testing of an adsorber - HEPA system substantial bypass of the adsorber bank was detected (72%). Previous visual inspection had not revealed system deficiencies which would suggest leakage of such magnitude. Several adsorber units were removed at random and manually shaken. The adsorbent level was checked with a flashlight and found to be settled between 2 to 8 inches. Further investigation revealed that the cells had been refilled on-site.

They had not been vibrated during or after filling and had not been leak tested as individual cells. Current standards such as AACC CS-8T and ANSI N509-76 require cells be filled to maximum packing density and leak and pressure drop tested. While it is usually permissible to refill a single cell from which a sample has been taken if all proper procedures are followed by properly trained personnel, entire bank refilling by plant personnel will almost certainly result in unacceptable results, if inadequate filling equipment is used.

Many cell designs do not provide for adequate filling access. Ideally the entire filling surface should be open for proper filling. The smaller the fill opening the more difficult to obtain an acceptable fill.

While it should be an obvious requirement, some cells are still seen with mild steel components. Through bolts are the most common offender. It is not know if this is a design or material control problem.

As mentioned in the deep bed section of this paper there is a rough and smooth side on perforated metal. This is an inherent attribute of the material and its method of production. The smooth side should always be facing the carbon. The rough side will abrade the carbon to fines due to system vibration. This is

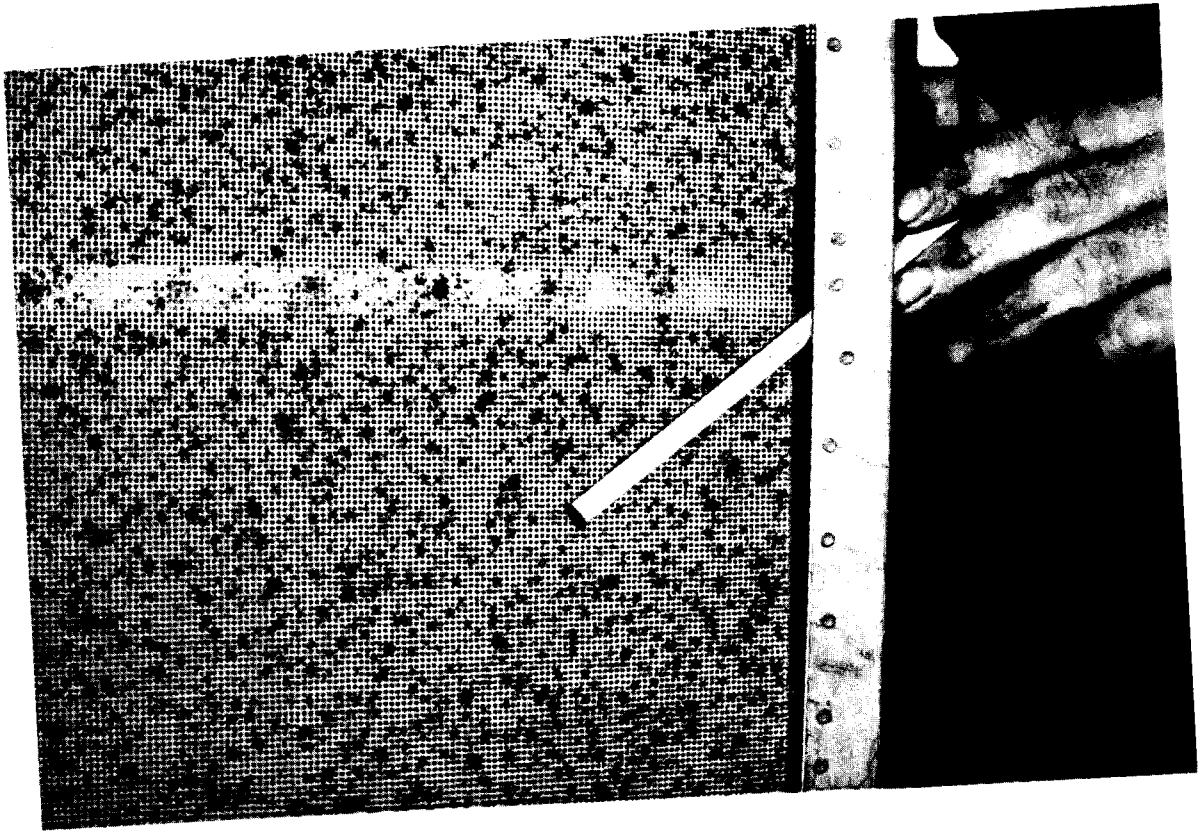


Figure 3 Mechanical failure of a tray type adsorber resulting from corrosion.

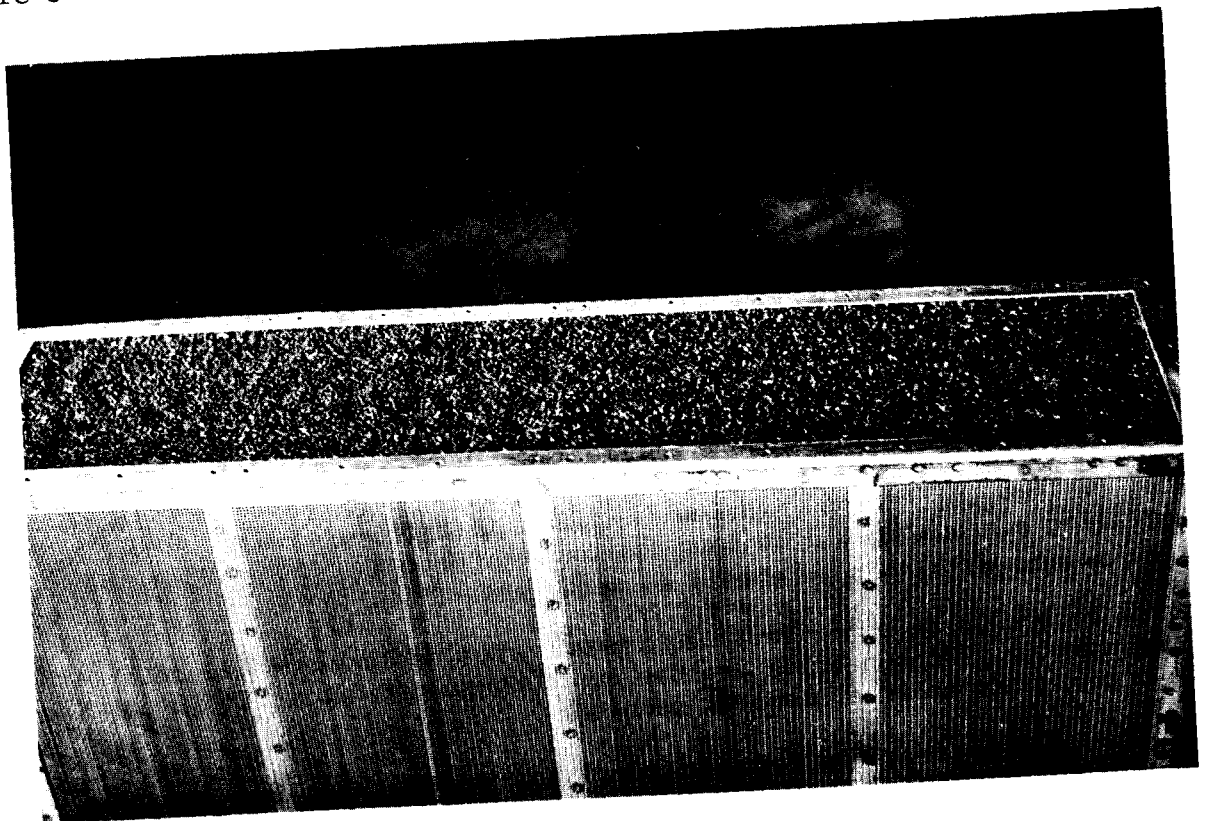


Figure 4 Stationary fill - tray type adsorber.

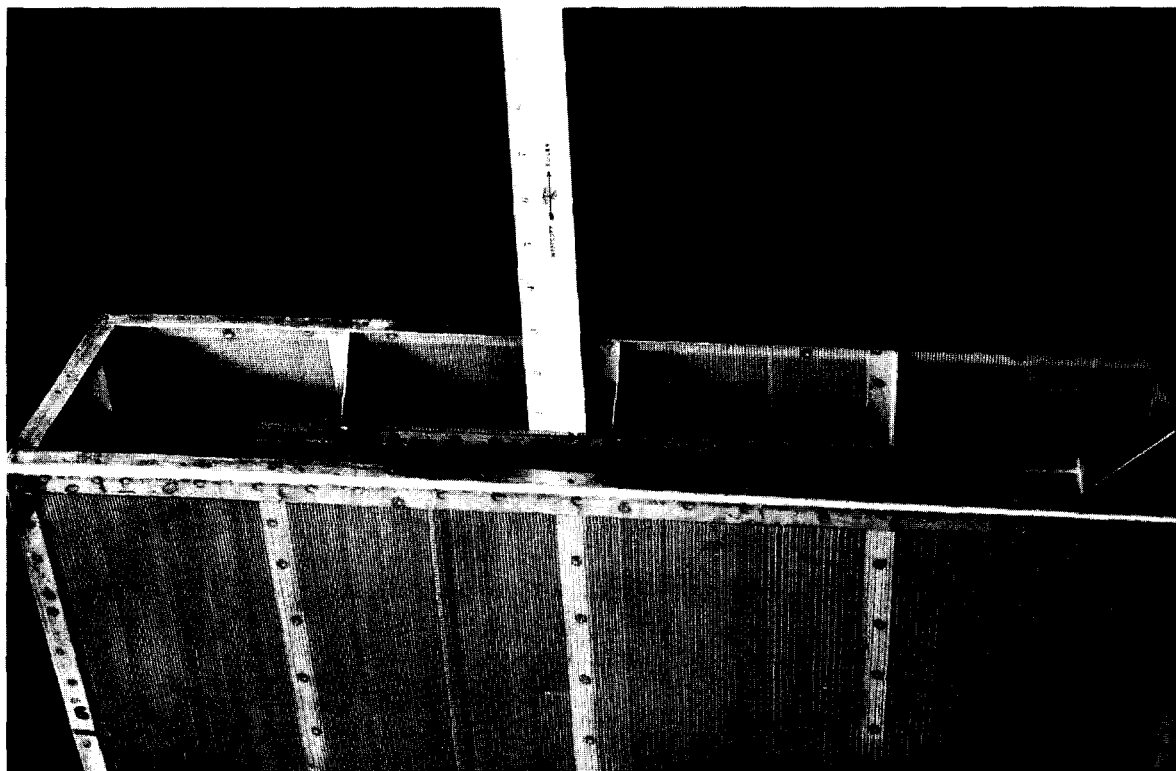


Figure 5 The same adsorber pictured in Figure 4 but after vibration to achieve maximum packing density.

15th DOE NUCLEAR AIR CLEANING CONFERENCE

particularly true if the packing is less than perfect. Experience has shown almost a random aspect perforated placement by some manufactures. In deep beds with guard beds there is an obvious problem if only a single sheet of material separates the two (2) beds.

Particular care must be taken in filling deep bed systems. With beds on the order of 6" deep and 10 ft high filling is extremely difficult. Filling must be performed with proper equipment and at the proper rate by trained personnel. Very large variations in packing density can and will occur if the carbon is simply dumped in from drums.

Although the point has been made many times by many people including papers at past Air Cleaning Conferences, there are still instances of large scale painting in areas ventilated by adsorbent systems with the system in operation.

Storage of adsorbent in bulk or in filled cells varies widely. There is general insufficient understanding of the requirements of clean heated (in cold climates) storage areas where there is minimum chemical contamination.

Two final points for consideration should be made. Some new plants still have either more than one size or simply nonstandard size adsorber cells which increase both cost and lead time on replacements. There is no technically valid reason for this design approach.

Another point is offered for consideration and possible study. Most plant Technical Specifications require filter system and adsorbent testing before refueling which certainly makes sense. The system may not be required to be retested until the next refueling cycle. Since refueling is usually the time for considerable maintenance it is also the time when there is a high probability of adsorbent contamination. We suggest that system testing after refueling is completed should be considered in addition to or instead of testing before refueling if the type of maintenance performed is conducive to organic contamination.

15th DOE NUCLEAR AIR CLEANING CONFERENCE

AECL IODINE SCRUBBING PROJECT

D.F. Torgerson and I.M. Smith
Atomic Energy of Canada Limited
Whiteshell Nuclear Research Establishment
Pinawa, Manitoba, R0E 1L0

Abstract

We describe a gas phase chemistry approach to organic iodide scrubbing which achieves large removal efficiencies for iodomethane and iodobenzene from air. Low energy electrons, ions, and reactive neutral species are generated using a corona discharge through which the gas flow is directed. Organic iodides are rapidly decomposed to form an inorganic, iodine-containing compound which precipitates from the flow. Electrons and negative ions appear to be the most effective scavengers for organic iodides since negative voltage discharges have the highest scrubbing efficiency. The iodine-containing precipitate is an amorphous iodine/oxygen compound which decomposes to form crystalline I_2O_5 on heating.

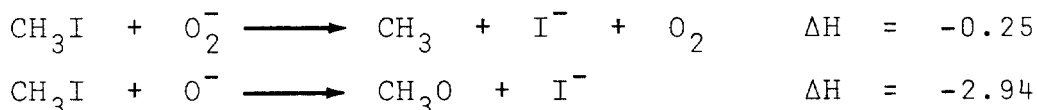
I. Introduction

In this paper, we discuss an approach to iodine scrubbing which uses gas phase chemistry to achieve large decontamination factors for iodomethane and iodobenzene. Airborne iodine can occur in a variety of chemical forms and the chemical distribution can be shifted by changes in conditions. Accordingly, we are interested in developing a procedure to scrub all possible species of iodine from air, including the highly penetrating organic forms. This paper summarizes some of the results to date.

II. Background

The basis for this work is the reaction of organic iodides with negative ions, electrons, and active neutral species. Iodomethane, for example, is an effective electron scavenger⁽¹⁾ and decomposes in the gas phase to form CH_3 and I^- . The cross-section for scavenging maximizes at an electron energy of 0.15 eV,⁽²⁾ and the reaction therefore requires low energy electrons.

The study of negative ion-molecule reactions is important in the fields of radiation chemistry, combustion, gas discharges, and atmospheric chemistry. Much valuable information has been obtained on negative ion-molecule reactions using the flowing afterglow technique⁽³⁾ and mass spectrometric methods.⁽⁴⁾ These studies have shown that ion-molecule reactions are orders of magnitude faster than gas phase reactions not involving ions. Reactions between iodomethane and negatively charged oxygen species are exothermic, as illustrated below for just two of several possible reactions:



15th DOE NUCLEAR AIR CLEANING CONFERENCE

Therefore, these reactions, along with direct electron capture, appeared to be reasonable bases for developing a CH_3I scrubbing procedure. Furthermore, since the organic moiety affects penetration of organic iodides through filter systems, decomposition to an inorganic iodine form seemed to have merit.

Although there are several conceivable ways to inject free electrons and negative ions into a gas stream, the simplest procedure is to use a low energy discharge. Corona discharges can be readily developed in air using a thin wire coaxially aligned with a hollow grounded cylinder. When negative high voltage is applied to the wire, the resulting discharge generates electrons having a broad energy spectrum as well as ionic species such as O^- and O_2^- .⁽⁵⁾ Therefore, by passing organic iodide-contaminated air streams through a corona discharge, it was hoped that sufficient reactive species would be present to effect efficient decomposition.

In addition to ions, discharges in air produce neutral reactive species such as O and O_3 . These can also contribute to organic iodide scavenging, but as noted earlier, neutral reactions are expected to be orders of magnitude slower than ionic reactions.

Finally, negative ions from nitrogen are unlikely to be formed in a corona discharge,⁽⁶⁾ and N_2 may simply act as an inert carrier gas.

III. Experimental Method

Testing of this concept was carried out using a corona discharge tube of 2.54 cm diameter and 63 cm long. The central electrode was a tungsten wire of 0.2 mm diameter operated at 6-10 kV depending on the discharge current desired between the electrode and the grounded cylinder wall. A 13 M Ω resistor was placed between the power supply and central electrode to act as a current limiter. Gas flow through the unit was controlled using rotameters and valves. Impurities were introduced into the air stream by diverting part of the flow through a vessel designed to saturate the gas with the appropriate species. The saturated gas was re-mixed with the main flow, and impurity levels could be changed by adjusting flow through the vessel. The reference flow for much of this work was 1000 cm^3/min containing 100 $\mu\text{g/g}$ iodomethane.

Chemical analyses of the gas stream were performed on-line using an Extranuclear quadrupole mass spectrometer. The mass spectrometer was controlled using a Tennecomp TP 5/11 analyser which was programmed to run the experiments automatically and to analyse data between runs. Since non-radioactive iodides were used, the decontamination factor was defined as (initial concentration)/(final concentration).

IV. Iodomethane Scrubbing

Effect of Discharge Current and Polarity

Figure 1 shows how the CH_3I decontamination factor changes with discharge current using both negative and positive electrode voltages.

15th DOE NUCLEAR AIR CLEANING CONFERENCE

Decontamination factors greater than 10^3 - 10^4 could not be measured owing to detection sensitivity limitations.

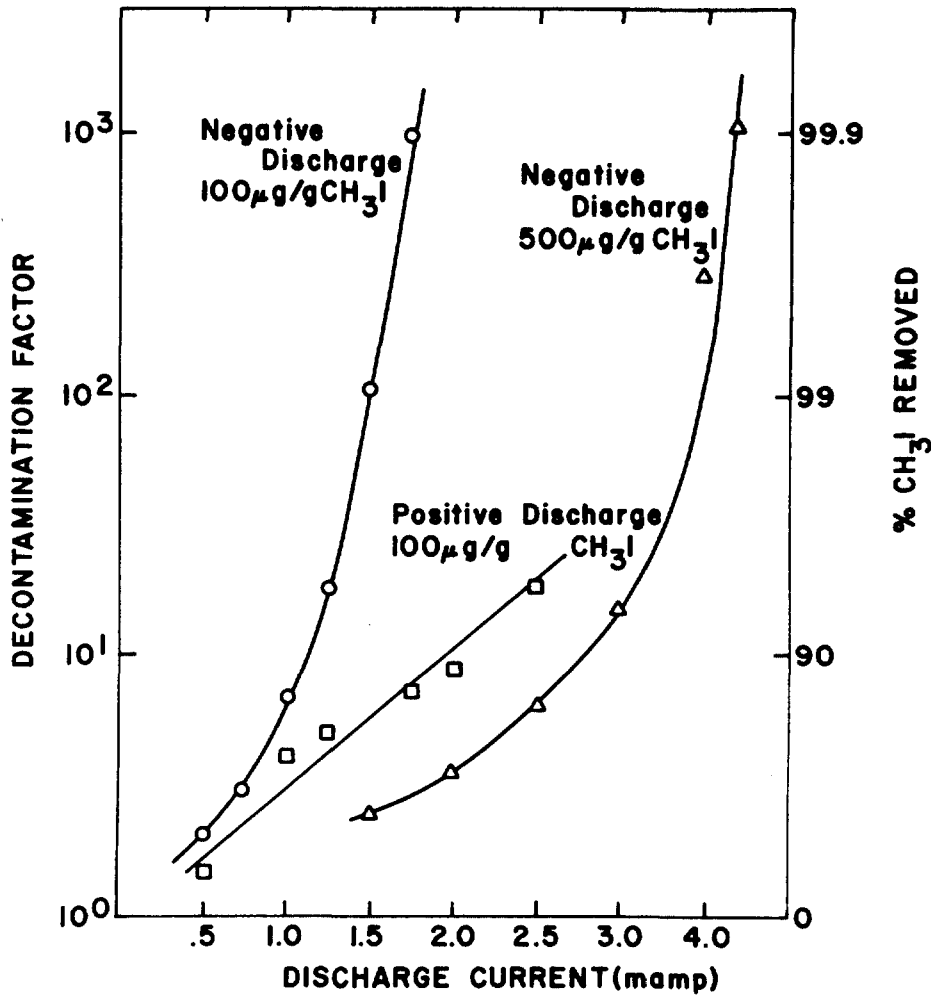


FIGURE 1
EFFECT OF DISCHARGE CURRENT ON CH₃I DF

The most striking feature of these curves is the rapid increase of DF with current when negative voltage is used. It is of interest, therefore, to consider the difference between positive and negative discharges.

Both negative and positive corona discharges produce a ~ 2 mm radius discharge region centered on the wire electrode. However, species produced outside this region are quite different for the two discharges. A positive discharge is developed when free electrons in the discharge region (always present owing to cosmic rays and background radiation) are accelerated towards the positively charged electrode, and produce more free electrons by ionization of neutral air molecules. Positive ions are repelled by the wire and migrate towards the cylinder wall. In contrast, negative discharges result from bombardment of the central electrode by positive ions, and free electrons are repelled towards the cylinder wall along with negatively-charged dissociated products. Since the mean electron energy

15th DOE NUCLEAR AIR CLEANING CONFERENCE

outside the discharge region is 1-2 eV for the experimental conditions used in this work, only electron capture processes are possible. It appears, therefore, that negative species (e^- , O_2^- , O^-) are somewhat superior to positive ions for CH_3I scavenging.

It is noted from Figure 1 that to attain the same DF for higher CH_3I loadings, a larger discharge current is required. This is an expected result and indicates that the current can be suitably adjusted for the DF desired over a range of CH_3I concentrations. Since the curves in Figure 1 for negative discharges are sharply rising at the detection limits, it is possible that very large decontamination factors can be achieved.

Effect of Oxygen Concentration

The role of oxygen in CH_3I decomposition can be further examined by varying the O_2 concentration. Table I compares decontamination factors for different gas compositions using a discharge current of 2.0 mA.

Table I. CH_3I removal as a function of oxygen concentration.

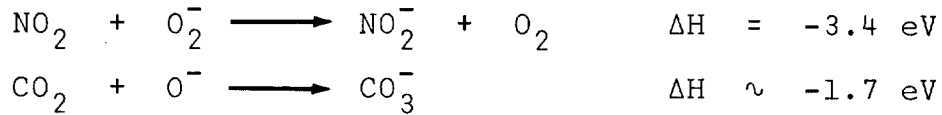
<u>Gas Composition</u>	<u>DF</u>	<u>% CH_3I Removal</u>
0 % O_2 /100 % N_2	2.5	60.5
2.6% O_2 / 97.4% N_2	682	99.85
5 % O_2 / 95 % N_2	5×10^3	99.98

In the absence of oxygen, free electrons account for virtually all negative current in the discharge tube. Thus, reaction with electrons is likely the dominant scrubbing mechanism. However, the presence of O_2 greatly enhances scrubbing efficiency. One possible explanation is that O^- and O_2^- are less mobile than electrons in the gas stream, thus increasing the probability of reactions with CH_3I . In addition, neutral reactive species are produced from O_2 which can contribute to CH_3I scrubbing for both positive and negative discharges.

Effect of Impurities

Impurities in the gas stream can have an effect on decontamination factors if the impurities compete for the active species. Some preliminary results indicate that water vapor does not affect the scrubbing process. At a flow of 500 cm^3/min , 100 $\mu g/g$ CH_3I loading, and 0.5 mA discharge current, the removal efficiencies are 97.9% in dry air and 97.6% in air containing 2.5% water vapor. This is an expected result since the reactions between H_2O and O^- or O_2^- are endothermic, and reactions with electrons have a threshold of ~ 3.8 eV. However, reactions of the type

15th DOE NUCLEAR AIR CLEANING CONFERENCE



suggest that nitrogen oxides and CO_2 may be poisoning agents in the discharge. Figure 2 shows the effect of these compounds on CH_3I removal efficiency.

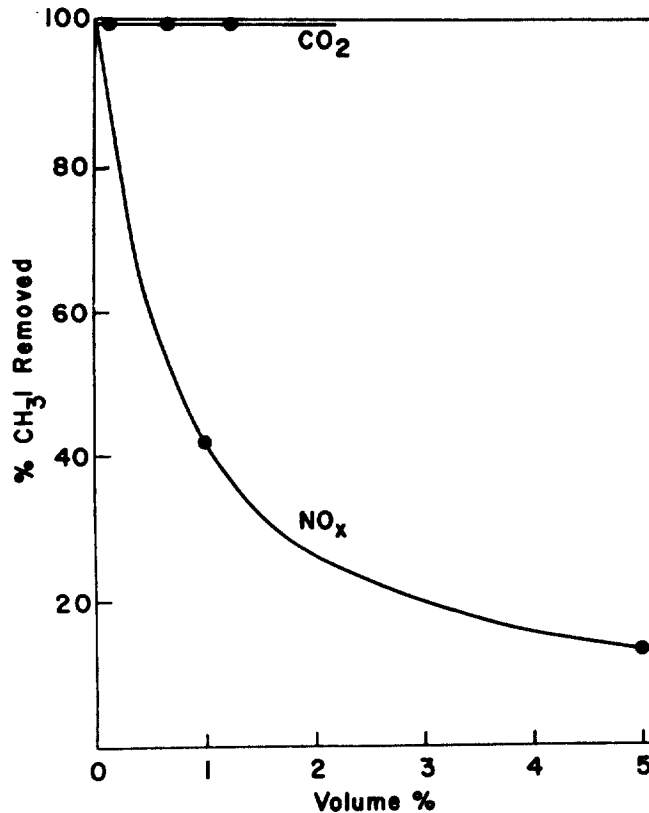
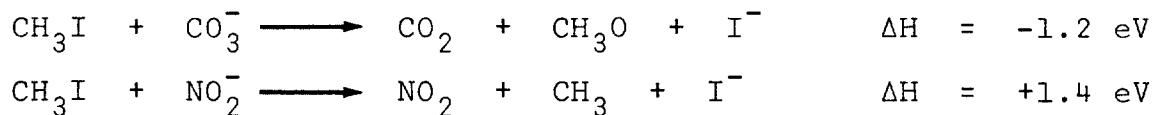


FIGURE 2
 CH_3I REMOVAL EFFICIENCY AS A FUNCTION OF CO_2 AND NO_x CONCENTRATION

As expected, nitrogen oxides significantly reduce the scrubbing efficiency, but CO_2 has no effect. The reason for this difference can be understood by considering the following reactions:



The fact that CO_3^- is not stable in the presence of CH_3I explains why CO_2 has no effect on the efficiency. On the other hand, reactions with NO_2^- are endothermic. Therefore, NO_2 effectively scavenges the negative charge and seriously interferes with the scrubbing process.

The NO_2^- ultimately transfers its electron to the walls of the discharge tube without initiating any further reactions.

Nature of the Iodine Precipitate

The iodine precipitate is a white hygroscopic solid which initially liberates I_2 when stored at room temperature. Samples of the fresh precipitate have been analysed by direct probe mass spectroscopy, X-ray diffraction, thermal gravimetric analysis, and differential thermal analysis. These studies show that the precipitate is an amorphous solid containing iodine and oxygen, with perhaps traces of organic contaminants. Typical DTA and TGA curves are shown in Figure 3.

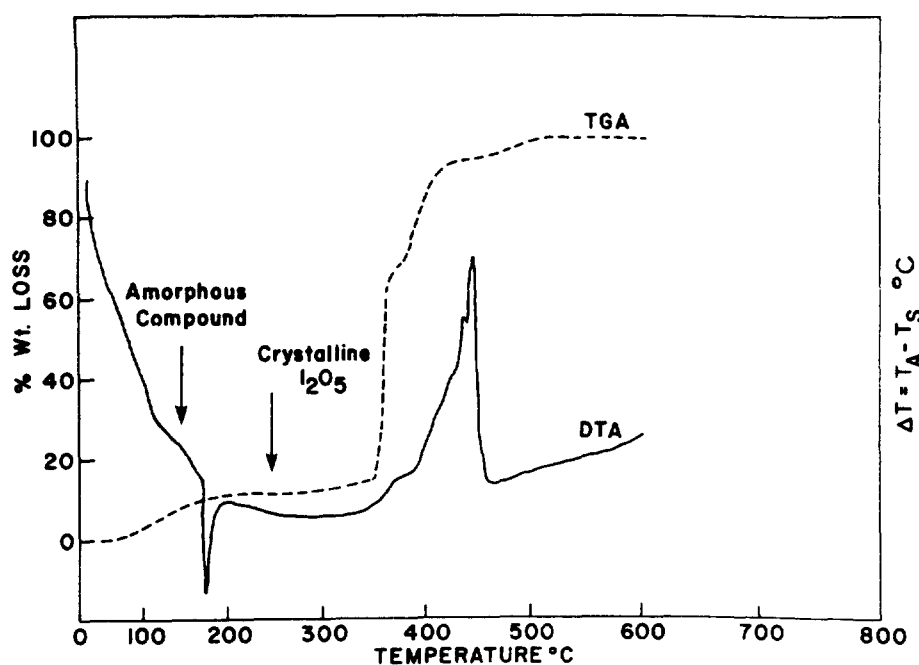
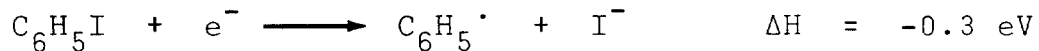


FIGURE 3
DTA (LEFT SCALE) AND TGA (RIGHT SCALE) CURVES
OBTAINED FOR THE IODINE PRECIPITATE

As shown by the TGA curve, the amorphous solid begins to decompose at $\sim 120^\circ\text{C}$ and loses $\sim 15\%$ of its weight. The DTA curve shows that this is an exothermic transition, leading to a crystalline product which has been identified as I_2O_5 by X-ray diffraction. At $\sim 350^\circ\text{C}$, the I_2O_5 begins to decompose to I_2 and O_2 in an endothermic reaction. This is the expected behaviour for I_2O_5 .⁽⁷⁾ Efforts to understand the chemical and physical properties of the amorphous solid are continuing.

V. Iodobenzene Scrubbing

Aromatic iodides have proven to be among the most difficult iodine species to remove from air using conventional filtering technology. However, enthalpies for the following reactions indicated that a gas phase chemistry approach might also be applicable to iodobenzene:



Again, this is by no means a complete list of possible reactions, and it is felt that iodobenzene could be removed at least as effectively as CH_3I .

Figure 4 shows a plot of DF versus discharge power for air containing $80 \mu\text{g/g}$ $\text{C}_6\text{H}_5\text{I}$. Although these results are preliminary, it is evident that $\text{C}_6\text{H}_5\text{I}$ removal is also feasible using a corona discharge.

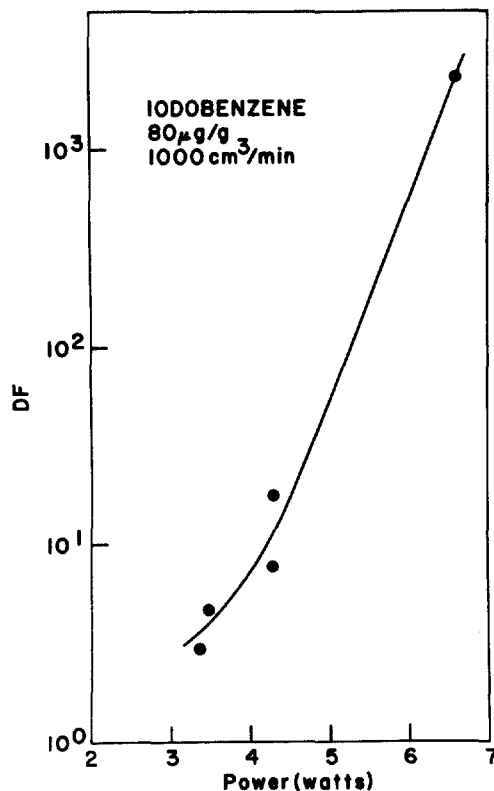


FIGURE 4
 $\text{C}_6\text{H}_5\text{I}$ DECONTAMINATION FACTOR AS A FUNCTION OF POWER
 FOR NEGATIVE DISCHARGE

VI. Conclusions

Gas phase chemistry is an appropriate mechanism for scrubbing organic iodides from air streams. Reaction enthalpies can be successfully used to predict the performance of the corona scrubber. Other iodine species (I_2 , HI, HOI) should also be amenable to removal by reactions similar to those discussed here. While much work remains to be done, we believe that gas phase scrubbing is a viable approach to airborne iodine control.

VII. Acknowledgements

We should like to thank A. Wikjord, L. Hachkowski, and P. Taylor for their dedication to the iodine precipitate characterization studies.

VIII. References

1. R.F. Claridge and J.E. Willard, "Production of trapped radicals from alkyl halides in organic glasses by dissociative electron attachment and by photo dissociation", J. Amer. Chem. Soc., 87, 4992 (1965).
2. J.A. Stockdale, F.J. Davis, R.N. Compton, and C.E. Klots, "Production of negative ions from CH_3X molecules by electron impact and by collisions with atoms in excited Rydberg states", J. Chem. Phys. 60, 11, 4279 (1974).
3. E.E. Ferguson, "Thermal-energy negative ion-molecule reactions", Acc. Chem. Res. 3, 402 (1970).
4. J.L. Franklyn and P.W. Harland, "Gaseous negative ions", Ann. Rev. Phys. Chem. 25, 485 (1974).
5. L.M. Chanin, A.V. Phelps, and M.A. Biondi, "Measurements of the attachment of low-energy electrons to oxygen molecules", Phys. Rev. 128, 219 (1962).
6. E.W. McDaniel, Collision Phenomena in Ionized Gases, Wiley & Sons, New York, 1964, pp. 373, 381.
7. F.A. Cotton and G. Wilkinson, Advanced Inorganic Chemistry, Interscience, New York, 1962, p. 445.

15th DOE NUCLEAR AIR CLEANING CONFERENCE

DISCUSSION

VAN BRUNT: Have you done any sizing of a packed electrochemical reactor for this system?

TORGERSON: We have not yet done any sizing studies. At this point, the research is exploratory in nature, and we have concentrated on demonstrating that the basic ideas work.

VAN BRUNT: Have you investigated any other anode or cathode materials?

TORGERSON: We have investigated many anode and cathode materials. The critical component is the central wire, and we have found that tungsten is the best choice in terms of chemical reactivity and mechanical strength.

DEMPSEY: Where do the gases go when they interact and precipitate? How might you collect and remove them in an engineered system?

TORGERSON: The iodine compound precipitates on the walls of the apparatus, and can be mechanically collected. It appears that the precipitate can collect on the walls indefinitely without affecting efficiency. Moreover, you can precipitate the compounds onto any removal surface you wish. If the outer electrode is a mesh, most of the product passes through and plates out on whatever you have behind the mesh. There are, therefore, many possible engineered removal systems. For example, if you did not want a solid, you could even collect the product in a thin film of solvent flowing down the outer wall. An interesting approach would be to engineer the device to be both the scrubber and the storage container, leaving the iodine in solid form.

15th DOE NUCLEAR AIR CLEANING CONFERENCE

DETERMINATION OF THE PHYSICO-CHEMICAL ^{131}I SPECIES IN THE EXHAUSTS AND STACK EFFLUENT OF A PWR POWER PLANT

H. Deuber, J.G. Wilhelm

Laboratorium für Aerosolphysik und Filtertechnik,
Kernforschungszentrum Karlsruhe GmbH,
Postfach 3640, D-7500 Karlsruhe 1, W. Germany

Abstract

To quantify the credit that can be granted in the assessment of the ^{131}I ingestion doses and the improvement that can be achieved in the ventilation systems if differences of the physico-chemical ^{131}I species with respect to the environmental impact are taken into account, the fractions of the ^{131}I species were determined in the stack effluent and in various exhausts of a 1300 MW_e PWR power plant during a period of 3 months. Based on these measurements, calculations for different cases of filtration of the main exhausts for iodine were carried out.

The average fractions of elemental and organic ^{131}I were about 70 and 30 % respectively in the stack effluent during the time indicated. Elem. ^{131}I originated mainly from the hoods in which samples of the primary coolant are taken and processed. Org. ^{131}I was mainly contributed by the equipment compartments. If the hood exhaust had been filtered, as was the case with the equipment compartment exhaust, the fractions of elem. and org. ^{131}I would have been on the order of 50 % each and the calculated ^{131}I ingestion doses would have been a factor of 3 lower.

I. Introduction

Of the radionuclides released from nuclear power plants ^{131}I is the decisive one with respect to the radiation exposure of the population in the vicinity.⁽¹⁾ The radiation exposure by radioiodine is caused primarily by ingestion via the pasture-cow-milk-pathway. It is therefore dependent on the fractions of the physico-chemical ^{131}I species which feature different deposition velocities for pastures. In the Federal Republic of Germany a fallout velocity ratio of 100 : 10 : 1 is used for elemental (I_2), particulate, and organic (CH_3I) ^{131}I , the main airborne species, in calculations pertaining to the assessment of the ingestion doses caused by the release of ^{131}I or of the ^{131}I release limits.⁽²⁾

An efficient improvement of the ventilation systems of nuclear power stations in terms of reduction of elem. ^{131}I release rates can be anticipated, if iodine ^{131}I filters are installed in the exhausts which constitute the main sources of elem. ^{131}I . To evaluate the range of an eventual improvement of the ventilation systems and the credit for differences of the ^{131}I species in the stack effluents with respect to the environmental impact, the fractions of the ^{131}I species have to be measured in the various exhausts within the nuclear power plants and in the stack effluents.

In the United States of America ^{131}I species measurements have been carried out in BWR power plants.⁽³⁾ In the Federal Republic of Germany ^{131}I species determinations over an extended period (12 and 6 months respectively) have been performed in the stack effluents of two modern PWR power plants of 1200 and 1300 MW_e respectively.^(4,5)

15th DOE NUCLEAR AIR CLEANING CONFERENCE

(The ^{131}I activities discharged per year via the stacks were in the order of 10 mCi each in the last years.) In one of the PWRs (PWR 2) the fraction of elem. ^{131}I was about 30 %, in the other PWR (PWR 3) it was about 60 %, the balance consisting nearly entirely of org. ^{131}I in both cases. The differences are difficult to account for, since the ventilation systems of the plants are similar in principle.

Besides the ^{131}I species measurements in the stack effluent, the ^{131}I species fractionation is now being determined in the main exhaust streams of PWR 3. The results obtained during the first 3 months of the comprehensive program are the basis of this paper.

II. Method of Measurements

The ^{131}I species measurements in the Federal Republic of Germany mentioned are performed with the radioiodine species sampler developed at the Karlsruhe Nuclear Research Center (KfK). (6) This sampler is suitable for the determination of part., elem. (I_2), and org. (CH_3I) radioiodine. It consists in principle of a stainless steel tube (5 cm inside diameter) in which particulate filters and beds of sorbents for the specific retention of the mentioned radioiodine species (from the air conducted through) are mounted (Fig. 1). Each sampler component (particulate filters, beds of sorbents) is twofold so that conclusions concerning the discrimination of the species can be drawn. (The employment of the second particulate filter, however, is usually dispensed with in routine work.) The volume of the beds is 75 or 150 cm^3 , the flow rate 3.6 or 7.2 m^3/h respectively, i.e. the residence time is kept at 0.075 s per bed. The sampling time is usually 1 week.

The retention of particles by the particulate filter GF/A is sufficiently high (a value of > 99.9 % has been measured under certain conditions), whereas the adsorption of I_2 and CH_3I is usually negligible.

The I_2 sorbent DSM 11 is obtained by impregnation (with a salt mixture) of a material consisting mainly of insoluble silicid acid with a certain pore structure. It exhibits a retention efficiency of > 99.9 % for I_2 and of < 0.5 % for CH_3I at a residence time of 0.1 s in the whole design parameter range (10 - 70°C, 20 - 80 % R.H.). (6) At the same residence time the removal efficiency of the KI impregnated carbon CG 0.8 for CH_3I is >> 99.9 % at 10 and 70°C in the case of 20 % R.H.; it is 89 and 96 % respectively at 10 and 70°C in the case of 80 % R.H. In the event of a high relative humidity a removal efficiency of > 99 % for CH_3I can be achieved by mounting additional beds of CG 0.8. Organic compounds of higher molecular weight, as for example $\text{C}_6\text{H}_5\text{I}$ (iodine benzene), are collected by CG 0.8 better than CH_3I .

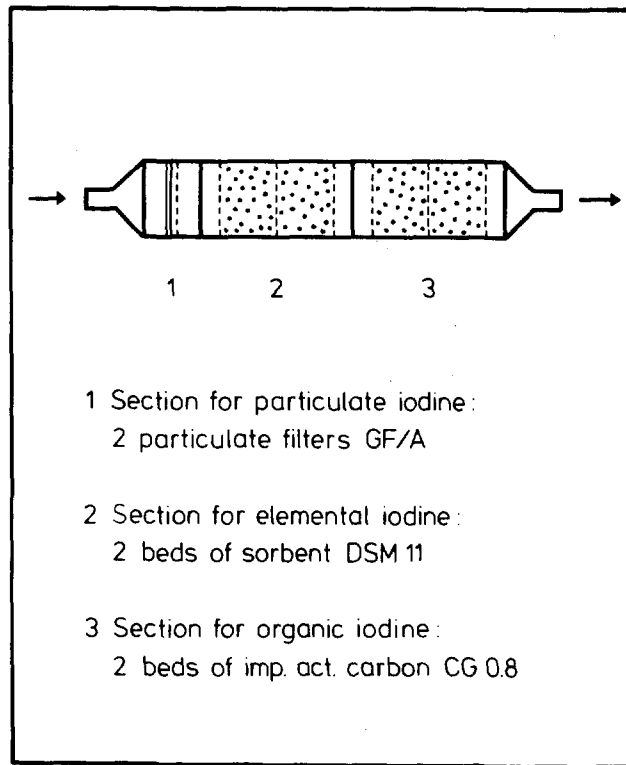
Counting of the ^{131}I activities of the sampler components is accomplished after demounting by Ge(Li) detectors. The detection limit as defined in this account (net counting rate equal to the standard deviation of the net counting rate) amounts to about 10^{-15} Ci $^{131}\text{I}/\text{m}^3$ at a sampling time of 1 week and a counting time of 1000 min. At a ^{131}I concentration of 10^{-13} Ci/ m^3 for example, it is possible to measure ^{131}I species whose fractions total 1 %.

In Figs. 2 and 3 the results of ^{131}I species measurements in exhausts containing high and low percentages of elem. ^{131}I respectively are demonstrated. In both cases the differentiation of elem. and org. ^{131}I was excellent.

The samplers used in the measurements shown in Figs. 2 and 3 feature a peculiarity: the employment of the sorbent IPH. This material is used in radioiodine species samplers for the specific retention of hypoiodous acid (HIO). (3, 8)

15th DOE NUCLEAR AIR CLEANING CONFERENCE

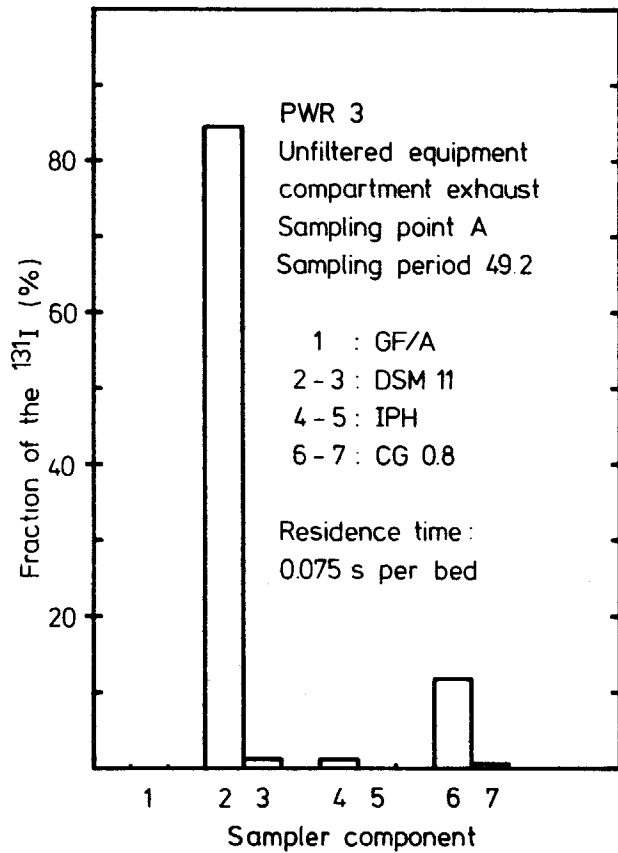
It has been employed in the KfK sampler on several occasions with results similar to those of Figs. 2 and 3, i.e. the percentages of ^{131}I on the IPH beds have been minimal. It is thus inferred that $\text{H}^{131}\text{I}\text{O}$ plays no significant part in the exhaust streams assayed here. No attempts are therefore made to detect $\text{H}^{131}\text{I}\text{O}$ in routine ^{131}I species measurements and the employment of IPH is dispensed with. If present, this species would be collected in the KfK sampler on CG 0.8, since the retention of $\text{H}^{131}\text{I}\text{O}$ by DSM 11 is negligible in a wide range of parameters. (7)



KfK
LAF II 10/88

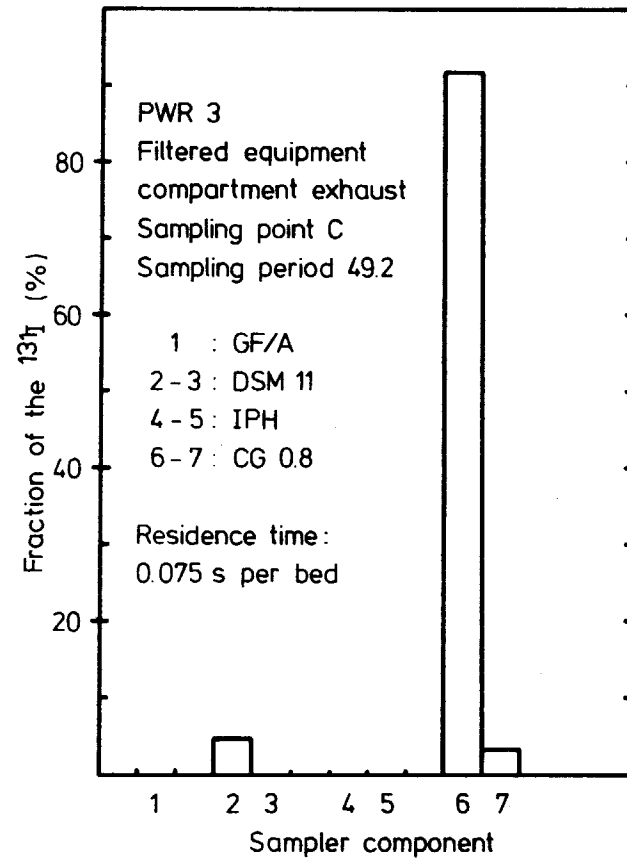
Radioiodine species sampler

Fig. 1



Distribution of the ^{131}I in the radioiodine
species sampler

Fig. 2



Distribution of the ^{131}I in the radioiodine
species sampler

Fig. 3

15th DOE NUCLEAR AIR CLEANING CONFERENCE

III. Essential Data of the Plant Studied (PWR 3)

The flow diagram, flow rates, and sampling points of the exhausts are given in Fig. 4 and Table I. The activity sources contributing to the stack effluent are located in the reactor building and auxiliary building. The turbine building, whose ventilation air contains practically no activities, is exhausted by roof vents.

The exhausts of the equipment and operating compartments of the reactor building are usually filtered - depending on the pressure in the equipment compartments - by 1 or 2 iodine filters (between sampling points A and B and C respectively). In special cases, for instance during refueling outages, two other iodine filters located in the operating compartments (near sampling point D) can be put in operation for filtration of the air of the equipment and operating compartments (containment purging). These filters can be operated in recirculation and exhaust air mode. (In Fig. 4 only the exhaust air mode has been taken into consideration.)

The annular compartment exhaust is normally filtered by particulate filters (near sampling point H). For accidents filtration of the annular compartment exhaust by an iodine filter is provided for, as shown in the diagram.

The auxiliary building exhausts are filtered by particulate filters (near sampling point H). The upper and lower parts of the equipment compartments of the auxiliary building are exhausted separately (sampling points G and H respectively).

With the sampling locations B, C, E, F, G, H, all the main exhaust streams are covered. Sampling point A has been included so as to enable the determination of the decontamination factors of the equipment compartment exhaust filters. At sampling point D special ^{131}I species investigations were provided for (not dealt with in this report).

The sample extraction at the various sampling points was carried out isokinetically except for the stack effluent sampling point. Here the samples had to be extracted nonisokinetically from a by-pass (inside diameter: 25 mm; length to the stack: 13 m; material: polyethylene). Conclusions on the reliability of the results of the measurements at the stack effluent sampling point prior to and during the time covered in this report can be drawn from a correlation of these results with those obtained at the other sampling locations.

During the time covered in this account, i.e. during the sampling periods 36 to 48, the plant operated nearly constantly at between 50 and 60 % of the rated power, short of the sampling periods 47 and 48. At the beginning of sampling period 47 the reactor was shut down for refueling and maintenance. At the commencement of sampling period 48 containment purging was started. 1 day before the end of this sampling period the reactor pressure vessel was opened for removal of the fuel elements.

15th DOE NUCLEAR AIR CLEANING CONFERENCE

Table I Flow rates and sampling points of the exhausts.

Exhaust	Flow rate (m ³ /h)	Sampling point
Equipment compartment exhaust ^a	1 200	A, B, C
Annular compartment exhaust ^b	61 500 ^f	E
Hood exhaust ^c	4 300	F
Auxiliary building exhaust ^d	41 000	G
Auxiliary building exhaust ^e	57 000	H
Stack effluent	165 000 ^f	I

^a Exhaust from the equipment and operating compartments of the reactor building.

^b Includes filtered air from the equipment and operating compartments of the reactor building, if the two iodine filters located in the operating compartments are operated in the exhaust air mode (containment purging).

^c Exhaust from the laboratory hoods and the primary coolant sampling hoods.

^d Exhaust from the upper parts of the equipment compartments of the auxiliary building, the staff rooms, and the laboratories.

^e Exhaust from the lower parts of the equipment compartments of the auxiliary building.

^f 74 500 and 178 000 m³/h respectively during sampling period 48 because of containment purging (refueling outage).

15th DOE NUCLEAR AIR CLEANING CONFERENCE

IV. Results of the ^{131}I Species Measurements and Calculations

The total ^{131}I concentrations, total ^{131}I release rates, and ^{131}I species fractions observed at the various sampling points during the sampling periods 36 to 48 are listed in Tables II to V. Table V includes the corresponding values for the stack effluent calculated from the results of the measurements in the various exhausts. Figs. 5 to 7 show the measured and calculated total ^{131}I concentrations and the elem. and org. ^{131}I species fractions for the individual sampling periods. The ^{131}I species contributions of the different exhausts to the stack effluent are presented in Tables VI to VIII and in Figs. 8 to 12.

The results reveal that during sampling period 48 a fundamental change occurred, attributable to the opening of the reactor pressure vessel and the containment purging. The total ^{131}I concentration of the annular compartment exhaust (which at sampling point E included filtered air from the equipment and operating compartments because of the containment purging) increased by more than 2 orders of magnitude. This resulted in a sharp increase of the ^{131}I species contribution of that exhaust and in a decrease of the ^{131}I contributions of the filtered equipment compartment and hood exhausts. The fraction of elem. ^{131}I in the stack effluent was smaller than 50 % in this sampling period, the first time during the sampling periods 36 to 48. This is in contrast with the findings for PWR 2, where the proportion of elem. ^{131}I increased to more than 90 % in the stack effluent when the reactor pressure vessel was opened. (4)

No increase of the total ^{131}I concentration in the equipment compartment exhaust occurred during sampling period 48, as would have been anticipated. Nor did a significant increase occur during the following sampling period. The proportion of elem. ^{131}I increased sharply, however, as can be seen in Fig. 2.

The average values of the results of the ^{131}I species measurements and calculations for the sampling periods 36 to 48 are given in Table IX and in Figs. 13 and 14. The averages of the measured fractions of elem. and org. ^{131}I in the stack effluent were about 68 and 31 % respectively. They agree to a high extent with those of the calculated fractions (69 and 29 % respectively). It is therefore inferred that the averages of the ^{131}I species fractions observed previously in the stack effluent of PWR 3 (60 and 39 % respectively) are reliable.

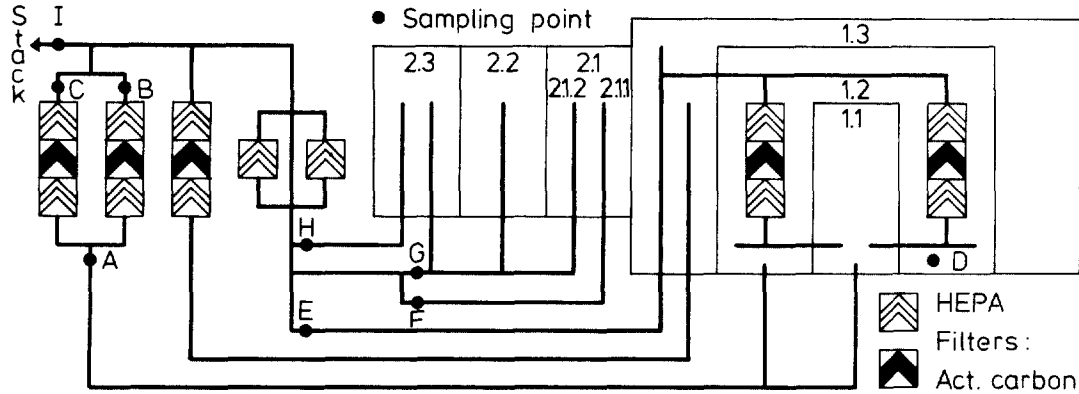
As for the averages of the measured and calculated total ^{131}I concentrations and release rates of the stack effluent, there is agreement within the standard deviations.

The main results concerning the contributions to the stack effluent are as follows:

- (a) The contribution of the filtered equipment compartment exhaust was of all the exhausts the smallest for elem. ^{131}I (nearly 0 %) and the largest for org. ^{131}I (36 %). The total ^{131}I contribution was 11 %.
- (b) In the case of the annular compartment exhaust all the individual contributions to the stack effluent were smaller than 10 %.
- (c) The hood exhaust was the main contributor with respect to elem. ^{131}I (68 %) and total ^{131}I (55 %). It accounted for 21 % of the org. ^{131}I .
- (d) All the individual contributions of the two auxiliary building exhausts were smaller than 25 %.

15th DOE NUCLEAR AIR CLEANING CONFERENCE

The dominant source of total ^{131}I was the equipment compartment exhaust. By filtration it was reduced by a factor of about 6 (Table IX). From Table X and Fig. 15 it can be seen that filter 1 (between sampling points A and B) was much less efficient for elem. and org. ^{131}I than filter 2 (between sampling points A and C). However the ratio of the average decontamination factors for elem. and org. ^{131}I was larger with filter 1 than with filter 2 (94 and 46 respectively). This means that the removal efficiency of filter 1 for elem. ^{131}I had decreased less than that for org. ^{131}I .



- | | |
|----------------------------|---|
| Reactor building : | Auxiliary building : |
| 1.1 Equipment compartments | 2.1 Laboratories (2.1.1 Hoods, 2.1.2 Rooms) |
| 1.2 Operating compartments | 2.2 Staff rooms |
| 1.3 Annular compartment | 2.3 Equipment compartments |



Simplified exhaust flow diagram of PWR 3

Fig. 4

15th DOE NUCLEAR AIR CLEANING CONFERENCE

Table II Results of the ^{131}I species measurements in the equipment compartment exhaust.

Sampling period	Total ^{131}I concentration ^a (Ci/m ³)	Total ^{131}I release rate (Ci/s)	Fraction of the ^{131}I species ^b (%)			Detection limit ^c (%)
			Part. ^{131}I	Elem. ^{131}I	Org. ^{131}I	
Unfiltered equipment compartment exhaust (sampling point A)						
36	1.1 (-10)	3.7 (-11)	< 1	9	91	< 1
37	1.2 (-10)	4.0 (-11)	< 1	6	94	< 1
38	4.1 (-11)	1.4 (-11)	-	10	90	< 1
39	3.8 (-11)	1.3 (-11)	-	9	91	< 1
40	5.4 (-11)	1.8 (-11)	-	7	93	< 1
41	4.0 (-11)	1.4 (-11)	< 1	8	92	< 1
42	2.7 (-11)	8.9 (-11)	< 1	9	90	< 1
43	2.3 (-11)	7.8 (-11)	-	7	93	< 1
44	6.3 (-11)	2.1 (-11)	-	6	94	< 1
45	3.7 (-11)	1.2 (-11)	< 1	22	78	< 1
46	6.0 (-11)	2.0 (-11)	< 1	23	77	< 1
47	1.5 (-10)	5.1 (-11)	< 1	31	69	< 1
48	1.3 (-10)	4.4 (-11)	< 1	30	70	< 1
Filtered equipment compartment exhaust (s. periods 36-41: s.point B; s. periods 42-48: s.point C)						
36	2.8 (-11)	9.3 (-12)	< 1	< 1	99	< 1
37	4.8 (-11)	1.6 (-11)	-	< 1	100	< 1
38	1.3 (-11)	4.2 (-12)	-	< 1	100	< 1
39	1.1 (-11)	3.6 (-12)	-	< 1	100	< 1
40	1.7 (-11)	5.6 (-12)	-	< 1	100	< 1
41	1.2 (-11)	3.9 (-12)	< 1	< 1	99	< 1
42	1.1 (-12)	3.5 (-13)	1	3	96	< 1
43	5.9 (-13)	2.0 (-13)	-	1	99	< 1
44	2.2 (-12)	7.5 (-13)	-	< 1	100	< 1
45	1.4 (-12)	4.8 (-13)	-	1	99	< 1
46	2.4 (-12)	7.8 (-13)	-	< 1	100	< 1
47	1.2 (-11)	4.0 (-12)	-	-	100	< 1
48	7.4 (-12)	2.5 (-12)	-	< 1	100	< 1

^a Powers of 10 represented by the exponents in parentheses.

^b Fractions smaller than the detection limits represented by dashes.

^c Detection limit of the ^{131}I species, related to total ^{131}I .

15th DOE NUCLEAR AIR CLEANING CONFERENCE

Table III Results of the ^{131}I species measurements in the annular compartment and hood exhausts.

Sampling period	Total ^{131}I concentration (Ci/m ³)	Total ^{131}I release rate (Ci/s)	Fraction of the ^{131}I species (%)			Detection limit (%)
			Part. ^{131}I	Elem. ^{131}I	Org. ^{131}I	
Annular compartment exhaust (sampling point E)						
36	3.7 (-14)	6.3 (-13)	-	39	61	3
37	9.4 (-15)	1.6 (-13)	-	44	56	12
38	1.5 (-14)	2.6 (-13)	-	38	62	7
39	1.0 (-14)	1.7 (-13)	-	36	64	11
40	3.8 (-15)	6.6 (-14)	-	-	100	29
41	1.4 (-13)	2.4 (-12)	6	34	60	< 1
42	1.6 (-14)	2.7 (-13)	-	36	64	7
43 ^a						
44	1.4 (-14)	2.4 (-13)	-	11	89	8
45	9.0 (-15)	1.5 (-13)	-	25	75	12
46 ^a						
47	3.6 (-15)	6.1 (-14)	-	100	-	32
48	1.2 (-12)	2.5 (-11)	-	49	51	< 1
Hood exhaust (sampling point F)						
36	7.1 (-11)	8.5 (-11)	< 1	88	11	< 1
37	1.0 (-11)	1.3 (-11)	< 1	86	14	< 1
38	1.6 (-11)	2.0 (-11)	2	92	6	< 1
39	7.6 (-12)	9.1 (-12)	1	87	12	< 1
40	1.3 (-11)	1.5 (-11)	1	86	13	< 1
41	1.3 (-11)	1.6 (-11)	2	93	5	< 1
42	3.7 (-12)	4.5 (-12)	2	89	8	< 1
43	9.2 (-12)	1.1 (-11)	2	93	5	< 1
44	1.4 (-11)	1.7 (-11)	2	94	4	< 1
45	6.6 (-12)	7.9 (-12)	2	91	7	< 1
46	5.1 (-12)	6.1 (-12)	4	88	8	< 1
47	1.2 (-11)	1.5 (-11)	2	79	19	< 1
48	7.1 (-12)	8.4 (-12)	3	60	37	< 1

^a No ^{131}I detected; total ^{131}I concentration corresponding to the detection limit and average of the ^{131}I species fractions of the preceding and subsequent sampling period used.

15th DOE NUCLEAR AIR CLEANING CONFERENCE

Table IV Results of the ^{131}I species measurements in the auxiliary building exhausts.

Sampling period	Total ^{131}I concentration (Ci/m ³)	Total ^{131}I release rate (Ci/s)	Fraction of the ^{131}I species (%)			Detection limit (%)
			Part. ^{131}I	Elem. ^{131}I	Org. ^{131}I	
Auxiliary building exhaust (sampling point G)						
36	2.8 (-12)	3.2 (-11)	-	71	29	< 1
37	1.4 (-12)	1.7 (-12)	-	63	37	< 1
38	3.6 (-13)	4.2 (-12)	-	94	6	< 1
39	3.5 (-13)	4.0 (-12)	2	73	25	< 1
40	7.5 (-13)	8.5 (-12)	2	68	30	< 1
41	6.9 (-13)	7.9 (-12)	4	65	31	< 1
42	2.8 (-13)	3.2 (-12)	5	77	18	< 1
43	4.1 (-13)	4.7 (-12)	4	84	12	< 1
44	1.2 (-13)	1.4 (-12)	-	65	35	2
45	1.0 (-13)	1.2 (-12)	-	65	35	2
46	1.3 (-13)	1.5 (-12)	-	58	42	2
47	9.4 (-13)	1.1 (-11)	2	93	4	< 1
48	9.2 (-13)	1.1 (-11)	-	32	68	< 1
Auxiliary building exhaust (sampling point H)						
36	1.0 (-13)	1.6 (-12)	-	9	91	2
37	1.3 (-13)	2.1 (-12)	2	15	83	2
38	1.1 (-13)	1.8 (-12)	-	-	100	2
39	2.8 (-14)	4.5 (-13)	-	57	43	8
40	3.7 (-14)	5.8 (-13)	13	16	71	6
41	1.5 (-13)	2.4 (-12)	9	28	63	1
42	6.1 (-14)	9.7 (-13)	-	45	55	4
43 ^a	3.7 (-14)	5.8 (-13)	32	31	37	6
44	1.5 (-14)	2.5 (-13)	-	-	100	14
45	7.1 (-14)	1.1 (-12)	-	22	78	3
46	6.6 (-14)	1.0 (-12)	-	25	75	3
47	1.2 (-13)	1.8 (-12)	-	18	82	2
48	3.2 (-13)	5.0 (-12)	-	55	45	< 1

^a Values questionable because of short counting time for part. ^{131}I .

15th DOE NUCLEAR AIR CLEANING CONFERENCE

Table V Results of the ¹³¹I species measurements and calculations for the stack effluent.

Sampling period	Total ¹³¹ I concentration (Ci/m ³)	Total ¹³¹ I release rate (Ci/s)	Fraction of the ¹³¹ I species (%)			Detection limit (%)
			Part. ¹³¹ I	Elem. ¹³¹ I	Org. ¹³¹ I	
Values measured (sampling point I)						
36	4.9 (-12)	2.3 (-10)	< 1	76	23	< 1
37	1.4 (-12)	6.6 (-11)	< 1	63	36	< 1
38	7.5 (-13)	3.4 (-11)	1	64	35	< 1
39	5.7 (-13)	2.6 (-11)	1	73	26	< 1
40	9.4 (-13)	4.3 (-11)	< 1	74	25	< 1
41	9.0 (-13)	4.1 (-11)	1	75	24	< 1
42	2.9 (-13)	1.3 (-11)	3	70	27	< 1
43	2.1 (-13)	9.5 (-12)	-	82	18	< 1
44	4.3 (-13)	2.0 (-11)	2	77	21	< 1
45	2.5 (-13)	1.1 (-11)	-	71	29	< 1
46	2.5 (-13)	1.2 (-11)	-	51	49	< 1
47	1.1 (-12)	4.8 (-11)	-	66	34	< 1
48	1.3 (-12)	6.3 (-11)	< 1	41	59	< 1
Values calculated from the results of the measurements at the sampling points B, C, E, F, G, H						
36	2.8 (-12)	1.3 (-10)	< 1	76	23	-
37	1.0 (-12)	4.7 (-11)	< 1	45	54	-
38	6.5 (-13)	3.0 (-11)	1	74	25	-
39	3.8 (-13)	1.7 (-11)	< 1	65	35	-
40	6.5 (-13)	3.0 (-11)	1	63	36	-
41	7.1 (-13)	3.3 (-11)	3	66	31	-
42	2.0 (-13)	9.3 (-12)	3	76	22	-
43	3.6 (-13)	1.7 (-11)	4	87	9	-
44	4.3 (-13)	2.0 (-11)	2	86	12	-
45	2.4 (-13)	1.1 (-11)	2	76	22	-
46	2.1 (-13)	9.5 (-12)	3	69	29	-
47	6.8 (-13)	3.1 (-11)	2	71	28	-
48	1.1 (-12)	5.2 (-11)	< 1	46	54	-

15th DOE NUCLEAR AIR CLEANING CONFERENCE

Table VI Contributions of the filtered equipment compartment exhaust to the stack effluent with respect to the ^{131}I species (s. periods 36-41: s. point B; s. periods 42-48: s. point C).

Sampling period	^{131}I species contribution (%)		
	Elem. ^{131}I	Org. ^{131}I	Total ^{131}I
36	< 1	31	7
37	< 1	62	34
38	< 1	56	14
39	< 1	60	21
40	< 1	52	19
41	< 1	38	12
42	< 1	17	4
43	< 1	13	1
44	< 1	32	4
45	< 1	20	4
46	< 1	29	8
47	< 1	46	13
48	< 1	9	5

15th DOE NUCLEAR AIR CLEANING CONFERENCE

Table VII Contributions of the annular compartment and hood exhausts to the stack effluent with respect to the ^{131}I species.

Sampling period	^{131}I species contribution (%)		
	Elem. ^{131}I	Org. ^{131}I	Total ^{131}I
Annular compartment exhaust (sampling point E)			
36	< 1	1	< 1
37	< 1	< 1	< 1
38	< 1	2	< 1
39	< 1	2	1
40	< 1	< 1	< 1
41	4	14	7
42	2	9	3
43	< 1	< 1	< 1
44	< 1	9	1
45	< 1	5	1
46	< 1	< 1	< 1
47	< 1	< 1	< 1
48	53	46	49
Hood exhaust (sampling point F)			
36	76	32	66
37	50	7	27
38	82	15	65
39	71	19	53
40	69	19	51
41	69	9	49
42	57	19	48
43	71	36	67
44	95	28	87
45	87	23	73
46	82	19	65
47	53	32	47
48	21	11	16

15th DOE NUCLEAR AIR CLEANING CONFERENCE

Table VIII Contributions of the auxiliary building exhausts to the stack effluent with respect to the ^{131}I species.

Sampling period	^{131}I species contribution (%)		
	Elem. ^{131}I	Org. ^{131}I	Total ^{131}I
Auxiliary building exhaust (sampling point G)			
36	23	31	25
37	48	24	35
38	18	3	14
39	26	17	23
40	31	24	29
41	24	24	24
42	35	29	35
43	28	37	29
44	5	20	7
45	10	17	11
46	13	24	16
47	46	5	34
48	14	26	20
Auxiliary building exhaust (sampling point H)			
36	< 1	5	1
37	2	7	4
38	< 1	23	6
39	2	3	3
40	< 1	4	2
41	3	15	7
42	6	27	11
43	1	14	4
44	< 1	11	1
45	3	36	10
46	4	29	11
47	2	17	6
48	12	8	10

Table IX Average values of the results of the ^{131}I species measurements and calculations for the various exhausts and the stack effluent.^a Sampling periods 36-48.

Exhaust	Total ^{131}I concentration (Ci/m ³)	Total ^{131}I release rate (Ci/s)	Fraction of the ^{131}I species (%) ^b		^{131}I species contribution to the stack effluent (%) ^b		
			Elem. ^{131}I	Org. ^{131}I	Elem. ^{131}I	Org. ^{131}I	Total ^{131}I
Unfilt.eq.comp.(A)	6.9 ± 1.2(-11)	2.3 ± 0.4(-11)	13.6 ± 2.6	86.4 ± 2.6	-	-	-
Filt.eq.comp.(B,C)	1.2 ± 0.4(-11)	4.0 ± 1.2(-12)	0.5 ± 0.2	99.3 ± 0.3	0.0 ± 0.0	35.6±5.1	11.2±2.5
Annular comp. (E)	1.1 ± 0.9(-13)	2.3 ± 1.9(-12)	38.3 ± 6.8	61.4 ± 6.8	4.7 ± 4.0	7.0±3.5	5.0±8.7
Hood (F)	1.5 ± 0.5(-11)	1.7 ± 0.6(-11)	86.6 ± 2.5	11.6 ± 2.4	67.9 ± 5.3	20.5±2.6	54.8±5.2
Aux.building (G)	7.2 ± 2.0(-13)	8.2 ± 2.3(-12)	69.8 ± 4.5	28.7 ± 4.7	24.6 ± 3.6	21.6±2.6	23.2±2.6
Aux.building (H)	9.6 ± 2.2(-14)	1.5 ± 0.3(-12)	24.8 ± 5.2	70.9 ± 5.9	2.7 ± 0.9	15.2±2.9	5.8±1.0
Stack (I)	1.0 ± 0.3(-12)	4.7 ± 1.6(-11)	67.8 ± 3.1	31.3 ± 3.2	-	-	-
Stack ^c	7.2 ± 1.9(-13)	3.3 ± 0.9(-11)	69.2 ± 3.6	29.2 ± 3.7	-	-	-

^a Uncertainties expressed as standard deviations.

^b Calculated as averages of the values of the various sampling periods; slightly different average values result from the average ^{131}I species release rates.

^c Calculated from the results of the measurements at the sampling points B, C, E, F, G, H.

15th DOE NUCLEAR AIR CLEANING CONFERENCE

Table X Decontamination factors of the equipment compartment exhaust filters ^a.
 Filter 1: s. points A and B; Filter 2: s. points A and C.

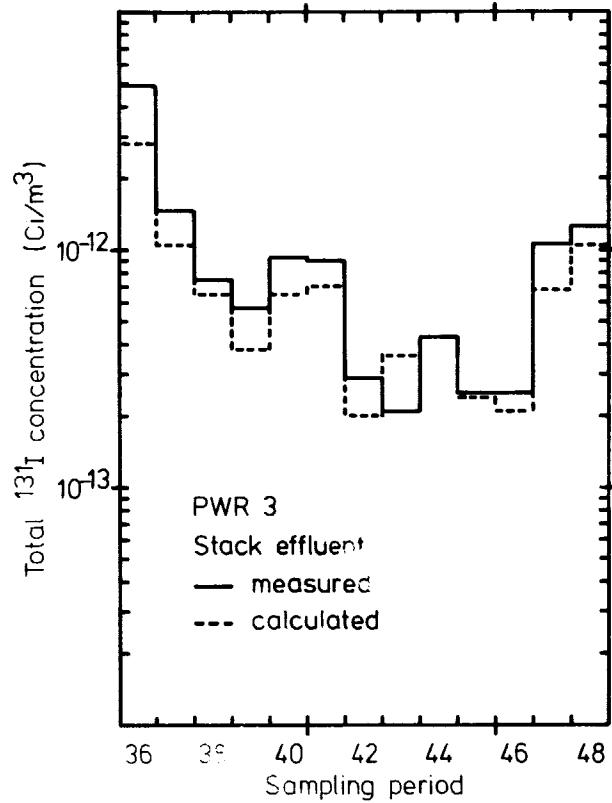
Filter	Sampling period	Decontamination factor		
		Elem. 131 _I	Org. 131 _I	Total 131 _I
1	36	510	3.6	4.0
	37	130	2.3	2.5
	38	450	2.9	3.2
	39	360	3.2	3.5
	40	280	3.0	3.3
	41	50	3.2	3.4
	36 - 41 ^b 36 - 41 ^c	290 ± 70	3.1 ± 0.2	3.3 ± 0.2
2	42	90	24	25
	43	210	38	40
	44	1 900	26	28
	45	560	20	26
	46	1 500	20	25
	47	> 10 000	9	13
	48	1 400	12	18
	42 - 48 ^b 42 - 48 ^c	960 ^d ± 310 ^d	21 ± 4	25 ± 3

^a Sorbent: KI impregnated carbon, 8 - 12 mesh (filled into the filters 2 years prior to the measurements);
 residence time: ~ 0,5 s;
 average relative humidity: 40 %;
 average temperature: 30°C.

^b Average value.

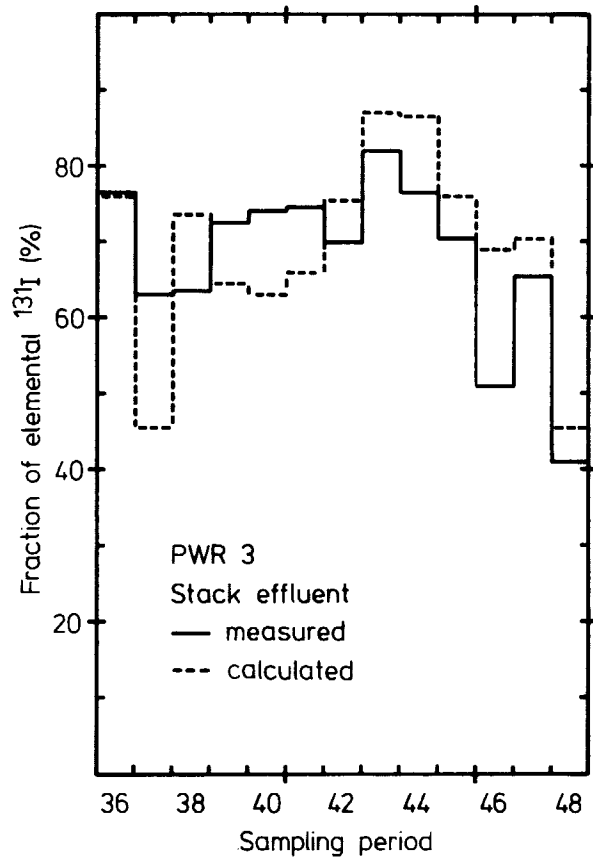
^c Standard deviation of the average value.

^d Calculated without consideration of sampling period 47.



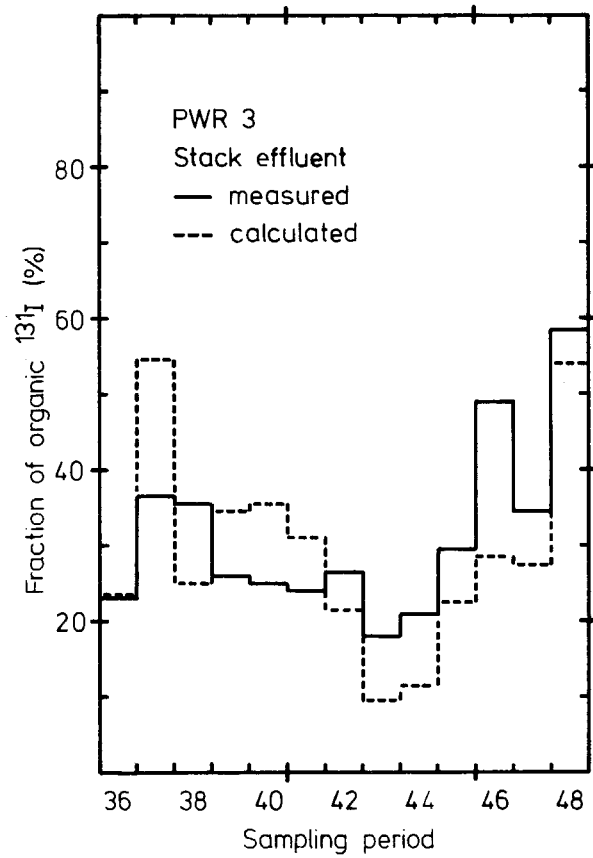
Total ^{131}I concentration as a function of time

Fig. 5



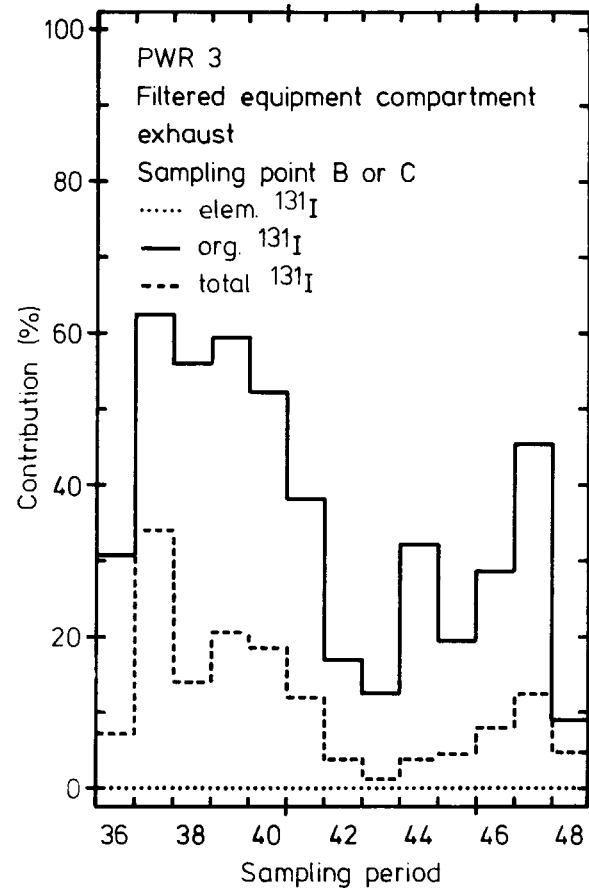
Fraction of elemental ^{131}I as a function of time

Fig. 6



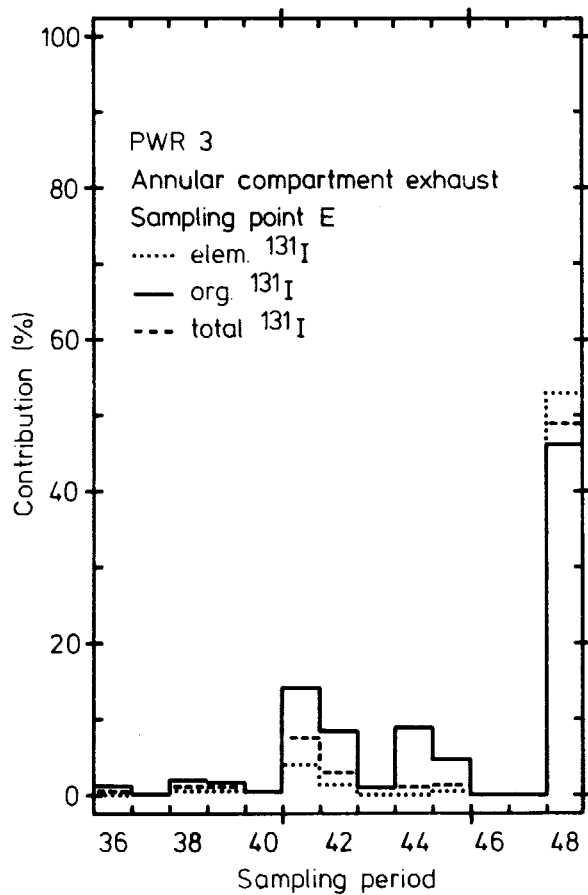
Fraction of organic ^{131}I
as a function of time

Fig. 7



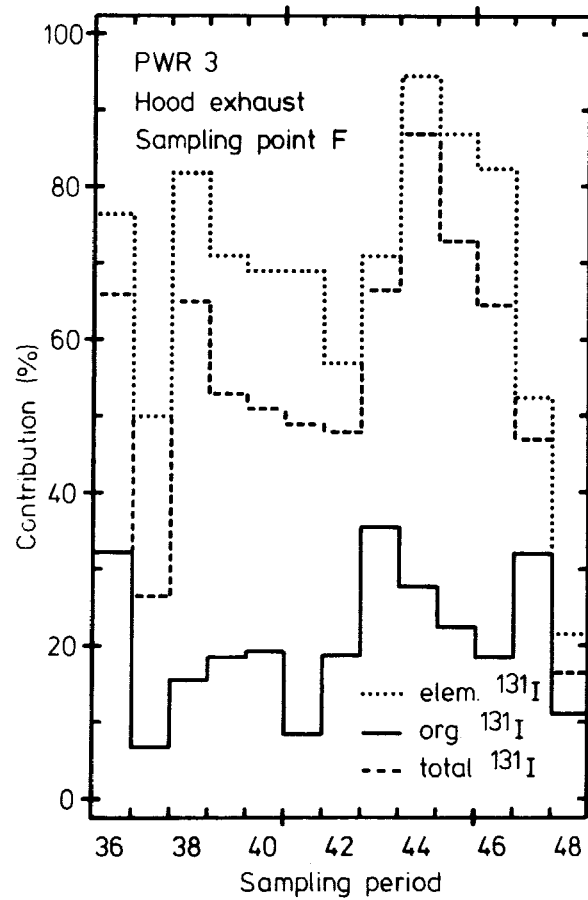
Contribution to the stack effluent with respect
to the ^{131}I species as a function of time

Fig. 8



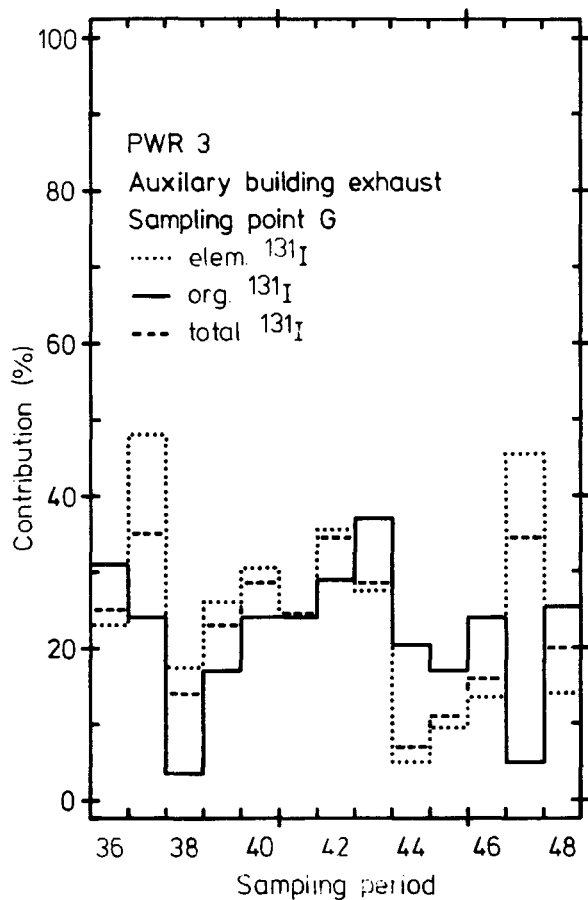
Contribution to the stack effluent with respect to the ^{131}I species as a function of time

Fig. 9



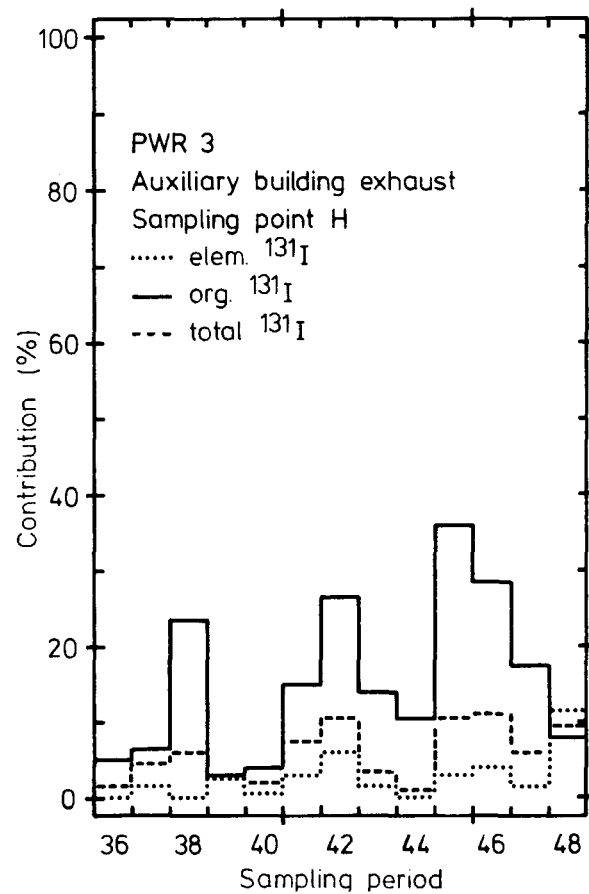
Contribution to the stack effluent with respect to the ^{131}I species as a function of time

Fig. 10



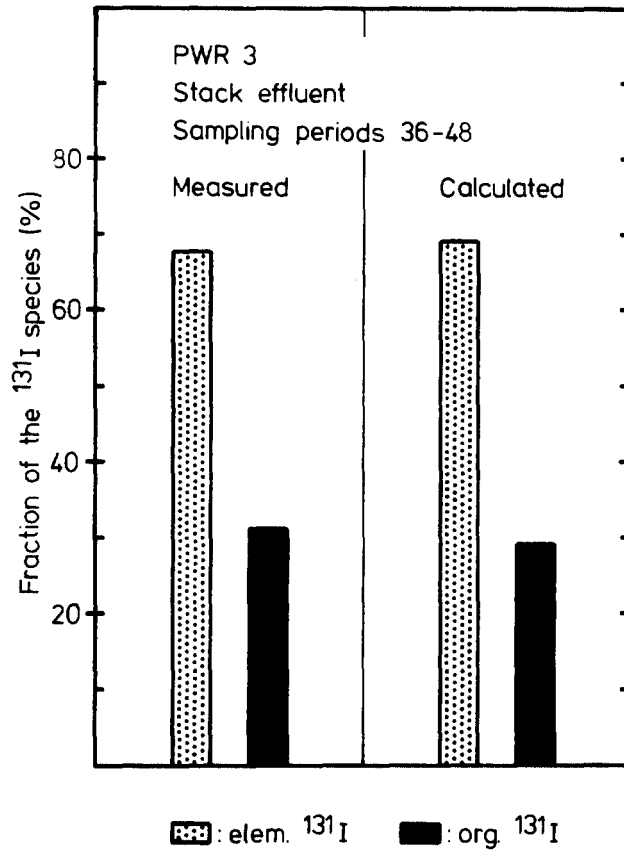
Contribution to the stack effluent with respect to the ^{131}I species as a function of time

Fig. 11



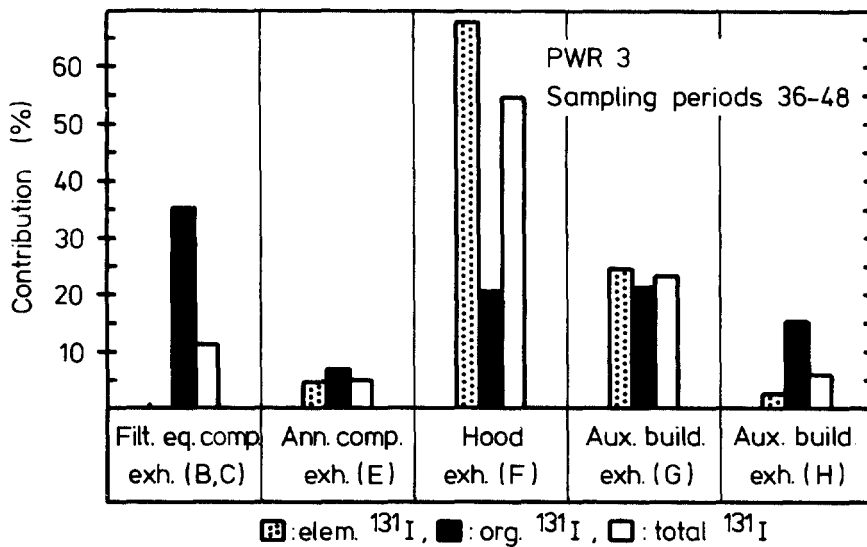
Contribution to the stack effluent with respect to the ^{131}I species as a function of time

Fig. 12



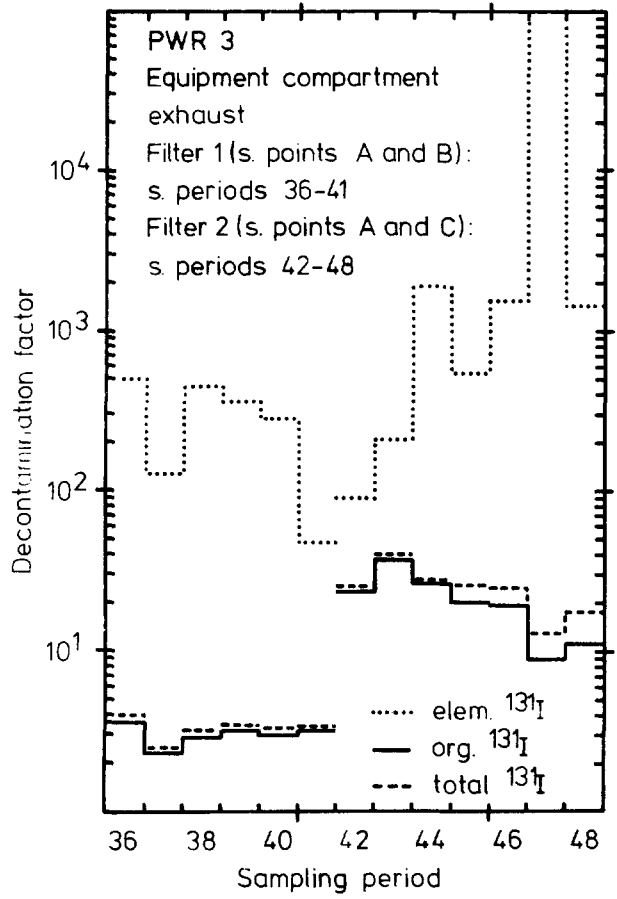
Average fractions of the ¹³¹I species

Fig. 13



Average contributions of the various exhausts to the stack effluent with respect to the ¹³¹I species

Fig. 14



LA-14978E

Decontamination factor as a function of time

Fig. 15

15th DOE NUCLEAR AIR CLEANING CONFERENCE

V. Calculation of Data Pertaining to the ^{131}I Stack Release for Various Cases of Filtration of the Equipment Compartment and Hood Exhausts

To generalize the experimental data of the sampling periods 36 to 48 to a certain extent various calculations were performed. In these calculations filtration of the major ^{131}I sources, i.e. the equipment compartment and hood exhausts, with different decontamination factors for the ^{131}I species, including decontamination factors of 1 for all species (no filtration), was assumed. The cases of filtration considered are shown in Table XI. For these cases the fractions of the ^{131}I species in the stack effluent, the ^{131}I species stack release rates, and the relative ingestion doses due to the total ^{131}I stack release were calculated.

The results are presented in Table XII and in Figs. 16 to 18. They may be summarized as follows:

- (a) The fractions of elem. and org. ^{131}I are about 50 % each in case 1 (no filtration). The relative amount of elem. ^{131}I increases (with the total ^{131}I release rate lower than without filtration) if the equipment compartment exhaust is filtered (cases 2, 3), it decreases in the event of filtration of the hood exhaust (cases 4, 5). The ^{131}I species proportions are on the order of 50 % if both the exhausts are filtered with the same decontamination factors (cases 6, 7).
- (b) The release rate of elem. ^{131}I diminishes to a small extent in the event of filtration of the equipment compartment exhaust (cases 2, 3), but to a high degree in the event of filtration of the hood exhaust (cases 4, 5). The highest diminution is obtained if both the exhausts are filtered.
- (c) The relative ingestion doses due to the total ^{131}I release are approximated by the ratios of the elem. ^{131}I release rates in the various cases if a weighting ratio of 100 : 10 : 1 for elem., part., and org. ^{131}I is used. If both the equipment compartment and the hood exhausts are filtered, the relative ingestion dose is 28 % or 27 % (100 % in the case of no filtration at all). Case 2 with a relative ingestion dose of 85 % approaches to the actual situation during the sampling periods 36 to 48. This means that by installation of an iodine filter in the hood exhaust with decontamination factors for part., elem. and org. ^{131}I of 100, 100, and 10 respectively, the actual ingestion dose would have been reduced by a factor of 3.

It is pointed out that the results obtained apply to specific conditions (of mainly power operation) only. Under other circumstances, especially in the case of an incident, different values may hold. In particular, the percentage of elem. ^{131}I may be high in unfiltered equipment compartment exhaust in the case of an incident so that the reduction of the elem. ^{131}I release rates and the ingestion doses achieved by filtration of this exhaust would be much higher than found above.

Table XI Different cases of filtration of the equipment compartment and hood exhausts used in the calculation of data pertaining to the stack release.

Case	Decontamination factor					
	Equipment compartment exhaust			Hood exhaust		
	Part. ^{131}I	Elem. ^{131}I	Org. ^{131}I	Part. ^{131}I	Elem. ^{131}I	Org. ^{131}I
1	1	1	1	1	1	1
2 ^a	100	100	10	1	1	1
3	100	1000	100	1	1	1
4	1	1	1	100	100	10
5	1	1	1	100	1000	100
6	100	100	10	100	100	10
7	100	1000	100	100	1000	100

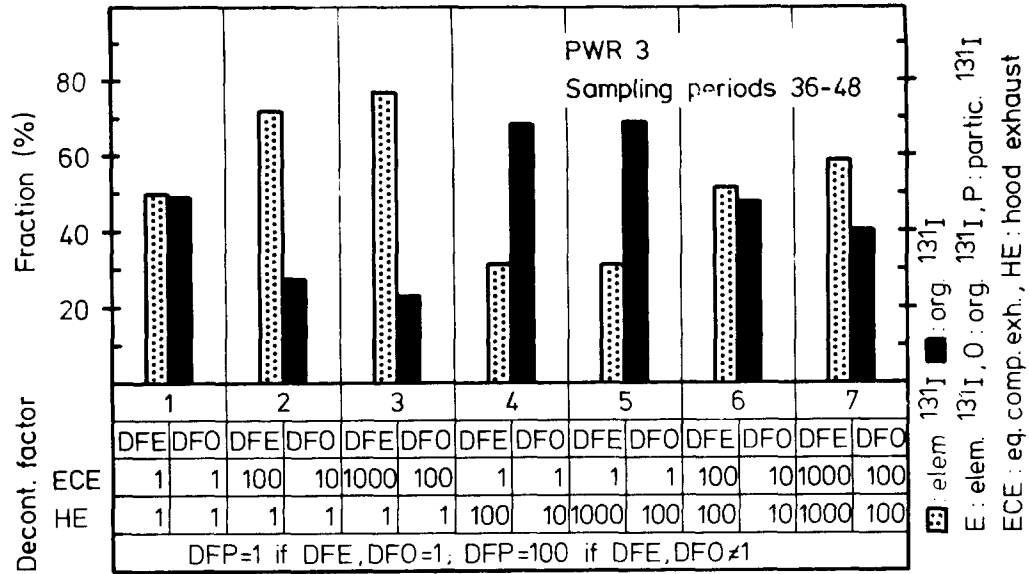
^a Approximates the actual situation (average decontamination factor of the equipment compartment exhaust filters about 13 for org. ^{131}I (Table X); no hood exhaust filter installed).

Table XII Calculated data pertaining to the stack release for various cases of filtration of the equipment compartment and hood exhausts.
Cases as indicated in Table XI; sampling periods 36-48.

Case	Fraction of the ^{131}I species (%) ^a		^{131}I species release rate (Ci/s)			Relative ingestion dose due to total ^{131}I release (%) ^b
	Elem. ^{131}I	Org. ^{131}I	Elem. ^{131}I	Org. ^{131}I	Total ^{131}I	
1	48.6 ± 2.6	50.4 ± 2.7	2.62 ± 0.67(-11)	2.58 ± 0.48(-11)	5.24 ± 1.07(-11)	100
2	71.8 ± 2.9	26.5 ± 3.0	2.24 ± 0.65(-11)	8.54 ± 2.36(-12)	3.14 ± 0.83(-11)	85.2 ± 24.5
3	77.0 ± 2.9	21.2 ± 3.1	2.24 ± 0.65(-11)	6.81 ± 2.16(-12)	2.96 ± 0.81(-11)	85.0 ± 24.5
4	28.7 ± 2.3	70.6 ± 2.4	1.11 ± 0.29(-11)	2.41 ± 0.43(-11)	3.53 ± 0.70(-11)	42.7 ± 10.9
5	28.5 ± 2.3	70.8 ± 2.4	1.09 ± 0.28(-11)	2.39 ± 0.43(-11)	3.50 ± 0.69(-11)	42.2 ± 10.9
6	49.3 ± 3.7	49.3 ± 4.0	7.32 ± 1.95(-12)	6.81 ± 1.94(-12)	1.43 ± 0.37(-11)	28.0 ± 7.4
7	59.0 ± 3.6	39.3 ± 4.0	7.15 ± 1.91(-12)	4.90 ± 1.72(-12)	1.22 ± 0.35(-11)	27.2 ± 7.3

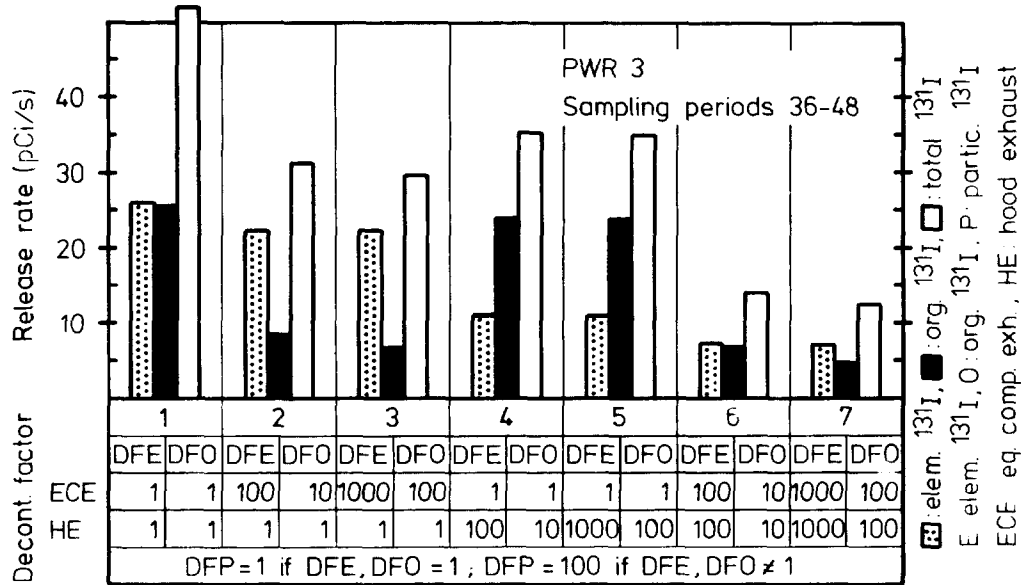
^a Calculated as averages of the fractions of the various sampling periods; slightly different fractions result from the ^{131}I species release rates, as shown in Fig. 16.

^b Weighting ratio of the ^{131}I species release rates:
elem. ^{131}I : part. ^{131}I : org. ^{131}I = 100 : 10 : 1.



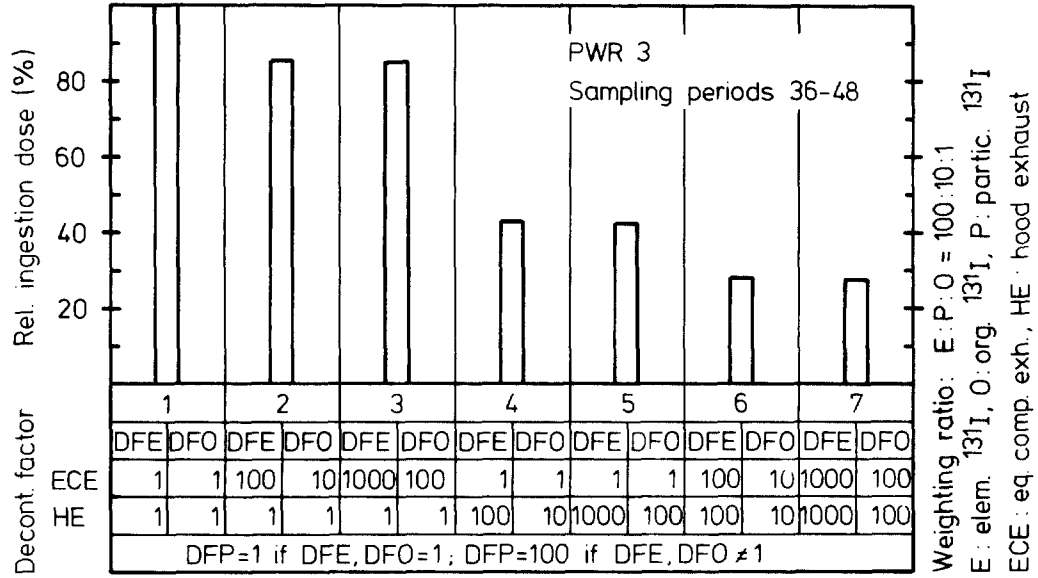
Calculated fractions of the ¹³¹I species in the stack effluent for various cases of filtration of the equipment compartment and hood exhaust

Fig. 16



Calculated stack release rates of the ¹³¹I species for various cases of filtration of the equipment compartment and hood exhaust

Fig. 17



KIK LAFII 141278 E

Calculated relative ingestion doses due to the total ¹³¹I stack release for various cases of filtration of the equipment compartment and hood exhaust (1st case:100%)

Fig. 18

15th DOE NUCLEAR AIR CLEANING CONFERENCE

VI. Conclusions

The credit for differences of the ^{131}I species in the stack effluents of PWRs with respect to the environmental impact may be based under favorable conditions on release rates of elemental and organic ^{131}I in the ratio of 1 : 1 or in even lower ratios. But as the fractions of the ^{131}I species may differ substantially from plant to plant and be strongly influenced by the mode of exhaust filtration, i.e. by the location of the iodine filters, the decision to grant the credit mentioned for a specific plant should be based on ^{131}I species measurements in the stack effluent of the plant in question.

A considerable improvement of the ventilation systems of PWRs in terms of reduction of elem. ^{131}I release rates under normal operating conditions may be possible.

Acknowledgements

We wish to express our appreciation to Messrs. K. Bleier, R. Butz, and K.H. Simice who performed or evaluated the laboratory and in-plant measurements.

The special sponsorship of the Federal Minister of Research and Technology of the Federal Republic of Germany is gratefully acknowledged.

References

1. Wilhelm, J.G., "Iodine filters in nuclear power stations," KFK 2449 (1977).
2. Bundesminister des Inneren, "Allgemeine Berechnungsgrundlagen für die Bestimmung der Strahlenexposition durch Emission radioaktiver Stoffe mit der Abluft," Empfehlung der Strahlenschutzkommission, p. 65 (1977).
3. Pelletier, C.A., et al., "Sources of radioiodine at boiling water reactors," EPRI NP-495 (1978).
4. Deuber, H., Wilhelm, J.G., "Bestimmung der physikalisch-chemischen Komponenten des Radiojods in der Kaminabluft von Kernkraftwerken," KFK-Ext. 30/78-1 (1978).
5. Deuber, H., "Bestimmung von Iodkomponenten in der Abluft kerntechnischer Anlagen," KFK 2700 (to be published).
6. Deuber, H., "Bestimmung von Jodkomponenten in der Abluft kerntechnischer Anlagen," KFK 2435, p. 127-139 (1977); KFK 2500, p. 132-145 (1977); KFK 2600 (to be published).
7. Birke, G., "Abscheidung von ^{131}I in Form von HI an verschiedenen Iod-Sorptionsmaterialien," KFK 2700 (to be published).
8. Emel, W.A., et al., "An airborne radioiodine species sampler and its application for measuring removal efficiencies of large charcoal adsorbers for ventilation exhaust air," CONF 760822, p. 389-431 (1976).

DISCUSSION

CARTER: A point of clarification, please; how long were the iodine filters in operation?

DEUBER: The first iodine filter had been in operation for about 2 years, the second one only occasionally prior to the measurements of the DFs.

CHAIRMAN BURCHSTED'S SUMMARY:

During the first half of this session a number of papers were presented which dealt with factors relating to the degradation of adsorbents. All of these factors had been discussed in earlier Air Cleaning Conferences at one time or another, but it is interesting to see that the empirical observations of earlier years are now yielding to mathematical treatment that gives us a better understanding of the mechanisms involved and lead to predictive possibilities and improved design in the future. Several factors also suggest the effects of different base carbons, activation methods, and impregnations that indicate the possibility of "designing" activated carbons for specific applications, e.g., stand-by treatment system service vs. continuously on-line system service, etc. The discussions of inherent characteristics that affect carbon degradation, as opposed to external (i.e., atmospheric) conditions that poison the carbon, led the Session Chairman to propose a distinctive nomenclature for use in the future: Aging as the generic term for degradation resulting from inherent factors (e.g., surface oxidation with time, inherent acid introduced during manufacture) and Weathering for degradation caused by external factors (i.e., atmospheric and environmental).

One of the papers by Dr. Dietz described a proposed test which defines the very important characteristic of attrition (often referred to as dusting). The results of that study were particularly interesting because they suggest a possibility of classifying adsorbents with respect to this characteristic. Finally, the paper by Romans suggests the possibility of testing activated carbons with a non-radioactive CH_3I challenge, a possibility that could simplify qualification, production, and surveillance testing in the future. However, Kovach pointed out that the test cannot reflect the isotopic exchange of ^{131}I for ^{127}I that is the primary mechanism for trapping the radioactive iodine fraction with KI and I_2 impregnated carbon. As the chairman noted, we don't really care if nonradioactive CH_3I comes off a carbon bed so long as we trap and hold the radioactive fraction. Wood points out, on the other hand, that the total CH_3I does have importance in the overall performance of the adsorption system. The papers not only suggest areas of further research in this field, but suggest many potential areas of interest to the engineer and designer.

15th DOE NUCLEAR AIR CLEANING CONFERENCE

SESSION VI

OFF-GAS TREATMENT

Tuesday, August 8, 1978

CHAIRMEN: R. R. Bellamy, R. Brown

BURNER AND DISSOLVER OFF-GAS TREATMENT IN HTR FUEL REPROCESSING

H. Barnert-Wiemer, M. Heidendael,
H. Kirchner, E. Merz, G. Schröder,
H. Vygen

AEROSOL AND IODINE REMOVAL SYSTEM FOR THE DISSOLVER OFF-GAS IN A LARGE FUEL RE-
PROCESSING PLANT

J. Furrer, J. G. Wilhelm, K. Jannakos

NOBLE GAS SEPARATION WITH THE USE OF INORGANIC ADSORBENTS

D. T. Pence, C. C. Chou, J. D. Christ-
ian, W. J. Paplawsky

NITROGEN OXIDE ABSORPTION INTO WATER AND DILUTE NITRIC ACID IN AN ENGINEERING-
SCALE SIEVE-PLATE COLUMN WITH PLATES DESIGNED FOR HIGH GAS-LIQUID INTERFACIAL
AREA

R. M. Counce, W. S. Groenier, J. A.
Klein, J. J. Perona

REMOVAL OF ^{14}C -CONTAMINATED CO_2 FROM SIMULATED LWR FUEL REPROCESSING OFF-GAS BY
UTILIZING THE REACTION BETWEEN CO_2 AND ALKALINE HYDROXIDES IN EITHER SLURRY OR
SOLID FORM

D. W. Holladay, G. L. Haag

MEASUREMENT OF RADIOACTIVE GASEOUS EFFLUENTS FROM VOLOXIDATION AND DISSOLUTION OF
SPENT NUCLEAR FUEL

J. A. Stone, D. R. Johnson

INVESTIGATION OF AIR CLEANING PROCESSES FOR REMOVING TRIBUTYL PHOSPHATE VAPORS FROM
FUEL REPROCESSING OFF-GAS STREAMS

G. B. Parker, L. C. Schwendiman

A REVIEW OF SOME U.K.A.E.A. WORK ON GAS CLEANING IN FUEL REPROCESSING PLANTS

M. N. Elliott, E. Lilleyman

ELIMINATION OF NO_x BY SELECTIVE REDUCTION WITH NH_3

A. Bruggeman, L. Meynedonckx,
W. R. A. Goossens

OPENING REMARKS OF SESSION CHAIRMAN:

BELLAMY: We will be hearing papers in this session concerning the treatment of offgases from fuel reprocessing plants. We expect the use of fuel reprocessing plants to become larger as the nuclear industry expands. We hope that will be the case for the future. The contaminants of concern that we will hear about this afternoon include gaseous fission products (iodine-129, tritium, carbon-14), gaseous NO_x compounds, carbon-14 as CO_2 , tributyl phosphate and tributyl phosphate vapors. We will also hear a paper that will discuss a technique for the measurement of these offgas pollutants.

15th DOE NUCLEAR AIR CLEANING CONFERENCE

BURNER AND DISSOLVER OFF-GAS TREATMENT IN HTR FUEL REPROCESSING

H. Barnert-Wiemer
M. Heidendael
H. Kirchner
E. Merz
G. Schröder
H. Vygen

Kernforschungsanlage Jülich GmbH
Jülich/Germany

Abstract

In the reprocessing of HTR fuel essentially all of the gaseous fission products are released during the head-end treatment, which includes burning of the graphite matrix and dissolving of the heavy metallic residues in THOREX reagent.

Three facilities for off-gas cleaning are described, the status of the facility development and test results are reported.

Hot tests with a continuous dissolver for HTR-type fuel (throughput 2 kg HM/d) with a closed helium purge loop have been carried out. The goals of these experiments were two-fold:

- the complete dissolver unit was to be tested before a similar one is built into the JUPITER facility
- the composition and some steps of an off-gas cleaning system were to be checked.

Preliminary results of these experiments are reported.

I. Facility development

In the Institute for Chemical Technology of KFA Jülich three facilities for off-gas cleaning during reprocessing of HTR-fuel are being developed:

- the AKUT II-facility for the burner off-gas
- the KRYOSEP I-facility for the off-gas from a discontinuous dissolver
- the KRYOSEP II-facility for the off-gas from a continuous dissolver with a closed purge gas loop.

The AKUT II-facility

The flowsheet of the AKUT II-facility (Fig. 1), consisting of the consecutive steps

filtering
catalytic burning
tritium removal
compression and liquefaction
distillation

has already been described previously ¹⁾.

AKUT - II
Flowsheet

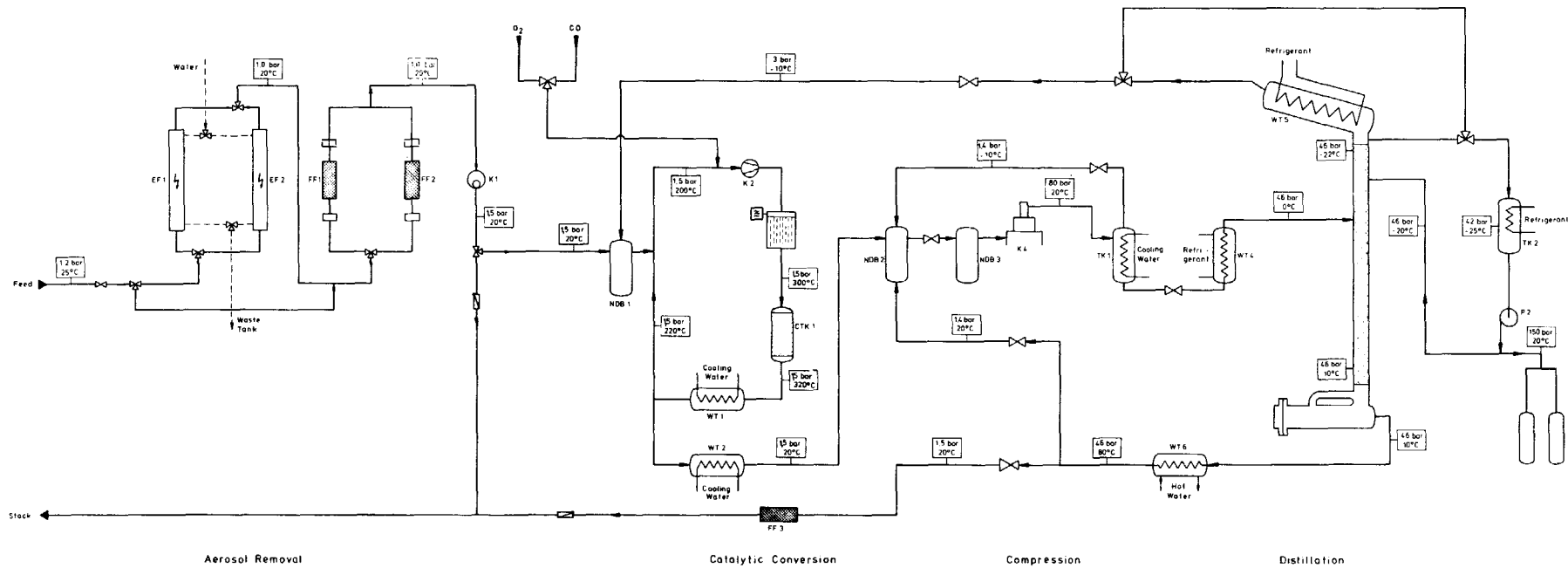


Fig. 1: Flowsheet of the AKUT II-facility

15th DOE NUCLEAR AIR CLEANING CONFERENCE

One of the electrostatic precipitators ¹⁾ is at this time being tested in the laboratory to check the influence of the Kr-85 concentration on the efficiency. The throughput is varied between 5 and 40 m³/h and the Kr-85 concentration between 0,5 and 25 Ci/m³. The efficiency of the filter is determined by adding cesium aerosols with Cs-137 as tracer to the gas stream. In further experiments graphite dust (particle size < 5 μm) in varying amounts (1 to 10 g/m³) is to be fed into the gas and the efficiency for graphite dust removal is to be evaluated.

The catalytic burning equipment (Fig. 2) has undergone preliminary testing.

The off-gas from the JUPITER fluidized bed burner is at steady state expected to be 7,5 m³/h consisting of CO₂ with 20 % CO. The maximum capacity of the catalytic burner is 10 m³/h off-gas consisting of 100 % CO. To handle the wide range of possible off-gas compositions the off-gas is fed into a recycled gas stream whose throughput can be varied by means of a blower between 75 and 325 m³/h according to the conditions of the off-gas. The catalyst bed contains 15,4 l of a palladium catalyst (0,1 % Pd on Al₂O₃) distributed in two 40 mm high layers. The catalyst can be operated at temperatures between 200 °C and 650 °C and space velocities up to 30 m³/h per liter catalyst.

In the tests the CO-concentration was increased to 14 % in the feed gas of 5 m³/h which resulted in a temperature increase in the catalyst bed from 250 °C to 281 °C, the recycle gas flow being 150 m³/h. Behind the catalyst no CO was detected, but the O₂-concentration was 0,25 %. The tests were discontinued because of a leak in the blower. In future tests the main task will be to improve the facility control, mainly the response of the O₂ supply valves to the CO concentration.

No data are available on iodine poisoning of the catalyst. But since the J₂ concentration in the off-gas is below 1 ppm the supplier of the catalyst expects no difficulties.

The AKUT II-facility (Fig. 3) as a whole is expected to be ready for preliminary testing in late fall, with the exception of the tritium removal system for which laboratory testing still needs to be done.

The KRYOSEP I-facility

During the dissolution of the heavy metal ash the remainder of the gaseous fission products is released into the off-gas.

Since only 20 l/h dissolver off-gas are produced by the JUPITER reprocessing pilot plant, this off-gas is compressed and filled in gas cylinders till enough gas has been collected to operate the KRYOSEP I-facility which has a throughput of 5 m³/h. KRYOSEP I consists of a pretreatment unit, a O₂/NO_x removal system and a cryogenic separation unit.

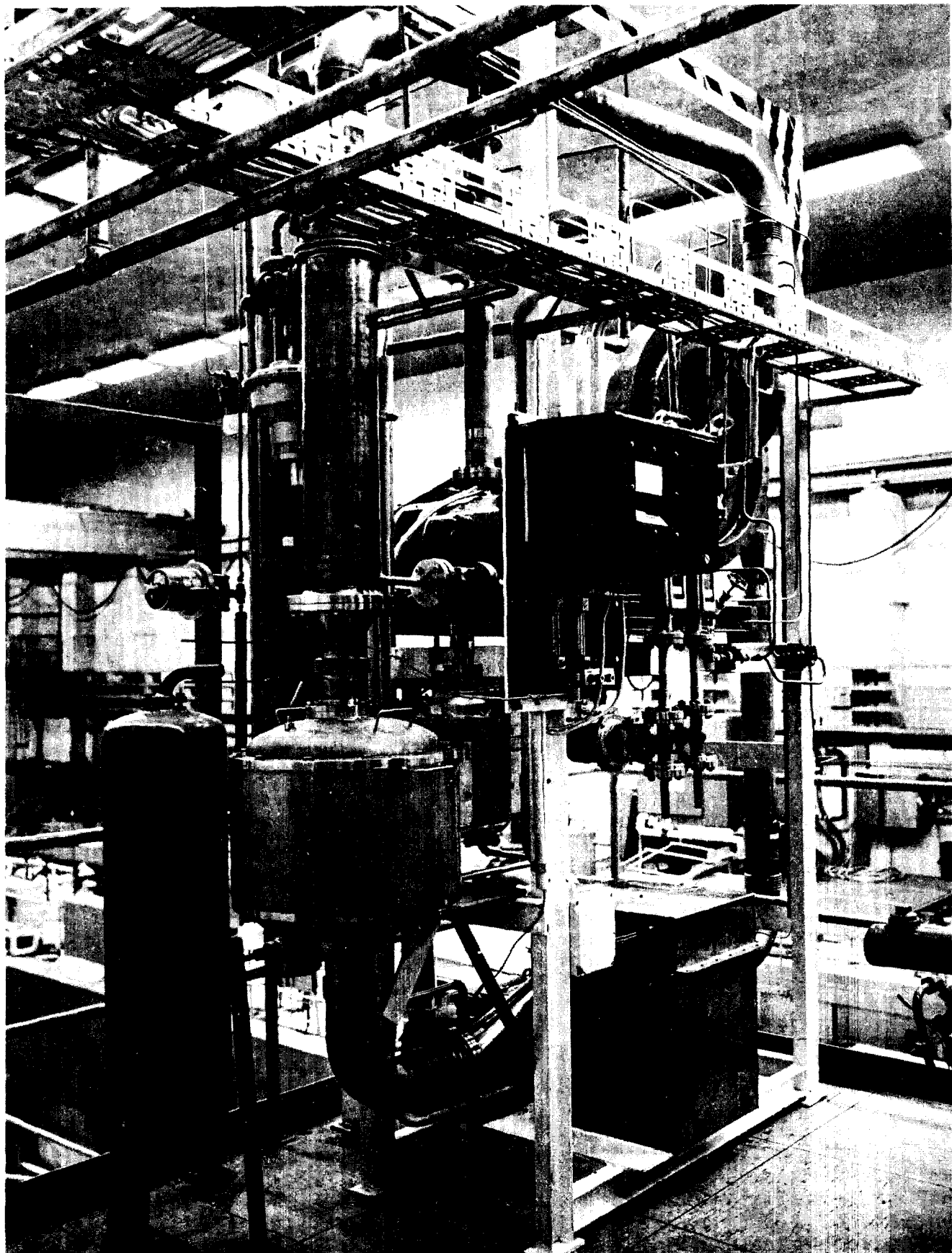


Fig. 2: The catalytic burning equipment of the AKUT II-facility

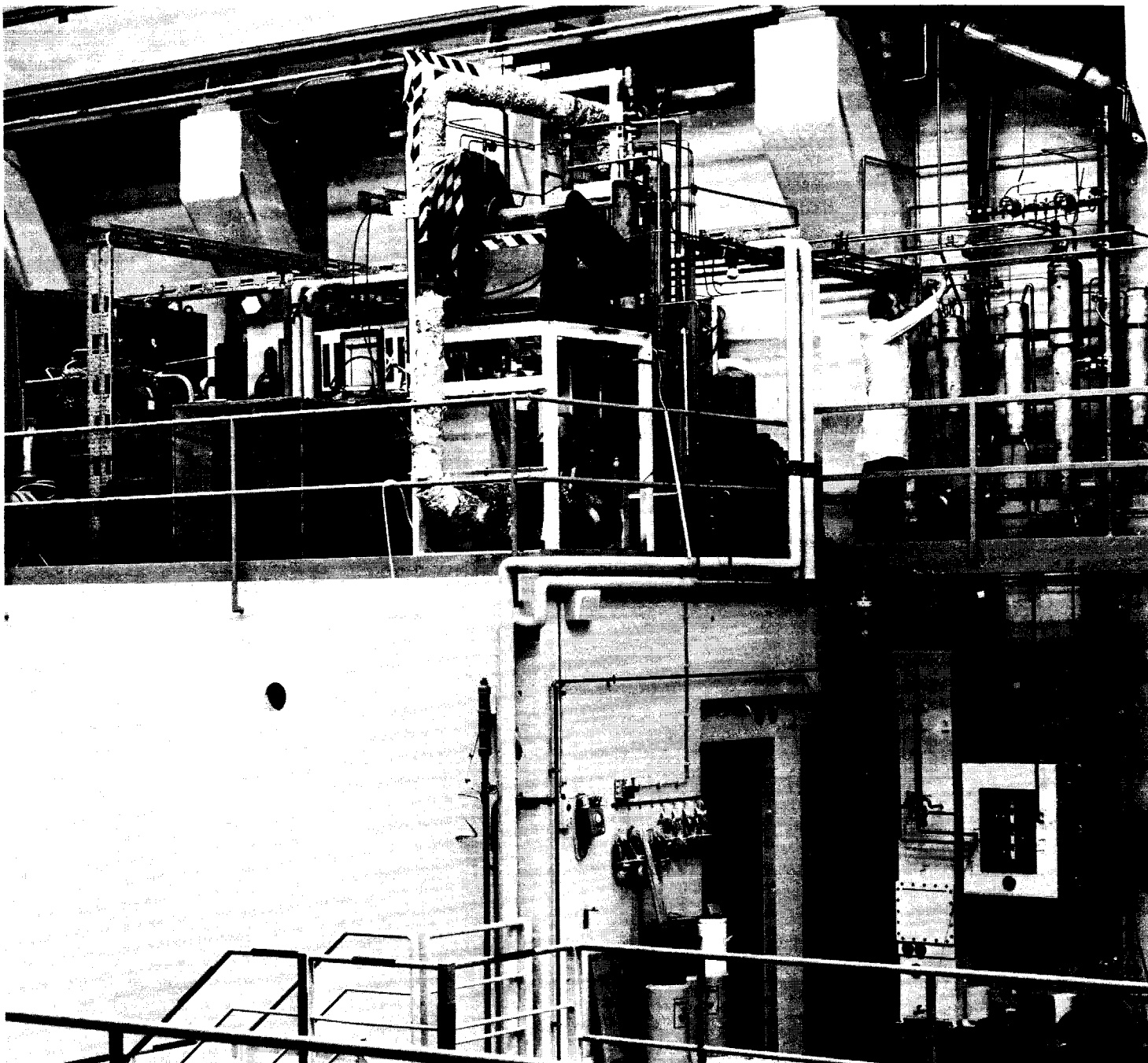


Fig. 3:

View of the
AKUT II-facility
during assembly

15th DOE NUCLEAR AIR CLEANING CONFERENCE

To prevent poisoning of the catalyst in the O₂/NO_x separation system iodine is removed quantitatively before the gas enters said system. This is achieved by fixation in two alternately operated filters filled with the sorption material AC-6120, an Ag-impregnated product on the basis of amorphous silicic acid.

The gas entering the O₂/NO_x removal system (Fig. 4) consists mainly of the following components:

N ₂	:	76,5	%
O ₂	:	20,6	%
NO _x	:	1,0	%
Ar	:	0,9	%
Xe	:	0,7	%
Kr	:	0,1	%.

To avoid the formation of ozone ($3 \text{ O}_2 \xrightarrow{h\nu} 2 \text{ O}_3$) in presence of a γ -radiation field and to exclude the latent risk of explosion when distilling liquid noble gas - oxygen mixtures, oxygen and nitrogen oxides are eliminated by reaction with hydrogen in the presence of a catalyst, whereby oxygen and nitrogen oxides are converted to elemental nitrogen, water and traces of ammonia. While direct conversion results in elevated temperatures of about 1100 °C, the same reaction takes place on precious metal catalyst at a temperature range of 200 - 300 °C. To operate outside the explosion limits, the relative high oxygen-content is lowered by feeding the off-gas into a recycle of oxygen free gas. Moreover, this dilution is necessary to avoid overheating of the catalyst, because each vol-% O₂ induces a rise of temperature in the catalyst bed of ~ 150 °C. A flow-sheet is shown in figure 5: NO_x-containing dissolver off-gas (5 m³/h) is diluted by nitrogen which is recycled by a blower (K1) with a throughput of 65 m³/h. Thereby the oxygen-content of the gas stream is decreased to about 2 vol-% O₂. The O₂-concentration given by a paramagnetic O₂-analyser, and the flow-rate given by a flow-meter control the hydrogen feed. Behind the catalyst bed (K.B.) the gas stream, primarily N₂, passes through a water-cooled condenser (WT1) to remove the water formed by the H₂-O₂-reaction. The surplus hydrogen (~ 2000 ppm) is subsequently removed by reaction with activated copper oxide (CuO-B1 or CuO-B2) and the water from that reaction is removed in a water-cooled heat exchanger (WT4). Before leaving the O₂/NO_x removal system the gas is dried by molecular sieves (MS-B1 or MS-B2) which also adsorb traces of impurities like CO₂, NO₂ and NH₃.

During cold tests it was found that the platinum catalyst caused nearly all of the NO_x to react with the hydrogen to form ammonia. Therefore laboratory tests are under way to find a catalyst suitable for O₂ and NO_x removal at the same time. Two ruthenium and one nickel catalyst are being tested at present.

The gas entering the cryogenic distillation unit (Fig. 6) where the separation of krypton and xenon from the gas stream and further purification of the xenon fraction is achieved, consists mainly of N₂, Ar, Xe and Kr.

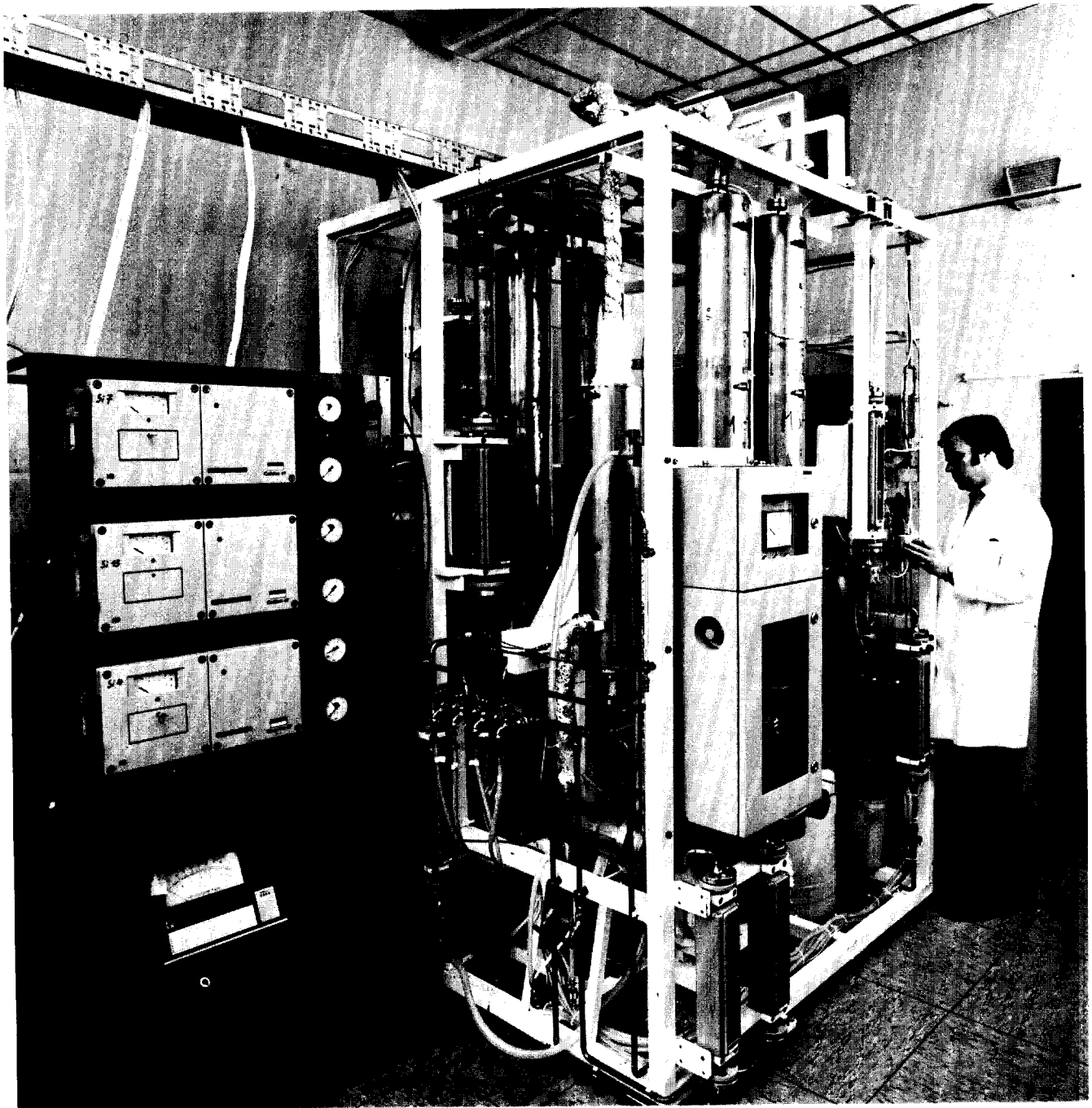


Fig. 4: View of the O_2/NO_x removal system

O₂/NO_x-Removal System

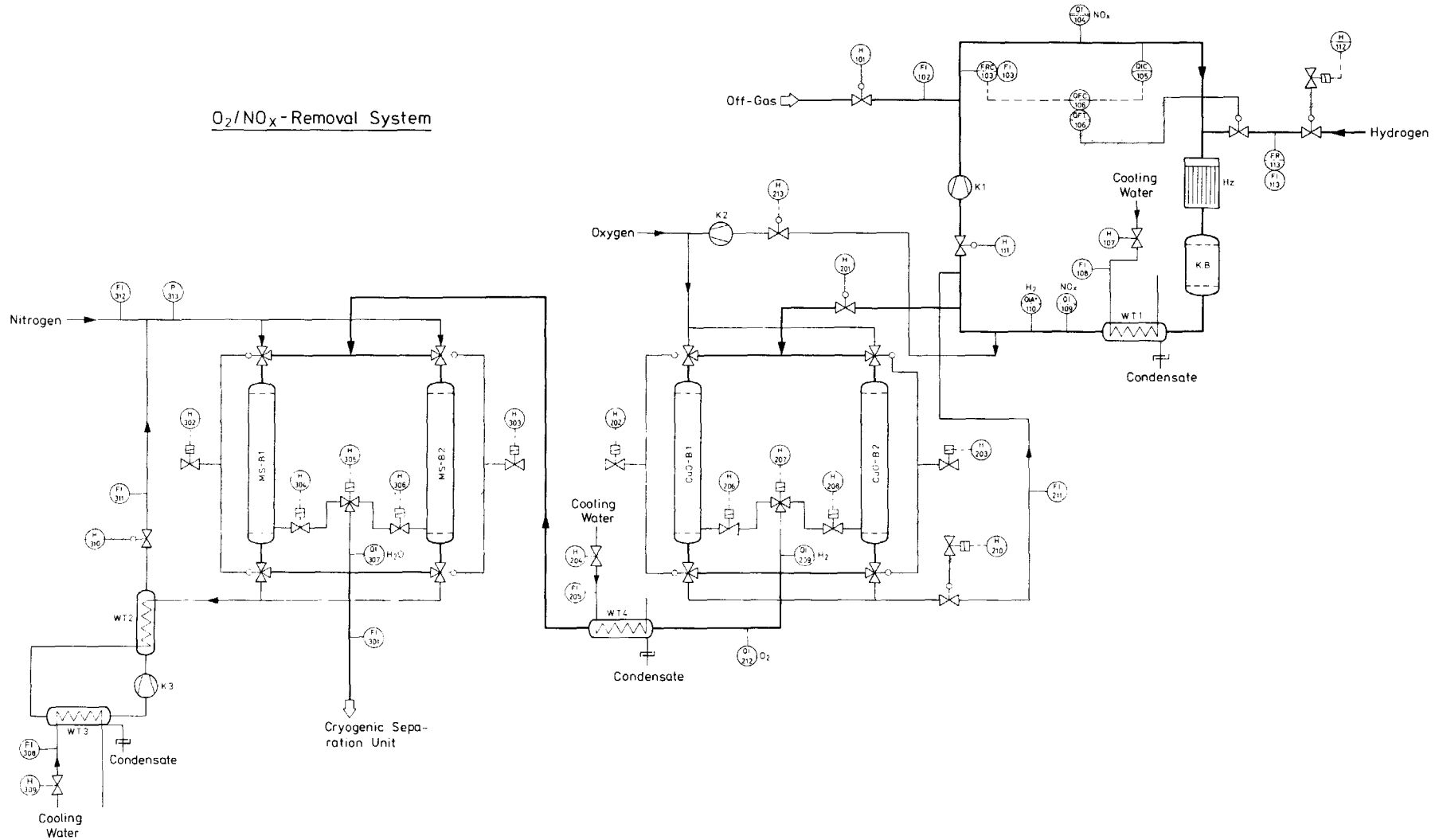


Fig. 5: Flowsheet of the O₂/NO_x removal system

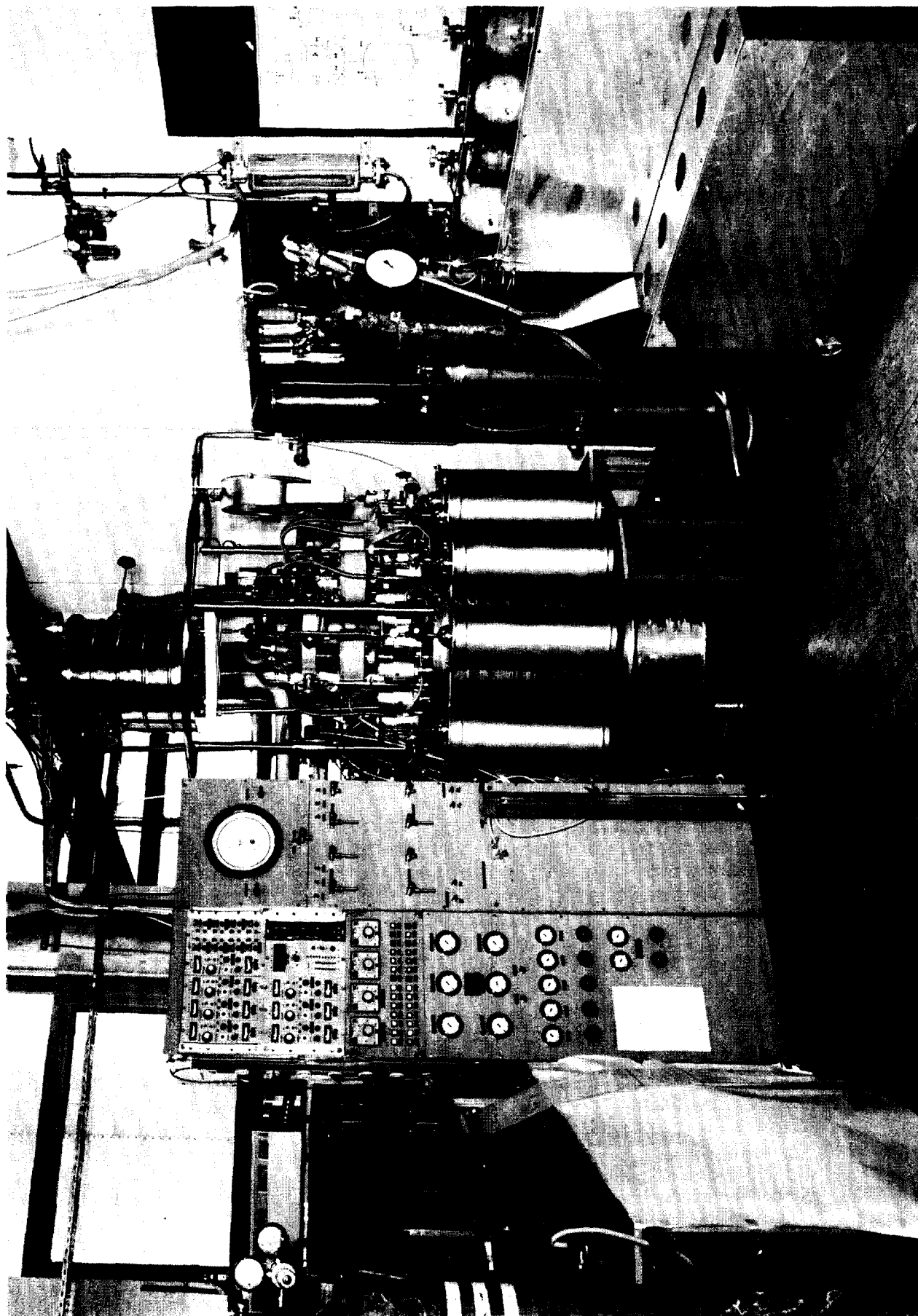


Fig. 6: View of the KRYOSEP I-facility

15th DOE NUCLEAR AIR CLEANING CONFERENCE

The components of the system are placed in a vacuum container (height: 3 m, diameter: 1 m) where a vacuum of 10^{-5} Torr is maintained.

Fig. 7 shows the flowsheet: Entering the cryogenic part of the separation unit the preconditioned gas stream passes a countercurrent heat-exchanger where it is precooled to 160 - 180 K by the effluent cold gas from the cooling system of the cold-traps.

In the upper part of two alternately operated cold-traps xenon is deposited at about 80 K in solid form adsorbing about 0,5 vol-% krypton. Simultaneously, the remaining gas components are liquified in the lower part of the Xe-separator and flow to a 200 l storage tank.

The liquified gas-mixture is fed by overpressure from the storage tank to the still. The column (height: 1600 mm, diameter: 38 mm) is packed with "Knitmesh Multifil" wire mesh which is similar in structure to Goodloe packing. At operating conditions the system pressure is 1,2 bar. The liquid levels in the reboiler and the 200 l storage tank are controlled by level indicators on the basis of capacity metering devices. Thermometry is achieved by resistance thermometers.

During operation an average rate of about 6 liters/h liquid enters the column. The decontaminated gas stream, primarily nitrogen, is discharged at the top of the column, while krypton is enriched in the bottom of the still. During the last two campaigns decontamination factors of $2 \cdot 10^3$ and $8 \cdot 10^3$ were achieved for krypton. The Kr-fraction, containing about 10 - 40 vol-% krypton is withdrawn batchwise from the bottom and filled in high-pressure steel cylinders.

To reduce the ultimate storage volume of the fission product noble gases or to get an extremely pure xenon for eventual industrial utilization Kr-85 contaminated xenon, previously deposited in the cold traps must be refined. This is done by batch distillation in the second column with the aim to obtain a Kr-85 content of $< 3 \mu$ Ci Kr-85 / m³ xenon. Therefore 4,5 kg xenon-charges bottled in high-pressure steel cylinders are transferred periodically to the still (volume: 1,5 l liquid xenon) to remove the contaminant by boiling under total reflux. Krypton and small amounts of xenon discharged from the top of the column are recycled to the primary process gas stream. Decontaminated xenon is withdrawn from the bottom to be bottled in steel cylinders for further use.

Up to now the batch distillation has rendered only unsatisfactory decontamination factors of 10^0 . To meet the specification of the purified xenon a decontamination factor better than $3 \cdot 10^0$ is necessary.

To reach this goal it is intended to add inactive Kr to the Xe-batch and repeat the distillation.

487

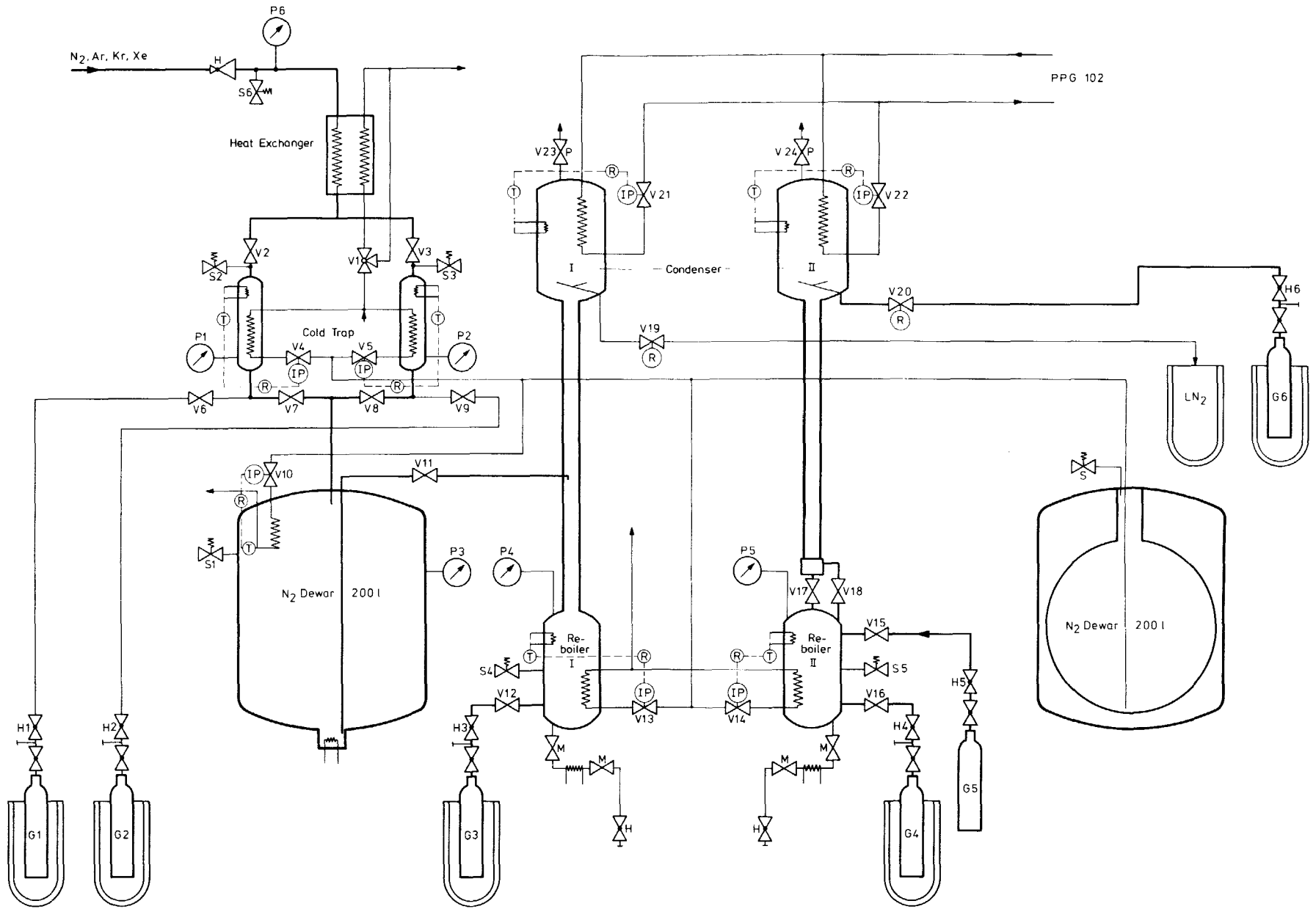


Fig. 7: Flowsheet of the KRYOSEP I-facility

The KRYOSEP II-facility

The KRYOSEP II-facility (Fig. 8) for cryogenic separation of Xe and Kr from the off-gas of a continuous dissolver with a closed helium-purge loop has the same pretreatment steps as the KRYOSEP I-facility, with the difference that only traces of O₂ (from inleaking air) have to be removed together with the NO_x. The facility has been described previously²⁾.

The KRYOSEP II-facility which is not intended for hot operation is at present being repaired and improved and is expected to be ready for start up in late fall.

II. Hot dissolver experiments

The dissolver (Fig. 9) is a round-bottomed in the lower part cylindrical, in the upper part conical stainless steel vessel with jackets for steam heating. The throughput is 2 kg HM/d.

The heavy metal ash is brought into the continuously operating dissolver (D 301) by an auger. The THOREX reagent is fed in near the bottom of the vessel. The fuel solution leaves the dissolver near the top and flows into the intermediate storage tank F 101. The concentration and the liquid level in the dissolver are measured by dip tubes. The helium from these measurements leaves the dissolver transporting the fission gases and the remainder of the NO_x and the water vapor which are not condensed in the heat exchanger D 201 to the off-gas cleaning facility (Fig. 10).

The radioactive components are semicontinuously monitored at four points (MS 1 - 4) by multichannel analysers. Gas samples can be taken before (GM - 1) and after (GM - 2) the off-gas clean-up. The gas first enters absorber columns to remove J₂ and NO_x. It is scrubbed with a 0,5 M HNO₃ / 0,1 % H₂O₂ solution in the first column (WK 1) and with a 5 M NaOH / 0,1 M Na₂S₂O₃ solution in the second column (WK 2). The NO_x concentration is measured before and after the absorber columns. The absorber columns are followed by demisters (DM WT 1 and 2) for water aerosol removal. Heated absolute filters (AF 1 and 2) are passed before the gas reaches the membrane gas pumps (GP 1 and 2). After adsorption of water and impurities like NO_x or CO₂ on molecular sieves (MSP 1 and 2) the oxygen is removed by reaction with copper catalysts (BTS 1 and 2) before the remainder of the iodine is removed by silver impregnated silica gel type AC 6120 (JOF 1 and 2). Xenon and part of the krypton are frozen out in the liquid nitrogen cooled cold traps (GF 1 and 2). Before the helium leaves the clean-up system the remainder of the impurities is separated in a liquid nitrogen cooled active charcoal bed.

In two runs 3,7 kg heavy metal ash have been dissolved. The U/Th ratio of the mixed oxide particles was 1 : 5. The burnup was 45 % fima and the cooling time 4 years. Assuming that 7 % of the fission gases had been released during the burning step, the particles still contained 2,7 Ci H-3 and 73 Ci Kr-85. To gain information on iodine removal newly irradiated particles were added to the ash.

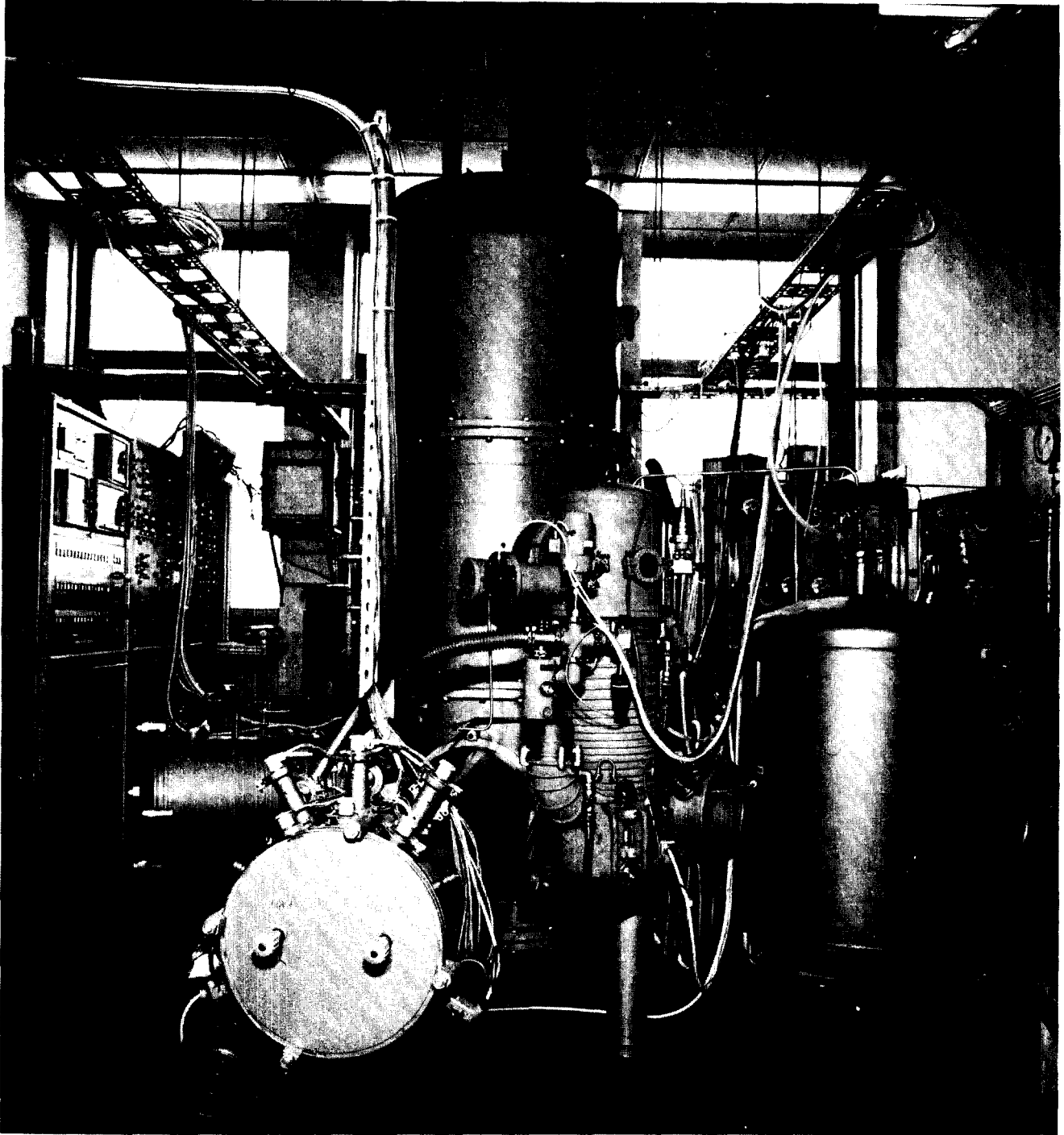


Fig. 8: View of the KRYOSEP II-facility

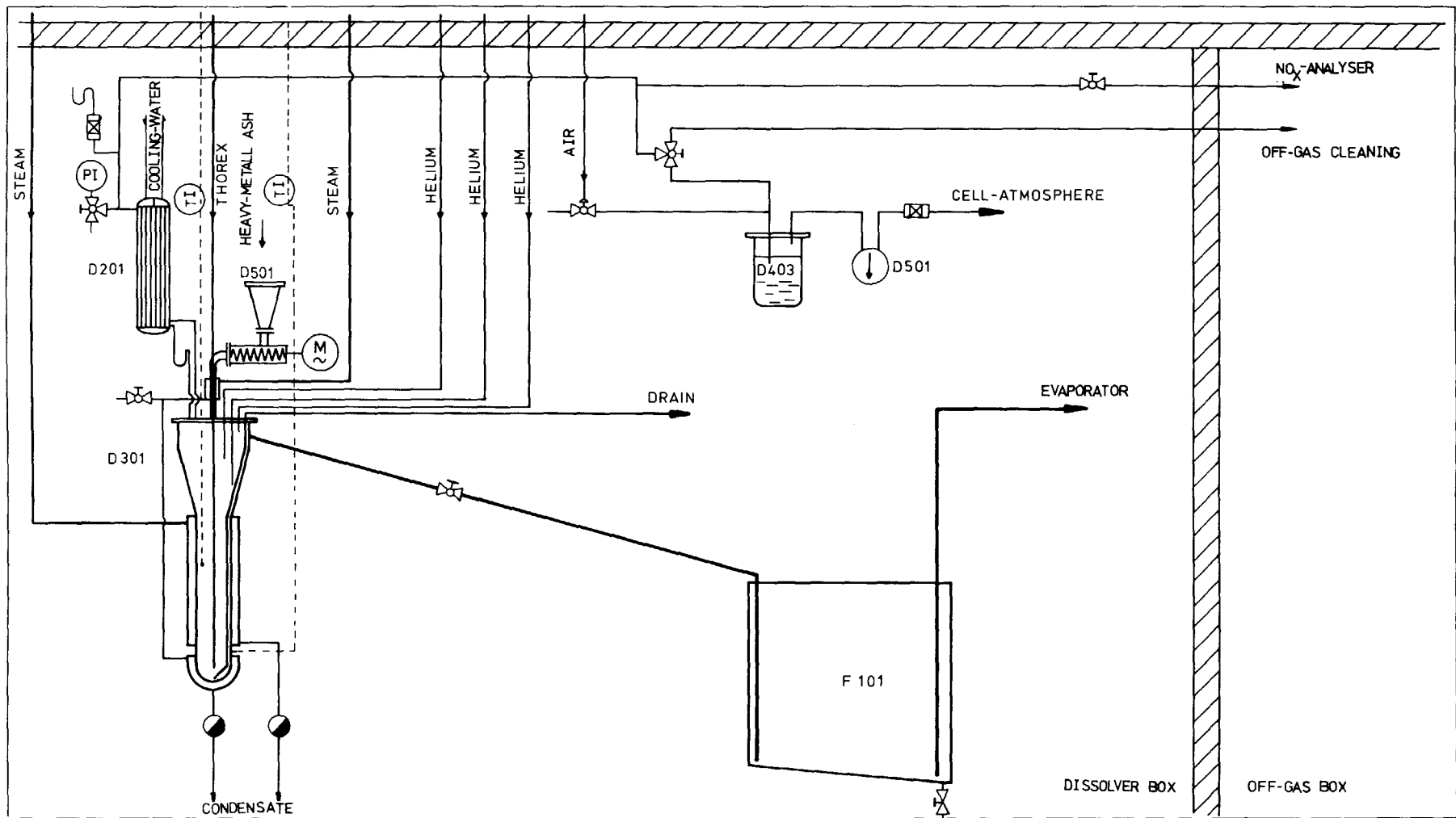


Fig. 9: Flowsheet of the dissolver equipment used for hot tests

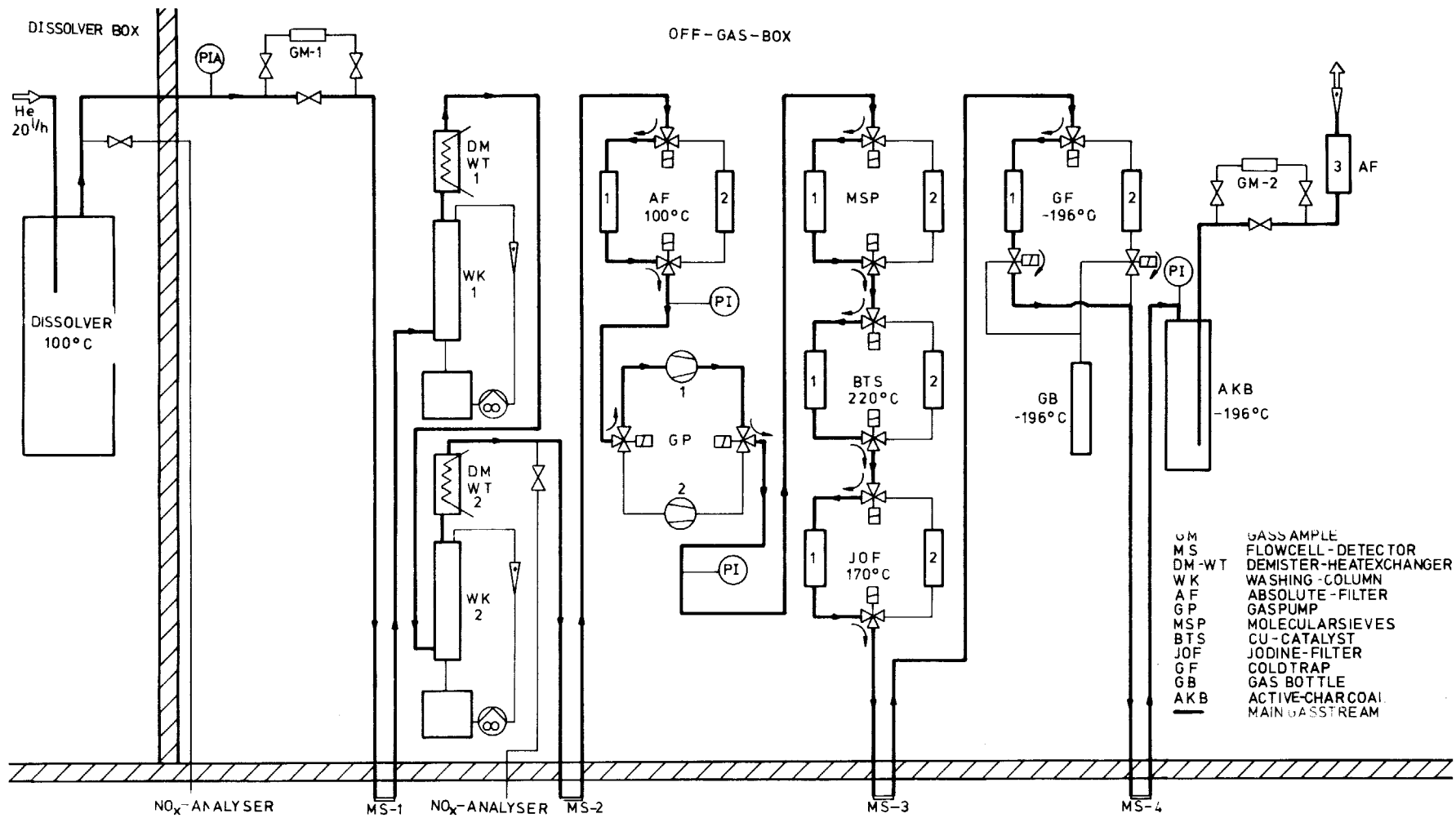


Fig. 10: Flowsheet of the off-gas equipment for the hot dissolver tests

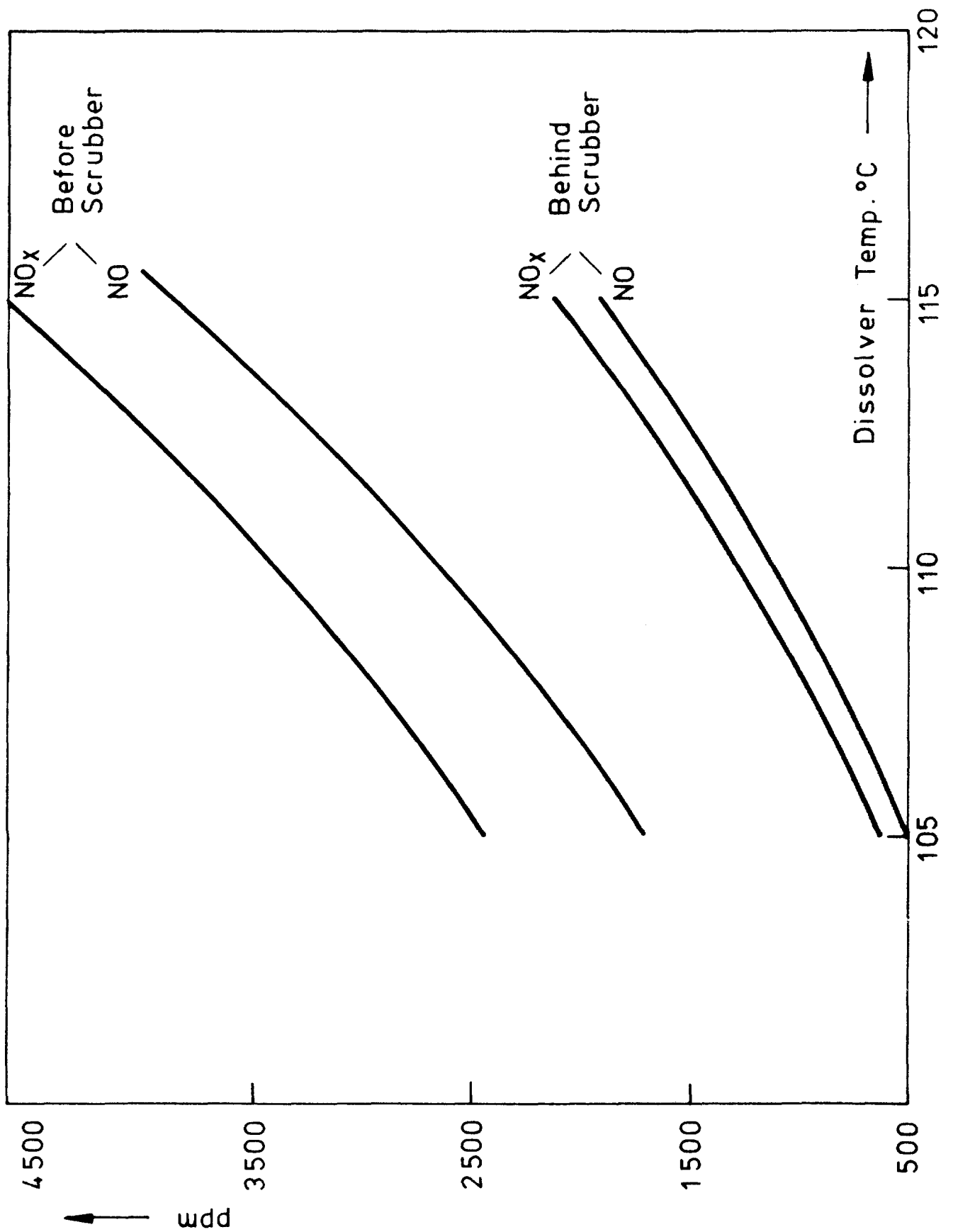


Fig. 11: NO_x concentration in the dissolver off-gas

15th DOE NUCLEAR AIR CLEANING CONFERENCE

The NO_x concentration in the off-gas was found to be dependent mainly on the dissolver temperature (Fig. 11). The NO_x concentration ranged between 2400 ppm and 4700 ppm for dissolver temperature between 105 °C and 115 °C. The main component of the off-gas being helium with only traces of oxygen present, the greater part of the NO_x was NO (~ 80 %). The efficiency of the scrubbers for NO_x was only 65 %, a fact that could be expected from the data in literature 3). For iodine the efficiency of the scrubbers was 99,7 %. 75 % of the absorbed iodine were found in the scrub solution of column WK 1 and 25 % in the solution of column WK 2.

2 % of the tritium inventory of the particles was found in the off-gas, 98,5 % of which were retained in the off-gas clean-up system, indicating that ~ 1,5 % of the tritium in the off-gas existed as 3H_2 . No ruthenium was found in the off-gas. The decontamination factors for Kr and Xe have not been determined yet.

References

1. H. Barnert-Wiemer, H. Beaujean, M. Laser, E. Merz, H. Vygen
14 th ERDA Air Cleaning Conf., Sun Valley, Idaho,
Aug. 2 - 4, 1976
2. J. Bohnenstingl, S.H. Djoa, M. Laser, St. Mastera, E. Merz
P. Morschl
14 th ERDA Air Cleaning Conf., Sun Valley, Idaho,
Aug. 2 - 4, 1976
3. ERDA - 76 - 43 V. 2 (1976) p. 13.44

15th DOE NUCLEAR AIR CLEANING CONFERENCE

AEROSOL AND IODINE REMOVAL SYSTEM FOR THE DISSOLVER OFF-GAS IN A LARGE FUEL REPROCESSING PLANT

J. Furrer, J. G. Wilhelm ⁺), *K. Jannakos* ⁺⁺)

⁺) Laboratorium für Aerosolphysik und Filtertechnik

⁺⁺) Abteilung Reaktorbetrieb und Technik

Kernforschungszentrum Karlsruhe GmbH
Postfach 3640, D-7500 Karlsruhe 1, Germany

Abstract

A newly developed filter combination for the dissolver off-gas in a reprocessing plant with a throughput of 1400 t/yr of heavy metal is presented and single filter components are described. The design principle chosen provides for remote handling and direct disposal in waste drums of 200 l volume. The optimization of housings and filter units is studied on true scale components in the simulated dissolver off-gas of a test facility named PASSAT. This facility will be described. PASSAT will be also used for final testing of the SORPTEX process which is under development. Its concept is included in the paper. The design and function of the new multiway sorption filter providing for complete loading of the iodine sorption material and maintaining continuously high decontamination factors will also be given.

Removal efficiencies measured for aerosols and iodine in an existing reprocessing plant are indicated.

I. Introduction

The risk potential of a reprocessing plant as regards its environment is based almost exclusively on the inventory of radioactive materials, especially fission products and actinides. Part of these materials is converted into off-gas and exhaust air by evaporation and further aerosol generating processes; the radio-nuclides present as gases in the fuel are immediately released into the off-gas during the process of fuel dissolution.

By several filter barriers the release of radioactive materials into the environment is reduced. In case of operation of a reprocessing plant according to the specifications the highest gas borne activity occurs in the dissolver off-gas. In this paper processes and equipment will be described for dissolver off-gas cleaning from iodine and from solid and liquid aerosols, which are being developed and tested, respectively, with a view to a planned German reprocessing plant.

II. Requirements to Off-Gas Cleaning

The requirements to the off-gas cleaning of the large German reprocessing plant are a result of recommendations prepared jointly in 1977 by the Reactor Safety Commission and the Radiation Protection Commission on behalf of the German Federal Minister of the Interior (1). It was specified that the emissions of ^{129}I should be limited to 0.2 Ci/yr, of α -aerosols to 0.05 Ci/yr, and of β -aerosols to 5 Ci/yr. Based on these values and on the emission values for T, C-14 and Kr-85 and applying the "bases of calculation for the determination of radiation exposure

15th DOE NUCLEAR AIR CLEANING CONFERENCE

through emission of radioactive substances with the exhaust air" presently valid in the Federal Republic of Germany, maximum radiation exposures of 4 mrem/yr for the whole body and of 18 mrem/yr for the thyroid are received at the most unfavorable point of exposure.

For an I-129 throughput of 57 Ci/yr in the planned reprocessing plant this implies for the removal of iodine practically completely present in the off-gas that a total removal efficiency of 99.65 % is required. Since iodine released with the vessel off-gas as well as released due to unforeseen handling operations and bypassing the removal devices have also to be taken into account, it is the objective of the work described to reliably guarantee a decontamination factor ≥ 99.9 % of the iodine sorption filter in the dissolver off-gas filter train during the service life of the facility.

The requirements to aerosol filtering depend on the activity concentration of the off-gases which are not only a function of the activity inventory of the plant but decisively of the type, design and number of aerosol generating components and of the way the process is run. As a rule, removal efficiencies ≥ 99.9 % are required.

III. Setup and Layout of the Filter Train for the Dissolver

Off-Gas

Prior to the removal of solid particulates by HEPA filters and before iodine removal the off-gas must undergo preliminary treatment. This preliminary off-gas treatment serves the following purposes:

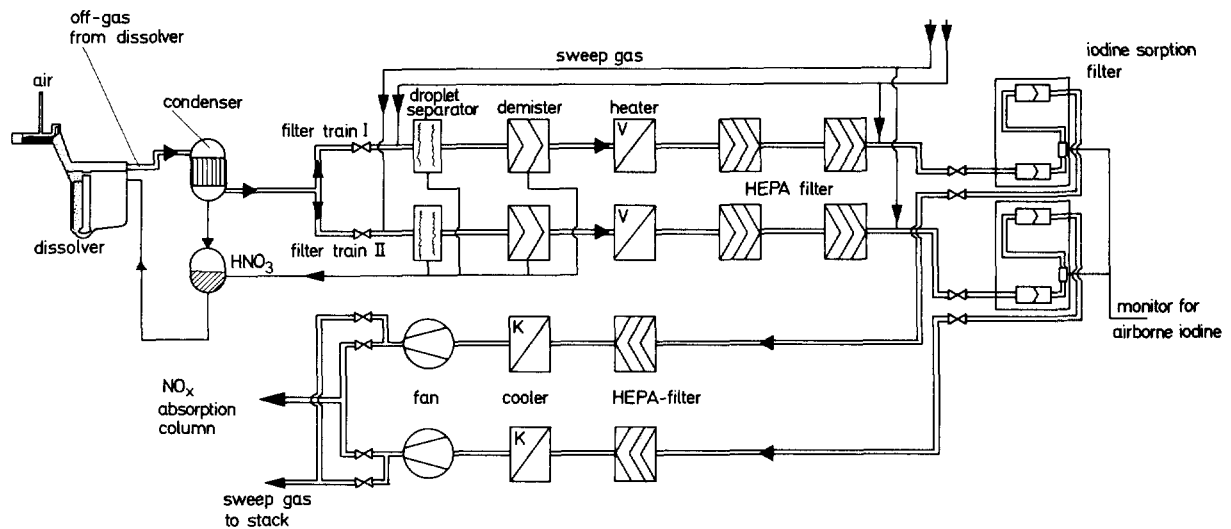
- (1) Reduction of the content of water vapor.
- (2) Removal of droplet aerosols, preliminary removal of solid particulates.
- (3) Reduction of the relative humidity and concentration of corrosive media to tolerable values such that the performance of HEPA filters is not impaired.

The task indicated under (1) is fulfilled by lowering the dew point temperature, possibly by a condenser. To achieve (2), special droplet separators have to be used which guarantee a high removal efficiency also for small droplets ($< 10 \mu\text{m}$ diameter) as well as particulates. To be able to manage variable mass concentrations as well as a broad spectrum of droplets, a distinction must be made between coarse and fine droplet separators. To achieve (3) heaters are provided in the off-gas stream downstream of droplet separators, the temperature rise must ensure the destruction of residual droplet aerosols or transformation into solid aerosols by evaporation.

The eligible corrosive media are above all those nitric oxides whose concentrations are usually reduced by a preceding scrubber (NO_2 absorption). Previous experience will not be sufficient to make statements about the longterm behavior of the HEPA filters at high NO_x concentrations. The planned iodine sorption filters can be conveniently used at a higher nitric oxide concentration.

The layout of the filter train for dissolver off-gas purification can be seen from Fig. 1. The filter train consists of a wave plate separator for coarse droplet removal, a packed-fiber mist eliminator for fine droplet removal, a heater, two HEPA and iodine sorption filters each connected in series, an additional HEPA filter following the iodine sorption filters, a cooler, and the off-gas ventilator. If appropriate, an additional heater is installed between the two first HEPA filters and the iodine sorption filters in order to be able to set the operating temperature of the HEPA filters sufficiently above the dew point temperature of the off-gas so as to avoid damage, although below the iodine sorption filter operating temperature

(130 - 150°C). Accordingly, a cooler should be provided upstream of the HEPA filter following the iodine sorption filters.



KfK
LAF II 52

FIGURE 1 SORPTEx-process for head end iodine removal in a reprocessing plant.

The whole filter train is presently still planned for installation downstream of an NO_2 absorption and an I_2 desorption column in the dissolver off-gas. With this configuration a major portion of the fission product iodine already present as vapor in the off-gas stream is absorbed by the acid recovered in the NO_2 absorption column. Via a downstream desorption column it has to be returned into the off-gas stream to be finally removed in the iodine sorption filters.

Installation of the whole filter train immediately downstream of the dissolver (with a preceding condenser so as to reduce the vapor content in the off-gas) would allow a much simplified flowsheet since the expenditure in terms of process engineering needed to release fission product iodine from the recombined acid can be avoided. The development of this so-called SORPTEx process will be the subject of future R&D activities. The higher activity and acid concentrations in the upstream gas preceding the filter train (due to the lack of removal efficiency of the columns with respect to aerosols) as well as the reduction of the pressure acting in the NO_2 column due to the pressure reduction in the preceding filter train, have to be regarded as drawbacks of this technique. On account of the pressure loss either a fan placed in-between or a greater number of trays in the NO_2 absorption column is required.

IV. Criteria of Selection and Requirements to the Filter Components

For the filter train only passive components are chosen which require little maintenance work and are characterized by a high removal efficiency. In case that a regular replacement was foreseeable during operation, only remotely handled

15th DOE NUCLEAR AIR CLEANING CONFERENCE

filters were eligible which fulfil the following requirements regarding this characteristic:

- Remotely handled filter replacement has to be carried out as far as possible without contaminating the joint room of installation.
- One single, easy to operate remote handling system (hoist unit) must be sufficient for replacement of all filter elements provided in the filter train.
- The filter elements must be capable of being remotely packed into 200 l waste drums without reduction of volume.
- The leaktightness of the filter seats must be capable of being continuously monitored during operation.
- The filter vessels must be capable of being decontaminated.
- The lids of the filter vessels should have the same outer dimensions and be equipped with identical closing systems.
- Provisions must be made that the lids can be closed and opened by the remotely handled hoist unit (in case of failure of the hydraulic closing system) which is also used for the replacement of filter elements (emergency handling).
- Independent lid locking devices must be available which prevent the filter vessels from opening in case of pressure pulses resulting from an incident.
- The lid openings of the filter vessels have to be provided at one level in a straight line of the room of installation in order to be able to perform all necessary work using a hoist unit.

V. Filter Components for Aerosol Removal

Fig. 2 shows the coarse droplet separator. A wave plate separator was designed which is equipped with a self-cleaning system and does not call for any maintenance work. For droplets $> 10 \mu\text{m}$ a removal efficiency $\geq 90\%$ is required. The design of the separator allows flanged connection to the off-gas line; on account of previous operating experience a remotely handled design proved to be superfluous. In case salt crusts are formed, diluted nitric acid is sprayed in by short spraying periods via a nozzle system provided at the gas inlet so that the crusts formed get detached again.

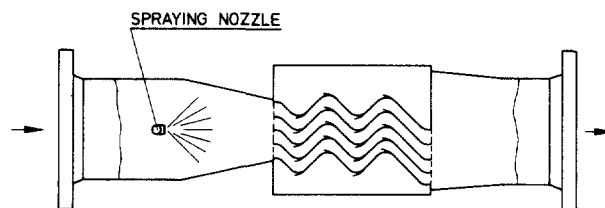


Fig.2 Wave-plate separator, component 1, droplet removal $> 10 \mu\text{m}$

Fig. 3 shows the remotely handled packed-fiber mist eliminator provided in the exhaust air of the wave plate separator. It is intended to remove liquid droplets $< 10 \mu\text{m}$ with a removal efficiency $\geq 99\%$. Moreover, it is to be used as a prefilter for particulates so as to increase the service life of the following HEPA filter. Since a greater surface is offered on the upstream gas side of the fiber package, flow from outside to inside is preferred.

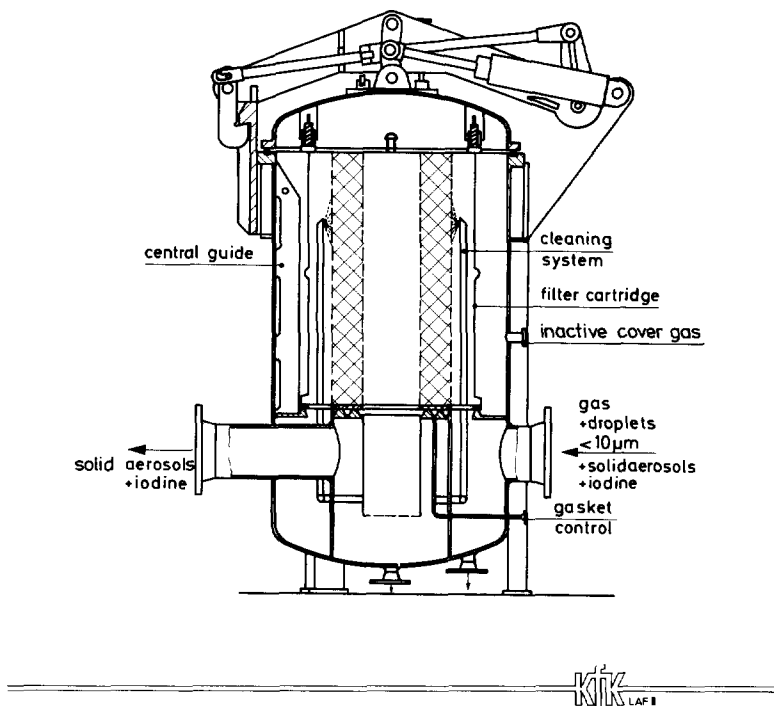


Fig.3 Passat packed fiber mist eliminator,- high efficiency element,- component II, for droplet removal $< 10 \mu\text{m}$

The demister consists of packed glass fibers of about $20 \mu\text{m}$ diameter with a statistically vertical orientation. Impinging droplets are retained by the fibers, combine into larger droplets, and due to gravity and pressure difference they migrate from top to bottom in the fiber layer to reach ultimately the sump in the filter vessel.

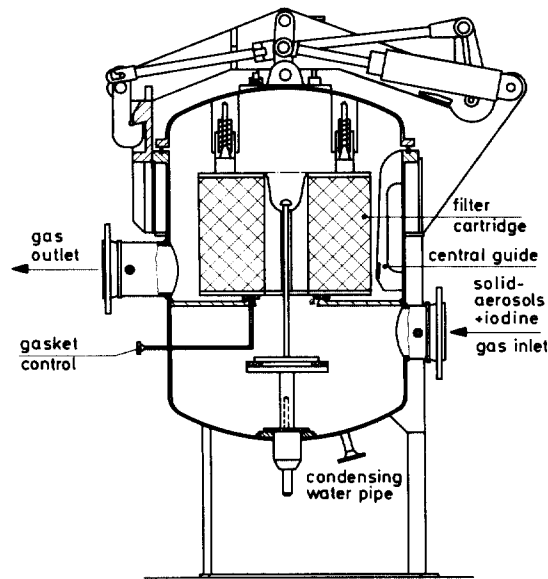
The fiber layer is placed in a sheet metal case open on the bottom and is replaced together with this case. The upstream and downstream gases are routed within this sheet metal case. Plating out of radioactive salts on the outer side of the case in the upper part of the filter vessel and on the inner side of the lid is prevented by sealing and an inactive cover gas. The leaktightness can be monitored continuously, as will be described for the HEPA filter. As soon as an unacceptable high pressure difference over the fiber layer is obtained, a spraying device is actuated which consists of a spray ring with six nozzles surrounding the fiber layer so as to wash out with diluted nitric acid the crystallized salts and the solid aerosols deposited. Steam condensate can possibly be formed by reducing the off gas temperature below the dew point temperature in front of the packed-fiber mist eliminator, which will result in continuous self-cleaning of the fiber layer.

15th DOE NUCLEAR AIR CLEANING CONFERENCE

Preliminary tests were made on a Brink packed-fiber mist eliminator supplied by Monsanto which was not yet delivered as a demister capable of remote handling as described above. The fiber layer was 150 mm deep and had a high packing density. For droplets between 3 and 10 μm a decontamination factor of > 75.000 was obtained which was calculated via the detection limit and with the mass concentration known. The packed-fiber mist eliminator yielded a removal efficiency $> 99\%$ for solid aerosols with particle diameters between 0.1 and 1 μm (uranine test)(2).

In the PASSAT technical-scale facility described at the end of this paper tests are planned for optimizing the remotely handled packed-fiber mist eliminator with a view to pressure reduction, depth of the fiber layer, and packing density for given removal efficiencies. Moreover, studies relate to the deterioration of the removal efficiency by loading with soluble and insoluble salts, to the effect of continuous and batchwise spraying with diluted nitric acid for clean up and to the self-cleaning behavior.

Fig. 4 shows the HEPA filter installed behind a heater in the off-gas stream. The filter vessel also complies with the requirements mentioned above. The filter element is exposed to internal flow so as to keep low the outside contamination with a view to filter replacement. Also in this case continuous monitoring of the leaktightness of the filter seat is possible during operation, inclusive of both the top and the bottom surfaces of the gasket between the filter element and the mounting frame in the filter vessel.



KIK
LAF II

Fig.4 Passat HEPA - filter, component III, removal of solid aerosols $\eta \geq 99.9\%$

15th DOE NUCLEAR AIR CLEANING CONFERENCE

A new HEPA filter element is presently developed. For the time being, an earlier design is used which allows replacement by means of a proven remote handling system. Attempts are made to simplify the design and to increase the temperature resistance to 150°C continuous temperature.

Measurement of the removal efficiencies of filter papers used in HEPA filter elements in the dissolver off-gases (Table I) of two reprocessing plants show that the standards for HEPA filters so far assumed with removal efficiencies > 99.97 % for aerosols in the dissolver off-gas of reprocessing plants are not observed. Removal efficiencies between 99 and 99.4 % were obtained in short-term and long-term investigations. Therefore, several HEPA filters were series connected in both plants.

In the off-gases of the Karlsruhe reprocessing pilot plant (WAK) still different filter papers are investigated. The best suited papers will be installed in newly conceived filter elements which can be bagged out into a 200 l standard waste drum.

In PASSAT an integral in-place filter testing method is to be tested by use of a uranyl nitrate test aerosol so that the safe use of aerosol filters can be ensured in the dissolver off-gases.

VI. Fission Product Iodine Removal

On account of excellent experience obtained with iodine sorption filters (3), using the AC 6120 iodine sorption material (4, 5) in WAK during 2.5 years of operation until now, removal of the total fission product iodine from the dissolver off-gas is planned to be achieved on the AC 6120 solid iodine sorption material. A multitude of measurements of the removal efficiency performed in the course of dissolving and standstill periods showed that with the help of the iodine sorption filter installed in WAK, which does not yet comply with the design described in the subsequent text, removal efficiencies of at least > 99.9 %, usually > 99.99 %, were achieved.

With this method silver in the amount of about 10 kg Ag/GW_{e1} · yr is used. Due to the relatively low consumption of silver, conversion is not planned of the silver iodide obtained in the sorption material while recovering the silver although would be quite feasible in additional process steps.

The iodine sorption filters, Figs. 5, 6 and 7, presented here were designed and built for removal of about 400 kg/yr of fission product iodine in filter elements, which can be transferred into the usual 200 l waste drums for radioactive waste without further conditioning or loss of drum volume.

This led to the selection of a filter element having the shape of a cylindrical deep bed filter with a diameter of the iodine sorption material layer of 50 cm and a bed depth of 69 cm. This bed depth is solely determined by the highest possible loading capacity, whilst the required removal efficiency is achieved already with a much lower bed depth (and residence time, respectively) (5).

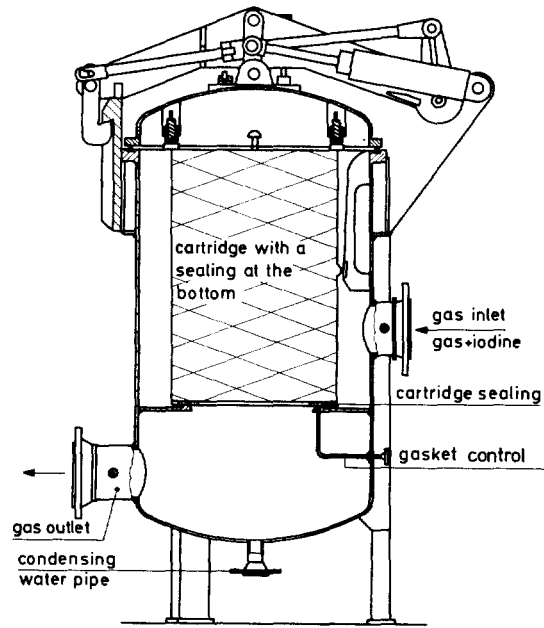
15th DOE NUCLEAR AIR CLEANING CONFERENCE

Table I Removal Efficiencies of HEPA-Filters in Dissolver Off Gases of Nuclear Fuel Reprocessing Plants (NFRP).

Operating conditions at the filter paper:

	NFRP I	NFRP II
type of filter paper	SS 6	Astrocel
temperature	150 ^o C	130 ^o C
NO _x -concentration	< 10 Vol.%	< 10 Vol.%
linear gas velocity	2,2 cm/s	4,2 cm/s

Test-No.	NFRP 1					NFRP II
	1	2	3	4	5	6
sampling place in relation to absorption column	up-stream	down-stream	down-stream	down-stream	up-stream	down-stream
sampling time (h)	6,5	6,25	8,5	8,5	6,75	960
removal efficiency (%)	99,3	99,03	99,27	99,23	99,0	99,24
decontamination factor	143	103	137	130	100	132



KFK
LAF 1

Fig.5 Passat iodine filters, components IV+V, removal of gaseous iodine compounds $\eta \approx 99.9\%$

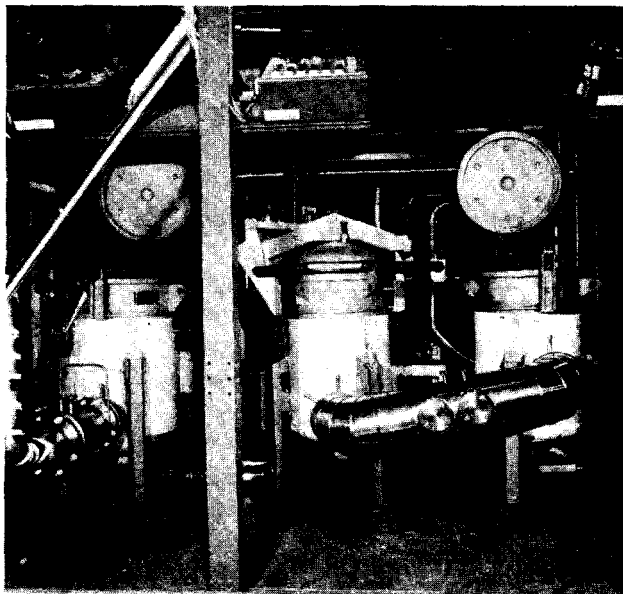


Fig. 6 Filter housings of mist eliminator (left) and two iodine sorption filters (right)

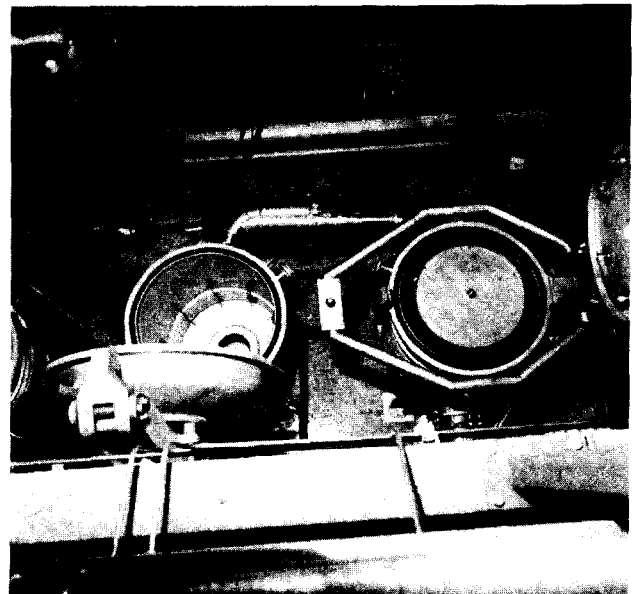


Fig. 7 Filter housings of iodine sorption filters, one cartridge loaded (right)

15th DOE NUCLEAR AIR CLEANING CONFERENCE

Although the design described causes a higher pressure loss during operation as compared with a ring layer of the sorption material, advantages were decisive, such as

- simple design,
- guaranteed leaktightness of the sorption layer (if the flow is directed from top),
- maximum quantity of sorption material filling, and
- complete utilization of the sorption material.

The service life of a filter element in the dissolver off-gas is limited by the maximum iodine load of 11.8 kg. This means that the filter element has to be replaced after about 10 days of filter operation, assuming a daily capacity of about 4 t of uranium. Therefore, a very stable design had to be chosen for the filter vessel in order to avoid tolerances occurring after many replacements. Due to the frequency of filter element replacements resulting from operation, the replacement itself must be an easy and fast process and, moreover, the tight seal of the filter element in the filter vessel must be inspected continuously. Therefore a design was selected which allows to apply a test pressure (compressed air) to the whole circumference of the gasket. The gasket (between the filter element and the mounting frame of the vessel) was attached as usual at the filter element and is replaced with the latter. If a filter element is used twice (in the first and second vessel of a two-stage filter) care was taken by use of a staggered arrangement of the sealing edges in the filter vessels that the sealing of the filter unit after relocation is achieved by a part of the gasket not previously compressed.

The already described high degree of preliminary aerosol removal is intended to avoid as much as possible contamination of the filter vessel and filter element by fission product aerosols (including hard γ -emitters). Nevertheless, plating out of radioactive aerosols in pipings, valves and filter vessels cannot be safely excluded for extended operation. Therefore, the design chosen for the iodine sorption filter allows remote filter replacement and remote packing of the filter element into the waste drum as well as bagging out.

To be able to fully use the iodine sorption material containing silver, two iodine sorption filters connected in series will be provided. The filter element located in the first vessel in the direction of flow is exhaustively loaded (Fig. 1), whilst the filter element in the second vessel is used only to remove the iodine occurring in the exhaust air stream of the first filter. This filter element is exhaustively loaded only after its relocation into the first vessel in flow direction. At the end of this period of use the relocated filter element shows practically no residual removal efficiency and the required total removal efficiency of $\geq 99.9\%$ must be obtained solely by the second iodine sorption filter. At this time any leak of the second filter can fully impair the removal efficiency achievable.

Since at the end of the service life of the filter element in the first vessel the iodine concentration in the downstream air is practically equal to that in the upstream filter air, the clean air side of this filter as well as the whole zone up to the sorption layer of the second filter element are contaminated by off-gas with a high iodine concentration. Prior to replacing the filter elements this contamination has to be removed by scavenging with air free from iodine or, if applicable, iodine release into the clean air must be avoided by flow reversal or sealing. Therefore, in the design of the filter vessel, the flow was routed such that dead spaces are largely excluded which cannot be flushed.

15th DOE NUCLEAR AIR CLEANING CONFERENCE

In addition to the relocation of filter elements for complete loading a piping is in discussion which allows alternate loading of the filter vessel (Fig. 8). An appropriate method involves the use of at least 7 valves which have to be controlled by a program and locked in order to avoid wrong connections. Besides, on account of unavoidable contamination of the "clean air side" of each of the two series connected filters in the course of switching over, loss of the removal efficiency must be expected, the more so since scavenging by filtered air is possible only during operating phases strictly limited in duration.

A major portion of the PASSAT test program will be devoted to testing the relocation and switching operation under realistic operating conditions, especially with a view to the iodine partial vapor pressure and the off-gas condition. For the quantitative determination of clean air contamination possibly occurring during filter replacement radioactively labeled iodine is used.

As an alternative to iodine removal by the assembly described the use of a multi-way sorption filter (MWS filter) is considered (6). However, use of this filter calls for a perfect flow behavior of the iodine sorption material, which can be proved only by several years of operating experience. The newly developed MWS filter offers the advantages of a countercurrent filter. The size of the surface and the filter bed depth can be broadly varied as opposed to the countercurrent filter; the influence of the sorption material pouring cone on the bed depth of the sorption material was completely eliminated (Fig. 9).

Fresh sorption material is introduced batchwise from top into the MWS filter and withdrawn at the bottom after passage through two or more filter chambers and complete loading. The off-gas stream to be cleaned is passed several times (at least twice) through the sorption material in the horizontal direction. In case of plane parallel withdrawal and appropriate design of the zone between the two filter chambers the sorption material can be completely loaded while maintaining a given removal efficiency. Mechanical leaks via the sorption layer can be excluded without requiring additional sorption material.

VII. Description of the PASSAT Technical Scale Test Facility

The performance of the filter train described calls for cooperation of quite a number of single units with no experience available on their performance and reliability under the conditions prevailing in the dissolver off-gas of a reprocessing plant. Due to its importance in safety technology the availability of the dissolver off-gas section directly influences the availability of the reprocessing plant. To avoid hazards in terms of safety and economy, extensive testing in cold and hot operation is therefore required. For cold testing of the whole filter train and for optimizing individual components the technical scale PASSAT facility was built which allows to simulate the dissolver off-gas of a reprocessing plant.

PASSAT consists of a room for filter installation, accommodating the entire filter train, the remote handling devices for filter replacement and packing, and the equipment for the production and circulation of the simulated dissolver off-gas.

Fig. 10 shows the block diagram for PASSAT. The volume flow of the simulated dissolver off-gas can be freely set between 50 and 250 Nm³/h and so includes the off-gas flows under discussion for the dissolver off-gas train of a reprocessing plant having a daily capacity of about 4 t of heavy metal.

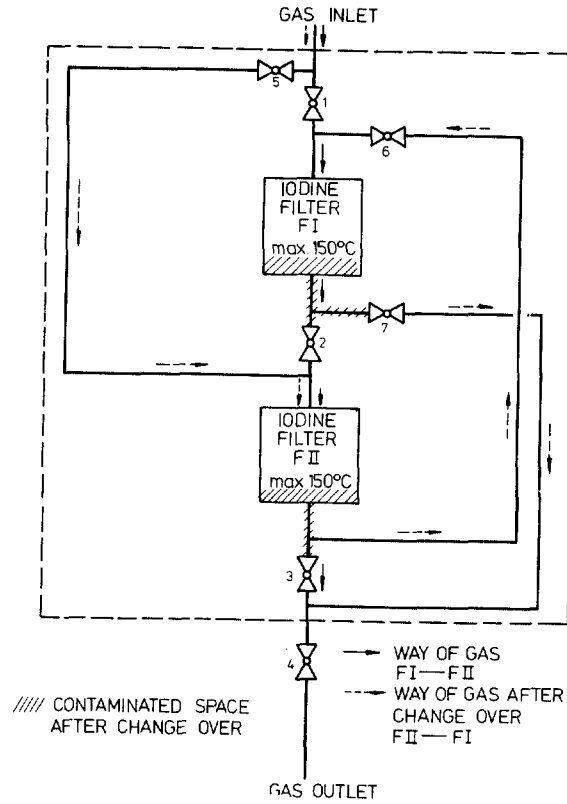


Fig. 8 Iodine filter switching system

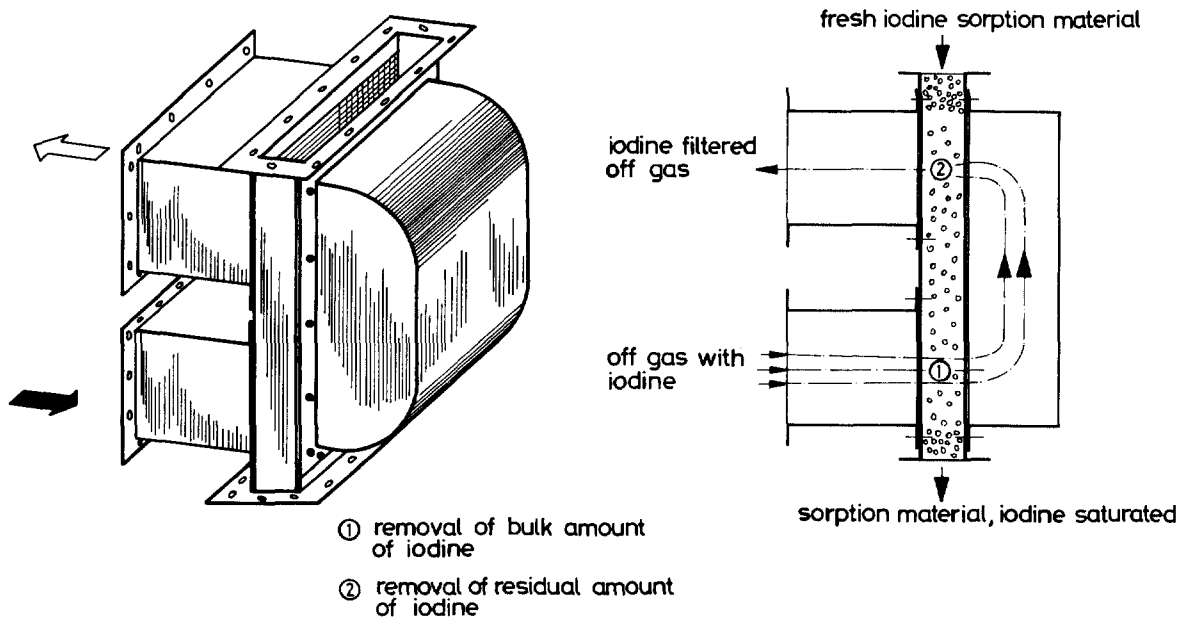
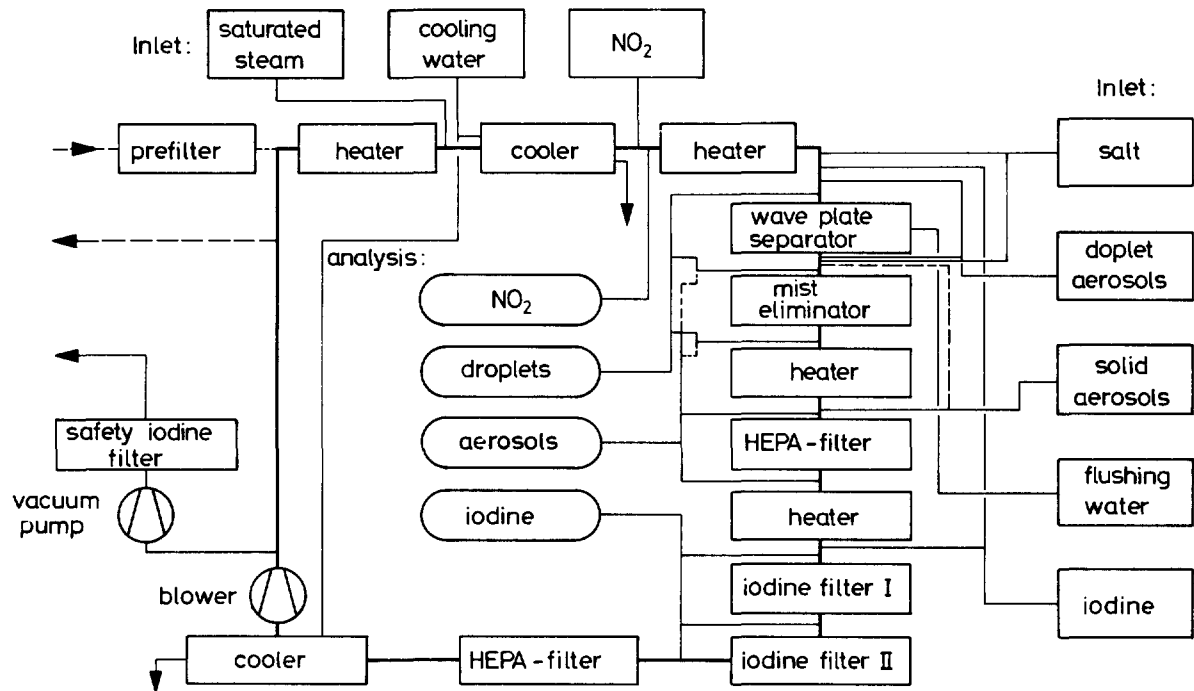


Fig.9 Multiway iodine sorption-filter



KfK LAF II 52 1977

Fig.10 Process flowsheet of the Passat test facilities

For reasons of safety and supply PASSAT can be operated with fresh gas or recycled gas depending on the operating conditions. Recycling is intended especially at higher nitric oxide concentrations and in cases where radioactively labeled iodine is fed into the system.

Upstream of the filter train an operating pressure of about 80 mbar below atmospheric pressure is set in order to simulate the specified inlet pressure of the filter train of a reprocessing plant. This pressure is determined by the pressure difference over the dissolver and the subsequent columns.

The gas upstream of the filter train may consist of an air-water vapor mixture of 30 - 100 % relative humidity kept within the temperature range from 30°C to 75°C. The temperature of the gas flow may be increased up to 160°C upstream of the HEPA and iodine filters. The NO₂ content in the upstream gas may reach up to 10 vol.%. The maximum pressure difference permitted over the whole facility is 0.5 bar.

Test droplet aerosols are fed into the droplet separators and measured according to the flowchart represented in Fig. 10, with droplet sizes > 10 μm attained with a single-component nozzle at the wave plate separator and droplet sizes of 1 - 10 μm attained with a two-component nozzle at the packed-fiber mist eliminator. Sampling and measurement are performed isokinetically at a constant pressure of the plant by use of a light scattering instrument calibrated with respect to droplets.

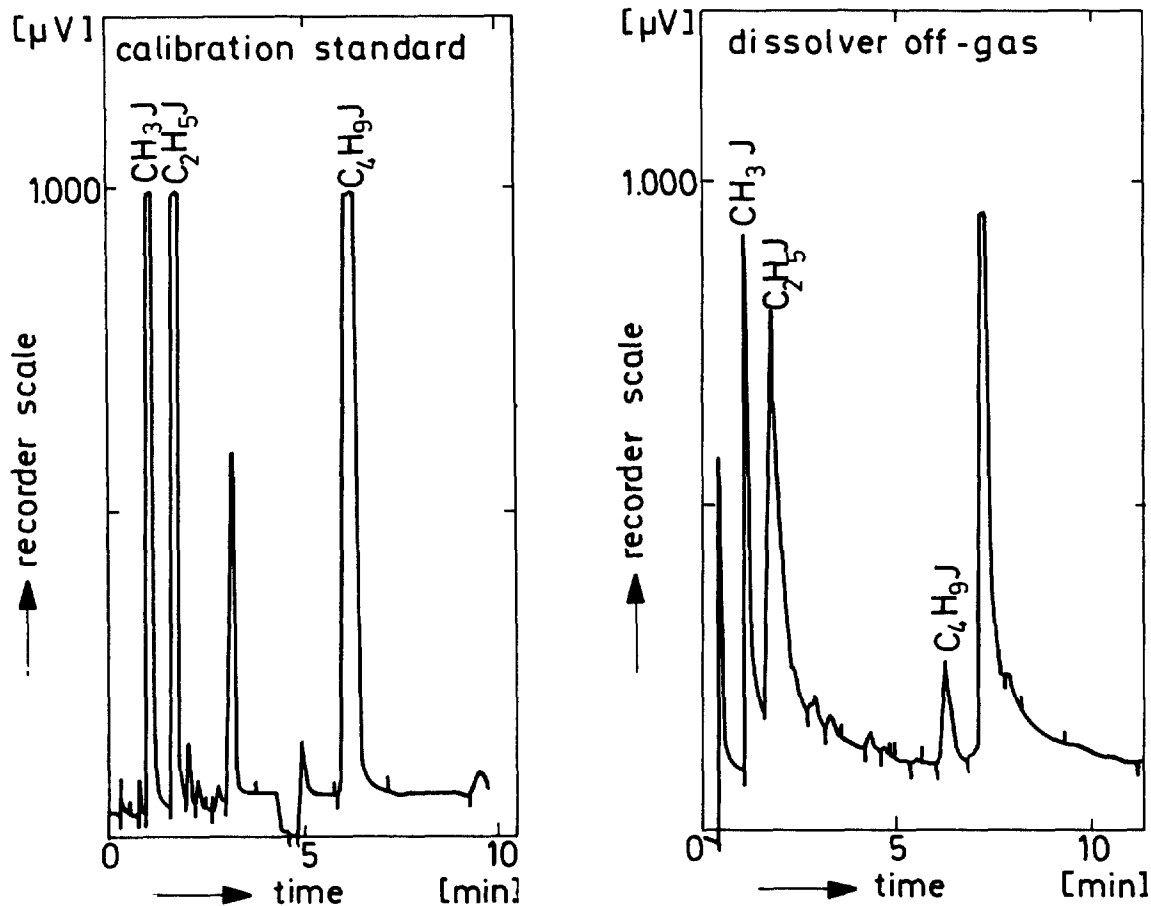
With respect to the HEPA filter, the removal of particulates with a diameter of about 0.1 μm will be tested. They are generated by an aerosol generator spraying a 1 % sodium fluoresceine solution (uranine) into the homogenizer where the droplets are dried. Sampling is made isokinetically upstream and downstream of the filter.

A partial gas stream is drawn through a measuring filter. The filters are evaluated with a spectral fluorimeter determining the mass concentration. The distribution of aerosol particle sizes is determined by pictures taken with the X-ray electron microscope; subsequently the particles are classified and counted.

The iodine released during dissolution of spent fuel elements mainly occurs as elemental iodine. Organic iodides are formed only at low concentrations by the recycled and recombined acid.

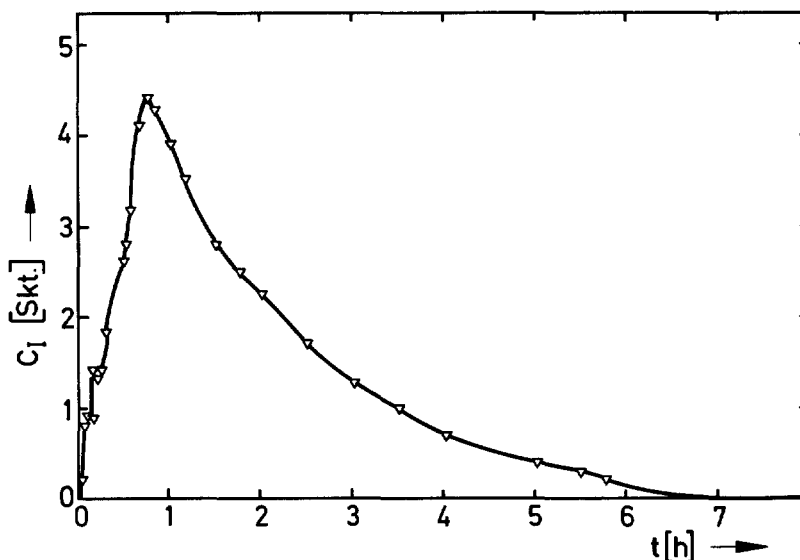
Fig. 11 shows the gas chromatogram of the dissolver off-gases of the WAK during a dissolution period (7). As compared with the iodine inventory of the dissolver of about 18 g and an off-gas throughput of 100 m³/h, the concentration of organic components was less than 0.05 % of the total inventory.

In Fig. 12 the iodine concentration curve has been plotted which is typical of a dissolution period in WAK. The iodine concentration was monitored with an iodine detector. The respective plots are obtained during Kr-85 measurement. The wet chemical method according to Duflos which is used in PASSAT and which relies on the reaction of an alkali iodide with ammonium ferric sulfate in sulfuric acid solution allows the momentaneous increase of iodine production by addition of the alkali iodide and thus the simulation of the iodine concentration curve in the dissolver off-gas (8).



KfK LAF II

Fig. 11 Gas-chromatogram of the calibration standard in toluene and of the dissolver off-gas



KfK LAF II 52 1977

Fig. 12 Iodine distribution in the WAK dissolver off-gas during dissolution

The decontamination factors of the individual filter stages are determined by gas sampling upstream of, between and downstream of the filters, accompanied by chemisorption of iodine on impregnated iodine sorption material and measurement of the ^{131}I activity added as a tracer.

Loading of the first filter stage is indicated by measurement of the iodine concentration after iodine penetration, using an iodine detector. After a given concentration has been reached, a signal is released for filter replacement.

The investigation program performed at PASSAT includes the development and testing of remotely handled devices for the replacement and bagging out of filter units (Fig. 13). In this program a remote handling device was developed and tested which includes a single track trolley and a hoist allowing easy performance of all manipulations without spreading the contamination into the filter cell. All the filter vessels were arranged in one line so that both replacement of the filter elements and emergency handling of the filter vessels can be performed with the same hoisting equipment.

One of the main problems during reloading is the contamination free transport of filter elements out of the cell of the filter train. A simple double lid lock was conceived which allows bagging in and bagging out of the filter elements with the help of the waste drum. For coupling the waste drum on the lock a lifting-swiveling mechanism was used instead of the previously employed coupling vehicle. These are the advantages of this mechanism:

- no tracks and track drive,
- no cable takeup reel and cables,
- no emergency handling of the vehicle drive,
- accurate positioning possible by manual operation.

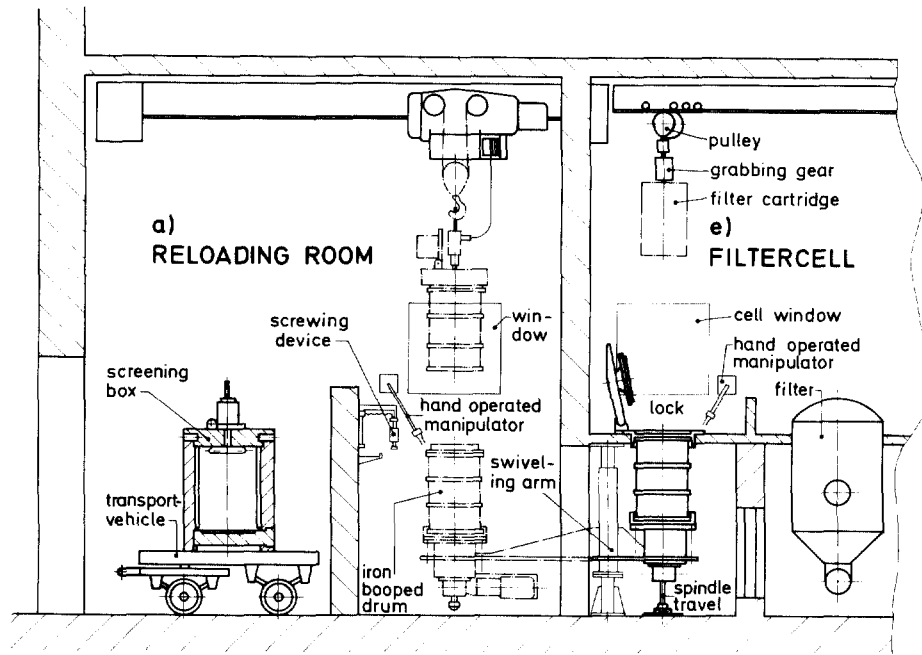


FIG.13 Lock for contaminated filter cartridges

The first true-scale cold tests with the cell lock have performed satisfactorily.

Acknowledgments

The authors express their gratitude to all the cooperators in the PASSAT project and particularly to Messrs. H.-G. Dillmann, R. Herrmann, R. Kaempffer, H. Mock, G. Potgeter, and M. Tuzek.

References

- 1) GRS: Grundsätzliche sicherheitstechnische Realisierbarkeit des Entsorgungszentrums. Beurteilung und Empfehlungen der Reaktorsicherheitskommission (RSK) und der Strahlenschutzkommission (SSK); (1977).
- 2) A. Briand, J. Dupoux: Mesure en laboratoire et en usine l'efficacité des éléments filtrantes et du papier filtre par la méthode à l'aérosol de fluorescéine sodée (uranine). Norme AFNOR NFX 44 011, V/835/77, p. 249.
- 3) V. Böhmer, G. Herrmann, H.-P. Wichmann: Messungen zur Bestimmung der Rückhaltung und Ableitung von I-129 bei der WAK, Conference paper of Reaktortagung 1977, p. 393.
- 4) J.G. Wilhelm, H. Schüttelkopf, An Inorganic Adsorber Material for Off-Gas Cleaning in Fuel Reprocessing Plants, CONF-720 823, p. 540 (1972).

15th DOE NUCLEAR AIR CLEANING CONFERENCE

- 5) J.G. Wilhelm, J. Furrer, E. Schultes, Head-end Iodine Removal from a Reprocessing Plant with a Solid Sorbent. CONF-760 822, p. 447 (1976).
- 6) M. Ohlmeyer, J.G. Wilhelm: Filteranlage zum Reinigen von Gas- oder Luftströmen, DT/OS 2540141, March 10, 1977.
- 7) J. Furrer, R. Kaempffer, R. Gerhard: Messung von Iodverbindungen im Abgas der WAK. KFK 2500, p. 121 (1977).

DISCUSSION

BURCHSTED: What fiber was used in your demister?

FURRER: We used in our demister packed glass fibers of about 20 μm diameter with a statistically vertical orientation.

BURCHSTED: What was the air temperature at the HEPA filter?

FURRER: At the HEPA filter, we work at 120°C up to 150°C.

BURCHSTED: I'd be interested in knowing the construction of that filter.

FURRER: A new HEPA filter element is presently developed. For the time being, an earlier design is used which allows replacement by means of a proven remote handling system. Attempts are made to simplify the design and to increase the temperature resistance to 150°C continuous temperature.

BELLAMY: I have a question along the same lines for the silver zeolite used. Could you tell us what the level of silver was on the silver zeolite and if there are plans to recover or regenerate that material?

FURRER: We don't want to regenerate. We don't think that the silver price for iodine removal is too high. With this method, silver in the amount of about 10 kg Ag/GW_{e1}.yr is used. Due to the relatively low consumption of silver, conversion of the silver iodate obtained in the sorption material is not planned. Nevertheless, recovering the silver would be quite feasible by additional steps.

GRADY: Would you explain a little more about the reason for putting HEPA filters before the iodine bed and, again, after the iodine bed but before the NO_x adsorber? Why do you need that much filtration in that part of the process?

FURRER: There may be aerosol generation in the filter beds; for example loss of silver nitrate impregnant. Therefore, we set a second HEPA filter behind the iodine filters as a safety filter for the following sand.

GRADY: I see, so you're saying that the particulates that are getting through the mist eliminator possibly will cause some problems in your iodine bed or downstream?

FURRER: Yes.

T. R. THOMAS: Did you mention that you would like to try the iodine adsorbent before the nitric acid scrubber?

FURRER: Yes.

15th DOE NUCLEAR AIR CLEANING CONFERENCE

T. R. THOMAS: What are the advantages?

FURRER: The advantages are: a) no iodine loading of the scrubber solutions; b) no contamination by aerosols of the scrubber solution; c) no further iodine desorption process.

T. R. THOMAS: Would you expect to have problems with nitric acid, NO_x , or particulates? Would you still remove particulates before the iodine adsorbent?

FURRER: Although we haven't tried it yet, we will try this material at very high concentrations because we expect concentrations up to 30 volume percent of NO_2 .

T. R. THOMAS: Is there an advantage to keeping iodine out of the nitric acid scrubber?

FURRER: We tried this method in the DOG of the French reprocessing plant in Marcoule with great success and high removal efficiencies.

T. R. THOMAS: Can you heat AC/6120 to a high enough temperature to regenerate (i.e., 400-500°C)? Doesn't the silver nitrate run off?

FURRER: The silver nitrate does not run off. We ran it up to 500°C and also some melting occurred on the surface, but the silver nitrate did not evaporate.

T. R. THOMAS: It doesn't melt or change the structure?

FURRER: It melts normally at 210°C, but it doesn't change the structure or removal efficiency.

T. R. THOMAS: From your experience with the WAK, how long have you had an AC/6120 bed in service and what is the iodine loading obtained?

FURRER: The sorption material was in for one year of continuous operation in a ring layer-filter. We reached a capacity of about 80% of iodine loading and had a removal efficiency of more than 99.9%.

15th DOE NUCLEAR AIR CLEANING CONFERENCE

NOBLE GAS SEPARATION WITH THE USE OF INORGANIC ADSORBENTS*

D. T. Pence, C. C. Chou, J. D. Christian, and W. J. Paplawsky
Science Applications, Inc.
4030 Sorrento Valley Boulevard
San Diego, California 92121

Abstract

A noble gas separation process is proposed for application to airborne nuclear fuel reprocessing plant effluents. The process involves the use of inorganic adsorbents for the removal of contaminant gases and noble gas separation through selective adsorption. Water and carbon dioxide are removed with selected zeolites that do not appreciably adsorb the noble gases. Xenon is essentially quantitatively removed with a specially developed adsorbent using conventional adsorption-desorption techniques. Oxygen is removed to low ppm levels with the use of a rapid cycle adsorption technique on a special adsorbent leaving a krypton-nitrogen mixture. Krypton is separated from nitrogen with a special adsorbent operated at about -80°C . Because the separation process does not require high pressures and oxygen is readily removed to sufficiently limit ozone formation to insignificant levels, appreciable capital and operating cost savings with this process are possible compared with other proposed processes. In addition, the proposed process is safer to operate.

I. Introduction

A number of techniques have been proposed for noble gas separation from airborne nuclear fuel reprocessing plant effluents. Cryogenic distillation has received the most attention because the required equipment is similar to that used in air separation technology. Also, a cryogenic distillation process for separating krypton and xenon from a reprocessing plant off-gas stream has been demonstrated at the Idaho Chemical Reprocessing Plant;^(1,2) however, the original design was intended for partial rather than complete removal of the noble gases.

A process is under development at Oak Ridge National Laboratory that involves the use of fluorocarbon absorption and selective distillation for product separation. This process has been described and discussed in several previous Air Cleaning Conference papers^(3,4) and requires some pressurization and low-temperature operation.

Several processes have been proposed that involve a pressure-swing technique using charcoal adsorbents for noble gas separation, but have not been developed for reprocessing plant application.^(5,6)

The process reported in this paper is being supported under a DOE-sponsored program for the development of an integrated off-gas treatment process for nuclear fuel reprocessing facilities. Because

*Work performed under USDOE (SRO) Contract EY-77-C-09-0979

15th DOE NUCLEAR AIR CLEANING CONFERENCE

the complete process scheme has only been recently developed and the patent application is still in progress, only a general description of the proposed process will be provided.

II. General Process Description

A schematic process flow diagram is shown in Figure 1.

NO_x and Semivolatile Removal

The dissolver off-gas is first passed through an NO_x adsorption tower and condenser where most of the NO₂ is converted to nitric acid for recycle to the dissolver. The remaining NO₂ and NO are then directed through an interchanger and a heater prior to entering an NO_x destructor.

The NO_x (primarily NO and NO₂) entering the destructor is catalytically reduced to nitrogen and water on a bed of hydrogen-form synthetic mordenite using ammonia as the reducing gas.^(7,8,9) The catalyst bed temperature is maintained at about 400 °C. Most of the semivolatile compounds, such as ruthenium, are expected to plate-out on the NO_x destructor catalyst. In our laboratory tests, it has been observed that volatilized ruthenium can be removed on the catalyst bed with a decontamination factor (DF) of greater than 200 at airborne ruthenium concentrations equivalent to 0.01% volatility of the ruthenium present in the dissolver solution. This amount of ruthenium is probably an order of magnitude or so higher than that which will actually become volatilized, so it is a conservative estimate.

The attainable semivolatile DF has not yet been defined because of the sensitivity of our analytical techniques. These techniques are being improved to increase the attainable sensitivities.

After the NO_x destructor, the off-gas flows through the interchanger where it is cooled to about 150 °C while it is heating the feed gas to the NO_x destructor. The cooled gas then enters the iodine adsorbent bed where the iodine is removed. The iodine adsorbent will either be the German-developed, silver nitrate-impregnated, amorphous silicic acid catalyst material, AC 6120,⁽¹⁰⁾ or silver-exchanged synthetic mordenite.⁽¹¹⁾ These materials, and others are being evaluated for this application in another recently initiated task of this DOE-sponsored program, and the results will be reported at a later meeting. Two iodine removal beds will be placed in parallel so one can be in service while the other can be replaced or regenerated.

It should be noted that the proposed component arrangement is conceptual and subject to change pending the results of the iodine adsorbent evaluation studies. There is some evidence⁽¹⁰⁾ indicating AC 6120 material may perform better if it is located prior to the NO_x absorption column. Also, the affect of iodine on the NO_x destructor catalyst has not yet been determined.

Water Removal

After the iodine adsorbent bed, the off-gas is cooled to near ambient temperature, and the bulk of the water removed with a

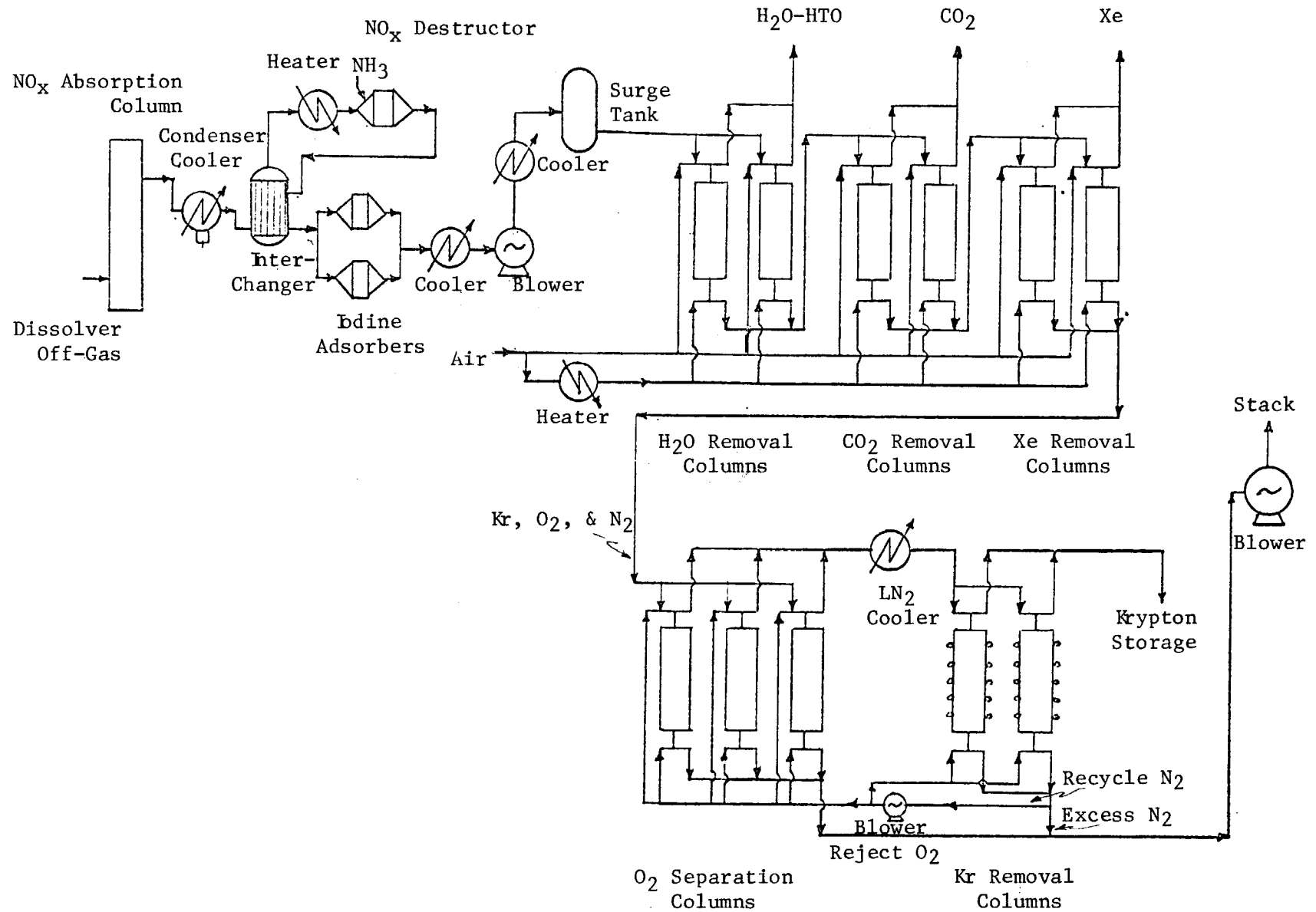


Figure 1. Schematic Flow Sheet For Noble Gas Separation With The Use Of Selective Inorganic Adsorbents.

15th DOE NUCLEAR AIR CLEANING CONFERENCE

condenser. Type 3A zeolite is then used to remove the remaining water to about 1 ppm. The Type 3A zeolite is used because it will not appreciably coadsorb any of the other remaining gaseous species. Two water removal columns will be operated in parallel so that one can be regenerated while the other is in service. Before the water is removed, the water-laden column is given a short purge of air in the feed direction to ensure no residual contaminant gases other than water remain in the column.

Carbon Dioxide Removal

Following water removal, carbon-14 containing carbon dioxide is then selectively removed with Type 4A zeolite. The physical arrangement using two parallel adsorption beds is similar to that of the water removal step. The other remaining gaseous species, nitrogen, oxygen, xenon, and krypton, do not appreciably coadsorb with the carbon dioxide and are readily purged from the CO₂-loaded column with air prior to the regeneration step; the purged gas is added to the feed to the xenon removal column. Carbon dioxide DFs of greater than 100 have been demonstrated in laboratory tests.

Xenon Removal

Xenon is selectively removed from the remaining gases with a specially developed adsorbent in the same parallel bed arrangement as that for water and carbon dioxide. The xenon-adsorbent interaction is strong enough at ambient temperature and pressure to allow adsorption of up to several weight percent before xenon breaks through the column. This allows the xenon adsorption column to be in service many hours before regeneration becomes necessary. DFs for xenon separation of greater than 10³ have been obtained using this technique. Unlike the water and carbon dioxide regeneration steps that require temperatures of about 250 °C and a gas stream purge for several hours, xenon can be readily desorbed from the adsorbent at a temperature of about 100 °C with a smaller gas purge. The size of the adsorbent bed is essentially the same as that for water and carbon dioxide.

Oxygen Separation

The next separation is oxygen from krypton and nitrogen which is also done by selective adsorption on a specially developed adsorbent material. Because the krypton-adsorbent interaction is stronger than the oxygen-adsorbent interaction, the krypton remains adsorbed on the column while oxygen passes through. Some of the nitrogen coadsorbs with the krypton limiting the loading capacity of the krypton on the adsorbent causing krypton breakthrough after a few minutes. Therefore, the separation is performed using a rapid adsorption-desorption technique. The best cycle time will depend on the selected operating conditions and adsorbent bed size. Preliminary results indicate the best cycle time is about 6 minutes while operating the bed near ambient temperature and pressure. A typical cycle would be feed for 3 minutes, forward purge with recycle nitrogen for 0.5-minute, and back-purge for about 2.5 minutes. To ensure adequate recovery of the adsorbed krypton, the back purge flow rate is about twice that of the feed. This will result in about a 67% dilution of the krypton, but it will reduce the oxygen content in the krypton-nitrogen mixture

to concentrations that limit ozone formation from oxygen radiolysis to an insignificant level. Oxygen concentrations in the krypton-nitrogen mixture on the order of 40 ppm and krypton DFs greater than 150 have been obtained using this technique through 15 cycles of operation without a measurable change in krypton DF or increase in oxygen concentration in the effluent. Because the cycle times are so short, accurate DFs are difficult to determine; and they may be considerably better than 150, but they are at least this great. A three-adsorbent bed arrangement is used for this separation to allow adequate purge of the krypton prior to being returned to service.

Krypton Removal

The separation of krypton from nitrogen is performed with the same adsorbent but operated at sub-ambient temperature and ambient pressure. Decontamination factors greater than 10^5 for the separation of krypton from nitrogen have been obtained with the adsorbent cooled to about -80°C . A dual bed arrangement is used to allow recovery of the krypton-rich fraction while the other adsorbent bed is in service. Loading times of several hours of continuous operation are obtainable with the adsorbent bed at -80°C . By heating the adsorbent bed to about ambient temperature with a slow purge, krypton concentration factors on the order of 10^4 are expected. Nitrogen is used as the purge gas for the krypton recovery beds; and after krypton is removed from the gas stream in the krypton removal beds, some of the nitrogen is recycled for desorption of the adsorbed krypton from the oxygen separation step. The cooled nitrogen will not be reheated prior to its use as a purge gas for krypton, and the oxygen separation beds will be cooled slightly. This procedure is expected to enhance the oxygen separation from the krypton.

If desired, the krypton can be purified further by collecting the desorbed krypton from the krypton removal beds with a liquid nitrogen-cooled krypton collection trap in a closed recirculating system.

III. Status Of Development

Initial evaluations for component-selective adsorption on various adsorbents were performed with the use of a modified gas chromatograph (GC). Small adsorption beds, 0.6-cm dia by 20-cm long columns, packed with adsorbents ground to 40-60 mesh were used. For the more promising adsorbents, the evaluations were performed with the same diameter but longer beds, 90-cm long columns. The GC was modified with additional switching valves so that several adsorption-desorption cycles could be performed.

Additional adsorbent evaluations were performed using 4.6-cm dia by 90-cm long columns packed with 10-20 mesh granular or beaded adsorbent materials. The flow rates used with the large columns were generally about 1 to 2 m^3/h . A test apparatus was constructed that allowed either single cycle or multicycle operation. Each of the separations has been demonstrated with the use of the large columns except the krypton-nitrogen separation at sub-ambient temperatures. A quadrupole mass spectrometer was used to verify the DFs. The feed gas composition used for the gaseous separations tests was as follows:

15th DOE NUCLEAR AIR CLEANING CONFERENCE

water, 40 °C dew point; carbon dioxide, about 300 ppm; oxygen, about 20%; xenon, 2500 ppm; krypton, 200 ppm; and the balance, nitrogen.

A small-scale engineering system is being designed that will provide integrated operation for the separation of water, carbon dioxide, xenon, oxygen, and krypton. The rapid cycle separation of the oxygen will be performed using microprocessor control of electronically operated valves.

IV. Comparison Of Proposed Separation Technique With Alternatives

The two main advantages of the proposed noble gas separation technique compared with alternative techniques are improved safety of operation and reduced capital and operating costs.

Improved safety of operation is obtained because none of the separation steps require high-pressure systems. The only pressures involved in the separations are the pressure drops across the adsorbent beds to maintain adequate flow. The only steps requiring pressurization in the process are: (1) the slight pressure buildup of the krypton recovery bed prior to venting and purging as it warms from sub-ambient to ambient temperature; and (2) pressurization for krypton storage, assuming steel cylinder storage.

Another, and perhaps the most important, improved safety feature of the proposed process, is the reduced ozone formation hazard. Because nearly all of the oxygen is removed from the feed stream before krypton is concentrated, the probability of ozone formation from radiolysis of oxygen by krypton-85 is reduced to essentially zero. This design would eliminate the need for including the oxygen recombiner currently being incorporated in many of the present designs to remove the oxygen prior to the cryogenic distillation unit.

The proposed noble gas separation process offers a number of economic advantages compared with other proposed processes:

1. Because high pressures are not required for the separations, considerable capital and operating cost savings can be realized by eliminating the need for pressure vessels and compressors.

2. The need for including an oxygen recombiner in the off-gas pretreatment train would be eliminated resulting in a substantial capital and operating cost savings.

3. Sub-ambient cooling is necessary for only one step in the process, and the lowest temperature required is about -80 °C, therefore reduced operating costs are expected compared with conventional cryogenic separation techniques.

4. Although a number of switching valves are involved, the separation columns are relatively simple in design and size and will have lower capital costs.

5. The separations process is readily amenable to remote operation and maintenance and requires less cell space. High maintenance

15th DOE NUCLEAR AIR CLEANING CONFERENCE

valves can be located for easy accessibility in a secondary containment-maintenance corridor.

At the completion of the small engineering-scale tests, the overall proposed system can be more clearly defined, and a more detailed cost analysis comparison will be performed.

V. References

1. C.L. Bendixsen and G.F. Offutt, Rare Gas Recovery Facility At The Idaho Chemical Reprocessing Plant, IN-1221, (April 1969).
2. C.L. Bendixsen and F.O. German, 1974 Operation Of The ICPP Rare Gas Recovery Facility, ICP-1057 (March 1975).
3. M.J. Stephenson, et al., "Absorption Process For Removing Krypton From Off-Gas From An LMFBR Fuel Processing Plant," Proceedings, 13th AEC Air Cleaning Conference, CONF 740807, p. 263 (August 1974).
4. M.J. Stephenson and R.S. Eby, "Development Of The FASTER Process For Removing Krypton-85, Carbon-14, And Other Contaminants From The Off-Gas Of Fuel Reprocessing Plants," Proceedings, 14th ERDA Air Cleaning Conference, CONF 760822, p. 1017 (August 1976).
5. T. Kanazawa, et al., "Development Of The Cryogenic Selective Adsorption-Desorption Process On Removal Of Radioactive Noble Gases," Proceedings, 14th ERDA Air Cleaning Conference, CONF 760822, p. 964 (August 1976).
6. Y. Yuasa, et al., "Selective Adsorption-Desorption Method For The Enrichment Of Krypton," Proceedings, 13th AEC Air Cleaning Conference, CONF 740807, p. 177 (August 1974).
7. D.T. Pence and T.R. Thomas, "NO_x Abatement Using Ammonia With Zeolite Catalyst," Proceedings Of The AEC Pollution Control Conference, CONF 721030, p. 115 (October 25, 1972).
8. D.T. Pence and T.R. Thomas, "NO_x Abatement At Nuclear Processing Plants," Proceedings Of The 2nd AEC Environmental Protection Conference, WASH-1332(74) (April 16, 1974).
9. T.R. Thomas and D.H. Munger, An Evaluation Of NO_x Abatement By NH₃ Over Hydrogen Mordenite For Nuclear Fuel Reprocessing Plants, ICP-1133 (January 1978).
10. J.G. Wilhelm and J. Furrer, "Head-End Iodine Removal From A Reprocessing Plant With A Solid Adsorbent," Proceedings, 14th ERDA Air Cleaning Conference, CONF 760822, p. 447 (August 1976).
11. T.R. Thomas, et al., Airborne Elemental Iodine Loading Capacities Of Metal Zeolites And A Method For Recycling Silver Zeolite, ICP-1119 (July 1977).

15th DOE NUCLEAR AIR CLEANING CONFERENCE

DISCUSSION

STEVENSON: You indicated that your equipment is small. Could you give us an idea of column diameter for a typical 5 to 10 ton per day reprocessing plant?

PENCE: The size of the columns depends, of course, on the flow rate of the offgas to be treated. Assuming a dissolver offgas flow rate of 200 m³/hr for a 5 MTHM/d reprocessing plant, the size of the columns would be on the order of 60 cm (2 ft) in diameter.

STEVENSON: Barnwell's flow rate is about 500 cfm.

PENCE: I know, but Barnwell's design is a little bit different from most of the proposed plants. I think the Exxon plant was 200 cfm and I think the European plants are normally in this range.

STEVENSON: What sort of velocity does this represent?

PENCE: Face velocities between 25 and 40 feet per minute.

STEVENSON: I was wondering then about heat transfer as heat transfer characteristics of packed beds are not very good and beds that size and larger don't do as well as small beds. You have only two traps shown. How fast can you cool down and heat up those traps in the krypton regeneration cycle? Is it feasible to cycle with only two traps?

PENCE: The desorption cycle time for water, carbon dioxide, and xenon removal steps are all shorter than the adsorption or leading times so that only two columns are required for separation. The desorption cycle for krypton during the oxygen separation step is nearly equal to that of the adsorption cycle so three adsorption beds will probably be required. We do not have enough information at this point to determine whether two or three beds will be required for the krypton recovery step.

STEVENSON: Your process is based on chromatographic separation. Have you considered the effect of radioactive heat of decay on the sorption-desorption characteristics of the solid sorbent?

PENCE: We do not expect the decay heat to significantly affect any of the removal or separation steps except the final concentration step because the adsorbed krypton concentration will always be quite low. In the final concentration step, the incoming gas and adsorption column will be cooled sufficiently to compensate for the decay heat.

STEVENSON: You indicated that your system does not require a process gas compressor. What is the difference between your "blower" and a gas compressor? What do you define as a high pressure process?

PENCE: I do not care to get into a discussion regarding the differences between a blower and a compressor, but in the presentation, I used the term "blower" rather than "compressor" to indicate the pressure drops in the system are on the order of cm (in.) of water rather than thousands of Pascals (tens to hundreds of psi). I would consider anything over about 10 KPa (~70 psi) as high pressure with regard to this discussion. Of course, this is an arbitrary definition on my part.

STEVENSON: Fluorocarbon-based systems have been running at an absorber pressure

15th DOE NUCLEAR AIR CLEANING CONFERENCE

of only 100 psig for the last two years, whereas the cryogenic process operates in the neighborhood of 60 pounds. These are not high pressure processes so I was wondering what you were comparing them against.

PENCE: Operating costs and the need for high pressure. If you have to compress, that's one of the biggest energy users we have. That's the point I was trying to make.

STEVENSON: We ran into the effect where you have radiation heat in a gas chromatograph that effects the loading characteristics of the components and the way the curves come off the chromatographic beds. I know your system is based primarily on the operation of a chromatograph. You've worked with cold krypton. Have you assessed the effect of hot krypton on the elution of the various peaks through the columns?

PENCE: I don't understand where there would be such an effect. The only time there would be a heating effect would be when krypton is concentrated and we don't concentrate the krypton until the final bed. Up to that point, the krypton is still around 200-250 ppm and we don't expect the heating of that to be significant because it's not absorbing. It's just a pass-through system.

STEVENSON: Where you hold the krypton on the bed, you can have a heat effect. It can warm it up and it can affect the desorption characteristics of the bed.

PENCE: It's possible this could occur on the final bed, but we don't load it at any step other than the oxygen separation. That could become a problem except that the enrichment factor is very small and it's very rapid.

STEVENSON: You cite low pressure as being a safety feature and yet you point out that your process requires a high pressure bottling step for final storage of the Kr-85. This step is the largest hazard normally associated with the other krypton removal processes, as it is for yours, also. Yet, you say your process is low pressure and is therefore safer than the others. Why?

PENCE: With regard to storage pressures, I assumed storage would be in high-pressure steel cylinders, but this does not really have anything to do with the separation and recovery processes used.

VON AMMON: I'm sure you are aware of the German development of the company Bachbahlforschren in Issen which developed an adsorbent material for the separation of nitrogen and oxygen on the basis of coal with molecular sieve properties. Now, my question is, could you give us a small hint concerning your adsorbent? Has it something to do with this coal based molecular sieve?

PENCE: The adsorbent material we use for the oxygen separation step is completely inorganic in nature.

CHENG: It wasn't clear to me from the flow charts how you plan to regenerate the oxygen removal beds.

PENCE: During the oxygen separation step, the adsorbent adsorbs krypton and nitrogen, and the oxygen is not significantly adsorbed, but passes on through the column. The krypton is recovered by back-purging with nitrogen. The back-purge flow rate is twice that of the column feed, and this increased flow strips the krypton from the oxygen separation column. The entire oxygen separation process cycle is performed near ambient pressure.

15th DOE NUCLEAR AIR CLEANING CONFERENCE

CHENG: Do you expect much carry-over of radioactive material from the purge stream?

PENCE: No, we don't.

WILHELM: How many valves do you need for this process?

PENCE: Five valves per column on the rapid cycle adsorption and, for the others, about the same, or maybe six. Five for each column and for most operations six. We have five in each column for the test setup we're using. We are only doing single column studies now.

WILHELM: That's what I'd like to comment on. I assume you need a total of about 100 valves. Each has to be leak tight and have a high reliability. I think that might be a problem for this process.

PENCE: There is only one place where trouble may occur and you need that many valves no matter what process you use. There are five valves per column and at this lower point you're down to krypton and nothing else. Since krypton doesn't contaminate anything permanently, if you have a defective valve you can back-purge it, bring it out, and do hands-on maintenance. I would expect a reasonable failure rate. I don't know what this is, but if the valves are easy to get at and repair, I think it would be acceptable.

WILHELM: I would expect some corrosion. Also, rubidium comes from the krypton and this will work on the valves, too.

VAN BRUNT: What about temperature effects and the effects of rapid recycling on the metal in the high radiation field? I assume that a large number of recycles might affect the wells and cause problems. Have you assessed that? I'm beginning to think you might have reliability problems that you might not otherwise have in a process that remains either cold or warm.

PENCE: I don't think we will have a materials problem because we don't concentrate the krypton until the last step. Until then, the columns operate under atmospheric conditions. We have not yet made an in-depth evaluation of this at this time. Because the temperature swing will only be about 120°C, we do not expect the problems to be unsolvable, though. Therefore, I don't see where this process will be any different than any of the others.

VAN BRUNT: I was referring to where you have temperature differences, because you're cycling so many times from -100 to room temperature.

BROWN: Will you be using the sensible heat of your very low purge in the krypton concentration system to heat up that system from -100 to room temperature or will you be using external heat transfer?

PENCE: Desorption of the krypton during the oxygen separation step is accomplished primarily by the change in partial pressure of the krypton-free purge gas rather than in the use of external heat.

BROWN: The combined time for the heating and cooling must be equal to or less than the time of your adsorption. Have you worked out what the energy balance is and the times required?

PENCE: No, we haven't gone to that detail for several reasons. First, we don't know for certain how long our cycle time will be. It may be anywhere from

15th DOE NUCLEAR AIR CLEANING CONFERENCE

1-3 hr. We're not certain at this point whether we'll have to use a third column or can work with two.

ALEXANDER: I was interested in the fact that you said you expected the ruthenium to plate out on your catalyst. Do you expect that to affect the performance of the catalyst adversely and do you have large quantities of ruthenium?

PENCE: Considering the expected amount of volatile ruthenium, we do not expect the catalyst material to lose its activity. However, we have observed some variation in the NO_x catalyst efficiency with increasing ruthenium plate-out. Unfortunately, we also experienced operational difficulties with our NO_x analyzer. We will repeat these experiments to verify the effect, if any, of the ruthenium plate-out on the catalyst material. In our initial experiments, we also used 10- to-100 times greater ruthenium concentrations than we expect in an actual reprocessing plant off-gas in order to ensure adequate sensitivities in our ruthenium analyses. We believe that we have refined the ruthenium analytical technique sufficiently so that we can use lower ruthenium concentrations in the off-gas.

DIETZ: I'd just like to point out that flake mineralogical graphite is a very good trap for rubidium and could be used to localize the krypton decay product. You can clean up your gas mixture if you have a little bit of powdered graphite in there. I have some evidence for it.

PENCE: Many of the zeolites would serve the same purpose and would probably be less expensive.

15th DOE NUCLEAR AIR CLEANING CONFERENCE

NITROGEN OXIDE ABSORPTION INTO WATER AND DILUTE NITRIC ACID IN AN ENGINEERING-SCALE SIEVE-PLATE COLUMN WITH PLATES DESIGNED FOR HIGH GAS-LIQUID INTERFACIAL AREA*

R. M. Counce, W. S. Groenier,
J. A. Klein, and J. J. Perona
Oak Ridge National Laboratory
Oak Ridge, Tennessee 37830

Abstract

The absorption of gaseous NO_x compounds into water and dilute HNO_3 was studied in a three-stage sieve-plate column with plates designed for high gas-liquid interfacial area. The performance of the column was measured while several operating parameters were varied. The results of the study indicate the importance of three mechanisms in the absorption of gaseous NO_x ($\text{NO}_2 + 2\text{N}_2\text{O}_4 + \text{NO}$) compounds: (1) the absorption of NO_2^* ($\text{NO}_2 + 2\text{N}_2\text{O}_4$) which results in production of liquid HNO_3 and HNO_2 ; (2) the dissociation of the liquid HNO_2 into HNO_3 and gaseous NO ; and (3) the gas-phase oxidation of NO to NO_2 . A mathematical model based on these mechanisms was developed and is presented to explain the observed phenomena.

I. Introduction

The removal of NO_x compounds from gas streams is important in the reprocessing of nuclear fuels because many of the off-gas streams in such a facility will contain these compounds in concentrations to interfere with further gas cleanup operations or exceed discharge limits. Composition of the feed-gas stream for these studies was prepared to simulate the product gas resulting from the fuel dissolution step. This product gas contains a large amount of steam as well as air and NO_x compounds. The mechanism of NO_x removal considered in this study is based on: (1) the absorption of NO_2^* ($\text{NO}_2 + 2\text{N}_2\text{O}_4$) into dilute HNO_3 , which results in the production of liquid HNO_3 and HNO_2 ; (2) the dissociation of liquid HNO_2 into liquid HNO_3 and gaseous NO ; and (3) the gas-phase oxidation of NO to NO_2 . This method is attractive for the proposed application because the HNO_3 produced could be recycled for use in the plant.

Commercial NO_x scrubbing equipment, usually bubble-cap columns, is based on HNO_3 -industry experience. Since the absorption reactions are exothermic, commercial scrubbers generally have cooling coils in the froth of each column stage. The absorber under development is intended for operation in a radioactive environment, and hence the design of the scrubber should be as simple as possible to facilitate maintenance. The scrubber system under investigation meets this requirement. In this system, dilute HNO_3 is recirculated through the column; the water input is provided by condensing steam from the feed gas. The column under development is designed to operate at high liquid flow rates, which eliminates the need for internal cooling. Heat associated with the absorption reactions and condensing steam is removed from the scrubber liquid in external heat exchangers.

*Research sponsored by the Nuclear Power Development Division, U.S. Department of Energy under contract W-7405-eng-26 with the Union Carbide Corporation.

15th DOE NUCLEAR AIR CLEANING CONFERENCE

II. Experimental Apparatus and Procedure

The flowsheet for the experiment is shown in Fig. 1. The NO_x scrubber is a three-stage sieve-plate column constructed of 0.076-m-ID by 0.254-m-long sections of Pyrex glass pipe. The plates and downcomers, shown in Fig. 2, are constructed of stainless steel.

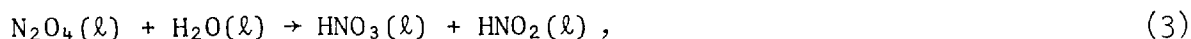
The free area per plate, 0.6%, is relatively low when compared with that of a typical sieve-plate column.⁽¹⁾ This is because the column was designed for high ratios of liquid flow rate to gas flow rate (L/G) in an attempt to dissipate the heat generated from the absorption reactions and the condensation of the steam with increased liquid flow rates; this also provides increased gas residence time in the column.

Other equipment used in the experiment include: a scrubber liquid holdup tank, pump, rotameter, and heat exchanger; a gaseous NO₂^{*} supply system; and process air, steam, and water supply systems. The gas-handling equipment includes a NO₂^{*}-air rotameter, an effluent gas holdup tank, an infrared analyzer to determine the concentrations of NO_x in the feed and effluent gas streams, a calibration gas supply system, and an exhaust gas system.

The system is normally operated by pumping the scrubber liquid from the scrubber liquid holdup tank and metering it through heat exchangers to the column. Upon leaving the column, the effluent liquid stream flows by gravity to the return tank. Gaseous NO₂^{*} is supplied to the system by vaporizing commercially obtained liquid NO₂^{*} in a temperature-regulated water bath. Process air is metered with the NO₂^{*} by a rotameter and is blended with steam in a common feed stream to the column. Steam flow is controlled by maintaining a constant differential pressure across a calibrated capillary tube. The system is allowed to reach steady-state conditions before data are taken. The system is considered to be at steady state when all gas and liquid flow rates, column temperatures, and NO_x concentrations in the feed and effluent streams have shown no change over a 30-min interval. The gas stream is sampled before and after leaving each stage. The gas-sample streams, with the exception of the feed stream, are passed through a sample holdup tank to provide sufficient time for the NO_x gases to reach the NO₂^{*} state for analysis. The sample streams are then metered to an infrared analyzer (Lira Model 202), which is specific for NO₂^{*} and requires a gas with a known air-NO₂^{*} content for the purpose of calibration. Samples of the scrubber liquid are taken entering and leaving the column. These liquid samples are analyzed for HNO₃ and HNO₂ by standard techniques. Plate and column efficiencies are then calculated from the gas concentration differences.

III. Theoretical Development

The overall chemical reactions involved in the steady-state absorption of NO_x compounds into water or dilute HNO₃ appear to be adequately represented as follows:



ORNL DWG 76-14582R3

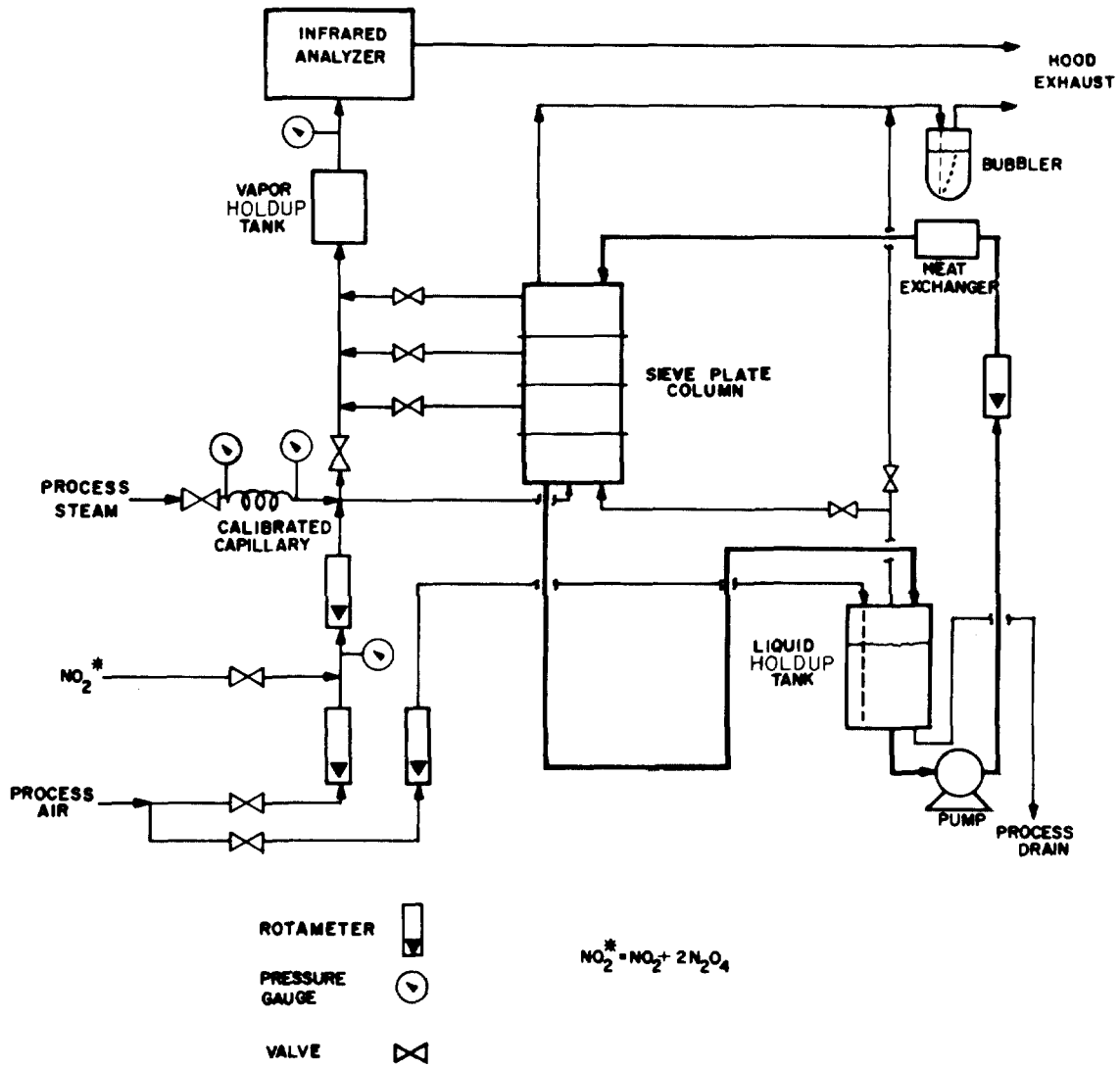
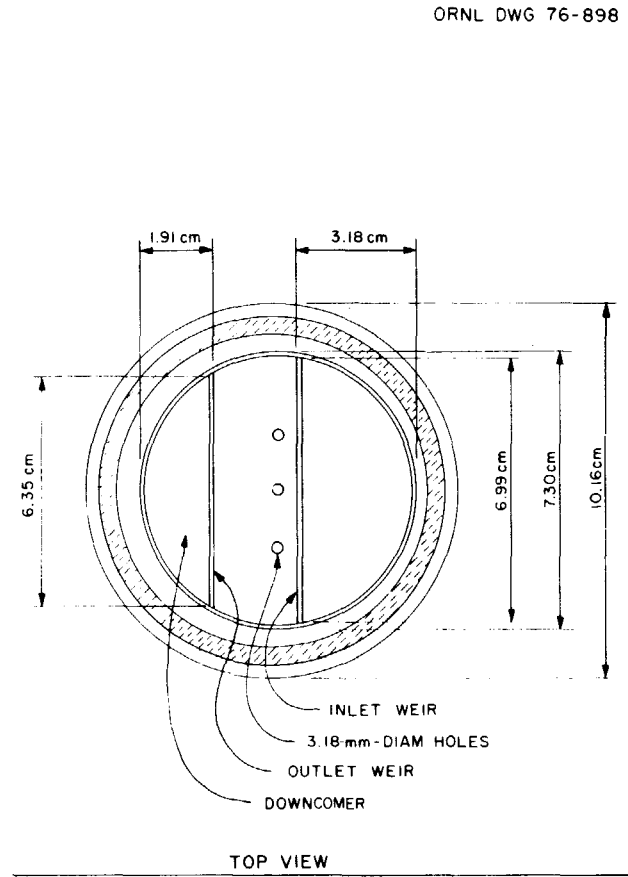
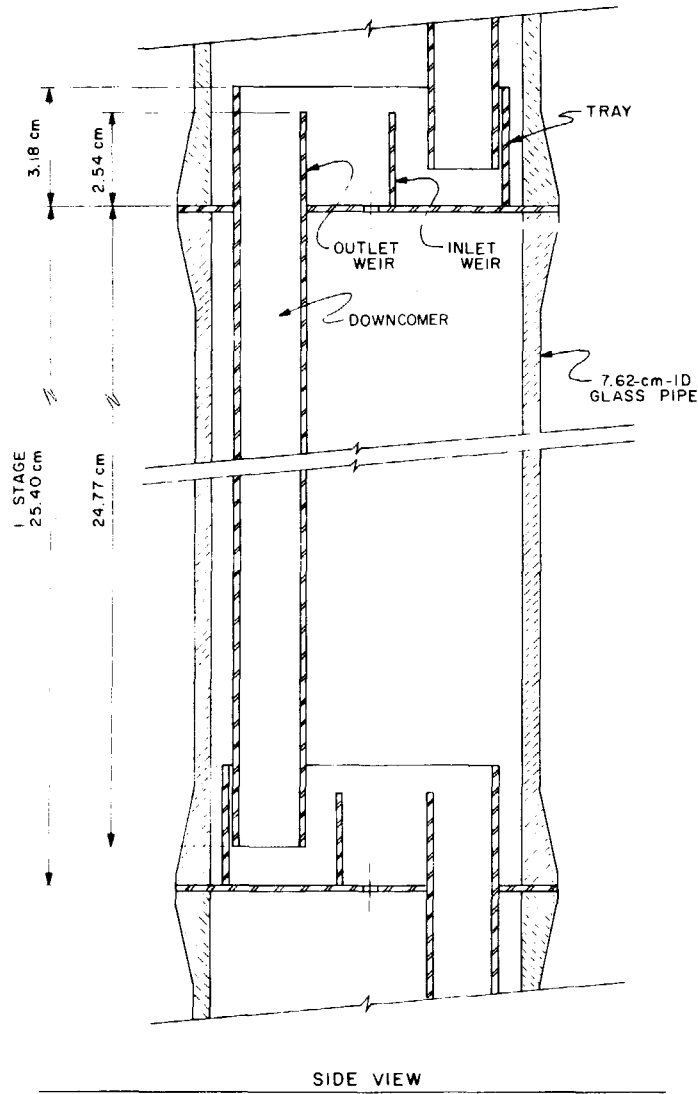


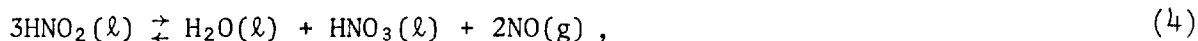
FIGURE 1
 FLOWSHEET OF EQUIPMENT USED IN NO_x SCRUBBING EXPERIMENT.



ORNL DWG 76-898

FIGURE 2
TYPICAL PLATE AND DOWNCOMER ARRANGEMENT FOR SIEVE-PLATE COLUMN.

15th DOE NUCLEAR AIR CLEANING CONFERENCE



where (g) and (l) indicate gas and liquid species respectively. A review of the literature indicates that the following assumptions about the overall reactions may be made:

1. The NO_2 and N_2O_4 are in continuous gas-phase equilibrium. ⁽²⁻⁴⁾
2. Reaction of N_2O_4 with water proceeds by means of a fast-first-order liquid-phase reaction. ⁽⁴⁻¹⁶⁾ (For NO_2^* partial pressures >0.01 atm, this is the predominant absorption reaction). ⁽¹⁷⁾
3. The HNO_2 decomposes exclusively by Eq. (4). ⁽¹⁸⁻²¹⁾
4. Oxidation of NO occurs as an overall third-order gas-phase reaction. ⁽²²⁻²⁷⁾

The following additional assumptions were made concerning the characteristics of the column gas and liquid phases:

1. The froth on the sieve plates is well mixed.
2. No backmixing occurs in the gas traveling through the sieve-plate froth.
3. The changes in gas flow rate through the froth and through the gas space between plates are considered to be negligible while in that particular phase.
4. The gases behave ideally.
5. The gas in the gas space between the plates is well mixed.

The NO_2 - N_2O_4 equilibrium and the absorption of gaseous N_2O_4 into water or dilute HNO_3 are simulated mathematically and combined into an equation for N_2O_4 absorption in the froth on the sieve plates. The dissociation of liquid HNO_2 to gaseous NO is also treated mathematically. By using the gas-phase reaction rate for NO oxidation, a mathematical expression is developed for the extent of this reaction in the gas space between the sieve plates. These three equations are combined in an overall mathematical model for NO_x removal in a multistage-plate column.

The equilibrium between N_2O_4 and NO_2 can be defined by ⁽²⁻⁴⁾

$$K_{p,1} = \frac{P_{\text{NO}_2}^2}{P_{\text{N}_2\text{O}_4}}, \quad (6)$$

where

$K_{p,1}$ = pressure equilibrium constant for reaction (1), atm;

15th DOE NUCLEAR AIR CLEANING CONFERENCE

P_{NO_2} = partial pressure of NO_2 , atm; and

$P_{N_2O_4}$ = partial pressure of N_2O_4 , atm.

If α represents the degree of dissociation of N_2O_4 and the partial pressures of N_2O_4 and NO_2 are expressed in terms of NO_2^* and α , then

$$P_{N_2O_4} = (1 - \alpha)P_{NO_2}^*/2 \quad (7)$$

and

$$P_{NO_2} = \alpha P_{NO_2}^* \quad (8)$$

where

$$P_{NO_2}^* = P_{NO_2} + 2P_{N_2O_4}, \text{ atm.}$$

Combination and rearrangement of the above equations results in the following equation for α :

$$\alpha = \frac{-K_{p,1} + K_{p,1} \sqrt{1 + 8P_{NO_2}^*/K_{p,1}}}{4P_{NO_2}^*} \quad (9)$$

The local absorption rate for NO_2^* into dilute HNO_3 , neglecting gas-phase resistance, can be expressed as:

$$\bar{R}_{NO_2}^* = 2\sqrt{(D_{N_2O_4, H_2O})k_3} (P_{N_2O_4}/He_{N_2O_4}), \quad (10)$$

where

$\bar{R}_{NO_2}^*$ = local absorption rate of NO_2^* per unit area, kg.moles/m² sec,

$D_{N_2O_4, H_2O}$ = diffusivity of N_2O_4 in H_2O , m²/sec,

k_3 = pseudo-first-order reaction rate constant, sec⁻¹; and

$He_{N_2O_4}$ = Henry's law constant for the solution of N_2O_4 in H_2O .

Utilizing Eq. (10) a balance for NO_2^* around a differential element of froth is developed, incorporating the following definition:

$$P_{NO_2}^* = P_{NO_2, in}^* (1 - X_{NO_2}^*), \quad (11)$$

where

$P_{NO_2}^*$ = partial pressure of NO_2^* , atm;

$P_{NO_2, in}^*$ = partial pressure of NO_2^* entering the froth, atm; and

$X_{NO_2}^*$ = conversion of NO_2^* , the ratio of the change in the partial pressure of NO_2^* to the partial pressure of NO_2^* entering the froth of a given plate;

and the equilibrium relationship between N_2O_4 and NO_2 into the differential NO_2^* balance. Integrating over the volume of froth per plate, the following equation may be obtained:

$$\frac{\phi \sqrt{(D_{N_2O_4, H_2O})^3 k_3} aRTV_{FR}}{GHe_{N_2O_4}} + \frac{2}{\phi} \left[\ln \left(\frac{\sqrt{1 + 2\phi - 2\phi X_{NO_2}^*} - 1}{\sqrt{1 + 2\phi} - 1} \right) + \frac{\sqrt{1 + 2\phi - 2\phi X_{NO_2}^*} - \sqrt{1 + 2\phi}}{(\sqrt{1 + 2\phi - 2\phi X_{NO_2}^*} - 1)(\sqrt{1 + 2\phi} - 1)} \right] = 0, \quad (12)$$

where

$\phi = 4P_{NO_2, in}^* / K_{p,1}$;

a = gas-liquid interfacial area per unit volume of froth, m^{-1} ;

R = gas constant, $m^3 \text{ atm/kg.mole K}$;

T = froth temperature, K;

V_{FR} = froth volume, m^3 ; and

G = superficial gas volumetric flow rate, m^3/sec .

Solution of this equation involves finding the root, $X_{NO_2}^*$, between zero and one.

The model for the decomposition of HNO_2 in the froth on the sieve plates presumes equilibrium of Eq. (4) as indicated by: (18-21)

15th DOE NUCLEAR AIR CLEANING CONFERENCE

$$K_{p,4} = \frac{(C_{H^+})(C_{NO_3^-})(P_{NO})^2}{C_{HNO_2}^3} \quad (13)$$

where

$K_{p,4}$ = pressure equilibrium constant for reaction (4), $m^3 \text{ atm}^2/\text{kg}\cdot\text{mole}$;

C_{H^+} = liquid concentration of H^+ , $\text{kg}\cdot\text{mole}/m^3$;

$C_{NO_3^-}$ = liquid concentration of NO_3^- , $\text{kg}\cdot\text{mole}/m^3$;

P_{NO} = partial pressure of NO, atm; and

C_{HNO_2} = liquid concentration of HNO_2 , $\text{kg}\cdot\text{mole}/m^3$.

Because the froth is considered to be perfectly mixed,

$$C_{HNO_2} = C_{HNO_2}^* \text{ in } (1 - X_{HNO_2}), \quad (14)$$

where

$C_{HNO_2}^* \text{ in}$ = concentration of liquid HNO_2 resulting from the HNO_2 in the incoming liquid stream and production from absorption reactions, $\text{kg}\cdot\text{mole}/m^3$; and

X_{HNO_2} = conversion of HNO_2 , the concentration decomposing per plate divided by $C_{HNO_2}^* \text{ in}$.

A mole of NO is produced for each 3/2 moles of HNO_2 decomposed; therefore, the following relationship may be used to predict the partial pressure of NO desorbed per plate:

$$\Delta P_{NO} = (2/3)(L/G) R T C_{HNO_2}^* \text{ in } X_{HNO_2} \quad (15)$$

where

L = liquid flow rate, m^3/sec .

Because equilibrium is approached by the decomposition of liquid HNO_2 , Eq. (13) may be rearranged into the following form, using relationships given in Eqs. (14) and (15):

15th DOE NUCLEAR AIR CLEANING CONFERENCE

$$K_{p,4} [C_{\text{HNO}_2, \text{in}}^* (1 - X_{\text{HNO}_2})]^3 - (C_{\text{H}^+})(C_{\text{NO}_3^-}) [P_{\text{NO}, \text{in}} + (2/3)(L/G)RTC_{\text{HNO}_2, \text{in}}^* X_{\text{HNO}_2}]^2 = 0, \quad (16)$$

where

$P_{\text{NO}, \text{in}}$ = partial pressure of NO entering the froth, atm .

The solution of the equation involves finding the positive and real root, X_{HNO_2} , of this third-degree polynomial.

The model for NO oxidation in the free volume between the sieve plates is based on the third-order gas-space reaction of NO and oxygen. The reaction rate is expressed as:

$$\bar{r}_{\text{NO}} = k_5 P_{\text{NO}}^2 P_{\text{O}_2}, \quad (17)$$

where

\bar{r}_{NO} = local reaction rate of the oxidation of NO, atm/sec;

k_5 = reaction rate constant for reaction (5), $\text{atm}^{-2} \text{sec}^{-1}$;

P_{NO} = partial pressure of NO, atm; and

P_{O_2} = partial pressure of O_2 , atm .

Utilizing Eq. (17) in developing a NO balance around a differential element of free space between the plates, and incorporating the following definitions:

$$P_{\text{NO}} = P_{\text{NO}, \text{in}} (1 - X_{\text{NO}}) \quad (18)$$

and

$$P_{\text{O}_2} = P_{\text{O}_2, \text{in}} [1 - (P_{\text{NO}, \text{in}} / 2P_{\text{O}_2, \text{in}}) X_{\text{NO}}], \quad (19)$$

where

$P_{\text{NO}, \text{in}}$ = the partial pressure of NO entering the gas space, atm;

X_{NO} = the conversion of NO in the free space between the sieve plates, ratio of the partial pressure of NO oxidized to the partial pressure of NO entering the gas space, dimensionless; and

15th DOE NUCLEAR AIR CLEANING CONFERENCE

$P_{O_2, in}$ = the partial pressure of O_2 entering the gas space, atm.

Integrating over the free space between the plates yields:

$$-X_{NO} + k_5 P_{NO, in} P_{O_2, in} \left[1 - \left(\frac{P_{NO, in}}{P_{O_2, in}} + 2 \right) X_{NO} + \left(\frac{P_{NO, in}}{P_{O_2, in}} + 1 \right) X_{NO}^2 - \left(\frac{P_{NO, in}}{2P_{O_2, in}} \right) X_{NO}^3 \right] \tau = 0, \quad (20)$$

where

τ = the gas residence time between the sieve plates, sec.

The solution of this equation involves finding the real and positive root, X_{NO} , of this polynomial.

The overall model for NO_x removal is based on the mathematical simulations developed earlier for the NO_2^* absorption and HNO_2 decomposition in the froth on a sieve plate and NO oxidation in the gas spaces between the sieve plates.

The steady-state acid molarities were calculated using the conversions of NO_2^* and HNO_2 and the stoichiometry of Eqs. (1-4). For calculations involving the recycle of the scrubber liquid, the liquid feed stream to the column was equal in concentration to the effluent-scrubber liquid stream. Steady-state acid concentrations are determined through repeated iterations of the column model, beginning with initial acid concentrations of near zero. Reaching steady state in the liquid phase coincided with establishing steady state in the gas phase for the described calculations. The model allows for adjustment of the gas density upon leaving the froth and again upon leaving the gas space. The subscripts j and k are used to indicate the stage number in a column and the position of the gas in a particular stage respectively. For gas entering the froth of plate j , $k = 1$; for gas leaving the froth of plate j , $k = 2$. The partial pressures of NO_2^* , NO , nitrogen, and oxygen of a gas stream entering the froth on stage j are indicated by $P_{NO_2^*, j, k=1}$, $P_{NO, j, k=1}$, $P_{N_2, j, k=1}$, and $P_{O_2, j, k=1}$ respectively. The model begins at the first plate and works upward. The partial pressures of the components leaving the froth are indicated by:

$$P_{NO_2^*, j, k=2} = P_{NO_2^*, j, k=1} (1 - X_{NO_2^*}) / (1 - \epsilon_{k=1} X_{NO_x}), \quad (21)$$

$$P_{NO, j, k=2} = [P_{NO, j, k=1} + \Delta P_{NO, j}] / (1 - \epsilon_{k=1} X_{NO_x}), \quad (22)$$

$$P_{N_2, j, k=2} = P_{N_2, j, k=1} / (1 - \epsilon_{k=1} X_{NO_x}), \quad (23)$$

and

$$P_{O_2, j, k=2} = P_{O_2, j, k=1} / (1 - \epsilon''_{k=1} X_{NO_x}) \quad (24)$$

where

X_{NO_x} = conversion of NO_x , the ratio of the change in the partial pressure of NO_x entering the froth of a given plate.

Those leaving the gas space of stage j or entering stage $j+1$ are indicated by:

$$P_{NO_2^*, j+1, k=1} = [P_{NO_2^*, j, k=2} + P_{NO, j, k=2} X_{NO}] / (1 - \epsilon''_{k=2} X_{NO}) \quad (25)$$

$$P_{NO, j+1, k=1} = P_{NO, j, k=2} (1 - X_{NO}) / (1 - \epsilon''_{k=2} X_{NO}) \quad (26)$$

$$P_{N_2, j+1, k=1} = P_{N_2, j, k=2} / (1 - \epsilon''_{k=2} X_{NO}) \quad (27)$$

and

$$P_{O_2, j+1, k=1} = P_{O_2, j, k=2} (1 - \frac{P_{NO, in}}{2P_{O_2, in}} X_{NO}) / (1 - \epsilon''_{k=2} X_{NO}) \quad (28)$$

The partial pressures of the gas components as well as the gas flow rates are corrected for bulk removal of the gas-phase components. This correction may be made by division or multiplication by $(1 - \epsilon'')$, where ϵ'' is the fractional volume change due to removal of the gas components ($k = 1$ for the froth and $k = 2$ for the gas space). The quantities $X_{NO_2^*}$, $\Delta P_{NO, j}$, and X_{NO} are found using Eqs. (12), (15), and (20). Solution of Eq. (15) requires prior solution of Eq. (16). A multistage column may be modeled by letting j assume values from one to the number of required stages, provided the basic removal mechanisms remain valid.

IV. Experimental Results

In order to calculate the column performance, it is necessary to have numerical values for the appropriate equilibrium, kinetic, and transfer constants. The values of $K_{p,1}$ used in this study were obtained from a correlation by Hoftyzer and Kwanten⁽⁴⁾ based on the work of Verhoek and Daniels.⁽³⁾ The values of $\sqrt{D_{N_2O_4, H_2O}^k / He_{N_2O_4}}$ used to calculate the absorption of N_2O_4 were also obtained from a correlation by Hoftyzer and Kwanten.⁽⁴⁾ Abel's equilibrium constant as a function of temperature was used to describe the decomposition of HNO_2 .⁽¹⁸⁻²¹⁾ The rate constant for the oxidation of NO was derived as a function of temperature from the work of Greig and Hall.⁽²⁷⁾ The gas-liquid interfacial area was determined experimentally for the case with no steam in the feed gas by utilizing

15th DOE NUCLEAR AIR CLEANING CONFERENCE

the absorption of CO_2 into NaOH solutions, as described by Danckwerts. (28) These results are summarized in Fig. 3. The interfacial area of the bottom tray for the case when steam is present in the feed gas was estimated utilizing Eq. (12), and the experimental data given in Table I for nominal run conditions.

The nominal run conditions were:

1. scrubber liquid flow rate, 0.175×10^{-4} or $0.350 \times 10^{-4} \text{ m}^3/\text{sec}$;
2. combined air and NO_2^* flow rates, $2.0 \times 10^{-4} \text{ m}^3/\text{sec}$;
3. steam flow rate, 3.7 kg of steam per m^3 of air and NO_2^* ;
4. inlet scrubber temperature, 298 K;
5. feed gas temperature, 363 K;
6. scrubber molarity, ~ 2.0 ;
7. feed gas partial pressure of NO_2^* , 0.31 atm;
8. total pressure, 1.1 atm.

A series of experiments was performed, as shown in Table I, in which the absorption of NO_2^* was studied using a single plate in order to evaluate the validity of Eq. (11) and the selected constants. This was accomplished by measuring the partial pressure of NO_2^* in N_2 before and after it was passed through the sieve-plate froth. The scrubber liquid for these runs was water flowing in a single pass through the column. These results are given in Table I. A representative experimental series showing experimental and model-predicted NO_2^* absorption or conversion is shown for various feed partial pressures of NO_2^* in Fig. 4. In general, NO_2^* conversion increases with increased partial pressures of NO_2^* and increased liquid flow rates and decreases with increased superficial gas flow rates. The presence of steam was shown to greatly enhance the absorption of NO_2^* in these experiments, involving a single sieve plate.

The removal of gaseous NO_x compounds depends not only on the absorption of NO_2^* , but also on the desorption and subsequent gas-phase oxidation of NO . The model predictions for the three-stage column performance provide for these phenomena as indicated previously.

The buildup of HNO_2 in the liquid phase for runs involving liquid recycle is shown in Fig. 5. The attainment of steady state appears to be closely related to reaching a steady-state concentration of HNO_2 in the recirculating scrubber liquid. As the concentration of HNO_2 increases in the scrubber liquid, the overall scrubber efficiency or conversion of NO_x is shown to decrease. The model-predicted conversion of NO_x behaves similarly as shown in Fig. 6, in which other conditions were approximately as experimental run 42 given in Tables II and III.

The model-predicted gaseous NO_x profile in the column is compared with that calculated from the experimental data of run 53 in Table IV. Plates are numbered from bottom to top. There was no steam in the feed gas for this experiment. The model-predicted profiles are very close to the experimentally determined profiles.

ORNL DWG-77-6091

535

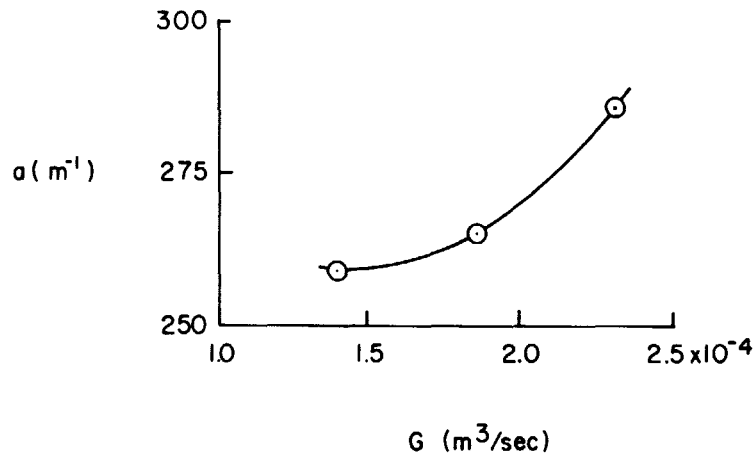


FIGURE 3
CORRELATION OF EXPERIMENTALLY DETERMINED GAS-LIQUID INTERFACIAL AREA VS GAS FLOW RATE FOR A SINGLE-STAGE SIEVE-PLATE COLUMN.

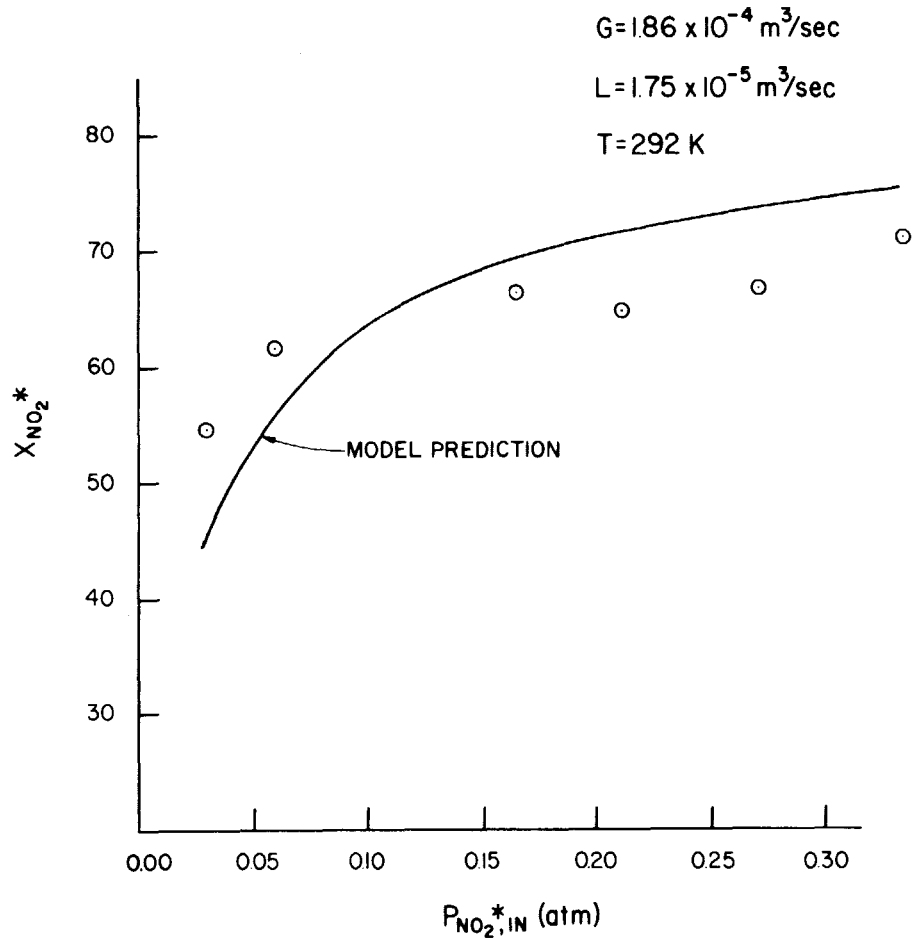
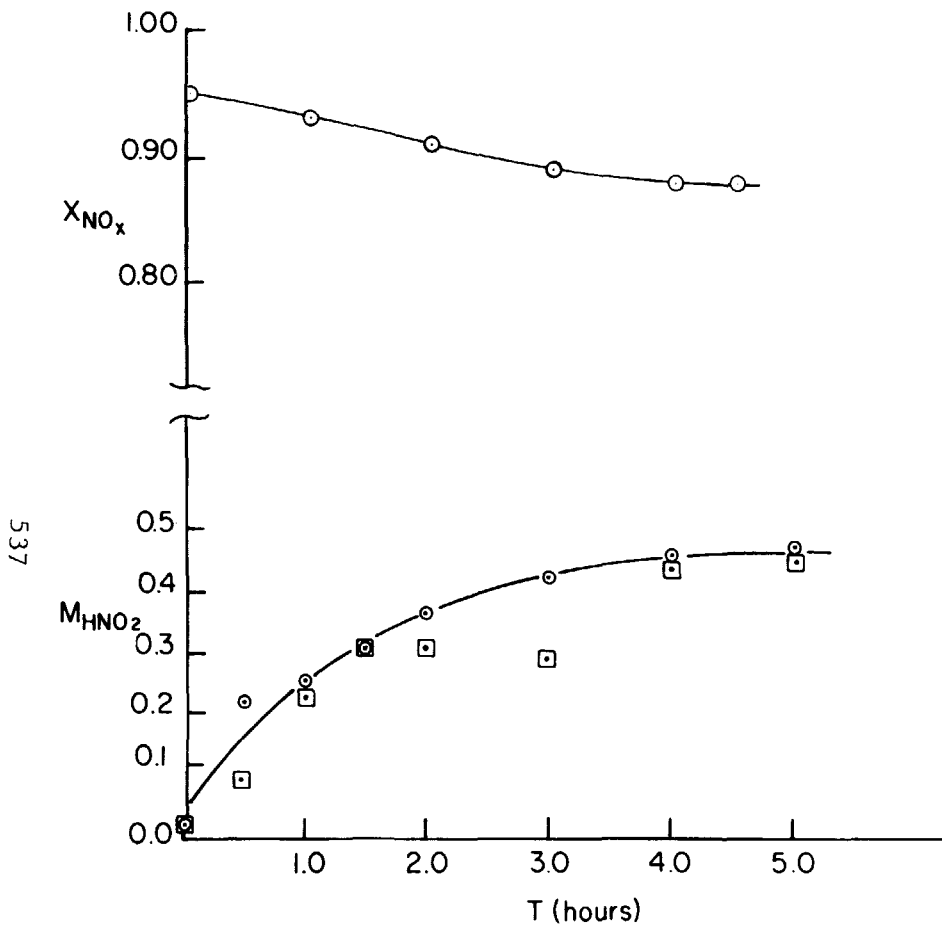


FIGURE 4
EXPERIMENTAL AND MODEL PREDICTED NO_2^* ABSORPTION VS THE PARTIAL PRESSURE OF NO_2^* ENTERING THE TRAY AT A TOTAL GAS FLOW RATE OF $1.86 \times 10^{-4} \text{ m}^3/\text{sec}$ IN A SINGLE-PLATE COLUMN.

15th DOE NUCLEAR AIR CLEANING CONFERENCE

Table I. Steady-state NO_2^* scrubbing data for a single sieve plate and a nonrecirculating scrubber liquid

Run No.	$P_{\text{NO}_2, \text{in}}^*$ (atm)	$P_{\text{NO}_2, \text{out}}^*$ (atm)	$T_{\text{G, in}}$ (K)	$T_{\text{G, out}}$ (K)	T_{L} (K)	G (std m^3/sec)	F_{STEAM} (kg/sec)	L (m^3/sec)	a (m^2/m^3)
55a	0.026	0.012	293	297	292	2.0×10^{-4}	0	1.75×10^{-5}	
55b	0.051	0.020	294	297	292	2.0×10^{-4}	0	1.75×10^{-5}	
55c	0.101	0.040	294	297	292	2.0×10^{-4}	0	1.75×10^{-5}	
55d	0.161	0.059	294	297	292	2.0×10^{-4}	0	1.75×10^{-5}	
55e	0.207	0.081	294	297	292	2.0×10^{-4}	0	1.75×10^{-5}	
55f	0.267	0.103	294	297	292	2.0×10^{-4}	0	1.75×10^{-5}	
55g	0.330	0.117	294	297	292	2.0×10^{-4}	0	1.75×10^{-5}	
56a	0.035	0.013	294	298	293	1.5×10^{-4}	0	1.75×10^{-5}	
56b	0.053	0.017	294	298	293	1.5×10^{-4}	0	1.75×10^{-5}	
56c	0.107	0.035	294	298	293	1.5×10^{-4}	0	1.75×10^{-5}	
56d	0.167	0.057	294	298	293	1.5×10^{-4}	0	1.75×10^{-5}	
56e	0.187	0.075	294	298	293	1.5×10^{-4}	0	1.75×10^{-5}	
56f	0.260	0.088	294	298	293	1.5×10^{-4}	0	1.75×10^{-5}	
56g	0.330	0.094	294	298	293	1.5×10^{-4}	0	1.75×10^{-5}	
57a	0.020	0.011	294	297	293	2.5×10^{-4}	0	1.75×10^{-5}	
57b	0.044	0.020	294	298	293	2.5×10^{-4}	0	1.75×10^{-5}	
57c	0.101	0.044	294	298	293	2.5×10^{-4}	0	1.75×10^{-5}	
57d	0.161	0.068	295	298	292	2.5×10^{-4}	0	1.75×10^{-5}	
57e	0.216	0.094	295	298	292	2.5×10^{-4}	0	1.75×10^{-5}	
57f	0.279	0.119	295	298	292	2.5×10^{-4}	0	1.75×10^{-5}	
57g	0.312	0.134	295	298	292	2.5×10^{-4}	0	1.75×10^{-5}	
58a	0.015	0.009	295	298	293	3.0×10^{-4}	0	1.75×10^{-5}	
58b	0.050	0.024	295	298	292	3.0×10^{-4}	0	1.75×10^{-5}	
58c	0.107	0.051	295	298	292	3.0×10^{-4}	0	1.75×10^{-5}	
58d	0.165	0.075	295	298	292	3.0×10^{-4}	0	1.75×10^{-5}	
58e	0.211	0.099	295	298	292	3.0×10^{-4}	0	1.75×10^{-5}	
58f	0.260	0.119	295	298	292	3.0×10^{-4}	0	1.75×10^{-5}	
59a	0.163	0.079	294	296	292	2.0×10^{-4}	0	0.44×10^{-5}	
59b	0.163	0.075	294	296	293	2.0×10^{-4}	0	0.88×10^{-5}	
59c	0.163	0.062	294	296	292	2.0×10^{-4}	0	2.60×10^{-5}	
59d	0.163	0.057	294	296	290	2.0×10^{-4}	0	3.50×10^{-5}	
63a	0.152	0.051	299	297	290	2.0×10^{-4}	0	1.75×10^{-5}	
63b	0.145	0.044	297	298	291	1.5×10^{-4}	0	1.31×10^{-5}	
63c	0.151	0.055	294	298	290	2.5×10^{-4}	0	2.19×10^{-5}	
63d	0.151	0.055	294	298	290	2.5×10^{-4}	0	2.19×10^{-5}	
64a	0.165	0.026	348	302	298	2.0×10^{-4}	1.67×10^{-4}	1.75×10^{-5}	622
64b	0.166	0.024	355	304	302	2.0×10^{-4}	3.67×10^{-4}	1.75×10^{-5}	724
64c	0.163	0.024	362	306	309	2.0×10^{-4}	7.83×10^{-4}	1.75×10^{-5}	850
64d	0.166	0.022	365	309	317	2.0×10^{-4}	11.83×10^{-4}	1.75×10^{-5}	1200
65a	0.141	0.031	368	316	337	2.0×10^{-4}	7.83×10^{-4}	0.44×10^{-5}	1650
65b	0.152	0.019	359	300	300	2.0×10^{-4}	7.83×10^{-4}	3.50×10^{-5}	781
65c	0.151	0.028	369	322	322	2.0×10^{-4}	7.83×10^{-4}	0.86×10^{-5}	1120



537

FIGURE 5

OVERALL NO_x CONVERSION IN THREE-STAGE SIEVE-PLATE COLUMN AND CONCENTRATION OF HNO_2 ($\text{kg}\cdot\text{moles}/\text{m}^3$) IN THE SCRUBBER LIQUID DURING THE APPROACH TO STEADY-STATE OPERATION (THE CIRCLE AND SQUARE DATA POINTS FOR HNO_2 CONCENTRATION ARE SCRUBBER LIQUID EFFLUENT AND FEED RESPECTIVELY).

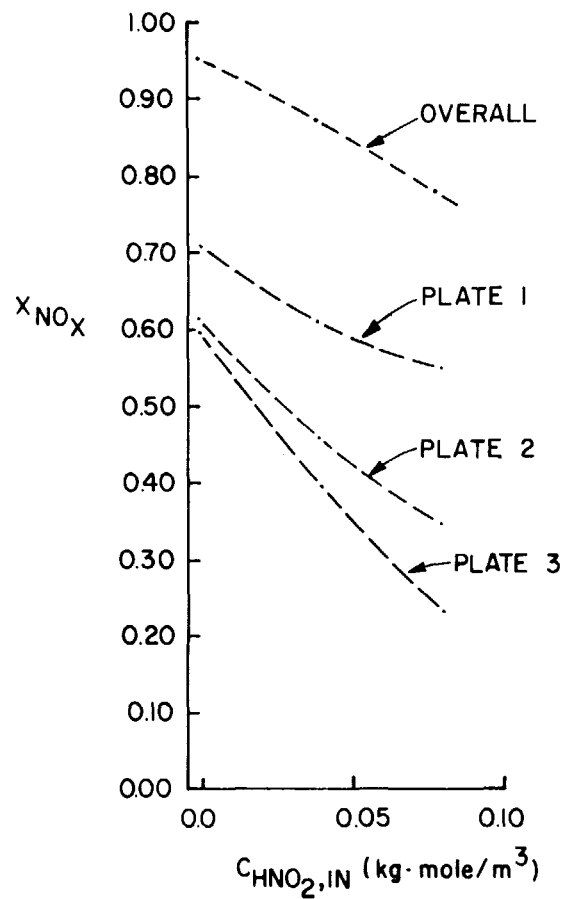


FIGURE 6

MODEL-PREDICTED CONVERSION OF NO_x FOR VARYING CONCENTRATIONS OF HNO_2 IN THE SCRUBBER LIQUID STREAM TO COLUMN AT REFERENCE CONDITIONS.

Table II. Steady-state NO_x scrubbing data for recirculating scrubber liquid

Run no.	NO _x partial pressure (atm)				Gas temperature (K)				Liquid temperature (K)		
	feed	stage 1	stage 2	stage 3	feed	stage 1	stage 2	stage 3	stage 1	stage 2	stage 3
Recirculating scrubber liquid											
9	0.308	0.106	0.067	0.051	352	314	306	305	310	298	297
10	0.312	0.114	0.068	0.053	353	312	305	303	310	297	297
11	0.299	0.114	0.073	0.058	353	312	304	304	310	297	297
12	0.295	0.110	0.068	0.053	351	309	305	304	310	297	297
13	0.273	0.012	0.073	0.062	353	312	305	303	310	297	297
15	0.341	0.128	0.073	0.051	353	313	305	304	312	297	297
16	0.310	0.141	0.084	0.070	298	302	303	305	297	297	297
17	0.293	0.100	0.057	0.040	352	312	304	303	310	297	297
18	0.332	0.103	0.057	0.042	351	312	304	303	309	297	297
19	0.0	0.0	0.0	0.0	351	303	299	299	310	297	297
20	0.310	0.117	0.066	0.042	351	316	305	303	309	297	297
31	0.341	0.125	0.079	0.057	353	312	305	304	310	297	297
32	0.352	0.117	0.070	0.051	353	313	305	304	310	297	297
42	0.306	0.141	0.088	0.062	364	320	307	305	320	298	297
44	0.295	0.136	0.095	0.066	365	320	308	306	320	298	297
45	0.301	0.150	0.097	0.084	299	303	306	299	298	297	297
46	0.301	0.125	0.088	0.070	357	311	306	305	310	298	297
47	0.301	0.143	0.097	0.068	368	322	308	305	331	299	298
48	0.350	0.141	0.090	0.068	363	315	307	305	313	299	297
49	0.301	0.107	0.069	0.051	363	317	305	304	309	298	297
50	0.312	0.171	0.112	0.075	367	333	310	305	337	299	297
51	0.145	0.066	0.048	0.040	362	317	304	303	318	298	297
52	0.215	0.127	0.110	0.105	298	300	300	301	298	297	297
53	0.317	0.183	0.123	0.103	299	303	307	309	298	297	297
54	0.321	0.132	0.101	0.079	365	317	306	305	318	296	295
60	0.293	0.129	0.079	0.057	366	317	306	303	310	298	297
61	0.400	0.174	0.101	0.070	366	315	305	303	311	297	296
62	0.308	0.114	0.068	0.050	357	336	313	300	310	297	297

Table III. Steady-state NO_x scrubbing data
(total pressure = 1.1 atm in all runs)

Run no.	Steam feed rate ^a (kg/sec × 10 ³)	Air feed rate ^a (m ³ /sec × 10 ⁴)	Liquid feed rate ^a (m ³ /sec × 10 ⁴)	HNO ₂ (M)	HNO ₃ (M)	Recycle of gas from liquid holdup tank	Liquid holdup tank sparge rate (m ³ /sec × 10 ⁶)	Liquid holdup volume (m ³ × 10 ²)
9	0.73	1.40	0.35	—	1.0	Yes	0.0	1.64
10	0.73	1.40	0.35	—	2.0	Yes	0.0	1.64
11	0.73	1.40	0.35	—	3.5	Yes	0.0	1.64
12	0.73	1.40	0.35	—	3.0	Yes	0.0	1.64
13	0.73	1.40	0.35	—	3.5	Yes	0.0	1.64
15	0.73	1.40	0.35	—	2.4	Yes	2.5	1.64
16	0.73	1.40	0.35	—	3.2	Yes	0.0	1.64
17	0.73	1.40	0.35	—	3.0	Yes	7.5	1.64
18	0.73	1.40	0.35	—	2.4	Yes	14.0	1.64
19	0.73	1.40	0.35	—	2.2	Yes	0.0	1.64
20	0.73	1.40	0.35	—	2.2	Yes	2.5	2.51
31	0.73	1.40	0.35	0.45	1.3	No	0.0	1.64
32	0.73	1.40	0.35	0.39	1.7	No	2.5	1.64
42	0.70	1.40	0.17	0.25	2.3	No	0.0	1.64
44	1.08	2.10	0.26	0.20	1.6	No	0.0	1.64
45	0.00	1.40	0.18	0.28	2.7	No	0.0	1.64
46	0.35	1.40	0.18	0.18	3.0	No	0.0	1.64
47	1.09	1.40	0.18	0.18	2.8	No	0.0	1.64
48	0.67	1.40	0.26	0.30	2.6	No	0.0	1.64
49	0.67	1.40	0.35	—	2.0	No	0.0	1.64
50	0.67	1.40	0.09	0.20	2.4	No	0.0	1.64
51	0.67	1.70	0.18	0.21	2.0	No	0.0	1.64
52	0.00	1.80	0.18	—	2.1	No	0.0	1.64
53	0.00	2.16	0.26	0.20	3.0	No	0.0	1.64
54	0.85	1.80	0.22	0.20	3.0	No	0.0	1.64
60	0.83	1.80	0.22	0.19	1.5	No	0.0	1.64
61	0.65	1.24	0.17	0.28	2.4	No	0.0	1.64
62	0.36	1.22	0.13	0.27	2.4	No	0.0	1.64

^aThe tabulated numbers in the columns have been multiplied by the indicated factor.

15th DOE NUCLEAR AIR CLEANING CONFERENCE

Table IV. A comparison of steady-state NO_x column profiles calculated from experimental data versus NO_x removal predicted by model for experiment 53

Experiment 53 (no steam in feed gas)

$P_T = 1.1 \text{ atm}$

$G_{\text{feed}} = 3.07 \times 10^{-4} \text{ m}^3/\text{sec}$

$L = 2.6 \times 10^{-5} \text{ m}^3/\text{sec}$

$M_{\text{HNO}_3} = 3.0$

$M_{\text{HNO}_2} = 0.20 \text{ (experimental), } 0.13 \text{ (calculated)}$

NO_x Profile in Column (atm)

	<u>Experimental</u>	<u>Calculated</u>
Feed	0.317	0.317
Stage 1	0.183	0.181
Stage 2	0.123	0.134
Stage 3	0.103	0.116

Table V. Calculated partial pressures of gaseous components for stage, i, and position, j, where j = 1 entering froth and j = 2 leaving froth for experiment 53

Stage (i,j)	P _{NO₂} *	P _{NO}	P _{O₂}	P _{N₂}
(1,1)	0.317	0.000	0.165	0.618
(1,2)	0.095	0.086	0.193	0.726
(2,1)	0.135	0.051	0.163	0.751
(2,2)	0.051	0.083	0.172	0.794
(3,1)	0.087	0.051	0.143	0.819
(3,2)	0.037	0.080	0.147	0.837

15th DOE NUCLEAR AIR CLEANING CONFERENCE

The steady-state HNO_2 concentration calculated by the model is slightly lower than that determined experimentally. The calculated partial pressures of the gaseous component are given for each plate (i) and for positions entering the froth (j=1) and leaving the froth (j=2) in Table V.

Experimentally determined NO_x conversions are compared with those predicted by the model in Fig. 7 for two different feed gas rates with no steam in feed gas. The NO_x conversions predicted by the model are then compared with those experimentally determined for varying scrubber liquid flow rates, feed gas flow rates, NO_x partial pressure in feed gas, and steam component in feed gas at reference conditions in Figures 8-11. In almost all cases, the model used to predict NO_x conversions in sieve plate columns is low with respect to absorption efficiencies. Consequently, the steady-state-predicted concentrations of HNO_2 (usually $\sim 0.1 \text{ kg}\cdot\text{mole}/\text{m}^3$) are always lower than the experimental values. The column overall NO_x conversion for varying HNO_3 molarities is given in Fig. 12.

Some researchers have consolidated the forward rates of Eqs. (3) and (4) producing one-third of a mole of NO for every mole of NO_2^* absorbed. No apparent difference in the revised model and the one described in this paper was detected when this mode was tested for the steady-state case involving recycle of the scrubber liquid. However, the use of this simple model does not account for the buildup of liquid HNO_2 in the system or for the reduced NO_x removal efficiency that results from its presence in the scrubber liquid. The model clearly demonstrates the observed phenomenon that the presence of HNO_2 in the scrubber liquid reduces the overall NO_x scrubbing efficiency of the system.

V. Conclusions

The following conclusions can be drawn from the results of this study:

1. The model adequately represents the experimental results for the experimental system over the range of variables studied.
2. The conversion of NO_x varies directly with the gas and liquid flow rates and the partial pressure of NO_2^* .
3. The model predicts a buildup of HNO_2 in the scrubber liquid and a corresponding decrease in scrubbing efficiency. This was verified in the experimental work.
4. These findings indicate that a method to destroy HNO_2 in the scrubber liquid before its recycle to the column will greatly increase the system NO_x removal efficiency.
5. Additional investigation will be necessary in order to verify the use of this model in predicting effluent-gas partial pressures of less than 0.01 atm.

VI. Acknowledgement

This work was performed in the Chemical Technology Division under the auspices of the Advanced Fuel Recycle Program of the Oak Ridge National Laboratory.

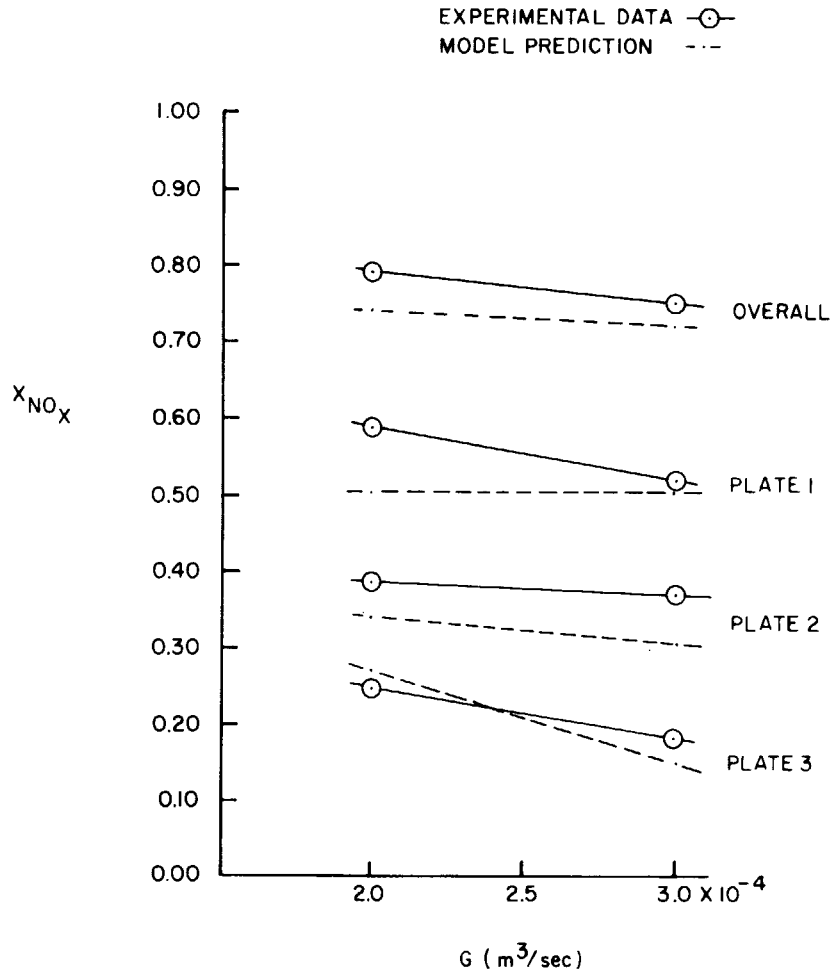


FIGURE 7
EXPERIMENTAL NO_x CONVERSIONS AND THOSE PREDICTED BY THE MODEL
FOR VARYING GAS FLOW RATES WITH NO STEAM IN FEED GAS AT
OTHERWISE REFERENCE CONDITIONS FOR STEADY-STATE,
THREE-STAGE, SIEVE-PLATE COLUMN OPERATION.

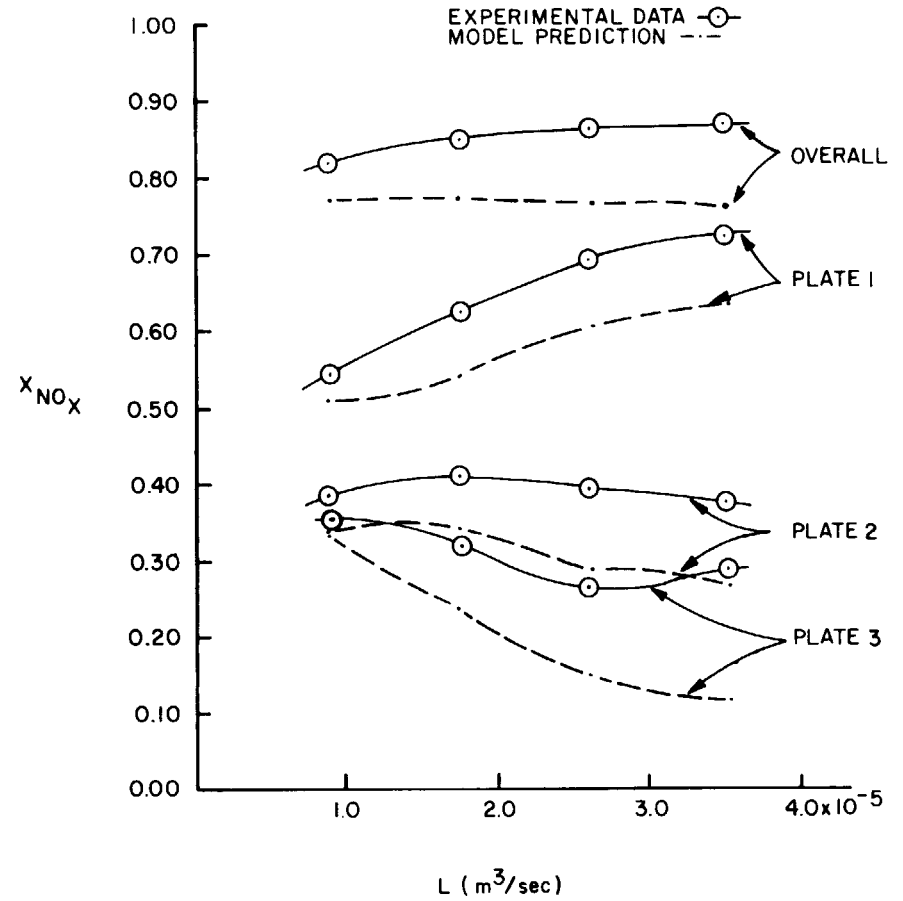


FIGURE 8
EXPERIMENTAL NO_x CONVERSIONS AND THOSE PREDICTED BY THE MODEL
FOR VARYING SCRUBBER LIQUID FLOW RATES AT OTHERWISE
REFERENCE CONDITIONS FOR STEADY-STATE THREE-STAGE COLUMN OPERATION.

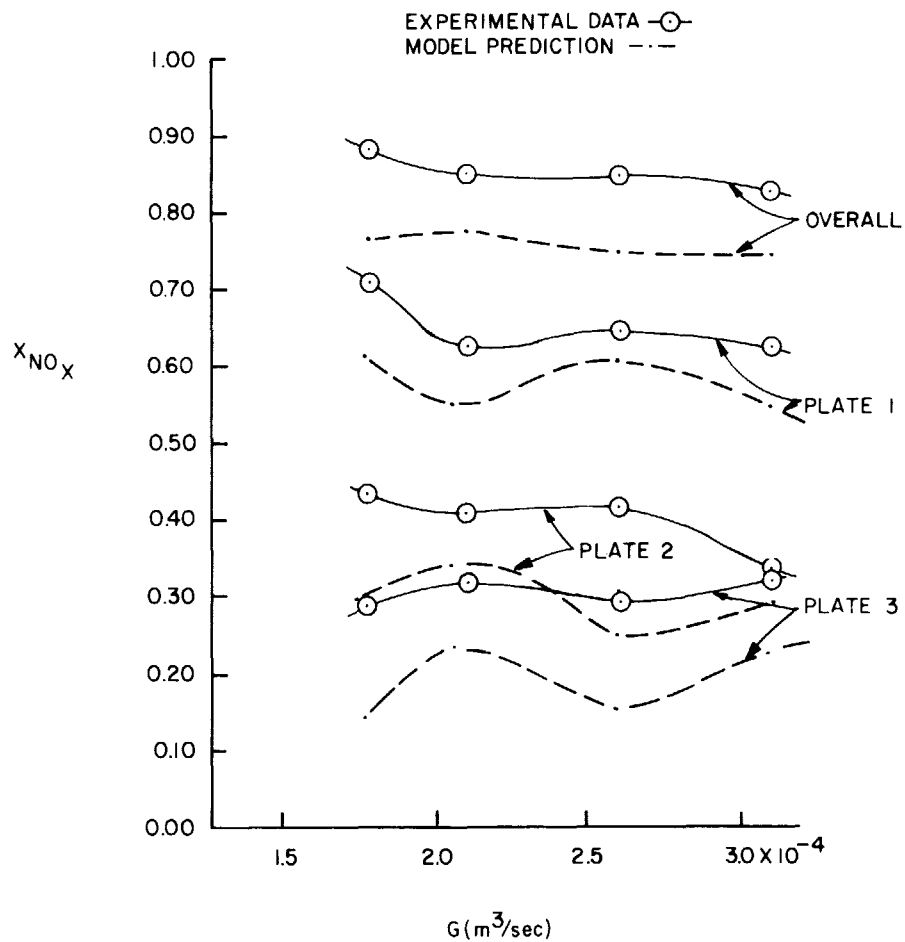


FIGURE 9
EXPERIMENTAL NO_x CONVERSIONS AND THOSE PREDICTED BY THE MODEL
FOR VARYING FEED GAS FLOW RATES AT OTHERWISE REFERENCE
CONDITIONS FOR STEADY-STATE THREE-STAGE COLUMN OPERATION.

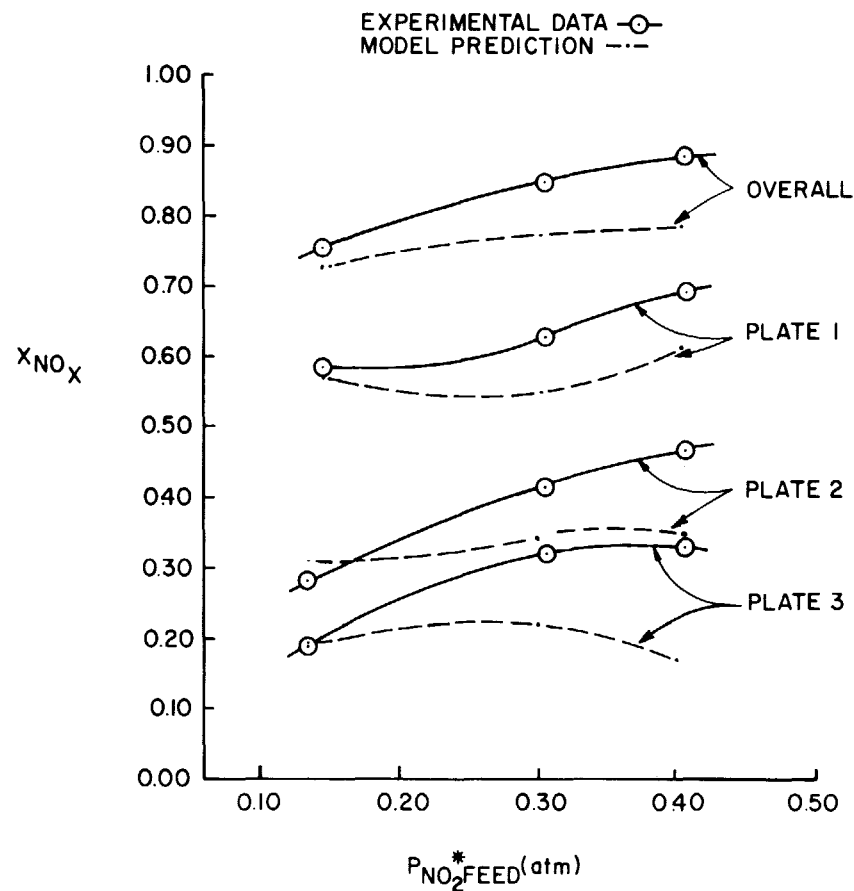


FIGURE 10
EXPERIMENTAL NO_x CONVERSIONS AND THOSE PREDICTED BY THE MODEL
FOR VARYING PARTIAL PRESSURE OF NO_x IN THE FEED GAS AT
OTHERWISE REFERENCE CONDITIONS FOR STEADY-STATE
THREE-STAGE COLUMN OPERATION.

ORNL DWG.78-1012

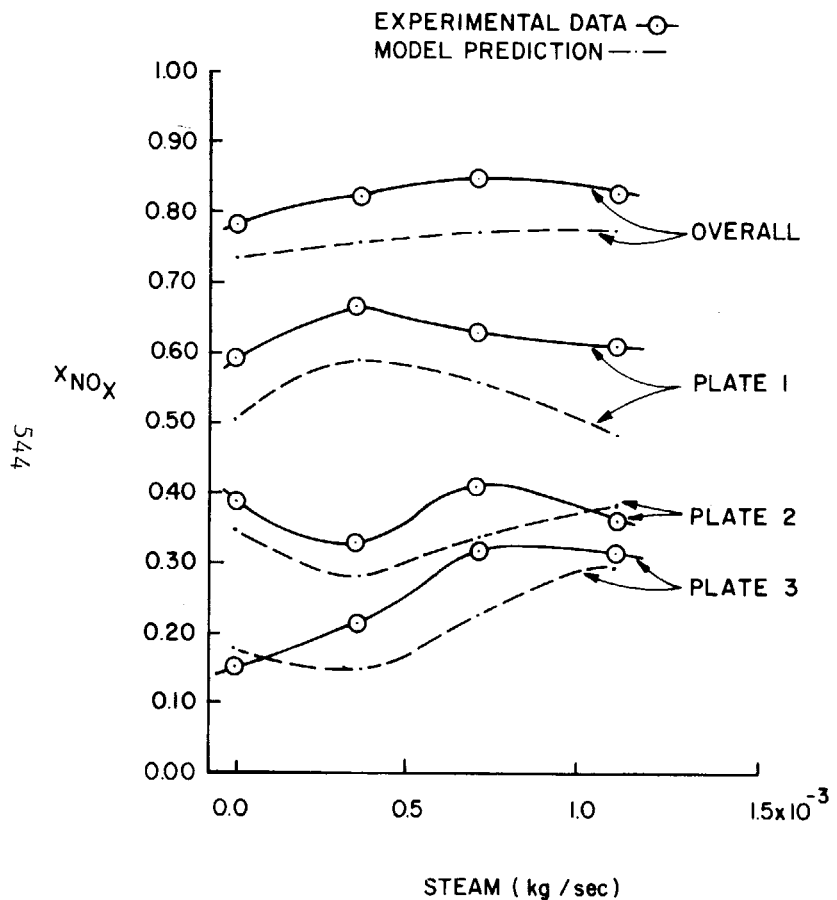


FIGURE 11
EXPERIMENTAL NO_x CONVERSIONS AND THOSE PREDICTED BY THE MODEL
FOR VARYING STEAM FLOW RATES AT OTHERWISE REFERENCE
CONDITIONS FOR STEADY-STATE THREE-STAGE COLUMN OPERATION.

ORNL DWG.77-443

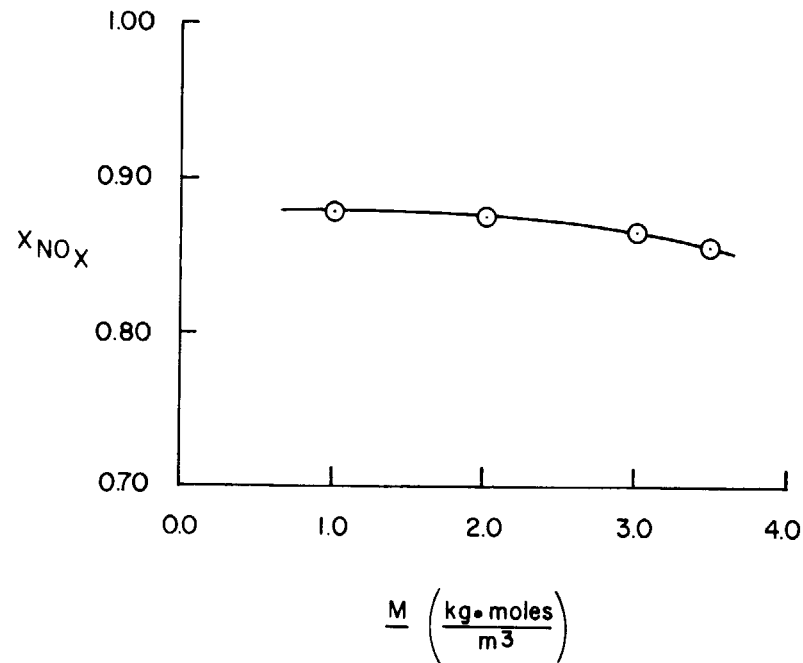


FIGURE 12
OVERALL NO_x REMOVAL IN THREE-STAGE SIEVE-PLATE COLUMN AS A
FUNCTION OF ACID MOLARITY IN SCRUBBER LIQUID.

15th DOE NUCLEAR AIR CLEANING CONFERENCE

VII. List of References

1. R. H. Perry and C. H. Chilton, "Chemical engineers' handbook," 5th ed., 18-8, McGraw-Hill, New York (1973).
2. M. Bodenstein, "Formation and decomposition of nitrous oxides of high volume," Z. Elektrochem. 100: 68-123 (1922).
3. F. H. Verhoek and F. J. Daniels, "The dissociation constants of nitrogen tetroxide and of nitrogen trioxide," J. Am. Chem. Soc. 53: 1250-63 (1931).
4. P. J. Hoftyzer and F. J. G. Kwanten, "Process for air pollution control," 2nd ed., 164-87, Chemical Rubber Co., Cleveland (1972).
5. K. G. Denbigh and A. J. Prince, "Kinetics of nitrous gas absorption in aqueous nitric acid," J. Chem. Soc. 53: 790-801 (1947).
6. P. G. Caudle and K. G. Denbigh, "Kinetics of the absorption of nitrogen peroxide into water and aqueous solutions," Trans. Faraday Soc., 49: 39-52 (1953).
7. M. M. Wendel and R. L. Pigford, "Kinetics of nitrogen tetroxide absorption in water," AIChE. J. 4: 249-56 (1958).
8. M. S. Peters and J. L. Holman, "Vapor- and liquid-phase reactions between nitrogen dioxide and water," Ind. Eng. Chem. 47: 2536-39 (1955).
9. J. J. Carberry, "Some remarks on chemical equilibrium and kinetics in the nitrogen oxides-water system," Chem. Eng. Sci. 9: 189-94 (1959).
10. W. A. Dekker, E. Snoeck, and H. Kramers, "The rate of absorption of NO₂ in water," Chem. Eng. Sci. 11: 61-71 (1959).
11. E. S. Koval and M. S. Peters, "How does nitric oxide affect reactions of aqueous nitrogen dioxide?," Ind. Eng. Chem. 52: 1011-14 (1960).
12. M. J. Moll, "The rate of hydrolysis of nitrogen tetroxide," Ph.D. Dissertation, Univ. of Washington (1966).
13. J. P. Detournay and R. H. Jadot, "Determination of the reactive phase during the absorption of nitrogen oxides in water," Chem. Eng. Sci. 28: 2099-2102 (1973).
14. M. S. Peters, C. P. Ross, and J. E. Klein, "Controlling mechanisms in the aqueous absorption of nitrogen oxides," AIChE. J. 1: 105-11 (1955).
15. H. Kramers, M. P. P. Blind, and E. Snoeck, "Absorption of nitrogen tetroxide by water jets," Chem. Eng. Sci. 14: 115-23 (1961).
16. T. K. Sherwood, R. L. Pigford, and C. R. Wilke, "Mass transfer," 346-361, McGraw-Hill Book Co., New York (1975).
17. S. P. Andrews and D. Hanson, "The dynamics of nitrous gas absorption," Chem. Eng. Sci. 14: 115-23 (1961).

15th DOE NUCLEAR AIR CLEANING CONFERENCE

18. E. Abel and H. Schmid, "Kinetics of nitrous acid," Z. Phys. Chem. 132: 55-77 (1928).
19. E. Abel and H. Schmid, "Kinetics of nitrous acid: kinetics of the decomposition of nitrous acid," Z. Phys. Chem. 134: 279-300 (1928).
20. E. Abel, H. Schmid, and S. Babad, "Kinetics of nitrous acid: kinetics of the formation of nitrous acid from nitric acid and nitric oxide," Z. Phys. Chem. 136: 135-45 (1928).
21. E. Abel, H. Schmid, and S. Babad, "Kinetics of nitrous acid: kinetics of the nitrous acid-nitric acid-nitric oxide reaction," Z. Phys. Chem. 136: 419-36 (1928).
22. M. Bodenstein, "Velocity of reaction between nitric oxide and oxygen," Z. Elektrochem. 24: 183-201 (1918).
23. R. L. Hasche and W. A. Patrick, "Studies on the rate of oxidation of nitric oxide; II the velocity of the reaction between nitric oxide and oxygen at 0° and 30°," J. Am. Chem. Soc. 47: 1207-14 (1925).
24. J. C. Treacy and F. Daniels, "Kinetic study of the oxidation of nitric oxide with oxygen in the pressure range 1-20 mm," J. Am. Chem. Soc. 77: 2033-36 (1955).
25. P. G. Ashmore, M. G. Burnett, and B. J. Tyler, "Reaction of nitric oxide and oxygen," Trans. Faraday Soc. 58: 685-91 (1962).
26. M. E. Morrison, R. C. Rinker, and W. H. Corcoran, "Rate and mechanism of gas-phase oxidation of parts-per-million concentrations of nitric oxide," Ind. Eng. Chem. Fundam. 5: 175-81 (1966).
27. J. D. Greig and P. G. Hall, "Thermal oxidation of nitric oxide at low concentrations," Trans. Faraday Soc. 63: 655-61 (1967).
28. P. V. Danckwerts, "Gas-liquid reactions," 96-150, 117-118, 227, McGraw-Hill, New York (1970).

15th DOE NUCLEAR AIR CLEANING CONFERENCE

REMOVAL OF ^{14}C -CONTAMINATED CO_2 FROM SIMULATED LWR FUEL REPROCESSING OFF-GAS BY UTILIZING THE REACTION BETWEEN CO_2 AND ALKALINE HYDROXIDES IN EITHER SLURRY OR SOLID FORM

D. W. Holladay and G. L. Haag
Oak Ridge National Laboratory
Oak Ridge, Tennessee 37830

Abstract

An important consideration in the design of a LWR fuel reprocessing plant is the removal of ^{14}C -contaminated CO_2 from the process off-gas. The separation and fixation of essentially all the CO_2 from the simulated off-gas can be accomplished by reaction with alkaline slurries in agitated tank-type contactors. Based on efficacy for CO_2 removal, consideration of reactant cost, and stability of the carbonate product as related to long-term storage requirements, the two most promising slurry reactants for CO_2 removal from low CO_2 -content feed gases are $\text{Ca}(\text{OH})_2$ and $\text{Ba}(\text{OH})_2$.

The removal of ^{14}C -contaminated CO_2 from simulated LWR off-gases was studied as a function of both operating conditions and varying sizes of bench-scale design. Parametrically, the effects on the CO_2 removal rate of feed composition (330 ppm - 4.74% CO_2), impeller speed (325-650 rpm), superficial velocity (5-80 cm/min), reactants [$\text{Mg}(\text{OH})_2$, $\text{Ca}(\text{OH})_2$, $\text{Ba}(\text{OH})_2$, NaOH], contactor size (20.3 cm and 27.3 cm ID), and type of operation (semibatch or continuous slurry) were determined.

The decontamination factors (DF, i.e. moles CO_2 in/moles CO_2 out) for CO_2 removal from gases containing 0.033 to 3% CO_2 , for fixed values of such parameters as gas superficial velocity, slurry temperature, and power consumption, varied directly with the solubility of the metal hydroxide employed. For 1.0 M $\text{Ca}(\text{OH})_2$ in the 27.3-cm-ID contactor, a power consumption of 21.0 kW/m³ ($n = 650$ rpm), a temperature of 15°C, and a 0.033% CO_2 -air feed, DFs were 2×10^3 to 10^2 for superficial velocities of 5 to 80 cm/min. For 0.4 M $\text{Ba}(\text{OH})_2$ in the 27.3-cm-ID contactor, a power consumption of 21.0 kW/m³ ($n = 650$ rpm), a temperature of 15°C, and a 0.033% CO_2 -air feed, DFs were 10^4 to 10^3 for superficial velocities of 20 to 80 cm/min. For 1.0 M NaOH in the 27.3-cm-ID contactor, a power consumption of 21.0 kW/m³ ($n = 650$ rpm), a temperature of 25°C, and a 0.033% CO_2 -air feed, DFs were 10^4 to 10^3 for superficial velocities of 40 to 80 cm/min. DFs obtained for CO_2 removal from 0.033% CO_2 -air mixtures were about a factor of 2 larger than those obtained for CO_2 removal from 1-3% CO_2 -air feed gases.

A very promising alternative process for removing CO_2 from off-gases with low CO_2 content is the reaction with solid $\text{Ba}(\text{OH})_2$ (mono- or octahydrate) in packed or fluidized beds. Decontamination factors $>10^4$ were obtained for CO_2 removal at ambient conditions from water-saturated gas feeds containing 4.5% CO_2 , and DFs of at least 10^3 were obtained for CO_2 removal from water-saturated air.

I. Introduction

Recently, the fact that ^{14}C may constitute a significant radiological hazard in the effluents from nuclear power facilities, particularly from fuel reprocessing plants, has become a matter of increasing concern. Since Bonka⁽¹⁾ and Magno⁽²⁾ first discussed the problem posed by ^{14}C which is produced in nuclear power reactors, studies have been conducted to measure the quantity of ^{14}C released at nuclear power plants [Kunz⁽³⁾] and to predict the behavior of the ^{14}C that would be released in LWR, HTGR, and LMFBR fuel reprocessing plants [Davis⁽⁴⁾, Croff⁽⁵⁾, and Killough⁽⁶⁾]. Among the studies conducted to predict the behavior of CO_2 in the atmosphere were those of Machta⁽⁷⁾, Killough⁽⁸⁾, and Snider and Kay⁽⁹⁾.

According to Davis⁽⁴⁾, ^{14}C is formed from neutron reactions with isotopes of elements that are normal or impurity components of the cooling water, fuel, and structural materials of LWRs. The neutron-induced reactions are: (1) $^{13}\text{C}(n,\gamma)^{14}\text{C}$, (2) $^{14}\text{N}(n,p)^{14}\text{C}$, (3) $^{15}\text{N}(n,d)^{14}\text{C}$, (4) $^{16}\text{O}(n,^3\text{He})^{14}\text{C}$, and (5) $^{17}\text{O}(n,\alpha)^{14}\text{C}$. Most of the ^{14}C will be formed by the fuel reactions $^{17}\text{O}(n,\alpha)^{14}\text{C}$ and $^{14}\text{N}(n,p)^{14}\text{C}$. Nitride nitrogen at a median concentration of 25 ppm was estimated to produce 14 and 15 Ci of $^{14}\text{C}/\text{GW}(\text{e})\text{-yr}$ in BWR and PWR fuels, respectively, while the contribution of ^{17}O in BWR and PWR fuels would be 3.3 and 3.5 Ci of $^{14}\text{C}/\text{GW}(\text{e})\text{-yr}$, respectively. The net contribution of all the possible neutron reactions was estimated to be in the range of 400 to 2200 Ci of ^{14}C per year for a LWR fuel reprocessing plant treating 1500 metric tons of heavy metal annually with a range of 40 to 240 ppb of $^{14}\text{CO}_2$ in a reference flow of 500-scfm off-gas.

Also, Kunz et al.⁽²⁾ have reported that for the BWR at Nine Mile Point [625 MW(e)], a release rate of 8 Ci of ^{14}C per year was observed. These authors also reported that 6 Ci/GW(e)-yr was measured in the emissions from Ginna, Indian Point 1, and Indian Point 2 PWRs. For the BWR, the ^{14}C was distributed as 95% CO_2 , 2.5% CO , and 2.5% in the hydrocarbons, while in the PWRs more than 80% of total gaseous ^{14}C activity was contained in CH_4 and C_2H_6 , with less than 5% as CO_2 and CO .

In view of the above-noted concentrations of $^{14}\text{CO}_2$ in LWR power plant and fuel reprocessing off-gases, a process evaluation was conducted to review the various technical methods for recovering $^{14}\text{CO}_2$, along with the more abundant normal CO_2 , from the LWR reprocessing plant dissolver off-gas stream and for immobilizing it in a stable leach-resistant solid matrix. An initial experimental program⁽¹⁰⁾ had shown that DFs of 10^2 for single-stage contacting and 10^4 for two-stage contacting in a gas-lime slurry [$\text{Ca}(\text{OH})_2$] agitated contactor were feasible for removing CO_2 from simulated HTGR fuel reprocessing off-gases. The product CaCO_3 , which could be easily recovered in an aqueous mixture containing 40 to 50 wt % CaCO_3 , offered a very attractive chemical form capable of maintaining acceptable stability under requisite long-term storage conditions. However, the simulated HTGR off-gases which were studied were very rich in CO_2 ($\sim 90\%$) so that it was necessary to conduct additional

15th DOE NUCLEAR AIR CLEANING CONFERENCE

experiments for simulated LWR fuel reprocessing off-gases for which probable CO₂ concentrations are in the range of 0.03-1.0%.

II. Experimental Apparatus

Mechanically Agitated Gas-Alkaline Slurry Contactor

Two continuous stirred-tank contactors were utilized in the studies concerning CO₂ removal from simulated LWR fuel reprocessing off-gases. The 20.3-cm-ID contactor has been previously described in detail(10), while the 27.3-cm-ID contactor was designed to be a geometrically similar scaled-up version, by about a factor of 2, of the smaller Rushton-type contactor. However, to simplify operation during studies utilizing continuous slurry flow, the disengaging section of the larger contactor was redesigned to allow the slurry to be removed through the top flange area of the contactor. To minimize troublesome flow interruption from slurry settling during intermittent operation, two input ports for the slurry were provided in the bottom flange of the 27.3-cm-ID contactor. Additional improvements to the original contactor were replacement of the shaft seal, consisting of pressure rings and a packing gland, with a more dependable Crane mechanical seal, and introduction of a 2-to-1 gear reduction in the Gast air-motor drive to enhance torque-loading capabilities of the turbine impeller. A schematic of the experimental equipment is shown in Fig. 1.

Beds of Hydrated Barium Hydroxide

The efficient removal of CO₂ from 0.033% CO₂-air feeds was also achieved in beds of barium hydroxide at ambient conditions (~21°C). Both packed beds and fluidized beds were useful for treatment of 0.033% CO₂-air feeds; higher velocities were achieved in the fluidized bed contactor. The packed beds had dimensions of 2.54 x 15.2 cm and contained up to 62 g of Ba(OH)₂ (mono- or octahydrate). The fluidized beds were tapered, varying from 2.54 to 7.62 cm ID over a 91-cm length. Neither column contactor was provided with means for controlling temperature.

III. Analytical Techniques

Background

In the initial stages of this experimental program, it quickly became apparent that the employment of sensitive analytical instrumentation to detect CO₂ effluent concentrations <1 ppm would be as important to the success of the program as the development of processes to achieve effluents of that quality. Brief discussions of three different analytical techniques which were investigated and, in some cases, successfully applied to analyzing CO₂ at the <1 ppm level are presented in the paragraphs that follow.

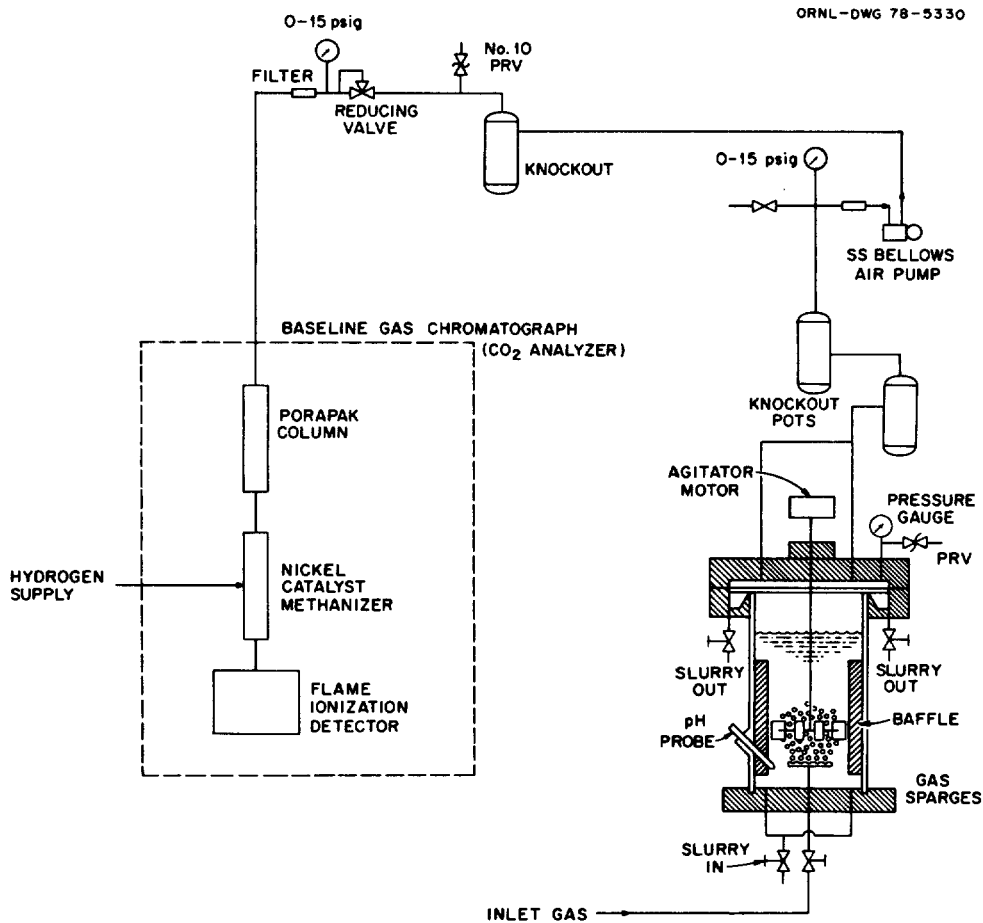


Fig. 1. Schematic of agitated-contactor experimental equipment and gas analysis system.

15th DOE NUCLEAR AIR CLEANING CONFERENCE

Liquid Scintillation Counting of Sorbed $^{14}\text{CO}_2$

In an alternative technique for measuring traces of $^{14}\text{CO}_2$ in both feed and product streams, the CO_2 can be sorbed from the appropriately sized thief-stream into a solvent capable of quantitative reaction with the CO_2 . The solvent is then mixed with the appropriate scintillant, and the bound $^{14}\text{CO}_2$ is detected in a liquid scintillation counter. Among the most widely used solvents for this analytical technique are the hydroxide of hyamine, ethanolamine-cellosolve mixtures, and phenethylamine(11-13).

The continuous reaction of CO when bubbled into a stirred solvent at a low flow rate appears to be the most promising technique for $^{14}\text{CO}_2$ trapping. Of course, any ambient CO_2 that is sorbed does not interfere with the $^{14}\text{CO}_2$ counting because nonradioactive CO_2 only consumes part of the solvent, which is supplied at sufficient excess to avoid depletion. We have been able to reproducibly count $^{14}\text{CO}_2$ -labeled air (330 ppm total CO_2) containing 10^6 - 10^7 cpm/liter and obtain an accountability of >95% of the available counts. However, a primary concern with this method has been to ensure that the continuous-bubbling organic solvent technique is capable of trapping CO_2 at levels below 1 ppm. This question has been studied by making controlled dilutions, with pure helium, of 1/100, 1/500, and 1/1000 of a 0.033% CO_2 -air feed for which the $^{14}\text{CO}_2$ content is known. Thus the ability of the organic solvent to trap 3 ppm or 0.3 ppm of CO_2 can be tested. Initial results with the gas containing 3 ppm of CO_2 with $^{14}\text{CO}_2$ tracer have indicated that at least 80% of the 3 ppm can be sorbed in the organic solvent bubbler. Experiments will be continued at the ppb level. Great care must be taken to ensure that such small quantities of CO_2 are not absorbed in the piping and glassware prior to the organic solvent bubbler.

Infrared Spectroscopy

A number of manufacturers can provide infrared spectrometers which are capable of measuring CO_2 in the 1-ppm range. We are in the process of evaluating infrared (IR) instrumentation which is capable of detecting CO_2 in the 100-ppb range. Thus far in our investigation, we have utilized IR to obtain data for CO_2 effluents in the 1-ppm range.

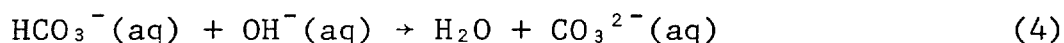
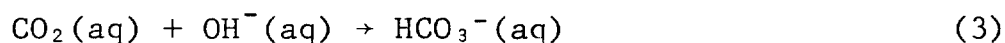
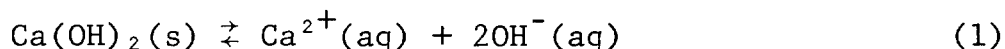
Flame Ionization Detection

The analytical system that has provided the most reliable determinations of CO_2 effluent stream concentrations below 1 ppm involves gas chromatography (GC) with analysis by flame ionization detection. Williams et al.(14) and Eaton et al.(15) have shown that, by utilization of a methanizer in conjunction with appropriate fractionating columns and a flame ionization detector (FID), CO_2 can be measured accurately at the 100-ppb level in ideal gas mixtures containing air with a known organic component. Our most reproducible results were obtained with a specially fitted GC instrument containing the three required elements: a fractionating column, a H_2 -nickel catalyst bed for carbon compound conversion to CH_4 , and the

FID unit. As much as 50% uncertainty may exist in measurements at the 100-ppb level. Some developmental work may be necessary to accurately obtain CO₂ levels below 1 ppm whenever actual or accurately simulated fuel reprocessing off-gases are studied, because such gases could contain trace organics at the 1-ppm level. A schematic of the methanizer and flame ionization detection system is shown in Fig. 1.

IV. Theoretical Considerations

Juvekar and Sharma⁽¹⁶⁾ have extensively discussed the mechanism for the absorption of CO₂ into a suspension of Ca(OH)₂ in both bubble columns and mechanically agitated contactors. They hypothesized that the overall process of carbonation of lime could be described by:



Because reactions (4) and (5) are instantaneous, the controlling mechanism is in reaction (1), (2), or (3). The gas-phase diffusional resistance could become important only for gases containing low concentrations of CO₂. After consideration of the rate equations for transport of CO₂ through the gas film, for the rate of dissolution of Ca(OH)₂, and for the rate of transport of CO₂ into the liquid and the reaction of CO₂ with hydroxyl ions, Juvekar derived the following rate expression:

$$R\alpha = \frac{\alpha H p_g [D_A k_2 (\text{OH}^{-})_s + k_L^2]^{0.5}}{1 + \frac{\alpha H [D_A k_2 (\text{OH}^{-})_s + k_L^2]^{0.5}}{k_G \alpha}} \quad (6)$$

where

- R = specific rate of absorption of CO₂, g-mole/sec-cm² dispersion,
- α = gas-liquid interfacial area, cm²/cm³ dispersion,
- p_g = partial pressure of CO₂ in the bulk gas, atm,
- D_A^g = diffusivity of CO₂ in aqueous solution, cm²/sec,
- k₂ = rate constant for the reaction between CO₂ and OH⁻ ions, cm³/(g-mole-sec),
- (OH⁻)_s = saturation concentration of OH⁻ ions in aqueous solution in equilibrium with solid Ca(OH)₂, g-ion/cm³,
- k_L = liquid-side mass transfer coefficient in the absence of chemical reaction, cm/sec,

15th DOE NUCLEAR AIR CLEANING CONFERENCE

$k_G\alpha$ = gas-side mass transfer coefficient, g-mole/(cm³ · dispersion-sec-atm),
 H = Henry's coefficient of solubility, g-mole/(cm³-atm).

This expression applies to about 80% of the reaction time (for semi-batch operation), which is called the "constant rate period" wherein hydroxyl concentration remains constant. Another expression is necessary to describe the "falling rate period" (in which the OH⁻ concentration and the rate of CO₂ reaction decrease). Operation of the process with continuous slurry flow allows for OH⁻ stabilization and thus eliminates the falling rate period.

Because the contactor design and operating conditions of this study were similar to those used by Juvekar and Sharma, we may adopt their value of $\sim 10^{-4}$ g-mole/(cm³-sec-atm) for $k_G\alpha$ (gas-side mass transfer coefficient for gas-phase control in an agitated contactor). In order for the gas-side resistance to contribute significantly to the overall mass transfer resistance, the following relationship should be satisfied:

$$\frac{\alpha H p_g [D_A k_2 (\text{OH}^-)_s + k_L^2]^{0.5}}{k_G\alpha} \geq 1 \quad (7)$$

Condition 7 is not satisfied for feed gases containing 1-5% CO₂ or 0.033% CO in air, so that the rate expression for CO₂ absorption in a lime suspension in the mechanically agitated contactor becomes:

$$R_a = \alpha H p_{DF} [D_A k_2 (\text{OH}^-)_s + k_L^2]^{0.5} \quad (8)$$

or, for dilute CO₂-air feed gases,

$$[\ln DF] R_a \cong \alpha H (p_i - p_o) [D_A k_2 (\text{OH}^-)_s + k_L^2]^{0.5} \quad (8a)$$

The rate expression given in Eq. 8 is generally assumed to be applicable at any point in the agitated contactor and thus the specific rate R_a can be directly related to the overall mass transfer rate for the total dispersed volume in the contactor. The proper form of the pressure term p_{DF} for the agitated contactor appears to be dependent on the nature of the solution or suspension in the contactor. The log-mean pressure was shown by Juvekar for dilute CO₂-air mixtures to be the proper form for the pressure driving force for the CO₂-Ca(OH)₂ reaction under the following conditions: (1) CO₂ reacting with a Ca(OH)₂ slurry; (2) CO₂ concentrations in air of about 10%; (3) a 12.5-cm-ID agitated contactor; (4) impeller speeds, n , of 1000 to 2000 rpm; and (5) gas superficial velocities, Q_s , of 2.2 to 4.6 cm/sec. For these conditions [(1) through (5)], utilization of the log-mean (based on natural log) form for pressure resulted in more "reasonable" values for the interfacial area than those calculated from the backmix model because the latter model would predict the illogical trend that the area increased as the flow rate decreased.

It is interesting to note that, for similar contactor design, operating conditions, and feed gas compositions, previous studies

(Mehta and Sharma⁽¹⁷⁾, Hanhart et al.⁽¹⁸⁾) have shown that both gas and liquid phases in an agitated gas-liquid dispersion are almost completely mixed when the speed of agitation exceeds a certain critical value. However, for CO₂ sorption into a slurry, several studies (Holladay⁽¹⁰⁾, Morris and Woodburn⁽¹⁹⁾, Juvekar and Sharma⁽¹⁶⁾) have shown that the system appears to be better represented by a plug flow model than by a backmix assumption. It is believed that the presence of the fine solids alters the coalescence behavior and flow pattern of the gas bubbles.

The data of this study differ from those of Juvekar and Sharma in two key respects: (1) a considerable number of the experiments were conducted with feed gas containing only 0.033% CO₂; (2) in order to achieve the primary goal of these studies, which was a high CO₂ removal efficiency, it was necessary to use superficial gas feed rates considerably lower than those studied by Juvekar. With regard to point 1, the similarity between DFs obtained for feed gases containing 0.033% CO₂ or 1-5% CO₂ in air would appear to eliminate the concern that there were different mass transfer control regimes for the two feed concentrations. However, the variation in flow rates is a major factor in the interpretation of our data with the model of Eq. 8. Whereas Juvekar noted no variation in interfacial area with superficial velocity, calculations of interfacial area a based on our studies indicate a very strong dependence of a on Q_s , even for agitation speeds well in excess of n_0 (as defined by Westerterp et al.⁽²⁰⁾). The log-mean model resulted in calculation of values of a from 0.2 to 2.0 cm²/cm³, while the backmix model predicted values from 30 to 50 cm²/cm³. The log-mean values of a varied directly with Q_s up to $Q_s \approx 2$ cm/sec and then appeared to level off in agreement with Juvekar's work.

Thus, Eq. 8 can be utilized to formulate qualitative predictions about the effects of such operating parameters as temperature, impeller speed, and gas superficial velocity on the rate, and more importantly the DF, which can be obtained for CO₂ removal in agitated contactors. Because the dissolution of Ba(OH)₂ and subsequent reaction with CO₂ in a sparged, agitated tank should follow the same reaction scheme as proposed in Eqs. 1-5, the same form of Eq. 8 should be relevant to the predictions of CO₂ reaction with Ba(OH)₂ slurries. The reaction between CO₂ and the NaOH solution should also be described by Eq. 8, with the backmix pressure term.

So in general for fixed H , D_A , k_2 , (OH^-) , and k_L , it is predicted by Eq. 8 that the DF will vary inversely with gas superficial velocity Q_s (because of the direct variation of R_a with Q_s) and directly with impeller speeds above the critical speed (because of the direct variation of interfacial area with n). DF will also vary directly with temperature for suspensions in which the solubility of the solids increases with temperature. The temperature variation occurs because the effects of the increase in rate constant and hydroxyl solubility are larger than the effect of the decrease in CO₂ solubility in aqueous solutions. Because of the inverse variation of Ca(OH)₂ solubility with temperature, Eq. 8 sometimes predicts a reduction in DF for an elevation in temperature for Ca(OH)₂ slurries for the log-mean case.

15th DOE NUCLEAR AIR CLEANING CONFERENCE

Yet the question remains concerning the precise form of Eq. 8 for application to the removal of CO₂ from 0.033% CO₂--air at low superficial velocities and high impeller speeds. The precise form of the residence time is unclear for the CO₂ in transit through the suspension; hence uncertainty remains about the proper form for the pressure driving force. The DFs predicted by the log-mean model for a Ba(OH)₂ slurry when compared to the DFs for a Ca(OH)₂ slurry under the same feed and operating conditions are higher than the actual measured data (it was assumed that α , H, T, D_A, and k₂ were held constant). The DFs predicted by the backmix model are lower than those obtained experimentally. Perhaps the ultimate solution to this quandary is to describe the DF by an expression which links both the kinetics as expressed in Eq. 8 and the effects of physical parameters such as power input, superficial velocity, impeller design, solution density, and viscosity through a multiparameter empirical model.

V. Experimental Results

Comparison of Decontamination Factors Obtained for CO₂ Removal in the 20.3- and 27.3-cm-ID Contactors

Two comparisons of the experimental data for removal of CO₂ from air containing 0.033% and 1-5% CO₂ are shown in Fig. 2. First, results were obtained for air feeds to the 20.3- and 27.3-cm-ID contactors to provide initial information concerning scale-up of the process. Second, the results for removal of CO₂ from air containing 0.033% or 1-5% CO₂ were obtained to determine the effect of two orders of magnitude of feed gas dilution on the efficiency of the process. The CO₂ contents in the contactor gaseous effluents were determined by GC with methanization and flame ionization detection for concentrations less than ~1 ppm and by IR spectroscopy and GC with thermal conductivity detection for concentrations \geq 1 ppm. As indicated in Fig. 2, a few of the high DF values at low superficial velocities were also corroborated by analysis utilizing sorption of ¹⁴CO₂ tracer from 0.033%--air feeds into organic solvents (ethanolamine-Cellosolve mixture) and subsequent counting by beta scintillation detection. The temperature of the suspension and solutions in the contactor was controlled in the range of 15-25°C.

The useful similarity between the DF curves for removing CO₂ from 0.033% CO₂-air or from 1-5% CO₂-air is apparent in Fig. 2. It is also evident from the data of Fig. 2 that there is reasonable agreement between the DF values obtained in the 20.3- and 27.3-cm-ID contactors for the same feed gas compositions, superficial velocities operating temperatures, and impeller speeds. All the DF curves appear to follow the same general pattern as a function of gas superficial velocity; that is, at low velocities, they tend to pinch toward asymptotically increasing values of DF. For gas superficial velocities in the range of 10-60 cm/min, the DF curves become essentially exponential functions of Q_S. At high superficial velocities, all curves appear to level off toward values which are probably associated with a rapid plug flow transit through the

ORNL-DWG 78-9912

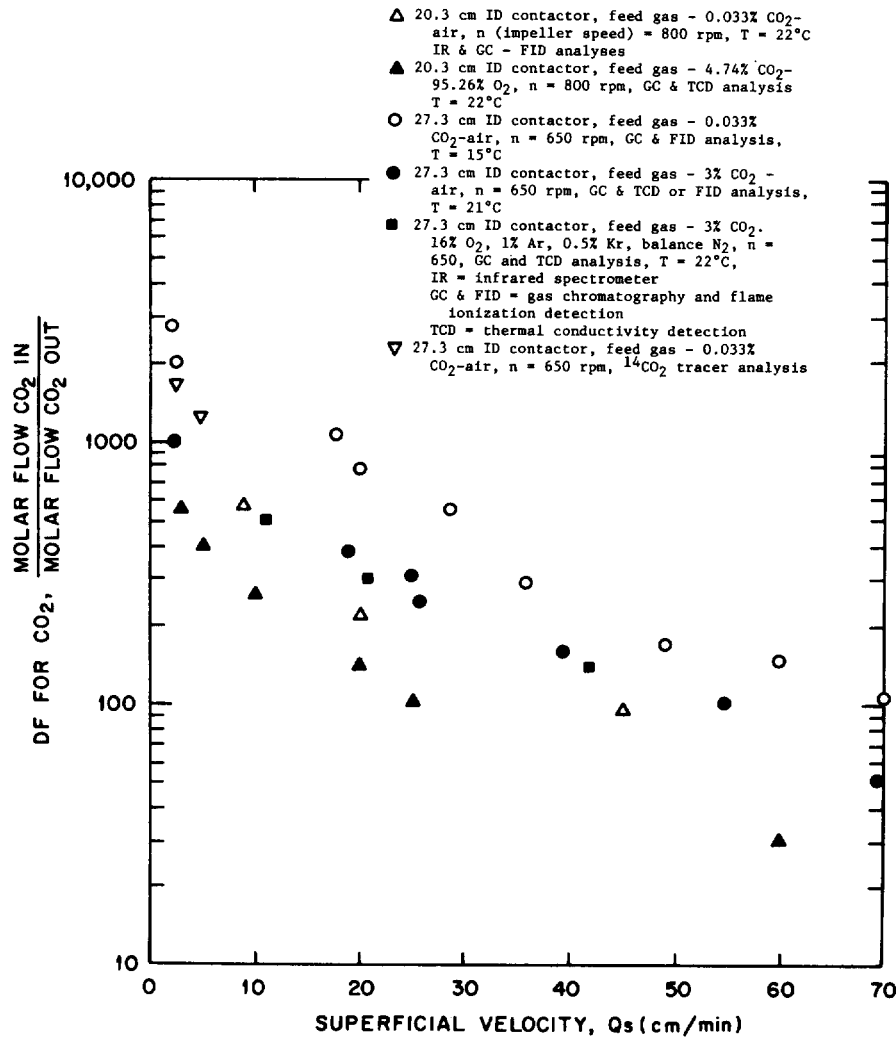


Fig. 2. Comparison of DFs for CO₂ removal from dilute gas streams utilizing a 1.0 m Ca(OH)₂ slurry in 20.3- and 27.3-cm-ID agitated contactors.

contactor. It is not clear whether all curves would tend to approach the same value at high superficial velocities. Further studies may be desirable at very high superficial velocities.

When a 0.033% CO₂--air feed was reacted with a 1.0 m Ca(OH)₂ slurry in the 27.3-cm-ID contactor, the DFs varied from 10³ to 10² as the superficial velocity was increased from 5 to 70 cm/min. In general, the DF values obtained for CO₂ removal from 1-5% CO₂--air were somewhat lower (about a factor of 2) than those obtained for 0.033% CO₂--air for similar operating conditions (i.e., equal impeller speed, slurry concentration and temperature, superficial velocity, and contactor size).

The higher DFs obtained in the 27.3-cm-ID contactor may have been due to a slightly better design which resulted in more efficient mixing and higher interfacial area and mass transfer for that contactor. The volumes of the two contactors were too similar to allow us to determine whether the most appropriate criterion for contactor scale-up should be maintenance of constant superficial velocity or constant retention time. Either case would require additional scaling criteria such as maintenance of constant interfacial area, maintenance of the constant $nD_I/D_T^{0.5}$ (D_I = impeller diameter, D_T = contactor diameter) [proposed by Westerterp(20,21)], or maintenance of constant power input per volume of contactor. The data obtained at this time for constant power inputs did appear to show more similarity when compared for equal residence times rather than for equal superficial velocities. However, the question of proper scaling factor remains to be solved at a larger scale of contactor design.

It is also apparent from the results of Fig. 2 that the presence of 0.5% krypton in the feed gas had no effect on removal of CO₂ from air streams containing 1-5% CO₂. Further studies are now being conducted with ⁸⁵Kr-traced feed gases to determine the distribution of krypton between the gas and slurry phases. If the distribution is such that only a very low level (e.g., krypton in slurry = 0.0001 krypton in gas) of krypton is included in the slurry, the CO₂ removal process could be placed upstream of the krypton removal operation during off-gas processing.

When CO₂ was removed from 0.033% CO₂-air with a 1.0 m Ca(OH)₂ slurry in a 27.3-cm-ID contactor for no mechanical agitation ($n = 0$), the DFs ranged from 10 to 1 as the gas superficial velocity was increased from 5 to 70 cm/min.

For most of the experiments in this study, DFs were obtained for removal of CO₂ from dilute CO₂-air feeds with semibatch operation of the agitated contactor (no slurry flow). For semibatch operation with 1.0 m Ca(OH)₂, gas flow was maintained through the agitated contactor until the pH began to drop below the 12.4-12.6 range (dependent on operating slurry temperature). The time at which the pH begin to fall coincided with about 90% conversion of the Ca(OH)₂. Semibatch operation with Ba(OH)₂ slurries was obtained in a similar manner, but the pH range was different. Semibatch operation with NaOH solution was obtained for only a small decrease in pH due to excess capacity of the solution relative to a feed gas containing

only 3% CO₂. In a few experiments, for the same operating conditions (that is, gas flow rate, slurry temperature, impeller speed, etc) in both modes of operation, it was shown that there was little difference in DFs obtained for CO₂ removal for either semibatch or continuous slurry operation. Because the feed gases studied were dilute in CO₂, only a very slow continuous flow of 1.0 m Ca(OH)₂ was needed to replace the Ca(OH)₂ depleted by reaction with CO₂.

Comparison of Decontaminated Factors Obtained for CO₂ Removal from 0.033% CO₂--Air and 1% CO₂--Air Feeds with Slurries of Ca(OH)₂ and Ba(OH)₂ or Solutions of NaOH

Figure 3 shows experimental results which indicate the effects of varying the metal hydroxide composition or the power input on the removal of CO₂ from dilute CO₂--air feed gases in the 27.3-cm-ID agitated contactor. The theoretical nonsparged power inputs in the 27.3-cm-ID contactor for impeller speeds of 325 and 650 rpm, for impeller diameters one-half the contactor diameter, are about 2.6 and 21.0 kW/m³ (0.1 and 0.8 hp/ft³), respectively. Although the DF values are presented as a function of gas superficial velocity, the latter variable can be converted to nominal residence time by reciprocation after division by the appropriate dispersed-phase height (32-34 cm). The quiescent slurry volume was about 17 liters, while the agitated dispersed volume was typically 19 to 20 liters.

According to Eq. 8, at fixed values of superficial gas velocity, temperature (H and k_2 fixed), and impeller speed, the pressure driving term should vary inversely with hydroxyl ion concentration, according to the particular metal hydroxide employed. Conversely, the process DF should vary directly with $[\text{OH}^-]$. For fixed operating conditions, an increase in $[\text{OH}^-]$ should result in an increase in $R\alpha$ but a decrease in p_{DF} . However, for operating conditions which result in DFs in excess of 10^2 , the rate $R\alpha$ becomes relatively constant, as there is little difference in 0.99 N_{CD}, 0.999 N_{CD}, or 0.9999 N_{CD} (where N_{CD} is CO₂ molar flow rate). Thus an increase in $[\text{OH}^-]$ concentration is manifested in a concomitant decrease in p_{DF} (and an increase in DF). Also, as previously discussed in Section IV, the process DF is predicted by Eq. 8 to vary inversely with superficial velocity, directly with impeller speed, and in most cases directly with slurry temperature. All of these predicted functional relationships are supported by the results in Fig. 3.

Under standard operating conditions of $T \approx 20^\circ\text{C}$ and $n = 650$ rpm, the lowest DFs obtained for CO₂ removal in the 27.3-cm-ID contactor were for 1.0 m Mg(OH)₂ suspensions. With fixed gas velocities, the DFs increased according to the solubilities of the hydroxyl species, varying in the order $\text{DF}(\text{NaOH}) > \text{DF}(\text{Ba}(\text{OH})_2) > \text{DF}(\text{Ca}(\text{OH})_2)$. The DFs obtained for Ba(OH)₂ and NaOH systems varied directly with temperature, while for Ca(OH)₂ the dependence was less due to an inverse relationship between Ca(OH)₂ solubility and temperature.

Doubling the impeller speed at fixed operating conditions resulted in a sizable increase in the DF for CO₂ removal, regardless

ORNL-DWG 78-9913

Reactant	Impeller speed	Gas composition	Analytical method	Temp
△ 1 m Mg(OH) ₂	650 rpm	0.033% CO ₂ -air	GC & TCD	21°C
▲ 1 m Ca(OH) ₂	325 rpm	1 and 3% CO ₂ -air	GC & TCD or FID	21°C
○ 1 m Ca(OH) ₂	650 rpm	0.033% CO ₂ -air	GC & FID	15°C
● 1 m Ca(OH) ₂	650 rpm	3% CO ₂ -air	GC & TCD or FID	21°C
▽ 1 m Ca(OH) ₂	650 rpm	0.033% CO ₂ -air	GC & FID	60°C
◻ 0.4 and 0.75 m Ba(OH) ₂	650 rpm	0.033% CO ₂ -air	GC & FID	15°C
■ 0.4 and 0.75 m Ba(OH) ₂	650 rpm	3% CO ₂ -air	GC & TCD or FID	25°C
▼ 1.0 N NaOH	650 rpm	3% CO ₂ -air	GC & TCD or FID	25°C

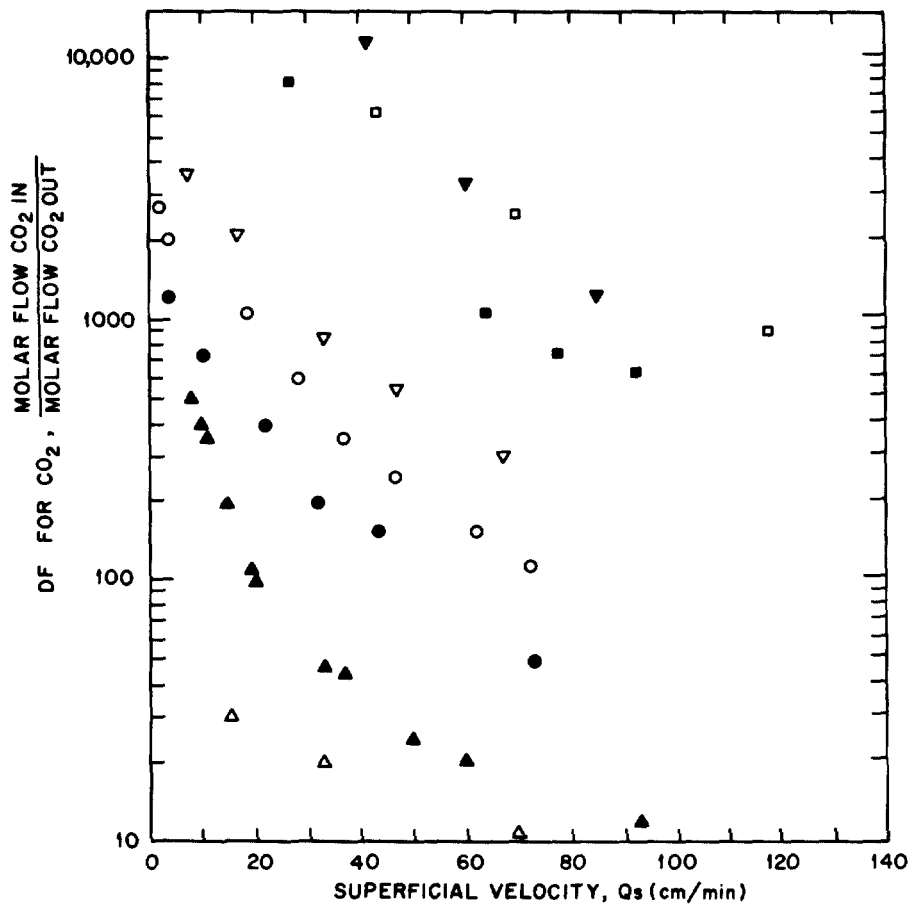
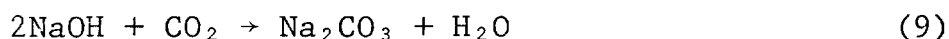


Fig. 3. DFs for CO₂ removal obtained for different metal hydroxide slurries at various impeller speeds, superficial velocities, and temperatures in the 27.3-cm-ID contactor.

of which metal hydroxide was used. Unfortunately, the improvement in process DF was accompanied by a penalty of about an eightfold increase in power input.

The similarity in the DFs obtained for CO₂ removal from feeds containing 0.033% CO₂--air and 1-5% CO₂--air is shown for both Ba(OH)₂ and Ca(OH)₂ suspensions. However, the DFs appear to be consistently higher for removal of CO₂ from the more dilute feed gas. Determination of DFs for CO₂ removal from gases containing 1-5% CO₂ was made for two reasons: (1) a need for treating a reprocessing off-gas containing as much as 1-5% CO₂ may arise in the future, (2) the similarity between DFs obtained for 0.033% and 1-5% CO₂ was useful because, even with the GC-flame ionization detection system, the practical lower limit for CO₂ detection was ~100 ppb. When such concentrations occurred in effluents from the contactor for 0.033% CO₂--air feeds at low gas velocities, approximate DF values for the 0.033% CO₂-air feed could be readily estimated from the effluents from the contactor for feed gases containing 1% CO₂. In that case, an effluent of 100 ppb corresponded to a DF of 10⁵.

Examination of the results of Fig. 3 indicates that there could be an advantage in utilizing a combination of NaOH solution with a Ca(OH)₂ or Ba(OH)₂ slurry to enhance the scrubbing efficiency for CO₂ removal from feed gases either dilute or rich in CO₂. Although no experiments have yet been conducted with this promising system, one might expect a set of reactions such as the following:



The total process could be conducted in one stirred contactor. Reactions 9 and 10 would be competing; however, the CaCO₃ would be a desirable end-product as it is for the CO₂-Ca(OH)₂ reaction alone. Any Na₂CO₃ formed by reaction 9 would react as in Eq. 11, resulting in the release of NaOH as an autocatalyst. The product would be filtered, the cake would be washed to remove any soluble salts, and the liquor containing primarily NaOH (with makeup Ca(OH)₂ added) could be recycled to the initial contactor operated in a continuous-flow mode.

Examination of the Group 2 elements in the periodic chart reveals that the metal hydroxide solubility increases, and the carbonate solubility decreases, with increasing atomic weight. However, when both cost and carbonate solubility are considered, Ba(OH)₂ appears to be the only other Group 2 hydroxide which could actually be competitive with slurried Ca(OH)₂.

CO₂ Removal from 0.033% CO₂--Air and 1-5% CO₂--Air Utilizing Fixed Beds and Fluidized Beds of Dry Hydrated Barium Hydroxides

Background. The efficacy of hydrated barium hydroxide in reacting with CO₂ at ambient conditions appears to have been ignored

in the search for techniques which serve to remove CO_2 from dilute CO_2 --air streams and simultaneously provide a product amenable to the extended storage time which is necessitated by the long half-life of ^{14}C . It has been known for years⁽²²⁾ that LiOH as a solid bed possessed excellent CO_2 removal characteristics. Although the solid Li_2CO_3 product would be quite resistant to thermal decomposition, it would be too soluble to qualify as a candidate for long-term storage. Holladay⁽¹⁰⁾ and Engel et al.⁽²³⁾ have shown previously that solid $\text{Ca}(\text{OH})_2$ does not readily react with CO_2 at ambient conditions; significant rates are achieved only by adding heat at approximately 400°C . Also, CO_2 does not readily react with CaO or BaO at ambient conditions because of rate limitations which arise from diffusional resistance produced by formation of carbonates on the surface of CaO or BaO particles.

The gas-solid carbonation reaction between CO_2 and CaO has been the subject of numerous studies. Depending on the experimental conditions used, the conversion of CaO and CaCO_3 has ranged from 10 to 80%. The rate of solid carbonation was enhanced by ensuring the presence of water vapor, by increasing the temperature in the range of 300 - 800°C , and by increasing the pressure at the higher temperatures. It has been reported that BaO reacts with CO_2 faster at lower temperatures than does CaO . The interested reader should consult the review conducted by Swanson⁽²⁴⁾, who has compiled a list of 71 references concerning the reaction between CO_2 and solid alkaline oxides, hydrated alkaline hydroxides, alkaline slurries, and other substances.

Experimental Results

The studies that have been performed to date for removing CO_2 at ambient conditions from dilute CO_2 --air feed gases with $\text{Ba}(\text{OH})_2$ hydrates in fixed and fluidized beds have been of a preliminary and scoping nature. Thus, only general information and process trends will be discussed. Much more in-depth information must be obtained before the process can be discussed from a mechanistic or theoretical perspective.

In initial experimental studies with $\text{Ba}(\text{OH})_2 \cdot 8\text{H}_2\text{O}$ reactant at room temperature, DFs in excess of 300 were obtained for CO_2 removal from 0.033% CO_2 --air with the reactant in both fixed and fluidized beds (DFs >300 could not be analytically detected in preliminary experiments). Results of these early studies showed that the DFs for CO_2 removal from 0.033% CO_2 --air were considerably enhanced when the feed gases were presaturated with water vapor. Therefore, all subsequent experiments were performed with water-saturated feed gases.

For the removal of CO_2 from feed gases containing 0.033%, 4.7%, and 88% CO_2 (balance as air), the highest DFs and bed conversions (routinely $>95\%$) were obtained with the $\text{Ba}(\text{OH})_2 \cdot \text{H}_2\text{O}$ species. A typical CO_2 sorption profile for a feed gas of 0.033% CO_2 --air contacted at room temperature with $\text{Ba}(\text{OH})_2 \cdot 8\text{H}_2\text{O}$ in a 2.54×15 cm glass column is shown in Fig. 4. For the initial 1 hr of contact time, DFs in excess of 3000 were obtained (100 ppb was the lower limit at which CO_2 could be accurately detected with the FID system). The DF then

ORNL DWG 78-9648 A

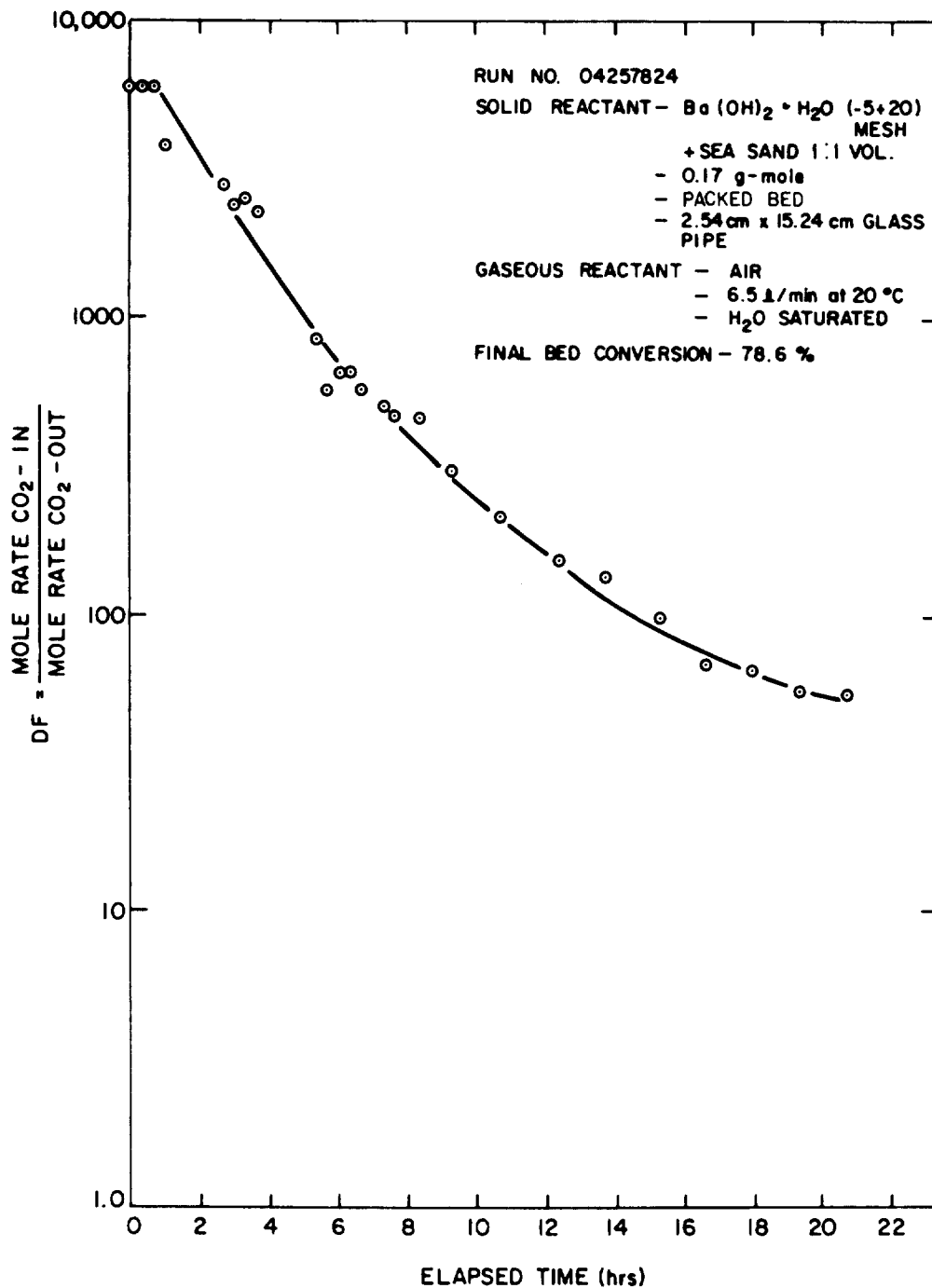


Fig. 4. Carbon dioxide removal capability of $Ba(OH)_2 \cdot H_2O$ in a fixed bed for treating a water-saturated feedstream containing 0.033% CO_2 -air.

15th DOE NUCLEAR AIR CLEANING CONFERENCE

decreased gradually as indicated, although a value of 10^2 could be obtained for 13 hr of operation or until about 40% of the bed had been converted. After 25 hr of operation, the bed conversion was 78%. The DFs for CO_2 removal from very dilute feed gases appear to be dependent on the movement of a mass transfer zone through the bed. Further studies will be necessary to characterize this mass transfer mechanism and, in particular, its dependence on such parameters as flow rate, feed gas composition, $\text{Ba}(\text{OH})_2$ species, and column design.

For the removal of CO_2 from a 4.78% CO_2 -air feed, the highest DFs and bed conversions were obtained with the $\text{Ba}(\text{OH})_2 \cdot \text{H}_2\text{O}$ species. The results of typical experiments for sorption of CO_2 from a 4.78% CO_2 -air feed at room temperature in packed beds of the three barium hydroxide species are shown in Fig. 5. DFs as high as 3×10^4 were obtained for 75% of the run time in the $\text{Ba}(\text{OH})_2 \cdot \text{H}_2\text{O}$ packed bed. Final bed conversion for processing 4.74% CO_2 -air was as much as 85%; however, in the latter portion of the operation, process DFs rapidly decreased below 10^3 as complete bed conversion was approached. When barium hydroxide hydrates are used for CO_2 removal, a common operational problem is an increase in pressure which results from the production of BaCO_3 fines. However, this effect can be at least partially reduced, if not eliminated, by increasing bed porosity with such measures as adding solids such as fly ash or sand to the bed or forming the $\text{Ba}(\text{OH})_2 \cdot \text{H}_2\text{O}$ into small pellets.

Fixed-bed treatments of 88% CO_2 --air feeds have been successful only for $\text{Ba}(\text{OH})_2 \cdot \text{H}_2\text{O}$ reactants. Conditions for a typical run consisted of processing 0.23 std liters/min of 88% CO_2 --air through 0.2 g-mole of $\text{Ba}(\text{OH})_2 \cdot \text{H}_2\text{O}$ in a 2.54 x 15 cm glass column. The maximum DF for a representative run was in excess of 10^5 . Conversion at the base of the bed was 95%. Because of the fast rate of reaction, sufficient heat was generated to increase the column temperature to $>70^\circ\text{C}$, which caused the $\text{Ba}(\text{OH})_2 \cdot \text{H}_2\text{O}$ in the upper portions of the bed to melt. The product formed in the presence of this high temperature was a hard solid which complicated product removal. The various heat-related process problems that occurred for treatment of the 88% CO_2 --air feed were alleviated when sand was added to the $\text{Ba}(\text{OH})_2 \cdot \text{H}_2\text{O}$. The presence of the sand changed the character of the product to a free-flowing solid. The DFs for removing CO_2 from 88% CO_2 --air feeds with $\text{Ba}(\text{OH})_2 \cdot 5\text{H}_2\text{O}$ and $\text{Ba}(\text{OH})_2 \cdot 8\text{H}_2\text{O}$ have been much lower than those obtained with $\text{Ba}(\text{OH})_2 \cdot \text{H}_2\text{O}$.

Based on the initial experimental studies with very dilute CO_2 --air feeds, the removal and permanent fixation of CO_2 from 0.033% CO_2 -air with $\text{Ba}(\text{OH})_2 \cdot \text{H}_2\text{O}$ in fluidized beds appear to be very promising. DFs in excess of 300 have been obtained at gas velocities considerably in excess of the minimum fluidization velocity (as much as five times the flow rate for the same DF in a packed bed). However, operation of the fluidized bed at the minimum fluidization velocity may sufficiently restrict the time and degree of gas-solid contact so as to produce poor overall mass transfer. Initial scoping data on laboratory-scale equipment have indicated that this may occur for a feed gas with 5% CO_2 concentration when it is contacted with 25-50 mesh $\text{Ba}(\text{OH})_2 \cdot \text{H}_2\text{O}$ in a tapered fluidized bed. Although entrainment of fines has caused operational difficulties, it is likely that

ORNL DWG 78-9650 A

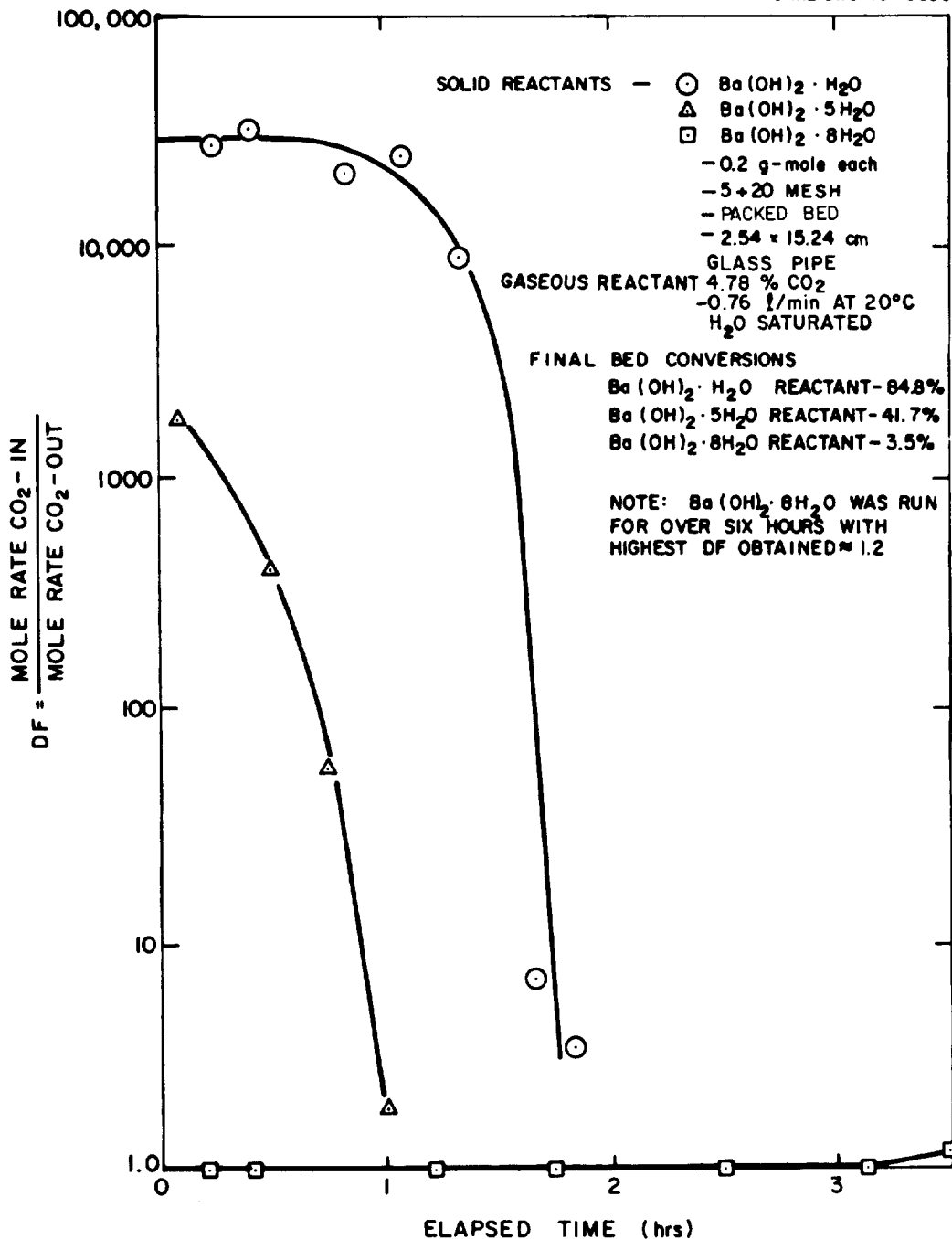


Fig. 5. Carbon dioxide removal capability of $\text{Ba}(\text{OH})_2 \cdot \text{H}_2\text{O}$ in a fixed bed for treating a water-saturated feedstream containing 4.78% CO_2 -air.

15th DOE NUCLEAR AIR CLEANING CONFERENCE

this problem can be resolved in larger-scale equipment through the use of cyclones and/or blowback filters.

The use of solid $\text{Ba}(\text{OH})_2$ offered possibilities of an operationally simpler and less expensive process than the $\text{Ca}(\text{OH})_2$ slurry contactor with its ancillary CaCO_3 recovery equipment. However, a distinct disadvantage of $\text{Ba}(\text{OH})_2$ was the expense relative to $\text{Ca}(\text{OH})_2$. Because reagent-grade $\text{Ba}(\text{OH})_2 \cdot 8\text{H}_2\text{O}$ was found to cost in excess of \$3.00/lb, a search for commercial suppliers of $\text{Ba}(\text{OH})_2$ was made. Discussions have been conducted with two vendors who will supply $\text{Ba}(\text{OH})_2$ in bulk quantities. Source 1 quoted $\text{Ba}(\text{OH})_2 \cdot 8\text{H}_2\text{O}$ in truckload quantities at \$0.50/lb (as of November 1977). Source 2 quoted truckload quantities of $\text{Ba}(\text{OH})_2 \cdot \text{H}_2\text{O}$, $\text{Ba}(\text{OH})_2 \cdot 5\text{H}_2\text{O}$, and $\text{Ba}(\text{OH})_2 \cdot 8\text{H}_2\text{O}$ at \$0.34, \$0.28, and \$0.235/lb, respectively (as of December 1977). Bulk $\text{Ca}(\text{OH})_2$ may be purchased at \$0.015/lb (as of May 1978). The various hydrates of $\text{Ba}(\text{OH})_2$ have been obtained from both vendors and are now being studied in fixed-bed experiments to ascertain their relative efficiencies in reacting with feed gases containing low concentrations of CO_2 .

VI. Conclusions

The removal of CO_2 from simulated LWR fuel reprocessing off-gases containing 0.033% CO_2 --air and 1-5% CO_2 --air has been shown to be feasible for gas processing with both alkaline slurries in agitated contactors and hydrated barium hydroxides in packed beds. It appears feasible to obtain CO_2 DFs of 10^2 to 10^3 for tractable sizes of equipment and operating conditions. However, the gas feeds that have been studied are those which simulate the composition of LWR fuel reprocessing off-gases as they would occur at the end of the off-gas processing train where I_2 , NO_x 's, and krypton would already have been removed. Thus, further experiments will be conducted to determine the effect of placing the CO_2 removal processes at optional sites in the off-gas processing train where such contaminants as I_2 and NO_x 's could complicate the operation and to determine the proper scaling factors for increasing the size of the agitated contactor process. Additional experiments will be conducted with $\text{Ba}(\text{OH})_2 \cdot x\text{H}_2\text{O}$ beds to optimize the parametric relationships among the following factors: degree of barium hydroxide hydration, bed particle size, bed temperature, gas flow rate, column design, and bed conversion and bed DF for CO_2 removal.

15th DOE NUCLEAR AIR CLEANING CONFERENCE

VII. References

1. H. Bonka et al., "Contamination of the Environment by Carbon-14 Produced in High Temperature Reactors," *Kerntechnik* 15(7), 297 (1973).
2. P. J. Magno, C. B. Nelson, and W. H. Ellett, "A Consideration of the Significance of Carbon-14 Discharges from the Nuclear Power Industry," p. 1047 in Proceedings of the Thirteenth AEC Air Cleaning Conference, San Francisco, Calif., CONF-740807 (August 12-15, 1974).
3. C. O. Kunz, W. E. Mahoney, and T. W. Miller, "Carbon-14 Gaseous Effluents from Boiling Water Reactors," *Trans. Am. Nucl. Soc.* 21, 91 (1975).
4. W. Davis, Jr., "Carbon-14 Production in Nuclear Reactors," ORNL/NUREG/TM-12 (February 1977).
5. A. G. Croff, "An Evaluation of Options Relative to the Fixation and Disposal of ^{14}C -Contaminated CO_2 as CaCO_3 ," ORNL/TM-5171 (April 1976).
6. G. G. Killough et al., "Progress Report on Evaluation of Potential Impact of ^{14}C Releases from an HTGR Reprocessing Facility," ORNL/TM-5284 (July 1976).
7. L. Machta, "Prediction of CO_2 in the Atmosphere," Carbon and the Biosphere, G. M. Woodwell and E. V. Pecan, Eds., Technical Information Center, Office of Information Services, U.S. Atomic Energy Commission (August 1973).
8. G. G. Killough, "A Diffusion-Type Model of the Global Carbon Cycle for the Estimation of Dose to the World Population from Releases of Carbon-14 to the Atmosphere," ORNL/TM-5269 (1977).
9. J. W. Snider and S. V. Kaye, "Process Behavior and Environmental Assessment of ^{14}C Releases from an HTGR Fuel Reprocessing Facility," Proceedings of the ANS-AIChE Topical Meeting, Sun Valley, Idaho, August 5-6, 1976.
10. D. W. Holladay, "Experiments with a Lime Slurry in a Stirred Tank for the Fixation of Carbon-14 Contaminated CO_2 from Simulated HTGR Fuel Reprocessing Off-Gas," ORNL/TM-5757 (1978).
11. E. Rapkin, "Hydroxide of Hyamine 10-X," Packard Technical Bulletin, revised 1961.
12. H. Jeffay and J. Alvarez, "Liquid Scintillation Counting of Carbon-14; Use of Ethanolamine-Ethylene Glycol Monomethyl Ether-Toluene," *Anal. Chem.* 33, 612 (1961).
13. F. H. Woeller, "Liquid Scintillation Counting of $^{14}\text{CO}_2$ with Phenethylamine," *Anal. Biochem.* 2, 508 (1961).

15th DOE NUCLEAR AIR CLEANING CONFERENCE

14. F. W. Williams, F. J. Woods, and M. E. Umstead, "Determination of Carbon Dioxide in the Parts-Per-Million Range with Gas Chromatography," J. Chromat. Sci. 10, 570 (1972).
15. H. G. Eaton, M. E. Umstead, and W. D. Smith, "A Total Hydrocarbon Analyzer for Use in Nuclear Submarines and Other Closed Environments," J. Chromat. Sci., 11, 275 (1973).
16. V. A. Juvekar and M. M. Sharma, "Absorption of CO₂ in a Suspension of Lime," Chem. Eng. Sci., 28, 825 (1973).
17. V. D. Mehta and M. M. Sharma, "Mass Transfer in Mechanically Agitated Gas-Liquid Contactors," Chem. Eng. Sci., 26, 461 (1971).
18. J. Hanhart, H. Kramers, and K. R. Westerterp, "The Residence Time Distribution of the Gas in an Agitated Gas-Liquid Contactor," Chem. Eng. Sci., 18, 503 (1963).
19. R. M. Morris and E. T. Woodburn, "Testing of Certain Design Equations for Predicting the Performance of a Calcium Hydroxide Carbonation Reactor, Part I: Gas Bubble Dynamics and Interfacial Areas in a Stirred Tank," South African Chem. Proc. (June-July 1967); "Part II: The Constant Rate Period," South African Chem. Proc. (August-September 1967); "Part III: The Falling Rate Period," South African Chem. Proc. (October-November 1967).
20. K. R. Westerterp, L. L. Van Dierendonck, and J. A. De Kraa, "Interfacial Areas in Agitated Gas-Liquid Contactors," Chem. Eng. Sci., 18, 157 (1963).
21. K. R. Westerterp, "Design of Agitators for Gas-Liquid Contacting," Chem. Eng. Sci., 18, 495 (1963).
22. R. M. Wright, J. M. Ruder, V. B. Dunn, and K. C. Hwang, "Development of Design Information for Molecular-Sieve Type Regenerative CO₂-Removal Systems," NASA-CR-2277, prepared by Airresearch Man. Co. (July 1973).
23. R. Engel, V. Decken, and B. Claus (Brown Boveri/Krupp Reaktorbau G.m.b.H.), "Method of Removing CO₂ and H₂O from a Gas Stream," U.S. Patent 3,519,384, granted July 7, 1970.
24. R. R. Swanson, "Literature Survey, Reaction of CO₂ with Solid CaO," Idaho Chemical Programs Operational Office, RRSW (October 1976).

15th DOE NUCLEAR AIR CLEANING CONFERENCE

DISCUSSION

KABAT: Have you tested the absorbent at higher temperatures and what is the maximum operational temperature you recommend for $\text{Ba}(\text{OH})_2$?

HAAG: Temperature is not a variable of significant importance as the reaction is kinetically feasible under ambient conditions. We are restricted to upper temperatures of 105°C for the $\text{Ba}(\text{OH})_2 \cdot \text{H}_2\text{O}$ and 78°C for the $\text{Ba}(\text{OH})_2 \cdot 8\text{H}_2\text{O}$, as these are melting points.

KABAT: It means that the temperature limit for this reaction would be roughly 100°C ?

HAAG: That would be the upper limit. We had been obtaining data at ambient conditions, i.e., 25°C , and this is the temperature I recommend for the process.

VAN BRUNT: Have you considered spouted beds and slowly moving beds?

HAAG: We have considered them. I should point out that the bulk of this work has been performed during the past nine months, and has been of an exploratory nature. Fluidized bed work has been put off primarily because of the problems we're having with entrainment of fines. The spouted bed looks good but we see some funny things, e.g., the minimum fluidization velocity seems to change and the bed conversion changes. Operation of a spouted fluidized bed could very definitely be an alternative in reducing the fines entrainment problem and we will examine it with further process development.

VAN BRUNT: You would expect the fines problem to be minimized at minimum fluidization.

HAAG: Yes.

BROWN: Do the advantages of the solid-state reactions appear large enough to justify halting the work on the aqueous system?

HAAG: This is difficult to answer at this time due to the different stages of development of the slurry and packed bed processes. I must point out that we have not conducted an in-depth examination of the effects of possible off-gas constituents, e.g. NO_x , I_2 , CH_3I , Kr, on the two systems. Furthermore, the location of this process in the overall offgas flowsheet is subject to change. This will affect the feed gas. Packed beds of $\text{Ba}(\text{OH})_2$ hydrates look very promising but they are in the initial stages of development. Based upon the expertise which we have developed with respect to the slurry system and its present stage of development, a nominal effort will complete the study. My choice, at this time, would be the packed bed approach but with the reservation that more data are required before a firm decision can be made. The size of a stirred tank reactor to treat 500 cfm would be excessive and the power input would be high.

BROWN: Would the disadvantage of handling the aqueous system and the subsequent clean-up be prohibitive?

HAAG: You are exactly right.

15th DOE NUCLEAR AIR CLEANING CONFERENCE

McDONALD: The authors should be aware that the Navy has been using LiOH canisters for several years to remove CO₂ from contained atmospheres. It is possible that these commercial systems have applicability in airborne nuclear wastes. At any rate, advantage may be taken of a large technical literature pertaining to the research and development and commercialization of these systems.

HAAG: I am aware of the open literature work of Dietz, Umstead, et al. at the Naval Research Lab that pertains to submarine environments and I would gladly welcome any information which would be beneficial in our process development. I understand LiOH was used by NASA in the early Mercury space flights for CO₂ removal from spacecraft environments and was eventually discontinued and replaced by molecular sieves due to weight limitation problems. Incidentally, our present analytical system, conversion of CO₂ to CH₄ over a nickel catalyst and subsequent FID analysis of the methane, may be referenced to some excellent work performed at NRL by Williams, Eaton, Umstead, et al.

15th DOE NUCLEAR AIR CLEANING CONFERENCE

MEASUREMENT OF RADIOACTIVE GASEOUS EFFLUENTS FROM VOLOXIDATION AND DISSOLUTION OF SPENT NUCLEAR FUEL*

J. A. Stone and D. R. Johnson
Savannah River Laboratory
E. I. du Pont de Nemours & Co.
Aiken, South Carolina 29801

Abstract

Laboratory-scale tests gave data on the release of tritium, ^{14}C , ^{85}Kr , and ^{129}I as radioactive gases from spent nuclear fuels during voloxidation and dissolution. Voloxidation, a proposed reprocessing step, is intended to remove tritium from fuel by oxidation of UO_2 to U_3O_8 prior to dissolution of the fuel with nitric acid. ^{14}C , ^{85}Kr , and ^{129}I may be evolved in both steps. Quantitative data from the tests may be used in designing off-gas treatment processes and equipment. The tests were performed in a shielded cell with a combination voloxidizer-dissolver. With a recirculating off-gas system, tritium and ^{14}C were trapped on molecular sieves; ^{129}I was trapped on silver-exchanged zeolite. ^{85}Kr was measured by online gamma-ray counting. Zircaloy-clad UO_2 fuels from H. B. Robinson-2, Oconee-1, and Saxton reactors, with burnups from ~ 100 to $\sim 28,000$ MWD/MTHM, were tested. The results confirm that voloxidation released most of the tritium but only small fractions of the ^{14}C , ^{85}Kr , and ^{129}I ; the remainder of these radioactive gases evolved when the voloxidized fuels were dissolved. Voloxidation off-gases typically contained $>99.8\%$ of the tritium, 17 to 22% of the ^{14}C , 7 to 17% of the ^{85}Kr , and $<8\%$ of the ^{129}I . Tritium evolved as HTO , with $<0.1\%$ as HT .

Introduction

In processing spent nuclear fuel to recover fissile material, volatile radionuclides such as tritium, ^{14}C , ^{85}Kr , and ^{129}I evolve into the off-gas system. Technology is available for trapping the gaseous radioactive species to prevent release to the environment. (1-3) However, proper design of off-gas facilities requires quantitative data on amounts evolved in each process step.

A reference flowsheet for head-end processing steps is shown in Figure 1. The spent fuel rods are sheared into short pieces, and then a voloxidation step drives tritium out of the fuel. The oxidized fuel is dissolved with nitric acid, and the clarified solution is fed to solvent-extraction steps. Most of the gaseous radionuclides enter the off-gas system during the voloxidation and dissolution steps.

* The information contained in this article was developed during the course of work under Contract No. AT(07-2)-1 with the U. S. Department of Energy.

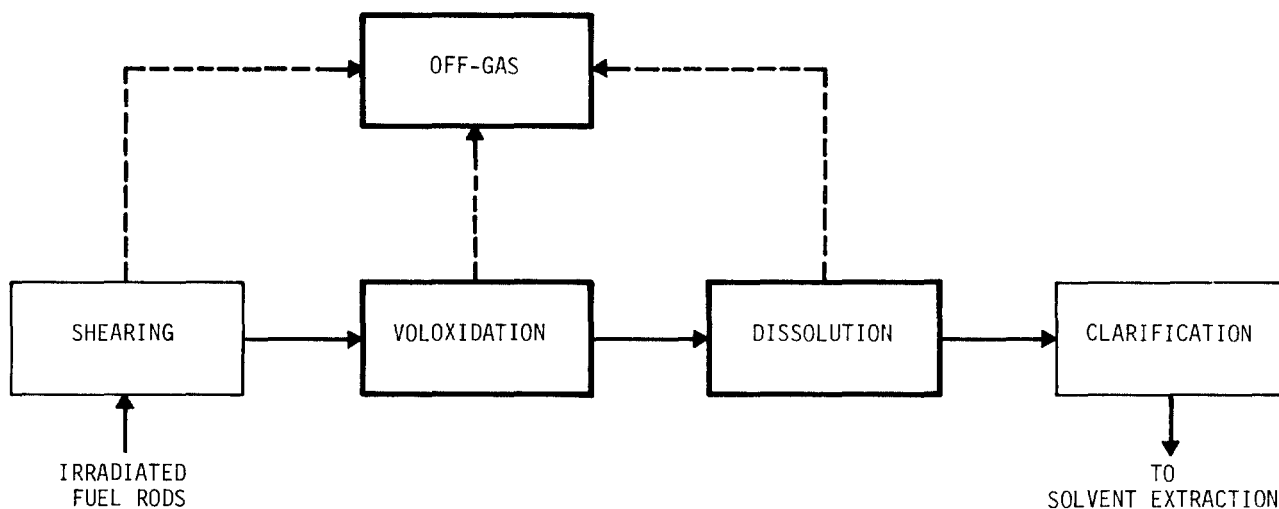


Figure 1. Head-end process operations.

In voloxidation, first developed at Oak Ridge National Laboratory,⁽⁴⁾ UO_2 fuel oxidizes to U_3O_8 at about 490°C , promoting evolution of tritium as HTO (water vapor). During oxidation, the fuel expands, disintegrates into fine powder, and separates from the cladding. Tritium removal before fuel dissolution is desirable to avoid extensive isotopic dilution by nontritiated water. Previous studies^(4,5) showed that even though tritium evolved quantitatively during voloxidation, species such as ^{85}Kr and ^{129}I evolved incompletely.

In this paper, new laboratory-scale measurements of tritium, ^{14}C , ^{85}Kr , and ^{129}I evolved during voloxidation and dissolution of irradiated power-reactor fuels are reported. We confirm the quantitative evolution of tritium during voloxidation and report the distribution of the other species between voloxidation and dissolution.

Experimental Procedure

Apparatus

Voloxidizer-Dissolver. A stainless-steel reaction vessel, shown in Figure 2, serves for both voloxidation and dissolution of irradiated fuel. The apparatus is in a shielded cell for remote operation and is connected to off-gas collection facilities. The voloxidizer-dissolver is a 2-liter reaction chamber equipped with numerous heaters, thermocouples, cooling coils, a rotary agitator, and orifices for off-gases. The reaction chamber rotates on a horizontal axis to provide two operating positions: 1) tilted as shown in Figure 2 for voloxidation or 2) vertically upright for dissolving. Gases emerge through a reflux condenser during dissolving or through another orifice during voloxidation.

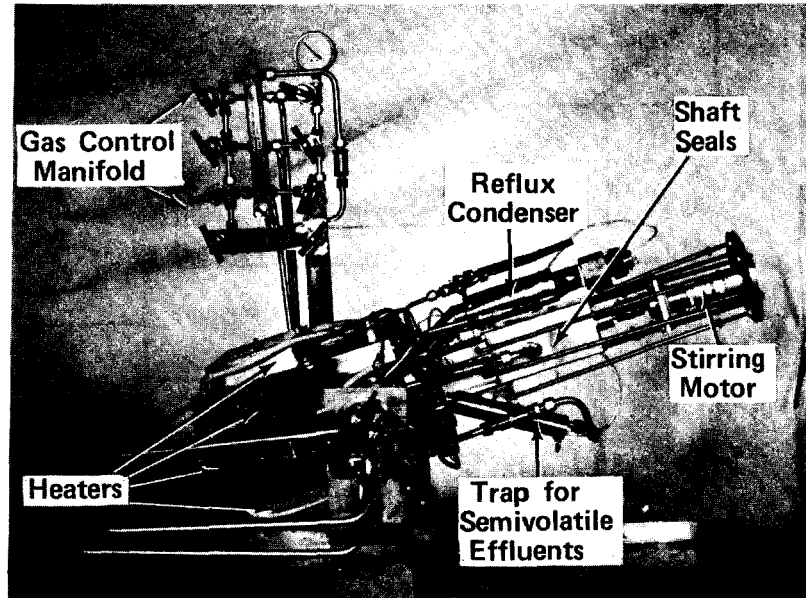


Figure 2. Voloxidizer-dissolver.

Off-Gas System. The voloxidizer-dissolver is coupled to laboratory-scale off-gas equipment both inside and outside the shielded cell; the arrangement for voloxidation is shown schematically in Figure 3. A small pump recirculates helium carrier gas through the closed system. Oxygen consumed in the system is replaced to maintain constant oxygen content in the recirculating gas. ^{85}Kr is measured by online gamma-ray counting; tritium, ^{14}C , and ^{129}I are collected on a series of molecular sieve traps for later analyses. The off-gas system was tested and calibrated with tracer amounts of radioactive gases.

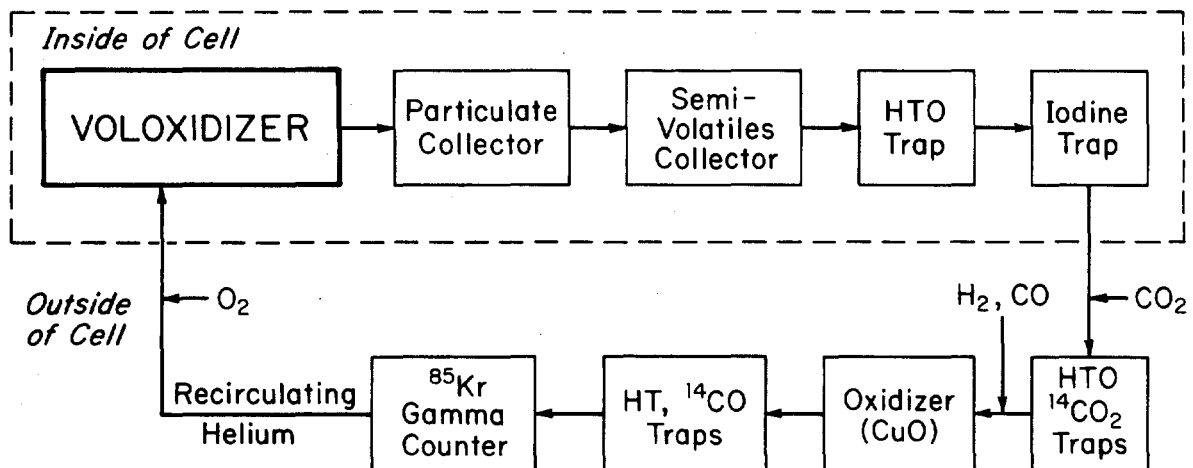


Figure 3. Off-gas system.

15th DOE NUCLEAR AIR CLEANING CONFERENCE

Particulates in the off-gas are collected on impacter plates at the mouth of the voloxidizer. Semivolatile elements such as cesium, antimony, and ruthenium may plate out along a temperature-gradient tube following the particulate collector. Data on particulates and semivolatiles are not discussed in this paper.

Three Type 3A molecular sieve traps collect tritium as HTO. One trap closely coupled to the voloxidizer collects evolved HTO quantitatively. Water vapor introduced into the off-gas recirculation line carries the HTO. The other two traps are in a hood outside the shielded cell, one upstream and one downstream from an oxidizing bed of CuO at 300°C. The upstream trap is a backup for collecting residual HTO, whereas the downstream trap collects HTO converted from HT in the off-gas. Hydrogen gas introduced upstream from the CuO bed carries any HT.

Two Type 13X molecular sieve traps collect ^{14}C as $^{14}\text{CO}_2$. These traps are also outside the shielded cell, one on each side of the heated CuO bed. Any ^{14}CO in the off-gas is oxidized to $^{14}\text{CO}_2$ and collected in the second trap. Carrier CO_2 is added before the first trap, and carrier CO is added before the CuO bed. As discussed in the following section, separation of CO and CO_2 in this system is not entirely satisfactory.

The off-gas circulates through a calibrated chamber for counting the 514-keV gamma ray of ^{85}Kr with a high-resolution Ge-Li detector. These rapid online measurements allowed the course of voloxidation and dissolution reactions to be monitored.

A bed of silver-exchanged zeolite ($\text{Ag}^0\text{-X}$) at 180°C traps iodine in the off-gas. During voloxidation, the iodine trap, although near the voloxidizer in the shielded cell, is downstream from the tritium trap. Because any ^{129}I that deposited in the upstream lines or in the tritium trap would not have been detected, the measured ^{129}I is possibly less than the total amount evolved.

The arrangement of the off-gas system for dissolution is similar to that shown in Figure 3. Equipment outside the shielded cell is identical. In the cell, dissolver off-gases pass through a reflux condenser directly to an iodine trap.

Analytical Methods

After each voloxidation or dissolution test, tritium, ^{14}C , and ^{129}I are removed from their primary sorbents by a heat treatment. The methods used are summarized in Table I. HTO and $^{14}\text{CO}_2$ are desorbed from molecular sieve pellets to obtain forms suitable for liquid scintillation beta-counting. Used pellets are discarded.

Because silver interferes with neutron-activation analysis for ^{129}I , the iodine is removed from silver zeolite as HI and resorbed on lead zeolite, which does not interfere. This method was adapted from the work of Staples, Murphy, and Thomas.^(6,7) The regenerated silver-zeolite traps are reused.

15th DOE NUCLEAR AIR CLEANING CONFERENCE

Table I. Analyses for gaseous radioactive species.

<u>Radionuclide</u>	<u>Primary Sorbent</u>	<u>Bakeout^a</u>	<u>Carrier Gas</u>	<u>Secondary Trap</u>	<u>Analytical Method</u>
³ H	3A	Yes	H ₂ O	Cold trap ^b	β counting
¹⁴ C	13X	Yes	CO ₂	CO ₂ mMET ^{c,d}	β counting
⁸⁵ Kr	-	-	He	-	Online γ counting
¹²⁹ I	Ag ⁰ -X	Yes ^e	H ₂	Pb-X(150°C)	Neutron activation

- a. Heat treatment at 500°C for 8 to 16 hours.
 b. Refrigerated to -50°C.
 c. Trademark of Amersham/Searle carbon dioxide trapping agent.
 d. Preceded by cold trap for H₂O.
 e. Heated at 500°C with flowing hydrogen gas.

Irradiated Fuels

Representative fuels with a wide range of burnups from three different light-water reactors, listed in Table II, were used for the tests described in this paper. Each of these fuels was UO₂ and was originally clad with Zircaloy. Fuels from H. B. Robinson-2 and Oconee-1 reactors were from single rods. Saxton fuel was contained in four rods with different irradiation histories. (8)

Similar unirradiated UO₂ fuel was tested in a control experiment to establish lower limits of detection for the gaseous radioactive species.

Table II. Characteristics of Zircaloy-clad UO₂ fuel rods.

<u>Reactor</u>	<u>Rod^a</u>	<u>Burnup, MWD/MTHM</u>	<u>Cooling Period, yr</u>	<u>Initial ²³⁵U Enrichment, %</u>
H. B. Robinson-2	-	~28,000	3	2.55
Oconee-1	-	~11,000	3	2.0
Saxton	A	~6,000	5	12.5
	B	~3,000	5	12.5
	C	~3,000	5	12.5
	D	~100	5	12.5

- a. Arbitrary designations.

Test Conditions

Voloxidation. About 200 g of irradiated UO_2 fuel in cladding and/or as loose fragments was charged to the voloxidizer. Cladding pieces were from 2.5 to 3.8 cm long. The fuel was heated for 4 hours at $490^\circ C$ and was tumbled with the rotary agitator at 3.5 rpm. Oxygen content of the recirculating gas was monitored periodically with an inline oxygen analyzer and was held at a nominal 20% in most tests, by adding oxygen as needed. Eleven tests were run with irradiated fuels. Control tests were run with unirradiated fuel and without fuel.

Figure 4 shows the behavior of a typical voloxidation test. Reaction temperature, incremental oxygen additions, and ^{85}Kr evolution were measured as a function of time. In this example, for Saxton fuel, the reaction appeared to be complete after one hour at $490^\circ C$. Part of the added oxygen was consumed in the off-gas system by reactions in the heated CuO bed; this fraction was determined in a separate blank experiment and was subtracted from the data to obtain the amount of oxygen consumed by voloxidation.

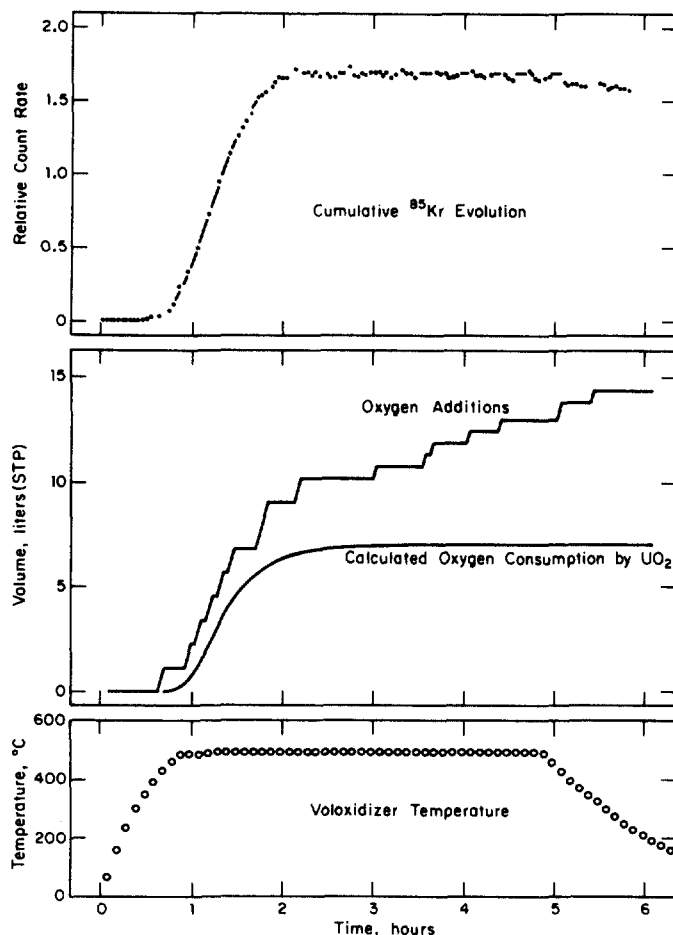


Figure 4. Typical voloxidation behavior (Saxton fuel).

15th DOE NUCLEAR AIR CLEANING CONFERENCE

Dissolution. Fuel dissolution was initiated at ambient temperature with a batch quantity of 1 to 3M HNO₃. As the dissolution proceeded, 10M HNO₃ was metered in over 60 to 75 minutes, to slowly increase acid concentration. Ninety minutes after the initial acid charge, the solution temperature was increased to 90°C to complete the dissolution. Gas circulated through the dissolver and off-gas system, and radioactive species were trapped as with voloxidation. Additional steps included leaching the spent cladding hulls and any undissolved residue with 10M HNO₃ and then rinsing with 1 to 3M HNO₃.

Figure 5 shows the behavior of a typical dissolution test. Dissolved uranium concentration and ⁸⁵Kr evolution were measured as a function of time. The data show that total dissolution time was about 200 minutes and that ⁸⁵Kr evolution correlated well with the fuel dissolution rate.

Each batch of voloxidized fuel (11 irradiated and 1 unirradiated) and single batches of unvoloxidized Robinson and Ocone fuels were dissolved. A few experiments⁽⁵⁾ in a glass apparatus with less complete off-gas facilities are reported for comparison. In a blank experiment, dissolving operations without fuel were also performed.

Dissolver solutions were analyzed for tritium, ¹⁴C, and ¹²⁹I. Negligible ¹⁴C or ¹²⁹I was found in solution. The tritium decontamination factor (DF) for voloxidation was calculated from the amount of tritium in the dissolver solution.

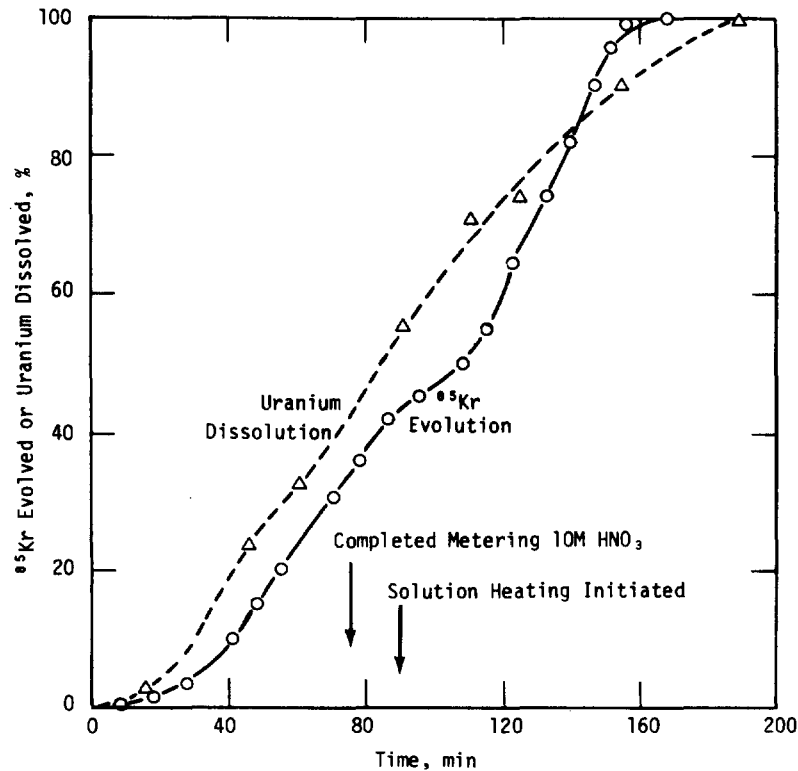


Figure 5. Typical dissolution behavior (Saxton fuel).

15th DOE NUCLEAR AIR CLEANING CONFERENCE

Results and Discussion

Tritium

Table III shows, for the cases studied, that nearly all of the tritium in spent fuel evolved during voloxidation, thus confirming the effectiveness of voloxidation for tritium removal. In most of the tests, >99.8% of tritium in the fuel was removed by voloxidation. The small amount of tritium remaining in the fuel after voloxidation was not released to off-gas by dissolution; it was found as HTO in the dissolver solution.

In two tests, the fraction of tritium evolved during voloxidation was somewhat low (87 and 98% released). Conversion of UO_2 to U_3O_8 was incomplete in both tests. In every test with complete conversion to U_3O_8 , the tritium DF exceeded 650.

The total amount of tritium for each test is the sum of amounts found in all off-gas traps and in the dissolver solution. Most of the total in each test was found in the trap nearest the voloxidizer, as expected. Duplicate tests with Saxton rods gave good reproducibility. Total tritium from Robinson and Saxton fuels appears to be correlated with burnup, but tritium from Oconee fuel is less than that expected on the basis of burnup.

Table III. Tritium distribution.

Fuel	Tritium, Ci/MTU			Voloxidation		
	Voloxidizer Off-gas	Dissolver Solution	Total	Tritium DF	Tritium, % of Total	HT, % ^a
Robinson	133 b,c	0.004 250	133 250	33,150 -	>99.9 -	0.03 -
Oconee	6 16 27 7 b b,c	0.91 0.002 0.013 0.035 35 7	7 16 27 7 35 7	8 ^d 6,560 2,170 195 - -	87.5 >99.9 >99.9 99.5 - -	0.05 0.02 0.01 0.07 - -
Saxton	A B B C C D	0.57 0.027 0.044 0.003 0.007 0.012	32 25 29 28 28 10	55 ^d 925 665 8,450 4,150 805	98.2 99.9 99.8 >99.9 >99.9 99.9	0.01 0.1 0.1 0.05 0.03 0.02
Unirradiated	0.2	0.033	0.2	-	-	-
Blank	1.2	0.008	1.2	-	-	-

a. Upper limit.

b. Unvoloxidized UO_2 fuel.

c. Dissolved in glass apparatus (Reference 5).

d. Incomplete oxidation.

15th DOE NUCLEAR AIR CLEANING CONFERENCE

Tritium in irradiated fuel arises principally from ternary fission and activation of ^6Li impurities. Thus, total tritium will depend upon the lithium impurity level and upon irradiation history of the fuel. A calculation with the ORIGEN code⁽⁹⁾ for Robinson fuel predicted about 470 Ci/MTU of tritium from fission and a comparable amount from activation. Observed amounts are less. Possible sources of variation in the results include: loss of tritium in earlier operations, such as shearing and storage; differences in burnup along a fuel rod; migration of tritium within a rod, because of thermal gradients; tritium trapped in the cladding.

Carbon-14

From 17 to 22% of the total ^{14}C in the fuels evolved during voloxidation in most of the tests (Table IV). The remainder of the ^{14}C was released to the off-gas system during dissolution. The amounts found were 1000 times greater than the limit of detection for ^{14}C , as determined by the control experiments. Duplicate tests with Saxton fuel showed that the measurements were reproducible.

Somewhat less than the typical ~20% of the ^{14}C evolved during the two voloxidation tests with incomplete conversion to U_3O_8 ; about 9% was released in these tests. Saxton fuel with very low burnup was another exception, evolving only 2% during voloxidation.

Table IV. Carbon-14 distribution.

Fuel	^{14}C , Ci/MTU			Voloxidation		Dissolution
	Voloxidizer Off-gas	Dissolver Off-Gas	Total	^{14}C , % of Total	^{14}CO , % ^a	^{14}CO , % ^a
Robinson	0.066	0.243	0.309	21.3	59	0.04
Oconee	0.010	0.104	0.114	9.1 ^b	22	72
	0.025	0.124	0.149	16.8	27	65
	0.024	0.104	0.128	18.7	2	31
	0.035	0.141	0.176	19.7	51	24
	c	0.081	0.081	-	-	0.2
Saxton						
A	0.0037	0.0389	0.0426	8.7 ^b	0.07	0.14
B	0.0055	0.0235	0.0290	19.1	75	29
B	0.0068	0.0234	0.0302	22.4	51	58
C	0.0053	0.0216	0.0269	19.7	64	29
C	0.0047	d	d	d	69	d
D	0.00001	0.0005	0.0005	2.0	76	4
Unirradiated	0.000005	0.00005	0.00005	-	50	55
Blank	0.000005	0.00003	0.00003	-	50	20

a. Upper limit (see text).

b. Incomplete oxidation.

c. Unvoloxidized UO_2 fuel.

d. Not determined.

15th DOE NUCLEAR AIR CLEANING CONFERENCE

^{14}C in irradiated fuels is formed primarily by the $^{14}\text{N}(n,p)^{14}\text{C}$ reaction on nitrogen impurities in the fuel and secondarily by the $^{17}\text{O}(n,\alpha)^{14}\text{C}$ reaction. Thus, the amount of ^{14}C produced depends upon the amount of nitrogen impurity and upon fuel burnup. A typical calculated value is 0.5 Ci/MTU for fuel with 20-ppm nitrogen irradiated to about 30,000 MWD/MTHM. The amounts of ^{14}C measured in Robinson, Oconee, and Saxton fuels are correlated with the burnups and are in the range expected for 10 to 20 ppm nitrogen in the fuels.

Krypton-85

Table V shows that, in most of the tests, 7 to 17% of the total ^{85}Kr in the fuels evolved during voloxidation. The dissolution tests confirmed that the major fraction of ^{85}Kr remained in voloxidized fuel but was totally released by dissolving. Duplicate tests with Saxton fuel agreed well. Again, somewhat lower results (4 to 6% released during voloxidation) were obtained for the two tests with incomplete conversion to U_3O_8 .

The small fraction of ^{85}Kr from voloxidation agrees with results of other workers with different fuels.⁽⁴⁾ Apparently, krypton from fission is dispersed throughout the fuel as individual atoms rather than accumulated as bubbles at the grain boundaries. Oxidation of UO_2 does not release much of the krypton from the matrix, even though a very fine U_3O_8 powder is formed. Since tritium is released completely under the same conditions, the results imply that krypton diffuses much slower than tritium in the U_3O_8 crystal lattice.

Table V. Krypton-85 distribution.

Fuel	^{85}Kr , Ci/MTU			Voloxidation ^{85}Kr , % of Total
	Voloxidizer Off-Gas	Dissolver Off-Gas	Total	
Robinson	137	1651	1788	7.7
Oconee	41	969	1010	4.1 ^a
	123	1087	1210	10.2
	77	1011	1088	7.1
	115	1058	1173	9.8
	b	1070	1070	-
Saxton				
A	62	944	1006	6.2 ^a
B	75	377	452	16.6
B	62	396	458	13.5
C	60	388	448	13.4
C	61	c	c	c
D	0.7	5.1	5.8	11.3
Unirradiated	0.07	1.00	1.07	-
Blank	0.07	0.08	0.15	-

a. Incomplete oxidation.

b. Unvoloxidized UO_2 fuel.

c. Not determined.

15th DOE NUCLEAR AIR CLEANING CONFERENCE

Total ^{85}Kr in fuel is related to burnup, cooling period, and perhaps previous thermal history. A calculation with the ORIGEN code predicted about 7000 Ci/MTU of ^{85}Kr for the Robinson fuel. The amounts of ^{85}Kr measured in Robinson, Oconee, and Saxton fuels correlate well with burnups but are somewhat lower than calculated values. An unknown amount of krypton may have been released on initial puncture of the rods and subsequent storage of the fuel.

Iodine-129

Table VI gives results for ^{129}I collected during voloxidation and/or dissolution of the fuels. The data are less consistent than for the other radioactive gases, possibly because of experimental difficulties. We conclude from our experience with these tests that separate experiments designed specifically to measure iodine will yield more accurate results.

In all of the tests, very little ^{129}I (from 0.02 to 1.7 g/MTU) was collected during voloxidation. These amounts also were small fractions of total ^{129}I found, ranging from 0.1 to 7.9% evolved during most of the voloxidation tests. In two tests, the fractions from voloxidation were 59 and 84%; however, material balances for iodine in these two tests did not agree well with amounts expected.

Table VI. Iodine-129 distribution.

Fuel	^{129}I , g/MTU			Voloxidation ^{129}I , % of Total	
	Voloxidizer Off-gas	Dissolver Off-gas	Total		
Robinson	0.18	58	58	0.3	
	a,b	171	171	-	
Oconee	0.03	27	27	0.1	
	0.76	31	32	2.4	
	1.7	20	22	7.9	
	a,b	104	104	-	
	a,c	102	c	c	
Saxton	A	1.5	27	28	5.4
	B	0.16	0.03	0.19	84
	C	0.03	c	c	c
	C	0.02	c	c	c
	D	1.1	0.8	1.9	59
Unirradiated	0.007	0.016	0.023	-	
Blank	0.014	0.009	0.023	-	

a. Dissolved in glass apparatus (Reference 5).

b. Unvoloxidized UO_2 fuel.

c. Not determined.

15th DOE NUCLEAR AIR CLEANING CONFERENCE

Also shown in Table VI are previously reported results⁽⁵⁾ for Robinson and Oconee fuels dissolved in a glass apparatus; the iodine was collected in an NaOH off-gas scrubber. About three times more ^{129}I was obtained with the glass apparatus than with the metal equipment used in this work. Reasons for the difference have not been determined, although results from the glass apparatus are believed to be more accurate. The earlier work showed little difference in ^{129}I evolved during dissolution of voloxidized or unvoloxidized Oconee fuel; this is consistent with the fraction of ^{129}I evolved during voloxidation being small.

Total ^{129}I should be proportional to burnup only. A typical calculated value for Robinson fuel is 187 g/MTU.

Chemical Species

Upper limits on the amounts of tritium evolved as HT and ^{14}C evolved as ^{14}CO were determined from tritium or ^{14}C found in the traps downstream from the oxidizing bed of CuO . Table III gives the fraction of tritium from voloxidation found in the downstream tritium trap. Table IV gives similar information for ^{14}C from both voloxidation and dissolution.

The results show that nearly all of the tritium from voloxidation was in the form of HTO, as expected. Less than 0.1% could have been in the form of HT. Although these amounts are 10 to 100 times greater than the background level of the system, they are within the range of possible leakage from upstream traps and therefore should be regarded as upper limits for HT. From dissolution of voloxidized fuel, no tritium as HT was observed; only background levels of tritium were found in the downstream trap.

The distribution between $^{14}\text{CO}_2$ and ^{14}CO is uncertain. During the required conditions of prolonged flow, some CO_2 desorbed from the upstream trap and collected in the downstream trap. This effect was shown in a calibration test with $^{14}\text{CO}_2$; the ^{14}C was found equally distributed between the two traps even though no ^{14}CO was in the system. In voloxidation tests, up to 76% (in a test with Saxton fuel) of the ^{14}C was found in the downstream trap. In dissolution tests, up to 72% (in a test with Oconee fuel) of the ^{14}C was found in the downstream trap. Because an unknown part of the ^{14}C on this trap was originally $^{14}\text{CO}_2$ and not ^{14}CO , the values shown represent only upper limits on ^{14}CO ; the actual amounts could have been much less. In one test with Saxton fuel, only about 0.1% of the ^{14}C from either voloxidation or dissolution appeared as ^{14}CO . Total ^{14}C evolved was accurately measured because the total capacity of the upstream and downstream traps for CO_2 was adequate for the quantities involved.

15th DOE NUCLEAR AIR CLEANING CONFERENCE

Conclusions

From the data of Tables III - VI, we conclude the following:

- Voloxidation of spent nuclear fuel releases tritium to the off-gas system quantitatively but releases only small fractions of the ^{14}C , ^{85}Kr , and ^{129}I in the fuel.
- Dissolution of voloxidized fuel in nitric acid releases the remaining ^{14}C , ^{85}Kr , and ^{129}I to the off-gas system.
- Typical values for the fractions evolved during voloxidation are >99.8% of the tritium, 17 to 22% of the ^{14}C , 7 to 17% of the ^{85}Kr , and <8% of the ^{129}I .
- Tritium is evolved as HTO during voloxidation; less than 0.1% is HT.

References

1. Proceedings - Controlling Airborne Effluents from Fuel Cycle Plants, Sun Valley, Idaho, August 5-6, 1976. American Nuclear Society (1976).
2. R. A. Brown, Ed. "Volatile radioisotope recovery and off-gas treatment." Alternatives for Managing Wastes from Reactors and Post-Fission Operations in the LWR Fuel Cycle. USERDA Report ERDA-76-43, Chapter 13, Vol. 2, pp 13.1-13.68, Washington, DC (1976).
3. O. O. Yarbrow, F. E. Harrington, and D. S. Joy. Effluent Control in Fuel Reprocessing Plants. USAEC Report ORNL-TM-3899, Oak Ridge National Laboratory, Oak Ridge, TN (1974).
4. J. H. Goode, Ed. Voloxidation - Removal of Volatile Fission Products from Spent LMFBR Fuels. USAEC Report ORNL-TM-3723, Oak Ridge National Laboratory, Oak Ridge, TN (1973).
5. D. R. Johnson and J. A. Stone. "Light water reactor fuel reprocessing: dissolution studies of voloxidized fuel." Paper presented at ANS Topical Meeting on the Back End of the LWR Fuel Cycle, Savannah, GA, March 19-22, 1978.
6. B. A. Staples, L. P. Murphy, and T. R. Thomas. "Airborne elemental iodine loading capacities of metal zeolites and a dry method for recycling silver zeolite." Proceedings of the Fourteenth ERDA Air Cleaning Conference, Sun Valley, Idaho, August 2-4, 1976. USERDA Report CONF-760822, pp 363-379 (1977).
7. T. R. Thomas, B. A. Staples, L. P. Murphy, and J. T. Nichols. Airborne Elemental Iodine Loading Capacities of Metal Zeolites and a Method for Recycling Silver Zeolite. USERDA Report ICP-1119, Idaho National Engineering Laboratory, Idaho Falls, ID (1977).

15th DOE NUCLEAR AIR CLEANING CONFERENCE

8. G. W. Gibson, et al. Characteristics of UO₂-Zircaloy Fuel Rod Materials from the Saxton Reactor for Use in Power Burst Facility. USNRC Report ANCR-NUREG-1321, Aerojet Nuclear Co., Idaho Falls, ID (1976).
9. M. J. Bell. ORIGEN - The ORNL Isotope Generation and Depletion Code. USAEC Report ORNL-4628, Oak Ridge National Laboratory, Oak Ridge, TN (1973).

DISCUSSION

EVANS: The amount of ¹²⁹I and ⁸⁵Kr released during the voloxidation step seems quite small compared to the assumed releases for DBA melt-down for reactors. Do you believe your numbers could be used as valid source terms for future accident analysis work?

STONE: The absolute quantities reported represent data for the fuels as received. Unknown amounts of gases may have been released in the prior history of the fuel, as, for example, in the initial puncture of the fuel rods and during their storage. The relative amounts released would probably be valid in air at the quoted temperature, 490°C. There are literature data that suggest that ⁸⁵Kr and ¹²⁹I will be completely released at higher temperatures (say, 1000°C).

LAMBERGER: You stated that more than 99.8% of the tritium in the fuel was released by voloxidation. Does this include tritium in cladding, in the gas plenum, or in the getter (if any)?

STONE: No, the fraction quoted is of total tritium found in the offgas system after voloxidation and dissolution, and in the dissolver solution.

LAMBERGER: Do you have any data on tritium distribution in clad, fuel, gas, and getter?

STONE: No.

SCHINDLER: In the dissolution step, did you look at the distribution of the iodine and the carbon-14 with respect to the offgas and the liquid? Did it all go out in the offgas or did some remain in the liquid?

STONE: Within the limits of our detection it all went out in the offgas. That is, greater than 98%. We don't know if a small amount was left that was beyond the limit of detection.

15th DOE NUCLEAR AIR CLEANING CONFERENCE

INVESTIGATION OF AIR CLEANING PROCESSES FOR REMOVING TRIBUTYL PHOSPHATE VAPORS FROM FUEL REPROCESSING OFF-GAS STREAMS*

Graham B. Parker
Lysle C. Schwendiman

Pacific Northwest Laboratory
Richland, Washington

Abstract

Tributyl Phosphate (TBP) is used as an extractant in combination with the solvent dodecane in the dissolution process in a conventional nuclear fuel reprocessing plant. When recycled acid is used in the process, the dissolver off-gas (DOG) may contain small amounts of TBP and dodecane vapor. The vessel off-gas (VOG) will also contain TBP vapors in even higher fractions. Under some conditions, TBP vapor in these gas streams adversely affects the performance of silver-loaded solid sorbent beds used in the treatment of these streams to remove iodine and organic iodide compounds. This study is investigating the use of inorganic solid sorbent beds located upstream of the silver-loaded sorbent beds to remove TBP and extend the useful life of the silver beds.

Laboratory scale experiments have been conducted using selected inorganic solid sorbent materials which have specific properties indicating their effectiveness for removing TBP or similar organic compounds. Screening studies of short duration were run using several materials to select the most promising materials for further parametric testing. Twelve materials (10 inorganic and 2 organic based) designated A through M were used in these initial studies. The materials were packed in a bed 2.5 cm diameter by 5 cm deep. Typical TBP concentrations ranged from 4×10^{-4} to 1×10^{-3} g/l in air flowing at 172 ml/min. Results indicated 4 inorganic materials (D, H, K, L) would retain greater than 95% of inlet TBP over a 3-hour run time.

These four materials are being tested in a small packed glass column arrangement using variations in TBP concentration, face velocity and column temperature. As a part of this work, a sensitive quantitative analysis technique was developed enabling continuous real time analysis of TBP vapor concentrations, as low as 1×10^{-7} g/l, so that breakthrough progression can be measured.

Of the three materials examined to date in parametric experiments (D, H and L), material H shows the highest retention efficiency for TBP. Material H will retain 15 times more TBP before detectable breakthrough than the next most efficient material. Concentrations of TBP in these experiments ranged from 6×10^{-5} to 4.5×10^{-4} g/l in air flowing at 0.45-2 l/min.

*Work performed under DOE Contract EY-76-C-1830

15th DOE NUCLEAR AIR CLEANING CONFERENCE

Material H will be used in further laboratory experiments to demonstrate TBP removal in a simulated process stream. The materials selected for this experiment will be used as protective beds upstream of iodine sorbent beds and iodine retention for protected and unprotected beds will be a measure of the effectiveness of the beds to remove TBP.

I. Introduction

Tributyl phosphate ($C_{12}H_{27}PO_4$) diluted with dodecane (or normal paraffin hydrocarbon, NPH) is the solvent used in the PUREX process to separate uranium and plutonium from fission products in spent LWR fuel. Most PUREX flow sheets used to date and those proposed for future reprocessing plants incorporate acid recycle. When the acid is recycled, small amounts of NPH and TBP vapor will be present in the dissolver off-gas and vessel off-gas. Both of these gas streams will contain other airborne fission products released during the reprocessing steps which must be removed by gas cleaning processes.

Iodine and organic iodides are major radioactive constituents of these gas streams. Current treatment methods proposed involve the use of silver-loaded inorganic sorbents to remove iodine. Laboratory and pilot plant studies have shown that the presence of TBP vapor in these gas streams reduce the capacity of the silver beds to remove iodine, thus resulting in more frequent replacement of the beds.⁽¹⁾

Little work addressing the problem has been done in the United States. The presence of TBP/NPH in the off-gas streams has been recognized as a possibility since the PUREX flow sheets were prepared and plants built at Hanford and Savannah River to reprocess spent fuel. The potential deleterious effect of TBP on silver sorbents has not been fully explored. Work has been done in this area in West Germany in conjunction with research involved in iodine removal from DOG and VOG streams using the Karlsruhe Reprocessing Pilot Plant (WAK).⁽¹⁾ Airborne TBP in concentrations of $\sim 6 \times 10^{-3}$ g/l significantly reduced iodine sorption capacity of AC 6120 material. Removal efficiency of AC 6120, however, could be restored by introducing NO_2 in the air stream. Dodecane was found to have no deleterious effect.

Use of NO_2 to reduce the effect of TBP contamination may be a viable option for AC 6120 silver-impregnated material because of its unique chemical composition. If materials such as silver-substituted zeolites (faujasite) or mordenites are used as iodine sorbents, this may not be feasible. Work with silver mordenites and silver zeolites has shown that the presence of NO_2 significantly reduces the loading of iodine.⁽²⁾ If off-gas treatment includes using silver zeolites or silver mordenites, then TBP must be removed prior to iodine removal to assure efficient use of the silver.

II. General Approach

A literature survey was conducted to identify possible inorganic sorbents having properties indicating their effectiveness to remove TBP or similar organic compounds. The required material would have a surface area of less than 500 m^2/g to minimize the water sorption, a

15th DOE NUCLEAR AIR CLEANING CONFERENCE

pore diameter greater than ~ 50 Å to accept a molecule the size of tributyl phosphate and must be able to be used at temperatures up to 170°C. Materials showing an affinity to "fix" phosphates such as alumina or iron-containing materials were considered. Candidate material selected for study include silica gels, aluminas, acid treated clays and zeolite molecular sieves.

Before any laboratory work could begin, a sensitive quantitative analysis technique for measuring very low concentrations of TBP was to be developed. Gas chromatography was successful for analysis of liquid TBP.⁽³⁾ The use of a gas chromatograph for direct vapor injections of airborne TBP was not successful in the current study. A continuous real time monitoring instrument was most desirable due to the nature of the planned experiments. A search for the best available analysis method was initiated.

A series of laboratory and pilot plant experiments was developed. Initial screening studies in the laboratory using packed beds of small amounts of material in short term TBP loading experiments were designed to identify promising materials for future work. The candidate material would be used in parametric experiments using only TBP in an air stream to identify the most promising material for further laboratory experiments. Tests using variations in flow rate, TBP loading rate, and bed temperature would be conducted. Final laboratory experiments would be conducted using a simulated reprocessing off-gas stream containing major constituents found in actual reprocessing streams.

The final phase of the study involves demonstrating the selected air cleaning system in the Nuclear Waste Vitrification pilot plant at PNL which can operate as a fuel reprocessing pilot plant. Part of this work will be to measure the typical TBP vapor concentrations found in off-gas streams. The demonstrated TBP removal system will be installed in an off-gas stream at an operating fuel reprocessing plant such as at Savannah River or Hanford to assess its effectiveness under actual operating conditions. Part of this task would also involve measuring TBP vapor concentrations under the various operating conditions.

III. Analysis Methods

Laboratory work was initiated to develop a sensitive method to quantitatively analyze low concentrations of TBP vapor (10^{-5} g/l). One method explored was to trap TBP vapor on charcoal-impregnated filter papers and analyze for the phosphorus by x-ray fluorescence. A series of experiments were conducted by placing charcoal filters in series in an air stream containing TBP vapor. The filters were analyzed to determine TBP trapping efficiency. A lower detection limit of 0.1 mg P/filter sample was established.

A phosphorus gradient on the filter papers from front to back was identified by the analyses. The amount of phosphorus detected was also inconsistent from one run to another. An attempt was made to macerate and homogenize the paper and press it into a suitable size for analysis to give a uniform phosphorus distribution. The sample preparation was not found to be suitable for x-ray analysis and consequently the effort was terminated.

15th DOE NUCLEAR AIR CLEANING CONFERENCE

An analysis method for organic phosphates outlined in the NIOSH standard procedures was explored for TBP analysis since TBP has many of the same chemical characteristics as the organophosphate pesticides.⁽⁴⁾⁽⁵⁾ This method involves collection of airborne TBP vapor in ethylene glycol using an impinger system. The TBP is extracted from the glycol into hexane and concentrated. The liquid concentrate is analyzed by a gas chromatograph equipped with a flame ionization phosphorus detector. The detector limit was 0.005 μl TBP. This method was successful for samples <10 mg TBP/50 ml glycol and was used in the initial laboratory screening experiments. This method was modified later in the experiments to eliminate the glycol by sparging the TBP laden air directly into hexane in a cold trap.

Direct injection of TBP vapor samples into a gas chromatograph was explored in an attempt to eliminate the hexane cold trap and give a faster turnaround time and a semicontinuous analysis. A Hewlett-Packard 5730 gas chromatograph with an N_2/P sensitive flame ionization detector and associated integrator was used. Optimum conditions for TBP liquid analysis were established in the chromatograph and highly reproducible results were obtained. Repeated TBP vapor injections gave a good response, however, they were not reproducible. TBP vapor pressure is very low (0.09 mm at 60°C) which may account for the difficulty in analysis.⁽⁶⁾

A continuous real time instrument for vapor phase phosphorus analysis was subsequently identified with the capability to detect phosphorus near 10^{-7} g/l. The instrument, a Meloy Laboratories, Inc. PA-460*, uses a patented flame photometric detector. The instrument was found suitable for TBP vapor analysis after slight modification. TBP was found to adsorb onto and degrade the teflon tubing used in the internals of the instrument. The pathway the TBP followed to the detector was altered to pass only through specially treated chromatographic grade stainless steel tubing. This instrument was used in the long term experiments to measure TBP retention of selected sorbents.

IV. Experimental Runs and Results

Initial Screening Studies

Several commercially available sorber materials identified through manufacturer's literature and known applications were obtained for use in the initial screening studies to evaluate TBP retention. The materials selected were either silicon oxide, aluminum oxide or combination of magnesium, silicon, alumina and iron oxides. Other materials (A and B) were either carbon based or contained activated charcoal and were used as a reference material for comparison with the other materials. These short studies were run at one set of conditions and were designed to identify sorbents showing a high TBP retention for use in further parametric long term loading experiments.

*Meloy Laboratories, Inc., Springfield, Virginia

15th DOE NUCLEAR AIR CLEANING CONFERENCE

The analyses of TBP in these experiments were performed using the NIOSH method. The reproducibility of the overall methods of generation, sampling and measurement were evaluated as part of these studies. A schematic of the experimental apparatus is shown in Figure 1.

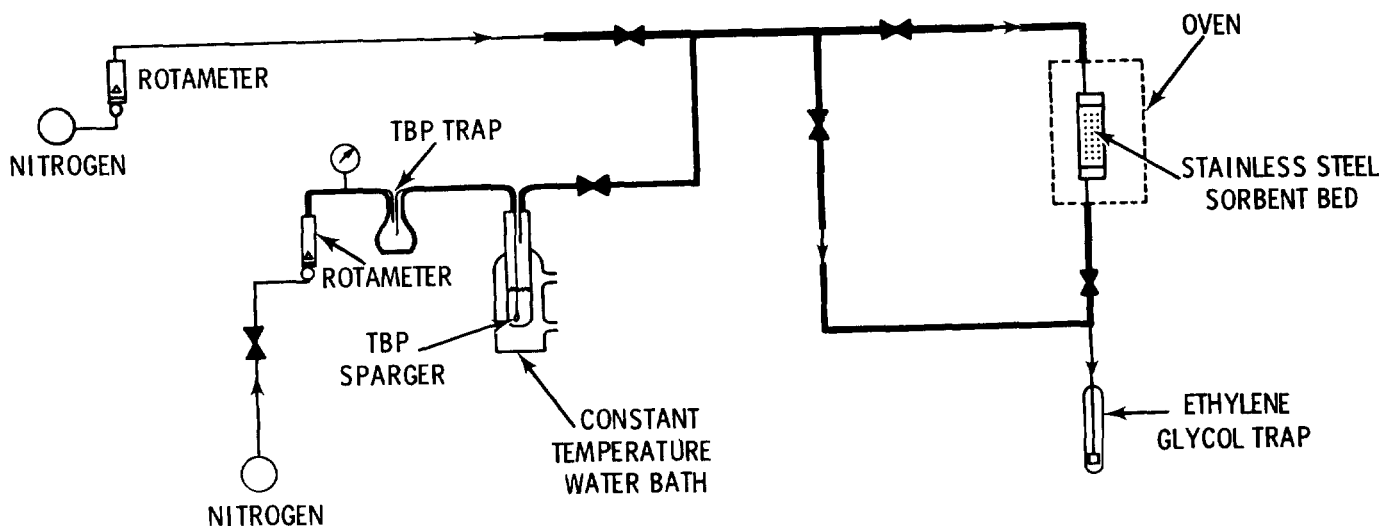


FIGURE 1
SCHEMATIC DIAGRAM OF APPARATUS USED IN
INITIAL SCREENING STUDIES OF TBP REMOVAL

Sorbents were packed into a 5 cm deep by 2.5 cm diameter stainless steel column which was placed in an oven maintained at 100°C. The feed stream to the column consisted of TBP vapor in dry nitrogen flowing at 172 ml/min. TBP vapor was generated by sparging the nitrogen at 72 ml/min through TBP liquid kept at a constant temperature. The constant temperature was set at a point between 80° and 90°C. A side stream of dry nitrogen flowing at 100 ml/min combined with the sparger stream to make up the feed stream. All feed lines in the system were standard grade stainless steel and heated where necessary to prevent condensation. Temperature and pressure were continuously monitored.

Prior to each experiment, samples were taken of the bed inlet feed stream by sparging the total stream through ethylene glycol to establish the inlet TBP concentration. Measured TBP concentration ranged from 4×10^{-4} to 1×10^{-3} g/l. Experiments were started by diverting the feed stream to the bed. The effluent from the bed was passed through the glycol. Samples were taken in 1 hour increments continuously for a total of 3 hours. In several test runs, a sample was also taken of the carrier gas (N_2) alone which was passed through the bed material for 1 hour at the end of the test run to measure any TBP eluting from the bed. Each ethylene glycol sample was analyzed for TBP. Efficiency of the material to remove TBP was determined by calculating the retained percentage of the total TBP metered to the bed. Table I is a summary of the results.

15th DOE NUCLEAR AIR CLEANING CONFERENCE

Table I Tributyl phosphate removal by sorbents.
Airflow 172 cc/min, bed temperature
100°C, bed 5 cm deep by 2.5 cm diameter.

Material	Inlet TBP, mg	Outlet TBP				Total, mg	TBP in N ₂ for 1 hr Flush Following Run, mg	% TBP Retention
		1st hr, mg	2nd hr, mg	3rd hr, mg				
Charcoal(a)	1.8	0.119	0.031	0.005	0.155	0.008	91.4	
A	1.8	<0.005	<0.005	<0.005	<0.015	<0.005	>99	
B	2.6	--	--	--	0.22(b)	--	91.5	
	1.9	0.14	0.008	0.808	0.156	0.008	91.8	
C	1.4	0.071	(c)	0.008	--	0.008	--	
D	1.5	0.015	<0.005	<0.005	<0.025	<0.005	>98.3	
E	2.6	0.14	0.01	<0.005	<0.155	<0.005	>94	
F	2.0	0.16	0.064	<0.005	<0.229	0.005	>89	
G	1.9	0.34	0.089	0.20	0.579	0.005	70	
H	1.6	0.006	<0.005	<0.005	<0.016	<0.005	>99	
J	2.4	0.16	0.038	0.019	0.217	0.006	91	
K	19.8	0.67	0.069	0.041	0.77	--	96.1	
L	19.8	0.37	0.061	0.029	0.47	--	97.7	
M	9.6	0.52	0.099	0.035	0.654	0.018	93.2	

(a) Coconut base

(b) Total of 4.5 hr run time

(c) Sample lost

The indicated inlet concentration of TBP in this series of experiments extending over a period of about 4 months had a standard deviation of 26% at the 95% confidence level. The reproducibility is largely determined by the errors in the extraction step and the gas chromatographic analyses. Furthermore, each screening test was performed over a relatively short time period during which more nearly constant conditions could be maintained. Thus, the bed removal efficiencies are more accurate than represented by the standard deviation determined over the full range of these experiments.

Parametric Studies

The most promising inorganic sorbents for TBP removal identified in the initial screening studies were selected for further experimentation. These experiments involve longer TBP loading at flow conditions more nearly approaching those likely to be found in actual reprocessing off-gas streams. These experiments were designed to evaluate materials under various operating conditions of temperature, flow and TBP concentration. The best material as determined early in these experiments will be used in experiments in the laboratory demonstration unit using a simulated process stream. The apparatus in use in these experiments is shown in Figure 2.

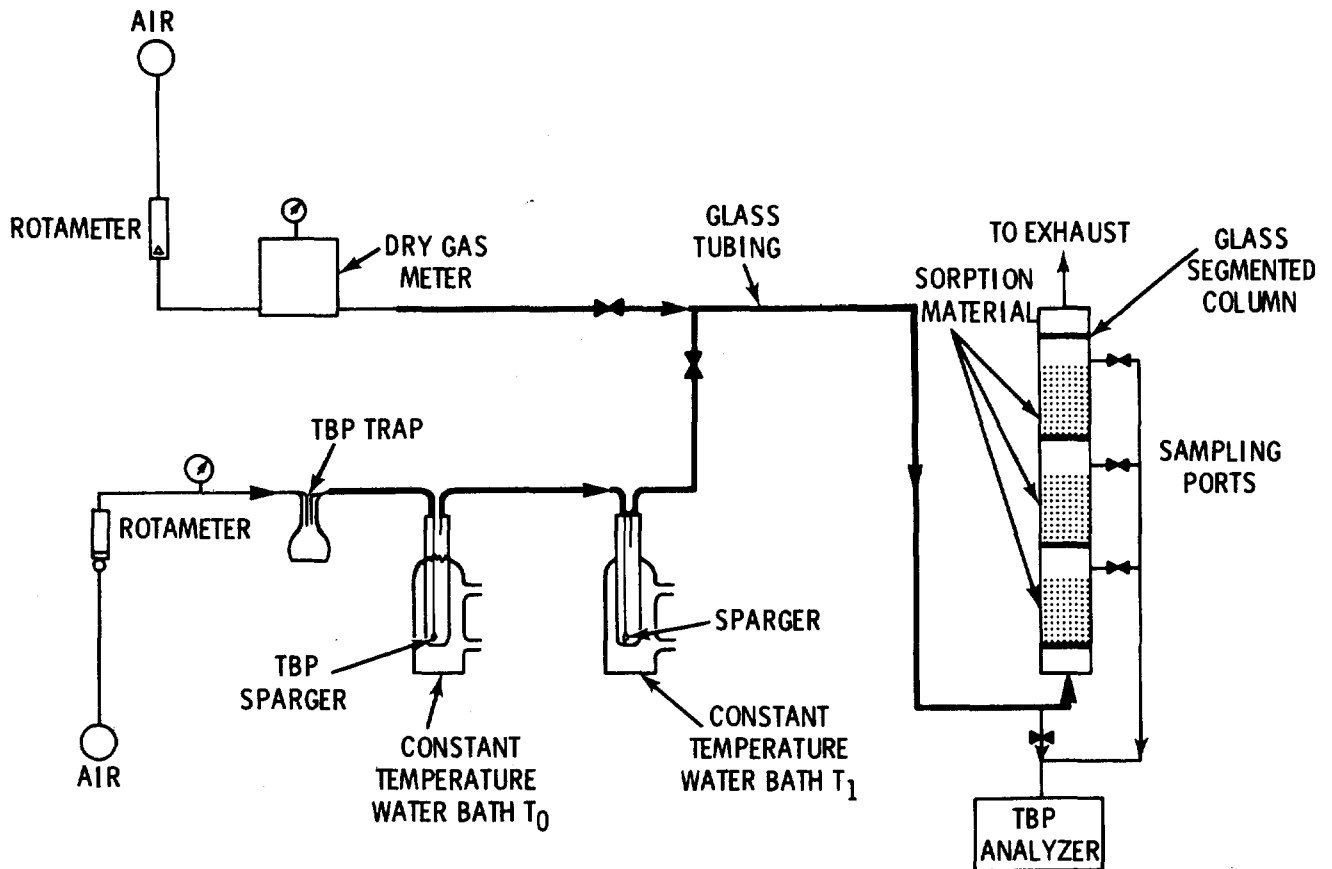


FIGURE 2
SCHEMATIC DIAGRAM OF APPARATUS USED IN PARAMETRIC EXPERI-
MENTS USING SELECTED SORBENT MATERIALS FOR TBP REMOVAL

TBP vapor is generated by sparging air at a low flow through two temperature controlled gas washing bottles in series. The first bottle is at 95°C and the second at 60°C. In this manner a saturated air stream containing a known TBP vapor concentration is reproducibly generated at 60°C. This configuration was necessary due to the low TBP vapor pressure. The TBP vapor stream is mixed with air which has passed through a dry gas meter. The flows are regulated by rotameters to obtain the desired airborne TBP feed concentration. After mixing, the feed stream flows through 6 mm glass tubing to the bed of material which is packed in glass column segments. Glass is used in the system because in early attempts to calibrate the PA-460 phosphorus analyzer using clean commercial grade stainless steel it was found that TBP adsorbed on the walls of the stainless steel tubing. Experiments showed no significant TBP adsorption on the glass tubing.

The material to be loaded with TBP is packed into the 2.5 cm diameter glass column shown in Figure 3.

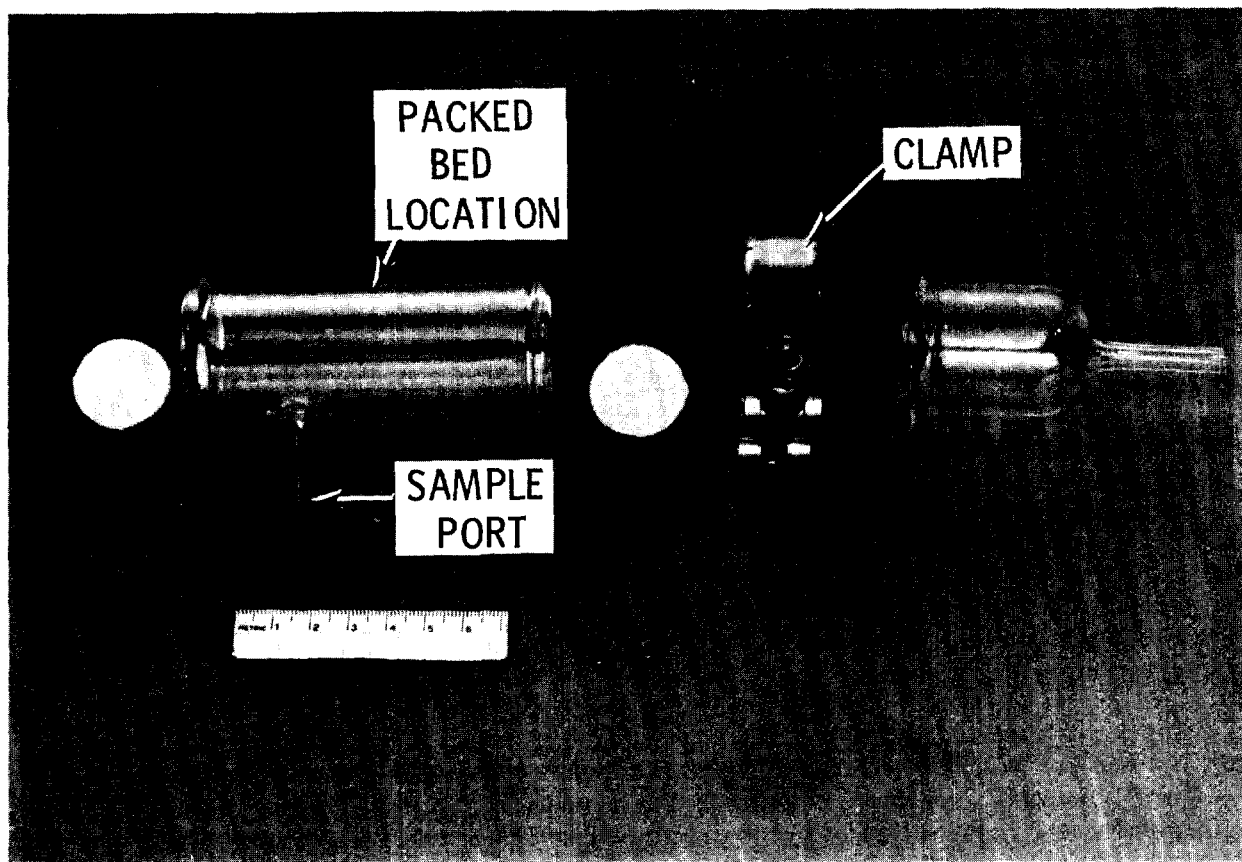


FIGURE 3
GLASS COLUMN ARRANGEMENT FOR HOLDING MATERIAL
IN PARAMETRIC STUDIES OF TBP REMOVAL

Approximately 3.8 cm of material is held in place by Gelman Type G glass fiber filters placed in front of stainless steel screens and snap rings to retain any fines purged from the material. A 1/4 inch sample port located just downstream of the material is used to sample the airstream leaving the bed segment. Airflow is upward through the system. As many as three column segments can be loaded with TBP during an experiment.

During an experimental run, TBP entering the inlet to the column is sampled via the sampling line to the PA-460. The PA-460 draws a portion of the total feed stream at 200 cc/min into the instrument. This inlet concentration (C_0) is sampled periodically. Samples of the airstream leaving each column segment are taken continuously to measure TBP concentration (C) breaking through the material: Sampling concentrates on the first column segment until significant breakthrough is measured. Subsequent samples are taken of each column segment as necessary to follow breakthrough progression through the entire column. A ratio of C/C_0 is calculated as a measure of breakthrough. The calculated standard deviation in breakthrough calculations is $\pm 25\%$ at a 95% confidence level. Largest

15th DOE NUCLEAR AIR CLEANING CONFERENCE

contributing errors in these calculations occur in instrument calibration in combination with the analysis of the inlet and outlet stream during experimentation.

Experiments with sorbent H. From the initial screening studies, sorbent H, an 8x14 mesh granular activated alumina material had the highest retention of the noncarbonaceous materials tested (material A contained an activated charcoal mix), and was selected for further parametric study. Three column segments containing 20 g of material H in each segment were loaded with TBP. The following conditions were employed.

Bed temperature: 100°C
Average airflow: 0.45 l/min
TBP concentration: 1×10^{-4} - 2.4×10^{-4} g/l
Preconditioning with air: 2.5 hours

After more than 277 hours of run time and 1.8 grams TBP metered to the columns, a breakthrough of $C/C_0 = 0.02\%$ in the first column segment was measured. No breakthrough in the other two column segments was detected. The concentration of TBP entering the columns was increased during the test run from 1×10^{-4} g/l to accelerate loading and breakthrough.

A second experiment using material H was prepared. A single column segment was packed with 19.1 g of material and loaded with TBP. Airflow was increased by a factor of 4 to assess the effect of this parameter. The following conditions were employed.

Bed temperature: 100°C
Average airflow: 1.9 l/min
TBP concentration: 1×10^{-4} - 4.5×10^{-4} g/l
Preconditioning with air: 2 hours

The material was loaded with 2.9 g TBP before any breakthrough ($>0.01\%$) was measured. A total of 8.96 g TBP was metered to the material over a period of 331.6 hours before the run was terminated. Breakthrough measured at the end of the run was $\sim 100\%$. The complete breakthrough curve is shown in Figure 4.

The capacity of the material to retain TBP was calculated from the breakthrough curve to be 377 mg TBP/g material. Because of the high TBP retention of material H in these experiments, it was decided to use the material in laboratory experiments **run under simulated offgas stream conditions.**

Experiments with sorbent D. TBP loading of 4x8 mesh spherical catalyst material D was initiated in late February 1978. A single column segment of material weighing 14.6 g was used in this first experiment. The following conditions were employed:

Bed temperature: 100°C
Average airflow: 1.9 l/min
TBP concentration: 1×10^{-4} g/l
Preconditioning with air: 2 hours

15th DOE NUCLEAR AIR CLEANING CONFERENCE

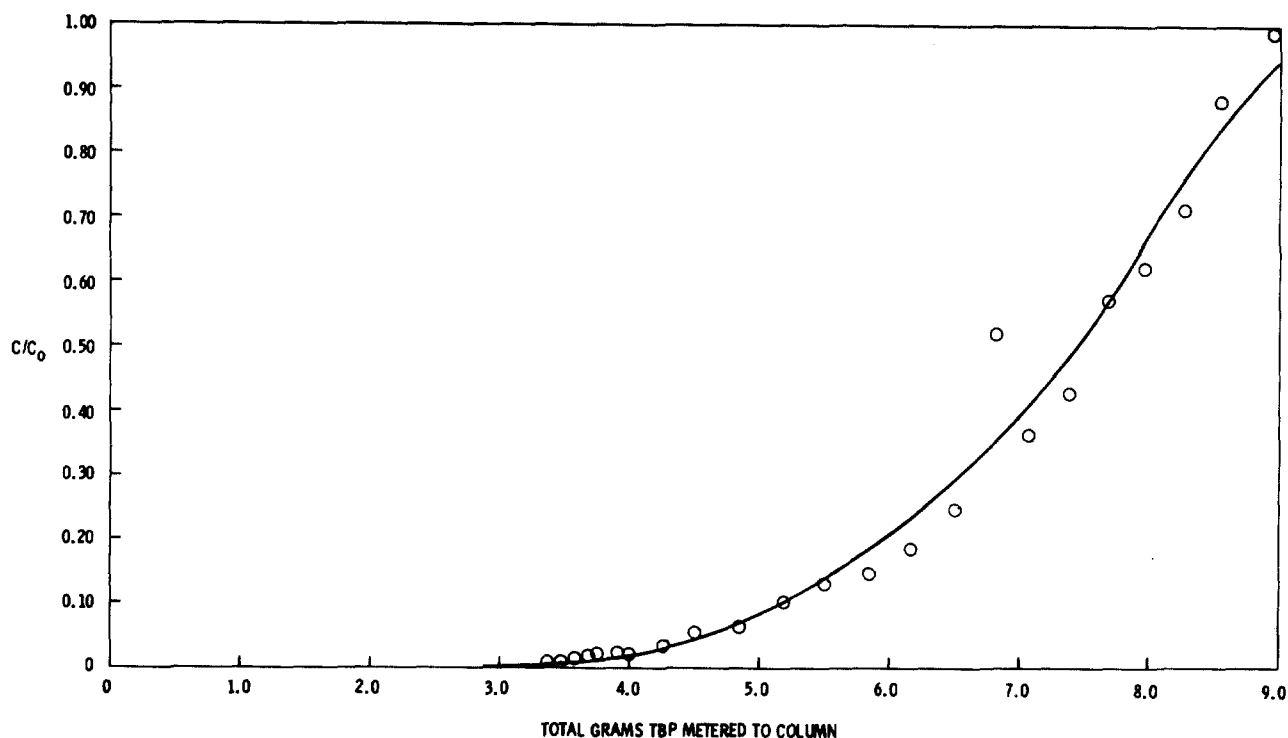


FIGURE 4
 BREAKTHROUGH HISTORY FOR TBP LOADING OF MATERIAL H.
 AIRFLOW 1.9 l/MIN, BED TEMPERATURE 100°C, TBP CON-
 CENTRATION $1-4.5 \times 10^{-4}$ g/l

Nearly instantaneous breakthrough was measured and 100% breakthrough was achieved after 37.6 hours of run time and 0.45 g TBP metered to the material. From the breakthrough curve in Figure 5, the capacity of the spherical material to retain TBP was calculated to be 11 mg TBP/g material, which is considerably less than the granular material H tested under nearly identical conditions.

This spherical material was crushed to 6x14 mesh in an effort to increase the surface area for reaction. The crushed material weighing 15.1 g was packed into a single glass column and TBP was loaded onto the material under identical conditions as those used for the spherical form of the material.

As in the experiment using the spherical form of material D, nearly instantaneous breakthrough was measured. The run was terminated after metering 0.97 g TBP to the material in 73.1 hours. The breakthrough curve for this material is shown in Figure 6. Calculated TBP retention of the crushed material is 39 mg TBP/g material.

Even though TBP retention was increased by 3.5, retention is significantly lower than that achieved with material H. Further experimentation with material D is not considered due to the very low TBP retention.

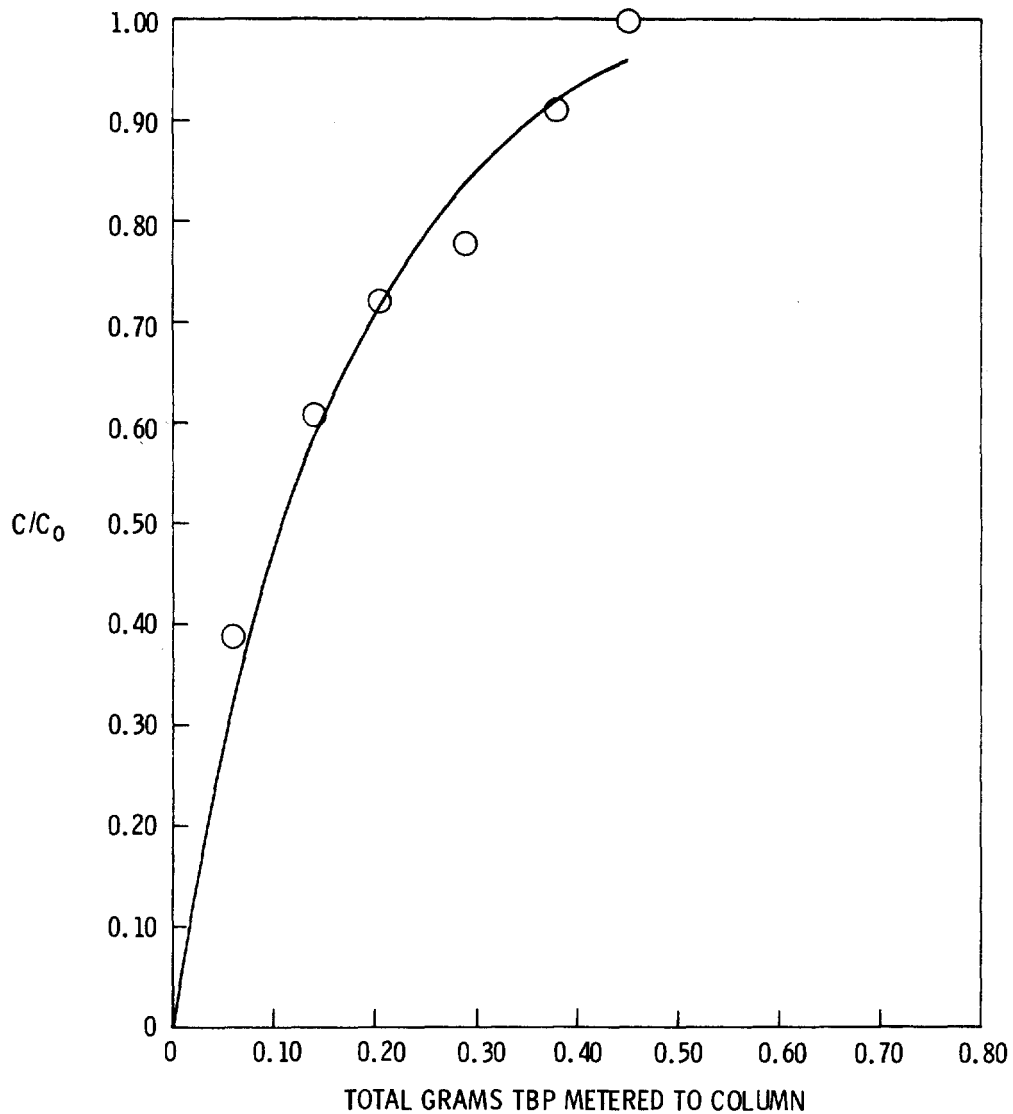


FIGURE 5
 BREAKTHROUGH HISTORY FOR TBP LOADING ONTO MATERIAL D
 (4x8 MESH SPHERICAL). BED TEMPERATURE 100°C, AIRFLOW
 1.9 l/MIN, TBP CONCENTRATION 1×10^{-4} g/l

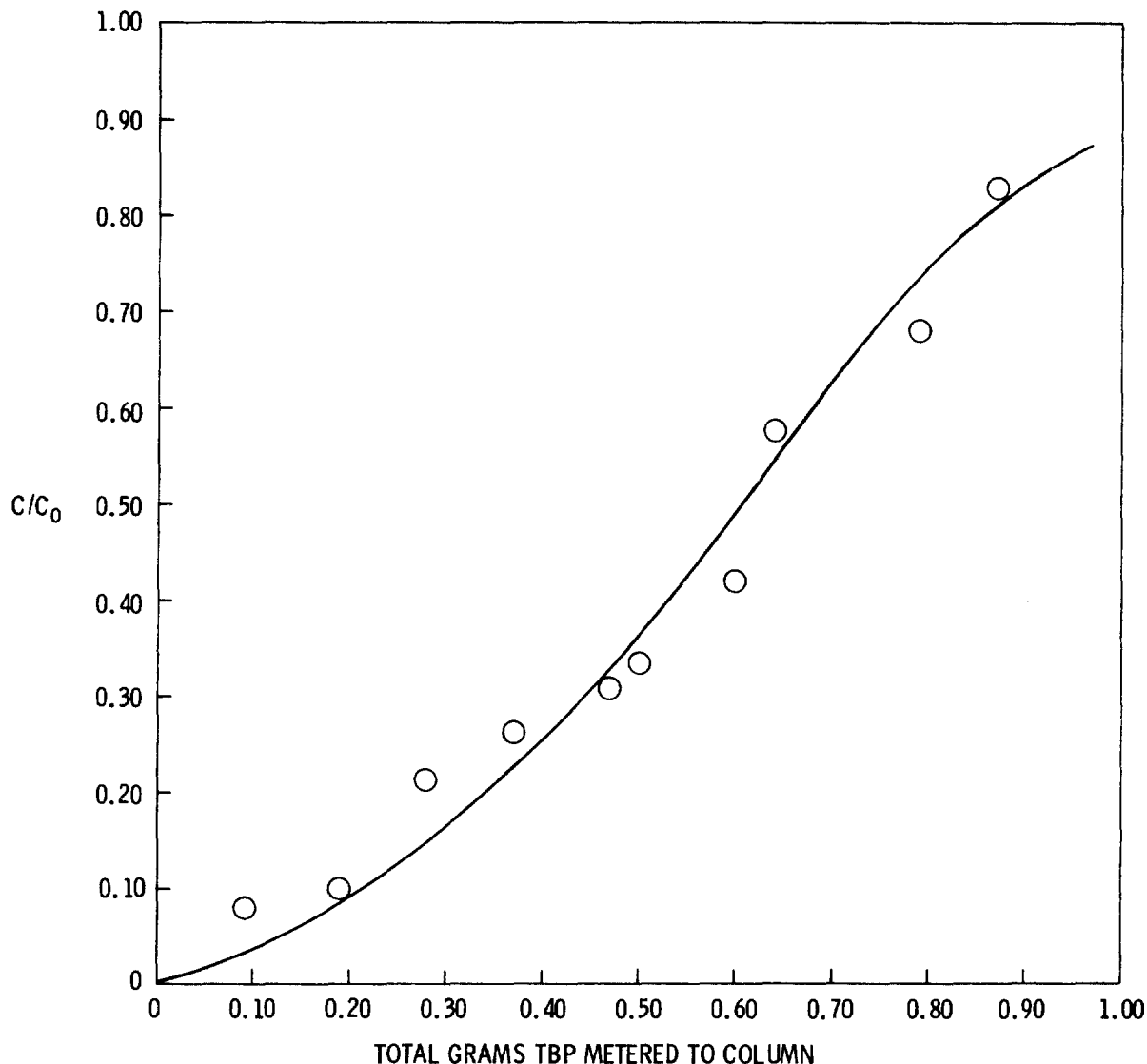


FIGURE 6
BREAKTHROUGH HISTORY FOR TBP LOADING ONTO MATERIAL D
(6x14 MESH GRANULAR). BED TEMPERATURE 100°C, AIRFLOW
1.9ℓ /MIN, TBP CONCENTRATION 1x10⁻⁴ g/ℓ

Experiments with sorbent L. The next material used in these experiments was sorbent L, an 8 x 30 mesh granular, silica, alumina, magnesia sorptive clay, which indicated the third highest TBP retention of the noncarbonaceous materials in the screening studies. Two 3.8 cm x 2.5 cm glass column segments were packed with material L and prepared for loading with TBP. Segment 1 contained 13.6 g and segment 2 contained 14.0 g. The following conditions were employed.

Bed temperature: 100°C
Average airflow: 2.0 ℓ/min
TBP concentration: 6x10⁻⁵ g/ℓ
Preconditioning with air: 2 hours

A breakthrough of 0.6% in segment 1 was measured after metering 0.19 TBP to the column. After metering 0.94 g of TBP to the material a breakthrough of 54% was measured in the first column segment at which time the run was terminated. No breakthrough was measured in the second column segment. The breakthrough curve for the first column segment is found in Figure 7.

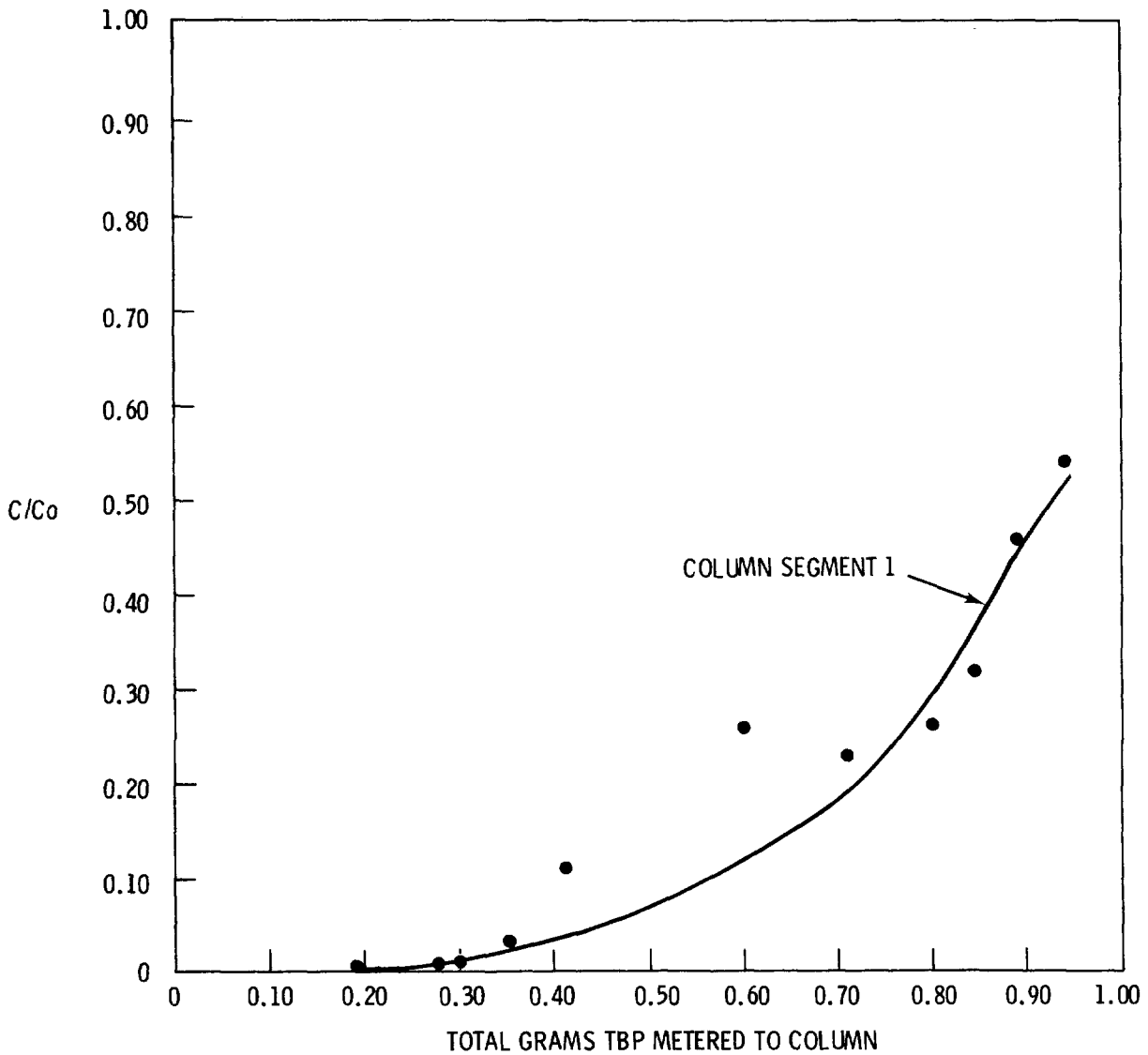


FIGURE 7
 BREAKTHROUGH HISTORY FOR TBP LOADING ONTO MATERIAL L. BED TEMPERATURE 100°C, AIRFLOW 2.0 l/MIN, TBP CONCENTRATION 6×10^{-5} g/l

Even though breakthrough was not followed to 100%, total capacity of the material can be estimated from the available breakthrough data. Approximated capacity of the material extrapolated to 100% breakthrough is 70 mg/g material which is greater than material D but considerably less than material H.

V Future Work

Material H will be used in laboratory demonstration experiments to determine the effectiveness of the material to remove TBP vapor and protect iodine sorbent beds downstream. The measure of effectiveness for TBP removal will be iodine retention of the iodine sorbent material. The experiments will be conducted using an air stream containing TBP, water vapor and other constituents likely to be present. Other candidate materials will be used in this demonstration unit as they are identified in the parametric experiments.

An alternative method to quantitatively measure TBP vapor using a remote optoacoustic laser analysis technique is being explored. The feasibility of such an analysis method is being studied by first examining the possible constituents present in the off-gas that could cause interference in this analysis method.

VI Summary and Conclusion

- It has been demonstrated that it is possible to quantitatively analyze low concentrations of airborne TBP using a modified real time continuous instrument. Based on vapor pressure calculations, concentrations as low as 1×10^{-7} g TBP/l air have been measured using this instrument.
- Several inorganic sorbents identified through literature have shown promise to retain TBP vapors in low flow, short duration sorption experiments. Four of the inorganic materials gave greater than 95% TBP retention and one of the four gave greater than 99% retention.
- Long duration parametric experiments have shown material H to be the most efficient sorbent for TBP removal. The first experiment at an airflow of 0.45 l/min gave a detectable TBP breakthrough after metering 1.8 g TBP to the material. Increasing the airflow by a factor of 4 increased TBP retention before measurable breakthrough by a factor of 1.6.
- No other material tested in nearly identical long duration experiments has shown as efficient TBP retention as material H. Material L, the next most efficient material showed a measurable TBP breakthrough in 3.8 cm of material after metering less than 0.19 g TBP. This is 1/15 the TBP which was metered to material H before measurable breakthrough in a nearly identical experiment.

15th DOE NUCLEAR AIR CLEANING CONFERENCE

References

- (1) Wilhelm, J. G. and J. Furrer, "Head-end iodine removal from a reprocessing plant with a solid sorbent," Proceedings of the 14th ERDA Air Cleaning Conference, CONF 760822 (1976).
- (2) Thomas, T. R., L. P. Murphy, B. A. Staples and J. T. Nichol, "Airborne iodine loading capacities of metal zeolites and a method for recycling silver zeolite," ERDA, Idaho Operations Office, ICP-1119, (1977).
- (3) Horton, A. D., "Gas chromatographic determination of tri-methyl phosphate, dimethyl phosphate, methyl dibutyl phosphate and tributyl phosphate," Journal of Chromatographic Science, 10:125 (1972).
- (4) NIOSH Method P&CAM 158, "Parathion in air," revised (1973).
- (5) EHS Procedure P-3, "Pesticide analysis of plant tissue" (1973).
- (6) Burger, L. L., "The chemistry of tributyl phosphate a review," HW-40910, U.S. A.E.C., Hanford Atomic Products Operation, Richland, Washington

DISCUSSION

VAN BRUNT: Have you performed experiments with other solvent constituents such as TDP or n-decane?

PARKER: Yes. In the bench scale experiment designed for testing the TBP sorbents as protective beds for iodine sorbents, TBP is used in combination with dodecane (NPH) in the field stream. I do not expect any deleterious effect from the dodecane, however.

VAN BRUNT: Do you expect that the TBP vapor from a knockout pot following the dissolver and from the VOG to be near your experimental conditions, i.e. at 100°C? I would expect a conservative temperature to be closer to 60°C.

PARKER: True, the TBP vapor temperature would be closer to 60°C than 100°C. But TBP removal beds can be operated at temperatures above 60°C (up to 150°C) if they are placed in the system in the same manner as the iodine sorbent beds. These TBP sorbent beds seem to operate more efficiently at the higher temperatures.

VAN BRUNT: Wouldn't you expect the TDP vapor pressure to be very low after a knock-out pot?

PARKER: TDP vapor pressure is just low, but some is still going to get into the air stream even at 50 or 60°C.

WILHELM: Did you try cold adsorption of elementary iodine on your material? I find it quite interesting and I would be happy if this material could be used in front of a silver adsorption bed. But you may have iodine adsorption on it

15th DOE NUCLEAR AIR CLEANING CONFERENCE

and you may not be able to desorb the iodine again. Because iodine is not in a chemical compound with no, or low, pressure, it may desorb slowly. This may generate a contamination and place restrictions on where you put the material which you use to remove tributyl phosphate.

PARKER: You're saying that possibly iodine could be adsorbed in a TBP adsorbent, also?

WILHELM: Yes.

PARKER: For the laboratory tests that we're running now with methyl iodide, the results are in the April, May, June quarterly report to the Department of Energy. The question you asked would be answered in that report but I can't answer it here because it's a limited distribution.

WILHELM: What about elemental iodine?

PARKER: Yes, I'd say there's a good possibility it could happen with elemental iodine. It would be something to explore. Of course, elemental iodine will plate out on just about everything in the world.

15th DOE NUCLEAR AIR CLEANING CONFERENCE

A REVIEW OF SOME U.K.A.E.A. WORK ON GAS CLEANING IN FUEL REPROCESSING PLANT

M.N. Elliot (UKAEA, Harwell)
E. Lilleyman (UKAEA, Dounreay)

Abstract

The efficiency of air cleaning systems for fuel reprocessing plant is of prime importance and present systems based upon HEPA filtration have proved very satisfactory in this respect. However, with the larger installations the associated handling and storage procedures are less attractive and new approaches are being developed for the changing levels of radioactivity and plant throughput. This paper presents an interim report of the work.

Improvements can be obtained from a reduction in the size or number of filter installations, an increase in filter life, and from simpler handling and storage procedures. Alternative schemes which can reduce the ventilation load or the number of separate filter installations are discussed. Prefiltration techniques can extend filter life and work on a condensation technique and electrostatic precipitation is described. Methods of volume reduction for storage or disposal of spent filters (by compaction, dismantling and incineration) are being examined and progress to date is reported. Filter sealing and change mechanisms vary with application and have some features in common with more conventional posting systems. Techniques in use or being considered for α and $\beta\gamma$ -active applications are discussed.

I. Introduction

An unconventional design approach is as necessary for the ventilation and filtration systems as for other sections of nuclear fuel reprocessing plant. However until comparatively recently this has not been fully acknowledged and conventional technology, modified to suit the process conditions, has largely been used.

The ideal gas cleaning system should:

- (a) guarantee highly efficient removal of radioactive particulates under both normal and incident conditions,
- (b) minimise handling operations and penetration of containment,
- (c) minimise the treatment and storage of contaminated filters.

Present well-sealed systems satisfy criterion (a) but the handling and storage procedures are cumbersome and costly. As the industry expands, filtration plant employing improved techniques will be required, and dealing with the 'back-end' of the system presents challenging development problems.

15th DOE NUCLEAR AIR CLEANING CONFERENCE

Many gas cleaning systems throughout the world are based upon once-through ventilation and HEPA filtration. For U.K. applications a filter efficiency of at least 99.95% is specified, the filters must be capable of continuous operation at 200°C and show an efficiency of 98% after exposure to 500°C for ten minutes. Steel cases are used and the pleated glass fibre medium is sealed by a layer of glass fibre wadding.

The filters are reproducibly highly efficient when correctly installed. However a single installation may contain some tens of individual 1700m³/h (1,000 cfm) units and a complete plant may require many such installations, grouped according to the plant layout and including primary, secondary and stand-by filter banks. The handling, particularly by remote means, of the large number of individual units is time-consuming and costly. Since approximately 75% of the unit volume is virtually void, storage and disposal of unprocessed filters is costly and wasteful.

Improvements seem possible in three main areas:

- (a) reduced installation size,
- (b) increased filter life,
- (c) improved handling and storage/disposal procedures.

This paper contains an interim report of some work in these areas, carried out within the UKAEA. However, before considering the three headings in detail, it is worthwhile completing the discussion of future trends.

Gas cleaning systems based upon sand beds have been successfully used at the Savannah River site for some years⁽¹⁾⁽²⁾. The avoidance of regular filter-changing procedures is very attractive but there is some uncertainty about their eventual decommissioning. A sealed, loaded sand bed does not conform strictly to the definition of a retrievable store and some provision for bed transfer may be necessary to satisfy the regulations. Thus whilst the application of such systems is under consideration, no firm conclusion has been reached.

II. Reduced Installation Size

A reduction in the ventilation load and hence in size of filter installation is an important objective of any design exercise. For example, the once-through air flow can be reduced by improving the leak-tightness of containment structures and penetrations and/or matching ventilation rates to specific process operations rather than to some general air change criterion. Such principles have been applied to the conversion of the Dounreay fast reactor (DFR) fuel reprocessing plant to prototype fast reactor (PFR) reprocessing, where it has proved possible to reduce the combined extracts from the fuel breakdown cave, process cell and vessel vents from the original design value of approximately 20,000m³/h (12,000cfm) to a normal operating flowrate of 1,700m³/h (1,000cfm).

However the size of an installation may be dictated by other factors which must be included in the design studies. For example, the rating is sometimes controlled by the forecast emergency situation and in this case

15th DOE NUCLEAR AIR CLEANING CONFERENCE

an assessment of procedures which might ease the burden of such a restriction is important. A fairly common example is the design of access arrangements to avoid the high air flows which result when the criterion of

1m/sec linear velocity through an opening is applied. Fluidic devices can be used to carefully control the pressure drop between contamination zones and to respond, but not over-react, to the emergency condition. By such measures the flowrate under incident conditions has been limited, in the case above, to approximately double the normal value.

Recirculating systems, already used for inert atmosphere glove-boxes can, in principle, be applied more widely. An example is the new fuel handling cave associated with the PFR reprocessing plant, designed to contain some hundreds of tons of liquid sodium and provided with a nitrogen blanket gas system including purification using a by-pass low temperature plant. The cave has a volume of 850m³ and a leak-rate of 0.05 volume % per hour has been achieved at the 13mm w.g. ($\frac{1}{2}$ ") working pressure differential. This despite many envelope penetrations including an 18m² area shielded access door (fitted with an inflatable seal).

Closed cycle ventilation using a condensible gas is now being studied experimentally at Dounreay⁽³⁾ and would seem most suitable for use on the head-end sections of a reprocessing plant. The concept offers the potential for greatly eased fission product gas removal and particulate removal but the early state of development excludes a more detailed discussion at present.

III. Increased Filter Life

The HEPA Filter is not a high dust-capacity device and even in moderate dust-loading situations the use of a prefilter is desirable. Although it has been shown that removal of the larger particulates results in a more rapid increase of pressure drop with dust loading, and hence in reduced dust capacity⁽⁴⁾, the filter life is very significantly increased because of the reduced incident aerosol concentration.

This is of clear benefit provided that the handling and storage problems are not greatly increased. Conventional prefilters do tend to present additional complications, however, and ideally devices which can be cleaned and maintained in-situ by remote means are required.

A technique which could be applied to the water-saturated air flows characteristic of scrubbed vessel vent streams has been studied at the laboratory scale (10m³/h total air flow)⁽⁵⁾. The process involves the condensation of water onto the particulate nuclei, followed by removal of the grown droplets using a wire mesh demister. In the laboratory, condensation was promoted by mixing saturated air at 45°C with chilled air at 5°C, and removal efficiencies > 90% were measured for naturally occurring airborne particulates larger than 0.3 μm.

As has been noted by others⁽⁶⁾, the process is not economically competitive if steam injection is necessary to form a saturated air stream. However humid vessel vent streams, saturated at approximately 45°C, present special problems due to the impingement of water droplets and condensation at the HEPA filter, and dehumidification by cooling is being investigated

15th DOE NUCLEAR AIR CLEANING CONFERENCE

for their protection. The recycle of part of the chilled air to promote condensation appears feasible and is to be tested, in conjunction with the dehumidification work, on the 2,000m³/h scale.

The demisting operation should be essentially self-cleaning but some spray wash could be incorporated if necessary to ensure remote functioning and cleaning.

Electrostatic precipitation is another technique which promises reliable remote operation for long periods and has a wider application. The satisfactory experience with the special electrostatic filters on the highly active storage tank off-gas systems at Windscale⁽⁷⁾ is encouraging.

A compact reliable unit is required which can be cleaned remotely and be easily removed in modules for maintenance. Ignition of solvent vapours which might be present must be avoided.

The present work is in two parts. Firstly a commercial unit is being installed in an inactive process area to obtain first-hand experience of reliability and cleaning methods with particulates similar to those of cell and cave extract streams. Electrical design parameters are also being examined to design a compact reliable multi-stage unit, using a spark energy limitation technique to avoid solvent ignition problems, as described by other workers⁽⁸⁾⁽⁹⁾. Filled, fibre reinforced laminates appear well-suited for use in the collection section.

IV. Improved Handling and Storage Procedures

4.1 Handling

The Dounreay experience of filter sealing and change systems associated with enriched uranium fuel reprocessing⁽¹⁰⁾, coupled with the move to a plutonium fuel cycle and a policy of minimising plastic waste generation called for a critical review of techniques. As a consequence, the following criteria have been applied to the design of filter housings for the PFR reprocessing plant:

- (1) the system should guarantee plutonium containment standards at all times and external radiation levels at the housing surface should not exceed 0.5 mrem/h during normal operation and filter change. Isolation during the filter change must therefore ensure no by-pass to the downstream ductwork.
- (2) secondary waste production should be minimised and (because of radiolytic production of HCl in retrievable storage), PVC bagging procedures should be excluded. Used filters should be packaged for delivery to a disposal facility or storage in an externally clean container.
- (3) provision for inspection and maintenance of the permanent sealing faces should be included.

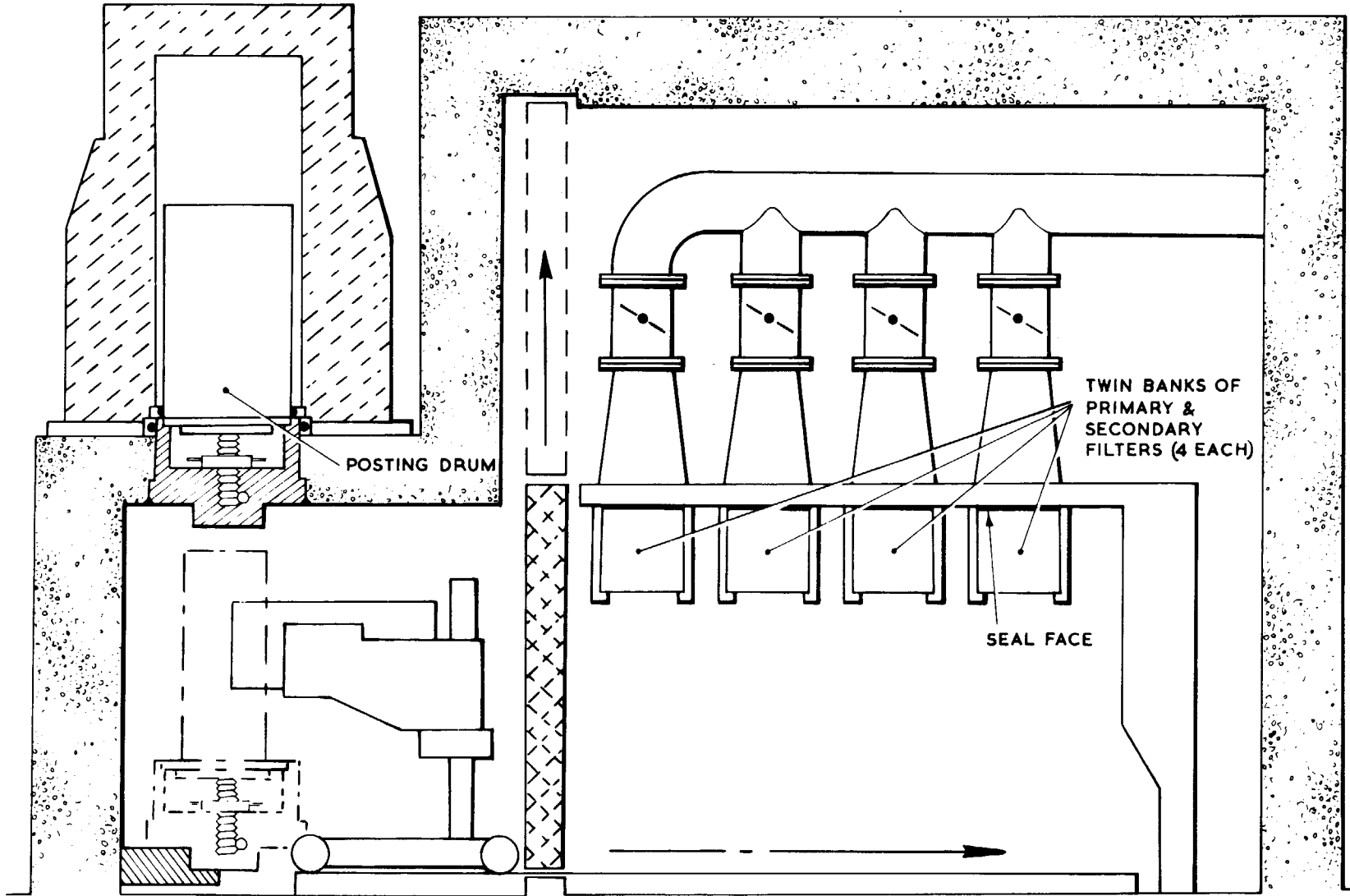


FIG 1 REMOTE ROBOT FILTER CHANGE SYSTEM

15th DOE NUCLEAR AIR CLEANING CONFERENCE

The first system designed to these criteria handles the combined extracts from the PFR reprocessing plant (figure 1). The primary and secondary filter banks, rated at $4000\text{m}^3/\text{h}$ ($2,400\text{fm}$) each, contain four filter units, installed in the same shielded enclosure. The filters are sealed to the cell roof and arranged with downflow through the primaries, upflow through the secondaries.

Clean and used filters are transferred in 200 litre posting drums contained in a shielded flask. The drum lid locates with the shield plug of the posting port to protect the external surfaces from contamination, as with other double door systems, of which the La Calhene posting system is an example. Similar posting facilities are provided at the waste handling and storage facility. Transfers between the posting and filter cells are carried out using a robot, and, once they are located, sealing pressure is applied to the filters by a separate remotely operated system. The operating sequence is then as follows:

1. Position posting drum containing new filter, locate lid and shield plug, lower the lid assembly and filter into the posting cell.
2. Transfer the filter to a stand-by position.
3. Transfer the robot (via a shielded access door) to the filter cell and engage with the used filter.
4. Release the sealing pressure and locate the sealing clamps in the filter withdrawal position.
5. Lower the used filter, transfer to the posting cell and insert with the lid assembly into the posting drum.
6. Transfer the clean filter, locate, actuate sealing clamps and withdraw robot.

Valves rather than dampers are used for isolation during the changing operation and a chemical to fix loose contamination can be sprayed onto the used filter before removal.

The design satisfies the criteria but is mechanically rather complex. For the waste handling facilities a filter change system has been developed which again uses the double door principle, but with operations carried out manually by means of rods through the shielding (figure 2)⁽¹¹⁾. The unit comprises three filters, rated at $425\text{m}^3/\text{h}$ (250fcm) each, one in use with two on permanent standby.

The rectangular filters are fitted with circular end pieces sealed by plugs which engage with corresponding plugs in the filter cell ducts. After sealing by manual lever, duct and filter plugs are engaged by rotation and then by further rotation are released so that both can be withdrawn to a parking position. Air is then free to pass through the filter.

For filter removal the filter and duct plugs are re-located, the former containing radioactive particulate within the filter and the latter isolating the filter cell from the inlet and outlet ducts. A high standard

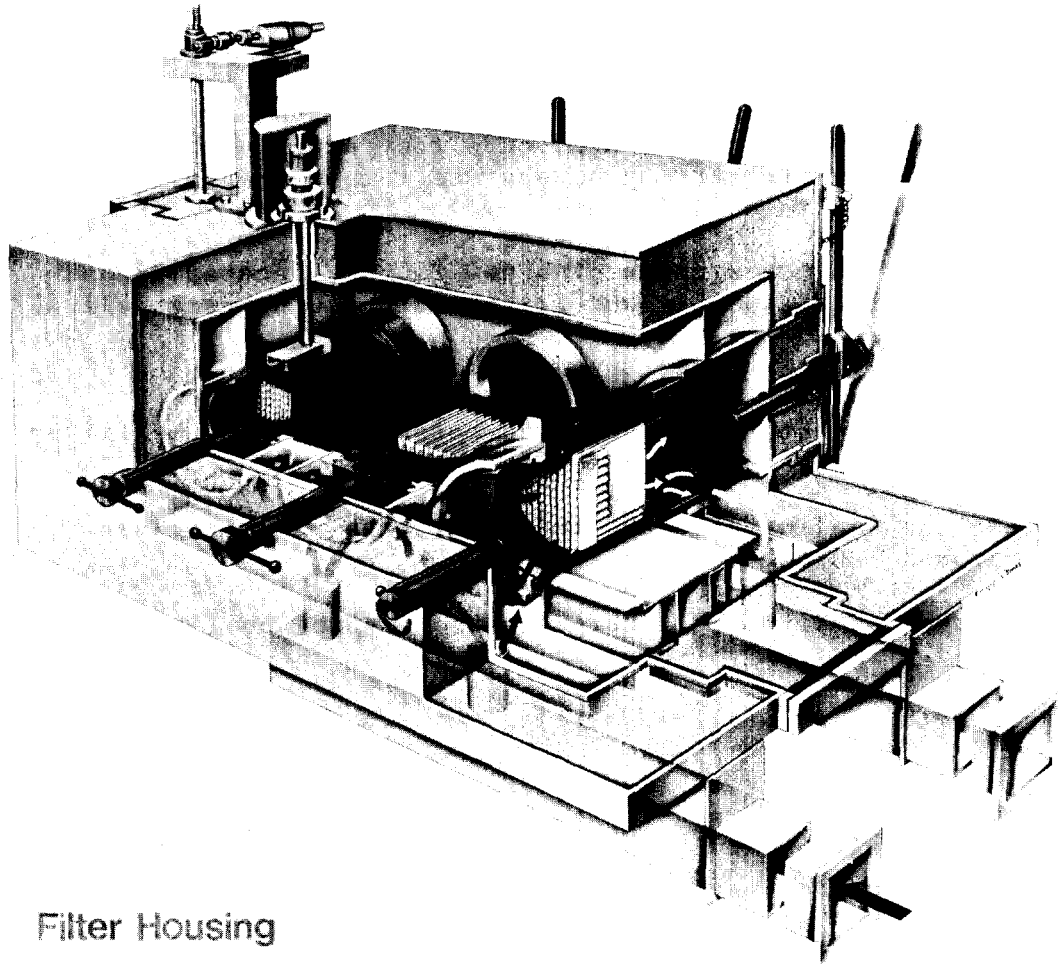


FIGURE 2
MANUALLY OPERATED SHIELDED FILTER CHANGE SYSTEM

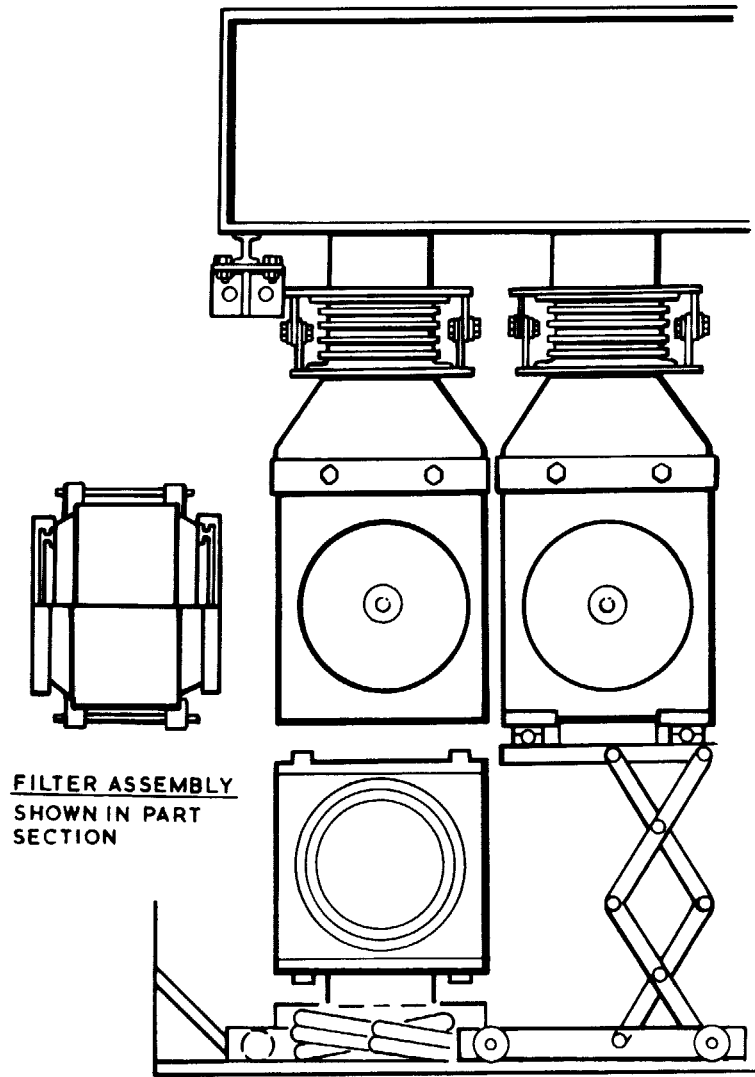
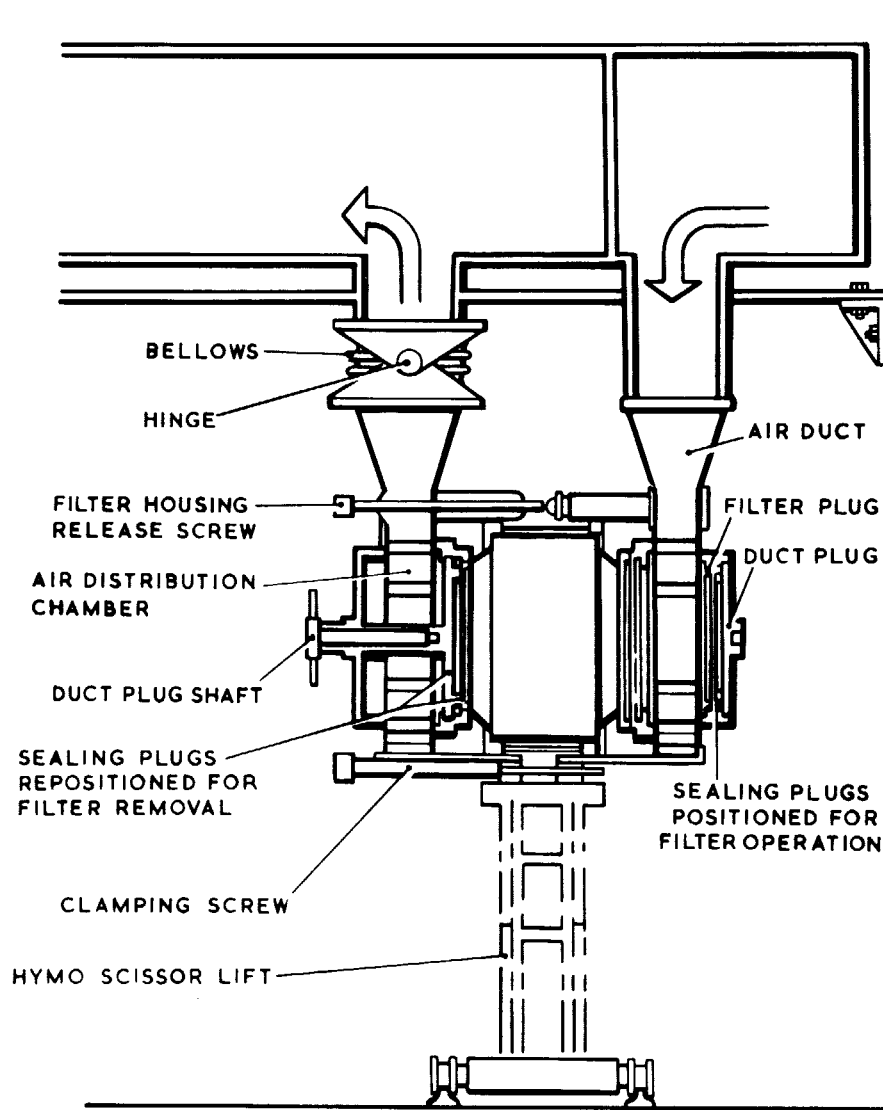


FIGURE 3
HIGH α LOW $\beta\gamma$ FILTER INSTALLATION

15th DOE NUCLEAR AIR CLEANING CONFERENCE

of containment can thus be obtained. Further, the use of both inlet and outlet sealing faces ensures a pressure differential between the cell and filter/ducting which avoids by-passing of the filter, irrespective of the condition of the seal faces.

A similar principle has been applied to unshielded systems, handling $1700\text{m}^3/\text{h}$ filters, to avoid the conventional bagging procedures and to provide good isolation during filter changes. A prototype unit is illustrated in figure 3 and an installation rated at $51,000\text{m}^3/\text{h}$ is being manufactured.

4.2 Storage or Disposal

The volume reduction of filters for retrievable storage or disposal is patently beneficial. Compression techniques such as baling are being evaluated elsewhere⁽¹²⁾⁽¹³⁾ but the handling and contamination problems can be quite formidable, and two alternatives which promise fewer remote handling problems are being studied at Harwell.

Firstly, for conventional metal-cased dry-sealed units, techniques based upon dismantling are being examined. Cases of riveted or bolted construction can be opened using power tools but their use is inconvenient and time-consuming and only suited for low levels of radioactivity. To facilitate rapid dismantling by either direct or remote handling, a method of construction using proprietary quick-release fasteners has been developed in conjunction with Vokes Ltd. A prototype filter is illustrated in figure 4. The filter efficiency is unimpaired by this method of construction and in-service testing of prototypes is planned. As an alternative, the use of carefully positioned, easily sheared rivets is being examined for the $425\text{m}^3/\text{h}$ units used with the shielded filter change system described previously.

In the simplest case, if the filter pack can be removed by hand, it can be readily processed without heavy engineering equipment. Recycle of the case appears feasible.

At higher levels of radioactivity, frogsuit or glove box manipulations may be restricted or shielded operations required, and for these situations mechanical removal of the paper is being developed⁽¹⁴⁾.

The technique is illustrated in figure 5. This involves removing one side of the case and the associated wadding to expose one edge of the pleated pack of glass fibre paper. The exposed edge is located in a driven spool which withdraws the paper, forming a tightly coiled roll which is easily handled even when removed from the spool. Spacers are separated during coiling and collected in trays on both sides of the machine. The separated fractions can be treated as required. Plutonium recovery from the paper is possible and it appears that the glass fibre and aluminium can readily be compacted or melted.

Using a laboratory model or the prototype machine shown in figure 6, over 20 inactive or slightly contaminated filters from installations at Harwell have been treated. The machines were installed in a PVC tent to monitor airborne contamination and this has proved to be very low. Some

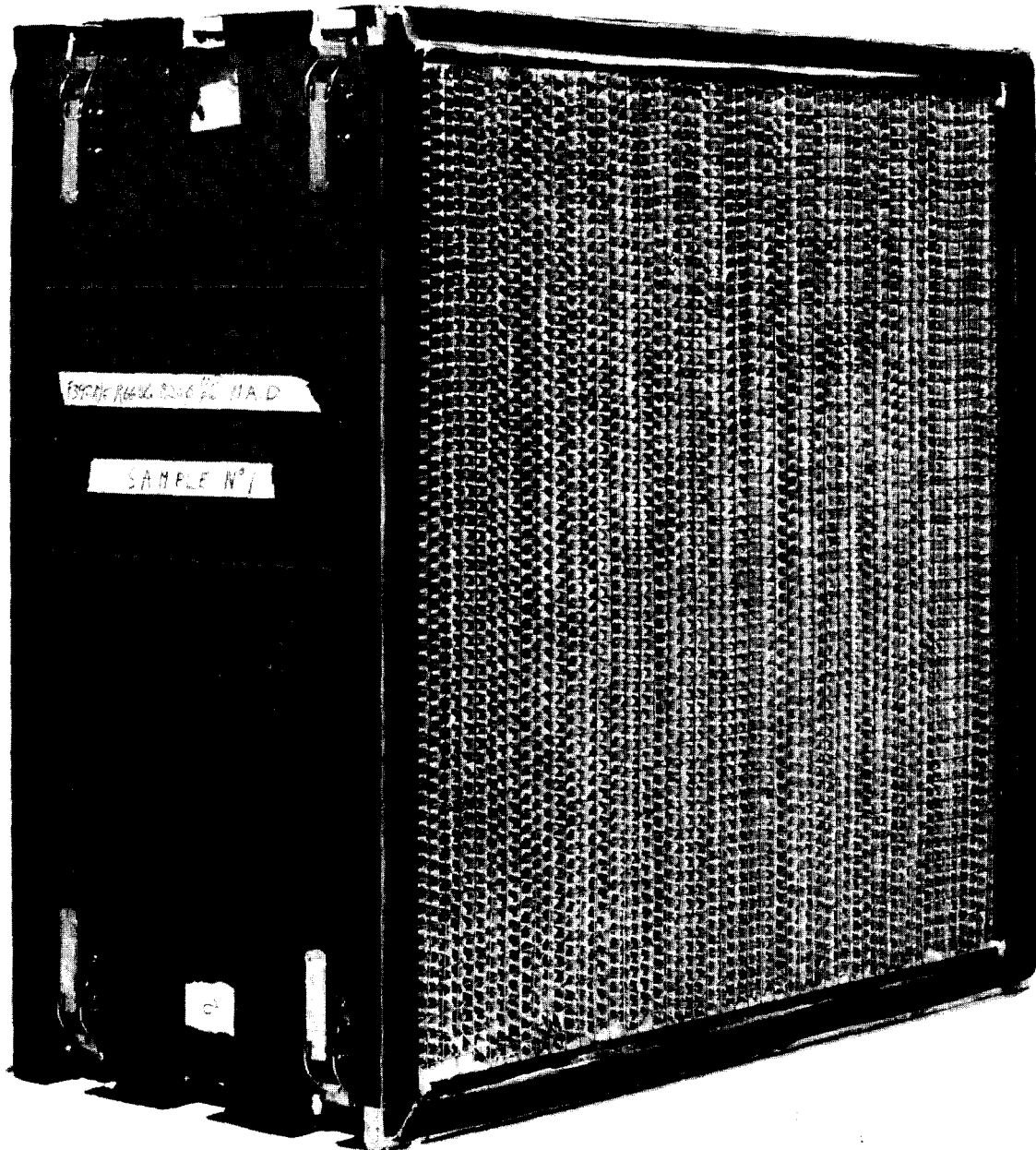


FIGURE 4
MODIFIED HEPA FILTER

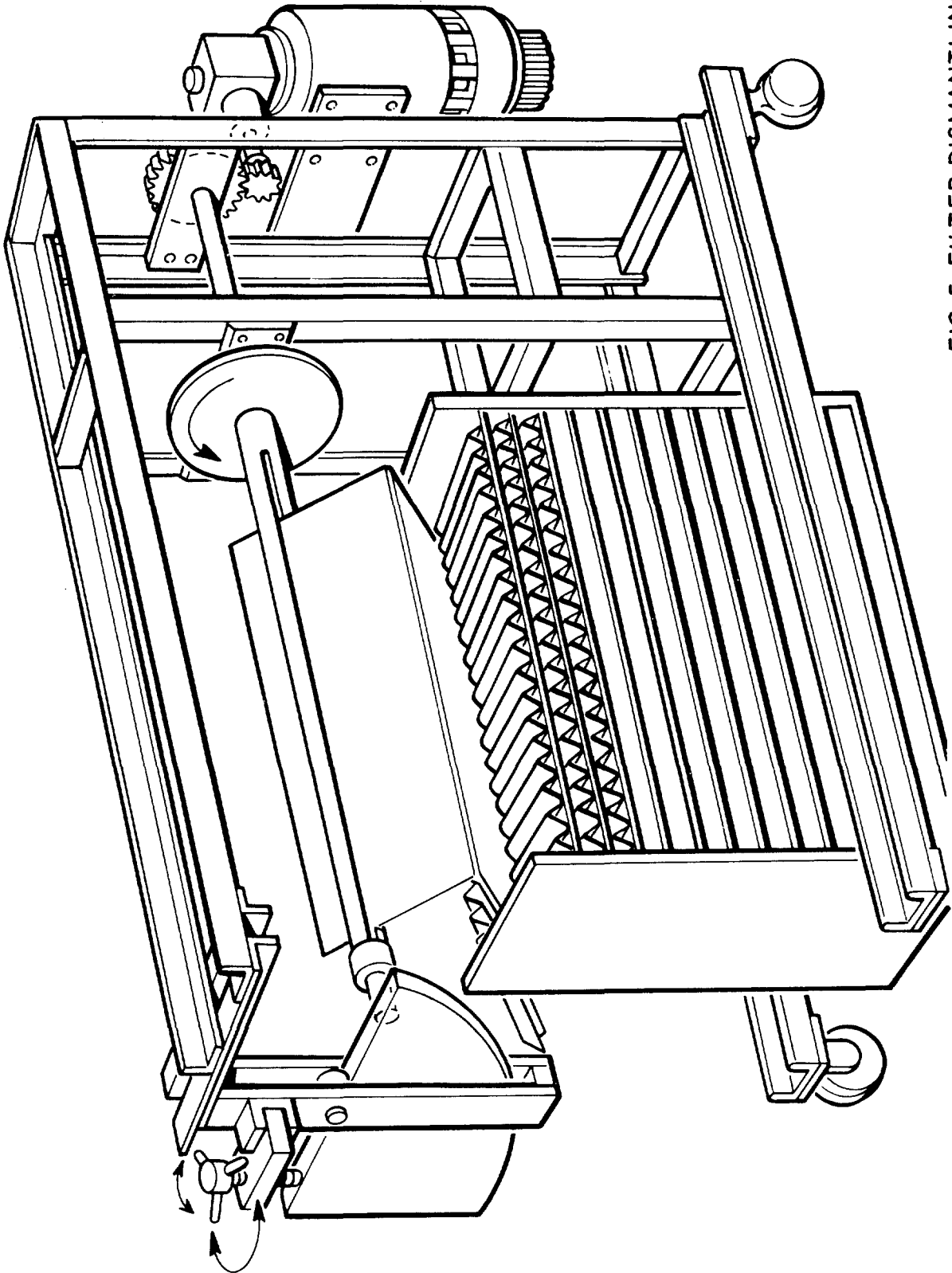


FIG 5 FILTER DISMANTLING MACHINE

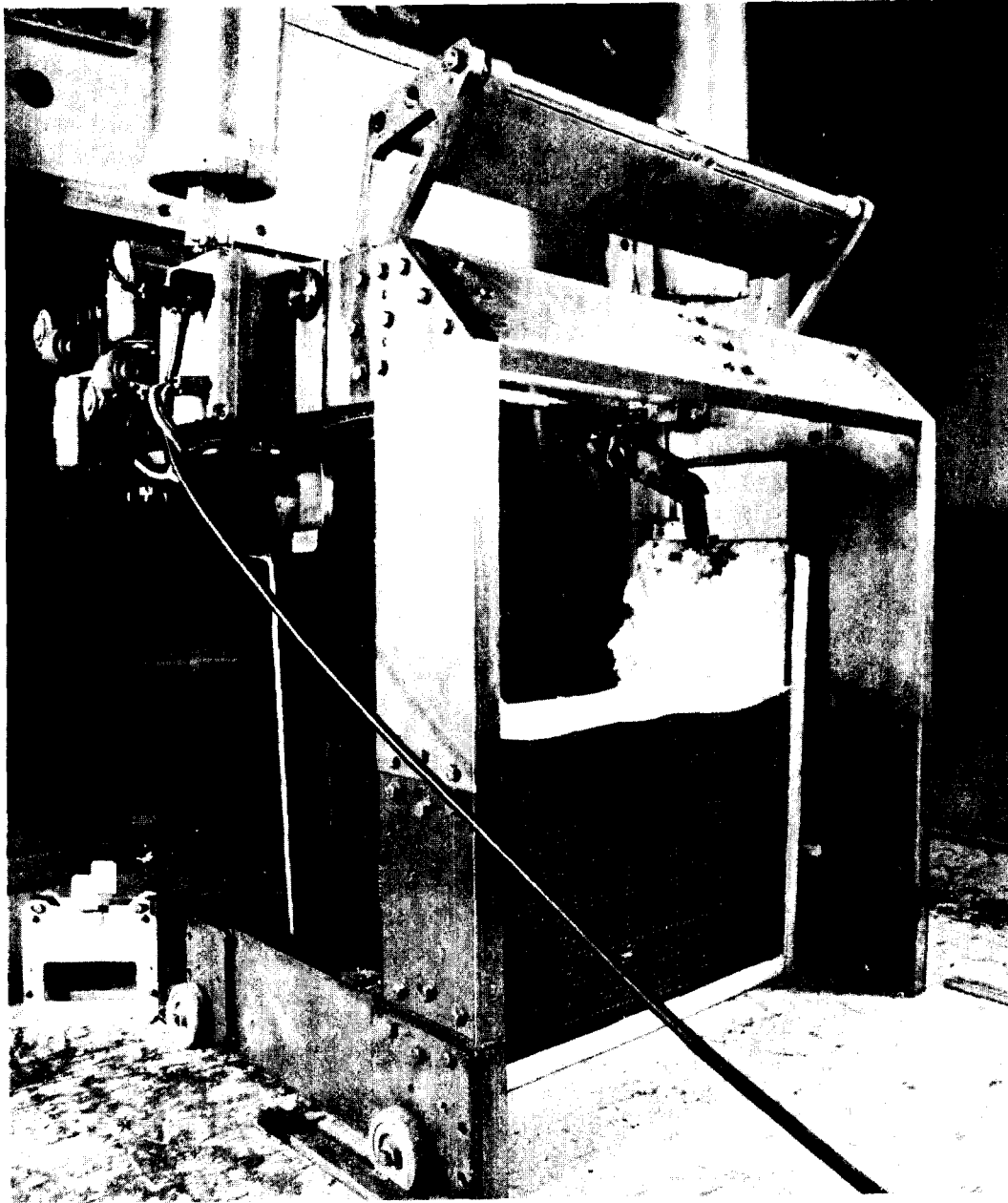


FIGURE 6
PROTOTYPE DISMANTLING MACHINE

15th DOE NUCLEAR AIR CLEANING CONFERENCE

surface contamination, in the form of agglomerated dust, has been observed but this is not readily dispersed. Used filters in good condition have been processed without difficulty but trouble was experienced with plenum filters from an office building. These were of indeterminate age and were found to be coated with a black deposit, possibly derived from vehicle exhaust, which caused the spacers to adhere very firmly to the filter paper. A prototype machine has also been installed at Dounreay for evaluation under radioactive conditions, and again the success of the technique has been found to depend upon the condition of the filter. In some cases badly corroded aluminium spacers, with the residue adhering to the paper, made coiling difficult, whilst in others the paper tore when coiling tension was applied. These weaknesses appeared to result from exposure to wet nitric acid vapours.

Evidence to date is that the technique is quite satisfactory for filters in reasonable condition. In radioactive service, actions should be taken to prevent the arising of heavily contaminated or badly deteriorated filters, and thus the requirement for easy dismantling is in line with good filter practice.

As a longer-term and perhaps more speculative alternative to dismantling, materials of construction are being examined at Harwell which, whilst satisfying the temperature performance criteria described in section 1, can be reduced in bulk by incineration or pyrolysis⁽¹⁵⁾. The materials properties specification is quite demanding and a survey of fibrous materials concluded that a replacement for the glass fibre paper was unlikely to be found. However, three promising resins have been identified which can be used with glass fibre reinforcement for the case and spacers. Preliminary costings show, not surprisingly, a considerable increase in the unit cost of filters and a response from potential users will be obtained before further work to fabricate and test prototypes is carried out.

V. Conclusions

An unconventional design and development approach is required for the ventilation and filtration systems of highly radioactive plant, particularly when due attention is given to the handling and storage procedures. Certain aspects of UKAEA work in this field have been reviewed in the paper, and some of these advances, necessary for heavier-duty plants and operations, will inevitably increase the immediate unit cost of installations. This will be balanced to some extent by reductions in the installation size and perhaps by savings in the waste management operations associated with discarded filters. The overall effect on fuel cycle costs will be insignificant but the influence on the acceptability of certain types of reprocessing and fuel fabrication operations could be quite important.

15th DOE NUCLEAR AIR CLEANING CONFERENCE

References

1. Sykes, G.H. and Harper, J.A. (1968) I.A.E.A. Symposium on the Treatment of Airborne Radioactive Wastes.
2. Moyer, R.A., Crawford, J.H. and Tatum, R.E. (1974) Proceedings of the 13th A.E.C. Air Cleaning Conference.
3. Williams, J.A. and Jackson, R.F. (1976) Unpublished study.
4. Adley, F.E. and Wisehart, D.E. (1961) Proceedings of the 7th A.E.C. Air Cleaning Conference.
5. Horsley, D.M.C. (A.E.R.E. Harwell), 1978, Unpublished work.
6. Davis, R.J. and Truitt, J. (1971) ORNL-4654.
7. Warner, B.F. (1967) Kerntechnik, 9, 249.
8. Thompson, J.K., Clark, R.C. and Fielding, G.H. (1976), Proceedings of the 14th U.S. E.R.D.A. Air Cleaning Conference.
9. Clark, R.C., Fielding, G.H., and Thompson, J.K. (1976). Proceedings of the Seminar on High Efficiency Aerosol Filtration, Aix-en-Provence, 605.
10. Bristow, H.A.S. and Lilleyman, E. (1976), Ibid, 483.
11. U.K. Patent Application No. 26336/78. Changing and storing of active filters.
12. Mallek, H. (1976). Proceedings of the Seminar on High Efficiency Aerosol Filtration, Aix-en-Provence, 495.
13. Sinhuber, D., Stiehl, H.H., and Schroth, W. (1976). Ibid 503.
14. Powell, R.M. (A.E.R.E. Harwell), 1978, Private Communication.
15. Macphail, I. (A.E.R.E. Harwell), 1978, Private Communication.

DISCUSSION

LOO: How will the robot used for filter changeout be maintained? I take it that the robot will be highly contaminated after a few filter changeouts in a real operating condition.

DYMENT: The robot is designed to work in the contaminated atmosphere, although it's the filters, themselves, which bear the vast quantity of the contamination that presents an external hazard. Maintenance will be carried out in an active servicing area which is shielded from the external radiation hazard in the filter cell. The robot would normally not be in the filter cell. It can be maintained there by a staff who can go into the active area without very much in the way of external radiation. The whole concept is to be as reliable as possible, but, of course, it is accepted that nothing is 100% reliable these days.

15th DOE NUCLEAR AIR CLEANING CONFERENCE

ELIMINATION OF NO_x BY SELECTIVE REDUCTION WITH NH₃

A. Bruggeman, L. Meynendonckx, W.R.A. Goossens
S.C.K./C.E.N., Mol, Belgium

Abstract

In nuclear reprocessing plants the nitrogen oxides generated during the dissolution of the fuel are only partially removed in the primary off-gas treatments. Further reduction to the ppm level is necessary as a preliminary step to the cryogenic retention and separation of the noble gases. If simultaneous oxygen removal is not required, selective reduction of NO (and NO₂) to N₂ and H₂O by NH₃ is a preferable method.

The feasibility of this method was investigated on a laboratory scale at atmospheric pressure. Since excess NH₃ has to be destroyed to get a suitable method, not only the catalytic NO reduction by NH₃ in air was studied, but also the catalytic destruction of NH₃ by the oxygen of the air. Hydrogen mordenite was used as catalyst in a packed bed with an internal diameter of 4.15 cm. At temperatures between 350 and 500 °C, NH₃ showed to react preferentially with NO rather than with oxygen. To drop the NO inlet concentration (up to 5,000 ppm v/v in air) to less than 1 ppm v/v at the reactor outlet, a residence time as low as 0.2 s was sufficient when the NH₃ inlet concentration was at least 1.5 times the NO influent concentration. Hence, the NH₃ oxidation in air being slower than the NO reduction by NH₃, the design of the catalytic reactor has to be based on the NH₃ oxidation rate. The experimental study proved that the NH₃ oxidation is a pseudo first order reaction with an Arrhenius activation energy of $2.4 \cdot 10^5 \text{ J mol}^{-1}$.

Although some physical decrepitation of the catalyst occurred, the catalytic activity was not observed to decrease during the experiments. No poisoning of the catalyst could be demonstrated when iodine was added to the process stream. In the absence of O₂ however, the reaction between NO and NH₃ slowed down extremely.

Based on these laboratory results a pilot denitro-unit has been designed and constructed as part of an integrated reprocessing off-gas purification test loop. The working pressure of this unit is $8 \cdot 10^5 \text{ Pa}$, the flow rate $25 \text{ m}^3 \text{ h}^{-1}$ and the maximum concentration 1 % v/v. Demonstration tests with this pilot unit are planned for the second half of 1978.

I. Introduction

In nuclear reprocessing plants the dissolver off-gas contains rather large amounts of nitrogen oxides generated during the dissolution of the fuel in nitric acid. Provided oxygen is present in excess these nitrogen oxides are partially removed in the wet primary off-gas treatments. Complete elimination is precluded due to the slow oxidation of nitric oxide at low concentrations and its reiterative formation from the reaction of nitrogen dioxide with water. The residual nitric oxide content of the off-gas is expected to be of the order of 0.1 to 1 % v/v.

15th DOE NUCLEAR AIR CLEANING CONFERENCE

If cryogenic processes are used to trap the noble gases from the off-gas, the residual concentration of nitrogen oxides has to be further reduced to the ppm level, probably by catalytic reduction to nitrogen. In the non selective reduction with hydrogen, where oxygen reacts first and the excess hydrogen is used for the reduction of nitric oxide, the high oxygen concentration consumes large quantities of hydrogen and excessive capacities of heat exchange are required. If simultaneous oxygen removal is not necessary the selective reduction of nitric oxide to nitrogen is the preferable method for economical as well as for safety reasons.

With proper temperature control and when ammonia is used as the reductant selective catalytic reduction of nitric oxide in the presence of oxygen is possible.⁽¹⁾ In this case the reaction between NH_3 and NO in air has to be faster than the oxidation of NH_3 by the oxygen of the air. The latter reaction however should preferably still be fast enough since excess NH_3 has to be destroyed. Thomas and Pence have reported favourable performances with hydrogen mordenite, an acid resistant molecular sieve, as a catalyst.^(2,3) Recently an evaluation of this method was published.⁽⁴⁾

II. Laboratory experiments and conclusions

Experimental Set Up

The laboratory loop built to investigate the feasibility of the elimination of NO in air by selective reduction with NH_3 at atmospheric pressure is schematically shown in Figure 1. The feeding part comprised pressure regulators, rotameters and regulating valves for the carrier gas, NO , NH_3 and interfering gas. An iodine generator made it possible to add continuously 1 g I_2 per hour to the carrier gas. For this purpose a small flow of 0.027 m^3 (at 20°C and 1 bar) h^{-1} N_2 was almost saturated with I_2 by passing it through a first column filled with I_2 crystals and thermostated at 61°C . Further stabilization of the I_2 flow rate was obtained by crystallization and sublimation in a second column thermostated at 55°C . To prevent crystallization the I_2 containing N_2 flow was then further heated before being added to the carrier gas.

If not otherwise stated, purified plant air with a water content of about 0.5 % v/v (atmospheric dew point of -1°C) was used as the carrier gas at flow rates of 1 to 5 m^3 (at 20°C and 1 bar) h^{-1} . The nitric oxide concentrations were of the order of 0.1 to 0.5 % v/v. The nitric oxide used had a purity of 99.85 % but some oxidation during the addition to the carrier air was observed.

Before entering the reactor the air - $\text{NO}(\text{NO}_x)$ mixture was preheated to the desired operating temperature in an externally heated electric preheater. Behind the preheater and close to the reactor NH_3 was added to this gas mixture. A cylindrical stainless steel reactor with an inner diameter of 41.5 mm and a height of 300 mm contained the catalyst. The reactor walls were also heated to the operating temperature. After leaving the reactor the hot gases were cooled consecutively by air and water.

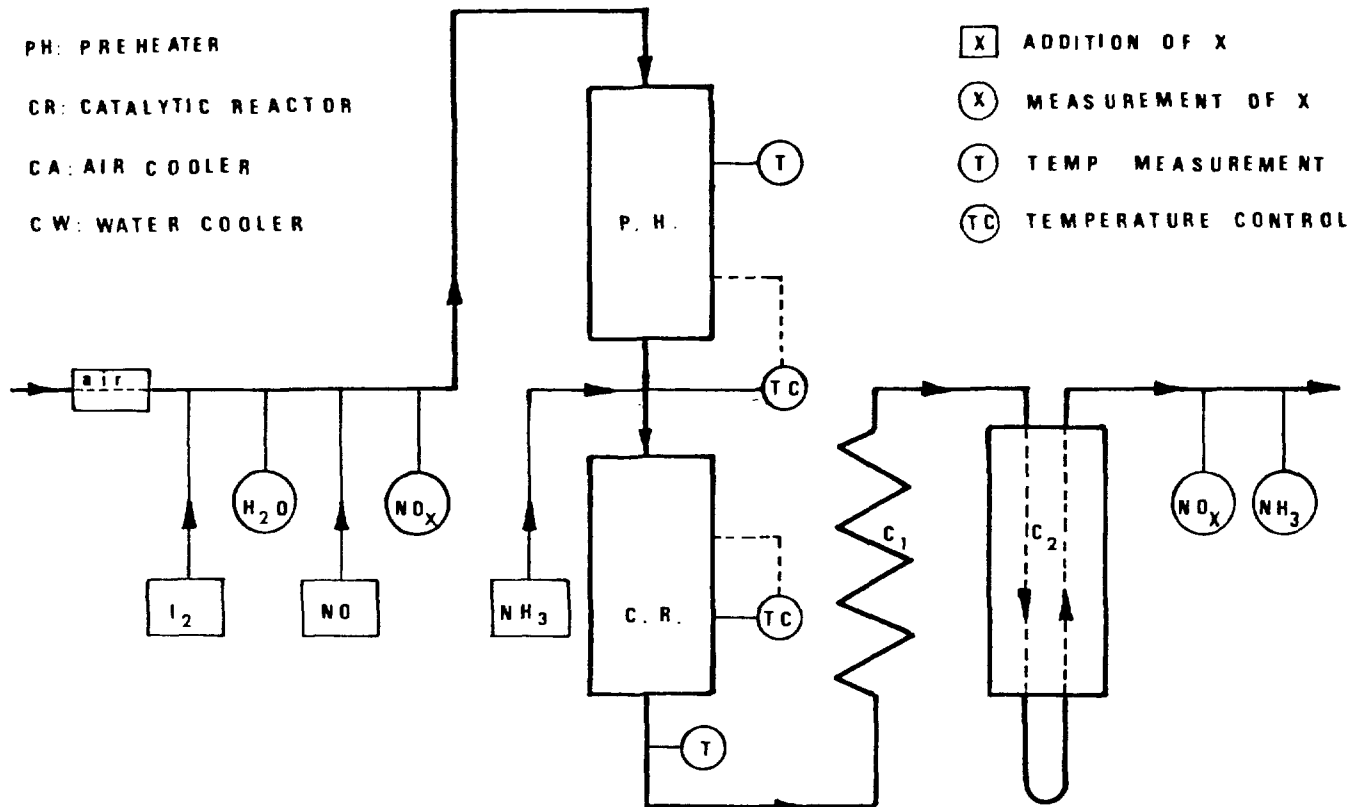


FIGURE 1
 SIMPLIFIED DIAGRAM OF EXPERIMENTAL LABORATORY APPARATUS

Sample ports were provided before the preheater and behind the water cooler. Some samples were also taken between preheater and reactor. Influent and effluent NO_x concentrations were measured with a calibrated chemiluminescence monitor (calibration range 0.01 to 5 ppm v/v) after appropriate dilution, if required. After absorption in 0.01 N H_2SO_4 the effluent NH_3 concentrations were determined colorimetrically by the indophenol method.⁽⁵⁾ For large NH_3 concentrations and when no NO_2 interferences were present, back titration with 0.01 N NaOH gave comparable results.

Catalyst

$\text{Fe}_2\text{O}_3\text{-Cr}_2\text{O}_3\text{-C}$, Pd on Al_2O_3 , Al_2O_3 and sodium mordenite catalysts were tested, but selective reduction of NO to the ppm level was only achieved with synthetic hydrogen mordenite. All the experiments reported below were carried out with 1.6 mm extrudates of hydrogen mordenite.

For the first experiments hydrogen mordenite was prepared by treating the available commercial sodium mordenite with HCl 2 M. After an exchange period of 2 hours the hydrogen mordenite was washed with distilled water until no more Cl^- ions could be detected in the wash water. After drying at 110 °C, further drying was carried out dynamically in the reactor. A second amount was prepared in nearly the same way but instead of HCl 2 M a warm 2 M solution of NH_4Cl was

15th DOE NUCLEAR AIR CLEANING CONFERENCE

used. After washing and drying this catalyst was loaded into the reactor and NH_3 was further expelled by heating. For the last experiments commercial hydrogen mordenite was used (Zeolon 900 H, manufactured by Norton Chemical Company). Some physical and chemical characteristics of this material, as given by the manufacturer are represented in Table I.⁽⁶⁾

Table I. Physical and chemical characteristics of Zeolon 900 H⁽⁶⁾

Chemical composition	$\text{H}_8 \text{ Al}_8 \text{ Si}_{40} \text{ O}_{96} \cdot 24 \text{ H}_2\text{O}$
Effective pore diameter	0.8 - 0.9 nm
Surface area	$450 \text{ m}^2 \text{ g}^{-1}$
Physical form	extrudates 1.6 mm diam.
Equivalent particle diameter	2.8 mm
Bulk packing density	720 kg m^{-3}
Static H_2O capacity	11 wt %

Results and discussion

Selective reduction of NO with NH_3 . The selective reduction of NO in air with NH_3 over hydrogen mordenite was investigated at temperatures between 300 and 500 °C, at space times between 0.2 and 1 s and at inlet NH_3 concentrations between 1 and 2 times the inlet NO concentration. As stated earlier the inlet NO concentration was varied between 1000 and 5000 ppm v/v.

In not any experiment a difference in catalytic activity between the 3 badges of hydrogen mordenite could be observed. The NO conversion increased with increasing NH_3/NO inlet ratio until the latter value was about 1.5. When the added NH_3 concentration was 1.5 times the inlet NO concentration or higher and when the reactor temperature was 400 °C or higher, the effluent NO_x concentration was always measured to be smaller than 1 ppm v/v, whereas the effluent NH_3 concentration decreased with decreasing excess of NH_3 used and with increasing temperature. It could thus be concluded that with hydrogen mordenite as a catalyst and under the conditions mentioned the reaction between NH_3 and NO in air is much faster than the oxidation of NH_3 by the oxygen of the air.

Oxidation of NH_3 in air. As not only NO_x but preferably also the NH_3 added has to be eliminated to the ppm level over the same hydrogen mordenite catalyst, the oxidation rate of the excess NH_3 determines the required reactor dimensions. The oxidation of NH_3 in air was thus studied in the conditions to be used for the selective reduction of NO with NH_3 . Therefore the breakthrough of NH_3 was measured as a function of the inlet NH_3 concentration.

As shown for two series of experiments at a superficial velocity of 80 cm s^{-1} and a temperature of respectively 350 °C and 400 °C in Figure 2, the data obtained in these experiments indicated a pseudo first-order irreversible reaction :

$$r = k_1 C_{\text{NH}_3} \quad (1)$$

where r is the reaction rate, C_{NH_3} the concentration of NH_3 and k_1 the apparent reaction rate constant.

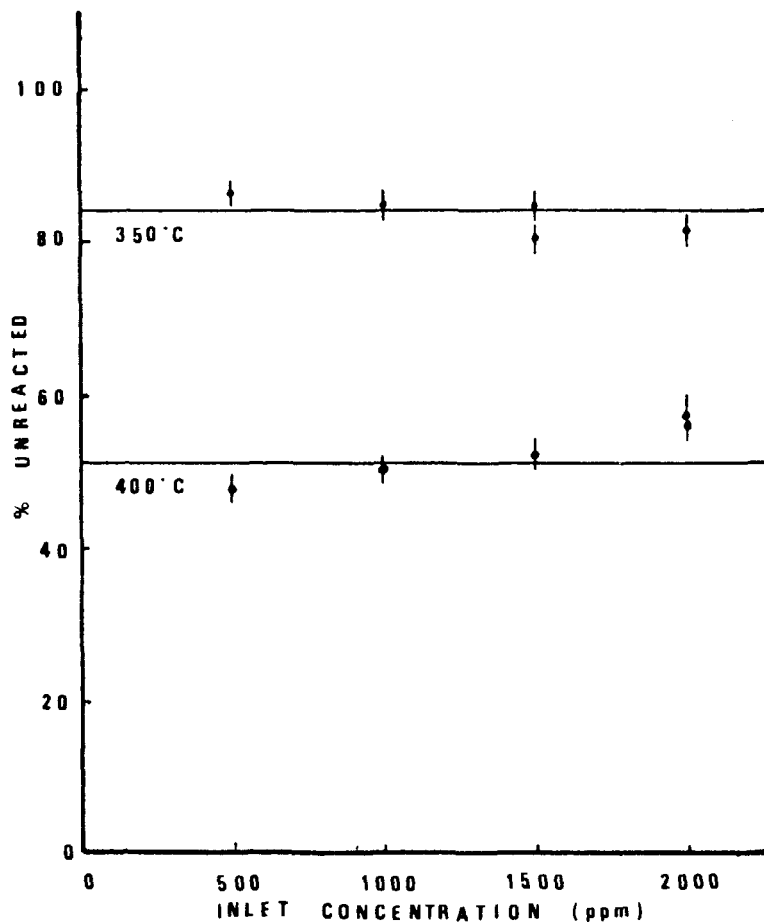


FIGURE 2
REACTION OF NH_3 IN AIR ON HYDROGEN MORDENITE :
UNREACTED NH_3 VS INLET CONCENTRATION

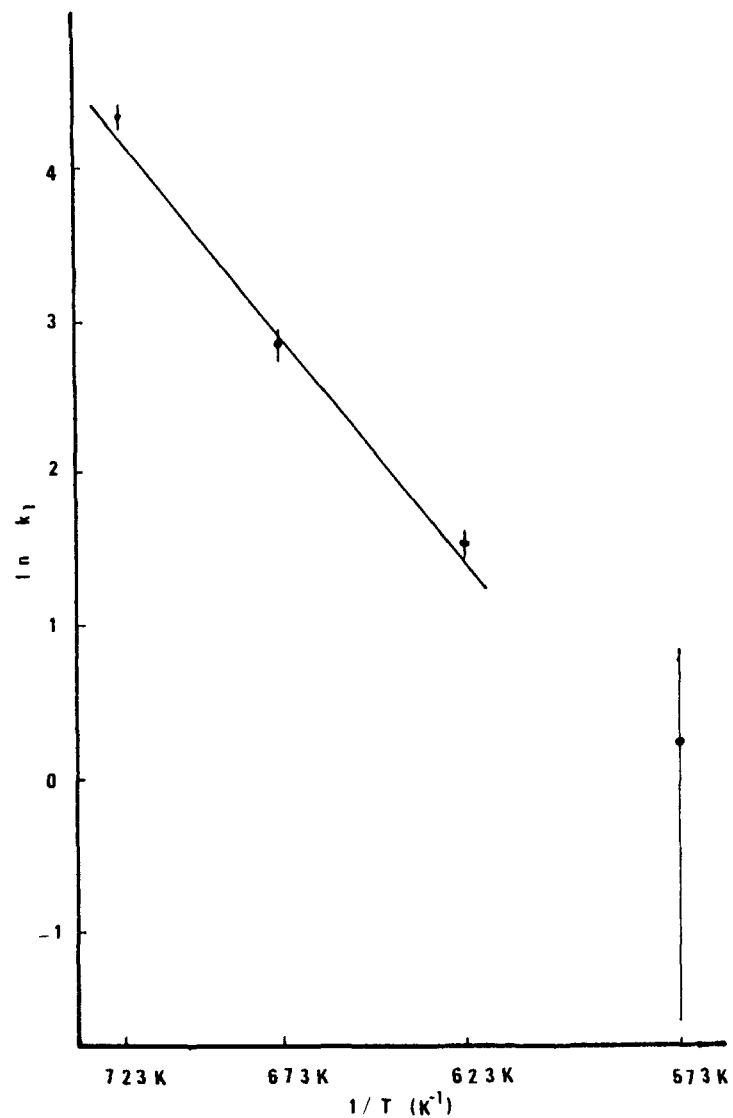


FIGURE 3
REACTION OF NH_3 IN AIR ON HYDROGEN MORDENITE :
TEMPERATURE DEPENDENCE OF THE REACTION RATE

15th DOE NUCLEAR AIR CLEANING CONFERENCE

Especially at higher temperature the apparent reaction rate constant was observed to decrease with decreasing linear velocity. A linear regression analysis yielded :

$k_1 \sim G^{0.54}$ at 450 °C, $k_1 \sim G^{0.43}$ at 400 °C and $k_1 \sim G^{0.21}$ at 350 °C, where G is the total flow rate. This behaviour suggested that the reaction rate was partially controlled by extragranular material transport, but even at 450 °C and 20 cm s⁻¹ a material balance for the hydrodynamic boundary layer around the catalyst pellets yielded a concentration gradient of only 1.2 %. In any case the expression for the reaction rate mentioned above is only an empirical first approximation.

Neglecting their variation with flow rate the apparent reaction rate constants (in m³ per hour and per kg catalyst) at each temperature were averaged. The natural logarithms of these mean values are plotted in Figure 3. When one does not take into account the values at 300 °C, where the experimental failures are too large, a linear regression according to the equation :

$$\ln k_1 = \ln K_A - \frac{E_A}{RT} , \quad (2)$$

where R is the universal gas constant, yields an Arrhenius activation energy, E_A , of $2.4 \cdot 10^5$ J mol⁻¹.

As a first approximation the weight W (kg) of 1.6 mm extrudates of hydrogen mordenite needed to obtain under atmospheric pressure and in air with a water content of 0.5 % v/v a given conversion of NH₃ at a given temperature can thus be calculated from the well known expression for a first-order irreversible reaction in a fixed bed reactor with plug flow :

$$W = \frac{G}{k_1} \ln \frac{C_i}{C_f} , \quad (3)$$

where C_i and C_f are the inlet and outlet concentrations of NH₃. The value of k_1 at the temperature T can be found from Figure 3.

Deterioration of the catalyst. With a new catalyst load the pressure drop over the catalyst bed increased during the first experiments but stabilized later on. When the reactor was unloaded some physical decrepitation of the catalyst was visible and the sieve was clearly more white than before. Porosity measurements revealed that both unused and used catalyst pellets contained practically no meso- or macropores and that the total microporous volume was almost unchanged⁽⁷⁾. The fine powder formed was insoluble in water or acids.

An analogous decrepitation of Norton Zeolon was observed when it was refluxed in HNO₃ 4 M. In this last case X-ray powder patterns of the untreated extrudate, of the powder removed by the refluxing and of the extrudates that had been refluxed indicated that in no case any structural changes had taken place⁽⁸⁾.

During the experiments the catalytic activity was not observed to decrease. After one month working at 450 °C the hydrogen mordenite catalyst still performed well.

15th DOE NUCLEAR AIR CLEANING CONFERENCE

Interference by iodine. Although I_2 will normally be eliminated from the dissolver off-gas before the NO_x abatement, the influence of I_2 on the selective reduction of NO in air with NH_3 over hydrogen mordenite was controlled by adding 0.33 g m^{-3} (at 20°C and 1 bar) of I_2 to the proces gas during 18 days. Even with such large amounts of I_2 only a very small increase of the effluent NO_x and NH_3 concentrations was observed, as represented in Figure 4.

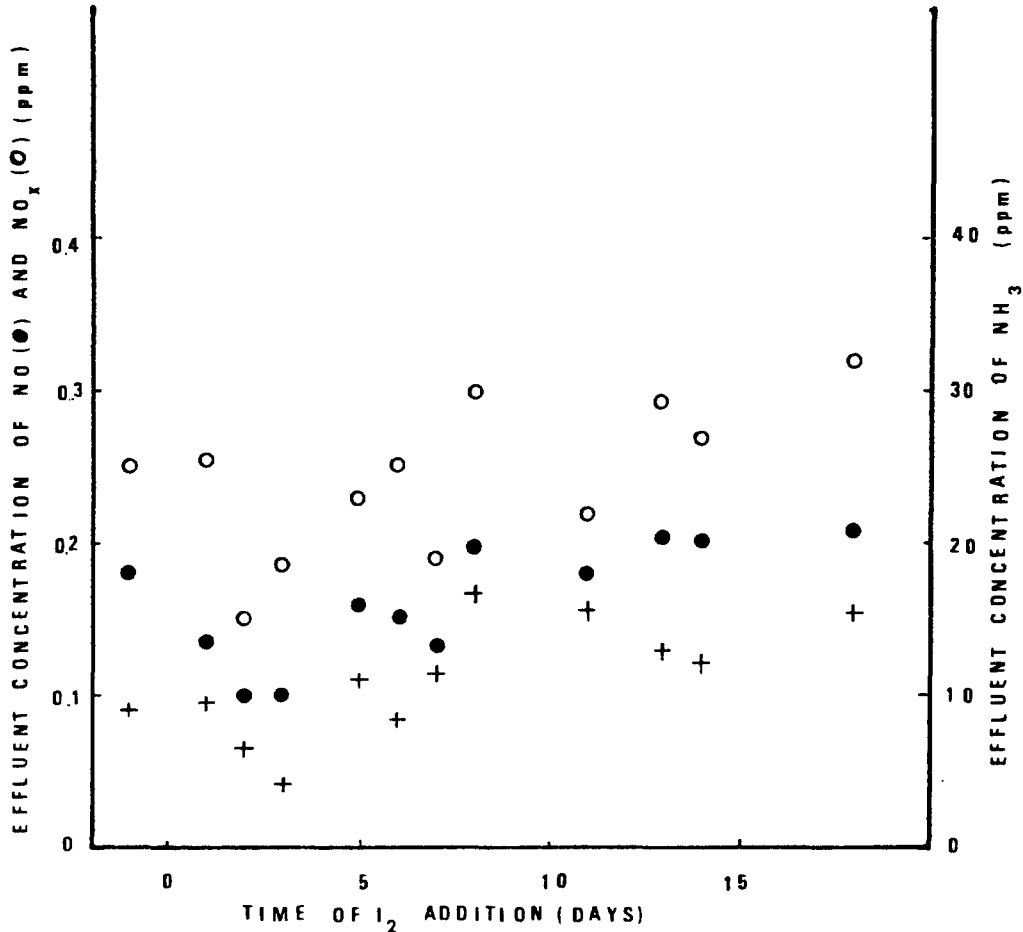


FIGURE 4
SELECTIVE REDUCTION OF NO IN AIR WITH NH_3 :
IODINE INTERFERENCE

Influence of oxygen. The influence of O_2 on the reaction of NO with NH_3 was not studied in detail but a few experiments were carried out with dry N_2 , wet N_2 and a mixture of 80 % v/v dry N_2 and 20 % v/v dry O_2 as the carrier gas. The results obtained with the mixture of N_2 and O_2 corresponded completely with the air results but in the absence of O_2 no reduction of NO by NH_3 could be demonstrated. The rate of the reaction of NO with NH_3 over hydrogen mordenite is thus strongly decreased by the absence of O_2 .

15th DOE NUCLEAR AIR CLEANING CONFERENCE

III. Design and construction of a pilot denitro-unit

Object

Based on the laboratory results discussed above, a pilot denitro-unit has been designed and constructed as part of an integrated reprocessing off-gas purification test loop. After fuel dissolution, nitric acid recovery, aerosol and iodine capture in the wet section of the integrated gas purification loop "Gaston", the off-gas is further purified in the conditioning section before being sent to the cryogenic distillation unit for the separation of krypton and xenon. The object of the denitro installation, which is part of the conditioning section, is the selective elimination beyond the ppm level of the nitrogen oxides from the oxygen containing off-gas, in which they are present for maximum 1 %.

Description

The denitro-unit is shown in Figure 5 and the flow sheet is represented in Figure 6. After compression to $8 \cdot 10^5$ Pa and after passing a cooler condenser and a demister the off-gas with a flow rate of about 25 m^3 (at $20 \text{ }^\circ\text{C}$ and 1 bar) h^{-1} and with a maximum NO_x concentration of 1 % v/v is first heated from about $25 \text{ }^\circ\text{C}$ to about $275 \text{ }^\circ\text{C}$

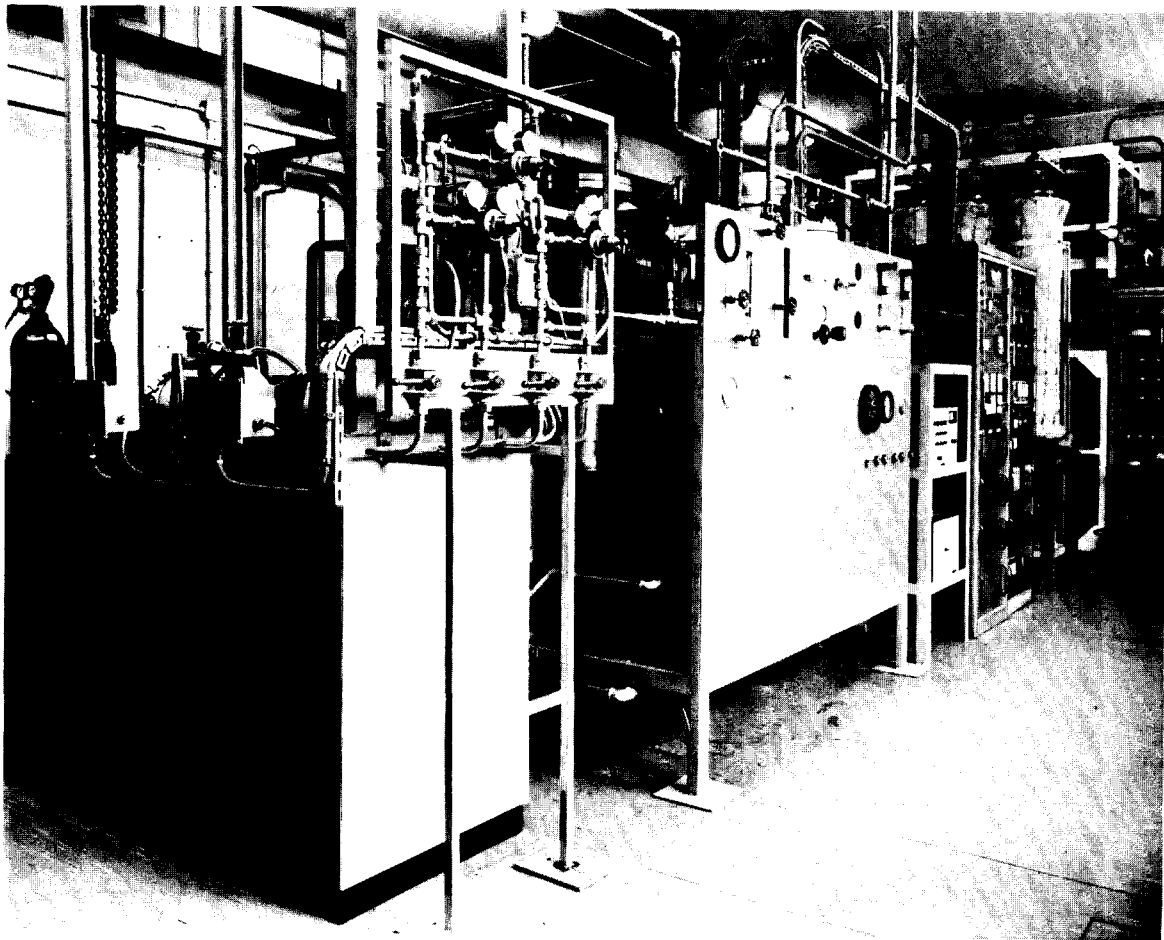


FIGURE 5
VIEW OF THE DENITRO INSTALLATION

15th DOE NUCLEAR AIR CLEANING CONFERENCE

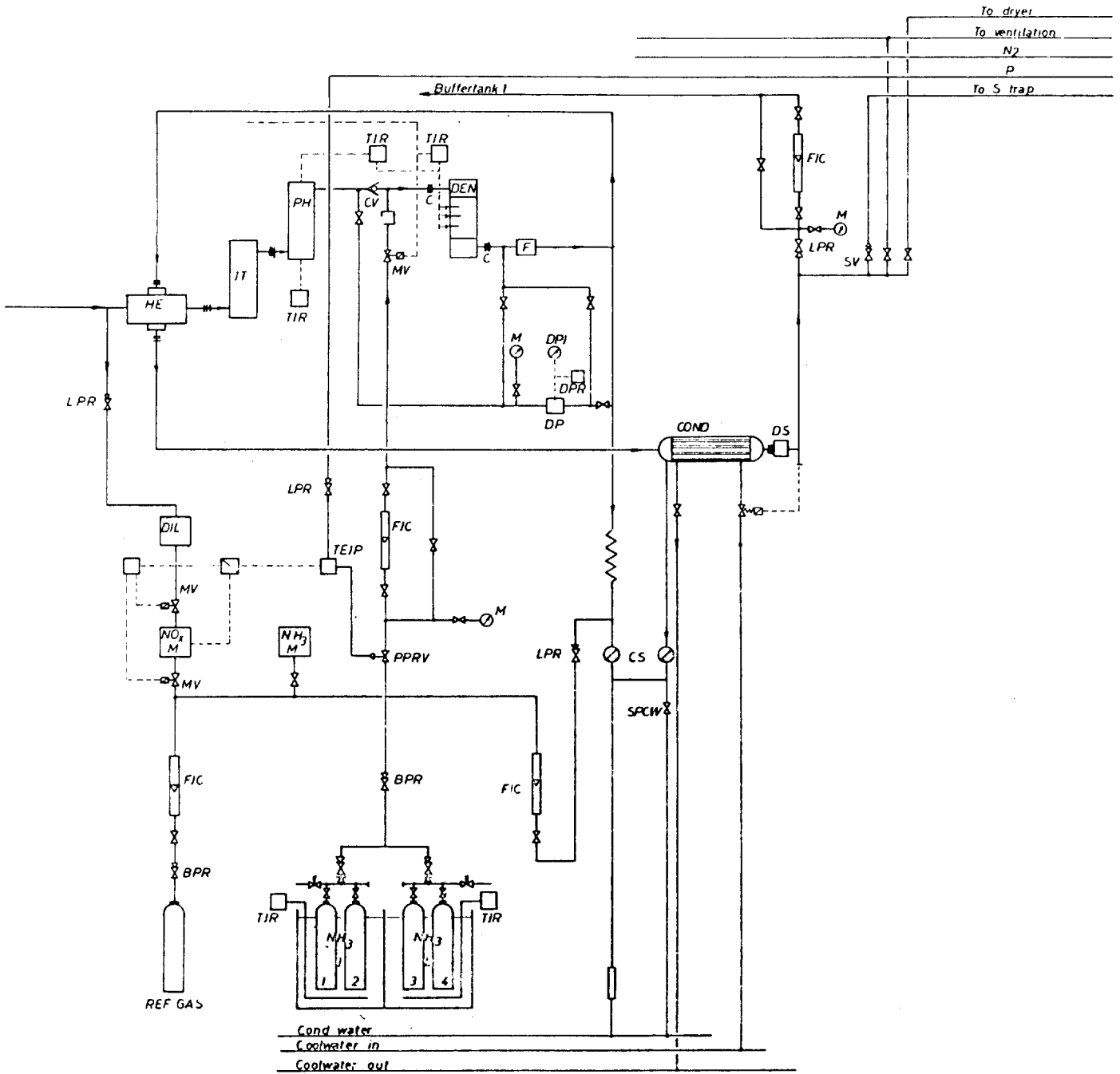


FIGURE 6
FLOW SHEET OF THE DENITRO INSTALLATION

by heat recuperation in a compact helix type heat exchanger. The warm gas passes through a final iodine trap filled with silver impregnated molecular sieves and is then further heated in an electric preheater.

After the preheater and just before the reactor NH₃ gas is added to the off-gas in an amount of 1.5 times the initial NO_x concentration. The addition of NH₃ is regulated by a valve, actuated in function of the NO_x concentration measured at the inlet of the installation. A semi-automatic manifold provides a continuous addition of NH₃. The

15th DOE NUCLEAR AIR CLEANING CONFERENCE

high pressure resisting NH_3 bottles are kept at a pressure of $15.5 \cdot 10^5$ Pa, by heating them in a thermostated water bath at 40°C .

The hot process gas mixed with NH_3 enters the denitro reactor which is filled with the hydrogen mordenite catalyst Zeolon 900 H, 1.6 mm extrudates. Here NO_x and the excess NH_3 have to be reduced to less than 1 ppm by conversion to N_2 and H_2O . The working temperature of the reactor is chosen at 500°C . To reduce heat losses from the reactor, the reactor wall is also heated at 500°C . The temperature in the reactor is measured and in spite of the varying NO_x (and thus also NH_3) concentration, this temperature is kept within a narrow range by a temperature regulator, which drives the preheater. To avoid the formation of dangerous NH_4NO_3 at too low temperatures and damage to the installation at too high temperatures, the NO_x containing off-gas from the wet section is automatically replaced by plant air when the reactor temperature is lower than 300°C or when it rises above 600°C .

A filter which collects dust particles larger than $10\ \mu\text{m}$ has been placed after the reactor. A pressure drop measurement is possible over the reactor, over the filter and over both. After the dust filter a sampling system for NH_3 and NO_x determination is provided. The filtered hot gas leaving the denitro reactor is cooled from 500°C to about 250°C in the previously mentioned heat exchanger and the heat is recuperated by the incoming gas. In the water cooler condenser the gas is further cooled to about 20°C . The cooling feed water is automatically adjusted by a regulation valve which is actuated in function of the temperature of the gas leaving the cooler condenser. The condens water can be sampled.

Finally the proces gas passes through a drop separator and can be sent either to a drying installation or to the vent. It is also possible to recycle a part of the gas over a pressure regulator and a rotameter before the compressor to dilute the incoming gas or to reduce the consumption of compressed air when the denitro installation works as a separate unit. A safety relief valve is placed in parallel on the exit line and will open at a pressure of $10.5 \cdot 10^5$ Pa, releasing the gas to the ventilation.

The mechanical and electrical construction of the pilot unit is completed and demonstration tests are planned for the following months.

IV. Conclusion

Laboratory experiments have confirmed the feasibility of eliminating NO from air beyond the ppm level by adding NH_3 over a hydrogen mordenite catalyst. At atmospheric pressure and with air (water content 0.5 % v/v) as a carrier gas selective catalytic reduction of NO to N_2 is easily achieved at temperatures up to 500°C . Under the same conditions dimensioning of the reactor for destruction of the excess NH_3 by the O_2 of the air is made possible. The activity of the catalyst remains rather constant even when large concentrations of I_2 are present. On the basis of the laboratory results a pilot installation has been designed and constructed which will demonstrate the process in an integrated gas purification loop at a pressure of $8 \cdot 10^5$ Pa during the next months.

15th DOE NUCLEAR AIR CLEANING CONFERENCE

Acknowledgements

The authors are very indebted to Dr. D.T. Pence of Science Applications Inc. and to Dr. L.H. Baetslé and Ir. G. Collard, for helpful discussions. The technical assistance of D. Smets, J. Van Dooren, E. Ooms and J. Boons was greatly appreciated.

References

1. H.C. Andersen, W.J. Green and D.R. Steele, "Catalytic treatment of nitric acid plant tail gas" Ind. Eng. Chem. vol. 53, no. 3, pp 199 (1961).
2. D.T. Pence and T.R. Thomas, "NO_x abatement at nuclear processing plants", Proceedings of the Second AEC Environmental Protection Conference, WASH-1332(74) (April 1974).
3. T.R. Thomas and D.T. Pence, "Reduction of NO_x with ammonia over zeolite catalyst", Proceedings of the 67th Annual Meeting of the Air Pollution Control Association, paper no. 75-258 (June 1974).
4. T.R. Thomas and D.H. Munger, "An evaluation of NO_x abatement by NH₃ over hydrogen mordenite for nuclear fuel reprocessing plants", ICP-1133 (January 1978).
5. Z. Marczenko, "Spectrophotometric determination of elements" pp. 392, Ellis Horwood Ltd, Chichester (1976).
6. Norton Chemical Process Products Division, "Zeolon acid resistant molecular sieves", Bulletin Z-50.
7. P. Henrion, S.C.K./C.E.N., personal communication.
8. L.C. Lewis "Evaluation of adsorbents for purification of noble gases in dissolver off-gas" IN-1402 (July 1970).

DISCUSSION

T. R. THOMAS: What was the dewpoint of your test gas and what was the effluent concentration of ammonia from your bed?

BRUGGEMAN: The dewpoint of the test gas was -1^oC, corresponding to about 0.5 volume-% of water. The concentration of ammonia was dependent on the working conditions, but the final working conditions were such that the ammonia concentration was below one part per million at the outlet of the reactor. These conditions do not seem difficult to fulfill, at least in the range of working conditions we have tested.

15th DOE NUCLEAR AIR CLEANING CONFERENCE

T. R. THOMAS: That agrees very well with our work. But, when the gas streams are wet, excess ammonia seems to come roaring through.

BRUGGEMAN: We didn't do experiments with wet gases. We used dry gases and then very dry gases and the results didn't change.

T. R. THOMAS: You mean you didn't get ammonia coming through with the wet gas?

BRUGGEMAN: No. We used gases that were drier. We used mixtures of dry oxygen and dry nitrogen and we used air with a dewpoint of -1°C . We didn't use gases with a higher dewpoint.

T. R. THOMAS: What was the temperature gradient in your bed and were you able to measure the inlet-outlet temperature?

BRUGGEMAN: In the laboratory experiments, we had no means to measure the temperature gradient. We will have them in the pilot unit.

T. R. THOMAS: Is your rate constant based on the outlet or inlet temperature of the bed? I always had a gradient of $40-50^{\circ}$ across the bed when I ran my tests.

BRUGGEMAN: In our low NO and NH_3 inlet experiments, the temperature at the inlet and the outlet was about the same because we heated the walls of the catalytic reactor to keep it at the same working temperature as the incoming gases from the preheater. At higher concentrations, temperature gradients are hard to avoid.

T. R. THOMAS: Have you looked at NO_2 in this reaction?

BRUGGEMAN: We measured NO_2 but we didn't use NO_2 at the inlet. We always used nitric oxide. We have seen some oxidation of nitric oxide, about 20% in some cases. In the preheater, we had a small reduction. At higher temperatures, we had a reduction of nitrogen dioxide to nitric oxide, so the first oxidation was opposite to the reduction in the preheater. We think that, at most, we had 10% nitrogen dioxide at the inlet of the reactor.

COWAN: Did you check to see if there's any N_2O in the offgas from the reaction of the ammonia and oxides of nitrogen?

BRUGGEMAN: We didn't measure N_2O because we used only a chemiluminescence monitor. The formation of N_2O in this reaction is possible, but we do not expect formation of N_2O at temperatures as high as 500°C .

T. R. THOMAS: I'd like to make a comment on this topic. We looked at that particular reaction very closely, and, in no case, could we find N_2O when only NO was introduced into the feed gas. It only occurs in the presence of NO_2 . There was very little NO_2 from this reaction. When starting with 5000 ppm NO , possibly 10% went to NO_2 but I never saw N_2O when only NO was introduced upstream of the reactor.

